MOLECULAR MECHANISMS IN CHRONIC KIDNEY DISEASE

EDITED BY: Claudia Torino, Evangelia Dounousi, Samar Abd ElHafeez and Nejra Prohic

PUBLISHED IN: Frontiers in Cell and Developmental Biology

frontiers Research Topics

Frontiers eBook Copyright Statement

The copyright in the text of individual articles in this eBook is the property of their respective authors or their respective institutions or funders. The copyright in graphics and images within each article may be subject to copyright of other parties. In both cases this is subject to a license granted to Frontiers.

The compilation of articles constituting this eBook is the property of Frontiers.

Each article within this eBook, and the eBook itself, are published under the most recent version of the Creative Commons CC-BY licence. The version current at the date of publication of this eBook is CC-BY 4.0. If the CC-BY licence is updated, the licence granted by Frontiers is automatically updated to the new version.

When exercising any right under the CC-BY licence, Frontiers must be attributed as the original publisher of the article or eBook, as applicable.

Authors have the responsibility of ensuring that any graphics or other materials which are the property of others may be included in the CC-BY licence, but this should be checked before relying on the CC-BY licence to reproduce those materials. Any copyright notices relating to those materials must be complied with.

Copyright and source acknowledgement notices may not be removed and must be displayed in any copy, derivative work or partial copy which includes the elements in question.

All copyright, and all rights therein, are protected by national and international copyright laws. The above represents a summary only. For further information please read Frontiers' Conditions for Website Use and Copyright Statement, and the applicable CC-BY licence.

ISSN 1664-8714
ISBN 978-2-88971-258-8
DOI 10.3389/978-2-88971-258-8

About Frontiers

Frontiers is more than just an open-access publisher of scholarly articles: it is a pioneering approach to the world of academia, radically improving the way scholarly research is managed. The grand vision of Frontiers is a world where all people have an equal opportunity to seek, share and generate knowledge. Frontiers provides immediate and permanent online open access to all its publications, but this alone is not enough to realize our grand goals.

Frontiers Journal Series

The Frontiers Journal Series is a multi-tier and interdisciplinary set of open-access, online journals, promising a paradigm shift from the current review, selection and dissemination processes in academic publishing. All Frontiers journals are driven by researchers for researchers; therefore, they constitute a service to the scholarly community. At the same time, the Frontiers Journal Series operates on a revolutionary invention, the tiered publishing system, initially addressing specific communities of scholars, and gradually climbing up to broader public understanding, thus serving the interests of the lay society, too.

Dedication to Quality

Each Frontiers article is a landmark of the highest quality, thanks to genuinely collaborative interactions between authors and review editors, who include some of the world's best academicians. Research must be certified by peers before entering a stream of knowledge that may eventually reach the public - and shape society; therefore, Frontiers only applies the most rigorous and unbiased reviews.
Frontiers revolutionizes research publishing by freely delivering the most outstanding research, evaluated with no bias from both the academic and social point of view. By applying the most advanced information technologies, Frontiers is catapulting scholarly publishing into a new generation.

What are Frontiers Research Topics?

Frontiers Research Topics are very popular trademarks of the Frontiers Journals Series: they are collections of at least ten articles, all centered on a particular subject. With their unique mix of varied contributions from Original Research to Review Articles, Frontiers Research Topics unify the most influential researchers, the latest key findings and historical advances in a hot research area! Find out more on how to host your own Frontiers Research Topic or contribute to one as an author by contacting the Frontiers Editorial Office: frontiersin.org/about/contact

MOLECULAR MECHANISMS IN CHRONIC KIDNEY DISEASE

Topic Editors:
Claudia Torino, Italian National Research Council, Italy
Evangelia Dounousi, University of Ioannina, Greece
Samar Abd ElHafeez, Alexandria University, Egypt
Nejra Prohic, Clinical Center University of Sarajevo, Bosnia and Herzegovina

Citation: Torino, C., Dounousi, E., ElHafeez, S. A., Prohic, N., eds. (2021). Molecular Mechanisms in Chronic Kidney Disease. Lausanne: Frontiers Media SA.
doi: 10.3389/978-2-88971-258-8

Table of Contents

05 ***Editorial: Molecular Mechanisms in Chronic Kidney Disease***
Claudia Torino, Evangelia Dounousi, Samar Abd ElHafeez and Nejra Prohic

09 ***NLRP2 Regulates Proinflammatory and Antiapoptotic Responses in Proximal Tubular Epithelial Cells***
Marianna N. Rossi, Antonia Pascarella, Valerio Licursi, Ivan Caiello, Anna Taranta, Laura R. Rega, Elena Levtchenko, Francesco Emma, Fabrizio De Benedetti and Giusi Prencipe

23 ***Unraveling Cardiovascular Risk in Renal Patients: A New Take on Old Tale***
Michele Provenzano, Giuseppe Coppolino, Luca De Nicola, Raffaele Serra, Carlo Garofalo, Michele Andreucci and Davide Bolignano

37 ***Dynamic Phenotypes and Molecular Mechanisms to Understand the Pathogenesis of Diabetic Nephropathy in Two Widely Used Animal Models of Type 2 Diabetes Mellitus***
Yanfei Liu, Hui Huang, Rui Gao and Yue Liu

53 ***Mechanisms of Cardiovascular Disorders in Patients With Chronic Kidney Disease: A Process Related to Accelerated Senescence***
Julia Carracedo, Matilde Alique, Carmen Vida, Guillermo Bodega, Noemí Ceprián, Enrique Morales, Manuel Praga, Patricia de Sequera and Rafael Ramírez

67 ***The Multi-Faced Extracellular Vesicles in the Plasma of Chronic Kidney Disease Patients***
Hara T. Georgatzakou, Efthimia G. Pavlou, Effie G. Papageorgiou, Issidora S. Papassideri, Anastasios G. Kriebardis and Marianna H. Antonelou

76 ***Paget's Disease and Secondary Hyperparathyroidism: Is Healing Possible?***
Vincenzo Antonio Panuccio and Rocco Tripepi

80 ***Urinary Neutrophil Gelatinase-Associated Lipocalin (NGAL) Predicts Renal Function Decline in Patients With Glomerular Diseases***
Giuseppe Coppolino, Nicola Comi, Davide Bolignano, Gemma Patella, Alessandro Comi, Michele Provenzano, Laura Rivoli, Michele Andreucci and Giorgio Fuiano

87 ***Induction of Autophagy by Pterostilbene Contributes to the Prevention of Renal Fibrosis via Attenuating NLRP3 Inflammasome Activation and Epithelial-Mesenchymal Transition***
Ying-Jan Wang, Yu-Ying Chen, Ching-Mao Hsiao, Min-Hsiung Pan, Bour-Jr Wang, Yu-Chi Chen, Chi-Tang Ho, Kuo-Ching Huang and Rong-Jane Chen

99 ***Elevated suPAR is an Independent Risk Marker for Incident Kidney Disease in Acute Medical Patients***
Esben Iversen, Morten Baltzer Houlind, Thomas Kallemose, Line Jee Hartmann Rasmussen, Mads Hornum, Bo Feldt-Rasmussen, Salim S. Hayek, Ove Andersen and Jesper Eugen-Olsen

108 ***Icariin Prevents Extracellular Matrix Accumulation and Ameliorates Experimental Diabetic Kidney Disease by Inhibiting Oxidative Stress via GPER Mediated p62-Dependent Keap1 Degradation and Nrf2 Activation***
Kai Wang, Xiulan Zheng, Zhenzhen Pan, Wenhui Yao, Xin Gao, Xiniao Wang and Xuansheng Ding

125 ***Insulin: Trigger and Target of Renal Functions***
Ana F. Pina, Diego O. Borges, Maria João Meneses, Patrícia Branco, Rita Birne, Antonio Vilasi and Maria Paula Macedo

140 ***DNA Methylation Associated With Diabetic Kidney Disease in Blood-Derived DNA***
Laura J. Smyth, Christopher C. Patterson, Elizabeth J. Swan, Alexander P. Maxwell and Amy Jayne McKnight

153 ***The Role of Disturbed Mg Homeostasis in Chronic Kidney Disease Comorbidities***
Cristian Rodelo-Haad, M. Victoria Pendón-Ruiz de Mier, Juan Miguel Díaz-Tocados, Alejandro Martin-Malo, Rafael Santamaria, Juan Rafael Muñoz-Castañeda and Mariano Rodríguez

168 ***O-GlcNAcylation Suppresses the Ion Current IClswell by Preventing the Binding of the Protein ICln to α-Integrin***
Roberta Costa, Alessia Remigante, Davide A. Civello, Emanuele Bernardinelli, Zoltán Szabó, Rossana Morabito, Angela Marino, Antonio Sarikas, Wolfgang Patsch, Markus Paulmichl, Tamás Janáky, Attila Miseta, Tamás Nagy and Silvia Dossena

191 ***The Aryl Hydrocarbon Receptor in Chronic Kidney Disease: Friend or Foe?***
Yenan Mo, Zhaoyu Lu, Lixin Wang, Chunlan Ji, Chuan Zou and Xusheng Liu

203 ***Transient Receptor Potential Channel 6 Knockout Ameliorates Kidney Fibrosis by Inhibition of Epithelial–Mesenchymal Transition***
Yanhong Zhang, Nina Yin, Anbang Sun, Qifang Wu, Wenzhu Hu, Xin Hou, Xixi Zeng, Min Zhu and Yanhong Liao

218 ***Fiber Derived Microbial Metabolites Prevent Acute Kidney Injury Through G-Protein Coupled Receptors and HDAC Inhibition***
Yunzi Liu, Yan J. Li, Yik W. Loh, Julian Singer, Weiping Zhu, Laurence Macia, Charles R. Mackay, Weiming Wang, Steven J. Chadban and Huiling Wu

235 ***The Pharmacological Effect and Mechanism of Lanthanum Hydroxide on Vascular Calcification Caused by Chronic Renal Failure Hyperphosphatemia***
Lulu Zhao, Shengnan Wang, Hong Liu, Xiaoli Du, Ren Bu, Bing Li, Ruilan Han, Jie Gao, Yang Liu, Jian Hao, Jianrong Zhao, Yan Meng and Gang Li

251 ***Renal Ciliopathies: Sorting Out Therapeutic Approaches for Nephronophthisis***
Marijn F. Stokman, Sophie Saunier and Alexandre Benmerah

frontiers in Cell and Developmental Biology

EDITORIAL
published: 29 June 2021
doi: 10.3389/fcell.2021.712834

Editorial: Molecular Mechanisms in Chronic Kidney Disease

Claudia Torino[1]*, *Evangelia Dounousi*[2], *Samar Abd ElHafeez*[3] *and Nejra Prohic*[4]

[1] *Institute of Clinical Physiology, National Research Council, Reggio Calabria, Italy,* [2] *School of Health Sciences, University of Ioannina, Ioannina, Greece,* [3] *High Institute of Public Health, Alexandria University, Alexandria, Egypt,* [4] *Clinical Center University of Sarajevo, Sarajevo, Bosnia and Herzegovina*

Keywords: CKD, ESRD, aetiology, biomarkers, risk factors

Editorial on the Research Topic

Molecular Mechanisms in Chronic Kidney Disease

Recent progress in the field of medicine, together with improved therapeutic resources, resulted in a significant lengthening of the life span, with the consequent increase in the prevalence of chronic diseases, typically associated with age. Among the non-transmissible diseases, Chronic Kidney Disease (CKD), represents a major public health problem, having reached a worldwide prevalence of 13% (Hill et al., 2016).

Molecular mechanisms underlying CKD have been investigated for long, unravelling the role of membrane proteins, inflammatory processes or even microbiota in the development and progression of this disease (**Figure 1**).

One example is given by Nod-like Receptor Pyrin domain containing proteins (NLRPs), expressed by resident renal cells. Rossi et al. investigated the possible role of NLRPs in cystinosis, a genetic disorder that affects kidney proximal tubular epithelial cells (PTEC). Analysing human control and cystinotic immortalised PTEC, they found that cystinotic cells had higher expression levels of NLRP2, suggesting that NLRP2 may have a key role in regulating proinflammatory, profibrotic, and antiapoptotic responses in PTEC, contributing to the pathogenesis of this disease. Focusing on inflammation, NLRP3 inflammasome activation plays a central role in renal damage. This process is negatively regulated by autophagy, investigated by Wang et al. in order to identify potential therapeutic approaches. Analysing the effect of pterostilbene (PT) on renal fibrosis, they found a significant reduction of renal fibrosis in CKD models, reduction due to the downregulation of NLRP3 inflammasome activation. Another mechanism involved in kidney fibrosis is the epithelial–mesenchymal transition (EMT). As the Transient Receptor Potential Channel 6 (TRPC6) knockout plays an anti-fibrotic role, Zhang et al. investigated this relationship in mice models. Limiting the search on diabetic nephropathy, O-GlcNAcylation, a post-translational modification of proteins, may be involved in the pathogenic process. In order to unravel mechanisms downstream this phenomenon, Costa et al. investigated his role in the impairment of the regulatory volume decrease (RVD) after cell swelling. Their study shows that O-GlcNAcylation affects RVD by influencing IClswell, i.e., the chloride current induced by cell swelling.

The recent advances in sequencing technologies have notably increased our knowledge of the gut-kidney axis. In their paper, Liu et al. explored the possible link between short-chain fatty acids (SCFAs), diet and gut microbiome, finding a partial protection against AKI and subsequent CKD in mice fed with a high content of fibre. This led to the conclusion that dietary manipulation of the gut microbiome protects against kidney disease onset and progression.

Among the new frontiers of genetics, epigenetics investigates modifications in gene expression (i.e., methylation) without changing the DNA sequence. Smyth at al. analysed DNA methylation in

OPEN ACCESS

Edited and reviewed by:
Masaru Katoh,
National Cancer Centre
(Japan), Japan

****Correspondence:***
Claudia Torino
ctorino@ifc.cnr.it

Specialty section:
This article was submitted to Molecular Medicine, a section of the journal Frontiers in Cell and Developmental Biology

Received: *21 May 2021*
Accepted: *07 June 2021*
Published: *29 June 2021*

Citation:
Torino C, Dounousi E, Abd ElHafeez S and Prohic N (2021) Editorial: Molecular Mechanisms in Chronic Kidney Disease. Front. Cell Dev. Biol. 9:712834. doi: 10.3389/fcell.2021.712834

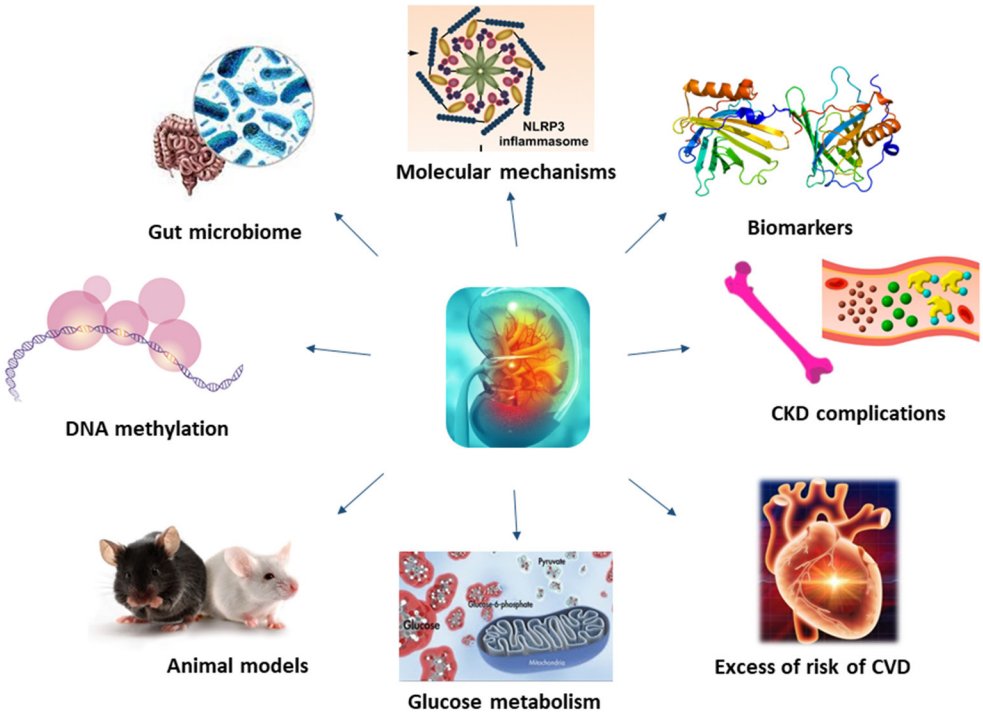

FIGURE 1 | Molecular mechanisms underlying CKD have not been fully understood. Recent studies, thanks to the application of new technology and more efficient animal models, have shed light on novel mechanisms and biomarkers of CKD, also unravelling the role of kidney on glucose metabolism, CKD and CVD complications.

677 diabetic patients with or without DKD, finding high methylation levels in 2 genes involved in RNA transcription and splicing (ZNF187 and CCNL1).

One of the difficulties in unravelling molecular mechanisms of CKD is that results obtained in animal models may diverge from that obtained in real patients. Nephronophthisis (NPH), an autosomal recessive ciliopathy, is an example. In their review, Stokman et al. summarise the most important findings of therapeutic approaches in NPH model systems. Looking at data available so far, in spite of many potential therapies identified, results are limited by the lack of animal models able to reproduce the juvenile NPH phenotype. Employment of non-orthologous animal models and developments in organoid technology can potentially fill this gap and provide new opportunities for personalised treatments. Better results were obtained with diabetic nephropathy (DN). Liu et al. explored its pathogenesis in two different animal models, finding that a spontaneous T2DM model, established by feeding KK-Ay mice with a high-fat diet, showed renal dysfunction and pathology before mice in which diabetes was chemically induced, with increased in severity over the length of the experiment. As KK-Ay mice showed earlier onset of the typical pathological characteristics associated with T2DM, together with renal lesions suggestive of kidney damage, they could be useful preclinical model for the development of anti-DN drugs. An example of therapeutic approach developed in animal models is given by Wang et al., who tested the efficacy of icariin, the flavonoids used in traditional Chinese medicine for kidney disease. They results showed an improvement of renal parameters, as well as positive histopathological changes of kidney, suggesting that the treatment could inhibit T1DM.

If effects of glucose on kidney are clear, kidney function in glucose metabolism is less known. In this review, Pina et al. summarise literature available on insulin and kidney, focusing on kidney dysmetabolism and hyperinsulinemia/insulin resistance (IR). It emerges a new role for kidney: not only a mere target of insulin action, but also damaged by IR, even in absence of diabetes. However, if IR is responsible for the onset and progression of CKD, or vice versa, need to be clarified.

Whilst some of the molecular mechanisms resulting in renal failure have been unravelled, those underlining CKD complications are more complex, being associated with coagulation abnormalities, endothelial dysfunction, vascular calcification, uremic toxins, oxidative and metabolic stress and inflammation (Culleton et al., 1999; Schillaci et al., 2001; De Leeuw et al., 2002; Anavekar et al., 2004; Shlipak et al., 2004; Weiner et al., 2004) (**Figure 1**). Among uremic toxins, those tryptophan-derived toxins are of particular interest because of their cardiovascular toxicity and its bound with the aryl hydrocarbon receptor (AhR), considered a potential target for new therapeutic interventions. In their review, Mo et al. showed the existing link between AhR and CKD complications, including cardiovascular disease (CVD), and its involvement in the enhancement of the intestinal barrier function to mitigate the effects of uremic toxins.

Among biomarkers potentially useful for monitoring kidney disease, Neutrophil Gelatinase-Associated Lipocalin (NGAL), holds promising capacities in predicting renal function worsening in various renal diseases. Starting from this hypothesis, Coppolino et al. tested the efficacy of urinary NGAL (uNGAL) in 61 patients affected by glomerulonephritides (GNs). They found that uNGAL levels were inversely correlated with eGFR, with progressor subjects showing exceedingly high baseline uNGAL values as compared with non-progressors. Furthermore, subjects with uNGAL values above the optimal cut-off of 107 ng/mL experienced a more rapid progression to the renal endpoint, indicating that this biomarker may represent a real-time indicator of renal damage and an independent predictor of renal disease progression. Another biomarkers thought to be involved in the pathogenesis and development of kidney disease is soluble urokinase plasminogen activator receptor (suPAR). Iversen et al., analysing retrospectively data from 25,000 patients, found that elevated suPAR was independently associated with incident chronic and acute kidney conditions, highlighting the potential for using suPAR in risk classification models to identify high-risk patients who could benefit from early clinical interventions.

CKD progression is strongly influenced by diabetes, hypertension, and CVD. Even though it is known in literature that hypomagnesemia is associated with the development and progression of these comorbidities, no indications on the usefulness of Mg supplementation in preventing adverse clinical outcomes are available. In their analysis, Rodelo-Haad et al. conclude that no strong evidence is available to make a formal recommendation to prescribe Mg supplements. However, some data strongly suggest the benefits of Mg on vascular calcification, CVD, and kidney function, indicating that Mg supplementation, if indicated, may slow down the development of such negative morbidities.

Patients with CKD have an almost uniquely high risk of death and cardiovascular disease, and with a rate of incident cardiovascular events strongly associated with the level of renal function (Zoccali, 2006; **Figure 1**). Contrarily to the general population, where as much as the 75% of excess risk for coronary heart disease could be explained by classical risk factors (Magnus and Beaglehole, 2001), the excess of risk of CVD in CKD patients it is not so easy to explain. Furthermore, as renal function deteriorates, the risk increases linearly (Weiner et al., 2004). To this proposal, Provenzano et al. report, in their review how albuminuria and eGFR reduction predict higher CV risk, independently from traditional risk factors. Furthermore, the addition of eGFR and albuminuria to risk prediction models including the traditional CV risk factors (i.e., Framingham risk score) improved the predictive accuracy, leading to consider CKD as an equivalent CV risk.

Among novel risk factors for complications in CKD, in their review Georgatzakou et al. focused on extracellular vesicles (EVs), membrane-enclosed nanoparticles released by most cells in body fluids and extracellular matrix, whose function is signal transduction. Plasma EVs may have significant roles in CKD as disease biomarkers, risk factors for the development of complications, repair or protective factors diffusing harmful stress signals, and finally, therapeutic factors. Development of therapeutic interventions have already been oriented to both block their negative effects and take advantage of their beneficial properties. EVs, as promoters of vascular damage and subsequent development of CVD, are also described in the review by Carracedo et al., who discussed several aspects that characterise CKD-associated CVDs, such as etiopathogenic elements that CKD patients share with the general population, changes in the cellular balance of reactive oxygen species (ROS), and the associated process of cellular senescence. In particular, they reported how uremia-associated ageing is associated to numerous changes both at the cellular and molecular level, changes similar to those observed in the normal process of physiologic ageing. Understanding the processes and factors involved in accelerated senescence and other abnormal intercellular signalling could lead to identify new therapeutic targets and lead to improved methods of diagnosis and monitoring for patients with CKD-associated CVDs.

CKD patients often present alterations in the bone and mineral metabolism, and in dialysis patients the existing association between bone fractures and cardiovascular comorbidities is well-known. Paget bone disease (PDB) is a cause of osteoporosis and bone fragility and exposes patients to a high incidence of bone fractures but, as secondary hyperparathyroidism is a frequent condition in dialysis patients, it can easily mask PDB diagnosis. As reported by Panuccio and Tripepi, there are limited reports on the treatment of patients with CKD and PBD. Furthermore, management of these patients is a challenge because these diseases act synergistically in affecting bone quality and increasing the risk of fractures. According to the 2017 KDIGO guideline, an aggressive control of serum parathyroid hormone, calcium, phosphorus, and vitamin D level for the CKD-MBD patient is strongly suggested. It is important to individualise therapy and to try to prevent falls with regular exercise to maintain joint mobility and bone strength.

Alterations in the bone and mineral metabolism, typical of CKD, has a direct consequence the onset of vascular calcification induced by hyperphosphatemia. Lanthanum drugs are commonly used ad phosphate binders in CKD patients, so Zhao et al. investigated, in animal models, their potential efficacy in the treatment of vascular P-induced calcifications in CKD patients. Comparing differently treated rats, authors found an improvement in biochemical and histopathological parameters in the lanthanum but not in the control group, indicating the efficacy of lanthanum hydroxide in postponing CRF progression and in protecting renal function. In addition, lanthanum hydroxide postponed hyperphosphatemia-mediated vascular calcification in CKD via the NF-κB signal transduction pathway, suggesting a protection against renal failure and high phosphorus level, thus postponing vascular calcification progression.

Understanding mechanisms underlying CKD is fundamental to develop novel treatments for this disease and its complications (**Figure 1**). In recent years, bioinformatics has emerged as a powerful tool for providing comprehensive

insights into the molecular mechanisms of disease and identifying potential biomarkers and therapeutic targets. Novel methods, such as bioinformatics analyses applied to genome and proteome, might help in identifying new, unknowns, pathways.

AUTHOR CONTRIBUTIONS

CT drafted the initial manuscript. All authors revised, approved the final version, and agree to be accountable for the content of the work.

REFERENCES

Anavekar, N. S., McMurray, J. J. V., Velazquez, E. J., Solomon, S. D., Kober, L., Rouleau, J.-L., et al. (2004). Relation between renal dysfunction and cardiovascular outcomes after myocardial infarction. *N. Engl. J. Med.* 351, 1285–1295. doi: 10.1056/NEJMoa041365

Culleton, B. F., Larson, M. G., Wilson, P. W., Evans, J. C., Parfrey, P. S., and Levy, D. (1999). Cardiovascular disease and mortality in a community-based cohort with mild renal insufficiency. *Kidney Int.* 56, 2214–2219. doi: 10.1046/j.1523-1755.1999.00773.x

De Leeuw, P. W., Thijs, L., Birkenhager, W. H., Voyaki, S. M., Efstratopoulos, A. D., Fagard, R. H., et al. (2002). Prognostic significance of renal function in elderly patients with isolated systolic hypertension: results from the Syst-Eur trial. *J. Am. Soc. Nephrol.* 13, 2213–2222. doi: 10.1097/01.asn.0000027871.86296.92

Hill, N. R., Fatoba, S. T., Oke, J. L., Hirst, J. A., O'Callaghan, C. A., Lasserson, D. S., et al. (2016). Global prevalence of chronic kidney disease - a systematic review and meta-analysis. *PLoS ONE* 11:e0158765. doi: 10.1371/journal.pone.0158765

Magnus, P., and Beaglehole, R. (2001). The real contribution of the major risk factors to the coronary epidemics: time to end the "only-50%" myth. *Arch. Intern. Med.* 161, 2657–2660. doi: 10.1001/archinte.161.22.2657

Schillaci, G., Reboldi, G., and Verdecchia, P. (2001). High-normal serum creatinine concentration is a predictor of cardiovascular risk in essential hypertension. *Arch. Intern. Med.* 161, 886–891. doi: 10.1001/archinte.161.6.886

Shlipak, M. G., Smith, G. L., Rathore, S. S., Massie, B. M., and Krumholz, H. M. (2004). Renal function, digoxin therapy, and heart failure outcomes: evidence from the digoxin intervention group trial. *J. Am. Soc. Nephrol.* 15, 2195–2203. doi: 10.1097/01.ASN.0000135121.81744.75

Weiner, D. E., Tighiouart, H., Amin, M. G., Stark, P. C., MacLeod, B., Griffith, J. L., et al. (2004). Chronic kidney disease as a risk factor for cardiovascular disease and all-cause mortality: a pooled analysis of community-based studies. *J. Am. Soc. Nephrol.* 15, 1307–1315. doi: 10.1097/01.asn.0000123691.46138.e2

Zoccali, C. (2006). Traditional and emerging cardiovascular and renal risk factors: an epidemiologic perspective. *Kidney Int.* 70, 26–33. doi: 10.1038/sj.ki.5000417

Conflict of Interest: The authors declare that the research was conducted in the absence of any commercial or financial relationships that could be construed as a potential conflict of interest.

Copyright © 2021 Torino, Dounousi, Abd ElHafeez and Prohic. This is an open-access article distributed under the terms of the Creative Commons Attribution License (CC BY). The use, distribution or reproduction in other forums is permitted, provided the original author(s) and the copyright owner(s) are credited and that the original publication in this journal is cited, in accordance with accepted academic practice. No use, distribution or reproduction is permitted which does not comply with these terms.

frontiers in Cell and Developmental Biology

ORIGINAL RESEARCH
published: 24 October 2019
doi: 10.3389/fcell.2019.00252

NLRP2 Regulates Proinflammatory and Antiapoptotic Responses in Proximal Tubular Epithelial Cells

*Marianna N. Rossi[1], Antonia Pascarella[1], Valerio Licursi[2,3], Ivan Caiello[1], Anna Taranta[4], Laura R. Rega[4], Elena Levtchenko[5], Francesco Emma[4], Fabrizio De Benedetti[1] and Giusi Prencipe[1]**

[1] Department of Laboratories, Immuno-Rheumatology Research Area, Bambino Gesù Children's Hospital, Rome, Italy, [2] Institute for Systems Analysis and Computer Science "Antonio Ruberti," National Research Council, Rome, Italy, [3] Department of Biology and Biotechnologies "Charles Darwin," Sapienza University of Rome, Rome, Italy, [4] Laboratory of Nephrology, Department of Rare Diseases, Bambino Gesù Children's Hospital, Rome, Italy, [5] Department of Paediatric Nephrology & Development and Regeneration, University Hospitals Leuven, Leuven, Belgium

Nod-like Receptor Pyrin domain containing proteins (NLRPs) expressed by resident renal cells may contribute to the pathogenesis of multiple renal diseases. Cystinosis is a genetic disorder that affects kidney and particularly proximal tubular epithelial cells (PTEC). Here, we investigated the expression of NLRP family members in human control and cystinotic conditionally immortalized PTEC. Among all the NLRPs tested, we found that NLRP2 is highly expressed in cystinostic PTEC, but not in PTEC from healthy subjects. The NLRP2 overexpression was confirmed in primary PTEC and in kidney biopsies from cystinotic patients. In order to elucidate the role of NLRP2 in PTEC, we stably transfected control PTEC with an NLRP2-containing plasmid. We showed that NLRP2 markedly increases the production of several NF-κB regulated cytokines and chemokines. Accordingly, we demonstrated that NLRP2 interacts with IKKa and positively regulates the DNA-binding activity of p50 and p65 NF-κB, by modulating the p65 NF-κB phosphorylation status in Serine 536. Transcriptome analysis revealed that NLRP2 also upregulates the expression of profibrotic mediators and reduces that of several interferon-inducible genes. Finally, NLRP2 overexpression decreased the apoptotic cell rate. Consistently, silencing of NLRP2 by small-interfering RNA in cystinotic PTEC resulted in a significant decrease in cytokine and chemokine production as well as in an increase in the apoptosis rate. Altogether, our data reveals a previously unrecognized role for NLRP2 in regulating proinflammatory, profibrotic and antiapoptotic responses in PTEC, through NF-κB activation. Moreover, our findings unveil a novel potential mechanism involving NLRP2 overexpression in the pathogenesis of cystinosis.

Keywords: NLRP2, proximal tubular epithelial cells, inflammation, cytokines, apoptosis, cystinosis

OPEN ACCESS

Edited by:
Claudia Torino,
Italian National Research Council, Italy

Reviewed by:
Saurabh Chattopadhyay,
The University of Toledo,
United States
Ross F. Collery,
Medical College of Wisconsin,
United States

***Correspondence:**
Giusi Prencipe
giusi.prencipe@opbg.net

Specialty section:
This article was submitted to Molecular Medicine, a section of the journal Frontiers in Cell and Developmental Biology

Received: *01 July 2019*
Accepted: *11 October 2019*
Published: *24 October 2019*

Citation:
Rossi MN, Pascarella A, Licursi V, Caiello I, Taranta A, Rega LR, Levtchenko E, Emma F, De Benedetti F and Prencipe G (2019) NLRP2 Regulates Proinflammatory and Antiapoptotic Responses in Proximal Tubular Epithelial Cells. Front. Cell Dev. Biol. 7:252. doi: 10.3389/fcell.2019.00252

INTRODUCTION

Nod-like receptors (NLRs) are intracellular pattern-recognition receptors that sense pathogen-associated molecular patterns and endogenous damage-associated molecular patterns and, similarly to Toll-like receptors (TLRs), play a crucial role in the prompt induction of immune responses during infection as well as during tissue injury (Komada and Muruve, 2019). In humans, the NLR

family consists of twenty-two proteins that are divided based on their N-terminal signaling domain, with the NLR pyrin domain-containing protein (NLRP) family comprising the largest group. The ligands and functions of most NLR family members remain to date unknown. Nevertheless, the activity of the best-understood NLRs can be classified into three categories, with some NLRs displaying more than one function: (a) regulation of IL-1β and IL-18 production by formation of the multimeric protein complex inflammasome (Malik and Kanneganti, 2017); (b) negative or positive regulation of inflammatory pathways by modulation of NF-κB activity (Thaiss et al., 2016), and (c) regulation of antiviral immunity (Moore et al., 2008; Cui et al., 2010; Lupfer and Kanneganti, 2013).

Proximal tubular epithelial cells (PTEC) are the most abundant cell type in the kidney (Liu et al., 2018). PTEC play an important role in renal repair and/or progression to chronic kidney diseases, since they not only insure tubular reabsorption in the proximal segments of the nephron, but also have endocrine and immunological functions (Schlondorff, 2008). More specifically, PTEC display innate immune characteristics, including the expression of NLRs and TLRs, that allow them to respond to a wide range of immunologic, metabolic, toxic and ischemic insults (Leemans et al., 2014; Liu et al., 2018). Indeed, upon exposure to urinary proteins as well as to TLRs/NLRs ligands and/or metabolic insults, PTEC synthesize extracellular matrix materials, growth factors and a repertoire of inflammatory molecules, including cytokines, chemokines and complement components (David et al., 1997; Gerritsma et al., 1998). The ensuing release of these bioactive mediators promotes the recruitment of immune cells, initiates tissue repair and activates adaptive immune responses aimed at regaining tissue integrity. Nevertheless, if the inflammatory reaction is inappropriate or chronic, maladaptive inflammatory and fibrogenic responses can develop, causing irreversible and progressive kidney damage (Meng et al., 2014). Indeed, a large body of evidence indicates that TLRs and NLRs expressed by different resident renal cell types, including tubular epithelial cells, may have important roles in the pathogenesis of multiple renal disorders, such as chronic kidney diseases, diabetic nephropathies, sepsis or toxic-mediated acute kidney injury (AKI) and crystal-related nephropathies (Gluba et al., 2010; Darisipudi and Knauf, 2016). Consistently, the absence of specific inflammasome components in murine models of acute or chronic kidney diseases has been demonstrated to protect mice from kidney failure (Shigeoka et al., 2010; Vilaysane et al., 2010; Zhuang et al., 2015).

Cystinosis is a rare autosomal recessive disorder caused by mutations in the *CTNS* gene, codifying for the lysosomal cystine-proton co-transporter cystinosin. PTEC are among the first affected cells in cystinosis: accumulation of cystine-crystals, changes in lysosomal morphology, oxidative stress, high susceptibility to apoptosis and dysregulation of autophagy have been demonstrated in these cells (Park et al., 2002; Laube et al., 2006; Festa et al., 2018; Luciani et al., 2018).

Based on our previous results demonstrating that cystine-crystals can act as an endogenous activator of the inflammasome and on additional data showing that endogenous uric acid crystals modulate the expression of NLRP in PTEC (Xiao et al., 2015), in this study we have investigated the expression of the best-known NLRP3 and of other members of the NLRP family in cystinotic PTEC. Having demonstrated that NLRP2 is markedly expressed in human cystinotic PTEC but not in control PTEC, we decided to investigate the functional role of NLRP2 in these cells. To this purpose, we stably transfected control PTEC with an NLRP2-containing plasmid. We found that NLRP2 upregulates the expression of proinflammatory, chemotactic and profibrotic mediators as well as reduces the apoptotic rate in PTEC, by modulating the activity of the transcription factor NF-κB. Our data reveals a previously unrecognized role for NLRP2 in PTEC and provide evidence of a novel mechanism involving NLRP2 overexpression in the pathogenesis of cystinosis.

MATERIALS AND METHODS

Cell Culture

Two control and three cystinotic conditionally immortalized PTEC lines (ciPTEC) were kindly provided by Dr. Elena. Levtchenko and cultured as described in Wilmer et al. (2005). Cystinotic cell lines 1 and 2 carried the 57 kb deletion of the *CTNS* gene, while the cystinotic cell line 3 carried the c.518-519delCA deletion (p.Tyr173X) in exon 8 and the c.1015G>A missense mutation (p.Gly339Arg) in exon 12. Primary tubular epithelial cells were isolated from urine of five cystinotic patients and one healthy subject as described previously (Wilmer et al., 2005). The patient chronic kidney disease stage was defined, at time of urine collection, according to the CKD Work Group KDIGO 2012 clinical practice guideline (Andrassy, 2013).

To generate PTEC stably expressing NLRP2, control ciPTEC were transfected with pEZ-M68 containing full length NLRP2 EX-Z7760-M68 or pEZ-M68 empty vector (Genecopoeia) by using Lipofectamine 2000 (Life Technologies), according to the manufacturer's procedure. After 48 hours of transfection, cells were subjected to 1 μM puromycin selection. Media was changed every 2–3 days. Cells were frozen as a polyclonal line.

For cell stimulation assays, cells were starved for 3 h in medium without serum and then stimulated with 10 ng/ml of Tumor necrosis factor alpha (TNF-α, R&D Systems), 10 mg/ml of Bovine serum albumin (BSA, Sigma), 10 μg/ml of Lipopolysaccharides (LPS, Sigma) or 10% of fetal bovine serum (FBS, GIBCO).

For treatment with NF-κB inhibitor, BAY 11-7082 (Cayman Chemicals) was added at the final concentration of 50 μM to the cell cultures. An aliquot of conditioned media was collected after 5 and 20 h since BAY 11-7082 addition for cytokine measurements. For studies of RNA expression, cells were cultured for 20 h in the presence of BAY 11-7082 and then were stimulated for 1 h with fresh medium containing TNF-α.

For apoptosis induction experiments, cells were treated with 30 ng/ml of TNF-α plus 2.5 μg/ml of Actinomycin D for 24 h. To analyze the apoptosis rate, the conditioned media of untreated or treated cells were collected and centrifuged to retrieve the floating cells. Adherent cells were detached by trypsin and combined with floating cells. After centrifugation and wash with PBS, cells were incubated with Calbiochem Annexin

V-FITC apoptosis detection kit, according to the manufacturer's procedure. Cells were analyzed by flow cytometry (FACSCanto II, BD Biosciences).

RNA Isolation and Quantitative Real-Time PCR

Total RNA was extracted using Trizol Reagent (Ambion), and cDNAs were obtained using the Superscript Vilo kit (Invitrogen). Real-time PCR assays were performed using TaqMan Universal PCR Master Mix and gene expression assays from Applied Byosystems. Gene expression was normalized using human *HPRT1* as endogenous control. Data were analyzed with the $2^{\Delta ct}$ method and are expressed as arbitrary units (AU) or as fold difference.

Immunohistochemistry

After moist heat–induced antigen retrieval with EnVision Flex Target Retrieval Solutions High pH (DakoCytomation), 2.5-μm kidney sections were incubated with antibody to NLRP2 (sc-166584 Santa Cruz Biotechnologies) overnight at 4°C. After washing, sections were incubated with appropriate horseradish peroxidase–conjugated secondary antibodies. Chromogen detection was carried out with the DAB chromogen kit (DakoCytomation). Nuclei were counterstained with hematoxylin, followed by dehydration and mounting.

Enzyme-Linked Immunosorbent Assays (ELISAs)

Cell culture supernatants were collected at the indicated time points and analyzed for cytokine and chemokine concentrations by using commercial ELISA kits, according to the manufacture's procedure. IL-6 (DY206), IL-8 (DY-208), MCP-1 (DY279), CXCL1 (DGR00B), and CXCL5 (DX000) kits were all purchased from R&D Systems; Serum Amyloid A (KA0518) and G-CSF (ELH-GCSF) were purchased from Abnova and RayBiotech, respectively. The detection limit of the assays were 9.38 (IL-6), 31.3 (IL-8), 15.6 (MCP-1), 31.3 (CXCL1), 31.3 (CXCL5), 2.5 (SAA), 0.69 (G-CSF) pg/ml.

Western Blotting and Immunoprecipitation

Cells were lysed in RIPA buffer (Cell Signaling) and protein concentration was measured with BCA Protein assay (Pierce). A total of 30 μg protein extracts were resolved by 10% SDS PAGE, transferred to nitrocellulose membranes (Amersham Life Sciences) and probed with antibody to NLRP2 (NALP2, 137569) from Abcam, NF-κB (8242), GAPDH (5174s), pS536- NF-κB (3033S), IKKα (11930S), all from Cell Signaling Technology. Blots were developed with the ECL system (Amersham Biosciences) according to the manufacturer's protocol.

For immunoprecipitation experiments, PTEC/NLRP2 and PTEC/EV were lysed with RIPA buffer and protein concentration was measured with BCA Protein assay (Pierce). 1.5 mg of total proteins for each sample were precleared with 20 μl Dynabeads Protein A for 1 h at 4°C in rotation. Precleared lysates were incubated overnight with 1 μg of anti-NLRP2 antibody or Rabbit IgG (Invitrogen). Then 20 μl Dynabeads Protein A were added and incubated for additional 2 h. Beads were washed three times with PBS plus 0.1% Tween and once with PBS. Immunoprecipitated proteins were eluted from beads with Laemmli sample buffer (Bio-Rad 161-0747) and loaded on polyacrylamide gel to be subjected to western blot analysis.

NF-κB DNA-Binding ELISAs

p52, p50, p65, RelB, c-Rel binding to DNA consensus sequences were assayed in nuclear lysates using the TransAm NF-κB family kit (Active Motif). Briefly, cells were lysed with NE-PER kit (Pierce) to obtain nuclear pellets. Nuclei were lysed in the Complete lysis Buffer and protein concentration was measured with Bradford assay (Bio-Rad). 50 μg of protein extracts were loaded on each well. After incubation with primary and secondary antibodies, absorbance was measured at 450 nm.

Small Interference RNA

Proximal tubular epithelial cells were transfected using a mixture of four chemically synthesized small interference RNA (siRNA) duplex against NLRP2 (SMART pool Dharmacon cod SO-2616566G) or on target plus control pool (Dharmacon D-001810-10-05), at a final concentration of 200 nM. 72 h after transfection, cells were collected for western blot analysis or RNA extraction. For cytokine release measurements, 72 h after transfection, media were replaced with fresh media and collected 24 h later.

RNA-Seq Trascriptomic Analysis

Total RNA was extracted and quantified as described above. RNA-seq libraries preparation and sequencing were performed by Lexogen Service using the QuantSeq 3' mRNA-Seq Library Prep Kit FWD for Illumina by using total RNA, according to manufacturer instructions. The final libraries for single-read sequencing of 76 base pairs were carried out on an Illumina HiSeq2000. Each sample produced about 50 millions of reads.

Reads quality was evaluated using FastQC (version 0.11.2, Babraham Institute Cambridge, United Kingdom) tool. Reads were then mapped to the human Ensembl GRCh38 build reference genome using STAR version 2.5.0a (Dobin et al., 2013). The Ensembl annotation release 91 was used to build a transcriptome index that was then provided to STAR during the alignment. The average percentage of uniquely mapped reads to the human genome was 85.7%. Read distribution coverage was uniform among samples and it was evaluated with *read_distribution.py* script from RSeQC package version 2.6.4. The average percentage values of mapped reads on CDS exons, 3′UTR Exon and Introns were 24.2% ± 0.6, 48.1% ± 0.3, and 7.8% ± 0.3, respectively.

The same gene annotations were used to quantify the gene-level read counts using HTSeq-count version 0.8.0 script (Anders et al., 2015). The differential analysis for gene expression was performed using Bioconductor R version 3.4.4 package DESeq2 version 1.18.1 (Gentleman et al., 2004; Love et al., 2014).

In order to understand biological meaning of the differentially expressed genes the resulting filtered [False discovery rate (FDR) adjusted p-value < 0.01] genes were clustered by enrichment pathway analysis using Bioconductor R packages *clusterProfiler*

(Yu et al., 2012), with annotation of Gene Ontology Database (Ashburner et al., 2000). RNA-Seq data accompanying this paper are available through Gene Expression Omnibus (GEO) repository, under accession number GSE123247.

Statistical Analysis

Results have been reported as mean ± Standard Error Mean (SEM). Values between at least three groups were compared by the parametric ANOVA test and, if significant, pairwise comparisons were evaluated by the unpaired *t*-test. All statistical analyses were performed using GraphPad Prism V software. Statistical significance is shown as $^{*}p < 0.05$ or $^{**}p < 0.01$ or $^{***}p < 0.001$.

RESULTS

NLRP2 Is Highly Expressed in Cystinotic PTEC

The mRNA expression of NLRP family members was analyzed by RT-qPCR in conditionally immortalized cystinotic and control PTEC. Among the 14 tested members (*NLRP1-14*), only *NLRP1*, *NLRP2*, and *NLRP3* showed detectable mRNA levels. *NLRP1* expression levels were comparable between cystinotic and control cells. *NLRP3* mRNA levels showed a mild increase only in one out of three cystinotic cell lines. Notably, we found that in all the three cystinotic PTEC analyzed the *NLRP2* gene was strongly expressed, compared to control PTEC (from 38 to 280 fold-difference), in which *NLRP2* mRNA levels were almost undetectable (**Figures 1A,B**). Accordingly, while the NLRP2 protein was barely expressed in control PTEC, it was detected in the cystinotic PTEC (**Figure 1C**). Further confirming the upregulation of NLRP2 in cystinosis, we observed markedly higher NLRP2 protein levels in primary PTEC obtained from five cystinotic patients compared to PTEC from a healthy subject (**Figure 1D**). Consistently, immunohistochemistry revealed strong staining for NLRP2 in PTEC of a cystinotic kidney (**Figures 1F,H**). In contrast, NLRP2 staining was very weak or absent in control kidney biopsies (**Figures 1E,G**). Collectively, these results highlights a specific and significant overexpression of NLRP2 in cystinotic PTEC *ex vivo* and *in vivo*.

Exogenous Overexpression of NLRP2 in Control PTEC Increases the Production of Proinflammatory Cytokines and Chemokines

To elucidate the functional role of increased NLRP2 expression in PTEC, we established an NLRP2 overexpressing control PTEC line (PTEC/NLRP2) by transfection with a NLRP2 containing plasmid. Control PTEC transfected with an empty vector (PTEC/EV) were used as control (**Figures 2A,B**). Based on previously published data demonstrating that NLRP2 can form an inflammasome complex in other cell types (Bruey et al., 2004; Minkiewicz et al., 2013), we first tested if NLRP2 could form an active inflammasome in PTEC. To this end, cystinotic PTEC, PTEC/NLRP2 and PTEC/EV were stimulated

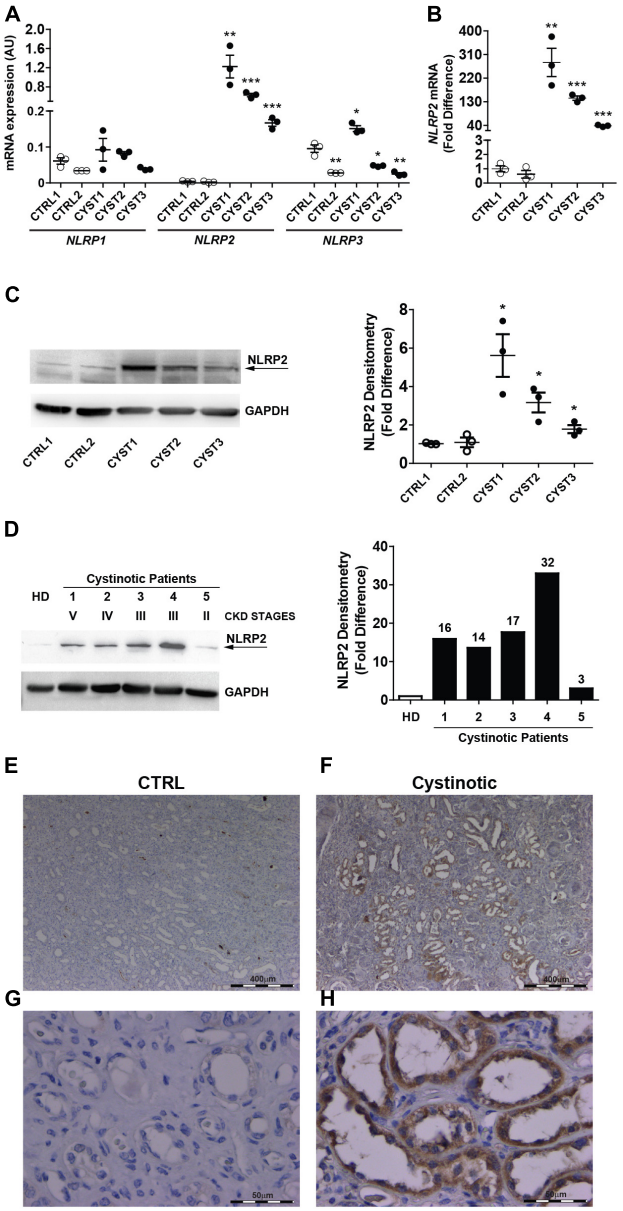

FIGURE 1 | NLRP2 expression is upregulated in cystinotic proximal tubular epithelial cells. **(A,B)** *NLRP1*, *NLRP2*, and *NLRP3* mRNA expression levels were evaluated by qPCR analysis in 2 control (CTRL1 and CTRL2) and 3 cystinotic (CYST1, CYST2, and CYST3) conditionally immortalized PTEC lines. Results are obtained after normalization with the housekeeping gene *HPRT1* and are expressed as arbitrary units (AU) **(A)** and for NLRP2 as fold difference **(B)** versus the CTRL1 cell line. Differences between groups were compared using the parametric ANOVA test ($p > 0.5$ for NLRP1 and $p < 0.0001$ for NLRP2 and NLRP3) and, if significant, unpaired *t*-test was applied, comparing each cell line versus the CTRL1 cell line. **(C)** Representative western blot showing NLRP2 protein upregulation in cystinotic PTEC compared to control PTEC. The arrow indicates the specific NLRP2 upper band. GAPDH is used as loading control (left panel). Densitometric analysis of NLRP2 normalized to the corresponding band intensity of GAPDH (right graph) confirmed the upregulation of NLRP2 in cystinotic cells. The data represent mean ± SEM from at least three independent experiments and are reported as fold difference versus CTRL1 cell line. **(D)** Western Blot and densitometric

(Continued)

FIGURE 1 | Continued
analysis of NLRP2 protein levels in primary PTEC isolated from urine of 5 cystinotic patients and 1 healthy subject (HD). For each patient, the chronic kidney disease (CKD) stage at time of urine collection is reported. Immunoblot data shown are representative of more than three independent experiments. $^{*}p < 0.05$ or $^{**}p < 0.01$ or $^{***}p < 0.001$. **(E,H)** Kidney biopsy specimens from one representative healthy subject (CTRL) and one cystinotic patient **(F,H)** were stained with an antibody against NLRP2, revealing a strong staining of NLRP2 specifically in proximal tubular epithelial cells of cystinotic kidney. **(E,F)** 5X magnification, **(G,H)** 60X magnification.

for 6 or 24 h with different stimuli, including TNF-α, LPS and BSA. The inflammasome-mediated secretion of IL-1β and IL-18 was assessed after exposure of cells to the canonical NLRP3 inflammasome stimulus ATP. Levels of both IL-1β and IL-18 in culture supernatants were undetectable in all tested experimental conditions (data not shown), which excludes a role for NLRP2 in IL-1β and IL-18 mediated inflammasome release. Based on *in vitro* evidence demonstrating that NLRP2 is able to regulate inflammation by inhibiting NF-κB activity in macrophage-like THP-1 cells (Bruey et al., 2004; Fontalba et al., 2007; Tilburgs et al., 2017), we evaluated the production of NF-κB-dependent cytokines, such as IL-6, IL-8, and MCP-1 in PTEC/NLRP2. Contrary to what was expected, we found that unstimulated PTEC/NLRP2 released significantly higher levels of all analyzed cytokines, compared to PTEC/EV (**Figures 2C,E,G**). Consistently with these results, a significant basal increase in the mRNA levels of *IL6* and *IL8* was also observed (**Figures 2D,F**). No significant differences in *MCP1* mRNA levels were found (**Figure 2H**). These results indicate that the overexpression of NLRP2 is able to modulate the production on NF-κB -regulated cytokines in PTEC.

NLRP2 Regulates NF-κB Activation and Interacts With IKKα

Our results strongly supported a role for NLRP2 in positive regulation of NF-κB transcriptional activity. In order to test this hypothesis, we evaluated whether the increased cytokine production observed in PTEC/NLRP2 was NF-κB driven. To this purpose, PTEC/NLRP2 and PTEC/EV were stimulated with TNF-α, a well-known activator of the NF-κB signaling pathway. A significant and marked increase in both mRNA (**Figures 3A,C**) and protein (**Figures 3B,D**) levels of IL-6 and IL-8 was found in PTEC/NLRP2 compared to PTEC/EV. Accordingly, when PTEC/NLRP2 were treated with a specific NF-κB inhibitor (BAY 11-7082), a strong reduction in the basal production of both IL-6 and IL-8 was observed in PTEC/NLRP2 (**Figures 3E,F**). In addition, we also found that treatment with the NF-κB inhibitor was able to lower *IL6* and *IL8* mRNA levels of TNF-α stimulated PTEC/NLRP2 to those observed in TNF-α stimulated PTEC/EV (**Figures 3G,H**), further supporting a role for NLRP2 in modulating NF-κB activation. Based on these results, we tested the DNA-binding activities of the NF-κB p65 (RelA), p50, p52, c-Rel, and RelB family members. We observed that under basal conditions the activities of p65 and p50 were significantly higher in PTEC/NLRP2 than in PTEC/EV

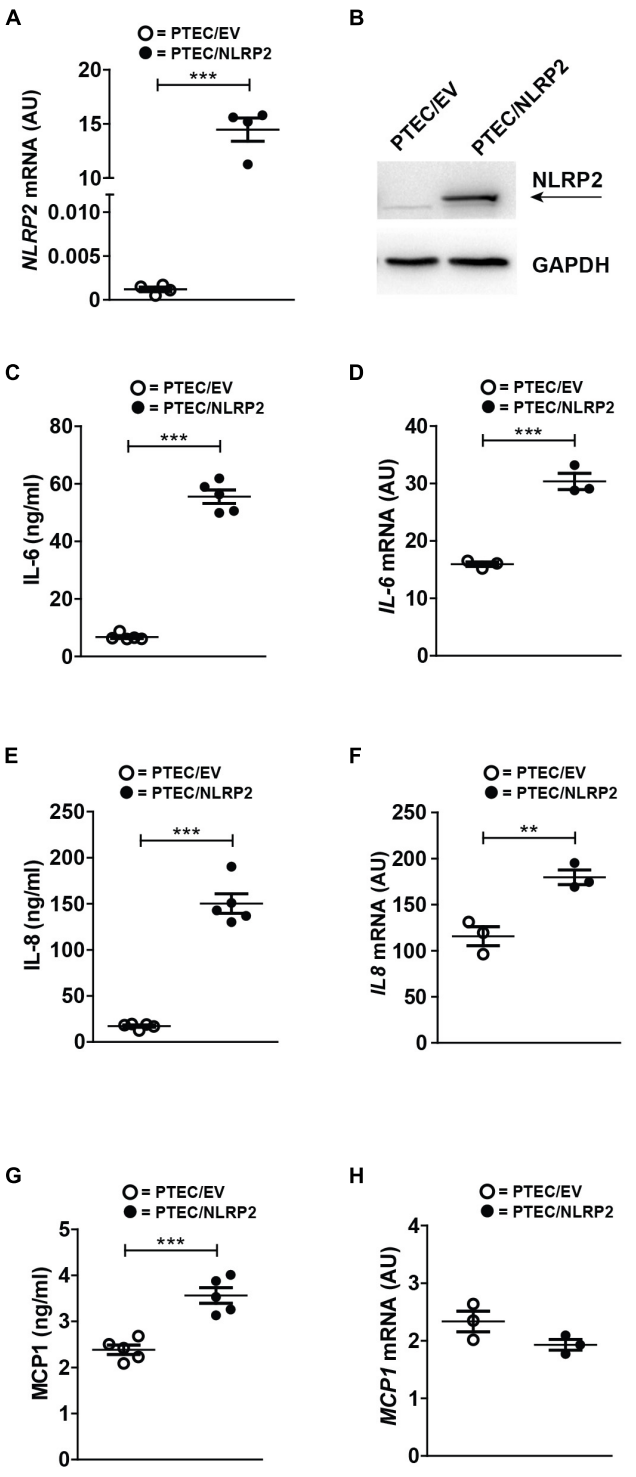

FIGURE 2 | In control PTEC overexpressing NLRP2, mRNA and protein levels of proinflammatory cytokines IL-6, IL-8 and MCP-1 are increased. **(A)** *NLRP2* mRNA expression levels were evaluated by qPCR analysis in PTEC/EV and PTEC/NLRP2. Results are obtained after normalization with the housekeeping gene *HPRT1* and are expressed as arbitrary units (AU). **(B)** NLRP2 protein levels were assessed by western blot analysis in PTEC/EV and PTEC/NLRP2. GAPDH is reported as loading control. Immunoblot data shown are
(Continued)

FIGURE 2 | Continued
representative of more than three independent experiments. **(C,E,G)** IL-6, IL-8, and MCP-1 levels were measured by ELISA in the conditioned media of PTEC/EV and PTEC/NLRP2 after 72 h of cell culture. **(D,F,H)** mRNA expression levels of *IL6*, *IL8*, and *MCP1* in PTEC/EV and PTEC/NLRP2 were evaluated by qPCR analysis. Results are obtained after normalization with the housekeeping gene *HPRT1* and are expressed as arbitrary units (AU). **(C–H)** The data represent mean ± SEM from at least three independent experiments. $^{**}p < 0.01$ or $^{***}p < 0.001$.

(**Figure 4A**). No differences in c-Rel activity were observed (**Figure 4A**), while RelB and p52 activities were undetectable (data not shown). To further investigate the mechanism by which NLRP2 modulate NF-κB p65 activation, we assessed the Serine 536 (S536) phosphorylation status in serum-starved cells unstimulated or stimulated with fetal bovine serum. Lower NF-κB p65 S536 phosphorylation levels were detected in unstimulated PTEC/NLRP2 ($p = 0.07$) and in PTEC/NLRP2 stimulated for 2 h with serum ($p = 0.03$), compared to PTEC/EV (**Figure 4B**). Similar results were obtained also by stimulating cells with TNF-α (data not shown). Since IKKα has been identified as one of the kinases involved in p65 S536 phosphorylation (Lawrence et al., 2005), we hypothesized that NLRP2 may exert its effects in PTEC by interacting with IKKα. To verify our hypothesis, we performed co-immunoprecipitation experiments and found that NLRP2 specifically interacts with IKKα (**Figure 4C**). Collectively, these results demonstrated that in PTEC overexpression of NLRP2 is associated with an increased NF-κB transcriptional activity and reduced levels of S536 phosphorylated p65 NF-κB.

NLRP2 Upregulates Biological Processes Involved in Immune Responses, Chemotaxis and Extracellular Matrix Organization and Downmodulates the Expression of Interferon-Inducible Genes

To reveal other potential genes and molecular pathways modulated by NLPR2 overexpression in PTEC, we performed an RNA-Seq transcriptomic analysis in PTEC/NLRP2 and PTEC/EV. After applying a FDR <0.01, 817 genes showed significant changes between PTEC/NLRP2 and PTEC/EV. Among them, 377 were upregulated and 440 were downregulated (**Figure 5A** and **Supplementary Table S1**). Gene Ontology biological process analyses of differentially expressed genes in PTEC/NLRP2 versus PTEC/EV were performed. The upregulated biological processes with the highest enrichment scores included items related to positive regulation of leukocyte migration and immune responses (**Figure 5B**). On the other hand, the downregulated gene clusters with the highest enrichment scores were all related to responses to Type I and Type II Interferons (**Figure 5B**). Altogether, these findings further demonstrate the role of NLRP2 in modulating the expression of a large number of mediators with a crucial role in inflammatory responses.

In order to validate the differential expression of several genes from our RNA-Seq data, we first evaluated the mRNA

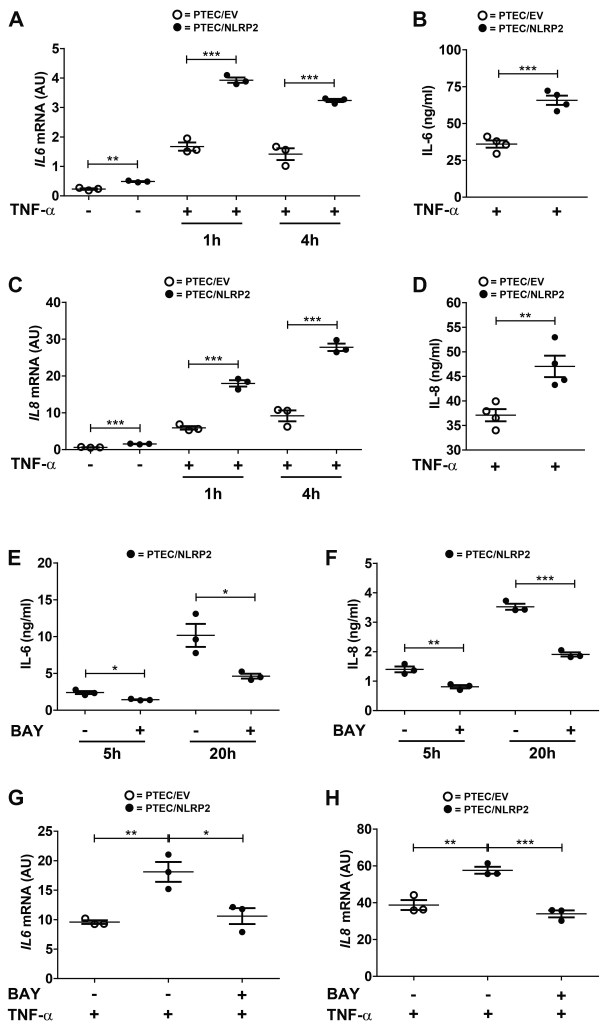

FIGURE 3 | IL-6 and IL-8 levels are increased in TNF-α stimulated PTEC/NLRP2 and are decreased by NF-κB inhibition. **(A,C)** The expression levels of *IL6* and *IL8* were evaluated by qPCR analysis in PTEC/EV and PTEC/NLRP2 unstimulated and after stimulation with TNF-α (10 ng/ml) for the indicated hours (h). Results are obtained after normalization with the housekeeping gene *HPRT1* and are expressed as arbitrary units (AU). **(B,D)** PTEC/EV and PTEC/NLRP2 were stimulated with TNF-α (10 ng/ml) for 24 h and IL-6 and IL-8 were measured in the conditioned media by ELISA. **(E,F)** PTEC/NLRP2 were treated for the indicated hours (h) with 50 μM BAY 11-7082 (BAY) and conditioned media were analyzed by ELISA for IL-6 and IL-8 release. **(G,H)** PTEC/NLRP2 were untreated or treated for 20 h with 50 μM BAY 11-7082 and then stimulated with 10 ng/ml of TNF-α for 1 h. The mRNA expression levels of *IL6* and *IL8* were evaluated by qPCR analysis. Data are also compared with results obtained in TNF-α stimulated PTEC/EV. Results are obtained after normalization with the housekeeping gene *HPRT1* and are expressed as arbitrary units (AU). **(A–H)** The data represent mean ± SEM from at least three independent experiments. $^{*}p < 0.05$, $^{**}p < 0.01$, $^{***}p < 0.001$.

and/or protein levels of selected upregulated genes with a known role in inflammation and chemotaxis. Six chemokines were found significantly upregulated (*CXCL1*, *CXCL2*, *CXCL3*, *CXCL5*, *CXCL6*, and *CXCL12*). Of these, we tested the mRNA and protein levels of CXCL1 and CXCL5. Not only did we confirmed their

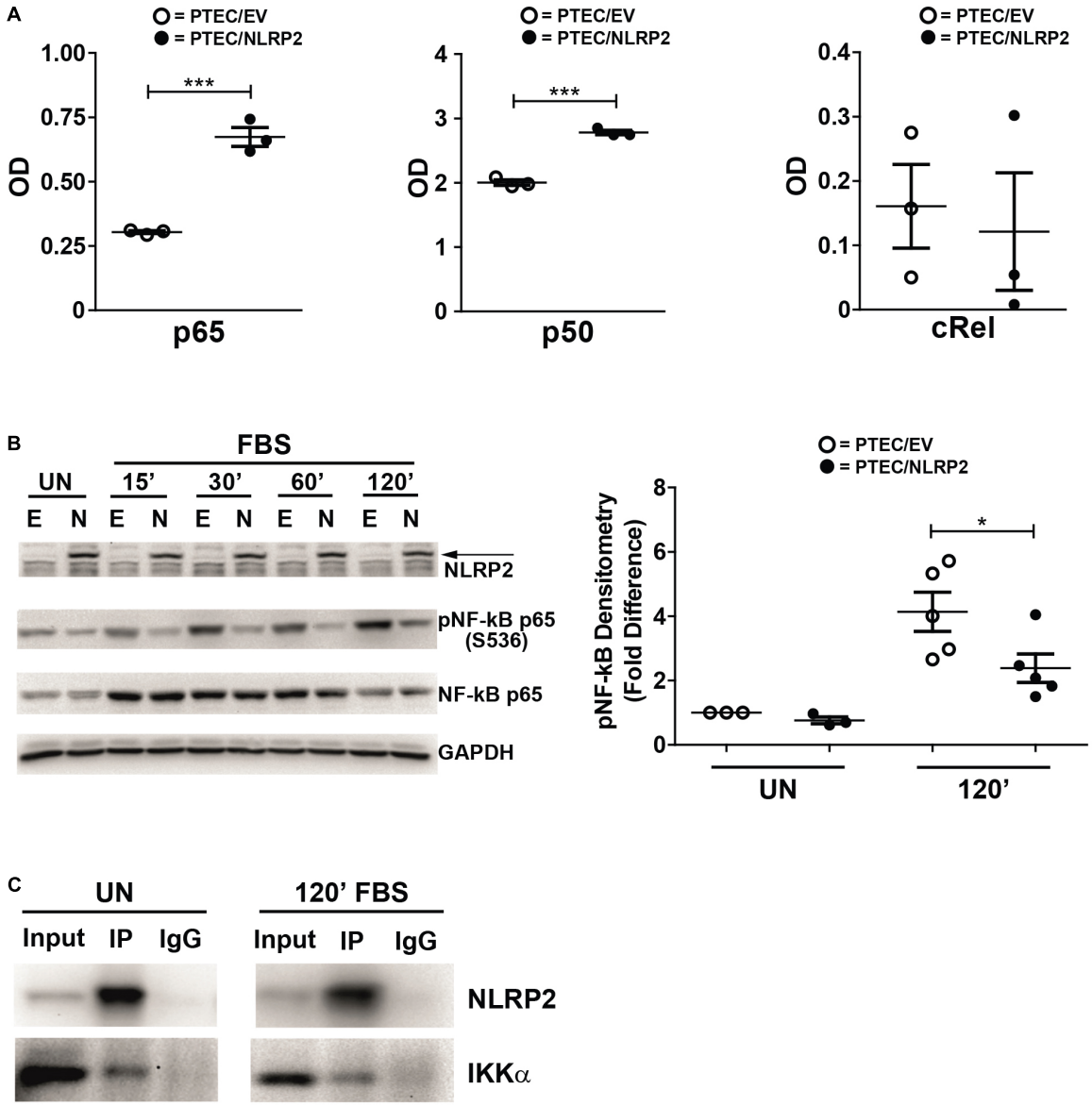

FIGURE 4 | NLRP2 regulates NF-κB DNA-binding activity, reduces NF-κB p65 phosphorylation in Serine 536 and interacts with IKKα. **(A)** PTEC/EV and PTEC/NLRP2 were cultured for 3 h in media without serum. Cells were lysed and nuclear extracts were assayed with the TransAm NF-κB family kit (Active Motive) to measure the binding of p65, p50 and cRel to their DNA consensus sequences. Data are shown as mean ± SEM of at least three independent experiments. OD = optical density. **(B)** PTEC/EV (E) and PTEC/NLRP2 (N) were starved for 3 h in media without FBS and lysed (unstimulated, UN) or stimulated with 10% FBS and lysed at the indicated time points (15, 30, 60, and 120 minutes). NLRP2, phosphorylated (S536) NF-κB p65 and total NF-κB p65 protein levels were assessed by Western blot analyses. GAPDH is used as loading control. Densitometric quantification of phosphoNF-κB p65 (S536) protein levels (right graph) is reported. The data represent mean ± SEM from at least three independent experiments. **(C)** PTEC/NLRP2 were left unstimulated (UN) or were starved for 3 h and then stimulated with 10% FBS for 120 minutes (120′ FBS). Lysates were immunoprecipitated with anti-NLRP2 antibody and proteins were detected as indicated. Input = total cell lysates; IP = samples immunoprecipitated with anti-NLRP2 antibody; IgG = samples immunoprecipitated with control anti-rabbit IgG. Immunoblot data shown are representative of three independent experiments. $^{*}p < 0.05$, $^{***}p < 0.001$.

higher mRNA levels in PTEC/NLRP2 (**Figure 6A**), but we also observed a markedly significant increase in the release of both chemokines (**Figure 6B**). To further validate RNA-Seq results, in conditioned media of PTEC/NLRP2 and PTEC/EV, we measured the levels of other two factors known to be regulated by NF-κB, the major acute-phase protein serum amyloid A (*SAA1/2* genes) and the Granulocyte Colony stimulating factor (G-CSF, *CSF3* gene) (Dunn et al., 1994; Jensen and Whitehead, 1998). Consistently, we found that PTEC/NLRP2 released significantly higher amounts of both mediators (**Figure 6C**).

Interestingly, biological processes involved in extracellular matrix organization were also enriched in PTEC/NLRP2. Indeed,

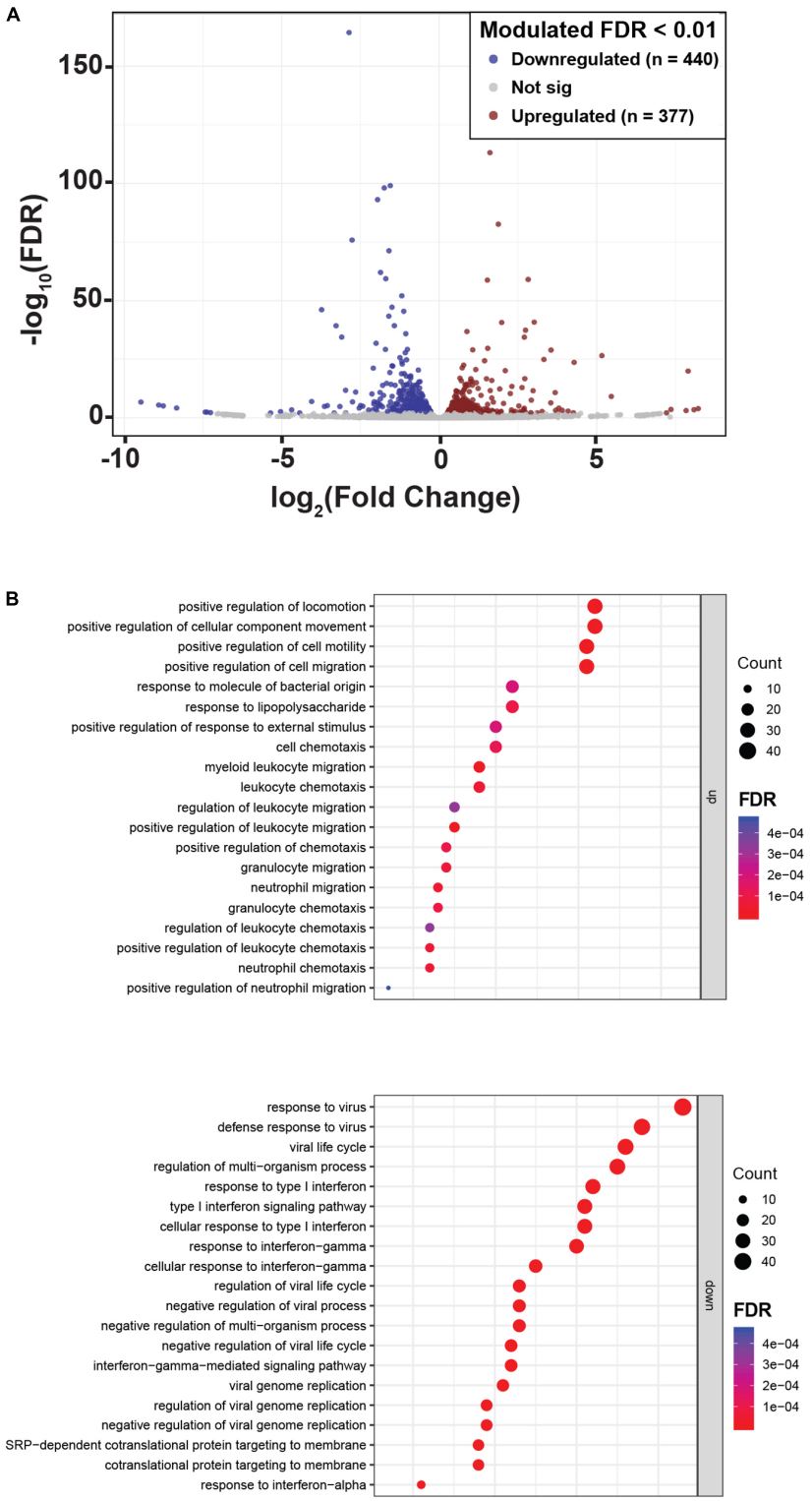

FIGURE 5 | NLRP2 upregulates biological processes that are mainly involved in immune responses and chemotaxis, and downmodulates the expression of interferon inducible genes. **(A)** A volcano plot displaying the 817 differentially expressed genes in PTEC/NLRP2 versus PTEC/EV. Axes show logarithmic transformation of fold change (*x*-axis) and *p*-values (false discovery rate, FDR). Genes upregulated and downregulated in PTEC/NLRP2 with a *p*-value < 0.01 are represented in red and in blue, respectively. **(B)** Genes with differential expression were subjected to gene ontology (GO) analyses. The top 20 most significantly upregulated (upper panel) and downregulated (lower panel) biological processes are shown.

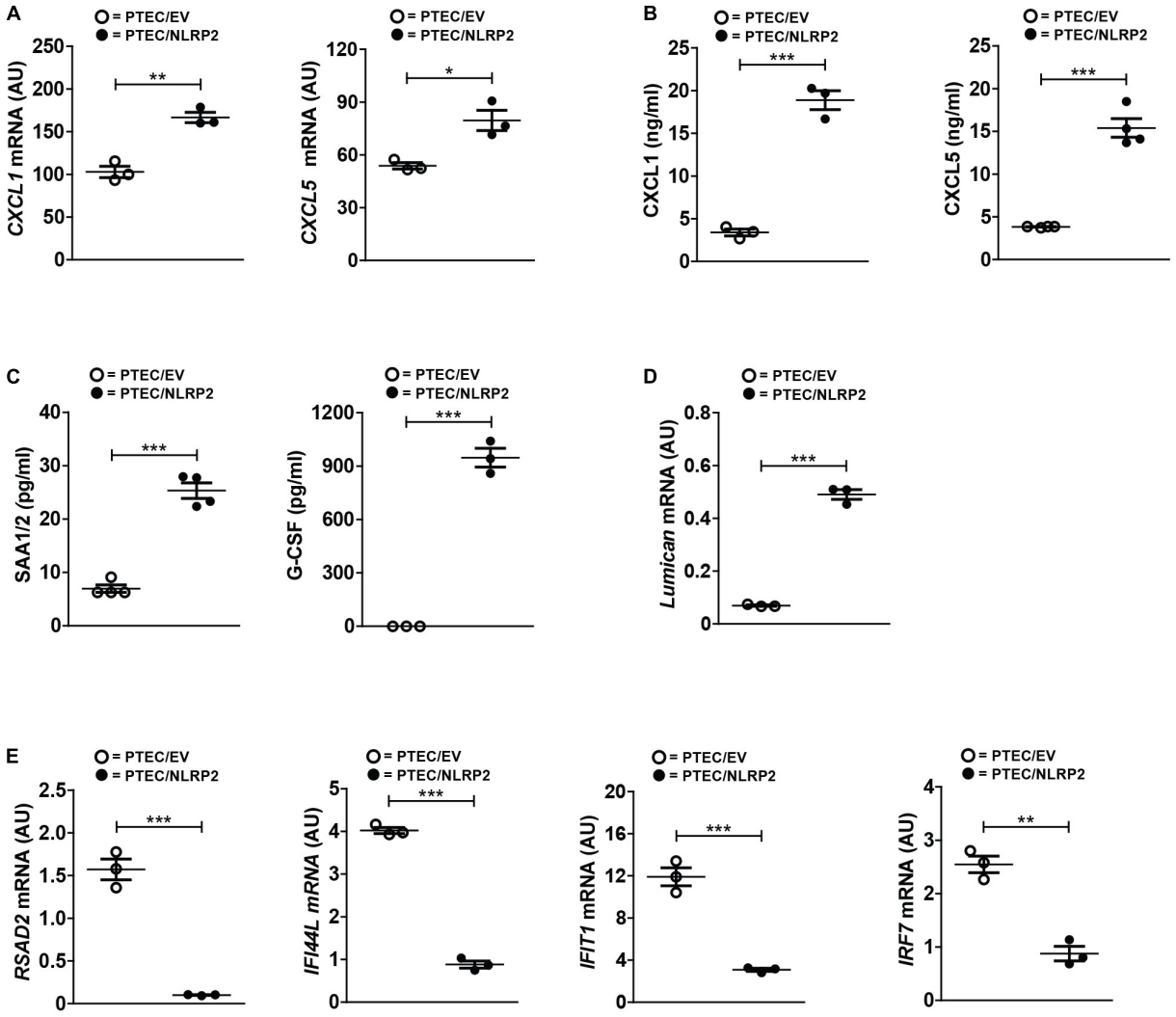

FIGURE 6 | NLRP2 significantly modulates mRNA and protein levels of multiple genes involved in inflammatory and Interferon responses. **(A,D,E)** The expression levels of the indicated genes were evaluated by qPCR analysis in PTEC/EV and PTEC/NLRP2. Results are obtained after normalization with the housekeeping gene *HPRT1* and are expressed as arbitrary units (AU). Data in the graphs represent mean ± SEM of at least three independent experiments. **(B,C)** After 48 h of culture, PTEC/EV and PTEC/NLRP2 conditioned media were collected and assayed for the indicated proteins by ELISA. For G-CSF measurements, in PTEC/EV cells, levels were under the lower standard curve detection limit (0.69 pg/ml). The data represent mean ± SEM from at least three independent experiments. $^{*}p < 0.05$ or $^{**}p < 0.01$ or $^{***}p < 0.001$.

multiple genes encoding for biologically active components of the extracellular matrix that have been demonstrated to be involved in the regulation of inflammatory and fibrotic renal disorders, including type IV collagen, metalloproteases, and small leucine-rich proteoglycans (lumican, biglycan, and decorin) were upregulated in PTEC/NLRP2, compared to PTEC/EV. A significant increase in lumican gene expression in PTEC/NLRP2 was confirmed by RT-qPCR (**Figure 6D**).

In addition, gene ontological grouping revealed a significant downmodulation of a large number of genes induced by type I and type II Interferons (IFNs). These results have been confirmed by RT-qPCR, evaluating 4 out of the 32 IFN-inducible genes that were found to be downmodulated in the RNA-Seq analysis (**Figure 6E**).

Taken together, these data indicate that overexpression of NLRP2 *per se* is able to induce in control PTEC the upregulation of genes mainly related to inflammatory/chemotactic responses as well as the downregulation of IFN responses-related genes.

NLRP2 Overexpression Exerts an Anti-apoptotic Effect in PTEC

Having demonstrated that NLRP2 acts in PTEC by upregulating the NF-κB activity, we decided to evaluate whether NLRP2 overexpression influenced the apoptotic response. Indeed, the role of NF-κB in suppressing apoptosis is largely known (Luo et al., 2005). To investigate this issue, PTEC/NLRP2 and PTEC/EV were left untreated or treated with the proapoptotic

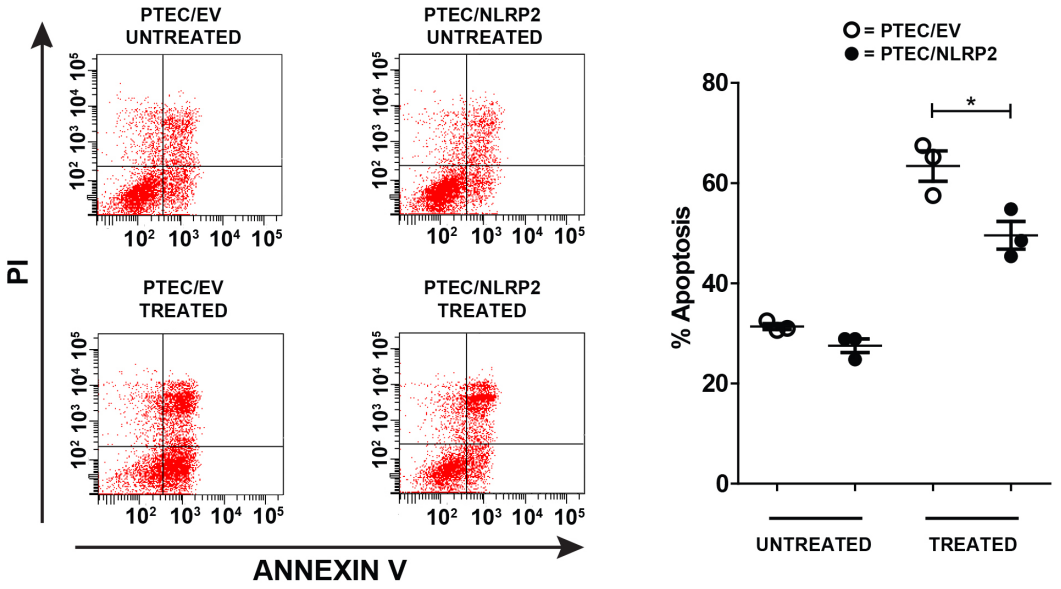

FIGURE 7 | The apoptosis rate is decreased in PTEC overexpressing NLRP2. PTEC/NLRP2 and PTEC/EV were left untreated or treated with 30 ng/ml of TNF-α plus 2.5 μg/ml of Actinomycin D for 24 h. Cells were double stained with Annexin V-FITC/Propidium Iodide and apoptosis percentage was analyzed by flow cytometry. Representative scatterplots depict the Annexin V/PI stain **(left panel)**. The apoptosis rate was calculated including early and late apoptotic cells **(right panel)**. The data represent mean ± SEM from at least three independent experiments. *$p < 0.05$.

stimuli Actinomycin- D and TNF-α. Consistently, PTEC/NLRP2 showed a significant lower apoptotic cell rate compared to PTEC/EV (**Figure 7**), suggesting an NF-κB mediated antiapoptotic role for NLRP2 in PTEC.

NLRP2 Silencing Reduces Cytokine and Chemokine Production as Well as Enhances Apoptosis in Cystinotic PTEC

Finally, in order to verify whether high NLRP2 levels in cystinotic cells regulated the expression of inflammatory-related genes, we performed experiments of *NLRP2* small interfering RNA (siRNA) in conditionally immortalized cystinotic PTEC. Although we observed a marked decrease in NLRP2 mRNA (>five-fold decrease) and protein levels (**Figures 8A,B**), *NLRP2* expression remained significantly higher than that observed in control PTEC. Nevertheless, we found that cystinotic PTEC silenced for *NLRP2* released significantly lower amounts of IL-6, IL-8 and CXCL5, compared to control siRNA cells (**Figures 8C–E**), supporting the proinflammatory role of NLRP2 in cystinotic cells. Moreover, consistent with our previous results, we found a significant increase in the apoptosis rate in NLRP2-silenced cystinotic PTEC compared to control siRNA-silenced cells exposed to proapoptotic stimuli (**Figure 8F**). Altogether, these results support the pro-inflammatory and antiapoptotic role of NLRP2 in cystinotic cells.

DISCUSSION

In this study, we report the overexpression of NLRP2 *ex vivo* and *in vivo* in cystinotic PTEC and identify a previously unrecognized role for NLRP2 in the regulation of proinflammatory, chemotactic, fibrotic and apoptotic responses in these cells.

NLR proteins are cytosolic receptors with key roles in innate immune responses and tissue homeostasis (Kufer and Sansonetti, 2011). Few data on NLRP2 expression and functions are available. Studies on NLRP2 knock out mice revealed that NLRP2 is selectively expressed in ovaries and, while it is dispensable for innate and adaptive immunity, it plays a key role in early embryogenesis and fertility (Kuchmiy et al., 2016; Mahadevan et al., 2017). Accordingly, a recent meta-analysis of endometrial gene expression profiles of patients with embryo implantation failure demonstrated that *NLPR2* mRNA levels are significantly reduced in these patients and that inflammatory responses are significantly downmodulated, providing evidence for a proinflammatory role of NLRP2 *in vivo* (Li et al., 2017). Conversely, results obtained *in vitro* in different cell types, such as THP1 macrophages or astrocytes, in which NLRP2 has been exogenously expressed, suggest a role of NLRP2 in repressing the activity of NF-κB (Bruey et al., 2004; Fontalba et al., 2007). In the present study, we have shown that NLRP2 is highly expressed in cystinotic PTEC, as demonstrated by analyses performed in conditionally immortalized cells as well as in primary cells and kidney biopsies from cystinotic patients, while it is almost undetectable in PTEC derived from healthy subjects. Moreover, we demonstrated that the exogenous expression of NLRP2 in control PTEC causes a marked increase in the expression and production of NF-κB driven cytokines, such as IL-6, IL-8, CXCL1, CXCL5. Accordingly, we found that NLRP2 upregulates the NF-κB p65 and p50 DNA-binding activities. These apparently conflicting results on the activatory and inhibitory activities of NLRP2 could be explained by different functionalities of NLRP2

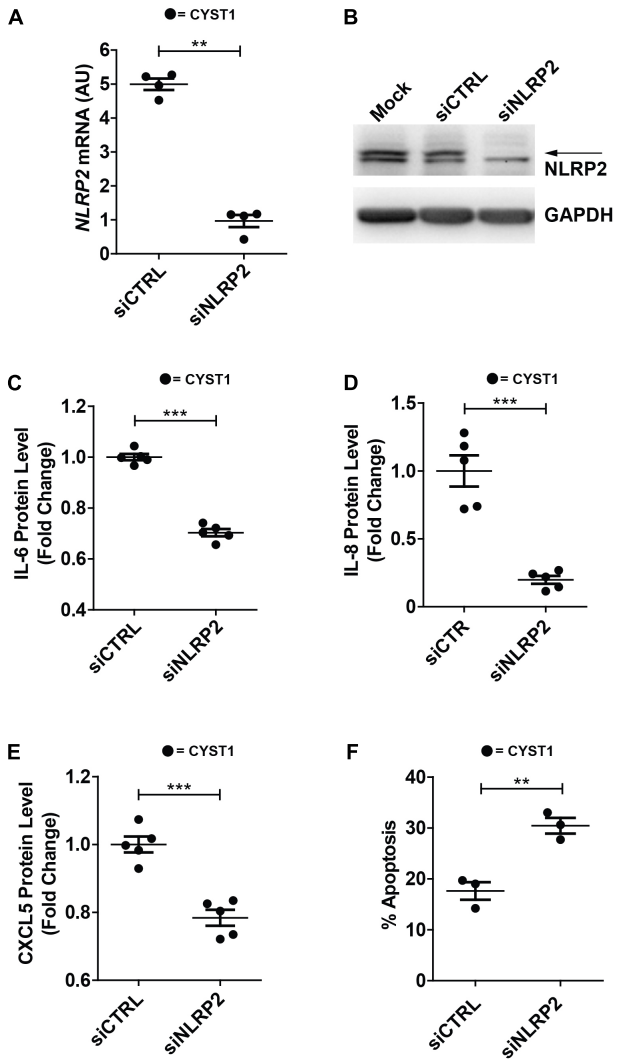

FIGURE 8 | Silencing of NLRP2 in cystinotic PTEC results in decreased cytokine production and increased apoptosis rate. **(A)** *NLRP2* mRNA expression levels were assessed in cystinotic PTEC (CYST1 cell line) by qPCR analysis after 72 h of transfection with "on target plus control pool" siRNA (siCTRL) or siRNA pool against NLRP2 (siNLRP2). Results are obtained after normalization with the housekeeping gene *HPRT1* and are expressed as arbitrary units (AU). **(B)** Western blot analysis of NLRP2 protein levels in mock, siCTRL and siNLRP2 cystinotic PTEC. GAPDH is used as loading control. Immunoblot data shown are representative of more than three independent experiments. **(C–E)** IL-6, IL-8 and CXCL5 levels were analyzed by ELISA in the conditioned media of cystinotic PTEC transfected for 96 h with siCTRL and siNLRP2. **(F)** The apoptosis rate was calculated in siCTRL and siNLRP2 cystinotic PTEC treated with 30 ng/ml of TNFα plus 2.5 μg/ml of Actinomycin D for 24 h. Cells were double stained with Annexin V-FITC/Propidium Iodide and apoptosis percentage was analyzed by flow cytometry. The apoptosis rate was calculated including early and late apoptotic cells. **(A–F)** The data represent mean ± SEM from at least three independent experiments. $^{**}p < 0.05$, $^{***}p < 0.001$.

in different cell types, as already demonstrated for other NLR family members (Li et al., 2018; Luan et al., 2018). In addition, most of the studies on NLRPs have been performed on immune cells and the full spectrum of NLRP functions in different tissues and cells is still limited. In this context, our study extends the knowledge of NLRP2 functions in PTEC.

NF-κB transcriptional activity is modulated through different mechanisms, among which phosphorylation is one of the best characterized (Christian et al., 2016). S536 is one of the best-understood phosphorylation targets in the transactivation domain of p65. Although several studies demonstrated that S536 phosphorylation is required for the activation and nuclear translocation of NF-κB, an important role for S536 phosphorylation in inhibiting NF-κB signaling has been recently demonstrated (Lawrence et al., 2005; Pradere et al., 2016), suggesting that the effects of S536 phosphorylation would appear to depend mainly on the physiological context. Indeed, phosphorylation of p65 S536 has been shown to promote the proteasomal degradation of p65 and, therefore, to limit NF-κB transcriptional responses. Moreover, Lawrence et al. (2005) identified IKKα as the kinase responsible for the phosphorylation of p65 S536 in macrophages. Consistent with this evidence, we found that the phosphorylation status of p65 S536 is decreased in unstimulated and serum-stimulated PTEC/NLRP2 and is associated with an increased NF-κB activity. In addition, we also found that NLRP2 interacts with IKKα, leading us to speculate that NLRP2 could modulate the NF-κB transcriptional activity by interacting with IKKα and interfering with the phosphorylation of p65 in S536.

To better understand the physiopathological role of NLRP2 in PTEC, we performed an RNA-Seq transcriptomic analysis comparing control cells transfected with the NLRP2 gene or with an EV. We found that NLRP2 *per se* is able to modulate the expression of a large number of genes involved in biological processes mainly related to inflammatory responses, chemotaxis as well as extracellular matrix organization. These results are in accordance with the evidence that NF-κB is the master regulator of the inflammatory responses as well as regulates the transcription of genes controlling proliferation and cell death (Lawrence, 2009). Although kidney cell-type specific NF-κB functions remain unknown, an increasing body of evidence demonstrated the involvement of this transcription factor in the pathogenesis of renal diseases, such as ischemia/reperfusion AKI, sepsis-induced AKI, glomerulonephritis, or allogenic renal transplantation (Sanz et al., 2010). Interestingly, a recent study performed in a mouse model with specific tubular epithelia-NF-κB suppression showed that post-ischemic NF-κB activation in PTEC aggravates tubular injury and exacerbates a dysregulated immune response by increasing cytokine and chemokine production (Marko et al., 2016). To date, the role of inflammation in the pathogenesis of cystinosis is not clearly established. Nevertheless, kidneys of *Ctns*$^{-/-}$ mice are characterized by tubular atrophy and interstitial inflammatory infiltrates. In addition, a preliminary observational analysis on a large number of cystinotic patients has shown an improved renal outcome in patients treated with the anti-inflammatory drug indomethacin that (Emma et al., 2016), incidentally, has been demonstrated to inhibit the NF-κB activity (Sung et al., 2004), therefore supporting a pathogenic role of inflammation in the progression of renal disease. In the light of these observations,

our data demonstrating the upregulation of NLRP2 in cystinotic PTEC and the reduction of proinflammatory cytokines and chemokines in cystinotic PTEC silenced for NLRP2 shed a new light on mechanisms causing inflammation in cystinosis.

A recent study has demonstrated that NLRP2 negatively regulates antiviral immunity by inhibiting the TANK-binding kinase 1 (TBK1)-dependent IFN signaling in human embryonic kidney 293T cells (Yang et al., 2018). In agreement with these results, we observed that also in PTEC NLRP2 markedly reduced mRNA expression levels of several IFNs-regulated genes. Our study did not address specifically the molecular mechanism involved in the NLPR2 response. However, it has been shown that IKKα is also critically involved in the activation of the interferon regulatory factor (IRF) 3 and IRF7, which are the major transcription factors in the regulation of IFN-inducible genes (Hoshino et al., 2006; Wang et al., 2008). The exact role of the activation of the IFN signaling pathway in PTEC needs to be established in future studies. Nevertheless, a common side effect of high-dose IFN therapy is the renal impairment that has been demonstrated to be associated with tubular cell dysfunction and tubular cell death (Izzedine et al., 2005). Likewise, IFNs involvement has been demonstrated in ischemic reperfusion–triggered pro-apoptotic pathways in PTEC (Lechner et al., 2008).

Whether upregulation of NLRP2 is restricted to cystinotic PTEC or is a common response in tubular damage needs further studies. In this respect, it is interesting to notice that a whole genome gene expression study performed in a large number of deceased donor kidney biopsies prior to engraftment has shown increased NLRP2 expression levels associated with acute tubular damage, further supporting a role of NLRP2 in proximal tubular dysfunction (Perco et al., 2009). These findings led us to speculate a model in which damaged/injured PTEC upregulate NLRP2 expression that, in turn, increases the production of cytokines, chemokines and extracellular matrix components and protects cells from apoptosis. Hypothetically, this response is aimed at recruiting immune cells, activating innate and adaptive immune responses, and promoting cell and tissue repair. In chronic or genetic diseases, including cystinosis, the sustained overexpression of NLRP2 could contribute to the progression of renal failure by creating a vicious inflammatory cycle.

Taken together, our findings demonstrated a novel role for NLRP2 in regulating proinflammatory, profibrotic and antiapoptotic responses in PTEC. Furthermore, our data shed light on a potential mechanism involving NLRP2 overexpression in the pathogenesis of cystinosis and other tubulopathies, providing the rationale for novel targeted anti-inflammatory therapeutic strategies that may complement presently available conventional therapies.

DATA AVAILABILITY STATEMENT

The datasets generated for this study can be found in the RNA-Seq data accompanying this manuscript are available through Gene Expression Omnibus (GEO) repository, under accession number GSE123247.

ETHICS STATEMENT

The studies involving human participants were reviewed and approved by the Bambino Gesù Children's Hospital Institutional Ethical Committees. Written informed consent to participate in this study was provided by the participants' legal guardian/next of kin.

AUTHOR CONTRIBUTIONS

MR, FD, and GP designed the study. MR, AP, and IC carried out the experiments. VL analyzed the RNA-seq data. AT, LR, and EL provided essential reagents and techniques for this study. MR, AP, and GP analyzed the data. FE and EL contributed to the study design. FD and GP supervised the research design. GP supervised the laboratory activities and drafted the manuscript. All authors contributed to the manuscript writing and approved the final version of the manuscript.

FUNDING

This work was supported by the Cystinosis Research Foundation (Grant CRFF-2016-006 to GP and FD; Grant CRFF-2016-004 to FE), the FWO Flandres (Grant 1801110N to EL), and the KU Leuven (Grant C1-17-00518 to EL).

SUPPLEMENTARY MATERIAL

The Supplementary Material for this article can be found online at: https://www.frontiersin.org/articles/10.3389/fcell.2019.00252/full#supplementary-material

REFERENCES

Anders, S., Pyl, P. T., and Huber, W. (2015). HTSeq–a Python framework to work with high-throughput sequencing data. *Bioinformatics* 31, 166–169. doi: 10.1093/bioinformatics/btu638

Andrassy, K. M. (2013). Comments on 'KDIGO 2012 clinical practice guideline for the evaluation and management of chronic kidney disease'. *Kidney Int.* 84, 622–623. doi: 10.1038/ki.2013.243

Ashburner, M., Ball, C. A., Blake, J. A., Botstein, D., Butler, H., Cherry, J. M., et al. (2000). Gene ontology: tool for the unification of biology. The gene ontology consortium. *Nat. Genet.* 25, 25–29. doi: 10.1038/75556

Bruey, J. M., Bruey-Sedano, N., Newman, R., Chandler, S., Stehlik, C., and Reed, J. C. (2004). PAN1/NALP2/PYPAF2, an inducible inflammatory mediator that regulates NF-kappaB and caspase-1 activation in macrophages. *J. Biol. Chem.* 279, 51897–51907. doi: 10.1074/jbc.M406741200

Christian, F., Smith, E. L., and Carmody, R. J. (2016). The regulation of NF-kappaB subunits by phosphorylation. *Cells* 5:E12. doi: 10.3390/cells5010012

Cui, J., Zhu, L., Xia, X., Wang, H. Y., Legras, X., Hong, J., et al. (2010). NLRC5 negatively regulates the NF-kappaB and type I interferon signaling pathways. *Cell* 141, 483–496. doi: 10.1016/j.cell.2010.03.040

Darisipudi, M. N., and Knauf, F. (2016). An update on the role of the inflammasomes in the pathogenesis of kidney diseases. *Pediatr. Nephrol.* 31, 535–544. doi: 10.1007/s00467-015-3153-z

David, S., Biancone, L., Caserta, C., Bussolati, B., Cambi, V., and Camussi, G. (1997). Alternative pathway complement activation induces proinflammatory activity in human proximal tubular epithelial cells. *Nephrol. Dial. Transplant.* 12, 51–56. doi: 10.1093/ndt/12.1.51

Dobin, A., Davis, C. A., Schlesinger, F., Drenkow, J., Zaleski, C., Jha, S., et al. (2013). STAR: ultrafast universal RNA-seq aligner. *Bioinformatics* 29, 15–21. doi: 10.1093/bioinformatics/bts635

Dunn, S. M., Coles, L. S., Lang, R. K., Gerondakis, S., Vadas, M. A., and Shannon, M. F. (1994). Requirement for nuclear factor (NF)-kappa B p65 and NF-interleukin-6 binding elements in the tumor necrosis factor response region of the granulocyte colony-stimulating factor promoter. *Blood* 83, 2469–2479. doi: 10.1182/blood.v83.9.2469.2469

Emma, F., Ariceta, G., Greco, M., Van'T Hoff, W., Niaudet, P., and Elena, L. (2016). Outcome and prognostic factors of nephropathic cystinosis: data from the eunefron cohort. *Pediatr. Nephrol.* 31, 1723–1748. doi: 10.1007/s00467-016-3466-6

Festa, B. P., Chen, Z., Berquez, M., Debaix, H., Tokonami, N., Prange, J. A., et al. (2018). Impaired autophagy bridges lysosomal storage disease and epithelial dysfunction in the kidney. *Nat. Commun.* 9:161. doi: 10.1038/s41467-017-02536-7

Fontalba, A., Gutierrez, O., and Fernandez-Luna, J. L. (2007). NLRP2, an inhibitor of the NF-kappaB pathway, is transcriptionally activated by NF-kappaB and exhibits a nonfunctional allelic variant. *J. Immunol.* 179, 8519–8524. doi: 10.4049/jimmunol.179.12.8519

Gentleman, R. C., Carey, V. J., Bates, D. M., Bolstad, B., Dettling, M., Dudoit, S., et al. (2004). Bioconductor: open software development for computational biology and bioinformatics. *Genome Biol.* 5:R80. doi: 10.1186/gb-2004-5-10-r80

Gerritsma, J. S., van Kooten, C., Gerritsen, A. F., van Es, L. A., and Daha, M. R. (1998). Transforming growth factor-beta 1 regulates chemokine and complement production by human proximal tubular epithelial cells. *Kidney Int.* 53, 609–616. doi: 10.1046/j.1523-1755.1998.00799.x

Gluba, A., Banach, M., Hannam, S., Mikhailidis, D. P., Sakowicz, A., and Rysz, J. (2010). The role of Toll-like receptors in renal diseases. *Nat. Rev. Nephrol.* 6, 224–235. doi: 10.1038/nrneph.2010.16

Hoshino, K., Sugiyama, T., Matsumoto, M., Tanaka, T., Saito, M., Hemmi, H., et al. (2006). IkappaB kinase-alpha is critical for interferon-alpha production induced by Toll-like receptors 7 and 9. *Nature* 440, 949–953. doi: 10.1038/nature04641

Izzedine, H., Launay-Vacher, V., and Deray, G. (2005). Antiviral drug-induced nephrotoxicity. *Am. J. Kidney Dis.* 45, 804–817. doi: 10.1053/j.ajkd.2005.02.010

Jensen, L. E., and Whitehead, A. S. (1998). Regulation of serum amyloid A protein expression during the acute-phase response. *Biochem. J.* 334(Pt 3), 489–503. doi: 10.1042/bj3340489

Komada, T., and Muruve, D. A. (2019). The role of inflammasomes in kidney disease. *Nat. Rev. Nephrol.* 15, 501–520. doi: 10.1038/s41581-019-0158-z

Kuchmiy, A. A., D'Hont, J., Hochepied, T., and Lamkanfi, M. (2016). NLRP2 controls age-associated maternal fertility. *J. Exp. Med.* 213, 2851–2860. doi: 10.1084/jem.20160900

Kufer, T. A., and Sansonetti, P. J. (2011). NLR functions beyond pathogen recognition. *Nat. Immunol.* 12, 121–128. doi: 10.1038/ni.1985

Laube, G. F., Shah, V., Stewart, V. C., Hargreaves, I. P., Haq, M. R., Heales, S. J., et al. (2006). Glutathione depletion and increased apoptosis rate in human cystinotic proximal tubular cells. *Pediatr. Nephrol.* 21, 503–509. doi: 10.1007/s00467-006-0005-x

Lawrence, T. (2009). The nuclear factor NF-kappaB pathway in inflammation. *Cold Spring Harb. Perspect. Biol.* 1:a001651. doi: 10.1101/cshperspect.a001651

Lawrence, T., Bebien, M., Liu, G. Y., Nizet, V., and Karin, M. (2005). IKKalpha limits macrophage NF-kappaB activation and contributes to the resolution of inflammation. *Nature* 434, 1138–1143. doi: 10.1038/nature03491

Lechner, J., Malloth, N., Seppi, T., Beer, B., Jennings, P., and Pfaller, W. (2008). IFN-alpha induces barrier destabilization and apoptosis in renal proximal tubular epithelium. *Am. J. Physiol. Cell Physiol.* 294, C153–C160. doi: 10.1152/ajpcell.00120.2007

Leemans, J. C., Kors, L., Anders, H. J., and Florquin, S. (2014). Pattern recognition receptors and the inflammasome in kidney disease. *Nat. Rev. Nephrol.* 10, 398–414. doi: 10.1038/nrneph.2014.91

Li, J., Liu, D., Wang, J., Deng, H., Luo, X., Shen, X., et al. (2017). Meta-analysis identifies candidate key genes in endometrium as predictive biomarkers for clinical pregnancy in IVF. *Oncotarget* 8, 102428–102436. doi: 10.18632/oncotarget.22096

Li, Q., Wang, Z., Zhang, Y., Zhu, J., Li, L., Wang, X., et al. (2018). NLRC5 deficiency protects against acute kidney injury in mice by mediating carcinoembryonic antigen-related cell adhesion molecule 1 signaling. *Kidney Int.* 94, 551–566. doi: 10.1016/j.kint.2018.02.031

Liu, B. C., Tang, T. T., Lv, L. L., and Lan, H. Y. (2018). Renal tubule injury: a driving force toward chronic kidney disease. *Kidney Int.* 93, 568–579. doi: 10.1016/j.kint.2017.09.033

Love, M. I., Huber, W., and Anders, S. (2014). Moderated estimation of fold change and dispersion for RNA-seq data with DESeq2. *Genome Biol.* 15:550. doi: 10.1186/s13059-014-0550-8

Luan, P., Zhuang, J., Zou, J., Li, H., Shuai, P., Xu, X., et al. (2018). NLRC5 deficiency ameliorates diabetic nephropathy through alleviating inflammation. *FASEB J.* 32, 1070–1084. doi: 10.1096/fj.201700511RR

Luciani, A., Festa, B. P., Chen, Z., and Devuyst, O. (2018). Defective autophagy degradation and abnormal tight junction-associated signaling drive epithelial dysfunction in cystinosis. *Autophagy* 14, 1157–1159. doi: 10.1080/15548627.2018.1446625

Luo, J. L., Kamata, H., and Karin, M. (2005). IKK/NF-kappaB signaling: balancing life and death–a new approach to cancer therapy. *J. Clin. Invest.* 115, 2625–2632. doi: 10.1172/jci26322

Lupfer, C., and Kanneganti, T. D. (2013). The expanding role of NLRs in antiviral immunity. *Immunol. Rev.* 255, 13–24. doi: 10.1111/imr.12089

Mahadevan, S., Sathappan, V., Utama, B., Lorenzo, I., Kaskar, K., and Van den Veyver, I. B. (2017). Maternally expressed NLRP2 links the subcortical maternal complex (SCMC) to fertility, embryogenesis and epigenetic reprogramming. *Sci. Rep.* 7:44667. doi: 10.1038/srep44667

Malik, A., and Kanneganti, T. D. (2017). Inflammasome activation and assembly at a glance. *J. Cell Sci.* 130, 3955–3963. doi: 10.1242/jcs.207365

Marko, L., Vigolo, E., Hinze, C., Park, J. K., Roel, G., Balogh, A., et al. (2016). Tubular Epithelial NF-kappaB Activity Regulates Ischemic AKI. *J. Am. Soc. Nephrol.* 27, 2658–2669. doi: 10.1681/ASN.2015070748

Meng, X. M., Nikolic-Paterson, D. J., and Lan, H. Y. (2014). Inflammatory processes in renal fibrosis. *Nat. Rev. Nephrol.* 10, 493–503. doi: 10.1038/nrneph.2014.114

Minkiewicz, J., de Rivero Vaccari, J. P., and Keane, R. W. (2013). Human astrocytes express a novel NLRP2 inflammasome. *Glia* 61, 1113–1121. doi: 10.1002/glia.22499

Moore, C. B., Bergstralh, D. T., Duncan, J. A., Lei, Y., Morrison, T. E., Zimmermann, A. G., et al. (2008). NLRX1 is a regulator of mitochondrial antiviral immunity. *Nature* 451, 573–577. doi: 10.1038/nature06501

Park, M., Helip-Wooley, A., and Thoene, J. (2002). Lysosomal cystine storage augments apoptosis in cultured human fibroblasts and renal tubular epithelial cells. *J. Am. Soc. Nephrol.* 13, 2878–2887. doi: 10.1097/01.asn.0000036867.49866.59

Perco, P., Kainz, A., Wilflingseder, J., Soleiman, A., Mayer, B., and Oberbauer, R. (2009). Histogenomics: association of gene expression patterns with histological parameters in kidney biopsies. *Transplantation* 87, 290–295. doi: 10.1097/TP.0b013e318191b4c0

Pradere, J. P., Hernandez, C., Koppe, C., Friedman, R. A., Luedde, T., and Schwabe, R. F. (2016). Negative regulation of NF-kappaB p65 activity by serine 536 phosphorylation. *Sci. Signal.* 9:ra85. doi: 10.1126/scisignal.aab2820

Sanz, A. B., Sanchez-Nino, M. D., Ramos, A. M., Moreno, J. A., Santamaria, B., Ruiz-Ortega, M., et al. (2010). NF-kappaB in renal inflammation. *J. Am. Soc. Nephrol.* 21, 1254–1262. doi: 10.1681/ASN.2010020218

Schlondorff, D. O. (2008). Overview of factors contributing to the pathophysiology of progressive renal disease. *Kidney Int.* 74, 860–866. doi: 10.1038/ki.2008.351

Shigeoka, A. A., Mueller, J. L., Kambo, A., Mathison, J. C., King, A. J., Hall, W. F., et al. (2010). An inflammasome-independent role for epithelial-expressed

Nlrp3 in renal ischemia-reperfusion injury. *J. Immunol.* 185, 6277–6285. doi: 10.4049/jimmunol.1002330

Sung, S., Yang, H., Uryu, K., Lee, E. B., Zhao, L., Shineman, D., et al. (2004). Modulation of nuclear factor-kappa B activity by indomethacin influences A beta levels but not A beta precursor protein metabolism in a model of Alzheimer's disease. *Am. J. Pathol.* 165, 2197–2206. doi: 10.1016/s0002-9440(10)63269-5

Thaiss, C. A., Levy, M., Itav, S., and Elinav, E. (2016). Integration of innate immune signaling. *Trends Immunol.* 37, 84–101. doi: 10.1016/j.it.2015.12.003

Tilburgs, T., Meissner, T. B., Ferreira, L. M. R., Mulder, A., Musunuru, K., Ye, J., et al. (2017). NLRP2 is a suppressor of NF-κB signaling and HLA-C expression in human trophoblastsdagger,double dagger. *Biol. Reprod.* 96, 831–842. doi: 10.1093/biolre/iox009

Vilaysane, A., Chun, J., Seamone, M. E., Wang, W., Chin, R., Hirota, S., et al. (2010). The NLRP3 inflammasome promotes renal inflammation and contributes to CKD. *J. Am. Soc. Nephrol.* 21, 1732–1744. doi: 10.1681/ASN.2010020143

Wang, R. P., Zhang, M., Li, Y., Diao, F. C., Chen, D., Zhai, Z., et al. (2008). Differential regulation of IKK alpha-mediated activation of IRF3/7 by NIK. *Mol. Immunol.* 45, 1926–1934. doi: 10.1016/j.molimm.2007.10.034

Wilmer, M. J., de Graaf-Hess, A., Blom, H. J., Dijkman, H. B., Monnens, L. A., van den Heuvel, L. P., et al. (2005). Elevated oxidized glutathione in cystinotic proximal tubular epithelial cells. *Biochem. Biophys. Res. Commun.* 337, 610–614. doi: 10.1016/j.bbrc.2005.09.094

Xiao, J., Zhang, X. L., Fu, C., Han, R., Chen, W., Lu, Y., et al. (2015). Soluble uric acid increases NALP3 inflammasome and interleukin-1beta expression in human primary renal proximal tubule epithelial cells through the Toll-like receptor 4-mediated pathway. *Int. J. Mol. Med.* 35, 1347–1354. doi: 10.3892/ijmm.2015.2148

Yang, Y., Lang, X., Sun, S., Gao, C., Hu, J., Ding, S., et al. (2018). NLRP2 negatively regulates antiviral immunity by interacting with TBK1. *Eur. J. Immunol.* 48, 1817–1825. doi: 10.1002/eji.201847589

Yu, G., Wang, L. G., Han, Y., and He, Q. Y. (2012). clusterProfiler: an R package for comparing biological themes among gene clusters. *OMICS* 16, 284–287. doi: 10.1089/omi.2011.0118

Zhuang, Y., Hu, C., Ding, G., Zhang, Y., Huang, S., Jia, Z., et al. (2015). Albumin impairs renal tubular tight junctions via targeting the NLRP3 inflammasome. *Am. J. Physiol. Renal Physiol.* 308, F1012–F1019. doi: 10.1152/ajprenal.00509.2014

Conflict of Interest: The authors declare that the research was conducted in the absence of any commercial or financial relationships that could be construed as a potential conflict of interest.

Copyright © 2019 Rossi, Pascarella, Licursi, Caiello, Taranta, Rega, Levtchenko, Emma, De Benedetti and Prencipe. This is an open-access article distributed under the terms of the Creative Commons Attribution License (CC BY). The use, distribution or reproduction in other forums is permitted, provided the original author(s) and the copyright owner(s) are credited and that the original publication in this journal is cited, in accordance with accepted academic practice. No use, distribution or reproduction is permitted which does not comply with these terms.

frontiers in Cell and Developmental Biology

REVIEW
published: 03 December 2019
doi: 10.3389/fcell.2019.00314

Unraveling Cardiovascular Risk in Renal Patients: A New Take on Old Tale

Michele Provenzano[1], Giuseppe Coppolino[1], Luca De Nicola[2], Raffaele Serra[3], Carlo Garofalo[2], Michele Andreucci[1] and Davide Bolignano[4]*

[1] Renal Unit, Department of Health Sciences, University "Magna Graecia" of Catanzaro, Catanzaro, Italy, [2] Renal Unit, University of Campania "Luigi Vanvitelli", Naples, Italy, [3] Interuniversity Center of Phlebolymphology (CIFL), University "Magna Graecia"of Catanzaro, Catanzaro, Italy, [4] Institute of Clinical Physiology, Italian National Research Council (CNR), Reggio Calabria, Italy

Chronic kidney disease (CKD), defined by an estimated glomerular filtration rate <60 ml/min/1.73 m^2 and/or an increase in urine protein excretion (i.e., albuminuria), is an important public health problem. Prevalence and incidence of CKD have risen by 87 and 89%, worldwide, over the last three decades. The onset of either albuminuria and eGFR reduction has found to predict higher cardiovascular (CV) risk, being this association strong, independent from traditional CV risk factors and reproducible across different setting of patients. Indeed, this relationship is present not only in high risk cohorts of CKD patients under regular nephrology care and in those with hypertension or type 2 diabetes, but also in general, otherwise healthy population. As underlying mechanisms of damage, it has hypothesized and partially proved that eGFR reduction and albuminuria can directly promote endothelial dysfunction, accelerate atherosclerosis and the deleterious effects of hypertension. Moreover, the predictive accuracy of risk prediction models was consistently improved when eGFR and albuminuria have been added to the traditional CV risk factors (i.e., Framingham risk score). These important findings led to consider CKD as an equivalent CV risk. Although it is hard to accept this definition in absence of additional reports from scientific Literature, a great effort has been done to reduce the CV risk in CKD patients. A large number of clinical trials have tested the effect of drugs on CV risk reduction. The targets used in these trials were different, including blood pressure, lipids, albuminuria, inflammation, and glucose. All these trials have determined an overall better control of CV risk, performed by clinicians. However, a non-negligible residual risk is still present and has been attributed to: (1) missed response to study treatment in a consistent portion of patients, (2) role of many CV risk factors in CKD patients not yet completely investigated. These combined observations provide a strong argument that kidney measures should be regularly included in individual prediction models for improving CV risk stratification. Further studies are needed to identify high risk patients and novel therapeutic targets to improve CV protection in CKD patients.

Keywords: cardiovascular risk, epidemiology, chronic kidney disease, risk score, smoking habit, statins, eGFR, proteinuria

OPEN ACCESS

Edited by:
Nejra Prohic,
Clinical Center University of Sarajevo,
Bosnia and Herzegovina

Reviewed by:
Laszlo Rosivall,
University of Debrecen, Hungary
Ingrid Inge Prkacin,
University of Zagreb, Croatia
Giuseppe Remuzzi,
Istituto Di Ricerche Farmacologiche
Mario Negri, Italy

****Correspondence:***
Giuseppe Coppolino
gcoppolino@unicz.it

Specialty section:
This article was submitted to
Molecular Medicine,
a section of the journal
Frontiers in Cell and Developmental
Biology

Received: *03 September 2019*
Accepted: *18 November 2019*
Published: *03 December 2019*

Citation:
Provenzano M, Coppolino G,
De Nicola L, Serra R, Garofalo C,
Andreucci M and Bolignano D (2019)
Unraveling Cardiovascular Risk
in Renal Patients: A New Take on Old
Tale. Front. Cell Dev. Biol. 7:314.
doi: 10.3389/fcell.2019.00314

INTRODUCTION

Chronic kidney disease (CKD) is defined as the presence of kidney damage, mainly albuminuria, and/or decreased kidney function (estimated glomerular filtration rate [eGFR] <60 mL/min/1.73 m^2) for at least 3 months (Levey and Coresh, 2012). Since the new onset of eGFR reduction and/or albuminuria is often asymptomatic, CKD is considered as part of non-communicable diseases, together with type 2 diabetes, hypertension and obesity (Jha et al., 2013). In the past decades, the epidemiology of communicable and non-communicable diseases has completely changed. From one side, the drop of mortality due to the main communicable diseases represented the "public health triumph" of the 20th century (Mensah et al., 2017). Indeed, by 1960, the improvement of Health System organization and the development of vaccines and new antibiotics have dramatically decreased mortality from infectious disease and raised life expectancy by an average of 20 years in the United States population (Murray and Lopez, 2013). From around the same period, a sharp decline in cardiovascular (CV) mortality has also been observed in the United States population and worldwide (Centers for Disease Control and Prevention, 1999). In United States, using the 1940 population as reference, the annual heart disease mortality rate declined by 56% in 1996, whereas the mortality rate for stroke fell by 70% in the same period. Similar findings were observed in many other populations (Lozano et al., 2012). The descending trend in CV mortality has been attributed to the improvement in specific prevention strategies, such as better blood pressure control, reduction in total cholesterol plasma levels, smoking cessation, increased physical activity (Ford et al., 2007). On the other side, the burden of non-communicable diseases has dramatically increased in the last quarter century. The number of adults with diabetes has raised from 108 million in 1980 to 422 million in 2014 and that of hypertensive subjects almost duplicated in the period 1975–2015 (NCD Risk Factor Collaboration [NCD-RisC], 2016, 2017). The increased prevalence of these comorbidities together with the population growth and aging, as the longer survival in CV disease, have shaped the CKD epidemiology trend. Indeed, the global prevalence and incidence of CKD has risen by 87 and 89%, respectively, over the period 1990–2016 (Xie et al., 2018). Intriguingly, although the age-standardized mortality rate has shown to be improved for most communicable and non-communicable disease (Ford et al., 2007; Lozano et al., 2012; Mortality and Causes of Death Collaborators, 2015), CKD is among a small number of diseases for which death rates have essentially risen in the last three decades. Specifically, age-standardized death rate due to CKD has increased by 4.39% from 1990 to 2017 (Xie et al., 2018). To date, it has been not completely clarified the specific role of clinical and demographic variables as risk factors for CKD development, maintenance and progression, as well as their effects on the three main endpoints measured in CKD patients: kidney function decline, mortality, CV events. This is, for example, the case of body mass index (BMI) and hypertension. Two recent meta-analyses showed that obesity and not only hypertension, but also pre-hypertension, were significant predictors of new onset CKD (Garofalo et al., 2016, 2017). Further analyses showed that high BMI increases also the risk for dialysis initiation but not for CV events (Russo et al., 2014). These important findings confirm that epidemiologic analyses may provide different results, given the different populations examined.

Aim of this Narrative Review article is to elucidate the main epidemiologic evidences about the association between Kidney damage and CV disease, the mechanisms responsible for this association, available strategies to reduce CV risk in patients suffering from CKD and future directions to answer the unmet needs around this topic.

CARDIOVASCULAR OUTCOMES IN CHRONIC KIDNEY DISEASE PATIENTS

Cardiovascular events remain responsible for a large proportion of unfavorable outcomes in CKD patients. Indeed, among several CKD cohorts, mortality overcomes End-Stage-Kidney-Disease (ESKD), which is considered the "natural" endpoint in these population (Go et al., 2004). Among patients with CKD alone or with CKD and type 2 diabetes of the United States Medicare population, risks of death and atherosclerotic vascular disease exceeded that of ESKD (Foley et al., 2005). Similar findings were reported from individuals with eGFR <60 ml/min/1.73 m^2 selected from insurance-based health organizations (i.e., Kaiser Permanente Northwest), or Veterans Affair elderly with proteinuria or type 2 diabetes (Keith et al., 2004; Patel et al., 2005). However, these cohorts included patients with advanced age. In the Medicare population, prevalence of patients older than 70, in the subset with CKD and diabetes or CKD alone, was 88 and 91%, respectively (Foley et al., 2005). Cohorts which enrolled patients with a broad range of age, primary renal diseases as well as cohorts of patients referred to Nephrologists (the so-called Nephrology care), showed different results. In a cohort of referred CKD, the rate of ESKD overcame death (including CV death) up to 60 years age or 65 years (only if eGFR was <30 ml/min/1.73 m^2), being the risk of death more frequent in patients older than 60 years with mild reduced kidney function. Thus, age and kidney function are the two main moderators of mortality and ESKD risks in CKD patients. Moreover, in patients under nephrology care, at variance with unreferred, the ESKD incidence rate is higher than mortality and CV rates (Coppolino et al., 2010; De Nicola et al., 2012, 2017). Nevertheless, CV risk remains relevant in this setting of patients in clinical studies that have been carried-out from different Countries. The presence of previous CV events, defined as myocardial infarction, stroke, heart failure, peripheral vascular disease or revascularization, ranged from 10 to 30% in the NephroTest (France), Mild-to-Moderate Kidney Disease (MMKD) study (Germany, Austria, and South Tyrol) and the British Columbia Study (Canada) (Levin et al., 2008; Dieplinger et al., 2009; Moranne et al., 2009). This prevalence rose to 30–50% in CKD populations of MASTERPLAN (Netherlands) (van Zuilen et al., 2006), CRIB

(Chronic Renal Impairment in Birmingham, United Kingdom) (Landray et al., 2001), AASK (African Americans) Study (Norris et al., 2006) and CKD-Multicohort (Italy) (Minutolo et al., 2018); in this latter study, which enrolled CKD patients referred to 40 Italian nephrology clinics, ESKD, CV fatal/non-fatal events and mortality rates were 5.26, 4.52, and 3.76 per 100/pt/years, respectively (Minutolo et al., 2018).

Although all these studies evidenced a significant association between CV disease and CKD, the frequency of CV risk varies due to the different inclusion criteria used to recruit patients, particularly with regards of eGFR and proteinuria levels (Astor et al., 2011). An extended estimate of the prevalence of CV risk in CKD patients has been recently realized by the Global Burden of Disease Investigators (Thomas et al., 2017). By analyzing more than 1,000 surveys of CKD patients from around the world, it was found that, in the year 2013, 1,207,453 out 2,163,699 deaths (more than half, 55.8%) were secondary to CV disease. Interestingly, the age-standardized CV disease mortality rate was slightly higher in developing vs. developed world (**Figure 1**). This phenomenon is partly related to the increase, in developing Countries, of risk factors that can accelerate CV disease development, such as the aging of the population and the change in dietary habit toward high caloric and fatty foods compared to still limited prevention and treatment strategies (Barquera et al., 2015). All these evidences confirm the burden of CV disease in CKD patients and reinforce the need to improve and better understanding how to reduce CV risk in these frailty patients (Piccoli et al., 2018) as well as to ameliorate health care access and infrastructure in developing countries (Perico et al., 2005). Moreover, these findings also encourage incorporating CV disease in the evaluation of the benefits of CKD screening worldwide. Indeed, cost-effectiveness CKD screening studies have concluded that screening is cost effective whether CV fatal and non-fatal events have been included in the analysis at variance with studies that measured the effect on ESKD only (Vos et al., 2010; Crews et al., 2011).

CHRONIC KIDNEY DISEASE IS AN INDEPENDENT RISK FACTOR FOR CARDIOVASCULAR EVENTS

In the past decades, several studies affirmed the importance of CKD as a risk factor for the onset of CV events such as myocardial infarction, stroke, chronic heart failure, peripheral vascular disease, CV death. These studies have been carried out in general population and high-risk cohorts (for example diabetic patients, CKD patients and those with a previous CV disease). In a recent meta-analysis, which enrolled more than 100,000 individuals from the general population, both a reduction in kidney function

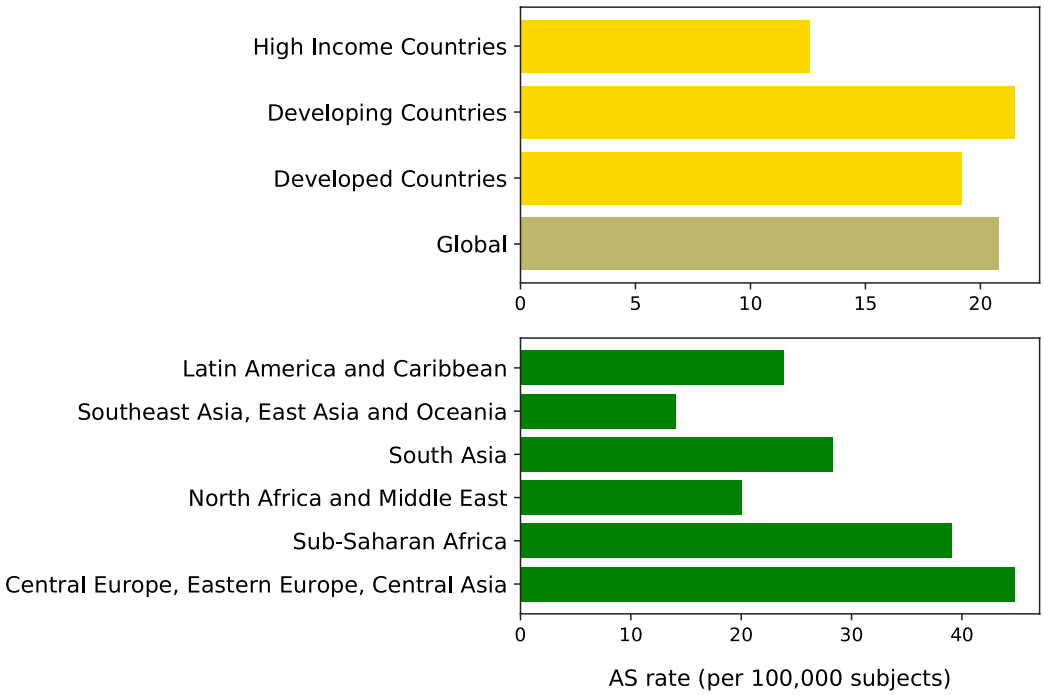

FIGURE 1 | Age-standardized (AS) cardiovascular diseases mortality rate (per 100,000 subjects) worldwide in CKD patients in 2013 (Thomas et al., 2017). Top plot shows rates by development status; bottom plot shows rates by geographic macro-areas. Global, which represents the average rate, is darkly colored. Developed countries are defined as sovereign states that have a developed economy and technologically advanced infrastructure when compared to other countries. (Definition and list at: http://worldpopulationreview.com/countries/developed-countries/). Developing countries are characterized by being less developed industrially with a lower Human Development Index when compared to other countries. (Definition and list at: http://worldpopulationreview.com/countries/developing-countries/). High-income refers to Asia Pacific, Australia, Western Europe, Southern Latin America, North America; sub-Saharan Africa refers to Central sub-Saharan Africa, Eastern sub-Saharan Africa, Southern sub-Saharan Africa, Western sub-Saharan Africa.

(eGFR) and the presence of kidney damage (albuminuria) were independently and strictly associated with an increased risk of death and CV death, regardless of many potential confounders such as age, gender, and traditional CV risk factors (Chronic Kidney Disease Prognosis Consortium Matsushita et al., 2010). In particular, mortality risk started to increase for eGFR level ≤60 ml/min/1.73 m^2 and was two-fold higher at 30–45 ml/min/1.73 m^2 as compared to normal eGFR levels. Regarding the albuminuria-related CV risk, this doubled by moving from 5 to 100 mg/g of urinary albumin/creatinine ratio, thus demonstrating that even a slight increase in albuminuria can herald patients' higher CV and mortality risk. Similar findings were obtained from high risk population with type 2 diabetes and hypertension (Fox et al., 2012; Mahmoodi et al., 2012; Simeoni et al., 2016; Coppolino et al., 2017). A large meta-analysis from the CKD-Prognosis Consortium assessed the risk of CV mortality by type 2 diabetes status. CV risk was higher in diabetic vs. non-diabetic patients across the whole range of eGFR and albuminuria. However, Authors reported that interaction between eGFR (or albuminuria) and diabetes for all-cause mortality and CV-mortality endpoints was not significant (Fox et al., 2012). This means that, after establishing a reference point on the eGFR or albuminuria scale, the relative risks of the two health outcomes did not differ in diabetic vs. non-diabetic patients. Similar results were obtained when comparing hypertensive vs. non-hypertensive patients (Mahmoodi et al., 2012). An observational analysis of the ADVANCE (Action in Diabetes and Vascular disease: preterAx and diamicroN-MR Controlled Evaluation) clinical trial provided additional useful evidences on CV risk in type 2 diabetes patients. In that study, where more than 10,000 type 2 diabetic patients aged 55 (or older) were enrolled, higher albuminuria and lower eGFR levels were associated with an increased risk of all CV events (CV death, non-fatal myocardial infarction and non-fatal stroke) (Ninomiya et al., 2009).

According to these previous studies, both the two kidney measures (i.e., albuminuria and eGFR) are both strongly associated to the development of CV events. This association is independent from the presence of hypertension and diabetes, thus confirming the crucial role of CKD *per se*.

LINK BETWEEN KIDNEY MEASURES AND CARDIOVASCULAR DAMAGE

A first pioneering hypothesis about how albuminuria may testify high CV risk came from the group of researchers of the Steno Memorial Hospital, in Denmark, and was thus called the *Steno hypothesis* (Deckert et al., 1989). Owing the observation that in diabetic patients with increased albuminuria, this marker was associated to an increased transcapillary escape rate of fibrinogen and increased levels of von Willebrand factor, they suggested that albuminuria might reflect a general endothelial dysfunction and systemic vascular damage. Indeed, the leakage of albumin in the vessel-wall may trigger an inflammatory response, thus accelerating the atherosclerotic process. More recently, multiple experimental and clinical studies elucidated that the presence of albuminuria witnesses abnormalities in endothelial glycocalyx, as well as other endothelial structures (Stehouwer et al., 1992; Coppolino et al., 2009; Perticone et al., 2016). Perticone et al. (2015) have also found a significant inverse relationship between alkaline phosphatase and endothelium-dependent vasodilation, which can be mediated by an increase in fibroblast growth factor-23, an early marker of endothelial dysfunction in CKD patients. Moreover, in patients at increased risk for CKD, such as diabetic or hypertensive patients, the microvascular pressure and flows are increased (Ruggenenti and Remuzzi, 2006). This (also called hemodynamic hypothesis) can contribute to the development of albuminuria and the concurrent vascular damage in other organs, such as the heart and the eyes, with the onset of impaired coronary hemodynamics, left ventricular hypertrophy and retinopathy, respectively (Gavin et al., 1998; Liang et al., 2013; De Nicola et al., 2015a).

The contribution of eGFR to the increased CV risk has not completely understood yet, but has raised at the same time an increasing levels of clinical research attention. Indeed, in a survey conducted in the metropolitan area of Kyushu Island, in Southern Japan, heart tissue obtained from 482 individuals who underwent autopsies was examined. The severity of coronary atherosclerosis correlated with the grade of impairment in their kidney function (Nakano et al., 2010). Moreover, the presence of a significant coronary artery stenosis has been found, by angiography, in about half of pre-dialysis patients with extremely low levels of eGFR (Ohtake et al., 2005). Improving management of atherosclerotic risk factors, before reaching an advanced CKD stage, is therefore becoming one of the main targets of Nephrology care.

CKD AS A RISK EQUIVALENT OF CARDIOVASCULAR EVENTS

A common way to measure a patient's risk of developing a CV event consists in calculating a 10-year risk based on a combination of some predictors. The Framingham risk score computes the 10-year risk (%) of coronary heart disease for a subject given the exact value of age, gender, systolic blood pressure, total and HDL cholesterol, and smoking status. Once the score has been computed, it should modify the clinical management in accordance to the 10-year CV risk: ≥ 10% defines a very-high risk of CV risk; 5–10% a high risk; 1–5% a moderate risk; < 1% a low risk. However, when the predictive value of the traditional scores have been tested in CKD patients, the risk estimation was suboptimal and, definitely, not well calibrated (Weiner et al., 2007). This means that, traditional CV risk factors are able to explain only a portion of the total CV risk in CKD patients. Therefore, research has recently focused on assessing whether adding the CKD measures (i.e., albuminuria and eGFR) can ameliorate prediction models. A recent meta-analysis of general and high-risk populations, has showed that adding eGFR, albumin-to creatinine ratio (ACR), or both, to the traditional CV risk factors significantly improves the model performance for the prediction of all CV endpoints: CV mortality, coronary heart disease, stroke, and heart failure (Matsushita et al., 2015). More interestingly, the contribution of

TABLE 1 | Observational studies examining rates of cardiovascular (CV) events among CKD patients.

Study	Population	Sample size	Outcome	Results
Kaiser Permanente Northwest (KPN) (Go et al., 2004)	General population (health care system insuring in Northern California, United States)	1.120.295	Death from any cause, CV events, and hospitalizations	Risks of death, CV events, and hospitalizations increased as the eGFR decreased below 60 ml/min/1.73 m^2 as compared to eGFR >60 ml/min/1.73 m^2
United States Medicare population (Foley et al., 2005)	General population (health insurance including 50 United States states)	1.091.201	Incidence of atherosclerotic vascular disease, congestive heart failure or renal replacement therapy	Rates of atherosclerotic vascular disease, congestive heart failure or renal replacement therapy were higher in patients with type 2 diabetes and CKD (or CKD alone) as compared to the groups without CKD. CKD accelerates the progression to all poor outcomes investigated
PREVEND (Brantsma et al., 2008)	General population (Netherlands)	8.496	CV events	Baseline albuminuria and change of albuminuria over time were good predictors of CV events.
Alberta Kidney Disease (Tonelli et al., 2012)	General population (Province of Alberta, Canada)	11.340	Admission to Hospital for myocardial infarction	Rate of incident myocardial infarction in people with diabetes was substantially lower than for those with CKD when defined by eGFR <45 mL/min/1.73 m^2 and severely increased proteinuria. CKD should be regarded as a coronary heart disease risk equivalent.
HUNT II (Hallan et al., 2007)	General population (Norway)	9.709	CV mortality	Reduced kidney function and microalbuminuria were risk factors for CV death, independent of each other and traditional risk factors.
ARIC (Kottgen et al., 2007)	General population (four US communities)	14.857	Determining the effect of decreased kidney function on HF incidence	The incidence of HF was three-fold higher for individuals with eGFR <60 ml/min/1.73 m^2 compared to the reference group with eGFR ≥90 ml/min/1.73 m^2.
Steno (Theilade et al., 2012)	High risk population (Denmark)	900	CV events, mortality, ESRD	Endothelial dysfunction was a predictor of CV events, mortality, ESRD in patients with type I diabetes.
Kaiser Permanente Northwest- CKD (Keith et al., 2004)	CKD patients selected from the KPN cohort	27.998	Renal replacement therapy, death, disenrollment from the health plan	Rate of renal replacement therapy over time was 1.1, 1.3, and 19.9%, respectively, for the CKD stages 2, 3, and 4 whereas the mortality rate was 19.5, 24.3, and 45.7% across CKD stages. Thus, death was far more common than dialysis at all CKD stages.
CKD-Multicohort *(Minutolo et al., 2018)	Referred CKD patients (40 renal clinics in Italy)	2.174	All-cause mortality, fatal and non-fatal CV events and ESRD	The amount of 24 h proteinuria increased the risk of CV events and ESRD and anticipated the onset of CV events in patients with type II diabetes and CKD.
SIR-SIN (De Nicola et al., 2015b)	Referred CKD patients (100 renal clinic in Italy)	1.306	MACE (CV death, non-fatal events requiring hospitalization; ESRD or 50% eGFR reduction)	eGFR, high LDL cholesterol, type 2 diabetes, old age and previous CV disease predicted CV events in CKD patients.
British Columbia (Levin et al., 2008)	Referred CKD patients (Canada)	4.231	Death, dialysis therapy start, or loss of GFR greater than 5 mL/min/1.73 m^2/year.	Different clinical or laboratory variables predict kidney disease progression or death in referred CKD patients.

** CKD-Multicohort included TArget BLood pressure LEvel in Chronic Kidney Disease (TABLE-CKD) (Minutolo et al., 2006), NEPHROlogy Second University of Naples (NEPHRO-SUN) (De Nicola et al., 2015a), ambulatory blood pressure in chronic kidney disease (ABP-CKD) (Minutolo et al., 2011) and REporting COmorbidities in Renal Disease in ITaly (RECORD-IT) (Minutolo et al., 2013); CV, cardiovascular; CKD, chronic kidney disease; HF, heart failure; ESRD, end stage renal disease.*

albuminuria, revealed as ACR, to the overall model performance was greater than the contribution of traditional risk factors. These results are particularly significant and suggest that in population with a higher CV risk, such as CKD patients, the assessment of both eGFR and albuminuria is the essential step. Two additional separate analyses, performed in the general

populations of Alberta kidney disease (AKD) and atherosclerosis risk in communities (ARIC), provided important evidences on the relevant contribution of CKD to the development of CV events. Indeed, the AKD showed that the rate of myocardial infarction was significantly higher in patients with CKD, but without diabetes (6.9 per 1,000 person-years), than in those with diabetes, but without CKD (5.4 per 1,000 person-years), being the results similar when the GFR, estimated by the MDRD equation, and sex-specific serum creatinine cutoff points were used to identify reduced GFR (Tonelli et al., 2012). Moreover, the ARIC study evidenced that the adjusted risk for heart failure (HF) was about two-fold higher in patients with eGFR <60 mL/min/1.73 m^2 compared to those with eGFR ≥90 mL/min/1.73 m^2 regardless of the presence of coronary heart disease at baseline (Kottgen et al., 2007). Details of the principal observational cohort studies assessing the risk for CV fatal and non-fatal events among CKD patients are shown in **Table 1**. These results have led guidelines to consider CKD as coronary heart disease risk equivalent. The 2016 ESC/ESH guidelines classified patients with eGFR reduction at high risk (10-year CV mortality risk ≥ 10%), even in absence of albuminuria (Ponikowski et al., 2016). Similarly, KDIGO considered CKD patients older than 50 years old at high risk for CV events (Kidney Disease Improving Global Outcomes Work Group, 2013). Despite the great enthusiasm of such discoveries, several concerns have been raised about considering CKD as a CV disease risk equivalent. Indeed, the CV risk, which was estimated in AKD and ARIC studies, is profoundly influenced by the presence of an established CV disease, that is the strongest cause of a new CV event. Therefore, debate is still ongoing on whether considering CKD as risk equivalent of CV disease or not; in that case more evidence must be obtained to reach that conclusion. We need, in fact, to develop more accurate (i.e., in CKD patients only) risk prediction models on patients' CV risk and their target treatment, based on these risk scores. New studies in referred CKD patients should comply with this scope.

THE TERTIARY NEPHROLOGY CARE SETTING

Chronic kidney disease patients under stable "Nephrology care" represent a specific high-risk population that differs from general population and other high-risk populations, such as patients with hypertension or diabetes, in terms of basal risk, management and prognosis. In a multi-cohort analysis of about 4,000 patients referred to Nephrology Units in Italy, we have investigated the frequency of comorbidities and prognosis (Provenzano et al., 2018). Population was characterized by old age on average (67 years), and a high prevalence of diabetes (29%) and CV disease [heart failure, myocardial infarction, peripheral vascular disease, and stroke (34%)]. Therefore, this CKD population, in a large portion of cases, suffers from other comorbidities and consequently is at extremely high risk of worse outcome (**Figure 2**). A higher CV disease frequency has been found among CKD patients, who were diagnosed on diabetic nephropathy or hypertensive nephropathy, thus demonstrating the presence of a combination of multiple risk factors simultaneously in these patients (**Figure 3**). On the other hand, among over 400,000 Italian patients, followed by general practitioners, the frequency of diabetes and CV disease was 4.7 and 7.9%, respectively (Minutolo et al., 2008).

Moreover, it has also been shown that in referred CKD patients, CV disease is poorly controlled. In the TABLE-CKD (TArget Blood Pressure Levels), a multicenter study which enrolled patients with stage 3–5 of CKD and at least

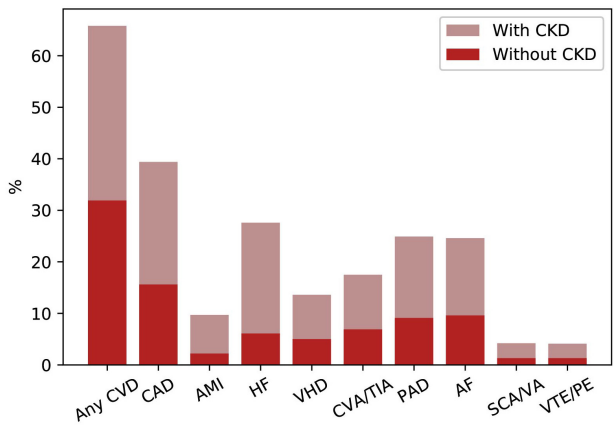

FIGURE 2 | Prevalence of common cardiovascular diseases in patients with or without CKD in United States (2015). AF, atrial fibrillation; AMI, acute myocardial infarction; CAD, coronary artery disease; CKD, chronic kidney disease; CVA/TIA, cerebrovascular accident/transient ischemic attack; CVD, cardiovascular disease; HF, heart failure; PAD, peripheral arterial disease; SCA/VA, sudden cardiac arrest and ventricular arrhythmias; VHD, valvular heart disease; VTE/PE, venous thromboembolism and pulmonary embolism.

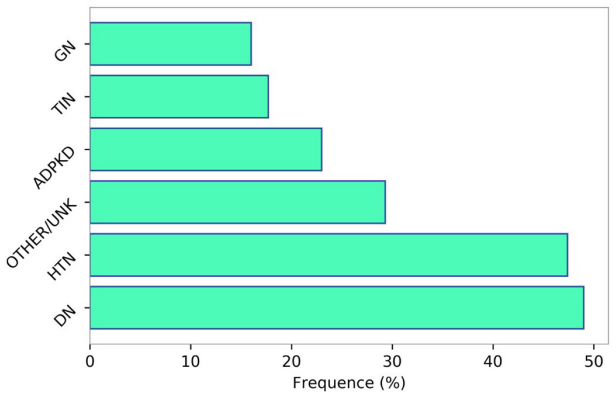

FIGURE 3 | Prevalence of cardiovascular disease (myocardial infarction, stroke, peripheral vascular disease, chronic heart failure, and angina) according to the primary renal disease categories. Data source: 3,957 patients selected from the Italian multicohort of CKD patients referred to nephrologists (Provenzano et al., 2018). HTN, hypertensive nephropathy; DN, diabetic nephropathy; GN, glomerulonephritis; TIN, tubulo-interstitial nephropaties; ADPKD, autosomal dominant polycystic kidney disease; OTHER/UNK, other or unknown diagnosis.

6-month follow up of Nephrology care, less than 15% of patients had blood pressure at target (<130/80 mmHg) and more than 80% patients showed an excessive salt intake not counterbalanced by an adequate treatment with loop diuretics, usually prescribed successfully by clinicians (Andreucci et al., 1999). However, the frequency of patients who had a better controlled hypertension significantly increased (up to 75% of patients) after 12 months of Nephrology care, which is generally considered a sufficient time interval for Nephrologists to intervene on the main co-morbidities (Russo et al., 2005; De Nicola et al., 2015a). Similarly, prevalence of hypercholesterolemia reached 50–60% depending on the stage of CKD (De Nicola et al., 2006). In another cohort of patients followed by Nephrologists, the SIR-SIN (Italian study on multiple predictors of outcome- epidemiology of chronic renal insufficiency in Italy) study, the therapeutic inertia for LDL control, defined as the percentage of patients not receiving statin prescription despite being recommended by current guideline, was as high as 61.3% (De Nicola et al., 2015b). These findings confirm, once again, the importance of referring high-risk patients to nephrologists.

As described for the general population and for diabetic/hypertensive patients, kidney measures have been confirmed as potent predictors of CV outcomes in tertiary nephrology care. The presence of proteinuria is an independent predictor of CV fatal and non-fatal events, with the risk starting to increase from 0.500 g/24 h and from 0.150 g/24 h in non-diabetic-CKD and diabetic-CKD patients, respectively (Coppolino et al., 2017; Minutolo et al., 2018). However, hazard ratio for CV events increased in all patients, selected from this cohort, also for slight increments of 24 h-proteinuria levels (**Figure 4**). This confirms how the effect of proteinuria on CV outcomes is consistent, strong and independent of other comorbidities, as described in the CKD-Prognosis Consortium. The risk of all-cause and CV death was increased as the eGFR declines (De Nicola et al., 2012). Smoking habit has been considered an independent predictor of CV events in general and high-risk cohorts (Cedillo-Couvert and Ricardo, 2016).

Moreover, current and former smokers have been found at increased risk of developing albuminuria over time as compared to never smokers in the general population (Halimi et al., 2000). However, even though a recent meta-analysis has also

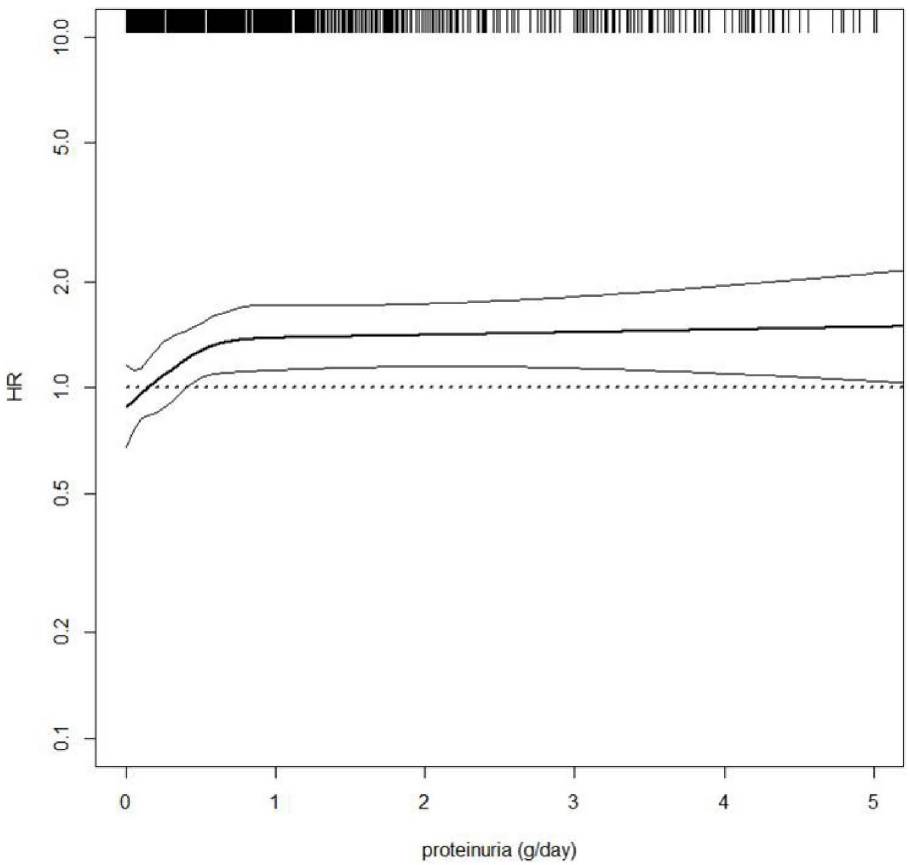

FIGURE 4 | Hazard ratio (HR, solid thick line) and 95% confidence intervals (solid thin lines) for cardiovascular (CV) fatal and non-fatal events (new onset of myocardial infarction, congestive heart failure, stroke, revascularization, peripheral vascular disease, non-traumatic amputation or CV death) by 24 h-proteinuria level. HR was modeled by means of restricted cubic spline (RCS) due to the non-linear association between proteinuria and CV events. Four knots were located at 0, 25th, 50th, and 75th percentiles of proteinuria, whereas HR estimate was adjusted for age, gender, and eGFR value. Rug plot on the *x* axis at the top represents the distribution of observations. Data source: pooled analysis of four cohorts of CKD patients referred to Italian nephrology clinics (Minutolo et al., 2018).

shown that smoking is a predictor of new onset of CKD in the general population, the prognostic role of cigarette smoking or the combination of smoking and albuminuria, in patients with already established CKD, remains not completely quantified (Orth and Hallan, 2008; Bolignano et al., 2015; Xia et al., 2017; Coppolino et al., 2018a).

By considering CKD as CV risk equivalent can lead to a reclassification of patients for CV prevention. However, the general opinion, given the differences in basal risks between CKD populations vs. general and high-risk cohorts, is that more studies clarifying the exact role of CV risk factors in referred CKD patients are needed (Nagler et al., 2014). Moreover, despite the fact that to compute a 10-year risk for each patient could be cumbersome, this method can have a greater accuracy in the prediction of CV events in the future, unlike to consider all CKD patients with any degree of proteinuria, eGFR and comorbidities with the same CV risk.

STRATEGIES FOR REDUCING CARDIOVASCULAR RISK IN CHRONIC KIDNEY DISEASE PATIENTS

In the last two decades, a growing number of intervention studies have been carried out, with the aim of achieving a better control of CV risk in CKD patients (Mann et al., 2001; Berl et al., 2003; Asselbergs et al., 2004; Norris et al., 2006; Rahman et al., 2006; Solomon et al., 2006; Brugts et al., 2007; Hallan et al., 2007; Kottgen et al., 2007; Perkovic et al., 2007; Bolignano et al., 2008, 2010; Anand et al., 2009; Heerspink et al., 2010; Shiga et al., 2010; Baigent et al., 2011; Parving et al., 2012; Tonelli et al., 2012; Wanner et al., 2016). This point is extremely important because, in the previous CV endpoints-trials, patients with impaired kidney function were regularly excluded (Zoccali et al., 2019). Nowadays, CV risk is also investigated with the aim to find novel biomarkers related to omics, imaging techniques and clinical data, which may help physicians in order to improve their knowledge and management (Serra et al., 2018).

The main intervention studies assessing the CV risk reduction in CKD patients, are listed in **Table 2**. Interventions differed between studies, with the effect of anti-hypertensive drugs, diuretics, albuminuria lowering agents and statins being tested (Bolignano et al., 2015). The CV benefits of drugs intervening in the renin-angiotensin-aldosterone-system (RAAS-I) are well established. The heart outcomes protection evaluation (HOPE) (Mann et al., 2001)and perindopril protection against recurrent stroke study (PROGRESS) (Perkovic et al., 2007) studies demonstrated, in patients with CKD, that blood pressure lowering using RAAS-I can significantly reduce the subsequent risk for CV events, such as stroke, coronary heart disease, and CV death. Intriguingly, the magnitude of the absolute risk reduction, achieved with that therapy, was greater in patients with CKD than in those without CKD, testifying that the obtained benefit is more pronounced if basal risk is higher. This concept contains a very important "public health" message, namely the priority of identifying CKD patients at increased CV risk that need more intensive management in terms of number of visits and therapy as well (Perkovic et al., 2007). This may also explain why several trials enrolling patients at less increased risk did not show any significant CV protection from the treatment with RAAS-I (Asselbergs et al., 2004; Norris et al., 2006; Bolignano et al., 2016). The most part of these trials have also shown that the risk reduction after blood pressure lowering intervention is strictly dependent on the concomitant albuminuria reduction. An observational analysis of the Reduction in Endpoints in Non-insulin dependent diabetes mellitus with the Angiotensin II Antagonist Losartan (RENAAL) study, a double-blind, randomized clinical trial testing the effect of losartan vs. placebo on cardio-renal outcomes, showed that the change in albuminuria, 6 months after the basal visit, was the strongest determinant of the CV risk reduction (de Zeeuw et al., 2004). Later on, a meta-analysis of 32 RCTs provided a stronger evidence by showing a 13% to 29% risk reduction of CV endpoints for each 10% decrease in albuminuria levels, following different treatments (Savarese et al., 2014). Hence, the CV risk effect of novel antialbuminuric drugs has been tested (Bolignano et al., 2015; Leporini et al., 2016). For this aim, Sodium–glucose cotransporter 2 (SGLT-2) inhibitors are promising agents (Savarese et al., 2014; Wanner et al., 2016; Coppolino et al., 2018b; Garofalo et al., 2019). SGLT-2 inhibitors act by reducing the reabsorption of glucose in the renal proximal tubule (Garofalo et al., 2019). They determine both hemodynamic and non-hemodynamic changes in the kidney, the first being mainly represented by the reduction in intraglomerular pressure and eGFR through tubuloglomerular feedback, whereas the second by a consistent reduction in oxidant stress (up to 60%), a reduction in NLRP3 inflammasome activity and an increase in intrarenal angiotensinogen levels (De Nicola et al., 2014; Bakris, 2019). Large randomized clinical trials assessing the effect of SGLT-2 inhibitors on CV and renal endpoints have shown that they not only can reduce CV risk, but also the progression of renal function decline in patients with CKD and type 2 diabetes. The Canagliflozin and Renal Events in Diabetes with Established Nephropathy Clinical Evaluation (CREDENCE) trial aimed at evaluating the effects of the SGLT2 inhibitor canagliflozin primarily on kidney endpoints in patients with type 2 diabetes and albuminuric CKD. The results of this study have been recently published (Perkovic et al., 2019) and showed that the risk of the primary endpoints (i.e., ESKD, doubling of creatinine, or death from kidney or CV causes) was reduced by 30% with canagliflozin treatment compared to placebo (hazard ratio: 0.70; 95% confidence interval: 0.59–0.82; $p < 0.001$). Findings for the kidney-specific composite endpoint (i.e., ESKD, doubling of creatinine, or kidney-related death) were positive as well (hazard ratio: 0.66; 95% confidence interval: 0.53–0.81; $p < 0.001$). Canagliflozin treatment was also associated with a lower risk for several CV related endpoints, such as the onset of CV death, myocardial infarction, hospitalization for heart failure or stroke (Perkovic et al., 2019).

Interestingly, since these drugs modify pathways (mainly the intraglomerular hypertension) that are shared between diabetic and non-diabetic CKD patients, it has been started the attempt of

TABLE 2 | Intervention studies assessing CV risk reduction in CKD patients.

Study	Population	Sample size	Intervention	Outcome	Results
PROGRESS study (Perkovic et al., 2007)	Cerebrovascular disease and CKD	6.105	Perindopril vs. placebo	Total stroke (fatal or non-fatal) and major vascular events.	Perindopril-based treatment reduced the risk of major vascular events by 30% and stroke by 35% among subjects with CKD, and the absolute effects of treatment were 1.7-fold greater for those with CKD than for those without.
CV outcomes in the irbesartan diabetic nephropathy trial (Berl et al., 2003)	Type 2 diabetic nephropathy and hypertension	1.715	Irbesartan, amlodipine, or placebo.	Doubling of serum creatinine levels, ESRD, and death from any cause.	The composite cardiovascular event rate did not differ in patients with type 2 diabetes and overt nephropathy treated with irbesartan, amlodipine, or placebo in addition to conventional antihypertensive therapy.
ALLHAT study (Rahman et al., 2006)	CKD and hypertension	31.797	Chlorthalidone vs. amlodipine vs. lisinopril.	To compare rates of CHD and ESRD; to determine whether GFR independently predicts risk for CHD; and to report the efficacy of first-step treatment with a CCB or an ARB each compared with a diuretic in modifying CV disease.	Older high-risk patients with hypertension and reduced GFR are more likely to develop CHD than to develop ESRD. A low GFR independently predicts increased risk for CHD. Neither amlodipine nor lisinopril is superior to chlorthalidone in preventing CHD, stroke, or combined CV disease, and chlorthalidone is superior to both for preventing heart failure.
ADVANCE study (Heerspink et al., 2010)	CKD and type 2 diabetes	10.640	Perindopril and indapamide vs. placebo	Major adverse cardiac event or MACE	The treatment benefits of a routine administration of a fixed combination of perindopril–indapamide to patients with type 2 diabetes on cardiovascular and renal outcomes, and death, are consistent across all stages of CKD at baseline. Absolute risk reductions are larger in patients with CKD highlighting the importance of blood pressure-lowering in this population.
SHARP study (Baigent et al., 2011)	CKD	9.270	Simvastatin and ezetimibe vs. placebo	Major adverse cardiac event or MACE	Reduction of LDL cholesterol with simvastatin 20 mg plus ezetimibe 10 mg daily safely reduced the incidence of major atherosclerotic events in a wide range of patients with advanced chronic kidney disease.
EMPA-REG OUTCOME study (Wanner et al., 2016)	Type 2 diabetes at high risk for cardiovascular events	7.020	10 mg Empagliflozin vs. 25 mg of empagliflozin vs. placebo	Incident or worsening nephropathy (progression to macroalbuminuria, doubling of the serum creatinine level, initiation of renal-replacement therapy, or death from renal disease) and incident albuminuria.	In patients with type 2 diabetes at high CV risk, empagliflozin was associated with slower progression of kidney disease and lower rates of clinically relevant renal events than was placebo when added to standard care.
CREDENCE study (Perkovic et al., 2019)	type 2 diabetes and albuminuric CKD	4.401	Canagliflozin 100 mg/day vs. placebo	Composite of end-stage kidney disease (dialysis, transplantation, or a sustained estimated GFR of <15 ml/min/1.73 m2), a doubling of the serum creatinine level, or death from renal or cardiovascular causes.	Relative risk (RR) for the primary outcome was 30% lower in canagliflozin group vs. placebo. Renal specific outcome RR was lower by 34% in canagliflozin group vs. placebo. Canagliflozin also reduced risk for cardiovascular death, myocardial infarction, or stroke and hospitalization for heart failure.

(Continued)

TABLE 2 | Continued

Study	Population	Sample size	Intervention	Outcome	Results
HIJ-CREATE study (Shiga et al., 2010)	High-risk hypertensive patients with CHD and CKD	1.022	Candesartan vs. non-ARB treatment	Major adverse cardiac event or MACE	There was no difference in MACE between the two arms in patients without impaired renal function. However, there was a lower incidence of MACE in the candesartan-based treatment arm than in the non-ARBs treatment arm in patients with impaired renal function.
ALTITUDE study (Parving et al., 2012)	Type 2 diabetes and CKD, CVD, or both	8.561	Aliskiren vs. placebo in addition to an ACE inhibitor or an ARB	Major adverse cardiac event or MACE ESRD, death attributable to kidney failure, or the need for renal-replacement therapy with no dialysis or transplantation available or initiated; or doubling of the baseline serum creatinine level.	The addition of aliskiren to standard therapy with renin-angiotensin system blockade in patients with type 2 diabetes who are at high risk for cardiovascular and renal events is not supported by the study and may even be harmful.
HOPE study (Mann et al., 2001)	CKD and non-CKD patients	9.287	Ramipril vs. vitamin E vs. placebo and vitamin E vs. placebo	Major adverse cardiac event or MACE; effect of ramipril on reducing CV risk.	In patients who had preexisting vascular disease or diabetes combined with an additional cardiovascular risk factor, mild CKD significantly increased the risk for subsequent cardiovascular events. Ramipril reduced CV risk without increasing adverse effects.
EUROPA study (Brugts et al., 2007)	CKD and non-CKD patients with stable CHD	12.056	Perindopril vs. Placebo	Major adverse cardiac event or MACE (cardiovascular death, non-fatal myocardial infarction, unstable angina, heart failure, stroke and other cardiovascular events requiring hospitalization).	Treatment benefits of perindopril were apparent in both patient groups either with eGFR $\geq$75 or eGFR $<$75. Has not been observed significant interaction between renal function and treatment benefit. The treatment benefit of perindopril is consistent and not modified by mild to moderate renal insufficiency.
PEACE study (Solomon et al., 2006)	CKD and non-CKD patients with stable CHD	8.290	Trandolapril vs. placebo	Major adverse cardiac event or MACE	Trandolapril was associated with a reduction in total mortality in patients with reduced renal function but not in patients with preserved renal function.
Val-HeFT study (Anand et al., 2009)	CKD and non-CKD patients with HF	5.010	Valsartan vs. placebo	Death and first morbid event, defined as death, sudden death with resuscitation, hospitalization for HF, or administration of intravenous inotropic or vasodilator drugs for 4 h or more.	Valsartan reduced the eGFR by the same amount in patients with and without CKD and reduced the risk of the first morbid event in patients with CKD, which suggests its beneficial effects in patients with HF and CKD.
AASK study (Norris et al., 2006)	African Americans with hypertensive nephrosclerosis.	1.094	Metoprolol vs. ramipril vs. Amlodipine	Major adverse cardiac event or MACE	Neither randomized class of antihypertensive therapy nor BP level had a significant effect on the occurrence of CV events. In multivariable analyses, seven baseline risk factors remained independently associated with increased risk for the CV events: BP level, duration of hypertension, abnormal ECG result, non-HDL cholesterol level, BUN, urine protein-creatinine ratio, urine sodium-potassium ratio, and low annual income.
PREVEND IT study (Asselbergs et al., 2004)	Microalbuminuric subjects	864	Fosinopril vs. placebo	Major adverse cardiac event or MACE	In microalbuminuric subjects, treatment with fosinopril had a significant effect on urinary albumin excretion. In addition, fosinopril treatment was associated with a trend in reducing cardiovascular events.
MASTERPLAN (Peeters et al., 2014)	multifactorial approach with the aid of nurse-practitioners reduces cardiovascular risk in patients with CKD	788	Nurse practitioner support added to physician care vs. physician care alone	Death, ESRD, and 50% increase in serum creatinine	The intervention reduced the incidence of the composite renal endpoint by 20% additional supporting that nurse practitioners may attenuate the decline of kidney function and improved renal outcome in patients with CKD

MACE defined as: cardiovascular death, non-fatal myocardial infarction, unstable angina, heart failure, stroke, and other cardiovascular events requiring hospitalization; CV, cardiovascular; CKD, chronic kidney disease; HF, heart failure; ESRD, end stage renal disease; CHD, coronary heart disease; CCB, calcium-channel blocker; ARB, angiotensin receptor blockers.

evaluating their benefits even in CKD patients without diabetes. Two large RCTs are actually ongoing and their results are eagerly expected. The Dapa-CKD clinical trial (ClinicalTrials.gov Identifier: NCT03036150) is testing the effects of the SGLT-2 inhibitor dapagliflozin on kidney endpoints and CV mortality in patients with CKD with and without type 2 diabetes vs. placebo, whereas the EMPA-KIDNEY trial is exploring empagliflozin vs. placebo in patients with CKD in order to answer the question whether SGLT-2 inhibitors are effective in a wide range of patients with CKD, such as patients with albuminuria or with reduced eGFR regardless of albuminuria levels (Herrington et al., 2018).

One of the reasons why the current available treatments for CKD patients can reduce, but not completely delete, the CV risk is due to the wide variability in response to treatments. It has been demonstrated from a pooled analysis of clinical trials that almost 30% of patients do not respond to antialbuminuric or blood pressure lowering drugs (Minutolo et al., 2000; Petrykiv et al., 2017). Statins have demonstrated to reduce CV risk in CKD patients. In the SHARP clinical trial, patients with CKD, who underwent statin treatment, were significantly protected from CV events as compared to placebo group, regardless of the basal level of LDL cholesterol (Baigent et al., 2011). KDIGO guidelines have therefore recommended to start treatment based on the CV risk and eGFR level, rather than on the LDL-cholesterol target. Evidences providing protective LDL targets, in CKD patients, deserve a further research effort.

CONCLUSION

In conclusion, knowledge on the association between CKD and CV risk has improved in the last years: (1) CKD is an independent risk factor of CV outcomes; the "public health" dimension of this concept is enormous because prevalence of CKD has dramatically increased (Provenzano et al., 2019); (2) identifying high risk patients is a priority; further observational studies are needed to gain more insights on the role of the main risk factors, specifically assessed in CKD; (3) common CV risk calculators are not useful in CKD patients; since CKD patients manifest different CV risk according to the presence of comorbidities, computing risk calculators specific to CKD is required. This may help in risk stratification and clinical decision making; (4) new clinical trials, aimed to reduce the CV risk excess in CKD patients are ongoing. In this regard, efforts are required to reduce variability in response to the available nephro- and cardio-protective treatments.

AUTHOR CONTRIBUTIONS

DB, GC, LD, RS, and CG contributed to the research idea. MP and GC wrote the manuscript. MA and DB critically revised the content of the manuscript.

REFERENCES

Anand, I. S., Bishu, K., Rector, T. S., Ishani, A., Kuskowski, M. A., and Cohn, J. N. (2009). Proteinuria, chronic kidney disease, and the effect of an angiotensin receptor blocker in addition to an angiotensin-converting enzyme inhibitor in patients with moderate to severe heart failure. *Circulation* 120, 1577–1584. doi: 10.1161/CIRCULATIONAHA.109.853648

Andreucci, M., Russo, D., Fuiano, G., Minutolo, R., and Andreucci, V. E. (1999). Diuretics in renal failure. *Miner Electrolyte Metab.* 25, 32–38. doi: 10.1159/000057416

Asselbergs, F. W., Diercks, G. F., Hillege, H. L., van Boven, A. J., Janssen, W. M., Voors, A. A., et al. (2004). Effects of fosinopril and pravastatin on cardiovascular events in subjects with microalbuminuria. *Circulation* 110, 2809–2816. doi: 10.1161/01.CIR.0000146378.65439.7A

Astor, B. C., Matsushita, K., Gansevoort, R. T., van der Velde, M., Woodward, M., Levey, A. S., et al. (2011). Lower estimated glomerular filtration rate and higher albuminuria are associated with mortality and end-stage renal disease. a collaborative meta-analysis of kidney disease population cohorts. *Kidney Int.* 79, 1331–1340. doi: 10.1038/ki.2010.550

Baigent, C., Landray, M. J., Reith, C., Emberson, J., Wheeler, D. C., Tomson, C., et al. (2011). The effects of lowering LDL cholesterol with simvastatin plus ezetimibe in patients with chronic kidney disease (study of heart and renal protection): a randomised placebo-controlled trial. *Lancet* 377, 2181–2192. doi: 10.1016/S0140-6736(11)60739-60733

Bakris, G. L. (2019). Major advancements in slowing diabetic kidney disease progression: focus on SGLT2 inhibitors. *Am. J. Kidney Dis.* 74, 573–575. doi: 10.1053/j.ajkd.2019.05.009

Barquera, S., Pedroza-Tobias, A., Medina, C., Hernandez-Barrera, L., Bibbins-Domingo, K., Lozano, R., et al. (2015). Global overview of the epidemiology of atherosclerotic cardiovascular disease. *Arch. Med. Res.* 46, 328–338. doi: 10.1016/j.arcmed.2015.06.006

Berl, T., Hunsicker, L. G., Lewis, J. B., Pfeffer, M. A., Porush, J. G., Rouleau, J. L., et al. (2003). Cardiovascular outcomes in the irbesartan diabetic nephropathy trial of patients with type 2 diabetes and overt nephropathy. *Ann. Intern. Med.* 138, 542–549. doi: 10.7326/0003-4819-138-7-200304010-200304010

Bolignano, D., Coppolino, G., Aloisi, C., Romeo, A., Nicocia, G., and Buemi, M. (2008). Effect of a single intravenous immunoglobulin infusion on neutrophil gelatinase-associated lipocalin levels in proteinuric patients with normal renal function. *J. Investig. Med.* 56, 997–1003. doi: 10.2310/JIM.0b013e31818e7e95

Bolignano, D., Coppolino, G., Romeo, A., Lacquaniti, A., and Buemi, M. (2010). Neutrophil gelatinase-associated lipocalin levels in chronic haemodialysis patients. *Nephrology* 15, 23–26. doi: 10.1111/j.1440-1797.2009.01163.x

Bolignano, D., D'Arrigo, G., Pisano, A., and Coppolino, G. (2015). Pentoxifylline for anemia in chronic kidney disease: a systematic review and meta-analysis. *PLoS One* 10:e0134104. doi: 10.1371/journal.pone.0134104

Bolignano, D., Pisano, A., and Coppolino, G. (2016). The dark side of blocking RAS in diabetic patients with incipient or manifested nephropathy. *Exp. Clin. Endocrinol. Diabetes* 124, 350–360. doi: 10.1055/s-0035-1550017

Brantsma, A. H., Bakker, S. J., de Zeeuw, D., de Jong, P. E., Gansevoort, R. T., and Group, P. S. (2008). Extended prognostic value of urinary albumin excretion for cardiovascular events. *J. Am. Soc. Nephrol.* 19, 1785–1791. doi: 10.1681/ASN.2007101065

Brugts, J. J., Boersma, E., Chonchol, M., Deckers, J. W., Bertrand, M., Remme, W. J., et al. (2007). The cardioprotective effects of the angiotensin-converting enzyme inhibitor perindopril in patients with stable coronary artery disease are not modified by mild to moderate renal insufficiency: insights from the EUROPA trial. *J. Am. Coll. Cardiol.* 50, 2148–2155. doi: 10.1016/j.jacc.2007.08.029

Cedillo-Couvert, E., and Ricardo, A. C. (2016). Smoking, vascular events, and ESRD in patients with CKD. *Am. J. Kidney Dis.* 68, 338–340. doi: 10.1053/j.ajkd.2016.06.004

Centers for Disease Control and Prevention, (1999). Decline in deaths from heart disease and stroke–United States, 1900-1999. *MMWR Morb. Mortal. Wkly. Rep.* 48, 649–656.

Chronic Kidney Disease Prognosis Consortium Matsushita, K., van der Velde, M., Astor, B. C., Woodward, M., Levey, A. S., et al. (2010). Association of estimated glomerular filtration rate and albuminuria with all-cause and cardiovascular mortality in general population cohorts: a collaborative meta-analysis. *Lancet* 375, 2073–2081. doi: 10.1016/S0140-6736(10)60674-60675

Coppolino, G., Buemi, A., Bolignano, D., Lacquaniti, A., La Spada, M., Stilo, F., et al. (2009). Perioperative iloprost and endothelial progenitor cells in uremic

patients with severe limb ischemia undergoing peripheral revascularization. *J. Surg. Res.* 157, e129–e135. doi: 10.1016/j.jss.2008.07.017

Coppolino, G., Leonardi, G., Andreucci, M., and Bolignano, D. (2018a). Oxidative stress and kidney function: a brief update. *Curr. Pharm. Des.* 24, 4794–4799. doi: 10.2174/1381612825666190112165206

Coppolino, G., Leporini, C., Rivoli, L., Ursini, F., di Paola, E. D., Cernaro, V., et al. (2018b). Exploring the effects of DPP-4 inhibitors on the kidney from the bench to clinical trials. *Pharmacol. Res.* 129, 274–294. doi: 10.1016/j.phrs.2017.12.001

Coppolino, G., Lucisano, G., Bolignano, D., and Buemi, M. (2010). Acute cardiovascular complications of hemodialysis. *Minerva Urol. Nefrol.* 62, 67–80.

Coppolino, G., Pisano, A., Rivoli, L., and Bolignano, D. (2017). Renal denervation for resistant hypertension. *Cochrane Database. Syst. Rev.* 2:CD011499. doi: 10.1002/14651858.CD011499.pub2

Crews, D. C., Boulware, L. E., Gansevoort, R. T., and Jaar, B. G. (2011). Albuminuria: is it time to screen the general population? *Adv. Chronic Kidney Dis.* 18, 249–257. doi: 10.1053/j.ackd.2011.06.004

De Nicola, L., Gabbai, F. B., Liberti, M. E., Sagliocca, A., Conte, G., and Minutolo, R. (2014). Sodium/glucose cotransporter 2 inhibitors and prevention of diabetic nephropathy: targeting the renal tubule in diabetes. *Am. J. Kidney Dis.* 64, 16–24. doi: 10.1053/j.ajkd.2014.02.010

De Nicola, L., Minutolo, R., Chiodini, P., Borrelli, S., Zoccali, C., Postorino, M., et al. (2012). The effect of increasing age on the prognosis of non-dialysis patients with chronic kidney disease receiving stable nephrology care. *Kidney Int.* 82, 482–488. doi: 10.1038/ki.2012.174

De Nicola, L., Minutolo, R., Chiodini, P., Zoccali, C., Castellino, P., Donadio, C., et al. (2006). Global approach to cardiovascular risk in chronic kidney disease: reality and opportunities for intervention. *Kidney Int.* 69, 538–545. doi: 10.1038/sj.ki.5000085

De Nicola, L., Provenzano, M., Chiodini, P., Borrelli, S., Garofalo, C., Pacilio, M., et al. (2015a). Independent role of Underlying Kidney disease on renal prognosis of patients with chronic kidney disease under nephrology care. *PLoS One* 10:e0127071. doi: 10.1371/journal.pone.0127071

De Nicola, L., Provenzano, M., Chiodini, P., D'Arrigo, G., Tripepi, G., Del Vecchio, L., et al. (2015b). Prognostic role of LDL cholesterol in non-dialysis chronic kidney disease: multicenter prospective study in Italy. *Nutr. Metab. Cardiovasc. Dis.* 25, 756–762. doi: 10.1016/j.numecd.2015.04.001

De Nicola, L., Provenzano, M., Chiodini, P., Borrelli, S., Russo, L., Bellasi, A., et al. (2017). Epidemiology of low-proteinuric chronic kidney disease in renal clinics. *PLoS One* 12:e0172241. doi: 10.1371/journal.pone.0172241

de Zeeuw, D., Remuzzi, G., Parving, H. H., Keane, W. F., Zhang, Z., Shahinfar, S., et al. (2004). Albuminuria, a therapeutic target for cardiovascular protection in type 2 diabetic patients with nephropathy. *Circulation* 110, 921–927. doi: 10.1161/01.CIR.0000139860.33974.28

Deckert, T., Feldt-Rasmussen, B., Borch-Johnsen, K., Jensen, T., and Kofoed-Enevoldsen, A. (1989). Albuminuria reflects widespread vascular damage. *Steno Hypothesis. Diabetol.* 32, 219–226. doi: 10.1007/bf00285287

Dieplinger, B., Mueller, T., Kollerits, B., Struck, J., Ritz, E., von Eckardstein, A., et al. (2009). Pro-A-type natriuretic peptide and pro-adrenomedullin predict progression of chronic kidney disease: the MMKD study. *Kidney Int.* 75, 408–414. doi: 10.1038/ki.2008.560

Foley, R. N., Murray, A. M., Li, S., Herzog, C. A., McBean, A. M., Eggers, P. W., et al. (2005). Chronic kidney disease and the risk for cardiovascular disease, renal replacement, and death in the United States Medicare population, 1998 to 1999. *J. Am. Soc. Nephrol.* 16, 489–495. doi: 10.1681/ASN.2004030203

Ford, E. S., Ajani, U. A., Croft, J. B., Critchley, J. A., Labarthe, D. R., Kottke, T. E., et al. (2007). Explaining the decrease in U.S. deaths from coronary disease, 1980-2000. *N. Engl. J. Med.* 356, 2388–2398. doi: 10.1056/NEJMsa053935

Fox, C. S., Matsushita, K., Woodward, M., Bilo, H. J., Chalmers, J., Heerspink, H. J., et al. (2012). Associations of kidney disease measures with mortality and end-stage renal disease in individuals with and without diabetes: a meta-analysis. *Lancet* 380, 1662–1673. doi: 10.1016/S0140-6736(12)61350-61356

Garofalo, C., Borrelli, S., Liberti, M. E., Andreucci, M., Conte, G., Minutolo, R., et al. (2019). SGLT2 inhibitors: nephroprotective efficacy and side effects. *Medicina* 55:E268. doi: 10.3390/medicina55060268

Garofalo, C., Borrelli, S., Minutolo, R., Chiodini, P., De Nicola, L., and Conte, G. (2017). A systematic review and meta-analysis suggests obesity predicts onset of chronic kidney disease in the general population. *Kidney Int.* 91, 1224–1235. doi: 10.1016/j.kint.2016.12.013

Garofalo, C., Borrelli, S., Pacilio, M., Minutolo, R., Chiodini, P., De Nicola, L., et al. (2016). Hypertension and prehypertension and prediction of development of decreased estimated GFR in the general population: a meta-analysis of cohort studies. *Am. J. Kidney Dis.* 67, 89–97. doi: 10.1053/j.ajkd.2015.08.027

Gavin, J. B., Maxwell, L., and Edgar, S. G. (1998). Microvascular involvement in cardiac pathology. *J. Mol. Cell Cardiol.* 30, 2531–2540. doi: 10.1006/jmcc.1998.0824

Go, A. S., Chertow, G. M., Fan, D., McCulloch, C. E., and Hsu, C. Y. (2004). Chronic kidney disease and the risks of death, cardiovascular events, and hospitalization. *N. Engl. J. Med.* 351, 1296–1305. doi: 10.1056/NEJMoa041031

Halimi, J. M., Giraudeau, B., Vol, S., Caces, E., Nivet, H., Lebranchu, Y., et al. (2000). Effects of current smoking and smoking discontinuation on renal function and proteinuria in the general population. *Kidney Int.* 58, 1285–1292. doi: 10.1046/j.1523-1755.2000.00284.x

Hallan, S., Astor, B., Romundstad, S., Aasarod, K., Kvenild, K., and Coresh, J. (2007). Association of kidney function and albuminuria with cardiovascular mortality in older vs younger individuals: the HUNT II study. *Arch. Intern. Med.* 167, 2490–2496. doi: 10.1001/archinte.167.22.2490

Heerspink, H. J., Ninomiya, T., Perkovic, V., Woodward, M., Zoungas, S., Cass, A., et al. (2010). Effects of a fixed combination of perindopril and indapamide in patients with type 2 diabetes and chronic kidney disease. *Eur. Heart J.* 31, 2888–2896. doi: 10.1093/eurheartj/ehq139

Herrington, W. G., Preiss, D., Haynes, R., von Eynatten, M., Staplin, N., Hauske, S. J., et al. (2018). The potential for improving cardio-renal outcomes by sodium-glucose co-transporter-2 inhibition in people with chronic kidney disease: a rationale for the EMPA-KIDNEY study. *Clin. Kidney J.* 11, 749–761. doi: 10.1093/ckj/sfy090

Jha, V., Garcia-Garcia, G., Iseki, K., Li, Z., Naicker, S., Plattner, B., et al. (2013). Chronic kidney disease: global dimension and perspectives. *Lancet* 382, 260–272. doi: 10.1016/S0140-6736(13)60687-X

Keith, D. S., Nichols, G. A., Gullion, C. M., Brown, J. B., and Smith, D. H. (2004). Longitudinal follow-up and outcomes among a population with chronic kidney disease in a large managed care organization. *Arch. Intern. Med.* 164, 659–663. doi: 10.1001/archinte.164.6.659

Kidney Disease Improving Global Outcomes Work Group (2013). Chapter 4: other complications of CKD: CVD, medication dosage, patient safety, infections, hospitalizations, and caveats for investigating complications of CKD. *Kidney Int. Suppl.* 3, 91–111. doi: 10.1038/kisup.2012.67

Kottgen, A., Russell, S. D., Loehr, L. R., Crainiceanu, C. M., Rosamond, W. D., Chang, P. P., et al. (2007). Reduced kidney function as a risk factor for incident heart failure: the atherosclerosis risk in communities (ARIC) study. *J. Am. Soc. Nephrol.* 18, 1307–1315. doi: 10.1681/ASN.2006101159

Landray, M. J., Thambyrajah, J., McGlynn, F. J., Jones, H. J., Baigent, C., Kendall, M. J., et al. (2001). Epidemiological evaluation of known and suspected cardiovascular risk factors in chronic renal impairment. *Am. J. Kidney Dis.* 38, 537–546. doi: 10.1053/ajkd.2001.26850

Leporini, C., Pisano, A., Russo, E., D Arrigo, G., de Sarro, G., Coppolino, G., et al. (2016). Effect of pentoxifylline on renal outcomes in chronic kidney disease patients: a systematic review and meta-analysis. *Pharmacol. Res.* 107, 315–332. doi: 10.1016/j.phrs.2016.03.001

Levey, A. S., and Coresh, J. (2012). Chronic kidney disease. *Lancet* 379, 165–180. doi: 10.1016/S0140-6736(11)60178-60175

Levin, A., Djurdjev, O., Beaulieu, M., and Er, L. (2008). Variability and risk factors for kidney disease progression and death following attainment of stage 4 CKD in a referred cohort. *Am. J. Kidney Dis.* 52, 661–671. doi: 10.1053/j.ajkd.2008.06.023

Liang, S., Zhang, X. G., Cai, G. Y., Zhu, H. Y., Zhou, J. H., Wu, J., et al. (2013). Identifying parameters to distinguish non-diabetic renal diseases from diabetic nephropathy in patients with type 2 diabetes mellitus: a meta-analysis. *PLoS One* 8:e64184. doi: 10.1371/journal.pone.0064184

Lozano, R., Naghavi, M., Foreman, K., Lim, S., Shibuya, K., Aboyans, V., et al. (2012). Global and regional mortality from 235 causes of death for 20 age groups in 1990 and 2010: a systematic analysis for the Global Burden of disease study 2010. *Lancet* 380, 2095–2128. doi: 10.1016/S0140-6736(12)61728-61720

Mahmoodi, B. K., Matsushita, K., Woodward, M., Blankestijn, P. J., Cirillo, M., Ohkubo, T., et al. (2012). Associations of kidney disease measures with mortality and end-stage renal disease in individuals with and without

hypertension: a meta-analysis. *Lancet* 380, 1649–1661. doi: 10.1016/S0140-6736(12)61272-61270

Mann, J. F., Gerstein, H. C., Pogue, J., Bosch, J., and Yusuf, S. (2001). Renal insufficiency as a predictor of cardiovascular outcomes and the impact of ramipril: the HOPE randomized trial. *Ann. Intern. Med.* 134, 629–636. doi: 10.7326/0003-4819-134-8-200104170-200104177

Matsushita, K., Coresh, J., Sang, Y., Chalmers, J., Fox, C., Guallar, E., et al. (2015). Estimated glomerular filtration rate and albuminuria for prediction of cardiovascular outcomes: a collaborative meta-analysis of individual participant data. *Lancet Diabetes Endocrinol.* 3, 514–525. doi: 10.1016/S2213-8587(15)00040-46

Mensah, G. A., Wei, G. S., Sorlie, P. D., Fine, L. J., Rosenberg, Y., Kaufmann, P. G., et al. (2017). Decline in cardiovascular mortality: possible causes and implications. *Circ. Res.* 120, 366–380. doi: 10.1161/CIRCRESAHA.116.309115

Minutolo, R., Agarwal, R., Borrelli, S., Chiodini, P., Bellizzi, V., Nappi, F., et al. (2011). Prognostic role of ambulatory blood pressure measurement in patients with nondialysis chronic kidney disease. *Arch. Intern. Med.* 171, 1090–1098. doi: 10.1001/archinternmed.2011.230

Minutolo, R., Andreucci, M., Balletta, M. M., and Russo, D. (2000). Effect of posture on sodium excretion and diuretic efficacy in nephrotic patients. *Am. J. Kidney Dis.* 36, 719–727. doi: 10.1053/ajkd.2000.17616

Minutolo, R., De Nicola, L., Mazzaglia, G., Postorino, M., Cricelli, C., Mantovani, L. G., et al. (2008). Detection and awareness of moderate to advanced CKD by primary care practitioners: a cross-sectional study from Italy. *Am. J. Kidney Dis.* 52, 444–453. doi: 10.1053/j.ajkd.2008.03.002

Minutolo, R., Gabbai, F. B., Provenzano, M., Chiodini, P., Borrelli, S., Garofalo, C., et al. (2018). Cardiorenal prognosis by residual proteinuria level in diabetic chronic kidney disease: pooled analysis of four cohort studies. *Nephrol. Dial. Transplant.* 33, 1942–1949. doi: 10.1093/ndt/gfy032

Minutolo, R., Locatelli, F., Gallieni, M., Bonofiglio, R., Fuiano, G., Oldrizzi, L., et al. (2013). Anaemia management in non-dialysis chronic kidney disease (CKD) patients: a multicentre prospective study in renal clinics. *Nephrol. Dial. Transplant.* 28, 3035–3045. doi: 10.1093/ndt/gft338

Minutolo, R., Sasso, F. C., Chiodini, P., Cianciaruso, B., Carbonara, O., Zamboli, P., et al. (2006). Management of cardiovascular risk factors in advanced type 2 diabetic nephropathy: a comparative analysis in nephrology, diabetology and primary care settings. *J. Hypertens.* 24, 1655–1661. doi: 10.1097/01.hjh.0000239303.93872.31

Moranne, O., Froissart, M., Rossert, J., Gauci, C., Boffa, J. J., Haymann, J. P., et al. (2009). Timing of onset of CKD-related metabolic complications. *J. Am. Soc. Nephrol.* 20, 164–171. doi: 10.1681/ASN.2008020159

Mortality, G. B. D., and Causes of Death Collaborators, (2015). Global, regional, and national age-sex specific all-cause and cause-specific mortality for 240 causes of death, 1990-2013: a systematic analysis for the Global Burden of disease study 2013. *Lancet* 385, 117–171. doi: 10.1016/S0140-6736(14)61682-61682

Murray, C. J., and Lopez, A. D. (2013). Measuring the global burden of disease. *N. Engl. J. Med.* 369, 448–457. doi: 10.1056/NEJMra1201534

Nagler, E. V., Webster, A. C., Bolignano, D., Haller, M. C., Nistor, I., van der Veer, S. N., et al. (2014). European renal best practice (ERBP) guideline development methodology: towards the best possible guidelines. *Nephrol. Dial. Transplant.* 29, 731–738. doi: 10.1093/ndt/gft407

Nakano, T., Ninomiya, T., Sumiyoshi, S., Fujii, H., Doi, Y., Hirakata, H., et al. (2010). Association of kidney function with coronary atherosclerosis and calcification in autopsy samples from Japanese elders: the Hisayama study. *Am. J. Kidney Dis.* 55, 21–30. doi: 10.1053/j.ajkd.2009.06.034

NCD Risk Factor Collaboration [NCD-RisC], (2016). Worldwide trends in diabetes since 1980: a pooled analysis of 751 population-based studies with 4.4 million participants. *Lancet* 387, 1513–1530.

NCD Risk Factor Collaboration [NCD-RisC], (2017). Worldwide trends in blood pressure from 1975 to 2015: a pooled analysis of 1479 population-based measurement studies with 19.1 million participants. *Lancet* 389, 37–55.

Ninomiya, T., Perkovic, V., de Galan, B. E., Zoungas, S., Pillai, A., Jardine, M., et al. (2009). Albuminuria and kidney function independently predict cardiovascular and renal outcomes in diabetes. *J. Am. Soc. Nephrol.* 20, 1813–1821. doi: 10.1681/ASN.2008121270

Norris, K., Bourgoigne, J., Gassman, J., Hebert, L., Middleton, J., Phillips, R. A., et al. (2006). Cardiovascular outcomes in the African American study of kidney disease and hypertension (AASK) trial. *Am. J. Kidney Dis.* 48, 739–751. doi: 10.1053/j.ajkd.2006.08.004

Ohtake, T., Kobayashi, S., Moriya, H., Negishi, K., Okamoto, K., Maesato, K., et al. (2005). High prevalence of occult coronary artery stenosis in patients with chronic kidney disease at the initiation of renal replacement therapy: an angiographic examination. *J. Am. Soc. Nephrol.* 16, 1141–1148. doi: 10.1681/ASN.2004090765

Orth, S. R., and Hallan, S. I. (2008). Smoking: a risk factor for progression of chronic kidney disease and for cardiovascular morbidity and mortality in renal patients–absence of evidence or evidence of absence? *Clin. J. Am. Soc. Nephrol.* 3, 226–236. doi: 10.2215/CJN.03740907

Parving, H. H., Brenner, B. M., McMurray, J. J., de Zeeuw, D., Haffner, S. M., Solomon, S. D., et al. (2012). Cardiorenal end points in a trial of aliskiren for type 2 diabetes. *N. Engl. J. Med.* 367, 2204–2213. doi: 10.1056/NEJMoa1208799

Patel, U. D., Young, E. W., Ojo, A. O., and Hayward, R. A. (2005). CKD progression and mortality among older patients with diabetes. *Am. J. Kidney Dis.* 46, 406–414. doi: 10.1053/j.ajkd.2005.05.027

Peeters, M. J., van Zuilen, A. D., van den Brand, J. A., Bots, M. L., van Buren, M., Ten Dam, M. A., et al. (2014). Nurse practitioner care improves renal outcome in patients with CKD. *J. Am. Soc. Nephrol.* 25, 390–398. doi: 10.1681/ASN.2012121222

Perico, N., Plata, R., Anabaya, A., Codreanu, I., Schieppati, A., Ruggenenti, P., et al. (2005). Strategies for national health care systems in emerging countries: the case of screening and prevention of renal disease progression in Bolivia. *Kidney Int. Suppl.* 97, S87–S94. doi: 10.1111/j.1523-1755.2005.09715.x

Perkovic, V., Jardine, M. J., Neal, B., Bompoint, S., Heerspink, H. J. L., Charytan, D. M., et al. (2019). Canagliflozin and renal outcomes in type 2 diabetes and nephropathy. *N. Engl. J. Med.* 380, 2295–2306. doi: 10.1056/NEJMoa1811744

Perkovic, V., Ninomiya, T., Arima, H., Gallagher, M., Jardine, M., Cass, A., et al. (2007). Chronic kidney disease, cardiovascular events, and the effects of perindopril-based blood pressure lowering: data from the PROGRESS study. *J. Am. Soc. Nephrol.* 18, 2766–2772. doi: 10.1681/ASN.2007020256

Perticone, F., Perticone, M., Maio, R., Sciacqua, A., Andreucci, M., Tripepi, G., et al. (2015). Serum alkaline phosphatase negatively affects endothelium-dependent vasodilation in naive hypertensive patients. *Hypertension* 66, 874–880. doi: 10.1161/HYPERTENSIONAHA.115.06117

Perticone, M., Maio, R., Sciacqua, A., Cimellaro, A., Andreucci, M., Tripepi, G., et al. (2016). Serum phosphorus levels are associated with endothelial dysfunction in hypertensive patients. *Nutr. Metab. Cardiovasc. Dis.* 26, 683–688. doi: 10.1016/j.numecd.2016.02.003

Petrykiv, S. I., de Zeeuw, D., Persson, F., Rossing, P., Gansevoort, R. T., Laverman, G. D., et al. (2017). Variability in response to albuminuria-lowering drugs: true or random? *Br. J. Clin. Pharmacol.* 83, 1197–1204. doi: 10.1111/bcp.13217

Piccoli, G. B., Breuer, C., Cabiddu, G., Testa, A., Jadeau, C., and Brunori, G. (2018). Where are you going, nephrology? considerations on models of care in an evolving discipline. *J. Clin. Med.* 7:E199. doi: 10.3390/jcm7080199

Ponikowski, P., Voors, A. A., Anker, S. D., Bueno, H., Cleland, J. G. F., Coats, A. J. S., et al. (2016). 2016 ESC guidelines for the diagnosis and treatment of acute and chronic heart failure: the task force for the diagnosis and treatment of acute and chronic heart failure of the European Society of Cardiology (ESC)developed with the special contribution of the Heart Failure Association (HFA) of the ESC. *Eur. Heart J.* 37, 2129–2200. doi: 10.1093/eurheartj/ehw128

Provenzano, M., Chiodini, P., Minutolo, R., Zoccali, C., Bellizzi, V., Conte, G., et al. (2018). Reclassification of chronic kidney disease patients for end-stage renal disease risk by proteinuria indexed to estimated glomerular filtration rate: multicentre prospective study in nephrology clinics. *Nephrol. Dial Transpl.* doi: 10.1093/ndt/gfy217 [Epub ahead of print].

Provenzano, M., Mancuso, C., Garofalo, C., De Nicola, L., and Andreucci, M. (2019). [Temporal variation of chronic kidney Disease's epidemiology]. *G. Ital. Nefrol.* 36:2019-vol2.

Rahman, M., Pressel, S., Davis, B. R., Nwachuku, C., Wright, JT Jr, Whelton, P. K., et al. (2006). Cardiovascular outcomes in high-risk hypertensive patients stratified by baseline glomerular filtration rate. *Ann. Intern. Med.* 144, 172–180. doi: 10.7326/0003-4819-144-3-200602070-200602075

Ruggenenti, P., and Remuzzi, G. (2006). Time to abandon microalbuminuria? *Kidney Int.* 70, 1214–1222. doi: 10.1038/sj.ki.5001729

Russo, D., Andreucci, M., De Blasio, A., Frattolillo, P., and Andreucci, V. E. (2005). Treatment of hypertension in Italian nephrology out-patient clinics: the THIN Study. *Semin. Nephrol.* 25, 431–434. doi: 10.1016/j.semnephrol.2005.05.015

Russo, D., Morrone, L. F., Errichiello, C., De Gregorio, M. G., Imbriaco, M., Battaglia, Y., et al. (2014). Impact of BMI on cardiovascular events, renal function, and coronary artery calcification. *Blood Purif.* 38, 1–6. doi: 10.1159/000362862

Savarese, G., Dei Cas, A., Rosano, G., D'Amore, C., Musella, F., Mosca, S., et al. (2014). Reduction of albumin urinary excretion is associated with reduced cardiovascular events in hypertensive and/or diabetic patients. a meta-regression analysis of 32 randomized trials. *Int. J. Cardiol.* 172, 403–410. doi: 10.1016/j.ijcard.2014.01.065

Serra, R., Ielapi, N., Barbetta, A., Andreucci, M., and de Franciscis, S. (2018). Novel biomarkers for cardiovascular risk. *Biomark. Med.* 12, 1015–1024. doi: 10.2217/bmm-2018-2056

Shiga, T., Kasanuki, H., Hagiwara, N., Sumiyoshi, T., Honda, T., Haze, K., et al. (2010). Angiotensin receptor blocker-based therapy and cardiovascular events in hypertensive patients with coronary artery disease and impaired renal function. *Blood Press.* 19, 359–365. doi: 10.3109/08037051003802475

Simeoni, M., Nicotera, R., Colao, M., Citraro, M. L., Pelagi, E., Cerantonio, A., et al. (2016). Direct inhibition of plasmatic renin activity with aliskiren: a promising but under-investigated therapeutic option for non-diabetic glomerulonephritis. *Int. Urol. Nephrol.* 48, 229–237. doi: 10.1007/s11255-015-1128-1124

Solomon, S. D., Rice, M. M., Solomon, K., Jose, P., Domanski, M., Sabatine, M., et al. (2006). Renal function and effectiveness of angiotensin-converting enzyme inhibitor therapy in patients with chronic stable coronary disease in the prevention of events with ACE inhibition (PEACE) trial. *Circulation* 114, 26–31. doi: 10.1161/CIRCULATIONAHA.105.592733

Stehouwer, C. D., Nauta, J. J., Zeldenrust, G. C., Hackeng, W. H., Donker, A. J., and den Ottolander, G. J. (1992). Urinary albumin excretion, cardiovascular disease, and endothelial dysfunction in non-insulin-dependent diabetes mellitus. *Lancet* 340, 319–323. doi: 10.1016/0140-6736(92)91401-s

Theilade, S., Lajer, M., Jorsal, A., Tarnow, L., Parving, H. H., and Rossing, P. (2012). Arterial stiffness and endothelial dysfunction independently and synergistically predict cardiovascular and renal outcome in patients with type 1 diabetes. *Diabet. Med.* 29, 990–994. doi: 10.1111/j.1464-5491.2012.03633.x

Thomas, B., Matsushita, K., Abate, K. H., Al-Aly, Z., Arnlov, J., Asayama, K., et al. (2017). Global cardiovascular and renal outcomes of reduced GFR. *J. Am. Soc. Nephrol.* 28, 2167–2179. doi: 10.1681/ASN.2016050562

Tonelli, M., Muntner, P., Lloyd, A., Manns, B. J., Klarenbach, S., Pannu, N., et al. (2012). Risk of coronary events in people with chronic kidney disease compared with those with diabetes: a population-level cohort study. *Lancet* 380, 807–814. doi: 10.1016/S0140-6736(12)60572-60578

van Zuilen, A. D., van der Tweel, I., Blankestijn, P. J., Bots, M. L., van Buren, M., ten Dam, M. A., et al. (2006). multifactorial approach and superior treatment efficacy in renal patients with the aid of nurse practitioners. design of the masterplan study [isrctn73187232]. *Trials* 7:8. doi: 10.1186/1745-6215-7-8

Vos, T., Carter, R., Barendregt, J., Mihalopoulos, C., Veerman, J. L., and Magnus, A. (2010). *Assessing Cost-Effectiveness in Prevention (ACE- Prevention): Final Report*. Melbourne: Brisbane and Deakin University.

Wanner, C., Inzucchi, S. E., Lachin, J. M., Fitchett, D., von Eynatten, M., Mattheus, M., et al. (2016). Empagliflozin and progression of Kidney Disease in Type 2 diabetes. *N. Engl. J. Med.* 375, 323–334. doi: 10.1056/NEJMoa1515920

Weiner, D. E., Tighiouart, H., Elsayed, E. F., Griffith, J. L., Salem, D. N., Levey, A. S., et al. (2007). The framingham predictive instrument in chronic kidney disease. *J. Am. Coll. Cardiol.* 50, 217–224. doi: 10.1016/j.jacc.2007.03.037

Xia, J., Wang, L., Ma, Z., Zhong, L., Wang, Y., Gao, Y., et al. (2017). Cigarette smoking and chronic kidney disease in the general population: a systematic review and meta-analysis of prospective cohort studies. *Nephrol. Dial. Transplant.* 32, 475–487. doi: 10.1093/ndt/gfw452

Xie, Y., Bowe, B., Mokdad, A. H., Xian, H., Yan, Y., Li, T., et al. (2018). Analysis of the global burden of disease study highlights the global, regional, and national trends of chronic kidney disease epidemiology from 1990 to 2016. *Kidney Int.* 94, 567–581. doi: 10.1016/j.kint.2018.04.011

Zoccali, C., Blankestijn, P. J., Bruchfeld, A., Capasso, G., Fliser, D., Fouque, D., et al. (2019). Children of a lesser god: exclusion of chronic kidney disease patients from clinical trials. *Nephrol. Dial. Transplant.* 34, 1112–1114. doi: 10.1093/ndt/gfz023

Conflict of Interest: The authors declare that the research was conducted in the absence of any commercial or financial relationships that could be construed as a potential conflict of interest.

The reviewer GR declared a past co-authorship with several of the authors MP, LD, and CG to the handling Editor.

Copyright © 2019 Provenzano, Coppolino, De Nicola, Serra, Garofalo, Andreucci and Bolignano. This is an open-access article distributed under the terms of the Creative Commons Attribution License (CC BY). The use, distribution or reproduction in other forums is permitted, provided the original author(s) and the copyright owner(s) are credited and that the original publication in this journal is cited, in accordance with accepted academic practice. No use, distribution or reproduction is permitted which does not comply with these terms.

frontiers in Cell and Developmental Biology

ORIGINAL RESEARCH
published: 19 March 2020
doi: 10.3389/fcell.2020.00172

Dynamic Phenotypes and Molecular Mechanisms to Understand the Pathogenesis of Diabetic Nephropathy in Two Widely Used Animal Models of Type 2 Diabetes Mellitus

Yanfei Liu[1,2,3†], Hui Huang[4†‡], Rui Gao[3] and Yue Liu[1‡]*

[1] Cardiovascular Diseases Center, Xiyuan Hospital of China Academy of Chinese Medical Sciences, Beijing, China, [2] Graduate School, Beijing University of Chinese Medicine, Beijing, China, [3] Institute of Clinical Pharmacology of Xiyuan Hospital, China Academy of Chinese Medical Sciences, Beijing, China, [4] Beijing Duan-Dian Pharmaceutical Research & Development Co., Ltd., Beijing, China

OPEN ACCESS

Edited by:
Evangelia Dounousi,
University Hospital of Ioannina,
Greece

Reviewed by:
Yannis Vasilios Simos,
University of Ioannina, Greece
Anil Duni,
University Hospital of Ioannina,
Greece
Yogesh A. Kulkarni,
SVKM's Narsee Monjee Institute of
Management Studies, India

***Correspondence:**
Yue Liu
liuyueheart@hotmail.com

† These authors have contributed equally to this work and share first authorship

‡ **ORCID:**
Yue Liu
orcid.org/0000-0002-0084-863X
Hui Huang
orcid.org/0000-0002-1992-3513

Specialty section:
This article was submitted to
Molecular Medicine,
a section of the journal
Frontiers in Cell and Developmental
Biology

Received: 23 September 2019
Accepted: 02 March 2020
Published: 19 March 2020

Citation:
Liu Y, Huang H, Gao R and Liu Y
(2020) Dynamic Phenotypes
and Molecular Mechanisms
to Understand the Pathogenesis
of Diabetic Nephropathy in Two
Widely Used Animal Models of Type 2
Diabetes Mellitus.
Front. Cell Dev. Biol. 8:172.
doi: 10.3389/fcell.2020.00172

Objective: We aimed to characterize the pathogenesis of diabetic nephropathy (DN) in two commonly used type 2 diabetes mellitus (T2DM) animal models and explore the preliminary molecular mechanisms underlying DN in two models.

Methods: To verify the effect of hyperglycemia on renal tissue, we observed the cell growth inhibition rate by adding different concentration of glucose to cell supernatant. After that, a chemically-induced T2DM model was established by administering streptozotocin (STZ) to Sprague Dawley (SD) rats in combination with high fat feeding. In addition, a spontaneous T2DM model was established by feeding 8 weeks old KK-Ay mice a high-fat diet during a period of over 20 weeks. Animal body weight, fasting blood glucose (FBG), insulin tolerance, lipid metabolism, renal function, and renal pathology were periodically measured (once every 2 or 4 weeks) over a duration of 20 weeks. At the 12th week, an Affymetrix gene chip assay was performed on the renal tissues extracted from the T2DM animal models and control animals. Through screening for the differentially expressed genes, some key genes were selected for PCR validation.

Results: High level of glucose could inhibit the growth of kidney cells. Besides, KK-Ay mice were found to have high FBG and abnormal insulin tolerance. Renal dysfunction and pathology were observed at the 4th week following the start of model creation, which increased in severity over the length of the experiment. The T2DM SD rats also showed high FBG, abnormal glucose tolerance and abnormal lipid metabolism, but the renal function and renal pathology changed only slightly within 20 weeks. Gene

profiling in animal kidneys and subsequent analyses and validation revealed differentially expressed genes and enriched pathways in DN.

Conclusion: KK-Ay mice with both high fasting glucose and insulin resistance were more likely to develop diabetic nephropathy than STZ-induced diabetic SD rats with low fasting glucose or only insulin resistance. The KK-Ay mice model showed earlier onset of the typical pathological characteristics associated with T2DM and obvious renal lesions suggestive of kidney damage.

Keywords: diabetic nephropathy, type 2 diabetes mellitus, pathogenesis, sprague dawley rat, KK-Ay mice

INTRODUCTION

Diabetes mellitus (DM) is a chronic disease caused by relative or absolute insufficiency of insulin secretion, a decrease in insulin sensitivity of target cells or structural defects in insulin itself, resulting in metabolic disorders (DeFronzo et al., 2015; Gheith et al., 2015). There are currently 400 million people with diabetes worldwide and the number of DM patients is increasing at a rate of 4 million per year (Wild et al., 2004; Forouhi and Wareham, 2014; Martínez-Castelao et al., 2015). Persistent hyperglycemia, insulin resistance and lipid metabolism disorders can lead to a series of complications such as diabetic retinopathy, diabetic nephropathy, diabetic foot and neuropathy (American Diabetes Association, 2009; Terry et al., 2012; Chawla et al., 2016).

Diabetic nephropathy (DN) is one of the most serious and common microvascular complications, and it is also one of the main causes of end-stage nephropathy and renal failure (Dronavalli et al., 2008). It is characterized by glomerular vascular injury, glomerulosclerosis, the formation of nodular lesions and deteriorating renal function that eventual leads to end-stage renal disease (Schena and Gesualdo, 2005; Kanwar et al., 2011). The incidence of diabetic nephropathy is about 33–40% among type 1 diabetics and 20–25% among type 2 diabetes (Khwaja et al., 2007; Olokoba et al., 2012). In recent years, clinical and experimental studies have shown that the pathogenesis of diabetic nephropathy is very complex. A growing number of studies have shown that glucose metabolism disorders, the formation of glycosylation end products, the activation of polyol pathway (Yamagishi et al., 2007), the increased activity of protein kinase C (Gnudi et al., 2003) and the changed renal hemodynamics collectively play an important role in the pathogenesis of diabetic nephropathy. Meanwhile, cytokines changed (Hellemons et al., 2012; Hao et al., 2013; Nakagawa et al., 2013), lipid metabolism disorders (Attman et al., 1998), genetic susceptibility (Schena and Gesualdo, 2005), oxidative stress (Forbes et al., 2008) and other factors are also involved.

Multiple DN animal models including those created by surgical excision of pancreas or chemical induction, spontaneous DN animals and transgenic DN animals have been used for the study of DN pathogenesis and the development of anti-DN drugs (King, 2012; Al-Awar et al., 2016). Two approaches to establish animal models of type 2 diabetes mellitus (T2DM) have been widely used: chemical induction with drugs such as streptozotocin (STZ) combined with high fat feeding in rats and spontaneous animal models with gene mutation like KK-Ay mice. STZ is a compound that has a preferential toxicity toward pancreatic β cells (Lenzen, 2008). The KK-Ay mouse was produced by transferring the yellow obese gene (Ay allele) into the KK/Ta mouse that spontaneously exhibited T2DM phenotypes associated with hyperglycemia, glucose intolerance, hyperinsulinemia, mild obesity and microalbuminuria (Suto et al., 1998; Tomino, 2012). The phenotypic characteristics of different types of T2DM models are different (King, 2012; Al-Awar et al., 2016), which indicates that the pathogenesis of DN, such as the onset, progress speed and degree of renal lesions in these models, might also be different. Therefore, the study of the characteristics and mechanisms of renal lesions using different T2DM animal models would likely contribute to the selection of suitable animal models for developing anti-DN drugs.

In this study, we established an animal model of T2DM SD rats using low dose STZ combined with high fat feeding and another animal model of spontaneous T2DM in KK-Ay mice with high fat feeding alone. The dynamic changes of glucose and lipid metabolic parameters, renal function-associated parameters, and pathological changes of kidneys along with the observation periods of 20 weeks in both T2DM SD rats and KK-Ay mice and their corresponding control animals were compared in a pairwise fashion. In addition, the molecular mechanisms underlying the differed pathogenesis of DN in these two models were preliminarily explored by gene profiling of renal tissues with microarrays.

MATERIALS AND METHODS

Cell Culture

Human renal proximal tubular cell line (HKC) and the stable MES 13 murine mesangial cells transformed with non-capsid-forming SV 40 virus were obtained from Institute of basic medicine, Chinese academy of medical sciences. All the cell lines were cultured in DMEM culture medium with 10% FBS and in a humidified atmosphere of 5% CO_2 at 37°. They were digested by

Abbreviations: AUC, Area Under the Curve; DM, Diabetes Mellitus; DN, Diabetic Nephropathy; FBG, Fasting Blood Glucose; ITT, Insulin Tolerance Test; LDL-C, Low-Density Lipoprotein-Cholesterol; OGCT, Oral Glucose Challenge Test; STZ, Streptozotocin; T2DM, Type 2 Diabetes Mellitus; TC, Total Cholesterol; TG, Triglyceride; UAE, Urinary Albumin Exclusion rate.

0.25% trypsin until they reached approximately 80% confluence. Cells that were after passages 2 were used in this study.

Measurements of Cell Growth Inhibition

After the digestion by trypsinization, the cell concentration of every cell line was adjusted to 2×10^4/mL and inoculated in three 96-well plates. Every hole contained 200 μL cell suspension solution or PBS. Each 96-well plates inoculated 50 holes which were divided into 10 groups, besides, PBS (200 μL in every hole) was add in the holes around them and the plates were cultured in a humidified incubator containing 5% CO_2 at 37°C. After 24 h, the medium of different groups was replaced with new medium containing different sugar concentrations and all the plates continued to culture in incubator for different time (24, 48, 72 h). At every point in time, each hole added 20 μL (5 mg/mL) MTT and put them back in the incubator for another 4 h. After that, the supernatant was abandoned and each hole added 150 μL DMSO and mixed by microporous plate thermostatic shaker for 15 min. The 96-well plates were placed in full spectrum enzyme marker at 570 nm for measuring the inhibition ratio.

$$\text{Inhibition ratio (\%)} = (\text{control group} - \text{treatment group}) / (\text{control group} - \text{background group}) \times 100\%$$

Animals

This study was performed in strict accordance with the recommendations in the Guide for the Care and Use of Laboratory Animals of the National Institute of Health. All procedures involving experimental animals were approved by the University Committee on the Use and Care of Animals (UCUCA) at the Beijing Yizhuang Biomedical Park Animal Center (approval number 2017S007).

Specific-pathogen-free (SPF) grade healthy SD rats (male, 170—190 g), C57BL/6J mice (male, 8 weeks old) and KK-Ay mice (male, 8 weeks old) were purchased from Beijing Huafukang Biotechnology Co. Ltd. (Beijing, China). The animals were housed at the experimental animal center of Beijing Yizhuang Biomedical Park Animal Center with a controlled temperature (22 ± 2°C) and humidity (50% ± 5%) on a 12 h alternate light-dark cycle. Food and water were provided *ad libitum* throughout the experiments.

The number of experimental animals in this study was calculated based on the study design of published related papers. We used the minimum sample size at each time point on the premise of ensuring statistical differences, to be specific, we included at least 6 animals at each time point for biochemical markers, urine analysis, body weight, et al. (Tahara and Takasu, 2018), and 3 animals of each group for kidney sampling and subsequent pathology (qualitative investigation) and sequencing at different time-point (Conesa et al., 2016).

Induction Methods of Type 2 Diabetic Models

Type 2 DM rats were induced by low dose STZ administration and high-fat-diet feeding (Gheibi et al., 2017). SD rats were randomly divided into "Control Rats" group (n = 15) and "T2DM Rats" group (n = 54).

After fasting for 10 h, rats in T2DM Rats were intraperitoneally injected with 1% STZ (Lot number WXBC3087V, Sigma-Aldrich, St. Louis, MO, United States) citrate buffer (pH = 4.2–4.5) at a dose of 30 mg/kg body weight in the first time (−3d, **Figure 1**). At 72 h after STZ injection, these rats fasted for 3 h before measurements of fasting blood glucose (FBG) were taken. The rats with FBG < 11.1 mmol/L were re-injected with the same dose of 1% STZ on the next day (1d, **Figure 1**). FBG was again measured after 72 h and continued to be measured for 20 weeks. Type 2 DM rats were fed with a high-fat diet (10% lard + 20% sucrose + 2.5% cholesterol + 1% cholate + 66.5% conventional chow) during the whole experimental process (Gheibi et al., 2017). Rats in the Control rats group were injected with the same amount of citrate buffer, and were fed with a normal diet.

Male C57BL/6J mice (n = 18) and KK-Ay mice (n = 18, SPF grade, 8 weeks old) were maintained in the individually ventilated cages (IVC) at the experimental animal center for 20 weeks (**Figure 1**). The KK-Ay mice model of spontaneous type 2 DM was established by feeding with high-fat diet (protein 16.5 kcal%, carbohydrate 37.9 kcal%, fat 45.6 kcal%) (Gheibi et al., 2017), while the C57BL/6J control mice were fed a normal diet. All feed was purchased from Beijing Huafukang Biotechnology Co. Ltd. with a license No. SCXK (Beijing) 2014-0008.

Biochemical Indicators Test

The body weight and FBG for rats and mice were recorded every 2 weeks. In the rat groups, the oral glucose tolerance test (OGTT) was performed at weeks 4, 8, and 20, while the insulin tolerance test (ITT) was performed at weeks 12 and 16. In the mouse groups, OGTT and ITT were performed every 4 weeks starting from week 4 (**Figure 1**).

The concentrations of urinary protein and urinary microalbumin were determined every 4 weeks starting from week 4, and 24 h urinary albumin excretion rate (UAE) was calculated (**Figure 1**). For urine samples collection, the beddings in cages were removed and homemade urine filters were placed on the bottom of the cages. After 24 h, urine at the bottom of the cage was collected with a disposable pipette and the amount of urine was recorded. After statically settled down overnight at 4°C, the supernatant was taken for detecting urine related indicators.

Every 4 weeks, three animals from the control groups and another three from the diabetic groups were randomly selected to measure the biomedical indicators using various kits. The following kits were from Nanjing Jiancheng Bioengineering Institute, Nanjing, China: Creatinine determination kits (batch number 20170209), albumin kit (batch number 20170222), blood urea nitrogen (BUN) kits(batch number 20170522), triglyceride (TG) kits (batch number 20170221), total cholesterol (T-CHO) kits (batch number 20170222), low-density lipoprotein-cholesterol (LDL-C) kits (batch number 20170519). Urine protein kit (batch number 20170821) and urinary microalbumin kit (batch number 20170227). The quantitation of these parameters was performed following the manufacturer's protocols. Blood glucose was monitored using blood glucose

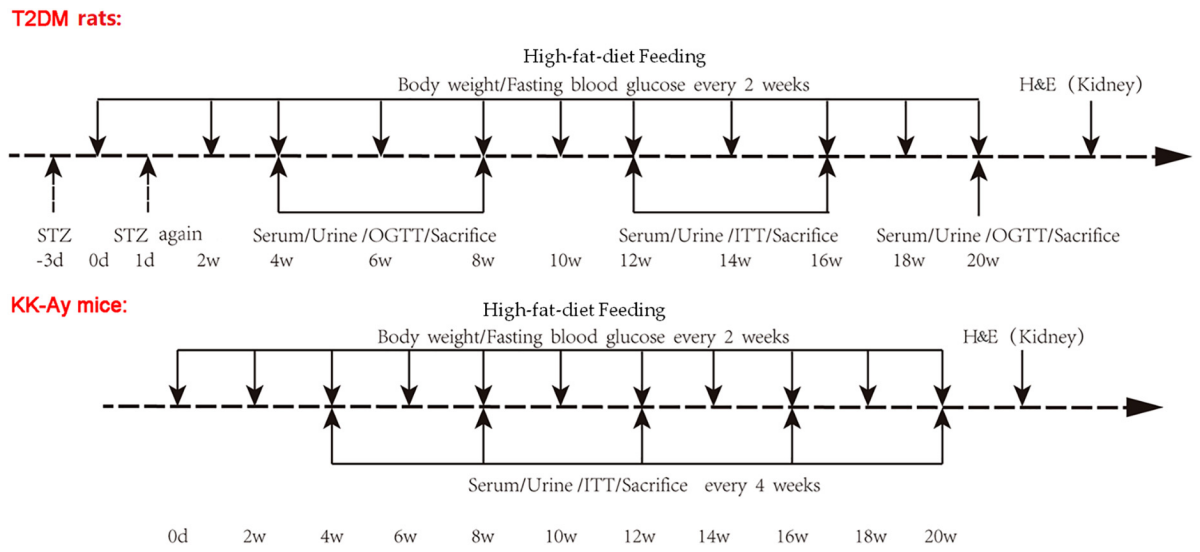

FIGURE 1 | Schematic representation of experimental design. Type 2 DM rats were induced by low dose STZ administration and high-fat-diet feeding. SD rats were randomly divided into Control rats group and T2DM rats group. After fasting for 10 h, rats in the T2DM rats group were intraperitoneally injected with 1% STZ citrate buffer at a dose of 30 mg/kg body weight in the first time (−3d). At 72 h after STZ injection, these rats were fasted for 3 h and subjected to measurements of FBG. The rats with FBG < 11.1 mmol/L were re-injected with the same dose of 1% STZ on the next day (1d). FBG was measured after 72 h and continued to be observed for 20 weeks. Type 2 DM rats were fed with high-fat-diet starting day 0. Rats in the Control rats group were injected with the same amount of citrate buffer, and were fed with normal diet. The KK-Ay mice model of spontaneous type 2 DM was established by feeding with high-fat-diet which was started at day 0, while the C57BL/6J control mice were fed with normal diet. The body weight and FBG for rats and mice were recorded every 2 weeks. Serum and urine samples were collected, and OGTT and ITT were performed, at the indicated time points after the initial of modeling. Animals were sacrificed at the indicated time points, and renal tissues were used for H&E staining. STZ, streptozotocin; FBG, fasting blood glucose; OGCT, oral glucose challenge test; ITT, insulin tolerance test.

meter (Roche, United States). Glucose (batch number 20170110) was obtained from Beijing Boaoxing Biotechnology Co., Ltd. (Beijing, China), and recombinant human insulin injection (Humulin, R) (batch number C553562D) was obtained from Lilly France.

Hematoxylin-Eosin Staining of Kidney

The unilateral kidney tissues of animals in the diabetic model group and the corresponding control group were extracted once every 4 weeks. The kidneys were fixed in 4% paraformaldehyde for 3 days and the following routine procedures were performed on the coronal tissue blocks, including dehydration, fixation, and paraffin embedding, and sectioning (3 μm). The sections were stained with hematoxylin and eosin (H&E) after dewaxing and rehydration. Pathological changes of kidney were observed under a light microscope. Three view fields were randomly selected for each slide, and were scored independently by two pathologists.

Gene Expression Profiles With Affymetrix 3′IVT Gene Chips

GeneChip^{TM} Rat Genome 230 2.0 Array chip and GeneChip^{TM} Mouse Genome 430 2.0 Array chip (Affymetrix, Inc., Santa Clara, CA, United States) were used to profile gene expressions of rat and mouse kidney tissues, respectively. Total RNA samples were extracted with the TRIzol reagent (Invitrogen, Carlsbad, CA, United States), and then quantified using a spectrophotometer. The integrity of RNA samples was tested by agarose gel electrophoresis. The samples with total RNA amount >1 μg, A260/A280 ≥ 1.80 and a brightness ratio of 28 s band: 18 s band greater than or close to 1:1 were judged to be samples qualified for microarray. The chip hybridizations were carried out following the manufacturer's specifications. The AGCC software was used to save the chip fluorescence scanning image into a.DAT file for analysis (Schroeder et al., 2006; Villegas-Ruiz et al., 2016).

Data Processing Methods of IVT Gene Expression Profiles

The results of gene chip were analyzed and plotted by R-Project software, and the data quality of gene chip was evaluated using chip signal intensity distribution statistics and relative logarithmic signal intensity statistics. The probes with the lowest 20% of signal intensity tested in all samples were filtered out as background noise. Genes with significant differential expression were screened according to the criteria of differential fold exchange ≥ 2.0 and $q \leq 0.05$. The above significant differentially expressed genes were classified by biological process, molecular function and cellular component aspect in the enrichment analysis by means of gene ontology (GO) annotation enrichment analysis with the software, CapitalBio® Molecule Annotation System V3.0. The significant enrichment level of a gene was evaluated by Fisher accurate test (Masuda et al., 2017).

Quantitative Real-Time PCR

Total RNA was extracted from the frozen kidneys with RNApure kit (Bioteke, Beijing, China) according to the instructions of

the manufacturer. Strand cDNA was synthesized by Plus All-in-one 1st Strand cDNA Synthesis SuperMix kit (NovoScript, Beijing, China) according to the instructions of the manufacturer. Twelve genes were selected to analyze their mRNA expression differences. The primers of these genes were listed in **Table 1**. The expression levels of genes were measured by 7500 FAST Real-Time PCR System (Thermo Fisher Scientific, United States). Gene expression levels were performed by 2 × Plus SYBR real-time PCR mixture according to the instructions of the manufacturer and quantified relatively to the expression of the GAPDH by using an optimized comparative Ct (△△Ct) value method which was calculated as 2^ (△△Ct) to compare the relative expression.

The whole process of biochemical indicators test, Hematoxylin-eosin staining and gene expression profiles of kidney at different time point of animal model of T2DM is shown in **Supplementary Table 1**.

Statistical Analysis

Data were analyzed by SPSS 16.0 software (IBM; Armonk, NY, United States), and were expressed as mean ± standard deviation (SD). The one-way analysis of variance (ANOVA) was used to compare the differences among groups. A $P < 0.05$ was considered to be statistically significant.

RESULTS

The Inhibition of Different Concentration of Glucose on Cell Growth

The inhibition of cell growth gradually increased with the increase of glucose concentration, but the maximum inhibition rate was less than 60%. On MES13, the inhibitory effect of different concentrations of glucose on cells achieved maximum at 48 h and then decreased (**Figures 2A–C**). However, this inhibition rate reached maximum at 72 h on HKC (**Figure 2C**). This experiment also showed that HKC was more sensitive to glucose concentration and duration than MES 13.

TABLE 1 | The primers of Twelve genes.

Gene	Primer sequences	Gene No.
Rat TGF-β F	5′-CAAGCAGAGTACACACAGCA-3′	59086
Rat TGF-β R	5′-GATGCTGGGCCCTCTCTCCAGC-3′	
Rat CTGF F	5-AAGACCTGTGGGATGGGC-3	64032
Rat CTGF R	5-TGGTGCAGCCAGAAAGCTC-3	
Rat PPARγ F	5-CAT AAA GTC CTT CCC GCT GA-3	25747
Rat PPARγ R	5-GAA ACTGGC ACC CTT GAA AA-3	
Rat P38 F	5′-CTGCGAGGGCTGAAGTAT-3′	81649
Rat P38 R	5′-TCCTCTTATCCGAGTCCAA-3′	
Rat Erk F	CTACACGCAGCTGCAGTACATC	24338
Rat Erk R	GTGCGCTGACAGTAGGTTTGA	
Rat Akt F	5′-TCAGGATGTGGATCAGCGAGA-3′	24185
Rat Akt R	5′- CTGCAGGCAGCGGATGATAA-3′	
Rat VEGF F	5′-CCACTTCTGTCTTGCCACACA-3′	83785
Rat VEGF R	5′-CCAACCAATTAAGACCTTCTG-3′	
Rat RAGE F	5- CAGGGTCACAGAAACCGG-3	81722
Rat RAGE R	5′-ATTCAGCTCTGCACGTTCCT-3′	
Rat β-actin F	3-GTAAAGACCTCTATGCCAACA-5	81822
Rat β-actin R	3-GGACTCATCGTACTCCTGCT-5	
Rat PI3K F	5′-CCCATGGGACAACATTCCAA-3′	25513
Rat PI3K R	R 5′-CATGGCGACAAGCTCGGTA-3′	
Rat Fst F	5′-GTGTATCAAAGCAAAGTCTTG-3′	24373
Rat Fst R	5′-GCTCATCGCAGAGAGCA-3′	
RatOPN_1F	5-AGGTCATCCCAGTTGCC-3	81644
RatOPN_1R	5-GGCCCTCTGCTTATACTCC-3	

The Dynamic Changes of Glucose and Lipid Metabolic Parameters in T2DM Rats and KK-Ay Mice

In rats with T2DM induced by low-dose STZ combined with high fat feeding, the glucose and lipid metabolism associated biochemical indexes were measured at different time points within 0–20 weeks after modeling. The body weight of the T2DM rats was significantly lower than that of the control rats at the all time points from week 4 to week 20 ($P < 0.05$; **Figure 3A**). A transient increase in FBG was observed after 3 days of the second injection of STZ (14.1 ± 6.9 mmol/L) in T2DM rats, and it remained at a low level during the next 4–8 weeks time points (FBG < 11.1 mmol/L). At the 12–20 weeks time points, a significant increase of FBG was identified (FBG > 11.1 mmol/L) (P < 0.05; **Figure 3B**). The OGTT results showed that at the 12th week, the percentage of blood glucose and the area under the curve (AUC) increased significantly ($P < 0.05$, data not shown) in 30 min in the T2DM rats after orally taking glucose solution when compared with the control group, and it also kept at a higher level at the 16th week ($P < 0.05$; **Figure 3C**). The ITT results showed that at the 12th week, the reduction percentage of blood glucose in 40 min after subcutaneous injection of insulin in the T2DM rats was significantly higher than that of the control rats. There was a slight ITT abnormality but no significant difference between the model and the normal rats at the 16th week (**Figure 3D**). Compared with the control rats, the T2DM rats demonstrated transient decrease of TG (**Figure 3E**) at week 16, and transient increase of TC (**Figure 3F**) and LDL-C (**Figure 3G**) at week 8 (all $P < 0.05$).

Compared to the control C57BL/6J mice, the body weight of KK-Ay mice increased significantly from 4 to 20 weeks after starting high-fat-diet feeding (**Figure 3A**). At week 4 there was a significant increase in FBG ($P < 0.05$) in the KK-Ay mice, and FBG values remained at 30 mmol/L during the first 12 weeks. Starting from week 16, the FBG values dropped to about 17 mmol/L (**Figure 3B**). Four weeks after modeling, OGTT results in the KK-Ay mice always showed a higher AUC value than the control mice (**Figure 3C**). The results of ITT showed that the reduction percentage of blood glucose in the model group was significantly less than the control group at all the time points between weeks 4 and 20 ($P < 0.05$; **Figure 3D**), which indicates an obvious insulin resistance phenomenon. The lipid metabolism indexes (TG, TC, and LDL-C) in the KK-Ay mice were significantly higher than those in the C57BL/6J mice starting from the 4th week ($P < 0.05$), and the difference between the two groups was most significant at the 12th week (**Figures 3E–G**). There was

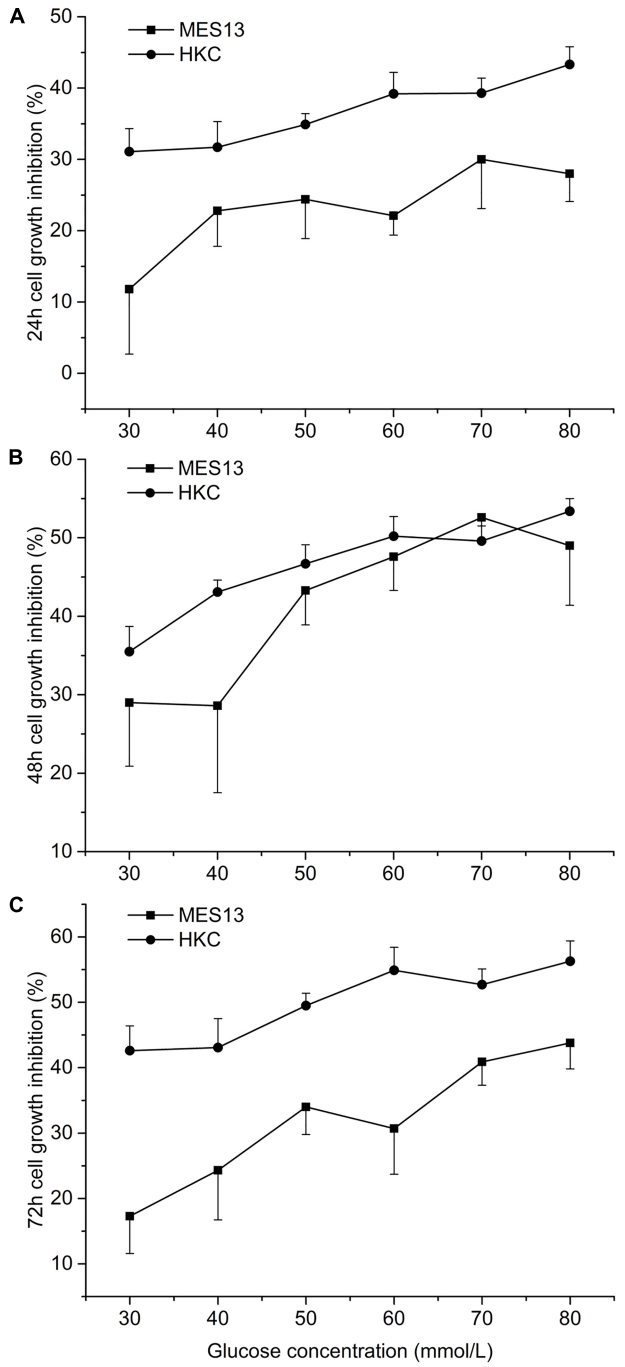

FIGURE 2 | Effects of different concentration of glucose on cell growth. After cell inoculation, cells were cultured for 24 h at incubator. Then each hole was added different concentration of glucose into the cell supernatant for 24 h **(A)**, 48 h **(B)**, or 72 h **(C)**. At the selected time point, the 96-well plate was taken out form the incubator for measuring the inhibition rate.

a recovery tendency of lipid metabolism over time, but the KK-Ay mice still have significantly higher lipid metabolism indexes (TG and TC) after the 16th week, compared with the C57BL/6J mice.

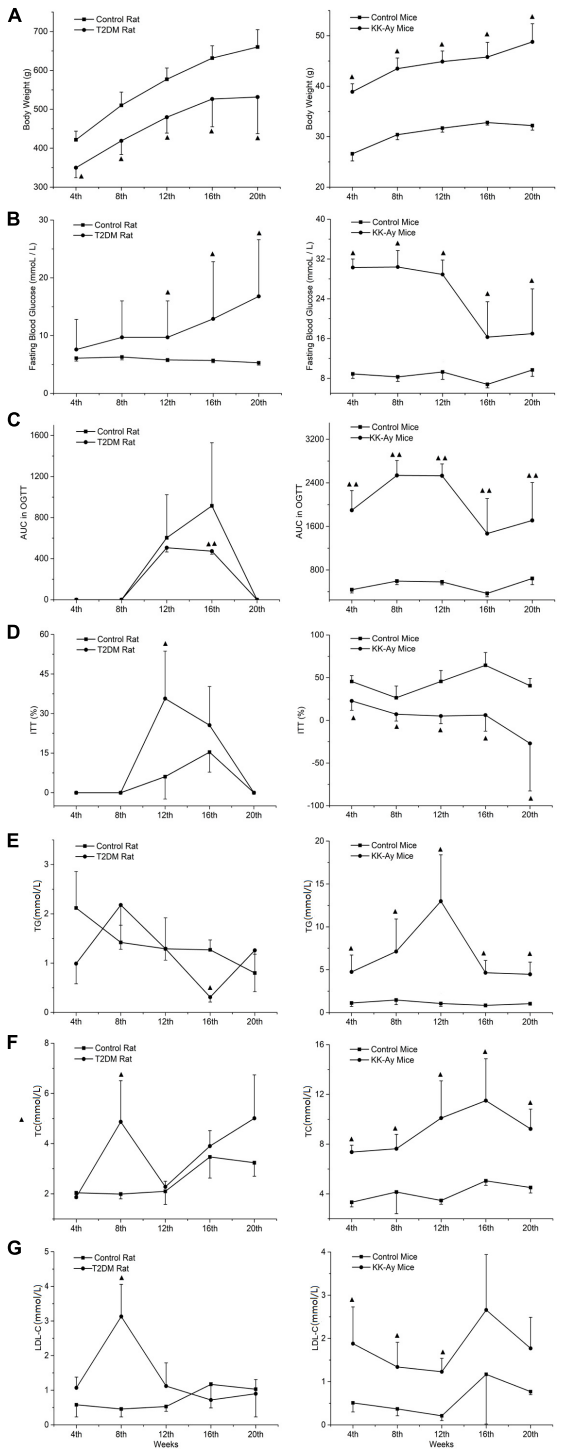

FIGURE 3 | Comparisons on the dynamic changes of glucose and lipid metabolic parameters in T2DM rats and KK-Ay mice. **(A–G)** The dynamic changes of body weight **(A)**, FBG **(B)**, AUC in OGCT **(C)**, percentage of ITT **(D)**, TG **(E)**, TC **(F)**, and LDL-C **(G)** in T2DM rats (left) and KK-Ay mice (right) along with the indicated time points after the initial of modeling are shown. ▲$P < 0.05$, ▲▲$P < 0.01$, compared with the corresponding control group at the same time point. FBG, fasting blood glucose; OGCT, oral glucose challenge test; ITT, insulin tolerance test; AUC, area under the curve; TG, triglyceride; TC, total cholesterol; LDL-C, low-density lipoprotein-cholesterol.

The Dynamic Changes of Renal Function-Associated Parameters in T2DM Rats and KK-Ay Mice

Renal function was evaluated by dynamic detection of urine biochemical indexes in the T2DM animal models and the normal control animals. Compared to the Control rats at the same time points, the urinary protein concentrations of T2DM rats decreased significantly at the 12th and 16th week ($P < 0.05$; **Figure 4A**). The concentration of urine microalbumin in T2DM rats increased significantly at the 16th week ($P < 0.05$; **Figure 4B**). Urinary albumin exclusion rate (UAE) also decreased significantly at the 8th and 12th week in T2DM rats, but it increased accidentally at the 16th week (**Figure 4C**). The concentrations of serum creatinine (**Figure 4D**) and urea nitrogen (**Figure 4E**) in T2DM rats were not significantly different from those in the control group at each time point, except that T2DM rats had significantly lower urea nitrogen levels at the 8th week (**Figure 4E**).

Compared to the control C57BL/6J mice at the same time points, the urine protein concentration (**Figure 4A**) and serum creatinine concentration (**Figure 4D**) of KK-Ay mice increased significantly ($P < 0.05$) and gradually increased in first 12th weeks. Urea nitrogen concentration in KK-Ay mice had a transient increase at the 16th week ($P < 0.05$; **Figure 4E**) and the urinary albumin exclusion rate (UAE) increased significantly at the 8th week ($P > 0.05$; **Figure 4C**), but there was no significant difference in terms of urinary microalbumin concentration (**Figure 4B**) between the two groups.

Comparisons on the Pathological Changes of Kidney in T2DM Rats and KK-Ay Mice

Renal pathology was examined at different time points in different T2DM models and the corresponding control groups by H&E staining. At 4 and 8 weeks after the start of model creation, there was no obvious pathological change in renal tissue of rats with T2DM, compared with the Control rats (**Figure 5**). At the 12th week, there was slight hyperplasia of glomerular mesangial cells in the kidney of one animal in the model group. At the 16th week, the renal histopathological changes associated with diabetic nephropathy were observed in T2DM rats, such as glomerular mesangial cell proliferation, glomerular mesangial matrix increase and the clear and empty cytoplasm of renal tubular epithelial cells (**Figure 5**). In addition to the above pathological changes, glomerular hypertrophy and thickening of glomerular capillary basement membrane were observed in the kidney of T2DM rats at the 20th week (**Figure 5**). The changes described above are typical pathological changes in the kidneys of diabetic animals. In addition, in each stage of modeling, a few kidneys, whole or in part, including those in the Control rats and T2DM rats, could be identified to display the renal tubule lumen protein flocculation, renal tubule dilatation, chronic progressive nephropathy (CPN, manifested as tubule basophilic degeneration), and pyelonephrosis, and these lesions are common spontaneous lesions in SD rats. There was no significant difference in the incidence and severity of these lesions between the control group and T2DM group (**Table 2**).

Compared to the control C57BL/6J mice at the same time points, the increase in mesangial matrix, the tubular epithelial cells vacuolar degeneration and CPN were observed in the kidney of KK-Ay mice during the full period (**Figure 5**). After 8 weeks of high fat feeding, some of the KK-Ay mice had the kidneys with renal pelvis dilatation. In the KK-Ay mice after 16 weeks of modeling, besides above lesions, glomerular hypertrophy, glomerular capillary basement membrane thickening, glomerular mesangial cell proliferation and glomerular segmental sclerosis were observed in their kidneys (**Figure 5**). At the 20th week, renal tubular epithelial cells in KK-Ay group were empty and blank, while tubule dilatation and protein flocculation in renal tubules were observed. In the above lesions, glomerular hypertrophy, thickening of glomerular capillary basement membrane, proliferation of glomerular mesangial cells, increase of glomerular mesangial matrix and glomerular segmental sclerosis were the characteristic pathological changes of diabetic kidney. Vacuolar degeneration of cortical renal tubular epithelial cells, CPN (characterized by basophilic degeneration of renal tubule, renal tubular hyaline and interstitial inflammatory cell infiltration), renal tubule dilatation, tubule protein flocculation and pelvis dilatation may be spontaneous lesions. The incidence of these lesions in the kidney of KK-Ay mice tended to be increased, compared with that in the control C57BL/6J mice (**Table 2**).

Comparisons on the Changes of Gene Expression Profiles in T2DM Rats and KK-Ay Mice

In order to reveal the molecular mechanisms underlying the pathological changes of kidneys in T2DM rats and KK-Ay mice, we performed gene expression profiling in kidney samples by Affymetrix 3′ IVT gene microarrays. As shown in the volcano plots in **Figure 6**, compared with the Control rats group, the T2DM rats group had 449 differentially expressed genes ($|\text{fold change}| \geq 2$, $q \leq 0.05$) in the renal tissues, among which 213 genes were up-regulated and 236 genes were down-regulated. Compared with the control C57BL/6J mice, KK-Ay mice had 1064 differentially expressed genes in the renal tissues, among which there were 334 up-regulated genes and 730 down-regulated genes. Of these, 73 differentially expressed genes were identified in both T2DM SD rats and spontaneous KK-Ay mice. The five most up-regulated genes and five most down-regulated genes in the renal tissues of T2DM SD rats and KK-Ay mice are listed in **Table 3**.

Further analyses on the differentially expressed genes between the model groups and the control groups suggested that the biological pathways and molecular functions of these genes were different (**Table 4**). The differentially expressed genes in the T2DM SD rats were primarily related to the pathways of glucose and lipid metabolism disorder, amino acid metabolism and angiogenesis. The dysregulation of glucose and lipid metabolism is consistently a characteristic of T2DM. Abnormal amino acid metabolism and angiogenesis are also the main characteristics

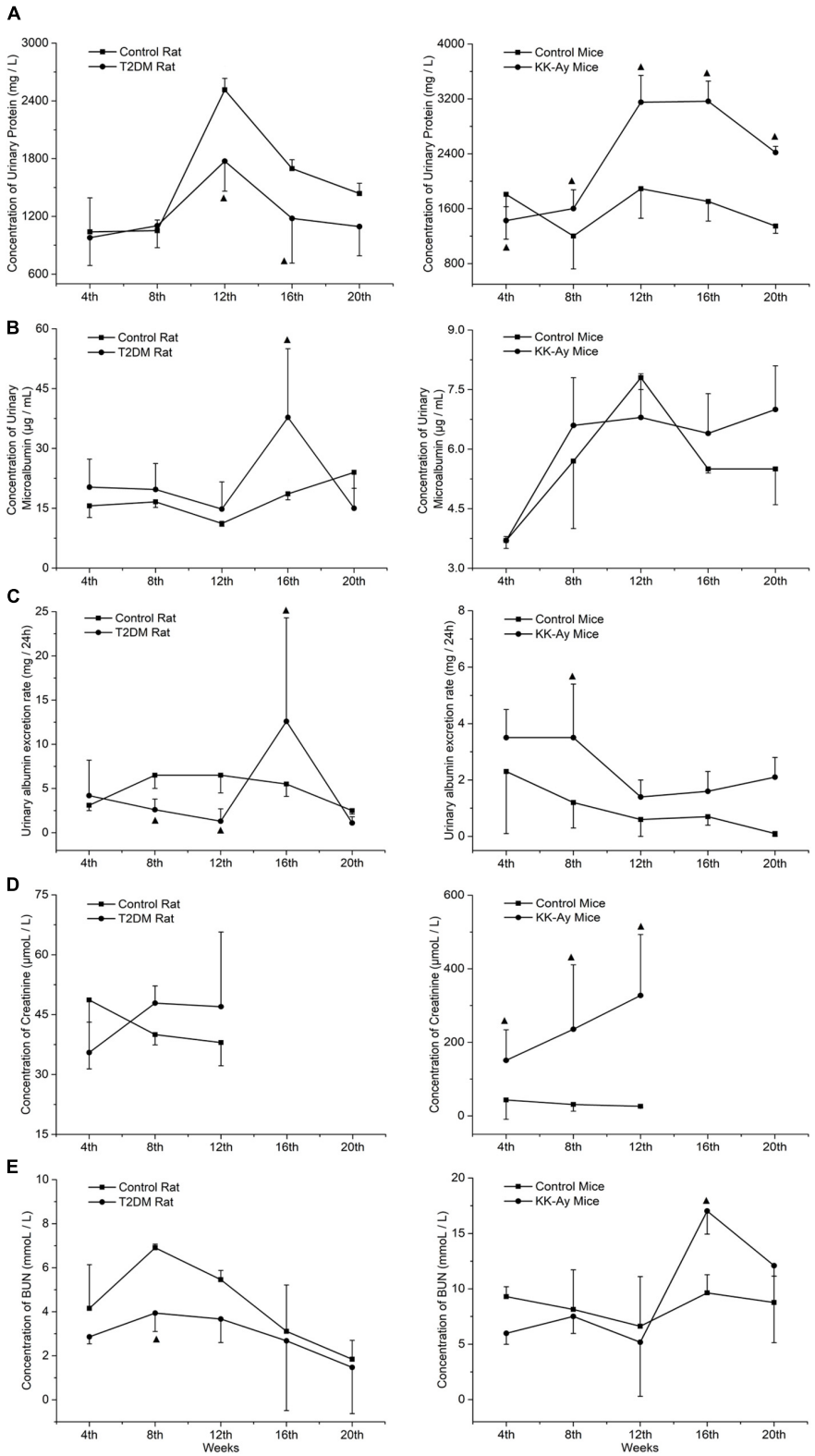

FIGURE 4 | Comparisons on the dynamic changes of renal function-associated parameters in T2DM rats and KK-Ay mice. **(A–E)** The dynamic changes in concentrations of urinary protein **(A)**, concentrations of urine microalbumin **(B)**, urinary albumin exclusion rate (UAE) **(C)**, concentrations of serum creatinine **(D)**, and concentrations of urea nitrogen **(E)** in T2DM rats (left) and KK-Ay mice (right) along with the indicated time points after the initial of modeling are shown ▲$P < 0.05$, compared with the corresponding control group at the same time point.

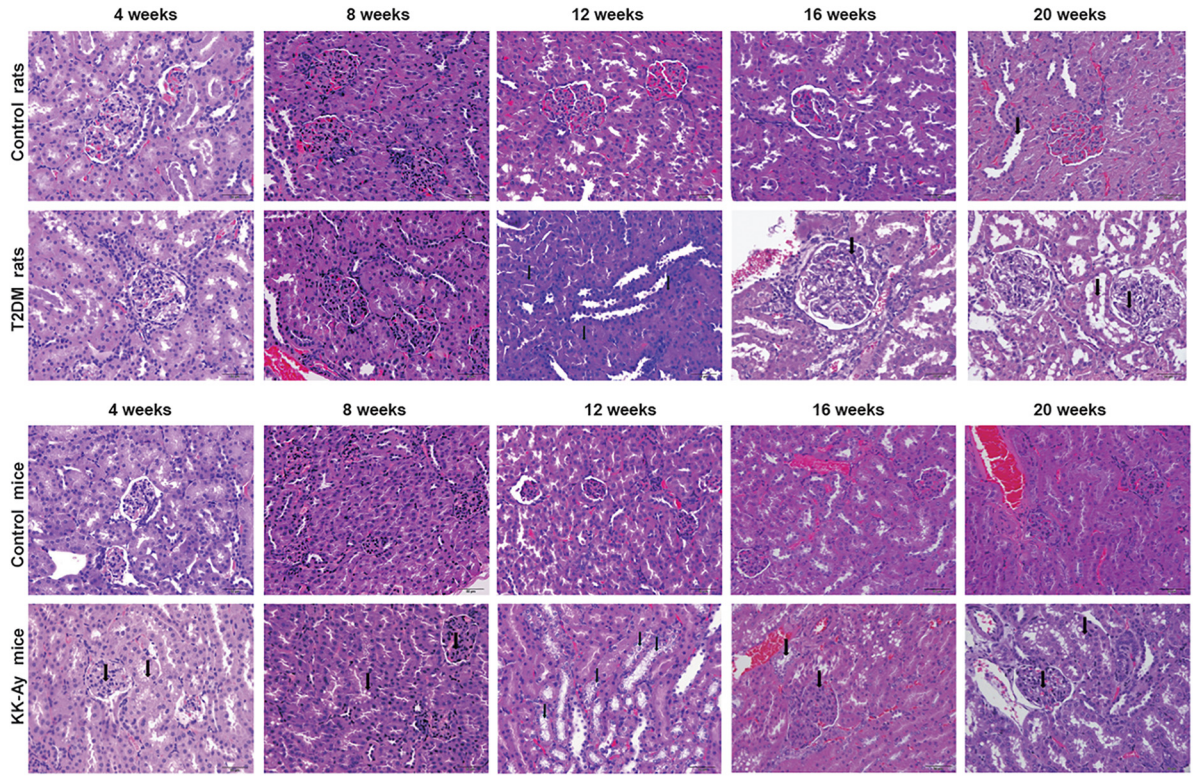

FIGURE 5 | Comparisons on the pathological changes of kidney in T2DM rats and KK-Ay mice. Representative H&E images show the pathological changes of kidneys from control/T2DM rats and control/KK-Ay mice at the indicated time points after the initial of modeling. Magnification, 40×.

of diabetic nephropathy. The differentially expressed genes in KK-Ay mice are mainly related to the amino acid metabolism pathway disorder, insulin secretion abnormality, glucose and lipid metabolism disorder and impaired coagulation function observed in the mice. The relative insufficiency of insulin secretion and insulin resistance are also typical characteristics of T2DM. The change in coagulation function may affect the renal hemodynamics and lead to renal lesion.

Expression of Possible Key Gene Relating of the Mechanism of Diabetes Mellitus

In those selected genes, there were only two genes (Erk and VEGF) having the same tendency in the gene expression. These two genes increased to different degrees in their respective models. That means Erk and VEGF were the shared gene in different models of this study. Some gene, such as OPN, TGF-β, RAGE, PPAR, showed highly expression in T2DM SD rats other than KK-Ay mice. Similarly, Akt, CTGF, and Fst were proved to have significantly increased expression in mice. PI3K and P38 were more interesting than other genes, and revealed opposite direction in two models. The results were shown in **Figure 7**.

The expression of choiced genes not exhibited the same variation between two selected models. PI3K and p38 owned the contrary increase direction ($P < 0.05$, $P<0.05$), but VEGF and Erk had the same variation ($P < 0.05$, $P < 0.05$; **Figure 7A**). Although the other choiced genes also had the high expression, they only changed obviously in one of the two models (**Figures 7B,C**).

The Predicted Interaction of Specific Proteins of Diabetes Mellitus Models

The Raf/MAPK/ERK pathway and Ras/PI3K/AKT pathways are both involved in cell cycle regulation. When Ras active Raf and PI3K, the further kinase (ERK and AKT) could be active respectively. Receptor-regulated SMAD that is an intracellular signal transducer and transcriptional modulator active by TGF-βand activin type 1 receptor kinases. Bind the TRE element in the promoter region of many genes that are regulated by TGF-β and, on formation of the SMAD2/SMAD4 or SMAD3/SMAD4 complex, activate transcription. Also can form a SMAD3/SMAD4/JUN/FOS complex at the AP-1/SMAD site to regulate TGF-β-mediated transcription. Follistatin could bind directly to activin and functions as an activin antagonist. TGF-β-activated RhoA/ROCK signaling could induce Mesenchymal stem cells (MSCs) differentiate into myofibroblasts that promotes formation of an extracellular matrix (ECM) complex consisting of connective tissue growth factor (CTGF), and vascular endothelial growth factor (VEGF). Interestingly, CTGF and OPN have the closely negative correlation in the laryngeal squamous cell carcinoma although OPN might involve in cell-cell tight junction. AGER mediates interactions of advanced glycosylation end products (AGE). These are non-enzymatically glycosylated

TABLE 2 | Pathological changes of kidney in different diabetes mellitus models.

Group	Time (week)	Increase of glomerular mesangial matrix	Vacuolar degeneration of cortical renal tubular epithelial cells	Tubular epithelial cells cytoplasmic shell	Tubular protein	Interstltial inflammatory cell infiltration	Basophilic degeneration of renal tubule	Distal convoluted tubule dilatation	Pyelectasia
Control rat	4th	−	−	/	−	/	±	/	−
	8th	−	−	−	−	−	−	−	−
	12th	−	−	−	−	−	−	−	−
	16th	−	−	−	−	−	+	±	−
	20th	−	−	−	−	−	+	±	−
T2DM rat	4th	−	−	/	−	/	−	/	Y
	8th	−	−	−	−	−	−	−	−
	12th	+	2+	2+	−	−	+	+∼2+	−
	16th	+	2+	2+	−	−	+	+	−
	20th	+	+	+	−	−	+	+	−
Control mice	4th	−	−	/	±	/	−	/	−
	8th	−	−	−	−	−	−	−	−
	12th	−	+	−	−	−	−	−	−
	16th	−	+	−	−	−	−	−	−
	20th	−	+	−	−	−	−	−	−
KK-Ay mice	4th	2+∼3+	2+	/	+	/	+	/	−
	8th	2+	+	−	+	+	+	−	Y
	12th	2+∼3+	+∼2+	+	+∼2+	+	+∼2+	+	Y
	16th	2+∼3+	+∼3+	+	−	−	−	−	3 +
	20th	3+	+∼3+	2+	−	−	−	−	3 + ∼4 +

N = 3∼5. ±, suspicious or extremely minor lesion; +, minor lesion; 2+, mild lesion; 3+, moderate lesion; 4+, severe lesion; Y, pathological changes regardless of grade;/, not determined. Data in the list was obtained from individuals with the most serious grade of pathological changes.

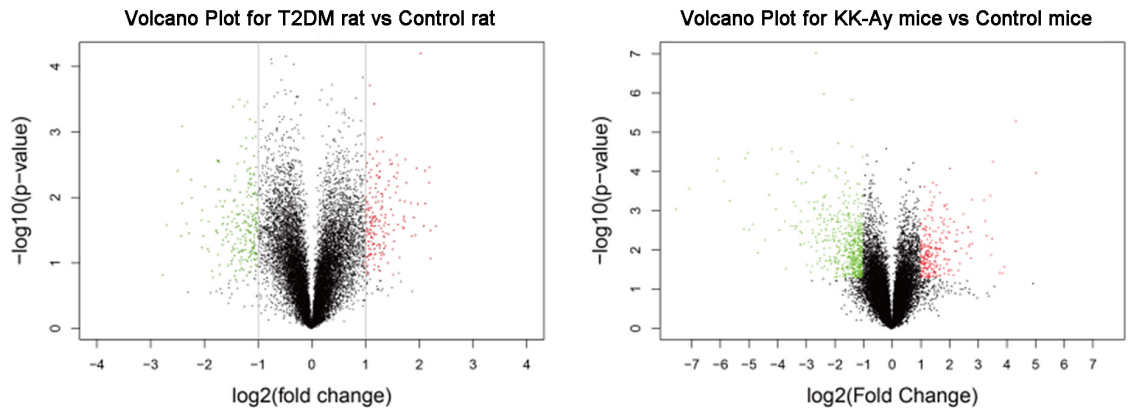

FIGURE 6 | Analyses of differentially expressed genes in kidneys from the T2DM animal models. Volcano plots of differentially expressed genes in the renal tissues from T2DM rats **(left)** and KK-Ay mice **(right)** are shown. The fold changes are represented in log2 scale as depicted on the x-axis, whereas the −log10 *P*-value is depicted on the y-axis. Genes with greater statistical significance are highlighted in the plots. The red/green dots represent genes that show differential expression with fold changes > 2 (red) or < 0.5 (green) and *P*-values < 0.05 between the T2DM renal tissues and normal control renal tissues.

proteins which accumulate in vascular tissue in aging and at an accelerated rate in diabetes. The results were shown in **Figure 8**.

DISCUSSION

Diabetic nephropathy is one of the most common chronic microvascular complications in diabetic patients and it is also leading cause of end-stage renal disease (Dronavalli et al., 2008). Experiments using DN animal models are significantly facilitating the development of anti-DN drugs. However, no model currently exhibits all the features of human DN (King, 2012; Al-Awar et al., 2016). Therefore, biochemical, pathological, and transcriptomic data in selecting the appropriate model to study the molecules and pathways of interest should be considered (Betz and Conway, 2016). Besides, unstable onset time

and uneven characteristics may significantly limit the stability of the models. Herein, we adopted the methods of inducing T2DM in rats by low-dose STZ combined with high fat diet and in KK-Ay mice with spontaneous type 2 diabetes. While examining the characteristics of DM, which included the dynamic changes of glucose and lipid metabolic parameters and renal function-associated parameters, we also studied the pathological changes in the kidneys during the whole process of renal lesion in these models. Furthermore, we explored the preliminary molecular mechanisms at the transcriptional level through gene profiling in renal tissues with microarrays. Our work provides an important reference for the evaluation of diabetic nephropathy models and contributes to our current understanding of the mechanisms of diabetic nephropathy of these T2DM animal models.

TABLE 3 | Summary of differentially expressed genes in kidney tissue of diabetic nephropathy animals (fold change ≥ 2 or ≤ 0.5, *q*-value ≤ 0.05).

Comparison	Gene symbol	*q*-value (%)	Fold change
T2DM rat vs. Control rat	Fst	0.88	4.98
	Cftr	1.46	4.64
	Gja1	0	3.95
	Sod3	1.40	2.62
	Pcdh9	0.88	3.82
	Smlr1	0	0.17
	Naglt1	0.62	0.15
	Angptl4	0	0.20
	Igfbp1	1.04	0.29
	F2	0.19	0.21
KK-Ay mice vs. Control mice	Lox	0	32.54
	Ighg	0.37	30.63
	Mela	0	20.10
	Lcn2	0.22	15.24
	Adgra1	0.09	11.10
	Spink1	0	0.01
	Ttr	0	0.01
	Stk4	0	0.02
	Serpina1f	0	0.02
	Methig1	0	0.05

Fold Change ≥2 means up -regulation; Fold Change ≤0.5 means down-regulation.

TABLE 4 | Enriched pathways from microarray detection of renal tissues in diabetic nephropathy.

DM	Enriched KEGG pathway	Input gene number
T2DM rat	Pentose and glucuronate interconversions	14
	Starch and sucrose metabolism	15
	Retinol metabolism	15
	Fatty acid degradation	7
	Beta-Alanine metabolism	6
	Tryptophan metabolism	6
	Complement and coagulation cascades	7
	Glycolysis/Gluconeogenesis	5
	Biosynthesis of amino acids	5
	PPAR signaling pathway	5
KK-Ay mice	PPAR signaling pathway	15
	Peroxisome	15
	Complement and coagulation cascades	14
	Tryptophan metabolism	9
	Protein digestion and absorption	13
	Retinol metabolism	11
	Fatty acid metabolism	8
	Fatty acid degradation	7
	Phenylalanine metabolism	4
	Arginine and proline metabolism	7

In our study, low-dose STZ combined with high fat feeding induced T2DM in SD rats, afterward which showed low FBG level and abnormal glucose tolerance. But there was no obvious abnormality in lipid metabolism and renal function. Renal lesions appeared in later time points and the main changes were glomerular mesangial matrix increasing, glomerular mesangial cell proliferation, glomerular hypertrophy and absence of tubular epithelial cells in cortex. The characteristics of renal lesions were closely related to insulin resistance. KK-Ay mice with spontaneous T2DM had the characteristics of high FBG, insulin resistance and abnormal lipid metabolism. For the renal function associated parameters, urinary protein excretion and serum creatinine were shown to have increased significantly. Renal lesions were displayed early onset and the main changes included increased glomerular mesangial matrix, glomerular mesangial cell proliferation, glomerular hypertrophy, glomerular capillary basement membrane thickening, glomerular segmental sclerosis, cortical renal tubular epithelial cells vacuolar degeneration, and CPN. The characteristics of renal lesions were closely related to high FBG, insulin resistance and abnormal lipid metabolism.

Different types of diabetes have different characteristics and pathogenesis that lead to different onset, progress speed and degree of renal lesions. Therefore, appropriate models should be selected to study the intervention of DN progression and to screen drugs for treating DN. Chemical induction of diabetes is widely used in DN animal models with the advantages of light injury, low mortality, high rate and low cost of model formation (Motshakeri et al., 2014). The animal model of spontaneous diabetic nephropathy reduces human factors to a certain extent, and the characteristics of renal lesions are similar to human DN. But the use of such model is limited due to its limited sources, high breeding conditions, low incidence of disease, long period of disease progression and high price (King, 2012; Al-Awar et al., 2016). Despite the essential differences in etiology of DM in the two animal models, our systemic in-depth analyses and comprehensive comparisons on the characteristics of DM and DN at different time points revealed some common factors of DN. For example, hyperglycemia was the key initial factor of DN, while renal hemodynamic changes and insulin resistance also played a key role in the formation of DN. In addition, hyperlipidemia also played a synergistic role in the occurrence and progression of DN.

Hyperglycemia Is the Initiating Factor of Diabetic Nephropathy

High FBG and elevated postprandial blood glucose are the main characteristics of diabetes mellitus. When the blood glucose

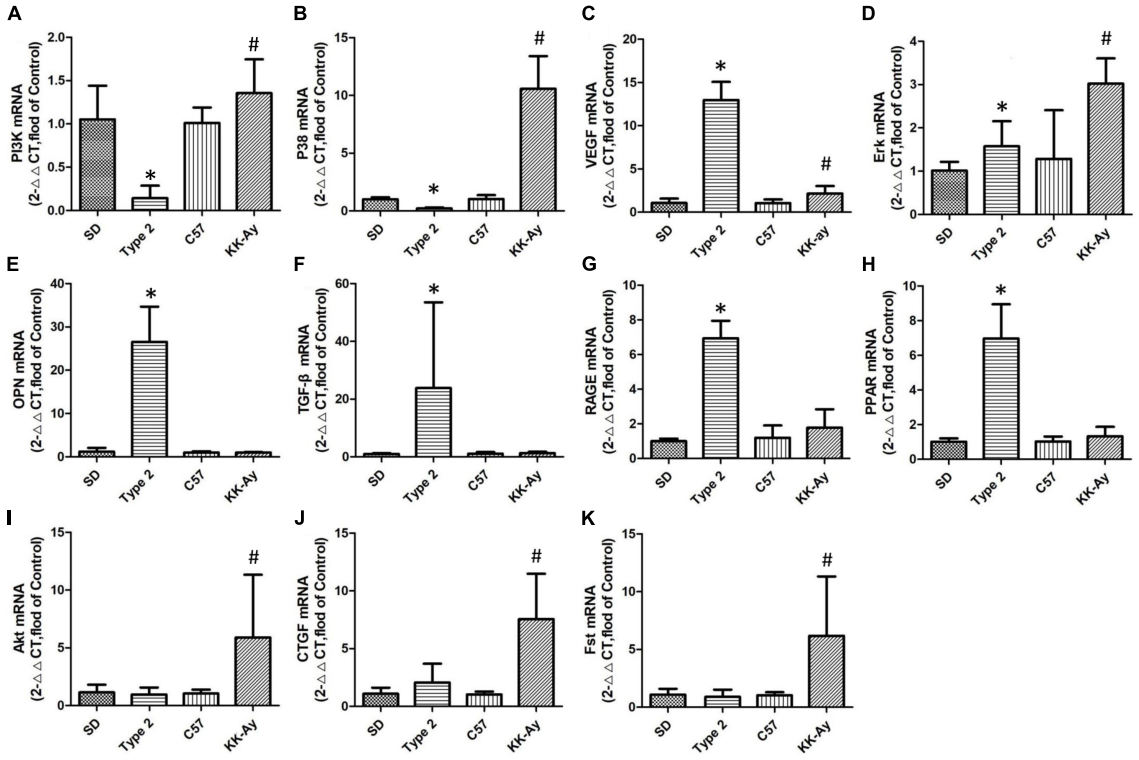

FIGURE 7 | Relative mRNA levels of selected genes in T2DM rats and KK-Ay mice. Quantitative real-time PCR of the 5 samples were conducted 3 times and normalized to GAPDH gene expression, measured with 2^ (−ΔΔCt) value. **(A)** PI3K mRNA, **(B)** P38 mRNA, **(C)** VEGF mRNA, **(D)** Erk mRNA, **(E)** OPN mRNA, **(F)** TGF-β mRNA, **(G)** RAGE mRNA, **(H)** PPAR mRNA, **(I)** Akt mRNA, **(J)** CTGF mRNA, and **(K)** Fst mRNA. Data are shown as the mean ± SE of 3 independent replicates. Significant differences (*$P < 0.05$, or #$P < 0.05$) between model group and corresponding control group.

concentration in the body is too high, the pressure on glucose metabolism in the kidney increases, leading to an increase in glomerular filtration rate and renal tubular reabsorption, this changes the biochemical composition of glomeruli, increases renal vascular permeability, causes the leakage of plasma protein, and leads to renal tubule sclerosis and proteinuria (Fukami et al., 2004). The results showed that the FBG in the model of KK-Ay mice continuously kept at a high level (25–30 mmol/L) until the 12th week after modeling initiation, and the metabolism of glucose in kidney was increased due to the severe hyperglycemia in the body, which leads to the increase of glomerular filtration rate, tubular reabsorption and vascular permeability. Therefore, urinary protein and urinary albumin were found to have significantly increased 4 weeks after the onset of hyperglycemia, which was accompanied with typical pathological changes of DN such as mild cortical tubular epithelial cell vacuolar degeneration and tubular basophilic degeneration.

Chronic hyperglycemia increases the activity of enzymes associated with glucose metabolism, resulting in the formation complexes consisting of enzymes and proteins; these deposit in the glomeruli, resulting in serious damage (Miyata et al., 1998). In addition, the increase of glucose concentration can also promote the non-enzymatic glycosylation of non-glycosylated substances to produce advanced glycosylation end-products (AGEs) (Goh and Cooper, 2008). The kidney is the main organ that clears AGEs. AGEs can mediate the production of Ang2 by binding to the specific receptor on mesangial cells. It also leads to the synthesis and secretion of a large number of cytokines, such as interleukin (IL), insulin-like growth factor (IGF) and transforming growth factor (TGF-β), which leads to cell hypertrophy, fibronectin synthesis and glomerular sclerosis. Our results from gene profiling consistently showed that there were observable abnormalities in amino acid synthesis and metabolic pathways in the two DM animal models, which indicated that the kidney had functional abnormalities. In KK-Ay mice, abnormal metabolism of starch and glycogen occurred, indicated by the excessive expression of SMAD and PPARγ in the PPAR signaling pathway (Dutchak et al., 2012). Moreover, the analysis of differential genes of these diabetic models has shown significant increases in the expression of IGF, Ang, and ICAM in renal tissues.

In conclusion, the FBG of KK-Ay mice remained high for a long time, and compared to the T2DM SD rats, the renal lesions for these mice appeared earlier and were more severe. A high degree of proteinuria, vacuolar degeneration of renal tubular epithelial cells, basophilic degeneration and other pathological changes appeared at the 4th week after the initiation of the model, and with the extension of time, the rate and degree of pathological changes became increasingly faster and more severe. At the 8th week, the UAE index increased significantly, and according to the

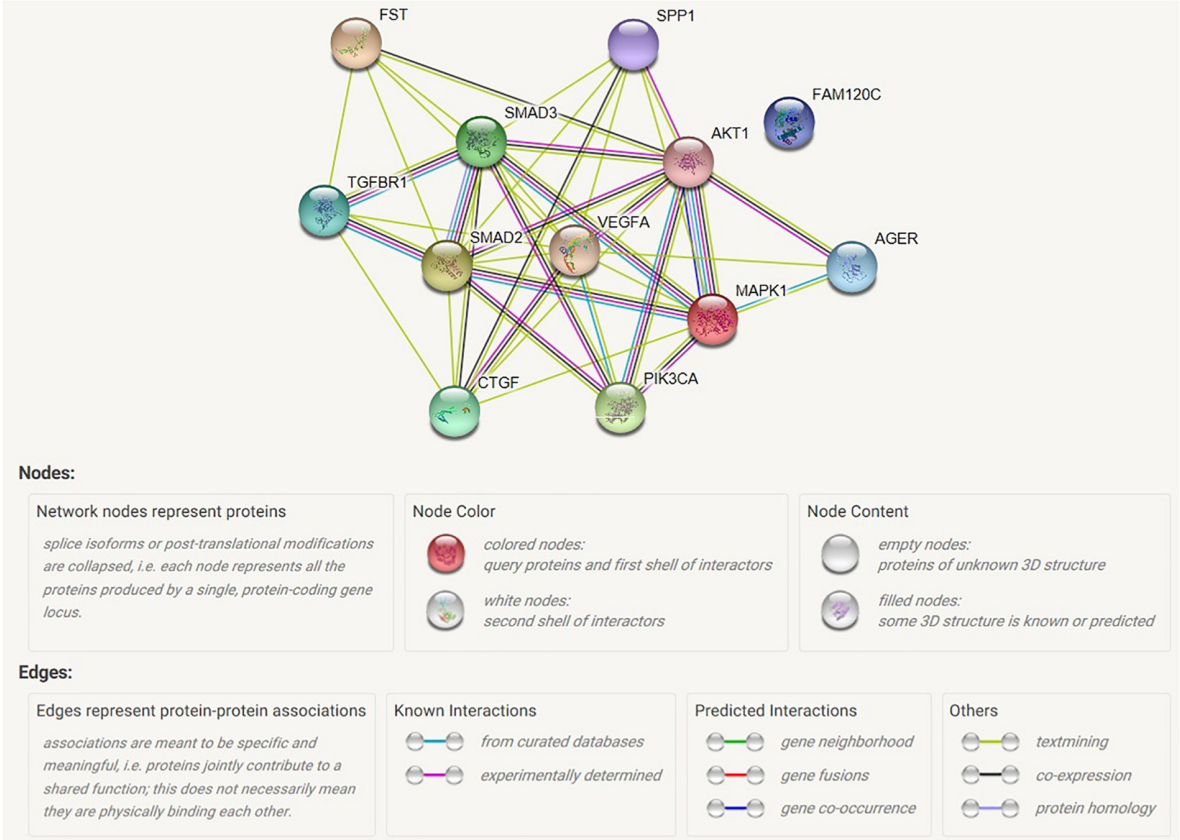

FIGURE 8 | Map of possible interaction between selected genes. AGER, advanced glycosylation end product-specific receptor; AKT1, serine/threonine kinase 1; CTGF, connective tissue growth factor; FAM120C, family with sequence similarity 120C; FST, follistatin; MAPK1, mitogen-activated protein kinase 1; PIK3CA, phosphatidylinositol; SMAD2, mothers against decapentaplegic homolog 2; SMAD3, mothers against decapentaplegic homolog 3; SPP1, secreted phosphoprotein 1; TGFBR1, TGF-beta receptor type-1; VEGFA, vascular endothelial growth factor A.

stage of Mogensen diabetic nephropathy, it can be classified as the stage 3. At every time point after modeling initiation, FBG level in the T2DM SD rats was lower than that in the KK-Ay mice. Therefore, onset time and degree of renal lesions in KK-Ay mice were more obvious than those in T2DM SD rats, which suggested that hyperglycemia was the initiator of diabetic nephropathy.

Insulin Resistance Is an Important Factor Causing Diabetic Nephropathy

The main cause of T2DM is the relative insufficiency of insulin secretion or the decrease of insulin sensitivity. The direct consequence of the deficiency of insulin secretion is the decrease of glucose uptake and utilization, which leads to increased postprandial blood sugar (DeFronzo et al., 2015). Insulin resistance causes bodily defects in both the inhibition of hepatic glucose output and stimulation of glucose uptake by peripheral muscle tissues, resulting in increased gluconeogenesis and glycogen output to further elevate blood glucose levels (DeFronzo et al., 2015). Hyperglycemia can lead to insulin resistance through post-insulin receptor defects. This is mainly due to the inhibition of serine-threonine phosphorylation of insulin receptor and insulin receptor substrate-1 (IRS-1) and subsequent decrease in the activity of phosphatidylinositol-3 kinase (PI3K). This causes inhibition of glucose transporter 4 (GLUT4) translocation, inhibition of glucose uptake and phosphorylation, reduction of intracellular ATP level and reduction of glycogen synthesis (Grundy et al., 2004). Marsha et al. found that glucose induced insulin resistance through hexosamine biosynthesis pathway, and hyperglycemia increased the activity of hexosamine pathway in the cell that induced the formation of insulin resistance in muscle and adipose tissue (Marshall et al., 1991). Insulin non-sensitive tissue may be involved in diabetic vascular complications by promoting the synthesis of certain growth factors, such as transforming growth factor β (TGF-β) (Kolm-Litty et al., 1998). When blood sugar is too high and exceeds the renal glucose threshold, glucose, which cannot be metabolized, is excreted from the urine, leading to glucosuria (Dutchak et al., 2012).

Insulin secretion was affected by many factors. Our results of glucose tolerance test and insulin tolerance test showed that compared to the control group, OGTT of T2DM rats increased significantly in 30 min after glucose loading. Compared to the control C57BL/6J mice, the KK-Ay mice had significantly decreased reduction percentage of blood glucose in 40 min

after administration of exogenous insulin. This indicates that the insulin secretion in the model animals was relatively insufficient and insulin resistance was present. The KK-Ay mice also had high FBG. In addition to the increase of FBG, KK-Ay also demonstrated insulin resistance characteristics. Moreover, urinary protein concentration and serum creatinine concentration in KK-Ay mice increased significantly. The pathological results also showed that the renal tissue of KK-Ay mice had mild or moderate level of glomerular mesangial matrix expansion, vacuolar degeneration of renal tubular epithelial cells and basophilic degeneration by week 4. Notably, our gene chip results showed that the PPAR signal pathway associated molecules Cyp4a1, Angptl4, Hmgcs2 were among the differentially expressed genes in both T2DM SD rats and KK-Ay mice.

In summary, the KK-Ay mice and T2DM SD rats not only have the characteristics of high FBG, but also have obvious characteristics of insulin resistance. The mice also showed the characteristics and progression of renal lesions. Together, these suggest that insulin resistance may be a key factor in the development of diabetic nephropathy but not the initiator.

Metabolic Disorders of Lipids Play a Synergistic Role in the Pathogenesis and Progression of Diabetic Nephropathy

In diabetic patients, glucose metabolic disorder is often accompanied by lipid metabolic disorders, which lead to dyslipidemia, obesity, cardiovascular and cerebrovascular diseases. Excessive glucose and fat can induce insulin resistance and destroy the function of islet cells. Hyperlipidemia is the pathophysiological basis of insulin resistance which can not only exacerbates hyperglycemia but also causes a series of vascular complications in diabetes (Hirano, 2018). The increase in blood lipid concentration leads to increased blood viscosity, slow blood rheology and decreased blood flow, so that fat stores in the kidney and other non-adipose tissues lead to glomerulosclerosis (Chen et al., 2005). The increase of blood lipid may also change the structure of the fatty acid in the kidney and increase the pressure in the glomerular capillaries. Hyperlipidemia reduces fibrinolytic activity, resulting in vascular embolization of glomerular capillaries (Wang et al., 2005). The lipid metabolism of T2DM SD rats only appeared transiently abnormal at the 8th week. The levels of TG, TC, and LDL-C in the serum of KK-Ay mice increased significantly by the 4th week, which were accompanied by proteinuria. The gene microarray results showed that the key genes in the fatty acid synthesis and decomposition pathway such as *Acaa2, Ehhadh, Echs1* were down-regulated in KK-Ay mice, which was also consistent with the above hypothesis.

In summary, the KK-Ay mice developed hyperlipidemia and manifested elevated FBG. As the pathophysiological basis of insulin resistance, hyperlipidemia can aggravate insulin resistance. For the T2DM SD rats with transiently abnormal lipid metabolism, the dysfunction of lipid metabolism did not play an important role in the formation of kidney lesions, as the related parameters seemed to be recovered to the normal ranges as the controls during the later period. Therefore, we hypothesized that hyperlipidemia caused by abnormal lipid metabolism has a synergistic effect on the pathogenesis and progression of DN.

Hemodynamic Changes Are One of the Important Pathogenesis of Diabetic Nephropathy

Abnormal renal hemodynamics is an important feature of the early stage diabetic nephropathy. Increased glomerular filtration rate plays a key role in the formation of diabetic nephropathy. This is primarily due to the increase in blood flow in each renal unit. The increase in the concentrations of blood glucose and lipid, the increase of blood viscosity, the slow blood rheology and the decrease of renal blood flow in diabetic patients lead to changes in renal hemodynamics and renal lesions aggravation (Wolf and Ziyadeh, 2007). A large number of studies have shown that renin-angiotensin system (RAS) is considered to be the main cause of renal injury and renal hemodynamic changes (Wada et al., 2011). Therefore, angiotensin convertase inhibitors are often used in the clinical treatment of renal diseases (Fernandez Juarez et al., 2013). The results of gene microarray showed that the expression of angiotensin II (Ang II), angiotensin convertase (ACE) and other factors in the two diabetic models were significantly increased. High glucose concentration can result in the increase of local Ang II in the kidney, which causes increased pressure in the glomerulus, the increase of renal glomerular filtration rate, and eventual glomerular damage (Lo et al., 2012). Ang II can also directly phosphorylate Smad protein by stimulating the expression of TGF-β in kidney and up-regulating the TGF-β receptor (Reudelhuber, 2010). ACE-2 is a key enzyme in the regulation and metabolism of angiotensin II (Ang 1-7) in RAS. It is also considered as an endogenous renal protective enzyme, which can effectively resist early onset proteinuria and alleviate glomerular pathological damage and renal fibrosis (Mori et al., 2014; Patel et al., 2014).

The following limitations of our study should be recognized. Firstly, we only observe the differences of renal lesions in two commonly used animal models of type 2 diabetes, but not included db/db mice, which are one of the most widely, used animal models of type 2 diabetic nephropathy for financial reasons. Secondly, the animal sample size is not large enough. Consider for its exploratory research, in the design of this experiment, there are only 54 type 2 diabetic rats and 18 kk-Ay mice were used as the starting point. At each time point, all the animals survived were tested for various indicators, and then three animals were randomly selected from each group for kidney sampling and subsequent pathology and sequencing. This can ensure the number of blood biochemical and urine biochemical indicators for each animal model, but also meet the requirements of three parallel samples for routine pathological and sequencing tests. Thirdly, the daily feed intake of animals was not measured, but body weight indirectly reflected the feed intake partly. Finally, animal species in this study. The bibliography supports that wistar rats maybe a better model for STZ-induced diabetes, while we selected the Sprague Dawley rats for my study, the main objective of this study was to compare the characteristics of DN between animal models of spontaneous type 2 diabetes and

animals with chemically induced type 2 diabetes, in the future, we can consider to carry out in-depth research on the differences of diabetic nephropathy between SD rats and Wistar rats, specially for early kidney damage. Using mice with a specific mutation as a model for DM and DM related nephropathy, which is also one of the limitations of this study that needs to be focused on.

CONCLUSION

Our study, for the first time, showed that KK-Ay mice with both high fasting glucose and insulin resistance, that had earlier onset with more uniform onset time and pathological characteristics compared with T2DM rats induced by low-dose STZ combining with high-fat-diet. The T2DM SD rats induced by low-dose STZ combining with high-fat-diet should not be used as a preclinical model for diabetic nephropathy because of the late onset time and unclear DN disease characteristics. Our systemic and comprehensive investigations on the occurrence and development of DN induced in these two common T2DM animal models, as well as our preliminary exploring on the underlying molecular mechanisms, provide significant guidance on the development of anti-DN drugs and valuable insight into the pathogenesis of DN in T2DM.

DATA AVAILABILITY STATEMENT

All datasets generated for this study are included in the article/**Supplementary Material**.

ETHICS STATEMENT

The animal study was reviewed and approved by University Committee on the Use and Care of Animals (UCUCA) at the Beijing Yizhuang Biomedical Park Animal Center.

AUTHOR CONTRIBUTIONS

YL designed the experiments. YfL and HH performed the experiments and wrote the manuscript. YfL, HH, and RG analyzed the data. All authors edited the manuscript and gave final approval for the final version to be published.

FUNDING

This work was supported by the Fundamental Research Funds for the Central Public Welfare Research Institutes of China Academy of Chinese Medical Sciences (ZZ13-YQ-001).

SUPPLEMENTARY MATERIAL

The Supplementary Material for this article can be found online at: https://www.frontiersin.org/articles/10.3389/fcell.2020.00172/full#supplementary-material

REFERENCES

Al-Awar, A., Kupai, K., Veszelka, M., Szűcs, G., Attieh, Z., Murlasits, Z., et al. (2016). Experimental diabetes mellitus in different animal models. *J. Diabetes Res.* 2016:9051426. doi: 10.1155/2016/9051426

American Diabetes Association, (2009). Diagnosis and classification of diabetes mellitus. *Diabetes Care* 32(Suppl. 1), S62–S67.

Attman, P. O., Knight-Gibson, C., Tavella, M., Samuelsson, O., and Alaupovic, P. (1998). The compositional abnormalities of lipoproteins in diabetic renal failure. *Nephrol. Dial. Transplant.* 13, 2833–2841. doi: 10.1093/ndt/13.11.2833

Betz, B., and Conway, B. R. (2016). An update on the use of animal models in diabetic nephropathy research. *Curr. Diab. Rep.* 16:18. doi: 10.1007/s11892-015-0706-2

Chawla, A., Chawla, R., and Jaggi, S. (2016). Microvasular and macrovascular complications in diabetes mellitus: distinct or continuum? *Indian J. Endocrinol. Metab.* 20, 546–551. doi: 10.4103/2230-8210.183480

Chen, H. C., Guh, J. Y., Chang, J. M., Hsieh, M. C., Shin, S. J., and Lai, Y. H. (2005). Role of lipid control in diabetic nephropathy. *Kidney Int.* 67(Suppl. 94) S60–S62.

Conesa, A., Madrigal, P., Tarazona, S., Gomez-Cabrero, D., Cervera, A., McPherson, A., et al. (2016). A survey of best practices for RNA-seq data analysis. *Genome Biol.* 17:13. doi: 10.1186/s13059-016-0881-8

DeFronzo, R. A., Ferrannini, E., Groop, L., Henry, R. R., Herman, W. H., Holst, J. J., et al. (2015). Type 2 diabetes mellitus. *Nat. Rev. Dis. Primers* 1:15019. doi: 10.1038/nrdp.2015.19

Dronavalli, S., Duka, I., and Bakris, G. L. (2008). The pathogenesis of diabetic nephropathy. *Nat. Clin. Pract. Endocrinol. Metab.* 4, 444–452. doi: 10.1038/ncpendmet0894

Dutchak, P. A., Katafuchi, T., Bookout, A. L., Choi, J. H., Yu, R. T., Mangelsdorf, D. J., et al. (2012). Fibroblast growth factor-21 regulates PPARγ activity and the antidiabetic actions of thiazolidinediones. *Cell* 148, 556–567. doi: 10.1016/j.cell.2011.11.062

Fernandez Juarez, G., Luño, J., Barrio, V., de Vinuesa, S. G., Praga, M., Goicoechea, M., et al. (2013). Effect of dual blockade of the renin-angiotensin system on the progression of type 2 diabetic nephropathy: a randomized trial. *Am. J. Kidney Dis.* 61, 211–218. doi: 10.1053/j.ajkd.2012.07.011

Forbes, J. M., Coughlan, M. T., and Cooper, M. E. (2008). Oxidative stress as a major culprit in kidney disease in diabetes. *Diabetes* 57, 1446–1454. doi: 10.2337/db08-0057

Forouhi, N. G., and Wareham, N. J. (2014). Epidemiology of diabetes. *Medicine (Abingdon)* 42, 698–702.

Fukami, K., Ueda, S., Yamagishi, S., Kato, S., Inagaki, Y., Takeuchi, M., et al. (2004). AGEs activate mesangial TGF-beta-Smad signaling via an angiotensin II type I receptor interaction. *Kidney Int.* 66, 2137–2147. doi: 10.1111/j.1523-1755.2004.66004.x

Gheibi, S., Kashfi, K., and Ghasemi, A. (2017). A practical guide for induction of type-2 diabetes in rat: incorporating a high-fat diet and streptozotocin. *Biomed. Pharmacother.* 95, 605–613. doi: 10.1016/j.biopha.2017.08.098

Gheith, O., Farouk, N., Nampoory, N., Halim, M. A., and Al-Otaibi, T. (2015). Diabetic kidney disease: worldwide difference of prevalence and risk factors. *J. Nephropharmacol.* 5, 49–56.

Gnudi, L., Viberti, G., Raij, L., Rodriguez, V., Burt, D., Cortes, P., et al. (2003). GLUT-1 overexpression: link between hemodynamic and metabolic factors in glomerular injury? *Hypertension* 42, 19–24. doi: 10.1161/01.hyp.0000075949.19968.ef

Goh, S.-Y., and Cooper, M. E. (2008). Clinical Review: the role of advanced glycation end products in progression and complications of diabetes. *J. Clin. Endocrinol. Metab.* 93, 1143–1152. doi: 10.1210/jc.2007-1817

Grundy, S. M., Brewer, H. B. Jr., Cleeman, J. I., Smith, S. C. Jr., Lenfant, C., American Heart Association, et al. (2004). Definition of metabolic

syndrome: report of the national heart, lung, and blood institute/american heart association conference on scientific issues related to definition. *Circulation* 109, 433–438. doi: 10.1161/01.cir.0000111245.75752.c6

Hao, J., Zhu, L., Li, F., Liu, Q., Zhao, X., Liu, S., et al. (2013). Phospho-mTOR: a novel target in regulation of renal lipid metabolism abnormality of diabetes. *Exp. Cell Res.* 319, 2296–2306. doi: 10.1016/j.yexcr.2013.06.013

Hellemons, M. E., Kerschbaum, J., Bakker, S. J., Neuwirt, H., Mayer, B., Mayer, G., et al. (2012). Validity of biomarkers predicting onset or progression of nephropathy in patients with Type 2 diabetes: a systematic review. *Diabet. Med.* 29, 567–577. doi: 10.1111/j.1464-5491.2011.03437.x

Hirano, T. (2018). Pathophysiology of diabetic dyslipidemia. *J. Atheroscler. Thromb.* 25, 771–782. doi: 10.5551/jat.RV17023

Kanwar, Y. S., Sun, L., Xie, P., Liu, F. Y., and Chen, S. (2011). A glimpse of various pathogenetic mechanisms of diabetic nephropathy. *Annu. Rev. Pathol.* 6, 395–423. doi: 10.1146/annurev.pathol.4.110807.092150

Khwaja, A., El Kossi, M., Floege, J., and El Nahas, M. (2007). The management of CKD: a look into the future. *Kidney Int.* 72, 1316–1323. doi: 10.1038/sj.ki.5002489

King, A. J. (2012). The use of animal models in diabetes research. *Br. J. Pharmacol.* 166, 877–894. doi: 10.1111/j.1476-5381.2012.01911.x

Kolm-Litty, V., Sauer, U., Nerlich, A., Lehmann, R., and Schleicher, E. D. (1998). High glucose-induced transforming growth factor beta1 production is mediated by the hexosamine pathway in porcine glomerular mesangial cells. *J. Clin. Invest.* 101, 160–169. doi: 10.1172/jci119875

Lenzen, S. (2008). The mechanisms of alloxan- and streptozotocin-induced diabetes. *Diabetologia* 51, 216–226. doi: 10.1007/s00125-007-0886-7

Lo, C. S., Liu, F., Shi, Y., Maachi, H., Chenier, I., Godin, N., et al. (2012). Dual RAS blockade normalizes angiotensin-converting enzyme-2 expression and prevents hypertension and tubular apoptosis in Akita angiotensinogen-transgenic mice. *Am. J. Physiol. Renal Physiol.* 302, F840–F852. doi: 10.1152/ajprenal.00340.2011

Marshall, S., Bacote, V., and Traxinger, R. (1991). Discovery of a metabolic pathway mediating glucose-induced desensitization of the glucose transport system. Role of hexosamine biosynthesis in the induction of insulin resistance. *J. Biol. Chem.* 266, 4706–4712.

Martínez-Castelao, A., Navarro-González, J. F., Górriz, J. L., and de Alvaro, F. (2015). The concept and the epidemiology of diabetic nephropathy have changed in recent years. *J. Clin. Med.* 4, 1207–1216. doi: 10.3390/jcm4061207

Masuda, Y., Yokose, S., and Sakagami, H. (2017). Gene expression analysis of cultured rat-endothelial cells after Nd: YAG laser irradiation by affymetrix genechip array. *In Vivo* 31, 51–54. doi: 10.21873/invivo.11024

Miyata, T., Ueda, Y., Horie, K., Nangaku, M., Tanaka, S., van Ypersele de Strihou, C., et al. (1998). Renal catabolism of advanced glycation end products: the fate of pentosidine. *Kidney Int.* 53, 416–422. doi: 10.1046/j.1523-1755.1998.00756.x

Mori, J., Patel, V. B., Ramprasath, T., Alrob, O. A., DesAulniers, J., Scholey, J. W., et al. (2014). Angiotensin 1-7 mediates renoprotection against diabetic nephropathy by reducing oxidative stress, inflammation, and lipotoxicity. *Am. J. Physiol. Renal Physiol.* 306, F812–F821. doi: 10.1152/ajprenal.00655.2013

Motshakeri, M., Ebrahimi, M., Goh, Y. M., Othman, H. H., Hair-Bejo, M., and Mohamed, S. (2014). Effects of brown seaweed (Sargassum polycystum) extracts on kidney, liver, and pancreas of type 2 diabetic rat model. *Evid. Based Complement Alternat. Med.* 2014:379407. doi: 10.1155/2014/379407

Nakagawa, T., Sato, W., Kosugi, T., and Johnson, R. J. (2013). Uncoupling of VEGF with endothelial NO as a potential mechanism for abnormal angiogenesis in the diabetic nephropathy. *J. Diabetes Res.* 2013:184539. doi: 10.1155/2013/184539

Olokoba, A. B., Obateru, O. A., and Olokoba, L. B. (2012). Type 2 diabetes mellitus: a review of current trends. *Oman. Med. J.* 27, 269–273. doi: 10.5001/omj.2012.68

Patel, V. B., Zhong, J. C., Fan, D., Basu, R., Morton, J. S., Parajuli, N., et al. (2014). Angiotensin-converting enzyme 2 is a critical determinant of angiotensin II-induced loss of vascular smooth muscle cells and adverse vascular remodeling. *Hypertension* 64, 157–164. doi: 10.1161/HYPERTENSIONAHA.114.03388

Reudelhuber, T. L. (2010). Prorenin, Renin, and their receptor: moving targets. *Hypertension* 55, 1071–1074. doi: 10.1161/hypertensionaha.108.120279

Schena, F. P., and Gesualdo, L. (2005). Pathogenetic mechanisms of diabetic nephropathy. *J. Am. Soc. Nephrol.* .16(Suppl. 1), S30–S33.

Schroeder, A., Mueller, O., Stocker, S., Salowsky, R., Leiber, M., Gassmann, M., et al. (2006). The RIN: an RNA integrity number for assigning integrity values to RNA measurements. *BMC Mol. Biol.* 7:3. doi: 10.1186/1471-2199-7-3

Suto, J., Matsuura, S., Imamura, K., Yamanaka, H., and Sekikawa, K. (1998). Genetic analysis of non-insulin-dependent diabetes mellitus in KK and KK-Ay mice. *Eur. J. Endocrinol.* 139, 654–661. doi: 10.1530/eje.0.1390654

Tahara, A., and Takasu, T. (2018). Prevention of progression of diabetic nephropathy by the SGLT2 inhibitor ipragliflozin in uninephrectomized type 2 diabetic mice. *Eur. J. Pharmacol.* 830, 68–75. doi: 10.1016/j.ejphar.2018.04.024

Terry, T., Raravikar, K., Chokrungvaranon, N., and Reaven, P. D. (2012). Does aggressive glycemic control benefit macrovascular and microvascular disease in type 2 diabetes? Insights from ACCORD, ADVANCE, and VADT. *Curr Cardiol. Rep.* 14, 79–88. doi: 10.1007/s11886-011-0238-6

Tomino, Y. (2012). Lessons from the KK-Ay mouse, a spontaneous animal model for the treatment of human type 2 diabetic nephropathy. *Nephrourol. Mon.* 4, 524–529. doi: 10.5812/numonthly.1954

Villegas-Ruiz, V., Moreno, J., Jacome-Lopez, K., Zentella-Dehesa, A., and Juarez-Mendez, S. (2016). Quality control usage in high-density microarrays reveals differential gene expression profiles in ovarian cancer. *Asian Pac. J. Cancer Prev.* 17, 2519–2525.

Wada, J., Sun, L., and Kanwar, Y. S. (2011). Discovery of genes related to diabetic nephropathy in various animal models by current techniques, in experimental models for renal diseases. *Contrib. Nephrol.* 169, 161–174. doi: 10.1159/000313951

Wang, Z., Jiang, T., Li, J., Proctor, G., McManaman, J. L., Lucia, S., et al. (2005). Regulation of renal lipid metabolism, lipid accumulation, and glomerulosclerosis in FVBdb/db mice with type 2 diabetes. *Diabetes* 54, 2328–2335. doi: 10.2337/diabetes.54.8.2328

Wild, S., Roglic, G., Green, A., Sicree, R., and King, H. (2004). Global prevalence of diabetes: estimates for the year 2000 and projections for 2030. *Diabetes Care* 27, 1047–1053. doi: 10.2337/diacare.27.5.1047

Wolf, G., and Ziyadeh, F. N. (2007). Cellular and molecular mechanisms of proteinuria in diabetic nephropathy. *Nephron. Physiol.* 106, 26–31.

Yamagishi, S., Fukami, K., Ueda, S., and Okuda, S. (2007). Molecular mechanisms of diabetic nephropathy and its therapeutic intervention. *Curr. Drug Targets* 8, 952–959. doi: 10.2174/138945007781386884

Conflict of Interest: HH was employed by the company Beijing Duan-Dian Pharmaceutical Research & Development Co., Ltd., Beijing, China.

The remaining authors declare that the research was conducted in the absence of any commercial or financial relationships that could be construed as a potential conflict of interest.

Copyright © 2020 Liu, Huang, Gao and Liu. This is an open-access article distributed under the terms of the Creative Commons Attribution License (CC BY). The use, distribution or reproduction in other forums is permitted, provided the original author(s) and the copyright owner(s) are credited and that the original publication in this journal is cited, in accordance with accepted academic practice. No use, distribution or reproduction is permitted which does not comply with these terms.

frontiers in Cell and Developmental Biology

REVIEW
published: 20 March 2020
doi: 10.3389/fcell.2020.00185

Mechanisms of Cardiovascular Disorders in Patients With Chronic Kidney Disease: A Process Related to Accelerated Senescence

Julia Carracedo[1], Matilde Alique[2]*, Carmen Vida[2], Guillermo Bodega[3], Noemí Ceprián[1], Enrique Morales[4,5], Manuel Praga[4,5], Patricia de Sequera[5,6] and Rafael Ramírez[2]*

[1] Departamento de Genética, Fisiología y Microbiología, Universidad Complutense/Instituto de Investigación Sanitaria Hospital 12 de Octubre (imas12), Madrid, Spain, [2] Departamento Biología de Sistemas, Facultad de Medicina y Ciencias de la Salud (IRYCIS), Universidad de Alcalá, Alcalá de Henares, Madrid, Spain, [3] Departamento de Biomedicina y Biotecnología, Facultad de Biología, Química y Ciencias Ambientales, Universidad de Alcalá, Alcalá de Henares, Spain, [4] Departamento de Nefrología, Hospital Universitario 12 de Octubre/Instituto de Investigación Sanitaria Hospital 12 de Octubre (imas12), Madrid, Spain, [5] Departamento de Medicina, Universidad Complutense de Madrid, Madrid, Spain, [6] Sección de Nefrología, Hospital Universitario Infanta Leonor, Madrid, Spain

OPEN ACCESS

Edited by:
Evangelia Dounousi,
University Hospital of Ioannina,
Greece

Reviewed by:
Stefanos Roumeliotis,
University General Hospital
of Thessaloniki AHEPA, Greece
Panagiotis I. Georgianos,
University General Hospital
of Thessaloniki AHEPA, Greece

***Correspondence:**
Julia Carracedo
julcar01@ucm.es
Matilde Alique
matilde.alique@uah.es

Specialty section:
This article was submitted to
Molecular Medicine,
a section of the journal
Frontiers in Cell and Developmental
Biology

Received: 18 December 2019
Accepted: 05 March 2020
Published: 20 March 2020

Citation:
Carracedo J, Alique M, Vida C, Bodega G, Ceprián N, Morales E, Praga M, de Sequera P and Ramírez R (2020) Mechanisms of Cardiovascular Disorders in Patients With Chronic Kidney Disease: A Process Related to Accelerated Senescence. Front. Cell Dev. Biol. 8:185. doi: 10.3389/fcell.2020.00185

Cardiovascular diseases (CVDs), especially those involving a systemic inflammatory process such as atherosclerosis, remain the leading cause of morbidity and mortality in patients with chronic kidney disease (CKD). CKD is a systemic condition affecting approximately 10% of the general population. The prevalence of CKD has increased over the past decades because of the aging of the population worldwide. Indeed, CVDs in patients with CKD constitute a premature form of CVD observed in the general population. Multiple studies indicate that patients with renal disease undergo accelerated aging, which precipitates the appearance of pathologies, including CVDs, usually associated with advanced age. In this review, we discuss several aspects that characterize CKD-associated CVDs, such as etiopathogenic elements that CKD patients share with the general population, changes in the cellular balance of reactive oxygen species (ROS), and the associated process of cellular senescence. Uremia-associated aging is linked with numerous changes at the cellular and molecular level. These changes are similar to those observed in the normal process of physiologic aging. We also discuss new perspectives in the study of CKD-associated CVDs and epigenetic alterations in intercellular signaling, mediated by microRNAs and/or extracellular vesicles (EVs), which promote vascular damage and subsequent development of CVD. Understanding the processes and factors involved in accelerated senescence and other abnormal intercellular signaling will identify new therapeutic targets and lead to improved methods of diagnosis and monitoring for patients with CKD-associated CVDs.

Keywords: chronic kidney disease, cardiovascular diseases, reactive oxygen species, extracellular vesicles, microRNAs, cellular senescence, epigenetic alterations, atherosclerosis

INTRODUCTION

Chronic kidney disease (CKD) is defined as a systemic pathology that affects approximately 10% of the population; however, data showed differences in the prevalence of CKD between countries (Hill et al., 2016). The prevalence of CKD has increased markedly over the past decades due to aging of the population worldwide and increase in incidence of diabetes mellitus, which has become the primary cause of CKD. Nowadays, CKD is considered a public health problem that causes high rates of mortality in the population due to the association with cardiovascular diseases (CVDs) (Go et al., 2004). Thus, CVDs are prevalent in patients with CKD, and subsequent CKD is a significant risk factor for CVDs. Furthermore, patients with CKD are at increased risk for cardiovascular events or death than for progression to end-stage renal disease (ESRD) (Keith et al., 2004). Multiple studies support the notion that patients with renal disease suffer accelerated aging, which precipitates the appearance of pathologies, including CVDs, usually associated with advanced age (Stenvinkel and Larsson, 2013).

Considerable efforts have been made to slow the progression of the disease and improve the quality of life in patients with CKD. New pharmacological strategies do slow the progression of CVDs, and reduce the morbidity and mortality of CKD patients (Merino et al., 2010). Likewise, methods of renal replacement therapy currently offer increased purification capacity and reduced adverse effects. However, the development of CVDs in patients with CKD has not yet been halted. This may be because when CKD is diagnosed, vascular pathology is already advanced and irreversible (Vanholder et al., 2005).

The causes of vascular damage in CKD are exceptionally complex. Among the theories proposed in recent years to explain the high frequency of CVDs in renal patients, one states that senescence of peripheral blood cells (known as immunosenescence) and vascular cells (known as vascular senescence) may be involved in the initiation and perpetuation of vascular pathology that appears early in patients with CKD (Merino et al., 2010, 2011; Carracedo et al., 2013).

Some therapies used successfully in other pathologies, such as CVDs have tested in trials to avoid the progression to ESRD. Statins with a clearly cardioprotective role present non-beneficial results in these CKD patients (Jun et al., 2011). However, recent studies demonstrated that statins in high doses might be improved the renal function (Sanguankeo et al., 2015). In this regard, antiplatelet agents may also be different effects in ESRD (Jun et al., 2011). Moreover, other therapies among them, antioxidants, angiotensin receptor blockers (ARBs) therapies, and angiotensin-converting enzyme (ACE) inhibitors, improve the kidney function in ESRD (Jun et al., 2011).

In this article, we review the cellular and molecular mechanisms, as well as processes involved, in increased risk for CKD-associated CVDs. Summarizing the current state of knowledge on CKD-associated CVDs will aid in early diagnosis and design of novel therapies that will improve the health and quality of life in renal patients.

INCREASED RISK FOR CVDs IN RENAL PATIENTS, THE CURRENT STATE OF THE PROBLEM

Cardiovascular diseases are the main cause of morbidity and mortality in CKD patients (Go et al., 2004). This may be because CKD itself is an independent risk factor for CVDs, and is associated with an increased prevalence of traditional and non-traditional risk factors for CVDs. Both estimated glomerular filtration rate (eGFR) and albuminuria are independently associated with cardiovascular outcomes (Matsushita et al., 2015). Even microalbuminuria without a decline in renal function is associated with a twofold to fourfold increase in the risk for CVD (Schiffrin et al., 2007). Furthermore, CVD alone, and numerous risk factors for CVD, exacerbate the progression of this condition and may be risk factors for CKD.

In patients with CKD, remodeling of the myocardium and blood vessels leads to several cardiovascular complications such as cardiomyopathy, atherosclerosis, arterial stiffness, calcification, and subsequent ischemic heart disease, heart failure, cerebrovascular and cardiovascular death, and progression of renal disease including ESRD (Chen et al., 2018). However, CKD patients present a high incidence of cardiovascular morbidity and mortality that is not fully accounted for by traditional risk factors and those mutual to CVDs and CKD such as age, hypertension, diabetes mellitus, obesity, hyperuricemia, dyslipidemia, tobacco use, family history, and male gender. Specific risk factors for renal impairment include albuminuria, anemia, mineral and bone disorders, malnutrition, toxic metabolites, endothelial dysfunction, inflammation, and oxidative stress (**Figure 1**).

Patients with CKD have numerous risk factors for the progression of cardiac dysfunction. Several non-traditional risk factors, such as volume overload, anemia, albuminuria, abnormal calcium-phosphate metabolism, inflammation, oxidative stress, and endothelial dysfunction, play critical roles in this process. Left ventricular hypertrophy (LVH) is closely related to the occurrence of heart failure (HF) and is known to be an independent risk factor for mortality (London et al., 2001). Among traditional risk factors, hypertension can be both a cause and a consequence of CKD, while dyslipidemia is another important risk factor for both CVDs and CKD.

INFLAMMATORY ALTERATIONS IN CKD AND THEIR RELATIONSHIP WITH THE DEVELOPMENT OF CVDs

Inflammation, which is a new non-traditional risk factor and consequence of reduced kidney function, is highly associated with elevated cardiovascular risk in patients with kidney disease (London et al., 2001). The inflammation transfers to the blood and generates damage in distal tissues in the progression of concomitant diseases such as CVDs (Cottone et al., 2008). Epidemiological and clinical studies have shown a close relationship between markers of inflammation and risk for cardiovascular events (Cottone et al., 2008).

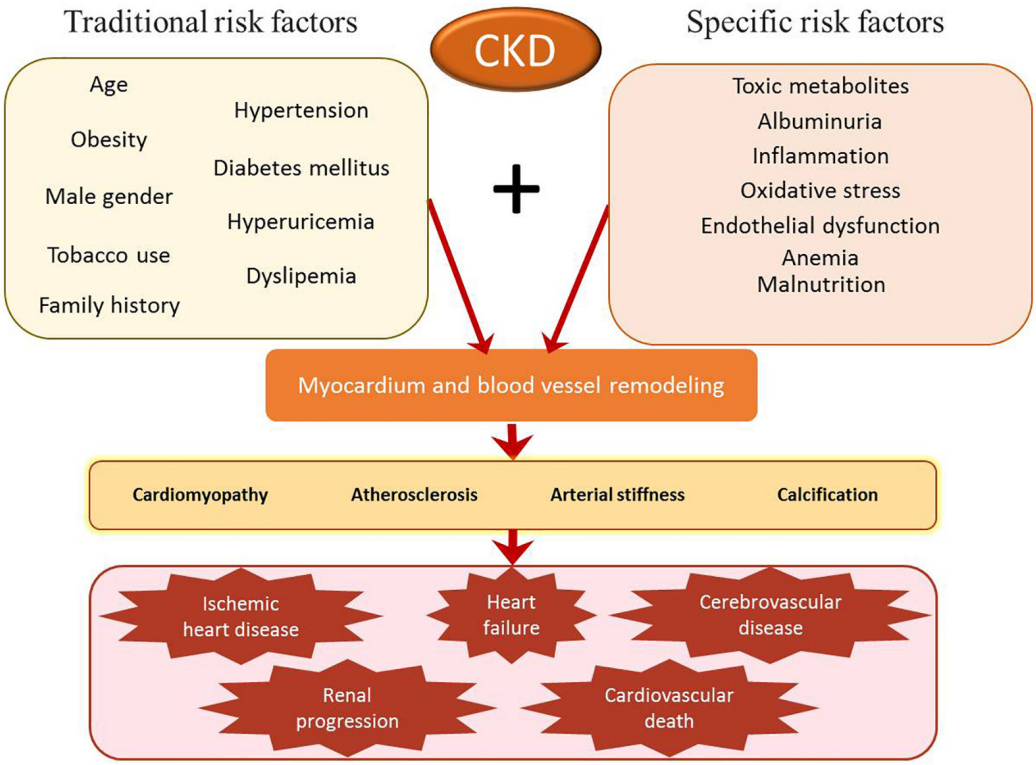

FIGURE 1 | Risk factors for cardiovascular morbidity and mortality in patients with chronic kidney disease (CKD). Traditional risk factors (such as hypertension and diabetes mellitus) and specific CKD risk factors (such as albuminuria or inflammation) lead to remodeling of the myocardium and blood vessels. This process may contribute to the development and progression of cardiomyopathy, atherosclerosis, arterial stiffness, and calcification. Without treatment, these alterations may progress to ischemic heart disease, heart failure, cerebrovascular disease, renal progression, and cardiovascular death.

In patients with CKD, traditional cardiovascular risk factors, such as hyperlipidemia and hypertension, are associated with an inflammatory process (Silverstein, 2009). Specific cardiovascular risk factors in CKD patients, such as accumulation of uremic toxins inherent to the use of renal replacement techniques, promote inflammation and are also associated with CVDs (Silverstein, 2009). The chronic, systemic, and low-grade inflammation usually observed in patients with CKD is a long and generalized process that shows no signs of acute inflammation and is mediated by moderate levels of cytokines and inflammatory mediators (Ramirez et al., 2006). The systemic nature and low intensity of this inflammatory response indicate lack of injury and no loss of functionality in these specific tissues; injury and loss of function are distinctive features in both acute and chronic inflammation (Furman et al., 2019). Conversely, the damage generated by systemic inflammation (SI) causes a deterioration in the general state, favoring tumor processes or degenerative diseases such as CVDs (Ungvari et al., 2018).

A similar SI process that is associated with aging is called *inflammaging* (Flynn et al., 2019). SI is considered an adaptive response that causes systemic damage, leading to the development of multiple pathologies, including CVDs (Oishi and Manabe, 2016).

Chronic, low-grade inflammation can be determined by measuring plasma levels of markers such as C reactive protein (CRP) (Sproston and Ashworth, 2018) and cytokines such as IL-6 and TNF-α. In a longitudinal analysis, CRP, measured at baseline during the Modification of Diet in Renal Disease (MDRD) study, was an independent predictor of all-cause and CVD-caused mortality (Levey et al., 1999). In dialysis patients, the association of CRP with mortality was main at low CRP levels, the lower CRP level, the lower mortality risk (Bazeley et al., 2011). Other pro- and anti-inflammatory cytokines, including IL-10 and TNF-α, may also play a role in the development of CKD-associated CVDs (Ekdahl et al., 2017; Mihai et al., 2018).

Although the mechanisms triggering innate immunity and associated inflammation in CKD are still scarce, in spite of some studies have shown that low levels of bacterial endotoxins reached the blood circulatory system in CKD patients, stimulate CKD-associated pathways. Endotoxemia is more prevalent in patients with CKD than in healthy population, and it is linked with CKD-associated CVDs (Ramezani and Raj, 2014; Sirich et al., 2014). Endotoxins, which act as pro-inflammatory stimuli, is linked to endothelial dysfunction, one of the earliest steps in the development of atherosclerosis. Highlighted that there is no data that described the mechanism in which the endotoxins from bacteria get into the circulation of CKD patients. In case the patient undergoes dialysis, the procedure may result the cause of the infection. However, endotoxemia is noted in stages of CKD that precede dialysis

(Wu et al., 2011), suggesting that factors unrelated to dialysis contribute to this process.

Disruption of the healthy intestinal barrier, among other factors, may facilitate the passage of bacterial endotoxins into circulation. Two protein-bound uremic toxins, indoxyl sulfate (IS), and p-cresyl sulfate, not removed by conventional dialysis induce inflammation and oxidative stress, causing vascular endothelial cell injury (Ramezani and Raj, 2014) and contributing to progression of renal impairment (Sirich et al., 2014) and CV-related mortality (Wu et al., 2011).

Therefore, physicians need to identify patients at risk and implement early prevention and treatment strategies in these patients. In practice, managing cardiovascular risk in patients with CKD mostly involves reducing modifiable risk factors such as hypertension, dyslipidemia, and disturbance of mineral and bone metabolism. Furthermore, dialysis adequacy and renal transplantation, preferably pre-emptive transplantation, are considered optimal therapies for the reduction of cardiovascular risk in these patients.

CHANGES IN CELLULAR BALANCE OF REACTIVE OXYGEN SPECIES CAN CAUSE CVDs IN CKD PATIENTS

Oxidative stress appears because of an imbalance between the production and elimination of reactive oxygen species (ROS). Moreover, oxidative stress is considered a hallmark feature of CKD-associated CVDs and contributes to all-cause mortality in this patient population. Also, physiological stress on the body of CKD patients is increased in very early stages of the disease, progresses parallel to the deterioration of renal function and is further exacerbated in patients undergoing dialysis (Liakopoulos et al., 2017, 2019b). In fact, ESRD patients on both hemodialysis (HD) and peritoneal dialysis (PD) manifest significantly enhanced oxidative stress compared with that of predialysis uremic patients (Liakopoulos et al., 2017, 2019a,b). However, the link between the initiation of CKD and oxidative stress remains debated.

Aging *per se* is a physiological process. However, aging is associated with several age-related diseases such as CVDs and CKD. According to the "oxidative stress theory of aging," aging and age-related diseases are precipitated by chronic oxidative stress (Sies, 1986). Therefore, because incidence of CKD is high in older persons and age is considered the most consistent risk factor for CVDs (O'Hare et al., 2007; Elewa et al., 2012), CKD is often examined in the context of aging (Nitta et al., 2013). Furthermore, other fundamental mechanisms that characterize biological aging (López-Otín et al., 2013), such as cellular senescence, mitochondrial dysfunction, loss of proteostasis, or altered intercellular communication (López-Otín et al., 2013), may also play central roles in the pathogenesis of CKD-associated CVDs (Shimizu and Minamino, 2019). In this context, several studies have shown that CKD promotes cellular senescence and accelerates premature aging via diverse mechanisms in the internal milieu such as redox state perturbations, oxidative damage, inflammation, toxicity, and localized signaling mediated by growth factors (Stenvinkel and Larsson, 2013; Dai et al., 2019).

Low-grade inflammation (involving increased levels of circulating inflammatory mediators in the absence of infection), which is another characteristic feature of aging and age-related diseases (De la Fuente and Miquel, 2009), is a crucial component of CKD (Mihai et al., 2018). Although the precise mechanisms contributing to the high prevalence of inflammation in CKD are not well established, ROS may potentially contribute to inflammation during declining renal function (Cachofeiro et al., 2008). Oxidative stress and inflammation are interlinked processes (De la Fuente and Miquel, 2009). The highly reactive ROS can alter cellular structures and functional pathways. This triggers a vicious cycle in which inflammatory cells, stimulated by cell damage caused by ROS, generate a state of oxidative stress and amplified oxidative damage (Mihai et al., 2018). Therefore, cross-talk between oxidative stress, inflammation, and aging/senescence represents a fundamental triad contributing to the development and progression of CKD-associated CVDs (Cachofeiro et al., 2008; Popolo et al., 2013).

In CKD patients, a pro-oxidative physiologic state leads to oxidative tissue damage (Cachofeiro et al., 2008; Puchades Montesa et al., 2009; Popolo et al., 2013). Indeed, oxidative stress and damage increase in later stages of CKD and become severe in ESRD patients undergoing HD and PD (Liakopoulos et al., 2017, 2019a,b). Several oxidative stress parameters gradually increase when renal disease progresses (**Table 1**), suggesting that a decline in renal function may have a direct effect on the worsening of oxidative stress (Dounousi et al., 2006; Khansari et al., 2009). HD and PD procedures further exacerbate oxidative stress via different underlying mechanisms. In HD patients, several factors, such as duration of dialysis, biocompatibility of dialyzer membrane and dialysate, intravenous iron administration, activation of leukocytes, retention of uremic toxins, or anemia, contribute to the development and accumulation of oxidative products. In addition, the composition of PD dialysate solutions (such as increased osmolarity, low pH, high-glucose content, and presence of lactate buffer) can trigger oxidative stress in PD patients (Liakopoulos et al., 2017, 2019a,b; Roumeliotis et al., 2019a). However, PD is considered to be more biocompatible than HD. Indeed, HD shows increased accumulation of pro−oxidants and depletion of antioxidants compared with PD (Liakopoulos et al., 2017, 2019a,b; Roumeliotis et al., 2019a).

Table 1 lists clinical studies on triggers of oxidative stress and damage in patients with CKD and ESRD undergoing HD or DP. The underlying mechanisms responsible for oxidative stress in CKD include: increased production and decreased clearance of ROS and other oxidant compounds, such as reactive nitrogen species or chlorinated oxidants; impaired function of antioxidant systems, including both enzymatic [i.e., catalase, superoxide dismutase (SOD), glutathione peroxidase (GPx)], and non-enzymatic [i.e., glutathione (GSH), thioredoxins, and vitamins C, E, and A] systems (Kobayashi et al., 2005; Popolo et al., 2013; Gondouin et al., 2015); increased oxidation of lipids, proteins, and DNA. Indeed, CKD patients show elevated levels of lipid-peroxidation

TABLE 1 | Factors participating in oxidative stress and damage in patients with CKD, ESRD, and those undergoing HD or DP.

Number of patients	Localization	Parameters	Results	References
31 HC	Whole blood	GSH	HC = mild > moderate > severe CRF = HD	Ceballos-Picot et al., 1996
83 mild CRF	Erythrocytes	GSSG	HC = mild < HD < moderate < severe CRF HC < HD < mild = moderate = severe CRF	
55 moderate CRF	Plasma	GPx	HD < HC < mild < moderate < severe CRF HD < HC = mild = moderate = severe CRF	
47 severe CRF		GSSG	HD < PD < severe < moderate < mild CRF < HC HD > PD > mild = moderate = severe CRF > HC	
18 HD		Cu/Zn-SOD		
30 PD		GSH		
		GSSG		
31 HC	Plasma	AOPPs	HC = mild < moderate < advance CRF	Witko-Sarsat et al., 1998
73 mild CRF		AGE-pentoside	HC < mild < moderate < advance CRF	
53 moderate CRF		MDA	HC < mild = moderate = advance CRF	
36 advanced CRF		GPx	HC > mild > moderate > advance CRF	
61 HC	Serum	TBARS; TAS	HC = CRF	Annuk et al., 2001
37 CRF	RBCs	LOOH	HC < CRF	
		GSH	HC > CRF	
		GSSG; GSSG/GSH	HC < CRF	
70 HC	Plasma	Thiols	HC > CKD	Oberg et al., 2004
60 CKD		Carbonyls	HC < CKD	
		F2-isoprotanes	HC < CKD	
		CRP	HC < CKD	
		IL-6	HC < CKD	
67 HC	Plasma	MDA	HC < CKD	Puchades Montesa et al., 2009
32 CKD (stage 4)		Carbonylated protein	HC < CKD	
		F2-isoprotanes	HC < CKD	
		GSH	HC > CKD	
		GSSG/GSH	HC < CKD	
		CAT; GR; GPx; SOD	HC > CKD	
		8-OH-dG	HC < CKD	
21 HC	PBMNs	ROS	HC < CKD	Fortuño et al., 2005
22 CKD (stages 1 and 2)		NADPH oxidase	HC < CKD	
38 HC	Plasma	Vitamin C	HC > CKD > HD	Gondouin et al., 2015
51 CKD (stages 3, 4 and 5) 50 HD	RBCs	Zn	HC > CKD = HD	
		SOD	HC = CKD > HD	
		XO	HC < CKD < HD	
		MDA	HC = CKD < HD	
1539 HD	Serum	AOPPs	HD > PD	Zhou et al., 2012
556 PD		MDA	HD > PD	

8-OHdG: 8-hydroxy deoxyguanosine; AGEs: advanced glycation end-products; AOPPs: advanced oxidation protein products; CAT: catalase; CKD: chronic kidney disease; CRP: C-reactive protein; Cu: copper; GPx: glutathione peroxidase; GR: glutathione reductase; GSH: reduced glutathione; GSSG: oxidized glutathione; GSSG/GSH: ratio of oxidized/reduced glutathione; HC: healthy controls; HD: hemodialysis; IL-6: interleukin 6; LOOH: lipid hydroperoxides; MDA: malondialdehyde; PBMNs: peripheral blood mononuclear cells; PD: peritoneal dialysis; RBCs: red blood cells; ROS: reactive oxygen species; Se: selenium; SOD: superoxide dismutase; TAS: total antioxidant status; TBARS: thiobarbituric acid reactive substances; XO: xanthine oxidase; Zn: zinc.

products [such as lipid hydroperoxides and malondialdehyde (MDA), thiobarbituric acid-reactive substances (TBARS), 4-hydroxynonenal (HNE), and F2-isoprostanes], oxidized LDL, protein carbonyls, advanced-oxidation protein products (AOPPs), advanced-glycation end products (AGEs), as well as 8-hydroxy-2′-deoxyguanosine (8-OH-dG) and 8-oxo-7,8-dihydro-2′-deoxyguanosine (8-oxo-dG). These factors contribute to atherosclerotic lesions in these patients (Popolo et al., 2013; Sung et al., 2013; Daenen et al., 2019). Moreover, genetic polymorphisms and mutations in DNA repair genes, such as *FAN1* or *hOGG1*, and DNA repair nucleases, are involved in increased accumulation of damaged nuclear DNA, which contributes to progressive loss of kidney function (Stenvinkel and Larsson, 2013; Sung et al., 2013). Uremic toxins, such as IS, homocysteine, and AGEs, contribute to early senescent of endothelial cells, and also play critical roles in the development

of CKD. In CKD patients, progressive deterioration of renal function leads to the accumulation of uremic toxins, which can promote oxidative stress and inflammatory pathways (Sung et al., 2013). For instance, IS induces uncoupling of endothelial nitric oxide synthase (eNOS) and increased expression and activity of nicotinamide adenine dinucleotide phosphate (NADPH) oxidases, leading to increased levels of ROS and endothelial dysfunction in patients with CKD (Yu et al., 2011; Daenen et al., 2019). High IS concentration is a risk factor for CKD-associated CVDs and accelerates the progression of CKD (Yu et al., 2011; Sung et al., 2013). Moreover, IS enhances the production of mitochondrial ROS and downregulates the expression of cellular protective factors by activating NF-κB and related signaling by nuclear factor erythroid-derived 2-like 2 (NRF2), hemeoxygenase-1 (HO-1), and NADPH quinone oxidoreductase-1. In addition to causing increased levels of ROS, this cascade also upregulates the production of pro-inflammatory cytokines (Dou et al., 2007; Zakkar et al., 2009; Masai et al., 2010; Hwang et al., 2019). Moreover, NRF-2 downregulates the expression of proteins involved in mitogen-activated protein kinase (MAPK) pathways, contributing to cellular apoptosis and senescence (Zakkar et al., 2009; Tebay et al., 2015). **Figure 2** shows the relationship between oxidative stress and CKD-associated CVDs.

In addition to formation and accumulation of pro-oxidant molecules, CKD patients, especially those undergoing dialysis, can also suffer a considerable downregulation in antioxidative and defensive mechanisms. This is associated with several factors, such as malnutrition, dietary restrictions, or loss of vitamins and trace elements occurring during HD or PD (Liakopoulos et al., 2017, 2019b; Roumeliotis et al., 2019a). Implementing lifestyle interventions, such as administration of exogenous antioxidants, in patients with CKD on dialysis may downregulate the inflammation and oxidative stress associated with CVD-linked morbidity and mortality even in early stages of CKD (Liakopoulos et al., 2019a,b; Roumeliotis et al., 2019b). Indeed, several studies have investigated the possible benefits of exogenous antioxidant administration in both HD and PD patients. Whether vitamins (B, C, D, and E), statins, coenzyme Q-10, N-acetylcysteine (NAC), omega-3 fatty acids, flavonoids, polyphenols, curcumin, green tea, and L-carnitine are beneficial in HD and PD patients remains controversial. Although these data are limited and mainly derived from animal studies or small observational trials, they have generally shown that daily intake of vitamin C and E, NAC, polyphenols, curcumin, or flavonoids, combined with a standard urate-lowering therapy, may act synergistically to ameliorate the deleterious effects of hyperuricemia and oxidative stress in

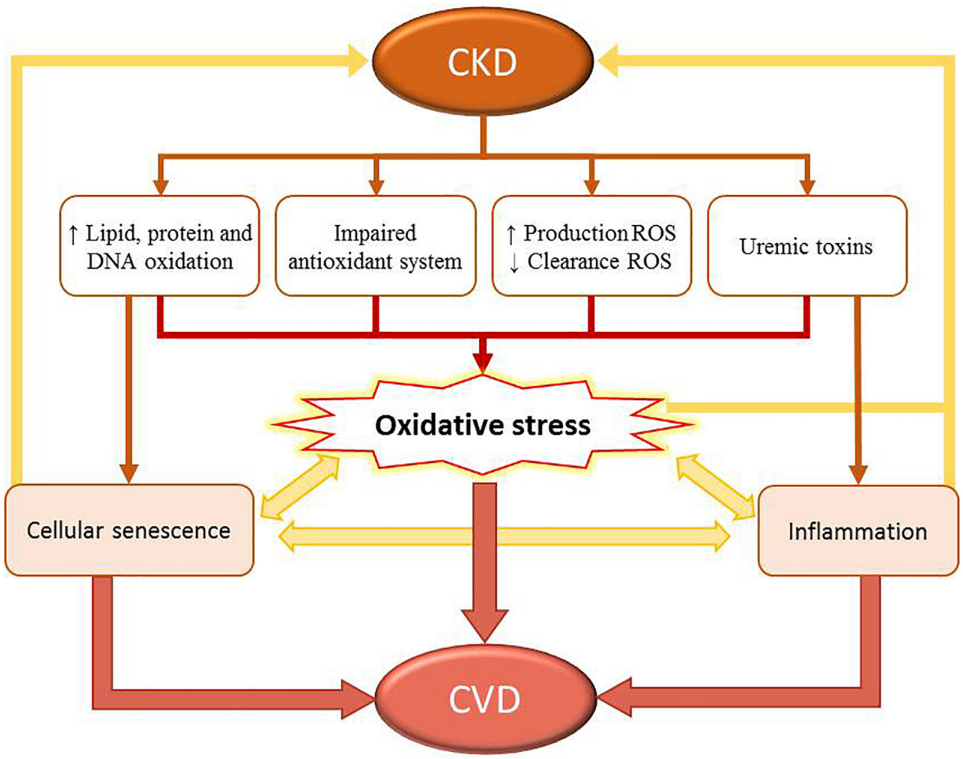

FIGURE 2 | Relationship between oxidative stress and CKD-associated cardiovascular disease (CVDs). CKD leads to increased damage of biomolecules (such as lipids, proteins, and DNA), impairment of the antioxidant system, increased levels of reactive oxygen species (ROS), decreased ROS clearance, and high concentration of uremic toxins in circulation. This process increases the levels of oxidative stress. CKD is also associated with systemic inflammation, mitochondrial dysfunction, loss of proteostasis, altered intercellular communication, and cellular senescence. Combined, these factors contribute to increased levels of oxidative stress in this patient population. However, cellular senescence and inflammation also participate in the development and progression of CVDs.

CKD (Liakopoulos et al., 2019a,b; Roumeliotis et al., 2019b). However, further studies in large cohorts of HD and PD patients are necessary to determine the causality between antioxidant supplementation and clinical hard end-points of CVDs and all-cause mortality.

IMMUNE ALTERATIONS IN PATIENTS WITH CKD AND THEIR RELATIONSHIP WITH VASCULAR PATHOLOGY

CKD is classically associated with immunodeficiency that contributes considerably to all-cause morbidity and mortality (Cohen and Hörl, 2012). Patients with CKD and those undergoing renal replacement therapy show quantitative alterations in components of the immune system and altered functionality of these components. Numerous studies have focused on relationships between immune-cell senescence and early onset of CKD-associated CVDs.

The number and function of lymphoid cells suffer a decrease associated with the loss of the renal function. This is characterized by loss of thymic function, shortening of telomeres, and expansion of memory T-cell populations, which is compatible with the concept of premature immune aging (Georgin-Lavialle et al., 2010).

Total lymphopenia is a marker of overall mortality in patients on hemodialysis (Pahl et al., 2010; Saad et al., 2014). Patients with ESRD or those undergoing renal replacement therapy show a decreased response to specific pathogens and vaccines. These patients also show an increased susceptibility to intracellular pathogens and increased incidence of tumors compared with the general population (Eleftheriadis et al., 2007). Different subtypes of lymphocyte populations and immunoglobulins play ambivalent roles in atherosclerosis. Some lymphocytes and immunoglobulins (T-helper lymphocytes, natural killer cells, T-cytotoxic lymphocytes, and B2 cells, and IgG- and IgE-secreting cells) play a pro-atherogenic role, while others [Tregs, B1a cells, innate response activator (IRA) B cells, Bregs, and natural IgM-secreting cells] show protective functions in healthy subjects (Tsiantoulas et al., 2015). A previous study has examined the roles of different subtypes of T lymphocytes and their cytokines in patients with CVDs and ESRD or those undergoing renal replacement therapy (Danyan et al., 2013). In patients with CKD, studies have focused on the roles of T lymphocytes, increased numbers of Th17 cells, and their proatherogenic activity (Danyan et al., 2013) (**Figure 3**).

The roles of B cells in the development of CKD-associated CVDs are unclear. Patients undergoing hemodialysis frequently develop lymphopenia B. This is due to increased cellular apoptosis that results from decreased Bcl-2 expression, and resistance to interleukin-7 (IL-7) and B-cell-activating factor of the TNF family (BAFF), which is necessary for the differentiation and survival of B lymphocytes (Fernández-Fresnedo et al., 2000; Pahl et al., 2010). B cells are classified into subtypes B1 (B1a and B1b) and B2 (**Figure 3**). Patients on hemodialysis have decreased numbers of both B1 (atherogenic B1a) and B2 (proatherogenic) lymphocytes, although the reduction in B1 lymphocytes is generally more significant (Pahl et al., 2010). This milieu causes a chronic imbalance favoring pro-endogenous B lymphocytes, which increase the incidence of cardiovascular pathology.

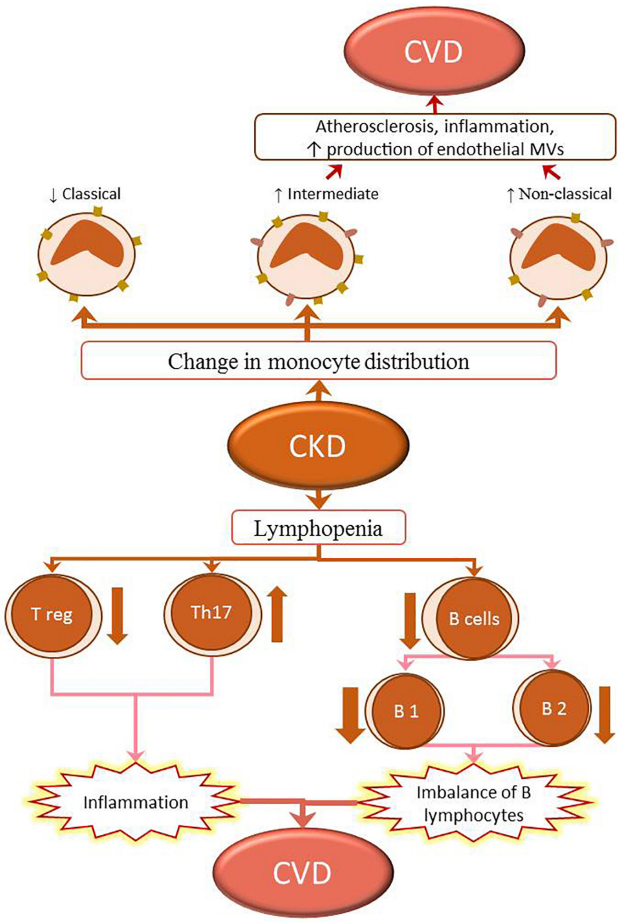

FIGURE 3 | Changes in the immune system in CKD lead to the development of CVD. The populations of classical (CD14++CD16-) monocytes in CKD decrease, while those of intermediate (CD14++CD16+) and non-classical (CD14+CD16+) monocytes increase. The intermediate (CD14++CD16+) and non-classical (CD14+CD16+) monocytes promote inflammation and proatherogenic milieu by upregulating the expression of adhesion molecules and production of microvesicles (MVs) in the endothelium; this contributes to the development of CVD in patients with CKD. Lymphopenia of both T and B lymphocytes is observed in CKD. The T lymphopenia is caused by the reduction of T regulatory cells (Treg), contrariwise the increase of pro-inflammatory T helper 17 lymphocytes (Th17). These changes in proportion of regulatory cells to proinflammatory cells can lead to inflammation. B lymphopenia is caused by decreased numbers of B1 and B2 cells. The numbers of B1 lymphocytes generally show a greater decline than those of B2, resulting in a B-lymphocyte imbalance. These two processes also participate in the development of CKD-associated CVD.

A recent study, examining the roles of different lymphocyte populations in the mortality of hemodialysis patients in Spain, has shown that the number of B lymphocytes is an independent risk factor for overall mortality in this patient population. The study has shown that cardiovascular pathology is the leading cause of mortality in these patients, and that

a relationship exists between decreased B-cell numbers and mortality from cardiovascular causes. The leading cause of mortality in this study was cardiovascular, and in this aspect, there was a relationship between the decrease in B cells and the mortality of cardiovascular causes, confirming this data with the determination of B lymphocytes at 12 months of follow-up. Conversely, patients with a CD56+ lymphopenia show a higher prevalence of mortality from infectious causes (Molina et al., 2018).

Patients with ESRD currently show high mortality; therefore, multiple parameters have been evaluated to predict the mortality of this population (Floege et al., 2015). CD19 lymphopenia may be a new marker for predicting the risk for morbidity and mortality in patients on hemodialysis. Therefore, accurate and timely diagnosis of CD19 lymphopenia in patients with ESRD and those undergoing dialysis may lead to new therapeutic targets against CKD.

The three subpopulations of peripheral blood monocytes, identified in the innate immune system, are: classical monocytes (CD14++/CD16-), existing mainly in healthy subjects; intermediate monocytes (CD14++/CD16+); and non-classical monocytes (CD14+/CD16+). Intermediate monocytes (CD14++/CD16+) may be involved in the development of atherosclerosis both in the general population and in patients with CKD (Georgin-Lavialle et al., 2010; Merino et al., 2011). CD14+/CD16+ monocytes are inflammatory cells with high capacity to produce pro-inflammatory cytokines and possess a robust dendritic-cell – like function. In peripheral blood of elderly individuals and patients with CKD, non-classical monocytes accumulate because of their increased resistance to apoptosis (Ramírez et al., 2005). CD14+/CD16+ cells express elevated levels of adhesion molecules and chemokines and show high adhesion capacity on endothelial cells (ECs). In ECs, CD14+/CD16+ cells induce increased expression of angiogenic factors and production of microvesicles (MVs), which are instrumental in induction of vascular damage (Merino et al., 2011). Therefore, accumulation of CD14+/CD16+ monocytes in peripheral blood plays a prominent role in inducing and perpetuating the inflammatory process in elderly individuals and patients with CKD and may have a direct relationship with the development of CVDs (**Figure 3**).

CELLULAR ALTERATIONS IN THE VASCULAR SYSTEM OF PATIENTS WITH CKD

The sustained microinflammatory milieu that persists in patients with CKD may be related to increased endothelial damage (Merino et al., 2010; Cohen and Hörl, 2012). Changes in endothelium are considered main factors indicating vascular deterioration in the early detection of CVDs (Heine et al., 2012). Endothelial aging, associated with age or induced by CKD, favors endothelial dysfunction (Ramírez et al., 2005). *In vitro* studies have shown that uremia determines a state of senescence in ECs, which is also associated with chronic inflammation (Carracedo et al., 2013). Therefore, both endothelial damage/dysfunction and inflammation likely play important roles in the initiation and progression of cardiovascular complications associated with CKD (Ross, 1999).

Endothelial damage is associated with increased production of extracellular vesicles (EVs). EVs serve as a signaling system between the factors involved in the function and homeostasis of the organism (Ekdahl et al., 2017). EVs are classified into three types based on their biogenesis: exosomes, MVs, and apoptotic bodies (Yáñez-Mó et al., 2015; van Niel et al., 2018). EVs are produced by most cell types, especially when cells are in contact with liquids. EVs are also produced under physiological and pathological conditions, although their number and molecular content differ under both conditions; indeed, of the potential use of EVs as pathological markers is based on these differences (Yuana et al., 2013). Aging and stress also induce changes in EVs. EVs are involved in the origin and development of various pathologies, and may be used as potential biomarkers or therapeutic agents in patients with CVDs (Amosse et al., 2017; Jansen et al., 2017; Dickhout and Koenen, 2018). EVs are involved in the development of renal dysfunction (Karpman et al., 2017; Lv et al., 2019), and can, therefore, be used in the diagnosis of, and therapy against, these diseases (Zhang et al., 2016). Elimination of EVs is currently used as a therapeutic strategy (Tang and Liu, 2019). Endothelial MVs can serve as useful biomarkers of CKD (Carmona et al., 2017a) because endothelial damage is associated with CKD, and the release of EVs is enhanced during endothelial injury. Uremic toxins (such as IS) also induce a release of endothelial MVs (Carmona et al., 2017b). Not only are plasma EVs modified in kidney diseases, but the release of EVs from renal cells (epithelial cells, podocytes, and tubular cells) is also altered. These kidney-derived EVs can be isolated from urine and used as biomarkers of CKD (Lv et al., 2019). Proteomic analyses have shown differences in urinary EVs obtained from patients with kidney diseases (Bruschi et al., 2019). These differences can be used to establish stages in the development of kidney (Stokman et al., 2019). In addition to serving as biomarkers, blood and urinary MVs play functional and therapeutic roles in renal diseases (Erdbrügger and Le, 2016; Kwon, 2019). For example, blood EVs influence renal physiology via intranephron communication (Lv et al., 2019), and their antibacterial (Hiemstra et al., 2014) and protective effects (Bruno et al., 2009, 2016; Rovira et al., 2017) have been demonstrated in kidney diseases. ROS are important in the origination and development of CKD, while MVs play antioxidative roles in this condition (Bodega et al., 2019).; However, the specific roles of blood and urinary MVs in redox dysregulation occurring in CKD have not been determined.

MVs microRNAs MEDIATE CKD-ASSOCIATED CVDs

MicroRNAs (miRNAs) are small, approximately 22-nucleotide long strands of small non-coding RNAs that regulate post-transcriptional processes (Ramshani et al., 2019; Rios et al., 2019). Unlike RNA, miRNAs show high stability in fluids and can be

reliably detected in the blood (Mitchell et al., 2008). MiRNAs levels differ in healthy and diseased tissues (Liu et al., 2019) and play a critical role in the maintenance of cardiovascular homeostasis (Pfeifer et al., 2015). EV-associated miRNAs have been studied extensively (Liu et al., 2019; Ramshani et al., 2019). Numerous studies have shown that miRNAs can be used as valuable pathological and therapeutic biomarkers in both cells and EVs (Bekris and Leverenz, 2015; Lei et al., 2017). Therefore, miRNAs may act as master regulators of signaling pathways involved in CKD-associated CVDs. Moreover, different profiles of EVs miRNAs in injured cells can be used as diagnostic markers in various pathologies such as cancer (Chen et al., 2019), viral infections (Yoshikawa et al., 2019), lung diseases (Chen et al., 2017), ischemic stroke (van Kralingen et al., 2019), CVDs (Bellin et al., 2019), and especially CKD-associated CVDs (Jansen et al., 2017; Blaser and Aikawa, 2018). Cells from vascular walls may selectively package miRNAs as molecular cargo in EVs (Rios et al., 2019).

CKD-associated CVDs are associated with premature aging. Accelerated aging of the vascular wall induces a senescent phenotype in vessel cells, and particularly in ECs (Carracedo et al., 2018a,b). EVs, released by senescent cells, are involved in mechanisms driving the acquisition of this senescent phenotype in ECs, which promotes the progression of CVDs. miRNA-loaded

TABLE 2 | Highlighted miRNAs mediate homeostasis of the vascular wall.

MiRNAs	Expression	Target	Function	Inverse (negative) regulated by	References
Healthy ECs					
miR-155	↓(Down)	Endothelial nitric oxide synthase (eNOS)	Endothelium, vascular relaxation	Inflammatory factor (TNF-α) (↑ miR-155)	Ballantyne et al., 2019; Chen et al., 2019
miR-126	↑(Up)	Vascular endothelial growth factor A (VEGF-A)	Angiogenesis	Sprouty-related EVH1 domain 1 (SPRED-1) (↓ miR-126)	Alique et al., 2019; Ballantyne et al., 2019
Physiological VSMC phenotype					
miR-21	↑(Up)	Phosphatase and tensin homolog (PTEN) B-cell lymphoma 2 (Bcl-2) expression	SMC proliferation and survival (anti-apoptotic)	Programmed cell death protein 4 (PDCD4)	Maegdefessel et al., 2015; Ballantyne et al., 2019
miR-143/145 cluster	↑(Up)	Transcription factors such as Kruppel-like factor (KLF)-4, (miR-145), KLF5, and ELK-1	VSMCs contractility and proliferation	Angiotensin-converting enzyme (ACE), KLF-4, myocardin	Maegdefessel et al., 2013; Maegdefessel et al., 2015; Metzinger-Le Meuth et al., 2017; Ballantyne et al., 2019; Vacante et al., 2019

TABLE 3 | MiRNAs involved in pathologies of the vasculature.

MiRNAs	Expression	Pathology	Effect	Via	References
Damage ECs					
miR-125b	↑(Up)	Stimulation or ischemia	Inhibition of *in vitro* tube formation	↓ VE-cadherin VEGF	Vosgha et al., 2018; Ballantyne et al., 2019
miR-126	↓ (Down)	Aging	Senescence	Hypoxia-inducible factor 1 (HIF-1)-α	Alique et al., 2019
		CKD	Endothelial dysfunction	CXCL12 V-CAM 1	Metzinger-Le Meuth et al., 2017
miR-34b-5p	↓ (Down)	Cancer	Proliferation and angiogenesis	VEGF-A	Maroof et al., 2017
miR-205	↑(Up)	Epithelial-to-mesenchymal transition (EMT) and cancer	Inhibition of tumor growth	VEGF-A	Vosgha et al., 2018
VSMCs phenotype regulation					
miR-21	↓ (Down)	Abdominal aortic aneurysms and atherosclerosis (unstable plaques in humans)	Antiproliferative	RE1-silencing transcription factor (REST)	Barwari et al., 2018
miR-143/145 cluster	↓ (Down)	Vascular injury (vascular remodeling), hypertension, atherosclerosis, and pulmonary-arterial hypertension	VSMC differentiation and phenotypic switch	↓ Jag-1/Notch ↓ SRF/Myocardin	Vacante et al., 2019
Alteractions in ECs and VSMCs					
miR-155	↓ (Down)	CKD osteoclastogenesis (vascular calcification)	Differentiation of monocytes/macrophages into osteoclast-like cells	↓TNF-α	Metzinger-Le Meuth et al., 2017
miR-223	↑(Up)	CKD (vascular calcification, osteoclastogenesis)	Transdifferentiation of VSMCs into an "osteoblast-like" phenotype	RhoB/MEF2C/SMαA	Metzinger-Le Meuth et al., 2017

EVs induce numerous injury-associated responses in other vascular cells, leading to the development of CVDs (Carracedo et al., 2018a). MiRNAs are essential to the homeostasis and maintenance of EC activity (Ballantyne et al., 2019). Some of the miRNAs involved in endothelial and vascular smooth muscle cell (VSMCs) homeostasis are described in **Table 2**.

MiRNAs modulation is critical in numerous disorders. For instance, miR-155 and miR-223 are responsible for the imbalance between calcium and phosphate that is observed in the vessels of patients with CKD. Moreover, patients with CKD show a dysregulation of miR-155 and miR-223, which causes their bones to lose calcium and phosphate; these ions are then accumulated in the vascular wall (Metzinger-Le Meuth et al., 2017). Recently, miR-223 has implied in the gene program of osteoclastogenesis and macrophage differentiation during the vascular calcification. This is a common complication in CKD that affects the vascular system due to pathological deposition of calcium and phosphate in the vessels (Metzinger-Le Meuth et al., 2017). Also, Ulbing et al. (2017) have shown that the expression of seric miR-223 is decreased in a murine model of CKD; decreased levels of seric miR-223 are also used to confirm CKD stage 4 and 5 diagnosis in patients with CKD. In this context, the levels of miR-155, miR-125b, and miR-145 are also decreased in stage 3-5D CKD patients (Chen et al., 2013).

Microvesicles (Hunter et al., 2008) and exosomes (Valadi et al., 2007) may actively play pathological roles in the development and progression of CVDs because they act as carriers of various miRNAs. miRNAs can be carried by RNA-binding proteins such as Argonaute 2 (Arroyo et al., 2011), or lipoprotein complexes such as HDL (Vickers et al., 2011). MiR-223 could be delivery, in part linked to HDL, toward to intima and media wall and could be transferred to ECs suppressing the expression of intercellular adhesion molecule 1 (ICAM-1) (Metzinger-Le Meuth et al., 2017). Accordingly, the results of our previous study show that both strands of miR-126 are encapsulated in endothelial MVs, and that vascular endothelial repair is mediated by miR-126 and HIF-1α (Alique et al., 2019). Results reported that miRNAs are involved in the senescence phenotype acquisition (Alique et al., 2017, 2019; Carracedo et al., 2018b). Several miRNAs–mediated pathological effects are described in **Table 3**.

MiR-145 is upregulated in the plasma of patients with stable coronary artery disease, stable or unstable angina, and acute myocardial infarction (Vacante et al., 2019). Nonetheless, EVs contain-associated miR-143 acts as a mediator of communication between ECs and VSMCs in CVDs. miR-143 in particular is associated with vascular remodeling in pulmonary arterial hypertension (Vacante et al., 2019), while the miR-143/145 cluster, released from VSMCs, modulates angiogenesis and EC proliferation (Climent et al., 2015; Vacante et al., 2019). These findings indicate that miR-143 and miR-145 regulate VSMCs phenotype and mediate the development of vascular diseases. Therefore, miRNA expression may be used as a biomarker of CKD-associated CVDs, while modulation of this expression can be used to develop novel therapeutic approaches against these diseases.

MiR-21 is linked with VSMCs physiological proliferation (Ballantyne et al., 2019) and kidney fibrosis because the abrogation of miR-21 has been described as a protector against the development of fibrosis (Metzinger-Le Meuth et al., 2017). Furthermore, miR-21 is upregulated in ECs collected from atheroma plaques and in progenitor cells obtained from patients with coronary artery disease (Pfeifer et al., 2015). Hence, the elimination of miR-21 could be a useful therapy to avoid the development of kidney fibrosis, whereas this effect could be hazardous for the normal VSMCs proliferation in the vessels. In this regard, the developing localized therapies in the kidney may reduce the risk of adverse events in this treatment approach (Barwari et al., 2018).

CONCLUSION AND FUTURE PERSPECTIVES

In this review, we discussed the cellular and molecular factors involved in accelerated senescence that is observed in patients with CKD. The aging process that occurs due to uremia is associated with numerous changes at the cellular and molecular level, which coincide with changes observed during the physiological aging process. These changes may explain some of the complications that typically occur in patients with CKD and CKD-associated CVDs. Expanding our understanding of the factors and molecules involved in accelerated senescence will serve to identify possible targets associated with this process. This will lead to improved methods of diagnosis and monitoring of these patients. Understanding the similarities between accelerated senescence and normal physiological aging will help establish new treatments. Further studies are needed to assess whether treatments aimed at delaying physiological aging can be applied in CKD.

AUTHOR CONTRIBUTIONS

JC chose the topic for this review and enlisted MA, CV, GB, NC, EM, MP, PS, and RR as coauthors. JC, MA, and RR defined the manuscript topic and outline conceived. All authors contributed to the writing and editing of this manuscript, and approved the final version of the manuscript.

FUNDING

This study has been funded by the Instituto de Salud Carlos III through the project "PI17/01029" and "PI19/00240" (co-funded by the European Regional Development Fund "A way to make Europe"), Santander/UCM PR41/17-20964, Sociedad Española de Nefrología, and Universidad de Alcalá grants (UAH-GP2018-4 and CCG2018/BIO-010). NC is a fellow of the program "Contratos Asociados a Proyectos de Investigación, Instituto de Investigación Sanitaria Hospital 12 de Octubre (imas12)," Madrid, Spain.

REFERENCES

Alique, M., Bodega, G., Giannarelli, C., Carracedo, J., and Ramírez, R. (2019). MicroRNA-126 regulates Hypoxia-Inducible Factor-1α which inhibited migration, proliferation, and angiogenesis in replicative endothelial senescence. *Sci. Rep.* 9:7381. doi: 10.1038/s41598-019-43689-3

Alique, M., Ruíz-Torres, M. P., Bodega, G., Noci, M. V., Troyano, N., Bohórquez, L., et al. (2017). Microvesicles from the plasma of elderly subjects and from senescent endothelial cells promote vascular calcification. *Aging* 9, 778–789. doi: 10.18632/aging.101191

Amosse, J., Martinez, M. C., and Le Lay, S. (2017). Extracellular vesicles and cardiovascular disease therapy. *Stem Cell Investig.* 4:102. doi: 10.21037/sci.2017.11.07

Annuk, M., Zilmer, M., Lind, L., Linde, T., and Fellström, B. (2001). Oxidative stress and endothelial function in chronic renal failure. *J. Am. Soc. Nephrol.* 12, 2747–2752.

Arroyo, J. D., Chevillet, J. R., Kroh, E. M., Ruf, I. K., Pritchard, C. C., Gibson, D. F., et al. (2011). Argonaute2 complexes carry a population of circulating microRNAs independent of vesicles in human plasma. *Proc. Natl. Acad. Sci. U.S.A.* 108, 5003–5008. doi: 10.1073/pnas.1019055108

Ballantyne, R. K. J., Stewart, M. D., Baker, D. J., and Schlosser, K. (2019). "MicroRNA and LncRNA in the Vascular System," in *Textbook of Vascular Medicine*, eds R. Touyz, and C. Delles (Cham: Springer), doi: 10.1007/978-3-030-16481-2_14

Barwari, T., Rienks, M., and Mayr, M. (2018). MicroRNA-21 and the vulnerability of atherosclerotic plaques. *Mol. Ther.* 26, 938–940. doi: 10.1016/j.ymthe.2018.03.005

Bazeley, J., Bieber, B., Li, Y., Morgenstern, H., de Sequera, P., Combe, C., et al. (2011). C-reactive protein and prediction of 1-year mortality in prevalent hemodialysis patients. *Clin. J. Am. Soc. Nephrol.* 6, 2452–2461. doi: 10.2215/CJN.00710111

Bekris, L. M., and Leverenz, J. B. (2015). The biomarker and therapeutic potential of miRNA in Alzheimer's disease. *Neurodegener. Dis. Manag.* 5, 61–74. doi: 10.2217/nmt.14.52

Bellin, G., Gardin, C., Ferroni, L., Chachques, J. C., Rogante, M., Mitrečić, D., et al. (2019). Exosome in cardiovascular diseases: a complex world full of hope. *Cells* 8:E166. doi: 10.3390/cells8020166

Blaser, M. C., and Aikawa, E. (2018). Roles and regulation of extracellular vesicles in cardiovascular mineral metabolism. *Front. Cardiovasc. Med.* 5:187. doi: 10.3389/fcvm.2018.00187

Bodega, G., Alique, M., Puebla, L., Carracedo, J., and Ramírez, R. M. (2019). Microvesicles ROS scavengers and ROS producers. *J. Extracell. Vesicles* 8:1626654. doi: 10.1080/20013078.2019.1626654

Bruno, S., Grange, C., Deregibus, M. C., Calogero, R. A., Saviozzi, S., Collino, F., et al. (2009). Mesenchymal stem cell-derived microvesicles protect against acute tubular injury. *J. Am. Soc. Nephrol.* 20, 1053–1067. doi: 10.1681/ASN.2008070798

Bruno, S., Porta, S., and Bussolati, B. (2016). Extracellular vesicles in renal tissue damage and regeneration. *Eur. J. Pharmacol.* 790, 83–91. doi: 10.1016/j.ejphar.2016.06.058

Bruschi, M., Granata, S., Santucci, L., Candiano, G., Fabris, A., Antonucci, N., et al. (2019). Proteomic analysis of urinary microvesicles and exosomes in medullary sponge kidney disease and autosomal dominant polycystic kidney disease. *Clin. J. Am. Soc. Nephrol.* 14, 834–843. doi: 10.2215/CJN.12191018

Cachofeiro, V., de Goicochea, M., Vinuesa, S. G., Oubiña, P., Lahera, V., and Luño, J. (2008). Oxidative stress and inflammation, a link between chronic kidney disease and cardiovascular disease. *Kidney Int.* 74, S4–S9. doi: 10.1038/ki.2008.516

Carmona, A., Agüera, M. L., Luna-Ruiz, C., Buendía, P., Calleros, L., García-Jerez, A., et al. (2017a). Markers of endothelial damage in patients with chronic kidney disease on hemodialysis. *Am. J. Physiol. Renal Physiol.* 312, F673–F681. doi: 10.1152/ajprenal.00013.2016

Carmona, A., Guerrero, F., Buendia, P., Obrero, T., Aljama, P., and Carracedo, J. (2017b). Microvesicles derived from Indoxyl sulfate treated endothelial cells induce endothelial progenitor cells dysfunction. *Front. Physiol.* 8:666. doi: 10.3389/fphys.2017.00666

Carracedo, J., Alique, M., Ramirez-Carracedo, R., Bodega, G., and Ramirez, R. (2018a). Endothelial extracellular vesicles produced by senescent cells: pathophysiological role in the cardiovascular disease associated with all types of diabetes mellitus. *Curr. Vasc. Pharmacol.* 17, 447–454. doi: 10.2174/1570161116666180820115726

Carracedo, J., Buendía, P., Merino, A., Soriano, S., Esquivias, E., Martín-Malo, A., et al. (2013). Cellular senescence determines endothelial cell damage induced by uremia. *Exp. Gerontol.* 48, 766–773. doi: 10.1016/j.exger.2013.04.004

Carracedo, J., Rafael, R.-C., Alique, M., and Ramírez-Chamond, R. (2018b). *Endothelial Cell Senescence in the Pathogenesis of Endothelial Dysfunction*. Rijeka: Intech.

Ceballos-Picot, I., Witko-Sarsat, V., Merad-Boudia, M., Nguyen, A. T., Thévenin, M., Jaudon, M. C., et al. (1996). Glutathione antioxidant system as a marker of oxidative stress in chronic renal failure. *Free Radic. Biol. Med.* 21, 845–853. doi: 10.1016/0891-5849(96)00233-x

Chen, J., Hu, C., and Pan, P. (2017). Extracellular vesicle microRNA transfer in lung diseases. *Front. Physiol.* 8:1028. doi: 10.3389/fphys.2017.01028

Chen, M., Xu, R., Rai, A., Suwakulsiri, W., Izumikawa, K., Ishikawa, H., et al. (2019). Distinct shed microvesicle and exosome microRNA signatures reveal diagnostic markers for colorectal cancer. *PLoS One* 14:e0210003. doi: 10.1371/journal.pone.0210003

Chen, N. X., Kiattisunthorn, K., O'Neill, K. D., Chen, X., Moorthi, R. N., Gattone, V. H., et al. (2013). Decreased microRNA is involved in the vascular remodeling abnormalities in chronic kidney disease (CKD). *PLoS One* 8:e64558. doi: 10.1371/journal.pone.0064558

Chen, S. C., Huang, J. C., Su, H. M., Chiu, Y. W., Chang, J. M., Hwang, S. J., et al. (2018). Prognostic cardiovascular markers in chronic kidney disease. *Kidney Blood Press Res.* 43, 1388–1407. doi: 10.1159/000492953

Climent, M., Quintavalle, M., Miragoli, M., Chen, J., Condorelli, G., and Elia, L. (2015). TGFβ triggers miR-143/145 transfer from smooth muscle cells to endothelial cells. Thereby Modulating Vessel Stabilization. *Circ. Res.* 116, 1753–1764. doi: 10.1161/CIRCRESAHA.116.305178

Cohen, G., and Hörl, W. H. (2012). Immune dysfunction in uremia—an update. *Toxins* 4, 962–990. doi: 10.3390/toxins4110962

Cottone, S., Lorito, M. C., Riccobene, R., Nardi, E., Mulè, G., Buscemi, S., et al. (2008). Oxidative stress, inflammation and cardiovascular disease in chronic renal failure. *J. Nephrol.* 21, 175–179.

Daenen, K., Andries, A., Mekahli, D., Van Schepdael, A., Jouret, F., and Bammens, B. (2019). Oxidative stress in chronic kidney disease. *Pediatr. Nephrol.* 34, 975–991. doi: 10.1007/s00467-018-4005-4

Dai, L., Qureshi, A. R., Witasp, A., Lindholm, B., and Stenvinkel, P. (2019). Early vascular ageing and cellular senescence in chronic kidney disease. *Comput. Struct. Biotechnol. J.* 17, 721–729. doi: 10.1016/j.csbj.2019.06.015

Danyan, C., Xiaolong, H., Song, L., Hua, G., Weixue, T., and Ke, L. (2013). The effects of rhBMP-2 and Treg/Th17 functional disequilibrium in uremic patients with cardiovascular complication after maintenance hemodialysis. *Int. J. Artif. Organs* 36, 464–472. doi: 10.5301/ijao.5000217

De la Fuente, M., and Miquel, J. (2009). An update of the oxidation-inflammation theory of aging: the involvement of the immune system in oxi-inflamm-aging. *Curr. Pharm. Des.* 15, 3003–3026. doi: 10.2174/138161209789058110

Dickhout, A., and Koenen, R. R. (2018). Extracellular vesicles as biomarkers in cardiovascular disease; chances and risks. *Front. Cardiovasc. Med.* 5:113. doi: 10.3389/fcvm.2018.00113

Dou, L., Jourde-Chiche, N., Faure, V., Cerini, C., Berland, Y., Dignat-George, F., et al. (2007). The uremic solute indoxyl sulfate induces oxidative stress in endothelial cells. *J. Thromb. Haemost.* 5, 1302–1308. doi: 10.1111/j.1538-7836.2007.02540.x

Dounousi, E., Papavasiliou, E., Makedou, A., Ioannou, K., Katopodis, K. P., Tselepis, A., et al. (2006). Oxidative stress is progressively enhanced with advancing stages of CKD. *Am. J. Kidney Dis.* 48, 752–760. doi: 10.1053/j.ajkd.2006.08.015

Ekdahl, K. N., Soveri, I., Hilborn, J., Fellström, B., and Nilsson, B. (2017). Cardiovascular disease in haemodialysis: role of the intravascular innate immune system. *Nat. Rev. Nephrol.* 13, 285–296. doi: 10.1038/nrneph.2017.17

Eleftheriadis, T., Antoniadi, G., Liakopoulos, V., Kartsios, C., and Stefanidis, I. (2007). Disturbances of acquired immunity in hemodialysis patients. *Semin. Dial.* 20, 440–451. doi: 10.1111/j.1525-139X.2007.00283.x

Elewa, U., Sanchez-Niño, M. D., Martin-Cleary, C., Fernandez-Fernandez, B., Egido, J., and Ortiz, A. (2012). Cardiovascular risk biomarkers in CKD: the

inflammation link and the road less traveled. *Int. Urol. Nephrol.* 44, 1731–1744. doi: 10.1007/s11255-012-0271-4

Erdbrügger, U., and Le, T. H. (2016). Extracellular vesicles in renal diseases: more than novel biomarkers? *J. Am. Soc. Nephrol.* 27, 12–26. doi: 10.1681/ASN.2015010074

Fernández-Fresnedo, G., Ramos, M. A., de González-Pardo, M. C., Francisco, A. L., López-Hoyos, M., and Arias, M. (2000). B lymphopenia in uremia is related to an accelerated in vitro apoptosis and dysregulation of Bcl-2. *Nephrol. Dial. Transplant* 15, 502–510. doi: 10.1093/ndt/15.4.502

Floege, J., Gillespie, I. A., Kronenberg, F., Anker, S. D., Gioni, I., Richards, S., et al. (2015). Development and validation of a predictive mortality risk score from a European hemodialysis cohort. *Kidney Int.* 87, 996–1008. doi: 10.1038/ki.2014.419

Flynn, M. G., Markofski, M. M., and Carrillo, A. E. (2019). Elevated inflammatory status and increased risk of chronic disease in chronological aging: Inflamm-aging or. *Aging Dis.* 10, 147–156. doi: 10.14336/AD.2018.0326

Fortuño, A., Beloqui, O., San José, G., Moreno, M. U., Zalba, G., and Díez, J. (2005). Increased phagocytic nicotinamide adenine dinucleotide phosphate oxidase-dependent superoxide production in patients with early chronic kidney disease. *Kidney Int. Suppl.* 22, S71–S75. doi: 10.1111/j.1523-1755.2005.09913.x

Furman, D., Campisi, J., Verdin, E., Carrera-Bastos, P., Targ, S., Franceschi, C., et al. (2019). Chronic inflammation in the etiology of disease across the life span. *Nat. Med.* 25, 1822–1832. doi: 10.1038/s41591-019-0675-0

Georgin-Lavialle, S., Aouba, A., Mouthon, L., Londono-Vallejo, J. A., Lepelletier, Y., Gabet, A. S., et al. (2010). The telomere/telomerase system in autoimmune and systemic immune-mediated diseases. *Autoimmun. Rev.* 9, 646–651. doi: 10.1016/j.autrev.2010.04.004

Go, A. S., Chertow, G. M., Fan, D., McCulloch, C. E., and Hsu, C. Y. (2004). Chronic kidney disease and the risks of death, cardiovascular events, and hospitalization. *N. Engl. J. Med.* 351, 1296–1305. doi: 10.1056/NEJMoa041031

Gondouin, B., Jourde-Chiche, N., Sallee, M., Dou, L., Cerini, C., Loundou, A., et al. (2015). Plasma xanthine oxidase activity is predictive of cardiovascular disease in patients with chronic kidney disease, independently of uric acid levels. *Nephron* 131, 167–174. doi: 10.1159/000441091

Heine, G. H., Ortiz, A., Massy, Z. A., Lindholm, B., Wiecek, A., Martínez-Castelao, A., et al. (2012). Monocyte subpopulations and cardiovascular risk in chronic kidney disease. *Nat. Rev. Nephrol.* 8, 362–369. doi: 10.1038/nrneph.2012.41

Hiemstra, T. F., Charles, P. D., Gracia, T., Hester, S. S., Gatto, L., Al-Lamki, R., et al. (2014). Human urinary exosomes as innate immune effectors. *J. Am. Soc. Nephrol.* 25, 2017–2027. doi: 10.1681/ASN.2013101066

Hill, N. R., Fatoba, S. T., Oke, J. L., Hirst, J. A., O'Callaghan, C. A., Lasserson, D. S., et al. (2016). Global prevalence of chronic kidney disease - a systematic review and meta-analysis. *PLoS One* 11:e0158765. doi: 10.1371/journal.pone.0158765

Hunter, M. P., Ismail, N., Zhang, X., Aguda, B. D., Lee, E. J., Yu, L., et al. (2008). Detection of microRNA expression in human peripheral blood microvesicles. *PLoS One* 3:e3694. doi: 10.1371/journal.pone.0003694

Hwang, H. V., Lin, Y., Rebuffatti, M. N., Tran, D. T., Lee, L., Gomes, A. V., et al. (2019). Impaired proteostasis in senescent vascular endothelial cells: a perspective on estrogen and oxidative stress in the aging vasculature. *Am. J. Physiol. Heart Circ. Physiol.* 316, H421–H429. doi: 10.1152/ajpheart.00318.2018

Jansen, F., Li, Q., Pfeifer, A., and Werner, N. (2017). Endothelial- and immune cell-derived extracellular vesicles in the regulation of cardiovascular health and disease. *JACC Basic Transl. Sci.* 2, 790–807. doi: 10.1016/j.jacbts.2017.08.004

Jun, M., Lv, J., Perkovic, V., and Jardine, M. J. (2011). Managing cardiovascular risk in people with chronic kidney disease: a review of the evidence from randomized controlled trials. *Ther. Adv. Chronic Dis.* 2, 265–278. doi: 10.1177/2040622311401775

Karpman, D., Ståhl, A. L., and Arvidsson, I. (2017). Extracellular vesicles in renal disease. *Nat. Rev. Nephrol.* 13, 545–562. doi: 10.1038/nrneph.2017.98

Keith, D. S., Nichols, G. A., Gullion, C. M., Brown, J. B., and Smith, D. H. (2004). Longitudinal follow-up and outcomes among a population with chronic kidney disease in a large managed care organization. *Arch. Intern. Med.* 164, 659–663. doi: 10.1001/archinte.164.6.659

Khansari, N., Shakiba, Y., and Mahmoudi, M. (2009). Chronic inflammation and oxidative stress as a major cause of age-related diseases and cancer. *Recent Pat. Inflamm. Allergy Drug Discov.* 3, 73–80. doi: 10.2174/187221309787158371

Kobayashi, M., Sugiyama, H., Wang, D. H., Toda, N., Maeshima, Y., Yamasaki, Y., et al. (2005). Catalase deficiency renders remnant kidneys more susceptible to oxidant tissue injury and renal fibrosis in mice. *Kidney Int.* 68, 1018–1031. doi: 10.1111/j.1523-1755.2005.00494.x

Kwon, S. H. (2019). Extracellular vesicles in renal physiology and clinical applications for renal disease. *Korean J. Intern. Med.* 34, 470–479. doi: 10.3904/kjim.2019.108

Lei, Q., Liu, T., Gao, F., Xie, H., Sun, L., Zhao, A., et al. (2017). Microvesicles as potential biomarkers for the identification of senescence in human mesenchymal stem cells. *Theranostics* 7, 2673–2689. doi: 10.7150/thno.18915

Levey, A. S., Bosch, J. P., Lewis, J. B., Greene, T., Rogers, N., and Roth, D. (1999). A more accurate method to estimate glomerular filtration rate from serum creatinine: a new prediction equation. Modification of Diet in Renal Disease Study Group. *Ann. Intern. Med.* 130, 461–470. doi: 10.7326/0003-4819-130-6-199903160-00002

Liakopoulos, V., Roumeliotis, S., Bozikas, A., Eleftheriadis, T., and Dounousi, E. (2019a). Antioxidant supplementation in renal replacement therapy patients: Is there evidence? *Oxid. Med. Cell. Longev.* 2019:9109473. doi: 10.1155/2019/9109473

Liakopoulos, V., Roumeliotis, S., Gorny, X., Eleftheriadis, T., and Mertens, P. R. (2017). Oxidative stress in patients undergoing peritoneal dialysis: a current review of the literature. *Oxid. Med. Cell. Longev.* 2017:3494867. doi: 10.1155/2017/3494867

Liakopoulos, V., Roumeliotis, S., Zarogiannis, S., Eleftheriadis, T., and Mertens, P. R. (2019b). Oxidative stress in hemodialysis: causative mechanisms, clinical implications, and possible therapeutic interventions. *Semin. Dial.* 32, 58–71. doi: 10.1111/sdi.12745

Liu, T., Zhang, Q., Zhang, J., Li, C., Miao, Y. R., Lei, Q., et al. (2019). EVmiRNA: a database of miRNA profiling in extracellular vesicles. *Nucleic Acids Res.* 47, D89–D93. doi: 10.1093/nar/gky985

London, G. M., Pannier, B., Guerin, A. P., Blacher, J., Marchais, S. J., Darne, B., et al. (2001). Alterations of left ventricular hypertrophy in and survival of patients receiving hemodialysis: follow-up of an interventional study. *J. Am. Soc. Nephrol.* 12, 2759–2767.

López-Otín, C., Blasco, M. A., Partridge, L., Serrano, M., and Kroemer, G. (2013). The hallmarks of aging. *Cell* 153, 1194–1217. doi: 10.1016/j.cell.2013.05.039

Lv, L. L., Feng, Y., Tang, T. T., and Liu, B. C. (2019). New insight into the role of extracellular vesicles in kidney disease. *J. Cell. Mol. Med.* 23, 731–739. doi: 10.1111/jcmm.14101

Maegdefessel, L., Rayner, K. J., and Leeper, N. J. (2015). MicroRNA regulation of vascular smooth muscle function and phenotype: early career committee contribution. *Arterioscler. Thromb. Vasc. Biol.* 35, 2–6. doi: 10.1161/ATVBAHA.114.304877

Maegdefessel, L., Spin, J. M., Adam, M., Raaz, U., Toh, R., Nakagami, F., et al. (2013). Micromanaging abdominal aortic aneurysms. *Int. J. Mol. Sci.* 14, 14374–14394. doi: 10.3390/ijms140714374

Maroof, H., Islam, F., Ariana, A., Gopalan, V., and Lam, A. K. (2017). The roles of microRNA-34b-5p in angiogenesis of thyroid carcinoma. *Endocrine* 58, 153–166. doi: 10.1007/s12020-017-1393-3

Masai, N., Tatebe, J., Yoshino, G., and Morita, T. (2010). Indoxyl sulfate stimulates monocyte chemoattractant protein-1 expression in human umbilical vein endothelial cells by inducing oxidative stress through activation of the NADPH oxidase-nuclear factor-κB pathway. *Circ. J.* 74, 2216–2224. doi: 10.1253/circj.cj-10-0117

Matsushita, K., Coresh, J., Sang, Y., Chalmers, J., Fox, C., Guallar, E., et al. (2015). Estimated glomerular filtration rate and albuminuria for prediction of cardiovascular outcomes: a collaborative meta-analysis of individual participant data. *Lancet Diabetes Endocrinol.* 3, 514–525. doi: 10.1016/S2213-8587(15)00040-6

Merino, A., Buendia, P., Martin-Malo, A., Aljama, P., Ramirez, R., and Carracedo, J. (2011). Senescent CD14+CD16+ monocytes exhibit proinflammatory and proatherosclerotic activity. *J. Immunol.* 186, 1809–1815. doi: 10.4049/jimmunol.1001866

Merino, A., Portolés, J., Selgas, R., Ojeda, R., Buendia, P., Ocaña, J., et al. (2010). Effect of different dialysis modalities on microinflammatory status and endothelial damage. *Clin. J. Am. Soc. Nephrol.* 5, 227–234. doi: 10.2215/CJN.03260509

Metzinger-Le Meuth, V., Burtey, S., Maitrias, P., Massy, Z. A., and Metzinger, L. (2017). microRNAs in the pathophysiology of CKD-MBD: Biomarkers and

innovative drugs. *Biochim. Biophys. Acta Mol. Basis Dis.* 1863, 337–345. doi: 10.1016/j.bbadis.2016.10.027

Mihai, S., Codrici, E., Popescu, I. D., Enciu, A. M., Albulescu, L., Necula, L. G., et al. (2018). Inflammation-related mechanisms in chronic kidney disease prediction, Progression, and outcome. *J. Immunol. Res.* 2018:2180373. doi: 10.1155/2018/2180373

Mitchell, P. S., Parkin, R. K., Kroh, E. M., Fritz, B. R., Wyman, S. K., Pogosova-Agadjanyan, E. L., et al. (2008). Circulating microRNAs as stable blood-based markers for cancer detection. *Proc. Natl. Acad. Sci. U.S.A.* 105, 10513–10518. doi: 10.1073/pnas.0804549105

Molina, M., Allende, L. M., Ramos, L. E., Gutiérrez, E., Pleguezuelo, D. E., Hernández, E. R., et al. (2018). CD19. *Front. Immunol.* 9:1221. doi: 10.3389/fimmu.2018.01221

Nitta, K., Okada, K., Yanai, M., and Takahashi, S. (2013). Aging and chronic kidney disease. *Kidney Blood Press Res.* 38, 109–120. doi: 10.1159/000355760

Oberg, B. P., McMenamin, E., Lucas, F. L., McMonagle, E., Morrow, J., Ikizler, T. A., et al. (2004). Increased prevalence of oxidant stress and inflammation in patients with moderate to severe chronic kidney disease. *Kidney Int.* 65, 1009–1016. doi: 10.1111/j.1523-1755.2004.00465.x

O'Hare, A. M., Choi, A. I., Bertenthal, D., Bacchetti, P., Garg, A. X., Kaufman, J. S., et al. (2007). Age affects outcomes in chronic kidney disease. *J. Am. Soc. Nephrol.* 18, 2758–2765. doi: 10.1681/ASN.2007040422

Oishi, Y., and Manabe, I. (2016). Macrophages in age-related chronic inflammatory diseases. *NPJ Aging Mech. Dis.* 2:16018. doi: 10.1038/npjamd.2016.18

Pahl, M. V., Gollapudi, S., Sepassi, L., Gollapudi, P., Elahimehr, R., and Vaziri, N. D. (2010). Effect of end-stage renal disease on B-lymphocyte subpopulations, IL-7, BAFF and BAFF receptor expression. *Nephrol. Dial. Transplant* 25, 205–212. doi: 10.1093/ndt/gfp397

Pfeifer, P., Werner, N., and Jansen, F. (2015). Role and function of microRNAs in extracellular vesicles in cardiovascular biology. *Biomed Res. Int.* 2015:161393. doi: 10.1155/2015/161393

Popolo, A., Autore, G., Pinto, A., and Marzocco, S. (2013). Oxidative stress in patients with cardiovascular disease and chronic renal failure. *Free Radic. Res.* 47, 346–356. doi: 10.3109/10715762.2013.779373

Puchades Montesa, M. J., Gonz Rico, M. A., Solís Salguero, M. A., Torregrosa Maicas, I., Tormos Muñoz, M. C., Saez Tormo, G., et al. (2009). [Study of oxidative stress in advanced kidney disease]. *Nefrologia* 29, 464–473. doi: 10.3265/Nefrologia.2009.29.5.5493.en.full

Ramezani, A., and Raj, D. S. (2014). The gut microbiome, kidney disease, and targeted interventions. *J. Am. Soc. Nephrol.* 25, 657–670. doi: 10.1681/ASN.2013080905

Ramirez, R., Carracedo, J., Berdud, I., Carretero, D., Merino, A., Rodríguez, M., et al. (2006). Microinflammation in hemodialysis is related to a preactivated subset of monocytes. *Hemodial. Int.* 10(Suppl. 1), S24–S27. doi: 10.1111/j.1542-4758.2006.01186.x

Ramírez, R., Carracedo, J., Soriano, S., Jiménez, R., Martín-Malo, A., Rodríguez, M., et al. (2005). Stress-induced premature senescence in mononuclear cells from patients on long-term hemodialysis. *Am. J. Kidney Dis.* 45, 353–359. doi: 10.1053/j.ajkd.2004.10.022

Ramshani, Z., Zhang, C., Richards, K., Chen, L., Xu, G., Stiles, B. L., et al. (2019). Extracellular vesicle microRNA quantification from plasma using an integrated microfluidic device. *Commun. Biol.* 2:189. doi: 10.1038/s42003-019-0435-1

Rios, T. R. M., Montezano, F. J., and Burger, A. C. (2019). "Microparticles and Exosomes in Cell-Cell Communication," in *Textbook of Vascular Medicine*, eds R. Touyz, and C. Delles (Cham: Springer).

Ross, R. (1999). Atherosclerosis–an inflammatory disease. *N. Engl. J. Med.* 340, 115–126. doi: 10.1056/NEJM199901143400207

Roumeliotis, S., Eleftheriadis, T., and Liakopoulos, V. (2019a). Is oxidative stress an issue in peritoneal dialysis? *Semin. Dial.* 32, 463–466. doi: 10.1111/sdi.12818

Roumeliotis, S., Roumeliotis, A., Dounousi, E., Eleftheriadis, T., and Liakopoulos, V. (2019b). Dietary antioxidant supplements and uric acid in chronic kidney disease: a review. *Nutrients* 11:E1911. doi: 10.3390/nu11081911

Rovira, J., Diekmann, F., Campistol, J. M., and Ramírez-Bajo, M. J. (2017). Therapeutic application of extracellular vesicles in acute and chronic renal injury. *Nefrologia* 37, 126–137. doi: 10.1016/j.nefro.2016.04.006

Saad, K., Elsayh, K. I., Zahran, A. M., and Sobhy, K. M. (2014). Lymphocyte populations and apoptosis of peripheral blood B and T lymphocytes in children with end stage renal disease. *Ren. Fail.* 36, 502–507. doi: 10.3109/0886022X.2013.875833

Sanguankeo, A., Upala, S., Cheungpasitporn, W., Ungprasert, P., and Knight, E. L. (2015). Effects of statins on renal outcome in chronic kidney disease patients: a systematic review and meta-analysis. *PLoS One* 10:e0132970. doi: 10.1371/journal.pone.0132970

Schiffrin, E. L., Lipman, M. L., and Mann, J. F. (2007). Chronic kidney disease: effects on the cardiovascular system. *Circulation* 116, 85–97. doi: 10.1161/CIRCULATIONAHA.106.678342

Shimizu, I., and Minamino, T. (2019). Cellular senescence in cardiac diseases. *J. Cardiol.* 74, 313–319. doi: 10.1016/j.jjcc.2019.05.002

Sies, H. (1986). Biochemistry of Oxidative Stress. *Angew. Chem. Int. Ed. Engl.* 25, 1058–1071. doi: 10.1002/anie.198610581

Silverstein, D. M. (2009). Inflammation in chronic kidney disease: role in the progression of renal and cardiovascular disease. *Pediatr. Nephrol.* 24, 1445–1452. doi: 10.1007/s00467-008-1046-0

Sirich, T. L., Meyer, T. W., Gondouin, B., Brunet, P., and Niwa, T. (2014). Protein-bound molecules: a large family with a bad character. *Semin. Nephrol.* 34, 106–117. doi: 10.1016/j.semnephrol.2014.02.004

Sproston, N. R., and Ashworth, J. J. (2018). Role of C-reactive protein at sites of inflammation and infection. *Front. Immunol.* 9:754. doi: 10.3389/fimmu.2018.00754

Stenvinkel, P., and Larsson, T. E. (2013). Chronic kidney disease: a clinical model of premature aging. *Am. J. Kidney Dis.* 62, 339–351. doi: 10.1053/j.ajkd.2012.11.051

Stokman, M. F., Bijnsdorp, I. V., Schelfhorst, T., Pham, T. V., Piersma, S. R., Knol, J. C., et al. (2019). Changes in the urinary extracellular vesicle proteome are associated with nephronophthisis-related ciliopathies. *J. Proteomics* 192, 27–36. doi: 10.1016/j.jprot.2018.07.008

Sung, C. C., Hsu, Y. C., Chen, C. C., Lin, Y. F., and Wu, C. C. (2013). Oxidative stress and nucleic acid oxidation in patients with chronic kidney disease. *Oxid. Med. Cell. Longev.* 2013:301982. doi: 10.1155/2013/301982

Tang, T. T., and Liu, B. C. (2019). Extracellular vesicles: opportunities and challenges for the treatment of renal fibrosis. *Adv. Exp. Med. Biol.* 1165, 693–709. doi: 10.1007/978-981-13-8871-2_34

Tebay, L. E., Robertson, H., Durant, S. T., Vitale, S. R., Penning, T. M., Dinkova-Kostova, A. T., et al. (2015). Mechanisms of activation of the transcription factor Nrf2 by redox stressors, nutrient cues, and energy status and the pathways through which it attenuates degenerative disease. *Free Radic. Biol. Med.* 88(Pt. B), 108–146. doi: 10.1016/j.freeradbiomed.2015.06.021

Tsiantoulas, D., Sage, A. P., Mallat, Z., and Binder, C. J. (2015). Targeting B cells in atherosclerosis: closing the gap from bench to bedside. *Arterioscler. Thromb. Vasc. Biol.* 35, 296–302. doi: 10.1161/ATVBAHA.114.303569

Ulbing, M., Kirsch, A. H., Leber, B., Lemesch, S., Münzker, J., Schweighofer, N., et al. (2017). MicroRNAs 223-3p and 93-5p in patients with chronic kidney disease before and after renal transplantation. *Bone* 95, 115–123. doi: 10.1016/j.bone.2016.11.016

Ungvari, Z., Tarantini, S., Donato, A. J., Galvan, V., and Csiszar, A. (2018). Mechanisms of vascular aging. *Circ. Res.* 123, 849–867. doi: 10.1161/CIRCRESAHA.118.311378

Vacante, F., Denby, L., Sluimer, J. C., and Baker, A. H. (2019). The function of miR-143, miR-145 and the MiR-143 host gene in cardiovascular development and disease. *Vascul. Pharmacol.* 112, 24–30. doi: 10.1016/j.vph.2018.11.006

Valadi, H., Ekström, K., Bossios, A., Sjöstrand, M., Lee, J. J., and Lötvall, J. O. (2007). Exosome-mediated transfer of mRNAs and microRNAs is a novel mechanism of genetic exchange between cells. *Nat. Cell Biol.* 9, 654–659. doi: 10.1038/ncb1596

van Kralingen, J. C., McFall, A., Ord, E. N. J., Coyle, T. F., Bissett, M., McClure, J. D., et al. (2019). Altered extracellular vesicle microRNA expression in ischemic stroke and small vessel disease. *Transl. Stroke Res.* 10, 495–508. doi: 10.1007/s12975-018-0682-3

van Niel, G., D'Angelo, G., and Raposo, G. (2018). Shedding light on the cell biology of extracellular vesicles. *Nat. Rev. Mol. Cell Biol.* 19, 213–228. doi: 10.1038/nrm.2017.125

Vanholder, R., Massy, Z., Argiles, A., Spasovski, G., Verbeke, F., Lameire, N., et al. (2005). Chronic kidney disease as cause of cardiovascular morbidity and mortality. *Nephrol. Dial. Transplant* 20, 1048–1056. doi: 10.1093/ndt/gfh813

Vickers, K. C., Palmisano, B. T., Shoucri, B. M., Shamburek, R. D., and Remaley, A. T. (2011). MicroRNAs are transported in plasma and delivered to recipient

cells by high-density lipoproteins. *Nat. Cell Biol.* 13, 423–433. doi: 10.1038/ncb2210

Vosgha, H., Ariana, A., Smith, R. A., and Lam, A. K. (2018). targets angiogenesis and EMT concurrently in anaplastic thyroid carcinoma. *Endocr. Relat. Cancer* 25, 323–337. doi: 10.1530/ERC-17-0497

Witko-Sarsat, V., Friedlander, M., Nguyen Khoa, T., Capeillère-Blandin, C., Nguyen, A. T., Canteloup, S., et al. (1998). Advanced oxidation protein products as novel mediators of inflammation and monocyte activation in chronic renal failure. *J. Immunol.* 161, 2524–2532.

Wu, I. W., Hsu, K. H., Lee, C. C., Sun, C. Y., Hsu, H. J., Tsai, C. J., et al. (2011). p-Cresyl sulphate and indoxyl sulphate predict progression of chronic kidney disease. *Nephrol. Dial. Transplant* 26, 938–947. doi: 10.1093/ndt/gfq580

Yáñez-Mó, M., Siljander, P. R., Andreu, Z., Zavec, A. B., Borràs, F. E., Buzas, E. I., et al. (2015). Biological properties of extracellular vesicles and their physiological functions. *J. Extracell. Vesicles* 4:27066. doi: 10.3402/jev.v4.27066

Yoshikawa, F. S. Y., Teixeira, F. M. E., Sato, M. N., and Oliveira, M. D. S. L. (2019). Delivery of microRNAs by extracellular vesicles in viral infections: Could the news be packaged? *Cells* 8:611. doi: 10.3390/cells8060611

Yu, M., Kim, Y. J., and Kang, D. H. (2011). Indoxyl sulfate-induced endothelial dysfunction in patients with chronic kidney disease via an induction of oxidative stress. *Clin. J. Am. Soc. Nephrol.* 6, 30–39. doi: 10.2215/CJN.05340610

Yuana, Y., Sturk, A., and Nieuwland, R. (2013). Extracellular vesicles in physiological and pathological conditions. *Blood Rev.*27, 31–39. doi: 10.1016/j.blre.2012.12.002

Zakkar, M., Van der Heiden, K., Luong, A., Chaudhury, H., Cuhlmann, S., Hamdulay, S. S., et al. (2009). Activation of Nrf2 in endothelial cells protects arteries from exhibiting a proinflammatory state. *Arterioscler. Thromb. Vasc. Biol.* 29, 1851–1857. doi: 10.1161/ATVBAHA.109.193375

Zhang, Q., Shang, M., Zhang, M., Wang, Y., Chen, Y., Wu, Y., et al. (2016). Microvesicles derived from hypoxia/reoxygenation-treated human umbilical vein endothelial cells promote apoptosis and oxidative stress in H9c2 cardiomyocytes. *BMC Cell Biol.* 17:25. doi: 10.1186/s12860-016-0100-1

Zhou, Q., Wu, S., Jiang, J., Tian, J., Chen, J., Yu, X., et al. (2012). Accumulation of circulating advanced oxidation protein products is an independent risk factor for ischaemic heart disease in maintenance haemodialysis patients. *Nephrology* 17, 642–649. doi: 10.1111/j.1440-1797.2012.01640.x

Conflict of Interest: The authors declare that the research was conducted in the absence of any commercial or financial relationships that could be construed as a potential conflict of interest.

Copyright © 2020 Carracedo, Alique, Vida, Bodega, Ceprián, Morales, Praga, de Sequera and Ramírez. This is an open-access article distributed under the terms of the Creative Commons Attribution License (CC BY). The use, distribution or reproduction in other forums is permitted, provided the original author(s) and the copyright owner(s) are credited and that the original publication in this journal is cited, in accordance with accepted academic practice. No use, distribution or reproduction is permitted which does not comply with these terms.

frontiers in Cell and Developmental Biology

MINI REVIEW
published: 15 April 2020
doi: 10.3389/fcell.2020.00227

The Multi-Faced Extracellular Vesicles in the Plasma of Chronic Kidney Disease Patients

*Hara T. Georgatzakou[1], Efthimia G. Pavlou[1], Effie G. Papageorgiou[1], Issidora S. Papassideri[2], Anastasios G. Kriebardis[1] and Marianna H. Antonelou[2]**

[1] Laboratory of Reliability and Quality Control in Laboratory Hematology (HemQcR), Department of Biomedical Sciences, School of Health & Welfare Sciences, University of West Attica, Athens, Greece, [2] Department of Biology, School of Science, National and Kapodistrian University of Athens (NKUA), Athens, Greece

Extracellular vesicles (EVs) are membrane-enclosed nanoparticles released by most cells in body fluids and extracellular matrix. They function as signal transducers in intercellular communication, contributing to the maintenance of cell and tissue integrity. EVs biogenesis is deregulated in various pathologies, in structural and functional connection to the pathophysiology of donor cells. Consequently, EVs are considered diagnostic and monitoring factors in many diseases. Despite consensus as to their activity in promoting coagulation and inflammation, there is evidence suggesting protective roles for EVs in stress states. Chronic kidney disease (CKD) patients are at high risk of developing cardiovascular defects. The pathophysiology, comorbidities, and treatment of CKD may individually and in synergy affect extracellular vesiculation in the kidney, endothelium, and blood cells. Oxidative and mechanical stresses, chronic inflammation, and deregulation of calcium and phosphate homeostasis are established stressors of EV release. EVs may affect the clinical severity of CKD by transferring biological response modifiers between renal, vascular, blood, and inflammatory cells. In this Review, we focus on EVs circulating in the plasma of CKD patients. We highlight some recent advances in the understanding of their biogenesis, the effects of dialysis, and pharmacological treatments on them and their potential impact on thrombosis and vascular defects. The strong interest of the scientific community to this exciting field of research may reveal hidden pieces in the pathophysiology of CKD and thus, innovative ways to treat it. Overcoming gaps in EV biology and technical difficulties related to their size and heterogeneity will define the success of the project.

Keywords: CKD, ESRD, extracellular vesicles, dialysis, biomarkers, therapy

OPEN ACCESS

Edited by:
Evangelia Dounousi, University Hospital of Ioannina, Greece

Reviewed by:
George Pissas, University of Thessaly, Greece
Kostas G. Stylianou, University Hospital of Heraklion, Greece

***Correspondence:**
Marianna H. Antonelou
manton@biol.uoa.gr

Specialty section:
This article was submitted to Molecular Medicine, a section of the journal Frontiers in Cell and Developmental Biology

Received: *13 December 2019*
Accepted: *17 March 2020*
Published: *15 April 2020*

Citation:
Georgatzakou HT, Pavlou EG, Papageorgiou EG, Papassideri IS, Kriebardis AG and Antonelou MH (2020) The Multi-Faced Extracellular Vesicles in the Plasma of Chronic Kidney Disease Patients. Front. Cell Dev. Biol. 8:227. doi: 10.3389/fcell.2020.00227

EXTRACELLULAR VESICLES: BIOVECTORS AND BIOMARKERS

Extracellular vesiculation is an evolutionary conserved fundamental activity of both normal and diseased cells (Gyorgy et al., 2011). As an integral part of cell growth, aging, or development (Johnstone et al., 1987), as a way to get rid of unneeded cellular material, or as a means of intercellular, interorgan, and interspecies crosstalk (Giricz et al., 2014), extracellular vesiculation is

a key homeostatic mechanism contributing to survival, function, remodeling, and repair processes (Bruno et al., 2009). As cells transfer materials inside or outside them by secretory and transport vesicles, absolutely healthy, stressed, or activated cells release nanosized membrane-enclosed extracellular vesicles (EVs) to the external environment. Within blood circulation, EVs have a short half-life (from a couple of minutes to a few hours), before being taken up by neighboring or distant cells.

The highly dynamic and omnipresent EV compartment consists of a heterogeneous group of small exosomes (typically <150 nm), medium sized microvesicles (MVs, or microparticles, typically <1 μm), large sized apoptotic bodies, and several other EV subtypes (Raposo and Stoorvogel, 2013). On a constitutive basis or in response to stimulation, a cell can produce a wide variety of EVs. Their phenotype, biophysical characteristics, and biogenesis may overlap so much between each other and with non-EV components (e.g., plasma protein aggregates) so EVs characterization or classification is often a brainteaser.

Release of membrane vesicles is not a stochastic process but rather a regulated, highly selective cellular ability. It may have negative effects when overactivated, for example, during inflammation. The EVs bear "real-time" molecular signatures of the physiological states of the parental cells and their microenvironment. Based on those compositional and functional correlations, EVs are considered noninvasive predictive, diagnostic, and biomonitoring factors for the development and propagation of several diseases, including cardiovascular events (Sinning et al., 2011) and structural renal injury (Zhou et al., 2006), among others.

Moreover, according to numerous *in vitro* and *in vivo* data, material delivered by plasma EVs to recipient cells may induce immunomodulation, inflammation, oxidative stress, thrombogenesis, and vascular senescence or dysfunction (Gyorgy et al., 2011; Burger et al., 2012; Zecher et al., 2014; Cai et al., 2015; Camus et al., 2015; Hosseinkhani et al., 2018). This is quite reasonable for competent carriers endowed by nature with a remarkable efficiency to preserve their cargo intact and active along their journeys. Secreted cytokines, for example, are more stable inside EVs than free in plasma (Fitzgerald et al., 2018). *Vice versa*, the levels of circulating EVs are increased in diseases associated with inflammation or coagulation (van Beers et al., 2009), while proinflammatory and procoagulant factors promote the extracellular vesiculation by healthy cells *in vitro*.

Cardiovascular abnormalities represent the leading cause of increased morbidity and mortality in patients with chronic kidney disease (CKD), which may result to end-stage kidney disease (ESKD) (Antonelou et al., 2014). The molecular mechanisms underlining CKD have been associated with a pathophysiological context of chronic inflammation, anemia, accumulation of uremic toxins, increased oxidative and metabolic stresses (Antonelou et al., 2011), deregulation of calcium and phosphate homeostasis, coagulation and vascular abnormalities, and chronic or acute [e.g., by hemodialysis (HD)] endothelial activation (Georgatzakou et al., 2016). Of note, all of these pathologies have also been related to EV biology, either as stress factors triggering EV release or as outcomes of EVs' effects on sensitive cell targets. Those bidirectional connections reflect the dual role of EVs as both biomarkers of cell dysfunction and vectors of bioactive molecules contributing to it (**Figure 1**). Not surprisingly, CKD patients have elevated concentration of EVs in body fluids (Amabile et al., 2005).

EVS IN THE PLASMA OF CKD PATIENTS: GENERAL OUTLINE OF OUR KNOWLEDGE

Endothelium and blood cells in CKD are characterized by increased rate of extracellular vesiculation. Significant proportion of EVs (in most studies, MVs) that are released following activation of the origin cells (Antonelou et al., 2011) expose phosphatidylserine (PS; Faure et al., 2006; Burton et al., 2013; Yu et al., 2018) and are prothrombotic, often more than the parent cells (Sinauridze et al., 2007), according to both morphological and biochemical evidence (Gao et al., 2015b; Yu et al., 2018). The intriguing finding that the platelet-derived MVs are less procoagulant than in other diseases (Trappenburg et al., 2012) (probably due to functional defects in platelets) does not break up the intimate relation of EVs with thrombosis in CKD, as uremic patients with thrombotic events have more MVs compared to those without events (Ando et al., 2002). Moreover, PS on plasma EVs may nucleate calcium phosphate, contributing to ectopic calcification reactions (Wu et al., 2013). Therefore, pharmacological blocking of the PS binding sites on cells and EVs or lipid lowering drugs (Almquist et al., 2016) have been considered as meaningful measures to prevent thrombosis and vascular calcification risk in CKD. Of note, CKD patients with vascular calcification have both more circulating endothelial MVs and less endothelial progenitor cells compared to patients without calcification. This looming imbalance in endothelial damage and repair processes is probably induced by the MV-mediated expression of osteocalcin (Soriano et al., 2014).

Several cross-talking factors seem to augment extracellular vesiculation in CKD (**Figure 1**). Uremic toxins constitute the central one. To support, the PS^+ EV levels *in vivo* are inversely correlated with the glomerular filtration rate (Almquist et al., 2016; Yu et al., 2018), but positively with uric acid and proteinuria levels (Yu et al., 2018). More procoagulant MVs are detected in diabetes mellitus patients with CKD compared to patients without it (Almquist et al., 2016), and in patients with extreme albuminuria than in those with lower or normal levels (Yu et al., 2018). To get a laboratory verification, incubation of normal endothelial cells or red blood cells (RBCs) with (i) patients' serum, (ii) uremic toxins at concentrations found in patients, or (iii) increased concentration of phosphate induce PS exposure on cells and EVs release (Faure et al., 2006; Abbasian et al., 2015; Gao et al., 2015a,b; Yu et al., 2018).

Another informative (inverse) correlation of endothelial MVs with shear stress is repeatedly detected in ESRD patients. It suggests that variations in shear-stress determinants and blood viscosity, including anemia and hemoconcentration arisen by the dialysis or erythropoietin (EpO) supplementation, may affect the vesiculation rate in the endothelium (Boulanger et al., 2007). Indeed, more endothelial cell-derived MVs have been

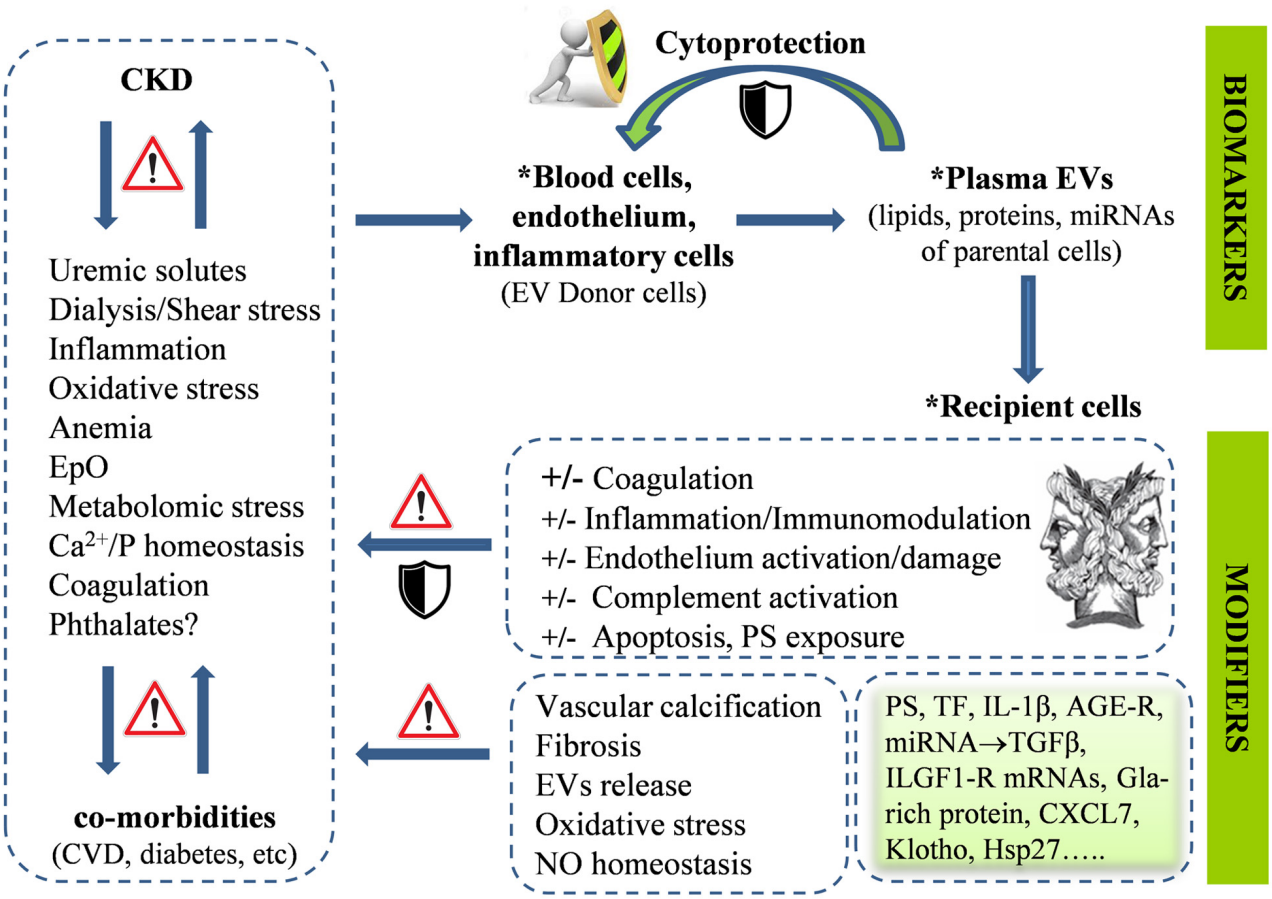

FIGURE 1 | The chronic kidney disease (CKD)-related pathophysiological factors, treatment modalities, and comorbidities affect the cellular stress and activation status of endothelium and blood cells, leading to augmented release of extracellular vesicles (EVs) in the plasma. EVs contain molecular components of parental cells, and thus, are considered biomarkers of disease phenotypes. EV release may represent a cytoprotective mechanism allowing, among other, removal of stress or death signals from donor cells. Interactions of plasma EVs with recipient cells and plasma components may be involved in the progress of the primary disease *per se* and its cardiovascular complications in both directions, either by transmitting and amplifying dangerous, cellular response modifiers or by counteracting them. The "Janus face" is a general feature of EVs functional potential, related to their complex biology, in both donor and recipient cells. Advances in EV research have provided sharper pictures of plasma EVs in CKD, identifying them as key parts of both problem and solution.

detected in child and adult dialysis patients with CKD, than in patients not getting dialysis (Dursun et al., 2009; Merino et al., 2010), but those findings may merely reflect the clinical severity of the disease. When comparing patients of similar clinical severity, both inflammation and repetitive mechanical stress, imposed on endothelium and blood cells by hemodialysis, still seem to augment vesiculation (Daniel et al., 2006). The same inducers modify the EV phenotypes and micro-RNA (miRNA) cargos, often in cell-specific (Faure et al., 2006; Trappenburg et al., 2012), or dialysis modal-specific ways (Cavallari et al., 2019). For instance, MV concentration is lower in patients treated by hemodiafiltration versus conventional hemodialysis (Georgatzakou et al., 2018). By examining the short-term effects of a single dialysis session on EV measurements, dialysis still triggers release of MVs but again, with marked differences between high-flux and low-flux dialyzers (de Laval et al., 2019). As to the accumulation of the PS-exposing MVs (Georgatzakou et al., 2018) and smaller EVs (Ruzicka et al., 2019), dialysis generally exerts a beneficial acute effect, mediated in part by EV absorbance to the dialysis membrane (Ruzicka et al., 2019), at least in patients with adequate response to EpO (Georgatzakou et al., 2017). Additionally, hemodialysis seems to be more effective in eliminating small compared to bigger EVs (Ruzicka et al., 2019). There is evidence that EpO affects platelet activation and promotes EV accumulation (Ando et al., 2002). This is quite interesting, because endothelium damage and cardiovascular disease appear more frequently in EpO resistance (Panichi et al., 2011). Despite that, several renal-protective EpO signaling pathways are proceeded through stimulating EV release by both mesenchymal stem cells (Wang et al., 2015) and bone marrow cells (Zhou et al., 2016). Finally, patients on hemodialysis are regularly exposed to considerable amounts of phthalates leaching by plastic tubing (Faouzi et al., 1999). Although the field is aware of the associated risks, the probable contribution of phthalates on comorbidities (Kataria et al., 2017) and extracellular vesiculation [extensively studied in stored blood (Serrano et al., 2016)], as well

as their probable dissemination to sensitive targets through EVs, have not been investigated so far in CKD.

WHAT IS THE MESSAGE OF CIRCULATING EVs IN CKD?

Like other pathologies, EVs represent phenotypic markers of cellular stress and activation in CKD. More importantly, their number and composition may also play a role in the pathophysiology of cardiovascular complications, and thus in mortality risk (Carmona et al., 2017a).

On one side, a wide panel of "incriminating" bioreactive phenotypes have been detected in plasma EVs of ESRD patients. Apart from PS, those phenotypes include platelet activation markers, tissue factor (TF), IL-1β, miRNAs (Shang et al., 2017), and advanced glycation end products (AGEs) receptor (Stinghen et al., 2016), which are potentially involved in coagulation, inflammation, oxidative stress, and endothelial activation/dysfunction (Stinghen et al., 2016; de Laval et al., 2019). Endothelial dysfunction, arterial stiffness, and atherosclerosis are determinants of cardiovascular risk in patients with or without CKD. Flow cytometry, functional measurements, and Kaplan–Meier survival analysis have showed that the concentration of endothelium-derived MVs in ESRD selectively correlates with arterial dysfunction *in vivo* (Amabile et al., 2005; Dursun et al., 2009), and further predicts cardiovascular mortality (Amabile et al., 2012). MVs released by cells exposed to uremic substances promote functional loss in endothelial progenitor cells (marked by overexpression of NF-κB and p53 proteins) (Carmona et al., 2017b) and TGFβ-mediated proliferation of vascular smooth muscle cells (Ryu et al., 2017), while isolated ESRD MVs can impair NO release and endothelium relaxation (Amabile et al., 2005). Endothelial dysfunction may be further related to activation of the alternative complement pathway and of note, endothelium-derived MVs in CKD do contain factor D and can activate the alternative pathway *in vitro* (Jalal et al., 2018).

Endothelial dysfunction and fibrosis may be promoted in CKD by EV-mediated miRNA transfer mechanisms (Xie et al., 2017). miRNA present in MVs induced by uremic toxins disturb signaling pathways involved in endothelial regeneration through oxidative stress and apoptosis (Carmona et al., 2017b). Indeed, a series of miRNAs that mostly target TGFβ signaling-related mRNAs in recipient cells have been found enriched or depleted in plasma and plasma-derived exosomes and MVs from patients with CKD (Muralidharan et al., 2017). miR-92a, for instance, is involved in atherosclerosis and cardiovascular disease as an effective suppressor of key endothelial-protective mRNAs. High serum levels of miR-92a have been associated with decreased kidney function. Moreover, endothelial MVs of uremic patients are enriched in miR-92a and uremic plasma upregulates its expression in cultured endothelial cells (Shang et al., 2017). Another miRNA, the miR-223 (which is abundant in resting platelets and further upregulated following platelet activation by pro-inflammatory factors), is enriched in platelet MVs of patients with nephritis, or atherosclerosis. It was found that miR-223 can promote apoptosis induced by AGEs in endothelial cells *in vitro* via targeting the insulin-like growth factor 1 receptor (Pan et al., 2014). Of note, a higher expression of miR-223 was found in the endothelial-derived exosomes and MVs of ESRD patients treated by bicarbonate hemodialysis compared to those treated by online hemodiafiltration and healthy subjects in close relation to variation in systemic inflammation markers (Cavallari et al., 2019).

Apart from the EV-delivered miR223, exosomes and MVs of ESRD patients with low levels of the Gla-rich protein (an anti-inflammatory factor and inhibitor of calcification in the cardiovascular system) can induce calcification in target vascular smooth muscle cells, by promoting osteogenic differentiation and inflammation (Viegas et al., 2018). There is evidence that monocyte and endothelial MVs induce podocyte phenotypic modifications *in vitro* [release of proinflammatory cytokines and vascular endothelial growth factor (VEGF)] typically associated with glomerular permeability and proteinuria (Eyre et al., 2011). Moreover, plasma platelet MVs can cause glomerular endothelial injury in animal models of diabetic nephropathy through transferring of chemokine ligand 7 (CXCL7) and activation of the mammalian target of rapamycin complex 1 (mTORC1) pathway in glomerular target cells (Zhang et al., 2018). Finally, recent studies revealed that plasma EVs in ESRD also contain the Klotho protein (de Laval et al., 2019), a transmembrane component of the distal convoluted tubule of the kidney. Klotho expression declines with reducing renal function, and its deficiency has been speculated to contribute to vascular calcification (Hu et al., 2012).

On the other side, EVs release is also an "alarm button" pressed by cells facing life-threatening provocations. In RBCs, for example, extracellular vesiculation increases by aging, oxidative stress, and cold storage-associated lesions (Kriebardis et al., 2008). Proteomic analyses of those EVs have suggested activity toward disposal of abnormal, nonfunctional, or dangerous materials (e.g., complement) that could otherwise signal premature elimination of releasing cells (Willekens et al., 2008; Tzounakas et al., 2016). In a similar way, release of caspase 3-containing EVs by endothelial cells *in vitro* protects them from apoptosis and detachment (Abid Hussein et al., 2007), suggesting that a similar mechanism may contribute to endothelial cell survival in CKD (**Figure 1**). Consequently, it is reasonable to assume that increased release of PS^+ RBC-derived EVs in CKD may counterbalance erythrophagocytosis leading to anemia (Georgatzakou et al., 2017). Complete phenotyping of EVs under various clinical and treatment conditions would test the accuracy of this assumption.

In addition, certain EVs may well induce anti-inflammatory responses in recipient cells (Gasser and Schifferli, 2004), although these responses may vary in pathological conditions including hyperglycemia (Jansen et al., 2015). miR-222 (Jansen et al., 2015) and Hsp27 (Shi et al., 2019) laden plasma EVs, for example, were found to reduce tumor necrosis factor-alpha-induced ICAM-1 expression (and monocyte adhesion) and stimulate the release of IL-10 and NF-kappa in endothelial and B cells, respectively, both *in vitro* and *in vivo*. Moreover, plasma MVs that are released by the dysfunctional endothelium of patients with unstable angina are enriched in the miR-19b and exert antithrombotic function

by inhibiting TF expression in endothelial cells (Li et al., 2014). Several other miRNAs that are potentially encapsulated in plasma EVs, such as the miR-23b (Zhao et al., 2016), have been shown to alleviate fibrosis and albuminuria in diabetic nephropathy, and thus, their levels are pathologically low in the serum and kidney of the patients. It is worth studying the degree of encapsulation of those cytoprotective miRNAs into the plasma EVs. Recent reports in animal models of kidney disease showed that miRNA expression is lower in plasma-derived exosomes compared to the plasma and that the miRNA levels may widely vary in each disease context (Xie et al., 2017). To sum up, plasma EVs may counteract proinflammatory and procoagulant signals instead of transmitting and amplifying them (**Figure 1**), and thus, part of them may protect the vascular and kidney functions in CKD.

HOW CAN WE READ THE FULL MESSAGE AND MOVE FORWARD?

EVs represent an exciting chapter of contemporary biology and medicine. The disproportionally high ratio of reviews to research articles dealing with plasma EVs in CKD (**Figure 2A**) reflects a major interest for understanding a subject that is, however, difficult to be studied. Generally, research on EVs is a challenge for the scientific community, mainly due to their size, heterogeneity, artificial generation during the preanalytical stages, and lack of standardized methods of working with them (Doyle and Wang, 2019). Let alone studying them in CKD patients characterized by extreme variabilities in primary lesions, comorbidities, and treatments, which individually and in synergy affect both their release and composition (Carmona et al., 2017a).

Despite that, research on EVs is critical for CKD for many reasons. First of all, we are now aware that EVs are key figures in the frame of this disease. They have to be taken into consideration, for instance, when measuring plasma cytokine levels in patients, because EV-encapsulated cytokines may not be detected by standard cytokine assays (Fitzgerald et al., 2018). Second, EVs have been associated with most of the cardiovascular risk factors (Hosseinkhani et al., 2018) and with poor clinical outcomes in CKD as in many other diseases. Third, regular recording of clinical/laboratory data of CKD patients drives physicians to make individual, intervening decisions on treatments per short intervals of time. Consequently, availability of sensitive tools to support biomonitoring of the disease progression and identification of patients at risk are highly desirable. Finally, similar to their release, EVs uptake is also a specific and regulated process. Since EVs can cross the glomerular basement membrane, the possibility of using them as therapeutic vehicles targeting the kidney cells *per se* (Oosthuyzen et al., 2016) open new prospects for CKD management.

Plasma EVs may provide peripheral biomarkers easily available for clinical diagnosis. The first step toward that is discovery of a reliable marker (or panel of markers) being related to a particular disease state, complication, or pathological condition. The candidate biomarker should then be appropriately validated *in vivo*, in animal disease models at first, and then, in cohorts of patients by clinical studies. Last is bridging of

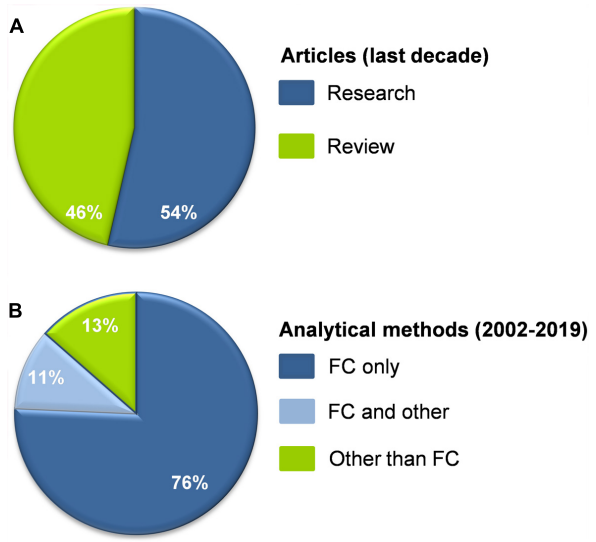

FIGURE 2 | (**(A)** Percentage of research and review articles dealing with plasma EVs in CKD published in the last decade (*N* = 56). **(B)** The vast majority of research data on plasma EVs in CKD derived in the period from 2002 till today (*N* = 37) were based exclusively on flow cytometry (FC). Fewer studies combined FC with other methodologies (immunoblotting, nanoparticle tracking analysis, proteomics, Elisa, electron microscopy) or they did not use FC at all. References are shown in the **Supplementary Material**.

those biomarkers' capabilities to clinical setting. Isolation of EVs, especially exosomes, is not a clinically friendly procedure; however, development of simple and quick innovative separation methods (like the microfluidic based techniques) provides candidates for potential use in the clinical setting.

Biomarker mining presupposes availability of reliable EV metrical, compositional, physicochemical, and uptake (Zaborowski et al., 2015) data. First of all, analytical methods able to detect and characterize the entire vesicular population, including the smaller (<200 nm) EVs, must be used. The majority of data reported on plasma EVs in CKD have been extracted by flow cytometry, the "gold standard" analytical method for EVs characterization (**Figure 2B**). However, conventional cytometry cannot detect vesicles < 300 nm, the area that harbors the majority of EVs in human blood (Yuana et al., 2011; Arraud et al., 2014). Apart from that, it is now well established that only few blood EVs expose PS, namely, the most commonly used tag for flow cytometry (Connor et al., 2010; Arraud et al., 2014). Despite insights provided by immobilizing smaller EVs on bead surfaces, and advances in the detection limits of new nanoscale instruments (100–200 nm) (Dragovic et al., 2011; Gomes et al., 2018), the fact is that the biology and functions of smaller plasma EVs are largely unknown in CKD (Kapustin et al., 2015), in opposite to those of urinary exosomes (Erdbrugger and Le, 2016). Of note, however, comparative proteomic analysis of RBC membrane in ESRD patients with good or poor response to EpO administration suggested release of small and/or PS-negative EVs in responders that are undetectable by the conventional flow cytometry (Georgatzakou et al., 2017).

Assessment of vesiculation by the protein concentration of a vesicular pellet is not accurate because pellets contain both disease specific and unspecific protein profiles, and moreover, they are unavoidably contaminated by plasma components (Doyle and Wang, 2019). To get insight into EVs size and concentration, sophisticated physical methods like nanoparticle tracking (Dragovic et al., 2011; Burton et al., 2013) and tunable resistive pulse sensing analyses, in combination with cryo-electron microscopy, are currently used in the EV research field (Hosseinkhani et al., 2018). Compositional analyses are more appropriately performed by immunoblotting, the much informative omics techniques, and by microfluidic devices allowing capture of EVs on a chip's surface and then lysis and probing of lysate, for identification of both surface and lumen components (He et al., 2014). Thermophoretic enrichment and profiling has been successfully tested for cancer detection and classification as an alternative method to detect surface proteins of plasma EVs, following labeling with fluorescent aptamers (Liu et al., 2019). Under such integrative characterization of plasma EVs, lack of specific protein markers to distinguish between their subtypes becomes less important.

Compositional analyses of EVs are of critical importance to understand the hows and whys of their biogenesis, stimuli, targets, and effects. Global and targeted mass spectrometry-based proteomic analysis is best suitable to suggest biomarker candidates (Zhou et al., 2006), the cellular destinations of EVs, and thus, the most suitable therapeutic targets in a given patient or disease context. However, analysis of one data type by itself is often limited to correlations resulting by reactive processes rather than by causative modifications. Integration of multiomics (Hasin et al., 2017), electron microscopy and physical characterization data (Thery et al., 2018) would rather reveal hidden aspects of EV biology and functions, offering the opportunity to understand the flow of material and information in CKD.

In a similar way, simple enumeration of EVs is not enough to establish a pathophysiological mechanism. Instead of it, time, place, and means of interactions (ligand binding, membrane fusion, or uptake by endocytosis), as well as identification of the specific molecular content(s) that mainly account for any given biological effect on target cells, are most critically connected to their desirable or harmful bioreactivity. However, this is also the hardest part in EV assessment. Incorporation of the guidelines suggested by the International Society for Extracellular Vesicles (Thery et al., 2018) would greatly benefit the emerging contemporary area of research on CKD-related EVs.

CONCLUSION

Plasma EVs may have significant roles in CKD as disease biomarkers, risk factors for the development of complications, repair or protective factors diffusing harmful stress signals, and finally, therapeutic factors. They seem to be part of the problem and part of the solution. At times when advanced technologies for EVs assessment are still evolving, understanding of their biology, from biogenesis to ultimate effects on recipient cells, is of key importance to reveal their clinical relevance to CKD. Development of therapeutic interventions have already been oriented to both block their negative effects and take advantage of their beneficial properties. Regulation of EVs release or uptake by drugs, including statins, antioxidants, and actin depolymerizing agents, and removal from plasma by immunoadsorption have been reported (Karpman et al., 2017). Those interventions may allow prognosis, better diagnosis, and individualized treatments for CKD patients.

AUTHOR CONTRIBUTIONS

HG and MA conceived the concept, wrote the manuscript, and designed the figures. EPav, EPap, IP, and AK provided input and direction in structuring of the manuscript.

SUPPLEMENTARY MATERIAL

The Supplementary Material for this article can be found online at: https://www.frontiersin.org/articles/10.3389/fcell.2020.00227/full#supplementary-material

REFERENCES

Abbasian, N., Burton, J. O., Herbert, K. E., Tregunna, B. E., Brown, J. R., Ghaderi-Najafabadi, M., et al. (2015). Hyperphosphatemia, phosphoprotein phosphatases, and microparticle release in vascular endothelial cells. *J. Am. Soc. Nephrol.* 26, 2152–2162. doi: 10.1681/ASN.2014070642

Abid Hussein, M. N., Boing, A. N., Sturk, A., Hau, C. M., and Nieuwland, R. (2007). Inhibition of microparticle release triggers endothelial cell apoptosis and detachment. *Thromb. Haemost.* 98, 1096–1107. doi: 10.1160/th05-04-0231

Almquist, T., Mobarrez, F., Jacobson, S. H., Wallen, H., and Hjemdahl, P. (2016). Effects of lipid-lowering treatment on circulating microparticles in patients with diabetes mellitus and chronic kidney disease. *Nephrol. Dial. Transplant.* 31, 944–952. doi: 10.1093/ndt/gfv337

Amabile, N., Guerin, A. P., Leroyer, A., Mallat, Z., Nguyen, C., Boddaert, J., et al. (2005). Circulating endothelial microparticles are associated with vascular dysfunction in patients with end-stage renal failure. *J. Am. Soc. Nephrol.* 16, 3381–3388. doi: 10.1681/ASN.2005050535

Amabile, N., Guerin, A. P., Tedgui, A., Boulanger, C. M., and London, G. M. (2012). Predictive value of circulating endothelial microparticles for cardiovascular mortality in end-stage renal failure: a pilot study. *Nephrol. Dial. Transplant.* 27, 1873–1880. doi: 10.1093/ndt/gfr573

Ando, M., Iwata, A., Ozeki, Y., Tsuchiya, K., Akiba, T., and Nihei, H. (2002). Circulating platelet-derived microparticles with procoagulant activity may be a potential cause of thrombosis in uremic patients. *Kidney Int.* 62, 1757–1763. doi: 10.1046/j.1523-1755.2002.00627.x

Antonelou, M. H., Georgatzakou, H. T., Tzounakas, V. L., Velentzas, A. D., Kokkalis, A. C., Kriebardis, A. G., et al. (2014). Blood modifications associated with end stage renal disease duration, progression and cardiovascular mortality: a 3-year follow-up pilot study. *J. Proteomics* 101, 88–101. doi: 10.1016/j.jprot.2014.02.009

Antonelou, M. H., Kriebardis, A. G., Velentzas, A. D., Kokkalis, A. C., Georgakopoulou, S. C., and Papassideri, I. S. (2011). Oxidative stress-associated shape transformation and membrane proteome remodeling in erythrocytes of end stage renal disease patients on hemodialysis. *J. Proteomics* 74, 2441–2452. doi: 10.1016/j.jprot.2011.04.009

Arraud, N., Linares, R., Tan, S., Gounou, C., Pasquet, J. M., Mornet, S., et al. (2014). Extracellular vesicles from blood plasma: determination of their morphology, size, phenotype and concentration. *J. Thromb. Haemost.* 12, 614–627. doi: 10.1111/jth.12554

Boulanger, C. M., Amabile, N., Guerin, A. P., Pannier, B., Leroyer, A. S., Mallat, C. N., et al. (2007). In vivo shear stress determines circulating levels of endothelial microparticles in end-stage renal disease. *Hypertension* 49, 902–908. doi: 10.1161/01.hyp.0000259667.22309.df

Bruno, S., Grange, C., Deregibus, M. C., Calogero, R. A., Saviozzi, S., Collino, F., et al. (2009). Mesenchymal stem cell-derived microvesicles protect against acute tubular injury. *J. Am. Soc. Nephrol.* 20, 1053–1067. doi: 10.1681/ASN.2008070798

Burger, D., Kwart, D. G., Montezano, A. C., Read, N. C., Kennedy, C. R., Thompson, C. S., et al. (2012). Microparticles induce cell cycle arrest through redox-sensitive processes in endothelial cells: implications in vascular senescence. *J. Am. Heart Assoc.* 1:e001842. doi: 10.1161/JAHA.112.001842

Burton, J. O., Hamali, H. A., Singh, R., Abbasian, N., Parsons, R., Patel, A. K., et al. (2013). Elevated levels of procoagulant plasma microvesicles in dialysis patients. *PLoS One* 8:e72663. doi: 10.1371/journal.pone.0072663

Cai, J., Guan, W., Tan, X., Chen, C., Li, L., Wang, N., et al. (2015). SRY gene transferred by extracellular vesicles accelerates atherosclerosis by promotion of leucocyte adherence to endothelial cells. *Clin. Sci* . 129, 259–269. doi: 10.1042/CS20140826

Camus, S. M., De Moraes, J. A., Bonnin, P., Abbyad, P., Le Jeune, S., Lionnet, F., et al. (2015). Circulating cell membrane microparticles transfer heme to endothelial cells and trigger vasoocclusions in sickle cell disease. *Blood* 125, 3805–3814. doi: 10.1182/blood-2014-07-589283

Carmona, A., Aguera, M. L., Luna-Ruiz, C., Buendia, P., Calleros, L., Garcia-Jerez, A., et al. (2017a). Markers of endothelial damage in patients with chronic kidney disease on hemodialysis. *Am. J. Physiol. Renal. Physiol.* 312, F673–F681. doi: 10.1152/ajprenal.00013.2016

Carmona, A., Guerrero, F., Buendia, P., Obrero, T., Aljama, P., and Carracedo, J. (2017b). Microvesicles derived from indoxyl sulfate treated endothelial cells induce endothelial progenitor cells dysfunction. *Front. Physiol.* 8:666. doi: 10.3389/fphys.2017.00666

Cavallari, C., Dellepiane, S., Fonsato, V., Medica, D., Marengo, M., Migliori, M., et al. (2019). Online hemodiafiltration inhibits inflammation-related endothelial dysfunction and vascular calcification of uremic patients modulating mir-223 expression in plasma extracellular vesicles. *J. Immunol.* 202, 2372–2383. doi: 10.4049/jimmunol.1800747

Connor, D. E., Exner, T., Ma, D. D., and Joseph, J. E. (2010). The majority of circulating platelet-derived microparticles fail to bind annexin V, lack phospholipid-dependent procoagulant activity and demonstrate greater expression of glycoprotein Ib. *Thromb. Haemost.* 103, 1044–1052. doi: 10.1160/th09-09-0644

Daniel, L., Fakhouri, F., Joly, D., Mouthon, L., Nusbaum, P., Grunfeld, J. P., et al. (2006). Increase of circulating neutrophil and platelet microparticles during acute vasculitis and hemodialysis. *Kidney Int.* 69, 1416–1423. doi: 10.1038/sj.ki.5000306

de Laval, P., Mobarrez, F., Almquist, T., Vassil, L., Fellstrom, B., and Soveri, I. (2019). Acute effects of haemodialysis on circulating microparticles. *Clin. Kidney J.* 12, 456–462. doi: 10.1093/ckj/sfy109

Doyle, L. M., and Wang, M. Z. (2019). Overview of extracellular vesicles, their origin, composition, purpose, and methods for exosome isolation and analysis. *Cells* 8:727. doi: 10.3390/cells8070727

Dragovic, R. A., Gardiner, C., Brooks, A. S., Tannetta, D. S., Ferguson, D. J., Hole, P., et al. (2011). Sizing and phenotyping of cellular vesicles using nanoparticle tracking analysis. *Nanomedicine* 7, 780–788. doi: 10.1016/j.nano.2011.04.003

Dursun, I., Poyrazoglu, H. M., Gunduz, Z., Ulger, H., Yykylmaz, A., Dusunsel, R., et al. (2009). The relationship between circulating endothelial microparticles and arterial stiffness and atherosclerosis in children with chronic kidney disease. *Nephrol. Dial. Transplant.* 24, 2511–2518. doi: 10.1093/ndt/gfp066

Erdbrugger, U., and Le, T. H. (2016). Extracellular vesicles in renal diseases: more than novel biomarkers? *J. Am. Soc. Nephrol.* 27, 12–26. doi: 10.1681/ASN.2015010074

Eyre, J., Burton, J. O., Saleem, M. A., Mathieson, P. W., Topham, P. S., and Brunskill, N. J. (2011). Monocyte- and endothelial-derived microparticles induce an inflammatory phenotype in human podocytes. *Nephron. Exp. Nephrol.* 119, e58–e66. doi: 10.1159/000329575

Faouzi, M. A., Dine, T., Gressier, B., Kambia, K., Luyckx, M., Pagniez, D., et al. (1999). Exposure of hemodialysis patients to di-2-ethylhexyl phthalate. *Int. J. Pharm,* 180, 113–121. doi: 10.1016/s0378-5173(98)00411-6

Faure, V., Dou, L., Sabatier, F., Cerini, C., Sampol, J., Berland, Y., et al. (2006). Elevation of circulating endothelial microparticles in patients with chronic renal failure. *J. Thromb. Haemost.* 4, 566–573. doi: 10.1111/j.1538-7836.2005.01780.x

Fitzgerald, W., Freeman, M. L., Lederman, M. M., Vasilieva, E., Romero, R., and Margolis, L. A. (2018). System of cytokines encapsulated in extracellular vesicles. *Sci. Rep.* 8:8973. doi: 10.1038/s41598-018-27190-x

Gao, C., Ji, S., Dong, W., Qi, Y., Song, W., Cui, D., et al. (2015a). Indolic uremic solutes enhance procoagulant activity of red blood cells through phosphatidylserine exposure and microparticle release. *Toxins* 7, 4390–4403. doi: 10.3390/toxins7114390

Gao, C., Xie, R., Yu, C., Ma, R., Dong, W., Meng, H., et al. (2015b). Thrombotic role of blood and endothelial cells in uremia through phosphatidylserine exposure and microparticle release. *PLoS One* 10:e0142835. doi: 10.1371/journal.pone.0142835

Gasser, O., and Schifferli, J. A. (2004). Activated polymorphonuclear neutrophils disseminate anti-inflammatory microparticles by ectocytosis. *Blood* 104, 2543–2548. doi: 10.1182/blood-2004-01-0361

Georgatzakou, H. T., Antonelou, M. H., Papassideri, I. S., and Kriebardis, A. G. (2016). Red blood cell abnormalities and the pathogenesis of anemia in end-stage renal disease. *Proteomics Clin. Appl.* 10, 778–790. doi: 10.1002/prca.201500127

Georgatzakou, H. T., Tzounakas, V. L., Kriebardis, A. G., Velentzas, A. D., Kokkalis, A. C., Antonelou, M. H., et al. (2018). Short-term effects of hemodiafiltration versus conventional hemodialysis on erythrocyte performance. *Can. J. Physiol. Pharmacol.* 96, 249–257. doi: 10.1139/cjpp-2017-0285

Georgatzakou, H. T., Tzounakas, V. L., Kriebardis, A. G., Velentzas, A. D., Papageorgiou, E. G., Voulgaridou, A. I., et al. (2017). Pathophysiological aspects of red blood cells in end-stage renal disease patients resistant to recombinant human erythropoietin therapy. *Eur. J. Haematol.* 98, 590–600. doi: 10.1111/ejh.12875

Giricz, Z., Varga, Z. V., Baranyai, T., Sipos, P., Paloczi, K., Kittel, A., et al. (2014). Cardioprotection by remote ischemic preconditioning of the rat heart is mediated by extracellular vesicles. *J. Mol. Cell Cardiol.* 68, 75–78. doi: 10.1016/j.yjmcc.2014.01.004

Gomes, J., Lucien, F., Cooper, T. T., Kim, Y., Williams, K. C., Liao, X., et al. (2018). Analytical considerations in nanoscale flow cytometry of extracellular vesicles to achieve data linearity. *Thromb. Haemost.* 118, 1612–1624. doi: 10.1055/s-0038-1668544

Gyorgy, B., Szabo, T. G., Pasztoi, M., Pal, Z., Misjak, P., Aradi, B., et al. (2011). Membrane vesicles, current state-of-the-art: emerging role of extracellular vesicles. *Cell Mol. Life Sci.* 68, 2667–2688. doi: 10.1007/s00018-011-0689-3

Hasin, Y., Seldin, M., and Lusis, A. (2017). Multi-omics approaches to disease. *Genome Biol.* 18:83. doi: 10.1186/s13059-017-1215-1

He, M., Crow, J., Roth, M., Zeng, Y., and Godwin, A. K. (2014). Integrated immunoisolation and protein analysis of circulating exosomes using microfluidic technology. *Lab Chip* 14, 3773–3780. doi: 10.1039/c4lc00662c

Hosseinkhani, B., Kuypers, S., van den Akker, N. M. S., Molin, D. G. M., and Michiels, L. (2018). Extracellular vesicles work as a functional inflammatory mediator between vascular endothelial cells and immune cells. *Front. Immunol* 9:1789. doi: 10.3389/fimmu.2018.01789

Hu, M. C., Kuro-o, M., and Moe, O. W. (2012). The emerging role of Klotho in clinical nephrology. *Nephrol. Dial. Transplant.* 27, 2650–2657. doi: 10.1093/ndt/gfs160

Jalal, D., Renner, B., Laskowski, J., Stites, E., Cooper, J., Valente, K., et al. (2018). Endothelial Microparticles and systemic complement activation in patients with Chronic kidney disease. *J. Am. Heart Assoc.* 7,:e007818. doi: 10.1161/JAHA.117.007818

Jansen, F., Yang, X., Baumann, K., Przybilla, D., Schmitz, T., Flender, A., et al. (2015). Endothelial microparticles reduce ICAM-1 expression in a microRNA-222-dependent mechanism. *J. Cell Mol. Med.* 19, 2202–2214. doi: 10.1111/jcmm.12607

Johnstone, R. M., Adam, M., Hammond, J. R., Orr, L., and Turbide, C. (1987). Vesicle formation during reticulocyte maturation. Association of plasma

membrane activities with released vesicles (exosomes). *J. Biol. Chem.* 262, 9412–9420.

Kapustin, A. N., Chatrou, M. L., Drozdov, I., Zheng, Y., Davidson, S. M., Soong, D., et al. (2015). Vascular smooth muscle cell calcification is mediated by regulated exosome secretion. *Circ. Res.* 116, 1312–1323. doi: 10.1161/CIRCRESAHA.116.305012

Karpman, D., Stahl, A. L., and Arvidsson, I. (2017). Extracellular vesicles in renal disease. *Nat. Rev. Nephrol.* 13, 545–562. doi: 10.1038/nrneph.2017.98

Kataria, A., Levine, D., Wertenteil, S., Vento, S., Xue, J., Rajendiran, K., et al. (2017). Exposure to bisphenols and phthalates and association with oxidant stress, insulin resistance, and endothelial dysfunction in children. *Pediatr. Res.* 81, 857–864. doi: 10.1038/pr.2017.16

Kriebardis, A. G., Antonelou, M. H., Stamoulis, K. E., Economou-Petersen, E., Margaritis, L. H., and Papassideri, I. S. R. B. C. - (2008). derived vesicles during storage: ultrastructure, protein composition, oxidation, and signaling components. *Transfusion* 48, 1943–1953. doi: 10.1111/j.1537-2995.2008.01794.x

Li, S., Ren, J., Xu, N., Zhang, J., Geng, Q., Cao, C., et al. (2014). MicroRNA-19b functions as potential anti-thrombotic protector in patients with unstable angina by targeting tissue factor. *J. Mol. Cell Cardiol.* 75, 49–57. doi: 10.1016/j.yjmcc.2014.06.017

Liu, C., Zhao, J., Tian, F., Cai, L., Zhang, W., Feng, Q., et al. (2019). Low-cost thermophoretic profiling of extracellular-vesicle surface proteins for the early detection and classification of cancers. *Nat. Biomed. Eng.* 3, 183–193. doi: 10.1038/s41551-018-0343-6

Merino, A., Portoles, J., Selgas, R., Ojeda, R., Buendia, P., Ocana, J., et al. (2010). Effect of different dialysis modalities on microinflammatory status and endothelial damage. *Clin. J. Am. Soc. Nephrol.* 5, 227–234. doi: 10.2215/CJN.03260509

Muralidharan, J., Ramezani, A., Hubal, M., Knoblach, S., Shrivastav, S., Karandish, S., et al. (2017). Extracellular microRNA signature in chronic kidney disease. *Am. J. Physiol. Renal. Physiol* 312, F982–F991. doi: 10.1152/ajprenal.00569.2016

Oosthuyzen, W., Scullion, K. M., Ivy, J. R., Morrison, E. E., Hunter, R. W., Starkey Lewis, P. J., et al. (2016). Vasopressin regulates extracellular vesicle uptake by kidney collecting duct cells. *J. Am. Soc. Nephrol.* 27, 3345–3355. doi: 10.1681/ASN.2015050568

Pan, Y., Liang, H., Liu, H., Li, D., Chen, X., Li, L., et al. (2014). Platelet-secreted microRNA-223 promotes endothelial cell apoptosis induced by advanced glycation end products via targeting the insulin-like growth factor 1 receptor. *J. Immunol.* 192, 437–446. doi: 10.4049/jimmunol.1301790

Panichi, V., Rosati, A., Bigazzi, R., Paoletti, S., Mantuano, E., Beati, S., et al. (2011). Anaemia and resistance to erythropoiesis-stimulating agents as prognostic factors in haemodialysis patients: results from the RISCAVID study. *Nephrol. Dial. Transplant.* 26, 2641–2648. doi: 10.1093/ndt/gfq802

Raposo, G., and Stoorvogel, W. (2013). Extracellular vesicles: exosomes, microvesicles, and friends. *J. Cell Biol.* 200, 373–383. doi: 10.1083/jcb.201211138

Ruzicka, M., Xiao, F., Abujrad, H., Al-Rewashdy, Y., Tang, V. A., Langlois, M. A., et al. (2019). Effect of hemodialysis on extracellular vesicles and circulating submicron particles. *BMC Nephrol.* 20:294. doi: 10.1186/s12882-019-1459-y

Ryu, J. H., Park, H., and Kim, S. J. (2017). The effects of indoxyl sulfate-induced endothelial microparticles on neointimal hyperplasia formation in an ex vivo model. *Ann. Surg. Treat. Res.* 93, 11–17. doi: 10.4174/astr.2017.93.1.11

Serrano, K., Levin, E., Chen, D., Hansen, A., Turner, T. R., Kurach, J., et al. (2016). An investigation of red blood cell concentrate quality during storage in paediatric-sized polyvinylchloride bags plasticized with alternatives to di-2-ethylhexyl phthalate (DEHP). *Vox. Sang.* 110, 227–235. doi: 10.1111/vox.12355

Shang, F., Wang, S. C., Hsu, C. Y., Miao, Y., Martin, M., Yin, Y., et al. (2017). MicroRNA-92a mediates endothelial dysfunction in CKD. *J. Am. Soc. Nephrol.* 28, 3251–3261. doi: 10.1681/ASN.2016111215

Shi, C., Ulke-Lemee, A., Deng, J., Batulan, Z., and O'Brien, E. R. (2019). Characterization of heat shock protein 27 in extracellular vesicles: a potential anti-inflammatory therapy. *FASEB J.* 33, 1617–1630. doi: 10.1096/fj.201800987R

Sinauridze, E. I., Kireev, D. A., Popenko, N. Y., Pichugin, A. V., Panteleev, M. A., Krymskaya, O. V., et al. (2007). Platelet microparticle membranes have 50- to 100-fold higher specific procoagulant activity than activated platelets. *Thromb. Haemost.* 97, 425–434. doi: 10.1160/th06-06-0313

Sinning, J. M., Losch, J., Walenta, K., Bohm, M., Nickenig, G., and Werner, N. (2011). Circulating CD31+/Annexin V+ microparticles correlate with cardiovascular outcomes. *Eur. Heart J.* 32, 2034–2041. doi: 10.1093/eurheartj/ehq478

Soriano, S., Carmona, A., Trivino, F., Rodriguez, M., Alvarez-Benito, M., Martin-Malo, A., et al. (2014). Endothelial damage and vascular calcification in patients with chronic kidney disease. *Am. J. Physiol. Renal. Physiol,* 307, F1302–F1311. doi: 10.1152/ajprenal.00114.2014

Stinghen, A. E., Massy, Z. A., Vlassara, H., Striker, G. E., and Boullier, A. (2016). uremic toxicity of advanced glycation end products in CKD. *J. Am. Soc. Nephrol.* 27, 354–370. doi: 10.1681/ASN.2014101047

Thery, C., Witwer, K. W., Aikawa, E., Alcaraz, M. J., Anderson, J. D., Andriantsitohaina, R., et al. (2018). Minimal information for studies of extracellular vesicles 2018 (MISEV2018): a position statement of the International Society for Extracellular Vesicles and update of the MISEV2014 guidelines. *J. Extracell. Vesicles* 7:1535750. doi: 10.1080/20013078.2018.1535750

Trappenburg, M. C., van Schilfgaarde, M., Frerichs, F. C., Spronk, H. M., ten Cate, H., de Fijter, C. W., et al. (2012). Chronic renal failure is accompanied by endothelial activation and a large increase in microparticle numbers with reduced procoagulant capacity. *Nephrol. Dial. Transplant.* 27, 1446–1453. doi: 10.1093/ndt/gfr474

Tzounakas, V. L., Kriebardis, A. G., Georgatzakou, H. T., Foudoulaki-Paparizos, L. E., Dzieciatkowska, M., Wither, M. J., et al. (2016). Glucose 6-phosphate dehydrogenase deficient subjects may be better "storers" than donors of red blood cells. *Free Radic. Biol. Med.* 96, 152–165. doi: 10.1016/j.freeradbiomed.2016.04.005

van Beers, E. J., Schaap, M. C., Berckmans, R. J., Nieuwland, R., Sturk, A., van Doormaal, F. F., et al. (2009). Circulating erythrocyte-derived microparticles are associated with coagulation activation in sickle cell disease. *Haematologica* 94, 1513–1519. doi: 10.3324/haematol.2009.008938

Viegas, C. S. B., Santos, L., Macedo, A. L., Matos, A. A., Silva, A. P., Neves, P. L., et al. (2018). Chronic kidney disease circulating calciprotein particles and extracellular vesicles promote vascular calcification: a role for GRP (Gla-Rich Protein). *Arterioscler. Thromb. Vasc Biol.* 38, 575–587. doi: 10.1161/ATVBAHA.117.310578

Wang, Y., Lu, X., He, J., and Zhao, W. (2015). Influence of erythropoietin on microvesicles derived from mesenchymal stem cells protecting renal function of chronic kidney disease. *Stem Cell Res. Ther.* 6:100. doi: 10.1186/s13287-015-0095-0

Willekens, F. L., Werre, J. M., Groenen-Dopp, Y. A., Roerdinkholder-Stoelwinder, B., de Pauw, B., and Bosman, G. J. (2008). Erythrocyte vesiculation: a self-protective mechanism? *Br. J. Haematol.* 141, 549–556. doi: 10.1111/j.1365-2141.2008.07055.x

Wu, C. Y., Martel, J., Cheng, W. Y., He, C. C., Ojcius, D. M., and Young, J. D. (2013). Membrane vesicles nucleate mineralo-organic nanoparticles and induce carbonate apatite precipitation in human body fluids. *J. Biol. Chem.* 288, 30571–30584. doi: 10.1074/jbc.M113.492157

Xie, J. X., Fan, X., Drummond, C. A., Majumder, R., Xie, Y., Chen, T., et al. (2017). MicroRNA profiling in kidney disease: plasma versus plasma-derived exosomes. *Gene* 627, 1–8. doi: 10.1016/j.gene.2017.06.003

Yu, M., Xie, R., Zhang, Y., Liang, H., Hou, L., Yu, C., et al. (2018). Phosphatidylserine on microparticles and associated cells contributes to the hypercoagulable state in diabetic kidney disease. *Nephrol. Dial. Transplant.* 33, 2115–2127. doi: 10.1093/ndt/gfy027

Yuana, Y., Bertina, R. M., and Osanto, S. (2011). Pre-analytical and analytical issues in the analysis of blood microparticles. *Thromb. Haemost.* 105, 396–408. doi: 10.1160/TH10-09-0595

Zaborowski, M. P., Balaj, L., Breakefield, X. O., and Lai, C. P. (2015). Extracellular vesicles: composition. biological relevance, and methods of study. *Bioscience* 65, 783–797. doi: 10.1093/biosci/biv084

Zecher, D., Cumpelik, A., and Schifferli, J. A. (2014). Erythrocyte-derived microvesicles amplify systemic inflammation by thrombin-dependent activation of complement. *Arterioscler. Thromb. Vasc Biol.* 34, 313–320. doi: 10.1161/ATVBAHA.113.302378

Zhang, Y., Ma, K. L., Gong, Y. X., Wang, G. H., Hu, Z. B., Liu, L., et al. (2018). Platelet microparticles mediate glomerular endothelial injury in early diabetic nephropathy. *J. Am. Soc. Nephrol.* 29, 2671–2695. doi: 10.1681/ASN.2018040368

Zhao, B., Li, H., Liu, J., Han, P., Zhang, C., Bai, H., et al. (2016). MicroRNA-23b targets ras GTPase-activating protein sh3 domain-binding protein 2 to alleviate fibrosis and albuminuria in diabetic nephropathy. *J. Am. Soc. Nephrol.* 27, 2597–2608. doi: 10.1681/ASN.2015030300

Zhou, H., Pisitkun, T., Aponte, A., Yuen, P. S., Hoffert, J. D., Yasuda, H., et al. (2006). Exosomal fetuin-A identified by proteomics: a novel urinary biomarker for detecting acute kidney injury. *Kidney Int.* 70, 1847–1857. doi: 10.1038/sj.ki.5001874

Zhou, Y., Fang, L., Yu, Y., Niu, J., Jiang, L., Cao, H., et al. (2016). Erythropoietin protects the tubular basement membrane by promoting the bone marrow to release extracellular vesicles containing tPA-targeting miR-144. *Am. J. Physiol. Renal. Physiol.* 310, F27–F40. doi: 10.1152/ajprenal.00303.2015

Conflict of Interest: The authors declare that the research was conducted in the absence of any commercial or financial relationships that could be construed as a potential conflict of interest.

Copyright © 2020 Georgatzakou, Pavlou, Papageorgiou, Papassideri, Kriebardis and Antonelou. This is an open-access article distributed under the terms of the Creative Commons Attribution License (CC BY). The use, distribution or reproduction in other forums is permitted, provided the original author(s) and the copyright owner(s) are credited and that the original publication in this journal is cited, in accordance with accepted academic practice. No use, distribution or reproduction is permitted which does not comply with these terms.

frontiers in Cell and Developmental Biology

BRIEF RESEARCH REPORT
published: 29 May 2020
doi: 10.3389/fcell.2020.00399

Paget's Disease and Secondary Hyperparathyroidism: Is Healing Possible?

Vincenzo Antonio Panuccio[1] and Rocco Tripepi[2]**

[1] Nephrology, Dialysis and Transplantation Unit G.O.M. "Bianchi Melacrino Morelli", Reggio Calabria, Italy, [2] Institute of Clinical Physiology (IFC-CNR), Research Unit of Reggio Calabria, Reggio Calabria, Italy

Paget bone disease (PDB) is often asymptomatic and incidentally diagnosed. It is a cause of osteoporosis and bone fragility and exposes patients to a high incidence of bone fractures. In Europe the prevalence varies according to the geographical area of origin, and increases with age. In patients with chronic renal disease, the prevalence is unknown and only few cases with PDB have been reported. We present a challenging case in an elderly patient with chronic kidney disease on peritoneal dialysis treatment. Our patients presented extremely high levels of alkaline phosphatase, suggesting a Paget bone disease. Secondary hyperparathyroidism was confirmed by the bone histological examination. The surprising biochemical and clinical response to active vitamin D confirms the well-known role on hyperparathyroidism and may indicate an additional role in the pathogenesis of Paget's disease.

Keywords: Paget bone disease, hyperparathyroidism, vitamin D, alkaline phosphatase, CKD

OPEN ACCESS

Edited by:
Samar Abd ElHafeez, Alexandria University, Egypt

Reviewed by:
Maria Fusaro, Institute of Clinical Physiology (CNR), Italy
John Charles Rotondo, University of Ferrara, Italy

****Correspondence:***
Vincenzo Antonio Panuccio
enzopanuccio@gmail.com
Rocco Tripepi
rocco.tripepi@ifc.cnr.it

Specialty section:
This article was submitted to Molecular Medicine, a section of the journal Frontiers in Cell and Developmental Biology

Received: *13 March 2020*
Accepted: *29 April 2020*
Published: *29 May 2020*

Citation:
Panuccio VA and Tripepi R (2020) Paget's Disease and Secondary Hyperparathyroidism: Is Healing Possible? Front. Cell Dev. Biol. 8:399. doi: 10.3389/fcell.2020.00399

INTRODUCTION

Paget bone disease (PDB) is a cause of osteoporosis and bone fragility and exposes patients to a high incidence of bone fractures (Dove, 1980; Melton et al., 2000). It is characterized by an imbalance between resorption and deposition of new bone tissue (Iaquinta et al., 2019) and by abnormal osteoclasts (OCL) that secrete high IL-6 levels and induce exuberant bone formation. The altered remodeling results in formation of unstructured, fibroblastic and mechanically fragile bone tissue. Its etiopathogenesis could be linked, at least in part, to infectious factors (Kurihara et al., 2011). A possible relationship between a mutation on chromosome 5 and Paget's disease of bone has recently been described (Michou et al., 2006). In Europe, the prevalence varies from 0.1 to 2% of the adult population, depending upon the geographical area of origin, and increases with age (Poór et al., 2006).

In a high proportion of cases, PDB is discovered incidentally on biochemical testing or radiography. It is possible to detect an isolated increase in alkaline phosphatase (ALP), proportional to the extension of bone disease. Though generally asymptomatic, pain at rest is the most common symptom. A very small percentage of patients may experience a dreadful complication of sarcomatous degeneration.

Paget bone disease can occur in two forms: monostotic if a single bone in involved, or polyostotic if several bone areas are affected. Any bone in the skeleton can be involved, the most frequent being the pelvis, spine, sacrum, skull, femora, and tibiae. In patients with chronic renal disease, the prevalence is unknown. Secondary hyperparathyroidism is a frequent condition in dialysis patients

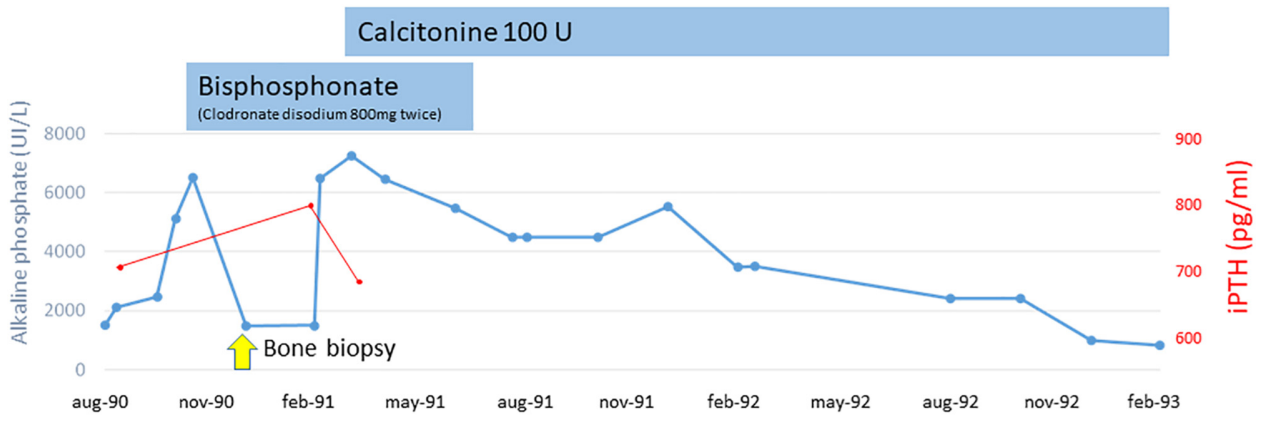

FIGURE 1 | Alkaline phosphatase and intact parathyroid hormone trend during pre-dialysis period.

and can easily mask PDB diagnosis. Furthermore, in dialysis patients, the existing association between bone fractures and cardiovascular comorbidities (Fusaro et al., 2013) is well known as is the predictive role of high iPTH levels and pro-inflammatory cytokines, such us TNF-α, in new bone fractures (Panuccio et al., 2012).

We present a challenging case of PBD in an elderly patient with chronic kidney disease (CKD) on peritoneal dialysis.

CASE REPORT

In 1989, a 60-year-old man with stage 4 CKD with a history of hypertension was referred to our Nephrology and Transplant unit for generalized bone pain and functional limitation. The patient had CKD stage 3b for 9 years until he was admitted in a Pulmonary Unit for tuberculosis disease treated with specific therapy. He also had uncomplicated diabetes mellitus on insulin therapy. Radiographs showed reduced kidney measures. Proteinuria was less than 1 gr/24 h. Koch bacillus in the urine was not detected. Differential diagnosis of the nephropathy was clinical and postulated as secondary to vascular damage, such as nephroangiosclerosis. Patient presented with hypocalcemia (7.6 mg/dl), normal phosphorus levels (average 3.6 mg/dl) and high iPTH (700 pg/ml) and Alkaline Phosphate (AP) (1600 UI/L) levels. He received a calcium-based phosphate binder and active vitamin D supplements thus reaching normalization of serum calcium levels but with a significant increase in phosphate and AP levels (the latter from 1600 to 6000 UI/L).

Bone pain become disabling and radiographs showed deformity of long bones and typical "cotton wool" appearance of the skull. Before excluding a possible neoplastic origin of high AP levels and, on the basis of the clinical and laboratory data, we suspected PDB and decided to treat our patient empirically with bisphosphonate (clodronate disodium 800 mg twice). We observed a rapid reduction of AP levels (to 1800 UI/L). A bone biopsy was suggestive of PDB with superimposed lesions typical of hyperparathiroidism. Alluminum staining was negative. After 3 months, we observed a new increase of AP levels (7000 UI/L) so clodronate was interrupted and nasal calcitonin was prescribed for 6 months resulting in a reduction of AP levels (1000 UI/L). AP and iPTH trends during the pre-dialysis period are shown in **Figure 1**.

In May, 1993, the patient started continuous ambulatory peritoneal dialysis (CAPD). Three months after suspension of calcitonin, the AP level returned near 5000 UI/L and bone pain remained severe. At this point, treatment was focused on the component of secondary hyperparathyroidism, and oral vitamin D boluses (calcitriol 1 mcg once day) were prescribed.

The AP and iPTH levels progressively decreased and reached normal range (AP about 80 UI/L and iPTH <250 pg/ml) at 6 months. **Figure 2** shows the calcium-phosphate product (CaxP) trend during the same period, after starting vitamin D treatment CaxP progressively decrease to became in the normal range. Treatment was stopped with a "watch and wait" approach; to our extreme surprise indicators of bone metabolism remained stable for more than 1 year (AP and iPTH trends during dialysis period are shown in **Figure 3**). To evaluate histological changes in bone turnover, we performed a second bone biopsy at the end of 1997. The bone framework was generally unchanged from the previous one, but with a decrease in severity of bone lesions.

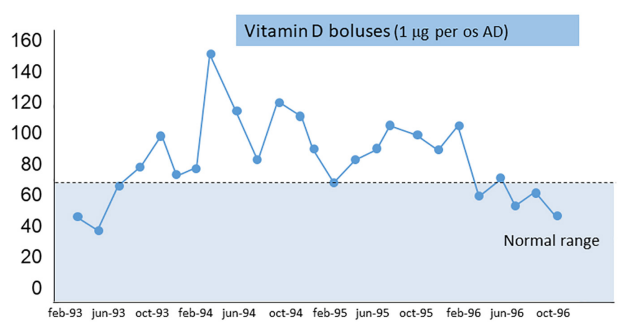

FIGURE 2 | Calcium-phosphate product (mg^2/dL^2) trend during vitamin D treatment.

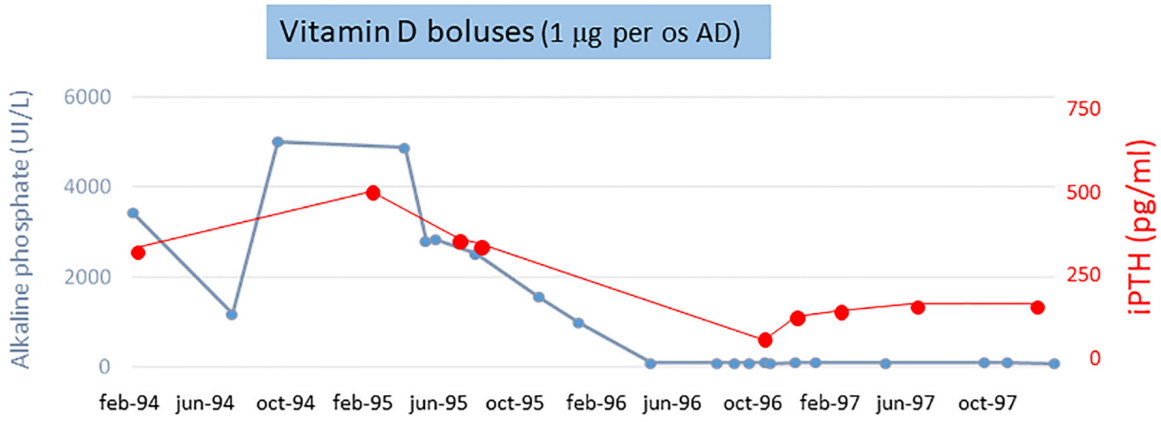

FIGURE 3 | Alkaline phosphatase and intact parathyroid hormone trend during dialysis period.

DISCUSSION

Severe bone pain associated with osteoarticular functional limitation in patients with chronic kidney disease is not common. The extremely high levels of alkaline phosphatase in our patient suggested a Paget bone disease. The peculiarity of our clinical case is that at the same time there was a serious secondary hyperparathyroidism, as confirmed by the bone histological examination. The surprising biochemical and clinical response to active vitamin D (Guillard Cumming et al., 1985; Beresford et al., 1986) may confirm his involvement importance in the pathogenesis of pagetic disease and naturally on the component of hyperparathyroidism. Active vitamin D represents a useful and manageable alternative to the bisphosphonate on the treatment of this patients on dialysis to treat these double disease that induces bone fragility and significantly increases the risk of bone fractures.

Serum ALP is recommended as a first line biochemical screening test, in combination with liver function tests, in screening for the presence of metabolically active PDB.

For the management of PDB, it is important to perform radionuclide bone scans, in addition to targeted radiographs, recommended as a means of fully and accurately defining the extent of metabolically active disease. Treatment in asymptomatic patients is controversial. In the randomized PRISM study, there was no benefit in terms of reducing the incidence of fractures, quality of life and bone pain in attempting to normalize ALP in asymptomatic patients (Langston et al., 2010). Anti-resorptive therapy consists of bisphosphonates for most patients with active PDB who are at risk for future complications. For those intolerant to bisphosphonates, subcutaneous calcitonin can be used for a limited period due to its associated risk of malignancy with long-term use (Ralston et al., 2019). Bisphosphonate treatment may be effective in preventing or slowing the progress of hearing loss and osteoarthritis in joints adjacent to PDB and may reverse paraplegia associated with spinal Paget disease. The adverse events that have been reported with bisphosphonate treatment relevant to the treatment of PDB are rare and include a typical femoral fractures, uveitis, osteonecrosis of the jaw, hypocalcemia, and impaired renal function. Case reports of the use of denosumab 60 mg by subcutaneous injection every 6 months in PDB patients in which bisphosphonates were poorly tolerated or contraindicated, a decrease in total ALP concentrations and an improvement of bone pain was observed (Ralston et al., 2019). There are limited reports on the treatment of patients with CKD and PBD. However, the 2017 KDIGO guideline suggests aggressive control of serum parathyroid hormone, calcium, phosphorus, and vitamin D level for the CKD-MBD patient (Isakova et al., 2017). In this field, calcium mimetics are useful to reach the targets for bone mineral metabolism parameters.

It is important to individualize therapy and to try to prevent falls with regular exercise to maintain joint mobility and bone strength. Patient management with PDB and CKD is a challenge because they are synergistic in affecting bone quality and increasing the risk of fractures.

DATA AVAILABILITY STATEMENT

The datasets generated for this study are available on request to the corresponding authors.

ETHICS STATEMENT

Written informed consent was obtained from the individual for the publication of any potentially identifiable images or data included in this article.

AUTHOR CONTRIBUTIONS

VP conceived the study. VP and RT collected information, drafted the manuscript and approved the final manuscript.

FUNDING

This study was supported by Association QoL-ONE.

ACKNOWLEDGMENTS

Many thanks to the Association QoL-ONE for its support.

REFERENCES

Beresford, J. N., Gallagher, J. A., and Russell, R. G. (1986). 1,25-Dihydroxyvitamin D3 and human bone-derived cells in vitro: effects on alkaline phosphatase, type I collagen and proliferation. *Endocrinology* 119, 1776–1785. doi: 10.1210/endo-119-4-1776

Dove, J. (1980). Complete fractures of the femur in paget's disease of bone. *J. Bone Joint Surg.* 62, 12–17. doi: 10.1302/0301-620x.62b1.7351428

Fusaro, M., Tripepi, G., Noale, M., Vajente, N., Plebani, M., Zaninotto, M., et al. (2013). High prevalence of vertebral fractures assessed by quantitative morphometry in hemodialysis patients, strongly associated with vascular calcifications. *Calcif Tissue Int.* 93, 39–47. doi: 10.1007/s00223-013-9722-x

Guillard Cumming, D. F., Beard, D. J., Douglas, D. L., Johnson, S. K., Awson Matthew, P. J., Russell, R. G. G., et al. (1985). Abnormal vitamin d metabolism in Paget's disease of bone. *Clin. Endocrinol.* 22, 559–566. doi: 10.1111/j.1365-2265.1985.tb00157.x

Iaquinta, M. R., Mazzoni, E., Bononi, I., Rotondo, J. C., Mazziotta, C., Montesi, M., et al. (2019). Adult stem cells for bone regeneration and repair. *Front. Cell Dev. Biol.* 12:268. doi: 10.3389/fcell.2019.00268

Isakova, T., NicKolas, T. L., Denburg, M., Yarlagadda, S., Weiner, D. E., Gutierrez, O. M., et al. (2017). KDIGO clinical practice guideline uptdate for the diagnosis, evaluation, prevention, and Treatment of Chronic Kidney Disease-Mineral and Bone Disorder (CKD-MBD). *AJKD* 70, 737–751. doi: 10.1053/j.ajkd.2017.07.019

Kurihara, N., Hiruma, Y., Yamana, K., Michou, L., Morissette, J., Galson, D. L., et al. (2011). Contributions of the measles virus nucleocapsid gene and the SQSTM1/p62P392L mutation to Paget's disease. *Cell Metab.* 13, 23–34. doi: 10.1016/j.cmet.2010.12.002

Langston, A. L., Campbell, M. K., Raser, W. D., MacLennan, G. S., Selby, R., Pelston, S. H., et al. (2010). Randomized trial of intensive bisphosphonate treatment versus symptomatic management in Paget's disease of bone. *J. Bone Miner. Res.* 25, 20–31. doi: 10.1359/jbmr.090709

Melton, L. J., Tiegs, R. D., Atkinson, E. J., and O'Fallon, W. M. (2000). Fracture risk among patients with Paget's disease: a population-based cohort study. *J. Bone Miner. Res.* 15, 2123–2128.

Michou, L., Collet, C., Laplanche, J. L., Orcel, P., and Cornélis, F. (2006). Genetics of Paget's disease of bone. *Joint Bone Spine* 73, 243–248.

Panuccio, V., Enia, G., Tripepi, R., Aliotta, R., Mallamaci, F., Tripepi, G., et al. (2012). Pro-inflammatory cytokines and bone fractures in CKD patients. An exploratory single centre study. *BMC Nephrol.* 9:134. doi: 10.1186/1471-2369-13-134

Poór, G., Donáth, J., Fornet, B., and Cooper, C. (2006). Epidemiology of Paget's disease in Europe: the prevalence is decreasing. *J. Bone Miner. Res.* 21, 1545–1549. doi: 10.1359/jbmr.060704

Ralston, S. H., Corral-Gudino, L., Cooper, C., Francis, R. M., Fraser, W. D., Gennari, L., et al. (2019). Diagnosis and management of Paget's disease of bone in adults: a clinical guideline. *J. Bone Miner. Res.* 34, 579–604.

Conflict of Interest: The authors declare that the research was conducted in the absence of any commercial or financial relationships that could be construed as a potential conflict of interest.

Copyright © 2020 Panuccio and Tripepi. This is an open-access article distributed under the terms of the Creative Commons Attribution License (CC BY). The use, distribution or reproduction in other forums is permitted, provided the original author(s) and the copyright owner(s) are credited and that the original publication in this journal is cited, in accordance with accepted academic practice. No use, distribution or reproduction is permitted which does not comply with these terms.

frontiers in Cell and Developmental Biology

BRIEF RESEARCH REPORT
published: 29 May 2020
doi: 10.3389/fcell.2020.00336

Urinary Neutrophil Gelatinase-Associated Lipocalin (NGAL) Predicts Renal Function Decline in Patients With Glomerular Diseases

Giuseppe Coppolino, Nicola Comi, Davide Bolignano, Gemma Patella, Alessandro Comi, Michele Provenzano, Laura Rivoli, Michele Andreucci and Giorgio Fuiano*

Renal Unit, "Magna Graecia" University, Catanzaro, Italy

Objective: Available biomarkers for monitoring primary glomerulonephritides (GNs), often lack the ability to assess longitudinal changes and have great variability with poor sensitivity. Accruing evidence has demonstrated that Neutrophil Gelatinase-Associated Lipocalin (NGAL), holds promising capacities in predicting renal function worsening in various renal diseases. We aimed at analyzing urinary NGAL (uNGAL) levels in a cohort of individuals with biopsy-proven GNs in order to evaluate its ability to reflect the entity of renal damage and to predict disease evolution overtime.

Methods: We enrolled 61 consecutive GNs patients still naïve to pathogenic therapy. uNGAL levels were measured at baseline and patients prospectively followed until the manifestation of a combined outcome of doubling of baseline serum creatinine and/or end-stage kidney disease requiring permanent dialysis support.

Results: Median uNGAL levels were 107[35–312] ng/mL. At univariate and multivariate analyses an inverse correlation was found between eGFR and uNGAL levels ($p = 0.001$). Progressor subjects showed exceedingly increased baseline uNGAL values as compared with non-progressors ($p < 0.001$). Twenty-one patients (34%) reached the composite renal endpoint. Subjects with uNGAL values above the optimal, ROC-derived, cut-off of 107 ng/mL experienced a more rapid progression to the renal endpoint ($p < 0.001$; HR: 5.47; 95% CI 2.31–12.95) with a mean follow-up time to progression of 73.4 vs 83.5 months.

Conclusion: In patients affected by primary glomerulonephritides, uNGAL may represent a real-time indicator of renal damage and an independent predictor of renal disease progression. Further studies on larger populations are warranted to confirm these findings.

Keywords: glomerulonefritis, CKD – chronic kidney disease, prediction, urinary NGAL, renal function

OPEN ACCESS

Edited by:
Claudia Torino,
Italian National Research Council, Italy

Reviewed by:
Francesco Pesce,
University of Bari Medical School, Italy
Massimo Senatore,
Ospedale Annunziata, Italy

****Correspondence:***
Giuseppe Coppolino
gcoppolino@unicz.it

Specialty section:
This article was submitted to Molecular Medicine, a section of the journal Frontiers in Cell and Developmental Biology

Received: *05 March 2020*
Accepted: *17 April 2020*
Published: *29 May 2020*

Citation:
Coppolino G, Comi N, Bolignano D, Patella G, Comi A, Provenzano M, Rivoli L, Andreucci M and Fuiano G (2020) Urinary Neutrophil Gelatinase-Associated Lipocalin (NGAL) Predicts Renal Function Decline in Patients With Glomerular Diseases. Front. Cell Dev. Biol. 8:336. doi: 10.3389/fcell.2020.00336

INTRODUCTION

The clinical management of primary glomerulonephritides (GNs) remains a major challenge for nephrologists. This particularly concerns their early identification, but also the choice of the optimal therapeutic pathway to procrastinate the evolution toward end-stage kidney disease (ESKD) (Floege and Amann, 2016). Renal biopsy represents the key-approach for diagnosis, risk stratification and

therapeutic management of patients affected by GNs (Fuiano et al., 2000). However, its invasive nature prevents a routinely use, particularly to monitor disease evolution and therapy success over short time periods.

The measurement of proteinuria has been proved to be a good marker in such regard. However, it often lacks of sensitivity, even if stratified for glomerular filtration rate (Provenzano et al., 2020a), and it is far from being an early indicator of renal impairment, as it usually reflects an already evident damage of the glomerular barrier (Simeoni et al., 2016; Provenzano et al., 2020b).

Hence, the search for alternative, surrogate markers able to predict the tendency of renal disease worsening in a non-invasive and easily reproducible manner remains an important research priority in renal medicine.

Biomarkers, which have been tested so far for monitoring GNs, often lack in the ability to assess longitudinal changes and have great variability with poor sensitivity, mostly due to the influence of concurrent conditions (Bolignano and Coppolino, 2014; Caliskan and Kiryluk, 2014; Rysz et al., 2017; Coppolino et al., 2018). To overcome this important limitation, a focus on markers specifically correlated to kidney disease pathology is desirable (Wasung et al., 2015).

During the last years, accruing evidence has demonstrated that Neutrophil Gelatinase-Associated Lipocalin (NGAL), a small 25-kD protein released in blood and urine from injured renal tubular cells, holds interesting capacities in anticipating renal function worsening in patients affected by chronic kidney disease (CKD) (Bolignano et al., 2008c). Interestingly, this capacity remained evident even after adjustment for a variety of potential confounders, including the severity of renal impairment itself (Bolignano et al., 2009). Furthermore, other reports evidenced the ability of urinary NGAL (uNGAL) to predict successful response to treatment in idiopathic membranous nephropathy, a frequent form of glomerular disease (Yavas et al., 2013).

With this background in mind, we aimed at analyzing uNGAL levels in a small cohort of individuals with biopsy-proven primitive glomerulonephritides still naïve to immunosuppressive therapy, in order to evaluate its ability to reflect the entity of renal damage and to predict disease evolution overtime.

MATERIALS AND METHODS

Patients and Baseline Data

We enrolled 61 consecutive patients with a biopsy-proven glomerulonephritis, who were referred to Renal Unit of the University-Hospital "Magna Graecia" of Catanzaro, Italy. The local Ethic Committee approved the study and all patients gave a written informed consent to participate. Inclusion criteria were the following: the presence of non-advanced renal impairment (intended as normal renal function or early renal insufficiency stages 1–3) and a stable renal function with no documented transitory or permanent doubling in serum creatinine levels over the last 6 months before starting the study. All patients were naïve to steroid or immunosuppressive therapy. Patients with active or previous history of malignancy, liver, inflammatory or infectious diseases, as well as those with altered blood glucose levels or active alterations in leucocyte count or formula, were excluded from the study. Patients' history and drug assumption were carefully collected by interview and confirmed by checking patients' record. Blood pressure was measured three times and the average value was recorded for analysis.

Laboratory Measurements

Blood samples were collected in the morning after an overnight fast, together with a second urine collection of the same day. Ten milliliters of fresh urine were then immediately mixed with 1 mL of 10 mM tris buffer, pH 8.6 with 0.05% Tween 20 and 0.01% of NaN_3 containing protease inhibitors (10 mM benzamidine, 10 mM aminocaproic acid, 20 mM ethylenediaminetetracetate and aprotinin). This mixture was centrifuged at 3000 rpm for 8 min at room temperature and then stored at −80°C until assayed.

Common laboratory parameters, including creatinine, uric acid, electrolytes, serum lipids, albumin, hemoglobin, 24-h proteinuria, fibrinogen and C-Reactive protein (CRP) were measured at baseline in all participants, according to routine standard methods. GFR was estimated by the Modification of Diet in Renal Disease formula, Eq. 7. Urinary NGAL levels were measured using an ABBOTT ARCHITECT® instrument for the rapid quantitative determination of Neutrophil Gelatinase-Associated Lipocalin (NGAL) according to the manufacturer's instructions. All specimens were often diluted to obtain the optimal density for analysis. The enzymatic reactions were quantified in an automatic microplate photometer. All measurements were made in a blinded, duplicate manner. NGAL levels were expressed as ng *per* mL. In order to minimize the potential influence of urine volume, all data analyses were checked by normalizing uNGAL for urinary creatinine.

Follow-Up and CKD Progression Endpoint

After the baseline measurements, patients were prospectively followed until the established end of the observation period or the occurrence of CKD progression, as defined by a combined outcome of doubling of baseline serum creatinine and/or the end-stage kidney disease (ESKD) requiring permanent dialysis support. Patients were directly contacted in case they missed any appointment and at study conclusion, in order to minimize loss to follow-up.

Statistical Analysis

Statistical analysis was performed with SPSS for Windows (version 24.0) and MedCalc (version 12.0). Estimating a 30% occurrence of the endpoint of CKD progression over 5 years in a population with non-advanced CKD and a correlation between uNGAL and the outcome of around 0.25, we computed a sample size of at least 54 participants to give approximately 80% power (alpha = 0.05, two-tailed) to reject the null hypothesis. Data were presented as mean ± SD, median (IQ range) or frequency as appropriate. Differences between groups were established by unpaired *t*-test for normally distributed values

and by Kruskal-Wallis analysis followed by Dunn's test for non-parametric values. Dichotomized values were compared using the X^2 test. Pearson or Spearman correlation coefficients were employed to test correlations between variables with all non-normally distributed values being log-transformed to better approximate normal distributions. Variables incorporated into the MDRD formula for GFR estimation were excluded from analysis. Receiver Operating Characteristics (ROC) analyses were performed to estimate the area under the curve (AUC) for uNGAL and to find the best NGAL cut-off values able to identify individuals who progressed to the endpoint. Kaplan-Meier curves were employed to evaluate renal survival in subjects with urinary NGAL values above and below the optimal ROC-calculated cut-off level. Adjusted risk estimates for progression endpoint were calculated using univariate Cox proportional hazard regression analysis including all variables which resulted significantly different at baseline between "CKD-progressor" and "non-CKD progressor" subjects. Variables significantly associated with the endpoint were then tested in a multivariate Cox model. All results were considered significant if p value was <0.05.

RESULTS

Baseline Data of the Study Cohort

Mean age of patients was 53 ± 17 yrs and 35 (57%) of them were male. Mean serum creatinine was 1.23 ± 0.6 mg/dL with a mean estimated GFR of 75.8 ± 22.1 mL/min/1.73 m^2. Median 24 h proteinuria levels were 3.3[1.1–7.2] g/24 h. Median Urinary NGAL levels were 107 [35–312] ng/mL. According to biopsy results, IgA nephropathy was the leading glomerular disease (25 pts, 41.0%), while three (4.9%) patients had minimal change disease, 20 (32.8%) had membranous nephropathy, 12 (19.7%) had focal glomerulosclerosis and only one subject (1.6%) had a membranoproliferative disease. There was no difference in uNGAL levels across different types of glomerulonephritis's (data not shown). **Table 1** summarizes the main baseline data of the study cohort.

Baseline Correlates of Renal Function

At univariate analyses, fibrinogen levels were directly correlated to eGFR (R: 0.25; p = 0.05) while an inverse correlation was found between eGFR and age (R: −0.28; p = 0.05), systolic blood pressure (R: −0.39; p = 0.006), diastolic blood pressure (R: −0.22; p = 0.03) and, particularly, uNGAL levels (R: −0.45; p = 0.001). In multivariate model including all significant predictors at univariate analyses, only fibrinogen (β: 0.35; p = 0.005), systolic BP (β:−0.32; p = 0.05) and uNGAL (β:−0.48; p < 0.001) remained significantly associated to eGFR. The model explained about 46% of the total variance of eGFR. **Supplementary Table 1** summarizes univariate and multivariate associations of baseline eGFR.

Prospective Follow-Up and Renal Outcome

Twenty-one patients (34%) reached the composite renal endpoint over a mean follow-up of 83.1 ± 24.5 mo. There was no regression

TABLE 1 | Baseline data of the study population.

Parameter	All patients n:61	CKD progressors n:21 (34%)	Non-progressors n:40 (66%)	*p*
Male gender (%)	57	45	55	0.15
Age (yrs)	53 ± 17	57 ± 19	52 ± 16	**0.03**
Systolic BP (mmHg)	136 ± 20	140 ± 21	133 ± 18	**0.05**
Diastolic BP (mmHg)	77 ± 12	79 ± 12	76 ± 13	0.51
eGFR (mL/min/1.73 m^2)	75.8 ± 22.1	51.6 ± 32.5	92.5 ± 39.8	**<0.001**
Serum Creatinine (mg/dL)	1.23 ± 0.6	1.58 ± 0.80	0.98 ± 0.35	**0.001**
Albumin (g/dL)	3.91 ± 1.20	3.9 ± 0.3	3.9 ± 0.3	0.82
Calcium (mg/dL)	9.08 ± 1.60	9.3 ± 0.6	9.0 ± 0.8	0.12
Phosphate (mg/dL)	5.00 ± 0.29	5.2 ± 1.7	4.9 ± 1.5	0.46
Hemoglobin (g/dL)	11.1 ± 1.44	11.0 ± 1.01	11.2 ± 1.36	0.58
Cholesterol (mg/dL)	228 ± 101	223 ± 60	230 ± 104	0.78
Triglycerides (mg/dL)	161 ± 109	187 ± 86	147 ± 75	0.15
C-Reactive Protein (mg/L)	3.05 [3.00–4.16]	5.01 [3.00–4.70]	3.80 [3.00–3.57]	0.29
Fibrinogen (mg/dL)	405.8 ± 109.8	417 ± 130	399 ± 98	**0.05**
Uric Acid (mg/dL)	5.90 ± 3.99	5.96 ± 1.48	5.87 ± 1.44	0.81
Proteinuria (g/24h/1.73 m^2)	3.3 [1.1–7.2]	4.77 [1.12–5.12]	4.69 [0.68–4.32]	0.59
Urinary NGAL (ng/mL)	107 [35–312]	253 [150–432]	118 [75–318]	**0.001**
Histology (%)				0.07
Minimal change	4.9	9.5	2.5	
Membranous nephropathy	32.8	14.3	15	
Focal	19.7	23.8	37.5	
IgA	41.0	47.7	42.5	
Membranoproliferative	1.6	4.7	0	

BP, blood pressure; eGFR, estimated glomerular filtration rate; NGAL, neutrophil gelatinase-associated lipocalin.

of serum creatinine to baseline levels in any of the individuals who progressed to the endpoint, therefore excluding a misleading manifestation of acute kidney injury instead of CKD progression.

The remaining 40 patients (66%) not experiencing a worsening in renal function completed the whole observational period (96 mo). At baseline, CKD-progressor subjects were significantly older and showed increased serum creatinine, systolic blood pressure and fibrinogen levels and lower eGFR values. On the contrary, they did not differ for other parameters such as gender, proteinuria, serum lipids (triglycerides and cholesterol), hemoglobin, CRP, electrolytes, uric acid, diastolic blood pressure and glomerulonephritis diagnosis. The main data and differences between patients experiencing or not-experiencing CKD progression are reported in **Table 1**.

Prognostic Value of uNGAL on Renal Outcome

Progressor subjects showed exceedingly increased baseline uNGAL values as compared with non-progressors (253 [150–432] vs 118 [75–318] ng/mL; $p < 0.001$). At ROC analyses (**Figure 1**), the Area Under the Curve (AUC) for uNGAL to identifying progressor subjects was 0.76 (95% CI 0.63–0.86). Of note, this AUC was virtually superimposable to that of eGFR (data not shown).

The optimal uNGAL cut-off value was 107 ng/mL (Sens. 80.9%, Spec. 67.5%). Interestingly, this coincided with the median value of uNGAL in the whole cohort.

Kaplan-Meier survival curves in individuals with uNGAL levels above or below this ROC-derived threshold are presented in **Figure 2**. Subjects with uNGAL values above 107 ng/mL experienced a more rapid progression to the renal endpoint ($p < 0.001$; HR: 5.47; 95% CI 2.31–12.95) with a mean follow-up time to progression of 73.4 mo (95% CI 62.8–84.6) vs 83.1 mo (95% CI 83.1–93.6).

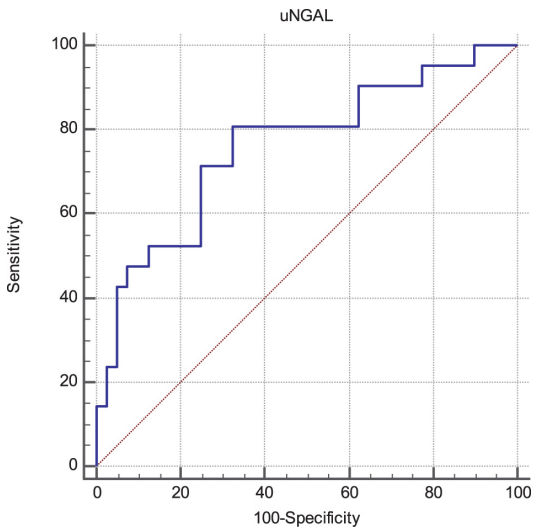

FIGURE 1 | Receiver Operating Characteristics (ROC) curves of uNGAL considering progression of CKD as status variable. The Area Under the Curve (AUC) was 0.76 (95% CI 0.63–0.86). The best cut-off values able to predict the progression of CKD was found to be 107 ng/mL with a sensibility of 80.9 (95% CI 58.1–94.6) and a specificity of 67.5 (95% CI 50.9–81.4).

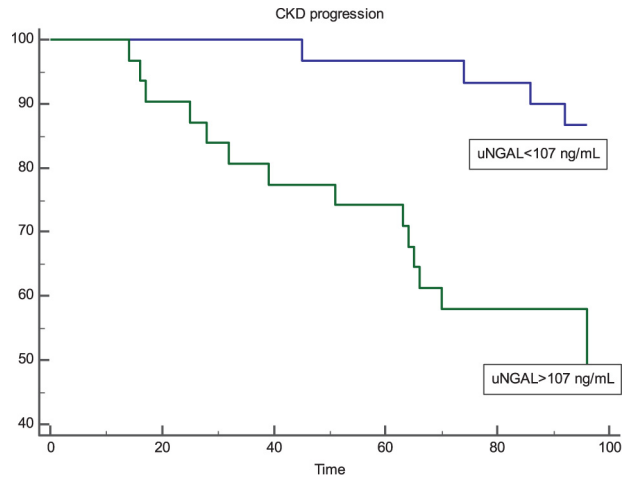

FIGURE 2 | Kaplan-Meier survival curves of renal end-point in patients with uNGAL levels above and below the optimal ROC cut-off level of 107 ng/mL. Patients with uNGAL >107 ng/mL showed a significantly faster progression to endpoint ($p < 0.001$; Log-Rank Test) with a Hazard Ratio of 5.47 (95% CI 2.31–12.95).

Univariate/Multiple Cox Regression Analysis and Renal Outcome

To detect possible risk factors associated with the renal outcome, we tested in a Cox regression analysis all variables that were different at baseline between CKD-progressors and non-progressors (age, systolic BP, eGFR, fibrinogen and uNGAL; **Supplementary Table 1**). Univariate analysis showed that only age (HR 0.99; 95% CI 0.68–0.986; p = 0.05), eGFR (HR 0.97; 95% CI 0.95–0.99; $p = 0.03$) and uNGAL (HR 1.01; 95% CI 1.01–1.07; $p = 0.004$) were significantly associated to the endpoint, while systolic BP and fibrinogen failed to reach statistical significance.

However, in a multiple Cox regression model including these three variables, only eGFR and uNGAL remained significantly associated to CKD progression while age apparently lost its predictive power. More in detail, an increase of 10 ng/mL of uNGAL was associated with a 4% increased risk of CKD progression (HR 1.04; 95% CI 1.01–1.08, $p = 0.03$), whereas an increase of 10 mL/min/1.73m^2 in eGFR reduced this risk by 3% (HR 0.97; 95% CI 0.96–0.99, $p = 0.04$). **Supplementary Table 1** summarizes data from univariate and multivariate Cox-regression analyses **Tables 2**, **3**.

DISCUSSION

The main aim of our study was to test the ability of urinary NGAL to predict progression of renal disease over a long follow-up period in a selected cohort of patients affected by primitive glomerulonephritides. Indeed, in this regard, we found a significant diagnostic capacity of NGAL

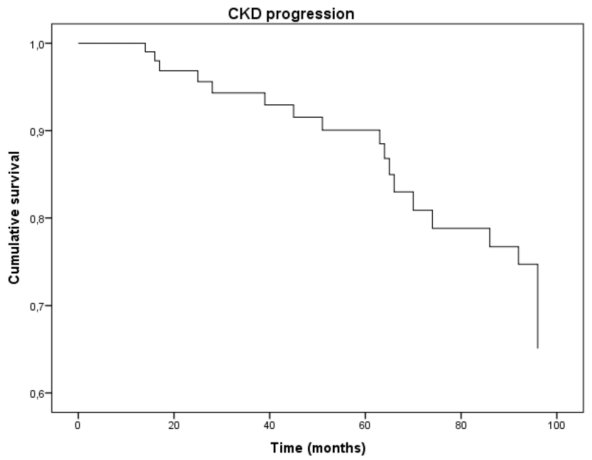

FIGURE 3 | Multiple Cox-derived survival curve to CKD progression.

TABLE 2 | Univariate Cox proportional hazards regression model for progression of CKD.

Variable	Units of increase	*HR*	*95% CI*	X^2	*p*
Age	**1 year**	**0.99**	**0.98–0.99**	**1.22**	**0.05**
Systolic BP	10 mm/Hg	0.99	0.97–1.02	0.17	0.80
eGFR	**10 mL/min/1.73 m^2**	**0.97**	**0.95–0.99**	**4.47**	**0.03**
Fibrinogen	10 mg/dL	1.00	0.99–1.00	0.55	0.45
uNGAL	**10 ng/mL**	**1.03**	**1.01–1.07**	**2.62**	**0.04**

BP, blood pressure; eGFR, estimated glomerular filtration rate; uNGAL, urinary NGAL.

TABLE 3 | Multivariate Cox proportional hazards regression model for progression of CKD.

Variable	Units of increase	*HR*	*95% CI*	X^2	*p*
Age	1 year	0.98	0.95–1.01	2.13	0.14
eGFR	**10 mL/min/1.73 m^2**	**0.97**	**0.96–0.99**	**5.02**	**0.04**
uNGAL	**10 ng/mL**	**1.04**	**1.01–1.08**	**2.13**	**0.03**

eGFR, estimated glomerular filtration rate; uNGAL, urinary NGAL.

which was independent from other important confounders, such as the type of glomerular disease and the baseline GFR itself. After diagnosis, besides the evaluation of proteinuria and GFR slopes overtime, only invasive procedures like renal biopsy are available to follow the natural history of GNs but routinely execution of biopsy is risky and unfeasible in common clinical practice. Hence, the search for early, non-invasive, alternative biomarkers able to stratify the risk to ESKD in this particular population setting remains a demanding priority. Similarly, the ability of these biomarkers to predict risk of relapses and response to different therapies would deserve targeted explorations. Unfortunately, the present study was not sufficiently powered to analyze also this aspect due to the relatively small cohort and the large variability of patients' diagnosis and characteristics.

In two recent studies, Bennett et al. (2012, 2017) demonstrated the capacity of NGAL to predict the degree of response to steroid therapy in children with idiopathic nephrotic syndrome, allowing to discriminate between steroid-sensitive and steroid-resistant individuals.

In our cohort, the majority of participants was affected by IgA nephropathy (41%). Hence, our findings were mostly in accordance with Ding et al. (2007), who also demonstrated that uNGAL is a powerful predictor of disease progression in patients with IgA nephropathy with tubulointerstitial injury. In contrast with these results, Neuhaus et al. (2018) failed to predict the progression of disease with a panel of urinary biomarkers including NGAL in a sub-cohort of the STOP-IgAN trial, although their first purpose was to identify subjects who could benefit from immunosuppression as compared to a supportive therapy alone. An et al. (2019) found higher urinary NGAL levels in patients with nephrotic range proteinuria as compared to those with sub-nephrotic range proteinuria. In our study, we did not find any correlation between uNGAL and proteinuria, perhaps due to the relatively limited sample size and the high heterogeneity of case-mix of our cohort. This also apparently contradicts findings from another previous paper, in which increased urinary NGAL levels resulted highly correlated with proteinuria in a larger cohort of proteinuric patients (Bolignano et al., 2008b). According to current knowledge, high urinary NGAL found in renal diseases is not merely an expression of circulating serum NGAL that is passively loss through the damaged glomerular membrane, but also the active response of tubular cells to a non-specific damage. From this point of view, in our study, the elevated levels of urinary NGAL would therefore represent a "real-time" indicator of how much damage and active suffering is present within the chronic renal impairment (Mori and Nakao, 2007; Bolignano et al., 2008a; Kuwabara et al., 2009). The measurement of urinary NGAL was demonstrated to be an early indicator of renal damage that anticipate common markers used in clinical practice like serum creatinine or cystatin C (George and Gounden, 2019). These common markers are practical and economically sustainable, but far from being a gold standard in terms of prognostic capacity. In fact, their implementation in determined algorithms allows the stadial categorization of renal impairment progression, but has the limit to hide the first phases of organ dysfunction. In fact, until more of the 50% of renal structures are destroyed, the estimated renal function may be normal or paradoxically increased due to hyperfiltration of the remnants glomeruli (Hostetter, 1995). Stressful activation of this functional compensatory effort is itself at the basis of pathological development of lesions, leading to accelerated worsening of renal function (Kliem et al., 1996). Our study has some strengths and limits that deserve mentioning. The main strength was the very long follow-up and the robust statistical analysis implant in which urinary NGAL remained an independent predictor of CKD progression even in a Cox proportional hazards model adjustment. Furthermore, all patients were still naïve to targeted drug approaches, therefore limiting the potential influence of pre-existing immunosuppressive therapy. Main limits are probably represented

by the small, single-center evaluation and by the heterogeneity of GNs, which could prevent application of findings to specific GN subpopulations.

CONCLUSION

We demonstrated that urinary NGAL represents a real-time indicator of renal damage and an independent predictor of renal disease progression in patients affected by primary glomerulonephritides. Future studies would be desirable to ascertain whether this biomarker could also be useful to guide therapeutic management of patients affected by GNs.

DATA AVAILABILITY STATEMENT

The datasets generated for this study are available on request to the corresponding author.

ETHICS STATEMENT

The studies involving human participants were reviewed and approved by University Magna Graecia of Catanzaro. The patients/participants provided their written informed consent to participate in this study.

AUTHOR CONTRIBUTIONS

GC, GF, NC, MA, and DB contributed to the research idea. DB and GC wrote the manuscript. GP, AC, LR, and MP collected the data.

SUPPLEMENTARY MATERIAL

The Supplementary Material for this article can be found online at: https://www.frontiersin.org/articles/10.3389/fcell.2020.00336/full#supplementary-material

REFERENCES

An, C., Akankwasa, G., Liu, J., Wang, D., Cheng, G., Zhang, J., et al. (2019). Urine markers of renal tubular injury in idiopathic membranous nephropathy: a cross sectional study. *Clin. Chim. Acta* 492, 7–11. doi: 10.1016/j.cca.2019.01.015

Bennett, M. R., Piyaphanee, N., Czech, K., Mitsnefes, M., and Devarajan, P. (2012). NGAL distinguishes steroid sensitivity in idiopathic nephrotic syndrome. *Pediatr. Nephrol.* 27, 807–812. doi: 10.1007/s00467-011-2075-7

Bennett, M. R., Pleasant, L., Haffner, C., Ma, Q., Haffey, W. D., Ying, J., et al. (2017). A novel biomarker panel to identify steroid resistance in childhood idiopathic nephrotic syndrome. *Biomark. Insights* 12:1177271917695832. doi: 10.1177/1177271917695832

Bolignano, D., and Coppolino, G. (2014). Biomarkers of cardio-renal damage in chronic kidney disease: one size cannot fit all. *Crit. Care* 18:134. doi: 10.1186/cc13834

Bolignano, D., Coppolino, G., Aloisi, C., Romeo, A., Nicocia, G., and Buemi, M. (2008a). Effect of a single intravenous immunoglobulin infusion on neutrophil gelatinase-associated lipocalin levels in proteinuric patients with normal renal function. *J. Investig. Med.* 56, 997–1003. doi: 10.2310/JIM.0b013e31818e7e95

Bolignano, D., Coppolino, G., Campo, S., Aloisi, C., Nicocia, G., Frisina, N., et al. (2008b). Urinary neutrophil gelatinase-associated lipocalin (NGAL) is associated with severity of renal disease in proteinuric patients. *Nephrol. Dial Transpl.* 23, 414–416. doi: 10.1093/ndt/gfm541

Bolignano, D., Donato, V., Coppolino, G., Campo, S., Buemi, A., Lacquaniti, A., et al. (2008c). Neutrophil gelatinase-associated lipocalin (NGAL) as a marker of kidney damage. *Am. J. Kidney Dis.* 52, 595–605. doi: 10.1053/j.ajkd.2008.01.020

Bolignano, D., Lacquaniti, A., Coppolino, G., Donato, V., Campo, S., Fazio, M. R., et al. (2009). Neutrophil gelatinase-associated lipocalin (NGAL) and progression of chronic kidney disease. *Clin. J. Am. Soc. Nephrol.* 4, 337–344. doi: 10.2215/CJN.03530708

Caliskan, Y., and Kiryluk, K. (2014). Novel biomarkers in glomerular disease. *Adv. Chron. Kidney Dis.* 21, 205–216. doi: 10.1053/j.ackd.2013.12.002

Coppolino, G., Leporini, C., Rivoli, L., Ursini, F., di Paola, E. D., Cernaro, V., et al. (2018). Exploring the effects of DPP-4 inhibitors on the kidney from the bench to clinical trials. *Pharmacol. Res.* 129, 274–294. doi: 10.1016/j.phrs.2017.12.001

Ding, H., He, Y., Li, K., Yang, J., Li, X., Lu, R., et al. (2007). Urinary neutrophil gelatinase-associated lipocalin (NGAL) is an early biomarker for renal tubulointerstitial injury in IgA nephropathy. *Clin. Immunol.* 123, 227–234. doi: 10.1016/j.clim.2007.01.010

Floege, J., and Amann, K. (2016). Primary glomerulonephritides. *Lancet* 387, 2036–2048. doi: 10.1016/S0140-6736(16)00272-5

Fuiano, G., Mazza, G., Comi, N., Caglioti, A., De Nicola, L., Iodice, C., et al. (2000). Current indications for renal biopsy: a questionnaire-based survey. *Am. J. Kidney Dis.* 35, 448–457. doi: 10.1016/s0272-6386(00)70197-1

George, J. A., and Gounden, V. (2019). Novel glomerular filtration markers. *Adv. Clin. Chem.* 88, 91–119.

Hostetter, T. H. (1995). Progression of renal disease and renal hypertrophy. *Annu. Rev. Physiol.* 57, 263–278. doi: 10.1146/annurev.ph.57.030195.001403

Kliem, V., Johnson, R. J., Alpers, C. E., Yoshimura, A., Couser, W. G., Koch, K. M., et al. (1996). Mechanisms involved in the pathogenesis of tubulointerstitial fibrosis in 5/6-nephrectomized rats. *Kidney Int.* 49, 666–678. doi: 10.1038/ki.1996.95

Kuwabara, T., Mori, K., Mukoyama, M., Kasahara, M., Yokoi, H., Saito, Y., et al. (2009). Urinary neutrophil gelatinase-associated lipocalin levels reflect damage to glomeruli, proximal tubules, and distal nephrons. *Kidney Int.* 75, 285–294. doi: 10.1038/ki.2008.499

Mori, K., and Nakao, K. (2007). Neutrophil gelatinase-associated lipocalin as the real-time indicator of active kidney damage. *Kidney Int.* 71, 967–970. doi: 10.1038/sj.ki.5002165

Neuhaus, J., Bauer, F., Fitzner, C., Hilgers, R. D., Seibert, F., Babel, N., et al. (2018). Urinary biomarkers in the prediction of prognosis and treatment response in IgA nephropathy. *Kidney Blood Press Res.* 43, 1563–1572. doi: 10.1159/000494442

Provenzano, M., Chiodini, P., Minutolo, R., Zoccali, C., Bellizzi, V., Conte, G., et al. (2020a). Reclassification of chronic kidney disease patients for end-stage renal disease risk by proteinuria indexed to estimated glomerular filtration rate: multicentre prospective study in nephrology clinics. *Nephrol. Dial Transplant* 35, 138–147. doi: 10.1093/ndt/gfy217

Provenzano, M., Garofalo, C., Chiodini, P., Mancuso, C., Barbato, E., De Nicola, L., et al. (2020b). Role of proteinuria in clinical research: for each old-answer, a new key-question. *Recenti Progressi Med.* 111, 74–81. doi: 10.1701/3309.32797

Rysz, J., Gluba-Brzozka, A., Franczyk, B., Jablonowski, Z., and Cialkowska-Rysz, A. (2017). Novel biomarkers in the diagnosis of chronic kidney disease and the prediction of its outcome. *Int. J. Mol. Sci.* 18:1702. doi: 10.3390/ijms18081702

Simeoni, M., Nicotera, R., Colao, M., Citraro, M. L., Pelagi, E., Cerantonio, A., et al. (2016). Direct inhibition of plasmatic renin activity with aliskiren: a promising but under-investigated therapeutic option for non-diabetic glomerulonephritis. *Int. Urol. Nephrol.* 48, 229–237. doi: 10.1007/s11255-015-1128-4

Wasung, M. E., Chawla, L. S., and Madero, M. (2015). Biomarkers of renal function, which and when? *Clin. Chim. Acta* 438, 350–357. doi: 10.1016/j.cca.2014.08.039

Yavas, H., Sahin, O. Z., Ersoy, R., Tasli, F., Gibyeli Genek, D., Uzum, A., et al. (2013). Prognostic value of NGAL staining in patients with IgA nephropathy. *Renal Fail.* 35, 472–476.

Conflict of Interest: The authors declare that the research was conducted in the absence of any commercial or financial relationships that could be construed as a potential conflict of interest.

Copyright © 2020 Coppolino, Comi, Bolignano, Patella, Comi, Provenzano, Rivoli, Andreucci and Fuiano. This is an open-access article distributed under the terms of the Creative Commons Attribution License (CC BY). The use, distribution or reproduction in other forums is permitted, provided the original author(s) and the copyright owner(s) are credited and that the original publication in this journal is cited, in accordance with accepted academic practice. No use, distribution or reproduction is permitted which does not comply with these terms.

frontiers in Cell and Developmental Biology

ORIGINAL RESEARCH
published: 03 June 2020
doi: 10.3389/fcell.2020.00436

Induction of Autophagy by Pterostilbene Contributes to the Prevention of Renal Fibrosis via Attenuating NLRP3 Inflammasome Activation and Epithelial-Mesenchymal Transition

Ying-Jan Wang[1,2†], Yu-Ying Chen[1], Ching-Mao Hsiao[1], Min-Hsiung Pan[3], Bour-Jr Wang[1,4,5], Yu-Chi Chen[6], Chi-Tang Ho[7], Kuo-Ching Huang[1,8†] and Rong-Jane Chen[9]*

[1] Department of Environmental and Occupational Health, College of Medicine, National Cheng Kung University, Tainan, Taiwan, [2] Department of Medical Research, China Medical University Hospital, China Medical University, Taichung, Taiwan, [3] Institute of Food Science and Technology, National Taiwan University, Taipei, Taiwan, [4] Department of Occupational and Environmental Medicine, National Cheng Kung University Hospital, Tainan, Taiwan, [5] Department of Cosmetic Science and Institute of Cosmetic Science, Chia Nan University of Pharmacy and Science, Tainan, Taiwan, [6] Department of Biotechnology, National Kaohsiung Normal University, Kaohsiung, Taiwan, [7] Department of Food Science, Rutgers University, New Brunswick, NJ, United States, [8] Division of Nephrology, Department of Internal Medicine, Chi Mei Hospital, Tainan, Taiwan, [9] Department of Food Safety/Hygiene and Risk Management, College of Medicine, National Cheng Kung University, Tainan, Taiwan

OPEN ACCESS

Edited by:
Claudia Torino,
Italian National Research Council, Italy

Reviewed by:
Marco Giammanco,
University of Palermo, Italy
Rossana Morabito,
University of Messina, Italy

***Correspondence:**
Rong-Jane Chen
janekhc@gmail.com

† These authors have contributed equally to this work

Specialty section:
This article was submitted to Molecular Medicine, a section of the journal Frontiers in Cell and Developmental Biology

Received: *13 March 2020*
Accepted: *08 May 2020*
Published: *03 June 2020*

Citation:
Wang Y-J, Chen Y-Y, Hsiao C-M, Pan M-H, Wang B-J, Chen Y-C, Ho C-T, Huang K-C and Chen R-J (2020) Induction of Autophagy by Pterostilbene Contributes to the Prevention of Renal Fibrosis via Attenuating NLRP3 Inflammasome Activation and Epithelial-Mesenchymal Transition. Front. Cell Dev. Biol. 8:436. doi: 10.3389/fcell.2020.00436

Chronic kidney disease (CKD) is recognized as a global public health problem. NLRP3 inflammasome activation has been characterized to mediate diverse aspect mechanisms of CKD through regulation of proinflammatory cytokines, tubulointerstitial injury, glomerular diseases, renal inflammation, and fibrosis pathways. Autophagy is a characterized negative regulation mechanism in the regulation of the NLRP3 inflammasome, which is now recognized as the key regulator in the pathogenesis of inflammation and fibrosis in CKD. Thus, autophagy is undoubtedly an attractive target for developing new renal protective treatments of kidney disease via its potential effects in regulation of inflammasome. However, there is no clinical useful agent targeting the autophagy pathway for patients with renal diseases. Pterostilbene (PT, trans-3,5-dimethoxy-4-hydroxystilbene) is a natural analog of resveratrol that has various health benefits including autophagy inducing effects. Accordingly, we aim to investigate underlying mechanisms of preventive and therapeutic effects of PT by reducing NLRP3 inflammasome activation and fibrosis through autophagy-inducing effects. The renal protective effects of PT were evaluated by potassium oxonate (PO)-induced hyperuricemia and high adenine diet-induced CKD models. The autophagy induction mechanisms and anti-fibrosis effects of PT by down-regulation of NLRP3 inflammasome are investigated by using immortalized rat kidney proximal tubular epithelial NRK-52E cells. To determine the role of autophagy induction in the alleviating of NLRP3

inflammasome activation and epithelial-mesenchymal transition (EMT), NRK-52E with Atg5 knockdown [NRK-Atg5-(2)] cells were applied in the study. The results indicated that PT significantly reduces serum uric acid levels, liver xanthine oxidase activity, collagen accumulation, macrophage recruitment, and renal fibrosis in CKD models. At the molecular levels, pretreatment with PT downregulating TGF-β-triggered NLRP3 inflammasome activation, and subsequent EMT in NRK-52E cells. After blockage of autophagy by treatment of Atg5 shRNA, PT loss of its ability to prevent NLRP3 inflammasome activation and EMT. Taken together, we suggested the renal protective effects of PT in urate nephropathy and proved that PT induces autophagy leading to restraining TGF-β-mediated NLRP3 inflammasome activation and EMT. This study is also the first one to provide a clinical potential application of PT for a better management of CKD through its autophagy inducing effects.

Keywords: autophagy, epithelial-mesenchymal transition, NLRP3 inflammasome, pterostilbene, renal fibrosis

INTRODUCTION

Chronic kidney disease (CKD) is now known as a major public health issue worldwide (Kumagai et al., 2017). Most forms of CKD are characterized by inflammation and progressive fibrosis in the final stage that eventually affects the structures and functions of kidney leading to an irreversible end-stage renal disease (Kim et al., 2014). Recent attention has focused on the contribution of NLRP3 [nucleotide-binding and oligomerization domain (NOD)-like receptors (NLRs) protein 3] inflammasome activation in the pathogenesis of inflammation and fibrosis in several CKD (Scarpioni and Obici, 2018). In response to damage-associated molecular patterns (DAMPs) such as uric acid (UA), NLRP3 proteins oligomerize, and recruit an ASC (apoptosis-associated speck-like protein containing a C-terminal caspase-recruitment domain), and pro-caspase-1 to complete the formation of the inflammasome (Chen et al., 2016). The inflammasome complexes then induce the caspase-1 activation thereby cleaves the pro-inflammatory cytokines into their active forms such as IL-1β and IL-18 leading to chronic inflammation and cellular damage (Chen et al., 2016). NLRP3 and ASC can be found in renal dendritic cells, infiltrating macrophages, epithelial cells, and tubules (Chang et al., 2014). A recent study indicated that UA could induce NLRP3 expression, caspase-1 activation, IL-1β, and ICAM-1 production in human renal proximal tubule epithelial cells (Xiao et al., 2015). In several CKD disease models, activation of NLRP3 inflammasome, production of IL-1β and activation of P-Smad 2/3 pathways were associated with renal inflammation, epithelial-mesenchymal transition (EMT), and fibrosis (Romero et al., 2017; Qi and Yang, 2018). These studies indicate that downregulation of NLRP3 inflammasome may attenuate renal inflammation and fibrosis; thus, NLRP3 inflammasome may serve as a potential new therapeutic target for CKD.

Recent studies prove the potential role of autophagy in the prevention of CKD (Lin et al., 2019). Autophagy is a highly regulated mechanism that occurs in four phases including induction, nucleation, elongation, and fusion that are tightly regulated by various signaling pathways such as 5′-adenosine monophosphate activated protein kinase (AMPK), autophagy proteins (Atgs) including Atg8 (LC3), Atg5, Atg12, and Atg16L1, and lysosomal enzymes (Chen et al., 2016). Defects in autophagy has been implicated in various diseases and health states, including CKD, neurodegeneration, aging, infectious disease, inflammation, and cancer (Chen et al., 2017b). Currently, autophagy was reported to negatively regulate the NLRP3 inflammasome activation through degradation of NLRP3, ASC, and caspase-1, and pro-inflammatory cytokines as well (Chen et al., 2016). In unilateral ureteral obstruction (UUO)-induced renal fibrosis model, autophagy induction protected fibrosis through regulation of the expression of NLRP3, TGF-β, and IL-1β. Therefore, autophagy is undoubtedly an attractive target for developing new protective treatments of CKD. However, there is no clinical useful agent targeting the autophagy pathway for patients with renal diseases.

Pterostilbene (PT, trans-3,5-dimethoxy-4-hydroxystilbene), a chemical classified as a stilbene, can be found in many foods and herbs such as blueberries, grapes, and tree wood (Chen et al., 2017b). Because of the presence of two methoxy groups, PT exhibits better bioavailability, more lipophilicity, as well as the higher cellular uptake and a longer half-life than its analog resveratrol (Chen et al., 2017b). PT has many health benefits including antioxidant activity, anti-inflammatory effects, anti-obesity, and chemopreventive effects attributed to its unique structure (Lee et al., 2019). Interestingly, PT has been recently demonstrated to effectively protect renal function in a potassium oxonate (PO)-induced hyperuricemia model through regulation of the renal mURAT1, mGLUT9, mABCG2, and mOAT1 (Shi et al., 2012). One other study also suggests that PT has renal protective actions and ameliorates fructose-induced hyperuricemia and fibrosis through suppression of the TGF-β/Smads pathway (Gu et al., 2019). More importantly, PT is now recognized as an effective autophagy inducer in cancer and normal cells (Chen et al., 2017b). The renal protective effects and mechanisms of PT regarding autophagy and NLRP3 inflammasome pathways have not yet been studied. In view of the autophagy inducing effects and the potential beneficial renal protective effects of PT; we try to put a forward a view-point

that autophagy induction is a novel mechanism modulating the PT-induced protective effects against CKD. In the present study, we provide the scientific basis of autophagy in the regulation of NLRP3 inflammasome and fibrosis in CKD. Our study also proves that PT could effectively prevent CKD via autophagy contributed to restraining TGF-β-mediated NLRP3 inflammasome activation and EMT in NRK-52E cells. To the best of our knowledge, this is the first study to provide a clinical potential application of PT for a better management of CKD through its autophagy inducing effects.

MATERIALS AND METHODS

Chemicals and Reagents

The uricase inhibitor PO, adenine (AD), and XOD inhibitor allopurinol (AP, urate lowering agent) were purchased from Sigma (St. Louis, MO, United States). TGF-β was obtained from R&D Systems, Inc. (Minneapolis, MN, United States). The NLRP3 inhibitor MCC950, UA assay kit and XOD fluorometric assay kit were purchased from Cayman Chemical Company (Michigan, United States). Pterostilbene (96% purity) was a gift from Sabinsa Corporation (East Winsor, NJ, United States). Primary antibodies against E-Cadherin, fibronectin, α-SMA, and Vimentin were purchased from Genetec Inc. (Montreal, QC, Canada). Antibodies against NLRP3, ASC, caspase-1, IL-1β, AMPK, phosphor-AMPK, mTOR, phosphor-mTOR, p62, LC3-II, and GAPDH were purchased from Cell Signaling (Beverly, MA, United States). The horseradish peroxidase (HRP)-conjugated anti-mouse and anti-rabbit secondary antibodies were obtained from Jackson ImmunoResearch (West Grove, PA, United States).

Animals

Four-week-old ICR male mice were purchased from BioLASCO Taiwan Co., Ltd (Taipei, Taiwan). They were housed (five mice per cage) in a pathogen-free environment, maintained on Lab Diet 5010 chow (PMI Feeds, Inc, St. Louis, MO, United States) at 24 ± 2°C and 50 ± 10% relative humidity, and subjected to a 12 h light/12 h dark cycle in the Laboratory Animal Center of the National Cheng Kung University Medical College. All animal studies were approved by the Laboratory Animal Center of the National Cheng Kung University Medical College (Approval No. 103293) and performed according to the local guidelines for animal care and protection.

PO-Induced Hyperuricemia Model

Establishment of the PO-induced hyperuricemia animal model was performed as our previous report (Chen et al., 2017a). Mice were divided into four groups of Control (0.9% normal saline), PO groups (400 mg/kg, hyperuricemia groups), PO + AP (positive treatment groups, AP: 10 mg/kg), or PO + PT (200 mg/kg) groups (**Figure 1A**).

XOD Activities of Mouse Livers

Mouse liver XOD activities were analyzed by XOD fluorometric assay kit (Chen et al., 2017a).

High Adenine Diet-Induced CKD Model

The CKD model is adapted by Diwan's study (Diwan et al., 2013). Briefly, male ICR mice at 5 weeks of age were randomly divided into four experimental groups treated for 10 days (n = 5 in each group). The control groups were given powdered mouse food. The PO + AD groups received high adenine diet (0.175% AD in powder) together with orally administration of PO (400 mg/kg/day). The PO + AD + AP and PO + AD + PT groups indicated the mice treated with AP (10 mg/kg) or PT (200 mg/kg) by gastric gavage for 10 days combined with PO + AD (**Figure 2A**). Urine were collected before the day of sacrificed. All mice were sacrificed 1 h after the last treatment, and blood samples were collected from cardiac puncture for analysis. Kidneys were removed and examined for the morphology at necropsy. The right kidneys were kept in liquid nitrogen for Western blotting analysis, and the left ones were preserved in 10% buffered formalin for immunohistochemistry study.

UA Analysis

The UA level of serum and urine was determined by the UA kit according to the manufacturer's instructions as previous reported (Chen et al., 2017a).

Renal Function Analysis

Mouse serum and urine samples were monitored by the biochemical indices including BUN (blood urea nitrogen), and CRE (creatinine) using commercial kits (FUJIFILM corporation, Tokyo, Japan).

H&E Staining, Masson Trichrome Staining, and Immunohistochemistry of Kidney Tissues

Serial tissue sections (4 μm) of kidneys were sliced from paraffin-embedded, formalin-fixed kidneys, and stained with hematoxylin and eosin (H&E). For Masson's trichrome staining, tissues were stained with aniline blue liquid and 1% acetic acid, followed by dehydration with ethanol. Staining showed collagen fibers in blue and cytoplasm in red color. For immunohistochemistry, the slides were incubated with primary and secondary antibodies then developed with the STARRTREK Universal HRP detection Kit (Biocare medical, Concord, CA, United States).

Cell Culture of Control and Atg5 Knockdown NRK-52E Cells

NRK-52E cells (immortalized rat kidney proximal tubular epithelial cells, CRL-1571) were purchased from Bioresource Collection and Research Center (Food Industry Research and Development Institute, Hsinchu, Taiwan) and were cultured in Dulbecco's modified Eagle's medium (DMEM) with 5% fetal bovine serum (HyClone, South Logan, UT, United States), 100 U/ml penicillin, and 100 μg/ml streptomycin (Life Technologies, Inc., Gaithersburg, MD, United States). The cells were treated with TGF-β (2.5 ng/ml), PT (2 μM), or in combination for indicated time points. To establish autophagy defect cells, NRK-52E cells were transfected with the Atg5 knockdown shRNA (TRCN0000327377) which was obtained

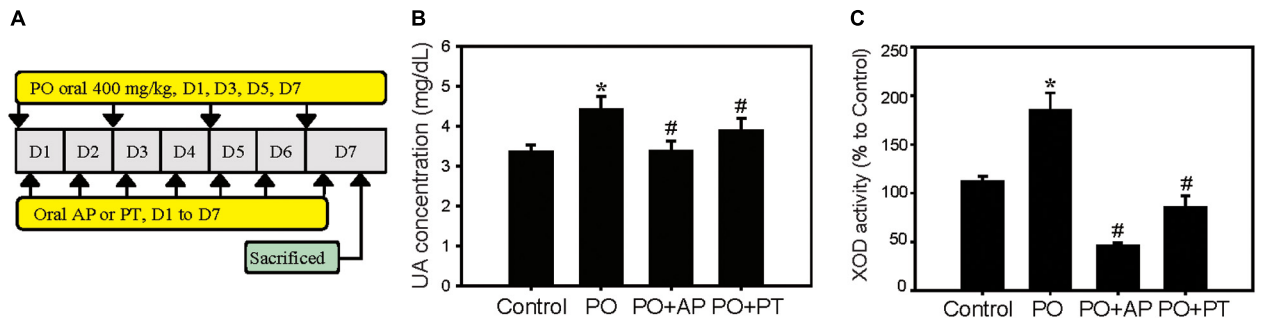

FIGURE 1 | Urate lowering effects of PT in a hyperuricemia animal model. **(A)** Scheme of PO-induced hyperuricemia model as described in the Materials and Methods. **(B)** UA concentration and **(C)** liver XOD activities of mice treated with Control, PO (400 mg/kg), PO + AP (10 mg/kg), or PO + PT (200 mg/kg) for 7 days (n = 3 in each group). Data represent the mean ± SD. $^{*}p < 0.05$ compared with the Control groups. $^{\#}p < 0.05$ compared with PO groups. PO: potassium oxonate, PT: pterostilbene, AP: allopurinol, and XOD: xanthine oxidase.

from the National RNA interference Core Facility located at the Institute of Molecular Biology/Genomic Research Centre, Academia Sinica (Nankang, Taipei, Taiwan). The stable Atg5 knockdown cells [NRK-Atg5(1), (2)] were maintained in DMEM contained with 2 μg/ml puromycin.

Cell Viability Assay

NRK-52E cells were seeded in a 96-well plate at a density of 1×10^4 cells/well for overnight then treated with TGF-β (2.5, 5, and 10 ng/ml), PT (0.5, 1, 2 μM), or TGF-β combined with PT for 24, 48, or 72 h and the viability was detected by MTT assay (Chen et al., 2010).

Detection of Autophagy by Flow Cytometry

NRK-52E and Atg5 knockdown cells were treated with TGF-β (2.5 ng/ml), PT (2 μM), or in combination for indicated time points and autophagy was detected by acridine orange (AO) staining and analyzed by flow cytometric analysis (FACScan, Becton Dickinson, San Jose, CA, United States) and quantified using FlowJo 7.6.1. software (Tree Star Inc, Ashland, OR, United States; Chen et al., 2010).

Western Blot Analyses

Randomized frozen kidney samples or NRK-52E cells from different treatment groups were homogenized and lysates were subjected to gel electrophoresis and immunoblotting (Chen et al., 2017c). Immunoreactive proteins were visualized with a chemiluminescent detection system (PerkinElmer Life Science, Inc. MA, United States) and BioMax LightFilm (Eastman Kodak Co., New Haven, CT, United States) according to the manufacturer's instructions.

Immunofluorescence Staining

After treatment with TGF-β, PT, or in combination for 72 h, cells were fixed, washed then incubated with primary and fluorophore-conjugated secondary antibodies for 1 h, mounted with Vectashield Mounting Medium with DAPI (Vector Laboratories, #H-1600, Peterborough, United Kingdom), and then analyzed using a fluorescence microscope.

Statistical Analysis

Results are expressed as mean ± standard error of the mean (SEM). Experimental data were analyzed using the Student's t test. Differences were considered to be statistically significant when the p value was less than 0.05.

RESULTS

Urate-Lowering Effect and XOD Inhibition Activity of PT in the Hyperuricemia Animal Model

Previous studies indicated that UA is the main risk factor for CKD (Kumagai et al., 2017). Accordingly, we first verify the urate-lowering effect of PT in the established PO-induced hyperuricemia model (**Figure 1A**). The results showed that PO significantly increased the UA concentration level (4.63 ± 0.32 mg/dL) when compared to the control groups (3.35 ± 0.19 mg/dL; **Figure 1B**), whereas PT administration followed by PO (PO + PT groups) effectively decreased UA levels (3.90 ± 0.31 mg/dL) compared to the PO groups. AP (therapy control) also significantly lowered serum UA levels in mice (PO + AP groups, 3.00 ± 0.23 mg/dL; **Figure 1B**). XOD activity was assayed using mouse livers and the inhibition of XOD activity by AP and PT showed 60.1% and 25%, respectively (**Figure 1C**). The results suggest the urate lowering effects of PT could partially depend on XOD inhibitory effects.

PT Reduced Renal Damage and Fibrosis in the High Adenine-Induced Renal Fibrosis Model

The renal protective mechanisms of PT were further investigated in the high AD diet-induced CKD model which has been reported related to the pathogenesis in human CKD (**Figure 2A**). Concomitant administration of PO and AD (PO + AD) reduced daily food intake and the final body weights in mice

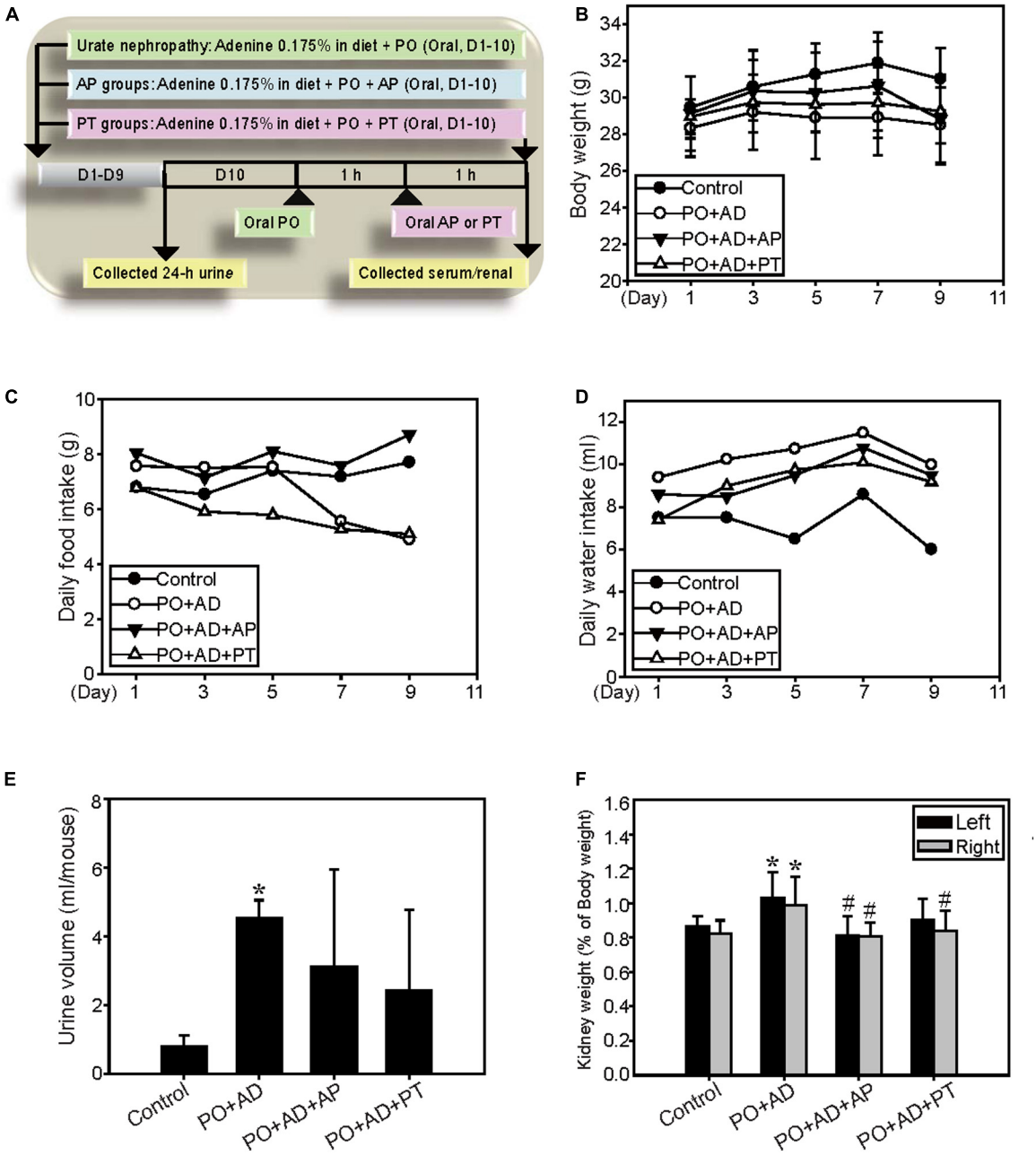

FIGURE 2 | Renal protective effects of PT in a high adenine-induced CKD model. **(A)** The high adenine-induced CKD model was performed as described in Materials and Method. **(B)** Changes of body weight, **(C)** daily food intake, and **(D)** daily water intake are demonstrated for ICR mice fed with 0.9% saline (Control), PO combined with 0.175% adenine (PO + AD), AP (10 mg/kg) combined with PO + AD (PO + AD + AP), or PT (200 mg/kg) combined with PO + AD (PO + AD + PT). Effects of PT on **(E)** 24-h urine output and **(F)** kidney relative weight (kidney weight/final body weight × 100) in mice. Each column and vertical bar are mean ± SD of 5 mice/group. *$p < 0.05$ compared with the control groups.

(**Figures 2B,C**) but increased water intake and urine output (**Figures 2D,E**). On the contrary, PT mitigates these actions as shown in **Figures 2B–E**. The weight of kidneys showed significantly increased in PO + AD groups, whereas PT prevents increased in kidney weights as shown in **Figure 2F**. Moreover, renal function analysis indicated the protective effects of PT comparted with PO + AD groups that mice treated with PT 200 mg/kg for 10 days (PO + AD + PT groups) decreased serum UA, CRE, and BUN levels compared to PO + AD groups (**Figures 3A,C,F**). Simultaneously, PT increased urine UA, CRE, and BUN levels (**Figures 3B,D,G**), and the clearance rate of CRE, and BUN as well (**Figures 3E,F**). Similar results were found in AP treated groups further confirmed the renal protective effects of PT.

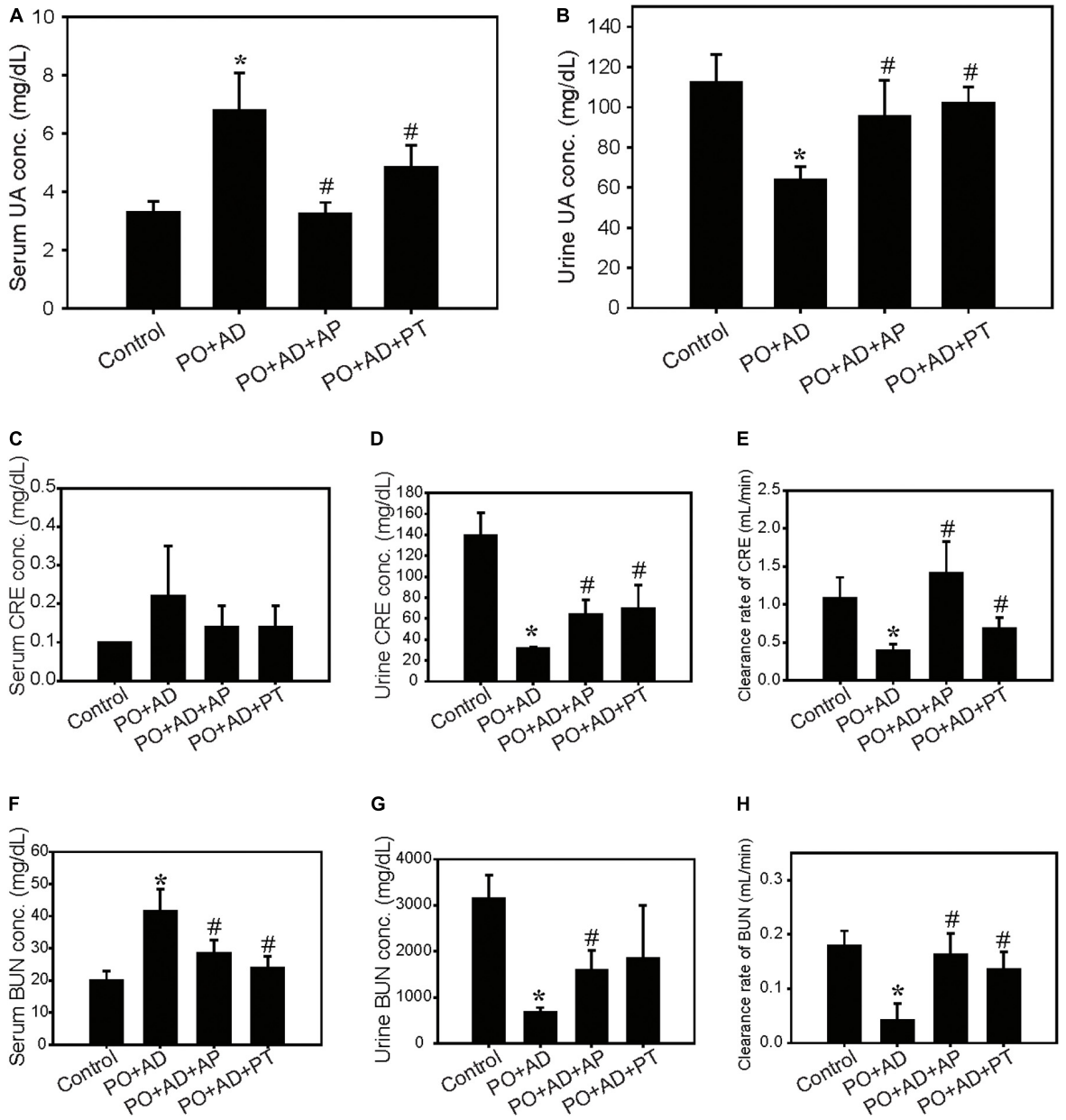

FIGURE 3 | Improvement of renal function by PT in the CKD model. Serum and urine levels of UA **(A,B)**, creatinine (CRE; **C,D)**, blood urea nitrogen (BUN; **F,G)**, and clearance rate of CRE **(E)**, and BUN **(H)** in the CKD model. Data were expressed as mean ± SD of 5 mice per group. *$p < 0.05$ compared with the control groups. #$p < 0.05$ compared with PO + AD groups.

Renal morphology examination showed critical roughness morphology in PO + AD groups compared with PT or AP treated groups (**Figure 4A**). H&E and immunohistochemistry staining further revealed obvious tubular-interstitial damage with tubular dilation, interstitial fibrosis (Masson Trichrome staining), infiltration of inflammatory cells (macrophages, $CD68^{+}$), and focal tubular atrophy in PO + AD groups (**Figure 4B**). With the treatment of PT, tubular interstitial damage, fibrosis, and infiltration of inflammatory cells were significantly alleviated (**Figure 4B**). Given the prominent role of TGF-β in renal fibrosis by inducing EMT leading to promotion of tubular epithelial cells to myoblast (Wang et al., 2015), the results of immunohistochemistry demonstrated that PT administration significantly reduced TGF-β expression compared to PO + AD groups (**Figure 4C**). EMT is characterized in which tubular cells loss the epithelial phenotypes such as E-cadherin, and acquire new characteristic features of mesenchymal properties such as ZO-1, Vimentin, fibronectin, and α-SMA (Bai et al., 2014). The

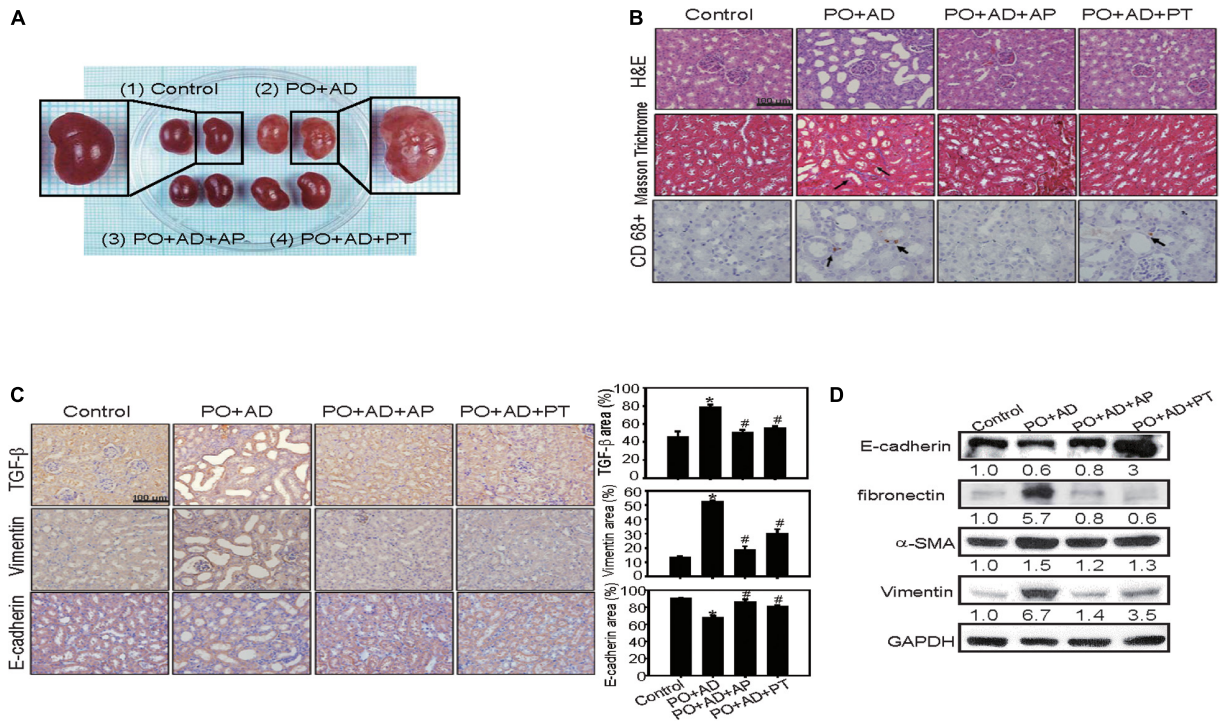

FIGURE 4 | PT alleviates inflammation and interstitial fibrosis in kidney tissues in the CKD model. **(A)** The size of kidney was increased in PO + AD groups. The appearance of kidney in PO + AD groups was rough and pale. **(B)** Renal tubular injury was assessed by H&E staining. The deposition of fibrosis in renal tissues was determined by Masson Trichrome staining. Blue color represents collagen fibers, red color represents muscle fibers. Infiltration of macrophages was detected by CD68 staining (brown color, arrow indicated). **(C)** Tubulointerstitial inflammation and EMT was assessed by staining of TGF-β, Vimentin, and E-cadherin. The results of immunohistochemistry were quantified by ImagJ ($n = 3$). Bar = 100 μm. *$p < 0.05$ compared with the control groups. #$p < 0.05$ compared with PO + AD groups. **(D)** Compared with PO + AD groups, PT increased the expression of E-cadherin, and decreased the expression of fibronectin, α-SMA, and Vimentin in renal tissues detected by Western blotting analysis. GAPDH was used as an internal control. Representative data from one of three independent experiments are shown. The number below each line indicates the relative intensity of protein expression compared to the control (defined as 1; **Figures 4–7**).

results of immunohistochemistry and Western blotting analysis showed that PT suppressed the expression of fibronectin while increased the expression of E-cadherin compared with PO + AD groups (**Figures 4C,D**). Taken together, the results of *in vivo* study strongly implicated the renal protective effects of PT, through the inhibition of UA synthesis, reducing inflammation, downregulation of TGF-β mediated EMT pathways and fibrosis (**Figures 1–4**).

PT Inhibits TGF-β-Induced EMT and Inflammasome Activation in NRK-52E Cells

The protective mechanisms of PT in alleviating fibrosis was further investigated in NRK-52E cells. Treatment with PT or TGF-β at lower concentration for 24 or 48 h did not induce cytotoxicity in NRK-52E cells (**Figures 5A,B**). However, treatment with TGF-β for 72 h, many NRK-52E cells became spindle fibroblast-like cells, meanwhile, the expression of fibronectin, ZO-1, and α-SMA were increased (**Figures 5C,D**). In contrast, pretreatment of PT for 1 h significantly attenuated TGF-β-induced EMT characteristics in cells (**Figures 5C,D**).

A previous study suggested that NLRP3 inflammasome activation in response to TGF-β could contribute to EMT, however, the role of NLRP3 inflammasome in EMT regulation is still obscured (Zhang et al., 2020). Then we determine the effects of PT on the regulation of NLRP3 inflammasome and found that NLRP3 expression increased in response to TGF-β, but significantly inhibited by the presence of PT (**Figure 6A**). Consequently, the expression of ASC and degraded form of caspase-1 were decreased leading to the reduction of maturation form of IL-1β after PT treatment (**Figure 6A**). Further, pretreatment with a potent NLRP3 inhibitor MCC950 significantly reduced the expression of NLRP3, caspase-1 activation, followed by reduced EMT markers including fibronectin and α-SMA expression, in which confirmed the role of NLRP3 inflammasome in EMT driven by TGF-β (**Figure 6B**). The results strongly implicated that PT downregulates NLRP3 inflammasome activation and consequently inhibits TGF-β-mediated EMT in NRK-52E cells.

PT Inhibits NLRP3 Inflammasome Activation by Augmenting Autophagy

Previous reports indicated that autophagy acts as a negative regulator to restrain NLRP3 activation from reducing the

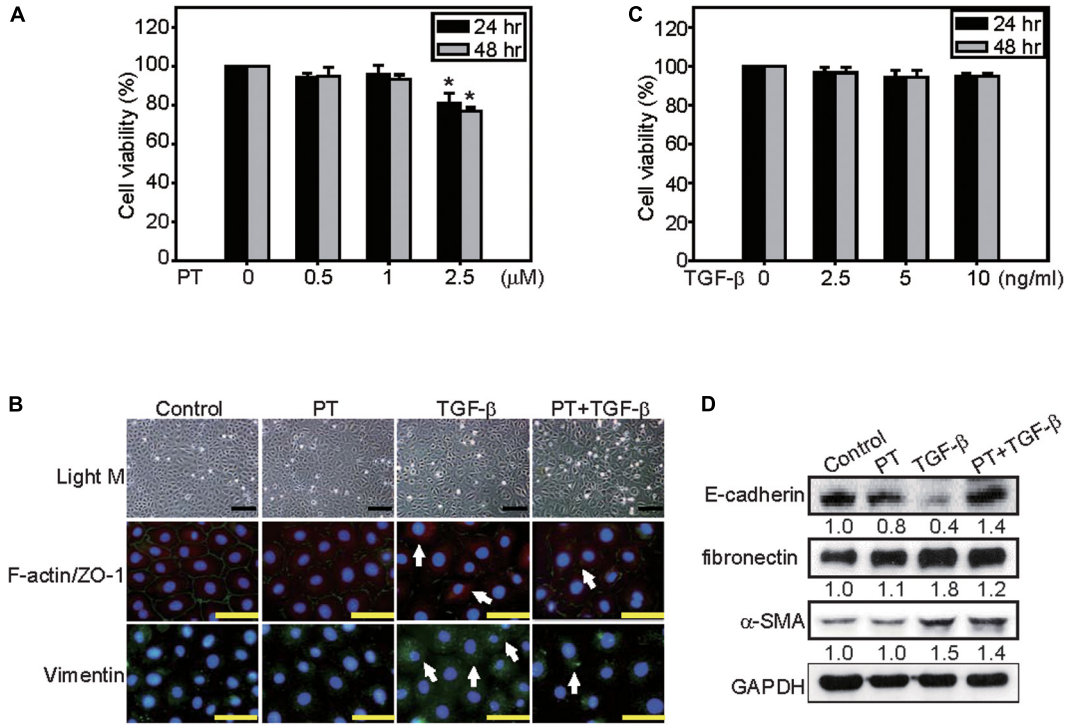

FIGURE 5 | PT inhibits TGF-β-triggered EMT in NRK-52E cells. NRK-52E cells were treated with **(A)** 0, 0.5, 1, or 2.5 μM PT, or **(B)** 0, 2.5, 5, or 10 ng/ml TGF-β for 24 or 48 h. Cell viability were detected by MTT assay. Mean ± SD; $n = 3$. **(C)** NRK-52E cells were treated with DMSO (Control), PT 2 μM, TGF-β 2.5 ng/ml, or PT combined with TGF-β for 72 h. The morphological changes of NRK-52E cells were recorded under a phase-contrast microscopy. F-actin/ZO-1 co-staining, or Vimentin staining were determined by immunofluorescence staining. Bar = 100 μm **(D)** The expression of E-cadherin, fibronectin, α-SMA, and Vimentin were determined by Western blotting analysis in NRK-52E cells treated with PT, TGF-β, or PT + TGF-β. The membrane was probed with anti-GAPDH to confirm equal loading of proteins. Immunoblots are representative of at least three independent experiments.

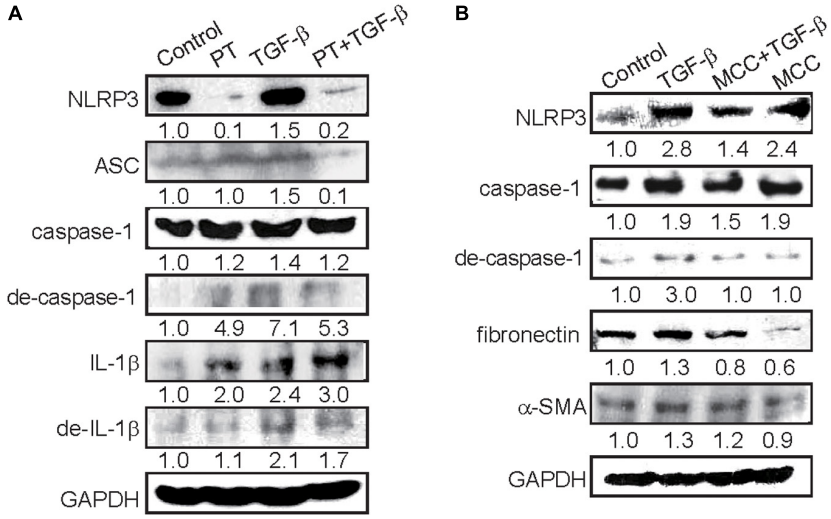

FIGURE 6 | PT and MCC950 attenuates TGF-β-induced NLRP3 inflammasome activation and EMT in NRK-52E cells. **(A)** Immunoblotting for NLRP3 inflammasome components NLRP3, ASC, caspase-1, degraded form of caspase-I, IL-1β, and degraded form of IL-1β in NRK-52E cells following treatment with DMSO (Control), PT 2 μM, TGF-β 2.5 ng/ml, or PT combined with TGF-β for 48 h (PT + TGF-β). **(B)** Immunoblotting for NLRP3, ASC, caspase-1, degraded form of caspase-1, and EMT markers fibronectin and α-SMA at 48 h following treatment with DMSO (Control), TGF-β 2.5 ng/ml, TGF-β combined with NLRP3 inhibitor MCC950 (MCC 10 nM), or MCC in NRK-52E cells. The membrane was probed with anti-GAPDH to confirm equal loading of proteins. Immunoblots are representative of at least three independent experiments.

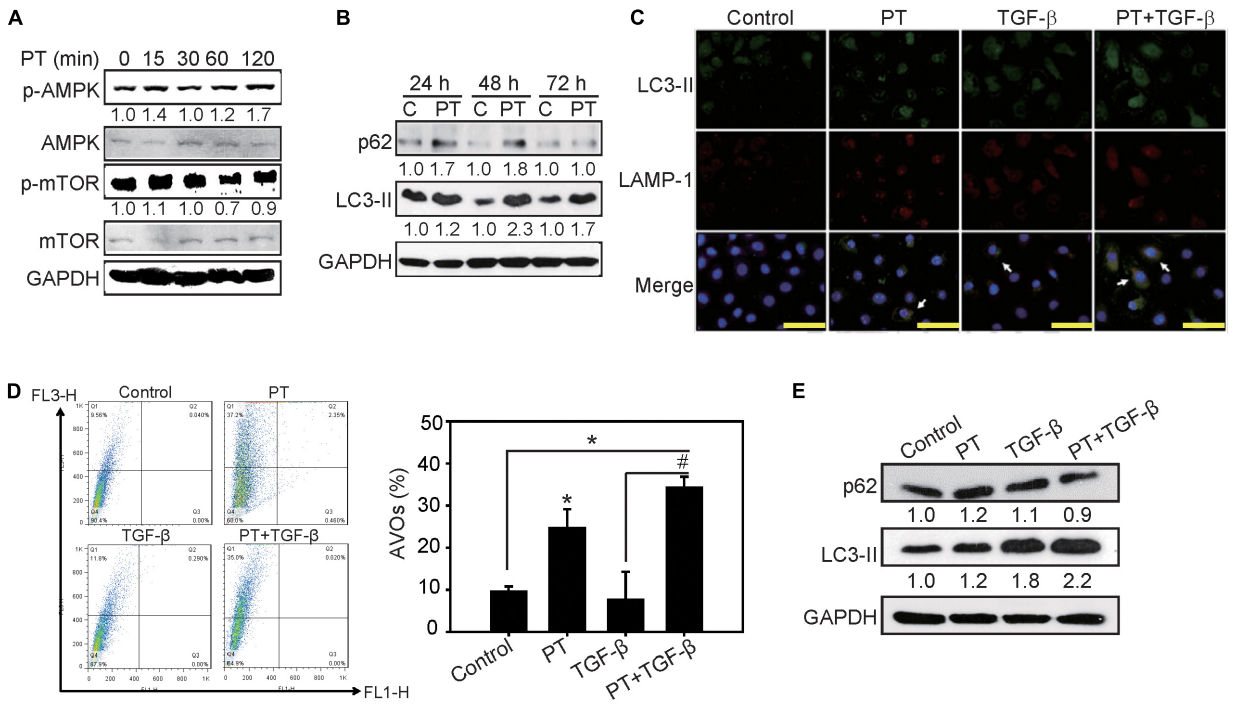

FIGURE 7 | Autophagy inducing effects of PT in NRK-52E cells. **(A)** PT 2 μM induced activation of AKT followed by inhibition of mTOR pathways in a time-dependent manner. **(B)** Autophagic markers p62 and LC3-II were determined using Western blotting analysis in NRK-52E cells treated with PT for 24, 48, and 72 h. **(C)** Immunofluorescence staining showed the autolysosomes co-stained with LC3-II and lysosomal marker LAMP-1 in PT treated groups (arrow indicated). Bars = 100 mm. **(D)** The induction of autophagy was measured by acidic vesicular organelles (AVOs) using flow cytometry. Quantification of AVOs in NRK-52E cells treated with DMSO (Control), PT 2 μM, TGF-β 2.5 ng/ml, or PT combined with TGF-β for 48 h. The data represent the means ± SD of three independent experiments; $^{*}P < 0.05$ compared with Control groups; and $^{\#}P < 0.05$ compared with TGF-β groups. **(E)** Immunoblotting for autophagy markers p62, and LC3-II in NRK-52E cells followed by the treatment of DMSO (Control), PT 2 μM, TGF-β 2.5 ng/ml, or PT + TGF-β for 48 h. The membrane was probed with anti-GAPDH to confirm equal loading of proteins. Immunoblots are representative of at least three independent experiments.

expression of inflammasome components (Chen et al., 2017b). To clarify whether PT downregulates NLRP3 inflammasome activation through autophagy induction, AMPK, and mTOR signaling pathways were examined firstly. PT time-dependently activates AMPK, leading to mTOR inhibition and autophagy induction as evidenced by LC3-II induction and p62 expression in NRK-52E cells (**Figures 7A,B**). To further confirm the complete autophagic flux induced by PT, the results of immunofluorescence staining showing that co-localization of LC3-II and the lysosome marker LAMP-1 could be observed in PT alone and PT + TGF-β treated groups (**Figure 7C**). In addition, the results of AO staining and Western blotting analysis further confirmed autophagy inducing effect of PT in NRK-52E cells (**Figures 7D,E**). To gain insight the role of autophagy in downregulation of NLRP3 inflammasome and the subsequent EMT pathways, NRK-52E cells with Atg5 knockdown [NRK-Atg5-(1) and (2)] was used. The expression of Atg5 (**Figure 8A**) was partially reduced in accordance with reduced autophagy after treated with PT (**Figures 8B,C**). Compared to NRK-52E cells, Atg5 knockdown cells [NRK-Atg5-(2) cells] revealed a significant increased expression of NLRP3, caspase 1, fibronectin, and α-SMA followed by the treatment with PT combined with TGF-β for 72 h (**Figure 8D**). Collectively, these results implicated the significant role of autophagy induced by PT in preventing NLRP3 inflammation activation and subsequently EMT in NRK-52E cells.

DISCUSSION

Chronic kidney disease is recognized as a global public health problem. Evidence has demonstrated that UA plays a crucial role in the CKD and using UA-lowering drugs may represent an effective therapeutic venue for delaying CKD progression (Kumagai et al., 2017). However, at present, the urate lowering agents such as AP or probenecid still possess a number of adverse side effects including allergic and hypersensitivity problems, nephropathy, and liver toxicity (Chen et al., 2017a). Therefore, the development of the effective and safety strategy at lowing UA thereby alleviating CKD is still necessary. In this study, we demonstrate a novel underlying urate lowering mechanisms and preventive effects of PT in renal inflammation and fibrosis. As shown in **Figure 8E**, high adenine treatment promotes urate nephropathy characterized by renal inflammation and fibrosis that is mainly regulated by TGF-β production and NLRP3 inflammasome activation. PT is effective in inhibiting XOD activity, reducing UA production, inflammation, and consequently renal fibrosis in mice. At molecular levels,

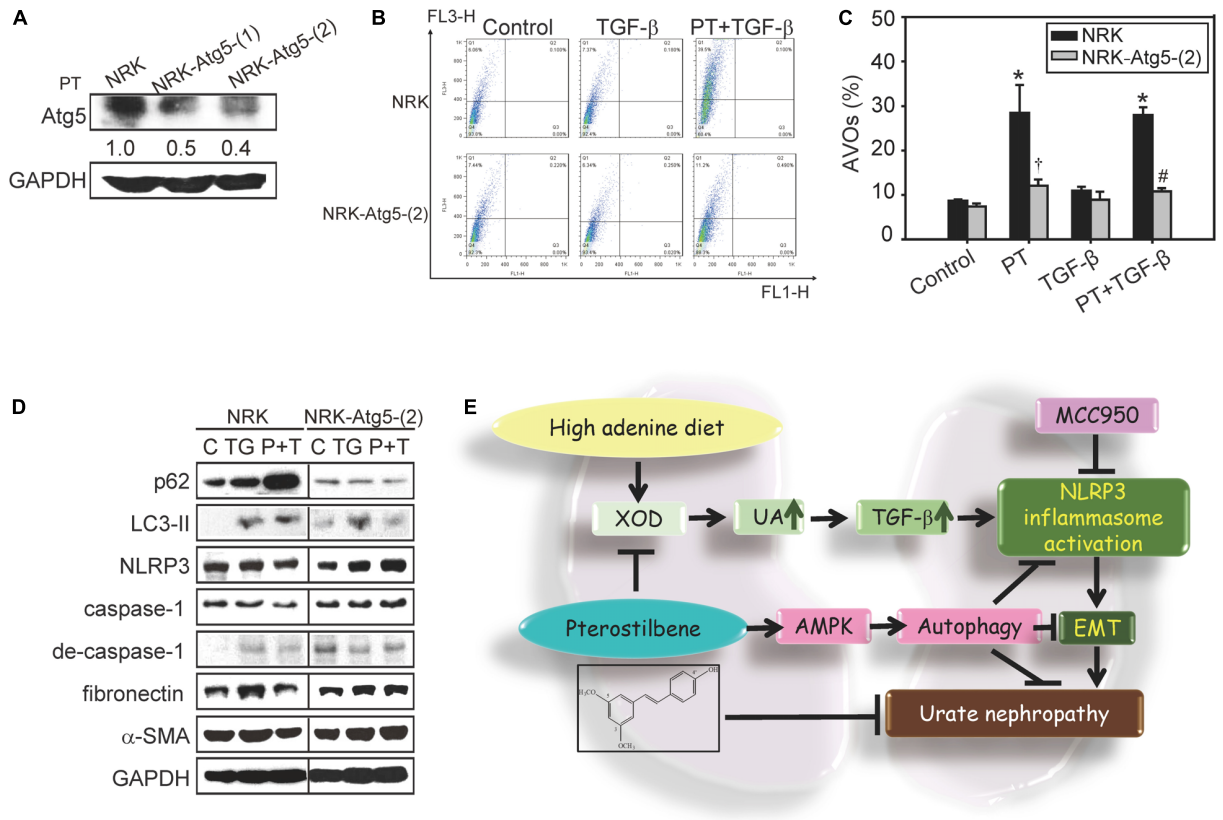

FIGURE 8 | Role of autophagy in attenuating NLRP3 activation and EMT in response to PT treatment. **(A)** Atg5 expression in NRK-52E cells stably transfected with Atg5 knockdown shRNA [Atg5-(1) and Atg5-(2)]. **(B)** The induction of autophagy by PT was measured by flow cytometry in NRK-52E and Atg5 knockdown NRK-Atg5-(2) cells. The data represent the means ± SD of three independent experiments; $^{*}P < 0.05$ compared with Control groups; $^{\#}P < 0.05$ compared with NRK-52E cells. **(C)** The percentage of acridine orange positive staining cells in NRK and NRK-Atg5-(2) treated with PT (2.5 μM), TGF-β, or PT + TGF-β for 48 h. **(D)** The protein expression of autophagy markers (p62 and LC3-II), NLRP3 inflammasome components (NLRP3, caspase-1 and degraded form of caspase-1), and EMT markers (fibronectin and α-SMA) were detected by Western blotting in NRK and NRK-Atg5-(2) cells following 48 h treatment with TGF-β (TG) or PT combined with TGF-β (P + T). The membrane was probed with anti-GAPDH to confirm equal loading of proteins. Immunoblots are representative of at least three independent experiments. **(E)** Proposed model for renal protective effects of PT. PT significantly reduces UA production and XOD activities, prevents renal dysfunction, and ameliorates renal fibrosis in animal models. The mechanistic studies implicate that PT induces autophagy through AMPK activation to restrain TGF–triggered NLRP3 inflammasome activation and EMT, subsequently contributing to the protection of renal fibrosis.

PT induces autophagy leading to restraining TGF-β-mediated NLRP3 inflammasome activation and EMT in NRK-52E cells. To the best of our knowledge, this is the first report investigating the protective effects of PT in CKD by attenuating NLRP3 inflammasome activation and EMT via autophagy induction.

Our previous study was the first to demonstrate that PT is a unique autophagy inducer (Chen et al., 2010). Through its autophagy inducing effects, PT could act as a promising protective agent for autophagy-defective diseases (Chen et al., 2017b). Notably, autophagy has a great impact on the maintenance of renal functions and homeostasis (Lin et al., 2019). For instance, autophagy has renal protective effects on the proximal tubular cells during acute kidney injury (AKI) in response to hypoxia and ROS (Wang et al., 2012). In addition, autophagy takes places in podocytes, mesangial cells, and tubular cells that helps repair and regenerates damaged kidneys (Lin et al., 2019). Impaired autophagy in kidneys resulted in podocyte loss, massive proteinuria, inflammation, and renal interstitial fibrosis in several CKD models (Lin et al., 2019). Xu et al. (2016) also indicated that autophagy defects can directly lead to excessive deposition of extracellular matrix such as fibronectin or indirectly activate renal fibrosis by enhancing oxidative stresses. Importantly, clinical studies indicated that patients with CKD have altered autophagy response (Chen et al., 2013). Our results also showed that depletion of autophagy by knockdown of Atg5 gene leads to increase the expression of NLRP3, degraded form of caspase-1, fibronectin, and α-SMA (**Figure 8D**). These studies indicated that autophagy induction is now considered an effective therapy for AKI or CKD but there is no clinical useful agent targeting the autophagy pathway for patients with renal diseases (Lin et al., 2019). As a result, our results firstly indicated that PT could act as an autophagy inducer resulting in downregulation of inflammasome and subsequent EMT thereby alleviating CKD (**Figure 8**).

In addition to autophagy regulation in CKD, NLRP3 inflammasome activation has been characterized to mediate

diverse aspect mechanisms of urate nephropathy through regulation of proinflammatory cytokines, tubulointerstitial injury, glomerular diseases, renal inflammation, and fibrosis pathways (Mulay et al., 2018). In the process of fibrosis, the tubular epithelial cells have the capacity to acquire an EMT in the injured kidney through the most important factor TGF-β (Chuang et al., 2013). A previous study of Wang et al. (2013) indicated that NLRP3 is required for optimal TGF-β signaling and its downstream P-Smad activation. Zhang et al. (2020) also indicated that TGF-β-mediated NLRP3 inflammasome activation may induce HMGB1 release and Gasdermin D cleavage contributing to renal fibrosis in Ang II-induced CKD. However, the regulation of NLRP3 in TGF-β mediated EMT process is largely unclear so far. In the present study, we demonstrated that TGF-β acts as a priming signal leads to NLRP3 protein induction, and the activated signal leads to caspase-1 activation and the following EMT (**Figure 5**). The role of NLRP3 in EMT is then confirmed by pretreatment with NLRP3 inhibitor MCC950. The results further implicated the protective role of PT in mitigating TGF-β induced EMT could be mediated by downregulation of NLRP3 protein expression and subsequently inhibition of IL-1β production (**Figure 6A**). Consistent with our findings, Nam et al. indicated that autophagy attenuates tubulointerstitial fibrosis through regulation of the expression of TGF-β, IL-1β, and NLRP3 inflammasome activation in UUO model. Therefore, we suggest that PT is effective in the prevention of NLRP3-inflammasome-mediated inflammation and EMT via autophagy.

As mentioned above, PT has attracted more attention for its beneficial health effects compared to its analog resveratrol because of its unique structure (Sun et al., 2016). PT has diverse pharmacological benefits for the prevention and treatment of variety of diseases such as cancer, diabetes, cardiovascular disease, dyslipidemia, and inflammation (Chen et al., 2018). In the present study, we are also the first one to demonstrate that PT could inhibit XOD activities that exerts as one of the urate lowering mechanisms of PT. XOD is a rate limiting enzyme for UA production and ROS production. Similar to our findings, a previous study also highlighted that flavonols such as quercetin had an inhibitory effect on XOD activities therefore modulate the activities of superoxide dismutase (Majo et al., 2014). These studies suggest the beneficial health effects of natural products in modulating of enzymes responsible for ROS production and inflammation (Majo et al., 2014). In clinical trials, PT could inhibit of PGE2 activity and reduce blood pressure in subjects (Riche et al., 2013). The results of clinical trials where the subjects took PT daily for 8 weeks with no serious adverse events indicated that PT is generally safe for use in humans up to 250 mg/day (Riche et al., 2013). In a preclinical study, mice fed with PT for 28 days at a dose up to 3000 mg/kg, equivalent to 50 times of human intake (250 mg/day) showed no significant toxic effects or adverse biochemical parameters compared to control (Lee et al., 2019). Consequently, PT is an attractive candidate for management of various diseases including CKD because of its low toxicity and wide health benefits. Taken together, we have provided a new evidence for a better understanding of the relationship between autophagy induction and NLRP3 inflammasome activation by PT in CKD models. These findings implicate that PT could be a novel preventive and therapeutic agent for CKD because of its ability of inhibiting NLRP3 activation and EMT by autophagy induction.

DATA AVAILABILITY STATEMENT

The raw data supporting the conclusions of this article will be made available by the authors, without undue reservation, to any qualified researcher.

ETHICS STATEMENT

The animal study was reviewed and approved by the Laboratory Animal Center of the National Cheng Kung University Medical College (Approval No. 103293).

AUTHOR CONTRIBUTIONS

R-JC, Y-YC, and C-MH carried out the animal studies, cell culture, drug treatment, flow cytometry analysis, immunohistochemistry, western blot analysis, and performed the statistical analysis. C-TH provided pterostilbene. Y-CC and K-CH precipitated in the animal and project submission. R-JC and Y-JW participated in the sequence alignment and drafted the manuscript. R-JC, B-JW, and M-HP participated in the design of the study and coordination and helped to draft the manuscript. All authors read and approved the final manuscript.

FUNDING

This work was supported by the Ministry of Science and Technology, Taiwan (MOST 107-2311-B-006-004-MY3 and MOST 106-2314-B-006-029-MY3), and Chi Mei Hospital, Liouying Dist, Tainan, Taiwan (CLFHR10731 and CLFHR10812). This research was also, in part, supported by the Ministry of Education, Taiwan, Republic of China. The Aim for the Top University Project to the National Cheng Kung University (NCKU).

REFERENCES

Bai, Y., Lu, H., Wu, C., Liang, Y., Wang, S., Lin, C., et al. (2014). Resveratrol inhibits epithelial-mesenchymal transition and renal fibrosis by antagonizing the hedgehog signaling pathway. *Biochem. Pharmacol.* 92, 484–493. doi: 10.1016/j.bcp.2014.09.002

Chang, A., Ko, K., and Clark, M. R. (2014). The emerging role of the inflammasome in kidney diseases. *Curr. Opin. Nephrol. Hypertens.* 23, 204–210. doi: 10.1097/01.mnh.0000444814.49755.90

Chen, R. J., Chen, M. H., Chen, Y. L., Hsiao, C. M., Chen, H. M., Chen, S. J., et al. (2017a). Evaluating the urate-lowering effects of different microbial fermented

extracts in hyperuricemic models accompanied with a safety study. *J. Food Drug Anal.* 25, 597–606. doi: 10.1016/j.jfda.2016.07.003

Chen, R. J., Lee, Y. H., Yeh, Y. L., Wu, W. S., Ho, C. T., Li, C. Y., et al. (2017b). Autophagy-inducing effect of pterostilbene: a prospective therapeutic/preventive option for skin diseases. *J. Food Drug Anal.* 25, 125–133. doi: 10.1016/j.jfda.2016.10.022

Chen, R. J., Wu, P. H., Ho, C. T., Way, T. D., Pan, M. H., Chen, H. M., et al. (2017c). P53-dependent downregulation of hTERT protein expression and telomerase activity induces senescence in lung cancer cells as a result of pterostilbene treatment. *Cell Death Dis.* 8:e2985. doi: 10.1038/cddis.2017.333

Chen, R. J., Ho, C. T., and Wang, Y. J. (2010). Pterostilbene induces autophagy and apoptosis in sensitive and chemoresistant human bladder cancer cells. *Mol. Nutr. Food Res.* 54, 1819–1832. doi: 10.1002/mnfr.201000067

Chen, R. J., Kuo, H. C., Cheng, L. H., Lee, Y. H., Chang, W. T., Wang, B. J., et al. (2018). Apoptotic and nonapoptotic activities of pterostilbene against cancer. *Int. J. Mol. Sci.* 19:E287. doi: 10.3390/ijms19010287

Chen, R. J., Lee, Y. H., Yeh, Y. L., Wang, Y. J., and Wang, B. J. (2016). The roles of autophagy and the inflammasome during environmental stress-triggered skin inflammation. *Int. J. Mol. Sci.* 17:E2063.

Chen, W. T., Hung, K. C., Wen, M. S., Hsu, P. Y., Chen, T. H., Wang, H. D., et al. (2013). Impaired leukocytes autophagy in chronic kidney disease patients. *Cardiorenal. Med.* 3, 254–264. doi: 10.1159/000356212

Chuang, P. Y., Menon, M. C., and He, J. C. (2013). Molecular targets for treatment of kidney fibrosis. *J. Mol. Med.* 91, 549–559. doi: 10.1007/s00109-012-0983-z

Diwan, V., Mistry, A., Gobe, G., and Brown, L. (2013). Adenine-induced chronic kidney and cardiovascular damage in rats. *J. Pharmacol. Toxicol. Methods* 68, 197–207. doi: 10.1016/j.vascn.2013.05.006

Gu, T. T., Chen, T. Y., Yang, Y. Z., Zhao, X. J., Sun, Y., Li, T. S., et al. (2019). Pterostilbene alleviates fructose-induced renal fibrosis by suppressing TGF-beta1/TGF-beta type I receptor/Smads signaling in proximal tubular epithelial cells. *Eur. J. Pharmacol.* 842, 70–78. doi: 10.1016/j.ejphar.2018.10.008

Kim, I. Y., Lee, D. W., Lee, S. B., and Kwak, I. S. (2014). The role of uric acid in kidney fibrosis: experimental evidences for the causal relationship. *Biomed. Res. Int.* 2014:638732.

Kumagai, T., Ota, T., Tamura, Y., Chang, W. X., Shibata, S., and Uchida, S. (2017). Time to target uric acid to retard CKD progression. *Clin. Exp. Nephrol.* 21, 182–192. doi: 10.1007/s10157-016-1288-2

Lee, Y. H., Chen, Y. Y., Yeh, Y. L., Wang, Y. J., and Chen, R. J. (2019). Stilbene compounds inhibit tumor growth by the induction of cellular senescence and the inhibition of telomerase activity. *Int. J. Mol. Sci.* 20:E2716. doi: 10.3390/ijms20112716

Lin, T. A., Wu, V. C., and Wang, C. Y. (2019). Autophagy in chronic kidney diseases. *Cells* 8:61. doi: 10.3390/cells8010061

Majo, D. D., Guardia, M. L., Leto, G., Crescimanno, M., Flandina, C., and Giammanco, M. (2014). Flavonols and flavan-3-ols as modulators of xanthine oxidase and manganese superoxide dismutase activity. *Int. J. Food Sci. Nutr.* 65, 886–892. doi: 10.3109/09637486.2014.931362

Mulay, S. R., Shi, C., Ma, X., and Anders, H. J. (2018). Novel insights into crystal-induced kidney injury. *Kidney Dis.* 4, 49–57. doi: 10.1159/000487671

Qi, R., and Yang, C. (2018). Renal tubular epithelial cells: the neglected mediator of tubulointerstitial fibrosis after injury. *Cell Death Dis.* 9:1126.

Riche, D. M., Mcewen, C. L., Riche, K. D., Sherman, J. J., Wofford, M. R., Deschamp, D., et al. (2013). Analysis of safety from a human clinical trial with pterostilbene. *J. Toxicol.* 2013:463595.

Romero, C. A., Remor, A., Latini, A., De Paul, A. L., Torres, A. I., and Mukdsi, J. H. (2017). Uric acid activates NRLP3 inflammasome in an in-vivo model of epithelial to mesenchymal transition in the kidney. *J. Mol. Histol.* 48, 209–218. doi: 10.1007/s10735-017-9720-9

Scarpioni, R., and Obici, L. (2018). Renal involvement in autoinflammatory diseases and inflammasome-mediated chronic kidney damage. *Clin. Exp. Rheumatol.* 36(Suppl. 110), 54–60.

Shi, Y. W., Wang, C. P., Liu, L., Liu, Y. L., Wang, X., Hong, Y., et al. (2012). Antihyperuricemic and nephroprotective effects of resveratrol and its analogues in hyperuricemic mice. *Mol. Nutr. Food Res.* 56, 1433–1444. doi: 10.1002/mnfr.201100828

Sun, Y., Wu, X., Cai, X., Song, M., Zheng, J., Pan, C., et al. (2016). Identification of pinostilbene as a major colonic metabolite of pterostilbene and its inhibitory effects on colon cancer cells. *Mol. Nutr. Food Res.* 60, 1924–1932. doi: 10.1002/mnfr.201500989

Wang, W., Wang, X., Chun, J., Vilaysane, A., Clark, S., French, G., et al. (2013). Inflammasome-independent NLRP3 augments TGF-beta signaling in kidney epithelium. *J. Immunol.* 190, 1239–1249. doi: 10.4049/jimmunol.1201959

Wang, Y., Liu, N., Su, X., Zhou, G., Sun, G., Du, F., et al. (2015). Epigallocatechin-3-gallate attenuates transforming growth factor-beta1 induced epithelial-mesenchymal transition via Nrf2 regulation in renal tubular epithelial cells. *Biomed. Pharmacother.* 70, 260–267. doi: 10.1016/j.biopha.2015.01.032

Wang, Y., Nartiss, Y., Steipe, B., Mcquibban, G. A., and Kim, P. K. (2012). ROS-induced mitochondrial depolarization initiates PARK2/PARKIN-dependent mitochondrial degradation by autophagy. *Autophagy* 8, 1462–1476. doi: 10.4161/auto.21211

Xiao, J., Zhang, X. L., Fu, C., Han, R., Chen, W., Lu, Y., et al. (2015). Soluble uric acid increases NALP3 inflammasome and interleukin-1beta expression in human primary renal proximal tubule epithelial cells through the Toll-like receptor 4-mediated pathway. *Int. J. Mol. Med.* 35, 1347–1354. doi: 10.3892/ijmm.2015.2148

Xu, G., Yue, F., Huang, H., He, Y., Li, X., Zhao, H., et al. (2016). Defects in MAP1S-mediated autophagy turnover of fibronectin cause renal fibrosis. *Aging* 8, 977–985. doi: 10.18632/aging.100957

Zhang, K., Fan, C., Cai, D., Zhang, Y., Zuo, R., Zhu, L., et al. (2020). Contribution of TGF-Beta-mediated NLRP3-HMGB1 activation to tubulointerstitial fibrosis in rat with angiotensin II-induced chronic kidney disease. *Front. Cell Dev. Biol.* 8:1. doi: 10.3389/fcell.2020.00001

Conflict of Interest: The authors declare that the research was conducted in the absence of any commercial or financial relationships that could be construed as a potential conflict of interest.

Copyright © 2020 Wang, Chen, Hsiao, Pan, Wang, Chen, Ho, Huang and Chen. This is an open-access article distributed under the terms of the Creative Commons Attribution License (CC BY). The use, distribution or reproduction in other forums is permitted, provided the original author(s) and the copyright owner(s) are credited and that the original publication in this journal is cited, in accordance with accepted academic practice. No use, distribution or reproduction is permitted which does not comply with these terms.

frontiers in Cell and Developmental Biology

ORIGINAL RESEARCH
published: 12 June 2020
doi: 10.3389/fcell.2020.00339

Elevated suPAR Is an Independent Risk Marker for Incident Kidney Disease in Acute Medical Patients

Esben Iversen[1,2†], Morten Baltzer Houlind[1,3,4†], Thomas Kallemose[1], Line Jee Hartmann Rasmussen[1,5], Mads Hornum[6,7], Bo Feldt-Rasmussen[6,7], Salim S. Hayek[8], Ove Andersen[1,7,9] and Jesper Eugen-Olsen[1]*

[1] Department of Clinical Research, Copenhagen University Hospital Amager and Hvidovre, Hvidovre, Denmark, [2] Icahn School of Medicine at Mount Sinai, New York, NY, United States, [3] Department of Drug Design and Pharmacology, University of Copenhagen, Copenhagen, Denmark, [4] Hospital Pharmacy, Copenhagen University Hospital Amager and Hvidovre, Hvidovre, Denmark, [5] Department of Psychology and Neuroscience, Duke University, Durham, NC, United States, [6] Department of Nephrology, Rigshospitalet, Copenhagen, Denmark, [7] Department of Clinical Medicine, Medical Sciences, University of Copenhagen, Copenhagen, Denmark, [8] Department of Medicine, Division of Cardiology, University of Michigan, Ann Arbor, MI, United States, [9] Emergency Department, Copenhagen University Hospital Amager and Hvidovre, Hvidovre, Denmark

OPEN ACCESS

Edited by:
Claudia Torino,
Institute of Clinical Physiology, Italian National Research Council, Italy

Reviewed by:
Christian Wandall Thorball,
Swiss Federal Institute of Technology Lausanne, Switzerland
Giovanni Tripepi,
Istituto Nanoscienze, Consiglio Nazionale delle Ricerche, Italy

***Correspondence:**
Esben Iversen
esbeniversen1@gmail.com

† These authors share first authorship

Specialty section:
This article was submitted to Molecular Medicine, a section of the journal Frontiers in Cell and Developmental Biology

Received: 13 December 2019
Accepted: 17 April 2020
Published: 12 June 2020

Citation:
Iversen E, Houlind MB, Kallemose T, Rasmussen LJH, Hornum M, Feldt-Rasmussen B, Hayek SS, Andersen O and Eugen-Olsen J (2020) Elevated suPAR Is an Independent Risk Marker for Incident Kidney Disease in Acute Medical Patients. Front. Cell Dev. Biol. 8:339. doi: 10.3389/fcell.2020.00339

Introduction: Identifying patients at high risk of developing kidney disease could lead to early clinical interventions that prevent or slow disease progression. Soluble urokinase plasminogen activator receptor (suPAR) is an inflammatory biomarker thought to be involved in the pathogenesis and development of kidney disease. We aimed to determine whether elevated plasma suPAR measured at hospital admission is associated with incident kidney disease in patients presenting to the emergency department.

Materials and Methods: This was a retrospective registry-based cohort study performed at the Emergency Department of Copenhagen University Hospital Amager and Hvidovre, Hvidovre, Denmark. Patients were included in the study from November 2013 to March 2017 and followed until June 2017. Patients were excluded if they were diagnosed with kidney disease or died prior to index discharge. Plasma suPAR was measured at hospital admission, and the main outcome was time to incident kidney disease, defined by ICD-10 diagnosis codes for both chronic and acute kidney conditions. Association between suPAR and time to incident kidney disease was assessed by Cox proportional hazard regression analysis.

Results: In total, 25,497 patients (median age 58.1 years; 52.5% female) were admitted to the emergency department and followed for development of kidney disease. In multivariable Cox regression analysis adjusting for age, sex, eGFR, CRP, cardiovascular disease, hypertension, and diabetes, each doubling in suPAR at hospital admission was associated with a hazard ratio of 1.57 (95% CI: 1.38–1.78, $P < 0.001$) for developing a chronic kidney condition and 2.51 (95% CI: 2.09–3.01, $P < 0.001$) for developing an acute kidney condition.

Discussion: In a large cohort of acutely hospitalized medical patients, elevated suPAR was independently associated with incident chronic and acute kidney conditions. This

highlights the potential for using suPAR in risk classification models to identify high-risk patients who could benefit from early clinical interventions. The main limitation of this study is its reliance on accurate reporting of ICD-10 codes for kidney disease.

Keywords: chronic kidney disease, acute kidney injury, dialysis, soluble urokinase plasminogen activator receptor, glomerular filtration rate, emergency department

INTRODUCTION

Chronic kidney disease (CKD) is a major health issue affecting 8–16% of people worldwide (Jha et al., 2013). Patients with CKD have increased rates of cardiovascular disease, end-stage renal disease (ESRD), hospitalization, and death (Go et al., 2004; Astor et al., 2011; Gansevoort et al., 2013). Identifying patients at high risk of developing CKD may lead to earlier medical interventions that reduce morbidity and mortality associated with disease progression (James et al., 2010; Akbari et al., 2014). However, current measures of kidney function, such as estimated glomerular filtration rate (eGFR) and proteinuria, are insensitive predictors of incident kidney disease (Levey et al., 2009; James et al., 2010; Eloot et al., 2011).

Soluble urokinase plasminogen activator receptor (suPAR) is an endogenous signaling molecule and biomarker of chronic inflammation, and elevated suPAR levels have been associated with a range of diseases and mortality (Eugen-Olsen et al., 2010). In 2015, suPAR was described as a novel biomarker for eGFR decline and CKD in a cohort of cardiovascular patients (Hayek et al., 2015). Subsequent studies have replicated these results in healthy middle-aged participants (Schulz et al., 2017), patients with type 1 diabetes (Curovic et al., 2019), and children (Schaefer et al., 2017). Another study demonstrated that high suPAR in patients undergoing cardiac surgery was a risk factor for postoperative acute kidney injury (Mossanen et al., 2017). There is growing evidence that suPAR may reflect the pathogenesis of kidney disease, and it has been proposed that suPAR itself causes kidney disease by damaging renal podocytes (Wei et al., 2011; Hayek et al., 2017).

Patients admitted through the emergency department are characterized by high age and disease burden (Juul-Larsen et al., 2017), and they are at elevated baseline risk of developing kidney disease after discharge (Rohun et al., 2011). Routine suPAR measurements in such high-risk patient populations may help identify patients at highest risk of developing kidney disease and ultimately lead to clinical interventions that slow or prevent disease progression. Therefore, we tested the hypothesis that elevated suPAR measured at hospital admission is associated with the development of kidney disease.

MATERIALS AND METHODS

Study Design and Setting

This was a retrospective observational cohort study performed at Copenhagen University Hospital Amager and Hvidovre. The initial patient population included all patients admitted to the Acute Medical Unit of the Emergency Department between November 18, 2013 and March 17, 2017 with follow-up data accessible in the Danish National Patient Registry (DNPR). Index admission was defined as the first recorded admission with a suPAR measurement within this study period. Patients were excluded from analysis if they were diagnosed with kidney disease, received dialysis, or died from any cause prior to index discharge. Patients with prior urolithiasis were not excluded. Data on prior kidney disease was obtained from the DNPR dating back to 1977. The study was approved by the Danish Data Protection Agency (ref. HVH-2014-018, 02767) and the Danish Health and Medicines Authority (ref. 3-3013-1061/1).

Measurements

Demographic information including age and sex was obtained from the Civil Registration System. Chronic disease status including cardiovascular disease, hypertension, and diabetes was described by two-year history of chronic diseases based on International Classification of Disease (ICD)-10 diagnosis codes from the DNPR (**Supplementary Table S1**). Blood samples were collected on admission to the Acute Medical Unit, and a standard panel of markers, including creatinine, C-reactive protein (CRP), and suPAR, was analyzed as part of routine evaluation at the Department of Clinical Biochemistry. Creatinine was measured on a Roche Cobas® c8000 701/702 (Roche Diagnostics, Mannheim, Germany) with a module instrument using the Roche Creatinine Plus version 2 IDMS-traceable enzymatic assay. CRP was measured on a Roche Cobas® 6000 (Roche Diagnostics, Mannheim, Germany). suPAR was measured on a Siemens BEP2000 using the suPARnostic® AUTO Flex ELISA (ViroGates A/S, Birkerød, Denmark) according to the manufacturer's instructions. Estimated GFR was calculated with the creatinine-based equation from the Chronic Kidney Diseases Epidemiology Collaboration (CKD-EPI) (Inker et al., 2012).

Outcomes

Information about disease status, hospital readmissions, and death was collected during a follow-up period beginning at index discharge and extending to a censor date (June 17, 2017) 90 days after the last patient was included (median follow-up time 755 days; range 90–1,307 days). Patients who left the country during the study period were censored at their last recorded hospitalization. Disease status during the study period was determined by ICD-10 codes obtained from the DNPR, which compiles information from all inpatient and outpatient activity within the Danish secondary healthcare system (Lynge et al., 2011). The quality of information within the DNPR has been described elsewhere (Schmidt et al., 2015). Kidney disease was defined as any ICD-10 diagnosis, procedure, or operation code suggesting renal

impairment (**Supplementary Table S2**). Kidney diseases were categorized as *chronic kidney condition* (CKD, glomerular disease, tubulointerstitial disease, or other renal disorder) or *acute kidney condition* (acute dialysis or acute kidney injury). Information on vital status at the end of follow-up was obtained from the Civil Registration System. The primary outcome was time to event during follow-up, which was defined as number of days from index discharge to first kidney disease diagnosis or death (whichever came first).

Statistics

Patient characteristics are presented with basic statistics: continuous variables as median with interquartile range, and discrete variables as number with percent of patients. Comparison between included and excluded patients was assessed by Wilcoxon rank sum test. Association between suPAR and incident kidney disease was assessed by Cox proportional hazard regression analysis and graphically represented by cumulative incidence plots. Association between suPAR and all-cause mortality was assessed by Cox proportional hazard regression analysis and graphically represented by a Kaplan-Meier plot.

An initial Cox regression model was generated with suPAR quartile as the explanatory variable and incident chronic kidney condition, acute kidney condition, or death as the endpoint. Start date was set to day of index discharge, censor date was set to June 17, 2017, and all endpoints were modeled as competing events for all other endpoints. Next, the analysis was repeated with suPAR modeled as a continuous variable. This was done first as a univariate model with $\log_2$(suPAR) as the sole explanatory variable and then as a multivariate model adjusted for age, sex, $\log_2$(eGFR), $\log_{10}$(CRP), cardiovascular disease, hypertension, and diabetes. In these models, suPAR, eGFR, and CRP were log-transformed for the purpose of interpretation and comparison with previous studies (Rasmussen et al., 2016; Rasmussen et al., 2018). Collinearity between $\log_2$(suPAR) and the covariates was assessed by variance inflation factor (VIF), and VIF greater than 5 was considered an indication of collinearity (Sheather, 2009). Association between $\log_2$(suPAR) and $\log_2$(eGFR) was further assessed by linear regression, and normality of residuals was evaluated by QQ-plot. Given the known association between suPAR and eGFR, an additional sensitivity analysis removing patients with eGFR less than 60 mL/min/1.73 m^2 was performed for the multivariate models. For a similar reason, sensitivity analysis removing patients with prior diagnosis of cardiovascular disease was also performed for the multivariate models.

To investigate differences in hazard ratio for specific etiologies of chronic kidney conditions, the continuous Cox regression models were repeated for these endpoints subdivided by disease type (CKD, glomerular disease, tubulointerstitial disease, or other renal disorder). To investigate differences in hazard ratio for specific etiologies of acute kidney conditions, the continuous Cox regression models were repeated for these endpoints subdivided by specific time periods from index discharge to diagnosis (<30 days, 30–90 days, or >90 days). In these time period specific models, patients who were censored or developed an event before each time period were excluded from the model for that time period, and patients who were censored or developed an event after each time period were censored at the end of that time period. Proportional hazard assumption of each regression model was evaluated by Schoenfeld residuals. $P < 0.05$ was taken to be statistically significant. SAS Enterprise Guide 7.1 (SAS Institute Inc, Cary, NC, United States) was used for statistical analysis and generation of figures.

RESULTS

Study Cohort

In total, 29,088 patients with follow-up data had suPAR measured at hospital admission during the study period. Of these, 2,836 patients were excluded due to prior kidney disease and 755 additional patients were excluded due to death from any cause prior to index discharge, resulting in a study cohort of 25,497 acute medical patients (**Supplementary Figure S1**). Baseline characteristics at index admission for the study cohort are shown in **Table 1**. Median age was 58.1 years, and 52.5% of patients were female. Compared with patients excluded due to prior kidney disease (n = 2,836), the study cohort had higher median eGFR (88.7 vs. 56.7 mL/min/1.73 m^2), lower median CRP (4.0 vs. 16.0 mg/L), and lower median suPAR (2.7 vs. 4.5 ng/mL) (all $P < 0.001$). Compared with patients excluded for any reason (n = 3,591), the study cohort had higher median eGFR (88.7 vs. 57.4 mL/min/1.73 m^2), lower median CRP (4.0 vs. 26.0 mg/L), and lower median suPAR (2.7 vs. 4.9 ng/mL) (all $P < 0.001$).

Outcomes During Follow-Up

During the follow-up period, 760 patients (3.0%) developed kidney disease, and 3,199 patients (12.5%) died without being diagnosed with kidney disease. Among patients who developed incident kidney disease, 570 patients (75%) developed a chronic kidney condition, and 190 patients (25%) developed an acute kidney condition (**Table 1**). Patients who developed kidney disease or died were older, had more comorbid conditions, more readmissions, lower eGFR, higher CRP, and higher suPAR at index admission compared with patients who were censored at follow-up. Basic statistics for patients developing each type of kidney condition are shown in **Table 2**. Among incident chronic kidney conditions, CKD was the most common diagnosis (263 cases), tubulointerstitial disease was the next most common (185 cases), and glomerular disease was the least common (23 cases). Among incident acute kidney conditions, 24 cases (12.6%) occurred within 30 days of index discharge, 29 cases (15.3%) occurred within 30–90 days, and 137 cases (72.1%) occurred after 90 days.

Association of suPAR With eGFR

There was no indication of collinearity between $\log_2$(suPAR) and the covariates, with the largest variance inflation for age (VIF 1.82) and $\log_2$(eGFR) (VIF 1.74). However, there was a significant association between $\log_2$(suPAR) and $\log_2$(eGFR) at

TABLE 1 | Patient characteristics by outcome.

	All patients *N* = 25,497	Incident chronic kidney condition *n* = 570	Incident acute kidney condition *n* = 190	Death without kidney disease *n* = 3,199	No event (censor) *n* = 21,538
Demographics					
Age in years, median (IQR)	58.1 (40.3–73.7)	72.5 (58.2–81.8)	68.5 (56.3–77.0)	79.4 (69.2–87.2)	54.0 (37.4–69.6)
Female, *n* (%)	13,373 (52.5%)	265 (46.5%)	73 (38.4%)	1,697 (53.0%)	11,338 (52.6%)
Chronic disease status					
Hypertension, *n* (%)	2,745 (10.8%)	131 (23.0%)	38 (20.0%)	624 (19.5%)	1,952 (9.1%)
Cardiovascular disease, *n* (%)	2,534 (9.9%)	123 (21.6%)	35 (18.4%)	745 (23.3%)	1,631 (7.6%)
Chronic pulmonary disease, *n* (%)	2,160 (8.5%)	67 (11.8%)	36 (18.9%)	595 (18.6%)	1,462 (6.8%)
Diabetes, *n* (%)	1,601 (6.3%)	108 (18.9%)	44 (23.2%)	362 (11.3%)	1,087 (5.0%)
Cancer, *n* (%)	1,291 (5.1%)	42 (7.4%)	11 (5.8%)	653 (20.4%)	585 (2.7%)
Dementia, *n* (%)	505 (2.0%)	13 (2.3%)	3 (1.6%)	264 (8.3%)	225 (1.0%)
Liver disease, *n* (%)	362 (1.4%)	11 (1.9%)	11 (5.8%)	76 (2.4%)	264 (1.2%)
Peptic ulcer disease, *n* (%)	226 (0.9%)	11 (1.9%)	5 (2.6%)	54 (1.7%)	156 (0.7%)
Other[a], *n* (%)	465 (1.8%)	19 (3.3%)	8 (4.2%)	100 (3.1%)	338 (1.6%)
Hospital admission					
Received surgery during hospitalization, *n* (%)	230 (0.9%)	3 (0.5%)	2 (1.1%)	24 (0.8%)	201 (0.9%)
Length of stay in days, median (IQR)	1 (0–3)	2 (1–6)	2 (1–7)	3 (1–8)	1 (0–2)
Acute readmission during follow-up:					
Within 30 days, *n* (%)	3,911 (15.3%)	154 (27.0%)	64 (33.7%)	1,119 (35.0%)	2,574 (12.0%)
Within 90 days, *n* (%)	6,058 (23.8%)	251 (44.0%)	101 (53.2%)	1,596 (49.9%)	4,110 (19.1%)
Biomarkers					
eGFR in mL/min/1.73 m^2, median (IQR)[b]	88.7 (69.8–104.7)	54.0 (36.3–84.6)	72.6 (49.7–93.2)	69.8 (50.0–87.7)	91.5 (74.7–106.7)
<60 mL/min/1.73 m^2, *n* (%)	3,987 (16.4%)	311 (57.2%)	68 (37.0%)	1,180 (38.2%)	2,428 (11.8%)
≥60 mL/min/1.73 m^2, *n* (%)	20,323 (83.6%)	233 (42.8%)	116 (63.0%)	1,908 (61.8%)	18,066 (88.2%)
CRP in mg/L, median (IQR)[b]	4 (1–22)	10 (3–50)	9 (3–55)	19 (5–70)	4 (1–15)
suPAR in ng/mL, median (IQR)[b]	2.7 (2.0–3.9)	4.2 (2.9–5.8)	4.6 (3.1–6.3)	4.5 (3.3–6.2)	2.5 (1.9–3.5)

[a]*Includes connective tissue disease, paraplegia/hemiplegia, and HIV/AIDS.* [b]*Measured at index admission; 1,187 patients (4.7%) missing value for eGFR and C-reactive protein. CRP, C-reactive protein; eGFR, estimated glomerular filtration rate; IQR, interquartile range; suPAR, soluble urokinase plasminogen activator receptor.*

TABLE 2 | Association of log_2(suPAR) with development of incident chronic and acute kidney conditions.

Endpoint	No. patients	Median (IQR) eGFR[a] (mL/min/1.73 m^2)	Median (IQR)[a] suPAR (ng/mL)	Hazard Ratio (95% CI)[b]	
				Univariate	Multivariate[c]
Chronic kidney condition	570	54.0 (36.3–84.6)	4.2 (2.9–5.8)	2.52 (2.31–2.75)	1.57 (1.38–1.78)
Chronic kidney disease	263	41.2 (30.6–58.4)	4.8 (3.6–6.3)	3.20 (2.84–3.60)	1.77 (1.47–2.13)
Glomerular disease	23	73.1 (52.8–98.0)	3.2 (2.0–5.8)	1.64 (1.00–2.67)	1.13 (0.60–2.14)
Tubulointerstitial disease	185	82.7 (56.8–107.0)	3.2 (2.2–4.6)	1.56 (1.31–1.86)	1.26 (1.00–1.59)
Other renal disorder	99	47.0 (33.6–71.5)	4.6 (3.5–6.3)	2.99 (2.46–3.65)	2.07 (1.56–2.76)
Acute kidney condition	190	72.6 (49.7–93.2)	4.6 (3.1–6.3)	2.96 (2.57–3.42)	2.51 (2.09–3.01)
<30 days from index	24	75.1 (59.3–93.5)	4.7 (3.9–6.3)	2.99 (2.01–4.44)	2.43 (1.45–4.06)
30–90 days from index	29	74.6 (54.0–93.6)	5.0 (3.1–7.4)	2.96 (2.06–4.26)	2.67 (1.70–4.20)
>90 days from index	137	69.9 (47.2–92.9)	4.6 (2.9–6.2)	2.96 (2.50–3.51)	2.49 (2.01–3.09)

[a]*Measured at index admission; 1,187 patients (4.7%) missing value for eGFR.* [b]*Hazard ratios represent the proportional risk of developing the given kidney condition for each doubling in suPAR and is evaluated for the entire duration of follow-up unless otherwise specified.* [c]*Adjusted for age, sex, log_2(eGFR), log_{10}(CRP), cardiovascular disease, hypertension, and diabetes. CI, confidence interval; eGFR, estimated glomerular filtration rate; IQR, interquartile range; suPAR, soluble urokinase plasminogen activator receptor.*

index admission, with $\beta = -0.32$ (**Supplementary Figure S2**). Patients with eGFR <60 mL/min/1.73 m^2 had significantly higher suPAR compared to patients with eGFR >60 mL/min/1.73 m^2 (median 4.5 vs 2.5 ng/mL, $P < 0.001$). Among patients with eGFR >60 mL/min/1.73 m^2, 349 patients (1.7%) developed kidney disease, and 1,908 patients (9.4%) died during follow-up. Among patients with eGFR <60 mL/min/1.73 m^2, 379 patients (9.5%) developed kidney disease, and 1,180 patients (29.6%) died during follow-up. For all categories of eGFR, patients who developed kidney disease or died during

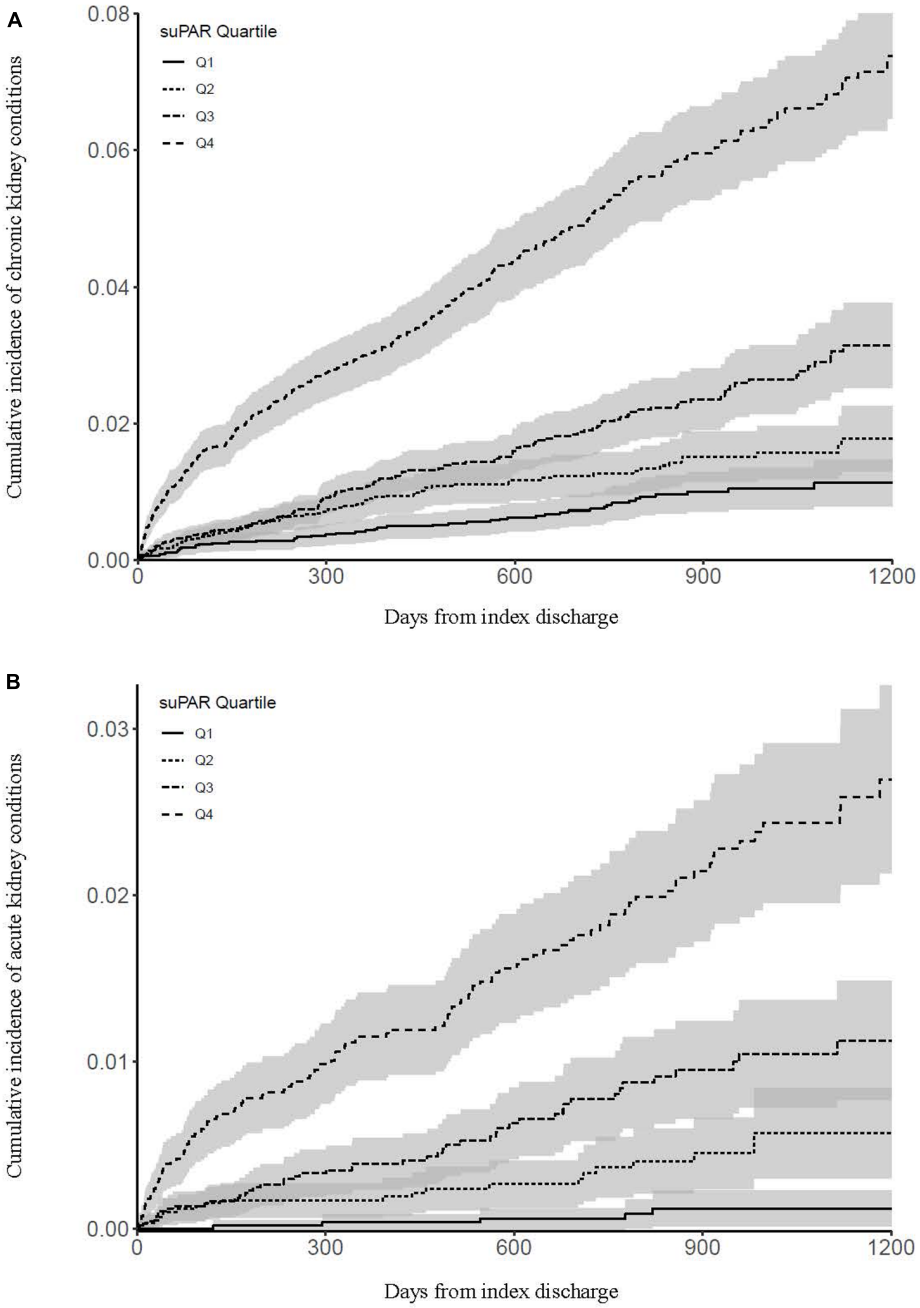

FIGURE 1 | Cumulative incidence of chronic kidney conditions **(A)** and acute kidney conditions **(B)** by suPAR quartile. Shaded areas indicate 95% confidence intervals.

follow-up had significantly higher suPAR at index admission (**Supplementary Figure S3**).

Association of suPAR With Chronic Kidney Conditions

Cumulative incidence of chronic kidney conditions by suPAR quartile is shown in **Figure 1A**. Compared with patients in the lowest suPAR quartile, patients in the 2nd quartile had a hazard ratio of 1.65 (95% CI: 1.15–2.37, $P = 0.007$) for developing an incident chronic kidney condition, patients in the 3rd quartile had a hazard ratio of 2.77 (95% CI: 1.99–3.86, $P < 0.001$), and patients in the highest suPAR quartile had a hazard ratio of 8.53 (95% CI: 6.31–11.54, $P < 0.001$).

Modeling suPAR as a continuous variable, each doubling in suPAR yielded an unadjusted hazard ratio of 2.52 (95% CI: 2.31–2.75, $P < 0.001$) and an adjusted hazard ratio of 1.57 (95% CI: 1.38–1.78, $P < 0.001$) for developing an incident chronic kidney

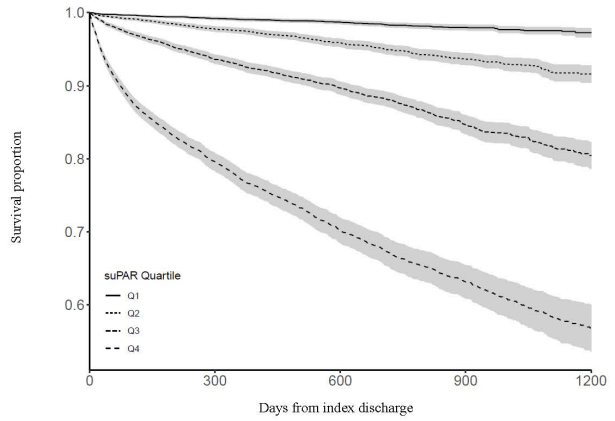

FIGURE 2 | Survival by suPAR quartile. Shaded areas indicate 95% confidence intervals.

condition (**Table 2**). Sensitivity analysis removing patients with eGFR <60 mL/min/1.73 m^2 resulted in an adjusted hazard ratio of 1.43 (95% CI: 1.17–1.73, $P < 0.001$), and sensitivity analysis removing patients with a prior diagnosis of cardiovascular disease resulted in an adjusted hazard ratio of 1.53 (95% CI: 1.33–1.77, $P < 0.001$) for developing an incident chronic kidney condition.

Association of suPAR With Acute Kidney Conditions

Cumulative incidence of acute kidney conditions by suPAR quartile is shown in **Figure 1B**. Compared with patients in the lowest suPAR quartile, patients in the 2nd quartile had a hazard ratio of 4.83 (95% CI: 1.82–12.82, $P = 0.002$) for developing an incident acute kidney condition, patients in the 3rd quartile had a hazard ratio of 10.43 (95% CI: 4.14–26.23, $P < 0.001$), and patients in the highest suPAR quartile had a hazard ratio of 30.47 (95% CI: 12.44–74.67, $P < 0.001$).

Modeling suPAR as a continuous variable, each doubling in suPAR yielded an unadjusted hazard ratio of 2.96 (95% CI: 2.57–3.42, $P < 0.001$) and an adjusted hazard ratio of 2.51 (95% CI: 2.09–3.01, $P < 0.001$) for developing an incident acute kidney condition (**Table 2**). Sensitivity analysis removing patients with eGFR <60 mL/min/1.73 m^2 resulted in an adjusted hazard ratio of 2.68 (95% CI: 2.17–3.32, $P < 0.001$), and sensitivity analysis removing patients with a prior diagnosis of cardiovascular disease resulted in an adjusted hazard ratio of 2.45 (95% CI: 2.01–3.00, $P < 0.001$) for developing an incident acute kidney condition.

Association of suPAR With All-Cause Mortality

Survival by suPAR quartile is shown in **Figure 2**. Compared with patients in the lowest suPAR quartile, patients in the 2nd quartile had a hazard ratio of 3.17 (95% CI: 2.54–3.96, $P < 0.001$) for dying during follow-up, patients in the 3rd quartile had a hazard ratio of 7.99 (95% CI: 6.53–9.79, $P < 0.001$), and patients in the highest suPAR quartile had a hazard ratio of 23.23 (95% CI: 19.10–28.24, $P < 0.001$).

Modeling suPAR as a continuous variable, each doubling in suPAR yielded an unadjusted hazard ratio of 2.89 (95% CI: 2.79–3.00, $P < 0.001$) and an adjusted hazard ratio of 1.99 (95% CI: 1.89–2.09, $P < 0.001$) for dying during follow-up. Sensitivity analysis removing patients with eGFR <60 mL/min/1.73 m^2 resulted in an adjusted hazard ratio of 2.02 (95% CI: 1.90–2.15, $P < 0.001$), and sensitivity analysis removing patients with a prior diagnosis of cardiovascular disease resulted in an adjusted hazard ratio of 2.01 (95% CI: 1.89–2.13, $P < 0.001$) for dying during follow-up.

DISCUSSION AND CONCLUSION

In a cohort of 25,497 acutely hospitalized medical patients without prior kidney disease, we found that elevated suPAR at hospital admission was significantly associated with higher incidence of kidney disease and all-cause mortality during a median follow-up of 2 years. These associations were independent of age, sex, eGFR, CRP, cardiovascular disease, hypertension, and diabetes at index admission. In the adjusted model, each doubling in suPAR increased the hazard of developing an incident chronic kidney condition by 57% and the hazard of developing an incident acute kidney condition by 151%.

Our study cohort had notably lower median suPAR (2.7 ng/mL) than what has been reported by similar studies in the emergency department, such as the 2016 TRIAGE III trial in Denmark that reported median suPAR of 4.1 ng/mL (Schultz et al., 2018). This can be explained in part by our selection criteria. Patients with prior kidney disease or who died during index admission had higher median suPAR than the initial patient population, so their exclusion resulted in a study cohort with lower median suPAR (**Supplementary Figure S1**). Differences in the assays used to measure suPAR may also contribute to variations in suPAR values. A recent study comparing the assay used by our hospital (suPARnostic® AUTO Flex ELISA) to another common assay (Quantikine® Human uPAR-Immunoassay) found that suPARnostic® yielded significantly lower suPAR in healthy controls and higher suPAR in patients with kidney disease (Winnicki et al., 2019).

While suPAR has previously been associated with kidney disease (Hayek et al., 2015; Mossanen et al., 2017; Schaefer et al., 2017; Schulz et al., 2017; Curovic et al., 2019), this is the first study to our knowledge to evaluate the association among patients in the emergency department. This is an important patient population to consider because these patients tend to be older and have multiple comorbid conditions (Juul-Larsen et al., 2017), putting them at greater risk of post-hospitalization kidney disease. Our results from a large population of acute medical patients suggest suPAR as a candidate to include in prediction models for kidney disease. If patients can be classified based on risk of developing kidney disease, then closer monitoring and early interventions in high

risk patients may slow kidney disease progression and avoid complications related to renal dysfunction. For example, a 2009 study from Sweden found that one third of all adverse drug reactions leading to hospitalization in older patients were related to improper dose adjustment according to renal function (Helldén et al., 2009), emphasizing the importance of medication review for patients at risk of developing impaired renal function.

In 2013, our hospital began measuring suPAR as a routine biomarker in the emergency department. For acute medical patients, we have previously reported that elevated suPAR at hospital admission is associated with increased rates of surgery (Meyer et al., 2018), future readmission (Rasmussen et al., 2016), and all-cause mortality independent of presenting symptoms (Rasmussen et al., 2018). However, while suPAR has been implicated in many medical conditions, its causal mechanisms have only been investigated in kidney disease. It is believed that formation of a complex between suPAR and $\alpha_v\beta_3$-integrin (a surface receptor on renal podocytes) can alter podocyte shape and disrupt the kidney's ability to retain large proteins such as albumin (Hayek et al., 2017). We did not find that elevated suPAR was associated more strongly with kidney diseases affecting podocyte function, but this does not exclude the possibility that suPAR may directly contribute to kidney damage.

It may be suggested that suPAR is simply a sensitive filtration marker for early kidney damage, as suPAR is freely filtered by the kidneys and can be measured in the urine. However, we found that the association of suPAR with incident kidney disease remained significant even after adjustment for eGFR, suggesting that elevated suPAR also reflects a feature of kidney disease separate from decreased filtration. Another possibility is that suPAR is related to a systemic chronic inflammatory state. It is well established that chronic inflammation may be responsible for insidious tissue damage (Furman et al., 2019), and elevated suPAR is associated with multiple organ failure and sepsis (Patrani et al., 2016; Zeng et al., 2016). Therefore, high suPAR may indicate a state of chronic low-grade inflammation that predisposes a patient to kidney damage. We adjusted for CRP in our analysis, but CRP is a marker of acute inflammation and likely produced through an inflammatory pathway separate from that of suPAR (Lyngbæk et al., 2013).

In any case, our results in the context of current literature clearly indicate that suPAR is related to aspects of kidney function that are unexplained by current kidney biomarkers. If suPAR is involved in kidney disease pathogenesis, then interventions to reduce suPAR could potentially prevent disease progression in high-risk patients. Haupt et al. (2019) found that current lifestyle as well as changes to diet, smoking, alcohol use, and exercise impacted suPAR over a five-year period, and suPAR levels attained at the end of this period were predictive of follow-up mortality. This finding demonstrates that suPAR is a modifiable risk factor, but it is unknown whether initiatives to reduce suPAR in humans would also reduce the incidence of kidney disease. More recently, Hayek et al. (2020) observed that suPAR overexpression in mice led to acute kidney injury, and pretreatment with uPAR antibody attenuated this injury. This is the latest evidence to suggest a causative role of suPAR in kidney disease as well as identify a potential therapeutic target.

The strength of our study is its large population size. Copenhagen University Hospital Amager and Hvidovre was the first hospital to implement routine suPAR measurements for all acute medical patients, affording us a head start in investigating the role of systemic chronic inflammation in disease progression. Furthermore, since the DNPR contains information about all hospital encounters, we were able to obtain follow-up medical records for >99% of patients in our initial cohort. The collection of routine suPAR measurements and unique access to national registry data enabled us to investigate the association between suPAR and specific disease diagnoses over a four-year period in a large patient cohort.

The main limitation of our study is its reliance on ICD-10 diagnosis codes for both the exclusion criteria and primary outcome of kidney disease. However, a 2011 study found high positive predictive value of ICD-10 codes for renal disease within the DNPR (Thygesen et al., 2011), and a 2013 study concluded that registration of acute admissions within the DNPR has high validity (Vest-Hansen et al., 2013). Still, discrepancies between kidney disease prevalence and diagnosis within Denmark indicate that kidney disease is likely underreported in the DNPR (Henriksen et al., 2018). This discrepancy may be even greater for patients admitted through the emergency department, since clinicians sometimes only record the primary discharge diagnosis.

Ideally, our registry data would be supported by repeated measurements of both eGFR and proteinuria, as well as results of kidney biopsy. Current guidelines from Kidney Disease Improving Global Outcomes (KDIGO) define CKD as eGFR <60 mL/min/1.73 m^2 or albuminuria >30 mg/day for a period of >3 months (Levin and Stevens, 2014). The lack of these endpoints within our cohort is an important limitation in the assessment of CKD, and our results rely largely on the accurate reporting of kidney disease in the DNPR. To address this issue, we performed a sensitivity analysis removing patients with eGFR <60 mL/min/1.73 m^2 and obtained similar results. However, using a single creatinine measurement to identify kidney disease is inaccurate and does not always reflect a patient's full clinical picture (Levey et al., 2015). For example, other conditions such as cardiovascular disease (Liu et al., 2014), hypertension (Lindeman et al., 1984), and diabetes (Alicic et al., 2017) are known to affect long-term kidney function. Therefore, we attempted to control for these conditions by including them in our analysis as potential confounders. We also performed a sensitivity analysis removing patients with known cardiovascular disease and obtained similar results.

In conclusion, we found that elevated suPAR in acute medical patients was independently associated with incident chronic and acute kidney conditions, as well as all-cause mortality. We propose suPAR as a candidate biomarker to include in risk classification models for kidney disease. Future studies are needed to evaluate whether early interventions in high risk

patients can slow disease progression or avoid complications related to renal dysfunction.

DATA AVAILABILITY STATEMENT

The datasets generated for this study are available on request to the corresponding author.

AUTHOR CONTRIBUTIONS

Each author was involved in data analysis or contributed important intellectual content during manuscript writing, accepts personal accountability for their contributions, and agreed to ensure that questions pertaining to the accuracy or integrity of any portion of the work are appropriately investigated and resolved.

FUNDING

This study was conducted at the Department of Clinical Research, Copenhagen University Hospital Amager and Hvidovre, Hvidovre, Denmark. The study did not receive any funding. LR was supported by a postdoctoral fellowship from the Lundbeck Foundation (grant R288-2018-380) and MH was supported by a clinical research associate professorship grant from the Lundbech Foundation (grant R187-2015-2148).

SUPPLEMENTARY MATERIAL

The Supplementary Material for this article can be found online at: https://www.frontiersin.org/articles/10.3389/fcell.2020.00339/full#supplementary-material

REFERENCES

Akbari, A., Clase, C. M., Acott, P., Battistella, M., Bello, A., Feltmate, P., et al. (2014). Canadian society of nephrology commentary on the KDIGO clinical practice guideline for CKD evaluation and management. *Am. J. Kidney Dis.* 65, 177–205. doi: 10.1053/j.ajkd.2014.10.013

Alicic, R. Z., Rooney, M. T., and Tuttle, K. R. (2017). Diabetic kidney disease. *Clin. J. Am. Soc. Nephrol. CJASN* 12, 2032–2045.

Astor, B. C., Matsushita, K., Gansevoort, R. T., van der Velde, M., Woodward, M., Levey, A. S., et al. (2011). Lower estimated glomerular filtration rate and higher albuminuria are associated with mortality and end-stage renal disease. A collaborative meta-analysis of kidney disease population cohorts. *Kidney Int.* 79, 1331–1340. doi: 10.1038/ki.2010.550

Curovic, V. R., Theilade, S., Winther, S. A., Tofte, N., Eugen-Olsen, J., Persson, F., et al. (2019). Soluble urokinase plasminogen activator receptor predicts cardiovascular events, kidney function decline, and mortality in patients with type 1 diabetes. *Diabetes Care* 42, 1112–1119. doi: 10.2337/dc18-1427

Eloot, S., Schepers, E., Barreto, D. V., Barreto, F. C., Liabeuf, S., Van Biesen, W., et al. (2011). Estimated glomerular filtration rate is a poor predictor of concentration for a broad range of uremic toxins. *Clin. J. Am. Soc. Nephrol.* 6, 1266–1273. doi: 10.2215/CJN.09981110

Eugen-Olsen, J., Andersen, O., Linneberg, A., Ladelund, S., Hansen, T. W., Langkilde, A., et al. (2010). Circulating soluble urokinase plasminogen activator receptor predicts cancer, cardiovascular disease, diabetes and mortality in the general population: suPAR: a novel risk marker for major disease and mortality. *J. Intern. Med.* 268, 296–308. doi: 10.1111/j.1365-2796.2010.02252.x

Furman, D., Campisi, J., Verdin, E., Carrera-Bastos, P., Targ, S., Franceschi, C., et al. (2019). Chronic inflammation in the etiology of disease across the life span. *Nat. Med.* 25, 1822–1832. doi: 10.1038/s41591-019-0675-0

Gansevoort, R. T., Correa-Rotter, R., Hemmelgarn, B. R., Jafar, T. H., Heerspink, H. J. L., Mann, J. F., et al. (2013). Chronic kidney disease and cardiovascular risk: epidemiology, mechanisms, and prevention. *Lancet* 382, 339–352. doi: 10.1016/S0140-6736(13)60595-4

Go, A. S., Chertow, G. M., Fan, D., McCulloch, C. E., and Hsu, C. (2004). Chronic kidney disease and the risks of death, cardiovascular events, and hospitalization. *N. Engl. J. Med.* 351, 1296–1305. doi: 10.1056/NEJMoa041031

Haupt, T. H., Rasmussen, L. J. H., Kallemose, T., Ladelund, S., Andersen, O., Pisinger, C., et al. (2019). Healthy lifestyles reduce suPAR and mortality in a Danish general population study. *Immun. Ageing A* 16:1. doi: 10.1186/s12979-018-0141-8

Hayek, S. S., Koh, K. H., Grams, M. E., Wei, C., Ko, Y. A., Li, J., et al. (2017). A tripartite complex of suPAR, APOL1 risk variants and $\alpha_v\beta_3$ integrin on podocytes mediates chronic kidney disease. *Nat. Med.* 23, 945–953. doi: 10.1038/nm.4362

Hayek, S. S., Leaf, D. E., Tahhan, A. S., Raad, M., Sharma, S., Waikar, S. S., et al. (2020). Soluble urokinase receptor and acute kidney injury. *N. Engl. J. Med.* 382, 416–426. doi: 10.1056/NEJMoa1911481

Hayek, S. S., Quyyumi, A. A., and Reiser, J. (2015). Soluble urokinase receptor and chronic kidney disease. *N. Engl. J. Med.* 373, 1916–1925.

Helldén, A., Bergman, U., von, Euler M, Hentschke, M., Odar-Cederlöf, I., and Ohlén, G. (2009). Adverse drug reactions and impaired renal function in elderly patients admitted to the emergency department: a retrospective study. *Drugs Aging* 26, 595–606. doi: 10.2165/11315790-000000000-00000

Henriksen, D. P., Damkier, P., Hallas, J., and Nybo, M. (2018). Sixteen years of creatinine measurements among 460 000 individuals-The Funen Laboratory Cohort (FLaC), a population-based pharmacoepidemiological resource to study drug-induced kidney disease. *Basic Clin. Pharmacol. Toxicol* 124, 582–590. doi: 10.1111/bcpt.13167

Inker, L. A., Schmid, C. H., Tighiouart, H., Eckfeldt, J. H., Feldman, H. I., Greene, T., et al. (2012). Estimating glomerular filtration rate from serum creatinine and cystatin C. *N. Engl. J. Med.* 367, 20–29. doi: 10.1056/NEJMoa1114248

James, M. T., Hemmelgarn, B. R., and Tonelli, M. (2010). Early recognition and prevention of chronic kidney disease. *Lancet* 375, 1296–1309. doi: 10.1016/S0140-6736(09)62004-3

Jha, V., Garcia-Garcia, G., Iseki, K., Li, Z., Naicker, S., Plattner, B., et al. (2013). Chronic kidney disease: global dimension and perspectives. *Lancet* 382, 260–272. doi: 10.1016/S0140-6736(13)60687-X

Juul-Larsen, H. G., Petersen, J., Sivertsen, D. M., and Andersen, O. (2017). Prevalence and overlap of disease management program diseases in older hospitalized patients. *Eur. J. Ageing* 14, 283–293. doi: 10.1007/s10433-017-0412-9

Levey, A. S., Becker, C., and Inker, L. A. (2015). Glomerular filtration rate and albuminuria for detection and staging of acute and chronic kidney disease in adults: a systematic review. *JAMA* 313, 837–846. doi: 10.1001/jama.2015.0602

Levey, A. S., Cattran, D., Friedman, A., Miller, W. G., Sedor, J., Tuttle, K., et al. (2009). Proteinuria as a surrogate Outcome in CKD: report of a scientific workshop sponsored by the national kidney foundation and the US food and drug administration. *Am. J. Kidney Dis.* 54, 205–226. doi: 10.1053/j.ajkd.2009.04.029

Levin, A., and Stevens, P. E. (2014). Summary of KDIGO 2012 CKD Guideline: behind the scenes, need for guidance, and a framework for moving forward. *Kidney Int.* 85, 49–61. doi: 10.1038/ki.2013.444

Lindeman, R. D., Tobin, J. D., and Shock, N. W. (1984). Association between blood pressure and the rate of decline in renal function with age. *Kidney Int.* 26, 861–868. doi: 10.1038/ki.1984.229

Liu, M., X-C, Li, Lu, L., Cao, Y., Sun, R.-R., Chen, S., et al. (2014). Cardiovascular disease and its relationship with chronic kidney disease. *Eur. Rev. Med. Pharmacol. Sci.* 18, 2918–2926.

Lyngbæk, S., Sehestedt, T., Marott, J. L., Hansen, T. W., Olsen, M. H., Andersen, O., et al. (2013). CRP and suPAR are differently related to anthropometry and subclinical organ damage. *Int. J. Cardiol.* 167, 781–785. doi: 10.1016/j.ijcard.2012.03.040

Lynge, E., Sandegaard, J. L., and Rebolj, M. (2011). The danish national patient register. *Scand. J. Public Health* 39, 30–33. doi: 10.1177/1403494811401482

Meyer, J., Alstrup, M., Rasmussen, L. J. H., Schultz, M., Ladelund, S., Haupt, T. H., et al. (2018). suPAR is associated with risk of future acute surgery and post-operative mortality in acutely admitted medical patients. *Scand. J. Trauma Resusc. Emerg. Med.* 26:11. doi: 10.1186/s13049-018-0478-1

Mossanen, J. C., Pracht, J., Jansen, T. U., Buendgens, L., Stoppe, C., Goetzenich, A., et al. (2017). Elevated soluble urokinase plasminogen activator receptor and proenkephalin serum levels predict the development of acute kidney injury after cardiac surgery. *Int. J. Mol. Sci* 18:1662. doi: 10.3390/ijms18081662

Patrani, M., Tsaganos, T., Kotzampassi, K., Paraschos, M., Katsenos, C., Giamarellos-Bourboulis, E. J., et al. (2016). Soluble urokinase plasminogen activator receptor informs on the progression course after multiple injuries. *Biomark. Biochem. Indic. Expo. Response Susceptibility Chem.* 21, 660–664. doi: 10.3109/1354750X.2016.1171911

Rasmussen, L. J., Ladelund, S., Haupt, T. H., Ellekilde, G., Poulsen, J. H., Iversen, K., et al. (2016). Soluble urokinase plasminogen activator receptor (suPAR) in acute care: a strong marker of disease presence and severity, readmission and mortality. A retrospective cohort study. *Emerg. Med. J. EMJ* 33, 769–775. doi: 10.1136/emermed-2015-205444

Rasmussen, L. J. H., Ladelund, S., Haupt, T. H., Ellekilde, G. E., Eugen-Olsen, J., and Andersen, O. (2018). Combining national early warning score with soluble urokinase plasminogen activator receptor (suPAR) improves risk prediction in acute medical patients: a registry-based cohort study. *Crit. Care Med.* 46, 1961–1968. doi: 10.1097/CCM.0000000000003441

Rohun, K., Kuliś, M., Pawłowska, A., Kierzkowska, I., Kwella, N., Kwella, B., et al. (2011). Identifying chronic kidney disease in an emergency department: a chance for an early diagnosis. *Pol. Arch. Med. Wewn.* 121, 23–28.

Schaefer, F., Trachtman, H., Wühl, E., Kirchner, M., Hayek, S. S., Anarat, A., et al. (2017). Association of serum soluble urokinase receptor levels with progression of kidney disease in children. *JAMA Pediatr.* 171:e172914. doi: 10.1001/jamapediatrics.2017.2914

Schmidt, M., Schmidt, S. A., Sandegaard, J. L., Ehrenstein, V., Pedersen, L., and Sørensen, H. T. (2015). The danish national patient registry: a review of content, data quality, and research potential. *Clin. Epidemiol.* 7, 449–490. doi: 10.2147/CLEP.S91125

Schultz, M., Rasmussen, L. J. H., Andersen, M. H., Stefansson, J. S., Falkentoft, A. C., Alstrup, M., et al. (2018). Use of the prognostic biomarker suPAR in the emergency department improves risk stratification but has no effect on mortality: a cluster-randomized clinical trial (TRIAGE III). *Scand. J. Trauma Resusc. Emerg. Med* 26:69. doi: 10.1186/s13049-018-0539-5

Schulz, C.-A., Persson, M., Christensson, A., Hindy, G., Almgren, P., Nilsson, P. M., et al. (2017). Soluble urokinase-type plasminogen activator receptor (suPAR) and impaired kidney function in the population-based malmö diet and cancer study. *Kidney Int. Rep.* 2, 239–247. doi: 10.1016/j.ekir.2016.11.004

Sheather, S. A. (2009). *A Modern Approach to Regression With R*. New York, NY: Springer-Verlag. doi: 10.1007/978-0-387-09608-7

Thygesen, S. K., Christiansen, C. F., Christensen, S., Lash, T. L., and Sørensen, H. T. (2011). The predictive value of ICD-10 diagnostic coding used to assess charlson comorbidity index conditions in the population-based danish national registry of patients. *BMC Med. Res. Methodol.* 11:83. doi: 10.1186/1471-2288-11-83

Vest-Hansen, B., Riis, A. H., and Christiansen, C. F. (2013). Registration of acute medical hospital admissions in the danish national patient registry: a validation study. *Clin. Epidemiol.* 5, 129–133. doi: 10.2147/CLEP.S41905

Wei, C., El Hindi, S., Li, J., Fornoni, A., Goes, N., Sageshima, J., et al. (2011). Circulating urokinase receptor as a cause of focal segmental glomerulosclerosis. *Nat. Med.* 17, 952–960. doi: 10.1038/nm.2411

Winnicki, W., Sunder-Plassmann, G., Sengoelge, G., Handisurya, A., Herkner, H., et al. (2019). Diagnostic and prognostic value of soluble urokinase-type plasminogen activator receptor (suPAR) in focal segmental glomerulosclerosis and impact of detection method. *Sci. Rep.* 9:13783. doi: 10.1038/s41598-019-50405-8

Zeng, M., Chang, M., Zheng, H., Li, B., Chen, Y., He, W., et al. (2016). Clinical value of soluble urokinase-type plasminogen activator receptor in the diagnosis, prognosis, and therapeutic guidance of sepsis. *Am. J. Emerg. Med.* 34, 375–380. doi: 10.1016/j.ajem.2015.11.004

Conflict of Interest: JE-O is a cofounder, shareholder, and Chief Scientific Officer of ViroGates A/S. JE-O and OA are named inventors on patents covering suPAR; the patents are owned by Copenhagen University Hospital Amager and Hvidovre, Hvidovre, Denmark and licensed to ViroGates A/S. LR has received funding for travel from ViroGates A/S.

The remaining authors declare that the research was conducted in the absence of any commercial or financial relationships that could be construed as a potential conflict of interest.

Copyright © 2020 Iversen, Houlind, Kallemose, Rasmussen, Hornum, Feldt-Rasmussen, Hayek, Andersen and Eugen-Olsen. This is an open-access article distributed under the terms of the Creative Commons Attribution License (CC BY). The use, distribution or reproduction in other forums is permitted, provided the original author(s) and the copyright owner(s) are credited and that the original publication in this journal is cited, in accordance with accepted academic practice. No use, distribution or reproduction is permitted which does not comply with these terms.

frontiers in Cell and Developmental Biology

ORIGINAL RESEARCH
published: 17 July 2020
doi: 10.3389/fcell.2020.00559

Icariin Prevents Extracellular Matrix Accumulation and Ameliorates Experimental Diabetic Kidney Disease by Inhibiting Oxidative Stress via GPER Mediated p62-Dependent Keap1 Degradation and Nrf2 Activation

*Kai Wang†, Xiulan Zheng†, Zhenzhen Pan, Wenhui Yao, Xin Gao, Xiniao Wang and Xuansheng Ding**

School of Basic Medicine and Clinical Pharmacy, China Pharmaceutical University, Nanjing, China

OPEN ACCESS

Edited by:
Claudia Torino,
Italian National Research Council, Italy

Reviewed by:
Jun Eguchi,
Okayama University, Japan
Heqing Huang,
Sun Yat-sen University, China
Rossana Morabito,
University of Messina, Italy

***Correspondence:**
Xuansheng Ding
1020030749@cpu.edu.cn

† These authors have contributed equally to this work

Specialty section:
This article was submitted to Molecular Medicine, a section of the journal Frontiers in Cell and Developmental Biology

Received: *28 February 2020*
Accepted: *11 June 2020*
Published: *17 July 2020*

Citation:
Wang K, Zheng X, Pan Z, Yao W, Gao X, Wang X and Ding X (2020) Icariin Prevents Extracellular Matrix Accumulation and Ameliorates Experimental Diabetic Kidney Disease by Inhibiting Oxidative Stress via GPER Mediated p62-Dependent Keap1 Degradation and Nrf2 Activation. Front. Cell Dev. Biol. 8:559. doi: 10.3389/fcell.2020.00559

The present study aimed to determine whether icariin could attenuate type 1 diabetic nephropathy (T1DN) induced by streptozotocin (STZ) after 4 weeks or not. Therefore, its therapeutic effect on diabetic kidney disease was investigated in view of reactive oxygen (ROS) and extracellular matrix (ECM) generation in human glomerular mesangial cells under high glucose. To establish the participation and the key role of GPER and Nrf2 in ECM deposition, a combination of G15 (antagonist of GPER) or siGPER and siNrf2 were performed, respectively. The results showed that T1DN can be significantly inhibited by oral icariin, evidenced by improvement of 24 h urinary volume, 24 h proteinuria, microalbuminuria, and histopathological changes of kidney. Icariin decreased the levels of intracellular superoxide anion, impeded the generation of fibronectin and increased the expression and activity of antioxidant enzymes in the human glomerular mesangial cells treated with high glucose. It acted as a GPER activator, increased dissociation of Nrf2/Keap1 complexes, combination of Keap1/p62 complexes, Nrf2 translocation to nuclear, Nrf2/ARE DNA binding activity, and ARE luciferase reporter gene activity in glomerular mesangial cells. The Nrf2 inhibitor ML385 or siNrf2 obviously abolished extracellular matrix (ECM) generation inhibited by icariin. Furthermore, icariin-induced Nrf2 activation was mainly dependent on p62-mediated Keap1 degradation, which functions as an adaptor protein during autophagy. The GPER antagonist G15 and siGPER obviously abolished the above effects by icariin. Taken together, the present study demonstrated that the therapeutic effects of icariin on type 1 diabetic nephropathy in rats via GPER mediated p62-dependent Keap1 degradation and Nrf2 activation.

Keywords: diabetic kidney disease, icariin, oxidative stress, extracellular matrix, GPER

INTRODUCTION

Diabetic nephropathy (DN), a common devastating complication of both types of diabetes and supervenes as the result of microvascular lesions in the renal glomeruli, is often associated with increased cardiovascular mortality and reduced life quality. According to previous studies, about 30% of patients with type 1 diabetes (T1D) and 20% of patients with type 2 diabetes (T2D) would ultimately be followed up with diabetic nephropathy. Approximately 25% of T1D occurred microalbuminuria after 15–20 years. By reporting, the end-stage renal disease incidence can be 4–17% within 25 years after the diagnoses of T1D. Over 20% of patients with T2D already have diabetic nephropathy at the same time of diabetes (Parving et al., 1988), of whom a further 35% develop DN mostly in next 10 years. Diabetic nephropathy, known as glomerulosclerosis, is associated with progressive, uninterrupted scarring of the glomerulus (Wolf and Ziyadeh, 1999; Zheng et al., 2004). Diabetic induce oxidative stress and excessive deposition of extracellular matrix (ECM) in the mesangium of the glomerulus (Mason and Wahab, 2003). The phenomenon is attributed to the loss of glomerular mesangial cell viability, which is a crucial-pathological change in the diabetes-mediated renal injury (Ortiz-Munoz et al., 2010; Loeffler et al., 2011).

Increasing evidence suggests the oxidative stress as a common feature connecting the changes of metabolic pathways in kidneys (Munoz et al., 2020). Renal oxidative stress is initiated by alterations of advanced glycation end products and glucose metabolism, leading to the antioxidant depletion and ROS production induced by pro-oxidant enzyme increasing (Jha et al., 2016). The investigation on regulation of the transcription factor Nrf2 has always been active. During the resting state, Nrf2 was regulated by Keap1 and kept its level low by ubiquitination and proteosomal degradation in cytoplasm (Loboda et al., 2016). In the case of stimulation, Nrf2 would induce the expression of protective, so-called phase 2 antioxidant genes, such as NQO1, HO-1, SOD2, and Trx1 by interacting with anti-oxidative response elements in the promoters for the maintenance of redox homeostasis (Rueda et al., 2007).

Icariin (**Figure 1A**) is the flavonoids used to remedy the kidney disease in traditional Chinese medicine, which is extracted from Epimedium species. Scientific research has found that icariin possesses multiple bioactivities such as protecting neurons from injury, improving osteoporosis, anti-inflammation, anti-tumor, anti-depression, and anti-oxidation functions (Yao et al., 2019). Recent studies have confirmed that icariin exerted preventive function of kidney disease in streptozotocin (STZ)-induced diabetic rats (Qi et al., 2011). In present, we investigated the potential of icariin in the treatment of DN and explored its mechanism of action from the perspective of ROS production in glomerular mesangial cells.

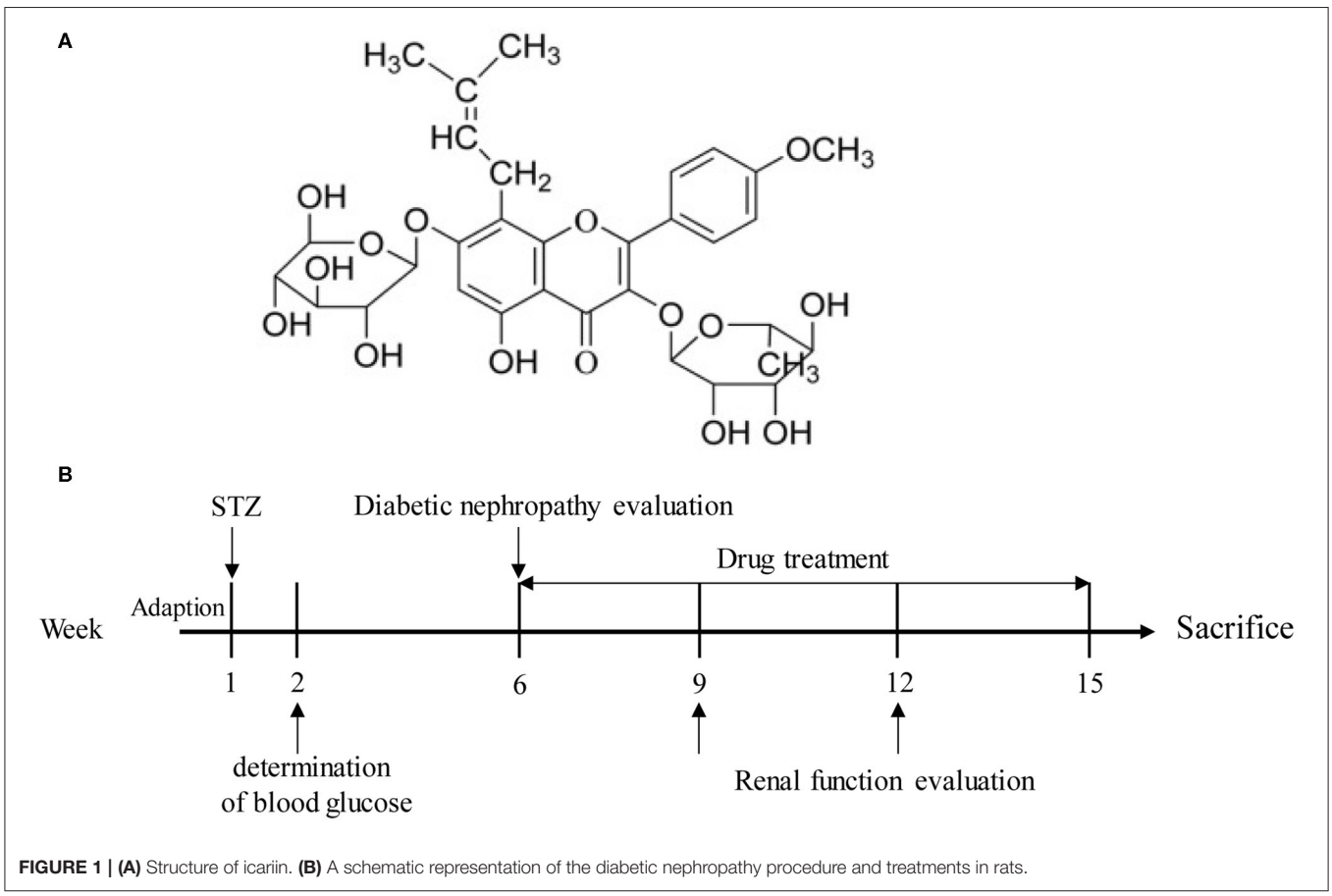

FIGURE 1 | (A) Structure of icariin. **(B)** A schematic representation of the diabetic nephropathy procedure and treatments in rats.

MATERIALS AND METHODS

Chemicals and Regents

Icariin was obtained from Yangtze River Pharm Co., Ltd. (Taizhou, China). Irbesartan was obtained from Sanofi San de la Fort Group Co., Ltd. (Paris, France). Streptozocin (STZ) was purchased from Sigma-Aldrich (St. Louis, MO, USA). Urine protein test kit, total cholesterol assay kit, low-density lipoprotein cholesterol assay kit, high-density lipoprotein cholesterol assay kit, triglyceride assay kit, creatinine assay kit, Heme oxygenase 1 (HO1), Quinone oxidoreductase 1 (NQO1) enzyme activity detection kits and malondialdehyde (MDA) were gained from Nanjing JianCheng Bioengineering Institute (Nanjing, China). Rat insulin ELISA kit was obtained from Jiangsu Yutong Biotechnology Co., Ltd (Nanjing, China). Blood glucose meter and Blood glucose test strips were obtained from Roche (Basel, Switzerland). Nuclear and cytoplasmic protein extraction kit and Phenylmethanesulfonyl fluoride (PMSF) were obtained from KeyGen Biotech (Nanjing, China). TRIzol reagent was purchased from Invitrogen (California, USA). DAPI, SOD, GPx, CAT enzyme activity detection kits and the goat anti-rabbit secondary antibodies were obtained from Beyotime Biotechnology (Shanghai, China). PI3K, Akt and mTOR antibodies were obtained from Cell Signaling Technology, Inc (Massachusetts, USA). ML385 was obtained from MCE (New Jersey, USA). Heme oxygenase 1 (HO1), superoxide dismutase 2 (SOD2) /MnSOD, and thioredoxin 1 (Trx1) antibodies were purchased from ProteinTech (Chicago, USA). Fibronectin, NQO1 and Nrf2 antibodies were purchased from Abcam (Chicago, USA). p62 antibody was obtained from Wanleibio (Shenyang, China). G15 was purchased from ApexBio (Houston, USA). Fetal bovine serum (FBS) was purchased from Biological Industries (BI, Israel). GAPDH and β-actin antibodies were purchased from Abways Technology (beijing, China). Dihydroethidium (DHE) was purchased from Yeasen (Shanghai, China). TRIzol reagent, qPCR SYBR® Green Master Mix and Enhanced chemiluminescent (ECL) plus reagent kit were purchased from Vazyme (Nanjing, China).

Animal Experiments

Female Spraque–Dawley rats (weighing between 180 to 200 g, $n = 104$) were obtained from Zhejiang Experimental Animal Center. Throughout experimental process, rats were housed in a controlled environment condition. The experimental protocol was reviewed and approved by Institutional Animal Care and Use committee of China Pharmaceutical University. The approved number of animal experiments was 2019-05-16.

For intraperitoneal injection, STZ was dissolved in citrate buffer (PH 4.5) and administered in a dose of 55 mg/kg. After 1 week of STZ administration, the rats with fasting blood glucose level over 11.1 mmol/L and persistent hyperglycemia over 16.7 mmol/L were considered as diabetic. Four weeks later, the serum urea nitrogen, urine protein and creatinine levels of rats were measured, and the rats ($n = 98$) meeting the requirements were selected for experimentation (**Figure 1B**). Rats were randomly divided into six groups: normal group, model group, icariin (20, 40, 80 mg/kg, i.g.) group and irbesartan (13.5 mg/kg, i.g.) group. After 9 weeks of administration, the blood and urine samples of all the rats were gathered. Finally, the rats were sacrificed, and their kidney tissues were obtained and weighed. For hematoxylin-eosin (H&E), Masson and PAS staining, part of kidney tissues were fixed in 4% paraformaldehyde. The rest of kidney tissues were preserved at −80°C for western blot analysis. The serum of rats was collected and stored for the detection of certain biochemical indexes.

Immunohistochemistry Assay

For immunohistochemistry assays, kidney tissues were fixed in 4% paraformaldehyde and embedded in paraffin. Then, the renal sections were daparaffinized, subjected to antigen retrieval and treated with 0.5% H_2O_2 to eliminate endogenous peroxidase activity. Next, the sections were incubated in blocking buffer (2% BSA) with primary antibody overnight at 4°C. Nrf2 and Fibronectin used at a dilution of 1:200 and 1:100, respectively.

TABLE 1 | Human Primers used in quantitative-polymerase chain reaction (Q-PCR).

Gene		Sequence (5′-3′)
GAPDH	Forward	TCGTGGAGGGACTTATGA
	Reverse	AGTGAGTGTCGCTGTTGA
GPER	Forward	CGTCATTCCAGACAGCACCGAG
	Reverse	CGAGGAGCCAGAAGCCACATC
Nrf2	Forward	CGGTATGCAACAGGACATTG
	Reverse	TTGGCTTCTGGACTTGGAAC
NQO1	Forward	CGCGACTCCCACAAGGTT
	Reverse	GTCCGACTCCACCACCTCC
Trx1	Forward	CGGAGAGGAGACTTCACAGAG
	Reverse	ATTTCCACGATTTCCCAGAG
SOD2	Forward	CAATAGAAGGCTGCCCTTTC
	Reverse	CACAGTGCACAGGAACACAG
HO-1	Forward	GGCAGAGGGTGATAGAAGAGG
	Reverse	AGCTCCTGCAACTCCTCAAA

TABLE 2 | Rat Primers used in quantitative-polymerase chain reaction (Q-PCR).

Gene		Sequence (5′-3′)
GAPDH	Forward	TGAACGGGAAGCTCACTG
	Reverse	GCTTCACCACCTTCTTGATG
NQO1	Forward	GGGGACATGAACGTCATTCTCT
	Reverse	AGTGGTGACTCCTCCCAGACAG
Trx1	Forward	ATGACTGCCAGGATGTTGCT
	Reverse	GTTAGCACCAGAGAACTCCCC
SOD2	Forward	GACGCCGCAGAGCAGAC
	Reverse	GACACAACATTGCTGAGGCG
HO-1	Forward	TGTCCCAGGATTTGTCCGAG
	Reverse	ACTGGGTTCTGCTTGTTTCGCT

ELISA Assay

To detect the levels of urea nitrogen and serum creatinine, ELISA assays were performed according to the manufacturer's instructions. All ELISA kits were purchased from Nanjing JianCheng Bioengineering Institute (Nanjing, China).

Cell Culture

Human mesangial cells (HMC) was obtained from ScienCell Research Laboratories, Inc. (San Diego, California, USA). Cells were cultured in Dulbecco's Modified Eagle's medium (DMEM) containing 10% FBS (fetal bovine serum) and Penicillin-Streptomycin Solution (1X) in an atmosphere of 5% CO_2 at 37°C. For the experimental study, HMCs were maintained in DMEM with normal glucose (5.6 mM glucose, NG), high glucose (30 mM glucose, HG), icariin of different concentrations and irbesartan of a certain concentration in the presence of high glucose for 48 h.

Western Blot Assay

The whole and nucleus proteins were lysed by certain lysis buffer containing 1% PMSF on the ice, and then clarified by centrifugation at 4Â°C. The samples were then separated by 10 % SDS-PAGE and electroblotted onto PVDF membranes. The membranes were blocked with 5% non-fat milk in TBST for 1.5 h, and incubated with Nrf2 (1:1,000), SOD2 (1:1,000), NQO1 (1:1,000), HO1 (1:1,000), Trx1 (1:1,000), Fibronectin (1:1,000), β-actin (1:1,000), and GAPDH (1:1,000) at 4°C overnight. Next, the membranes were washed and incubated with goat anti-rabbit IgG (1:5,000) for 1.5 h at room temperature. Finally, using ECL reagent (vazyme) to make the membrane visible and analytical, and all these images were quantified by ImageJ Software (Media Cybernetics, Silver Spring, MD, USA). Data were expressed as the ratio of integrated optical density to area.

Immunofluorescence Assay

HMC (1×10^6 cells per well) were plated on glass coverslips. The cells were fixed in 4% paraformaldehyde, permeabilized

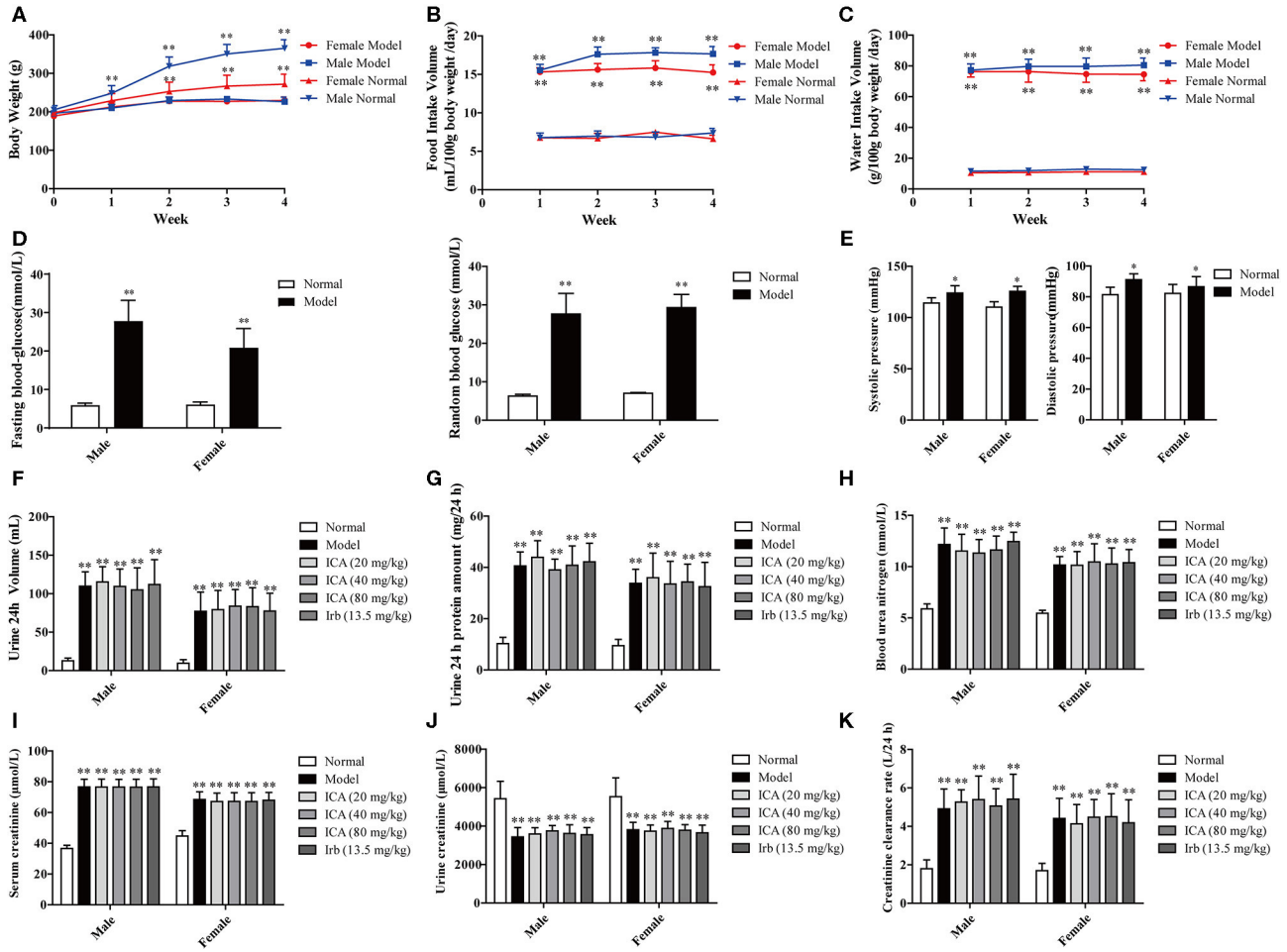

FIGURE 2 | Renal function in STZ-induced diabetic rats before administration. Four weeks after STZ administration, diabetic nephropathy models were examined based on general indicators. **(A)** Weight loss. **(B)** Food intake. **(C)** Water intake. **(D)** Blood glucose. **(E)** Blood pressure. **(F)** 24 h urine volume, **(G)** 24 h proteinuria, **(H)** Blood urea nitrogen (BUN), **(I)** Serum creatinine (Src), and **(J)** Urine creatinine (Ucr) were measured by ELISA. **(K)** Creatinine clearance rate. Data are expressed as mean ± SD. $^*p < 0.05$, $^{**}p < 0.01$, compared with the normal group.

with 0.3% Triton X-100 in PBS for 20 min at room temperature and incubated in blocking buffer (1% BSA) for 1 h. Then, Nrf2 antibody (1:200) was added in the glass coverslips at 4°C overnight. After washing cells with PBS for 3 times, goat anti-rabbit IgG H&L (FITC) was added and incubated for 1 h at room temperature. For nuclear staining, cells were incubated with DAPI (1:100,000) for 10 min. Finally, the images of cells were gathered by fluorescence microscope (Olympus, Japan) in the China Pharmaceutical University.

Co-immunoprecipitation Assay

HMC were treated with indicated drugs for 48 h, washed with cold phosphate-buffered saline (PBS) three times, and harvested by centrifugation. Then, the nuclear and cytoplasmic fractions were prepared by commercial nuclear and cytoplasmic extraction reagents. Proteins isolated from HMC were incubated with Nrf2 or Keap1 antibody at 4°C overnight. Next, the proteins were precipitated using protein A/G-agarose beads for 4 h at room temperature. After washing the precipitated proteins with PBS for 3 times, SDS-PAGE was used to separate proteins as illustrated in the western blot assay.

siRNA Transfection

Before transfection, 1×10^6 HMC cells were seeded in 6-well. 24 h later, the cells were transfected with the Control siRNA, siNrf2 or siGPER by lipofectamine 2000 reagent (Invitrogen, Carlsbad, CA, USA) and culture in opti-MEM reduced serum medium for 4 h. Next, the opti-MEM reduced serum transfection medium was removed from plates and DMEM with 10% FBS was added for 36 h incubation. Then, cells were treated by indicated drugs and harvested. Lastly, the samples were subjected to Q-PCR assay or western blot assay according to manufacturer's instruction with some modification.

Quantitative-Polymerase Chain Reaction (Q-PCR)

Kidneys cortexes from control and diabetic mice were collected or HMC cells were isolated to extract RNA using Trizol followed by the manufacturer's instructions. Total RNA was dissolved in the DEPC water. The RNA concentration was determined with a spectrophotometer (Nano 1000, Thermo Fisher Scientific, Waltham, MA, USA) by absorbance at 260 nm. Then, the reverse transcription of purified total RNA (1 μg) was conducted by HiScript™ reverse transcriptase kit and then reverse transcriptase–polymerase chain reaction was conducted on ABI 7500 (Applied Biosystems, Foster City, CA, USA) with Hieff™ qPCR SYBR® Green Master Mix. GAPDH was used as a

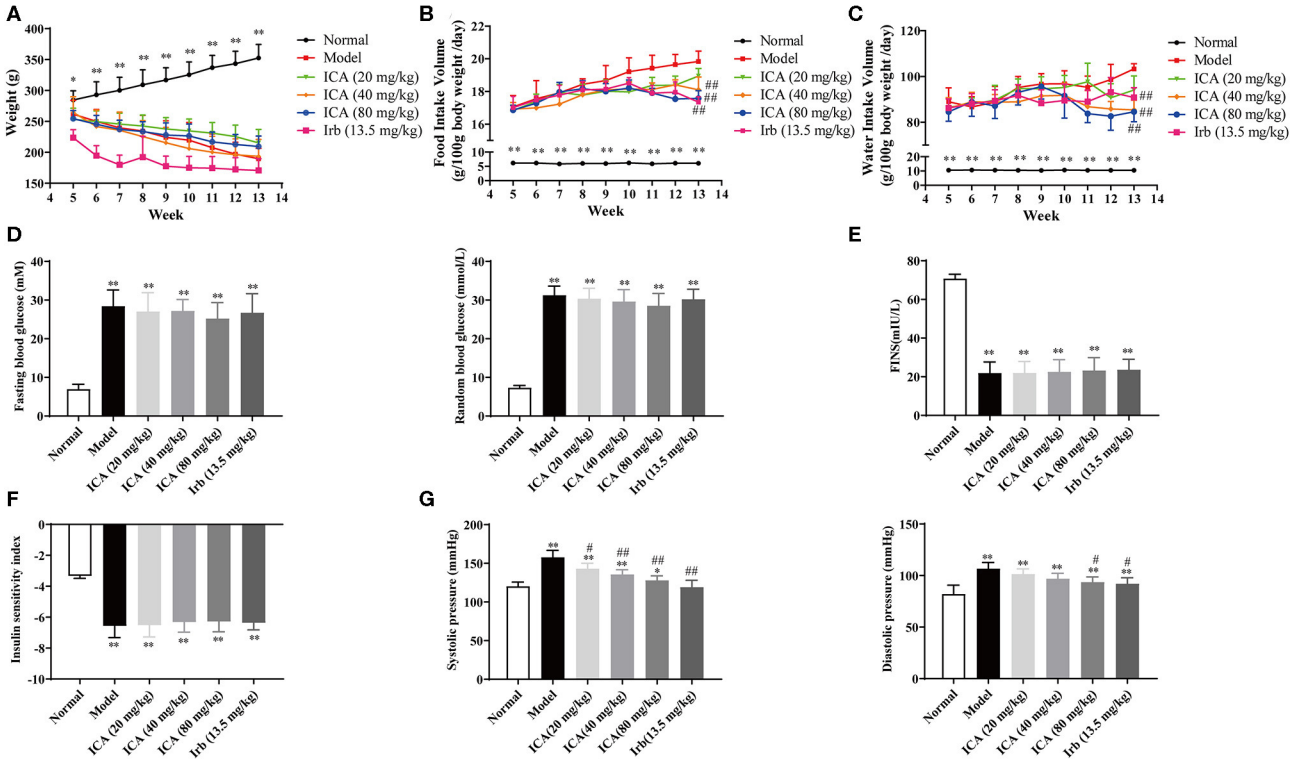

FIGURE 3 | Icariin prevented the development of diabetes in STZ-induced diabetic rats. Rats were subjected to diabetic nephropathy, and orally administered with icariin (20, 40, 80 mg/kg) or irbesartan (13.5 mg/kg) daily for 9 weeks. Rats were sacrificed, and kidneys were isolated. **(A)** Body weight. **(B)** Food intake. **(C)** Water intake. **(D)** Blood glucose. **(E)** Fasting serum insulin. **(F)** Insulin sensitivity index. **(G)** Blood pressure. Data are expressed as mean ± SD. $^{*}p < 0.05$, $^{**}p < 0.01$, compared with the normal control group; $^{\#}p < 0.05$, $^{\#\#}p < 0.01$, compared with the Model group ($n = 10$).

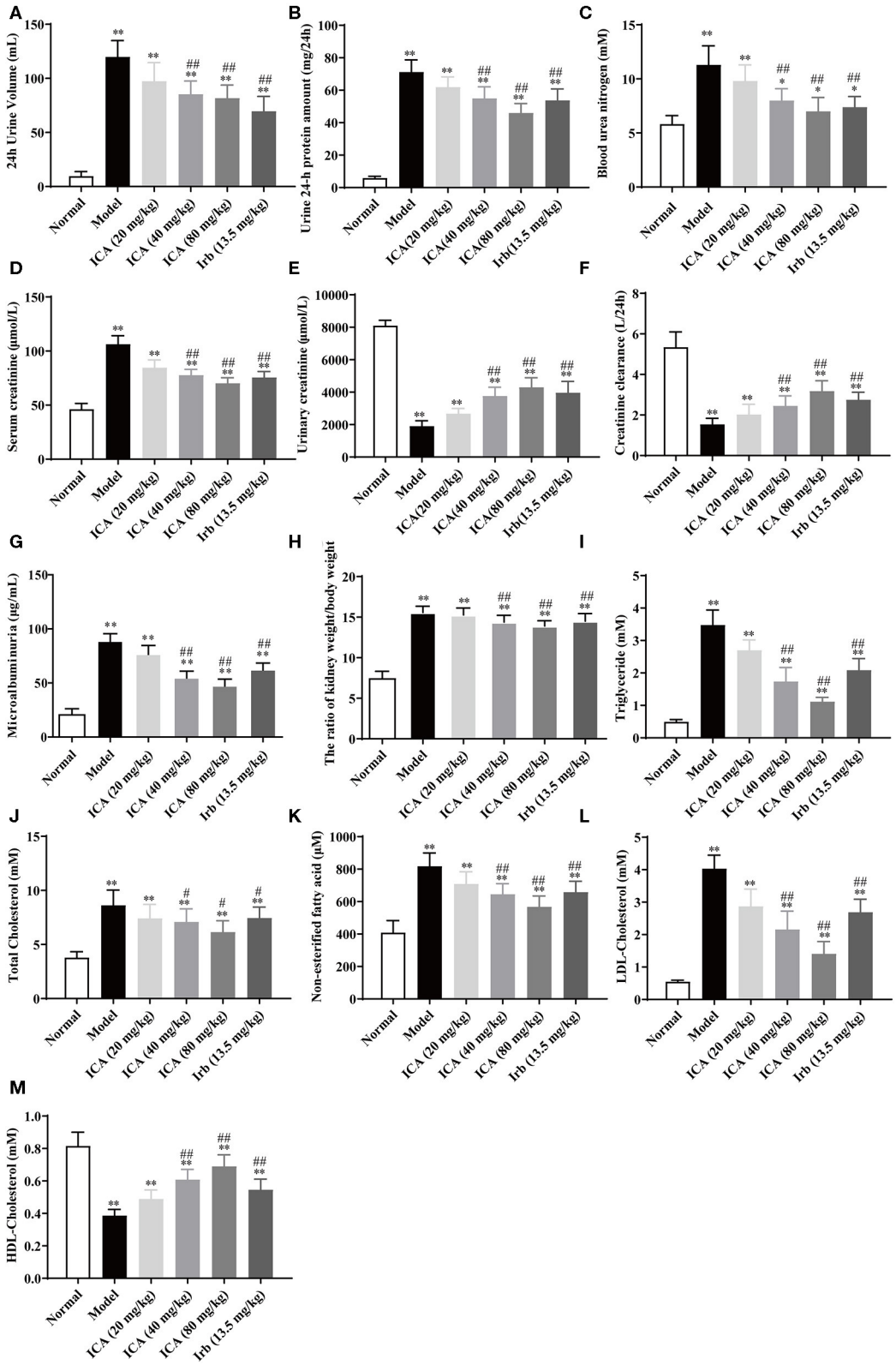

FIGURE 4 | Effects of icariin on metabolic parameters in kidney damage rats. **(A)** The 24 h urinary volume, **(B)** 24 h proteinuria, **(C)** Blood urea nitrogen (BUN), **(D)** Serum creatinine (Src), **(E)** Urinary creatinine, **(F)** Creatinine clearance, and **(G)** 24 h urinary albumin excretion were measured by ELISA. **(H)** The ratio of kidney weight to body weight. **(I)** Triglyceride, **(J)** Total Cholesterol, **(K)** Non-esterified fatty acid, **(L)** LDL-Cholesterol and **(M)** HDL-Cholesterol were measured by ELISA. Data are expressed as mean ± SD ($n = 10$). $^{*}p < 0.05$, $^{**}p < 0.01$, compared with the normal control group; $^{\#}p < 0.05$, $^{\#\#}p < 0.01$, compared with the Model group.

control for target gene. The sequences of primers were listed in **Tables 1**, **2**.

Superoxide Measurement

To detect the superoxide, HMC were treated with irbesartan (1 μM) and icariin (1, 3, 10 μM) for 48 h with or without high glucose. The final concentration of dihydroethidium (DHE) was 10 μM (Yeasen, Shanghai, China) with serum-free medium. Remove the cell culture medium, add appropriate volume of DHE, and incubate in 37°C cell incubator for 30 min. After washing cells with serum-free cell culture solution for 3 times, cells were collected and treated according to the manufacturer's instructions. Lastly, cells were detected by flow cytometry (Macsqant, Germany) in the China Pharmaceutical University.

To detect the superoxide level in the kidney tissues of rats, frozen slides were incubated with 10 μM DHE for 30 min at 37°C in dark. After washing slices with PBS for 3 times, they were photographed by fluorescence microscope.

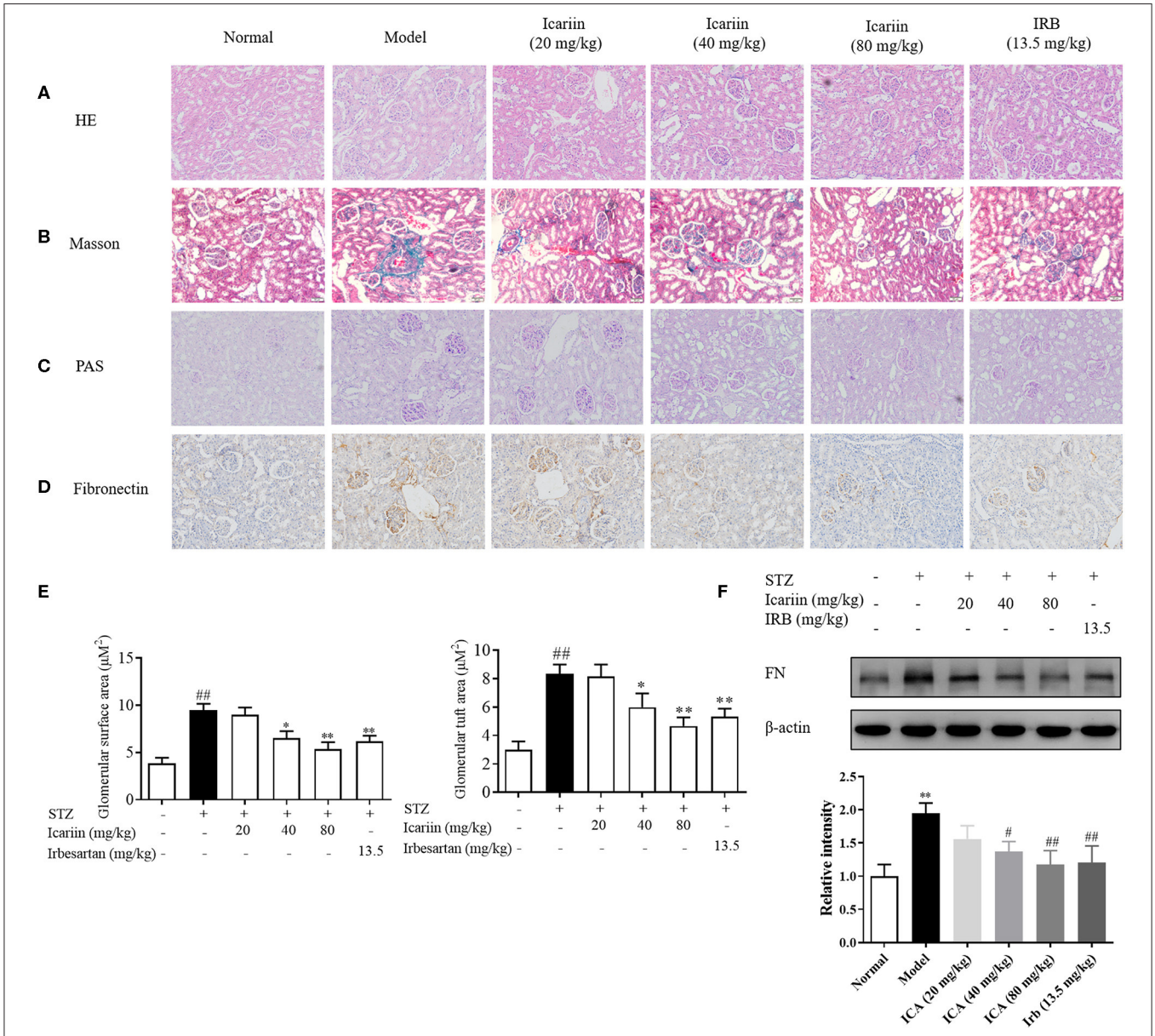

FIGURE 5 | Effect of icariin on the generation of ECM in STZ-induced diabetic rat. **(A)** The histopathology analysis of glomeruli using HE staining (200×). **(B)** The histopathology analysis of glomeruli using PAS staining (200×). **(C)** The histopathology analysis of glomeruli using Masson staining (200×). **(D)** Expression of FN in glomeruli through immunohistochemical (200×). **(E)** Glomerular surface area and glomerular tuft area were quantified using 30 glomeruli per mouse using ImageJ Software. **(F)** Expression of FN protein expression by western blot. Data are expressed as mean ± SD. $^{*}p < 0.05$, $^{**}p < 0.01$, compared with the normal control group; $^{\#}p < 0.05$, $^{\#\#}p < 0.01$, compared with the Model group.

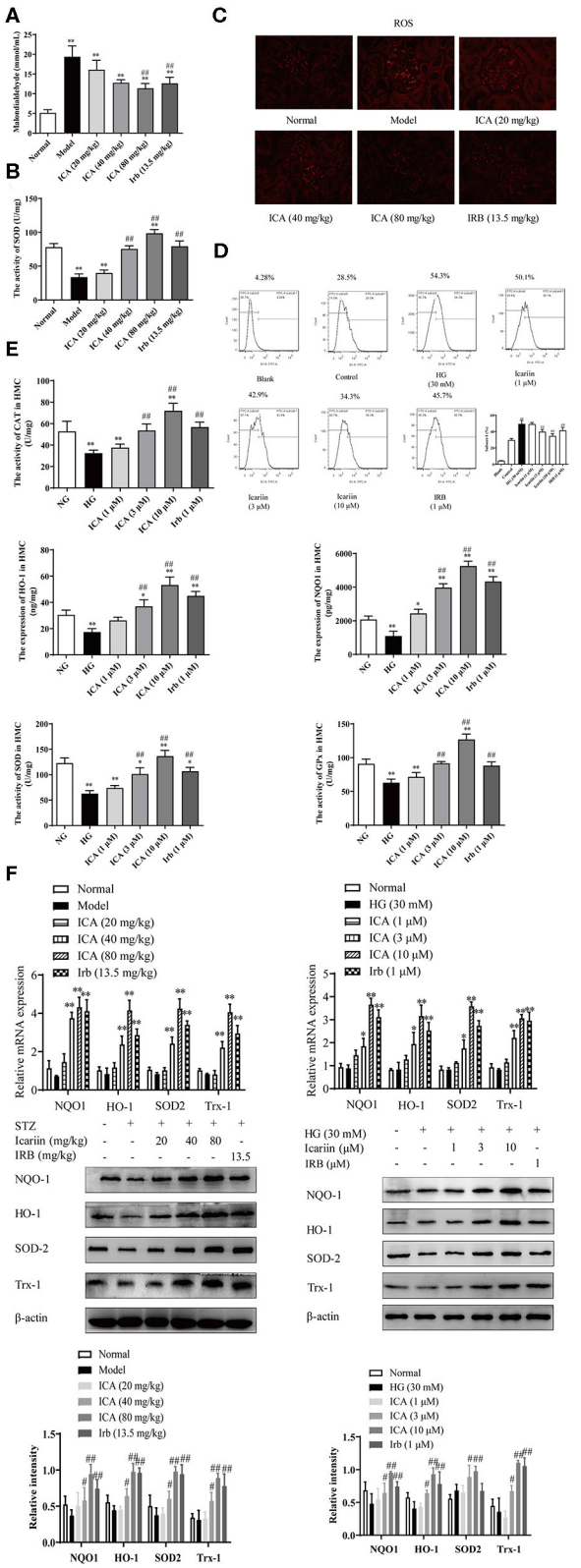

FIGURE 6 | Effect of icariin on oxidative stress in the kidneys of STZ-induced diabetic rats and HMC. **(A)** Malondialdehyde content (MDA). **(B)** Superoxide dismutase (SOD) activity. **(C)** The levels of superoxide anion were detected by

(Continued)

FIGURE 6 | dihydroethidium (DHE) staining in kidney. The images were taken at 200× magnification. **(D)** Effect of icariin on the levels of ROS induced by high glucose in HMC and the superoxide anion was detected by flow cytometry. **(E)** Effect of icariin on the activity of antioxidant enzymes CAT, HO-1, NQO1, SOD, and GPx in HMC. **(F)** Effect of icariin on the mRNA and protein level of antioxidant enzymes HO-1, NQO1, SOD and Trx1 in STZ-induced diabetic rats and HMC. Data are expressed as mean ± SD. $^{*}p < 0.05$, $^{**}p < 0.01$, compared with the normal control group; $^{\#}p < 0.05$, $^{\#\#}p < 0.01$, compared with the Model group.

Detection of Antioxidant Enzyme Activity

HMC cells (1×10^6 cells per well) were cultured in a 6-well plate at the logarithmic growth stage. The cells were completely adherent to the wall. Added low sugar culture medium to the normal group, high sugar culture medium (30 mM) to the model group, and treat the administration group with corresponding concentration of drugs and high sugar culture medium, respectively. After 48 h of administration, discarded the culture medium, washed the residual complete culture medium twice with PBS, and discarded all the residual PBS as much as possible. The activities of SOD, HO-1, NQO1, GPx and CAT antioxidant enzymes were detected according to the product manual of commodity manufacturer.

Electrophoretic Mobility Shift Assay (EMSA)

EMSA was performed to detect the DNA binding activity of Nrf2 by a commercial kit (Pierce, Rockford, IL, USA). Briefly, HMC (1×10^6 cells per well) were cultured in 6-well plates and treated with indicated drugs for 48 h and the nuclear proteins were extracted. Then, the proteins were incubated with biotin-labeled Nrf2-specific oligonucleotides, poly (dI-dC) and binding buffer for 20 min at room temperature. Next, the protein-DNA complexes were separated on a 5% non-denatured polyacrylamide gels and transferred onto PVDF membranes. Lastly, the biotin end-labeled DNA was detected by chemiluminescence.

Luciferase Reporter Assay

For Luciferase reporter assay, HMC were co-transfected with pGL3-ARE reporter gene plasmid by Lipofectamine 2000 for 8 h. Then, fresh medium with indicated drugs were added for another 48 h. Lastly, the relative luciferase activity was detected by the Luciferase assay kit.

Statistical Analysis

All experiments were performed for at least 3 times and the data was shown as mean ± SD. Data among groups were analyzed by *T*-test (two groups) or one-way ANOVA (multiple groups) by using SPSS statistical software (SPSS, Chicago, IL, USA). $p < 0.05$ was considered as statistically significant.

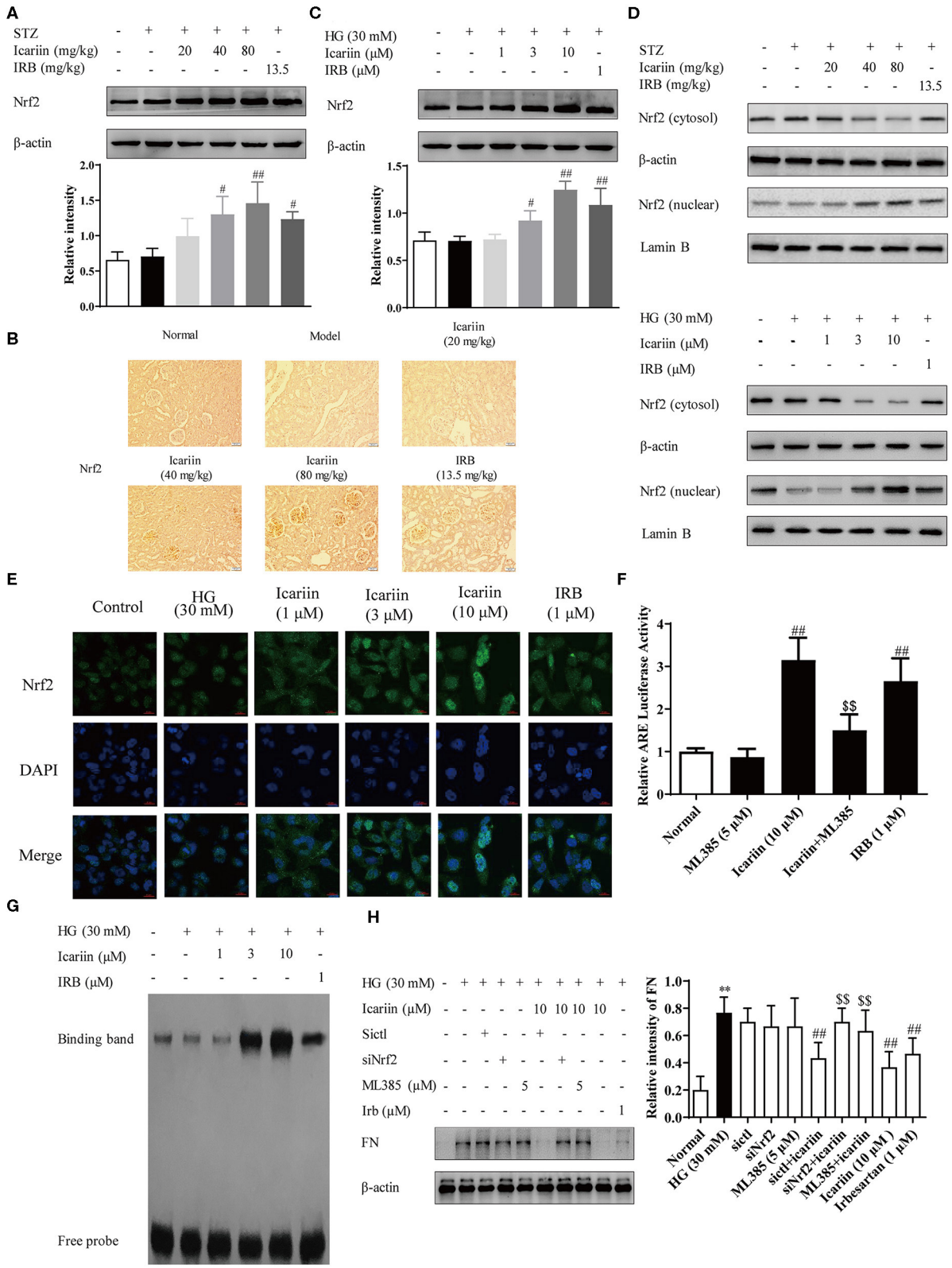

FIGURE 7 | Effect of icariin on Nrf2 activation and ECM generation in DN rats and HMC induced by high glucose. **(A)** Effect of icariin on the total expressions of Nrf2 in DN rats was detected by western blot assy. **(B)** Effect of icariin on Nrf2 protein level in DN rats was detected by immunohistochemical staining. Scale bar: 50 μm

(Continued)

FIGURE 7 | (C) Effect of icariin on Nrf2 protein level in high glucose induced HMC was detected by western blot assay. **(D)** Effect of icariin on the nuclear expressions of Nrf2 in STZ-induced diabetic rat kidney and high glucose induced HMC was detected by western blot assay. **(E)** Distribution of Nrf2 in HMC through Immunofluorescence. Bar: 20 μm. green fluorescence indicates localization of Nrf2. **(F)** Transcriptional activity of Nrf2 was measured by luciferase reporter assay. **(G)** DNA binding activity of Nrf2 was determined by electrophoretic mobility shift assay. **(H)** Effect of siNrf2 and ML385 on the inhibition of FN by icariin in HMC. Data are expressed as mean ± SD. $^{**}p < 0.01$, compared with the normal control group; $^{\#}p < 0.05$, $^{\#\#}p < 0.01$, compared with the Model group or HG group; $^{\$\$}p < 0.01$, compared with the icariin group.

RESULTS

Evaluation of Diabetic Nephropathy Model in STZ-Induced Diabetic Rats Before Administration

Four weeks after STZ injection, diabetic rats showed a remarkably increase in food intake (**Figure 2B**), water intake (**Figure 2C**), blood glucose (**Figure 2D**), blood pressure (**Figure 2E**), 24 h urine volume (**Figure 2F**), 24 h proteinuria (**Figure 2G**), blood urea nitrogen (BUN) (**Figure 2H**), serum creatinine (Src) (**Figure 2I**), and creatinine clearance rate (**Figure 2K**) while reduction in urine creatinine (Ucr) (**Figure 2J**) and weight (**Figure 2A**) when compared with the normal rats. The result showed that diabetic rats were developed with diabetes nephropathy. Subsequently, healthy rats with the injection of 0.1 M citrate buffer and successful established DN rats were divided into six groups.

Icariin Prevented the Development of DN in STZ-Induced Diabetic Rats

Body weight, food intake and water intake were recorded every day during the 9-weeks period. Diabetes is often associated with weight loss and increased water and food intake. Our results showed that diabetic rats took more water and food, along with the hyperglycemia and high blood pressure, indicating that a DN animal model was successfully established. Interestingly, icariin dose-dependently attenuated the progression of DN, as exhibited by decreased weight loss (**Figure 3A**) and inhibited the increase in water (**Figure 3C**), food intake (**Figure 3B**) and blood pressure (**Figure 3G**), but no significant changes in blood glucose (**Figure 3D**), fasting insulin level (**Figure 3E**) and insulin sensitivity index (**Figure 3F**) were observed in the different groups, which suggested that the improvement of diabetes symptoms by oral icariin was probably independent of glycemic control.

Icariin Dose-Dependently Ameliorated Renal Function and Corrected of Dyslipidemia in STZ-Induced Diabetic Rats

Nine weeks after being grouped, kidneys in diabetes mellitus (DM) rats in model group were heavier than those in other groups (**Figure 4H**). However, these indicators of kidney function were dose-dependently increased in icariin treatment groups of diabetic rats. The 24 h urinary volume (**Figure 4A**), 24 h proteinuria (**Figure 4B**), blood urea nitrogen (BUN) (**Figure 4C**), serum creatinine (Src) (**Figure 4D**), and 24 h urinary albumin excretion (**Figure 4G**) were all significantly higher in five groups of diabetic rats than those in normal group. These values were decreased dose-dependently in icariin treatment groups. Compared with the irbesartan treatment group, the ratio of kidney weight to body weight, serum creatinine, and 24 h urinary albumin excretion were all further decreased, whereas urinary creatinine (**Figure 4E**) and creatinine clearance (**Figure 4F**) were increased in icariin (40, 80 mg/kg) groups but these values did not differ between the two groups. Dyslipidemia often occurs in diabetic nephropathy, including increased triglyceride (TG) (**Figure 4I**), total cholesterol (**Figure 4J**), non-esterified fatty acid (**Figure 4K**), low density lipoprotein cholesterol (LDL-C) (**Figure 4L**) and decreased high density lipoprotein cholesterol (HDL-C) (**Figure 4M**), these values were dose-dependently improved in icariin (40, 80 mg/kg) groups.

Icariin Attenuated the Pathological Changes in STZ-Induced Diabetic Rats

Glomerular lesions are characterized by extracellular matrix deposition in the mesangium and glomerular hypertrophy. In order to observe renal cortical morphological changes in diabetic rats, the representative photomicrographs of rat kidneys in HE, PAS and Masson's trichrome-stained from the six groups were performed. As shown in **Figures 5A–C**, in model group, the glomerular exhibited alterations in several aspects including extracellular matrix deposition, mesangial region enlargement and basement membrane thickening compared with normal group. Icariin treatment obviously attenuated glomerular hypertrophy and mesangial matrix expansion in diabetic rats. Similarly, the HE staining exhibited increased ECM deposition in the glomeruli of model group, after icariin treatment, the renal injury dose-dependently improved (**Figure 5E**). Furthermore, the Masson stain also manifested that icariin-decreased collagen deposition in the glomeruli of diabetic rat. Fibronectin (FN), the major component of glomerular ECM, play a key role in promoting glomerular fibrotic lesions. In this study, icariin significantly dampened the increase in FN protein expression in the diabetic rat's kidney by immunohistochemical stain (**Figure 5D**) and western blot (**Figure 5F**) assay. Overall, these results showed that icariin alleviated renal damage by reducing the ECM deposition.

Icariin Attenuated Oxidative Stress in DN Rats and Glomerular Mesangial Cells Induced by High Glucose

Oxidative stress has been considered to be one of the main causes of excessive generation of ECM and consequent leading to damage to kidney function and structure in DN. To explore the effects of icariin on oxidative stress in DN, the malondialdehyde (MDA) content (**Figure 6A**), superoxide dismutase (SOD) activity (**Figure 6B**) and superoxide anion (**Figure 6C**) as determined by DHE staining in kidney were detected. Compared with normal group, MDA content and superoxide anion were

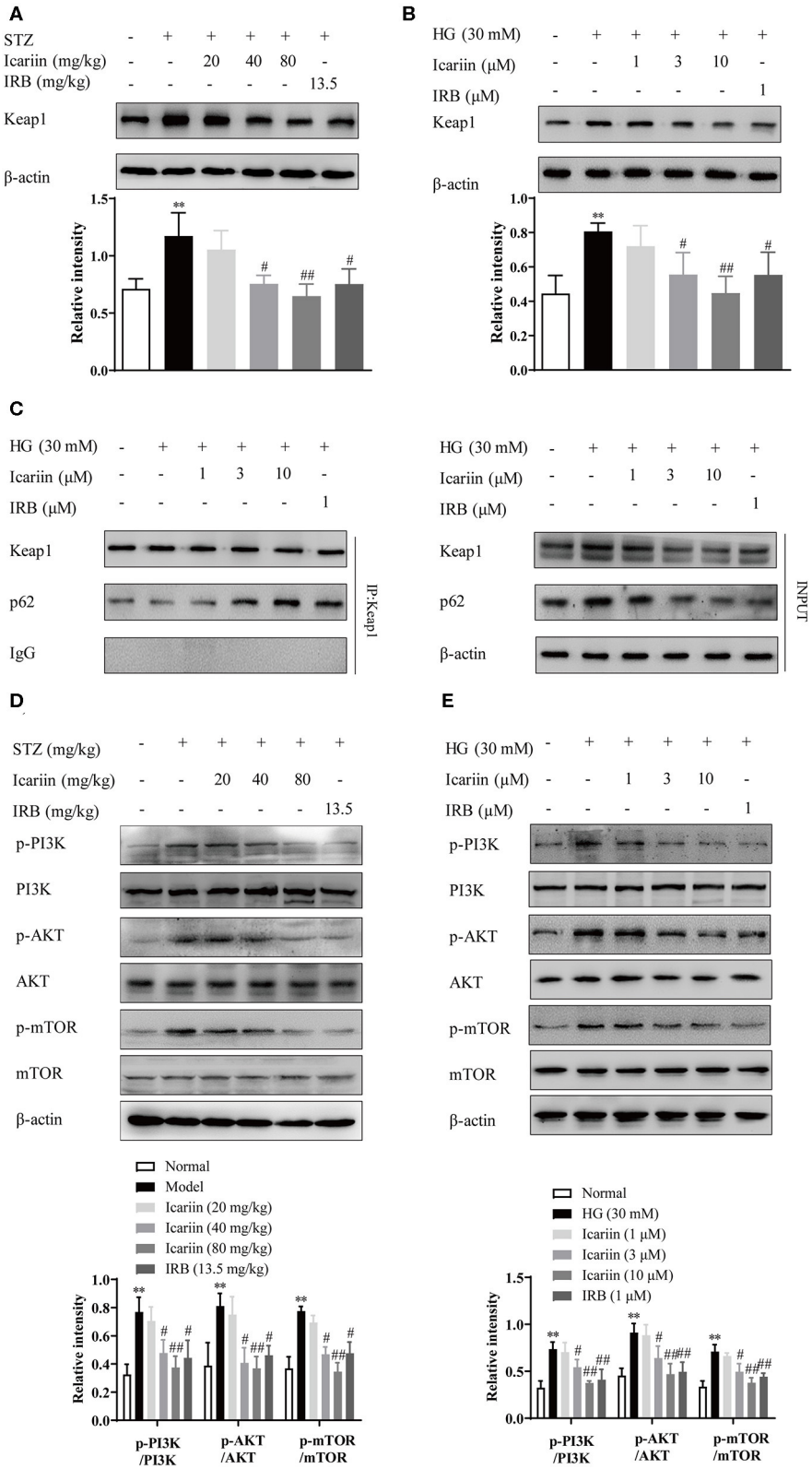

FIGURE 8 | Effect of icariin on HG-induced degradation of Nrf2 by promoting p62-dependent Keap1 degradation. **(A,B)** Effect of icariin on Keap1 protein level in STZ-induced diabetic rat kidney and high glucose induced HMC. **(C)** Effect of icariin on the interaction between p62 and Keap1 induced by high glucose in HMC. **(D,E)** Effect of icariin on phosphorylated and total PI3K, Akt, and mTOR1 protein level *in vivo* and *in vito*. Data are expressed as mean ± SD. $^{**}p < 0.01$, compared with the normal control group; $^{\#}p < 0.05$, $^{\#\#}p < 0.01$, compared with the Model group or HG group.

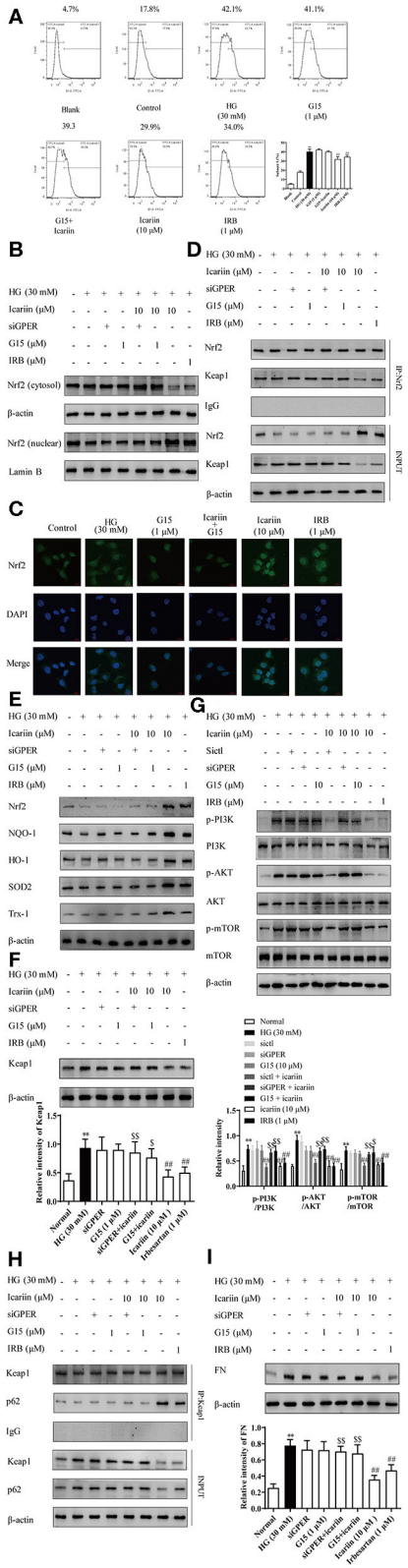

FIGURE 9 | Effect of icariin on GPER mediated p62-dependent Keap1 degradation and Nrf2 activation. The cells were treated with NG (5.6 mM), HG (30 mM), HG (30 mM) + G15 (1 μM), HG (30 mM) + siGPER, HG (30 mM) + *(Continued)*

FIGURE 9 | icariin (10 μM) + G15 (1 μM), HG (30 mM) + icariin (10 μM) + siGPER, HG (30 mM) + icariin (10 μM) and HG (30 mM) +IRB (1 μM) for 48 h. **(A)** The ROS was detected by flow cytometry. **(B)** the nuclear expressions of Nrf2 induced by high glucose in HMC by western blot. **(C)** Distribution of Nrf2 in HMC through Immunofluorescence **(D)** the interaction between Nrf2 and Keap1 induced by high glucose in HMC. **(E)** The expression of Nrf2 and antioxidant enzymes HO-1, NQO1, SOD2 and Trx1 in HMC. **(F)** Keap1 protein level induced by high glucose in HMC. **(G)** Effect of icariin on phosphorylated and total PI3K, Akt, and mTOR1 protein level induced by high glucose in HMC. **(H)** The interaction between Nrf2 and p62 induced by high glucose in HMC. **(I)** Expression of FN protein expression by western blot. Data are expressed as mean ± SD. $^{**}p < 0.01$, compared with the normal control group; $^{\#}p < 0.05$, $^{\#\#}p < 0.01$, compared with the Model group or HG group; $^{\$}p < 0.05$, $^{\$\$}p < 0.01$, compared with the icariin group.

higher, while SOD activity were significantly lower in model group. In contrast, the level of MDA and superoxide anion were markedly lowered, whereas the activity of SOD increased dose-dependently in icariin groups.

The level of ROS in HMC-induced by high glucose, as determined by DHE staining, was markedly increased. The content of superoxide anion (**Figure 6D**) was dose-dependently attenuated by icariin (1, 3, 10 μM) detected by flow cytometry. During the progression of DN, the antioxidant scavenging system does not work, accompanying by decreased activity and expression of antioxidase, including catalase (CAT), heme oxygenase (HO-1), NADPH: quinone acceptor oxidoreductase 1 (NQO1), superoxide dismutase (SOD) and glutathione peroxidase (GPx). As illustrated in **Figure 6E**, the stimulation with high glucose significantly decreased the activity of the scavenging system against reactive species in HMC, while icariin promoted the activity of antioxidant enzymes. Moreover, Q-PCR and western blot assays indicated that icariin (1, 3, 10 μM) significantly increased the mRNA and protein expressions of HO-1, NQO1, SOD and Trx1 (**Figure 6F**) in HMC.

Icariin-Induced Nrf2 Activation to Inhibit the Oxidative Stress and ECM Generation in DN Rats and Glomerular Mesangial Cells Induced by High Glucose

To illuminate the mechanism of icariin on anti-oxidative stress with its effect on the expression and activation of Nrf2, a key regulator of antioxidative stress system was firstly investigated. As shown in the **Figures 7A–C**, icariin increased the Nrf2 protein level *in vivo* and *in vitro*. Subsequently, we investigated whether icariin played a role in the regulation of Nrf2, and the protein levels of Nrf2 in the nucleus and cytoplasm were detected by western blot assay. The results showed that icariin exerted promotion effects on Nrf2 nuclear translocation compared with the HG group and also in icariin treatment groups of diabetic rats (**Figure 7D**). To further confirm that icariin promoted HG-induced distribution of Nrf2 in HMC, immunofluorescence staining was performed by laser scanning confocal microscopy to investigate the distribution of Nrf2 (**Figure 7E**). The images indicated that icariin could significantly increase Nrf2 staining (green) in the nucleus, suggesting that icariin promote the nuclear translocation of Nrf2, and the results were consistent

with the western blot. In addition, the DNA binding activity and the transcriptional activity of Nrf2 were detected by EMSA and luciferase reporter gene assay, respectively. As shown in **Figures 7F,G**, HG stimulation had no effect on the binding activity and luciferase activity of Nrf2 in HMC, while icariin significantly increased the DNA-binding activity of Nrf2 and Nrf2 luciferase activity. The massive deposition of fibronectin (FN) plays an important role in the diabetic glomerular pathology, therefore, inhibition of ECM accumulation in kidneys would repress the glomerulopathy and delay the progression of DN. **Figure 7H** illustrated that Nrf2 siRNA and ML385 (Nrf2 Inhibitor) also abolished the inhibitory effect of icariin on ECM deposition. Therefore, icariin might alleviate the oxidative stress and ECM generation in HG-induced HMC by activating the Nrf2 signaling pathway.

Icariin Inhibited HG-Induced Degradation of Nrf2 by Promoting p62-Dependent Keap1 Degradation

Under normal conditions, the degradation of Keap1 mainly through the proteasomal degradation and autophagy-lysosome pathway (Tkachev et al., 2011). In this process, p62 compete with the Keap1-binding site on Nrf2, subsequently the Keap1-p62 complex is recruited to the autophagosome by LC3, and degraded by autophagy (Fan et al., 2010; Taguchi et al., 2012). To explore the mechanisms by which icariin stimulates Nrf2 activation under high glucose conditions, the protein level of Keap1 was detected by western blot assay (**Figures 8A,B**). The result showed that Keap1 was significantly increased in model group and HG group as well as it significantly decreased in icariin treatment group. To further confirm that Keap1 is degraded through p62-dependent pathway, the level of co-immunoprecipitated p62 significantly increased after treat with icariin in HMC (**Figure 8C**), suggesting that p62 was involved in the enhancement effect of icariin on Nrf2 level in HMC under high glucose conditions. In addition, the protein levels of total and phosphorylated PI3K, Akt, and mTOR1 (**Figures 8D,E**) were examined by western blot assay. Icariin treatment decreased the phosphorylation levels of PI3K, Akt, and mTOR in diabetic rats, these findings revealed that PI3K/Akt/mTOR signal pathway mediated autophagy inhibition is activated by icariin.

Icariin Reduced the Levels of Superoxide Anion and ECM via the GPER Mediated p62-Dependent Keap1 Degradation and Nrf2 Activation

We have previously demonstrated that icariin attenuated high glucose-induced TGF-β production through G protein-coupled estrogen receptor 1 (GPER) (Li et al., 2013). Here, we additionally demonstrated significant increases in ROS accumulation as indices of oxidative stress during the progression of DN, and explored associated mechanisms. To confirm the key role of GPER played in icariin mediated protection of DN, the level of ROS (**Figure 9A**) was detected by flow cytometry. The results showed that icariin markedly reduced the superoxide anion in HMC, while G15 (a selective antagonist of GPER) prevented icariin decreasing ROS. Then, the protein levels of Nrf2 in the nucleus and cytoplasm (**Figures 9B,C**), the interaction between Nrf2 and Keap1 (**Figure 9D**), the antioxidant enzymes (**Figure 9E**), Keap1 (**Figure 9F**), PI3K/Akt pathway (**Figure 9G**), the interaction between p62 and Keap1 (**Figure 9H**), and FN

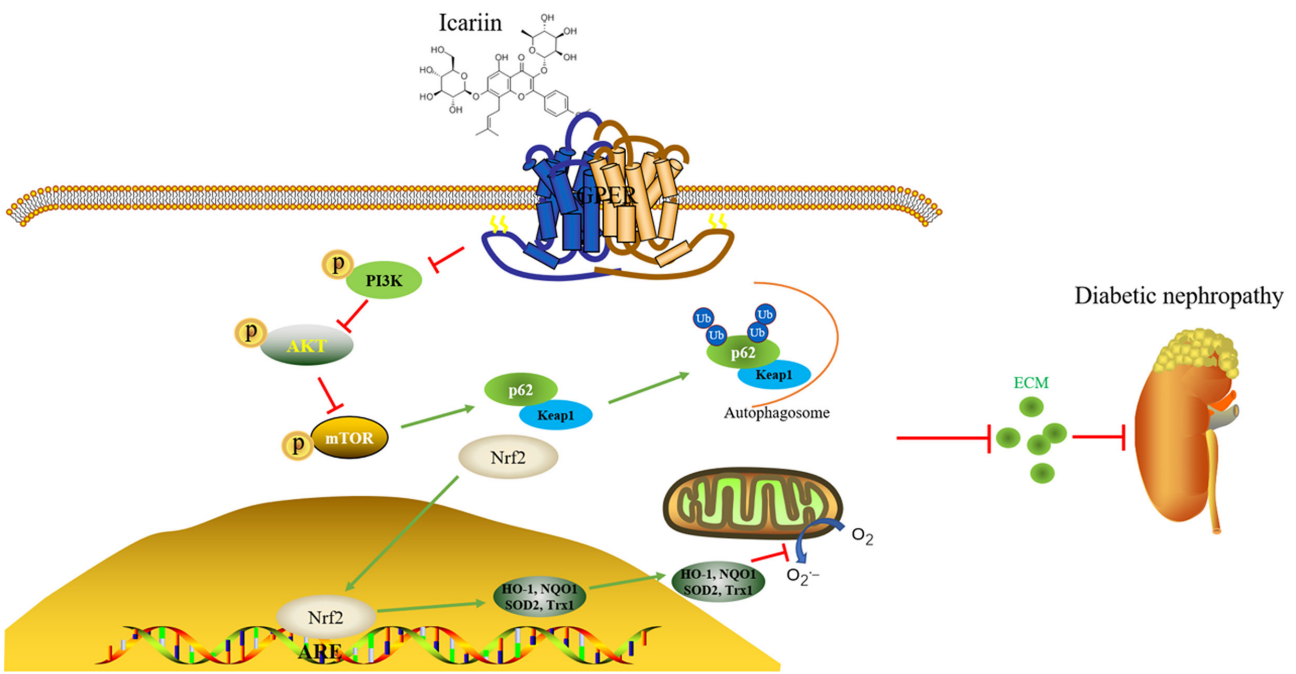

FIGURE 10 | Mechanisms for the anti-diabetic kidney disease (CKD) effect of icariin.

(**Figure 9I**) were detected. siGPER and G15 significantly reduced the inhibitory effects of icariin on Keap1, PI3K/Akt pathway, p62 and FN expression. In addition, icariin also significantly up-regulated the Nrf2 and the antioxidant enzymes protein level, increased the dissociation of Nrf2 and Keap1, association of Nrf2 and p62 in HMC, while these effects could be abolished by siGPER and G15. The main mechanisms about anti-CKD effect of icariin has been showed in (**Figure 10**).

DISCUSSION

Diabetic kidney disease (DKD) is a major cause of mortality worldwide in diabetic, and decreased kidney function can be formed by many different reasons including hypertensive nephrosclerosis and acute kidney failure (Groop et al., 2009; Gregg et al., 2014). Diabetic nephropathy (DN) is a diagnosis that indicates functional changes and specific pathologic structural in the kidneys of type 1 or type 2 DM patients. These changes would lead to clinical manifestations which characterized by proteinuria, hypertension, and gradual decline in kidney function (Umanath and Lewis, 2018). Multiple mechanisms have been proposed to mediate adverse hyperglycemic effects, including the increased production of sorbitol, methylglyoxal, diacylglycerol, reactive oxygen species, and advanced glycation end products (Lee et al., 1989; Giacco et al., 2014). However, the precise pathogenesis of DN remains unclear.

Previous studies suggested that icariin could be beneficial to the prevention of DN due to its ability to reduce serum creatinine (Cr), blood urea nitrogen (BUN), TGF-β1 protein expression in STZ-induced diabetic rats (Qi et al., 2011), and block TGF-β1-Smads pathway of mesangial cells induced by high glucose, which is beneficial to the prevention of DN (Li et al., 2013). Unlike previous studies, our present work mainly explore the therapeutic effect of icariin on DN and its underlying mechanism through focusing on oxidative stress. In this study, a rat model of diabetes was induced by STZ, a method which has been widely used to create diabetes models in rodents with pathological features similar to human diabetes (Tesch and Allen, 2007). One week after STZ injection, blood glucose was assessed with the result that about 94 % of female rats and 85% of male rats developed diabetes. It has been reported that the evaluation of drugs' effects on diabetic nephropathy should not be examined until 3 weeks after STZ injection when the kidney gets out of the acute mild nephrotoxic (Kraynak et al., 1995). Therefore, the diabetic nephropathy model, as exhibited by weight loss, food intake, water intake, blood glucose, 24 h urine volume, 24 h proteinuria, blood urea nitrogen (BUN), serum creatinine (Src), urine creatinine (Ucr), and blood pressure in **Figure 2**, had been evaluated at 4 weeks after intraperitoneal injection of STZ. The result showed that about 92 % of female rats and 82% of male rats developed diabetes nephropathy. Compared with normal rats, diabetic rats showed a significant increase in food and water intake, blood glucose, 24 h urine volume, 24 h proteinuria, blood urea nitrogen (BUN), serum creatinine (Src) and blood pressure with the reduction of urine creatinine (Ucr) and weight.

After the evaluation, the healthy rats and successfully-established DN rats were divided into six groups. Body weight, food intake, water intake and blood glucose were recorded and the effects of icariin on renal function, as exhibited by 24 h urine volume, 24 h proteinuria, urine creatinine (Ucr), were measured every 3 weeks during the 9-weeks experimental period. Results showed that icariin (40, 80 mg/kg) could decrease the 24 h urine volume and 24 h proteinuria with urine creatinine (Ucr) increased right from the first detection after 3-weeks administration (date not shown). Then, we demonstrated that icariin reduced DN progression in a dose-dependent manner, as exhibited by reducing weight loss, water intake, food intake and blood pressure during the process of 9-weeks administration. Diabetic rats presented with severe renal dysfunction manifested as increased urine volume in 24 h, proteinuria in 24 h, blood urea nitrogen (BUN), serum creatinine (Src), urinary albumin excretion in 24 h and the ratio of kidney weight to body weight, as well as urinary creatinine and creatinine clearance decreased. These values were decreased in a dose-dependent manner in all treatment groups, whereas the urinary creatinine and creatinine clearance rate were markedly increased only in icariin (40, 80 mg/kg) treatment groups. In addition, icariin treatment markedly attenuated glomerular hypertrophy, mesangial matrix expansion and the renal damage, as well as collagen deposition in the glomeruli of diabetic rats decreased. These results reported the therapeutic effects of icariin on DN rats by attenuating glomerular hyperfiltration, kidney structure deterioration and decreasing collagen deposition. Furthermore, we found that the treatment of icariin and irbesartan had no effect on STZ-induced hyperglycemia in type 1 diabetic rats, suggesting that the renal protective effects of icariin and irbesartan were probably independent of blood glucose control, providing support for glycemic control and lent support to previous studies (Cheng et al., 2001; Shao et al., 2008).

Typical pathological features of DN are glomerular hypertrophy and mesangial matrix expansion. We found that ECM was significantly increased in model group as compared with rats in normal group. There are complicated mechanisms in the increased ECM of the glomeruli, including hemodynamic change, lipid and glucose metabolisms abnormalities, multiple cytokines and inflammatory factors along with oxidative stress (Kanwar et al., 2011; Jha et al., 2017). Oxidative stress is a crucial pathogenic factor of vascular complications in metabolic disease including diabetic nephropathy, which leads to the development and progression of kidney injury (Forbes et al., 2008; Sharma, 2016). Mesangial cells generated a mass of ROS induced by high glucose, which might promote the ECM deposition by promoting the production of plasminogen activator inhibitor (Zheng et al., 2011), activating TGF-β1-Smad signaling pathway (Chen et al., 2019) and the protein kinase C pathway (Ji et al., 2016). In the present study, icariin inhibited the expression of FN, the main component of ECM, in HMC induced by high glucose. The levels of ROS are regulated by the balance of endogenous antioxidants and anti-oxidases, which indirectly reflect the ability to eliminate ROS (Cao et al., 2016). MDA, an end-product of lipid peroxidation, directly reflect the extent of lipid peroxidation (Huang et al., 2013). At the same time, icariin

treatment restored SOD activities, decreased MDA and ROS levels compared with model group. In addition, icariin increased the activities and promoted the protein levels of antioxidant enzymes, thus inhibiting the oxidative stress and reducing the intracellular levels of ROS in cells. These results indicated that icariin could alleviate oxidative stress in diabetic rats and mesangial cells induced by high glucose.

Nrf2, as a redox-sensitive transcription factor, is a key transcription factor that regulates the expression of various antioxidant enzymes to maintain cellular redox homeostasis and prevent oxidative stress (Saito, 2013; Suzuki and Yamamoto, 2017). In the rest time, Nrf2 is anchored in the cytoplasm. In the presence of external stimuli, Nrf2 accumulates and transports to the nucleus, and then interacts with antioxidant-response element (ARE) to initiate the response (Kaspar et al., 2009). Sulforaphane, a Nrf2 activator, could reduce renal damage and protect renal function in diabetic mice, suggesting that Nrf2 might be a promising therapeutic target for DN (Zheng et al., 2011). In addition, there is evidence that Nrf2 knockout mice or silencing of Nrf2 in renal cells might increase the accumulation of ECM deposition in diabetes (de Haan, 2011). In this study, icariin and irbesartan were found to promote the total protein levels and nuclear translocation of Nrf2, thus promoting the protein expression of HMC antioxidant enzymes under high glucose treatment. Herein, the studies showed that nuclear translocation, DNA binding activity and transcriptional activity of Nrf2 decreased and FN protein level increased in HG-induced HMC. Moreover, further studies confirmed that icariin upregulated of nuclear Nrf2 DNA binding activity and Nrf2 transcription activity in HG-induced HMC. In combination with siNrf2 and ML385, icariin mediated reduction of FN was almost abolished, which meant that icariin needed to active Nrf2 to inhibit the oxidative stress and ECM production of DN rats and mesangial cells induced by high glucose.

In response to oxidative stress, electrophilic damage targets the Nrf2-Keap1 complex, separates Nrf2 from Keap1, enable Nrf2 to translocate into the nucleus to transactivate target genes and facilitates the degradation of Keap1 (Suzuki and Yamamoto, 2017). The degradation of Keap1 is mainly goes through ubiquitin-proteasome and autophagy-lysosome pathway (Tkachev et al., 2011). P62, the selective autophagy substrate and the protein levels are generally considered to be inversely proportional to autophagy activity, keeps a binding site for Keap 1 and promotes autophagic degradation of Keap1, releasing Nrf2, and transporting Nrf2 into the nucleus to transcript antioxidant genes to prevent oxidative stress (Komatsu et al., 2010). Indeed, our study provided direct evidence to demonstratd that icariin would reduce the protein level of keap1 and p62 but increased the correlation level between p62 and Keap1 and subsequent degradation level of Keap1, indicating that icariin was found significantly, but not completely, to prevent the diabetes-induced up regulation of Keap1. Impaired autophagy activity contributes to the pathogenesis of DN, and the recovery of autophagy activity may be a promising therapeutic target for DN. Currently, the latest studies have confirmed that the inhibition of PI3K/Akt/mTOR signaling pathway restored autophagy and ameliorate DN (Tu et al., 2019; Wang et al., 2019). Result showed that the phosphorylation levels of PI3K, Akt, and mTOR in diabetic rats and mesangial cells induced by high glucose were obviously decreased by icariin treatment.

GPER has been shown to play a part in the rapid non-genomic signaling events of E2 widely observed in cells and tissues (Revankar et al., 2005). Using isolated perfused hearts subjected to ischemia/reperfusion, pretreatment with the GPER agonist, G1, confers cardioprotective effects via PI3K pathways (Bopassa et al., 2010). In order to confirm the crucial role of GPER in the *in vivo* and *in vitro* protection of DN-mediated by icariin, combined use with G15 demonstrated the involvement of GPER in the inhibition of icariin on ROS generation. These findings suggested that GPER might involve in the regulation of icariin on intracellular homeostasis. Further studies demonstrated that siGPER or G15 could eliminate the promotion of icariin on the antioxidant enzymes protein level and the dissociation of Nrf2 and Keap1, indicating that icariin inhibited the degradation of Nrf2 depend on GPER in HMC. Moreover, the combined use of siGPER and G15 nearly eliminated the attenuation of icariin on the association of Keap 1 with p62 and ECM generation in HMC, illustrating that Nrf2 pathway GPER was also important in the icariin inhibition of the oxidative stress and the ECM generation in high glucose-stimulated HMC.

CONCLUSION

Overall, icariin, a potential activator of GPER, reduced the levels of ROS and ECM generation in the kidney of diabetic rats, and ameliorated the symptoms of DN through, at least partially, GPER mediated p62-dependent Keap1 degradation and Nrf2 activation.

DATA AVAILABILITY STATEMENT

The datasets generated for this study are available on request to the corresponding author.

ETHICS STATEMENT

The animal study was reviewed and approved by the Animal Ethics Committee of China Pharmaceutical University.

AUTHOR CONTRIBUTIONS

XD and KW designed the study. KW, XZ, ZP, WY, and XW performed experiments. XD and KW contributed significantly to analysis and manuscript preparation. KW, XZ, and XG wrote the manuscript. All authors contributed to the article and approved the submitted version.

FUNDING

This work was supported by research grants from the National New Drug Innovation Program of China

(No. 2017ZX09301004), the National Natural Science Foundation of China (Grant No. 81873131), and Postgraduate Innovative Project of Jiangsu Province (KYCX19_0688).

ACKNOWLEDGMENTS

We would like show sincere appreciation to our colleagues for their valuable efforts and comments on this paper.

REFERENCES

Bopassa, J. C., Eghbali, M., Toro, L., and Stefani, E. (2010). A novel estrogen receptor GPER inhibits mitochondria permeability transition pore opening and protects the heart against ischemia-reperfusion injury. *Am. J. Physiol. Heart Circ. Physiol.* 298, H16–H23. doi: 10.1152/ajpheart.00588.2009

Cao, A., Wang, L., Chen, X., Guo, H., Chu, S., Zhang, X., et al. (2016). Ursodeoxycholic acid ameliorated diabetic nephropathy by attenuating hyperglycemia-mediated oxidative stress. *Biol. Pharm. Bull.* 39, 1300–1308. doi: 10.1248/bpb.b16-00094

Chen, R. R., Fan, X. H., Chen, G., Zeng, G. W., Xue, Y. G., Liu, X. T., et al. (2019). Irisin attenuates angiotensin II-induced cardiac fibrosis via Nrf2 mediated inhibition of ROS/ TGFbeta1/Smad2/3 signaling axis. *Chem. Biol. Interact.* 302, 11–21. doi: 10.1016/j.cbi.2019.01.031

Cheng, Z. J., Vaskonen, T., Tikkanen, I., Nurminen, K., Ruskoaho, H., Vapaatalo, H., et al. (2001). Endothelial dysfunction and salt-sensitive hypertension in spontaneously diabetic Goto-Kakizaki rats. *Hypertension* 37, 433–439. doi: 10.1161/01.HYP.37.2.433

de Haan, J. B. (2011). Nrf2 activators as attractive therapeutics for diabetic nephropathy. *Diabetes* 60, 2683–2684. doi: 10.2337/db11-1072

Fan, W., Tang, Z., Chen, D., Moughon, D., Ding, X., Chen, S., et al. (2010). Keap1 facilitates p62-mediated ubiquitin aggregate clearance via autophagy. *Autophagy* 6, 614–621. doi: 10.4161/auto.6.5.12189

Forbes, J. M., Coughlan, M. T., and Cooper, M. E. (2008). Oxidative stress as a major culprit in kidney disease in diabetes. *Diabetes* 57, 1446–1454. doi: 10.2337/db08-0057

Giacco, F., Du, X., D'Agati, V. D., Milne, R., Sui, G., Geoffrion, M., et al. (2014). Knockdown of glyoxalase 1 mimics diabetic nephropathy in nondiabetic mice. *Diabetes* 63, 291–299. doi: 10.2337/db13-0316

Gregg, E. W., Li, Y., Wang, J., Burrows, N. R., Ali, M. K., Rolka, D., et al. (2014). Changes in diabetes-related complications in the United States, 1990-2010. *N. Engl. J. Med.* 370, 1514–1523. doi: 10.1056/NEJMoa1310799

Groop, P. H., Thomas, M. C., Moran, J. L., Waden, J., Thorn, L. M., Makinen, V. P., et al. (2009). The presence and severity of chronic kidney disease predicts all-cause mortality in type 1 diabetes. *Diabetes* 58, 1651–1658. doi: 10.2337/db08-1543

Huang, K., Huang, J., Xie, X., Wang, S., Chen, C., Shen, X., et al. (2013). Sirt1 resists advanced glycation end products-induced expressions of fibronectin and TGF-beta1 by activating the Nrf2/ARE pathway in glomerular mesangial cells. *Free Radic. Biol. Med.* 65, 528–540. doi: 10.1016/j.freeradbiomed.2013.07.029

Jha, J. C., Banal, C., Chow, B. S., Cooper, M. E., and Jandeleit-Dahm, K. (2016). Diabetes and kidney disease: role of oxidative stress. *Antioxid. Redox Signal.* 25, 657–684. doi: 10.1089/ars.2016.6664

Jha, J. C., Banal, C., Okabe, J., Gray, S. P., Hettige, T., Chow, B., et al. (2017). NADPH oxidase Nox5 accelerates renal injury in diabetic nephropathy. *Diabetes* 66, 2691–2703. doi: 10.2337/db16-1585

Ji, X., Li, C., Ou, Y., Li, N., Yuan, K., Yang, G., et al. (2016). Andrographolide ameliorates diabetic nephropathy by attenuating hyperglycemia-mediated renal oxidative stress and inflammation via Akt/NF-kappaB pathway. *Mol. Cell. Endocrinol.* 437, 268–279. doi: 10.1016/j.mce.2016.06.029

Kanwar, Y. S., Sun, L., Xie, P., Liu, F. Y., and Chen, S. (2011). A glimpse of various pathogenetic mechanisms of diabetic nephropathy. *Annu. Rev. Pathol.* 6, 395–423. doi: 10.1146/annurev.pathol.4.110807.092150

Kaspar, J. W., Niture, S. K., and Jaiswal, A. K. (2009). Nrf2:INrf2 (Keap1) signaling in oxidative stress. *Free Radic. Biol. Med.* 47, 1304–1309. doi: 10.1016/j.freeradbiomed.2009.07.035

Komatsu, M., Kurokawa, H., Waguri, S., Taguchi, K., Kobayashi, A., Ichimura, Y., et al. (2010). The selective autophagy substrate p62 activates the stress responsive transcription factor Nrf2 through inactivation of Keap1. *Nat. Cell Biol.* 12, 213–223. doi: 10.1038/ncb2021

Kraynak, A. R., Storer, R. D., Jensen, R. D., Kloss, M. W., Soper, K. A., Clair, J. H., et al. (1995). Extent and persistence of streptozotocin-induced DNA damage and cell proliferation in rat kidney as determined by in vivo alkaline elution and BrdUrd labeling assays. *Toxicol. Appl. Pharmacol.* 135, 279–286. doi: 10.1006/taap.1995.1234

Lee, T. S., Saltsman, K. A., Ohashi, H., and King, G. L. (1989). Activation of protein kinase C by elevation of glucose concentration: proposal for a mechanism in the development of diabetic vascular complications. *Proc. Natl. Acad. Sci. U.S.A.* 86, 5141–5145. doi: 10.1073/pnas.86.13.5141

Li, Y. C., Ding, X. S., Li, H. M., and Zhang, C. (2013). Icariin attenuates high glucose-induced type IV collagen and fibronectin accumulation in glomerular mesangial cells by inhibiting transforming growth factor-beta production and signalling through G protein-coupled oestrogen receptor 1. *Clin. Exp. Pharmacol. Physiol.* 40, 635–643. doi: 10.1111/1440-1681.12143

Loboda, A., Damulewicz, M., Pyza, E., Jozkowicz, A., and Dulak, J. (2016). Role of Nrf2/HO-1 system in development, oxidative stress response and diseases: an evolutionarily conserved mechanism. *Cell. Mol. Life Sci.*73, 3221–3247. doi: 10.1007/s00018-016-2223-0

Loeffler, I., Hopfer, U., Koczan, D., and Wolf, G. (2011). Type VIII collagen modulates TGF-beta1-induced proliferation of mesangial cells. *J. Am. Soc. Nephrol.* 22, 649–663. doi: 10.1681/ASN.2010010098

Mason, R. M., and Wahab, N. A. (2003). Extracellular matrix metabolism in diabetic nephropathy. *J. Am. Soc. Nephrol.* 14, 1358–1373. doi: 10.1097/01.ASN.0000065640.77499.D7

Munoz, M., Lopez-Oliva, M. E., Rodriguez, C., Martinez, M. P., Saenz-Medina, J., Sanchez, A., et al. (2020). Differential contribution of Nox1, Nox2 and Nox4 to kidney vascular oxidative stress and endothelial dysfunction in obesity. *Redox Biol.* 28:101330. doi: 10.1016/j.redox.2019.101330

Ortiz-Munoz, G., Lopez-Parra, V., Lopez-Franco, O., Fernandez-Vizarra, P., Mallavia, B., Flores, C., et al. (2010). Suppressors of cytokine signaling abrogate diabetic nephropathy. *J. Am. Soc. Nephrol.* 21, 763–772. doi: 10.1681/ASN.2009060625

Parving, H. H., Hommel, E., Mathiesen, E., Skott, P., Edsberg, B., Bahnsen, M., et al. (1988). Prevalence of microalbuminuria, arterial hypertension, retinopathy and neuropathy in patients with insulin dependent diabetes. *Br. Med. J. (Clin. Res. Ed).* 296, 156–160. doi: 10.1136/bmj.296.6616.156

Qi, M. Y., Kai-Chen, L.iu, H. R., Su, Y. H., and Yu, S.Q. (2011). Protective effect of Icariin on the early stage of experimental diabetic nephropathy induced by streptozotocin via modulating transforming growth factor beta1 and type IV collagen expression in rats. *J. Ethnopharmacol.* 138, 731–736. doi: 10.1016/j.jep.2011.10.015

Revankar, C. M., Cimino, D. F., Sklar, L. A., Arterburn, J. B., and Prossnitz, E. R. (2005). A transmembrane intracellular estrogen receptor mediates rapid cell signaling. *Science* 307, 1625–1630. doi: 10.1126/science.1106943

Rueda, B., Oliver, J., Robledo, G., Lopez-Nevot, M. A., Balsa, A., Pascual-Salcedo, D., et al. (2007). HO-1 promoter polymorphism associated with rheumatoid arthritis. *Arthritis Rheum.* 56, 3953–3958. doi: 10.1002/art.23048

Saito, H. (2013). Toxico-pharmacological perspective of the Nrf2-Keap1 defense system against oxidative stress in kidney diseases. *Biochem. Pharmacol.* 85, 865–872. doi: 10.1016/j.bcp.2013.01.006

Shao, Y., He, M., Zhou, L., Yao, T., Huang, Y., and Lu, L. M. (2008). Chronic angiotensin (1-7) injection accelerates STZ-induced diabetic renal injury. *Acta Pharmacol. Sin.* 29, 829–837. doi: 10.1111/j.1745-7254.2008.00812.x

Sharma, K. (2016). Obesity and diabetic kidney disease: role of oxidant stress and redox balance. *Antioxid. Redox Signal.* 25, 208–216. doi: 10.1089/ars.2016.6696

Suzuki, T., and Yamamoto, M. (2017). Stress-sensing mechanisms and the physiological roles of the Keap1-Nrf2 system during cellular stress. *J. Biol. Chem.* 292, 16817–16824. doi: 10.1074/jbc.R117.800169

Taguchi, K., Fujikawa, N., Komatsu, M., Ishii, T., Unno, M., Akaike, T., et al. (2012). Keap1 degradation by autophagy for the maintenance of redox homeostasis. *Proc. Natl. Acad. Sci. U. S. A.* 109, 13561–13566. doi: 10.1073/pnas.1121572109

Tesch, G. H., and Allen, T. J. (2007). Rodent models of streptozotocin-induced diabetic nephropathy. *Nephrology (Carlton).* 12, 261–266. doi: 10.1111/j.1440-1797.2007.00796.x

Tkachev, V. O., Menshchikova, E. B., and Zenkov, N. K. (2011). Mechanism of the Nrf2/Keap1/ARE signaling system. *Biochem. Mosc.* 76, 407–422. doi: 10.1134/S0006297911040031

Tu, Q., Li, Y., Jin, J., Jiang, X., Ren, Y., and He, Q. (2019). Curcumin alleviates diabetic nephropathy via inhibiting podocyte mesenchymal transdifferentiation and inducing autophagy in rats and MPC5 cells. *Pharm. Biol.* 57, 778–786. doi: 10.1080/13880209.2019.1688843

Umanath, K., and Lewis, J. B. (2018). Update on diabetic nephropathy: core curriculum 2018. *Am. J. Kidney Dis.* 71, 884–895. doi: 10.1053/j.ajkd.2017.10.026

Wang, X., Gao, Y., Gao, J., Li, M., Zhou, M., Wang, J., et al. (2019). Rheb1 loss leads to increased hematopoietic stem cell proliferation and myeloid-biased differentiation *in vivo*. *Haematologica* 104, 245–255. doi: 10.3324/haematol.2018.194811

Wolf, G., and Ziyadeh, F. N. (1999). Molecular mechanisms of diabetic renal hypertrophy. *Kidney Int.* 56, 393–405. doi: 10.1046/j.1523-1755.1999.00590.x

Yao, X., Jing, X., Guo, J., Sun, K., Deng, Y., Zhang, Y., et al. (2019). Icariin protects bone marrow mesenchymal stem cells against iron overload induced dysfunction through mitochondrial fusion and fission, PI3K/AKT/mTOR and MAPK pathways. *Front. Pharmacol.* 10:163. doi: 10.3389/fphar.2019.00163

Zheng, H., Whitman, S. A., Wu, W., Wondrak, G. T., Wong, P. K., Fang, D., et al. (2011). Therapeutic potential of Nrf2 activators in streptozotocin-induced diabetic nephropathy. *Diabetes* 60, 3055–3066. doi: 10.2337/db11-0807

Zheng, S., Noonan, W. T., Metreveli, N. S., Coventry, S., Kralik, P. M., Carlson, E. C., et al. (2004). Development of late-stage diabetic nephropathy in OVE26 diabetic mice. *Diabetes* 53, 3248–3257. doi: 10.2337/diabetes.53.12.3248

Conflict of Interest: The authors declare that the research was conducted in the absence of any commercial or financial relationships that could be construed as a potential conflict of interest.

Copyright © 2020 Wang, Zheng, Pan, Yao, Gao, Wang and Ding. This is an open-access article distributed under the terms of the Creative Commons Attribution License (CC BY). The use, distribution or reproduction in other forums is permitted, provided the original author(s) and the copyright owner(s) are credited and that the original publication in this journal is cited, in accordance with accepted academic practice. No use, distribution or reproduction is permitted which does not comply with these terms.

frontiers in Cell and Developmental Biology

REVIEW
published: 29 July 2020
doi: 10.3389/fcell.2020.00519

Insulin: Trigger and Target of Renal Functions

*Ana F. Pina[1,2,3], Diego O. Borges[1,4], Maria João Meneses[1,2], Patrícia Branco[5,6], Rita Birne[5,6], Antonio Vilasi[7] and Maria Paula Macedo[1,3,6]**

[1] Centro de Estudos de Doenças Crónicas, NOVA Medical School/Faculdade de Ciências Médicas, Universidade Nova de Lisboa, Lisbon, Portugal, [2] ProRegeM Ph.D. Programme, NOVA Medical School/Faculdade de Ciências Médicas, Universidade Nova de Lisboa, Lisbon, Portugal, [3] Department of Medical Sciences, University of Aveiro, Aveiro, Portugal, [4] Molecular Biosciences Ph.D. Programme, Instituto de Tecnologia Química e Biológica António Xavier, Universidade Nova de Lisboa, Oeiras, Portugal, [5] Department of Nephrology, Centro Hospitalar Lisboa Ocidental, Lisbon, Portugal, [6] Portuguese Diabetes Association – Education and Research Center (APDP-ERC), Lisbon, Portugal, [7] Institute of Clinical Physiology – National Research Council, Reggio Calabria Unit, Reggio Calabria, Italy

Kidney function in metabolism is often underestimated. Although the word "clearance" is associated to "degradation", at nephron level, proper balance between what is truly degraded and what is redirected to *de novo* utilization is crucial for the maintenance of electrolytic and acid–basic balance and energy conservation. Insulin is probably one of the best examples of how diverse and heterogeneous kidney response can be. Kidney has a primary role in the degradation of insulin released in the bloodstream, but it is also incredibly susceptible to insulin action throughout the nephron. Fluctuations in insulin levels during fast and fed state add another layer of complexity in the understanding of kidney fine-tuning. This review aims at revisiting renal insulin actions and clearance and to address the association of kidney dysmetabolism with hyperinsulinemia and insulin resistance, both highly prevalent phenomena in modern society.

Keywords: diabetic nephropathy, insulin, insulin resistance, insulin clearance, albuminuria

OPEN ACCESS

Edited by:
Samar Abd ElHafeez, Alexandria University, Egypt

Reviewed by:
Sonia Michael Najjar, Ohio University, United States
Karem Salem, Fayoum University, Egypt

***Correspondence:**
Maria Paula Macedo
paula.macedo@nms.unl.pt

Specialty section:
This article was submitted to Molecular Medicine, a section of the journal Frontiers in Cell and Developmental Biology

Received: *18 March 2020*
Accepted: *02 June 2020*
Published: *29 July 2020*

Citation:
Pina AF, Borges DO, Meneses MJ, Branco P, Birne R, Vilasi A and Macedo MP (2020) Insulin: Trigger and Target of Renal Functions. Front. Cell Dev. Biol. 8:519. doi: 10.3389/fcell.2020.00519

INTRODUCTION

Insulin is a vital hormone with several functions among which its central role in energy and glucose homeostasis is fundamental (Plum, 2006). Beyond the traditional crosstalk between the most recognized insulin-responsive organs (liver, adipose tissue, and skeletal muscle), kidney insulin action and resistance have recently been suggested as critical components of metabolic and

Abbreviations: ADP, adenosine diphosphate; ATP, adenosine triphosphate; CEACAM-1, carcinoembryonic antigen-related cell adhesion molecule 1; cGMP, cyclic guanosine monophosphate; CKD, chronic kidney disease; CV, cardiovascular; DKD, diabetic kidney disease; DNL, *de novo* lipogenesis; eGFR, estimated glomerular filtration rate; ENaC, epithelial sodium channel; ER, endoplasmic reticulum; FFA, free fatty acid; FoxO1, forkhead box O1; GBM, glomerular basement membrane; GIT, glutathione-insulin transhydrogenase; GLUT1, glucose transporter 1; GLUT2, glucose transporter 2; GLUT4, glucose transporter 4; GRB2, growth factor receptor-bound protein 2; GSK3, glycogen synthase kinase 3; GSV, GLUT storage vesicle; IDE, insulin-degrading enzyme; INSR, insulin receptor; IR, insulin resistance; IRS1, insulin receptor substrate 1; IRS2, insulin receptor substrate 2; MAPK, mitogen activated protein kinase; mTOR, mammalian target of rapamycin; NAFLD, non-alcoholic fatty liver disease; NBCe1, sodium bicarbonate cotransporter 1; NHE-3, sodium/hydrogen exchanger 3; NKCC2, sodium-potassium chloride cotransporter-2; PGC1α, peroxisome proliferator-activated receptor-γ coactivator 1α; PI3K, phosphatidylinositol 3-kinase; PIP2, phosphatidylinositol 4,5 biphosphate; PIP3, phosphatidylinositol 3,4,5 triphosphate; PKB, protein kinase B; PKG, cGMP-dependent protein kinase G; PKGI, cGMP-dependent protein kinase G isoform I; PPARγ, peroxisome proliferator-activated receptor γ; PT, proximal tubule; PTEN, phosphatase and tensin homolog; PTP1B, protein tyrosine-phosphatase 1B; SGK1, serum/glucocorticoid regulated kinase 1; SGLT, sodium-glucose transport proteins; SGLT2, sodium-glucose co-transporter 2; SGLT2i, sodium-glucose co-transporter-2 inhibitors; SHIP2, SH2-domain-containing inositol phosphatase 2; SREBP-1c, sterol regulatory element binding protein-1c; T1DM, type 1 diabetes mellitus; T2DM, type 2 diabetes mellitus; TZDs, thiazolidinediones; Vamp2, vesicle-associated membrane protein 2.

dysmetabolic states (Artunc et al., 2016). The important role of insulin in the kidney is further corroborated by the increased prevalence of chronic kidney disease in subjects with type 2 diabetes mellitus (T2DM) and non-alcoholic fatty liver disease (NAFLD; Musso et al., 2014; Kim et al., 2018; Mok et al., 2019; Kiapidou et al., 2020). Furthermore, the kidney can adjust the levels of essential players of nutrient homeostasis such as glucose and insulin (Krebs, 1963; Chamberlain and Stimmler, 1967).

First reports of insulin actions in the kidney were originated in the 1950s (Farber et al., 1951). Since then, the knowledge acquired has dramatically increased, nonetheless much remains unveiled. It is now known that insulin impacts on tubular glucose reabsorption (Nakamura et al., 2015). In fact, a whole therapeutic class based on this mechanism was recently developed. Additionally, hyperinsulinemia driven by pancreatic hypersecretion and/or impairments in hepatic insulin clearance could explain changes in glomerular filtration rates and increased renal gluconeogenesis, which in turn causes fatty liver deposition and, as a direct consequence, may lead to dysglycemia (Bril et al., 2014; Naderpoor et al., 2017; Jung et al., 2018; Bergman et al., 2019).

Kidney is, in fact, the most critical organ responsible for insulin clearance after the liver (Elgee and Williams, 1954; Narahara et al., 1958); still, its relevance in the maintenance of proper insulinemia and insulin sensitivity is underestimated. The control of insulin clearance/action exerted by the kidney is complex. Furthermore, the diversity of insulin actions is only possible thanks to the differentiation of specific kidney segments in which insulin regulates different pathways. In this review, we will briefly describe insulin production and its main actions in the liver, adipose tissue, and skeletal muscle. Moreover, we will focus on kidney and on renal insulin actions as well as insulin clearance/degradation. Overall, this work aims at highlighting the critical role of kidney-insulin interplay in the development of dysmetabolism.

OVERVIEW OF INSULIN BIOSYNTHESIS AND NON-RENAL ACTION AND METABOLISM

The insulin gene (*INS*) is represented by only one copy in the human genome, and its transcription is mainly regulated by the same enhancers of other glucose-related genes (Andrali et al., 2008; Gao et al., 2014). In pancreas β-cell, *INS* is first transcribed as preproinsulin and, after cleavage and folding in the rough endoplasmic reticulum (ER), proinsulin is formed (Hutton, 1994). The conversion into insulin occurs after the removal of the c-peptide in the Golgi apparatus, with a final maturation achieved by c-terminal amino acid elimination (Steiner, 2004). Mature insulin is composed of A and B chains linked by two disulfide bonds, with a third bond within A chain (Mayer et al., 2007). For storage, insulin is complexed in hexamers with zinc, and an actin network is involved in the organization of mature insulin granules for first and second insulin secretion phases (Kalwat and Thurmond, 2013).

Insulin secretion is triggered by cytoplasmic increments in ATP levels, derived from glucose internalization and subsequent metabolism (Prentki and Matschinsky, 1987). This increase in ATP shuts down membrane ATP-sensitive K^+ channels, depolarizing plasma membrane, and activating voltage-gated calcium channels (Detimary et al., 1998). Indeed, the resultant Ca^{2+} influx seems to be necessary for the fusion of insulin granules with the plasma membrane, ending up in its secretion (Hou et al., 2009). The first wave of insulin secretion is composed of primed granules that are in close proximity with plasma membrane (Olofsson et al., 2002). However, most of these granules remain more distant from the plasma membrane and are further boosted with newly synthesized insulin that will culminate in 75–95% of total insulin secretion in the second phase (Kou et al., 2014).

With the insulin pools ready to be released, insulin secretion does not occur in a constant manner, but in waves of 4–5 min interval (Song et al., 2000). The pulsatile secretion profile is considered primordial for proper insulin responsiveness, as constant release would result in down-regulation of insulin receptor (INSR) expression (Matveyenko et al., 2012). After binding and activation of its receptor, insulin, as an anabolic hormone, promotes increased biosynthesis of macromolecules further needed to maintain energetic balance during nutrient privation (Bedinger and Adams, 2015).

At cellular level, insulin mostly relies on the specific bind to its transmembrane receptor to perform its actions (**Figure 1**). Insulin receptor is a tyrosine kinase receptor with two extracellular α subunits and two transmembrane β subunits (Ye et al., 2017). Insulin binding to INSR produces an autophosphorylation that leads to the internalization of the complex and activation of downstream effectors. INSR substrate 1 (IRS1) and 2 (IRS2) are the main targets that intracellularly coordinate insulin action (Thirone et al., 2006; Kubota et al., 2016). In the liver, the activity of these proteins is differently controlled by insulin. Although both IRS1 and IRS2 are degraded after insulin activation, only IRS2 is transcriptionally repressed by insulin activation (Hirashima et al., 2003). Further transduction of insulin signaling occurs via phosphatidylinositol 3-kinase (PI3K)/AKT phosphorylation. AKT or Protein kinase B (PKB) are considered the main effectors of metabolic insulin actions (Taniguchi et al., 2006; Molinaro et al., 2019). On the other hand, AKT1 and 3 are the leading players of mitogenic effects of insulin by RAS/mitogen activated protein kinase (MAPK) cascade and crosstalk with growth hormones (Xu et al., 2006; Xu and Messina, 2009; Qiu et al., 2017).

Given the scope of this review, we will summarize insulin actions on non-renal target organs, but detailed information is available in recent reviews (Gancheva et al., 2018; Tokarz et al., 2018). The first organ to be reached by insulin is the liver, where 50–70% is removed at first pass (Duckworth et al., 1998). In hepatocytes, insulin signaling recruits forkhead box transcription factor 1 (FoxO1) to the cytoplasm, inhibiting the transcription of gluconeogenic enzymes (Ling et al., 2018). In such an abundance of glucose, insulin also stimulates the synthesis of glycogen by phosphorylation of glycogen synthase kinase 3 (GSK3), which leads to dephosphorylation and activation of glycogen synthase

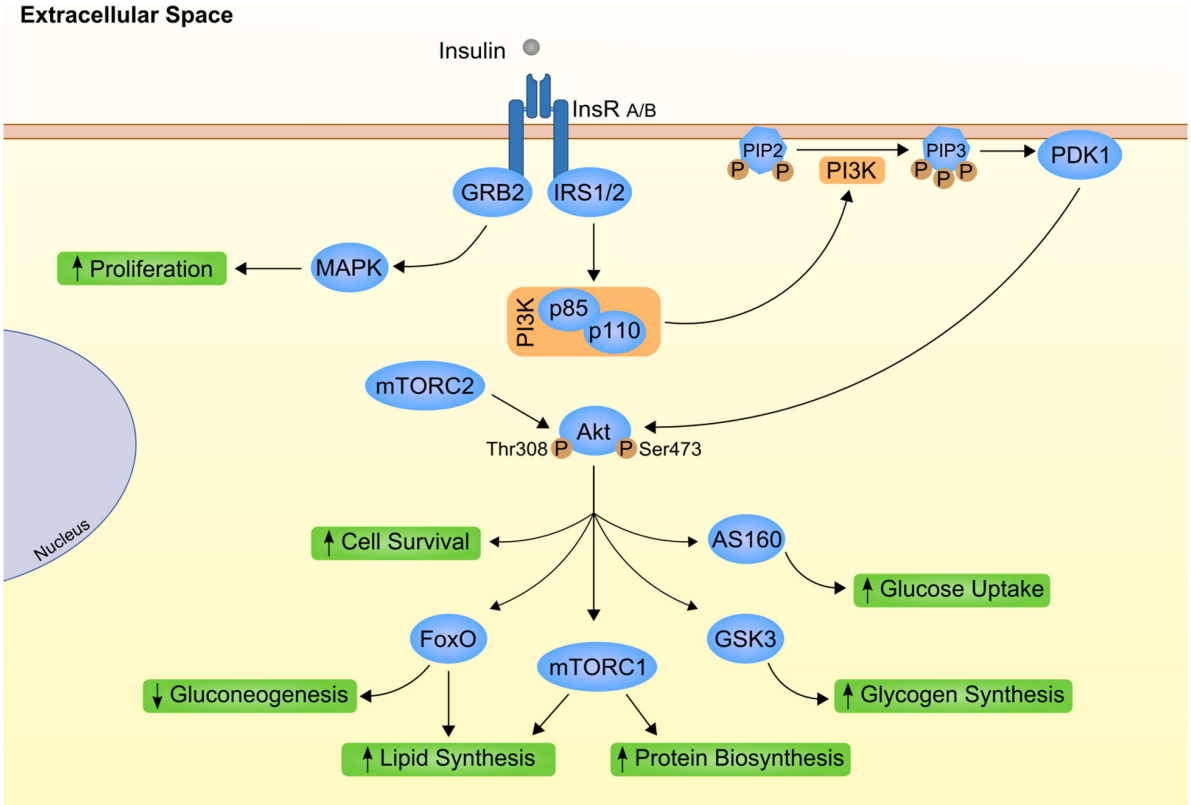

FIGURE 1 | Canonical insulin signaling cascade. Insulin (gray circle) binds to its transmembrane kinase receptor at cell membrane and triggers insulin signaling cascade. Insulin receptor present two isoforms with distinct affinity for insulin already associated to differential insulin internalization (INSR A and INSR B; Calzi et al., 1997). Binding of insulin auto-phosphorylates INSR at Tyr-960. Further recruitment and phosphorylation of insulin receptor substrate (IRS) 1 and 2 will mostly result in subsequent activation of phosphoinositide-dependent kinase 1 (PDK1) through phosphoinositide-3 kinase (PI3K; Yamada et al., 2002). PDK1 is responsible for propagation of insulin signal to one of the most important downstream effectors, Akt. Importantly, Akt has two distinct phosphorylation sites, Thr308 activated by PDK1 (Alessi et al., 1997) and Ser473 phosphorylated by mammalian target of rapamycin complex (mTORC) 2 protein (Bayascas and Alessi, 2005). Finally, fully activated Akt can interact with different proteins, eliciting different effects as stimulation of glucose uptake and glycogen synthesis by AS160 and glycogen synthase kinase 3 (GSK3), respectively (Ng et al., 2008). On the other hand, INRS activation also promote growth factor receptor-bound protein 2 (GRB2) interaction with Shc proteins and activation of mitogen activated protein kinases (MAPK; Skolnik et al., 1993; Xu et al., 2006). This as part of the insulin-mediated proliferative stimuli. PIP2, phosphatidylinositol 4,5 biphosphate; PIP3, phosphatidylinositol 3,4,5 triphosphate.

(McManus et al., 2005). After the replenishment of liver glycogen stores in the fed state, glucose starts to be degraded to pyruvate, which is the precursor of lipid biosynthesis via *de novo* lipogenesis (DNL; Sanders and Griffin, 2016). Herein, insulin signaling is also crucial for upregulation of sterol regulatory element binding protein 1c (SREPB1c), a transcription factor associated to further transcription of DNL (Oh et al., 2003; Roder et al., 2007; Krycer et al., 2010).

Only a fraction of the insulin that reaches the liver will get to the periphery, to perform its action at skeletal muscle, adipose tissue, and other insulin-sensitive organs. Skeletal muscle is the greater insulin-dependent "kidnapper" of glucose, it is responsible for ∼60 to 80% of whole-body glucose disposal (DeFronzo et al., 1976; Fernandes et al., 2011). Insulin signals to myocytes through classical signaling, promoting glucose uptake by the dynamic translocation of glucose transporter 4 (GLUT4; Zorzano et al., 1996). Glucose is here mainly used for glycolysis or stored as glycogen as already described for the liver.

During the fed state, a clear inhibitory effect in lipolysis and consequent blunt of free fatty acid (FFA) release is mediated by insulin acting on adipocytes (Dimitriadis et al., 2011). The resultant decrease in FFA availability reduces its hepatic uptake and fatty acid oxidation, changing the disposal of substrates that are mostly used for gluconeogenesis (Galgani et al., 2008). Not exclusively for liver, the effect of insulin in reducing adipose tissue FFA release is important for other organs that, at fed state, change energy source to glucose and recover glycogen stores contributing to normoglycemia (Petersen and Shulman, 2018). In this context, glucose uptake is also stimulated by insulin in the fed state at adipocytes. Furthermore, translocation of glucose transporters to the membrane of adipocytes was very well characterized in 3T3-L1 adipocytes by activation of the canonical PI3K/AKT2 pathway (Ng et al., 2008).

As mentioned above, all these organs expressing INSR are responsible for insulin clearance and local degradation. However, a significant part of insulin degradation is played in

the liver (50–70%) by its specialized machinery of internalization and degradation (Najjar and Perdomo, 2019). In the case of internalization, carcinoembryonic antigen-related cell adhesion molecule 1 (CEACAM-1) phosphorylation by insulin promotes rapidly receptor-mediated uptake (Poy et al., 2002). Carcinoembryonic antigen-related cell adhesion molecule 1 expression occurs preferentially in liver, and restoration of its function only at liver of null CEACAM-1 mice reverse the hyperinsulinemia and fatty liver deposition observed in global knockout CEACAM-1 model (Russo et al., 2017). Regarding degradation, insulin-degrading enzyme (IDE) is considered the most critical protease to cleave insulin intracellularly and is highly expressed in the liver (Kuo et al., 1993).

The amount of insulin that remains in circulation after liver first pass (30–50%) will be mostly degraded by the kidney (Elgee and Williams, 1954; Narahara et al., 1958). However, the kidney is not just an endpoint for insulin degradation, as insulin also acts throughout the entire nephron. Whereas hepatic insulin clearance is regaining attention as the very first alteration leading to hyperinsulinemia, compensatory mechanisms that could emerge from the kidney are not well known. Impairments in hepatic insulin clearance increase peripheral insulinemia, and very little is described regarding the exact effects of the increased amount of insulin that will further reach the kidney.

KIDNEY AND INSULIN ACTIONS

Kidney works together with the liver for maintenance of optimal insulin levels. In humans, kidney removes 6–8 U of insulin per day by two major routes (**Figure 2**), that apparently have distinct preferential physiological goals: post-glomerular secretion (insulin signaling) and glomerular filtration (nutrient conservation and homeostasis) (Ritz et al., 2013). In the kidney, insulin acts at multiple sites along the nephron, from the glomerulus (Coward et al., 2005; Welsh et al., 2010; Mima et al., 2011; Lay and Coward, 2014) to the renal tubule (Tiwari et al., 2008, 2013; Li et al., 2013), to modulate different functions such as glomerular filtration, gluconeogenesis, renal sodium handling, among others.

Many alterations in insulin associated mechanisms in the kidney are driven by insulin resistance (IR), leading to diabetic nephropathy if not reestablished (Svensson and Eriksson, 2006). In the Asiatic population, it was described that the prevalence of diabetic nephropathy with impaired estimated glomerular filtration rate (eGFR) (with or without albuminuria) was 31.6%, and the prevalence of albuminuria (with or without impaired eGFR) was 16.9 and 22.0%, respectively (Mok et al., 2019). Patients may already show diabetic kidney disease (DKD) at the time of T2DM diagnosis. Nevertheless, 10 years after the diagnosis of T2DM, low-level albuminuria is present in 24.9% of the patients and 5.3% already present macroalbuminuria (Adler et al., 2003).

Glomerular Insulin Actions

Podocytes are the primary constituent cell of the glomerulus, with their long finger-like projections to the glomerular capillaries at the glomerular basement membrane (GBM). These cells have intercellular junctions that form filtration barriers to help maintaining normal renal function. When damaged, podocytes lose their arrangement resulting in a reduction in barrier function. Indeed, one of the DKD features is the podocyte loss with consequent albuminuria (Pagtalunan et al., 1997; Wolf et al., 2005). Lately, it has been unveiled the role of insulin in podocytes (**Figure 3**); in other words, podocyte IR gives rise to the albuminuric feature.

Podocytes reveal to express proteins of the insulin signaling canonical pathway, namely the INSR, and both IRS1 and IRS2 (Coward et al., 2005; Santamaria et al., 2015), with IRS2 being the most prevalent one. Coward et al. (2005) depicted the effect of insulin in human podocytes, which results in glucose uptake not only through GLUT4 but also through glucose transporter 1 (GLUT1; **Figure 3**). As insulin promotes the translocation of GLUT4 to the membrane through the activation of PI3K-AKT2-PkB pathway, there is a remodeling of the cortical actin of the cytoskeleton with subsequent contraction (Welsh et al., 2010). In compliance, podocytes-specific deletion of INSR in mice revealed DKD features based on substantial albuminuria and histological features as podocyte foot structure loss and glomerulosclerosis (Welsh et al., 2010). AKT seems to play a central role as its phosphorylation appears to be severely affected in several models of both type 1 diabetes mellitus (T1DM; streptozotocin-induced T1DM) and T2DM (db/db mice, Zucker rats) (Tejada et al., 2008; Mima et al., 2011). Moreover, AKT isoform 2 deletion results in serious glomerular lesions in mice. This can lead to rapid disease progression, also associated with tubular dilatation and microalbuminuria (Canaud et al., 2013). Other relevant players that might contribute to podocyte IR is SH2-domain-containing inositol phosphatase 2 (SHIP2), a down regulator of the PI3K signaling pathway shown to be upregulated in the Zucker rats. Moreover, protein tyrosine-phosphatase 1B (PTP1B), a negative regulator of the INSR activity, or phosphatase and tensin homolog when increased, appears to also compromise the insulin signaling pathway (Mima et al., 2011; Garner et al., 2018).

Podocytes also present an insulin-dependent alternative pathway, the cyclic guanosine monophosphate(cGMP)-dependent protein kinase G (PKG), from which the PKG isoform I-alpha levels are increased in glomeruli of the hyperinsulinemic Zucker rats (Piwkowska et al., 2013). These high insulin levels increase glomerular barrier albumin permeability through a PKGI-reliant mechanism via the NAD(P)H-dependent generation of superoxide anion.

An important player in podocytes physiology is the protein nephrin, a podocyte-specific protein, which is responsible for the maintenance of the integrity of the filtration barrier. In fact, nephrin mutations are involved in severe nephrotic syndrome (Lenkkeri et al., 1999). Nephrin appears to play a most outstanding role in the trafficking of GLUT4 and GLUT1 by interacting with Vamp2 as well as by interacting with insulin-stimulated actin remodeling (Coward et al., 2007; Lay et al., 2017). Of interest, nephrin can also induce phosphorylation of p70S6K in a PI3K-dependent manner independently of INSR/AKT2 activation (Villarreal et al., 2016; **Figure 3**).

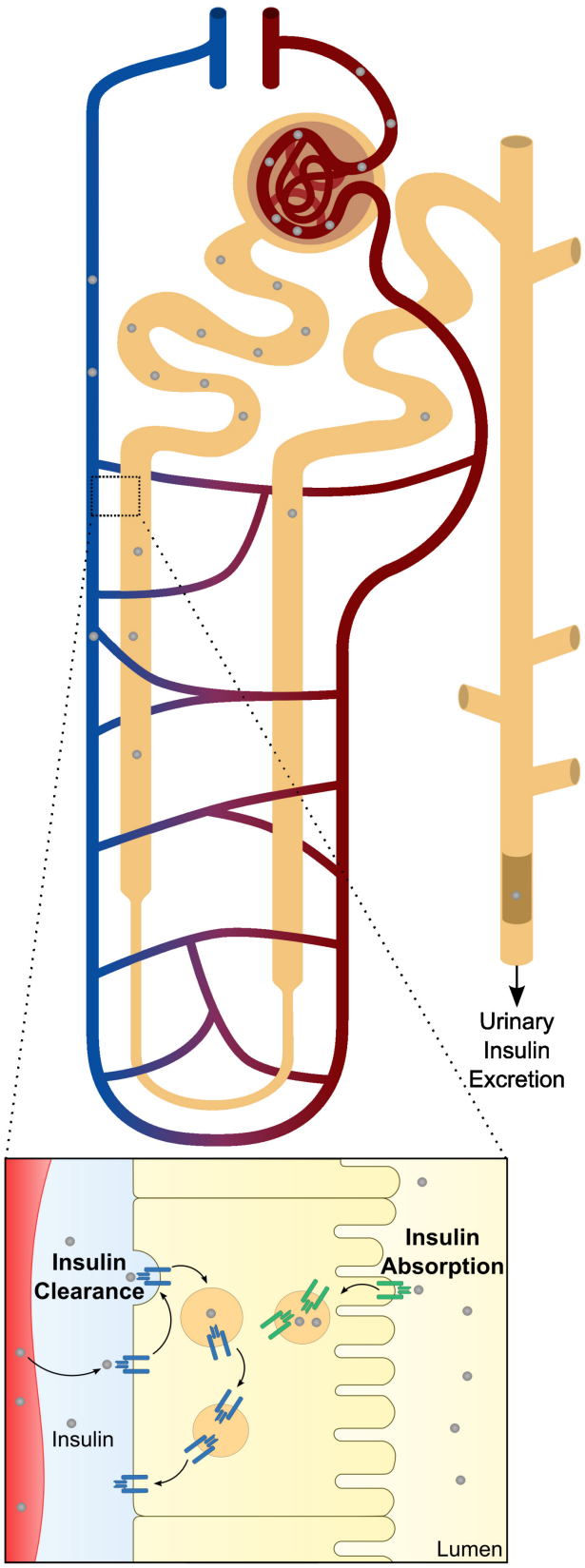

FIGURE 2 | Continued

FIGURE 2 | Schematic representation of renal insulin handling. Insulin is depicted in gray circles at different portions of the nephron. As insulin is a small molecule, it will be fully filtered by the glomerular system until it reaches the proximal tubule. At proximal tubule cells, almost all the filtered insulin will be absorbed at the luminal membrane. In physiological conditions, only a small percentage will be excreted in urine. Beyond glomerular filtration, insulin also raise from the perivenous capillaries. In a closer look to the proximal tubule cells is represented both mechanisms of insulin clearance. The increased levels of insulin receptor (INSR) and consequent increased uptake of insulin at the basolateral membrane is also depicted.

The development of glomerular IR is triggered by several factors: high glucose and/or insulin levels, increased FFAs levels, or an inflammatory milieu. Moreover, insulin signaling appears to be relevant for the adaptative ER stress response in DKD; this is the case for mice with podocyte-specific heterozygous INSR deletion (Madhusudhan et al., 2015). In support of this view, stable overexpression of INSR or knock-down of PTP1B was protective against ER stress (Garner et al., 2018). Podocyte mitochondria play an essential role in cellular metabolism. When dysfunctional as a result of reactive oxygen species production, mitochondria triggers apoptosis, which can also be observed along with a compromised IR state (Susztak et al., 2006). Certainly, the preservation or reestablishment of podocyte integrity is essential in the prevention of the onset and development of DKD.

INSULIN TUBULAR ACTIONS

In the kidney tubule, insulin has several roles: metabolism, electrolyte and acid-base regulation and absorption of filtered substances. However, the exact mechanisms by which insulin performs these distinct roles is not fully understood. Nonetheless, it seems that, at least some of them, are mediated by INSR, and can be explained by the recruitment of specific IRS, as recently shown by Nakamura et al. (2020) specifically for gluconeogenesis and sodium reabsorption regulation. Still, there are overlapping mediators in downstream pathways. In the following paragraphs we will summarize the most relevant and well-known insulin actions in the tubular segment.

Insulin receptor is present throughout the entire nephron (Butlen et al., 1988; Stechi et al., 1994), however, insulin binding capacity of luminal and basolateral membrane tubule cells is different. There is evidence showing same affinity of INSR in both membrane sides of the cell, nonetheless its abundance is asymmetrical (Hammerman, 1985). In fact, the binding capacity of the contraluminal compared to luminal membrane seems to be several times greater due to higher expression of INSR (Talor et al., 1982). **Figure 4** summarizes insulin signaling in proximal tubule (PT), regarding its actions in both gluconeogenesis and sodium reabsorption. Additionally, insulin actions through INSR are thought to be different in the proximal and distal nephron regions. Tiwari et al. (2013) demonstrated, in a mouse model with deletion of INSR in the kidney tubule cells, that depending on the segment targeted with INSR deletion, there were different phenotypes further described. In case of decreased INSR at PT,

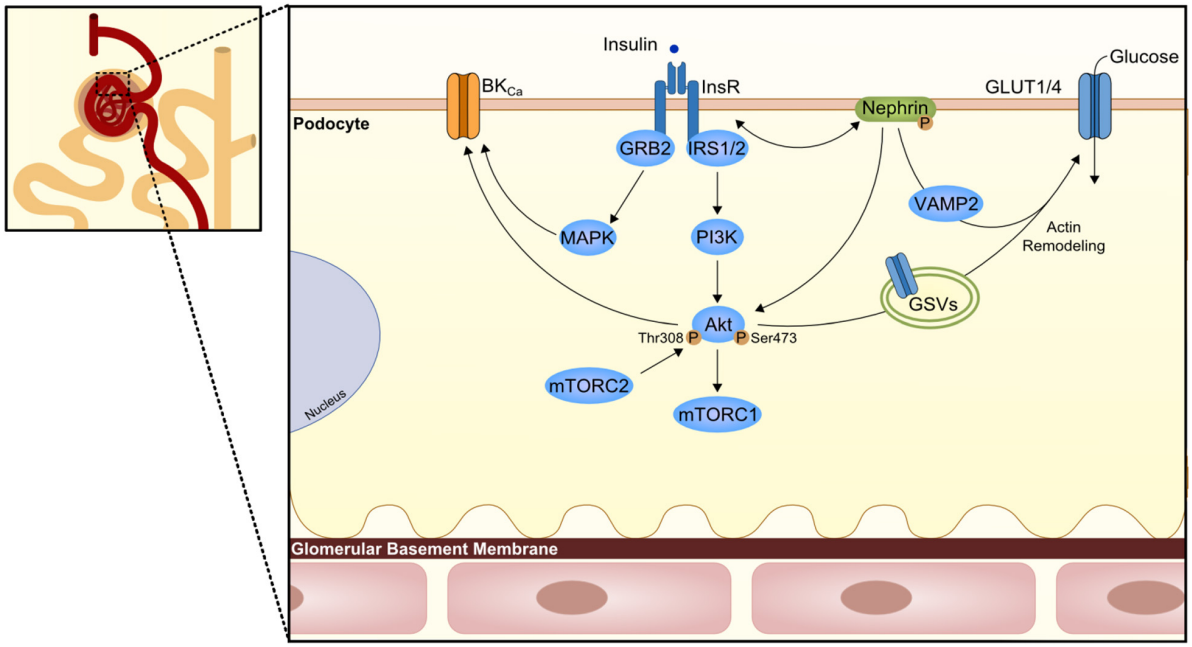

FIGURE 3 | Podocyte insulin signaling. Podocytes are the first cells to interact with insulin at the nephron and express several proteins of the canonical insulin signaling pathway. However, here the podocyte-specific protein nephrin is known to have a role in the trafficking of glucose transporters (GLUT1 or GLUT4) to podocyte membrane and consequently promote glucose uptake. The trafficking seems to involve Vamp2 and actin remodeling. On the other branch of insulin signaling, an effect in the large-conductance Ca^{2+}-activated K^{+} channels (BK_{Ca}) is also important for maintenance of podocyte integrity and proper glomerular filtration. GRB2, growth factor receptor-bound protein 2; GSV, GLUT storage vesicle; VAMP2, Vesicle-associated membrane protein 2.

animals had a mild diabetic phenotype, without increased IR when compared to control. These animals shown to have an higher activity of gluconeogenesis enzymes (Tiwari et al., 2013). On the other hand, in animals with the deletion of INSR targeted to distal parts of the tubule, elevated blood pressure and impaired sodium excretion was observed (Tiwari et al., 2008).

Glucose Reabsorption

Glucose is reabsorbed by the PT cells from the kidney tubule lumen to the bloodstream (**Figure 4A**). In the kidney, GLUT2 is in the basolateral membrane and diffuses glucose out of the cell, contrary to the liver, where GLUT2 acts in glucose uptake. Sodium-glucose transporter proteins (SGLT) are responsible for glucose and sodium co-transport by the luminal membrane of kidney cells. Sodium-glucose co-transporter 2 (SGLT2) is a high-capacity/low affinity sodium-glucose cotransporter present in the apical membrane of proximal convoluted tubule cells (Vallon et al., 2011). These transporters are responsible for approximately 90% of filtered glucose reabsorption, and an important target for T2DM therapy (SGLT2 inhibitors; DeFronzo et al., 2012). The remaining 10% of glucose in the tubule is absorbed by SGLT1, a low capacity and high affinity sodium-glucose cotransporter (Wright et al., 2011). Kidney has a threshold for glucose excretion which, in healthy conditions, relates to a glycemic value around 180 mg/dl (**Figure 4B**). This threshold, however, can be altered in diabetes (Rave et al., 2006). It is not clear if SGLT2 glucose transport is or not directly dependent on insulin signaling (Ferrannini et al., 2020). Nonetheless, SGLT2 expression was shown to be upregulated by insulin on human cultured PT cells, in a dose-dependent manner (Nakamura et al., 2015). Therefore, in hyperinsulinemic states, frequently observed in prediabetes and T2DM, an excessive glucose absorption can be observed. Of notice, glucose is still highly absorbed by SGLT2 in IR states, suggesting that this mechanism is not affected by IR, though it is upregulated by hyperinsulinemia. In this case, a vicious cycle can happen where increased insulin levels drive an increase in glucose SGLT2 overexpression increasing glycemic levels which in turn will increment the insulin secretion (**Figure 4C**). Therefore, SGLT2 overexpression inhibition is a potential new target for highly prevalent hyperinsulinemia related conditions, namely some dysglycemic phenotypes and obesity. In this case, lowering insulin levels could be paramount to prevent SGLT2 overexpression. Thus, SGLT2 inhibitors might become a relevant therapeutic approach for hyperinsulinemia related conditions, other than T2DM, namely obesity and prediabetes.

Gluconeogenesis Regulation

Kidney has a major role in gluconeogenesis along with the liver and the intestine. Gluconeogenesis occurs mainly in PT cells essentially from lactate and glutamine (**Figure 4A**). Moreover, PT cells do not use glucose, as they get their energy mostly from fatty acid oxidation (Gerich et al., 1963). Insulin regulates gluconeogenesis in PT cells to meet the fluctuating needs of the body. While in the fasting state the kidney contributes in 40% to overall gluconeogenesis, in the post-absorptive state its contribution drops to 20% (Gerich et al., 1963; **Figure 4B**).

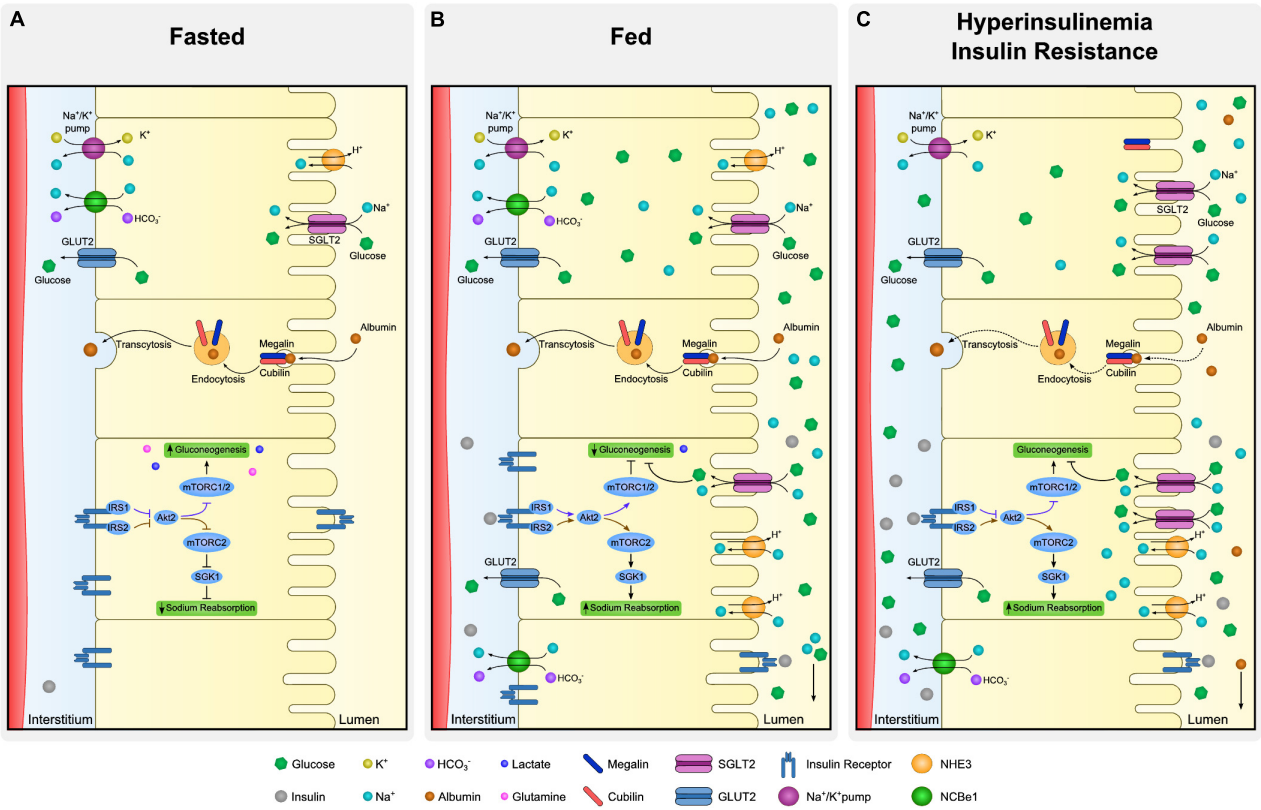

FIGURE 4 | Dynamics of proximal tubule cells at fasting, fed and insulin resistant states. Proximal tubule cells are subjected to distinct microenvironments (lumen and interstitium) and the regulation of absorption and reabsorption of molecules is complex. Although all the described processes occur in every cell of the proximal tubule simultaneously, each specific process is illustrated in a different cell. At fasting **(A)**, low levels of insulin allow expression of gluconeogenic enzymes whereas sodium reabsorption is downregulated. Expression of glucose transporter 2 (GLUT2) at basolateral membrane is mostly associated to glucose output and not to its uptake. Moreover, albumin absorption is performed by megalin and cubilin at luminal membrane and transcytosis allow albumin to be rerouted back to the organism. At fed state **(B)**, increased availability of insulin and glucose promote drastic changes in proximal tubule dynamics. In the case of insulin, luminal uptake is mostly associated to degradation and basolateral to signaling activation. Insulin receptor (INSR) activation downregulates gluconeogenesis and increases sodium reabsorption by different proteins as type 3 Na-H exchanger (NHE-3) and sodium-glucose transport protein 2 (SGLT2). Together with sodium, SGLT2 also co-transport glucose from the lumen. Finally, hyperinsulinemia is linked to perturbations of proximal tubule cells in many aspects **(C)**. As in many other organs, insulin signaling desensitization is associated to inefficient inhibition of gluconeogenesis contributing to maintenance of increased levels of glucose. Derangements at podocyte level increases filtration of albumin and overloads luminal capacity of reabsorption. Such impairment in albumin reabsorption culminates with albuminuria, frequent observed in hyperinsulinemic states.

Nakamura et al. (2020) demonstrated that insulin directly inhibits gluconeogenesis in isolated PT through IRS1/AKT2/mTORC1/2, and that mTORC1 positively regulates insulin signaling (Nakamura et al., 2020). Specifically, in the fasting state, suppressed insulin signaling increases FoxO1 activity, increasing the expression of gluconeogenic genes, such as PEPCK and glucose-6-phosphatase. In parallel, decreased glucose reabsorption via SGLT2 on the luminal membrane downregulates the NADH/NAD$^+$ ratio, activating sirtuin 1 and peroxisome proliferator-activated receptor-gamma coactivator 1α (PGC1α), a coactivator of FoxO1. Therefore, these two mechanisms lead to enhanced gluconeogenesis. On the contrary, in the fed state, the increased insulin levels and glucose reabsorption result in the suppression of gluconeogenesis through downregulation of the previously mentioned gluconeogenic genes (Nakamura et al., 2015; Sasaki et al., 2017). Whereas glucose is reabsorbed by the luminal membrane, insulin interacts with the basolateral membrane, thus gluconeogenesis regulation results from the integration of signals from distinct cell microenvironment.

Sodium

Insulin impacts on the fine-tuning of several electrolytes by the kidney. Among them sodium handling is probably the best described (DeFronzo et al., 1975). However, the insulin role on sodium retention in normoglycemia is not completely established. Regulation of sodium absorption is paramount to maintain the extracellular volume in a physiological range. Kidney is the principal organ involved in sodium excretion, responding and adapting to sodium intake (Krekels et al., 2015). Additionally, sodium has a major role in driving electrochemical forces that support kidney primary role in fine-tuning body composition. Sodium reabsorption and excretion results from the integration of a complex network of sensors,

neural-hormonal stimuli and hemodynamic and metabolic mechanisms (Frame and Wainford, 2017).

Contrary to glucose, sodium is absorbed along the nephron by distinct apical sodium transport proteins. Usually, approximately 65% of filtered sodium is reabsorbed in the PT along with water, mainly through type 3 Na-H exchanger (NHE-3) and SGLT proteins. In addition, the thick ascending limb is responsible for approximately 25% of reabsorption through sodium-potassium chloride cotransporter-2 (NKCC2). Finally, 5–10% of sodium is reabsorbed in the collecting duct by epithelial sodium channel (ENaC) and less than 10% is excreted in urine (Esteva-Font et al., 2012).

The association of insulin with sodium absorption was suggested almost a century ago (Atchley et al., 1933), nonetheless discrimination of insulin- and glucose-mediated effects has not been clarified (DeFronzo et al., 1976; Manhiani et al., 2011). It is still under debate if insulin has a causal effect on hypertension under normoglycemia. Nevertheless, it is known that insulin stimulates sodium absorption in all the tubule segments where it takes place (Kirchner, 1988; Friedberg et al., 1991; Ghezzi and Wright, 2012). In the PT, insulin regulates several sodium transporters, in both luminal (NHE-3, SGLT2) and basolateral membrane (Na/K-ATPase, NBCe1; **Figure 4A**; Gesek and Schoolwerth, 1991; Feraille et al., 1994; Ruiz et al., 1998). Recently, Nakamura et al. (2020) showed that, regarding sodium absorption in PT, insulin recruits an IRS (IRS2) different from the one orchestrating gluconeogenesis (IRS1). Insulin receptor substrate 2 acts through the AKT2/mTORC2 pathway (Nakamura et al., 2020; **Figure 4A**). In fact, mTORC2 is known to activate serum/glucocorticoid regulated kinase 1 (SGK1), that will then stimulate ENaC and NHE-3, increasing sodium reabsorption (Satoh et al., 2015). It has been suggested that, in healthy conditions, with rising insulin levels in fed state, IRS2 desensitize, suppressing sodium reabsorption at PT and increasing its delivery in the distal convoluted tubule (**Figure 4B**). Moreover, with IR, the desensitizing mechanism is abolished and therefore sodium will not reach the distal tubule (Ecelbarger, 2020; **Figure 4C**). Of notice, by recruiting distinct IRS, kidney cells can somehow dissociate pathways performing distinct functions.

Finally, it must be kept in mind that insulin can interact with intrarenal and systemic renin-angiotensin-aldosterone system in several ways (Muscogiuri et al., 2008) and therefore, indirectly interfere with sodium reabsorption in different mechanism out of the scope of this review.

Albumin Absorption

The luminal membrane of PT cells is primarily responsible for the reabsorption of proteins that are freely filtered in the glomerulus by receptor-mediated endocytosis (**Figure 4A**; Christensen and Gburek, 2004). This is the case of albumin reabsorption that can have an important role in energy conservation. It has been suggested that albumin endocytosis is a regulated process, dependent on membrane receptors megalin and cubilin (Christensen and Birn, 2001). More recent evidence suggest that insulin might also have a role in the regulation of tubular albumin absorption (Kumari et al., 2019).

Albuminuria is of major clinical relevance in diagnosis and follow-up of kidney disease including subjects with diabetes. Insulin resistance was found to be associated with decreased INSR expression in tubular cells in rat models (Wang et al., 2005). In these observations, Kumari et al. (2019) analyzed urine samples from mice with targeted deletion of INSR from the renal PT. These mice had an impaired uptake of albumin, without any glomerulopathy. They also demonstrated that in healthy humans, albumin absorption capacity and excretion vary from the fast to the fed state. Moreover, IR was associated with microalbuminuria even in normoglycemia as described in the RISC study (Pilz et al., 2014) and thus can be present regardless of diabetes diagnosis. Altogether, these evidences suggest that albuminuria might be an important marker of kidney tubular dysfunction and might reflect tubule cells IR (**Figure 4C**). These reinforces the kidney contribution to diabetes development and highlights insulin and albumin dynamics prior and regardless of the development of diabetes.

KIDNEY INSULIN CLEARANCE

In the systemic circulation, besides insulin metabolization by the liver, the kidney is the major site of insulin clearance (around 25%) (Elgee and Williams, 1954; Narahara et al., 1958); its action might be required to limit excessive insulin levels. Evidences supporting this theory started to rise in the middle of the 20th century (Zubrod et al., 1951; Elgee and Williams, 1954; Narahara et al., 1958; Ricketts and Wildberger, 1962). In a study from 1966, Beck et al. (1966) found that when insulin was injected intravenously in mice, it concentrated in liver and kidney; however, with higher insulin doses, raised insulin levels were found in rat's kidney, while these levels were found to be reduced in liver. Nevertheless, this early study has some methodological limitations. Indeed, kidney insulin clearance remains constant in spite of insulinemia variations, but varies with creatinine clearance (Rubenstein et al., 1967). Globally, these evidences suggest that kidney insulin clearance is a non-saturable process, although dependent on glomerular filtration rate.

Insulin freely filtered in the glomerulus is absorbed by the lining cells of the PT (**Figure 2**). Upon entering the cell, insulin is transported through the luminal membrane into the PT cells and is degraded. Luminal insulin reabsorption limits urine insulin excretion, thus less than 2% of insulin reaches the urine in normal fasting conditions (Rubenstein and Spitz, 1968). Insulin is transported through the luminal membrane by a receptor-mediated endocytic mechanism (Rabkin et al., 1984). Endocytic internalization of insulin seems to be more related to insulin degradation than to insulin biological actions (**Figure 2**).

While glomerular filtration of insulin could not account for its total estimated renal extraction, a second mechanism was postulated. In this context, it was observed that a significant amount of insulin was cleared by the post-glomerular peritubular capillaries into the tubule cells (Chamberlain and Stimmler, 1967). In humans, this route represents around one-third of cleared insulin in the kidney, where it enters tubule cells not

just by endocytosis, but also by INSR mediated uptake. In this case, through INSR binding, insulin signal to the kidneys' tubular apparatus is crucial to maintain central physiologic functions, similarly to what happens in extra-renal tissues, namely regarding glucose homeostasis and blood pressure.

Insulin degrading activity has been observed at cytosol, lysosomes and mitochondria in addition to the membrane, indicating that it occurs in distinct cell sites. Degradation at the membrane level, however, seems to represent less than 2% of total degrading activity (Rabkin et al., 1984). Insulin can be initially hydrolyzed by an insulin protease followed by the action of plasma-membrane-associated or lysosomal proteases. This pathway can degrade insulin entering through both luminal and contraluminal membrane. In another possible pathway, endocytic vesicles containing insulin fuse with lysosomes. This pathway comprehends glutathione-insulin transhydrogenase (GIT) action, followed by hydrolysis of intact A and B chains by lysosomal proteases, and seems to need insulin internalization. It may act primarily on insulin delivered by luminal uptake and it is most active when supraphysiological levels of insulin are present (Rabkin et al., 1984).

Azizi et al. (2015) demonstrated that, in a culture of human adipose microvascular endothelial cells, insulin can go through microvascular endothelial cells by transcytosis (Azizi et al., 2015). Regarding insulin handling in the kidney tubule, Dahl et al. (1989) hypothesized that insulin molecules could also pass tubular cells by a retroendocytic pathway instead of being degraded. The authors demonstrated that cultured opossum kidney cells exhibited a retroendocytic pathway for insulin (Dahl et al., 1989). Using the same model, the authors later demonstrated that inhibition of insulin degradation diverted intact insulin from the degradative to the retroendocytic pathway (Dahl et al., 1990). Although captivating, especially regarding a potential contribution to hyperinsulinemic states, this hypothesis was not further explored.

Whether insulin clearance mechanisms attributed to other organs affects renal function and insulin clearance it is not clear. For example, the lack of CEACAM-1, a key protein enrolled in hepatic insulin clearance driving hyperinsulinemia, in the kidney leads to increased renin levels contributing to a potentiation of the RAS system and hypertension. These effects are exacerbated upon high fat diet exposure. Hence, the described CEACAM-1 renal effects can be due to the lack of its expression as well as the observed hyperinsulinemia (Huang et al., 2013; Li et al., 2015).

Despite early conflicting results, further studies showed that insulin is excreted in urine. However, in physiological conditions, it represents a minimal proportion of insulin filtered in the glomerulus. In health, a minor amount of insulin appears in the urine, as the majority is absorbed in PT. Tubule absorbing capacity of insulin does not saturate and thus the insulin fraction excreted in urine is constantly small, regardless of insulin levels. However, the amount of insulin excreted in urine varies physiologically (e.g., fasting and post-prandial) and in pathological conditions (obesity, diabetes) depending on the affected nephron region (e.g., glomerulopathy vs. tubulopathy) (Rubenstein and Spitz, 1968). Considering that insulin is internalized in the apical membrane by a receptor-mediated endocytic mechanism, the increased urinary insulin excretion might represent a tubular dysfunction. Subjects with tubulopathy show large amounts of insulin in urine approximating the amount that is filtered (Rabkin et al., 1984). Conversely, subjects with nephrotic syndrome show normal amounts of insulin in urine. When both glomerular and tubule lesion occur urine insulin excretion increase (Rabkin et al., 1984).

CLINICAL INSIGHTS ON INSULIN DYSREGULATION

Insulin resistance is a common feature in chronic kidney disease (CKD) patients, even in absence of diabetes (DeFronzo et al., 1981; Shinohara et al., 2002; Becker et al., 2005; Kobayashi et al., 2005; Landau et al., 2011), and it is a risk factor for CKD progression (Fox et al., 2004). Its prevalence in CKD ranges from 30 to 50%, and this mainly depends on the adopted method of measurement (Spoto et al., 2016). Insulin resistance can be detected at the very early stages, when eGFR is still within the normal range, suggesting a potential role in triggering CKD (Fliser et al., 1998). A large study based on the Atherosclerosis Risk in Communities (ARICs) cohort confirmed that CKD development increases in strict parallelism with the number of metabolic syndrome criteria measured in non-diabetic adults, and this relationship remains significant even after controlling for the development of diabetes and hypertension (Kurella et al., 2005). Insulin resistance has also been associated with prevalent CKD and rapid decline in renal function in elderly, non-diabetic, Asian individuals (Cheng et al., 2012), and with microalbuminuria in the general population (Mykkänen et al., 1998), and in patients with T1DM (Yip et al., 1993; Ekstrand et al., 1998) and T2DM (Groop et al., 1993), indicating that this relationship is independent of diabetes (Mykkänen et al., 1998; Chen et al., 2003, 2004). The proposed mechanism by which IR contributes to kidney damage involves the worsening of renal hemodynamics through activation of the sympathetic nervous system (Rowe et al., 1981), sodium retention, decreased Na^+, K^+-ATPase activity, and increased GFR (Gluba et al., 2013).

The etiology of IR in CKD is multifactorial, depending on classical and CKD-peculiar risk factors, such as physical inactivity, inflammation and oxidative stress, adipokine derangements, vitamin D deficiency, metabolic acidosis, anemia and microbial toxins (Spoto et al., 2016).

Long-term hemodialysis has a positive effect on IR (DeFronzo et al., 1978), but there is little clinical data regarding the effect of peritoneal dialysis.

In addition to being a risk factor for CKD onset and progression, IR is also involved in the increased cardiovascular (CV) risk in this population. IR may be responsible for high blood pressure via direct stimulation of renin–angiotensin–aldosterone system (Nickenig et al., 1998), activation of sympathetic system (Sowers et al., 2001) and downregulation of the natriuretic peptide system (Sarzani et al., 1999).

However, the association between IR and CV complications in CKD patients is still to be clarified, as well as the relationship between IR and all-cause and CV mortality.

A positive association between IR and all-cause mortality was found in smokers and physically inactive CKD patients (Xu et al., 2014) and in a small cohort of 170 Japanese, non-diabetic, dialysis patients (Shinohara et al., 2002), whereas association with CV mortality was found in a cohort of peritoneal patients. However, no association was found in the ULSAM cohort, including 3-4 stage CKD patients (Jia et al., 2014) and in a small study performed in peritoneal dialysis patients (Sánchez-Villanueva et al., 2013).

Even though the prognostic value of IR for death and CV events need to be clarified, the association with CKD is well established. Even in this case, however, if IR is responsible of the onset and progression of CKD, or if CKD is responsible for IR is still to be clarified. A possible answer to this question could derive from clinical trials aiming at assessing the effect of drugs used for IR treatment on kidney function.

Thiazolidinediones (TZDs) are a class of oral diabetic medications that increase insulin sensitivity by acting on PPARγ (Yki-Järvinen, 2004). The effect of TZDs on kidney function has been previously described in mice models (Fujii et al., 1997). Treatment with TZDs has been demonstrated to improve insulin sensitivity in patients with T2DM after a 3-month treatment, and to reduce albuminuria, the last effect likely mediated by the concurrent increase in serum adiponectin concentration (Miyazaki et al., 2007). These results were confirmed in a meta-analysis of 15 double-blind, randomized, clinical trials involving diabetic patients (Sarafidis et al., 2010) and in a large study involving 4351 diabetic patients (Lachin et al., 2011). Even though a meta-analysis reported an increase in cardiovascular mortality linked to the use of TZDs in dialysis patients (Nissen and Wolski, 2007), no definitive proof are available on the risk related to this medication in this population.

Another interesting class of hypoglycemic drugs with positive kidney outcomes are the SGLT2 inhibitors (SGLT2i) which inhibit glucose and sodium reabsorption in the PT (Ferrannini, 2017). These drugs have a renoprotective effect in patients with T2DM (Perkovic et al., 2019) independently of glycemic control (Cherney et al., 2017). The renal protective effect can also be attributed to altered hemodynamics, reduced inflammation and fibrosis as well as controlled blood pressure and weight loss (Williams et al., 2020). In rats treated with SGLT2i the glycemic improvement was accompanied by a decrease in insulin and lipid levels (Huang et al., 2020). Moreover, the actions of SGLT2i are associated with increased insulin sensitivity and decreased albuminuria (Cherney et al., 2017). Interestingly, Jaikumkao et al. observed that in an animal model of diet induced obesity characterized by IR and impaired renal function dapagliflozin treatment resulted in improved IR, renal function and renal insulin signaling (Jaikumkao et al., 2018).

CONCLUSION

Insulin is a hormone which acts not only on the most recognized insulin-responsive organs (liver, adipose tissue, and skeletal muscle), but also on the kidney. Moreover, the kidney has a primordial role in insulin clearance and may impact on insulin plasma levels. Whereas its main action is mainly related to homeostasis of glucose, including modulation of gluconeogenesis and lipolysis, in kidney the effects of insulin and IR change according to whether the target is in glomeruli or tubules. More specifically, if in glomerular podocytes insulin promotes glucose uptake, with an involvement in barrier permeability, in tubules it contributes to glucose reabsorption and gluconeogenesis regulation, and plays an important role in sodium homeostasis.

Importantly, insulin intervenes in albumin reabsorption at tubular level. Moreover, IR has been associated with microalbuminuria even in normoglycemia, and thus can be present regardless of diabetes diagnosis. These findings reinforce the kidney contribution to diabetes development and highlights insulin and albumin dynamics prior and regardless of the development of diabetes.

Insulin is cleared in the PT of kidney by two major routes, either by absorption of filtered insulin, or by post-glomerular capillary secretion, and only a minor amount appears to be excreted in urine. A decreased renal insulin clearance might lead to higher insulin levels, in the organ or systemically, favoring IR. Nonetheless, the impact of renal insulin clearance affection in the kidney or in insulin plasma levels still needs to be further unveiled.

It is clear now that kidney is not a mere target of insulin action, but insulin, more precisely IR, is also able to trigger CKD even in absence of diabetes. IR has been associated with prevalent CKD, rapid decline in renal function and microalbuminuria in the general population and in diabetic patients. In addition to being a risk factor for CKD onset and progression, IR is also involved in the increased cardiovascular risk in this population. However, if IR is responsible for the onset and progression of CKD, or if CKD is responsible for IR is still to be clarified. Preliminary confirmations come from clinical trials aiming at exploring the effect of TZDs, a class of oral diabetic medications, on kidney function. However, more focused studies, aiming also at testing the safety of these medications in CKD patients, are needed to better understand if treatment of IR may improve renal function in this population.

AUTHOR CONTRIBUTIONS

AP and MPM conceptualized the study. All authors originally drafted the manuscript, reviewed, edited, and critically approved the final version of the manuscript.

FUNDING

This work was supported by "Fundação para a Ciência e a Tecnologia" – FCT to AP (PD/BD/136887/2018); MJM (PD/BD/114256/2016), MPM (PTDC/DTP-EPI/0207/2012), DOB e MPM (PTDC/BIM-MET/2115/2014); iNOVA4Health (UIDB/Multi/04462/2020), by the European Commission Marie Skłodowska-Curie Actions H2020 (grant agreements nos. 722619 and 734719), and by the Sociedade Portuguesa de Diabetologia.

REFERENCES

Adler, A. I., Stevens, R. J., Manley, S. E., Bilous, R. W., Cull, C. A., Holman, R. R., et al. (2003). Development and progression of nephropathy in type 2 diabetes: The United Kingdom Prospective Diabetes Study (UKPDS 64). *Kidney Int.* 63, 225–232. doi: 10.1046/j.1523-1755.2003.00712.x

Alessi, D. R., James, S. R., Downes, C. P., Holmes, A. B., Gaffney, P. R. J., Reese, C. B., et al. (1997). Characterization of a 3-phosphoinositide-dependent protein kinase which phosphorylates and activates protein kinase Bα. *Curr. Biol.* 7, 261–269. doi: 10.1016/S0960-9822(06)00122-9

Andrali, S. S., Sampley, M. L., Vanderford, N. L., and Özcan, S. (2008). Glucose regulation of insulin gene expression in pancreatic β-cells. *Biochem. J.* 415, 1–10. doi: 10.1042/BJ20081029

Artunc, F., Schleicher, E., Weigert, C., Fritsche, A., Stefan, N., and Häring, H. (2016). The impact of insulin resistance on the kidney and vasculature. *Nat. Publ. Gr.* 12, 721–737. doi: 10.1038/nrneph.2016.145

Atchley, D. W., Loeb, R. F., Richards, D. W., Benedict, E. M., and Driscoll, M. E. (1933). ON DIABETIC ACIDOSIS: a detailed study of electrolyte balances following the withdrawal and reestablishment of insulin therapy. *J. Clin. Invest.* 12, 297–326. doi: 10.1172/JCI100504

Azizi, P. M., Zyla, R. E., Guan, S., Wang, C., Liu, J., Bolz, S. S., et al. (2015). Clathrin-dependent entry and vesicle-mediated exocytosis define insulin transcytosis across microvascular endothelial cells. *Mol. Biol. Cell* 26, 740–750. doi: 10.1091/mbc.E14-08-1307

Bayascas, J. R., and Alessi, D. R. (2005). Regulation of Akt/PKB Ser473 Phosphorylation. *Mol. Cell* 18, 143–145. doi: 10.1016/j.molcel.2005.03.020

Beck, L. V., Zaharko, D. S., Roberts, N., and King, C. (1966). On insulin I-131 metabolism in mice. Modifying effects of anti-insulin serum and of total insulin dosage. *Diabetes* 15, 336–341. doi: 10.2337/diab.15.5.336

Becker, B., Kronenberg, F., Kielstein, J. T., Haller, H., Morath, C., Ritz, E., et al. (2005). Renal insulin resistance syndrome, adiponectin and cardiovascular events in patients with kidney disease: the mild and moderate kidney disease study. *J. Am. Soc. Nephrol.* 16, 1091–1098. doi: 10.1681/ASN.2004090742

Bedinger, D. H., and Adams, S. H. (2015). Metabolic, anabolic, and mitogenic insulin responses: a tissue-specific perspective for insulin receptor activators. *Mol. Cell. Endocrinol.* 415, 143–156. doi: 10.1016/j.mce.2015.08.013

Bergman, R. N., Piccinini, F., Kabir, M., Kolka, C. M., and Ader, M. (2019). Hypothesis: role of reduced hepatic insulin clearance in the pathogenesis of type 2 diabetes. *Diabetes Metab. Res. Rev.* 68, 1709–1716. doi: 10.2337/db19-0098

Bril, F., Lomonaco, R., Orsak, B., Ortiz-Lopez, C., Webb, A., Tio, F., et al. (2014). Relationship between disease severity, hyperinsulinemia, and impaired insulin clearance in patients with nonalcoholic steatohepatitis. *Hepatology* 59, 2178–2187. doi: 10.1002/hep.26988

Butlen, D., Vadrot, S., Roseau, S., and Morel, F. (1988). Insulin receptors along the rat nephron: [125I] Insulin binding in microdissected glomeruli and tubules. *Pflügers Arch. Eur. J. Physiol.* 412, 604–612. doi: 10.1007/BF00583761

Calzi, S. L., Choice, C. V., and Najjar, S. M. (1997). Differential effect of pp120 on insulin endocytosis by two variant insulin receptor isoforms. *Am. J. Physiol. Metab.* 273, E801–E808. doi: 10.1152/ajpendo.1997.273.4.E801

Canaud, G., Bienaimé, F., Viau, A., Treins, C., Baron, W., Nguyen, C., et al. (2013). AKT2 is essential to maintain podocyte viability and function during chronic kidney disease. *Nat. Med.* 19, 1288–1296. doi: 10.1038/nm.3313

Chamberlain, M. J., and Stimmler, L. (1967). The renal handling of insulin. *J. Clin. Invest.* 46, 911–919. doi: 10.1172/JCI105597

Chen, J., Muntner, P., Hamm, L. L., Fonseca, V., Batuman, V., Whelton, P. K., et al. (2003). Insulin resistance and risk of chronic kidney disease in nondiabetic US adults. *J. Am. Soc. Nephrol.* 14, 469–477. doi: 10.1097/01.ASN.0000046029.53933.09

Chen, J., Muntner, P., Hamm, L. L., Jones, D. W., Batuman, V., Fonseca, V., et al. (2004). The metabolic syndrome and chronic kidney disease in U.S. adults. *Ann. Intern. Med.* 140, 167–174. doi: 10.7326/0003-4819-140-3-200402030-00007

Cheng, H. T., Huang, J. W., Chiang, C. K., Yen, C. J., Hung, K. Y., and Wu, K. D. (2012). Metabolic syndrome and insulin resistance as risk factors for development of chronic kidney disease and rapid decline in renal function in elderly. *J. Clin. Endocrinol. Metab.* 97, 1268–1276. doi: 10.1210/jc.2011-2658

Cherney, D. Z. I., Zinman, B., Inzucchi, S. E., Koitka-Weber, A., Mattheus, M., von Eynatten, M., et al. (2017). Effects of empagliflozin on the urinary albumin-to-creatinine ratio in patients with type 2 diabetes and established cardiovascular disease: an exploratory analysis from the EMPA-REG OUTCOME randomised, placebo-controlled trial. *Lancet Diabetes Endocrinol.* 5, 610–621. doi: 10.1016/S2213-8587(17)30182-1

Christensen, E. I., and Birn, H. (2001). Megalin and cubilin: synergistic endocytic receptors in renal proximal tubule. *Am. J. Physiol. Physiol.* 280, F562–F573. doi: 10.1152/ajprenal.2001.280.4.F562

Christensen, E. I., and Gburek, J. (2004). Protein reabsorption in renal proximal tubule - Function and dysfunction in kidney pathophysiology. *Pediatr. Nephrol.* 19, 714–721. doi: 10.1007/s00467-004-1494-0

Coward, R. J. M., Welsh, G. I., Koziell, A., Hussain, S., Lennon, R., Ni, L., et al. (2007). Nephrin is critical for the action of insulin on human glomerular podocytes. *Diabetes Metab. Res. Rev.* 56, 1127–1135. doi: 10.2337/db06-0693

Coward, R. J. M., Welsh, G. I., Yang, J., Tasman, C., Lennon, R., Koziell, A., et al. (2005). The human glomerular podocyte is a novel target for insulin action. *Diabetes Metab. Res. Rev.* 54, 3095–3102. doi: 10.2337/diabetes.54.11.3095

Dahl, D. C., Tsao, T., Duckworth, W. C., Frank, B. H., and Rabkin, R. (1990). Effect of bacitracin on retroendocytosis and degradation of insulin in cultured kidney epithelial cell line. *Diabetes Metab. Res. Rev* 39, 1339–1346. doi: 10.2337/diab.39.11.1339

Dahl, D. C., Tsao, T., Duckworth, W. C., Mahoney, M. J., and Rabkin, R. (1989). Retroendocytosis of insulin in a cultured kidney epithelial cell line. *Am. J. Physiol. Cell Physiol.* 257, C190–C196. doi: 10.1152/ajpcell.1989.257.2.c190

DeFronzo, R. A., Alvestrand, A., Smith, D., Hendler, R., Hendler, E., and Wahren, J. (1981). Insulin resistance in uremia. *J. Clin. Invest.* 67, 563–568. doi: 10.1172/JCI110067

DeFronzo, R. A., Cooke, C. R., Andres, R., Faloona, G. R., and Davis, P. J. (1975). The effect of insulin on renal handling of sodium, potassium, calcium, and phosphate in man. *J. Clin. Invest.* 55, 845–855. doi: 10.1172/JCI107996

DeFronzo, R. A., Davidson, J. A., and del Prato, S. (2012). The role of the kidneys in glucose homeostasis: a new path towards normalizing glycaemia. *Diabetes Obes. Metab.* 14, 5–14. doi: 10.1111/j.1463-1326.2011.01511.x

DeFronzo, R. A., Goldberg, M., and Agus, Z. S. (1976). The effects of glucose and insulin on renal electrolyte transport. *J. Clin. Invest.* 58, 83–90. doi: 10.1172/JCI108463

DeFronzo, R. A., Tobin, J. D., Rowe, J. W., and Andres, R. (1978). Glucose intolerance in uremia. Quantification of pancreatic beta cell sensitivity to glucose and tissue sensitivity to insulin. *J. Clin. Invest.* 62, 425–435. doi: 10.1172/JCI109144

Detimary, P., Gilon, P., and Henquin, J.-C. (1998). Interplay between cytoplasmic Ca2+ and the ATP/ADP ratio: a feedback control mechanism in mouse pancreatic islets. *Biochem. J.* 333, 269–274. doi: 10.1042/bj3330269

Dimitriadis, G., Mitrou, P., Lambadiari, V., Maratou, E., and Raptis, S. A. (2011). Insulin effects in muscle and adipose tissue. *Diabetes Res. Clin. Pract.* 93, S52–S59. doi: 10.1016/S0168-8227(11)70014-6

Duckworth, W. C., Bennett, R. G., and Hamel, F. (1998). Insulin degradation: progress and potential. *Endocr. Rev.* 19, 608–624.

Ecelbarger, C. M. (2020). Refining insulin signaling in the proximal tubule at the level of the substrate. *Kidney Int.* 97, 256–258. doi: 10.1016/j.kint.2019.11.018

Ekstrand, A. V., Groop, P. H., and Grönhagen-Riska, C. (1998). Insulin resistance precedes microalbuminuria in patients with insulin-dependent diabetes mellitus. *Nephrol. Dial. Transplant.* 13, 3079–3083. doi: 10.1093/ndt/13.12.3079

Elgee, N. J., and Williams, R. H. (1954). Degradation of Insulin-I131 by Liver and Kidney in vivo. *Exp. Biol. Med.* 87, 352–355. doi: 10.3181/00379727-87-21380

Esteva-Font, C., Ballarin, J., and Fernández-Llama, P. (2012). Molecular biology of water and salt regulation in the kidney. *Cell. Mol. Life Sci.* 69, 683–695. doi: 10.1007/s00018-011-0858-4

Farber, S. J., Berger, E. Y., and Earle, D. P. (1951). Effect of diabetes and insulin on the maximum capacity of the renal tubules to reabsorb glucose. *J. Clin. Invest.* 30, 125–129. doi: 10.1172/JCI102424

Feraille, E., Carranza, M. L., Rousselot, M., and Favre, H. (1994). Insulin enhances sodium sensitivity of Na-K-ATPase in isolated rat proximal convoluted tubule. *Am. J. Physiol. Ren. Fluid Electrolyte Physiol.* 267, F55–F62. doi: 10.1152/ajprenal.1994.267.1.f55

Fernandes, A. B., Patarrão, R. S., Videira, P. A., and Macedo, M. P. (2011). Understanding postprandial glucose clearance by peripheral organs: the role of the hepatic parasympathetic system. *J. Neuroendocrinol.* 23, 1288–1295. doi: 10.1111/j.1365-2826.2011.02226.x

Ferrannini, E. (2017). Sodium-glucose co-transporters and their inhibition: clinical physiology. *Cell Metab.* 26, 27–38. doi: 10.1016/j.cmet.2017.04.011

Ferrannini, E., Pereira-Moreira, R., Seghieri, M., Rebelos, E., Souza, A. L., Chueire, V. B., et al. (2020). Insulin enhances renal glucose excretion: relation to insulin sensitivity and sodium-glucose cotransport. *BMJ Open Diabetes Res. Care* 8:e001178. doi: 10.1136/bmjdrc-2020-001178

Fliser, D., Pacini, G., Engelleiter, R., Kautzky-Willer, A., Prager, R., Franek, E., et al. (1998). Insulin resistance and hyperinsulinemia are already present in patients with incipient renal disease. *Kidney Int.* 53, 1343–1347. doi: 10.1046/j.1523-1755.1998.00898.x

Fox, C. S., Larson, M. G., Leip, E. P., Culleton, B., Wilson, P. W. F., and Levy, D. (2004). Predictors of new-onset kidney disease in a community-based population. *J. Am. Med. Assoc.* 291, 844–850. doi: 10.1001/jama.291.7.844

Frame, A. A., and Wainford, R. D. (2017). Renal sodium handling and sodium sensitivity. *Kidney Res. Clin. Pract.* 36, 117–131. doi: 10.23876/j.krcp.2017.36.2.117

Friedberg, C. E., Van Buren, M., Bijlsma, J. A., and Koomans, H. A. (1991). Insulin increases sodium reabsorption in diluting segment in humans: evidence for indirect mediation through hypokalemia. *Kidney Int.* 40, 251–256. doi: 10.1038/ki.1991.207

Fujii, M., Takemura, R., Yamaguchi, M., Hasegawa, G., Shigeta, H., Nakano, K., et al. (1997). Troglitazone (CS-045) ameliorates albuminuria in streptozotocin-induced diabetic rats. *Metabolism* 46, 981–983. doi: 10.1016/S0026-0495(97)90264-X

Galgani, J. E., Moro, C., and Ravussin, E. (2008). Metabolic flexibility and insulin resistance. *Am. J. Physiol. Metab.* 295, E1009–E1017. doi: 10.1152/ajpendo.90558.2008

Gancheva, S., Jelenik, T., Álvarez-Hernández, E., and Roden, M. (2018). Interorgan metabolic crosstalk in human insulin resistance. *Physiol. Rev.* 98, 1371–1415. doi: 10.1152/physrev.00015.2017

Gao, T., McKenna, B., Li, C., Reichert, M., Nguyen, J., Singh, T., et al. (2014). Pdx1 Maintains β cell identity and function by repressing an α cell program. *Cell Metab.* 19, 259–271. doi: 10.1016/j.cmet.2013.12.002

Garner, K. L., Betin, V. M. S., Pinto, V., Graham, M., Abgueguen, E., Barnes, M., et al. (2018). Enhanced insulin receptor, but not PI3K, signalling protects podocytes from ER stress. *Sci. Rep.* 8:3902. doi: 10.1038/s41598-018-22233-9

Gerich, J. E., Meyer, C., Hans, W. J., and Stumvoll, M. (1963). Renal gluconeogenesis. *Adv. Enzyme Regul.* 1, 385–400. doi: 10.1016/0065-2571(63)90034-7

Gesek, F. A., and Schoolwerth, A. C. (1991). Insulin increases Na(+)-H+ exchange activity in proximal tubules from normotensive and hypertensive rats. *Am. J. Physiol. Physiol.* 260, F695–F703. doi: 10.1152/ajprenal.1991.260.5.F695

Ghezzi, C., and Wright, E. M. (2012). Regulation of the human Na+-dependent glucose cotransporter hSGLT2. *Am. J. Physiol. Cell Physiol.* 303, 348–354. doi: 10.1152/ajpcell.00115.2012

Gluba, A., Mikhailidis, D. P., Lip, G. Y. H., Hannam, S., Rysz, J., and Banach, M. (2013). Metabolic syndrome and renal disease. *Int. J. Cardiol.* 164, 141–150. doi: 10.1016/j.ijcard.2012.01.013

Groop, L., Ekstrand, A., Forsblom, C., Widén, E., Groop, P. H., Teppo, A. M., et al. (1993). Insulin resistance, hypertension and microalbuminuria in patients with Type 2 (non-insulin-dependent) diabetes mellitus. *Diabetologia* 36, 642–647. doi: 10.1007/BF00404074

Hammerman, M. R. (1985). Interaction of insulin with the renal proximal tubular cell. *Am. J. Physiol. Physiol.* 249, F1–F11. doi: 10.1152/ajprenal.1985.249.1.F1

Hirashima, Y., Tsuruzoe, K., Kodama, S., Igata, M., Toyonaga, T., Ueki, K., et al. (2003). Insulin down-regulates insulin receptor substrate-2 expression through the phosphatidylinositol 3-kinase/Akt pathway. *J. Endocrinol.* 179, 253–266. doi: 10.1677/joe.0.1790253

Hou, J. C., Min, L., and Pessin, J. E. (2009). "Chapter 16 insulin granule biogenesis, trafficking and exocytosis," in *Vitamins and Hormones*, ed. G. Litwack (Amsterdam: Elsevier Inc), 473–506. doi: 10.1016/S0083-6729(08)00616-X

Huang, J., Ledford, K. J., Pitkin, W. B., Russo, L., Najjar, S. M., and Siragy, H. M. (2013). Targeted Deletion of Murine CEACAM 1 Activates PI3K-Akt signaling and contributes to the expression of (pro)renin receptor via CREB Family and NF-κB transcription factors. *Hypertension* 62, 317–323. doi: 10.1161/HYPERTENSIONAHA.113.01324

Huang, Z., Huang, L., Wang, C., Zhu, S., Qi, X., Chen, Y., et al. (2020). SUN-672 SGLT2 inhibitor reduces hyperinsulinemia and restores pulsatile growth hormone secretion in Obese MC4RKO mice. *J. Endocr. Soc.* 4:672. doi: 10.1210/jendso/bvaa046.1158

Hutton, J. C. (1994). Insulin secretory granule biogenesis and the proinsulin-processing endopeptidases. *Diabetologia* 37, S48–S56. doi: 10.1007/BF00400826

Jaikumkao, K., Pongchaidecha, A., Chueakula, N., Thongnak, L., Wanchai, K., Chatsudthipong, V., et al. (2018). Renal outcomes with sodium glucose cotransporter 2 (SGLT2) inhibitor, dapagliflozin, in obese insulin-resistant model. *Biochim. Biophys. Acta Mol. Basis Dis.* 1864, 2021–2033. doi: 10.1016/j.bbadis.2018.03.017

Jia, T., Huang, X., Qureshi, A. R., Xu, H., Ärnlöv, J., Lindholm, B., et al. (2014). Validation of insulin sensitivity surrogate indices and prediction of clinical outcomes in individuals with and without impaired renal function. *Kidney Int.* 86, 383–391. doi: 10.1038/ki.2014.1

Jung, S.-H., Jung, C.-H., Reaven, G. M., and Kim, S. H. (2018). Adapting to insulin resistance in obesity: role of insulin secretion and clearance. *Diabetologia* 61, 681–687. doi: 10.1007/s00125-017-4511-0

Kalwat, M. A., and Thurmond, D. C. (2013). Signaling mechanisms of glucose-induced F-actin remodeling in pancreatic islet β cells. *Exp. Mol. Med.* 45:e37. doi: 10.1038/emm.2013.73

Kiapidou, S., Liava, C., Kalogirou, M., Akriviadis, E., and Sinakos, E. (2020). Chronic kidney disease in patients with non-alcoholic fatty liver disease: what the Hepatologist should know? *Ann. Hepatol.* 19, 134–144. doi: 10.1016/j.aohep.2019.07.013

Kim, K.-S., Park, S. W., Cho, Y.-W., and Kim, S.-K. (2018). Higher prevalence and progression rate of chronic kidney disease in elderly patients with Type 2 diabetes mellitus. *Diabetes Metab. J.* 42, 224–232. doi: 10.4093/dmj.2017.0065

Kirchner, K. A. (1988). Insulin increases loop segment chloride reabsorption in the euglycemic rat. *Am. J. Physiol. Ren. Fluid Electrolyte Physiol.* 255, F1206–F1213. doi: 10.1152/ajprenal.1988.255.6.f1206

Kobayashi, S., Maesato, K., Moriya, H., Ohtake, T., and Ikeda, T. (2005). Insulin resistance in patients with chronic kidney disease. *Am. J. Kidney Dis.* 2012:691369.doi: 10.1053/j.ajkd.2004.09.034

Kou, S.-W., Hu, Y.-H., and Wu, D.-A. (2014). The response of first and second phase insulin secretion in newly diagnosed type 2 Diabetes Mellitus. *Int. J. Diabetes Clin. Diagnosis* 1:103. doi: 10.15344/2394-1499/2014/103

Krebs, H. A. (1963). Renal gluconeogenesis. *Adv. Enzyme Regul.* 1, 385–400.

Krekels, M., Kroon, A., and de Leeuw, P. (2015). Sodium intake as a modulator of kidney function. *Curr. Hypertens. Rev.* 11, 57–60. doi: 10.2174/1573402111666150530204512

Krycer, J. R., Sharpe, L. J., Luu, W., and Brown, A. J. (2010). The Akt–SREBP nexus: cell signaling meets lipid metabolism. *Trends Endocrinol. Metab.* 21, 268–276. doi: 10.1016/j.tem.2010.01.001

Kubota, N., Kubota, T., Kajiwara, E., Iwamura, T., Kumagai, H., Watanabe, T., et al. (2016). Differential hepatic distribution of insulin receptor substrates causes selective insulin resistance in diabetes and obesity. *Nat. Commun.* 7:12977. doi: 10.1038/ncomms12977

Kumari, M., Sharma, R., Pandey, G., Ecelbarger, C. M., Mishra, P., and Tiwari, S. (2019). Deletion of insulin receptor in the proximal tubule and fasting augment albumin excretion. *J. Cell. Biochem.* 120, 10688–10696. doi: 10.1002/jcb.28359

Kuo, W. L., Montag, A. G., and Rosner, M. R. (1993). Insulin-degrading enzyme is differentially expressed and developmentally regulated in various rat tissues. *Endocrinology* 132, 604–611. doi: 10.1210/endo.132.2.7678795

Kurella, M., Lo, J. C., and Chertow, G. M. (2005). Metabolic syndrome and the risk for chronic kidney disease among nondiabetic adults. *J. Am. Soc. Nephrol.* 16, 2134–2140. doi: 10.1681/ASN.2005010106

Lachin, J. M., Viberti, G., Zinman, B., Haffner, S. M., Aftring, R. P., Paul, G., et al. (2011). Renal function in type 2 diabetes with rosiglitazone,metformin, and glyburide monotherapy. *Clin. J. Am. Soc. Nephrol.* 6, 1032–1040. doi: 10.2215/CJN.09291010

Landau, M., Kurella-Tamura, M., Shlipak, M. G., Kanaya, A., Strotmeyer, E., Koster, A., et al. (2011). Correlates of insulin resistance in older individuals with and without kidney disease. *Nephrol. Dial. Transplant.* 26, 2814–2819. doi: 10.1093/ndt/gfq817

Lay, A., and Coward, R. J. (2014). Recent advances in our understanding of insulin signalling to the podocyte. *Nephrol. Dial. Transplant.* 29, 1127–1133. doi: 10.1093/ndt/gft471

Lay, A. C., Hurcombe, J. A., Betin, V. M. S., Barrington, F., Rollason, R., Ni, L., et al. (2017). Prolonged exposure of mouse and human podocytes to insulin induces insulin resistance through lysosomal and proteasomal degradation of the insulin receptor. *Diabetologia* 60, 2299–2311. doi: 10.1007/s00125-017-4394-0

Lenkkeri, U., Männikkö, M., McCready, P., Lamerdin, J., Gribouval, O., Niaudet, P., et al. (1999). Structure of the Gene for Congenital Nephrotic Syndrome of the Finnish Type (NPHS1) and Characterization of Mutations. *Am. J. Hum. Genet.* 64, 51–61. doi: 10.1086/302182

Li, C., Culver, S. A., Quadri, S., Ledford, K. L., Al-Share, Q. Y., Ghadieh, H. E., et al. (2015). High-fat diet amplifies renal renin angiotensin system expression, blood pressure elevation, and renal dysfunction caused by Ceacam1 null deletion. *Am. J. Physiol. Metab.* 309, E802–E810. doi: 10.1152/ajpendo.00158.2015

Li, L., Garikepati, R. M., Tsukerman, S., Kohan, D., Wade, J. B., Tiwari, S., et al. (2013). Reduced ENaC activity and blood pressure in mice with genetic knockout of the insulin receptor in the renal collecting duct. *Am. J. Physiol. Physiol.* 304, F279–F288. doi: 10.1152/ajprenal.00161.2012

Ling, A. V., Gearing, M. E., Semova, I., Shin, D.-J., Clements, R., Lai, Z. W., et al. (2018). FoxO1 is required for most of the metabolic and hormonal perturbations produced by hepatic insulin receptor deletion in male mice. *Endocrinology* 159, 1253–1263. doi: 10.1210/en.2017-00870

Madhusudhan, T., Wang, H., Dong, W., Ghosh, S., Bock, F., Thangapandi, V. R., et al. (2015). Defective podocyte insulin signalling through p85-XBP1 promotes ATF6-dependent maladaptive ER-stress response in diabetic nephropathy. *Nat. Commun.* 6:6496. doi: 10.1038/ncomms7496

Manhiani, M. M., Cormican, M. T., and Brands, M. W. (2011). Chronic sodium-retaining action of insulin in diabetic dogs. *Am. J. Physiol. Ren. Physiol.* 300, 957–965. doi: 10.1152/ajprenal.00395.2010

Matveyenko, A. V., Liuwantara, D., Gurlo, T., Kirakossian, D., Dalla Man, C., Cobelli, C., et al. (2012). Pulsatile portal vein insulin delivery enhances hepatic insulin action and signaling. *Diabetes Metab. Res. Rev* 61, 2269–2279. doi: 10.2337/db11-1462

Mayer, J. P., Zhang, F., and DiMarchi, R. D. (2007). Insulin structure and function. *Biopolymers* 88, 687–713. doi: 10.1002/bip.20734

McManus, E. J., Sakamoto, K., Armit, L. J., Ronaldson, L., Shpiro, N., Marquez, R., et al. (2005). Role that phosphorylation of GSK3 plays in insulin and Wnt signalling defined by knockin analysis. *EMBO J.* 24, 1571–1583. doi: 10.1038/sj.emboj.7600633

Mima, A., Ohshiro, Y., Kitada, M., Matsumoto, M., Geraldes, P., Li, C., et al. (2011). Glomerular-specific protein kinase C-β-induced insulin receptor substrate-1 dysfunction and insulin resistance in rat models of diabetes and obesity. *Kidney Int.* 79, 883–896. doi: 10.1038/ki.2010.526

Miyazaki, Y., Cersosimo, E., Triplitt, C., and DeFronzo, R. A. (2007). Rosiglitazone decreases albuminuria in type 2 diabetic patients. *Kidney Int.* 72, 1367–1373. doi: 10.1038/sj.ki.5002516

Mok, K. Y., Chan, P. F., Lai, L. K. P., Chow, K. L., and Chao, D. V. K. (2019). Prevalence of diabetic nephropathy among Chinese patients with type 2 diabetes mellitus and different categories of their estimated glomerular filtration rate based on the Chronic Kidney Disease Epidemiology Collaboration (CKD-EPI) equation in primary car. *J. Diabetes Metab. Disord.* 18, 281–288. doi: 10.1007/s40200-018-00382-y

Molinaro, A., Becattini, B., Mazzoli, A., Bleve, A., Radici, L., Maxvall, I., et al. (2019). Insulin-Driven PI3K-AKT signaling in the hepatocyte is mediated by redundant PI3Kα and PI3Kβ activities and is promoted by RAS. *Cell Metab.* 29:1400-1409.e5. doi: 10.1016/j.cmet.2019.03.010

Muscogiuri, G., Chavez, A., Gastaldelli, A., Perego, L., Tripathy, D., Saad, M., et al. (2008). The crosstalk between insulin and renin-angiotensin-aldosterone signaling systems and its effect on glucose metabolism and diabetes prevention. *Curr. Vasc. Pharmacol.* 6, 301–312. doi: 10.2174/157016108785909715

Musso, G., Gambino, R., Tabibian, J. H., Ekstedt, M., Kechagias, S., Hamaguchi, M., et al. (2014). Association of non-alcoholic fatty liver disease with chronic kidney disease: a systematic review and meta-analysis. *PLoS Med.* 11:e1001680. doi: 10.1371/journal.pmed.1001680

Mykkänen, L., Zaccaro, D. J., Wagenknecht, L. E., Robbins, D. C., Gabriel, M., and Haffner, S. M. (1998). Microalbuminuria is associated with insulin resistance in nondiabetic subjects: the insulin resistance atherosclerosis study. *Diabetes Metab. Res. Rev.* 47, 793–800. doi: 10.2337/diabetes.47.5.793

Naderpoor, N., Lyons, J. G., Mousa, A., Ranasinha, S., de Courten, M. P. J., Soldatos, G., et al. (2017). Higher glomerular filtration rate is related to insulin resistance but not to obesity in a predominantly obese non-diabetic cohort. *Sci. Rep.* 7:45522. doi: 10.1038/srep45522

Najjar, S. M., and Perdomo, G. (2019). Hepatic insulin clearance: mechanism and physiology. *Physiology* 34, 198–215. doi: 10.1152/physiol.00048.2018

Nakamura, M., Tsukada, H., Seki, G., Satoh, N., Mizuno, T., Fujii, W., et al. (2020). Insulin promotes sodium transport but suppresses gluconeogenesis via distinct cellular pathways in human and rat renal proximal tubules. *Kidney Int.* 97, 316–326. doi: 10.1016/j.kint.2019.08.021

Nakamura, N., Matsui, T., Ishibashi, Y., and Yamagishi, S. (2015). Insulin stimulates SGLT2-mediated tubular glucose absorption via oxidative stress generation. *Diabetol. Metab. Syndr.* 7:48. doi: 10.1186/s13098-015-0044-1

Narahara, H. T., Everett, N. B., Simmons, B. S., and Williams, R. H. (1958). Metabolism of Insulin-I 131 and Glucagon-I 131 in the Kidney of the Rat. *Am. J. Physiol. Content* 192, 227–231. doi: 10.1152/ajplegacy.1958.192.2.227

Ng, Y., Ramm, G., Lopez, J. A., and James, D. E. (2008). Rapid Activation of Akt2 is sufficient to stimulate GLUT4 translocation in 3T3-L1 adipocytes. *Cell Metab.* 7, 348–356. doi: 10.1016/j.cmet.2008.02.008

Nickenig, G., Röling, J., Strehlow, K., Schnabel, P., and Böhm, M. (1998). Insulin induces upregulation of vascular receptor gene expression by posttranscriptional mechanisms. *Circulation* 98, 2453–2460. doi: 10.1161/01.CIR.98.22.2453

Nissen, S. E., and Wolski, K. (2007). Effect of rosiglitazone on the risk of myocardial infarction and death from cardiovascular causes. *N. Engl. J. Med.* 356, 2457–2471. doi: 10.1056/NEJMoa072761

Oh, S.-Y., Park, S.-K., Kim, J.-W., Ahn, Y.-H., Park, S.-W., and Kim, K.-S. (2003). Acetyl-CoA Carboxylase β gene is regulated by sterol regulatory element-binding protein-1 in liver. *J. Biol. Chem.* 278, 28410–28417. doi: 10.1074/jbc.M300553200

Olofsson, C. S., Göpel, S. O., Barg, S., Galvanovskis, J., Ma, X., Salehi, A., et al. (2002). Fast insulin secretion reflects exocytosis of docked granules in mouse pancreatic B-cells. *Pflügers Arch.* 444, 43–51. doi: 10.1007/s00424-002-0781-5

Pagtalunan, M. E., Miller, P. L., Jumping-Eagle, S., Nelson, R. G., Myers, B. D., Rennke, H. G., et al. (1997). Podocyte loss and progressive glomerular injury in type II diabetes. *J. Clin. Invest.* 99, 342–348. doi: 10.1172/JCI119163

Perkovic, V., Jardine, M. J., Neal, B., Bompoint, S., Heerspink, H. J. L., Charytan, D. M., et al. (2019). Canagliflozin and Renal Outcomes in Type 2 Diabetes and Nephropathy. *N. Engl. J. Med.* 380, 2295–2306. doi: 10.1056/NEJMoa1811744

Petersen, M. C., and Shulman, G. I. (2018). Mechanisms of Insulin Action and Insulin Resistance. *Physiol. Rev.* 98, 2133–2223. doi: 10.1152/physrev.00063.2017

Pilz, S., Rutters, F., Nijpels, G., Stehouwer, C. D. A., HØjlund, K., Nolan, J. J., et al. (2014). Insulin sensitivity and albuminuria: the risc study. *Diabetes Care* 37, 1597–1603. doi: 10.2337/dc13-2573

Piwkowska, A., Rogacka, D., Kasztan, M., Angielski, S., and Jankowski, M. (2013). Insulin increases glomerular filtration barrier permeability through dimerization of protein kinase G type Iα subunits. *Biochim. Biophys. Acta Mol. Basis Dis.* 1832, 791–804. doi: 10.1016/j.bbadis.2013.02.011

Plum, L. (2006). Central insulin action in energy and glucose homeostasis. *J. Clin. Invest.* 116, 1761–1766. doi: 10.1172/JCI29063

Poy, M. N., Yang, Y., Rezaei, K., Fernström, M. A., Lee, A. D., Kido, Y., et al. (2002). CEACAM1 regulates insulin clearance in liver. *Nat. Genet.* 30, 270–276. doi: 10.1038/ng840

Prentki, M., and Matschinsky, F. M. (1987). Ca2+, cAMP, and phospholipid-derived messengers in coupling mechanisms of insulin secretion. *Physiol. Rev.* 67, 1185–1248. doi: 10.1152/physrev.1987.67.4.1185

Qiu, H., Yang, J.-K., and Chen, C. (2017). Influence of insulin on growth hormone secretion, level and growth hormone signalling. *Sheng Li Xue Bao* 69, 541–556. doi: 10.13294/j.aps.2017.0062

Rabkin, R., Ryan, M. P., and Duckworth, W. C. (1984). The renal metabolism of insulin. *Diabetologia* 27, 351–357. doi: 10.1007/BF00304849

Rave, K., Nosek, L., Posner, J., Heise, T., Roggen, K., and van Hoogdalem, E. J. (2006). Renal glucose excretion as a function of blood glucose concentration in subjects with type 2 diabetes - Results of a hyperglycaemic glucose clamp study. *Nephrol. Dial. Transplant.* 21, 2166–2171. doi: 10.1093/ndt/gfl175

Ricketts, H. T., and Wildberger, H. L. (1962). The effect of renal disease on the degradation of insulin. *Trans. Am. Clin. Climatol. Assoc.* 74, 102–108.

Ritz, E., Adamczak, M., and Wiecek, A. (2013). *Carbohydrate Metabolism in Kidney Disease and Kidney Failure*. Amsterdam: Elsevier Inc, doi: 10.1016/B978-0-12-391934-2.00002-3

Roder, K., Zhang, L., and Schweizer, M. (2007). SREBP-1c mediates the retinoid-dependent increase in fatty acid synthase promoter activity in HepG2. *FEBS Lett.* 581, 2715–2720. doi: 10.1016/j.febslet.2007.05.022

Rowe, J. W., Young, J. B., Minaker, K. L., Stevens, A. L., Pallotta, J., and Landsberg, L. (1981). Effect of insulin and glucose infusions on sympathetic nervous system activity in normal man. *Diabetes Metab. Res. Rev.* 30, 219–225. doi: 10.2337/diab.30.3.219

Rubenstein, A. H., Lowy, C., Welborn, T. A., and Fraser, T. R. (1967). Urine insulin in normal subjects. *Metabolism* 16, 234–244. doi: 10.1016/0026-0495(67)90172-2

Rubenstein, A. H., and Spitz, I. (1968). Role of the kidney in insulin metabolism and excretion. *Diabetes Metab. Res. Rev.* 17, 161–169. doi: 10.2337/diab.17.3.161

Ruiz, O. S., Qiu, Y.-Y., Cardoso, L. R., and Arruda, J. A. L. (1998). Regulation of the renal Na–HCO3 cotransporter: IX. Modulation by insulin, epidermal growth factor and carbachol. *Regul. Pept.* 77, 155–161. doi: 10.1016/S0167-0115(98)00115-3

Russo, L., Muturi, H. T., Ghadieh, H. E., Ghanem, S. S., Bowman, T. A., Noh, H. L., et al. (2017). Liver-specific reconstitution of CEACAM1 reverses the metabolic abnormalities caused by its global deletion in male mice. *Diabetologia* 60, 2463–2474. doi: 10.1007/s00125-017-4432-y

Sánchez-Villanueva, R., Estrada, P., Del Peso, G., Grande, C., Díez, J. J., Iglesias, P., et al. (2013). Repeated analysis of estimated insulin resistance using the HOMAIR index in nondiabetic patients on peritoneal dialysis and its relationship with cardiovascular disease and mortality. *Nefrologia* 33, 85–92. doi: 10.3265/Nefrologia.pre2012.Nov.11430

Sanders, F. W. B., and Griffin, J. L. (2016). De novo lipogenesis in the liver in health and disease: more than just a shunting yard for glucose. *Biol. Rev.* 91, 452–468. doi: 10.1111/brv.12178

Santamaria, B., Marquez, E., Lay, A., Carew, R. M., González-Rodríguez, Á, Welsh, G. I, et al. (2015). IRS2 and PTEN are key molecules in controlling insulin sensitivity in podocytes. *Biochim. Biophys. Acta Mol. Cell Res.* 1853, 3224–3234. doi: 10.1016/j.bbamcr.2015.09.020

Sarafidis, P. A., Stafylas, P. C., Georgianos, P. I., Saratzis, A. N., and Lasaridis, A. N. (2010). Effect of thiazolidinediones on albuminuria and proteinuria in diabetes: a meta-analysis. *Am. J. Kidney Dis.* 55, 835–847. doi: 10.1053/j.ajkd.2009.11.013

Sarzani, R., Dessì-Fulgheri, P., Salvi, F., Serenelli, M., Spagnolo, D., Cola, G., et al. (1999). A novel promoter variant of the natriuretic peptide clearance receptor gene is associated with lower atrial natriuretic peptide and higher blood pressure in obese hypertensives. *J. Hypertens.* 17, 1301–1305. doi: 10.1097/00004872-199917090-00010

Sasaki, M., Sasako, T., Kubota, N., Sakurai, Y., Takamoto, I., Kubota, T., et al. (2017). Dual regulation of gluconeogenesis by insulin and glucose in the proximal tubules of the kidney. *Diabetes Metab. Res. Rev* 66, 2339–2350. doi: 10.2337/db16-1602

Satoh, N., Nakamura, M., Suzuki, M., Suzuki, A., Seki, G., and Horita, S. (2015). Roles of Akt and SGK1 in the regulation of renal tubular transport. *Biomed Res. Int.* 2015, 1–8. doi: 10.1155/2015/971697

Shinohara, K., Shoji, T., Emoto, M., Tahara, H., Koyama, H., Ishimura, E., et al. (2002). Insulin resistance as an independent predictor of cardiovascular mortality in patients with end-stage renal disease. *J. Am. Soc. Nephrol.* 13, 1894–1900. doi: 10.1097/01.ASN.0000019900.87535.43

Skolnik, E. Y., Batzer, A., Li, N., Lee, C. H., Lowenstein, E., Mohammadi, M., et al. (1993). The function of GRB2 in linking the insulin receptor to Ras signaling pathways. *Science* 260, 1953–1955. doi: 10.1126/science.8316835

Song, S. H., McIntyre, S. S., Shah, H., Veldhuis, J. D., Hayes, P. C., and Butler, P. C. (2000). Direct measurement of pulsatile insulin secretion from the portal vein in human subjects 1. *J. Clin. Endocrinol. Metab.* 85, 4491–4499. doi: 10.1210/jcem.85.12.7043

Sowers, J. R., Epstein, M., and Frohlich, E. D. (2001). Diabetes, hypertension, and cardiovascular disease an update. *Hypertension* 37, 1053–1059. doi: 10.1161/01.HYP.37.4.1053

Spoto, B., Pisano, A., and Zoccali, C. (2016). Insulin resistance in chronic kidney disease: a systematic review. *Am. J. Physiol. Renal Physiol.* 311, F1087–F1108. doi: 10.1152/ajprenal.00340.2016

Stechi, L. A., De Carll, S., and Bartoll, E. (1994). In situ characterization of renal insulin receptors in the rat. *J. Recept. Res.* 14, 347–356. doi: 10.3109/10799899409101509

Steiner, D. F. (2004). The proinsulin c-peptide—a multirole model. *Exp. Diabesity Res.* 5, 7–14. doi: 10.1080/15438600490424389

Susztak, K., Raff, A. C., Schiffer, M., and Bottinger, E. P. (2006). Glucose-induced reactive oxygen species cause apoptosis of podocytes and podocyte depletion at the onset of diabetic nephropathy. *Diabetes Metab. Res. Rev* 55, 225–233. doi: 10.2337/diabetes.55.01.06.db05-0894

Svensson, M., and Eriksson, J. W. (2006). Insulin resistance in diabetic nephropathy — cause or consequence? *Diabetes. Metab. Res. Rev.* 22, 401–410. doi: 10.1002/dmrr.648

Talor, Z., Emmanouel, D. S., and Katz, A. I. (1982). Insulin binding and degradation by luminal and basolateral tubular membranes from rabbit kidney. *J. Clin. Invest.* 69, 1136–1146. doi: 10.1172/JCI110549

Taniguchi, C. M., Emanuelli, B., and Kahn, C. R. (2006). Critical nodes in signalling pathways: insights into insulin action. *Nat. Rev. Mol. Cell Biol.* 7, 85–96. doi: 10.1038/nrm1837

Tejada, T., Catanuto, P., Ijaz, A., Santos, J. V., Xia, X., Sanchez, P., et al. (2008). Failure to phosphorylate AKT in podocytes from mice with early diabetic nephropathy promotes cell death. *Kidney Int.* 73, 1385–1393. doi: 10.1038/ki.2008.109

Thirone, A. C. P., Huang, C., and Klip, A. (2006). Tissue-specific roles of IRS proteins in insulin signaling and glucose transport. *Trends Endocrinol. Metab.* 17, 70–76. doi: 10.1016/j.tem.2006.01.005

Tiwari, S., Sharma, N., Gill, P. S., Igarashi, P., Kahn, C. R., Wade, J. B., et al. (2008). Impaired sodium excretion and increased blood pressure in mice with targeted deletion of renal epithelial insulin receptor. *Proc. Natl. Acad. Sci. U.S.A.* 105, 6469–6474. doi: 10.1073/pnas.0711283105

Tiwari, S., Singh, R. S., Li, L., Tsukerman, S., Godbole, M., Pandey, G., et al. (2013). Deletion of the insulin receptor in the proximal tubule promotes hyperglycemia. *J. Am. Soc. Nephrol.* 24, 1209–1214. doi: 10.1681/ASN.2012060628

Tokarz, V. L., MacDonald, P. E., and Klip, A. (2018). The cell biology of systemic insulin function. *J. Cell Biol.* 217, 2273–2289. doi: 10.1083/jcb.201802095

Vallon, V., Platt, K. A., Cunard, R., Schroth, J., Whaley, J., Thomson, S. C., et al. (2011). SGLT2 mediates glucose reabsorption in the early proximal tubule. *J. Am. Soc. Nephrol.* 22, 104–112. doi: 10.1681/ASN.2010030246

Villarreal, R., Mitrofanova, A., Maiguel, D., Morales, X., Jeon, J., Grahammer, F., et al. (2016). Nephrin contributes to insulin secretion and affects mammalian target of rapamycin signaling independently of insulin receptor. *J. Am. Soc. Nephrol.* 27, 1029–1041. doi: 10.1681/ASN.2015020210

Wang, X. L., Lu, J. M., Pan, C. Y., Tian, H., and Li, C. L. (2005). A comparison of urinary albumin excretion rate and microalbuminuria in various glucose tolerance subjects. *Diabet. Med.* 22, 332–335. doi: 10.1111/j.1464-5491.2004.01408.x

Welsh, G. I., Hale, L. J., Eremina, V., Jeansson, M., Maezawa, Y., Lennon, R., et al. (2010). Insulin signaling to the glomerular podocyte is critical for normal kidney function. *Cell Metab.* 12, 329–340. doi: 10.1016/j.cmet.2010.08.015

Williams, D. M., Nawaz, A., and Evans, M. (2020). Renal outcomes in type 2 diabetes: a review of cardiovascular and renal outcome trials. *Diabetes Ther.* 11, 369–386. doi: 10.1007/s13300-019-00747-3

Wolf, G., Chen, S., and Ziyadeh, F. N. (2005). From the periphery of the glomerular capillary wall toward the center of disease: podocyte injury comes of age in diabetic nephropathy. *Diabetes Metab. Res. Rev.* 54, 1626–1634. doi: 10.2337/diabetes.54.6.1626

Wright, E. M., Loo, D. D. F., and Hirayama, B. A. (2011). Biology of Human Sodium Glucose Transporters. *Physiol. Rev.* 91, 733–794. doi: 10.1152/physrev.00055.2009

Xu, H., Huang, X., Ärnlöv, J., Cederholm, T., Stenvinkel, P., Lindholm, B., et al. (2014). Clinical correlates of insulin sensitivity and its association with mortality among men with CKD stages 3 and 4. *Clin. J. Am. Soc. Nephrol.* 9, 690–697. doi: 10.2215/CJN.05230513

Xu, J., Keeton, A. B., Franklin, J. L., Li, X., Venable, D. Y., Frank, S. J., et al. (2006). Insulin enhances growth hormone induction of the MEK/ERK signaling pathway. *J. Biol. Chem.* 281, 982–992. doi: 10.1074/jbc.M505484200

Xu, J., and Messina, J. L. (2009). "Crosstalk between growth hormone and insulin signaling," in *Vitamins and Hormones*, Ed. G. Litwack (Amsterdam: Elsevier Inc), 125–153. doi: 10.1016/S0083-6729(08)00606-7

Yamada, T., Katagiri, H., Asano, T., Tsuru, M., Inukai, K., Ono, H., et al. (2002). Role of PDK1 in insulin-signaling pathway for glucose metabolism in 3T3-L1 adipocytes. *Am. J. Physiol. Metab.* 282, E1385–E1394. doi: 10.1152/ajpendo.00486.2001

Ye, L., Maji, S., Sanghera, N., Gopalasingam, P., Gorbunov, E., Tarasov, S., et al. (2017). Structure and dynamics of the insulin receptor: implications for receptor activation and drug discovery. *Drug Discov. Today* 22, 1092–1102. doi: 10.1016/j.drudis.2017.04.011

Yip, J., Mattock, M. B., Morocutti, A., Sethi, M., Trevisan, R., and Viberti, G. (1993). Insulin resistance in insulin-dependent diabetic patients with microalbuminuria. *Lancet* 342, 883–887. doi: 10.1016/0140-6736(93)91943-G

Yki-Järvinen, H. (2004). Thiazolidinediones. *N. Engl. J. Med.* 351, 1106–1118. doi: 10.1056/NEJMra041001

Zorzano, A., Munoz, P., Camps, M., Mora, C., Testar, X., and Palacin, M. (1996). Insulin-Induced Redistribution of GLUT4 Glucose Carriers in the Muscle Fiber: in Search of GLUT4 Trafficking Pathways. *Diabetes* 45, S70–S81. doi: 10.2337/diab.45.1.S70

Zubrod, C. G., Eversole, S. L., and Dana, G. W. (1951). Amelioration of diabetes and striking rarity of acidosis in patients with kimmelstiel-wilson lesions. *N. Engl. J. Med.* 245, 518–525. doi: 10.1056/NEJM195110042451402

Conflict of Interest: The authors declare that the research was conducted in the absence of any commercial or financial relationships that could be construed as a potential conflict of interest.

Copyright © 2020 Pina, Borges, Meneses, Branco, Birne, Vilasi and Macedo. This is an open-access article distributed under the terms of the Creative Commons Attribution License (CC BY). The use, distribution or reproduction in other forums is permitted, provided the original author(s) and the copyright owner(s) are credited and that the original publication in this journal is cited, in accordance with accepted academic practice. No use, distribution or reproduction is permitted which does not comply with these terms.

frontiers in Cell and Developmental Biology

ORIGINAL RESEARCH
published: 15 October 2020
doi: 10.3389/fcell.2020.561907

DNA Methylation Associated With Diabetic Kidney Disease in Blood-Derived DNA

*Laura J. Smyth[1], Christopher C. Patterson[1], Elizabeth J. Swan[1], Alexander P. Maxwell[1,2] and Amy Jayne McKnight[1]**

[1] Centre for Public Health, Queen's University Belfast, Belfast, United Kingdom, [2] Regional Nephrology Unit, Belfast City Hospital, Belfast, United Kingdom

A subset of individuals with type 1 diabetes will develop diabetic kidney disease (DKD). DKD is heritable and large-scale genome-wide association studies have begun to identify genetic factors that influence DKD. Complementary to genetic factors, we know that a person's epigenetic profile is also altered with DKD. This study reports analysis of DNA methylation, a major epigenetic feature, evaluating methylome-wide loci for association with DKD. Unique features (n = 485,577; 482,421 CpG probes) were evaluated in blood-derived DNA from carefully phenotyped White European individuals diagnosed with type 1 diabetes with (cases) or without (controls) DKD (n = 677 samples). Explicitly, 150 cases were compared to 100 controls using the 450K array, with subsequent analysis using data previously generated for a further 96 cases and 96 controls on the 27K array, and *de novo* methylation data generated for replication in 139 cases and 96 controls. Following stringent quality control, raw data were quantile normalized and beta values calculated to reflect the methylation status at each site. The difference in methylation status was evaluated between cases and controls; resultant P-values for array-based data were adjusted for multiple testing. Genes with significantly increased (hypermethylated) and/or decreased (hypomethylated) levels of DNA methylation were considered for biological relevance by functional enrichment analysis using KEGG pathways. Twenty-two loci demonstrated statistically significant fold changes associated with DKD and additional support for these associated loci was sought using independent samples derived from patients recruited with similar inclusion criteria. Markers associated with *CCNL1* and *ZNF187* genes are supported as differentially regulated loci ($P < 10^{-8}$), with evidence also presented for *AFF3*, which has been identified from a meta-analysis and subsequent replication of genome-wide association studies. Further supporting evidence for differential gene expression in CCNL1 and ZNF187 is presented from kidney biopsy and blood-derived RNA in people with and without kidney disease from NephroSeq. Evidence confirming that methylation sites influence the development of DKD may aid risk prediction tools and stimulate research to identify epigenomic therapies which might be clinically useful for this disease.

Keywords: epigenetic, diabetes, kidney, renal, methylation, association

OPEN ACCESS

Edited by:
Masaru Katoh,
National Cancer Center, Japan

Reviewed by:
Lucas A. Salas,
Dartmouth College, United States
Harvest F. Gu,
China Pharmaceutical University, China

***Correspondence:**
Amy Jayne McKnight
a.j.mcknight@qub.ac.uk

Specialty section:
This article was submitted to Molecular Medicine, a section of the journal Frontiers in Cell and Developmental Biology

Received: *14 May 2020*
Accepted: *15 September 2020*
Published: *15 October 2020*

Citation:
Smyth LJ, Patterson CC, Swan EJ, Maxwell AP and McKnight AJ (2020) DNA Methylation Associated With Diabetic Kidney Disease in Blood-Derived DNA. Front. Cell Dev. Biol. 8:561907. doi: 10.3389/fcell.2020.561907

INTRODUCTION

Diabetes and associated complications are major personal and public health concerns, with diabetic kidney disease (DKD) contributing a substantial financial burden to healthcare providers (Franciosi et al., 2013; Campbell et al., 2017; Arredondo et al., 2018; Disease et al., 2018; Kawaguchi et al., 2020). DKD develops in approximately one-third of individuals with diabetes and remains the most common primary diagnosis of chronic kidney disease (CKD) leading to end-stage kidney disease (ESKD) worldwide (Hill et al., 2014; US Renal and Data System., 2018; Lassalle et al., 2019; UK Renal Registry, 2019). Current treatments are based on modification of risk factors and include the reduction in elevated blood pressure, hyperglycemia and hyperlipidemia. Epidemiological evidence confirms that heritable factors play a major role in the development and progression of DKD, but despite the identification of several genetic loci associated with DKD most of the inherited risk factors remain unknown (Sandholm et al., 2012, 2013, 2014, 2017; Canadas-Garre et al., 2018, 2019; van Zuydam et al., 2018; Fu et al., 2019; Salem et al., 2019).

Emerging evidence for epigenetic phenomena has transformed investigations of heritable influences on disease and, complementary to genome-wide association studies (GWAS), it is now cost-effective to perform population-based studies of the epigenome (Rakyan et al., 2011b; Canadas-Garre et al., 2018; Kato and Natarajan, 2019; Kerr et al., 2020). Epigenetic modifications modulate gene expression without changing the DNA sequence; these may be either stably inherited or dynamic epigenetic marks. Methylation is a key epigenetic feature that plays an important role in chromosomal integrity and regulation of gene expression with different methylation profiles now being associated with many complex diseases (Murphy and Mill, 2014; Greenberg and Bourc'his, 2019; Bayoumi et al., 2020; Hoang et al., 2020). Epigenome-wide association studies (EWAS) have revealed methylation features associated with type 1 diabetes (Rakyan et al., 2011a; Stefan et al., 2014; Elboudwarej et al., 2016), gestational diabetes (Haertle et al., 2017; Dias et al., 2019; Howe et al., 2020), and type 2 diabetes (Florath et al., 2016; Walaszczyk et al., 2018; Ochoa-Rosales et al., 2020). EWAS have also identified methylation features associated with chronic kidney disease (Smyth et al., 2014a,b, 2018; Chu et al., 2017; Qiu et al., 2018).

Differential DNA methylation has been associated with "metabolic memory" of glycemic control and with a higher risk of developing DKD (Swan et al., 2015; Keating et al., 2018; Aranyi and Susztak, 2019; Gluck et al., 2019; Gu, 2019; Jia et al., 2019; Park et al., 2019). As DKD is not clinically detectable until significant organ damage has developed (albuminuria and/or reduced eGFR), more effective diagnostic tools and treatments, guided by a better understanding of pathophysiology, are urgently required. The identification of novel epigenetic risk markers and biological pathways influencing DKD would contribute more to the understanding of this serious diabetic complication. This manuscript describes an EWAS from carefully phenotyped individuals who were specifically recruited to investigate molecular risk factors for DKD in people with type 1 diabetes, followed by *in silico* and *de novo* replication. Our overarching aim is to identify differentially methylated CpG sites associated with DKD.

MATERIALS AND METHODS

Participants

All recruited individuals provided written, informed consent and this study was approved by a United Kingdom Multicentre Research Ethics Committee (MREC/98/6/71). The discovery group comprised a subset of individuals (150 cases compared to 100 controls) selected from an established United Kingdom case-control collection that was recruited specifically to investigate risk factors for DKD (McKnight et al., 2010). One-third of the case group had end stage renal disease (ESRD). All individuals were White, from the United Kingdom and were diagnosed with type 1 diabetes prior to the age of 31 years. Participants in the case group had persistent proteinuria (>0.5 g protein/24 h) at least 10 years after diagnosis of diabetes, hypertension (BP > 135/85 mmHg or treatment with antihypertensive agents) and diabetic retinopathy. Individuals in the control group had at least 15 years duration of type 1 diabetes with normal renal function and were not receiving antihypertensive treatment. Cases and controls in the discovery group were matched for age, gender and duration of diabetes. The *in silico* replication groups comprised independent samples from the remainder of this collection and had similar characteristics to those involved in the discovery group. Similarly, all individuals included in the *de novo* typing phase were selected using blood-derived DNA from the larger collection (**Table 1**).

Methylation Typing

482,421 unique CpG features were evaluated in the discovery group. Existing blood-derived DNA [extracted using the salting-out method as previously described (Bell et al., 2010)] was accurately quantitated using PicoGreen®, normalized, and bisulfite treated using the EZ-96 DNA Methylation-Gold™ Kit (Zymo Research, Irvine, CA, United States) with case and control samples randomly distributed across plates. The Infinium Human Methylation 450K BeadChip (Sandoval et al., 2011) (Illumina Inc., San Diego, CA, United States) was employed according to manufacturer's instructions. Raw data were adjusted for dye bias and quantile normalized at the probe level with data derived from sites using Infinium I or Infinium II assay chemistry considered separately. This high-throughput platform enables quantitative evaluation of methylation levels with single nucleotide resolution, generating a methylation score per individual (a β value ranging from 0 for unmethylated to 1 representing complete methylation) for each CpG site.

In silico support for candidate loci was sought using normalized data available at the Gene Expression Omnibus accession GSE20067 (Bell et al., 2010). We previously analyzed 27,578 CpGs based on data from the Illumina Infinium® HumanMethylation27 BeadChip in 192 individuals diagnosed as having type 1 diabetes with and without nephropathy using time to event (duration of diabetes until nephropathy) analysis (Bell et al., 2010).

TABLE 1 | Clinical characteristics of individuals participating in this study.

	Discovery		*In silico* replication		*De novo* typing†	
	case	control	case	control	case	control
N	150	100	96	96	139	96
Age at diagnosis (year)	15.8 ± 7.3	16.0 ± 7.1	16.2	16.3	16.86 ± 7.9	12.5 ± 7.3
Duration of diabetes (year)	26.6 ± 8.8	27.1 ± 8.6	27.5	27.8	30.1 ± 8.8	23.2 ± 7.4
HBA_{1c} (%)	8.9 ± 2.0	8.8 ± 1.6	Not reported	Not reported	10.1 ± 2.0	9.5 ± 1.6
HBA_{1c} (mmol/mol from www.ngsp.org/convert1.asp)	74	73			87	80
Male (%)	49	49	50.0	49.0	54.0	41.7

†De novo genotyping group includes several individuals that were part of the in silico replication for cg02399570 and cg04861640 markers, which were not analyzed on the HumanMethylation27 BeadChip.

De novo replication was performed using Sequenom Epityper assays (Sequenom Inc., Hamburg, Germany). Sequenom facilitates the quantitative analysis of DNA methylation using matrix-assisted laser desorption ionization time-of-flight mass spectrometry. Assays were designed using the default settings (except mass window range changed to 1500–8000) at www.epidesigner.com. Amplicons were carefully designed to cover target sites, results were generated following the manufacturer's protocol and data analyzed using Epityper viewer 1.2 (Sequenom). An additional 235 independent individuals were typed as part of the replication population for *de novo* confirmation with the threshold for significance set at $P < 0.05$ without adjustment for multiple testing (**Table 1**).

Analysis

For the discovery cohort, stringent quality control included evaluation of bisulfite conversion efficiency, staining, hybridization, target removal, extension, dye specificity and 600 integral negative controls. Samples were excluded where more than 10% of probes did not generate useful data and all sites with poor detection *P*-values (detection $P \geq 0.05$) were set to "missing." Known non-CpG targeting probes (n = 3,091) were excluded from all results (Chen et al., 2013; Zhou et al., 2017). Probes on autosomes were evaluated for association with DKD adjusted for sex, duration of diabetes, age at diagnosis, and HBA_{1c} with subgroup analysis performed for cases with ESRD. Sex-specific analysis was performed for probes on chromosome X. Converting intensity levels to beta values and initial preprocessing were performed using the default settings within GenomeStudio's methylation module v1.9 (Illumina) (Smyth et al., 2014b). Principal component analysis and multi-dimensional scaling were employed and potential outliers from gender, non-White ethnicity or experimental batch effects were excluded from further investigation. Proportional white cell counts from whole blood (B cells, granulocytes, monocytes, NK cells, and T cells subsets) were estimated using Houseman's and Reinius' approaches (Houseman et al., 2012; Reinius et al., 2012). Microarray quality control metrics reports were generated using the arrayQualityMetrics package with the recommended parameters in Bioconductor (Kauffmann and Huber, 2010); arrays that did not pass the default quality control thresholds were excluded from further analysis. After correction for dye bias, raw data were normalized using quantile normalization using methylumi[1]. The Bioconductor package Limma (Wettenhall and Smyth, 2004; Ritchie et al., 2015) was used to generate association results. Significance values for the 450K array-based analysis were adjusted for multiple testing using the Benjamini & Hochberg, "fdr" adjustment, implemented in limma and reported as adjusted *p*-values.

For *in silico* replication, previously generated association data from the Illumina Infinium® HumanMethylation27 BeadChip for 192 individuals diagnosed as having type 1 diabetes with and without kidney disease (Bell et al., 2010) was "looked up."

For *de novo* replication, new genotype data was generated using Sequenom's MassARRAY® System. Sequenom-based data were analyzed by the large samples *z* test statistic with regression analysis to adjust for sex, duration of diabetes, age at diagnosis, and $HBA_{1c.}$ The area under the receiver operating characteristic (ROC) curve was generated using SPSS (version 15) to assess the ability of a CpG to distinguish between cases and controls.

In silico functional support for replicated loci was sought from datasets within NephroSeq (last accessed 14th September 2020)[2] for publicly available gene expression data using a *p*-value threshold of 0.05 and a fold change of at least 1.5.

To investigate if SNPs from our GWAS for DKD were located near differentially methylated CpG probes, SNPs in key chromosomal locations (5 kb flanking top ranked markers or their associated genes) were evaluated for association with DKD using publicly available data from our genome-wide association study (dbGAP phs000389.v1.p1); for SNP-based association analysis of this GWAS data, *P*-values were corrected by genomic control and adjusted for age at diagnosis, duration of diabetes, gender, biochemistry center and the first ten components of the study specific principal component analysis (Sandholm et al., 2012).

Provisionally significant genes (adjusted $P < 0.0001$) were analyzed for enrichment of KEGG pathway membership; enrichment was assessed for genes that showed increased or decreased methylation values separately. Additionally, DAVID Bioinformatics Resources 6.7 was interrogated for top-ranked gene results in the genetic association database, Online Mendelian Inheritance in Man, Kyoto Encyclopedia of Genes and

[1]http://tinyurl.com/methylumi

[2]www.nephroseq.org

Genomes (KEGG) pathways and articles recorded in PubMed (Huang da et al., 2009).

RESULTS

Greater than 99% concordance was observed between duplicate samples and experimentally defined genders matched each individual submitted for analysis based on Y-chromosome specific loci. Experimental controls generated expected results, but 5 arrays were identified as outliers and were thus removed from all subsequent analyses. There was no significant difference in the estimated proportional white cell counts between case and control groups (**Supplementary Table 1**). *In silico* adjustment for white cell composition does not alter the top-ranked genes associated with DKD in this study. As the discovery collection included 250 individuals, only CpGs with a sizable, significant difference in DNA methylation ($\Delta\beta$) were considered for subsequent analysis (**Figure 1**). Twenty-two unique sites were identified with $\Delta\beta \geq 0.2$ and $P < 10^{-8}$ where significance values were adjusted for multiple testing using the Benjamini & Hochberg method for controlling the false discovery rate (FDR). These sites are primarily "promoter associated" and affect 22 genes (**Table 2**); all 22 sites were taken forward for *in silico* and wet-lab replication. Subgroup analysis comparing those individuals who received a kidney transplant for DKD with controls show that 20 of these 22 sites were also highlighted in the ESRD focused dataset (**Table 2**). Sex-specific analyses for cg26399113 on the X chromosome was significant from female only ($P = 1 \times 10^{-12}$) and male only ($P = 8.9 \times 10^{-11}$) analyses. The discovery group generated results for 15 CpGs in the *CCNL1* gene, of which 12 showed an increase in methylation between cases and controls. Similarly for *ZNF187*, nine CpGs were examined of which eight showed differential methylation and all were in the same direction as the index marker.

Functional enrichment analysis for differentially regulated loci (adjusted $P < 0.0001$) in the discovery group revealed both hypermethylation and hypomethylation across several pathways. Top ranked pathways enriched with significant probes include genes in Wnt signaling pathway (04310, enrichment $P = 3.9 \times 10^{-5}$), focal adhesion (04510, enrichment $P = 7.9 \times 10^{-5}$), MAPK signaling (04010, enrichment $P = 1.0 \times 10^{-10}$) pathways. Annotation from DAVID Bioinformatics Resources 6.7 for top-ranked genes is presented in **Supplementary Table 2**.

Several SNPs from our British - Irish genome-wide association study revealed nominal significance for SNPs in the region of interest from the 450K discovery analysis. The SNP demonstrating most evidence for association with DKD within 5 kb flanking top-ranked methylation probes are presented in **Supplementary Table 3**. Rs16888186 showed the most evidence for association in the *DST* gene with $P = 0.0008$.

In silico replication data were available for six probes on the 27K array (cg25418748, cg07979357, cg21935083, cg21829265, cg24115040, cg26399113), but none of these sites confirmed differential methylation levels between cases and controls. *De novo* replication gave *z* test *P*-values supporting the association of two loci: cg02399570 on 3q25.31 in the *CCNL1* gene, $P = 7.2 \times 10^{-14}$ and cg04861640 on 6p21.31 in the *ZNF187* gene, $P = 1.5 \times 10^{-15}$ (**Figure 2**). Selecting a β level of 25% (as standard for unmethylated loci), the area under the ROC curve was 0.74 for cg02399570 and 0.81 for cg04861640 (**Figure 2**).

Multiple significant analyses for *CCNL1* gene expression associated with kidney function were returned from NephroSeq (**Supplementary Figure 1**). Higgins et al. (2004) observed that *CCNL1* is more highly expressed in renal glomeruli than other

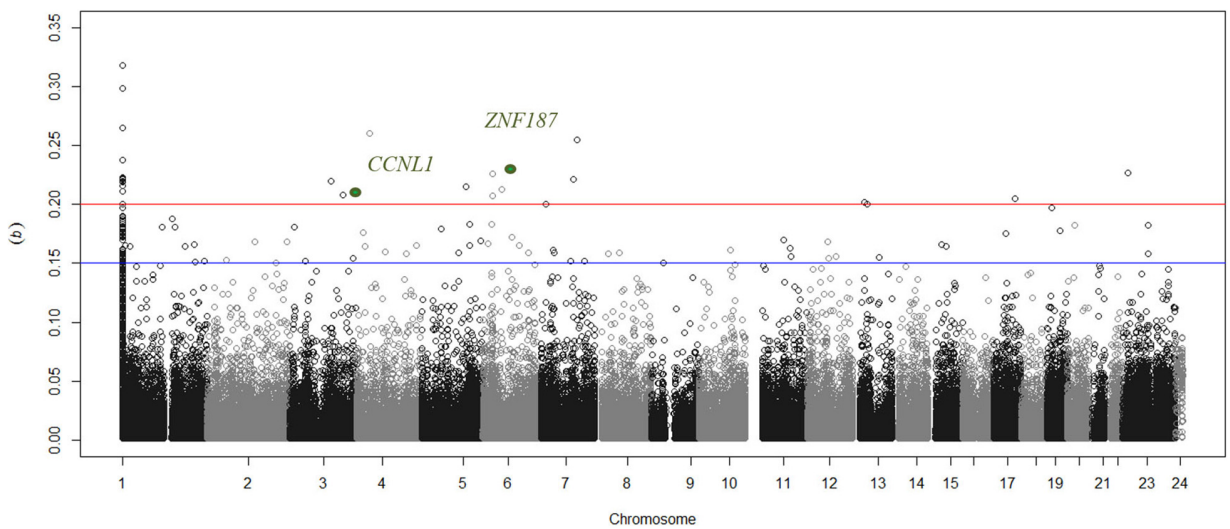

FIGURE 1 | Manhattan plot showing distribution of delta beta values for uniquely mapped sites across all chromosomes. The blue line discriminates sites that have suggestive differences in methylation between cases with nephropathy compared to non-nephropathic individuals in the control group. Circles above the red line are loci where a substantial difference in beta values (>0.2) were observed and the two markers supported in the replication group are highlighted in green. Markers that are not uniquely mapped to a chromosome position based on Illumina's updated bead pool manifest are assigned to chromosome 1 in this figure.

TABLE 2 | Details for markers showing significant (FDR adjusted *P*-value), substantial differences in mean methylation (Δβ) between case and control groups in the discovery phase.

Locus	Sequence position	Cytogenetic location	Symbol	Role from Entrez Gene	Δβ DN vs. DC	*P* DN vs. DC	Δβ ESRD vs. DC	*P* ESRD vs. DC
cg04861640	28234605	6p21.31	ZNF187 (ZSCAN26)	Transcriptional regulation	0.23	3.70E-24	0.22	3.80E-13
cg16203607	62500946	17q21	DDX5	Transcriptional regulation, differentiation, apoptosis	0.21	2.10E-23	0.21	1.90E-13
cg21829265	56911139	6p12.1	KIAA1586	Nucleic acid binding	0.21	4.10E-23	0.21	5.50E-13
cg20419181	38063874	4p14	TBC1D1	Regulation of cell growth, differentiation, protein organization	0.26	5.20E-23	0.27	9.00E-14
cg21935083	131892314	5q31	RAD50	Multiple including telomere maintenance and DNA repair/recombination	0.22	5.40E-23	0.23	3.10E-14
cg21739208	80280621	6	NA	NA	0.22	6.80E-23	0.22	8.10E-13
cg07242860	140739522	5q31	PCDHG@	Calcium ion binding	0.22	7.20E-23	0.23	1.20E-13
cg07979357	14142353	19p13.11	IL27RA	Immunity	0.2	1.80E-22	Not significant	Not significant
cg24115040	96652375	7q22	DLX5	Multiple, including transcriptional regulation, positive regulation of canonical Wnt receptor signaling pathway, and cell proliferation/differentiation	0.22	2.10E-22	0.23	4.70E-13
cg02339392	28234615	6p21.31	ZNF187 (ZSCAN26)	Transcriptional regulation	0.21	2.20E-22	0.21	7.90E-13
cg10463299	54987330	20q13.31	CASS4	Cell adhesion, cytoskeletal organization	0.23	2.30E-22	0.24	2.40E-13
cg00618312	41556559	13q13	ELF1	Protein acts as both an enhancer and a repressor to regulate transcription	0.2	2.40E-22	0.2	3.20E-12
cg15189015	72707255	17q25.1	RAB37;CD300LF	GTP binding; receptor activity	0.22	3.00E-22	0.23	6.40E-13
cg25418748	178977236	5q35.3	RUFY1	Endocytosis/protein transport	0.21	5.00E-22	0.21	1.20E-12
cg02399570	156877196	3q25.31	CCNL1	Transcription/RNA processing.	0.21	8.60E-22	0.21	3.30E-12
cg10905876	56716656	6p12.1	DST	Cell adhesion, cytoskeletal organization	0.22	8.90E-22	0.21	9.80E-12
cg16595484	122512170	3q21.1	HSPBAP1	Cell growth and differentiation	0.22	2.40E-21	0.22	1.30E-11
cg01667324	34392045	13q13.2	RFC3	Multiple including telomere maintenance and DNA repair/replication	0.2	5.30E-21	Not significant	Not significant
cg08779777	106505772	7q22.3	PIK3CG	Multiple. Associated with blood pressure variation (PMID: 21909110)	0.26	1.50E-20	0.25	6.10E-11
cg03037561	16459464	7p21.2	ISPD (CRPPA)	Nucleotidyltransferase activity, isoprenoid biosynthetic process	0.2	3.20E-18	0.24	1.50E-09
cg11671265	78722517	4q13.3	CNOT6L	Gene expression, RNA metabolic processing	0.24	5.00E-18	0.22	6.30E-09
cg26399113*	70752639	Xq13	OGT	Multiple, including response to insulin	0.22	1.00E-12	0.23	2.30E-07

*Differential methylation between individuals with DKD (DN, n = 150) compared to controls (DC, n = 100) with diabetes but no evidence of renal disease are highlighted, alongside differential methylation and significance values for the smaller ESRD versus control dataset. *Results presented from female cases compared to female controls.*

renal tissues. Downregulation of *CCNL1* gene expression was reported in multiple datasets comparing people with kidney disease versus controls without kidney disease [P = 3.55E-09 for thin basement membrane disease, based on 199 micro-dissected glomerular samples from CKD patients and living donors analyzed on Affymetrix Human U133 Plus 2.0 and Affymetrix Human U133A (altCDF v10) platforms, and P = 1.84E-05 for 53 kidney biopsies from people with chronic kidney disease tubular damage compared to healthy controls analyzed on Agilent Whole Human Genome Microarrays (Nakagawa et al., 2015)]. Gunther et al. (2014) reported a slight increase in blood-derived *CCNL1* gene expression (P = 0.006, fold change 1.6) for kidney transplant recipients with acute rejection compared to kidney transplant recipients with no rejection based on analysis of RNA from 40 samples on the Affymetrix Human Genome U133 Plus 2.0 array. Cox et al. (2015) explored blood-derived gene expression changes associated with glomerular filtration rate in eight patients with IgA nephropathy compared to nine healthy

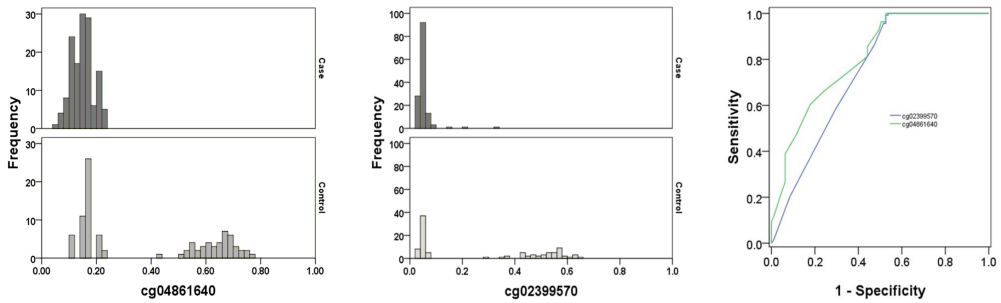

	cg02399570 (CCNL1)		cg04861640 (ZNF187)	
	Case (n=139)	**Control (n=95)**	**Case (n=139)**	**Control (n=96)**
Median (Interquartile range)	0.04 (0.04 – 0.05)	0.06 (0.04 – 0.52)	0.15 (0.12 – 0.18)	0.21 (0.17 – 0.65)
***P* (z-test)**	7.2×10^{-14}		1.5×10^{-15}	
Methylation <25%				
Sensitivity (95%CI)	99% (96%, 100%) 138/139	47% (37%, 58%) 45/95	100% (97%, 100%) 139/139	47% (37%, 57%) 45/96
Specificity (95%CI)				
Odds ratio† (95% CI)	100 (13 – 796)		∞	
Area under ROC curve	0.74		0.81	

FIGURE 2 | Histograms highlighting differences in the pattern of methylation between cases and controls for the two top ranked markers in the replication population. ROC curve demonstrating sensitivity and specificity of each marker. †Adjusted for age, HbA1c and gender. Neither age at diagnosis, nor duration of diabetes significantly influenced the model.

control participants, observing only a small change in expression for CCNL1 ($P = 0.02$).

Multiple significant analyses were returned from NephroSeq *ZNF187* kidney gene expression data from dissected renal lobes of five adult human kidneys using cDNA microarrays representing ∼30,000 different human genes (Higgins et al., 2004). ZNF187 is more highly expressed in renal glomeruli than other renal tissues (Higgins et al., 2004; Lindenmeyer et al., 2010). The most significant result returned from searching NephroSeq for ZNF187 was for tissue type [$P = 1.7 \times 10^{-5}$ comparing tubulointerstitium to glomerular tissue in six transplant living donors (Lindenmeyer et al., 2010)] and acute rejection following kidney transplantation from 48 patients [$P = 2.8 \times 10^{-5}$ (Sarwal et al., 2003)]. Gene expression changes were associated with glomerular filtration rate in kidney biopsy samples from people with IgA nephropathy ($P = 6.27 \times 10^{-4}$) (Reich et al., 2010), diabetes ($P = 0.008$) (Woroniecka et al., 2011), and blood derived gene expression from healthy individuals who had no evidence of kidney disease ($P = 0.018$) (Flechner et al., 2004). Focusing in on available data from 22 racially diverse microdissected human kidney samples with type 2 DKD measured on the Affymetrix U133A 2.0 array, visualizes decreased renal function associated with a decrease in ZNF187 gene expression ($P = 0.008$) (Woroniecka et al., 2011).

DISCUSSION

Using the Infinium Human Methylation 450K BeadChip (Sandoval et al., 2011) we identified differentially methylated CpG sites associated with DKD. To minimize false positive associations in our discovery cohort, we applied stringent quality control and adjusted association analyses; we used both a genome-wide significance threshold and a clear absolute methylation difference ($\Delta\beta \geq 0.2$) to minimize artifactual associations and ensure the selection of differentially methylated CpG probes (Dedeurwaerder et al., 2014). No SNPs are reported to affect methylation probes for *ZNF187*, however, one SNP resides 40 bases from the 3′ end of the probe for the *CCNL1* gene. This SNP (rs75624594, NP_064703.1:p.His112 = His, synonymous coding) has a reported minor allele frequency of 50% in African individuals, but only 4% in the US NHLBI Exome Sequencing Project (dbSNP ss342150967)[3] so is unlikely to account for the differential methylation observed in this study.

The majority of probes evaluated using the 27K array were also present on the 450K array ($n = 25{,}978$), and demonstrate good correlation for many, but not all, CpG probes. For this reasons

[3]https://esp.gs.washington.edu/drupal/

we sought supporting data from a previous study exploring DKD using the 27K array. It is clearly only possible to seek support for top-ranked markers that were present across both the 27K and 450K arrays and unfortunately data was only available for seven probes, none of which supported an association. Acknowledging the limitations of the 27K array to support top-ranked markers in this study (primarily that the majority of our top-ranked markers were not present on that much smaller array) and in the absence of a replication cohort with 450K data available for a population with similar phenotype characteristics, we sought independent replication. Pragmatically, independent replication was sought using all available samples with high molecular weight DNA (139 cases and 96 controls) for the 22 loci that were significantly associated with DKD from the 450K array-based discovery analysis using $\Delta\beta \geq 0.2$ and FDR adjusted $P < 10^{-8}$ thresholds. Importantly, the replication population was recruited with similar phenotypic characteristics to that of the discovery cohort and we used a completely different wet-lab approach (mass spectrometry) to validate the microarray-based data, which minimizes artifacts due to the microarray analysis. Only two of these CpG sites were supported by the new methylation data generated in our replication population – this is not unusual in genome-wide studies and may be due to false positives in the original EWAS or due to the fact that our replication population was not sufficiently powered to identify significant associations with all loci. Both discovery and *de novo* replication using a different experimental platform (mass spectrometry by Sequenom analyzed using EpiTyper software) to generate new laboratory data and an independent population strongly support the association of *CCNL1* and *ZNF187* genes with methylome-wide significance from 450K array-based (microarray by Illumina's iScan) discovery association results. RNA-based gene expression data also supports a functional influence of *CCNL1* and *ZNF187* in kidney disease.

Methylation patterns for *CCNL1* and *ZNF187* genes showed a striking higher methylation level for controls compared to individuals in the case group (**Figure 2**). It should be noted that DNA samples available for replication were not age and gender matched in this study, rather they were pragmatically selected as all available samples with high quality DNA and careful phenotyping. Cases were older, diagnosed with type 1 diabetes later, and had higher HBA_{1c} values with a longer duration of diabetes than individuals in the control group. Differential methylation between cases and controls was significant in both the *CCNL1* and *ZNF187* genes following adjustment for age, duration of diabetes, HBA1c and gender.

The *CCNL1* gene encodes cyclin L1, which is localized in nuclear speckles (splicing factor storage compartment) (Herrmann et al., 2007), is functionally related to the spliceosome, and is involved in pre-mRNA splicing activities (Chen et al., 2007; Tannukit et al., 2008). The transcription start site for *CCNL1* is located 89 bp upstream of the initiation codon and the first two exons overlap the CpG island (Dickinson et al., 2002; **Figure 2**). *CCNL1* was consistently hypomethylated in cases compared to controls. Overexpression (usually associated with hypomethylation) of *CCNL1* has been associated with cancer (Sticht et al., 2005; Mitra et al., 2010; Peng et al., 2011). The discovery group generated results for 15 CpGs in the *CCNL1* gene, of which 12 showed an increase in methylation between cases and controls. Replication using independent samples and a different wet-lab experimental approach supported the association of *CCNL1* with DKD. Based on published gene expression data from the Affymetrix® GeneChip® Whole Transcript Expression Arrays, *CCNL1* was one of four genes differentially expressed in patients with kidney stones compared to controls (2.6 fold change, downregulated, $P = 6.58E\text{-}05$) (Liang et al., 2019). Based on gene expression data within NephroSeq, differential gene expression was observed for *CCNL1* in kidney biopsy tissues from people with kidney disease compared to controls (Gunther et al., 2014; Ju et al., 2015; Nakagawa et al., 2015); no adjustment was made for cell heterogeneity in the disease compared to control collections for these gene expression datasets. *CCNL1* resides in chromosome band 3q25, which has been previously suggested to harbor risk loci for DKD (McKnight et al., 2009). Of particular interest, the *CCNL1* gene was ranked 4th from a meta-analysis for association with severe diabetic retinopathy ($P = 7.1 \times 10^{-7}$), but was no longer top-ranked for association with diabetic retinopathy when individuals with nephropathy were removed from the case group (Grassi et al., 2011). Subsequent studies have highlighted *CCNL1* SNPs associated with retinopathy and measures of renal function (Lin et al., 2016). Genetic variation near the *CCNL1* gene is robustly associated with low birth weight in European individuals (Freathy et al., 2010; Yaghootkar and Freathy, 2012; Horikoshi et al., 2013), specifically with growth restriction from early pregnancy onward (Mook-Kanamori et al., 2011). Another study suggests that individuals who carry a risk allele for rs900400 (near *CCNL1*) are more vulnerable to stress impacting on birth weight (Ali Khan et al., 2012). The relationship between birth weight and kidney disease has been debated with some groups suggesting that low birth weight is a risk factor for DKD (Rossing et al., 1995) while others report that low birth weight does not increase the risk of DKD (Fagerudd et al., 2006). The birth weight lowering effect rs900400 C allele has also been associated with increased insulin response following oral glucose stimulation in a meta-analysis based on Danish and Finnish non-diabetic individuals (Andersson et al., 2011). Published literature suggests that *CCNL1* may affect an individual's inherited and dynamic responses to their environment, perhaps reflecting both genetic and epigenetic contributions. While the molecular mechanism for *CCNL1* influencing DKD remains to be resolved, this is clearly a candidate gene that warrants further investigation having demonstrated genetic (SNPs), epigenetic (methylation) and transcriptomic (gene expression) associations with kidney disease across multiple collections.

In the discovery cohort, nine CpGs were examined for ZNF187; eight of these showed differential methylation and all were in the same direction as the index marker. Replication demonstrated strong support for association of ZNF187 with DKD. Analysis within NephroSeq revealed gene expression changes associated with glomerular filtration rate in kidney biopsy and blood-derived samples from people with IgA nephropathy (Reich et al., 2010), diabetes (Woroniecka et al., 2011), and renal function in healthy individuals

(Flechner et al., 2004; **Supplementary Figure 1**). ZNF187 is involved with transcriptional regulation, but there are few publications describing this gene. The *ZNF187* gene is was located at 6p21.31 and encodes the zinc finger protein 187. Gene ontology suggests that *ZNF187* is involved with transcriptional regulation, but there are no specific publications for this gene (or any aliases) in PubMed (accessed 12/05/20)[4]. The protein coding *ZNF187* gene has been renamed as *ZSCAN26* (zinc finger and SCAN domain containing 26), but we have retained the *ZNF187* nomenclature throughout this manuscript to keep the methylation array information consistent and facilitate easier searching and replication within methylation and gene expression datasets.

Both CCNL1 and ZNF187 were more highly expressed in renal glomeruli than other renal tissues, which may be consistent with DKD in people with type 1 diabetes primarily affecting the glomerulus (Higgins et al., 2004). The results for both significantly replicated genes in our methylation dataset are hypomethylated in cases compared to controls, while publicly available gene expression evidence for both genes suggests there is less RNA product in samples from people with kidney disease. This may be because less gene is expressed, or because the mRNA measured on arrays is not present for long, or because different isoforms are not captured by the gene expression array. cg02399570 is in the body of CCNL1 while cg04861640 is within the transcription start site of ZNF187. Most promoters and CpG sites in gene bodies that are hypomethylated are basically expressed, but gene regulation is complex and genes may be hypomethylated and "overexpressed" in disease states (Haney et al., 2016; Li et al., 2017). Significant further research is required in populations that have blood derived, kidney biopsy derived and *in vitro* models with SNP, CpG, and gene expression data available for the same individuals to tease out the molecular signatures of these genes (*CCNL1* and *ZNF187*) for kidney disease.

Pathway analysis revealed significant gene enrichment in the focal adhesion, Wnt and MAPK signaling pathways. These pathways have been previously top-ranked as differentially regulated in renal tubuli of individuals with DKD compared to healthy tissue from living kidney donors (Woroniecka et al., 2011). The focal adhesion pathway also demonstrates enrichment in the glomeruli of individuals with DKD (Woroniecka et al., 2011) and is a key molecular pathway in the formation and progression of the cardiorenal system (Muhlberger et al., 2012). The Wnt signally pathway has been shown to influence survival of glomerular mesangial cells exposed to high glucose (Lin et al., 2006) (41) and dysregulation of the Wnt pathway may represent and important pathogenic mechanism of DKD (Kavanagh et al., 2011; Zhou et al., 2012).

We incorporated existing GWAS data (Sandholm et al., 2012) with this novel methylation data to provide exploratory analysis seeking a provisional assessment of functionality. i.e., are SNPs demonstrating suggestive association with DKD from GWAS near CpG probes that are differentially methylated using the same case-control study population. As SNPs may have a functional role for each gene at a considerable genetic distance, we pragmatically selected 5 kb flanking each probe for this analysis. No strong associations were identified for SNPs near top-ranked differentially methylated genes. We also considered a similar analysis by looking up CpG sites for association near top-ranked GWAS SNPs (Sandholm et al., 2012). Meta-analysis of genome-wide association studies for DKD revealed novel association ($P = 1.2 \times 10^{-8}$) with SNPs in the *AFF3* gene, a transcriptional activator that influences renal fibrosis through the TGFβ1 pathway, in individuals who had progressed to end stage renal disease (Sandholm et al., 2012). Additionally, the top-ranked marker associated with DKD was in the *ERBB4* gene ($P = 2.1 \times 10^{-7}$) (Sandholm et al., 2012). Significant differential methylation was observed at both of these loci when comparing cases and controls on the 450K array (**Table 3**) suggesting that a combined genetic-epigenetic factor may influence the risk of DKD.

The role of epigenetics in common, complex diseases is beginning to be unraveled at a population level using relatively high throughput tools. Evidence is increasing that inter-individual epigenetic variation, in particular DNA methylation, may help explain some of the "missing heritability" that has not been identified through genome-wide association and resequencing approaches. Illumina's 450K BeadChip was proposed as the method of choice for cost-effective, high throughput epigenome-wide association studies with single-base resolution (Rakyan et al., 2011b). The content of this array (485,764 sites distributed across all chromosomes) was selected based on input from 22 methylation experts across the world. Included are unique markers that cover 99% of RefSeq genes with an average of 17 CpG sites per gene region distributed across the promoter, 5′ untranslated region, first exon, gene body, and 3′ untranslated region. This array also includes dedicated content for CpG sites outside CpG islands and microRNA promoter regions. Illumina have released a higher density EPIC array, the Infinium MethylationEPIC BeadChip, which facilitates evaluation of 862,927 sites at significantly increased financial cost. More comprehensive analysis of the methylome may be conducted through whole-methylome-sequencing, but this is financially prohibitive for most researchers using cohorts of more than 200 participants. However, technological and analytical advances now offer the potential for targeted, high throughput bisulfite sequencing with deep coverage as an attractive option for technical validation and replication. Using high density methylation arrays is currently the most cost-effective approach for EWAS using population-based study designs. Stringent quality control, strong significance values, and independent replication are essential to minimize false positive findings when investigating sequence changes to elucidate the genetic architecture of multifactorial disease.

Although this epigenetic study does not include the large sample numbers traditionally associated with genome-wide association studies, we have applied rigorous analysis approaches throughout and gained support using independent samples by a different technology – important to minimize technical artifacts.

[4]www.ncbi.nlm.nih.gov/pubmed

TABLE 3 | Methylation probes of interest associated with genes identified from recent meta-analysis of genome-wide association studies for DKD.

Locus	Gene	Description	Δβ DN vs. DC	*P* DN vs. DC
cg15934776	AFF3	AF4/FMR2 family, member 3	−0.024	1.40E-13
cg13353679	AFF3	AF4/FMR2 family, member 3	−0.045	3.40E-12
cg23118464	AFF3	AF4/FMR2 family, member 3	−0.022	1.50E-10
cg11577355	AFF3	AF4/FMR2 family, member 3	0.019	3.00E-10
cg22039234	AFF3	AF4/FMR2 family, member 3	−0.017	4.60E-08
cg01286950	AFF3	AF4/FMR2 family, member 3	−0.01	1.70E-07
cg11451506	AFF3	AF4/FMR2 family, member 3	0.013	1.10E-06
cg03393607	AFF3	AF4/FMR2 family, member 3	0.0057	1.10E-06
cg03816062	AFF3	AF4/FMR2 family, member 3	0.0038	2.00E-06
cg25798409	ERBB4	v-erb-a erythroblastic leukemia viral oncogene homolog 4 (avian)	−0.025	4.80E-14
cg24768649	ERBB4	v-erb-a erythroblastic leukemia viral oncogene homolog 4 (avian)	−0.012	1.20E-06

A sample size of only 65 heavy smokers and 56 non-smokers was sufficient to identify differential patterns of methylation ($P = 2.68^{-31}$) associated with smoking using the Illumina Human Methylation 27K BeadChip (Breitling et al., 2011). Similarly, a type 1 diabetes-methylation variation position signature was detected by assaying a relatively modest number of samples ($n = 15$ monozygotic twin pairs discordant for type 1 diabetes) on the 27K array (Bell et al., 2010; Rakyan et al., 2011a). Associations using the 450K array have been reported from 11 cell lines for rheumatoid arthritis (Nakano et al., 2013), 48 individuals for irritable bowel disease (Harris et al., 2012), and 165 females for alcohol use (Philibert et al., 2012), although study sizes are now increasing. Previous studies exploring blood-derived DNA methylation used an EWAS approach for DKD focused on the 27K array (Sapienza et al., 2011), the mitochondrial genome (Swan et al., 2015) or renal function decline in 181 Pima Indians with diabetes (Qiu et al., 2018). Targeted DNA methylation studies have been conducted using blood-derived DNA (Aldemir et al., 2017; Smyth et al., 2018), cell models of DKD (Brennan et al., 2010; Li et al., 2019) and an EWAS reported on kidney biopsy samples from 91 individuals of whom 45% had diabetes (Gluck et al., 2019) and 11 individuals with diabetes (Ko et al., 2013). The case and control population employed in this study has >60% power to detect a true positive (defined as detected CpGs with a meaningful difference in mean blood derived DNA methylation ±0.2 with a false discovery rate $P \leq 0.05$) association using pwrEWAS (Graw et al., 2019). More comprehensive whole genome bisulfite sequencing has been reported for kidney biopsy samples from five individuals with DKD compared to one person with diabetes without kidney disease, and four people with neither diabetes nor kidney disease (Park et al., 2019).

Careful phenotyping is critically important for methylation studies, as is the consistent extraction and storage of DNA. We and others have previously demonstrated that differences in DNA extraction approaches and storage methods significantly alter methylation profiles. Importantly for this study, all DNA was extracted using the same approach in the same laboratory (by two persons) with extracted DNA stored at −80°C in multiple aliquots with only one freeze-thaw cycle. Individuals were carefully phenotyped by consultant nephrologists using internationally agreed phenotype criteria. We restricted analysis to individuals with type 1 diabetes and known kidney function to minimize phenotypic heterogeneity and used a matched design for the discovery population.

Many cell types have unique methylation profiles so where possible it is important to adjust for cell heterogeneity in all studies using blood-derived or kidney-derived DNA. In our study, there was no significant difference in proportional white cell counts from whole blood (B cells, granulocytes, monocytes, NK cells, and T cells subsets) and adjusting for cell composition does not change the top-ranked association results for this study. While adjusting for white cell subpopulations is critically important for cancer studies, immune-mediated responses, and case-control approaches not matched for age and gender, this is a result that we and others have reported previously for carefully phenotyped populations with stringent wet-lab protocols from blood sampling through to array scanning. The proportion of these cell types may also reflect changing disease pathology (Lappalainen and Greally, 2017; Johnson et al., 2020). Epigenetic signatures may display tissue specificity linked to disease mechanisms, however, obtaining kidney biopsy material is invasive and is not performed as part of routine clinical practice in people with DKD and T1D in the United Kingdom. Peripheral blood-based methylation biomarkers have shown promise in several clinical fields (Moore et al., 2014; Agha et al., 2019; Cardenas et al., 2019; DiTroia et al., 2019; Henderson-Smith et al., 2019; Kerr et al., 2019a,b, 2020; Ladd-Acosta and Fallin, 2019; Zhou et al., 2019) including kidney disease (Smyth et al., 2014b, 2018; Swan et al., 2015; Aranyi and Susztak, 2019; Gluck et al., 2019; Kato and Natarajan, 2019; Kerr et al., 2019b; Park et al., 2019). We have previously demonstrated that blood-derived differential methylation is also reflected in kidney-derived differential methylation for CKD (Smyth et al., 2014b). Blood-derived DNA methylation offers clinical utility in biomarker development, incorporating a minimally invasive approach that could be cost-effectively implemented in a routine clinical setting. Indeed, ROC curve analysis suggests that 25% methylation for the two key *CCNL1* and *ZNF187* markers is reasonably good at differentiating individuals in case and control

groups. This is particularly critical for translation in DKD given the difficulty obtaining serial renal biopsies to establish diagnosis, track progression, and monitor response (Kim et al., 2018). Array-based approaches using blood-derived DNA have previously identified risk factors and biomarkers associated with complex phenotypes (Sandholm et al., 2013, 2017; Keating et al., 2018; Canadas-Garre et al., 2019; Gu, 2019; Park et al., 2019).

Interpreting epigenetic factors as disease-causing or consequences of disease processes, alongside genetic and/or environmental heterogeneity, are a significant problem for complex disease. Nevertheless, this study demonstrates that using high density methylation arrays are an appropriate, cost-effective tool to identify differential methylation profiles that may deliver minimally invasive biomarkers that are relevant for diabetic complications. We have identified CCNL1 and ZNF187 as differentially methylated genes associated with DKD in multiple cohorts. Larger EWAS exploring more markers with larger sample sizes will deliver the same gains identifying molecular biomarkers as has been observed for GWAS in recent years. Using longitudinal cohort designs will allow researchers to observe how DNA methylation changes over time. More complex analytical tools are being developed for DNA methylation such as MethylNet (Levy et al., 2020), which offers further opportunities for novel discoveries and improved understanding. The integration of multi-omic profiling will lead to a better understanding of inherited susceptibility to DKD and biomarkers for this common disease.

DATA AVAILABILITY STATEMENT

The data supporting the conclusion of this article will be made available by the authors, without undue reservation.

ETHICS STATEMENT

The studies involving human participants were reviewed and approved by the South and West Multicentre Research Ethics Committee (MREC/98/6/71). The patients/participants provided their written informed consent to participate in this study.

AUTHOR CONTRIBUTIONS

AMcK had full access to the data in the study and takes responsibility for the integrity of the data and the accuracy of the data analysis. LS, AM, and AMcK conceived and designed the study. LS and ES performed sample analysis. CP performed the statistical analyses in the replication group. All authors provided important intellectual content and agreed the final version of this manuscript.

FUNDING

Funding was provided by the Science Foundation Ireland and the Department for the Economy, Northern Ireland (15/IA/3152), the Medical Research Council (MC_PC_15025), and the NI Public Health Agency R&D Division as part of a US Ireland award (STL/4760/13). LS is the recipient of a Northern Ireland Kidney Research Fund Fellowship. ES is the recipient of Diabetes UK Ph.D. Studentship BDA 10/0004154.

ACKNOWLEDGMENTS

We appreciate the support provided by Fraser Morton at Fios Genomics who conducted independent analysis of the 450K array data, which was generated by Hologic Gen-Probe Inc. The Warren3/United Kingdom GoKinD Study Group was jointly funded by Diabetes UK and the Juvenile Diabetes Research Foundation and includes the following individuals: Prof. AM, Prof. AMcK, Dr. D. A. Savage (Belfast), Dr. J. Walker (Edinburgh), Dr. S. Thomas, Prof. G. C. Viberti (London), Prof. A. J. M. Boulton (Manchester), Prof. S. Marshall (Newcastle), Prof. A. G. Demaine, Dr. B. A. Millward (Plymouth), and Prof. S. C. Bain (Swansea).

SUPPLEMENTARY MATERIAL

The Supplementary Material for this article can be found online at: https://www.frontiersin.org/articles/10.3389/fcell.2020.561907/full#supplementary-material

REFERENCES

Agha, G., Mendelson, M. M., Ward-Caviness, C. K., Joehanes, R., Huan, T., Gondalia, R., et al. (2019). Blood leukocyte DNA methylation predicts risk of future myocardial infarction and coronary heart disease. *Circulation* 140, 645–657.

Aldemir, O., Turgut, F., and Gokce, C. (2017). The association between methylation levels of targeted genes and albuminuria in patients with early diabetic kidney disease. *Ren. Fail.* 39, 597–601. doi: 10.1080/0886022x.2017.1358180

Ali Khan, A., Rodriguez, A., Sebert, S., Kaakinen, M., Cauchi, S., Froguel, P., et al. (2012). The interplay of variants near LEKR and CCNL1 and social stress in relation to birth size. *PLoS One* 7:e38216. doi: 10.1371/journal.pone.0038216

Andersson, E. A., Harder, M. N., Pilgaard, K., Pisinger, C., Stancakova, A., Kuusisto, J., et al. (2011). The birth weight lowering C-allele of rs900400 near LEKR1 and CCNL1 associates with elevated insulin release following an oral glucose challenge. *PLoS One* 6:e27096. doi: 10.1371/journal.pone.0027096

Aranyi, T., and Susztak, K. (2019). Cytosine methylation studies in patients with diabetic kidney disease. *Curr. Diab. Rep.* 19:91.

Arredondo, A., Orozco, E., Duarte, M. B., Cuadra, M., Recaman, A. L., and Azar, A. (2018). Trends and challenges in diabetes for middle-income countries: evidence from Mexico. *Glob. Public Health* 14, 227–240. doi: 10.1080/17441692.2018.1498115

Bayoumi, A., Gronbaek, H., George, J., and Eslam, M. (2020). The epigenetic drug discovery landscape for metabolic-associated fatty liver disease. *Trends Genet.* 36, 429–441. doi: 10.1016/j.tig.2020.03.003

Bell, C. G., Teschendorff, A. E., Rakyan, V. K., Maxwell, A. P., Beck, S., and Savage, D. A. (2010). Genome-wide DNA methylation analysis for diabetic nephropathy in type 1 diabetes mellitus. *BMC Med. Genom.* 3:33. doi: 10.1186/1755-8794-3-33

Breitling, L. P., Yang, R., Korn, B., Burwinkel, B., and Brenner, H. (2011). Tobacco-smoking-related differential DNA methylation: 27K discovery and replication. *Am. J. Hum. Genet.* 88, 450–457. doi: 10.1016/j.ajhg.2011.03.003

Brennan, E. P., Ehrich, M., O'Donovan, H., Brazil, D. P., Crean, J. K., Murphy, M., et al. (2010). DNA methylation profiling in cell models of diabetic nephropathy. *Epigenetics* 5, 396–401. doi: 10.4161/epi.5.5.12077

Campbell, J. A., Bishu, K. G., Walker, R. J., and Egede, L. E. (2017). Trends of medical expenditures and quality of life in US adults with diabetes: the medical expenditure panel survey, 2002-2011. *Health Qual. Life Outcomes* 15:70.

Canadas-Garre, M., Anderson, K., Cappa, R., Skelly, R., Smyth, L. J., McKnight, A. J., et al. (2019). Genetic susceptibility to chronic kidney disease - some more pieces for the heritability puzzle. *Front. Genet.* 10:453. doi: 10.3389/fgene.2019.00453

Canadas-Garre, M., Anderson, K., McGoldrick, J., Maxwell, A. P., and McKnight, A. J. (2018). Genomic approaches in the search for molecular biomarkers in chronic kidney disease. *J. Transl. Med.* 16:292.

Cardenas, A., Lutz, S. M., Everson, T. M., Perron, P., Bouchard, L., and Hivert, M. F. (2019). Placental DNA methylation mediates the association of prenatal maternal smoking on birth weight. *Am. J. Epidemiol.* 188, 1878–1886. doi: 10.1093/aje/kwz184

Chen, H. H., Wong, Y. H., Geneviere, A. M., and Fann, M. J. (2007). CDK13/CDC2L5 interacts with L-type cyclins and regulates alternative splicing. *Biochem. Biophys. Res. Commun.* 354, 735–740. doi: 10.1016/j.bbrc.2007.01.049

Chen, Y. A., Lemire, M., Choufani, S., Butcher, D. T., Grafodatskaya, D., Zanke, B. W., et al. (2013). Discovery of cross-reactive probes and polymorphic CpGs in the Illumina Infinium HumanMethylation450 microarray. *Epigenetics* 8, 203–209. doi: 10.4161/epi.23470

Chu, A. Y., Tin, A., Schlosser, P., Ko, Y. A., Qiu, C., Yao, C., et al. (2017). Epigenome-wide association studies identify DNA methylation associated with kidney function. *Nat. Commun.* 8:1286.

Cox, S. N., Serino, G., Sallustio, F., Blasi, A., Rossini, M., Pesce, F., et al. (2015). Altered monocyte expression and expansion of non-classical monocyte subset in IgA nephropathy patients. *Nephrol. Dial. Transplant.* 30, 1122–1232. doi: 10.1093/ndt/gfv017

Dedeurwaerder, S., Defrance, M., Bizet, M., Calonne, E., Bontempi, G., and Fuks, F. (2014). A comprehensive overview of infinium humanmethylation450 data processing. *Brief Bioinform.* 15, 929–941. doi: 10.1093/bib/bbt054

Dias, S., Adam, S., Rheeder, P., Louw, J., and Pheiffer, C. (2019). Altered genome-wide DNA methylation in peripheral blood of south african women with gestational diabetes mellitus. *Int. J. Mol. Sci.* 20:5828. doi: 10.3390/ijms20235828

Dickinson, L. A., Edgar, A. J., Ehley, J., and Gottesfeld, J. M. (2002). Cyclin L is an RS domain protein involved in pre-mRNA splicing. *J. Biol. Chem.* 277, 25465–25473. doi: 10.1074/jbc.m202266200

Disease, G. B. D., Injury, I., and Prevalence, C. (2018). Global, regional, and national incidence, prevalence, and years lived with disability for 354 diseases and injuries for 195 countries and territories, 1990-2017: a systematic analysis for the Global Burden of Disease Study 2017. *Lancet* 392, 1789–1858.

DiTroia, S. P., Percharde, M., Guerquin, M. J., Wall, E., Collignon, E., Ebata, K. T., et al. (2019). Maternal vitamin C regulates reprogramming of DNA methylation and germline development. *Nature* 573, 271–275. doi: 10.1038/s41586-019-1536-1

Elboudwarej, E., Cole, M., Briggs, F. B., Fouts, A., Fain, R., Quach, H., et al. (2016). Hypomethylation within gene promoter regions and type 1 diabetes in discordant monozygotic twins. *J. Autoimmun.* 68, 23–29. doi: 10.1016/j.jaut.2015.12.003

Fagerudd, J., Forsblom, C., Pettersson-Fernholm, K., Saraheimo, M., Waden, J., Ronnback, M., et al. (2006). Low birth weight does not increase the risk of nephropathy in Finnish type 1 diabetic patients. *Nephrol. Dial. Transplant.* 21, 2159–2165. doi: 10.1093/ndt/gfl217

Flechner, S. M., Kurian, S. M., Head, S. R., Sharp, S. M., Whisenant, T. C., Zhang, J., et al. (2004). Kidney transplant rejection and tissue injury by gene profiling of biopsies and peripheral blood lymphocytes. *Am. J. Transplant.* 4, 1475–1489. doi: 10.1111/j.1600-6143.2004.00526.x

Florath, I., Butterbach, K., Heiss, J., Bewerunge-Hudler, M., Zhang, Y., Schottker, B., et al. (2016). Type 2 diabetes and leucocyte DNA methylation: an epigenome-wide association study in over 1,500 older adults. *Diabetologia* 59, 130–138. doi: 10.1007/s00125-015-3773-7

Franciosi, M., Lucisano, G., Amoretti, R., Capani, F., Bruttomesso, D., and Di Bartolo. (2013). Nicolucci, A., Costs of treatment and complications of adult type 1 diabetes. *Nutr. Metab Cardiovasc. Dis.* 23, 606–611. doi: 10.1016/j.numecd.2012.03.002

Freathy, R. M., Mook-Kanamori, D. O., Sovio, U., Prokopenko, I., Timpson, N. J., Berry, D. J., et al. (2010). Variants in ADCY5 and near CCNL1 are associated with fetal growth and birth weight. *Nat. Genet.* 42, 430–435.

Fu, H., Liu, S., Bastacky, S. I., Wang, X., Tian, X. J., and Zhou, D. (2019). Diabetic kidney diseases revisited: a new perspective for a new era. *Mol. Metab* 30, 250–263. doi: 10.1016/j.molmet.2019.10.005

Gluck, C., Qiu, C., Han, S. Y., Palmer, M., Park, J., Ko, Y. A., et al. (2019). Kidney cytosine methylation changes improve renal function decline estimation in patients with diabetic kidney disease. *Nat. Commun.* 10:2461.

Grassi, M. A., Tikhomirov, A., Ramalingam, S., Below, J. E., Cox, N. J., and Nicolae, D. L. (2011). Genome-wide meta-analysis for severe diabetic retinopathy. *Hum. Mol. Genet.* 20, 2472–2481. doi: 10.1093/hmg/ddr121

Graw, S., Henn, R., Thompson, J. A., and Koestler, D. C. (2019). pwrEWAS: a user-friendly tool for comprehensive power estimation for epigenome wide association studies (EWAS). *BMC Bioinform.* 20:218. doi: 10.1186/s12859-019-2804-7

Greenberg, M. V. C., and Bourc'his, D. (2019). The diverse roles of DNA methylation in mammalian development and disease. *Nat. Rev. Mol. Cell Biol.* 20, 590–607. doi: 10.1038/s41580-019-0159-6

Gu, H. F. (2019). Genetic and epigenetic studies in diabetic kidney disease. *Front. Genet.* 10:507. doi: 10.3389/fgene.2019.00507

Gunther, O. P., Shin, H., Ng, R. T., McMaster, W. R., McManus, B. M., Keown, A., et al. (2014). Novel multivariate methods for integration of genomics and proteomics data: applications in a kidney transplant rejection study. *OMICS* 18, 682–695. doi: 10.1089/omi.2014.0062

Haertle, L., El Hajj, N., Dittrich, M., Muller, T., Nanda, I., Lehnen, H., et al. (2017). Epigenetic signatures of gestational diabetes mellitus on cord blood methylation. *Clin. Epigenet.* 9:28.

Haney, S. L., Upchurch, G. M., Opavska, J., Klinkebiel, D., Hlady, R. A., Suresh, A., et al. (2016). Promoter hypomethylation and expression is conserved in mouse chronic lymphocytic leukemia induced by decreased or inactivated Dnmt3a. *Cell Rep.* 15, 1190–1201. doi: 10.1016/j.celrep.2016.04.004

Harris, R. A., Nagy-Szakal, D., Pedersen, N., Opekun, A., Bronsky, J., Munkholm, P., et al. (2012). Genome-wide peripheral blood leukocyte DNA methylation microarrays identified a single association with inflammatory bowel diseases. *Inflamm. Bowel. Dis.* 18, 2334–2341. doi: 10.1002/ibd.22956

Henderson-Smith, A., Fisch, K. M., Hua, J., Liu, G., Ricciardelli, E., Jepsen, K., et al. (2019). DNA methylation changes associated with Parkinson's disease progression: outcomes from the first longitudinal genome-wide methylation analysis in blood. *Epigenetics* 14, 365–382. doi: 10.1080/15592294.2019.1588682

Herrmann, A., Fleischer, K., Czajkowska, H., Muller-Newen, G., and Becker, W. (2007). Characterization of cyclin L1 as an immobile component of the splicing factor compartment. *FASEB J.* 21, 3142–3152. doi: 10.1096/fj.07-8377com

Higgins, J. P., Wang, L., Kambham, N., Montgomery, K., Mason, V., Vogelmann, S. U., et al. (2004). Gene expression in the normal adult human kidney assessed by complementary DNA microarray. *Mol. Biol. Cell* 15, 649–656. doi: 10.1091/mbc.e03-06-0432

Hill, C. J., Cardwell, C. R., Patterson, C. C., Maxwell, A. P., Magee, G. M., Young, R. J., et al. (2014). Chronic kidney disease and diabetes in the national health service: a cross-sectional survey of the U.K. national diabetes audit. *Diabet. Med.* 31, 448–454. doi: 10.1111/dme.12312

Hoang, T. T., Sikdar, S., Xu, C. J., Lee, M. K., Cardwell, J., Forno, E., et al. (2020). Epigenome-Wide association study of DNA methylation and adult asthma in the agricultural lung health study. *Eur. Respir. J.* 56:2000217.

Horikoshi, M., Yaghootkar, H., Mook-Kanamori, D. O., Sovio, U., Taal, H. R., Hennig, B. J., et al. (2013). New loci associated with birth weight identify genetic links between intrauterine growth and adult height and metabolism. *Nat. Genet.* 45, 76–82.

Houseman, E. A., Accomando, W. P., Koestler, D. C., Christensen, B. C., Marsit, C. J., Nelson, H. H., et al. (2012). DNA methylation arrays as surrogate measures of cell mixture distribution. *BMC Bioinform.* 13:86. doi: 10.1186/1471-2105-13-86

Howe, C. G., Cox, B., Fore, R., Jungius, J., Kvist, T., Lent, S., et al. (2020). Maternal gestational diabetes mellitus and newborn DNA methylation: findings from the pregnancy and childhood epigenetics consortium. *Diabetes Care* 43, 98–105.

Huang, da, W., Sherman, B. T., and Lempicki, R. A. (2009). Systematic and integrative analysis of large gene lists using DAVID bioinformatics resources. *Nat. Protoc.* 4, 44–57. doi: 10.1038/nprot.2008.211

Jia, Y., Reddy, M. A., Das, S., Oh, H. J., Abdollahi, M., Yuan, H., et al. (2019). Dysregulation of histone H3 lysine 27 trimethylation in transforming growth factor-beta1-induced gene expression in mesangial cells and diabetic kidney. *J. Biol. Chem.* 294, 12695–12707. doi: 10.1074/jbc.ra119.007575

Johnson, R. K., Vanderlinden, L. A., Dong, F., Carry, M., Seifert, J., Waugh, K., et al. (2020). Longitudinal DNA methylation differences precede type 1 diabetes. *Sci. Rep.* 10:3721.

Ju, W., Nair, V., Smith, S., Zhu, L., Shedden, K., Song, P., et al. (2015). Tissue transcriptome-driven identification of epidermal growth factor as a chronic kidney disease biomarker. *Sci. Transl. Med.* 7:316ra193.

Kato, M., and Natarajan, R. (2019). Epigenetics and epigenomics in diabetic kidney disease and metabolic memory. *Nat. Rev. Nephrol.* 15, 327–345. doi: 10.1038/s41581-019-0135-6

Kauffmann, A., and Huber, W. (2010). Microarray data quality control improves the detection of differentially expressed genes. *Genomics* 95, 138–142. doi: 10.1016/j.ygeno.2010.01.003

Kavanagh, D. H., Savage, D. A., Patterson, C. C., McKnight, A. J., Crean, J. K., Maxwell, A. P., et al. (2011). Warren 3 Uk GoKin. association analysis of canonical wnt signalling genes in diabetic nephropathy. *PLoS One* 6:e23904. doi: 10.1371/journal.pone.0023904

Kawaguchi, H., Moriyama, M., and Hashimoto, H. (2020). Does disease management for diabetic nephropathy reduce medical expenditure? evidence from a three-period difference-in-differences analysis. *BMC Health Serv. Res.* 20:403. doi: 10.1186/s12913-020-05297-0

Keating, S. T., van Diepen, J. A., Riksen, N. P., and El-Osta, A. (2018). Epigenetics in diabetic nephropathy, immunity and metabolism. *Diabetologia* 61, 6–20. doi: 10.1007/s00125-017-4490-1

Kerr, K., McAneney, A., Smyth, L., Flanagan, C., Silvestri, J., and Nesbitt, M. A. (2019a). A systematic review of differential methylation in rare ophthalmic diseases. *BMJ Open Opthalmol.* 4:e000342. doi: 10.1136/bmjophth-2019-000342

Kerr, K., McAneney, H., Flanagan, C., Maxwell, A. P., and McKnight, A. J. (2019b). Differential methylation as a diagnostic biomarker of rare renal diseases: a systematic review. *BMC Nephrol.* 20:320. doi: 10.1186/s12882-019-1517-5

Kerr, K., McAneney, H., Smyth, L. J., Bailie, C., McKee, S., and McKnight, A. J. (2020). A scoping review and proposed workflow for multi-omic rare disease research. *Orphanet. J. Rare Dis.* 15:107.

Kim, H., Wang, X., and Jin. (2018). Developing DNA methylation-based diagnostic biomarkers. *J. Genet. Genom.* 45, 87–97. doi: 10.1016/j.jgg.2018.02.003

Ko, Y. A., Mohtat, D., Suzuki, M., Park, A. S., Izquierdo, M. C., Han, S. Y., et al. (2013). Cytosine methylation changes in enhancer regions of core pro-fibrotic genes characterize kidney fibrosis development. *Genome Biol.* 14:R108.

Ladd-Acosta, C., and Fallin, M. D. (2019). DNA methylation signatures as biomarkers of prior environmental exposures. *Curr. Epidemiol. Rep.* 6, 1–13. doi: 10.1007/s40471-019-0178-z

Lappalainen, T., and Greally, J. M. (2017). Associating cellular epigenetic models with human phenotypes. *Nat. Rev. Genet.* 18, 441–451. doi: 10.1038/nrg.2017.32

Lassalle, M., Monnet, E., Ayav, C., Hogan, J., Moranne, O., Couchoud, C., et al. (2019). 2017 Annual report digest of the Renal Epidemiology Information Network (REIN) registry. *Transpl. Int.* 32, 892–902. doi: 10.1111/tri.13466

Levy, J. J., Titus, A. J., Petersen, C. L., Chen, Y., Salas, L. A., and Christensen, B. C. (2020). MethylNet: an automated and modular deep learning approach for DNA methylation analysis. *BMC Bioinform.* 21:108. doi: 10.1186/s12859-020-3443-8

Li, W., Sargsyan, D., Wu, R., Li, S., Wang, L., Cheng, D., et al. (2019). DNA Methylome and transcriptome alterations in high glucose-induced diabetic nephropathy cellular model and identification of novel targets for treatment by tanshinone IIA. *Chem. Res. Toxicol.* 32, 1977–1988. doi: 10.1021/acs.chemrestox.9b00117

Li, Z., Zhuang, X., Zeng, J., and Tzeng, C. M. (2017). Integrated analysis of DNA methylation and mrna expression profiles to identify key genes in severe oligozoospermia. *Front. Physiol.* 8:261. doi: 10.3389/fphys.2017.00261

Liang, X., Lai, Y., Wu, W., Chen, D., Zhong, F., Huang, J., et al. (2019). LncRNA-miRNA-mRNA expression variation profile in the urine of calcium oxalate stone patients. *BMC Med. Genom.* 12:57. doi: 10.1186/s12920-019-0502-y

Lin, C. L., Wang, J. Y., Huang, Y. T., Kuo, Y. H., Surendran, K., and Wang, F. S. (2006). Wnt/beta-catenin signaling modulates survival of high glucose-stressed mesangial cells. *J. Am. Soc. Nephrol.* 17, 2812–2820. doi: 10.1681/asn.2005121355

Lin, X., Wang, J., Yun, L., Jiang, S., Li, L., Chen, X., et al. (2016). Association between LEKR1-CCNL1 and IGSF21-KLHDC7A gene polymorphisms and diabetic retinopathy of type 2 diabetes mellitus in the Chinese Han population. *J. Gene Med.* 18, 282–287. doi: 10.1002/jgm.2926

Lindenmeyer, M. T., Eichinger, F., Sen, K., Anders, H. J., Edenhofer, I., Mattinzoli, D., et al. (2010). Systematic analysis of a novel human renal glomerulus-enriched gene expression dataset. *PLoS One* 5:e11545. doi: 10.1371/journal.pone.0011545

McKnight, A. J., O'Donoghue, D., and Maxwell, A. (2009). Annotated chromosome maps for renal disease. *Hum. Mutat.* 30, 314–320. doi: 10.1002/humu.20885

McKnight, A. J., Patterson, C. C., Pettigrew, K. A., Savage, D. A., Kilner, J., Murphy, M., et al. (2010). A GREM1 gene variant associates with diabetic nephropathy. *J. Am. Soc. Nephrol.* 21, 773–781. doi: 10.1681/asn.2009070773

Mitra, S., Mazumder Indra, D., Basu, S., Mondal, R. K., Roy, A., Roychoudhury, S., et al. (2010). Amplification of CyclinL1 in uterine cervical carcinoma has prognostic implications. *Mol. Carcinog* 49, 935–943. doi: 10.1002/mc.20671

Mook-Kanamori, D. O., Marsh, J. A., Warrington, N. M., Taal, H. R., Newnham, J. P., Beilin, L. J., et al. (2011). Variants near CCNL1/LEKR1 and in ADCY5 and fetal growth characteristics in different trimesters. *J. Clin. Endocrinol. Metab* 96, E810–E815.

Moore, K., McKnight, A. J., Craig, D., and O'Neill, F. (2014). Epigenome-wide association study for Parkinson's disease. *Neuromol. Med.* 16, 845–855. doi: 10.1007/s12017-014-8332-8

Muhlberger, I., Monks, K., Fechete, R., Mayer, G., Oberbauer, R., Mayer, B., et al. (2012). Molecular pathways and crosstalk characterizing the cardiorenal syndrome. *OMICS* 16, 105–112. doi: 10.1089/omi.2011.0121

Murphy, T. M., and Mill, J. (2014). Epigenetics in health and disease: heralding the EWAS era. *Lancet* 383, 1952–1954. doi: 10.1016/s0140-6736(14)60269-5

Nakagawa, S., Nishihara, K., Miyata, H., Shinke, H., Tomita, E., Kajiwara, M., et al. (2015). Molecular markers of tubulointerstitial fibrosis and tubular cell damage in patients with chronic kidney disease. *PLoS One* 10:e0136994. doi: 10.1371/journal.pone.0136994

Nakano, K., Whitaker, J. W., Boyle, D. L., Wang, W., and Firestein, G. S. (2013). DNA methylome signature in rheumatoid arthritis. *Ann. Rheum. Dis.* 72, 110–117. doi: 10.1136/annrheumdis-2012-201526

Ochoa-Rosales, C., Portilla-Fernandez, E., Nano, J., Wilson, R., Lehne, B., Mishra, P., et al. (2020). Epigenetic link between statin therapy and Type 2 diabetes. *Diabetes Care* 43, 875–884.

Park, J., Guan, Y., Sheng, X., Gluck, C., Seasock, M. J., Hakimi, A. A., et al. (2019). Functional methylome analysis of human diabetic kidney disease. *JCI Insight* 4:e128886.

Peng, L., Yanjiao, M., Ai-guo, W., Pengtao, G., Jianhua, L., Ju, Y., et al. (2011). A fine balance between CCNL1 and TIMP1 contributes to the development of breast cancer cells. *Biochem. Biophys. Res. Commun.* 409, 344–349. doi: 10.1016/j.bbrc.2011.05.021

Philibert, R. A., Plume, J. M., Gibbons, F. X., Brody, G. H., and Beach, S. R. (2012). The impact of recent alcohol use on genome wide DNA methylation signatures. *Front. Genet.* 3:54. doi: 10.3389/fgene.2012.00054

Qiu, C., Hanson, R. L., Fufaa, G., Kobes, S., Gluck, C., Huang, J., et al. (2018). Cytosine methylation predicts renal function decline in American Indians. *Kidney Int.* 93, 1417–1431. doi: 10.1016/j.kint.2018.01.036

Rakyan, V. K., Beyan, H., Down, T. A., Hawa, M. I., Maslau, S., Aden, D., et al. (2011a). Identification of type 1 diabetes-associated DNA methylation variable positions that precede disease diagnosis. *PLoS Genet.* 7:e1002300. doi: 10.1371/journal.pgen.1002300

Rakyan, V. K., Down, T. A., Balding, D. J., and Beck, S. (2011b). Epigenome-wide association studies for common human diseases. *Nat. Rev. Genet.* 12, 529–541. doi: 10.1038/nrg3000

Reich, H. N., Tritchler, D., Cattran, D. C., Herzenberg, A. M., Eichinger, F., Boucherot, A., et al. (2010). A molecular signature of proteinuria in glomerulonephritis. *PLoS One* 5:e13451. doi: 10.1371/journal.pone.0013451

Reinius, L. E., Acevedo, N., Joerink, M., Pershagen, G., Dahlen, S. E., Greco, D., et al. (2012). Differential DNA methylation in purified human blood cells: implications for cell lineage and studies on disease susceptibility. *PLoS One* 7:e41361. doi: 10.1371/journal.pone.0041361

Renal, U. S., and Data System. (2018). *2018 USRDS Annual Data Report: Epidemiology of Kidney Disease in the United States*. Amsterdam: Elsevier.

Ritchie, M. E., Phipson, B., Wu, D., Hu, Y., Law, C. W., Shi, W., et al. (2015). limma powers differential expression analyses for RNA-sequencing and microarray studies. *Nucleic Acids Res.* 43:e47. doi: 10.1093/nar/gkv007

Rossing, P., Tarnow, L., Nielsen, F. S., Hansen, B. V., Brenner, B. M., and Parving, H. H. (1995). Low birth weight. a risk factor for development of diabetic nephropathy?. *Diabetes* 44, 1405–1407. doi: 10.2337/diabetes.44.12.1405

Salem, R. M., Todd, J. N., Sandholm, N., Cole, J. B., Chen, W. M., Andrews, D., et al. (2019). Genome-Wide association study of diabetic kidney disease highlights biology involved in glomerular basement membrane collagen. *J. Am. Soc. Nephrol.* 30, 2000–2016.

Sandholm, N., Forsblom, C., Makinen, V. P., McKnight, A. J., Osterholm, A. M., He, B., et al. (2014). Genome-wide association study of urinary albumin excretion rate in patients with type 1 diabetes. *Diabetologia* 57, 1143–1153.

Sandholm, N., McKnight, A. J., Salem, R. M., Brennan, E. P., Forsblom, C., Harjutsalo, V., et al. (2013). Chromosome 2q31.1 associates with ESRD in women with type 1 diabetes. *J. Am. Soc. Nephrol.* 24, 1537–1543. doi: 10.1681/asn.2012111122

Sandholm, N., Salem, R. M., McKnight, A. J., Brennan, E. P., Forsblom, C., Isakova, T., et al. (2012). New susceptibility loci associated with kidney disease in type 1 diabetes. *PLoS Genet.* 8:e1002921. doi: 10.1371/journal.pgen.1002921

Sandholm, N., Van Zuydam, N., Ahlqvist, E., Juliusdottir, T., Deshmukh, H. A., Rayner, N. W., et al. (2017). The Genetic Landscape of Renal Complications in Type 1 Diabetes. *J. Am. Soc. Nephrol.* 28, 557–574.

Sandoval, J., Heyn, H., Moran, S., Serra-Musach, J., Pujana, M. A., Bibikova, M., et al. (2011). Validation of a DNA methylation microarray for 450,000 CpG sites in the human genome. *Epigenetics* 6, 692–702. doi: 10.4161/epi.6.6.16196

Sapienza, C., Lee, J., Powell, J., Erinle, O., Yafai, F., Reichert, J., et al. (2011). DNA methylation profiling identifies epigenetic differences between diabetes patients with ESRD and diabetes patients without nephropathy. *Epigenetics* 6, 20–28. doi: 10.4161/epi.6.1.13362

Sarwal, M., Chua, M. S., Kambham, N., Hsieh, S. C., Satterwhite, T., Masek, M., et al. (2003). Molecular heterogeneity in acute renal allograft rejection identified by DNA microarray profiling. *N. Engl. J. Med.* 349, 125–138. doi: 10.1056/nejmoa035588

Smyth, L. J., Duffy, S., Maxwell, A. P., and McKnight, A. J. (2014a). Genetic and epigenetic factors influencing chronic kidney disease. *Am. J. Physiol. Renal. Physiol.* 307, F757–F776.

Smyth, L. J., McKay, G. J., Maxwell, A. P., and McKnight, A. J. (2014b). DNA hypermethylation and DNA hypomethylation is present at different loci in chronic kidney disease. *Epigenetics* 9, 366–376. doi: 10.4161/epi.27161

Smyth, L. J., Maxwell, A. P., Benson, K. A., Kilner, J., McKay, G. J., and McKnight, A. J. (2018). Validation of differentially methylated microRNAs identified from an epigenome-wide association study; sanger and next generation sequencing approaches. *BMC Res. Notes* 11:767. doi: 10.1186/s13104-018-3872-x

Stefan, M., Zhang, W., Concepcion, E., Yi, Z., and Tomer, Y. (2014). DNA methylation profiles in type 1 diabetes twins point to strong epigenetic effects on etiology. *J. Autoimmun.* 50, 33–37. doi: 10.1016/j.jaut.2013.10.001

Sticht, C., Hofele, C., Flechtenmacher, C., Bosch, F. X., Freier, K., Lichter, P., et al. (2005). Amplification of Cyclin L1 is associated with lymph node metastases in head and neck squamous cell carcinoma (HNSCC). *Br. J. Cancer* 92, 770–774. doi: 10.1038/sj.bjc.6602400

Swan, E. J., Maxwell, A. P., and McKnight, A. J. (2015). Distinct methylation patterns in genes that affect mitochondrial function are associated with kidney disease in blood-derived DNA from individuals with Type 1 diabetes. *Diabet. Med.* 32, 1110–1115. doi: 10.1111/dme.12775

Tannukit, S., Wen, X., Wang, H., and Paine, M. L. (2008). TFIP11, CCNL1 and EWSR1 Protein-protein Interactions, and Their Nuclear Localization. *Int. J. Mol. Sci.* 9, 1504–1514. doi: 10.3390/ijms9081504

UK Renal Registry (2019). *UK Renal Registry 21st Annual Report – Data to 31/12/2017*, Bristol, UK. Available online at: https://www.renalreg.org/publications-reports/

van Zuydam, N. R., Ahlqvist, E., Sandholm, N., Deshmukh, H., Rayner, N. W., Abdalla, M., et al. (2018). A genome-wide association study of diabetic kidney disease in subjects with Type 2 diabetes. *Diabetes* 67, 1414–1427.

Walaszczyk, E., Luijten, M., Spijkerman, A. M. W., Bonder, M. J., Lutgers, H. L., et al. (2018). DNA methylation markers associated with type 2 diabetes, fasting glucose and HbA1c levels: a systematic review and replication in a case-control sample of the lifelines study. *Diabetologia* 61, 354–368. doi: 10.1007/s00125-017-4497-7

Wettenhall, J. M., and Smyth, G. K. (2004). limmaGUI: a graphical user interface for linear modeling of microarray data. *Bioinformatics* 20, 3705–3706. doi: 10.1093/bioinformatics/bth449

Woroniecka, K. I., Park, A. S., Mohtat, D., Thomas, D. B., Pullman, J. M., and Susztak, K. (2011). Transcriptome analysis of human diabetic kidney disease. *Diabetes* 60, 2354–2369. doi: 10.2337/db10-1181

Yaghootkar, H., and Freathy, R. M. (2012). Genetic origins of low birth weight. *Curr. Opin. Clin. Nutr. Metab. Care* 15, 258–264. doi: 10.1097/mco.0b013e328351f543

Zhou, F., Wang, R., Yuan, P., Ren, Y., Mao, Y., Li, R., et al. (2019). Reconstituting the transcriptome and DNA methylome landscapes of human implantation. *Nature* 572, 660–664. doi: 10.1038/s41586-019-1500-0

Zhou, T., He, X., Cheng, R., Zhang, B., Zhang, R. R., Chen, Y., et al. (2012). Implication of dysregulation of the canonical wingless-type MMTV integration site (WNT) pathway in diabetic nephropathy. *Diabetologia* 55, 255–266. doi: 10.1007/s00125-011-2314-2

Zhou, W., Laird, W., and Shen, H. (2017). Comprehensive characterization, annotation and innovative use of Infinium DNA methylation BeadChip probes. *Nucleic Acids Res.* 45:e22.

Conflict of Interest: The authors declare that the research was conducted in the absence of any commercial or financial relationships that could be construed as a potential conflict of interest.

Copyright © 2020 Smyth, Patterson, Swan, Maxwell and McKnight. This is an open-access article distributed under the terms of the Creative Commons Attribution License (CC BY). The use, distribution or reproduction in other forums is permitted, provided the original author(s) and the copyright owner(s) are credited and that the original publication in this journal is cited, in accordance with accepted academic practice. No use, distribution or reproduction is permitted which does not comply with these terms.

frontiers in Cell and Developmental Biology

REVIEW
published: 12 November 2020
doi: 10.3389/fcell.2020.543099

The Role of Disturbed Mg Homeostasis in Chronic Kidney Disease Comorbidities

Cristian Rodelo-Haad[1,2,3,4†], M. Victoria Pendón-Ruiz de Mier[1,2,3,4†], Juan Miguel Díaz-Tocados[1,2], Alejandro Martin-Malo[1,2,3,4], Rafael Santamaria[1,2,3,4], Juan Rafael Muñoz-Castañeda[1,2,3,4*‡] and Mariano Rodríguez[1,2,3,4‡]*

[1] Maimonides Biomedical Research Institute of Cordoba (IMIBIC), Córdoba, Spain, [2] University of Córdoba, Córdoba, Spain, [3] Nephrology Service, Reina Sofia University Hospital, Córdoba, Spain, [4] Spanish Renal Research Network (REDinREN), Institute of Health Carlos III, Madrid, Spain

OPEN ACCESS

Edited by:
Roland Wohlgemuth, Lodz University of Technology, Poland

Reviewed by:
Martin Kolisek, Comenius University, Slovakia
Said Kamel, INSERM U1088 Mécanismes Physiopathologiques et Conséquences des Calcifications Cardiovasculaires: Rôle des Remodelages Cardiovasculaires et Osseux, France

***Correspondence:**
Rafael Santamaria
rsantamariao@gmail.com
Juan Rafael Muñoz-Castañeda
juanr.munoz.exts@juntadeandalucia.es

†These authors share first authorship
‡These authors share last authorship

Specialty section:
This article was submitted to Molecular Medicine, a section of the journal Frontiers in Cell and Developmental Biology

Received: *15 March 2020*
Accepted: *09 October 2020*
Published: *12 November 2020*

Citation:
Rodelo-Haad C, Pendón-Ruiz de Mier MV, Díaz-Tocados JM, Martin-Malo A, Santamaria R, Muñoz-Castañeda JR and Rodríguez M (2020) The Role of Disturbed Mg Homeostasis in Chronic Kidney Disease Comorbidities. Front. Cell Dev. Biol. 8:543099. doi: 10.3389/fcell.2020.543099

Some of the critical mechanisms that mediate chronic kidney disease (CKD) progression are associated with vascular calcifications, disbalance of mineral metabolism, increased oxidative and metabolic stress, inflammation, coagulation abnormalities, endothelial dysfunction, or accumulation of uremic toxins. Also, it is widely accepted that pathologies with a strong influence in CKD progression are diabetes, hypertension, and cardiovascular disease (CVD). A disbalance in magnesium (Mg) homeostasis, more specifically hypomagnesemia, is associated with the development and progression of the comorbidities mentioned above, and some mechanisms might explain why low serum Mg is associated with negative clinical outcomes such as major adverse cardiovascular and renal events. Furthermore, it is likely that hypomagnesemia causes the release of inflammatory cytokines and C-reactive protein and promotes insulin resistance. Animal models have shown that Mg supplementation reverses vascular calcifications; thus, clinicians have focused on the potential benefits that Mg supplementation may have in humans. Recent evidence suggests that Mg reduces coronary artery calcifications and facilitates peripheral vasodilation. Mg may reduce vascular calcification by direct inhibition of the Wnt/β-catenin signaling pathway. Furthermore, Mg deficiency worsens kidney injury induced by an increased tubular load of phosphate. One important consequence of excessive tubular load of phosphate is the reduction of renal tubule expression of α-Klotho in moderate CKD. Low Mg levels worsen the reduction of Klotho induced by the tubular load of phosphate. Evidence to support clinical translation is yet insufficient, and more clinical studies are required to claim enough evidence for decision-making in daily practice. Meanwhile, it seems reasonable to prevent and treat Mg deficiency. This review aims to summarize the current understanding of Mg homeostasis, the potential mechanisms that may mediate the effect of Mg deficiency on CKD progression, CVD, and mortality.

Keywords: magnesium, chronic kidney disease, hypomagnesemia, cardiovascular disease, mineral metabolism and bone disease

INTRODUCTION

Magnesium (Mg) is required to maintain cell function, and it has a fundamental role in biological processes such as cell signaling, energy production, metabolism, cell growth and proliferation, synthesis of biomacromolecules, apoptosis, membrane fluidity, and control of cell motility (Romani, 2007). Mg is also required to stabilize RNA and DNA, by the time it facilitates the mechanisms of DNA repair, and it serves as a cofactor for many enzymes (de Baaij et al., 2015). Also, Mg is necessary for appropriate regulation of sodium and potassium transport (Bara et al., 1993).

Over the last decade, the study of Mg disturbances has gained attention given the several molecular processes involving Mg. Both Mg deficiency and hypermagnesemia have been associated with different fatal and non-fatal clinical outcomes.

The kidney plays a key role in Mg handling. Mg deficiency may be observed at any stage of chronic kidney disease (CKD). In the context of CKD, Mg disturbances are associated with an increase in oxidative stress, the production of inflammatory cytokines, sympathetic overactivity, increased adhesion of molecules, inflammation, and the development of cardiovascular disease (CVD). In fact, Mg deficiency has been associated with an increased risk of non-fatal and fatal cardiovascular events. Such association may be supported by the fact that low Mg is related to the development of high blood pressure (BP), renal dysfunction either in native or after kidney transplantation (KT), and vascular calcifications, all of which are determinants of CVD outcomes.

The aim of the present review is to describe the scientific evidence that supports the relationship between Mg and CKD and also the development of different comorbidities associated with CKD. First, a brief description of Mg transport and homeostasis will be presented. Second, an up-to-date description of the current understanding of Mg deficiency and its association with different abnormalities in parathyroid hormone (PTH) secretion, mineral metabolism, bone turnover, and development of CKD will be addressed. Both experimental and human data supporting such an association will be described. Then, the role of Mg in the development of CVD, vascular calcification, and death from cardiovascular causes will be reviewed. Special attention is made to the relationship between Mg disturbances and endothelial dysfunction, coronary artery calcifications (CACs), arrhythmias, and heart failure. Finally, we discuss the limited number of clinical studies on Mg supplementation and future perspectives.

Mg TRANSPORT AND HOMEOSTASIS

The total amount of Mg in the body is approximately 22.6 g, and the concentration in serum ranges from 2.1 to 3.1 mg/dL. Approximately 1% of the total Mg in the body is located in the extracellular space; 60% is ionized or "free," 30% is bound to proteins and 10% as phosphate, citrate, or oxalate salts (Kolisek et al., 2019), and bone is an important reservoir of Mg (around 66%) (Green, 1994).

Most Mg is within the intracellular compartment, and the passage to the extracellular space is slow. It is interesting to mention that the Mg concentration in the cytosol and the extracellular space is similar; this is in contrast with other divalent anions such as calcium with an intracellular concentration approximately 20,000-fold lower than in the extracellular compartment.

The Mg gradient between cytosol and cell organelles is almost non-existent (Romani and Scarpa, 2000; Schweigel-Röntgen and Kolisek, 2014). Intracellular Mg is regulated by different types of Mg transporters: transient receptor potential melastatin 7 channel (TRPM7), SLC41A1, SLC41A2, MRS2, TRPM6, and CNNM2 (de Baaij et al., 2015). Although MagT1 was initially described as Mg transporter, most recent evidence indicates that MagT1 gene sequence differs from other known Mg transporter and acts as oxidoreductase subunits of the ER-localized STT3B [catalytic subunit of the oligosaccharyltransferase (OST complex)] (Cherepanova et al., 2014; Shrimal et al., 2015). Different studies have shown the intracellular localization of MagT1 in the endoplasmic reticulum. MagT1 is not expressed in STTB3-B (−/−) HEK293 derived cells, which make unlikely its role as membrane transporter. In addition, the overexpression of MagT1 does not increase intracellular Mg concentration. Therefore, it has been hypothesized that the role of MagT1 in Mg transport is indirect, so STT3-B complex glycosylation mediated by MagT1 is the mechanism through which MagT1 promotes Mg transport activity (Cherepanova and Gilmore, 2016; Cherepanova et al., 2016). Similarly, there is some controversy on whether CNNM2 and CNNM4 act as Mg transporters or exclusively as sensors for other components that finally transport Mg (Kolisek et al., 2019). CNNM2 is highly expressed in the brain, heart, kidney, and liver, and it is of particular interest because its expression is mediated by the amount of Mg contained in the food. Concerning the kidney expression of CNNM2, it is known that variants of human CNNM2 have been implicated in the development of Mg wasting syndrome (dominant hypomagnesemia), which support the role of CNNM2 as Mg transporter (Funato et al., 2017; Kolisek et al., 2019), whereas the deletion of the CNNM2 gene in the brain is associated with disturbed brain development and hypomagnesemia. This information on CNNM2 as Mg transporter has been validated in animal models in which CNNM2 knockout mice present hypomagnesemia and reduced kidney Mg reabsorption (Funato et al., 2017). However, other authors suggest that rather than a transporter itself, CNNM2 acts as a regulator of Mg transport, perhaps through the activation of TRPM7 (Arjona et al., 2014; Sponder et al., 2016). The current understanding of CNNM1 and CNNM3 is scarce, and the specific role is yet to be elucidated.

Homeostasis of Mg is maintained by a controlled balance between the intestinal absorption and renal excretion with a serum concentration ranging from 1.3 to 2.7 mg/dL, although this range may vary between the different laboratories (Pérez González et al., 2009).

Daily intake of Mg is around 300 to 400 mg, and 50% is absorbed in the gastrointestinal tract (ileum and proximal jejunum). Proximal renal tubules reabsorb only 15 to 25% of the filtered Mg; 60–70% is reabsorbed in the ascending limb of the loop of Henle, and the distal tubule reabsorbs

a 5 to 10% (Pérez González et al., 2009; de Baaij et al., 2015). Hypomagnesemia is defined as serum Mg concentrations lower than 1.7 mg/dL, whereas hypermagnesemia is considered if serum Mg levels are higher than 2.5 mg/dL.

The primary sources of Mg are seeds, cereals, walnuts, green vegetables, and some types of meat and seafood. There are two processes responsible for intestinal Mg absorption. The first is active transport, which depends on a TRPM6. The second is a passive process that occurs by a paracellular pathway (Pérez González et al., 2009). Renal absorption of Mg occurs in the proximal tubule (15–20%); in the thick ascending loop of Henle, 65 to 70% of Mg is reabsorbed, and a small percentage is reabsorbed in the distal tubule (5–10%) through active transport via the apical TRPM6 pathway. With respect to the active mechanism of Mg transport, TRPM6 channels are located in the basolateral membrane of the cells in the thick ascending limb of Henle loop. However, recent evidence suggests the participation of a sodium-dependent exchange mechanism where Na^+/K^+-ATPase pump participates together with low concentrations of Na^+ (Schlingmann et al., 2002). A large proportion of Mg is reabsorbed in the ascending limb of the loop of Henle through paracellular pathway driven by an electrogenic gradient (positive lumen voltage) generated by the secretion of potassium into the lumen after its reabsorption through the Na-K-2Cl cotransporter.

Increased renal or gastrointestinal losses may cause hypomagnesemia (plasma Mg concentration <1.3 mg/dL or 0.75 mM) (**Figure 1**), decreased intake, or a disbalance between extracellular to intracellular Mg (Ahmed and Mohammed, 2019). Bartter and Gitelman syndrome, familial hypomagnesemia with hypercalciuria, and nephrocalcinosis are some of the pathologies associated with an increased renal loss of Mg. There are nephrotoxic drugs [aminoglycoside, amphotericin B, cisplatin, pentamidine, proton-pump inhibitors, calcineurin inhibitors (CNIs) (cyclosporine and tacrolimus), or epidermal growth factor receptor inhibitors] that are known to increase urinary excretion of Mg and thus be the cause of hypomagnesemia (de Baaij et al., 2015).

Hypomagnesemia is also common in alcoholic patients with a prevalence of approximately 30%. These are poorly nourished patients with a large intracellular shift of Mg ions into cells associated with carbohydrate feeding (Crook et al., 2001).

Hypomagnesemia, through several mechanisms, may produce pathophysiological changes responsible for many CKD-associated comorbidities. Low Mg level is frequently observed in CKD, hypertension, cardiac arrhythmias, sudden cardiac death, coronary artery disease, dyslipidemia, or metabolic syndrome (Severino et al., 2019). It has also been described that Mg plays an essential role in the regulation of insulin actions and glucose homeostasis. Hypomagnesemia has been associated with type 2 diabetes mellitus and insulin resistance (Kostov, 2019). More recently, Mg has been linked to energy production. In this regard, Mg binds to ATP to serve as a cofactor during glucose oxidation and modulates some enzymes that participate in the citric acid cycle (Yamanaka et al., 2016). Moreover, Mg enhances mitochondrial isocitrate dehydrogenase, 2-oxoglutarate dehydrogenase, and pyruvate dehydrogenase, all of which participate in energy production. More interestingly, the dysregulation of Mg modifies mitochondrial morphology, so ATP concentration is reduced. This fact is highly relevant because abnormal mitochondrial morphology has been linked to cancer, obesity, type 2 diabetes, and neurodegenerative disorders (Westermann, 2010; Imai and Lu, 2011; Yamanaka et al., 2016).

Low serum Mg levels have also been related to neurological diseases such as migraine, epilepsy, Parkinson disease, or depression (de Baaij et al., 2015).

Magnesium also has notable anti-inflammatory properties; therefore, hypomagnesemia is linked to a state of chronic systemic inflammation and oxidative stress (Weglicki, 2012). Mg is an active modulator of the expression and release of proinflammatory neuropeptide substance P, a compound involved in the perception of pain that is promoted by nuclear factor-κB (NF-κB) and the expression of proinflammatory genes and cytokines such as tumor necrosis factor α (TNF-α) (Nielsen, 2018). Hypermagnesemia is not frequent, and so far, no genetic causes have been identified (**Figure 2**). It may cause nausea, vomiting, flushing, or lethargy. Very high levels of Mg may produce severe cardiac dysfunction with hypotension, asystole, or even death by cardiac arrest.

Hypermagnesemia has been described in claudin 10 knockout mice; claudin 10 is expressed in the thick ascending limb of Henle loop that facilitates paracellular transport of Na^+. The absence of claudin causes an increase in positive charge (Na^+) in the lumen, which promotes paracellular Mg transport resulting in hypermagnesemia and nephrocalcinosis (Breiderhoff et al., 2012; de Baaij et al., 2015).

HYPOMAGNESEMIA AND CKD

Experimental and human data have been published relative to the association between serum Mg levels, the impairment of kidney function, and renal outcomes in CKD. The abnormal handling of Mg by the kidney may result in either hypomagnesemia or hypermagnesemia (Cunningham et al., 2012; Massy and Drüeke, 2015).

Strong evidence exists, linking hypomagnesemia and CVD. CVD and CKD share risk factors, so Mg likely impairs kidney function indirectly through the worsening of classic CVD risk factors. Indirect effects may be based on the higher risk of hypertension observed in patients with low Mg (Ascherio et al., 1992). Also, Mg deficiency indirectly impairs kidney function by promoting diabetes and endothelial dysfunction through increasing oxidative stress, inflammation, and the expression of different atherothrombotic factors (**Figure 3**) that affects different organs and systems such as parathyroid glands, immune system (inflammation), mineral metabolism, bone, kidney, and the cardiovascular system. In the following sections, we will describe the relation between Mg and these systems.

Mg and the PTH

During CKD, Mg status needs to be taken into consideration to achieve optimal management of mineral metabolism disorders and due to serum Mg has direct effects on PTH regulation and bone.

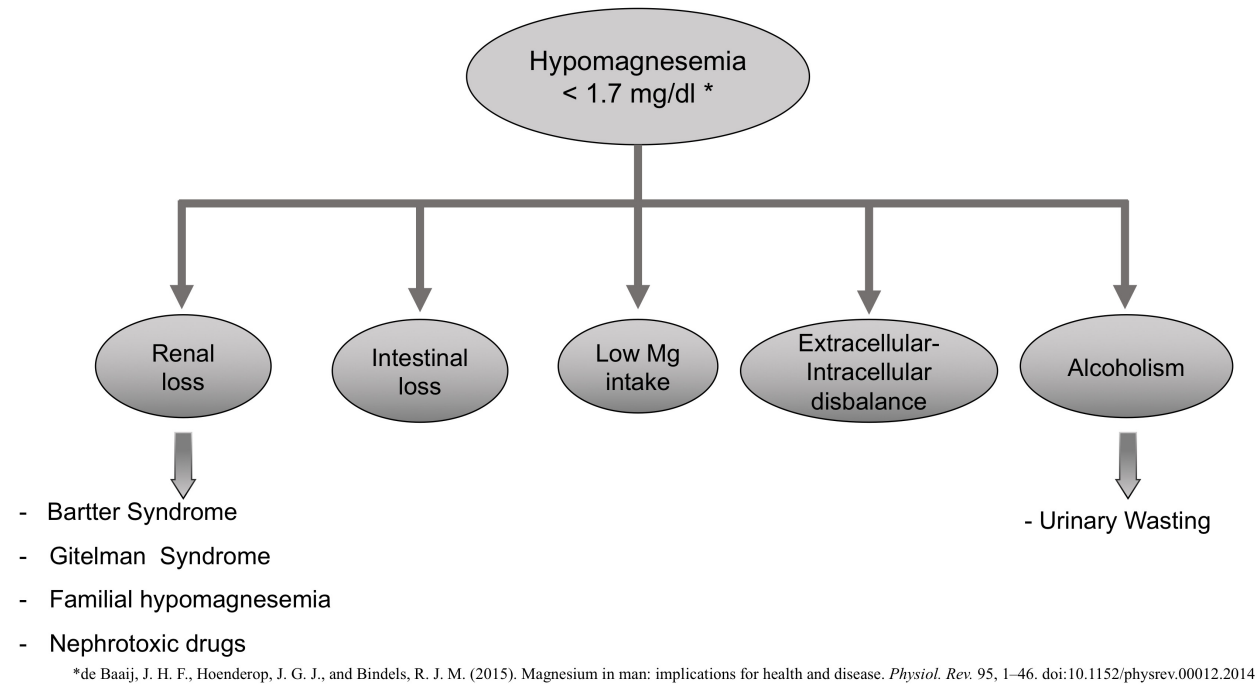

FIGURE 1 | Potential causes of Hypomagnesemia.

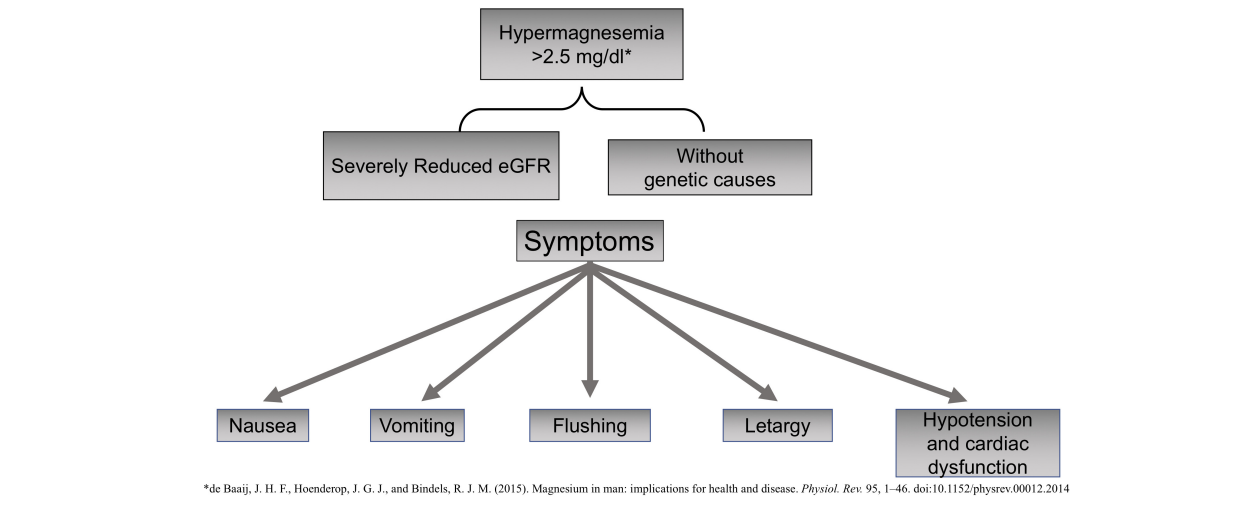

FIGURE 2 | Causes and Symptoms of Hypomagnesemia.

Cholst et al. (1984) described a case of asymptomatic hypocalcemia in pregnant women after treatment with intravenous Mg sulfate for premature onset of labor. This hypocalcemia was associated with a concomitant increase in plasma Mg and a decrease in PTH levels, bringing up the key role of Mg in the regulation of PTH secretion. Interestingly, plasma calcium remained low despite the normalization of PTH levels after 3 h of Mg infusion.

In incubated intact parathyroid glands, an increase in extracellular Mg reduced PTH secretion, and this effect is magnified if PTH is being stimulated by low calcium (Rodríguez-Ortiz et al., 2014; **Figure 4**). The inhibitory effects of Mg on PTH secretion is mediated through the calcium-sensing receptor (CaSR) (Quinn et al., 2013). Essentially, Mg ions target CaSR in the parathyroid glands, activating the downstream signaling pathway and reducing PTH release (Brown et al., 1987; Zhang C. et al., 2016).

Marked hypomagnesemia also reduces PTH levels even in the presence of hypocalcemia; this phenomenon is referred to as "paradoxical blockade of PTH secretion." With serum Mg below

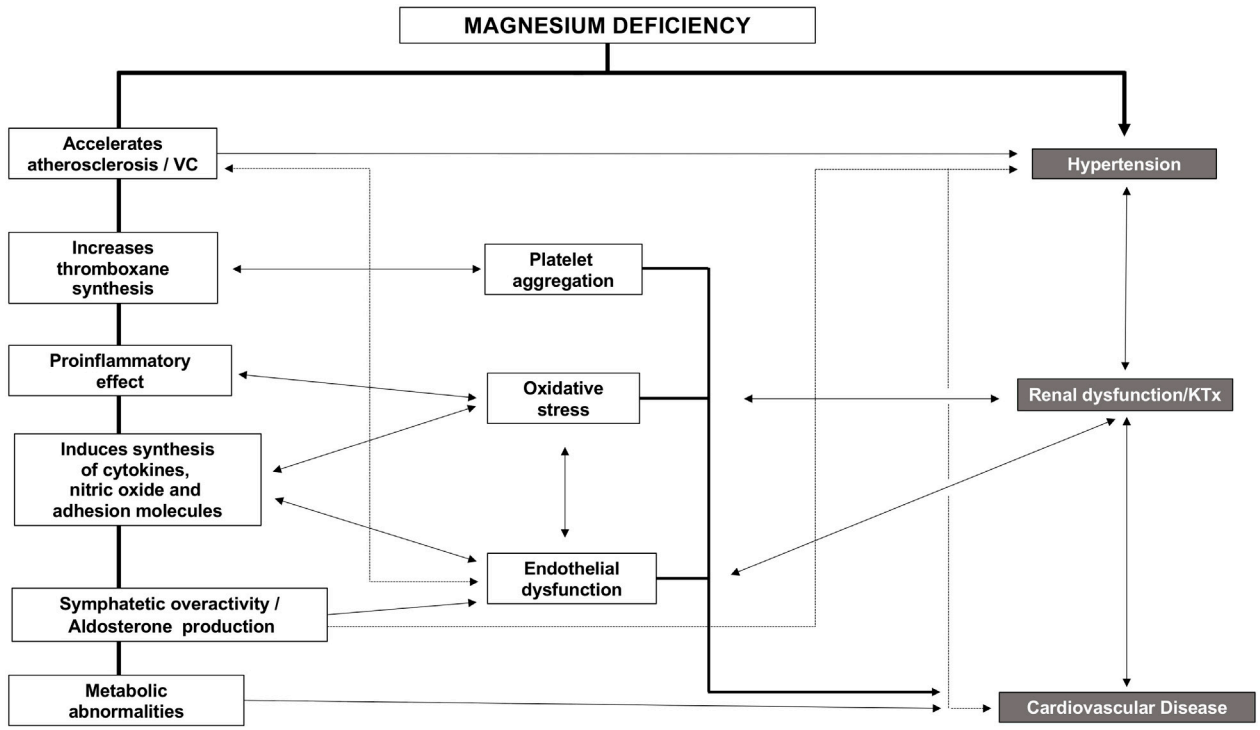

FIGURE 3 | Consequences of Hypomagnesemia.

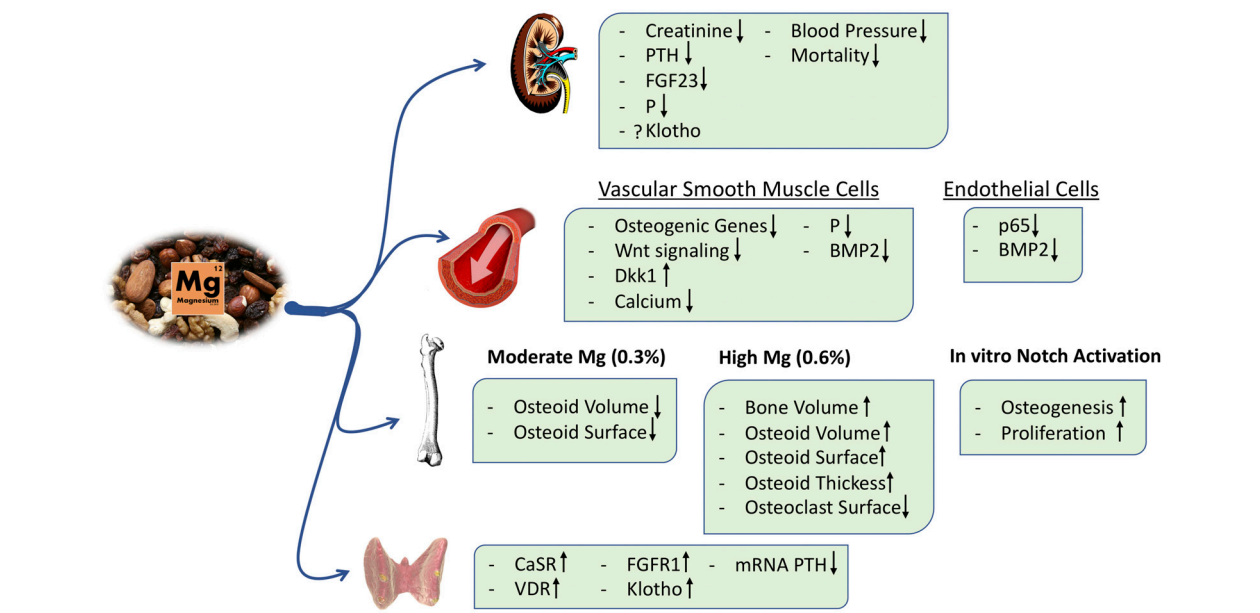

FIGURE 4 | Main effects of Mg Supplementation.

1.2 mg/dL, there is a disinhibition of Gα-subunits, which mimics activation of the CaSR and reduction of PTH secretion (Quitterer et al., 2001; Vetter and Lohse, 2002).

In patients undergoing regular hemodialysis, high levels of Mg are associated with low PTH values (Navarro et al., 1999). Sakaguchi et al. (2014, 2018c) showed that, in HD patients, hypomagnesemia was related to high serum PTH, frequent hip fractures, and increased cardiovascular and non-cardiovascular mortality. Very high concentrations of Mg were associated with excessive suppression of PTH. In this

respect, plasma Mg concentration appears to be key in the management of CKD-MBD.

The Effect of Mg on Bone

Around 60% of Mg is located in bone (Gröber et al., 2015). Alfrey and Miller (1973) demonstrated that serum Mg reflects the content of Mg in bone, and the existence of two different pools of Mg in bone was shown, one exchangeable between blood and bone and another that persists in the bone. Additionally, they suggested a role of bone Mg accumulation on renal osteodystrophy. However, there is limited information on the effects of Mg on bone in CKD patients.

Morinière et al. (1988) showed no significant changes in any bone histomorphometric parameter after 8 months of treatment with Mg hydroxide; however, they showed clear tendencies to increase osteoid and decrease osteoclasts resorption surface. In this line of research, Gonella et al. (1988) showed that osteomalacia was prevented by reducing Mg concentration in the dialysis bath. A Mg concentration of >4.5 mg/dL might prevent the *in vitro* formation of hydroxyapatite (Ennever and Vogel, 1981).

In animals, Rude et al. showed that as compared with the control Mg diet (0.063%), an Mg-deficient diet (0.002%) increased plasma calcium concentration and decreased PTH and calcitriol levels. Rats fed a low-Mg diet showed lower trabecular bone volume associated with more osteoclasts and reduced osteoblast activity (Rude, 1998). These findings suggest that, in addition to PTH and vitamin D, Mg is critical for bone remodeling. Other studies by the same group reported similar results in rats fed on diets with sequential Mg depletion, and these bone changes were associated with the presence of a higher amount of proinflammatory and pro-osteoclastogenic cytokines in bone (Rude et al., 2004, 2006, 2009). Thus, Mg supplementation might decrease osteoclast number, being beneficial in a bone disease with high bone resorption, as observed with hyperparathyroidism.

Magnesium promotes passive and active mechanisms that might affect calcium phosphate crystallization. A reduced concentration of Mg ions has a marked effect on nucleation and growth of calcium phosphate crystals. Mg delays the conversion of amorphous calcium precipitates to the more stable apatite phase and promotes the formation of whitlockite, which is a calcium/Mg orthophosphate that may alter bone and soft tissue mineralization. In addition to this passive phenomenon, other studies are showing a direct active role of Mg in the bone that will be exposed later (Ennever and Vogel, 1981; Verberckmoes et al., 2007).

More recently, in a *post hoc* analysis of the CALMAG study, the authors investigated whether there were changes in serum bone turnover markers in a cohort of hemodialysis patients receiving an Mg-based phosphate binder (calcium acetate/Mg carbonate) or the non-calcium-containing phosphate binder, sevelamer. Calcium acetate/Mg carbonate administration increased the serum levels of both calcium and Mg and reduced serum phosphate after 9 weeks of treatment. In this period, Mg-based phosphate binder administration decreased the serum β-crosslap collagen type I C-telopeptides, a marker of bone resorption, and increased the bone-specific alkaline phosphatase. These effects were not observed in the sevelamer group, although both groups showed a similar reduction in PTH levels (Covic et al., 2013). With respect to the active effects of Mg on bone, we have shown that Mg exerts a direct pro-osteogenic effect in an *in vitro* model of mesenchymal stem cells (MSCs) differentiated into osteoblasts, and this effect is at least partially mediated by the activation of the canonical Notch signaling pathway. Furthermore, the Mg transport through the cell membrane via the TRPM7 channel is required to observe Mg effects on osteogenesis, and inhibition of TRPM7 with 2-APB abolished MSC differentiation into osteoblasts (Díaz-Tocados et al., 2017; **Figure 4**). In addition, in a rat model of renal insufficiency, it was observed that dietary Mg supplementation maintains the number of osteoblasts despite a concomitant reduction in plasma PTH levels; however, excessive amounts of Mg may produce an accumulation of the osteoid in bone (Díaz-Tocados et al., 2017). Extremely high Mg may decrease hydroxyapatite formation in favor of whitlockite (Jang et al., 2015). Thus, Mg supplementation modulates PTH secretion, but it also directly stimulates osteoblast differentiation and maintains osteoclast number in bone; the exact mechanisms are not fully understood, and contemporary studies are needed to clarify the potential effects of Mg on bone and mineral metabolism and the safety of Mg treatment in clinical practice (Muñoz-Castañeda et al., 2018).

A direct effect of Mg on the prevention of renal and CVDs has also been reported in animal models and clinical studies.

Mg and Kidney Function

Experimental and human data have been published regarding the association between serum Mg levels, the impairment of kidney function, and renal outcomes in CKD. As mentioned, the abnormal handling of Mg by the kidney may result in either hypomagnesemia or hypermagnesemia (Cunningham et al., 2012; Massy and Drüeke, 2015).

Experimental Data Related to Hypomagnesemia and Kidney Injury

Since the early 1990s, low-Mg diets were described to induce nephrocalcinosis and impairment of kidney function (Van Camp et al., 1990). Subsequent studies in rats showed proximal renal tubules electron-dense granules in the brush border after only 12 h of Mg-deficient diet. After 7 days, the tubular injury was settled down, as shown by calcium deposits and necrosis of the tubular epithelial (Matsuzaki et al., 2002).

Increased serum phosphate concentration and an excessive tubular load of phosphate induce renal damage through renal tubular injury, interstitial fibrosis, and inflammation (Neves et al., 2004; Sakaguchi et al., 2012, 2018a; Gorostidi et al., 2018; Santamaría et al., 2018). Interestingly, a recent *in vitro* study demonstrated that Mg reduces renal cell toxicity associated with hyperphosphatemia (Sakaguchi et al., 2015; **Figure 4**). Furthermore, in animal models of CKD, an Mg-deficient diet aggravates tubular damage and down-regulates α-Klotho expression irrespective of serum phosphate levels (Sakaguchi et al., 2018b). It is likely that an Mg-deficient diet results in the up-regulation of mRNA expression of NPT2A cotransporters in

proximal tubules, promoting a positive phosphate balance and thus renal tubular injury. Despite the kidney damage and the consequent phosphate overload, a low-Mg diet was associated with low levels of FGF23 (Sakaguchi et al., 2018b), suggesting a deficient phosphate excretion. However, other experiments in animals have shown that dietary Mg supplementation was associated with a decrease in FGF23 levels, perhaps due to a reduction of serum phosphate levels and an increase in renal expression of Klotho (Diaz-Tocados et al., 2017; **Figure 4**). In Klotho knockout mice, a high Mg intake prevented vascular calcification despite increased serum levels of phosphate and FGF23 (Braake et al., 2019), suggesting other effects of Mg independent of Klotho and phosphate.

Studies in 5/6 nephrectomized rats clearly showed that renal function was better preserved in animals on a diet supplemented with Mg as compared to rats fed a basal Mg diet (0.1%). Different mechanisms could be involved, such as the reduction in intestinal absorption of phosphate mediated by an increase in the dietary intake of Mg, which is also associated with a reduction in vascular calcifications, lower systolic and diastolic BP, and an improvement in endothelial function (**Figure 3**). However, the beneficial effect of Mg on kidney function seems unlikely to be exclusively due to the reduction of intestinal absorption of phosphate because parenteral administration of Mg was able to reduce vascular calcification without a change in serum phosphate levels (Diaz-Tocados et al., 2017).

Clinical Studies Related to Hypomagnesemia and Kidney Injury

The incidence of CKD is increasing worldwide. It would be desirable to identify the factors and mechanisms that may delay CKD progression. In this line, hypomagnesemia has emerged as a factor that should be corrected as a strategy to reduce the progression of CKD. However, most of the information regarding the association between hypomagnesemia and CKD progression is based on observational studies (Joosten et al., 2015; Tin et al., 2015). In a study from the United States, estimated glomerular filtrate rate (eGFR) >60 mL/min/1.73 m^2 and a low dietary Mg intake (<101 mg/1,000 kcal) were associated with a more rapid decrease in kidney function. This association was maintained irrespective of sociodemographic variables, household income, baseline eGFR, diabetes, and hypertension (Rebholz et al., 2016). In other studies from Iran and Australia, adults with a high intake of Mg had a lower incidence of CKD (Strippoli et al., 2011; Farhadnejad et al., 2016). Diabetic patients with a low Mg intake also showed a more rapid decline in eGFR, together with an increase in proteinuria independently of glycemic control and the use of angiotensin-converting enzyme (ACE) inhibitor/angiotensin receptor blocker (Pham et al., 2005). In a subanalysis of the ARIC study, more than 13,000 African-American patients with eGFR >60 mL/min/1.73 m^2 were followed up for more than 20 years to prospectively evaluate the incidence of CKD and end-stage of kidney disease (ESKD). Patients with serum Mg less than 1.82 mg/dL showed a two-fold more risk of incident CKD compared to those with serum Mg greater than 2.1 mg/dL irrespective of gender, ethnicity, being diabetic, being hypertensive, and having other comorbidities (Tin et al., 2015). Concerning ESKD, low Mg levels increased by six-fold the risk of ESKD compared to patients with Mg within the normal range. Similarly, another study that included patients with different stages of CKD showed that in those with baseline serum Mg below 1.8 mg/dL, the yearly decline in eGFR was 9.6% higher as compared with 3.5% in subjects with higher values of serum Mg (Van Laecke et al., 2013).

Proteinuria is widely accepted as an independent risk factor for CKD. Proteinuria is also independently associated with hypomagnesemia as it enhances renal Mg wasting (Oka et al., 2018). As such, a combination of proteinuria and hypomagnesemia would aggravate the decline of kidney function.

In critically ill patients with acute kidney injury, there is an association between low Mg and the risk of non-recovery of kidney function (Alves et al., 2013). In this study, the prevalence of hypomagnesemia was significantly higher in patients who did not recover kidney function. These results may be based on the ability of Mg to reduce the negative impact of some medications on the kidney by promoting vasodilation or by reducing inflammation, oxidative stress, and preserving endothelial integrity (Alves et al., 2013). Another possible explanation is the development of endothelial dysfunction that indirectly increases vasoconstriction, BP, and sympathetic nerve overactivity, three well-known risk factors for kidney function impairment (Murasato et al., 1999; Ferrè et al., 2010).

It is important to mention the high prevalence of hypomagnesemia following KT (Nijenhuis et al., 2004). Evidence suggests that the leading cause of hypomagnesemia in this population is the treatment with CNIs as tacrolimus (FK506) and cyclosporine A (CsA). CNIs cause hypercalciuria and hypermagnesuria through the down-regulation of TPRV5, TPRM6, and calbindin-D_{28k} (Nijenhuis et al., 2004). In patients on CsA, hypomagnesemia is associated with a progressive decline of kidney function and a reduction of kidney graft survival. Also, it is suggested that Mg deficiency may exacerbate CsA nephrotoxicity (Holzmacher et al., 2005). In the long term, CNIs also increase the odds of post-transplant diabetes. Consequently, in kidney grafts, the CNI-induced hypomagnesemia and diabetes may contribute to kidney graft function deterioration (Van Laecke et al., 2009). Also, in KT recipients, hypomagnesemia is negatively correlated with pulse wave velocity and thus vascular stiffness, which may contribute to renal function impairment (Van Laecke et al., 2011).

Mg and CVD

Chronic kidney disease progression is associated with CVD. Actually, a high percentage of mortality in CKD patients is related to cardiovascular causes. Kidney and heart are interconnected organs; dysfunction in one organ may affect the function of the other. This close relationship is defined as cardiorenal syndrome. The mechanism underlying the cardiorenal connection in pathologic conditions remains incompletely understood. Some of the pathophysiological mechanisms whereby kidney and heart are interconnected might be associated with alterations in Mg homeostasis.

Several mechanisms may explain the adverse effects of hypomagnesemia on CVD (**Figure 3**). Mg deficiency accelerates

the atherosclerotic process, increases thromboxane synthesis stimulating platelet aggregation, produces oxidative stress due to its proinflammatory effect, and also induces the synthesis of other cytokines, nitric oxide, and adhesion molecules [vascular cell adhesion molecule 1 (VCAM-1) and intercellular adhesion molecule 1], all of which ends in endothelial dysfunction (Bo and Pisu, 2008). In patients with high cardiovascular risk, low serum Mg is associated with carotid atherosclerosis, independently of other traditional cardiovascular risk factors (Rodríguez-Ortiz et al., 2019).

Additionally, low Mg is associated with metabolic abnormalities such as insulin resistance, hyperglycemia, or dyslipidemia. Mg regulates cellular glucose metabolism and intervenes in phospholipid metabolism and mitochondrial oxidation of long-chain fatty acids (Severino et al., 2019). Serum Mg concentrations ranging from 1.73 to 2.16 mg/dL are associated with a linear decrease in the risk of cardiovascular events. At the same time, Mg intake has a non-linear inverse association with cardiovascular events (Qu et al., 2013).

Pathophysiological processes such as vascular calcifications, hypertension, arrhythmias, heart failure, endothelial dysfunction, and even cardiovascular death are possibly related to abnormal Mg homeostasis. In the following sections, the role of Mg deficiency on cardiovascular disorders is discussed.

Endothelial Dysfunction

Magnesium potentiates the production of local vasodilator mediators (prostacyclin and nitric oxide) and facilitates the vascular response to vasoactive substances (endothelin-1, angiotensin II, and catecholamines). The levels of antioxidants (vitamin C, vitamin E, selenium, glutathione peroxidase, superoxide dismutase, and catalase) are also decreased in the context of Mg deficiency (Kostov and Halacheva, 2018). It has been shown that hypomagnesemia decreases endothelial cell proliferation, stimulates the adhesion of monocytes, and potentiates the development of endothelial dysfunction via activation of NF-κB (Kostov and Halacheva, 2018). This correlates with a marked down-regulation of the levels of CDC25B, a member of the CDC25 family of phosphatases that controls the transition from G2 to the M phase of the cell cycle. These modifications are not permanent and are the result of Mg deprivation.

Low Mg causes endothelial dysfunction by generating a proinflammatory, prothrombotic, and proatherogenic environment (Maier et al., 2004b). Maier et al. (2004a) demonstrated a direct effect of Mg in maintaining endothelial function due to its protective effect against atherosclerosis and its role in promoting the growth of collateral vessels in chronic ischemia. High Mg might facilitate the re-endothelialization of damaged vessels.

In the vascular wall, Mg regulates collagen and elastin turnover, as well as matrix metalloproteinase activity; it also reduces calcium deposition in the elastic fibers, so the elasticity of the vessels is maintained. It has been described that hypomagnesemia may increase BP through several mechanisms: vasoconstriction, endothelial dysfunction, low-grade vascular inflammation, atherosclerosis, vascular remodeling, vascular aging, low-stress tolerance, and sodium retention. These changes result in arterial stiffness and hypertension (Kostov and Halacheva, 2018). We have reported that recombinant TNF-α increases the levels of mRNA and protein of BMP2 and p65 in human umbilical vein endothelial cells (HUVECs); the addition of $MgCl_2$ at 1.4 and 2.6 mM reduced significantly the levels of both proteins providing an additional mechanism by which Mg may protect against endothelial dysfunction (Diaz-Tocados et al., 2017). Similarly, in HUVECs incubated with different concentrations of Mg (low: 0.1 mM, control: 1 mM, high: 5 mM), the inflammatory response to LPS was increased in cells cultured in low Mg and suppressed in high Mg. This effect is mediated through the toll-like receptor 4/NF-κB pathway (Almousa et al., 2018).

Mg and Vascular Calcification

A wide number of factors are responsible for the development of arterial calcifications in CKD. In addition to high calcium, phosphate, the Ca-P product, uremic toxins, and other abnormalities, low Mg is also involved in the development of vascular calcifications. Indeed, in a group of patients receiving peritoneal dialysis followed up for more than 3 years, the serum Mg concentration discriminated patients with vascular calcification irrespective of the Ca-P product (Meema et al., 1987).

There are many cases of hyperphosphatemia and Mg deficiency. The administration of phosphate binders containing Mg reduces serum phosphate levels and improves hypomagnesemia, and they may help to reduce vascular calcifications. In experimental animals, dietary Mg supplementation improves phosphate handling and prevents calcifications (Diaz-Tocados et al., 2017).

Low serum Mg level is also associated with CAC, even in a population without previous evidence of CVD (Lee et al., 2015; Posadas-Sánchez et al., 2016; Rosique-Esteban et al., 2018). In CKD G4 patients, Mg supplementation reduces CAC progression (Sakaguchi et al., 2019). In stage G3-4 CKD patients, Mg could be an efficient strategy to improve outcomes given the demonstrated effect of Mg oxide (MgO) supplementation in the reduction of CAC progression. In this population, MgO reduced the percent change in CAC scores as compared with controls. However, no benefit was observed on thoracic aorta calcification, which warrants further investigation (Sakaguchi et al., 2019).

Experimental studies also observed a beneficial effect of Mg supplementation on vascular calcification. We have shown *in vitro* that Mg supplementation prevented phosphate-induced calcification in VSMC; this is mediated by the inhibition of a potent osteogenic cell signaling, the Wnt/β-catenin pathway (Montes de Oca et al., 2014). This effect is independent of hydroxyapatite formation because it is prevented by the blockade of cellular transport of Mg (Montezano et al., 2010; Kircelli et al., 2012; Louvet et al., 2013; Montes de Oca et al., 2014). *In vivo*, we observed that dietary Mg supplementation prevents and even reverse vascular calcification in an experimental model of 5/6 nephrectomy (Diaz-Tocados et al., 2017; **Figure 4**).

Mg and Hypertension

Experimental, clinical, and epidemiological studies have shown an inverse relationship between Mg and BP level, suggesting a relevant role of hypomagnesemia in the pathogenesis of hypertension (Touyz et al., 2002), but the mechanisms are not clear. Hypertensive patients with high renin activity have significantly lower serum Mg levels than normotensive subjects, and plasma renin activity is inversely related to the serum Mg (Resnick et al., 1983). Hypertensive patients with uncontrolled BP might have hypomagnesemia (Cunha et al., 2012).

Another meta-analysis supports the evidence of an inverse dose–response relationship between dietary Mg intake and the risk of hypertension. However, the evidence about the relationship between serum Mg concentration and hypertension is limited (Han et al., 2017).

The antihypertensive effects of Mg supplementation have been widely suggested. In a meta-analysis, Zhang X. et al. (2016) showed that Mg supplementation at a median dose of 368 mg/d for a median duration of 3 months significantly reduced systolic BP by 2.0 mmHg (95% confidence interval, 0.43–3.58) and diastolic BP by 1.78 mmHg (95% confidence interval, 0.73–2.82); these reductions were accompanied by an increase in serum Mg of 0.12 mg/dL (95% confidence interval, 0.07, 0.17 mg/dL) as compared with placebo (Zhang X. et al., 2016).

As previously mentioned, Mg may modulate BP through different mechanisms (Teo and Yusuf, 1993). In a spontaneously hypertensive animal model, it has been observed that Mg supplementation reduced the increase in BP induced by CsA (Pere et al., 2000). More importantly, Mg deficiency aggravated renal CsA-induced nephrotoxicity, whereas Mg supplementation prevented renal morphological changes and reduced proteinuria by 65% (Mervaala et al., 1997; Pere et al., 2000).

The exact mechanisms mediating the antihypertensive effect of Mg supplementation are not entirely known. Mg transport into the vascular smooth muscle cells may be the main determinant to reduce the contraction capacity of the VSMC. Increased concentrations of extracellular Mg promote vasodilation and decrease agonist-induced vasoconstriction. By contrast, low Mg concentrations cause VSMC contraction and enhance agonist-induced vasoconstriction (Touyz, 2003). Mg may also modify vascular tone through changes in Na^+/K^+ ATPase activity, which control Na^+ and K^+ transport and the levels of the vasodilators cyclic AMP and GMP (Touyz et al., 1991). Mg also decreases endothelin-1 and enhances vasodilation by augmenting nitric oxide (de Baaij et al., 2015). Additionally, animal studies have shown abnormalities in aldosterone regulation associated with hypomagnesemia. Hypomagnesemia promotes the up-regulation of aldosterone, which in turn worsens Mg deficiency through the down-regulation of TRPM7 transporters resulting in high BP. On the contrary, the supplementation of Mg decreases serum aldosterone levels (Sontia et al., 2008).

Arrhythmias

The antiarrhythmic effects of Mg have been well documented; this effect of Mg is mediated by changes in the activity of sodium, calcium, and potassium ionic channels with significant consequences on the duration of the action potential, cell excitability, and contractility (Agus and Agus, 2001). Numerous studies have evaluated the role of Mg in maintaining cardiac rhythm and preventing arrhythmias. An association between low serum Mg levels and the development of atrial fibrillation has been described (Khan et al., 2013). In a systematic review and meta-analysis, the post-operative administration of Mg appears to reduce the risk of atrial fibrillation after cardiothoracic surgery (Fairley et al., 2017), and it has been recently reported that the use of intraoperative Mg is associated with a reduction in post-operative arrhythmias (Mohammadzadeh et al., 2018; Salaminia et al., 2018). A meta-analysis suggests that Mg sulfate can be used safely and effectively in the prevention of arrhythmias (Salaminia et al., 2018). In another clinical trial, Mg administration did not significantly improve the incidence of arrhythmias in patients with hypomagnesemia or normomagnesemia after coronary artery bypass grafting. There was no significant correlation between post-operative serum levels of Mg and arrhythmia (Carpenter et al., 2018). Nevertheless, more studies are needed to demonstrate the effectiveness of Mg administration, dose, and length of treatment, in preventing arrhythmias.

The mechanisms whereby Mg intervenes in arrhythmias are not well defined yet. During hypomagnesemia, tachyarrhythmias, prolonged repolarization time, and electrocardiographic disturbances are frequently observed (Topf and Murray, 2003). *In vitro*, data demonstrate that Mg is involved in the generation and maintenance of resting membrane potential and regulating action potential through its effect on multiple ion channels (Leenders and Vervloet, 2019). Hypomagnesemia also predisposes to hypokalemia, enhancing the possibility of arrhythmias (Dinicolantonio et al., 2018).

Mg, Heart Failure, and Cardiovascular Death

Hypomagnesemia produces a decrease in cardiac contractility and increases the vascular tone. The administration of furosemide and digoxin is often used to treat heart failure and increase the renal excretion of Mg with a worsening of hypomagnesemia (Kunutsor et al., 2016; Dinicolantonio et al., 2018). Furthermore, low serum Mg is independently associated with the risk of developing heart failure (Kunutsor et al., 2016). However, baseline Mg level does not predict a worse outcome in patients with heart failure (Vaduganathan et al., 2013).

In the general population, it has been observed a protective effect of Mg against CVD (Del Gobbo et al., 2013). Lower serum Mg levels were associated with an increased risk of cardiovascular death (Reffelmann et al., 2011; Kieboom et al., 2016; Zhang et al., 2018). In a meta-analysis performed in elderly patients with CKD and reduced left ventricular systolic function, it was observed that high serum Mg levels (>2.55 mg/dL) were associated with an increased risk of cardiovascular death (Angkananard et al., 2016). However, Vaduganathan et al. (2013) have shown that the excess risk of cardiovascular death associated with higher Mg levels is likely attributable to older age, renal dysfunction, and worse baseline New York Heart Association functional class rather than Mg levels *per se*.

In CKD and ESKD patients, the relationship between hypomagnesemia and CVD and mortality has been increasingly reported in observational studies, although as renal function

deteriorates, the renal Mg excretion decreases, resulting in higher serum Mg levels (Ikee, 2018). There is an independent inverse association between serum Mg and all-cause mortality in European hemodialysis patients (de Roij van Zuijdewijn et al., 2015). Likewise, Lacson et al. (2015) found that, in American hemodialysis patients, elevated serum Mg levels (>2.5 mg/dL) were associated with better survival than low serum Mg levels (<1.56 mg/dL). In Japanese non-diabetic hemodialysis patients, serum Mg levels higher than 2.5 mg/dL were associated with improved survival and a 62% reduction of mortality risk. Kaplan–Meier analysis showed a significantly higher incidence of death in patients with serum Mg levels lower than 2.5 mg/dL (Shimohata et al., 2019). Furthermore, in a prospective study in Japanese hemodialysis patients, hypomagnesemia showed significantly worse 3-year cumulative survival for all-cause mortality; however, hypomagnesemia was not an independent risk factor for mortality, and it was associated with malnutrition (Mizuiri et al., 2019). In recent systematic review and meta-analysis of 20 publications, there was a strong association between hypomagnesemia and the risk of all-cause mortality in patients with CKD and ESKD (Xiong et al., 2019).

Finally, it has been documented that some beneficial effects of Mg may be achieved through the protection of organs against the injury induced by inflammation.

THE EFFECTS OF Mg SUPPLEMENTATION, CURRENT EVIDENCE

The protective effect of dietary Mg on CVD is based on the inverse association between Mg intake and insulin resistance, hyperglycemia, dyslipidemia, hypertension, and decreased markers of inflammation. A meta-analysis, including two independent American and Japanese cohort studies, has shown a strong inverse association between Mg intake and heart failure (Fang et al., 2016b). Sakaguchi et al. (2019) have recently published that Mg supplementation prevents CAC progression in CKD patients.

Supplements of Mg protect against the hemodynamic instability associated with the electrolyte abnormalities observed in heart failure where treatments with furosemide, digitalis, and ACE inhibitors could favor Mg excretion (Carpenter et al., 2018). Nevertheless, reports on the associations between dietary intake or supplements of Mg and arrhythmias are scarce. A low Mg intake may result in Mg depletion and arrhythmias (atrial fibrillation and flutter) in postmenopausal women and that Mg supplementation reverses these arrhythmias (Nielsen et al., 2007). However, a more recent prospective study, including American participants, has not shown a significant relationship between Mg intake and the incidence of atrial fibrillation (Misialek et al., 2013). Nevertheless, some authors recommend that hypomagnesemia should be corrected by oral Mg supplementation to prevent cardiac rhythm disorders (Carpenter et al., 2018).

Maintenance of optimal Mg status may also be an appropriate strategy to help control the BP (Kostov and Halacheva, 2018). A negative correlation between dietary Mg intake and BP has been observed, and supplementary oral Mg intake significantly reduced systolic and diastolic BP (Cunha et al., 2017; Carpenter et al., 2018) and ameliorated subclinical atherosclerosis (Cunha et al., 2017). Concerning cardiovascular death, in a meta-analysis, which included 400,000 adults, the dietary Mg intake was inversely associated with the risk of coronary heart disease, heart failure, and sudden cardiac death (Fang et al., 2016a). Repletion of Mg has been found to reduce the risk of arrhythmias and death after acute myocardial infarction, and it may also reduce sudden cardiac death (Dinicolantonio et al., 2018). Moreover, in a meta-analysis evaluating dose–response of prospective cohort studies, increasing dietary Mg intake was associated with a reduced risk of heart failure and all-cause mortality (Fang et al., 2016b). In a Mediterranean population with high cardiovascular risk, a randomized clinical trial showed that dietary Mg intake was inversely related to the mortality risk. However, no significant association was observed between Mg intake and major cardiovascular events (Guasch-Ferré et al., 2014).

Supplementation of Mg may be a therapeutic strategy for the management of CVD (Severino et al., 2019). The majority of recent studies show an inverse correlation between dietary Mg intake and serum Mg levels with the risk of CVD and mortality (Muñoz-Castañeda et al., 2018). High Mg intake is associated with a lower risk of major cardiovascular risk factors (mainly metabolic syndrome, diabetes, and hypertension) and less incidence of stroke and CVD (Rosique-Esteban et al., 2018). Mg supplementation should be considered in patients with a high risk of Mg deficiency and even more if they have high cardiovascular risk.

Several randomized, double-blind, placebo-controlled trial has also shown an improvement in endothelial function after oral Mg supplementation using different doses and duration of treatment. Mg supplementation has been used successfully in patients with coronary artery disease (Shechter et al., 2000), in hypertensive women (Cunha et al., 2017), and diabetic elderly patients (Barbagallo et al., 2010). A systematic review and meta-analysis showed that the use of oral Mg might improve flow-mediated dilation (Darooghegi Mofrad et al., 2018). However, Mg supplements did not improve endothelial function and cardiovascular risk markers in overweight and obese middle-aged and elderly adults (Joris et al., 2017). Supplementation of choline plus Mg oxide was more effective in improving inflammation and endothelial dysfunction in diabetic patients than supplementation with choline or Mg alone (Rashvand et al., 2019). Also, with respect to inflammation, in a large cohort of postmenopausal women, dietary Mg intake was inversely associated with the values of C-reactive protein (CRP), interleukin 6 (IL-6), TNF-α, VCAM-1, and E-selectin (Chacko et al., 2010).

One main effect of Mg supplementation is obtained through the decrease in inflammation. The protection of Mg against cardiovascular and renal inflammatory actions of aldosterone was demonstrated by Sontia et al. (2008). Treatment with recombinant aldosterone plus 0.9% of NaCl in drinking water promoted renal and cardiovascular expression of IL-6, VCAM-1, and COX2 in C57B6 mice. Aldosterone overload also decreased

renal expression of the TRPM7 channel. Dietary Mg (0.75%) attenuated renal and cardiac IL-6 content and decreased renal VCAM-1 and cardiac COX2 expression and increased renal expression of TRPM7.

Chronic systemic inflammation and oxidative stress are also common features of CKD and are associated with alterations in mineral metabolism (Stenvinkel et al., 2005). In uremia, there is an increase in the production of reactive oxygen species and cytokines, which favor calcification in CKD rats (Agharazii et al., 2015). Oxidative stress may be linked to hypomagnesemia, even at the very early stages of CKD (**Figure 3**).

In vitro, low Mg promotes the up-regulation of NF-κB (Van Laecke et al., 2012) and also increases the levels of IL-1β and TNF-α (Massy and Drüeke, 2015). *In vivo*, Mg deficiency mediates leukocyte activation and the release of several proinflammatory cytokines (Tejero-Taldo et al., 2006). In humans, hypomagnesemia is also associated with an elevation in CRP and worsens insulin resistance in diabetic patients (Kim et al., 2010).

CONCLUSION AND FINAL REMARKS

To date, the decision-making of prescribing Mg supplements to patients with Mg deficiency remains uncertain. Still, there is no evidence strong enough to make a formal recommendation to prescribe Mg supplements. However, there are data available that strongly suggest the benefits of Mg on vascular calcification, CVD, and kidney function. Thus, it appears that Mg supplementation, if indicated, may slow down the development of such negative morbidities.

From this ample bibliography related to Mg, one idea prevails; it is necessary to control the levels of Mg so that low levels of serum Mg should not be left untreated. The deleterious effects of Mg deficiency have been sufficiently demonstrated. However, it is also mandatory to learn what patients will benefit most from Mg supplementation and what the best protocol is to this end. It is likely that, in elderly patients with ESKD, Mg supplementation should be done carefully to avoid Mg accumulation due to the reduced renal function; for this reason, more clinical and experimental studies are necessary to learn when and how we must manage Mg to treat hypomagnesemia.

AUTHOR CONTRIBUTIONS

CR-H, MVP-R, JMD-T, AM-M, RS, JRM-C, and MR wrote the article. All authors contributed to the article and approved the submitted version.

FUNDING

JRM-C is a senior researcher supported by the Nicolás Monardes Program from Consejeria de Salud-SAS (Junta de Andalucía). This study was supported by grants from the National Institute of Health Carlos III (FIS 17/01010, and FIS 18/0138), the Consejeria de Salud of Junta de Andalucía (PI-0136-2016), the REDinREN from the National Institute of Health Carlos III, the EUTox Workgroup, and the EDTA CKD-MBD group. The sponsors had no influence in study design, data collection, and analysis, decision to publish, or preparation of the manuscript.

REFERENCES

Agharazii, M., St-Louis, R., Gautier-Bastien, A., Ung, R.-V., Mokas, S., Larivière, R., et al. (2015). Inflammatory cytokines and reactive oxygen species as mediators of chronic kidney disease-related vascular calcification. *Am. J. Hypertens.* 28, 746–755. doi: 10.1093/ajh/hpu225

Agus, M. S., and Agus, Z. S. (2001). Cardiovascular actions of magnesium. *Crit. Care Clin.* 17, 175–186. doi: 10.1016/s0749-0704(05)70158-5

Ahmed, F., and Mohammed, A. (2019). Magnesium: the forgotten electrolyte—a review on hypomagnesemia. *Med. Sci.* 7:56. doi: 10.3390/medsci7040056

Alfrey, A. C., and Miller, N. L. (1973). Bone magnesium pools in uremia. *J. Clin. Invest.* 52, 3019–3027. doi: 10.1172/JCI107500

Almousa, L. A., Salter, A. M., and Langley-Evans, S. C. (2018). Varying magnesium concentration elicits changes in inflammatory response in human umbilical vein endothelial cells (HUVECs). *Magnes. Res.* 31, 99–109. doi: 10.1684/mrh.2018.0439

Alves, S. C., Tomasi, C. D., Constantino, L., Giombelli, V., Candal, R., Bristot, M., et al. (2013). Hypomagnesemia as a risk factor for the non-recovery of the renal function in critically ill patients with acute kidney injury. *Nephrol. Dial. Transplant.* 28, 910–916. doi: 10.1093/ndt/gfs268

Angkananard, T., Anothaisintawee, T., Eursiriwan, S., Gorelik, O., McEvoy, M., Attia, J., et al. (2016). The association of serum magnesium and mortality outcomes in heart failure patients: a systematic review and meta-analysis. *Med. Baltim.* 95:e5406. doi: 10.1097/MD.0000000000005406

Arjona, F. J., Baaij, J. H. F., de Schlingmann, K. P., Lameris, A. L. L., van Wijk, E., Flik, G., et al. (2014). CNNM2 mutations cause impaired brain development and seizures in patients with hypomagnesemia. *PLoS Genet.* 10:e1004267. doi: 10.1371/journal.pgen.1004267

Ascherio, A., Rimm, E. B., Giovannucci, E. L., Colditz, G. A., Rosner, B., Willett, W. C., et al. (1992). A prospective study of nutritional factors and hypertension among US men. *Circulation* 86, 1475–1484. doi: 10.1161/01.cir.86.5.1475

Bara, M., Guiet-Bara, A., and Durlach, J. (1993). Regulation of sodium and potassium pathways by magnesium in cell membranes. *Magnes. Res.* 6, 167–177.

Barbagallo, M., Dominguez, L. J., Galioto, A., Pineo, A., and Belvedere, M. (2010). Oral magnesium supplementation improves vascular function in elderly diabetic patients. *Magnes. Res.* 23, 131–137. doi: 10.1684/mrh.2010.0214

Bo, S., and Pisu, E. (2008). Role of dietary magnesium in cardiovascular disease prevention, insulin sensitivity and diabetes. *Curr. Opin. Lipidol.* 19, 50–56. doi: 10.1097/MOL.0b013e3282f33ccc

Braake, A. D., ter Smit, A. E., Bos, C., Herwaarden, A. E., van Alkema, W., van Essen, H. W., et al. (2019). Magnesium prevents vascular calcification in Klotho deficiency. *Kidney Int.* 97, 487–501. doi: 10.1016/j.kint.2019.09.034

Breiderhoff, T., Himmerkus, N., Stuiver, M., Mutig, K., Will, C., Meij, I. C., et al. (2012). Deletion of claudin-10 (Cldn10) in the thick ascending limb impairs paracellular sodium permeability and leads to hypermagnesemia and nephrocalcinosis. *Proc. Natl. Acad. Sci. U.S.A.* 109, 14241–14246. doi: 10.1073/pnas.1203834109

Brown, E., Enyedi, P., LeBoff, M., Rotberg, J., Preston, J., and Chen, C. (1987). High extracellular Ca2+ and Mg2+ stimulate accumulation of inositol phosphates in bovine parathyroid cells. *FEBS Lett.* 218, 113–118. doi: 10.1016/0014-5793(87)81029-3

Carpenter, D. O., Zehra, R., and Fatmi, S. S. (2018). Dietary magnesium intake and heart health. *J. Food Nutr. Metab.* 2018, 1–5. doi: 10.31487/j.JFNM.2018.01.001

Chacko, S. A., Song, Y., Nathan, L., Tinker, L., de Boer, I. H., Tylavsky, F., et al. (2010). Relations of dietary magnesium intake to biomarkers of inflammation

and endothelial dysfunction in an ethnically diverse cohort of postmenopausal women. *Diabetes Care* 33, 304–310. doi: 10.2337/dc09-1402

Cherepanova, N., Shrimal, S., and Gilmore, R. (2016). N-linked glycosylation and homeostasis of the endoplasmic reticulum. *Curr. Opin. Cell Biol.* 41, 57–65. doi: 10.1016/j.ceb.2016.03.021

Cherepanova, N. A., and Gilmore, R. (2016). Mammalian cells lacking either the cotranslational or posttranslocational oligosaccharyltransferase complex display substrate-dependent defects in asparagine linked glycosylation. *Sci. Rep.* 6:20946. doi: 10.1038/srep20946

Cherepanova, N. A., Shrimal, S., and Gilmore, R. (2014). Oxidoreductase activity is necessary for N-glycosylation of cysteine-proximal acceptor sites in glycoproteins. *J. Cell Biol.* 206, 525–539. doi: 10.1083/jcb.201404083

Cholst, I. N., Steinberg, S. F., Tropper, P. J., Fox, H. E., Segre, G. V., and Bilezikian, J. P. (1984). The influence of hypermagnesemia on serum calcium and parathyroid hormone levels in human subjects. *N. Engl. J. Med.* 310, 1221–1225. doi: 10.1056/NEJM198405103101904

Covic, A., Passlick-Deetjen, J., Kroczak, M., Büschges-Seraphin, B., Ghenu, A., Ponce, P., et al. (2013). A comparison of calcium acetate/magnesium carbonate and sevelamer-hydrochloride effects on fibroblast growth factor-23 and bone markers: post hoc evaluation from a controlled, randomized study. *Nephrol. Dial. Transpl.* 28, 2383–2392. doi: 10.1093/ndt/gft203

Crook, M. A., Hally, V., and Panteli, J. V. (2001). The importance of the refeeding syndrome. *Nutrition* 17, 632–637. doi: 10.1016/S0899-9007(01)00542-1

Cunha, A. R., D'El-Rei, J., Medeiros, F., Umbelino, B., Oigman, W., Touyz, R. M., et al. (2017). Oral magnesium supplementation improves endothelial function and attenuates subclinical atherosclerosis in thiazide-treated hypertensive women. *J. Hypertens.* 35, 89–97. doi: 10.1097/HJH.0000000000001129

Cunha, A. R., Umbelino, B., Correia, M. L., and Neves, M. F. (2012). Magnesium and vascular changes in hypertension. *Int. J. Hypertens.* 2012:e754250. doi: 10.1155/2012/754250

Cunningham, J., Rodriguez, M., and Messa, P. (2012). Magnesium in chronic kidney disease Stages 3 and 4 and in dialysis patients. *Clin. Kidney J.* 5, i39–i51. doi: 10.1093/ndtplus/sfr166

Darooghegi Mofrad, M., Djafarian, K., Mozaffari, H., and Shab-Bidar, S. (2018). Effect of magnesium supplementation on endothelial function: a systematic review and meta-analysis of randomized controlled trials. *Atherosclerosis* 273, 98–105. doi: 10.1016/j.atherosclerosis.2018.04.020

de Baaij, J. H. F., Hoenderop, J. G. J., and Bindels, R. J. M. (2015). Magnesium in man: implications for health and disease. *Physiol. Rev.* 95, 1–46. doi: 10.1152/physrev.00012.2014

de Roij van Zuijdewijn, C. L. M., Grooteman, M. P. C., Bots, M. L., Blankestijn, P. J., Steppan, S., Büchel, J., et al. (2015). Serum magnesium and sudden death in european hemodialysis patients. *PLoS One* 10:e0143104. doi: 10.1371/journal.pone.0143104

Del Gobbo, L. C., Imamura, F., Wu, J. H. Y., de Oliveira Otto, M. C., Chiuve, S. E., and Mozaffarian, D. (2013). Circulating and dietary magnesium and risk of cardiovascular disease: a systematic review and meta-analysis of prospective studies. *Am. J. Clin. Nutr.* 98, 160–173. doi: 10.3945/ajcn.112.053132

Díaz-Tocados, J. M., Herencia, C., Martínez-Moreno, J. M., Montes de Oca, A., Rodríguez-Ortiz, M. E., Vergara, N., et al. (2017). Magnesium chloride promotes osteogenesis through notch signaling activation and expansion of mesenchymal stem cells. *Sci. Rep.* 7:7839. doi: 10.1038/s41598-017-08379-y

Diaz-Tocados, J. M., Peralta-Ramirez, A., Rodríguez-Ortiz, M. E., Raya, A. I., Lopez, I., Pineda, C., et al. (2017). Dietary magnesium supplementation prevents and reverses vascular and soft tissue calcifications in uremic rats. *Kidney Int.* 92, 1084–1099. doi: 10.1016/j.kint.2017.04.011

Dinicolantonio, J. J., Liu, J., and Keefe, J. H. O. (2018). Magnesium for the prevention and treatment of cardiovascular disease. *Open Heart* 5:e000775. doi: 10.1136/openhrt-2018-000775

Ennever, J., and Vogel, J. J. (1981). Magnesium inhibition of apatite nucleation by proteolipid. *J. Dent. Res.* 60, 838–841. doi: 10.1177/00220345810600041301

Fairley, J. L., Zhang, L., Glassford, N. J., and Bellomo, R. (2017). Magnesium status and magnesium therapy in cardiac surgery: a systematic review and meta-analysis focusing on arrhythmia prevention. *J. Crit. Care* 42, 69–77. doi: 10.1016/j.jcrc.2017.05.038

Fang, X., Liang, C., Li, M., Montgomery, S., Fall, K., Aaseth, J., et al. (2016a). Dose-response relationship between dietary magnesium intake and cardiovascular mortality: a systematic review and dose-based meta-regression analysis of prospective studies. *J. Trace Elem. Med. Biol.* 38, 64–73. doi: 10.1016/j.jtemb.2016.03.014

Fang, X., Wang, K., Han, D., He, X., Wei, J., Zhao, L., et al. (2016b). Dietary magnesium intake and the risk of cardiovascular disease, type 2 diabetes, and all-cause mortality: a dose-response meta-analysis of prospective cohort studies. *BMC Med.* 14:210. doi: 10.1186/s12916-016-0742-z

Farhadnejad, H., Asghari, G., Mirmiran, P., Yuzbashian, E., and Azizi, F. (2016). Micronutrient intakes and incidence of chronic kidney disease in adults: tehran lipid and glucose Study. *Nutrients* 8:217. doi: 10.3390/nu8040217

Ferrè, S., Baldoli, E., Leidi, M., and Maier, J. A. M. (2010). Magnesium deficiency promotes a pro-atherogenic phenotype in cultured human endothelial cells via activation of NFkB. *Biochim. Biophys. Acta* 1802, 952–958. doi: 10.1016/j.bbadis.2010.06.016

Funato, Y., Yamazaki, D., and Miki, H. (2017). Renal function of cyclin M2 Mg2+ transporter maintains blood pressure. *J. Hypertens.* 35, 585–592. doi: 10.1097/HJH.0000000000001211

Gonella, M., Ballanti, P., Della Rocca, C., Calabrese, G., Pratesi, G., Vagelli, G., et al. (1988). Improved bone morphology by normalizing serum magnesium in chronically hemodialyzed patients. *Min. Electrolyte Metab.* 14, 240–245.

Gorostidi, M., Sánchez-Martínez, M., Ruilope, L. M., Graciani, A., de la Cruz, J. J., Santamaría, R., et al. (2018). Chronic kidney disease in Spain: prevalence and impact of accumulation of cardiovascular risk factors. *Nefrologia* 38, 606–615. doi: 10.1016/j.nefro.2018.04.004

Green, J. (1994). The physicochemical structure of bone: cellular and noncellular elements. *Miner. Electrolyte Metab.* 20, 7–15.

Gröber, U., Schmidt, J., and Kisters, K. (2015). Magnesium in prevention and therapy. *Nutrients* 7, 8199–8226. doi: 10.3390/nu7095388

Guasch-Ferré, M., Bulló, M., Estruch, R., Corella, D., Martínez-González, M. A., Ros, E., et al. (2014). Dietary magnesium intake is inversely associated with mortality in adults at high cardiovascular disease risk. *J. Nutr.* 144, 55–60. doi: 10.3945/jn.113.183012

Han, H., Fang, X., Wei, X., Liu, Y., Jin, Z., Chen, Q., et al. (2017). Dose-response relationship between dietary magnesium intake, serum magnesium concentration and risk of hypertension: a systematic review and meta-analysis of prospective cohort studies. *Nutr. J.* 16:26. doi: 10.1186/s12937-017-0247-4

Holzmacher, R., Kendziorski, C., Michael Hofman, R., Jaffery, J., Becker, B., and Djamali, A. (2005). Low serum magnesium is associated with decreased graft survival in patients with chronic cyclosporin nephrotoxicity. *Nephrol. Dial. Transplant.* 20, 1456–1462. doi: 10.1093/ndt/gfh831

Ikee, R. (2018). Cardiovascular disease, mortality, and magnesium in chronic kidney disease: growing interest in magnesium-related interventions. *Ren. Replace. Ther.* 4:1. doi: 10.1186/s41100-017-0142-7

Imai, Y., and Lu, B. (2011). Mitochondrial dynamics and mitophagy in Parkinson's disease: disordered cellular power plant becomes a big deal in a major movement disorder. *Curr. Opin. Neurobiol.* 21, 935–941. doi: 10.1016/j.conb.2011.10.016

Jang, H. L., Lee, H. K., Jin, K., Ahn, H.-Y., Lee, H.-E., and Nam, K. T. (2015). Phase transformation from hydroxyapatite to the secondary bone mineral, whitlockite. *J. Mater. Chem. B* 3, 1342–1349. doi: 10.1039/C4TB01793E

Joosten, M. M., Gansevoort, R. T., Bakker, S. J. L., and Prevend Study Group (2015). Low plasma magnesium and risk of developing chronic kidney disease: results from the PREVEND Study. *Kidney Int.* 87, 1262–1263. doi: 10.1038/ki.2015.33

Joris, P. J., Plat, J., Bakker, S. J. L., and Mensink, R. P. (2017). Effects of long-term magnesium supplementation on endothelial function and cardiometabolic risk markers: a randomized controlled trial in overweight/obese adults. *Sci. Rep.* 7:106. doi: 10.1038/s41598-017-00205-9

Khan, A. M., Lubitz, S. A., Sullivan, L. M., Sun, J. X., Levy, D., Vasan, R. S., et al. (2013). Low serum magnesium and the development of atrial fibrillation in the community: the framingham heart Study. *Circulation* 127, 33–38. doi: 10.1161/CIRCULATIONAHA.111.082511

Kieboom, B. C. T., Niemeijer, M. N., Leening, M. J. G., Franco, O. H., Deckers, J. W., Hofman, A., et al. (2016). Serum magnesium and the risk of death from coronary heart. *J. Am. Heart Assoc.* 5:e002707. doi: 10.1161/JAHA.115.002707

Kim, D. J., Xun, P., Liu, K., Loria, C., Yokota, K., Jacobs, D. R., et al. (2010). Magnesium intake in relation to systemic inflammation, insulin resistance, and the incidence of diabetes. *Diabetes Care* 33, 2604–2610. doi: 10.2337/dc10-0994

Kircelli, F., Peter, M. E., Sevinc Ok, E., Celenk, F. G., Yilmaz, M., Steppan, S., et al. (2012). Magnesium reduces calcification in bovine vascular smooth muscle cells in a dose-dependent manner. *Nephrol. Dial. Transpl.* 27, 514–521. doi: 10.1093/ndt/gfr321

Kolisek, M., Sponder, G., Pilchova, I., Cibulka, M., Tatarkova, Z., Werner, T., et al. (2019). Magnesium extravaganza: a critical compendium of current research into cellular Mg2+ transporters other than TRPM6/7. *Rev. Physiol. Biochem. Pharmacol.* 176, 65–105. doi: 10.1007/112_2018_15

Kostov, K. (2019). Effects of magnesium deficiency on mechanisms of insulin resistance in type 2 diabetes: focusing on the processes of insulin secretion and signaling. *Int. J. Mol. Sci.* 20:1351. doi: 10.3390/ijms20061351

Kostov, K., and Halacheva, L. (2018). Role of magnesium deficiency in promoting atherosclerosis, endothelial dysfunction, and arterial stiffening as risk factors for hypertension. *Int. J. Mol. Sci.* 19:1724. doi: 10.3390/ijms19061724

Kunutsor, S. K., Khan, H., and Laukkanen, J. A. (2016). Serum magnesium and risk of new onset heart failure in men: the kuopio ischemic heart disease Study. *Eur. J. Epidemiol.* 31, 1035–1043. doi: 10.1007/s10654-016-0164-4

Lacson, E., Wang, W., Ma, L., and Passlick-Deetjen, J. (2015). Serum magnesium and mortality in hemodialysis patients in the united states: a cohort study. *Am. J. Kidney Dis.* 66, 1056–1066. doi: 10.1053/j.ajkd.2015.06.014

Lee, S. Y., Hyun, Y. Y., Lee, K. B., and Kim, H. (2015). Low serum magnesium is associated with coronary artery calcification in a Korean population at low risk for cardiovascular disease. *Nutr. Metab. Cardiovasc. Dis. NMCD* 25, 1056–1061. doi: 10.1016/j.numecd.2015.07.010

Leenders, N. H. J., and Vervloet, M. G. (2019). Magnesium: a magic bullet for cardiovascular disease in chronic kidney disease?. *Nutrients* 11:455. doi: 10.3390/nu11020455

Louvet, L., Büchel, J., Steppan, S., Passlick-Deetjen, J., and Massy, Z. A. (2013). Magnesium prevents phosphate-induced calcification in human aortic vascular smooth muscle cells. *Nephrol. Dial. Transpl.* 28, 869–878. doi: 10.1093/ndt/gfs520

Maier, J. A. M., Bernardini, D., Rayssiguier, Y., and Mazur, A. (2004a). High concentrations of magnesium modulate vascular endothelial cell behaviour in vitro. *Biochim. Biophys. Acta* 1689, 6–12. doi: 10.1016/j.bbadis.2004.02.004

Maier, J. A. M., Malpuech-Brugère, C., Zimowska, W., Rayssiguier, Y., and Mazur, A. (2004b). Low magnesium promotes endothelial cell dysfunction: implications for atherosclerosis, inflammation and thrombosis. *Biochim. Biophys. Acta* 1689, 13–21. doi: 10.1016/j.bbadis.2004.01.002

Massy, Z. A., and Drüeke, T. B. (2015). Magnesium and cardiovascular complications of chronic kidney disease. *Nat. Rev. Nephrol.* 11:432.

Matsuzaki, H., Ohdachi, J., Fuchigami, M., Masuyama, R., Uehara, M., Nakamura, K., et al. (2002). Changes in N-acetyl-beta-D-glucosaminidase activity in the urine and urinary albumin excretion in magnesium deficient rats. *Biosci. Biotechnol. Biochem.* 66, 192–194. doi: 10.1271/bbb.66.192

Meema, H. E., Oreopoulos, D. G., and Rapoport, A. (1987). Serum magnesium level and arterial calcification in end-stage renal disease. *Kidney Int.* 32, 388–394. doi: 10.1038/ki.1987.222

Mervaala, E. M., Pere, A. K., Lindgren, L., Laakso, J., Teräväinen, T. L., Karjala, K., et al. (1997). Effects of dietary sodium and magnesium on cyclosporin A-induced hypertension and nephrotoxicity in spontaneously hypertensive rats. *Hypertens. Dallas Tex.* 1979, 822–827. doi: 10.1161/01.hyp.29.3.822

Misialek, J. R., Lopez, F. L., Lutsey, P. L., Huxley, R. R., Peacock, J. M., Chen, L. Y., et al. (2013). Serum and dietary magnesium and incidence of atrial fibrillation in whites and in African Americans–Atherosclerosis Risk in Communities (ARIC) study. *Circ. J. Off. J. Jpn. Circ. Soc.* 77, 323–329. doi: 10.1253/circj.cj-12-0886

Mizuiri, S., Nishizawa, Y., Yamashita, K., Naito, T., Ono, K., Tanji, C., et al. (2019). Hypomagnesemia is not an independent risk factor for mortality in Japanese maintenance hemodialysis patients. *Int. Urol. Nephrol.* 51, 1043–1052. doi: 10.1007/s11255-019-02073-w

Mohammadzadeh, A., Towfighi, F., and Jafari, N. (2018). Effect of magnesium on arrhythmia incidence in patients undergoing coronary artery bypass grafting. *ANZ J. Surg.* 88, 612–615. doi: 10.1111/ans.14056

Montes de Oca, A., Guerrero, F., Martinez-Moreno, J. M., Madueño, J. A., Herencia, C., Peralta, A., et al. (2014). Magnesium inhibits Wnt/β-catenin activity and reverses the osteogenic transformation of vascular smooth muscle cells. *PLoS One* 9:e89525. doi: 10.1371/journal.pone.0089525

Montezano, A. C., Zimmerman, D., Yusuf, H., Burger, D., Chignalia, A. Z., Wadhera, V., et al. (2010). Vascular smooth muscle cell differentiation to an osteogenic phenotype involves TRPM7 modulation by magnesium. *Hypertension* 56, 453–462. doi: 10.1161/HYPERTENSIONAHA.110.152058

Morinière, P., Vinatier, I., Westeel, P. F., Cohemsolal, M., Belbrik, S., Abdulmassih, Z., et al. (1988). Magnesium hydroxide as a complementary aluminium-free phosphate binder to moderate doses of oral calcium in uraemic patients on chronic haemodialysis: lack of deleterious effect on bone mineralisation. *Nephrol. Dial. Transpl.* 3, 651–656.

Muñoz-Castañeda, J. R., Pend, V., Mier, D., and Rodr, M. (2018). Magnesium replacement to protect cardiovascular and kidney damage? *Lack Prospect. Clin. Trials* 19:664. doi: 10.3390/ijms19030664

Murasato, Y., Harada, Y., Ikeda, M., Nakashima, Y., and Hayashida, Y. (1999). Effect of magnesium deficiency on autonomic circulatory regulation in conscious rats. *Hypertens. Dallas Tex.* 1979, 247–252. doi: 10.1161/01.hyp.34.2.247

Navarro, J. F., Mora, C., Jiménez, A., Torres, A., Macía, M., and García, J. (1999). Relationship between serum magnesium and parathyroid hormone levels in hemodialysis patients. *Am. J. Kidney Dis.* 34, 43–48. doi: 10.1053/AJKD03400043

Neves, K. R., Graciolli, F. G., dos Reis, L. M., Pasqualucci, C. A., Moysés, R. M. A., and Jorgetti, V. (2004). Adverse effects of hyperphosphatemia on myocardial hypertrophy, renal function, and bone in rats with renal failure. *Kidney Int.* 66, 2237–2244. doi: 10.1111/j.1523-1755.2004.66013.x

Nielsen, F. H. (2018). Magnesium deficiency and increased inflammation: current perspectives. *J. Inflamm. Res.* 11, 25–34. doi: 10.2147/JIR.S136742

Nielsen, F. H., Milne, D. B., Klevay, L. M., Gallagher, S., and Johnson, L. (2007). Dietary magnesium deficiency induces heart rhythm changes, impairs glucose tolerance, and decreases serum cholesterol in postmenopausal women. *J. Am. Coll. Nutr.* 26, 121–132. doi: 10.1080/07315724.2007.10719593

Nijenhuis, T., Hoenderop, J. G. J., and Bindels, R. J. M. (2004). Downregulation of Ca(2+) and Mg(2+) transport proteins in the kidney explains tacrolimus (FK506)-induced hypercalciuria and hypomagnesemia. *J. Am. Soc. Nephrol. JASN* 15, 549–557. doi: 10.1097/01.asn.0000113318.56023.b6

Oka, T., Hamano, T., Sakaguchi, Y., Yamaguchi, S., Kubota, K., Senda, M., et al. (2018). Proteinuria-associated renal magnesium wasting leads to hypomagnesemia: a common electrolyte abnormality in chronic kidney disease. *Nephrol. Dial. Transplant.* 34, 1154–1162. doi: 10.1093/ndt/gfy119

Pere, A. K., Lindgren, L., Tuomainen, P., Krogerus, L., Rauhala, P., Laakso, J., et al. (2000). Dietary potassium and magnesium supplementation in cyclosporine-induced hypertension and nephrotoxicity. *Kidney Int.* 58, 2462–2472. doi: 10.1046/j.1523-1755.2000.00429.x

Pérez González, E., Santos Rodríguez, F., and Coto García, E. (2009). Magnesium homeostasis. Etiopathogeny, clinical diagnosis and treatment of hypomagnesaemia. A case study. *Nefrol. Engl. Ed.* 29, 518–524. doi: 10.3265/Nefrologia.2009.29.6.5534.en.full

Pham, P. C. T., Pham, P. M. T., Pham, P. A. T., Pham, S. V., Pham, H. V., Miller, J. M., et al. (2005). Lower serum magnesium levels are associated with more rapid decline of renal function in patients with diabetes mellitus type 2. *Clin. Nephrol.* 63, 429–436.

Posadas-Sánchez, R., Posadas-Romero, C., Cardoso-Saldaña, G., Vargas-Alarcón, G., Villarreal-Molina, M. T., Pérez-Hernández, N., et al. (2016). Serum magnesium is inversely associated with coronary artery calcification in the Genetics of Atherosclerotic Disease (GEA) study. *Nutr. J.* 15:22. doi: 10.1186/s12937-016-0143-3

Qu, X., Jin, F., Hao, Y., Li, H., Tang, T., Wang, H., et al. (2013). Magnesium and the risk of cardiovascular events: a meta-analysis of prospective cohort studies. *PLoS One* 8:e57720. doi: 10.1371/journal.pone.0057720

Quinn, S. J., Thomsen, A. R. B., Egbuna, O., Pang, J., Baxi, K., Goltzman, D., et al. (2013). CaSR-mediated interactions between calcium and magnesium homeostasis in mice. *Am. J. Physiol. Endocrinol. Metab.* 304, E724–E733. doi: 10.1152/ajpendo.00557.2012

Quitterer, U., Hoffmann, M., Freichel, M., and Lohse, M. J. (2001). Paradoxical block of parathormone secretion is mediated by increased activity of G alpha subunits. *J. Biol. Chem.* 276, 6763–6769. doi: 10.1074/jbc.M007727200

Rashvand, S., Mobasseri, M., and Tarighat-Esfanjani, A. (2019). The effects of choline and magnesium co-supplementation on metabolic parameters, inflammation, and endothelial dysfunction in patients with type 2 diabetes mellitus: a randomized, double-blind, placebo-controlled trial. *J. Am. Coll. Nutr.* 38, 714–721. doi: 10.1080/07315724.2019.1599745

Rebholz, C. M., Tin, A., Liu, Y., Kuczmarski, M. F., Evans, M. K., Zonderman, A. B., et al. (2016). Dietary magnesium and kidney function decline: the healthy aging in neighborhoods of diversity across the life span study. *Am. J. Nephrol.* 44, 381–387. doi: 10.1159/000450861

Reffelmann, T., Ittermann, T., Dörr, M., Völzke, H., Reinthaler, M., Petersmann, A., et al. (2011). Low serum magnesium concentrations predict cardiovascular and all-cause mortality. *Atherosclerosis* 219, 280–284. doi: 10.1016/j.atherosclerosis.2011.05.038

Resnick, L. M., Laragh, J. H., Sealey, J. E., and Alderman, M. H. (1983). Divalent cations in essential hypertension. Relations between serum ionized calcium, magnesium, and plasma renin activity. *N. Engl. J. Med.* 309, 888–891. doi: 10.1056/NEJM198310133091504

Rodríguez-Ortiz, M. E., Canalejo, A., Herencia, C., Martínez-Moreno, J. M., Peralta-Ramírez, A., Perez-Martinez, P., et al. (2014). Magnesium modulates parathyroid hormone secretion and upregulates parathyroid receptor expression at moderately low calcium concentration. *Nephrol. Dial. Transplant.* 29, 282–289. doi: 10.1093/ndt/gft400

Rodríguez-Ortiz, M. E., Gómez-Delgado, F., Arenas de Larriva, A. P., Canalejo, A., Gómez-Luna, P., Herencia, C., et al. (2019). Serum Magnesium is associated with Carotid Atherosclerosis in patients with high cardiovascular risk (CORDIOPREV Study). *Sci. Rep.* 9:8013. doi: 10.1038/s41598-019-44322-z

Romani, A. M., and Scarpa, A. (2000). Regulation of cellular magnesium. *Front. Biosci. J. Virtual Libr.* 5, D720–D734. doi: 10.2741/romani

Romani, A. M. P. (2007). Magnesium homeostasis in mammalian cells. *Front. Biosci. J. Virtual Libr.* 12, 308–331. doi: 10.2741/2066

Rosique-Esteban, N., Guasch-ferr, M., Hern, P., and Salas-salvad, J. (2018). Dietary magnesium and cardiovascular disease: a review with emphasis in epidemiological studies. *Nutrients* 10:168. doi: 10.3390/nu10020168

Rude, R. K. (1998). Magnesium deficiency: a cause of heterogeneous disease in humans. *J. Bone Min. Res.* 13, 749–758. doi: 10.1359/jbmr.1998.13.4.749

Rude, R. K., Gruber, H. E., Norton, H. J., Wei, L. Y., Frausto, A., and Kilburn, J. (2006). Reduction of dietary magnesium by only 50% in the rat disrupts bone and mineral metabolism. *Osteoporos. Int.* 17, 1022–1032. doi: 10.1007/s00198-006-0104-3

Rude, R. K., Gruber, H. E., Norton, H. J., Wei, L. Y., Frausto, A., and Mills, B. G. (2004). Bone loss induced by dietary magnesium reduction to 10% of the nutrient requirement in rats is associated with increased release of substance P and tumor necrosis factor-alpha. *J. Nutr.* 134, 79–85. doi: 10.1093/jn/134.1.79

Rude, R. K., Singer, F. R., and Gruber, H. E. (2009). Skeletal and hormonal effects of magnesium deficiency. *J. Am. Coll. Nutr.* 28, 131–141.

Sakaguchi, Y., Fujii, N., Shoji, T., Hayashi, T., Rakugi, H., and Isaka, Y. (2014). Hypomagnesemia is a significant predictor of cardiovascular and non-cardiovascular mortality in patients undergoing hemodialysis. *Kidney Int.* 85, 174–181. doi: 10.1038/ki.2013.327

Sakaguchi, Y., Hamano, T., and Isaka, Y. (2018a). Magnesium and progression of chronic kidney disease: benefits beyond cardiovascular protection? *Adv. Chronic Kidney Dis.* 25, 274–280. doi: 10.1053/j.ackd.2017.11.001

Sakaguchi, Y., Hamano, T., Matsui, I., Oka, T., Yamaguchi, S., Kubota, K., et al. (2018b). Low magnesium diet aggravates phosphate-induced kidney injury. *Nephrol. Dial. Transplant.* 34, 1310–1319. doi: 10.1093/ndt/gfy358

Sakaguchi, Y., Hamano, T., Wada, A., Hoshino, J., and Masakane, I. (2018c). Magnesium and risk of hip fracture among patients undergoing hemodialysis. *J. Am. Soc. Nephrol.* 29, 991–999. doi: 10.1681/ASN.2017080849

Sakaguchi, Y., Hamano, T., Obi, Y., Monden, C., Oka, T., Yamaguchi, S., et al. (2019). A randomized trial of magnesium oxide and oral carbon adsorbent for coronary artery calcification in predialysis CKD. *J. Am. Soc. Nephrol.* 30, 1073–1085. doi: 10.1681/ASN.2018111150

Sakaguchi, Y., Iwatani, H., Hamano, T., Tomida, K., Kawabata, H., Kusunoki, Y., et al. (2015). Magnesium modifies the association between serum phosphate and the risk of progression to end-stage kidney disease in patients with non-diabetic chronic kidney disease. *Kidney Int.* 88, 833–842. doi: 10.1038/ki.2015.165

Sakaguchi, Y., Shoji, T., Hayashi, T., Suzuki, A., Shimizu, M., Mitsumoto, K., et al. (2012). Hypomagnesemia in type 2 diabetic nephropathy: a novel predictor of end-stage renal disease. *Diabetes Care* 35, 1591–1597. doi: 10.2337/dc12-0226

Salaminia, S., Sayehmiri, F., Angha, P., Sayehmiri, K., and Motedayen, M. (2018). Evaluating the effect of magnesium supplementation and cardiac arrhythmias after acute coronary syndrome: a systematic review and meta-analysis. *BMC Cardiovasc. Disord.* 18:129. doi: 10.1186/s12872-018-0857-6

Santamaría, R., Díaz-Tocados, J. M., Pendón-Ruiz, de Mier, M. V., Robles, A., Salmerón-Rodríguez, M. D., et al. (2018). Increased phosphaturia accelerates the decline in renal function: a search for mechanisms. *Sci. Rep.* 8:13701. doi: 10.1038/s41598-018-32065-2

Schlingmann, K. P., Weber, S., Peters, M., Niemann Nejsum, L., Vitzthum, H., Klingel, K., et al. (2002). Hypomagnesemia with secondary hypocalcemia is caused by mutations in TRPM6, a new member of the TRPM gene family. *Nat. Genet.* 31, 166–170. doi: 10.1038/ng889

Schweigel-Röntgen, M., and Kolisek, M. (2014). SLC41 transporters–molecular identification and functional role. *Curr. Top. Membr.* 73, 383–410. doi: 10.1016/B978-0-12-800223-0.00011-6

Severino, P., Netti, L., Mariani, M. V., Maraone, A., D'Amato, A., Scarpati, R., et al. (2019). Prevention of cardiovascular disease: screening for magnesium deficiency. *Cardiol. Res. Pract.* 2019:4874921. doi: 10.1155/2019/4874921

Shechter, M., Sharir, M., Labrador, M. J., Forrester, J., Silver, B., and Bairey Merz, C. N. (2000). Oral magnesium therapy improves endothelial function in patients with coronary artery disease. *Circulation* 102, 2353–2358. doi: 10.1161/01.cir.102.19.2353

Shimohata, H., Yamashita, M., Ohgi, K., Tsujimoto, R., Maruyama, H., Takayasu, M., et al. (2019). The relationship between serum magnesium levels and mortality in non-diabetic hemodialysis patients: a 10-year follow-up study. *Hemodial. Int. Int. Symp. Home Hemodial.* 23, 369–374. doi: 10.1111/hdi.12759

Shrimal, S., Cherepanova, N. A., and Gilmore, R. (2015). Cotranslational and posttranslocational N-glycosylation of proteins in the endoplasmic reticulum. *Semin. Cell Dev. Biol.* 41, 71–78. doi: 10.1016/j.semcdb.2014.11.005

Sontia, B., Montezano, A. C. I., Paravicini, T., Tabet, F., and Touyz, R. M. (2008). Downregulation of renal TRPM7 and increased inflammation and fibrosis in aldosterone-infused mice: effects of magnesium. *Hypertens. Dallas Tex.* 1979, 915–921. doi: 10.1161/HYPERTENSIONAHA.107.100339

Sponder, G., Mastrototaro, L., Kurth, K., Merolle, L., Zhang, Z., Abdulhanan, N., et al. (2016). Human CNNM2 is not a Mg(2+) transporter per se. *Pflugers Arch.* 468, 1223–1240. doi: 10.1007/s00424-016-1816-7

Stenvinkel, P., Ketteler, M., Johnson, R. J., Lindholm, B., Pecoits-Filho, R., Riella, M., et al. (2005). IL-10, IL-6, and TNF-alpha: central factors in the altered cytokine network of uremia–the good, the bad, and the ugly. *Kidney Int.* 67, 1216–1233. doi: 10.1111/j.1523-1755.2005.00200.x

Strippoli, G. F. M., Craig, J. C., Rochtchina, E., Flood, V. M., Wang, J. J., and Mitchell, P. (2011). Fluid and nutrient intake and risk of chronic kidney disease. *Nephrol. Carlton Vic.* 16, 326–334. doi: 10.1111/j.1440-1797.2010.01415.x

Tejero-Taldo, M. I., Kramer, J. H., Mak, I. T., Komarov, A. M., and Weglicki, W. B. (2006). The nerve-heart connection in the pro-oxidant response to Mg-deficiency. *Heart Fail. Rev.* 11, 35–44. doi: 10.1007/s10741-006-9191-7

Teo, K. K., and Yusuf, S. (1993). Role of magnesium in reducing mortality in acute myocardial infarction. A review of the evidence. *Drugs* 46, 347–359. doi: 10.2165/00003495-199346030-00002

Tin, A., Grams, M. E., Maruthur, N. M., Astor, B. C., Couper, D., Mosley, T. H., et al. (2015). Results from the atherosclerosis risk in communities study suggest that low serum magnesium is associated with incident kidney disease. *Kidney Int.* 87, 820–827. doi: 10.1038/ki.2014.331

Topf, J. M., and Murray, P. T. (2003). Hypomagnesemia and hypermagnesemia. *Rev. Endocr. Metab. Disord.* 4, 195–206. doi: 10.1023/a:1022950321817

Touyz, R. M. (2003). Role of magnesium in the pathogenesis of hypertension. *Mol. Aspects Med.* 24, 107–136. doi: 10.1016/s0098-2997(02)00094-8

Touyz, R. M., Marshall, P. R., and Milne, F. J. (1991). Altered cations and muscle membrane ATPase activity in deoxycorticosterone acetate-salt spontaneously hypertensive rats. *J. Hypertens.* 9, 737–750. doi: 10.1097/00004872-199108000-00007

Touyz, R. M., Pu, Q., He, G., Chen, X., Yao, G., Neves, M. F., et al. (2002). Effects of low dietary magnesium intake on development of hypertension in stroke-prone spontaneously hypertensive rats: role of reactive oxygen species. *J. Hypertens.* 20, 2221–2232. doi: 10.1097/00004872-200211000-00022

Vaduganathan, M., Greene, S. J., Ambrosy, A. P., Mentz, R. J., Fonarow, G. C., Zannad, F., et al. (2013). Relation of serum magnesium levels and postdischarge outcomes in patients hospitalized for heart failure (from the EVEREST Trial). *Am. J. Cardiol.* 112, 1763–1769. doi: 10.1016/j.amjcard.2013.07.020

Van Camp, I., Ritskes-Hoitinga, J., Lemmens, A. G., and Beynen, A. C. (1990). Diet-induced nephrocalcinosis and urinary excretion of albumin in female rats. *Lab. Anim.* 24, 137–141. doi: 10.1258/002367790780890086

Van Laecke, S., Maréchal, C., Verbeke, F., Peeters, P., Van Biesen, W., Devuyst, O., et al. (2011). The relation between hypomagnesaemia and vascular stiffness in renal transplant recipients. *Nephrol. Dial. Transplant.* 26, 2362–2369. doi: 10.1093/ndt/gfq728

Van Laecke, S., Nagler, E. V., Verbeke, F., Van Biesen, W., and Vanholder, R. (2013). Hypomagnesemia and the risk of death and GFR decline in chronic kidney disease. *Am. J. Med.* 126, 825–831. doi: 10.1016/j.amjmed.2013.02.036

Van Laecke, S., Van Biesen, W., and Vanholder, R. (2012). Hypomagnesaemia, the kidney and the vessels. *Nephrol. Dial. Transplant.* 27, 4003–4010. doi: 10.1093/ndt/gfs126

Van Laecke, S., Van Biesen, W., Verbeke, F., De Bacquer, D., Peeters, P., and Vanholder, R. (2009). Posttransplantation hypomagnesemia and its relation with immunosuppression as predictors of new-onset diabetes after transplantation. *Am. J. Transplant.* 9, 2140–2149. doi: 10.1111/j.1600-6143.2009.02752.x

Verberckmoes, S. C., Persy, V., Behets, G. J., Neven, E., Hufkens, A., Zebger-Gong, H., et al. (2007). Uremia-related vascular calcification: more than apatite deposition. *Kidney Int.* 71, 298–303. doi: 10.1038/sj.ki.5002028

Vetter, T., and Lohse, M. J. (2002). Magnesium and the parathyroid. *Curr. Opin. Nephrol. Hypertens.* 11, 403–410. doi: 10.1097/00041552-200207000-00006

Weglicki, W. B. (2012). Hypomagnesemia and inflammation: clinical and basic aspects. *Annu. Rev. Nutr.* 32, 55–71. doi: 10.1146/annurev-nutr-071811-150656

Westermann, B. (2010). Mitochondrial fusion and fission in cell life and death. *Nat. Rev. Mol. Cell Biol.* 11, 872–884. doi: 10.1038/nrm3013

Xiong, J., He, T., Wang, M., Nie, L., Zhang, Y., Wang, Y., et al. (2019). Serum magnesium, mortality, and cardiovascular disease in chronic kidney disease and end-stage renal disease patients: a systematic review and meta-analysis. *J. Nephrol.* 32, 791–802. doi: 10.1007/s40620-019-00601-6

Yamanaka, R., Tabata, S., Shindo, Y., Hotta, K., Suzuki, K., Soga, T., et al. (2016). Mitochondrial Mg(2+) homeostasis decides cellular energy metabolism and vulnerability to stress. *Sci. Rep.* 6:30027. doi: 10.1038/srep30027

Zhang, C., Zhang, T., Zou, J., Miller, C. L., Gorkhali, R., Yang, J.-Y., et al. (2016). Structural basis for regulation of human calcium-sensing receptor by magnesium ions and an unexpected tryptophan derivative co-agonist. *Sci. Adv.* 2:e1600241. doi: 10.1126/sciadv.1600241

Zhang, X., Li, Y., Del Gobbo, L. C., Rosanoff, A., Wang, J., Zhang, W., et al. (2016). Effects of magnesium supplementation on blood pressure. *Hypertension* 68, 324–333. doi: 10.1161/HYPERTENSIONAHA.116.07664

Zhang, X., Xia, J., Del Gobbo, L. C., Hruby, A., Dai, Q., and Song, Y. (2018). Serum magnesium concentrations and all-cause, cardiovascular, and cancer mortality among U.S. adults: results from the NHANES I epidemiologic follow-up study. *Clin. Nutr. Edinb. Scotl.* 37, 1541–1549. doi: 10.1016/j.clnu.2017.08.021

Conflict of Interest: The authors declare that the research was conducted in the absence of any commercial or financial relationships that could be construed as a potential conflict of interest.

Copyright © 2020 Rodelo-Haad, Pendón-Ruiz de Mier, Díaz-Tocados, Martin-Malo, Santamaria, Muñoz-Castañeda and Rodríguez. This is an open-access article distributed under the terms of the Creative Commons Attribution License (CC BY). The use, distribution or reproduction in other forums is permitted, provided the original author(s) and the copyright owner(s) are credited and that the original publication in this journal is cited, in accordance with accepted academic practice. No use, distribution or reproduction is permitted which does not comply with these terms.

frontiers in Cell and Developmental Biology

ORIGINAL RESEARCH
published: 19 November 2020
doi: 10.3389/fcell.2020.607080

O-GlcNAcylation Suppresses the Ion Current IClswell by Preventing the Binding of the Protein ICln to α-Integrin

Roberta Costa[1†‡], Alessia Remigante[1,2†‡], Davide A. Civello[1], Emanuele Bernardinelli[1], Zoltán Szabó[3], Rossana Morabito[2], Angela Marino[2], Antonio Sarikas[1], Wolfgang Patsch[1], Markus Paulmichl[4], Tamás Janáky[3], Attila Miseta[5], Tamás Nagy[5]* and Silvia Dossena[1]*

[1] Institute of Pharmacology and Toxicology, Paracelsus Medical University, Salzburg, Austria, [2] Department of Chemical, Biological, Pharmaceutical and Environmental Sciences, University of Messina, Messina, Italy, [3] Department of Medical Chemistry, Faculty of Medicine, University of Szeged, Szeged, Hungary, [4] Department of Personalized Medicine, Humanomed, Klagenfurt, Austria, [5] Department of Laboratory Medicine, Medical School, University of Pécs, Pécs, Hungary

O-GlcNAcylation is a post-translational modification of proteins that controls a variety of cellular processes, is chronically elevated in diabetes mellitus, and may contribute to the progression of diabetic complications, including diabetic nephropathy. Our previous work showed that increases in the *O*-GlcNAcylation of cellular proteins impair the homeostatic reaction of the regulatory volume decrease (RVD) after cell swelling by an unknown mechanism. The activation of the swelling-induced chloride current IClswell is a key step in RVD, and ICln, a ubiquitous protein involved in the activation of IClswell, is *O*-GlcNAcylated. Here, we show that experimentally increased *O*-GlcNAcylation of cellular proteins inhibited the endogenous as well as the ICln-induced IClswell current and prevented RVD in a human renal cell line, while decreases in *O*-GlcNAcylation augmented the current magnitude. In parallel, increases or decreases in *O*-GlcNAcylation, respectively, weakened or stabilized the binding of ICln to the intracellular domain of α-integrin, a process that is essential for the activation of IClswell. Mutation of the putative YinOYang site at Ser67 rendered the ICln-induced IClswell current unresponsive to *O*-GlcNAc variations, and the ICln interaction with α-integrin insensitive to *O*-GlcNAcylation. In addition, exposure of cells to a hypotonic solution reduced the *O*-GlcNAcylation of cellular proteins. Together, these findings show that *O*-GlcNAcylation affects RVD by influencing IClswell and further indicate that hypotonicity may activate IClswell by reducing the *O*-GlcNAcylation of ICln at Ser67, therefore permitting its binding to α-integrin. We propose that disturbances in the regulation of cellular volume may contribute to disease in settings of chronically elevated *O*-GlcNAcylation, including diabetic nephropathy.

Keywords: *O*-GlcNAcylation, IClswell, ICln, α-integrin, regulatory volume decrease, kidney, protein–protein interaction

OPEN ACCESS

Edited by:
Claudia Torino,
Italian National Research Council, Italy

Reviewed by:
Tiziano Verri,
University of Salento, Italy
Eleanor DeLand Lederer,
University of Texas Southwestern Medical Center, United States

****Correspondence:***
Silvia Dossena
silvia.dossena@pmu.ac.at
Tamás Nagy
nagy.tamas@pte.hu

†Present address:
Roberta Costa,
Aptuit Srl, Verona, Italy
Alessia Remigante,
Institute of Biophysics, National Research Council, Genoa, Italy

‡These authors have contributed equally to this work

Specialty section:
This article was submitted to Molecular Medicine, a section of the journal Frontiers in Cell and Developmental Biology

Received: *16 September 2020*
Accepted: *23 October 2020*
Published: *19 November 2020*

Citation:
Costa R, Remigante A, Civello DA, Bernardinelli E, Szabó Z, Morabito R, Marino A, Sarikas A, Patsch W, Paulmichl M, Janáky T, Miseta A, Nagy T and Dossena S (2020) O-GlcNAcylation Suppresses the Ion Current IClswell by Preventing the Binding of the Protein ICln to α-Integrin. Front. Cell Dev. Biol. 8:607080. doi: 10.3389/fcell.2020.607080

INTRODUCTION

O-GlcNAcylation is a dynamic and abundant post-translational modification of cytosolic, nuclear, mitochondrial, and membrane proteins, which consists of the addition of a single monosaccharide (*O*-linked β-D-*N*-acetylglucosamine or *O*-GlcNAc) to hydroxyl groups of serine and/or threonine residues. The substrate for *O*-GlcNAcylation is uridine diphosphate-β-*N*-acetylglucosamine (UDP-GlcNAc), the end product of the hexosamine biosynthetic pathway (HBP), and its abundance controls the efficiency of protein *O*-GlcNAcylation. Approximately 2–5% of cellular glucose is diverted to the HBP, which is consequently strongly connected to the nutrient availability and carbohydrate metabolism (Wells et al., 2001, 2003b; Zachara and Hart, 2006; Zachara et al., 2015; Fisi et al., 2017). *O*-GlcNAc modification is reversible and specific and is tightly controlled by the activity of the enzymes *O*-GlcNAc-transferase (OGT) and *O*-GlcNAcase (OGA), which catalyze the addition and the removal of *O*-GlcNAc from target proteins, respectively (Gloster and Vocadlo, 2010; Yang and Qian, 2017).

O-GlcNAcylation may compete and establish a dynamic interplay with other post-translational modifications, including phosphorylation, by occurring on same sites or adjacent sites (Slawson and Hart, 2011). Amino acids that are either phosphorylated or *O*-GlcNAcylated in a mutually exclusive manner are called YinOYang sites and are crucially involved in controlling protein activity (Zeidan and Hart, 2010).

O-GlcNAcylation regulates a variety of cellular and molecular processes including intracellular signaling, gene transcription, protein–protein interaction, and stability, localization and expression of proteins (Butkinaree et al., 2010). Consequently, *O*-GlcNAc plays a role in numerous physiological and pathological conditions, including the response to stress, cancer, neurodegeneration, and diabetes mellitus (Wells et al., 2001; Zachara et al., 2004; Hart et al., 2007; Fardini et al., 2013). Specifically, strong positive correlations between protein *O*-GlcNAc levels and insulin resistance, glucose toxicity (McClain and Crook, 1996; Copeland et al., 2008), and chronic complications of diabetes mellitus (Brownlee, 2001; Buse, 2006; McLarty et al., 2013) have been well established in cell culture and animal models (Buse, 2006; Dias and Hart, 2007; Nagy et al., 2007) as well as in patients (Wang et al., 2009; Park et al., 2010; Springhorn et al., 2012; Myslicki et al., 2014; Pagesy et al., 2018). Among the multiple and diverse functions of *O*-GlcNAcylation, one of the least studied is the modulation of the regulation of cellular volume.

The regulation of cellular volume is a homeostatic reaction essential to normal cell function (Lang et al., 1998; Hoffmann et al., 2009). Variations of the cellular volume are due to an imbalance between the intra- and the extracellular osmolality; may induce alterations in cell morphology, function, and survival; and therefore require counterbalance. In mammalian cells, swelling activates a rapid release of KCl and/or non-essential organic osmolytes accompanied by cellular water (Jakab et al., 2002). This process is called regulatory volume decrease (RVD) and permits swollen cells to regain their original volume. The main conductive pathway leading to the release of Cl^- during RVD is called IClswell (Furst et al., 2002a), and the respective main molecular entity was identified as the leucine-rich repeat containing protein 8A (LRRC8A) (Qiu et al., 2014; Voss et al., 2014; Pedersen et al., 2016), although other channels may also play a role in this context (Liu et al., 2019; Okada et al., 2019).

Our previous study established a link between *O*-GlcNAcylation and RVD. Increasing the cellular *O*-GlcNAc levels by a hour pretreatment with glucosamine, PUGNAc, or high glucose (30 mM) altered the response of Jurkat cells to a hypotonic stimulus. Specifically, the swelling observed following exposure of cells to a hypotonic extracellular medium was augmented and the intracellular water diffusion was reduced (Nagy et al., 2010). However, the molecular mechanism by which augmented *O*-GlcNAcylation affects RVD remains to be established.

ICln is a ubiquitous, highly conserved, multifunctional protein that plays a fundamental role in RVD (Paulmichl et al., 1992; Furst et al., 2006). During a hypotonic stimulus, ICln is transposed toward the plasma membrane and facilitates the activation of IClswell (Ritter et al., 2003; Dossena et al., 2011). Binding of cytosolic ICln to the intracellular domain of α-integrin is an essential prerequisite for ICln association with the plasma membrane and IClswell activation and requires a direct molecular interaction between highly conserved amino acid motifs of both proteins (Schedlbauer et al., 2019). Specifically, the sequence (61)ISLHA(65) (single-letter amino acid code; numbers refer to the amino acid position within the human ICln protein sequence), located in the β4–β5 loop and β5 sheet of the pleckstrin homology-like N-terminal portion of ICln (Furst et al., 2005), appears to be essential for binding to α-integrin as well as for the ICln-induced activation of IClswell. Interestingly, ICln is *O*-GlcNAcylated (Hahne et al., 2013); however, the ICln *O*-GlcNAc modification site(s) as well as their physiological significance are not assessed.

The aim of the present study was to explore the mechanism by which *O*-GlcNAcylation affects RVD. Here, we show that augmented *O*-GlcNAcylation prevents RVD by reducing the magnitude of the ion current IClswell. IClswell inhibition results from *O*-GlcNAcylation of the protein ICln on serine 67, which prevents its binding to the intracellular domain of the integrin α chain. These findings suggest that dysfunction of cellular volume regulation may contribute to diseases associated with chronic elevation of *O*-GlcNAcylation.

MATERIALS AND METHODS

Cell Culture and Transfection

Human embryonic kidney (HEK) 293 Phoenix (DiCiommo et al., 2004) and HeLa cells [human cervical adenocarcinoma, CCL-2, obtained from American Type Cell Culture Collection (ATCC), Manassas, VA, United States] were cultured in Minimum Essential Eagle Medium (Sigma-Aldrich, St. Louis, MO, United States) supplemented with 10% fetal bovine serum (GIBCO, Thermo Fisher, Waltham, MA, United States), 2 mM L-glutamine, 100 U/ml penicillin, 100 μg/ml streptomycin, and 1 mM pyruvic acid (sodium salt). NIH/3T3 cells (mouse

embryonic fibroblasts, CRL-1658, obtained from ATCC) were cultured in Dulbecco's Modified Eagle's Medium (Sigma-Aldrich) supplemented with 10% bovine calf serum (GIBCO), 100 U/ml penicillin and 100 μg/ml streptomycin. The cells were maintained at 37°C, 5% CO_2, 95% air, and 100% humidity. Subcultures were routinely established every second to third day by seeding the cells into 100-mm diameter Petri dishes following trypsin/ethylenediaminetetraacetic acid (EDTA) treatment.

For transfection, cells were seeded into six-well plates or 30-mm diameter Petri dishes, grown overnight to ∼50% confluence, and transiently transfected with 1–3 μg of plasmid DNA by the calcium phosphate co-precipitation method (HEK 293 Phoenix) or 1.5–3 μg of plasmid DNA and 3–6 μl METAFECTENE PRO® (Biontex, Munich, Germany), following the manufacturer's instructions (HeLa and NIH/3T3). For co-transfection experiments, equimolar amounts of two vectors were used. Medium was replaced 6–8 h after transfection.

Plasmid Constructs

For electrophysiology experiments, the open reading frames (ORFs) coding for human ICln (hICln, NCBI Reference Sequence: NP_001284.1); *Canis familiaris* ICln (from Madin-Darby Canine Kidney cells, MDCK ICln, NP_001003288.1); and the long (OGA-L, NP_036347.1) or short (OGA-S, NP_001135906.1) isoforms of OGA, OGT (NP_858051.1; all from HEK 293 Phoenix cells), or integrin αIIbshort (amino acids 987–1039 of the human integrin αIIb chain, NP_000410.2) were cloned into the bicistronic mammalian expression vectors pIRES2EGFP or pIRES2dsRedExpress (Clontech, Mountain View, CA, United States). The use of a vector bearing the internal ribosome entry site (IRES) allows for the simultaneous expression of the protein of interest (either OGT, OGA, integrin αIIbshort, or ICln) and the transfection marker (either the enhanced green fluorescent protein EGFP or the red fluorescent protein dsRED) as two individual proteins from the same bicistronic mRNA, without the production of fusion proteins (Morgan et al., 1992). Control experiments were conducted in cells transfected with the pIRES2EGFP-EGFP vector, where an additional EGFP coding sequence was cloned into the pIRES2EGFP expression vector. Consequently, the control vector contained two EGFP coding sequences (one in the multiple cloning site and one downstream of the IRES sequence).

Plasmids encoding for ICln Ser67Ala, Thr223Ala, and Ser193* were obtained by site-directed mutagenesis of vectors bearing the wild-type ICln cDNA with the QuikChange Site-Directed Mutagenesis Kit (Agilent, Santa Clara, CA, United States). Mutagenesis primers were designed in-house (Gene Runner, version 5.0.993 Beta) and obtained from Microsynth AG (Balgach, Switzerland).

To produce fusion proteins for fluorescence resonance energetic transfer (FRET) experiments, hICln, MDCK ICln, hOGT, hOGA, or integrin αIIbshort ORFs were cloned into the pEYFPC1, pEYFPN1, pECFPC1, or pECFPN1 mammalian expression vectors (Clontech) in frame with the ORF of the enhanced yellow fluorescent protein (EYFP) or enhanced cyan fluorescent protein (ECFP).

All plasmid inserts were sequenced prior to their use in experiments (Microsynth AG).

Manipulation of *O*-GlcNAcylation of Cellular Proteins

To increase the *O*-GlcNAcylation levels of cellular proteins, cells were incubated for 1 h in complete medium with 20 mM D-glucose, 5 mM glucosamine, 100 μM *O*-(2-acetamido-2-deoxy-D-glucopyranosylidene)amino *N*-phenyl carbamate (PUGNAc; Sigma Aldrich), 100 μM PUGNAc, and 5 mM glucosamine (Nagy et al., 2010) or were transfected for 24 h with OGT. To reduce the *O*-GlcNAcylation levels of proteins, cells were transfected for 24 h with OGA. PUGNAc was dissolved in 100% dimethyl sulfoxide (DMSO) and stored at −20°C. To obtain equal osmolarity of control incubation media, 20 mM mannitol and 5 mM D-glucose were used instead of 20 mM D-glucose and 5 mM glucosamine.

Patch Clamp

Cells were transferred to glass coverslips (10-mm diameter) 8 h after transfection, and electrophysiology measurements were performed 24–32 h after transfection. Single cells expressing the transfection marker EGFP, dsRed, or both could be identified by fluorescence microscopy using FITC (excitation: 480/30x, dicroic: 505 dclp, and emission: 535/40 m) and TRITC (excitation: 540/25x, dicroic: 565 dclp, and emission: 605/55 m) filter sets. Selected cells were voltage-clamped using the whole-cell patch-clamp technique as previously described (Gandini et al., 2008; Dossena et al., 2011; Tamma et al., 2011; Morabito et al., 2017; Schedlbauer et al., 2019). The resistance of the glass pipettes was 3–8 MΩ when filled with the pipette solution (CsCl 125 mM, $MgCl_2$ 5 mM, EGTA 11 mM, ATP Mg^{2+} salt 2 mM, HEPES 10 mM, pH 7.2 adjusted with CsOH, and 300 mOsm/kg H_2O). Fast exchange of the isotonic bath solution (NaCl 125 mM, $CaCl_2$ 2.5 mM, $MgCl_2$ 2.5 mM, HEPES 10 mM, mannitol 40 mM, pH 7.4 adjusted with NaOH, and 300 mOsm/kg H_2O) with a hypotonic bath solution (NaCl 125 mM, $CaCl_2$ 2.5 mM, $MgCl_2$ 2.5 mM, HEPES 10 mM, pH 7.4 adjusted with NaOH, and 260 mOsm/kg H_2O) was obtained using a perfusion system with a flow rate of 5 ml/min and a bath volume of ∼300 μl. For data acquisition, an EPC10 USB amplifier (HEKA Elektronik, Lambrecht, Germany) controlled by a Macintosh computer running the Patch Master (v2x32, HEKA Elektronik) software was used. Access resistance was monitored throughout the recordings and never exceeded thrice the recording electrode resistance. Fast and slow capacitance were compensated. All current measurements were filtered at 2.9 kHz and digitized at 50 kHz. To monitor the activation of the swelling-activated chloride current (IClswell), cells were held at 0 mV and step pulses of 400-ms duration were applied from 0 to 40 mV every 20 s. To establish the current to voltage (IV) relationship, step pulses of 500-ms duration were applied every 5 or 10 min from −120 to +100 mV in 20-mV increments from a holding potential of 0 mV. For data analysis, Fit Master (v2x32, HEKA Elektronik) and Excel (Microsoft, United States) software were used. The current values (pA) were normalized to the membrane capacitance (pF) to obtain the current density

(pA/pF). Each data set was obtained from cells from at least three independent subcultures with control experiments in cells of the same subculture.

Western Blotting

Cells were washed twice with ice-cold phosphate-buffered saline (PBS) and lysed on ice in a buffer containing 20 mM Tris-HCl, 150 mM NaCl, 1 mM EDTA, 0.1% NP40, and protease inhibitor cocktail (Roche, Basel, Switzerland). Subsequently, cellular debris was discarded by centrifugation at 16,000 × *g* for 30 min at 4°C and the supernatant was collected. Typically, 10 μg of total proteins were separated by a 7.5% polyacrylamide gel containing 0.1% SDS and electroblotted using a polyvinylidene fluoride membrane (Bio-Rad, Basel, Switzerland) by applying a constant voltage (75 V) for 2 h at 4°C. Membranes were blocked for 1 h at room temperature in 5% bovine serum albumin (BSA) diluted in Tris-buffered saline (150 mM NaCl and 15 mM Tris-HCl) containing 0.1% Tween 20 (TBST) and incubated overnight at 4°C with the following primary antibodies: mouse monoclonal IgM CTD110.6 (Cell Signaling Technology, Inc., Danvers, MA, United States), highly specific for *O*-glycosylated proteins (Kneass and Marchase, 2004), diluted 1:1,000, or rabbit polyclonal IgG against amino acids 151–164 of CLNS1A (Sigma Aldrich), diluted 1:2,000. The housekeeping proteins GAPDH or β-actin were detected with a goat (GenScript, Piscataway, NJ, United States) or rabbit (Cell Signaling) polyclonal antibody, respectively, both diluted 1:1,000. Membranes were washed three times in TBST and incubated for 1 h at room temperature with the secondary antibodies diluted 1:10,000 in PBS and 5% BSA (goat anti-mouse IgM, IRD-680 RD, donkey anti-goat, IRD-800 CW, or goat anti-rabbit, IRD-800 CW, all from LI-COR, Lincoln, NE, United States). The signal of immunocomplexes was revealed using the Odyssey (LI-COR) infrared imaging system. Densitometric analysis was done using the ImageJ (1.49v) software.

Acceptor Photobleaching Fluorescence Resonance Energy Transfer

Cells were transferred to round 3-cm diameter glass slides 32 h post-transfection and fixed for 30 min with 4% paraformaldehyde in Hanks' Balanced Salt Solution (HBSS) 48 h post-transfection. Imaging was performed in HBSS at room temperature. The FRET acceptor EYFP was excited with the 514-nm line of the Argon laser, and the emission was detected in the 525–600-nm range. The FRET donor ECFP was excited with the 405-nm laser, and the emission was detected in the 450–490-nm range. Imaging was performed by sequential acquisition with FRET AB-Wizard with a Leica TCS SP5II AOBS confocal microscope (Leica Microsystems, Wetzlar, Germany) equipped with a HCX PL APO 63x/1.20 Lambda blue water immersion objective and controlled by the LAS AF software (version 2.7.3.9723, Leica Microsystems). EYFP photobleaching in whole cells was obtained with 15 sequential illuminations at 514 nm (zoom factor 8×). FRET efficiency was calculated using the following formula:

$$\text{FRET efficiency} = 1 - \text{ECFPpre}/\text{ECFPpost} \quad (1)$$

ECFPpre and ECFPpost refer to the ECFP intensity before and after EYFP photobleaching, respectively, and were determined either in the bleaching regions of interest (ROI) or in plasma membrane ROIs, as indicated. In the latter case, ROIs were drawn within the bleaching ROI, on the pre-bleaching EYFP image, in areas with a clear targeting of αIIbs-EYFP at the cell periphery.

Cell Volume Measurements

Cell volume measurements were performed as previously described (Morabito et al., 2013, 2014, 2017). Briefly, HEK 293 Phoenix cells were transferred to round 3-cm diameter glass slides and successively placed in a perfusion chamber. Cell volume measurements were performed on cells sequentially exposed to the following: isotonic solution for 1 min and hypotonic solution (∼15% reduction of osmolality by omission of mannitol) for 2–3 min. Cell volume measurements were performed on roundish cells. For each experiment, 100–150 images/cell (1 image/1,293 s) were taken with a phase contrast microscope (Leica DMI 6000, with a HCX PL APO 63x/1.20 Lambda blue water immersion objective; Leica Microsystems). Cell diameter was measured for each image and, assuming the cell as a sphere, cell volume was calculated and expressed as V/V_0, where V and V_0 represent the volume of a cell at a given time and the average volume of the same cell in isotonic solution, respectively.

Immunoprecipitation and Mass Spectrometry

For immunoprecipitation, cells were lysed on ice for 30 min in IP buffer (25 mM Tris-HCl, pH 7.4, 150 mM NaCl, 1 mM EDTA, 1% Triton X-100, 5% glycerol, 0.05% Na-azide, protease inhibitor cocktail, and 50 μM of PUGNAc). Next, the samples were sonicated for 5 s at 30% power (Bandelin Sonopuls). Finally, the samples were centrifuged at 4°C for 10 min at 3,000 rpm, and the supernatants were incubated with anti-ICln antibodies #1 or #2 at 4°C overnight on a rotary shaker. Anti-ICln #1 is a polyclonal antibody raised in rabbits against amino acids 214–237 of human ICln, while anti-ICln #2 (Santa Cruz Biotechnology, Cat. No.: SC-393525) is a mouse monoclonal antibody. Protein A-Sepharose beads (Sigma-Aldrich) were prepared as follows: beads were washed in 800 μl IP buffer and incubated for 30 min in 3% BSA/IP buffer at 4°C on a shaker to block non-specific binding sites. Next, immunoprecipitates were incubated with the Protein A beads on a rotary shaker at 4°C for 3 h. Next, the beads were washed in 1 ml of IP buffer twice, the last wash buffer was removed carefully, and 50 μl of elution buffer (0.1 M glycine, pH 2.8) was added to the beads and incubated for 10 min at room temperature. The eluate (IP) was kept and 6 μl of 1.5 M Tris-HCl (pH 8.8) was added to neutralize the pH. During the process, lysates including the antibodies (input) and flow-through (FT) from the beads were collected. All of the collected samples (input, FT, and IP) were adjusted with 4X sample buffer and processed on 7.5% polyacrylamide gel electrophoresis. The proteins were either transferred to PVDF membranes for western blot analysis or the gel was directly

stained with Coomassie Brilliant Blue R-250 for further mass spectrometry analysis.

For mass spectrometry (MS), the protein bands of interest were cut out from the Coomassie-stained gels and digested by trypsin using the in-gel digestion protocol as described (Szabo et al., 2012). Briefly, excised gel bands were cut into small pieces, destained in 25 mM NH_4HCO_3 and 50% acetonitrile, dehydrated with acetonitrile, and dried. The gel pieces were rehydrated in 12.5 ng/μl trypsin (Promega, Madison, WI, United States) solution (in 25 mM NH_4HCO_3) and incubated overnight at 37°C. Peptides were extracted with 5% formic acid and twice with 60% acetonitrile in 1% formic acid.

Digested protein samples were analyzed using a Waters nanoACQUITY UPLC System coupled with a Thermo Q Exactive plus mass spectrometer. Forty-five-minute long gradients from 3% to 40% acetonitrile/water were applied on a Waters BEH130 C18 75 μm × 100 mm column with 1.7 μm particle size C18 packing. The mass spectrometer was operated in DDA mode, and the 12 most intensive peptides were selected for fragmentation in each MS scan.

From all acquired data, peaklists were generated by the Msconvert tool from ProteoWizard (Chambers et al., 2012). All MS/MS samples were analyzed using Mascot 2.2.06 (Matrix Science, London, UK). Mascot was set up to search the UniProt Human proteome database (2017.03 release, 70,942 entries) assuming digestion by trypsin and allowing up to two missed cleavage sites. Database searching was carried out with a fragment ion mass tolerance of 0.1 Da and a parent ion tolerance of 10 ppm. The iodoacetamide derivative of cysteine was specified as a fixed modification, and oxidation of methionine, N-acetyl-glycosylation of serine and threonine, acetylation of protein N-terminal, and formylation of peptide N-terminal were specified as a variable modification in Mascot. Database search results were validated, and MS/MS spectra were annotated in PeptideShaker 1.16.45 (Vaudel et al., 2015).

Immunocytochemistry

HeLa cells were grown on coverslips until ∼50% confluence and treated with either 100 μM PUGNAc and 5 mM glucosamine or the vehicle for 1 h at 37°C. Following this, the cells were exposed to 300 mOsmol isotonic (mannitol 100 mM, NaCl 87.5 mM, $CaCl_2$ 2.5 mM, $MgCl_2$ 2.5 mM, HEPES 10 mM, pH 7.4) or 200 mOsmol hypotonic (NaCl 87.5 mM, $CaCl_2$ 2.5 mM, $MgCl_2$ 2.5 mM, HEPES 10 mM, pH 7.4) solution for 15 min. Next, cells were fixed in 10 *v*/*v*% PBS-buffered formaldehyde for 30 min at room temperature. To avoid formaldehyde autofluorescence, the coverslips were quenched with 50 mM ammonium chloride for 10 min. The cells were permeabilized with 0.25 *v*/*v*% Triton-X 100 for 10 min. Non-specific sites were blocked with 5% bovine serum albumin (Sigma-Aldrich) in PBS for 30 min, and then, the coverslips were incubated at room temperature with the primary antibodies in 5 *w*/*v*% BSA/PBS for 2 h. The primary antibodies and their dilutions were the following: CTD110.6 (1:200) and rabbit anti-ICln (1:100). After rinsing three times with PBS, samples were incubated with the corresponding secondary antibodies for 1 h in the dark. Finally, coverslips were mounted with VECTASHIELD (Vector Laboratories, Burlingame, CA, United States) mounting medium. Image acquisition was performed with a Zeiss LSM 710 confocal scanning microscope (Carl Zeiss AG, Oberkochen, Germany) equipped with the ZEN software (ver2.3, Carl Zeiss AG, Oberkochen, Germany) and a 63× objective. Alexa Fluor 488 (ICln) and Texas Red (CTD110.6) fluorescence channels were used for image acquisition (excitation 488 and 594 nm, emission 518 and 624 nm, respectively).

Bioinformatic Analysis

The amino acid sequence of human ICln (NP_001284.1) was analyzed with the YinOYang WWW server (http://www.cbs.dtu.dk/services/YinOYang/), which produces neural network predictions for O-β-GlcNAc attachment sites in eukaryotic protein sequences (Gupta and Brunak, 2002). This server can also use NetPhos, which predicts serine, threonine, or tyrosine phosphorylation sites in eukaryotic proteins, to identify possible phosphorylated sites that, when coinciding with *O*-GlcNAcylation sites, represent "YinOYang" sites (Blom et al., 2004). In addition, the *GlycoMine* (http://glycomine.erc.monash.edu/Lab/GlycoMine/) bioinformatics tool was used to predict O-linked glycosylation (Li et al., 2015).

Statistical Analysis

All data are expressed as arithmetic means ± standard errors of the mean. For statistical analysis and graphics, GraphPad Prism (version 5.0b for Mac OS, San Diego, CA, United States) and Excel (Microsoft) software were used. Significant differences between mean values were determined by the unpaired Student's *t*-test or ANOVA with Bonferroni's or Dunnett's post-test, as appropriate. Statistically significant differences were determined at $^{*}p < 0.05$, $^{**}p < 0.01$, $^{***}p < 0.001$; (*n*) corresponds to the number of independent measurements.

RESULTS

Manipulation of *O*-GlcNAcylation of Cellular Proteins

Incubation of cells with *O*-GlcNAc precursors such as D-glucose or glucosamine, pharmacological inhibition of OGA with PUGNAc, as well as overexpression of OGT or OGA have formerly been used to experimentally increase or decrease *O*-GlcNAcylation levels of cellular proteins (Champattanachai et al., 2008; Yuzwa and Vocadlo, 2014; Ferron et al., 2018). Here, incubation of HEK 293 Phoenix cells for 1 h with 20 mM D-glucose, 5 mM glucosamine, or 100 μM PUGNAc failed to significantly increase *O*-GlcNAcylation levels of cellular proteins (**Figures 1A–C** and **Table 1**). However, combining 100 μM PUGNAc with 5 mM glucosamine increased *O*-GlcNAcylation up to 3.6-fold of control levels (**Figure 1D** and **Table 1**). Transfection of cells with OGT was the most effective maneuver and increased *O*-GlcNAcylation of 6.5-fold compared to cells

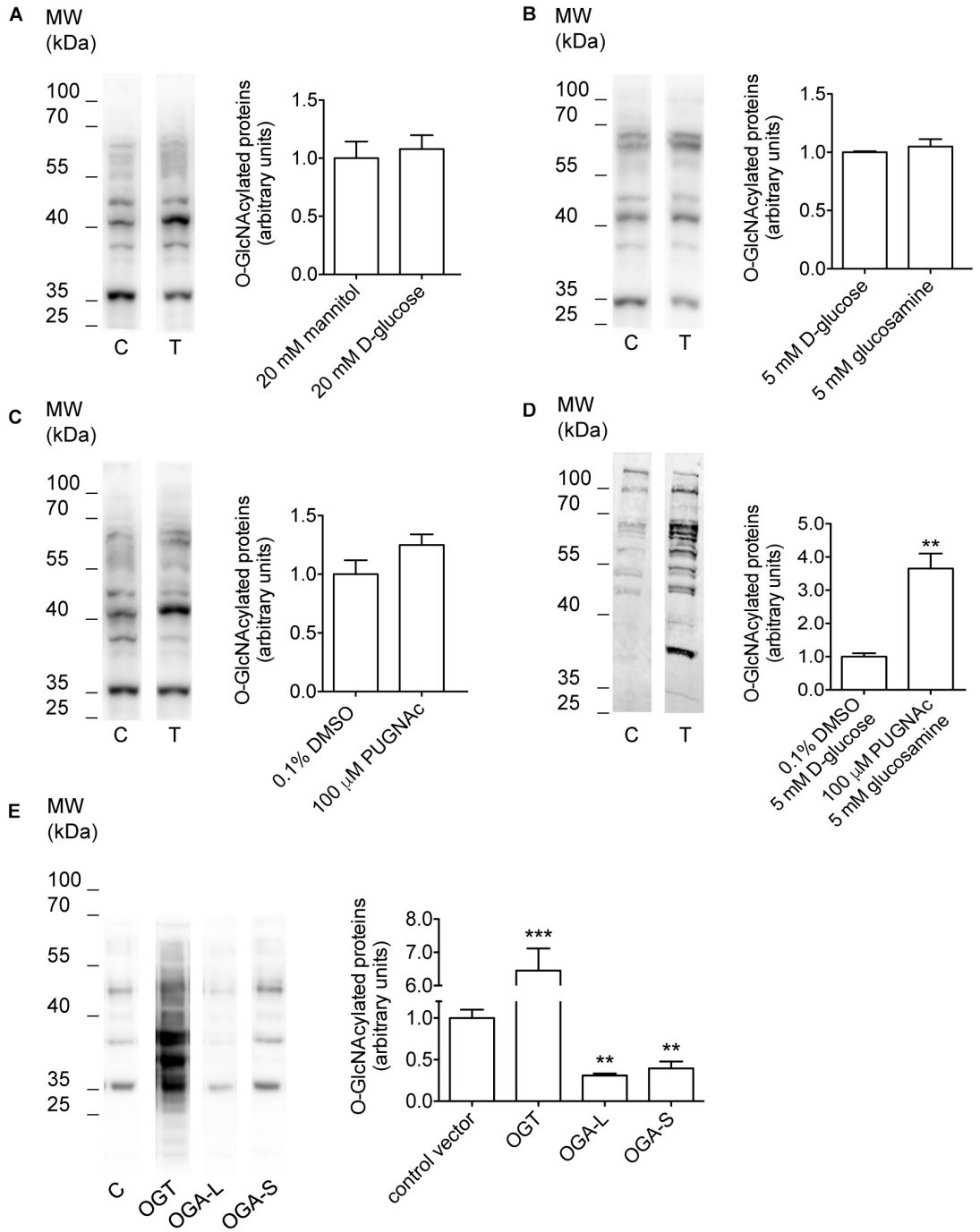

FIGURE 1 | Manipulation of *O*-GlcNAcylation levels of cellular proteins. HEK 293 Phoenix cells were incubated for 1 h in complete medium with **(A)** 20 mM mannitol (control) or D-glucose, **(B)** 5 mM D-glucose (control) or glucosamine, **(C)** 0.1% DMSO (control) or 100 μM PUGNAc, **(D)** 0.1% DMSO plus 5 mM D-glucose (control) or 100 μM PUGNAc plus 5 mM glucosamine, or **(E)** were transfected for 24 h with the pIRES2EGFP vector coding for OGT, OGA-L, or OGA-S or with the pIRES2EGFP-EGFP vector as a control. The expression levels of cellular *O*-GlcNAc-modified proteins determined via western blot were quantified by densitometry and normalized to the housekeeping protein β-actin. $n = 3$, $^{**}p < 0.01$, $^{***}p < 0.001$, two-tailed, unpaired Student's *t*-test or one-way ANOVA with Dunnett's post-test. (*n*) refers to the number of independent samples. C, control; T, treatment; DMSO, dimethyl sulfoxide; OGT, *O*-GlcNAc-transferase; OGA, *O*-GlcNAcase.

transfected with a control vector (**Figure 1E** and **Table 1**). Conversely, cells expressing either OGA-L or its splicing variant OGA-S showed a significant reduction in *O*-GlcNAcylation of cellular proteins, which was more pronounced with OGA-L (**Figure 1E** and **Table 1**). Hence, the catalytic activity of OGA-S was found to be lower than that of OGA-L

TABLE 1 | Effect of manipulation of *O*-GlcNAcylation of cellular proteins on the current IClswell.

Treatment	% variation in *O*-GlcNAcylation	Effect on IClswell		
		Native cells	Cells transfected with ICln wild type	Cells transfected with ICln Ser67Ala
20 mM D-glucose	+8% (n.s.)	n.s.	n.s.	n.p.
5 mM glucosamine	+5% (n.s.)	n.s.	n.s.	n.p.
100 μM PUGNAc	+25% (n.s.)	n.s.	n.s.	n.p.
100 μM PUGNAc plus 5 mM glucosamine	+265%	n.s.	−55%	n.s.
OGT	+545%	−38%	−58%	−38%
OGA-S	−60%	n.s.	n.p.	n.p.
OGA-L	−69%	n.s.	+158%	n.s.

*The % variation in O-GlcNAcylation was calculated from western blot data shown in **Figure 1**. The % variation in IClswell intensity was calculated at +100 mV. + and − denote an increase and decrease compared to the corresponding control, respectively. n.s., not significant; n.p., not performed.*

(Kim et al., 2006). Therefore, only OGA-L was used in further experiments.

Increased *O*-GlcNAcylation of Cellular Proteins Inhibits the Endogenous IClswell Current

To assess the possible influence of *O*-GlcNAc on the endogenous swelling-activated chloride current IClswell, the patch-clamp technique in whole-cell configuration was used in untransfected cells in which the *O*-GlcNAcylation of cellular proteins was experimentally increased or decreased. Cells were initially kept in an extracellular isotonic solution. In these conditions, currents were very small and undistinguishable from leakage currents. Exposure of cells to an extracellular hypotonic solution activated a current with outward rectification and slow time-dependent inactivation at voltages higher than +40 mV. The reversal potential (Erev) of this current was 0 mV, which corresponds to the equilibrium potential of chloride with the experimental solutions used and is therefore indicative of a chloride selective current (**Supplementary Figure S1**). All of the above-mentioned characteristics represent the biophysical fingerprints of IClswell (Furst et al., 2002a). Pre-incubation of HEK 293 Phoenix cells for 1 h with 20 mM D-glucose, 5 mM glucosamine, or 100 μM PUGNAc failed to increase *O*-GlcNAcylation of cellular proteins (**Figures 1A–C**) and did not modify the endogenous IClswell current (**Supplementary Figures S1–S3** and **Table 1**). Pre-incubating cells with 100 μM PUGNAc plus 5 mM glucosamine, which was effective in increasing *O*-GlcNAcylation levels in these cells (**Figure 1D**), also did not significantly modify the endogenous IClswell current (**Supplementary Figure S4** and **Table 1**). In contrast, in cells transfected with OGT, which was twice as effective as 100 μM PUGNAc plus 5 mM glucosamine in increasing *O*-GlcNAcylation levels, IClswell magnitude was significantly reduced and the activation in time was delayed in comparison to control conditions (**Figure 2** and **Table 1**). In cells transfected with OGA-L, IClswell showed a tendency to an increase, which, however, was not statistically significant (**Supplementary Figure S5**).

Increased *O*-GlcNAcylation of Cellular Proteins Inhibits the ICln-Induced IClswell Current

Overexpression of the heterologous protein ICln up-regulates IClswell in several cell types (Paulmichl et al., 1992; Hubert et al., 2000; Furst et al., 2002b; Dossena et al., 2011; Schedlbauer et al., 2019) (**Supplementary Figure S6**). In these cells, the apparent IClswell is the sum of the endogenous IClswell and the ICln-induced IClswell. Similarly to what was observed for the endogenous IClswell current, pre-incubation of cells with 20 mM D-glucose, 5 mM glucosamine, or 100 μM PUGNAc failed to modify IClswell in ICln-transfected cells (**Supplementary Figures S7–S9** and **Table 1**). In contrast, treatment with 100 μM PUGNAc plus 5 mM glucosamine, as well as OGT overexpression, significantly inhibited IClswell (**Figures 3, 4** and **Table 1**). As 5 mM glucosamine plus 100 μM PUGNAc had no effect on the endogenous current, the 55% inhibition of IClswell that was observed in ICln-transfected cells (**Table 1**) must have arisen from inhibition of the ICln-induced current. Similarly, the OGT-induced IClswell inhibition in ICln-transfected cells (58%) most likely represents the sum of inhibition of (i) the endogenous IClswell (38%, **Table 1**) and (ii) the ICln-induced current. Conversely, IClswell was significantly up-regulated by OGA-L in ICln-transfected cells (**Figure 5** and **Table 1**).

Increased *O*-GlcNAcylation of Cellular Proteins Prevents RVD

To assess the effects of an increased *O*-GlcNAcylation on RVD, HEK 293 Phoenix cells were treated with 100 μM PUGNAc plus 5 mM glucosamine or 0.1% DMSO plus 5 mM glucose as control. The cell size was monitored before and during an osmotic stress, and cell volume changes were expressed as V/V_0. As expected, the hypotonic shock promptly induced cell swelling followed by RVD activation in control cells, which regained their original volume. In contrast, in cells treated with 100 μM PUGNAc and 5 mM glucosamine, cell swelling was more prominent and, importantly, was not followed by an RVD phase (**Figure 6**).

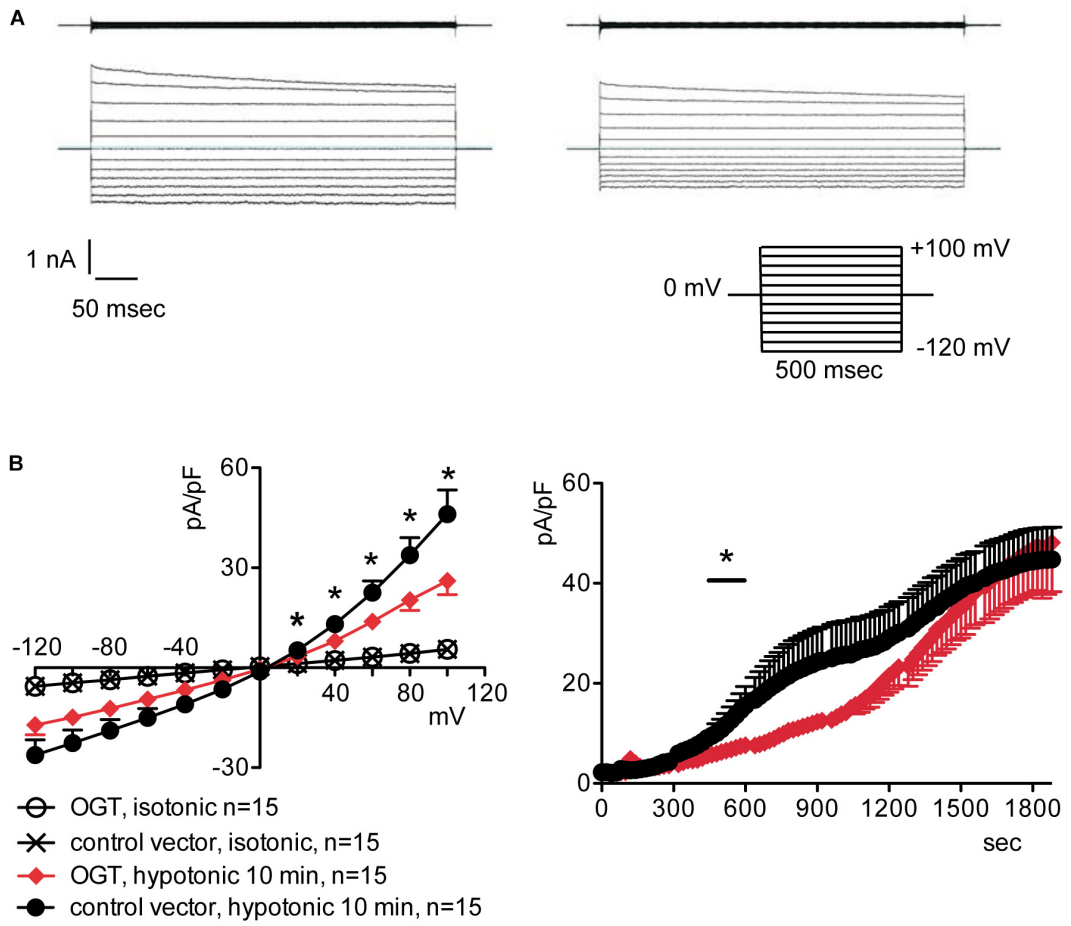

FIGURE 2 | *O*-GlcNAc elevation obtained by OGT overexpression blunts IClswell in native cells. IClswell activation was monitored in HEK 293 Phoenix cells transfected for 24 h with OGT and the transfection marker EGFP as separate proteins or a control vector. Single transfected cells were selected and voltage clamped using the whole-cell patch-clamp technique. **(A)** Original recordings obtained in isotonic (upper panels) and hypotonic (lower panels) extracellular solutions in control (left panels) or OGT-transfected (right panels) cells stimulated with voltage increments of 20 mV from −120 to +100 mV applied from a holding potential of 0 mV (lower right inset). **(B)** Current density-to-voltage relationship determined after a 10-min exposure to the extracellular hypotonic solution (left) and current density-to-time relationship (right) of IClswell in OGT-transfected and control cells. $^*p < 0.05$, unpaired Student's *t*-test. (*n*) refers to the number of cells. OGT, *O*-GlcNAc-transferase; EGFP, enhanced green fluorescent protein.

The C-Terminus of ICln Is *O*-GlcNAc Modified

Mass spectrometry was used to identify the ICln amino acids that are *O*-GlcNAcylated. After overexpressing ICln in HEK 293 Phoenix cells and treating the cells with 100 μM PUGNAc and 5 mM glucosamine, we successfully identified the ICln protein from immunoprecipitated samples with up to 90% sequence coverage. Out of the 32 individual peptides found, we detected *O*-GlcNAc modification on peptide 187–205. **Figure 7A** reports the analysis of the charge state 3+ of this peptide. The *O*-GlcNAc-modified peptide has a mass/charge (*m*/*z*) value of 754.014 while its unmodified counterpart has an *m*/*z* value of 696.3258. **Supplementary Figure S10** demonstrates the analysis of the same peptide with a charge state of 2+. Unfortunately, no b- or y-ions that carried the *O*-GlcNAc modification could be found; therefore, the exact *O*-GlcNAc site could not be discerned (there are four Ser representing potential *O*-GlcNAcylation sites on this peptide, **Figure 7B**). However, it is worth noting that both analyses found peaks that corresponded to the *m*/*z* value of GlcNAc residues and probably resulted from a loss of GlcNAc from the parent ion. In addition, we detected phosphorylation at Ser223 on peptide 206–236 (**Figure 7B**).

O-GlcNAcylation of the C-Terminus of ICln Is Not Involved in Modulating IClswell

Based on the MS results, two mutations were designed in order to prevent ICln *O*-GlcNAcylation, i.e., Ser193* (nucleotides coding for Ser193 were substituted by a STOP codon) and Thr223Ala (**Figure 7B**). The first mutation leads to an early termination of translation with consequent protein truncation. The mutant protein lacks all *O*-GlcNAcylation sites, including Ser193. Thr223 is a phosphorylated amino acid with high likelihood of *O*-Glycosylation (**Supplementary Figures S11, S12**)

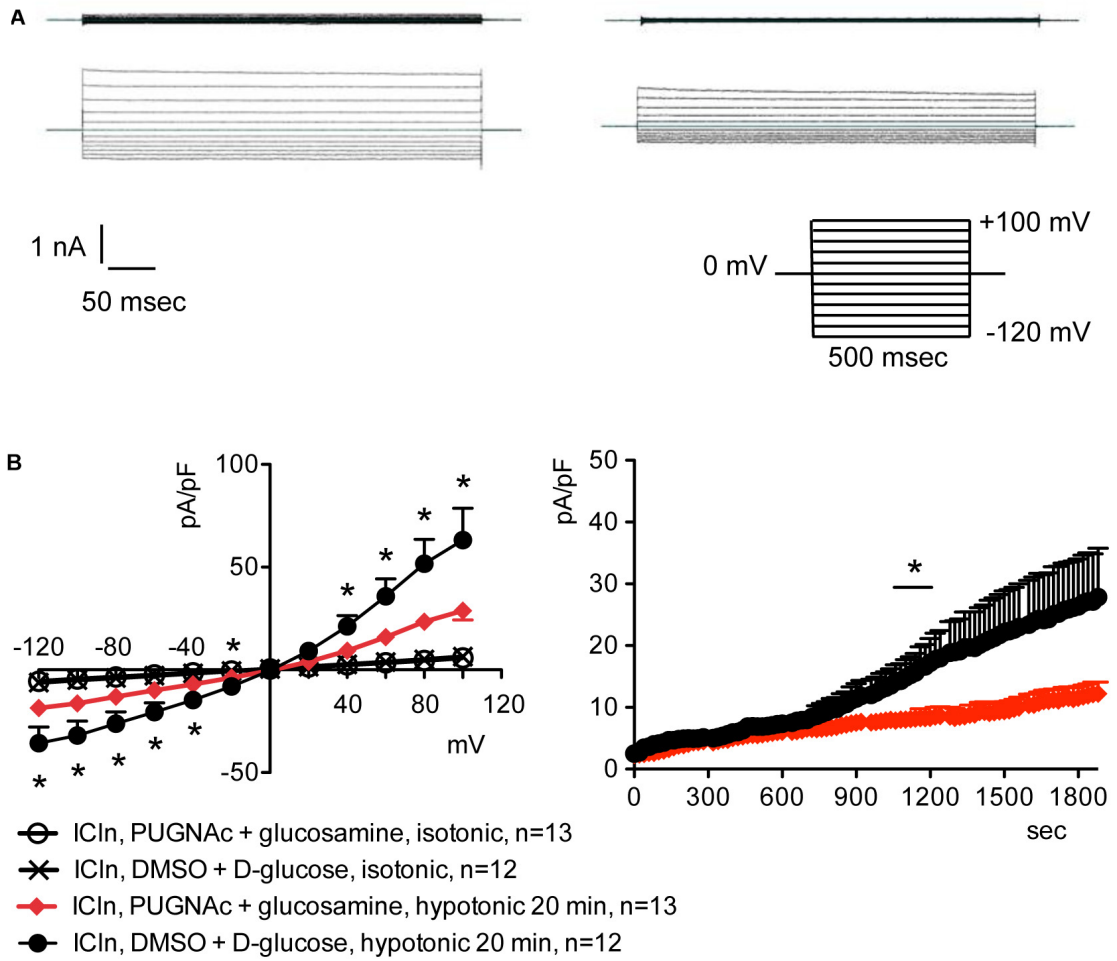

FIGURE 3 | *O*-GlcNAc elevation obtained by pre-incubation of cells with PUGNAc and glucosamine blunts IClswell in ICln-transfected cells. IClswell activation was monitored in HEK 293 Phoenix cells transfected for 24 h with ICln as well as the transfection marker EGFP as separate proteins. Single transfected cells were selected and voltage clamped using the whole-cell patch-clamp technique. **(A)** Original recordings obtained in isotonic (upper panels) and hypotonic (lower panels) extracellular solutions in cells pre-incubated for 1 h with 0.1% DMSO plus 5 mM D-glucose (left panels) or 100 μM PUGNAc plus 5 mM glucosamine (right panels) and stimulated with voltage increments of 20 mV from –120 to +100 mV applied from a holding potential of 0 mV (lower right inset). **(B)** Current density-to-voltage relationship determined after a 20-min exposure to the extracellular hypotonic solution (left) and current density-to-time relationship (right) of IClswell in cells pre-incubated with 100 μM PUGNAc plus 5 mM glucosamine or the vehicle. *$p < 0.05$, unpaired Student's *t*-test. (*n*) refers to the number of cells. EGFP, enhanced green fluorescent protein.

and therefore a potential YinOYang site. The second mutation converts this amino acid in the non-modifiable Ala. First, the expression of the ICln mutants and their ability of up-regulating IClswell were verified. Subsequently, the effect of an increased *O*-GlcNAcylation of cellular proteins was probed on the mutant ICln-induced current.

ICln expression in cells transfected with ICln Thr223Ala and Ser193* was doubled compared to the expression of the endogenous ICln in untransfected cells and was indistinguishable from that of cells transfected with wild-type ICln (**Figure 8A**). ICln Thr223Ala was fully functional, i.e., able of up-regulating IClswell to the level of ICln wild type (**Figure 8B**). In contrast, ICln Ser193* lost most of its activity, and only a small residual current, which was above the level of the endogenous IClswell, could be measured in transfected cells (**Figure 8C**).

Similarly to what was observed for the wild-type ICln-induced current, the ICln Thr223Ala-induced IClswell, as well as the residual ICln Ser193*-induced current, were inhibited by increases in the *O*-GlcNAcylation of cellular proteins induced by incubation of cells with PUGNAc and glucosamine (**Figure 9**). As pre-incubation of cells with PUGNAc plus glucosamine had no effect on the endogenous IClswell (**Supplementary Figure S4**), the inhibitory effect observed in cells transfected with ICln Thr223Ala or ICln Ser193* must arise from inhibition of the mutant ICln-induced current. These data clearly show that *O*-GlcNAcylation of ICln on Ser193 or Thr223 is not involved in suppressing IClswell and strongly suggest that the *O*-GlcNAcylation site involved in controlling the ICln-induced current is located upstream of Ser193.

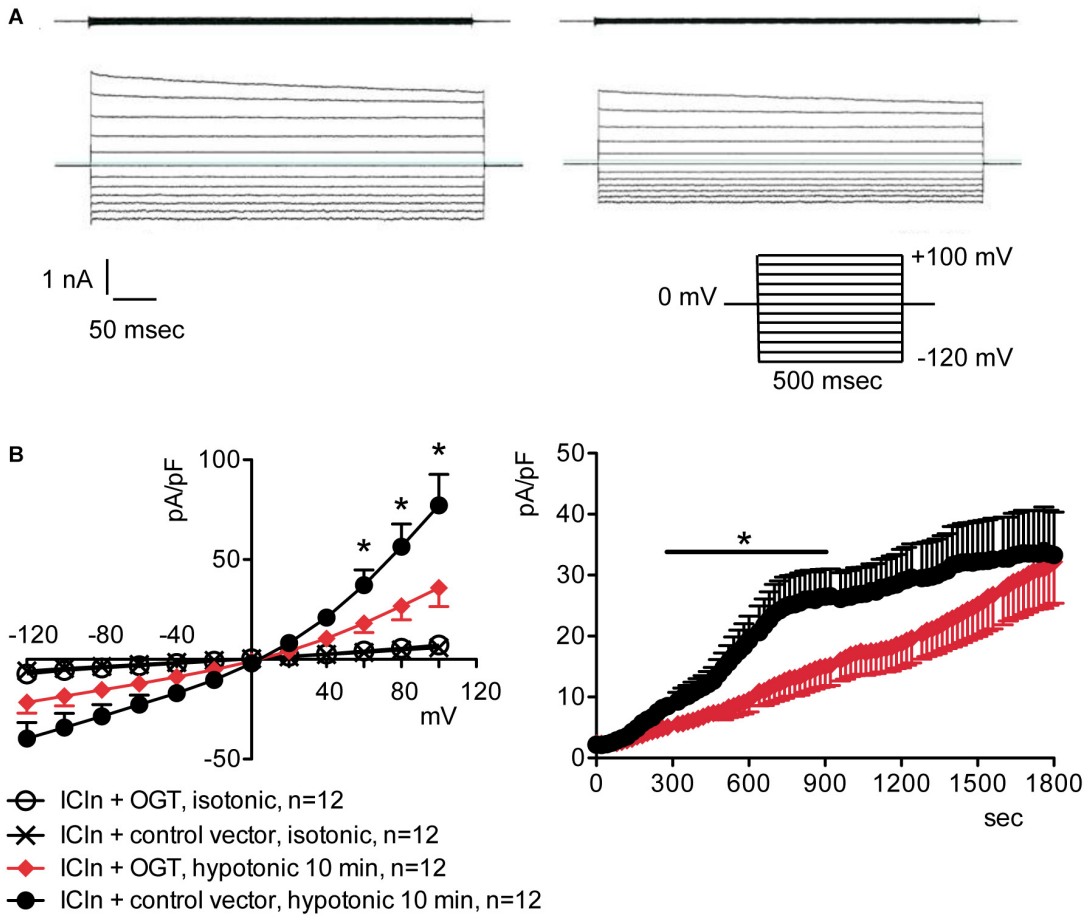

FIGURE 4 | *O*-GlcNAc elevation obtained by OGT overexpression blunts IClswell in ICln-transfected cells. IClswell activation was monitored in HEK 293 Phoenix cells transfected for 24 h with ICln and OGT or ICln and a control vector. Transfection markers were dsRed for ICln and EGFP for OGT. Single cells expressing both transfection markers were selected and voltage clamped using the whole-cell patch-clamp technique. **(A)** Original recordings obtained in isotonic (upper panels) and hypotonic (lower panels) extracellular solutions in control (left panels) or OGT-transfected (right panels) cells stimulated with voltage increments of 20 mV from –120 to +100 mV applied from a holding potential of 0 mV (lower right inset). **(B)** Current density-to-voltage relationship determined after a 10-min exposure to the extracellular hypotonic solution (left) and current density-to-time relationship (right) of IClswell in OGT-transfected and control cells. $^*p < 0.05$, unpaired Student's *t*-test. (*n*) refers to the number of cells. OGT, *O*-GlcNAc-transferase; EGFP, enhanced green fluorescent protein.

Ser67 Confers to ICln Sensitivity to *O*-GlcNAcylation

Upstream of ICln Ser193, there is a predicted YinOYang site at Ser67 (**Supplementary Figure S11**). This latter site is of particular interest as it lies in close proximity to the (61)ISLHA(65) motif, which is crucially involved in ICln binding to the intracellular domain of α-integrin and controls ICln function (Schedlbauer et al., 2019). Therefore, we decided to determine whether this site is involved in modulating ICln function following variation of *O*-GlcNAc levels. ICln Ser67Ala is fully functional, i.e., capable of up-regulating IClswell to an extent indistinguishable from that of wild-type ICln (**Figure 8D**). However, the current induced by this ICln mutant is insensitive to increases or decreases in the *O*-GlcNAcylation of cellular proteins (**Figure 10**). In particular, OGT overexpression induced a non-significant decrease (38%) in IClswell (**Figure 10B** and **Table 1**), which reflected the inhibition of the endogenous current (**Figure 2** and **Table 1**). These experiments strongly suggest that *O*-GlcNAcylation of ICln at Ser67 inhibits IClswell.

ICln Interacts With OGT

Conjugation of *O*-GlcNAc to a protein requires a direct molecular interaction with OGT. To study this phenomenon, FRET between OGT and ICln was measured. This technique requires the transfection of the proteins of interest fused to fluorophores serving as the FRET donor and acceptor. In this study, ECFP and EYFP were used as the FRET donor and acceptor, respectively. EYFP fusion to the N-terminus of OGT did not affect its catalytic activity (**Figure 11A**) and was therefore used in experiments. EYFP-OGT gave a significant FRET with ICln-ECFP, which was reduced following mutation of Ser67. In contrast, FRET between EYFP-OGA and ICln did not exceed the stochastic FRET of the negative control. These results indicate that, in unstimulated cells, ICln preferentially interacts with OGT rather than OGA,

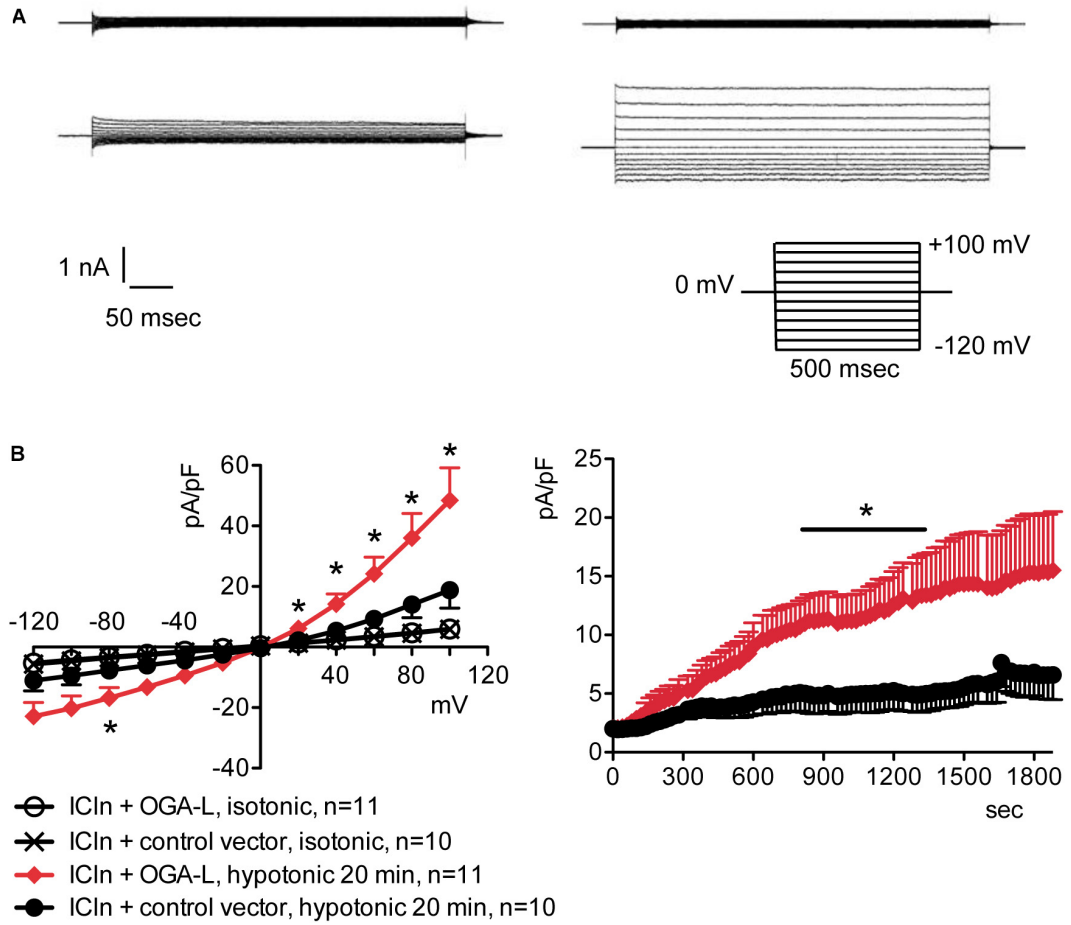

FIGURE 5 | *O*-GlcNAc reduction obtained by OGA-L overexpression upregulates IClswell in ICln-transfected cells. IClswell activation was monitored in HEK 293 Phoenix cells transfected for 24 h with ICln and OGA-L or ICln and a control vector. Transfection markers were dsRed for ICln and EGFP for OGA-L. Single cells expressing both transfection markers were selected and voltage clamped using the whole-cell patch-clamp technique. **(A)** Original recordings obtained in isotonic (upper panels) and hypotonic (lower panels) extracellular solutions in control (left panels) or OGA-L-transfected (right panels) cells stimulated with voltage increments of 20 mV from −120 to +100 mV applied from a holding potential of 0 mV (lower right inset). **(B)** Current density-to-voltage relationship determined after a 20-min exposure to the extracellular hypotonic solution (left) and current density-to-time relationship (right) of IClswell in OGA-L-transfected and control cells. $^*p < 0.05$, unpaired Student's *t*-test. (*n*) refers to the number of cells. EGFP, enhanced green fluorescent protein; OGA, *O*-GlcNAcase.

thus suggesting that ICln is constitutively *O*-GlcNAcylated. The ICln–OGT interaction is destabilized by mutation of Ser67, which may therefore represent the ICln *O*-GlcNAcylation site. The relatively small signal-to-noise ration of ICln–OGT FRET indicates that the interaction between the two proteins is dynamic and transient, which is consistent with the characteristics of a reversible interaction between an enzyme and its target.

O-GlcNAcylation of ICln at Ser67 Prevents Its Interaction With α-Integrin

ICln establishes a direct molecular interaction with the intracellular domain of α-integrin (Larkin et al., 2004, 2009; Daxecker et al., 2008) (**Figure 12**), and perturbation of this interaction affects IClswell activation (Schedlbauer et al., 2019). Surprisingly, the interaction between the non-glycosylatable/non-phosphorylatable ICln Ser67Ala and αIIb integrin measured by FRET was stronger than the interaction between wild-type ICln and αIIb integrin (**Figure 12B**). This finding suggests that post-translational modification of Ser67 weakens the binding of ICln to α-integrin. To further substantiate this hypothesis, the interaction between wild type and Ser67Ala ICln was measured following increases or decreases in the *O*-GlcNAcylation of cellular proteins obtained by incubation of cells with PUGNAc and glucosamine or transfection with OGA-L, respectively. In line with the hypothesis, elevation of *O*-GlcNAcylation reduced the FRET between wild-type ICln and α-integrin but, importantly, did not affect the FRET between Ser67Ala ICln and α-integrin (**Figure 12C**). This confirms that *O*-GlcNAcylation of Ser67 reduces the ICln/integrin interaction and further suggests that a fraction of the ICln protein pool is constitutively *O*-GlcNAcylated. In line with these hypotheses, reduction of *O*-GlcNAcylation increased the FRET between wild-type ICln and α-integrin. Again, Ser67Ala ICln was unresponsive to *O*-GlcNAcylation changes (**Figure 12D**).

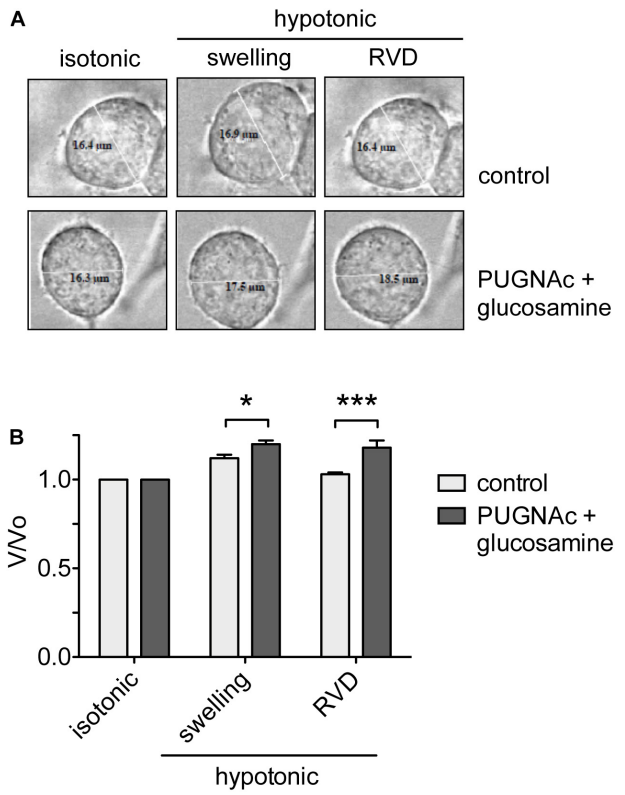

FIGURE 6 | *O*-GlcNAc elevation affects RVD. **(A)** HEK 293 Phoenix cells were incubated for 1 h with 100 μM PUGNAc plus 5 mM glucosamine (n = 4) or 0.1% DMSO plus 5 mM glucose as the control (n = 5), initially kept in extracellular isotonic solution and then submitted to hypotonic stress. **(B)** V/V_0 values determined in extracellular isotonic solution and 30 s (swelling) and 160 s (RVD) after exposure to the hypotonic solution. (n) refers to the number of cells. Data are representative of two independent experiments leading to similar results. $^*p < 0.05$, $^{***}p < 0.001$, two-way ANOVA with Bonferroni's post-test. RVD, regulatory volume decrease.

Hypotonicity Reduces *O*-GlcNAcylation of Cellular Proteins

To assess the dynamic nature of protein *O*-GlcNAc modification upon direct changes during cell volume regulation, we exposed HeLa cells to 200 mOsmol hypotonic challenge. As shown in **Figure 13**, hypotonicity significantly reduced the fluorescence intensity corresponding to *O*-GlcNAc levels. Interestingly, this effect was also detected when *O*-GlcNAc levels were previously elevated by PUGNAc and glucosamine treatment.

DISCUSSION

Since the discovery of *O*-GlcNAc modification, more than ∼4,000 protein targets have been identified (Ma and Hart, 2014). A large number of *O*-GlcNAcylated proteins are involved in the regulation of many cellular events, including intracellular signaling, gene transcription, cellular metabolism, and stress responses (Butkinaree et al., 2010; Hart, 2014); therefore, it is not surprising that improper *O*-GlcNAcylation contributes to the development of disease (Hart et al., 2011). Indeed, *O*-GlcNAcylation is associated with an increasing number of pathological states, such as type II diabetes mellitus, diabetic complications (Vaidyanathan and Wells, 2014; Peterson and Hart, 2016), insulin resistance (Wells et al., 2003a), cancer (Stowell et al., 2015), and neurodegeneration (Lagerlof and Hart, 2014; Banerjee et al., 2016; Hart, 2019). Therefore, uncovering the involvement of *O*-GlcNAcylation in a given pathological process and the identification of the respective protein targets could open the way to novel therapeutic strategies.

The alteration of RVD by increases in the *O*-GlcNAcylation of cellular proteins was first reported in Jurkat cells, an immortalized line of human T lymphocytes (Nagy et al., 2010). In this study, exposure of cells for 1 h to 30 mM D-glucose or 5 mM glucosamine was sufficient to significantly alter the levels of *O*-GlcNAcylated proteins as well as the osmotic response of cells to hypotonicity, leading to an increased swelling and delayed RVD. In HEK 293 Phoenix cells, significant increases in *O*-GlcNAc levels required incubation with 100 μM PUGNAc plus 5 mM glucosamine for 1 h (**Figure 1D**). In agreement with the above-mentioned study, these cells swelled more than control cells when stimulated by hypotonicity, and their RVD was abrogated (**Figure 6**). These data show that alteration of osmotic resistance by increases in the *O*-GlcNAcylation of cellular proteins is not a feature restricted to Jurkat cells and consists of two components, i.e., increased swelling and inefficient or absent RVD. Jurkat cells seem more sensitive to *O*-GlcNAc precursors than HEK 293 Phoenix cells. This may be linked to differential expression of glucose transporters and/or metabolic enzymes and particularly to the very high expression of the sodium-glucose co-transporter SGLT2 and the glucose transporter GLUT1 in Jurkat cells (Kaji et al., 2018), which may drive efficient glucose intake in these cells.

Inefficient RVD following increases in the *O*-GlcNAcylation of cellular proteins was linked to reduced intracellular water diffusion (Nagy et al., 2010). During RVD, K^+, Cl^-, and other intracellular osmolytes are lost, generating an osmotic water efflux that permits cells to reduce their volume (Friedrich et al., 2006). As water follows ions, one may speculate that reduced intracellular water diffusion may arise from impaired ion fluxes. Accordingly, pharmacological inhibition of swelling-activated ion channels leads to increased cell swelling after hypotonic stress and prevents RVD (Furst et al., 2002a), thus mimicking the effect of an increased *O*-GlcNAcylation. Therefore, we hypothesized that *O*-GlcNAcylation may alter RVD by inhibiting ion transport. The finding that the protein ICln, essential in the activation of the swelling-activated Cl^- current IClswell, is *O*-GlcNAc-modified (Hahne et al., 2013) further corroborated this hypothesis. As expected, incubation of cells for 1 h with 100 μM PUGNAc plus 5 mM glucosamine significantly inhibited the ICln-induced IClswell (**Figure 3**), with no effect on the endogenous IClswell (**Supplementary Figure S4**). Further increase in *O*-GlcNAcylation obtained by OGT overexpression inhibited both the ICln-induced current and the endogenous IClswell current (**Figures 2**, **4**). These findings suggest that the majority of endogenous ICln is *O*-GlcNAcylated in basal conditions and consequently unresponsive to relatively mild

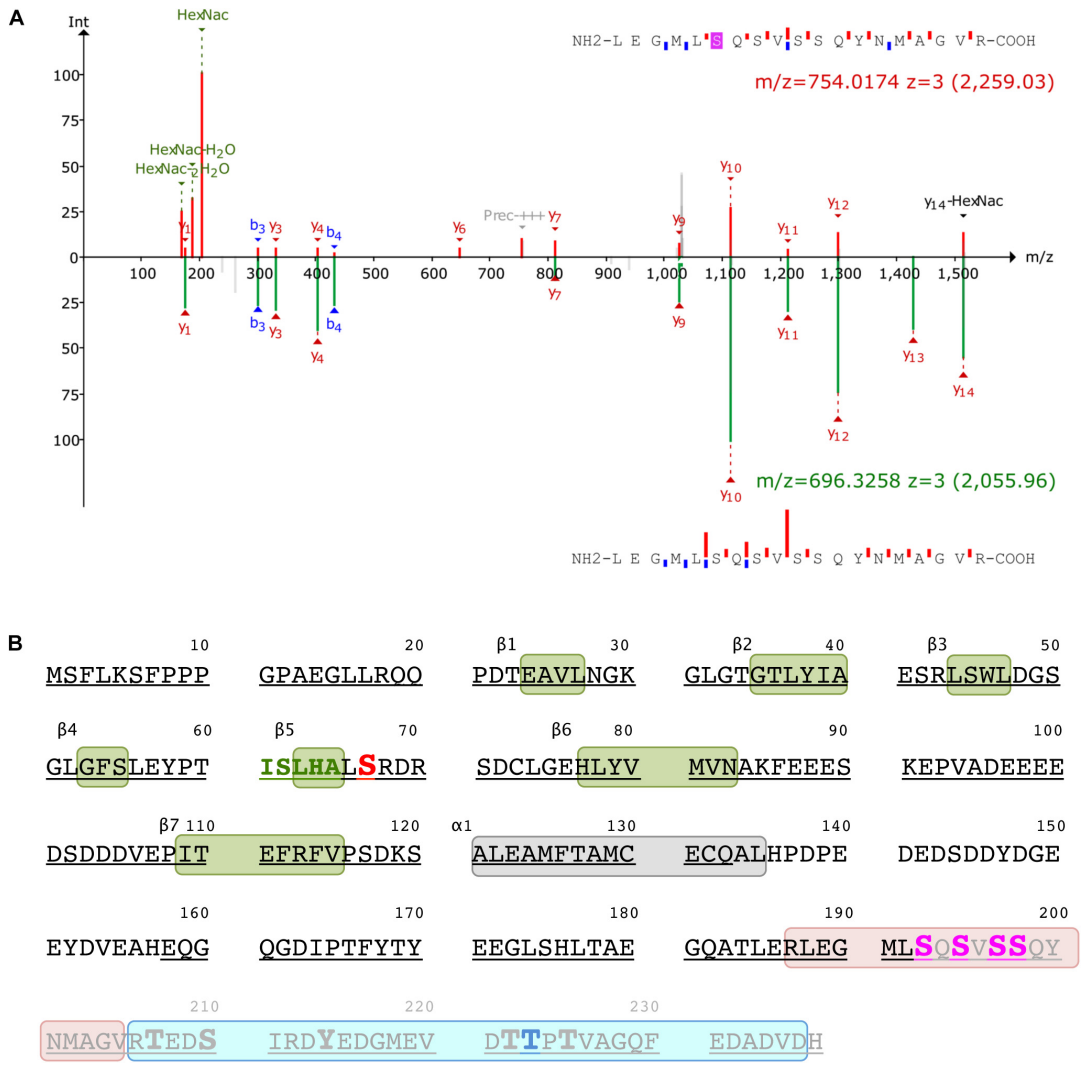

FIGURE 7 | Post-translational modification of ICln. **(A)** Identification of the *O*-GlcNAc site on ICln by LC-MS/MS. Product-ion spectra peptide 187–205 is displayed. Fragmentation products of the *O*-GlcNAc-modified peptide is shown at the top (red) while the unmodified peptide fragments are shown on at the bottom (green) with their corresponding monoisotopic mass *m/z* and charge-state (3+). The b- and y-ions are indicated with blue and red, respectively. **(B)** Amino acid sequence of human ICln (NP_001284). Green and gray boxes represent β sheets and α helix secondary structure motifs of the pleckstrin-homology-like domain, respectively. The predicted YinOYang site is in red and the amino acid sequence involved in the interaction with α-integrin is in green. Potential *O*-GlcNAcylation residues within the *O*-GlcNAcylated fragment (187–205, highlighted in rose) are indicated in magenta, and the residue with the highest likelihood of phosphorylation (Thr223) within the phosphorylated fragment (206–236, highlighted in cyan) is indicated in blue. Possible additional phosphorylation sites within this latter fragment are represented as enlarged letters. The amino acids covered by MS are underlined and the fragment missing in the ICln mutant Ser193* is grayed out. MS, mass spectrometry.

increases in *O*-GlcNAcylation, while heterologous ICln is largely unmodified. Experimental conditions that did not significantly increase the *O*-GlcNAcylation levels of cellular proteins as assessed by western blot (**Figures 1A–C**) failed to suppress the ICln-induced current (**Supplementary Figures S7–S9**) as well as the endogenous IClswell current (**Supplementary Figures S1–S3**).

The identification of the *O*-GlcNAcylated proteins and *O*-GlcNAcylated residues of a protein can be challenging. *O*-GlcNAc modifications have low stoichiometry and generally low abundance, and the extremely labile nature of *O*-GlcNAc makes the determination of modification sites by conventional tandem MS (MS/MS) difficult (Wang et al., 2014). Anti-*O*-GlcNAc antibodies did not recognize ICln immunoprecipitated from HEK 293 Phoenix cells, even following elevation of *O*-GlcNAc levels (data not shown). Therefore, computational methods remain an extremely useful tool in the identification of potential *O*-GlcNAcylation sites (Jia and Zuo, 2018). While MS evidenced that ICln is *O*-GlcNAc modified on its C-terminus, this is unlikely involved in the suppression of the ICln-induced current, as mutation or deletion of the C-terminus did not abrogate responsiveness of the ICln-induced current to *O*-GlcNAc elevation (**Figure 9**). Therefore, we assume that the ICln *O*-GlcNAcylated site

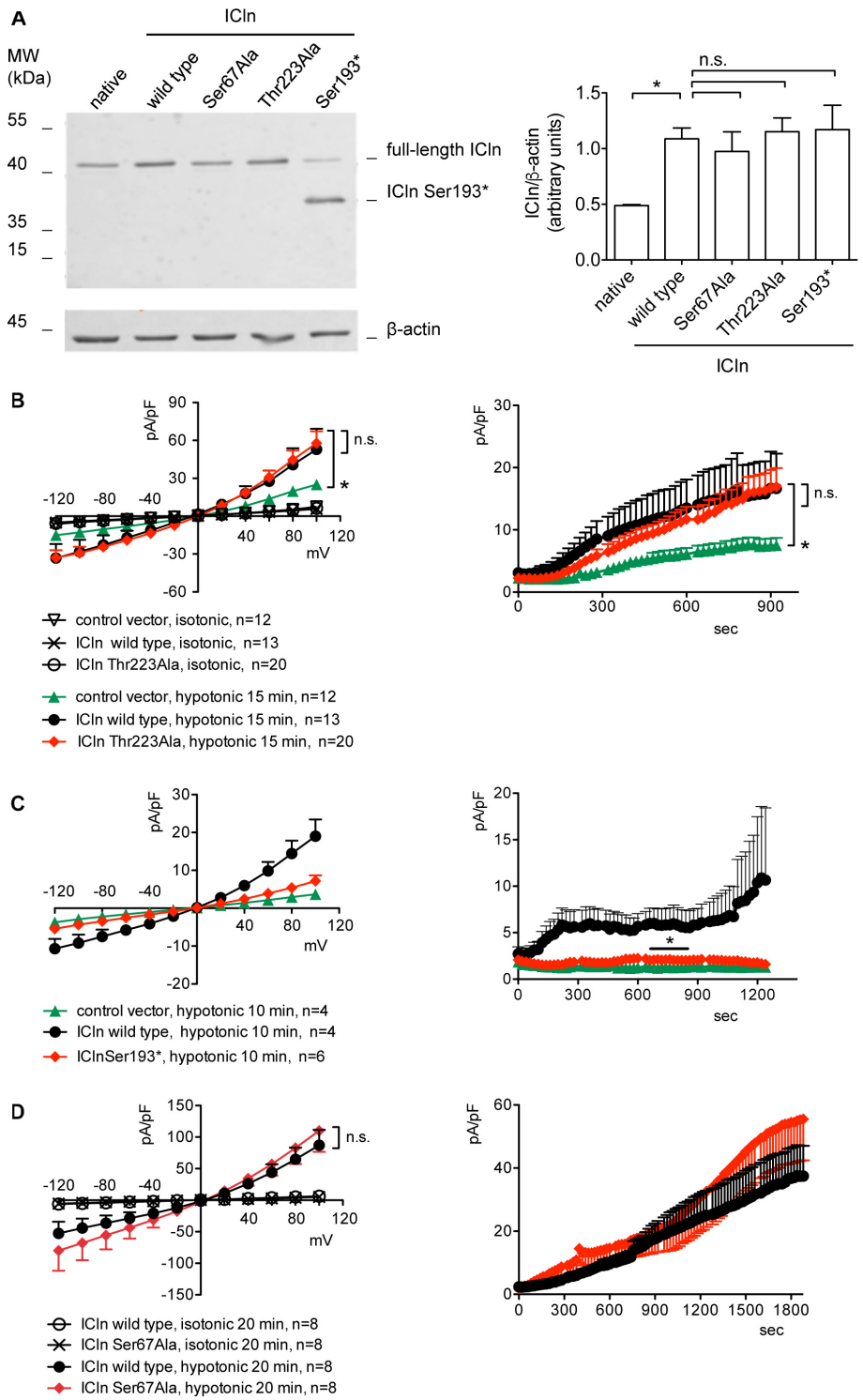

FIGURE 8 | Expression and function of ICln mutants. **(A)** HEK 293 Phoenix cells were transfected for 24 h with the indicated ICln mutants, wild-type ICln, or left untransfected. The expression levels of ICln determined via western blot (left panel) were quantified by densitometry and normalized to the housekeeping protein β-actin (right panel). $n = 3$ independent samples, $^*p < 0.05$, one-way ANOVA with Dunnett's post-test. **(B–D)** IClswell activation was monitored in HEK 293 Phoenix cells transfected for 24 h with wild-type or mutant ICln or a control vector, as indicated. Single transfected cells were selected based on the fluorescence of the transfection marker EGFP and voltage clamped using the whole-cell patch-clamp technique. The current density-to-voltage relationship (left panels) and the current density-to-time relationship (right panels) determined after exposure to the extracellular hypotonic solution are shown. $^*p < 0.05$, unpaired Student's *t*-test. n.s., not significant. (*n*) refers to the number of cells. EGFP, enhanced green fluorescent protein.

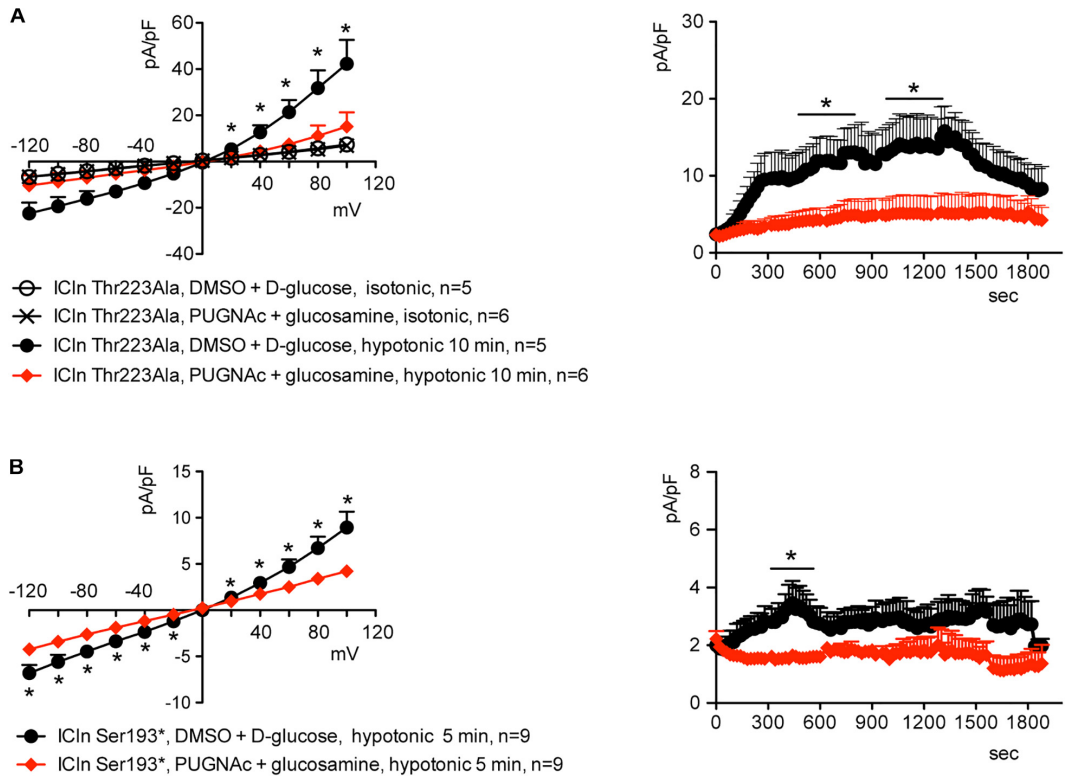

FIGURE 9 | *O*-GlcNAc elevation inhibits IClswell in cells transfected with non-*O*-glycosylatable forms of ICln. IClswell activation was monitored in HEK 293 Phoenix cells transfected for 24 h with **(A)** ICln Thr223Ala or **(B)** ICln Ser193* as well as the transfection marker EGFP as separate proteins and pre-incubated for 1 h with 100 μM PUGNAc plus 5 mM glucosamine or 0.1% DMSO plus 5 mM D-glucose as the control. Single transfected cells were selected and voltage clamped using the whole-cell patch-clamp technique. The current density-to-voltage relationships determined in an extracellular hypotonic solution (left) and the current density-to-time relationships (right) of IClswell in cells pre-incubated with 100 μM PUGNAc plus 5 mM glucosamine or the vehicle are shown. *$p < 0.05$, unpaired Student's *t*-test. (*n*) refers to the number of cells. EGFP, enhanced green fluorescent protein.

involved in the inhibition of the ICln-induced current could not be detected by MS as the *O*-GlcNAc moiety was most likely lost during sample preparation. In line with this hypothesis, mutation of the predicted YinOYang site on Ser67 conferred resistance of the ICln-induced current to *O*-GlcNAc increases or decreases (**Figure 10**), strongly suggesting that ICln is *O*-GlcNAc modified at Ser67. The non-significant 38% decrease in the ICln Ser67Ala-induced current observed in cells transfected with OGT most likely reflected the effect of *O*-GlcNAc elevation on the endogenous ICln (**Figure 10B** and **Table 1**).

The identification of a direct molecular interaction between ICln and OGT confirmed that ICln is *O*-GlcNAc modified. Mutation of Ser67 destabilized the interaction, suggesting that this amino acid comes in close contact with OGT (**Figure 11**). Substitution of Ser67 with an Ala should have minimal impact on protein conformation, as the expression levels and activity of ICln Ser67Ala are very similar to that of the wild-type protein (**Figures 8A,D**). Therefore, alterations in interaction with OGT and insensitivity of the ICln Ser67Ala-induced current to *O*-GlcNAc are unlikely linked to a variation in protein folding or stability and most likely reflect an impaired *O*-GlcNAcylation following substitution of Ser67.

Intriguingly, Ser67 lies in close proximity with the amino acid sequence (61)ISLHA(65), which binds the motif KXGFFKR of the intracellular domain of α-integrin as an essential step in IClswell activation (Schedlbauer et al., 2019). This observation prompted us to investigate whether *O*-GlcNAcylation controls the binding of ICln to integrin αIIb. Surprisingly, the FRET efficiency between the non-glycosylatable ICln Ser67Ala and integrin αIIb was approximately thrice that of the wild-type ICln, thus implying a strong interaction (**Figure 12A**). This finding suggests that *O*-GlcNAcylation prevents the interaction between wild-type ICln and α-integrin and further confirms that wild-type ICln is, at least in part, constitutively *O*-GlcNAcylated. While an increase in the *O*-GlcNAcylation of cellular proteins significantly reduced the direct molecular interaction between wild-type ICln and αIIb, it did not affect ICln Ser67Ala (**Figure 12C**). In parallel, a decrease in the *O*-GlcNAcylation of cellular proteins significantly increased the interaction between wild-type ICln and αIIb, but did not affect ICln Ser67Ala (**Figure 12D**). The unresponsiveness of the interaction between ICln Ser67Ala and α-integrin to changes in the *O*-GlcNAcylation levels reflects the insensitivity of the ICln Ser67Ala-induced current to the same conditions (**Figure 10**). Altogether, these results show that increases in the *O*-GlcNAcylation of cellular proteins affect RVD by inhibiting

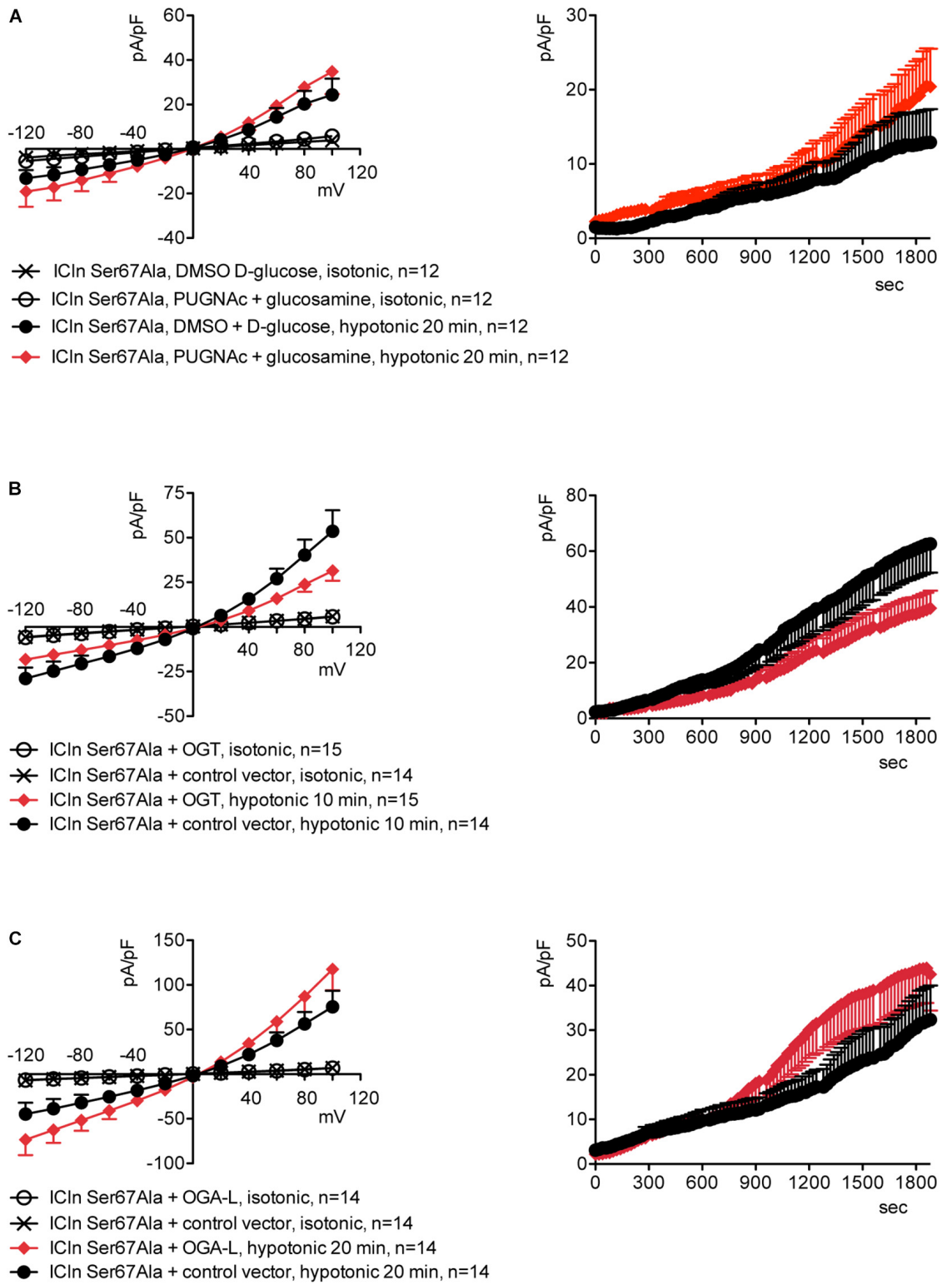

FIGURE 10 | The ICln Ser67Ala-induced ICIswell is unresponsive to variations in *O*-glycosylation of cellular proteins. ICIswell activation was monitored in HEK 293 Phoenix cells transfected for 24 h with ICln Ser67Ala and the transfection marker dsRed as separate proteins and **(A)** pre-incubated for 1 h with 100 μM PUGNAc plus 5 mM glucosamine or 0.1% DMSO plus 5 mM D-glucose as the control or **(B)** co-transfected with OGT or **(C)** OGA-L and the transfection marker EGFP. The current density-to-voltage relationships determined in an extracellular hypotonic solution (left panels) and the current density-to-time relationships (right panels) of ICIswell are shown. (*n*) refers to the number of cells. DMSO, dimethyl sulfoxide; EGFP, enhanced green fluorescent protein. OGT, *O*-GlcNAc transferase; OGA, *O*-GlcNAcase.

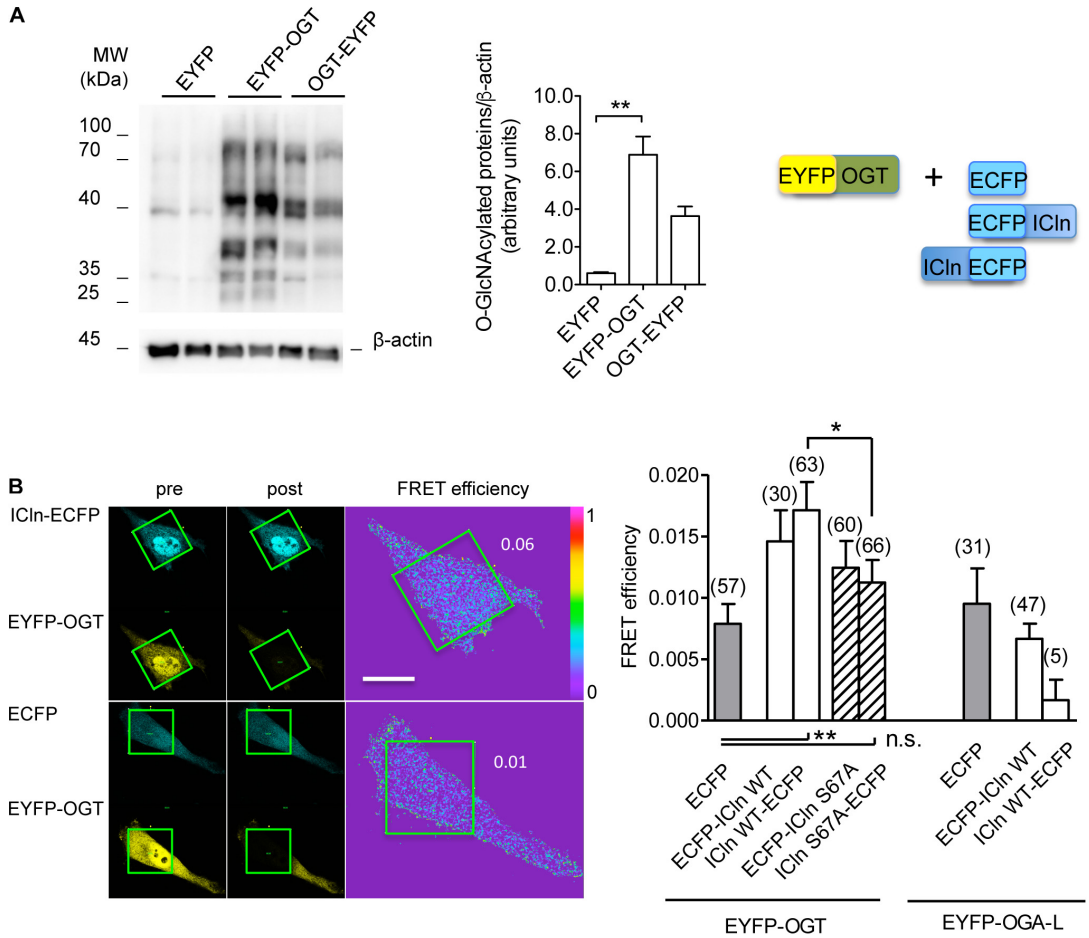

FIGURE 11 | ICln interacts with OGT. HeLa cells were transfected for 48 h with the FRET acceptors EYFP-OGT, OGT-EYFP, or EYFP as a negative control. **(A)** The expression levels of *O*-GlcNAc-modified cellular proteins were determined via western blot (left panel), quantified by densitometry and normalized to the housekeeping protein β-actin (middle panel). $n = 3$ independent samples. The protein pairs selected for FRET experiments are shown (right panel). **(B)** Left panel: single cells transfected with the indicated FRET protein pairs were imaged before (pre) and after (post) photobleaching of the FRET acceptor. Green squares correspond to the bleaching ROI and numbers correspond to the FRET efficiency determined in those ROIs. Scale bar: 10 μm. Right panel: FRET efficiency determined within the bleaching ROIs between the indicated protein pairs. (*n*) refers to the number of cells from four subcultures. $^{**}p < 0.01$, $^{*}p < 0.05$, one-way ANOVA with Dunnett's post-test. n.s., not significant; OGT, *O*-GlcNAc-transferase; FRET, fluorescence resonance energy transfer; EYFP, enhanced yellow fluorescent protein; ROI, region of interest.

IClswell; IClswell inhibition may derive from *O*-GlcNAcylation of the protein ICln, with consequent loss of function due to destabilization of the interaction with α-integrin; Ser67 controls the ICln binding to integrin by conferring responsiveness of this interaction to *O*-GlcNAcylation, thus indicating that this or another amino acid located in close proximity most likely represent an *O*-GlcNAcylation site.

An increase in the extracellular osmolarity resulted in an increase in the *O*-GlcNAcylation levels of cellular proteins in mouse embryonic fibroblasts (Zachara et al., 2004), while exposure of HEK293T cells and primary mouse cortical neurons to a hypotonic medium decreased *O*-GlcNAcylation, as a result of a decline in OGT expression (Kommaddi et al., 2011). Accordingly, we found that exposure of HeLa cells to hypotonicity significantly reduced cellular *O*-GlcNAcylation abundance (**Figure 13**). This event would permit an activation of ICln and, hence, IClswell and RVD, following hypotonic stress. As detailed above, several points of evidence indicate that, in the absence of hypotonic stress, ICln is kept inactive by constitutive *O*-GlcNAcylation. This concept is further supported by the existence of a significant FRET between ICln and OGT in an isotonic environment, while an interaction with OGA could not be detected in the same condition (**Figure 11**). Altogether, our findings indicate that hypotonicity would lead to IClswell activation via reduction of ICln *O*-GlcNAcylation at Ser67, which would permit its direct binding to α-integrin through the neighboring (61)ISLHA(65) motif.

The amino acid sequence (61)ISLHA(65) appears to be crucial in controlling the interaction between ICln and its molecular partners. As multifunctional protein and connector hub, ICln exerts multiple roles within distinct functional modules by interacting with heterogeneous protein targets

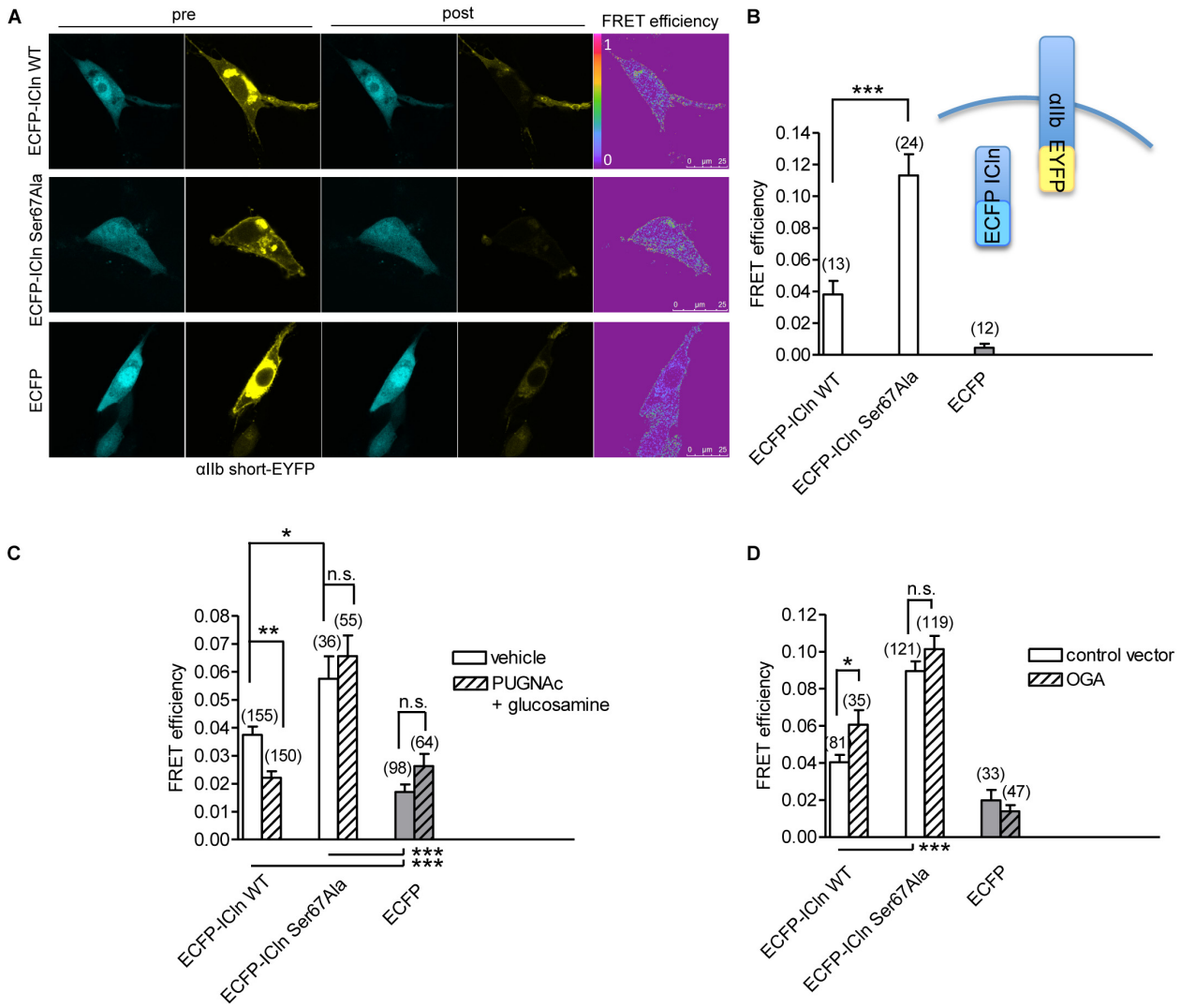

FIGURE 12 | *O*-GlcNAcylation controls the interaction of ICln with α-integrin. **(A)** NIH/3T3 cells were transfected for 48 h with the FRET acceptor αIIbshort-EYFP and ECFP-ICln wild type or Ser67Ala, or with ECFP as a control, and imaged before (pre) and after (post) photobleaching of the FRET acceptor. FRET efficiency was determined in three–four regions of interest (ROIs) of the plasma membrane of each cell. **(B)** The *O*-GlcNAcylation levels were left unmodified or **(C)** increased by incubation of cells with 100 μM PUGNAc plus 5 mM glucosamine for 1 h. The vehicle was 0.1% DMSO plus 5 mM D-glucose. **(D)** The *O*-GlcNAcylation levels were reduced by co-transfection of cells with OGA-L and the transfection marker dsRed as separated proteins. (*n*) refers to the number of ROIs of cells from at least four subcultures. ***$p < 0.001$, **$p < 0.01$, *$p < 0.05$, one-way ANOVA with Dunnett's post-test. FRET, fluorescence resonance energy transfer; EYFP, enhanced yellow fluorescent protein; ECFP, enhanced cyan fluorescent protein; DMSO, dimethyl sulfoxide.

(Furst et al., 2006). In addition to its function in the regulation of cellular volume, ICln acts as an assembly chaperone and Smith antigen (Sm) protein mimic and enables the assembly of the 6S core of the small nuclear ribonucleoproteins (snRNP), which are a key component of the spliceosome (Grimm et al., 2013). Within the ring structure of the 6S complex, ICln establishes a direct molecular interaction with SmD1 and SmG. The ICln–SmD1 interaction interface is centered on the antiparallel β-strand pair represented by the SmD1 β4 and the ICln β5. This interaction involves the formation of five backbone–backbone H-bonds involving the residues (61)ISLHA(65) of ICln. A sixth H-bond is formed between the side-chain hydroxyl group of ICln Ser67 and the backbone carbonyl of SmD1 Gln54. Therefore, it is likely that *O*-GlcNAcylation of Ser67 also affects the interaction between ICln and SmD1.

In line with our findings, other studies have shown that RVD and IClswell magnitude were reduced in mouse models of diabetes mellitus, a condition where *O*-GlcNAc is chronically elevated. For example, in white adipocytes isolated from yellow Kuo Kondo (KKA^y) diabetic mice, RVD rate and IClswell magnitude were lower than those measured in adipocytes of normal C57BL/6 or KK mice, a parental strain of KKA^y mice that do not manifest diabetes until an older age (Inoue et al., 2010).

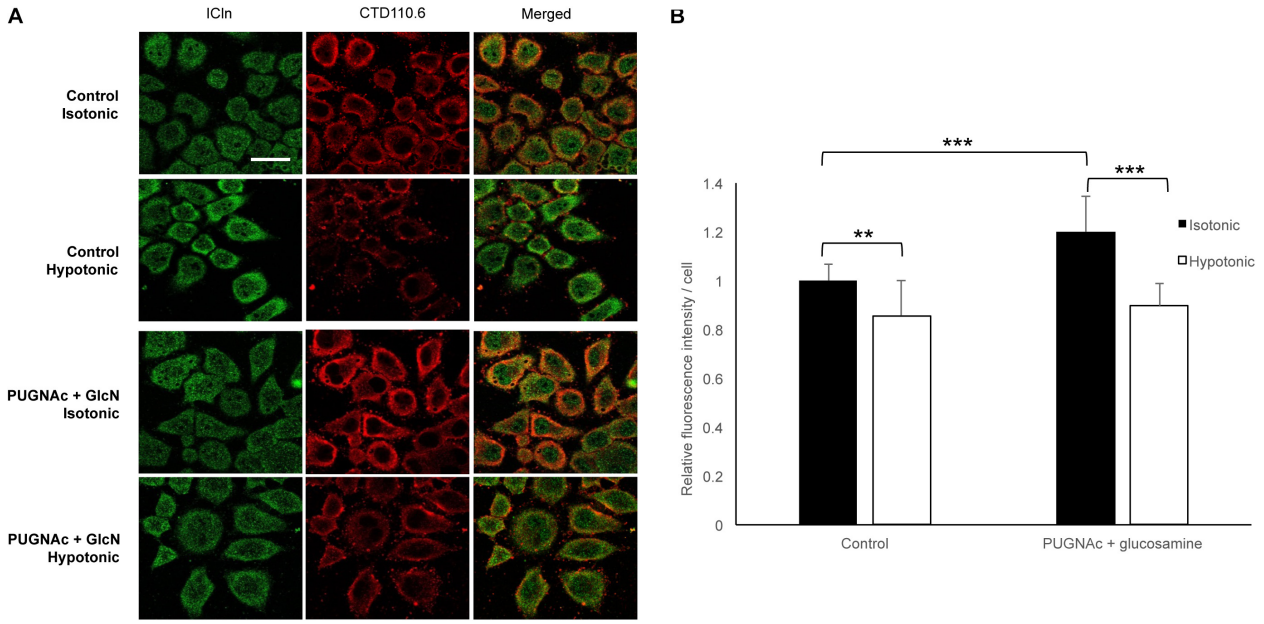

FIGURE 13 | Hypotonicity reduces the cellular *O*-GlcNAcylation levels. Immunofluorescence images of ICln and *O*-GlcNAc proteins in HeLa cells exposed to hypotonic stress. HeLa cells were pre-treated with the vehicle or 100 μM PUGNAc and 5 mM glucosamine (GlcN) and then exposed to normotonic (300 mOsmol) or hypotonic (200 mOsmol) conditions. **(A)** Representative confocal images of cells labeled with anti-ICln (green) and CTD110.6 (anti-*O*-GlcNAc, red) antibodies and corresponding merged images. Scale bar: 20 μM. **(B)** Bar graph shows the average fluorescence intensity of cells normalized to control levels. Each bar represents the average fluorescence of at least 60 cells. Data are shown as means ± SD, $^{**}p < 0.01$, $^{***}p < 0.001$, one-way ANOVA with Dunnett's post-test.

Accordingly, RVD was almost lost and IClswell magnitude was significantly reduced in ventricular myocytes of streptozotocin-induced mice, a well-established model of type 1 diabetes (Yamamoto et al., 2009). Importantly, the RVD rate was heavily reduced also in platelets derived from diabetic patients (Margalit et al., 1995). However, the cellular *O*-GlcNAc levels in these three latter studies were not measured, and the possible link between increased *O*-GlcNAc and impaired RVD was not assessed.

As already mentioned, *O*-GlcNAc modification is involved in the development of insulin resistance and chronic complications of diabetes mellitus (Vaidyanathan and Wells, 2014; Peterson and Hart, 2016), which could in principle be correlated to an impairment of RVD and/or IClswell. Diabetic nephropathy is a clinical syndrome characterized by kidney damage and may result in renal failure (Sun et al., 2013). The cellular and molecular mechanisms leading to diabetic nephropathy are complex and only partially understood. Although the glomerulus has historically been considered as the primary site of diabetic kidney injury, it is becoming increasingly evident that hyperglycemia-induced tubular lesions are prominent components of diabetic nephropathy (Bagby, 2007; Tang and Lai, 2012). The kidney plays the crucial function of controlling the systemic blood pressure and electrolyte balance and is often subjected to osmotic stress during the phenomena of diuresis and anti-diuresis. In addition, in diabetes mellitus, high levels of glucose in the glomerular filtrate lead to an increased reabsorption of glucose and sodium by SGLT2 and SGLT1 in the proximal tubule, along with passive reabsorption of chloride and water (Vallon and Thomson, 2020). It is well known that cells in absorptive epithelia need to efficiently regulate their volume following increases in the intracellular concentration of osmo-active substances, including glucose (van der Wijk et al., 2000). Therefore, although pathological changes like renal fibrosis, mesangial expansion, glomerular hypertrophy, inflammation, and oxidative stress seem to be the main events leading to diabetic nephropathy (Bhattacharjee et al., 2016), we suggest that an impaired or insufficient RVD of kidney tubular cells, which leads to necrotic cell death (Okada et al., 2001, 2019), may contribute to the development of kidney damage in the context of uncontrolled or poorly controlled diabetes mellitus.

Former studies exploring the role of *O*-GlcNAc in diabetic nephropathy mimicked hyperglycemic conditions by exposing various cell types to 20–35 mM D-glucose for 24–48 h (Park et al., 2014; Eleftheriadis et al., 2016, 2020; Gellai et al., 2016). The relatively short incubation time used in the present work (1 h) aimed at disclosing early pathophysiological changes prior overt derangements of cell homeostatic functions occurred. HEK 293 cells, which originate from embryonic kidney, are probably largely undifferentiated but show characteristics of renal epithelial cells and express markers of the proximal tubule, such as SGLT1 (Kaji et al., 2018). HEK 293 cells behavior did not significantly differ from that of HK2 cells—an immortalized proximal tubule epithelial cell line, in an *in vitro* model of diabetic nephropathy (Masola et al., 2011). Other cells used in the present work were chosen as a convenient overexpression system of ectopic proteins. It would be important to confirm the findings

presented here, and especially a GlcNAc-induced alteration in RVD, in better models of kidney tubular cells, such as primary human renal proximal tubular epithelial cells.

ICln interacts with multiple partner proteins to participate in multiple cellular functions (Furst et al., 2006). It is tempting to speculate that phosphorylation of Thr223 and/or *O*-GlcNAc modification of the C-terminus of ICln might control its interactome. Further studies are needed to explore this hypothesis.

In conclusion, an increased *O*-GlcNAcylation of cellular proteins leads to impairment of the homeostatic reaction of RVD by suppressing the swelling-activated chloride current IClswell. IClswell suppression is linked to an inhibition of function of the protein ICln subsequent to *O*-GlcNAcylation at Ser67, which leads to destabilization of its direct interaction with the intracellular domain of α-integrin. These results underscore the essential role of *O*-GlcNAc modification in governing basic cell homeostatic functions by controlling protein–protein interactions, and further suggest that reducing ICln *O*-GlcNAcylation may represent a novel strategy in the prevention or treatment of diseases where an RVD derangement might be involved, including chronic complications of diabetes mellitus such as diabetic nephropathy.

DATA AVAILABILITY STATEMENT

The original contributions presented in the study are included in the article/**Supplementary Material**, further inquiries can be directed to the corresponding author. The mass spectrometry proteomics data from this study were deposited in the ProteomeXchange Consortium via the jPOST (Okuda et al., 2017) partner repository with the dataset identifier PXD022389 and doi: 10.6019/PXD022389.

AUTHOR CONTRIBUTIONS

TN, MP, and SD conceived the study. TN, SD, MP, WP, AS, TJ, AMi, RM, and AMa designed the experiments and interpreted the results. RC, AR, DAC, EB, ZS, TN, and SD performed the experiments and analyzed the data. MP, AMi, AMa, WP, and TJ acquired funding. SD wrote the original draft. WP edited and all authors reviewed and approved the final version of the manuscript.

FUNDING

AR was supported by the Programma Operativo Nazionale (PON) Ricerca e Innovazione, "Dottorati Innovativi con caratterizzazione Industriale" 2014–2020, Fondo Sociale Europeo fellowship. DC was supported by the Harvard/Salzburg-Stipendium 02/00/28060/2013/064 (Stadt Salzburg).

ACKNOWLEDGMENTS

The authors acknowledge the expert secretarial assistance of Elisabeth Mooslechner.

SUPPLEMENTARY MATERIAL

The Supplementary Material for this article can be found online at: https://www.frontiersin.org/articles/10.3389/fcell.2020.607080/full#supplementary-material

REFERENCES

Bagby, S. P. (2007). Diabetic nephropathy and proximal tubule ROS: challenging our glomerulocentricity. *Kidney Int.* 71, 1199–1202. doi: 10.1038/sj.ki.5002286

Banerjee, P. S., Lagerlof, O., and Hart, G. W. (2016). Roles of O-GlcNAc in chronic diseases of aging. *Mol. Aspects Med.* 51, 1–15. doi: 10.1016/j.mam.2016.05.005

Bhattacharjee, N., Barma, S., Konwar, N., Dewanjee, S., and Manna, P. (2016). Mechanistic insight of diabetic nephropathy and its pharmacotherapeutic targets: an update. *Eur. J. Pharmacol.* 791, 8–24. doi: 10.1016/j.ejphar.2016.08.022

Blom, N., Sicheritz-Ponten, T., Gupta, R., Gammeltoft, S., and Brunak, S. (2004). Prediction of post-translational glycosylation and phosphorylation of proteins from the amino acid sequence. *Proteomics* 4, 1633–1649. doi: 10.1002/pmic.200300771

Brownlee, M. (2001). Biochemistry and molecular cell biology of diabetic complications. *Nature* 414, 813–820. doi: 10.1038/414813a

Buse, M. G. (2006). Hexosamines, insulin resistance, and the complications of diabetes: current status. *Am. J. Physiol. Endocrinol. Metab.* 290, E1–E8. doi: 10.1152/ajpendo.00329.2005

Butkinaree, C., Park, K., and Hart, G. W. (2010). O-linked beta-N-acetylglucosamine (O-GlcNAc): extensive crosstalk with phosphorylation to regulate signaling and transcription in response to nutrients and stress. *Biochim. Biophys. Acta* 1800, 96–106. doi: 10.1016/j.bbagen.2009.07.018

Chambers, M. C., Maclean, B., Burke, R., Amodei, D., Ruderman, D. L., Neumann, S., et al. (2012). A cross-platform toolkit for mass spectrometry and proteomics. *Nat. Biotechnol.* 30, 918–920. doi: 10.1038/nbt.2377

Champattanachai, V., Marchase, R. B., and Chatham, J. C. (2008). Glucosamine protects neonatal cardiomyocytes from ischemia-reperfusion injury via increased protein O-GlcNAc and increased mitochondrial Bcl-2. *Am. J. Physiol. Cell Physiol.* 294, C1509–C1520. doi: 10.1152/ajpcell.00456.2007

Copeland, R. J., Bullen, J. W., and Hart, G. W. (2008). Cross-talk between GlcNAcylation and phosphorylation: roles in insulin resistance and glucose toxicity. *Am. J. Physiol. Endocrinol. Metab.* 295, E17–E28. doi: 10.1152/ajpendo.90281.2008

Daxecker, H., Raab, M., Bernard, E., Devocelle, M., Treumann, A., and Moran, N. (2008). A peptide affinity column for the identification of integrin alpha IIb-binding proteins. *Anal. Biochem.* 374, 203–212. doi: 10.1016/j.ab.2007.11.033

Dias, W. B., and Hart, G. W. (2007). O-GlcNAc modification in diabetes and Alzheimer's disease. *Mol. Biosyst.* 3, 766–772. doi: 10.1039/b704905f

DiCiommo, D. P., Duckett, A., Burcescu, I., Bremner, R., and Gallie, B. L. (2004). Retinoblastoma protein purification and transduction of retina and retinoblastoma cells using improved alphavirus vectors. *Invest. Ophthalmol. Vis. Sci.* 45, 3320–3329. doi: 10.1167/iovs.04-0140

Dossena, S., Gandini, R., Tamma, G., Vezzoli, V., Nofziger, C., Tamplenizza, M., et al. (2011). The molecular and functional interaction between ICln and HSPC038 proteins modulates the regulation of cell volume. *J. Biol. Chem.* 286, 40659–40670. doi: 10.1074/jbc.M111.260430

Eleftheriadis, T., Pissas, G., Tsogka, K., Nikolaou, E., Liakopoulos, V., and Stefanidis, I. (2020). A unifying model of glucotoxicity in human renal proximal tubular epithelial cells and the effect of the SGLT2 inhibitor dapagliflozin. *Int. Urol. Nephrol.* 52, 1179–1189. doi: 10.1007/s11255-020-02481-3

Eleftheriadis, T., Tsogka, K., Pissas, G., Antoniadi, G., Liakopoulos, V., and Stefanidis, I. (2016). Activation of general control nonderepressible 2 kinase protects human glomerular endothelial cells from harmful high-glucose-induced molecular pathways. *Int. Urol. Nephrol.* 48, 1731–1739. doi: 10.1007/s11255-016-1377-x

Fardini, Y., Dehennaut, V., Lefebvre, T., and Issad, T. (2013). O-GlcNAcylation: a new cancer hallmark? *Front. Endocrinol.* 4:99. doi: 10.3389/fendo.2013.00099

Ferron, M., Denis, M., Persello, A., Rathagirishnan, R., and Lauzier, B. (2018). Protein O-GlcNAcylation in cardiac pathologies: past. present, future. *Front. Endocrinol.* 9:819. doi: 10.3389/fendo.2018.00819

Fisi, V., Miseta, A., and Nagy, T. (2017). The role of stress-induced O-GlcNAc protein modification in the regulation of membrane transport. *Oxid. Med. Cell Longev.* 2017:1308692. doi: 10.1155/2017/1308692

Friedrich, B., Matskevich, I., and Lang, F. (2006). Cell volume regulatory mechanisms. *Contrib. Nephrol.* 152, 1–8. doi: 10.1159/000096284

Furst, J., Botta, G., Saino, S., Dopinto, S., Gandini, R., Dossena, S., et al. (2006). The ICln interactome. *Acta Physiol.* 187, 43–49. doi: 10.1111/j.1748-1716.2006.01549.x

Furst, J., Gschwentner, M., Ritter, M., Botta, G., Jakab, M., Mayer, M., et al. (2002a). Molecular and functional aspects of anionic channels activated during regulatory volume decrease in mammalian cells. *Pflug. Arch* 444, 1–25. doi: 10.1007/s00424-002-0805-1

Furst, J., Ritter, M., Rudzki, J., Danzl, J., Gschwentner, M., Scandella, E., et al. (2002b). ICln ion channel splice variants in Caenorhabditis elegans: voltage dependence and interaction with an operon partner protein. *J. Biol. Chem.* 277, 4435–4445. doi: 10.1074/jbc.m107372200

Furst, J., Schedlbauer, A., Gandini, R., Garavaglia, M. L., Saino, S., Gschwentner, M., et al. (2005). ICln159 folds into a pleckstrin homology domain-like structure. Interaction with kinases and the splicing factor LSm4. *J. Biol. Chem.* 280, 31276–31282. doi: 10.1074/jbc.m500541200

Gandini, R., Dossena, S., Vezzoli, V., Tamplenizza, M., Salvioni, E., Ritter, M., et al. (2008). LSm4 associates with the plasma membrane and acts as a co-factor in cell volume regulation. *Cell Physiol. Biochem.* 22, 579–590. doi: 10.1159/000185542

Gellai, R., Hodrea, J., Lenart, L., Hosszu, A., Koszegi, S., Balogh, D., et al. (2016). Role of O-linked N-acetylglucosamine modification in diabetic nephropathy. *Am. J. Physiol. Renal Physiol.* 311, F1172–F1181. doi: 10.1152/ajprenal.00545.2015

Gloster, T. M., and Vocadlo, D. J. (2010). Mechanism, structure, and inhibition of O-GlcNAc processing enzymes. *Curr. Signal Transduct. Ther.* 5, 74–91. doi: 10.2174/157436210790226537

Grimm, C., Chari, A., Pelz, J. P., Kuper, J., Kisker, C., Diederichs, K., et al. (2013). Structural basis of assembly chaperone- mediated snRNP formation. *Mol. Cell* 49, 692–703. doi: 10.1016/j.molcel.2012.12.009

Gupta, R., and Brunak, S. (2002). Prediction of glycosylation across the human proteome and the correlation to protein function. *Pac. Symp. Biocomput.* 2002, 310–322.

Hahne, H., Sobotzki, N., Nyberg, T., Helm, D., Borodkin, V. S., van Aalten, D. M., et al. (2013). Proteome wide purification and identification of O-GlcNAc-modified proteins using click chemistry and mass spectrometry. *J. Prot. Res.* 12, 927–936. doi: 10.1021/pr300967y

Hart, G. W. (2014). Three Decades of Research on O-GlcNAcylation - a major nutrient sensor that regulates signaling, transcription and cellular metabolism. *Front. Endocrinol.* 5:183. doi: 10.3389/fendo.2014.00183

Hart, G. W. (2019). Nutrient regulation of signaling and transcription. *J. Biol. Chem.* 294, 2211–2231. doi: 10.1074/jbc.AW119.003226

Hart, G. W., Housley, M. P., and Slawson, C. (2007). Cycling of O-linked beta-N-acetylglucosamine on nucleocytoplasmic proteins. *Nature* 446, 1017–1022. doi: 10.1038/nature05815

Hart, G. W., Slawson, C., Ramirez-Correa, G., and Lagerlof, O. (2011). Cross talk between O-GlcNAcylation and phosphorylation: roles in signaling, transcription, and chronic disease. *Annu. Rev. Biochem.* 80, 825–858. doi: 10.1146/annurev-biochem-060608-102511

Hoffmann, E. K., Lambert, I. H., and Pedersen, S. F. (2009). Physiology of cell volume regulation in vertebrates. *Physiol. Rev.* 89, 193–277. doi: 10.1152/physrev.00037.2007

Hubert, M. D., Levitan, I., Hoffman, M. M., Zraggen, M., Hofreiter, M. E., and Garber, S. S. (2000). Modulation of volume regulated anion current by I(Cln). *Biochim.Biophys.Acta* 1466, 105–114. doi: 10.1016/s0005-2736(00)00177-2

Inoue, H., Takahashi, N., Okada, Y., and Konishi, M. (2010). Volume-sensitive outwardly rectifying chloride channel in white adipocytes from normal and diabetic mice. *Am. J. Physiol. Cell Physiol.* 298, C900–C909. doi: 10.1152/ajpcell.00450.2009

Jakab, M., Furst, J., Gschwentner, M., Botta, G., Garavaglia, M. L., Bazzini, C., et al. (2002). Mechanisms sensing and modulating signals arising from cell swelling. *Cell Physiol. Biochem.* 12, 235–258. doi: 10.1159/000067895

Jia, C., and Zuo, Y. (2018). Computational Prediction of Protein O-GlcNAc Modification. *Methods Mol. Biol.* 1754, 235–246. doi: 10.1007/978-1-4939-7717-8_14

Kaji, K., Nishimura, N., Seki, K., Sato, S., Saikawa, S., Nakanishi, K., et al. (2018). Sodium glucose cotransporter 2 inhibitor canagliflozin attenuates liver cancer cell growth and angiogenic activity by inhibiting glucose uptake. *Int. J. Cancer* 142, 1712–1722. doi: 10.1002/ijc.31193

Kim, E. J., Kang, D. O., Love, D. C., and Hanover, J. A. (2006). Enzymatic characterization of O-GlcNAcase isoforms using a fluorogenic GlcNAc substrate. *Carbohydr. Res.* 341, 971–982. doi: 10.1016/j.carres.2006.03.004

Kneass, Z. T., and Marchase, R. B. (2004). Neutrophils exhibit rapid agonist-induced increases in protein-associated O-GlcNAc. *J. Biol. Chem.* 279, 45759–45765. doi: 10.1074/jbc.M407911200

Kommaddi, R. P., Dickson, K. M., and Barker, P. A. (2011). Stress-induced expression of the p75 neurotrophin receptor is regulated by O-GlcNAcylation of the Sp1 transcription factor. *J. Neurochem.* 116, 396–405. doi: 10.1111/j.1471-4159.2010.07120.x

Lagerlof, O., and Hart, G. W. (2014). O-GlcNAcylation of neuronal proteins: roles in neuronal functions and in neurodegeneration. *Adv. Neurobiol.* 9, 343–366. doi: 10.1007/978-1-4939-1154-7_16

Lang, F., Bush, G. L., Ritter, M., Völkl, H., Waldegger, S., Gulbins, E., et al. (1998). Functional significance of cell volume regulatory mechanisms. *Physiol. Rev.* 78, 247–306. doi: 10.1152/physrev.1998.78.1.247

Larkin, D., Murphy, D., Reilly, D. F., Cahill, M., Sattler, E., Harriott, P., et al. (2004). ICln, a novel integrin alphaIIbbeta3-associated protein, functionally regulates platelet activation. *J. Biol. Chem.* 279, 27286–27293. doi: 10.1074/jbc.m402159200

Larkin, D., Treumann, A., Murphy, D., DeChaumont, C., Kiernan, A., and Moran, N. (2009). Compartmentalization regulates the interaction between the platelet integrin alpha IIb beta 3 and ICln. *Br.J.Haematol.* 144, 580–590. doi: 10.1111/j.1365-2141.2008.07483.x

Li, F., Li, C., Wang, M., Webb, G. I., Zhang, Y., Whisstock, J. C., et al. (2015). GlycoMine: a machine learning-based approach for predicting N-. C- and O-linked glycosylation in the human proteome. *Bioinformatics* 31, 1411–1419. doi: 10.1093/bioinformatics/btu852

Liu, Y., Zhang, H., Men, H., Du, Y., Xiao, Z., Zhang, F., et al. (2019). Volume-regulated Cl(-) current: contributions of distinct Cl(-) channels and localized Ca(2+) signals. *Am. J. Physiol. Cell Physiol.* 317, C466–C480. doi: 10.1152/ajpcell.00507.2018

Ma, J., and Hart, G. W. (2014). O-GlcNAc profiling: from proteins to proteomes. *Clin. Prot.* 11:8. doi: 10.1186/1559-0275-11-8

Margalit, A., Gilutz, H., and Granot, Y. (1995). Original article: low regulatory volume decrease rate in platelets from ischemic patients: a possible role

for hepoxilin a(3) in thrombogenicity. *Platelets* 6, 371–376. doi: 10.3109/09537109509078474

Masola, V., Gambaro, G., Tibaldi, E., Onisto, M., Abaterusso, C., and Lupo, A. (2011). Regulation of heparanase by albumin and advanced glycation end products in proximal tubular cells. *Biochim. Biophys. Acta* 1813, 1475–1482. doi: 10.1016/j.bbamcr.2011.05.004

McClain, D. A., and Crook, E. D. (1996). Hexosamines and insulin resistance. *Diabetes* 45, 1003–1009. doi: 10.2337/diab.45.8.1003

McLarty, J. L., Marsh, S. A., and Chatham, J. C. (2013). Post-translational protein modification by O-linked N-acetyl-glucosamine: its role in mediating the adverse effects of diabetes on the heart. *Life Sci.* 92, 621–627. doi: 10.1016/j.lfs.2012.08.006

Morabito, R., Costa, R., Rizzo, V., Remigante, A., Nofziger, C., La Spada, G., et al. (2017). Crude venom from nematocysts of Pelagia noctiluca (Cnidaria: Scyphozoa) elicits a sodium conductance in the plasma membrane of mammalian cells. *Sci. Rep.* 7:41065. doi: 10.1038/srep41065

Morabito, R., La Spada, G., Dossena, S., and Marino, A. (2014). Oxidative stress affects responsiveness to hypotonicity of renal cells. *J. Biol. Res.* 87:4811.

Morabito, R., Marino, A., Lauf, P. K., Adragna, N. C., and La Spada, G. (2013). Sea water acidification affects osmotic swelling, regulatory volume decrease and discharge in nematocytes of the jellyfish Pelagia noctiluca. *Cell Physiol. Biochem.* 32, 77–85. doi: 10.1159/000356629

Morgan, R. A., Couture, L., Elroy-Stein, O., Ragheb, J., Moss, B., and Anderson, W. F. (1992). Retroviral vectors containing putative internal ribosome entry sites: development of a polycistronic gene transfer system and applications to human gene therapy. *Nucl. Acids Res.* 20, 1293–1299. doi: 10.1093/nar/20.6.1293

Myslicki, J. P., Shearer, J., Hittel, D. S., Hughey, C. C., and Belke, D. D. (2014). O-GlcNAc modification is associated with insulin sensitivity in the whole blood of healthy young adult males. *Diabetol. Metab. Syndr.* 6:96. doi: 10.1186/1758-5996-6-96

Nagy, T., Balasa, A., Frank, D., Rab, A., Rideg, O., Kotek, G., et al. (2010). O-GlcNAc modification of proteins affects volume regulation in Jurkat cells. *Eur. Biophys. J.* 39, 1207–1217. doi: 10.1007/s00249-009-0573-3

Nagy, T., Miseta, A., and Kovacs, G. L. (2007). Protein-associated O-GlcNAc, a multifunctional mechanism in cell signaling and its role in the pathogenesis of diabetes, stress and malignant diseases. *Biochem. Medica* 17, 162–177. doi: 10.11613/bm.2007.015

Okada, Y., Maeno, E., Shimizu, T., Dezaki, K., Wang, J., and Morishima, S. (2001). Receptor-mediated control of regulatory volume decrease (RVD) and apoptotic volume decrease (AVD). *J. Physiol.* 532(Pt. 1), 3–16. doi: 10.1111/j.1469-7793.2001.0003g.x

Okada, Y., Numata, T., Sato-Numata, K., Sabirov, R. Z., Liu, H., Mori, S. I., et al. (2019). Roles of volume-regulatory anion channels, VSOR and Maxi-Cl, in apoptosis, cisplatin resistance, necrosis, ischemic cell death, stroke and myocardial infarction. *Curr. Top. Membr.* 83, 205–283. doi: 10.1016/bs.ctm.2019.03.001

Okuda, S., Watanabe, Y., Moriya, Y.,Kawano, S., Yamamoto, T., Matsumoto, M. et al. (2017). jPOSTrepo: an international standard data repository for proteomes. *Nucl. Acids Res.* 45, D1107–D1111. doi: 10.1093/nar/gkw1080

Pagesy, P., Tachet, C., Mostefa-Kara, A., Larger, E., and Issad, T. (2018). Increased OGA expression and activity in leukocytes from patients with diabetes: correlation with inflammation markers. *Exp. Clin. Endocrinol. Diabetes* 127, 517-523. doi: 10.1055/a-0596-7337

Park, K., Saudek, C. D., and Hart, G. W. (2010). Increased expression of beta-N-acetylglucosaminidase in erythrocytes from individuals with pre-diabetes and diabetes. *Diabetes* 59, 1845–1850. doi: 10.2337/db09-1086

Park, M. J., Kim, D. I., Lim, S. K., Choi, J. H., Han, H. J., Yoon, K. C., et al. (2014). High glucose-induced O-GlcNAcylated carbohydrate response element-binding protein (ChREBP) mediates mesangial cell lipogenesis and fibrosis: the possible role in the development of diabetic nephropathy. *J. Biol. Chem.* 289, 13519–13530. doi: 10.1074/jbc.M113.530139

Paulmichl, M., Li, Y., Wickman, K., Ackerman, M., Peralta, E., and Clapham, D. (1992). New mammalian chloride channel identified by expression cloning. *Nature* 356, 238–241. doi: 10.1038/356238a0

Pedersen, S. F., Okada, Y., and Nilius, B. (2016). Biophysics and physiology of the volume-regulated anion channel (VRAC)/volume-sensitive outwardly rectifying anion channel (VSOR). *Pflug. Arch.* 468, 371–383. doi: 10.1007/s00424-015-1781-6

Peterson, S. B., and Hart, G. W. (2016). New insights: a role for O-GlcNAcylation in diabetic complications. *Crit. Rev. Biochem. Mol. Biol.* 51, 150–161. doi: 10.3109/10409238.2015.1135102

Qiu, Z., Dubin, A. E., Mathur, J., Tu, B., Reddy, K., Miraglia, L. J., et al. (2014). SWELL1, a plasma membrane protein, is an essential component of volume-regulated anion channel. *Cell* 157, 447–458. doi: 10.1016/j.cell.2014.03.024

Ritter, M., Ravasio, A., Jakab, M., Chwatal, S., Furst, J., Laich, A., et al. (2003). Cell swelling stimulates cytosol to membrane transposition of ICln. *J. Biol. Chem.* 278, 50163–50174. doi: 10.1074/jbc.m300374200

Schedlbauer, A., Tamma, G., Rodighiero, S., Civello, D. A., Tamplenizza, M., Ledolter, K., et al. (2019). Binding of the protein ICln to alpha-integrin contributes to the activation of IClswell current. *Sci. Rep.* 9:12195. doi: 10.1038/s41598-019-48496-4

Slawson, C., and Hart, G. W. (2011). O-GlcNAc signalling: implications for cancer cell biology. *Nat. Rev. Cancer* 11, 678–684. doi: 10.1038/nrc3114

Springhorn, C., Matsha, T. E., Erasmus, R. T., and Essop, M. F. (2012). Exploring leukocyte O-GlcNAcylation as a novel diagnostic tool for the earlier detection of type 2 diabetes mellitus. *J. Clin. Endocrinol. Metab.* 97, 4640–4649. doi: 10.1210/jc.2012-2229

Stowell, S. R., Ju, T., and Cummings, R. D. (2015). Protein glycosylation in cancer. *Annu. Rev. Pathol.* 10, 473–510. doi: 10.1146/annurev-pathol-012414-040438

Sun, Y. M., Su, Y., Li, J., and Wang, L. F. (2013). Recent advances in understanding the biochemical and molecular mechanism of diabetic nephropathy. *Biochem. Biophys. Res. Commun.* 433, 359–361. doi: 10.1016/j.bbrc.2013.02.120

Szabo, Z., Szomor, J. S., Foeldi, I., and Janaky, T. (2012). Mass spectrometry-based label free quantification of gel separated proteins. *J. Proteomics* 75, 5544–5553. doi: 10.1016/j.jprot.2012.07.036

Tamma, G., Dossena, S., Nofziger, C., Valenti, G., Svelto, M., and Paulmichl, M. (2011). EGF stimulates IClswell by a redistribution of proteins involved in cell volume regulation. *Cell Physiol. Biochem.* 28, 1191–1202. doi: 10.1159/000335851

Tang, S. C., and Lai, K. N. (2012). The pathogenic role of the renal proximal tubular cell in diabetic nephropathy. *Nephrol. Dial Transpl.* 27, 3049–3056. doi: 10.1093/ndt/gfs260

Vaidyanathan, K., and Wells, L. (2014). Multiple tissue-specific roles for the O-GlcNAc post-translational modification in the induction of and complications arising from type II diabetes. *J. Biol. Chem.* 289, 34466–34471. doi: 10.1074/jbc.R114.591560

Vallon, V., and Thomson, S. C. (2020). The tubular hypothesis of nephron filtration and diabetic kidney disease. *Nat. Rev. Nephrol.* 16, 317–336. doi: 10.1038/s41581-020-0256-y

van der Wijk, T., Tomassen, S. F., de Jonge, H. R., and Tilly, B. C. (2000). Signalling mechanisms involved in volume regulation of intestinal epithelial cells. *Cell Physiol. Biochem.* 10, 289–296. doi: 10.1159/000016359

Vaudel, M., Burkhart, J. M., Zahedi, R. P., Oveland, E., Berven, F. S., Sickmann, A., et al. (2015). PeptideShaker enables reanalysis of MS-derived proteomics data sets. *Nat. Biotechnol.* 33, 22–24. doi: 10.1038/nbt.3109

Voss, F. K., Ullrich, F., Munch, J., Lazarow, K., Lutter, D., Mah, N., et al. (2014). Identification of LRRC8 heteromers as an essential component of the volume-regulated anion channel VRAC. *Science* 344, 634–638. doi: 10.1126/science.1252826

Wang, S., Yang, F., Camp, D. G. II, Rodland, K., Qian, W. J., Liu, T., et al. (2014). Proteomic approaches for site-specific O-GlcNAcylation analysis. *Bioanalysis* 6, 2571–2580. doi: 10.4155/bio.14.239

Wang, Z., Park, K., Comer, F., Hsieh-Wilson, L. C., Saudek, C. D., and Hart, G. W. (2009). Site-specific GlcNAcylation of human erythrocyte proteins: potential biomarker(s) for diabetes. *Diabetes* 58, 309–317. doi: 10.2337/db08-0994

Wells, L., Vosseller, K., and Hart, G. W. (2001). Glycosylation of nucleocytoplasmic proteins: signal transduction and O-GlcNAc. *Science* 291, 2376–2378. doi: 10.1126/science.1058714

Wells, L., Vosseller, K., and Hart, G. W. (2003a). A role for N-acetylglucosamine as a nutrient sensor and mediator of insulin resistance. *Cell Mol. Life Sci.* 60, 222–228. doi: 10.1007/s000180300017

Wells, L., Whelan, S. A., and Hart, G. W. (2003b). O-GlcNAc: a regulatory post-translational modification. *Biochem. Biophys. Res. Commun.* 302, 435–441. doi: 10.1016/s0006-291x(03)00175-x

Yamamoto, S., Ichishima, K., and Ehara, T. (2009). Reduced volume-regulated outwardly rectifying anion channel activity in ventricular myocyte of type 1 diabetic mice. *J. Physiol. Sci.* 59, 87–96. doi: 10.1007/s12576-008-0012-8

Yang, X., and Qian, K. (2017). Protein O-GlcNAcylation: emerging mechanisms and functions. *Nat. Rev. Mol. Cell Biol.* 18, 452–465. doi: 10.1038/nrm.2017.22

Yuzwa, S. A., and Vocadlo, D. J. (2014). O-GlcNAc and neurodegeneration: biochemical mechanisms and potential roles in Alzheimer's disease and beyond. *Chem. Soc. Rev.* 43, 6839–6858. doi: 10.1039/c4cs00038b

Zachara, N., Akimoto, Y., and Hart, G. W. (2015). "The O-GlcNAc Modification," in *Essentials of Glycobiology*, eds A. Varki, R. D. Cummings, J. D. Esko, P. Stanley, G. W. Hart, M. Aebi, et al. (New York, NY: Cold Spring Harbor), 239–251.

Zachara, N. E., and Hart, G. W. (2006). Cell signaling, the essential role of O-GlcNAc! *Biochim. Biophys. Acta* 1761, 599–617. doi: 10.1016/j.bbalip.2006.04.007

Zachara, N. E., O'Donnell, N., Cheung, W. D., Mercer, J. J., Marth, J. D., and Hart, G. W. (2004). Dynamic O-GlcNAc modification of nucleocytoplasmic proteins in response to stress. A survival response of mammalian cells. *J. Biol. Chem.* 279, 30133–30142. doi: 10.1074/jbc.M403773200

Zeidan, Q., and Hart, G. W. (2010). The intersections between O-GlcNAcylation and phosphorylation: implications for multiple signaling pathways. *J. Cell Sci.* 123(Pt. 1), 13–22. doi: 10.1242/jcs.053678

Conflict of Interest: The authors declare that the research was conducted in the absence of any commercial or financial relationships that could be construed as a potential conflict of interest.

Copyright © 2020 Costa, Remigante, Civello, Bernardinelli, Szabó, Morabito, Marino, Sarikas, Patsch, Paulmichl, Janáky, Miseta, Nagy and Dossena. This is an open-access article distributed under the terms of the Creative Commons Attribution License (CC BY). The use, distribution or reproduction in other forums is permitted, provided the original author(s) and the copyright owner(s) are credited and that the original publication in this journal is cited, in accordance with accepted academic practice. No use, distribution or reproduction is permitted which does not comply with these terms.

frontiers in Cell and Developmental Biology

REVIEW
published: 07 December 2020
doi: 10.3389/fcell.2020.589752

The Aryl Hydrocarbon Receptor in Chronic Kidney Disease: Friend or Foe?

Yenan Mo[1,2†], Zhaoyu Lu[1,2†], Lixin Wang[2], Chunlan Ji[1,2], Chuan Zou[2] and Xusheng Liu[2]*

[1] The Second Clinical College of Guangzhou University of Chinese Medicine, Guangzhou, China, [2] Department of Nephrology, The Second Affiliated Hospital of Guangzhou University of Chinese Medicine, Guangzhou, China

The aryl hydrocarbon receptor (AhR) is a ligand-activated transcription factor that promotes cell responses to small molecules derived from the diet, microorganisms, metabolism and pollutants. The AhR signal regulates many basic cellular processes, including cell cycle progression, adhesion, migration, apoptosis and cell proliferation. Many studies have shown that AhR is associated with chronic kidney disease (CKD) and its complications. This article reviews the current knowledge about the role of AhR in CKD, showing that AhR mediates CKD complications, including cardiovascular disease, anemia, bone disorders, cognitive dysfunction and malnutrition, and that it influences drug metabolism in individuals with CKD. AhR enhances the intestinal barrier function to reduce the harmful effects of uremic toxins. Therefore, understanding the complex roles of AhR during CKD is important to be able to target this transcription factor safely and effectively for CKD prevention and treatment.

Keywords: aryl hydrocarbon receptor, chronic kidney disease, tryptophan metabolism, uremic toxin, CKD complications, intestine homeostasis

OPEN ACCESS

Edited by:
Evangelia Dounousi, University Hospital of Ioannina, Greece

Reviewed by:
Henricus A. M. (Rick) Mutsaers, Aarhus University, Denmark
Bin Yang, University of Leicester, United Kingdom

***Correspondence:**
Xusheng Liu
liuxu801@126.com

† These authors have contributed equally to this work

Specialty section:
This article was submitted to Molecular Medicine, a section of the journal Frontiers in Cell and Developmental Biology

Received: *31 July 2020*
Accepted: *18 November 2020*
Published: *07 December 2020*

Citation:
Mo Y, Lu Z, Wang L, Ji C, Zou C and Liu X (2020) The Aryl Hydrocarbon Receptor in Chronic Kidney Disease: Friend or Foe? Front. Cell Dev. Biol. 8:589752. doi: 10.3389/fcell.2020.589752

INTRODUCTION

Chronic kidney disease (CKD) has become an emerging global disease during the past decade. The all-age prevalence of CKD increased 29.3% worldwide from 1990 to 2017, involving 697.5 million cases in 2017 (representing a global prevalence of 9.1%) (Bikbov et al., 2020). CKD results in irreversible kidney structural and functional alterations that lead to end-stage renal disease, with patients ultimately requiring dialysis or renal transplantation.

Chronic kidney disease is characterized by the accumulation of a mixture of uremic toxins/solutes that persist even after standard dialysis (Vanholder and Glorieux, 2014; Sirich, 2017). These toxins are divided into three categories: small soluble compounds, middle molecules and protein-bound molecules (Duranton et al., 2012). Tryptophan-derived toxins are of particular interest because they exhibit cardiovascular toxicity and are ligands of the aryl hydrocarbon receptor (AhR) (Heath-Pagliuso et al., 1998; Schroeder et al., 2010). Multiple sensors detect changes in the cellular milieu to adapt to toxic environments and generate responses to molecular environment changes due to diet, symbiotic microbiome and host metabolism factors. One of these sensors is AhR, a ligand-activated transcription factor involved in various cellular processes, such as cell cycle, epithelial barrier function and neurological signaling, as well as responses to antioxidants and xenobiotics (Murray et al., 2014).

Aryl hydrocarbon receptor regulation and its role during CKD has gained interest as a potential source of biological processes that may guide the development of new therapeutic interventions.

In this review, we summarize the current knowledge on the role of AhR in CKD and/or its complications, and we address the potential role of AhR as a therapeutic target.

AHR SIGNALING AND ITS LIGANDS

AhR Signaling Pathway

Aryl hydrocarbon receptor belongs to the periodic-AhR nuclear translocator-single-minded protein (PER-ARNT-SIM [PAS]) superfamily. The PAS domain senses both endogenous factors (such as cellular metabolites) and exogenous factors (such as environmental toxins) (McIntosh et al., 2010).

As shown in **Figure 1**, there are two AhR signaling pathways. One is the xenobiotic-responsive element (XRE)-dependent control of gene expression by AhR, also called canonical AhR signaling. Prior to AhR activation, AhR is inactive as part of a protein complex that consists of two molecules of heat-shock protein 90, one X-associated protein 2 (also known as an AhR-interacting protein), one co-chaperon p23 and the protein kinase Sarcoma (SRC) in the cytoplasm. The AhR chaperone complex stabilizes AhR in the cytoplasm and keeps it in a conformation that has high affinity for its ligands (Pongratz et al., 1992). Once a ligand binds to AhR, the molecule undergoes a conformational change to expose its N-terminal nuclear localization sequence, facilitating translocation of the liganded AhR protein complex into the nucleus. In the nucleus, AhR binds to ARNT (also known as HIF-1β) through its PAS domain, forming a ligand-bound AhR-ARNT dimer. The dimer gets recruited to a DNA-specific sequence (referred to as a DRE or XRE for a dioxin- or xenobiotic-responsive element) located within the promoters of target genes, to promote transcription of a wide variety of genes, such as cytochrome P450, family 1, member 1A (Cyp1A1); cytochrome P450, family 1, member 2A; cytochrome P450, family 1, subfamily B; AhR repressor (AhRR) and cyclooxygenase-2 (Denison and Nagy, 2003). AhR-dependent gene transcription ends upon separation of the AhR-ARNT complex from the DRE. The N-terminal nuclear export sequence mediates AhR export from the nucleus into the cytoplasm, where ubiquitin-mediated AhR proteasome degradation occurs (Pollenz, 2002). The other AhR signaling pathway is non-canonical AhR signaling, which controls AhR gene expression through non-XRE DNA-response elements. AhR can also interact with additional transcription factors such as nuclear factor-κB (NF-κB), programmed death ligand 1, signal transducer and activator of transcription (STAT) and nuclear factor-erythroid-2-related factor 2 by binding to them and modulating the expression of their target genes through a non-genomic pathway that does not require ARNT (Kimura et al., 2008; Puga et al., 2009; Wakamatsu et al., 2018; Singh et al., 2019; Wang et al., 2019). Moreover, AhR functions as an E3 ubiquitin ligase, regulating the half-life of other transcription factors. For example, indoxyl sulphate (IS) directly activates AhR, extending the half-life of tissue factor (TF) by inhibiting its ubiquitination in vascular smooth muscle cells; TF is a crucial mediator of injury-related thrombosis (Shivanna et al., 2016). In addition, AhR activation triggers phosphorylation cascades driven by SRC kinase released from the AhR chaperone complex. For instance, SRC phosphorylates a broad variety of target proteins including indoleamine 2,3-dioxygenase 1 (IDO1) (Bessede et al., 2014), which promotes tryptophan transformation into kynurenine, a ligand of AhR.

AhR Ligands

Aryl hydrocarbon receptor was discovered to be a receptor binding to 2,3,7,8-tetrachlorodibenzo-p-dioxin (TCDD) (also known as dioxin) with high affinity. The receptor can be hyperactivated in a sustained manner, resulting in numerous toxicological outcomes. In addition, many commercial and consumer products, vegetables, fruits, and spices have exhibited AhR activation potential (Jeuken et al., 2003; Zhao et al., 2013) and can facilitate the induction or repression of the expression of a range of genes, thereby regulating a diverse spectrum of biological and toxic effects. Environment pollutants and myriad endogenous molecules such as microbial metabolites (e.g., indolic solutes) and naturally occurring flavonoids (e.g., resveratrol and quercetin) are also AhR ligand candidates (Murray et al., 2014; Gutierrez-Vazquez and Quintana, 2018; Rothhammer and Quintana, 2019; **Table 1**).

For patients with CKD, the most important AhR ligands are uremic toxins, especially those derived from tryptophan metabolism. This essential aromatic amino acid is a biosynthetic precursor of a large number of microbial and host metabolites (Alkhalaf and Ryan, 2015). Tryptophan metabolism follows three major pathways in the gastrointestinal tract: (1) the indolic pathway in intestinal microorganisms that directly transforms tryptophan into several AhR ligand molecules, such as indole-3-acid-acetic (IAA), indole-3-aldehyde, indole-3-acetaldehyde, and indole-3-propionic acid (Zelante et al., 2013; Hubbard et al., 2015; Alexeev et al., 2018); (2) the kynurenine pathway via the rate-limiting enzyme IDO1 that produces kynurenine and downstream products such as quinolinic acid and kynurenic acid (Clarke et al., 2012; Cervenka et al., 2017; Kennedy et al., 2017) and (3) the serotonin pathway in enterochromaffin cells that involves tryptophan hydroxylase-1 (Yano et al., 2015). Some tryptophan metabolites such as IS, IAA and kynurenine represent both important uremic toxins and potent AhR ligands. We will summarize the associations between AhR and uremic toxins in CKD below.

ACTIVATED AHR AGGRAVATES RENAL DAMAGE

Patients with CKD are exposed to a variety of uremic toxins, which are agonists of AhR. Early Lu et al. (2006) provided evidence for a positive correlation between renal AhR expression and CKD severity, suggesting that AhR activation has a pathogenic effect in both male and female rats that have undergone nephrectomy. Compared with healthy controls, CKD patients and 5/6 of nephrectomy mice exhibited increased serum AhR-activating potential, which was strongly correlated with IS concentration and estimated glomerular filtration rate, and which upregulated expression of the AhR target genes AhRR and Cyp1A1 (Dou et al., 2018). Kim et al. (2020) reported higher

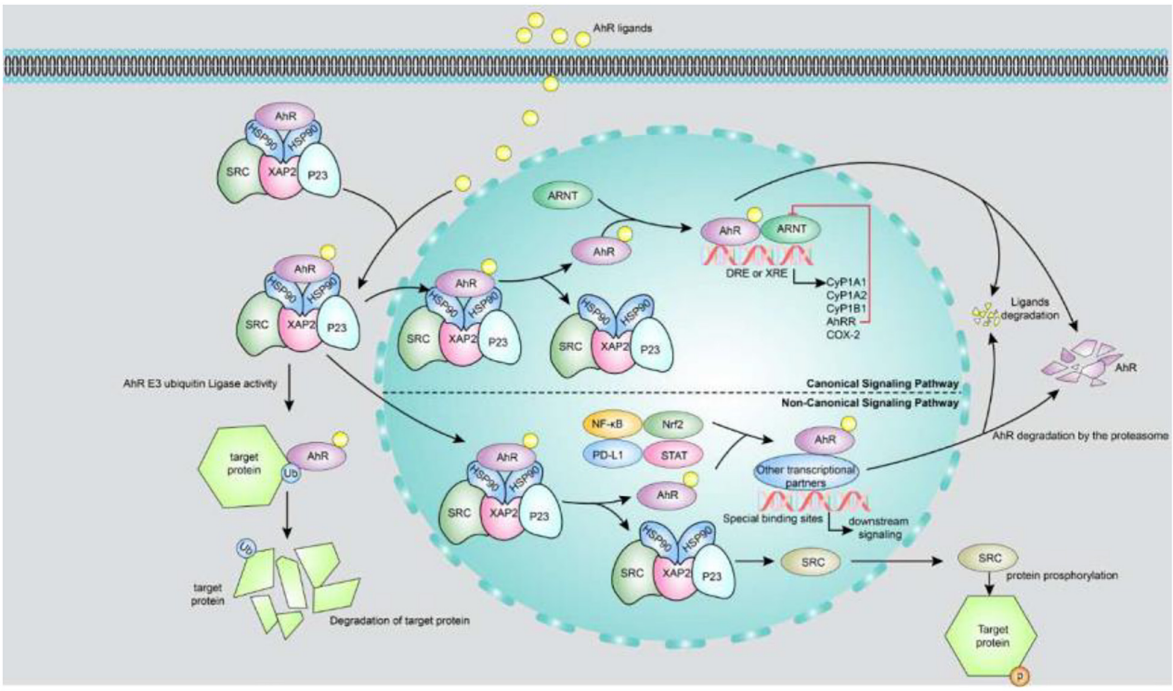

FIGURE 1 | Canonical and non-canonical signaling pathways of AhR. The upper part of the figure is a canonical AhR signal pathway. Prior to AhR activation, AhR is inactive as part of a protein complex that consists of two molecules of HSP90, XAP2, p23 and the protein kinase SRC in the cytoplasm. Once a ligand binds to AhR, the molecule undergoes a conformational change to expose its N-terminal nuclear localization sequence, facilitating translocation of the liganded AhR protein complex into the nucleus. In the nucleus, AhR binds to ARNT through its PAS domain, forming a ligand-bound AhR-ARNT dimer. The dimer gets recruited to a DNA-specific sequence located within the promoters of target genes, to promote transcription of a wide variety of genes, such as Cyp1A1, CyP1B1, AhRR, and COX-2. AhR activity is strictly controlled by three different negative feedback loops, including: (i) degradation of AhR by proteasome, (ii) clearance of ligand by metabolic pathway, (iii) destruction of AhR/ARNT complex by AhRR. The lower part of figure shows the non-canonical AhR signaling: (i) AhR can also interact with NF-κB, Nrf2, PD-L1 and STAT proteins or other transcription factors to bind their specific binding sites and consequently modulate the activity and expression of their target genes. (ii) AhR functions as an E3 ubiquitin ligase to regulate the half-life of other transcription factors. (iii) AhR activation triggers phosphorylation cascades driven by SRC kinase when it releases from the AhR chaperone complex. AhR, aryl hydrocarbon receptor; AhRR, AhR repressor; ARNT, aryl hydrocarbon receptor nuclear translocator; COX-2, cyclooxygenase-2; Cyp1A1, cytochrome P450; family 1, member 1A; Cyp1A2, cytochrome P450; family 1, member 2A; Cyp1B1, cytochrome P450; family 1, sub family B; DRE or XRE, dioxin-or xenobiotic-responsive element; HSP90, heat-shock protein 90; NF-κB, nuclear factor-κB; Nrf2, nuclear factor-erythroid-2-related factor 2; P23, co-chaperon p23; PD-L1, programmed death ligand 1; STAT, signal transducer and activator of transcription; XAP2, X-associated protein 2.

AhR transactivating (AhRT) activity in patients with CKD than in controls, and they showed that peritoneal dialysis treatment was more effective at reducing this AhRT activity than haemodialysis.

Aryl hydrocarbon receptor signaling regulates many fundamental cellular processes, such as cell cycle progression, apoptosis and cell proliferation by regulating P53, FasR, Bcl-2 and cell cycle kinases (Zaher et al., 1998; Mohammadi et al., 2017). Exposure to adenine and IS increases AhR activity in the periglomerular region as well as in proximal and distal renal tubules, leading to renal fibrosis (Walker et al., 2020). AhR activated by IS induces podocyte injury, progressive glomerular damage and a pro-inflammatory phenotype *in vitro* and *in vivo* (Ichii et al., 2014). IS downregulates the expression of the Mas receptor, which is associated with the inhibition of the renin-angiotensin system, via the organic anion transporter 3/AhR/STAT3 pathway to upregulate TGF-β in proximal tubular cells, thereby aggravating CKD (Ng et al., 2014). A possible connection between AhR and renal fibrosis has been further supported by the association between indole solutes and renal fibrosis (Mutsaers et al., 2015b), which may be mediated by AhR signaling.

In patients with diabetes mellitus, AhRT activity has been positively correlated with the progression of diabetic nephropathy (DN) and the severity of renal insufficiency (Kim et al., 2013). Lee et al. (2016) investigated the role of AhR in the pathophysiological processes of DN using AhR-knockout and pharmacological-inhibitor α-naphthoflavone models, and they found that AhR mediated renal oxidative stress in a diabetic mouse model, resulting in macrophage infiltration, extracellular matrix accumulation and mesangial cell activation.

Translocation of microbial antigens due to gut barrier breakdown has been associated with gut microbiota and the presence of systemic lupus erythematosus (SLE) and lupus nephritis in animal and human studies. Clinical studies have shown reduced gut microbiota diversity in patients with SLE, and gut-derived pathobionts including *Enterococcus gallinarum* have been detected in the liver (Manfredo Vieira et al., 2018). Animal studies have shown that gut-derived *E. gallinarum* can reach

TABLE 1 | exogenous and endogenous AhR ligands.

Ligand		Biochemical pathway
Xenobiotic	2,3,7,8-tetrachlorodibenzo-p-dioxin (TCDD)	Halogenated aromatic hydrocarbons
	3-methylcholanthrene	
	Benzanthracenes	
	Benzoflavones	
	Benzo[a]pyrene	
	Biphenyls	
	Dibenzofurans	
	Polyaromatic hydrocarbons	
	Leflutamide	Pharmaceuticals
	Tranilast	
	Omeprazole	
	6,2′,4′,-trimethoxyflavone	Compound from chemical library
	CH-223191	
	GNF351	
	StemRegenin 1 (SR1)	
	Indirubin	Phytochemicals from plants
	Indigo	
Diet	Galangin	Flavonoids
	Quercetin	
	Kaempferol	
	Resveratrol	Polyphenol
	Indole-3-acetonitrile	Dietary metabolite of cruciferous vegetables
	Indole-3-carbinole	
	Indolo[3,2-b]carbazole (ICZ)	
	3,3′-diindolylmethane (DIM)	
Tryptophan metabolites	3-Methylindole (Skatole)	Microbiota metabolism
	Indole-3-acetaldehyde	
	Indole-3 acetic acid (IAA)	
	Indole-3-aldehyde (IAld)	
	Tryptamine (TA)	
	5-hydroxy-tryptophan (5HTP)	Host metabolism
	Cinnabarinic acid (CA)	
	Kynurenic acid (KA)	
	Kynurenine (Kyn)	
	Xanthurenic acid	
	Indoxyl sulfate (IS)	Microbiota and host metabolism
	6-formylindolo[3,2-b]carbazole (FICZ)	Photo-oxidation
Other metabolites	Bilirubin	Haem metabolism
	Biliverdin	
	Lipoxin 4A	Arachidonic Acid Metabolism
	Prostaglandin PGG2	
	Hydroxyeicosatrienoic acid ([12(R)-HETE])	
	1,4-dihydroxy-2-naphtoic acid	Microbiota metabolism
	3-methylindole	
	7-ketocholesterol	
	Indirubin	
	Malassezin	
	Trypthantrin	

the liver and induce the development of lupus autoantibodies, partly via activation of the AhR/CYP1A1 pathway to trigger Th17 and T follicular helper cell activation, crucial steps for the production of systemic autoantibodies including anti-dsDNA antibodies (Manfredo Vieira et al., 2018).

Therefore, AhR may be a therapeutic target in CKD. In fact, resveratrol, a natural AhR antagonist, inhibits proteinuria, hypoalbuminemia and hyperlipidemia in nephritic rats (Nihei et al., 2001). Atrazine exposure has been shown to cause environmental nephrosis via direct kidney injury, whereas

supplementary lycopenes provide significant protection against atrazine-induced renal injury and environmental nephrosis via their inhibition of the activation of AhR and the expression of cytochrome P450 isoforms (Xia et al., 2018). On the other hand, ARNT, a transcriptional co-activator of AhR, has been implicated in renal fibrosis and is sought as a therapeutic target in CKD; strong experimental support exists for a mechanistic model in which FK506 induces renoprotection (Tampe et al., 2018; Haase, 2019).

AHR ACTIVATION MEDIATES VARIOUS COMPLICATIONS IN INDIVIDUALS WITH CKD

AhR and Cardiovascular Disease

Cardiovascular disease is a major cause of mortality in patients with CKD. AhR is an important receptor for various toxins and can activate pro-thrombotic and pro-inflammatory pathways; thus, there is a close association between the accumulation of uremic toxins and the cardiovascular complications of CKD (Vanholder et al., 2016). In fact, even under non-uremic conditions, AhR activation is associated with increased cardiovascular risks (Sallee et al., 2014). Accordingly, individuals exposed to AhR agonists are prone to increased cardiovascular risks (Humblet et al., 2008). For example, individuals exposed to the TCDD compound in Agent Orange during the Vietnam War have been shown to have associated cardiovascular complications ranging from coronary heart disease to stroke (Lowenstein, 2014).

The accumulation of uremic toxins has effects similar to those of AhR antagonists, making patients with CKD more prone to cardiovascular disease through a series of possible mechanisms. Ito et al. (2016) proved that AhR activated by IS can stimulate the transcriptional activity of activator protein-1 and induce the expression of E-selectin in vascular endothelial cells, thereby increasing the level of vascular inflammation and leukocyte adhesion. Assefa et al. (2019) showed that IS-activated AhR upregulates the activity of SRC to mediate the activity of vascular endothelial cadherin, thereby increasing endothelium permeability and promoting atherosclerosis. In human hepatoma HepG2 cells, IS-induced AhR activation inhibits the expression of fetuin-A, a liver-derived circulating protein that effectively suppresses calcification. Therefore, IS-activated AhR may increase the incidence of vascular calcification and cardiovascular mortality (Ochi et al., 2015). In human umbilical vein endothelial cells, AhR also mediates IS-induced cellular senescence (Koizumi et al., 2014; Eckers et al., 2016) and stimulates the expression of monocyte chemoattractant protein-1, a chemokine recruiting monocytes from the bloodstream into the subendothelial space to participate in the early stages of atherosclerosis (Watanabe et al., 2013). AhR further plays a key role during platelet production (Lindsey and Papoutsakis, 2011; Strassel et al., 2016) and function (Lindsey et al., 2014). AhR agonists enhance platelet aggregation by activating the AhR/p38MAPK pathway in platelets (Pombo et al., 2015). In addition, activated AhR increases the expression and activity of TF to induce a procoagulant state in vascular smooth muscle and endothelial cells (Gondouin et al., 2013; Shivanna et al., 2016); moreover, it enhances the activation of the pro-inflammatory enzyme cyclooxygenase-2 in endothelial cells (Dou et al., 2015). Vascular dysfunction caused by AhR activation may lead to atherosclerotic thrombosis, thus increasing the risk of myocardial infarction, stroke and peripheral artery disease in patients with CKD (Vanholder et al., 2016).

These summarized mechanisms of AhR activation in CKD support efforts to target AhR and limit the detrimental effects of uremic toxins on vascular outcomes. AhR has been considered a therapeutic target for improving the management of the cardiovascular complications of CKD (Shivanna et al., 2016). In Gondouin's study, IS and IAA elevated the production of TF in peripheral blood mononuclear and endothelial cells after AhR activation, generating a "dioxin-like" effect (Gondouin et al., 2013). Addi et al. (2019) confirmed that CH223191, an AhR-specific antagonist, could decrease the expression of TF in a process mediated by IAA in human endothelial cells. Meanwhile, Assefa et al. (2019) showed that resveratrol inhibits the activation of SRC and downregulates the activity and permeability of the vascular endothelium by blocking the IS/AhR pathway, thereby provoking protective effects.

AhR and Anemia

Renal anemia is common in CKD patients and is an important risk factor for CKD progression and mortality (Mohanram et al., 2004; Levin et al., 2006). The prevalent cause of renal anemia is the insufficient production of erythropoietin (EPO) that results from renal interstitial fibrosis (Souma et al., 2015). The transcription of EPO mRNA is mediated by a hypoxia-inducible transcription factor (HIF) formed by HIF-αs (including HIF-1α and HIF-2α) and ARNT. The expression of HIF-αs is strictly regulated by the concentration of cellular oxygen molecules. HIF-α degradation is inhibited under hypoxic conditions, and the resulting nuclear accumulation of HIF-α and its dimerization with ARNT promotes the expression of target genes including EPO. Because both HIF and AhR are members of the PAS-domain protein family and contain basic helix loops, AhR competes with HIF-α subunits to combine with ARNT and form heterodimeric transcription factor complexes in the nucleus (Soshilov and Denison, 2008). In individuals with CKD, uremic toxins elevate AhR levels and may provoke the accumulation of AhR-ARNT complexes while inhibiting the formation of HIF-α-ARNT complexes in the nucleus, leading to abnormal intracellular HIF signal transduction and the transition of renal interstitial EPO-producing tissues into a pathological fibrotic state associated with impaired EPO production capacity (Souma et al., 2013, 2016; Mascanfroni et al., 2015).

Asai et al. (2016), first reported that IS suppresses hypoxic HIF activation and inhibits the production of EPO in rats and HepG2 cells, confirming the presence of IS-impaired HIF signaling due to AhR activation in renal anemia. Later, the same researchers found that indole glucuronic acid inhibits the expression of HIF-dependent EPO by activating AhR, whereas the drug antagonist

CH-223191 blocks AhR and abolishes the inhibiting effect of indole glucuronide on HIF (Asai et al., 2018).

Renal anemia has the same signs as iron deficiency anemia, which is caused by impaired iron utilization. Hepcidin, a liver-secreted protein, is essential for iron metabolism regulation (Park et al., 2001); it induces the internalization and degradation of a cellular iron exporter called ferroportin that regulates intracellular iron efflux (Nemeth et al., 2004). Therefore, the increased hepcidin levels associated with CKD cause duodenal iron absorption disorder and intracellular iron retention, which aggravate the functional iron deficiency state in CKD. Hamano et al. (2018) showed that the expression of hepcidin is increased by IS in a dose-dependent manner and suppressed by AhR silencing in HepG2 cells.

AhR and Bone Disorders

Chronic kidney disease mineral and bone disorders are generally characterized by changes in bone metabolism. These systemic disorders are common in patients with CKD and are characterized by calcium and phosphorus abnormalities, vitamin D deficiency, vascular calcification, secondary hyperparathyroidism and bone abnormalities (Kidney Disease: Improving Global Outcomes (KDIGO) CKD-MBD Update Work Group, 2017).

Vidal et al. (2015) observed that the amount of tryptophan degraded through the kynurenine pathway increases significantly during the formation of osteoblasts and that osteoblast formation is inhibited when IDO1, the enzyme that stimulates the conversion of tryptophan to kynurenine, is blocked. Data published by Refaey et al. (2017) showed that intragastric or intraperitoneal kynurenine administration impairs osteoblast differentiation and increases osteoclast absorption to accelerate age-related bone loss.

Aryl hydrocarbon receptor is a cytoplasmic receptor of several low-molecular-weight exogenous and endogenous molecules that can control bone homeostasis by regulating osteoclast differentiation through the RANKL/AhR/c-Fos signaling axis (Izawa et al., 2016). Exposure to TCDD (the most widely known exogenous AhR ligand) weakens the mechanical strength of bone, hardens the bone matrix and makes the cortical bone thinner and looser in wild-type mice, but these effects are diminished in AhR-knockout mice (Herlin et al., 2013). In addition, AhR-knockout mice exhibit decreased bone resorption and increased bone mass. Kynurenine has been identified as an endogenous AhR agonist (Opitz et al., 2011). Kalaska et al. (2017) observed that the level of peripheral kynurenine is negatively correlated with bone biomechanical variables, bone geometric variables and bone mineral density, and that high peripheral kynurenine levels cause pathological changes in bone microstructure and strength through the AhR pathway in CKD rats that had undergone subtotal nephrectomy.

AhR and Cognitive Dysfunction

The severity of cognitive impairment varies from mild cognitive impairment to severe dementia and is characterized by the loss of independence in daily activities (American Psychiatric Association, 2013). Cognitive impairment may already be present during the early stages of CKD, and it becomes more severe as CKD progresses (Bugnicourt et al., 2013; Brodski et al., 2019). In a 6-year longitudinal study conducted in the general population, the impact of CKD on the risk of mild cognitive impairment and dementia exceeded the impacts of long-term use of anti-anxiety drugs, stroke or genetic factors (Lipnicki et al., 2017).

Factors such as white matter damage, asymptomatic infarction and microhaemorrhages may be involved in cognitive impairment (Bugnicourt et al., 2013), but vascular injury is the basic factor underlying all these pathological manifestations. AhR is thought to play an essential role in the vascular dysfunctions seen in patients with cardiovascular disease.

Aryl hydrocarbon receptor is expressed in the cerebral cortex, hippocampus, cerebellum and other sites of the brain (Lin et al., 2008), and the receptor is thought to be associated with cognitive dysfunction caused by oxidative stress or excitotoxicity (Kim and Yang, 2005; Williamson et al., 2005). Walker et al. (2020) found that activated AhR in brain microvascular endothelial cells in CKD models induced by adenine and IS treatment (in an uremic environment) plays a role in the biology and pathology of central nervous system endothelium. An increase in the production of reactive oxygen species (ROS) aggravates inflammation in patients with neurodegenerative diseases (Hsieh and Yang, 2013). In Adesso's study, increased expression of AhR in primary astrocytes and mixed glial cells was found after IS treatment; in addition, ROS production was significantly reduced after the addition of an AhR inhibitor, showing that the AhR/ROS pathway is activated by IS in the central nervous system of patients with CKD (Adesso et al., 2018).

AhR and Protein Energy Waste (PEW)

Protein energy waste (PEW) is a common complication with adverse consequences in patients with CKD. PEW is characterized by the gradual loss of protein and energy fuels stored in the body (i.e., body muscle and fat mass) (Ikizler et al., 2013). The loss of body muscle mass is caused by many factors, including insufficient energy and protein intake, protein loss in the urine and chronic inflammation (Carrero et al., 2013).

Enoki et al. (2016) demonstrated that IS activates the AhR/NADPH oxidase/NF-κB pathway, leading to increased ROS production, which then triggers the production of inflammatory markers and increases the expression of atrogin-1, myostatin, IL-6 and TNF-α to cause muscle atrophy. AhR inhibitors (e.g., CH-223191) and AhR-siRNA significantly inhibit the production of inflammatory cytokines (ROS and atrophy-related genes in C2C12 myoblasts), suggesting that the activation of AhR in cells is associated with muscle atrophy (Enoki et al., 2016).

AhR and Drug Metabolism

Patients with CKD have high rates of complications and comorbidities. Thus, they require the prescription of numerous medications. However, the pharmacokinetics of drugs in these patients are changed by the uremic environment, making drug dosage adjustments challenging and drug-related adverse events frequent. However, the cellular and molecular mechanisms involved remain unclear. There are more than 200 P450 proteins, and AhR signaling regulates three of them (CYP1B1, CYP1A1,

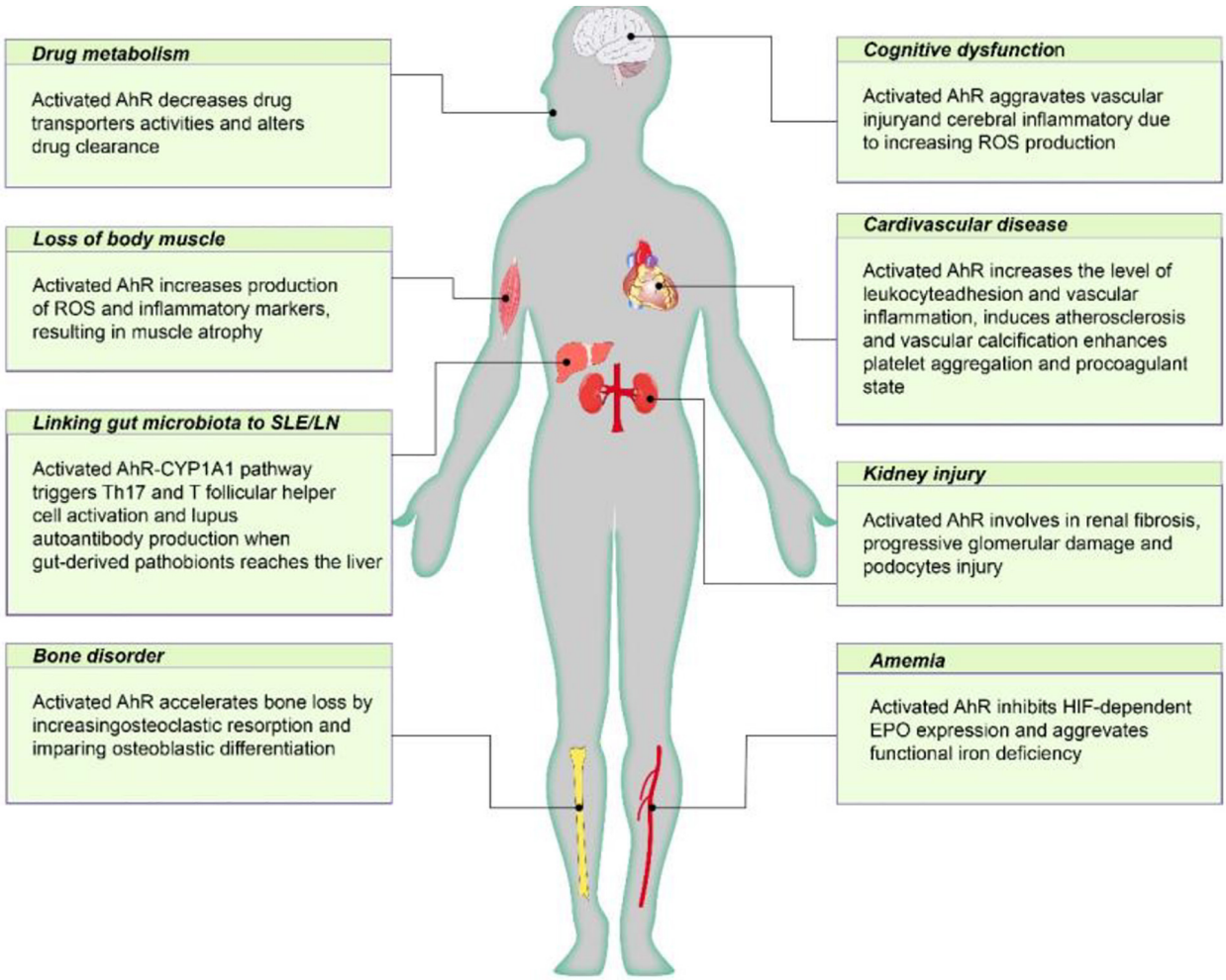

FIGURE 2 | The negative effect of AhR poses on CKD individuals. Active AhR aggravates renal damage, mediates various CKD complications, including cardiovascular disease, anemia, bone disorders, cognitive dysfunction, protein energy wasting, and influences drug metabolism. AhR, aryl hydrocarbon receptor; Cyp1A1, cytochrome P450; family 1, member 1A; EPO, erythropoietin; HIF, hypoxia inducible factor; ROS, reactive oxygen species.

and CYP1A2) (Fujii-Kuriyama and Mimura, 2005). Mutsaers et al. (2015a) showed that uremic toxins reduce the activity of some drug transporters. Santana et al. (2018) proved that IS affects the blood levels of cyclosporine by regulating transport proteins such as P-glycoprotein through AhR activation. Therefore, AhR seems to be associated with the altered drug clearance seen in CKD. The regulation of AhR activity may be a target for improving drug clearance in patients with CKD.

AHR ENHANCES INTESTINAL BARRIER FUNCTION

As discussed above, AhR mediates renal damage and CKD complications and seems to be harmful in CKD patients (**Figure 2**). However, AhR is thought to play an active role in intestinal homeostasis (**Figure 3**). AhR was found to be expressed in almost all colonic muscularis layers, whereas it was absent from the duodenal and jejunal muscular layers. At the same time, only relatively weak signals were detected in ileum terminal neurons, suggesting that AhR expression in intestinal neurons is synchronous with the intestinal microbial load (Obata et al., 2020). AhR influences different aspects of intestinal barrier function. First, AhR is considered important for specific monitoring pathways of the intestinal nervous system that regulate intestinal responses to colonization, the maintenance of intestinal functions and host defenses (Obata et al., 2020). Therefore, pharmacological or dietary interventions that modulate AhR activity in the cellular circuitry to control intestinal peristalsis offer a realistic strategy for the management of conditions associated with gut dysmotility, including the constipation due to slow colonic transit common in patients with CKD.

In addition to the role of AhR in neurogenic motility, AhR-dependent transcriptional procedures are also essential for the barrier function of intestinal epithelial cells (IECs)

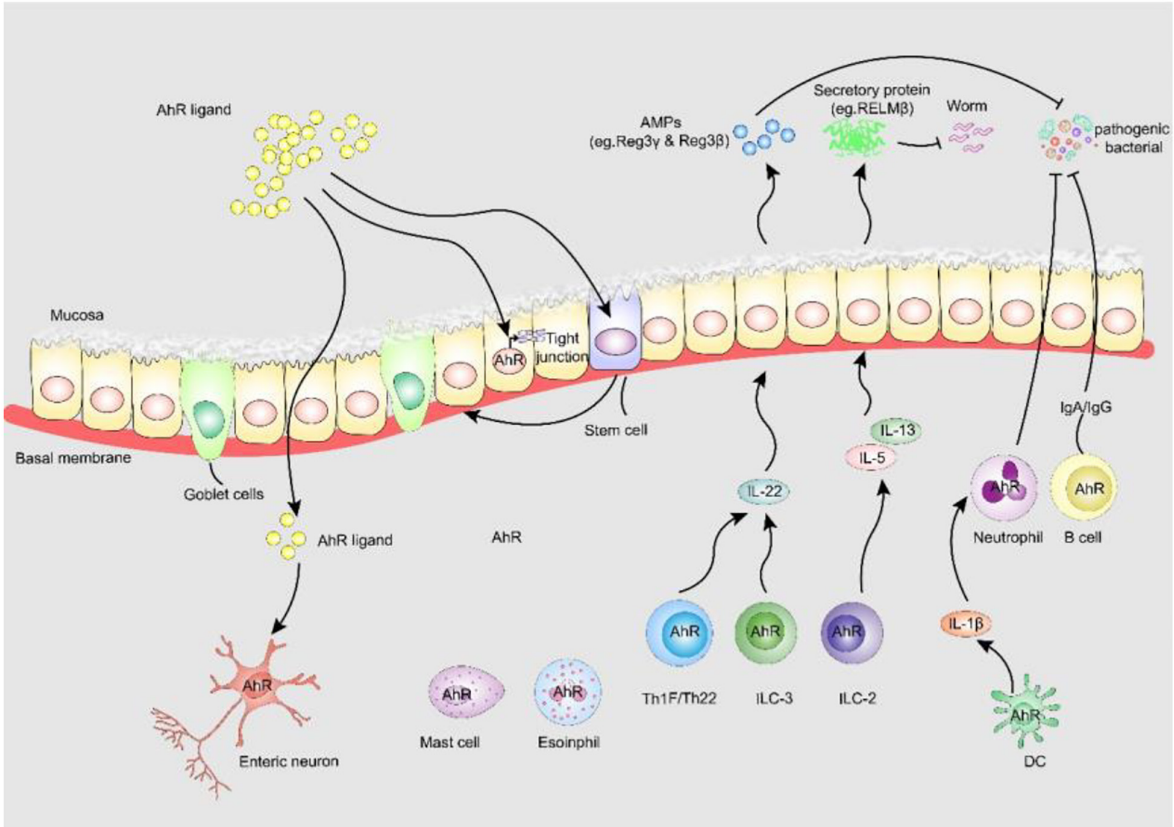

FIGURE 3 | AhR enhances intestinal barrier function. (i) AhR is identified as fulcrum of an enteric nervous system-specific surveillance pathway that regulates intestinal peristalsis in response to microbial colonization, maintaining gut homeostasis and host defense. (ii) AHR in ISC stabilizes gut epithelial barrier function and controls the regeneration of gut ILEs. (iii) AhR upregulates epithelial tight junction protein the tight junction between IECs. (iv) AhR is expressed by many adaptive and innate immune cells in the lamina propria, including macrophages, mast cells, eosinophils, DCs, B cells and T cells, AhR signaling is pivotal to the regulation of mucosal intestinal immune responses. AhR, aryl hydrocarbon receptor; AMPs, anti-microbial peptides; RELM-β, resistin-like molecule β; Reg3-γ, regenerating Islet Derived Protein-γ; Reg3-β, regenerating Islet Derived Protein-β.

(Metidji et al., 2018; Rothhammer and Quintana, 2019). AhR in intestinal stem cells stabilizes intestinal epithelial barrier function and controls the regeneration of IECs. Lack of IEC-specific AhR results in the failure to protect against *Citrobacter rodentium* infection due to reduced quantities of mucus-producing goblet cells (Metidji et al., 2018). AhR activation by dietary ligands may restore barrier homeostasis and protect the stem cell niche. Furthermore, AhR can upregulate epithelial tight junctions. 6-formylindolo[3,2-b]carbazole (FICZ), a high-affinity endogenous ligand of AhR, prevents the decrease of ZO-1, occludin and claudin-1 to modulate intestinal epithelial barrier function in dextran sulfate sodium-induced IECs (Yu et al., 2018). A metabolite of *Lactobacillus*, indole-3-aldehyde, stimulates lamina propria lymphocytes to secrete AhR/IL-22 pathway products and induces the phosphorylation of STAT3 to accelerate intestinal epithelial proliferation, thereby healing damaged intestinal mucosae (Hou et al., 2018).

Furthermore, the expression of AhR by many adaptive and innate immune cells in the lamina propria, including macrophages, mast cells, eosinophils, dendritic cells (DCs), B cells and T cells, suggests that AhR signaling is essential for the regulation of intestinal mucosal immune responses. DCs are prototypic targets of environmental exposure and endogenous AhR ligands (Quintana et al., 2015). Macrophages and DCs produce high levels of IL-1β, which promotes neutrophil recruitment and pathogen elimination. AhR is also essential for the function of innate lymphoid cells (ILCs) and Th17/Th22 cells that control symbiosis and pathogens through IL-22-pSTAT3 (Wang et al., 2014; Piccinni et al., 2019) and mediate the production of antimicrobial peptides by IECs (Sonnenberg et al., 2011). Antimicrobial peptides can also participate in colonization resistance against pathogens by shaping the microbiota, which compete with pathogens for nutrients. Genetic AhR ablation enhances gut ILC2 function during anti-helminth immunity, and cell-specific activation of AhR enhances gut ILC3 function for anti-bacterial immunity, suggesting the central role of AhR expression for gut adaptation and ILC2-ILC3 balance (Li et al., 2018).

Since Meijers proposed the existence of a gut-kidney axis (Meijers and Evenepoel, 2011), some studies have discovered that damage to the gut barrier function induced by intestinal dysbiosis in CKD allows the translocation of endotoxin and

bacterial metabolites into the circulation, which causes uremic toxicity, inflammation, CKD progression and cardiovascular disease (Meijers et al., 2019). As our understanding of the association between the gut and the kidney continues to grow, various therapies targeting the colonic microenvironment in CKD have been developed, such as regulating gut microbiota, blocking lipopolysaccharides, attenuating inflammation or targeting uremic toxin end-products of microbial fermentation (Ramezani and Raj, 2014). Although few therapies target AhR to improve intestinal barrier function in patients with CKD, the potential exists to uncover many novel avenues to delay CKD progress; for example, baicalein, a flavonoid from *Scutellaria baicalensis* used in Chinese herbal medicine, induces regulatory T-cell differentiation through AhR and enhances intestinal barrier function through its regulation of tight junctions in a mouse model of food allergies (Bae et al., 2016).

CONCLUDING REMARKS

Initial studies on AhR were focused on its role as a chemical sensor signaling molecule responding to environment pollutants, but the range of subjects researched has gradually expanded to include diseases such as cancer and cardiovascular and kidney disorders. AhR mediates CKD progression and its complications, including cardiovascular disease, anemia, bone disorders, cognitive dysfunction and malnutrition, and it affects the drug metabolism of individuals with CKD. On the other hand, AhR enhances intestinal barrier function and reduces the harmful effects of uremic toxins. Therefore, whether AhR helps patients with CKD to deal with the pathological changes they face or increases their risk for pathologic complications remains unclear. Based on the available data, we could not draw a definite conclusion about a positive role for AhR in intestinal homeostasis, but we know that it mediates renal damage and CKD complications outside the gastrointestinal tract. AhR-mediated detoxification mechanisms stimulate the clearance of endobiotics and xenobiotics by the kidney. AhR may help individuals to survive in changing environments or promote self-recovery during the early stages of disease, but once the normal physiological or protective responses of the AhR pathway are interrupted, the severity of disease increases. Regulating the AhR pathway is without a doubt an attractive treatment strategy for CKD. However, more studies are needed to overcome the interpretation challenges of the current data.

First, AhR ligands have different sources and structures, present diverse receptor affinities and produce different downstream signal transduction effects. Whether a certain type of AhR ligand is beneficial or detrimental under a specific situation needs to be determined. New metabolomics methods are helping researchers to discover, isolate and identify new exogenous and endogenous AhR ligands. An effective AhR ligand may not be able to play a "one size fits all" role throughout the entire CKD treatment process. In fact, even in a single model, an AhR-ligand combination may be temporarily effective in terms of protecting the body, but as the disease progresses, the interaction may turn harmful, or vice versa. In view of the conflicting observations on whether AhR promotes or inhibits inflammation, identifying and developing specific high-affinity AhR ligands to slow down the development of CKD and its complications is difficult. The ligands need to display targeted absorption, distribution, metabolism and excretion characteristics.

Second, a food-as-medicine approach could be used as a strategy based on bioactive nutrients to target the AhR pathway in patients with CKD. Natural bioactive compounds, including galangin, quercetin, kaempferol, resveratrol and dietary metabolites of cruciferous vegetables, are AhR ligands and potential nutritional therapeutic agents that may modulate the expression of pro-inflammatory factors. Suitable diet-derived AhR ligands should be considered during the dietary management of nutrients in patients with CKD, to put the ancient adage of "let food be thy medicine" into practice. Moreover, bioactive nutrients such as flavonoids and polyphenol compounds are widely distributed in natural products such as medicinal plants, tea, fruits and vegetables. In view of the important roles of the above-mentioned compounds in regulating AhR activity, further studies should address the regulation of AhR activity by natural compounds, to reveal their potential as therapeutic agents for CKD and demonstrate their molecular mechanisms.

Third, inducing the organism to produce appropriate AhR ligands is also a potential therapeutic strategy. Both indole-3-pyruvate (IPYA) and IS are derived from gut bacterial metabolism of the essential amino acid tryptophan. IPYA depends on AhR; it protects the intestine against excessive permeability by maintaining the integrity of apical junctional complexes and the associated actin regulatory proteins (Mafra et al., 2020), whereas IS induces intestinal barrier injury by impairing IRF1/DRP1 axis-mediated mitophagy (Huang et al., 2020). Therefore, inhibiting or promoting certain enzyme activities or regulating the intestinal flora for the metabolism of some key substances may induce the production of AhR ligands that are beneficial to the body.

Finally, although AhR is a promising target for clinical applications, most of the knowledge about its physiological and pathological functions in CKD comes from animal models, and the translation of experimental results into clinical applications for patients with CKD is difficult. Therefore, further research is needed to better understand the complex roles AhR plays in individuals with CKD, so as to be able to use it as a safe and effective target for CKD prevention and treatment.

AUTHOR CONTRIBUTIONS

XL: conceptualization. YM, ZL, CJ, and XL: literature search. YM, ZL, and XL: writing, formatting, and figures. LW, CZ, and XL: review and editing. All authors read and approved the final manuscript.

FUNDING

This study was supported by the National Natural Science Foundation of China (No. 81873261).

REFERENCES

Addi, T., Poitevin, S., McKay, N., El Mecherfi, K. E., Kheroua, O., Jourde-Chiche, N., et al. (2019). Mechanisms of tissue factor induction by the uremic toxin indole-3 acetic acid through aryl hydrocarbon receptor/nuclear factor-kappa B signaling pathway in human endothelial cells. *Arch. Toxicol.* 93, 121–136. doi: 10.1007/s00204-018-2328-3

Adesso, S., Paterniti, I., Cuzzocrea, S., Fujioka, M., Autore, G., Magnus, T., et al. (2018). AST-120 reduces neuroinflammation induced by Indoxyl sulfate in Glial cells. *J. Clin. Med.* 7:365. doi: 10.3390/jcm7100365

Alexeev, E. E., Lanis, J. M., Kao, D. J., Campbell, E. L., Kelly, C. J., Battista, K. D., et al. (2018). Microbiota-derived indole metabolites promote human and Murine intestinal homeostasis through regulation of interleukin-10 receptor. *Am. J. Pathol.* 188, 1183–1194. doi: 10.1016/j.ajpath.2018.01.011

Alkhalaf, L. M., and Ryan, K. S. (2015). Biosynthetic manipulation of tryptophan in bacteria: pathways and mechanisms. *Chem. Biol.* 22, 317–328. doi: 10.1016/j.chembiol.2015.02.005

American Psychiatric Association (2013). *Diagnostic and Statistical Manual of Mental Disorders (DSM-5)*. Washington, DC: APA.

Asai, H., Hirata, J., Hirano, A., Hirai, K., Seki, S., and Watanabe-Akanuma, M. (2016). Activation of aryl hydrocarbon receptor mediates suppression of hypoxia-inducible factor-dependent erythropoietin expression by indoxyl sulfate. *Am. J. Physiol. Cell Physiol.* 310, C142–C150.

Asai, H., Hirata, J., and Watanabe-Akanuma, M. (2018). Indoxyl glucuronide, a protein-bound uremic toxin, inhibits hypoxia-inducible factordependent erythropoietin expression through activation of aryl hydrocarbon receptor. *Biochem. Biophys. Res. Commun.* 504, 538–544. doi: 10.1016/j.bbrc.2018.09.018

Assefa, E. G., Yan, Q., Gezahegn, S. B., Salissou, M. T. M., He, S., Wu, N., et al. (2019). Role of resveratrol on indoxyl sulfate-induced endothelial hyperpermeability via Aryl hydrocarbon receptor (AHR)/Src-dependent pathway. *Oxid. Med. Cell. Longev.* 2019:5847040.

Bae, M. J., Shin, H. S., See, H. J., Jung, S. Y., Kwon, D. A., and Shon, D. H. (2016). Baicalein induces CD4(+)Foxp3(+) T cells and enhances intestinal barrier function in a mouse model of food allergy. *Sci. Rep.* 6: 32225.

Bessede, A., Gargaro, M., Pallotta, M. T., Matino, D., Servillo, G., Brunacci, C., et al. (2014). Aryl hydrocarbon receptor control of a disease tolerance defence pathway. *Nature* 511, 184–190.

Bikbov, B., Purcell, C. A., Levey, A. S., Smith, M., Abdoli, A., Abebe, M., et al. (2020). Global, regional, and national burden of chronic kidney disease, 1990–2017: a systematic analysis for the Global Burden of Disease Study 2017. *Lancet* 395, 709–733.

Brodski, J., Rossell, S. L., Castle, D. J., and Tan, E. J. (2019). A systematic review of cognitive impairments associated with kidney failure in adults before natural age-related changes. *J. Int. Neuropsychol. Soc.* 25, 101–114. doi: 10.1017/s1355617718000917

Bugnicourt, J. M., Godefroy, O., Chillon, J. M., Choukroun, G., and Massy, Z. A. (2013). Cognitive disorders and dementia in CKD: the neglected kidney-brain axis. *J. Am. Soc. Nephrol.* 24, 353–363. doi: 10.1681/asn.2012050536

Carrero, J. J., Stenvinkel, P., Cuppari, L., Ikizler, T. A., Kalantar-Zadeh, K., Kaysen, G., et al. (2013). Etiology of the protein-energy wasting syndrome in chronic kidney disease: a consensus statement from the International Society of Renal Nutrition and Metabolism (ISRNM). *J. Ren. Nutr.* 23, 77–90. doi: 10.1053/j.jrn.2013.01.001

Cervenka, I., Agudelo, L. Z., and Ruas, J. L. (2017). Kynurenines: Tryptophan's metabolites in exercise, inflammation, and mental health. *Science* 357:eaaf9794. doi: 10.1126/science.aaf9794

Clarke, G., McKernan, D. P., Gaszner, G., Quigley, E. M., Cryan, J. F., and Dinan, T. G. (2012). A distinct profile of tryptophan metabolism along the kynurenine pathway downstream of toll-like receptor activation in irritable bowel syndrome. *Front. Pharmacol.* 3:90. doi: 10.3389/fphar.2012.00090

Denison, M. S., and Nagy, S. R. (2003). Activation of the aryl hydrocarbon receptor by structurally diverse exogenous and endogenous chemicals. *Annu. Rev. Pharmacol. Toxicol.* 43, 309–334.

Dou, L., Poitevin, S., Sallee, M., Addi, T., Gondouin, B., McKay, N., et al. (2018). Aryl hydrocarbon receptor is activated in patients and mice with chronic kidney disease. *Kidney Int.* 93, 986–999. doi: 10.1016/j.kint.2017.11.010

Dou, L., Sallee, M., Cerini, C., Poitevin, S., Gondouin, B., Jourde-Chiche, N., et al. (2015). The cardiovascular effect of the uremic solute indole-3 acetic acid. *J. Am. Soc. Nephrol.* 26, 876–887. doi: 10.1681/asn.2013121283

Duranton, F., Cohen, G., De Smet, R., Rodriguez, M., Jankowski, J., Vanholder, R., et al. (2012). Normal and pathologic concentrations of uremic toxins. *J. Am. Soc. Nephrol.* 23, 1258–1270. doi: 10.1681/asn.2011121175

Eckers, A., Jakob, S., Heiss, C., Haarmann-Stemmann, T., Goy, C., Brinkmann, V., et al. (2016). The aryl hydrocarbon receptor promotes aging phenotypes across species. *Sci. Rep.* 6:19618.

Enoki, Y., Watanabe, H., Arake, R., Sugimoto, R., Imafuku, T., Tominaga, Y., et al. (2016). Indoxyl sulfate potentiates skeletal muscle atrophy by inducing the oxidative stress-mediated expression of myostatin and atrogin-1. *Sci. Rep.* 6:32084.

Fujii-Kuriyama, Y., and Mimura, J. (2005). Molecular mechanisms of AhR functions in the regulation of cytochrome P450 genes. *Biochem. Biophys. Res. Commun.* 338, 311–317. doi: 10.1016/j.bbrc.2005.08.162

Gondouin, B., Cerini, C., Dou, L., Sallee, M., Duval-Sabatier, A., Pletinck, A., et al. (2013). Indolic uremic solutes increase tissue factor production in endothelial cells by the aryl hydrocarbon receptor pathway. *Kidney Int.* 84, 733–744. doi: 10.1038/ki.2013.133

Gutierrez-Vazquez, C., and Quintana, F. J. (2018). Regulation of the immune response by the Aryl hydrocarbon receptor. *Immunity* 48, 19–33. doi: 10.1016/j.immuni.2017.12.012

Haase, V. H. (2019). ARNT as a novel antifibrotic target in CKD. *Am. J. Kidney Dis.* 73, 281–284. doi: 10.1053/j.ajkd.2018.08.009

Hamano, H., Ikeda, Y., Watanabe, H., Horinouchi, Y., Izawa-Ishizawa, Y., Imanishi, M., et al. (2018). The uremic toxin indoxyl sulfate interferes with iron metabolism by regulating hepcidin in chronic kidney disease. *Nephrol. Dial. Transplant.* 33, 586–597. doi: 10.1093/ndt/gfx252

Heath-Pagliuso, S., Rogers, W. J., Tullis, K., Seidel, S. D., Cenijn, P. H., Brouwer, A., et al. (1998). Activation of the Ah receptor by tryptophan and tryptophan metabolites. *Biochemistry* 37, 11508–11515. doi: 10.1021/bi980087p

Herlin, M., Finnila, M. A., Zioupos, P., Aula, A., Risteli, J., Miettinen, H. M., et al. (2013). New insights to the role of aryl hydrocarbon receptor in bone phenotype and in dioxin-induced modulation of bone microarchitecture and material properties. *Toxicol. Appl. Pharmacol.* 273, 219–226. doi: 10.1016/j.taap.2013.09.002

Hou, Q., Ye, L., Liu, H., Huang, L., Yang, Q., Turner, J. R., et al. (2018). Lactobacillus accelerates ISCs regeneration to protect the integrity of intestinal mucosa through activation of STAT3 signaling pathway induced by LPLs secretion of IL-22. *Cell Death Differ.* 25, 1657–1670. doi: 10.1038/s41418-018-0070-2

Hsieh, H. L., and Yang, C. M. (2013). Role of redox signaling in neuroinflammation and neurodegenerative diseases. *BioMed Res. Int.* 2013:484613.

Huang, Y., Zhou, J., Wang, S., Xiong, J., Chen, Y., Liu, Y., et al. (2020). Indoxyl sulfate induces intestinal barrier injury through IRF1-DRP1 axis-mediated mitophagy impairment. *Theranostics* 10, 7384–7400. doi: 10.7150/thno.45455

Hubbard, T. D., Murray, I. A., and Perdew, G. H. (2015). Indole and tryptophan metabolism: endogenous and dietary routes to Ah receptor activation. *Drug Metab. Dispos.* 43, 1522–1535. doi: 10.1124/dmd.115.064246

Humblet, O., Birnbaum, L., Rimm, E., Mittleman, M. A., and Hauser, R. (2008). Dioxins and cardiovascular disease mortality. *Environ. Health Perspect.* 116, 1443–1448. doi: 10.1289/ehp.11579

Ichii, O., Otsuka-Kanazawa, S., Nakamura, T., Ueno, M., Kon, Y., Chen, W., et al. (2014). Podocyte injury caused by indoxyl sulfate, a uremic toxin and aryl-hydrocarbon receptor ligand. *PLoS One* 9:e108448. doi: 10.1371/journal.pone.0108448

Ikizler, T. A., Cano, N. J., Franch, H., Fouque, D., Himmelfarb, J., Kalantar-Zadeh, K., et al. (2013). Prevention and treatment of protein energy wasting in chronic kidney disease patients: a consensus statement by the International Society of Renal Nutrition and Metabolism. *Kidney Int.* 84, 1096–1107. doi: 10.1038/ki.2013.147

Ito, S., Osaka, M., Edamatsu, T., Itoh, Y., and Yoshida, M. (2016). Crucial role of the Aryl hydrocarbon receptor (AhR) in indoxyl sulfate-induced vascular inflammation. *J. Atheroscler. Thromb.* 23, 960–975. doi: 10.5551/jat.34462

Izawa, T., Arakaki, R., Mori, H., Tsunematsu, T., Kudo, Y., Tanaka, E., et al. (2016). The nuclear receptor AhR controls bone homeostasis by regulating osteoclast differentiation via the RANK/c-Fos signaling axis. *J. Immunol.* 197, 4639–4650. doi: 10.4049/jimmunol.1600822

Jeuken, A., Keser, B. J., Khan, E., Brouwer, A., Koeman, J., and Denison, M. S. (2003). Activation of the Ah receptor by extracts of dietary herbal supplements, vegetables, and fruits. *J. Agric. Food Chem.* 51, 5478–5487. doi: 10.1021/jf030252u

Kalaska, B., Pawlak, K., Domaniewski, T., Oksztulska-Kolanek, E., Znorko, B., Roszczenko, A., et al. (2017). Elevated levels of peripheral kynurenine decrease bone strength in rats with chronic kidney disease. *Front. Physiol.* 8:836. doi: 10.3389/fphys.2017.00836

Kennedy, P. J., Cryan, J. F., Dinan, T. G., and Clarke, G. (2017). Kynurenine pathway metabolism and the microbiota-gut-brain axis. *Neuropharmacology* 112, 399–412. doi: 10.1016/j.neuropharm.2016.07.002

Kidney Disease: Improving Global Outcomes (KDIGO) CKD-MBD Update Work Group (2017). KDIGO 2017 clinical practice guideline update for the diagnosis, evaluation, prevention, and treatment of chronic kidney disease-mineral and bone disorder (CKD-MBD). *Kidney Int. Suppl.* 7, 1–59. doi: 10.1016/j.kisu.2017.04.001

Kim, J. T., Kim, S. H., Min, H. K., Jeon, S. J., Sung, S. A., Park, W. H., et al. (2020). Effect of dialysis on Aryl hydrocarbon receptor transactivating activity in patients with chronic kidney disease. *Yonsei Med. J.* 61, 56–63.

Kim, J. T., Kim, S. S., Jun, D. W., Hwang, Y. H., Park, W. H., Pak, Y. K., et al. (2013). Serum arylhydrocarbon receptor transactivating activity is elevated in type 2 diabetic patients with diabetic nephropathy. *J. Diabetes Investig.* 4, 483–491. doi: 10.1111/jdi.12081

Kim, S. Y., and Yang, J. H. (2005). Neurotoxic effects of 2,3,7,8-tetrachlorodibenzo-p-dioxin in cerebellar granule cells. *Exp. Mol. Med.* 37, 58–64. doi: 10.1038/emm.2005.8

Kimura, A., Naka, T., Nohara, K., Fujii-Kuriyama, Y., and Kishimoto, T. (2008). Aryl hydrocarbon receptor regulates Stat1 activation and participates in the development of Th17 cells. *Proc. Natl. Acad. Sci. U.S.A.* 105, 9721–9726. doi: 10.1073/pnas.0804231105

Koizumi, M., Tatebe, J., Watanabe, I., Yamazaki, J., Ikeda, T., and Morita, T. (2014). Aryl hydrocarbon receptor mediates indoxyl sulfate-induced cellular senescence in human umbilical vein endothelial cells. *J. Atheroscler. Thromb.* 21, 904–916. doi: 10.5551/jat.23663

Lee, W. J., Liu, S. H., Chiang, C. K., Lin, S. Y., Liang, K. W., Chen, C. H., et al. (2016). Aryl hydrocarbon receptor deficiency attenuates oxidative stress-related mesangial cell activation and macrophage infiltration and extracellular matrix accumulation in diabetic nephropathy. *Antioxid. Redox Signal.* 24, 217–231. doi: 10.1089/ars.2015.6310

Levin, A., Djurdjev, O., Duncan, J., Rosenbaum, D., and Werb, R. (2006). Haemoglobin at time of referral prior to dialysis predicts survival: an association of haemoglobin with long-term outcomes. *Nephrol. Dial. Transplant.* 21, 370–377. doi: 10.1093/ndt/gfi209

Li, S., Bostick, J. W., Ye, J., Qiu, J., Zhang, B., Urban, J. F. Jr., et al. (2018). Aryl hydrocarbon receptor signaling cell intrinsically inhibits intestinal group 2 innate lymphoid cell function. *Immunity* 49, 915–928.e5.

Lin, C. H., Juan, S. H., Wang, C. Y., Sun, Y. Y., Chou, C. M., Chang, S. F., et al. (2008). Neuronal activity enhances aryl hydrocarbon receptor-mediated gene expression and dioxin neurotoxicity in cortical neurons. *J. Neurochem.* 104, 1415–1429. doi: 10.1111/j.1471-4159.2007.05098.x

Lindsey, S., Jiang, J., Woulfe, D., and Papoutsakis, E. T. (2014). Platelets from mice lacking the aryl hydrocarbon receptor exhibit defective collagen-dependent signaling. *J. Thromb. Haemost.* 12, 383–394. doi: 10.1111/jth.12490

Lindsey, S., and Papoutsakis, E. T. (2011). The aryl hydrocarbon receptor (AHR) transcription factor regulates megakaryocytic polyploidization. *Br. J. Haematol.* 152, 469–484. doi: 10.1111/j.1365-2141.2010.08548.x

Lipnicki, D. M., Crawford, J., Kochan, N. A., Trollor, J. N., Draper, B., Reppermund, S., et al. (2017). Risk factors for mild cognitive impairment, dementia and mortality: the sydney memory and ageing study. *J. Am. Med. Dir. Assoc.* 18, 388–395.

Lowenstein, J. (2014). Agent Orange and heart disease: Is there a connection? *FASEB J.* 28, 1531–1533. doi: 10.1096/fj.14-0402ufm

Lu, H., Lei, X., and Klaassen, C. (2006). Gender differences in renal nuclear receptors and aryl hydrocarbon receptor in 5/6 nephrectomized rats. *Kidney Int.* 70, 1920–1928. doi: 10.1038/sj.ki.5001880

Mafra, D., Borges, N. A., Lindholm, B., Shiels, P. G., Evenepoel, P., and Stenvinkel, P. (2020). Food as medicine: targeting the uraemic phenotype in chronic kidney disease. *Nat. Rev. Nephrol.* doi: 10.1038/s41581-020-00345-8 [Epub ahead of print].

Manfredo Vieira, S., Hiltensperger, M., Kumar, V., Zegarra-Ruiz, D., Dehner, C., Khan, N., et al. (2018). Translocation of a gut pathobiont drives autoimmunity in mice and humans. *Science* 359, 1156–1161. doi: 10.1126/science.aar7201

Mascanfroni, I. D., Takenaka, M. C., Yeste, A., Patel, B., Wu, Y., Kenison, J. E., et al. (2015). Metabolic control of type 1 regulatory T cell differentiation by AHR and HIF1-alpha. *Nat. Med.* 21, 638–646. doi: 10.1038/nm.3868

McIntosh, B. E., Hogenesch, J. B., and Bradfield, C. A. (2010). Mammalian Per-Arnt-Sim proteins in environmental adaptation. *Annu. Rev. Physiol.* 72, 625–645. doi: 10.1146/annurev-physiol-021909-135922

Meijers, B., Evenepoel, P., and Anders, H. J. (2019). Intestinal microbiome and fitness in kidney disease. *Nat. Rev. Nephrol.* 15, 531–545. doi: 10.1038/s41581-019-0172-1

Meijers, B. K., and Evenepoel, P. (2011). The gut-kidney axis: indoxyl sulfate, p-cresyl sulfate and CKD progression. *Nephrol. Dial. Transplant.* 26, 759–761. doi: 10.1093/ndt/gfq818

Metidji, A., Omenetti, S., Crotta, S., Li, Y., Nye, E., Ross, E., et al. (2018). The environmental sensor AHR protects from inflammatory damage by maintaining intestinal stem cell homeostasis and barrier integrity. *Immunity* 49, 353–362.e5.

Mohammadi, S., Seyedhosseini, F. S., Behnampour, N., and Yazdani, Y. (2017). Indole-3-carbinol induces G1 cell cycle arrest and apoptosis through aryl hydrocarbon receptor in THP-1 monocytic cell line. *J. Recept. Signal Transduct. Res.* 37, 506–514. doi: 10.1080/10799893.2017.1360351

Mohanram, A., Zhang, Z., Shahinfar, S., Keane, W. F., Brenner, B. M., and Toto, R. D. (2004). Anemia and end-stage renal disease in patients with type 2 diabetes and nephropathy. *Kidney Int.* 66, 1131–1138. doi: 10.1111/j.1523-1755.2004.00863.x

Murray, I. A., Patterson, A. D., and Perdew, G. H. (2014). Aryl hydrocarbon receptor ligands in cancer: friend and foe. *Nat. Rev. Cancer* 14, 801–814. doi: 10.1038/nrc3846

Mutsaers, H. A., Caetano-Pinto, P., Seegers, A. E., Dankers, A. C., van den Broek, P. H., Wetzels, J. F., et al. (2015a). Proximal tubular efflux transporters involved in renal excretion of p-cresyl sulfate and p-cresyl glucuronide: implications for chronic kidney disease pathophysiology. *Toxicol. In Vitro* 29, 1868–1877. doi: 10.1016/j.tiv.2015.07.020

Mutsaers, H. A., Stribos, E. G., Glorieux, G., Vanholder, R., and Olinga, P. (2015b). Chronic kidney disease and fibrosis: the role of uremic retention solutes. *Front. Med.* 2:60. doi: 10.3389/fmed.2015.00060

Nemeth, E., Tuttle, M. S., Powelson, J., Vaughn, M. B., Donovan, A., Ward, D. M., et al. (2004). Hepcidin regulates cellular iron efflux by binding to ferroportin and inducing its internalization. *Science* 306, 2090–2093. doi: 10.1126/science.1104742

Ng, H. Y., Yisireyili, M., Saito, S., Lee, C. T., Adelibieke, Y., Nishijima, F., et al. (2014). Indoxyl sulfate downregulates expression of Mas receptor via OAT3/AhR/Stat3 pathway in proximal tubular cells. *PLoS One* 9:e91517. doi: 10.1371/journal.pone.0091517

Nihei, T., Miura, Y., and Yagasaki, K. (2001). Inhibitory effect of resveratrol on proteinuria, hypoalbuminemia and hyperlipidemia in nephritic rats. *Life Sci.* 68, 2845–2852. doi: 10.1016/s0024-3205(01)01061-x

Obata, Y., Castano, A., Boeing, S., Bon-Frauches, A. C., Fung, C., Fallesen, T., et al. (2020). Neuronal programming by microbiota regulates intestinal physiology. *Nature* 578, 284–289. doi: 10.1038/s41586-020-1975-8

Ochi, A., Mori, K., Nakatani, S., Emoto, M., Morioka, T., Motoyama, K., et al. (2015). Indoxyl sulfate suppresses hepatic fetuin-A expression via the aryl hydrocarbon receptor in HepG2 cells. *Nephrol. Dial. Transplant.* 30, 1683–1692. doi: 10.1093/ndt/gfv250

Opitz, C. A., Litzenburger, U. M., Sahm, F., Ott, M., Tritschler, I., Trump, S., et al. (2011). An endogenous tumour-promoting ligand of the human aryl hydrocarbon receptor. *Nature* 478, 197–203. doi: 10.1038/nature10491

Park, C. H., Valore, E. V., Waring, A. J., and Ganz, T. (2001). Hepcidin, a urinary antimicrobial peptide synthesized in the liver. *J. Biol. Chem.* 276, 7806–7810. doi: 10.1074/jbc.m008922200

Piccinni, M. P., Lombardelli, L., Logiodice, F., Kullolli, O., Maggi, E., and Barkley, M. S. (2019). Medroxyprogesterone acetate decreases Th1, Th17, and increases Th22 responses via AHR signaling which could affect susceptibility to infections

and inflammatory disease. *Front. Immunol.* 10, 642. doi: 10.3389/fimmu.2019.00642

Pollenz, R. S. (2002). The mechanism of AH receptor protein down-regulation (degradation) and its impact on AH receptor-mediated gene regulation. *Chem. Biol. Interact.* 141, 41–61. doi: 10.1016/s0009-2797(02)00065-0

Pombo, M., Lame, M. W., Walker, N. J., Huynh, D. H., and Tablin, F. (2015). TCDD and omeprazole prime platelets through the aryl hydrocarbon receptor (AhR) non-genomic pathway. *Toxicol. Lett.* 235, 28–36. doi: 10.1016/j.toxlet.2015.03.005

Pongratz, I., Mason, G. G., and Poellinger, L. (1992). Dual roles of the 90-kDa heat shock protein hsp90 in modulating functional activities of the dioxin receptor. Evidence that the dioxin receptor functionally belongs to a subclass of nuclear receptors which require hsp90 both for ligand binding activity and repression of intrinsic DNA binding activity. *J. Biol. Chem.* 267, 13728–13734.

Puga, A., Ma, C., and Marlowe, J. L. (2009). The aryl hydrocarbon receptor cross-talks with multiple signal transduction pathways. *Biochem. Pharmacol.* 77, 713–722. doi: 10.1016/j.bcp.2008.08.031

Quintana, F. J., Yeste, A., and Mascanfroni, I. D. (2015). Role and therapeutic value of dendritic cells in central nervous system autoimmunity. *Cell Death Differ.* 22, 215–224. doi: 10.1038/cdd.2014.125

Ramezani, A., and Raj, D. S. (2014). The gut microbiome, kidney disease, and targeted interventions. *J. Am. Soc. Nephrol.* 25, 657–670. doi: 10.1681/asn.2013080905

Refaey, M. E., McGee-Lawrence, M. E., Fulzele, S., Kennedy, E. J., Bollag, W. B., Elsalanty, M., et al. (2017). Kynurenine, a tryptophan metabolite that accumulates with age, induces bone loss. *J. Bone Miner. Res.* 32, 2182–2193. doi: 10.1002/jbmr.3224

Rothhammer, V., and Quintana, F. J. (2019). The aryl hydrocarbon receptor: an environmental sensor integrating immune responses in health and disease. *Nat. Rev. Immunol.* 19, 184–197. doi: 10.1038/s41577-019-0125-8

Sallee, M., Dou, L., Cerini, C., Poitevin, S., Brunet, P., and Burtey, S. (2014). The aryl hydrocarbon receptor-activating effect of uremic toxins from tryptophan metabolism: a new concept to understand cardiovascular complications of chronic kidney disease. *Toxins* 6, 934–949. doi: 10.3390/toxins6030934

Santana, M. T., Poitevin, S., Paul, P., McKay, N., Jourde-Chiche, N., Legris, T., et al. (2018). Indoxyl sulfate upregulates liver P-glycoprotein expression and activity through aryl hydrocarbon receptor signaling. *J. Am. Soc. Nephrol.* 29, 906–918.

Schroeder, J. C., Dinatale, B. C., Murray, I. A., Flaveny, C. A., Liu, Q., Laurenzana, E. M., et al. (2010). The uremic toxin 3-indoxyl sulfate is a potent endogenous agonist for the human aryl hydrocarbon receptor. *Biochemistry* 49, 393–400. doi: 10.1021/bi901786x

Shivanna, S., Kolandaivelu, K., Shashar, M., Belghasim, M., Al-Rabadi, L., Balcells, M., et al. (2016). The Aryl hydrocarbon receptor is a critical regulator of tissue factor stability and an antithrombotic target in uremia. *J. Am. Soc. Nephrol.* 27, 189–201. doi: 10.1681/asn.2014121241

Singh, R., Chandrashekharappa, S., Bodduluri, S. R., Baby, B. V., Hegde, B., Kotla, N. G., et al. (2019). Enhancement of the gut barrier integrity by a microbial metabolite through the Nrf2 pathway. *Nat. Commun.* 10:89.

Sirich, T. L. (2017). Obstacles to reducing plasma levels of uremic solutes by hemodialysis. *Semin. Dial.* 30, 403–408. doi: 10.1111/sdi.12609

Sonnenberg, G. F., Fouser, L. A., and Artis, D. (2011). Border patrol: regulation of immunity, inflammation and tissue homeostasis at barrier surfaces by IL-22. *Nat. Immunol.* 12, 383–390. doi: 10.1038/ni.2025

Soshilov, A., and Denison, M. S. (2008). Role of the Per/Arnt/Sim domains in ligand-dependent transformation of the aryl hydrocarbon receptor. *J. Biol. Chem.* 283, 32995–33005. doi: 10.1074/jbc.m802414200

Souma, T., Nezu, M., Nakano, D., Yamazaki, S., Hirano, I., Sekine, H., et al. (2016). Erythropoietin synthesis in renal myofibroblasts is restored by activation of hypoxia signaling. *J. Am. Soc. Nephrol.* 27, 428–438. doi: 10.1681/asn.2014121184

Souma, T., Suzuki, N., and Yamamoto, M. (2015). Renal erythropoietin-producing cells in health and disease. *Front. Physiol.* 6:167. doi: 10.3389/fphys.2015.00167

Souma, T., Yamazaki, S., Moriguchi, T., Suzuki, N., Hirano, I., Pan, X., et al. (2013). Plasticity of renal erythropoietin-producing cells governs fibrosis. *J. Am. Soc. Nephrol.* 24, 1599–1616. doi: 10.1681/asn.2013010030

Strassel, C., Brouard, N., Mallo, L., Receveur, N., Mangin, P., Eckly, A., et al. (2016). Aryl hydrocarbon receptor-dependent enrichment of a megakaryocytic precursor with a high potential to produce proplatelets. *Blood* 127, 2231–2240. doi: 10.1182/blood-2015-09-670208

Tampe, B., Tampe, D., Nyamsuren, G., Klopper, F., Rapp, G., Kauffels, A., et al. (2018). Pharmacological induction of hypoxia-inducible transcription factor ARNT attenuates chronic kidney failure. *J. Clin. Investig.* 128, 3053–3070. doi: 10.1172/jci89632

Vanholder, R., Fouque, D., Glorieux, G., Heine, G. H., Kanbay, M., Mallamaci, F., et al. (2016). Clinical management of the uraemic syndrome in chronic kidney disease. *Lancet Diabetes Endocrinol.* 4, 360–373.

Vanholder, R., and Glorieux, G. (2014). Introduction: uremic toxicity - state of the Art 2014. *Semin. Nephrol.* 34, 85–86. doi: 10.1016/j.semnephrol.2014.02.001

Vidal, C., Li, W., Santner-Nanan, B., Lim, C. K., Guillemin, G. J., Ball, H. J., et al. (2015). The kynurenine pathway of tryptophan degradation is activated during osteoblastogenesis. *Stem Cells* 33, 111–121. doi: 10.1002/stem.1836

Wakamatsu, T., Yamamoto, S., Ito, T., Sato, Y., Matsuo, K., Takahashi, Y., et al. (2018). Indoxyl sulfate promotes macrophage IL-1beta production by activating Aryl hydrocarbon receptor/NF-kappa/MAPK cascades, but the NLRP3 inflammasome Was Not Activated. *Toxins* 10:124. doi: 10.3390/toxins10030124

Walker, J. A., Richards, S., Belghasem, M. E., Arinze, N., Yoo, S. B., Tashjian, J. Y., et al. (2020). Temporal and tissue-specific activation of aryl hydrocarbon receptor in discrete mouse models of kidney disease. *Kidney Int.* 97, 538–550. doi: 10.1016/j.kint.2019.09.029

Wang, G. Z., Zhang, L., Zhao, X. C., Gao, S. H., Qu, L. W., Yu, H., et al. (2019). The Aryl hydrocarbon receptor mediates tobacco-induced PD-L1 expression and is associated with response to immunotherapy. *Nat. Commun.* 10:1125.

Wang, X., Ota, N., Manzanillo, P., Kates, L., Zavala-Solorio, J., Eidenschenk, C., et al. (2014). Interleukin-22 alleviates metabolic disorders and restores mucosal immunity in diabetes. *Nature* 514, 237–241. doi: 10.1038/nature13564

Watanabe, I., Tatebe, J., Namba, S., Koizumi, M., Yamazaki, J., and Morita, T. (2013). Activation of aryl hydrocarbon receptor mediates indoxyl sulfate-induced monocyte chemoattractant protein-1 expression in human umbilical vein endothelial cells. *Circ. J.* 77, 224–230. doi: 10.1253/circj.cj-12-0647

Williamson, M. A., Gasiewicz, T. A., and Opanashuk, L. A. (2005). Aryl hydrocarbon receptor expression and activity in cerebellar granule neuroblasts: implications for development and dioxin neurotoxicity. *Toxicol. Sci.* 83, 340–348. doi: 10.1093/toxsci/kfi031

Xia, J., Lin, J., Li, X. N., Zhang, C., Li, N., Du, Z. H., et al. (2018). Atrazine-induced environmental nephrosis was mitigated by lycopene via modulating nuclear xenobiotic receptors-mediated response. *J. Nutr. Biochem.* 51, 80–90. doi: 10.1016/j.jnutbio.2017.09.006

Yano, J. M., Yu, K., Donaldson, G. P., Shastri, G. G., Ann, P., Ma, L., et al. (2015). Indigenous bacteria from the gut microbiota regulate host serotonin biosynthesis. *Cell* 161, 264–276. doi: 10.1016/j.cell.2015.02.047

Yu, M., Wang, Q., Ma, Y., Li, L., Yu, K., Zhang, Z., et al. (2018). Aryl hydrocarbon receptor activation modulates intestinal epithelial barrier function by maintaining tight junction integrity. *Int. J. Biol. Sci.* 14, 69–77. doi: 10.7150/ijbs.22259

Zaher, H., Fernandez-Salguero, P. M., Letterio, J., Sheikh, M. S., Fornace, A. J. Jr., Roberts, A. B., et al. (1998). The involvement of aryl hydrocarbon receptor in the activation of transforming growth factor-beta and apoptosis. *Mol. Pharmacol.* 54, 313–321. doi: 10.1124/mol.54.2.313

Zelante, T., Iannitti, R. G., Cunha, C., De Luca, A., Giovannini, G., Pieraccini, G., et al. (2013). Tryptophan catabolites from microbiota engage aryl hydrocarbon receptor and balance mucosal reactivity via interleukin-22. *Immunity* 39, 372–385. doi: 10.1016/j.immuni.2013.08.003

Zhao, B., Bohonowych, J. E., Timme-Laragy, A., Jung, D., Affatato, A. A., Rice, R. H., et al. (2013). Common commercial and consumer products contain activators of the aryl hydrocarbon (dioxin) receptor. *PLoS One* 8:e56860. doi: 10.1371/journal.pone.0056860

Conflict of Interest: The authors declare that the research was conducted in the absence of any commercial or financial relationships that could be construed as a potential conflict of interest.

Copyright © 2020 Mo, Lu, Wang, Ji, Zou and Liu. This is an open-access article distributed under the terms of the Creative Commons Attribution License (CC BY). The use, distribution or reproduction in other forums is permitted, provided the original author(s) and the copyright owner(s) are credited and that the original publication in this journal is cited, in accordance with accepted academic practice. No use, distribution or reproduction is permitted which does not comply with these terms.

frontiers in Cell and Developmental Biology

ORIGINAL RESEARCH
published: 15 January 2021
doi: 10.3389/fcell.2020.602703

Transient Receptor Potential Channel 6 Knockout Ameliorates Kidney Fibrosis by Inhibition of Epithelial–Mesenchymal Transition

Yanhong Zhang [1,2,3†], Nina Yin [1,2†], Anbang Sun [1,3], Qifang Wu [1,3], Wenzhu Hu [1,3], Xin Hou [1,3], Xixi Zeng [1,3], Min Zhu [4] and Yanhong Liao [1,3*]*

[1] Department of Anatomy, Tongji Medical College, Huazhong University of Science and Technology, Wuhan, China, [2] Department of Anatomy, College of Basic Medicine, Hubei University of Chinese Medicine, Wuhan, China, [3] Key Laboratory of Neurological Diseases of Ministry of Education, Tongji Medical College, Huazhong University of Science and Technology, Wuhan, China, [4] Department of Thoracic Surgery, Tongji Hospital, Tongji Medical College, Huazhong University of Science and Technology, Wuhan, China

OPEN ACCESS

Edited by:
Samar Abd ElHafeez,
Alexandria University, Egypt

Reviewed by:
Guoping Zheng,
The University of Sydney, Australia
Rossana Morabito,
University of Messina, Italy

***Correspondence:**
Yanhong Liao
yhliao1@hust.edu.cn
Min Zhu
mzhu@tjh.tjmu.edu.cn

[†] These authors have contributed equally to this work

Specialty section:
This article was submitted to Molecular Medicine, a section of the journal Frontiers in Cell and Developmental Biology

Received: 04 September 2020
Accepted: 30 November 2020
Published: 15 January 2021

Citation:
Zhang Y, Yin N, Sun A, Wu Q, Hu W, Hou X, Zeng X, Zhu M and Liao Y (2021) Transient Receptor Potential Channel 6 Knockout Ameliorates Kidney Fibrosis by Inhibition of Epithelial–Mesenchymal Transition. Front. Cell Dev. Biol. 8:602703. doi: 10.3389/fcell.2020.602703

Kidney fibrosis is generally confirmed to have a significant role in chronic kidney disease, resulting in end-stage kidney failure. Epithelial–mesenchymal transition (EMT) is an important molecular mechanism contributing to fibrosis. Tubular epithelial cells (TEC), the major component of kidney parenchyma, are vulnerable to different types of injuries and are a significant source of myofibroblast by EMT. Furthermore, TRPC6 knockout plays an anti-fibrotic role in ameliorating kidney damage. However, the relationship between TRPC6 and EMT is unknown. In this study, TRPC6$^{-/-}$ and wild-type (WT) mice were subjected to a unilateral ureteric obstruction (UUO) operation. Primary TEC were treated with TGF-β1. Western blot and immunofluorescence data showed that fibrotic injuries alleviated with the inhibition of EMT in TRPC6$^{-/-}$ mice compared to WT mice. The activation of AKT-mTOR and ERK1/2 pathways was down-regulated in the TRPC6$^{-/-}$ mice, while the loss of Na^+/K^+-ATPase and APQ1 was partially recovered. We conclude that TRPC6 knockout may ameliorate kidney fibrosis by inhibition of EMT through down-regulating the AKT-mTOR and ERK1/2 pathways. This could contribute to the development of effective therapeutic strategies on chronic kidney diseases.

Keywords: EMT, TRPC6, TEC, UUO, kidney fibrosis, TGF-β1

INTRODUCTION

Kidney fibrosis is the end-stage of all progressive chronic kidney diseases, which can be caused by urinary obstruction and may develop into end-stage renal disease (Paniagua-Sierra and Galvan-Plata, 2017). Kidney fibrosis, including interstitial fibrosis, is characterized by proliferation of tubular epithelial cells (TEC) and interstitial cells, loss of glomerular and peritubular capillary architecture, and accumulation of the extracellular matrix (ECM) (Liu, 2011). Furthermore, the reduction of kidney parenchyma function is strongly related to the kidney fibrosis, which leads to compromised kidney insufficiency (Zeisberg and Kalluri, 2013). TEC, the major component of kidney parenchyma, often suffer ill-effects from different types of kidney injuries (Liu, 2004). As such, an increasing number of studies on kidney fibrosis have been devoted to the exploration of TEC.

Previous studies have shown that exploring the complex cellular mediators and molecular mechanisms of kidney fibrosis could offer new treatment avenues for chronic kidney disease (Bechtel et al., 2010; Sugimoto et al., 2012; LeBleu et al., 2013). However, no effective treatment to inhibit the onset or progress of chronic kidney disease has been discovered, and the occurrence of kidney fibrosis is still on the rise. Therefore, further investigation in kidney fibrosis is urgently needed.

In recent years, kidney fibrosis studies have shown that TEC, rather than being victims or bystanders, are likely an originator of the interstitial fibrosis reaction to a variety of injuries (Gewin, 2018; Liu et al., 2018). Importantly, TEC, as a vital source of myofibroblasts, contribute to kidney fibrosis by transitioning cells to mesenchymal characteristics (Iwano et al., 2002; Kalluri and Weinberg, 2009). The process is known as epithelial–mesenchymal transition (EMT) and may be induced by TGF-β1 (Hay, 1995). Many studies have suggested that EMT is a significant process in kidney fibrosis (Lovisa et al., 2015, 2016). Generally speaking, during EMT, epithelial cells lose their junctions, break apical–basal polarity, remodel their cytoskeleton, and experience signal process changes that define cell shape and reset gene expression (Thiery and Sleeman, 2006; Thiery et al., 2009). Epithelial cells then reveal some plasticity and lose epithelial markers such as E-cadherin (E-cad) and Cadherin-16 (Cadh16). Cadh16, as a kidney-specific cadherin, is present in kidney tubular epithelial cells (Grande et al., 2015). Simultaneously, other changes occur, such as the development of spindle-shaped morphology, which is characteristic of mesenchymal cell lines, and the improved producing capacity of extracellular matrix. In addition, during EMT, cells express mesenchymal-related molecular markers, such as α-SMA and vimentin (Radisky et al., 2007; Quaggin and Kapus, 2011), and the transcription factor snail1 is activated, which inhibits the expression of epithelial genes (Barrallo-Gimeno and Nieto, 2005; Peinado et al., 2007; Xu et al., 2009), especially E-cad and Cadh16 (Horikawa et al., 2011; Lin X. et al., 2019).

It is well-known that EMT has been observed in tissue modeling and remodeling (Katz et al., 2002; Coresh et al., 2007) and is integral to embryonic development and the physiopathology mechanism reactivated in wound healing, fibrosis, and cancer progression (Chapman, 2011; Liu et al., 2014; Gewin, 2018). Of note, EMT is triggered by pleiotropic signaling factors, including the TGFβ superfamily, epidermal growth factor (EGF), Sonic Hedgehog (Shh), fibroblast growth factor (FGF), and Wnt/β-catenin. TGF-β1 is an especially powerful inducer of EMT *in vitro* and *in vivo* and has been shown to be important in the activation and maintenance of fibrosis (Tamaki et al., 1994; Eddy, 1996; Holian et al., 2008). Fibrosis were initiated by TGF-β1 through Smad-dependent (canonical) and Smad-independent (non-canonical) pathways. Several Smad-independent pathways were activated in the process of EMT including the phosphatidylinositol-3′-kinase (PI3K), AKT (Pillow et al., 2014), ERK1/2, p38, and Ras- and Rho-GTPases (Moustakas and Heldin, 2005; Zhang, 2018). Furthermore, the AKT-mTOR pathway is activated to produce the transcriptional factor snail1, which can suppress the expression of E-cad in the process of EMT (Grille et al., 2003). ERK1/2 pathway is also activated in EMT and induced by TGF-β1 (Grande et al., 2002; Xie et al., 2004). Appropriate EMT induced by injury is beneficial; however, exaggerated EMT caused by healing can lead to tissue scarring or fibrosis. In addition to findings in experimental animal models, EMT of TEC was also detected in human fibrotic kidneys and was associated with disease progression (Rastaldi, 2006; Hertig et al., 2008).

Transient receptor potential channels (TRPCs) were first observed in *Drosophila*, in which the photoreceptors exhibited a transient voltage response when treated with a continuous light as trp gene mutations equipped (Minke, 1977; Montell et al., 1985). Distinct from other ion channels, TRPCs are classified by their homology and not by the function of ligand or selectivity, as TRPCs are too complex to elucidate their function. TRPC1 forms heteromeric channels with TRPC4 and/or TRPC5 and was the first mammalian TRPC reported (Wes et al., 1995). TRPC3, TRPC6, and TRPC7 proteins share 75% identity and are sensitive to the intracellular concentration of Ca^{2+}. TRPC2 seems to be a pseudogene in humans. TRPC6 is strongly involved in kidney diseases on the basis of wide expression in kidney cells, such as podocytes, glomerular mesangial cells, and TEC (Shen et al., 2013, 2014; Schlondorff, 2017; Wu et al., 2017). Mutation in TRPC6 would also cause kidney dysfunction. A single-point mutation in TRPC6, P112Q, is sufficient to lead to focal segmental glomerular sclerosis FSGS (Winn et al., 2005). Other mutations in TRPC6 that lead to nephrosis have been identified (Moller et al., 2007). In addition, it has been found that TRPC6 inactivation or inhibition is involved in the protective role of severe nephrosis (Kim et al., 2018; Lin B. L. et al., 2019). Therefore, increasing interest has been focused on TPRC6 as a potential therapeutic target of acquired kidney diseases.

EMT can be elicited in fibrotic kidney after unilateral ureteral obstruction (Iwano et al., 2002; Klahr and Morrissey, 2003). Inhibition of TRPC6 ameliorates fibrotic damage and contributes to kidney protection (Wu et al., 2017). Yet, the relationship between TRPC6 and EMT in kidney fibrosis is poorly understood. Moreover, the vast majority of studies on fibrosis of EMT were conducted on the animal models and cell lines, while few studies have been performed on the primary culture cells. Therefore, we aimed to study the important role of TRPC6 in the process of EMT after fibrotic injury in animal models and primary TEC.

In the current study, we found that TRPC6 knockout could alleviate kidney tubulointerstitial fibrosis mediated by EMT after unilateral ureteric obstruction (UUO) *in vivo*. We also found that EMT is more down-regulated in primary TEC induced by TGF-β1 from $TRPC6^{-/-}$ mice than from the wild-type (WT) mice *in vitro*. The pathways of the AKT-mTOR and ERK1/2 were both activated in the obstructed kidney and the primary TEC treated with TGF-β1, and down-regulation of AKT-mTOR and ERK1/2 signaling pathways were found in $TRPC6^{-/-}$ mice. We

Abbreviations: EMT, epithelial–mesenchymal transition; TEC, tubular epithelial cells; UUO, unilateral ureteric obstruction; TRPCs, transient receptor potential channels; E-cad, E-cadherin; Cadh16, Cadherin16; NO, non-obstructed; O, obstructed.

thus hypothesized that TRPC6 knockout may inhibit EMT to ameliorate the kidney injury by down-regulating the AKT-mTOR and ERK1/2 signaling pathways.

MATERIALS AND METHODS

Chemicals and Reagents

Sources of antibodies and reagents were as follows:

Anti-AKT (Cell Signaling Technology, Danvers, MA, USA), anti-p-AKT (Ser473) (Cell Signaling Technology, Danvers, MA, USA), anti-p-ERK1/2 (Cell Signaling Technology, Danvers, MA, USA), anti-ERK1/2 (Cell Signaling Technology, Danvers, MA, USA), anti-p-mTOR (Cell Signaling Technology, Danvers, MA, USA), anti-mTOR (Cell Signaling Technology, Danvers, MA, USA), anti-E-cad (Cell Signaling Technology, Danvers, MA, USA), anti-Cadh16 (Proteintech, Chicago, Illinois, USA), anti-snail1(Cell Signaling Technology:3879s), anti-α-SMA (Boster, Wuhan, Hubei, China), anti-AQP1 (Proteintech, Chicago, Illinois, USA), anti-ATP (Proteintech, Chicago, Illinois, USA), anti-TGF-β1 (Proteintech, Chicago, Illinois, USA), anti-GAPDH (Proteintech, Chicago, Illinois, USA), anti-TRPC6 (Alomone, Jerusalem, Israel), anti-TRPC3 (Alomone:ACC-016), anti-mouse IgG (KeRui, Wuhan, Hubei, China), anti-rabbit IgG antibody (KeRui, Wuhan, Hubei, China), recombinant human TGF-β1 (Cell Signaling Technology, Danvers, MA, USA), HYP9 (MedChem, Shanghai, China), and type-2 collagenase (Worthington Biochemical Corporation, Lakewood, Colorado, USA).

DMEM/f12 and FBS were purchased from Invitrogen (Chicago, California, USA). The whole sagittal section of the kidney was scanned by Biossci Biotechnology Company (Wuhan, Hubei, China).

Mice Models

TRPC6$^{-/-}$ mice on a 129SvEv background were reconstituted at the Comparative Medicine Branch (CMB) of the National Institute of Environmental Health Sciences (NIEHS), North Carolina, USA. WT mice, which served as controls for the knockout mice, were also obtained from NIEHS. Mice were permitted *ad libitum* access to food and water. Mice were kept on a 12-h light/12-h dark cycle in a temperature-controlled room. The protocols were conducted on adult male 8–10-week-old TRPC6$^{-/-}$ mice weighing 20–25 g and their age-matched WT 129SvEv controls. The experiments were carried out in strict accordance with the standard biosecurity and institutional safety procedures of the Laboratory of Huazhong University of Science and Technology. The animal study was reviewed and approved by the Institutional Animal Care and Use Committee at Tongji Medical College, Huazhong University of Science and Technology.

Experimental Unilateral Ureteric Obstruction

Animals were anesthetized with chloral hydrate before surgery. The surgery of UUO was performed as reported previously (Pang et al., 2009, 2010). Briefly, the left ureter was exposed via a midline abdominal incision under general anesthesia, ligated in two places using 4–0 surgical silk, and cut off between two ligatures. The right ureter was kept intact. In the study, the obstructed left kidney was used for fibrosis analysis, and the contralateral, non-obstructed kidney was used as controls (Masterson et al., 2004). UUO mice were sacrificed on days 3, 7, or 15 after UUO. Kidneys were immediately removed, decapsulated, and cut into small pieces for subsequent protein studies or stored at −80°C. One portion of the kidneys was collected and fixed in 4% neutral-buffered formalin for subsequent histologic and immunohistochemical staining.

Isolation and Primary Culture of Kidney TEC

Under sterile conditions, primary TEC were extracted and cultured from age-matched male mice on the basis of established culture methods in our lab (Barrallo-Gimeno and Nieto, 2005; Hou et al., 2018). Mice were sacrificed by cervical dislocation, and kidney tissues were collected. After carefully removing the capsule, the cortical tissues were isolated from the kidney, cut into small pieces, and mixed with the type-2 collagenase [DS with 0.1% (wt/vol)] to fully digest in a shaking temperature-controlled water bath kettle for 15 min about three–four times at 37°C. After removal of the supernatant, digestive liquid was added into an equal volume of pre-cold DMEM/F12 supplemented with 10% FBS to terminate digestion and then filtered by two nylon sieves (pore sizes 180 and 75 μm, Bio-Swamp, Wuhan, Hubei, China). The kidney tubular fragments were collected from the 75-μm sieve and resuspended in culture medium after centrifugation for 5 min at 500 g. The culture medium contained DMEM/F12 supplemented with 10% FBS, 1% penicillin/streptomycin, HEPES 15 mM, insulin 10 μg/ml, L-glutamine 2.5 mM, selenium 5 μg/ml (Sigma, St. Louis, Missouri, USA), transferrin 5.5 μg/ml, and sodium pyruvate 0.55 mM (Bio-Swamp, Wuhan, Hubei, China). The fragment tissues were maintained in a standard humidified incubator (Thermo Fisher Scientific, Waltham, MA, USA) at 37°C and in 5% CO_2-95% air, with culture medium being changed initially at day 3 and subsequently every 2 days. About 5 days later, primary outgrowth cells from tubular fragment were developed as a confluent monolayer and trypsinized for following experiments.

Occasionally, the fragments were seeded onto polylysine-coated glass slides for following cell immunofluorescence analysis.

Cell Culture and Treatments

Primary TEC were cultured in DMEM/F12 supplemented with 10% FBS and other nutrient factors. After the standard culture of 3 days, the TEC were treated with 5 ng/ml TGF-β1 for 72 h to induce EMT *in vitro* (Zhou T. et al., 2018). Culture medium with TGF-β1 was replaced every 2 days, and 10 Mm of HYP9 was added into the culture medium for 1.5 h prior to the treatment of TGF-β1 in experiments (Zhou L. F. et al., 2018).

Histology and Histopathology

Morphology changes of the kidney were examined by hematoxylin and eosin (HE), Masson, and Sirius Red staining. Kidneys were collected and fixed with 4% paraformaldehyde, dehydrated by sucrose, and embedded in OCT compound,

then sectioned in 6-μm thickness. The kidney cryosections were washed three times with PBS at room temperature and stained, respectively, with relevant reagents of HE, Masson, and Sirius red by standard protocol. The staining sections were detected by an optical microscope (Olympus, Tokyo, Japan) at ×200 magnification to analyze the interstitial fibrosis of UUO. Kidney injury was confirmed by interstitial fibrosis and tubular damage, which were defined by the structure, integrity of the basal membrane, and of the brush border and the dimension, compared to the healthy kidney tubule.

Immunofluorescence Staining

Immunofluorescence analysis was conducted according to the standard protocol. For immunofluorescence staining, 4% paraformaldehyde-fixed, sucrose-dehydrated, and OCT-embedded kidney tissues were sectioned to 6-μm thick. Primary TEC adhered to coverslips were fixed with 4% paraformaldehyde for 15 min at room temperature and immersed in 0.5% Triton X-100 for 15–30 min with the same operation of kidney cryosections. To detect the expression of EMT markers and the aquaporins of kidney tubule epithelial cell, kidney cryosections and pre-treated primary TEC adhered to coverslips were incubated at 37°C for 1 h in a humidified chamber with relevant primary antibody (dilution 1:50) of E-cad, Cadh16, α-SMA, snail1, and so on. Samples were then incubated with FITC-conjugated anti-mouse or rabbit secondary antibody (1:200) for 2 h at room temperature. Immunolabelled kidney cells were counterstained with DAPI (Sigma) for 10 min to show nuclear morphology. Stained slides were viewed and scanned at ×200 magnification by a confocal microscope (Olympus, Tokyo, Japan).

Western Blot Analysis

Fresh kidney samples were solubilized with the lysis buffer of RIPA containing 100 mg/ml PMSF and 1% protease inhibitor cocktail on ice for 30 min, while TEC were solubilized in a lysis mixture containing 50 mM Tris-HCl (pH 6.8), 1 mM PMSF, 1 mM EDTA, 150 mM NaCl, and 1% NP-40 and incubated on ice for 30 min. The tissue and cell lysates were centrifuged at 12,000 g for 15 min at 4°C. After the protein concentration was assessed by BCA protein assay kit, the supernatants were mixed with 4× SDS sample buffer, boiled for 10 min at 95°C, separated through 8–12% SDS–PAGE gels, and then transferred to a PVDF membrane (Roche, USA) by electroblotting in mini trans-blot cell (Bio-Rad). After being blocked in TBS-Tween buffer consisting of 5% (*w*/*v*) fat-free, dried milk for 30 min, the membrane was incubated with the appropriate primary antibodies (diluted 1:1,000) in skim milk at 4°C overnight and then incubation with the relevant HRP-conjugated secondary antibodies (diluted 1:3,000) in TBST followed. Finally, each protein band was visualized with Pierce ECL (Thermo Fisher Scientific, USA) reagents. Molecular weights were confirmed by comparison with pre-stained SDS–PAGE molecular weight standards (Thermo Fisher Scientific, USA). Densitometry of the western blots was analyzed using the Quantity One software (Bio-Rad, Hercules, CA, USA). Expression of EMT markers was normalized to GAPDH, and phospho-ERK1/2, p-AKT, and p-mTOR were normalized to total ERK1/2, AKT, and mTOR.

Statistical Analyses

All experiments were performed in triplicate at least three times, and the data results were expressed as mean ± sem (standard error of the mean). The statistical differences between groups were assessed by using one-way analysis of variance (ANOVA) depending on the number of comparisons being made and the data distribution. When p-values were <0.05, the differences were considered significant.

RESULTS

Kidney Fibrosis Increases TRPC6 Expression and Activates EMT Program

After UUO, fibrotic damages occurred in the obstructed kidney (Martinez-Klimova et al., 2019). Compared to the non-obstructed (NO) contralateral kidneys in UUO mice, which has a normal kidney structure, an obvious cavity can be observed in the coronal plane of the obstructed (O) kidney, while the cavity size markedly increased with the obstructed time extending after UUO (**Figure 1A**). A mass of extracellular matrix is produced in the process of kidney fibrosis, which is characteristic of fibrosis (Duffield, 2014). Therefore, HE, Masson, and Sirius red staining were conducted to explore histopathologic changes and accumulation of matrix and fibers related to fibrosis. The images revealed that a significant tubular impairment became worse by HE staining, and a higher degree of tubulointerstitial fibrosis was increased in the obstructed kidneys of WT mice, on days 3, 7, and 15 after UUO, relative to the non-obstructed kidney by Masson staining (collagen fibers, blue) and by Sirius red staining (collagen fibers, red) (**Figure 1B**). In order to better understand whether TRPC6 plays a key role in kidney fibrosis, we inspected the expression level of TRPC6 by western blot. Results showed that TRPC6 had a time-dependent increase in obstructed kidneys (**Figure 1C**), while the expression of TGF-β1, an important inducer to fibrosis, was also increased in the fibrotic kidney after UUO (**Supplementary Figure 1A**). So as to determine the participation of EMT in kidney fibrosis after UUO, EMT markers, such as E-cad, Cadh16, α-SMA, and snail1, were examined at the protein level by western blot. The expression levels of E-cad and Cadh16 were down-regulated, and α-SMA and snail1 were markedly upregulated in obstructed kidneys induced by UUO compared with the non-obstructed group (**Figure 1D**). These phenomena suggest that there may exist some connections between TRPC6 and EMT activation in kidney fibrosis.

TRPC6 Knockout Partially Inhibits EMT to Alleviate Kidney Injury

To investigate the relationship between TRPC6 and EMT in kidney fibrosis, the TRPC6$^{-/-}$ mice were used in the study. On day 15 after UUO, the size of the cavity in obstructed kidneys became overtly smaller in TRPC6$^{-/-}$ mice compared to WT mice (**Figure 2A**), and the swelling of the obstructed kidney was obviously alleviated (**Supplementary Figure 1B**). The

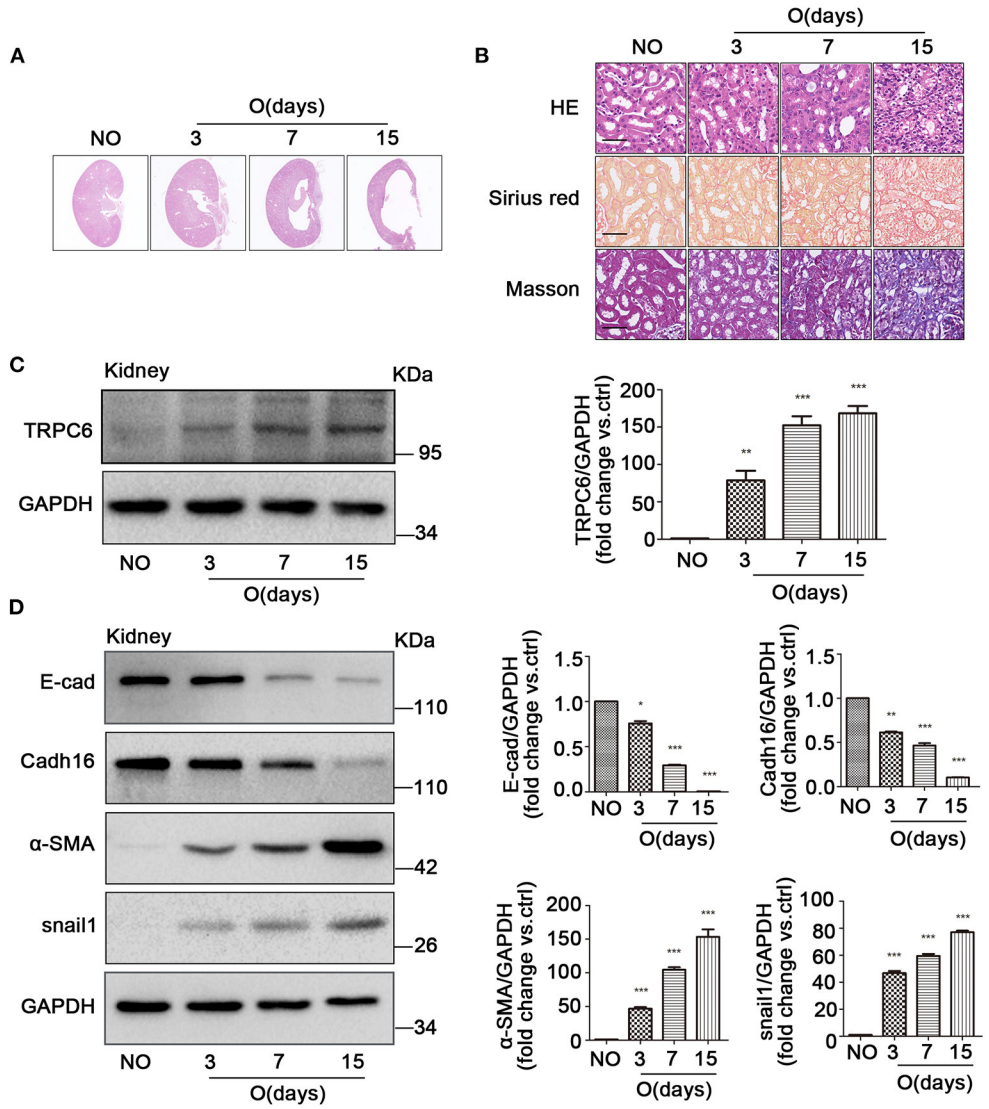

FIGURE 1 | The increase of TRPC6 and activation of EMT in fibrotic kidney tissues. **(A)** Representative scanning images of kidney coronal plane showing the cavity caused by fibrosis injury in the contralateral non-obstructed (NO) and obstructed (O) kidneys from WT mice on days 3, 7, and 15 after UUO. **(B)** Representative images of similar kidney sections stained by HE, Masson, and Sirius red showing the interstitial fibrosis change of kidney tissues from the above groups. Scale bars, 20 μm. **(C)** Expression level of TRPC6 from the above groups detected by western blot. Data are presented as mean ± sem, $n = 3$; an unpaired two-tailed *t*-test was used. $^{**}P < 0.01$, $^{***}P < 0.001$. **(D)** Expression level of EMT markers E-cad, Cadh16, α-SMA, and snail1 from the above groups detected by western blot. Data are presented as mean ± sem, $n = 3$; an unpaired two-tailed *t*-test was used. $^{*}P < 0.05$, $^{**}P < 0.01$, $^{***}P < 0.001$.

result showed that TRPC6 knockout could improve kidney health obviously in obstructed kidney. Then, the data of HE, Masson, and Sirius red staining also revealed a lower degree of injury and tubulointerstitial fibrosis in TRPC6$^{-/-}$ mice after UUO (**Figure 2B**). The tubular impairment was obviously alleviated and the accumulation of collagen fibers decreased apparently. In order to explore the EMT activation in kidney fibrosis, we examined the expression of EMT markers through immunofluorescent staining and western blot. The staining results showed that TRPC6 knockout could partially inhibit EMT and have an anti-fibrosis effect in obstructed kidney induced by UUO (**Figure 2C**). The decrease of E-cad and Cadh16 expression was prevented in obstructed kidneys of TRPC6$^{-/-}$ mice compared to that of WT mice, while the increase of α-SMA and snail1 expression was also inhibited in TRPC6$^{-/-}$ mice. To further confirm the result, the levels of EMT markers were detected by western blot (**Figure 2D**). All of the results showed that TRPC6 knockout plays a protective role along with the inhibition of EMT in kidney fibrosis.

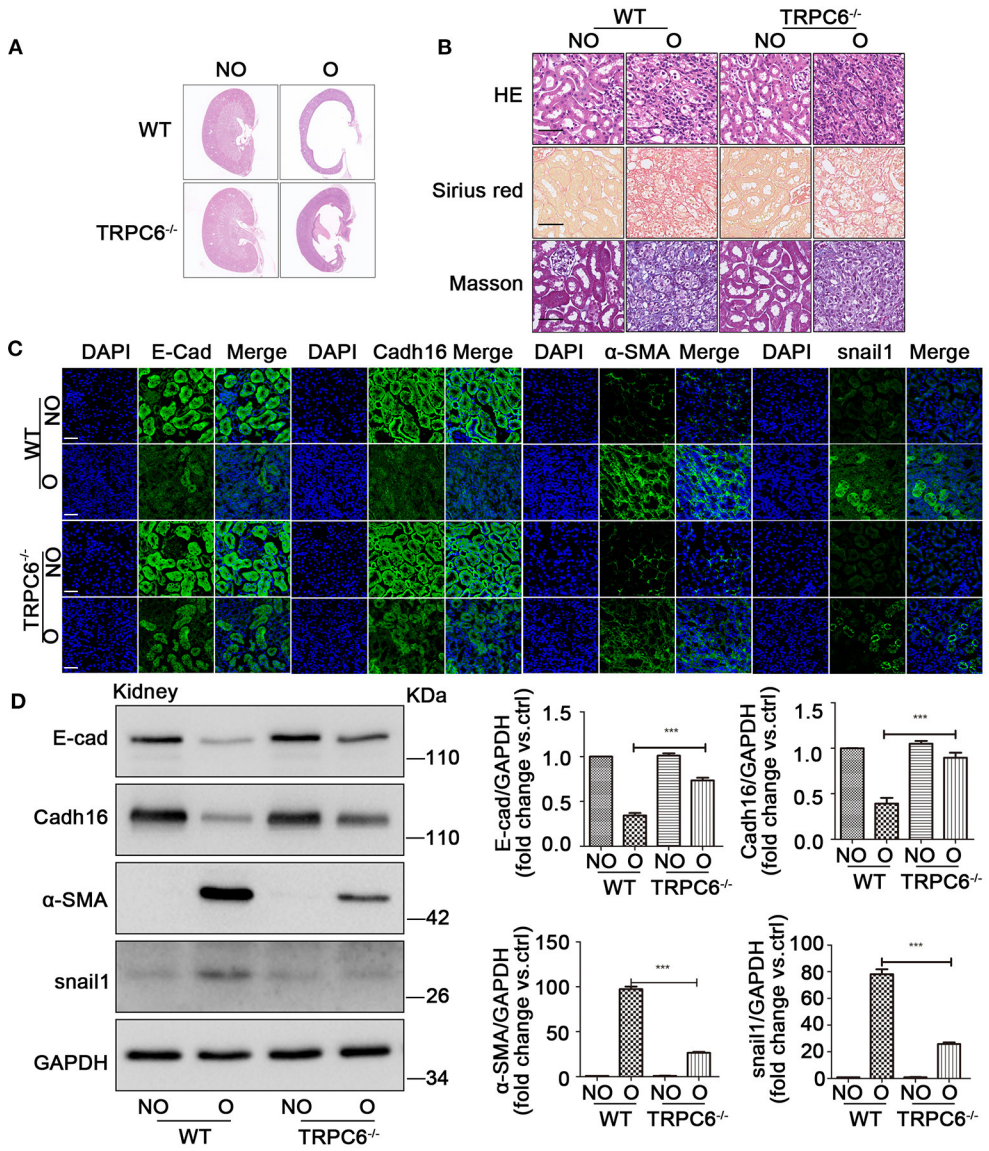

FIGURE 2 | TRPC6 knockout partially inhibits EMT to alleviate the kidney injury. **(A)** Representative scanning images of kidney coronal plane showing the cavity caused by fibrotic injury in NO and O kidneys from TRPC6 knockout and WT mice on day 15 after UUO. **(B)** Representative images of kidney sections stained by HE, Masson, and Sirius red showing interstitial fibrosis change of kidney tissues from the above groups. Scale bars, 20 μm. **(C)** Expression level of EMT markers (green) E-cad, Cadh16, α-SMA, and snail1 as well as nuclear stain DAPI (blue) from the above groups detected by immunofluorescence analysis. Scale bars, 20 μm. **(D)** Expression level of EMT markers E-cad, Cadh16, α-SMA, and snail1 in NO and O kidneys from the above groups detected by western blot. Data are presented as mean ± sem, $n = 3$; an unpaired two-tailed t-test was used. $^{***}P < 0.001$.

TRPC6 Increases in TEC After TGF-β1 Treatment Along With the Activation of EMT

Several studies have demonstrated that TGF-β1 is the master inducer of EMT in kidney fibrosis (Meng et al., 2016); therefore, we next examined the change of EMT in primary TEC after stimulation with TGF-β1. Primary TEC were treated with TGF-β1 for different times (12, 24, 48, and 72 h) at a concentration of 5 ng/ml and had an obvious phenotype change with the extended stimulation time. Under normal culture conditions, the primary TEC grew from the kidney tissue and fused to monolayer on day 5 (**Supplementary Figure 1C**). After treatment with TGF-β1 for 72 h, the cells exhibited morphology changes (**Supplementary Figure 1D**). It is known that TRPC3, TRPC6, and TRPC7 are in a homologous group and always work together in various pathological courses (Chen et al., 2017; He et al., 2017). Due to the lack of TRPC7 expression in the kidney (Liu et al., 2017), we examined the expression levels of TRPC3 and TRPC6 in primary TEC induced by TGF-β1. We discovered that the level of TRPC6 expression was enhanced, but the

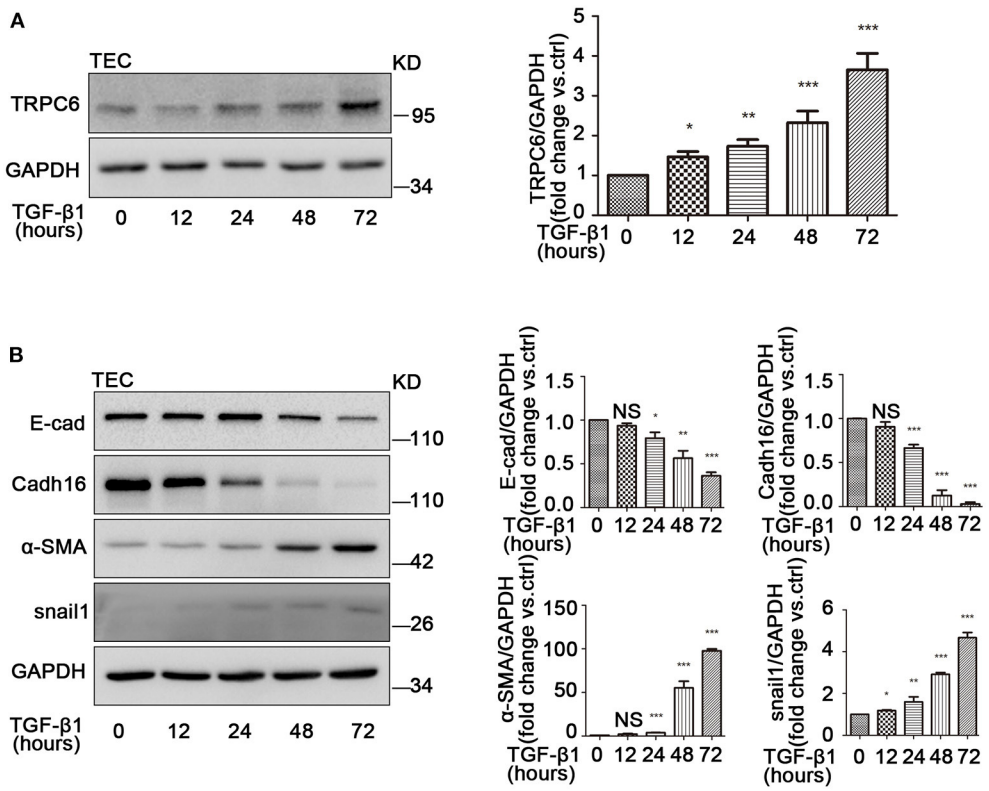

FIGURE 3 | The increase of TRPC6 and activation of EMT in primary TEC stimulated with TGF-β1. **(A)** Expression of TRPC6 in primary TEC without and with TGF-β1 (5 ng/ml in 20 mM citric acid, pH 3.0) stimulation at 12, 24, 48, and 72 h detected by western blot. Data are presented as mean ± sem, $n = 3$; an unpaired two-tailed *t*-test was used. $^{*}P < 0.05$, $^{**}P < 0.01$, $^{***}P < 0.001$. **(B)** Relative expression of the EMT markers including E-cad, Cadh16, α-SMA, and snail1 in primary TEC with and without TGF-β1 stimulation for 72 h detected by western blot. Data are presented as mean ± sem, $n = 3$; an unpaired two-tailed *t*-test was used. NS, not significant; $^{*}P < 0.05$, $^{**}P < 0.01$, $^{***}P < 0.001$.

level of TRPC3 expression had no obvious change in primary TEC stimulated by TGF-β1 (**Supplementary Figure 2A**). In our lab, we had previously confirmed that TEC from TRPC6$^{-/-}$ mice lack TRPC6 expression but had normal TRPC3 isoforms compared with TEC from the control group, and TRPC6 has a functional significance in TEC as a store-operated Ca^{2+} channel in primary TEC from WT mice (Hou et al., 2018). Western blot showed that TRPC6 expression increased gradually in primary TEC induced by TGF-β1 (**Figure 3A**). This highlighted that TRPC6 played a key role in primary TEC from WT mice treated with TGF-β1. It is also well-known that TGF-β1 is a common stimulator of EMT induction in cell lines. Next, we investigated whether the EMT was activated in primary TEC stimulated by TGF-β1. The markers of EMT, including E-cad, Cadh16, α-SMA and snail1, were examined by western blot. The data showed that the time-course of E-cad and Cadh16 expression decreased distinctly, while that of α-SMA and snail1 increased markedly (**Figure 3B**). This demonstrated that EMT was also activated in the primary TEC stimulated with TGF-β1 in line with the result of animal model. These results suggested that TRPC6 has a close link with EMT activation in primary TEC after treatment.

TRPC6 Knockout Partially Inhibits EMT Induced by TGF-β1 in Primary TEC

To explore the anti-fibrosis effect of TRPC6 in EMT-mediated kidney fibrosis, primary TEC of WT and TRPC6$^{-/-}$ mice were stimulated with 5 ng/ml TGF-β1 for 72 h to mimic obstructed injury *in vitro*. The TEC from the WT mice displayed typical cobblestone-like morphology without stimulation of TGF-β1 under the inverted microscope, exhibited polygon or fusiform morphology, and even stretched out some long pseudopods after treatment with TGF-β1 for 72 h (**Figure 4A**). The TEC from the TRPC6$^{-/-}$ mice, however, showed a lesser degree of change in the same treatment condition than TEC from the WT mice, and it was rather difficult to see the pseudopods around the cells in the TRPC6 knockout group. To explore the phenomena further, immunofluorescent staining was used to test the expression levels of EMT markers. As expected, it showed that the activation of EMT in TEC from TRPC6$^{-/-}$ mice was markedly prevented. The decrease of E-cad expression and increase of α-SMA and snail1 in treatment groups of TEC from TRPC6$^{-/-}$ mice were reversed compared to that of WT mice (**Figure 4B**). Cadh16 was lost in the original microenvironment of the kidney in cultured

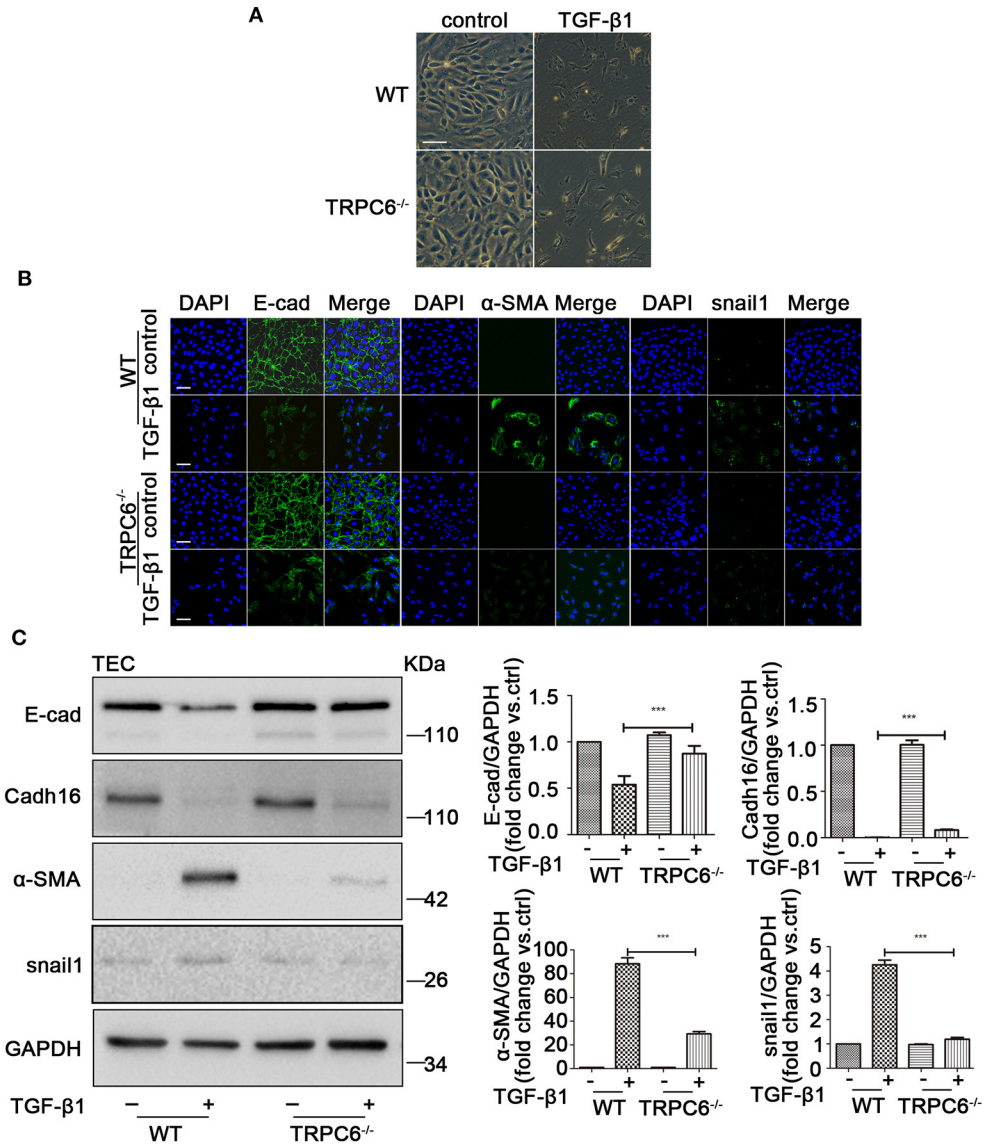

FIGURE 4 | The process of EMT was inhibited in primary TEC stimulated with TGF-β1 inTRPC6$^{-/-}$ mice. **(A)** Morphological changes of primary TEC from WT and TRPC6$^{-/-}$ mice with and without TGF-β1 stimulation for 72 h. **(B)** Expression level of EMT markers (green) E-cad, α-SMA, and snail1 as well as nuclear stain DAPI (blue) from the above groups detected by immunofluorescence analysis. Scale bars, 20 μm. **(C)** Expression level of EMT markers E-cad, Cadh16, α-SMA, and snail1 from the above groups detected by western blot. Data are presented as mean ± sem, $n = 3$; an unpaired two-tailed t-test was used. ***$P < 0.001$.

primary TEC, so it cannot be inspected by immunofluorescent staining. As further evidence, the expression levels of EMT markers were detected by western blot, and a consistent result was seen (**Figure 4C**). The results further confirmed that TRPC6 knockout has a protective effect with the inhibition of EMT in TEC treated with TGF-β1.

TRPC6 Knockout Negatively Regulates the AKT-mTOR and ERK1/2 Signaling Pathways

AKT kinase is likely a critical regulator in cellular activity including cell proliferation, differentiation, and apoptosis. Moreover, AKT/mTOR is a vital signaling pathway mediated many physiological and pathological processes of the kidney (Yoo et al., 2011; Yang et al., 2015). In addition, it was previously reported that ERK1/2 could be activated and have an important role in the program of fibrosis. We presumed that an AKT/mTOR-related or/and ERK1/2-related response could be activated in UUO-induced kidney fibrosis and cultured primary TEC treated with TGF-β1. As expected, the phosphorylation ratio of AKT (Ser473), mTOR (Ser2448), and ERK1/2 was increased during the process of EMT activation in the obstructed kidneys (**Figure 5A**) and the primary TEC stimulated by TGF-β1 (**Figure 5C**). Additionally, the obstructed kidney of TRPC6$^{-/-}$

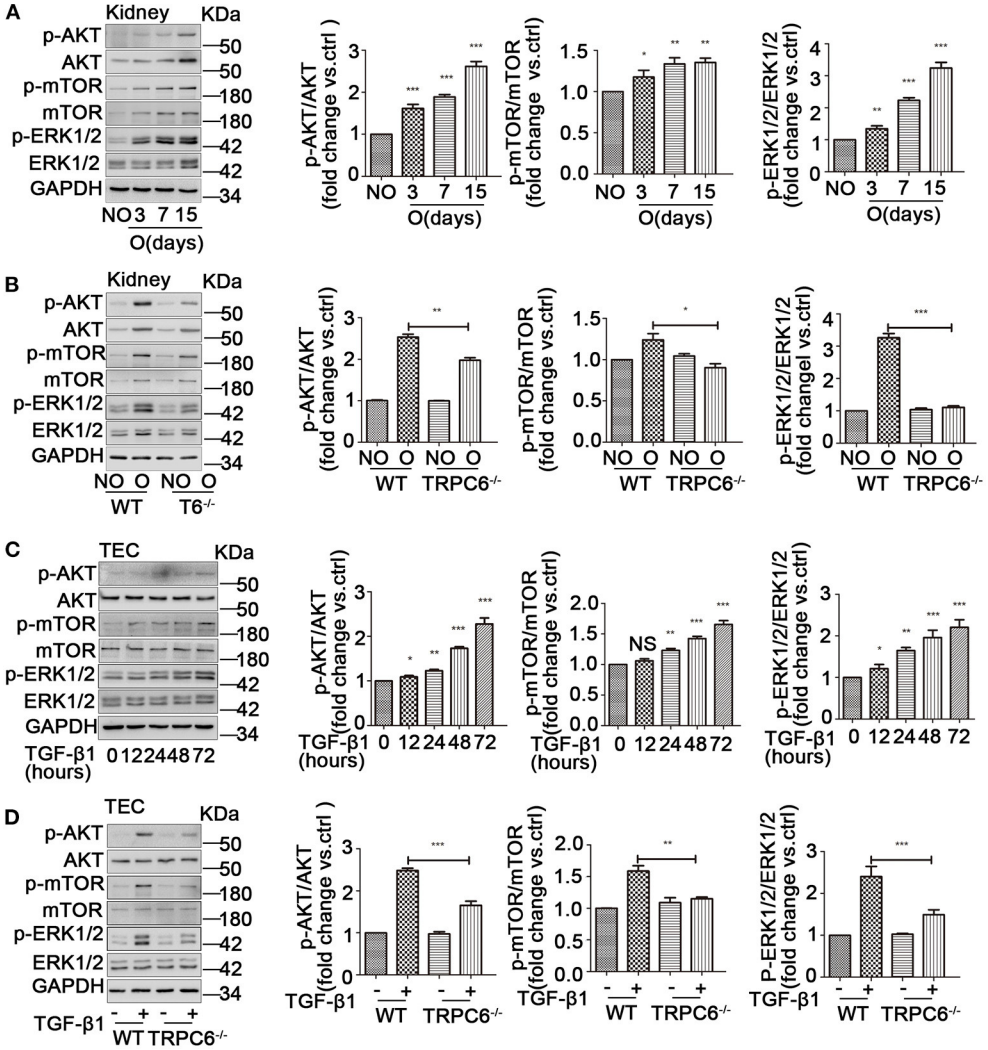

FIGURE 5 | The activation of AKT-mTOR and ERK1/2 signaling pathways was down-regulated in TRPC6$^{-/-}$ mice. **(A)** Expression level of the phosphorylated and total protein of AKT, mTOR, and ERK1/2 in NO and O kidneys from WT mice on days 3, 7, and 15 after UUO detected by western blot. Data are presented as mean ± sem, $n = 3$; an unpaired two-tailed *t*-test was used. $^{*}P < 0.05$, $^{**}P < 0.01$, $^{***}P < 0.001$. **(B)** Expression level of the phosphorylated and total protein of AKT, mTOR, and ERK1/2 in NO and O kidneys from TRPC6$^{-/-}$ and WT mice on day 15 after UUO detected by western blot. Data are presented as mean ± sem, $n = 3$; an unpaired two-tailed *t*-test was used. $^{*}P < 0.05$, $^{**}P < 0.01$, $^{***}P < 0.001$. **(C)** Expression level of the phosphorylated and total protein of AKT, mTOR, and ERK1/2 in primary TEC without and with TGF-β1 stimulation at 12, 24, 48, and 72 h detected by western blot. Data are presented as mean ± sem, $n = 3$; an unpaired two-tailed *t*-test was used. NS, not significant; $^{*}P < 0.05$, $^{**}P < 0.01$, $^{***}P < 0.001$. **(D)** Expression level of the phosphorylated and total protein of AKT, mTOR, and ERK1/2 in primary TEC from WT and TRPC6$^{-/-}$ mice with and without TGF-β1 stimulation for 72 h detected by western blot. Data are presented as mean ± sem, $n = 3$; an unpaired two-tailed *t*-test was used. $^{**}P < 0.01$, $^{***}P < 0.001$.

mice showed lower ratio of p-AKT, p-mTOR, and p-ERK1/2 than that of WT mice (**Figure 5B**). This result suggested the AKT-mTOR or/and ERK1/2 signaling pathways were activated in kidney fibrosis and were down-regulated in TRPC6$^{-/-}$ mice. TRPC6 knockout may alleviate kidney fibrosis through negative regulation of AKT-mTOR or/and ERK1/2 signaling pathways. In order to ascertain whether the hypothesis is the same with the EMT activation of primary TEC treated by TGF-β1, we examined the protein expression of related signaling molecules by western blot. We found that the ratio of p-AKT, p-mTOR, and p-ERK1/2 in treated TEC from TRPC6$^{-/-}$ mice was markedly lower than their WT counterparts (**Figure 5D**). This observation is in line with the consequence of TRPC6$^{-/-}$ mice models by UUO.

TRPC6 Knockout Improves the Loss of Na^{+}/K^{+}-ATPase and AQP1 in the Kidney

The realization of kidney function relies on the channel protein, and the loss of channel protein would significantly affect normal filtration function and lead to kidney dysfunction, which is harmful to our engine body. A specific reduction in the expression of Na^{+}/K^{+}-ATPase (ion channel protein) and

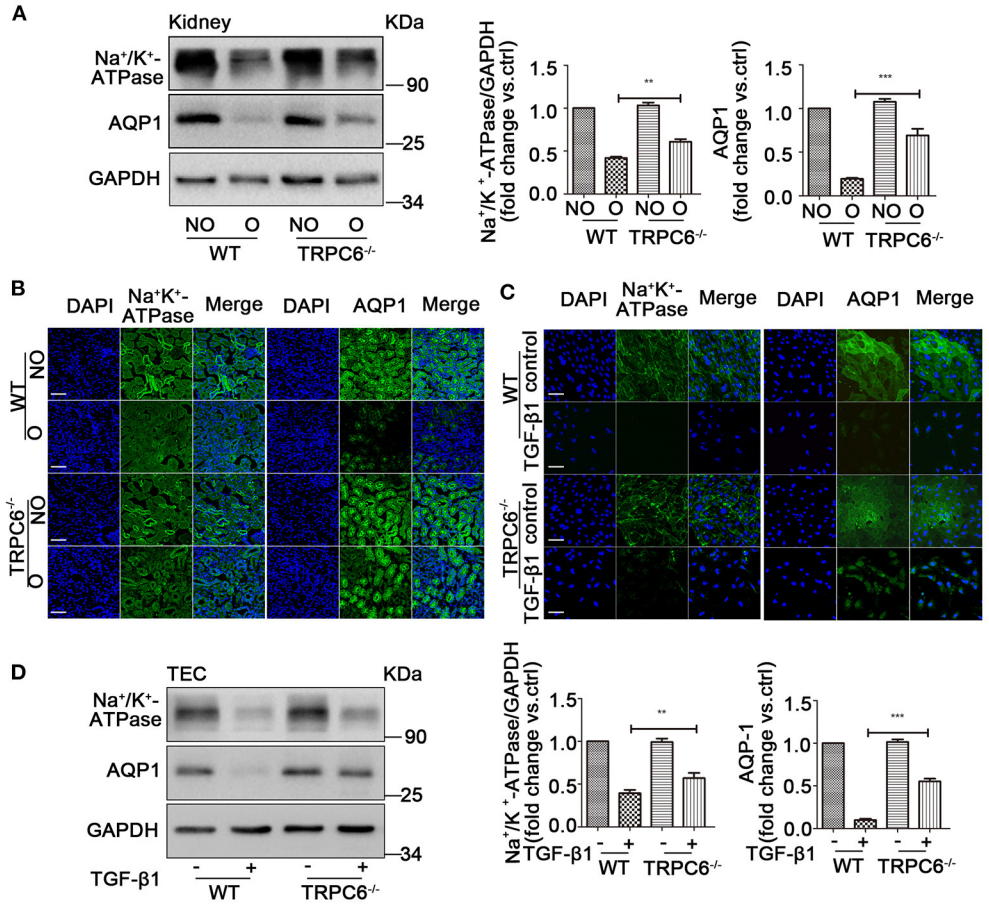

FIGURE 6 | TRPC6 knockout improves the loss of channel proteins on kidney tubulars and TEC. **(A)** Expression level of Na^+/K^+-ATPase and AQP1 in NO and O kidneys from TRPC6 knockout and WT mice on day 15 after UUO detected by western blot. Data are presented as mean ± sem, $n = 3$; an unpaired two-tailed *t*-test was used. $^{**}P < 0.01$, $^{***}P < 0.001$. **(B)** Expression level of Na^+/K^+-ATPase and AQP1 (green) as well as nuclear stain DAPI (blue) in NO and O kidneys from $TRPC6^{-/-}$ and WT mice on day 15 after UUO detected by immunofluorescent staining. Scale bars, 20 μm. **(C)** Expression level of Na^+/K^+-ATPase and AQP1 (green) as well as nuclear stain DAPI (blue) in primary TEC with and without TGF-β1 stimulation for 72 h detected by immunofluorescent staining. Scale bars, 20 μm. **(D)** Expression level of Na^+/K^+-ATPase solute transporter and AQP1 in primary TEC with and without TGF-β1 stimulation for 72 h detected by western blot. Data are presented as mean ± sem, $n = 3$; an unpaired two-tailed *t*-test was used. $^{**}P < 0.01$, $^{***}P < 0.001$.

aquaporin1 (AQP1) is shown in obstructed kidney tissues after UUO compared to contralateral kidneys, as well as an obvious improvement in $TRPC6^{-/-}$ mice compared to WT mice, which is evident by western blotting and immunofluorescent staining (**Figures 6A,B**). In order to verify the assumption that the effect is no different in culture TEC, the same tests were done by western blot and immunofluorescent staining. A consistent result was detected in TEC treated with TGF-β1 compared to controls from WT mice, and $TRPC6^{-/-}$ mice showed a reversal of the decrease compared to WT mice (**Figures 6C,D**). These results, therefore, show that TRPC6 knockout would ameliorate kidney dysfunction caused by kidney fibrosis.

DISCUSSION

Fibrosis is normally beneficial as a tissue repair process; however, if excessive, it leads to relentless tissue damage and failure of organ function in severe cases. In the process of kidney fibrosis, the myofibroblast plays a central role and its aberrant growth contributes to the over-production of extracellular matrix (Liu, 2004; Neilson, 2006; Wynn, 2008; Zubair and Ahmad, 2019). Generally, the myofibroblast is derived from the proliferation and differentiation of the fibroblast. The TEC, another important origin of myofibroblast, has been of interest to researchers recently. That epithelial cell could translate to the myofibroblast by EMT. Studies have found that EMT is of profound significance in fibrosis and pervasive in different organs, such as the lungs, lens, liver, and kidney (Liang et al., 2014; Kong et al., 2015; Yang et al., 2019; Yao et al., 2019). Furthermore, EMT has been observed to improve the onset of kidney fibrosis, and fibrotic damages could be alleviated by repressing the process of EMT (Du et al., 2012; Geng et al., 2019). Clinical studies have suggested that EMT, as the early onset element of interstitial fibrosis in the kidney, is confirmed in diabetic patients (Hills and Squires, 2011; Carew et al., 2012). The direct role of EMT of TEC in kidney fibrosis remains controversial. In 2015, Grande and Lovisa et al.

independently pinpointed a partial epithelial-to-mesenchymal transition as a mechanism driving the development of kidney fibrosis. They observed that TEC undergo an incomplete EMT; TEC with partial EMT remain attached in the basement of membrane and promote kidney fibrosis via following three mechanisms. In cell-autonomous manner, a partial EMT causes cell-cycle arrest, halting further proliferation and repair; the partial EMT secretes growth factors such as TGF-β and drives myofibroblast proliferation; pathological secretome promotes kidney chronic inflammation(Grande et al., 2015; Lovisa et al., 2015).

TRPCs have a close correlation with kidney disease and are located in the glomeruli and tubules of the kidney (Woudenberg-Vrenken et al., 2009; Liu et al., 2010, 2011). More specifically, TRPC3 and TRPC6 are homologous in structure, but compose heteromultimers in different cell types. TRPC6 is widely present in podocytes, vascular smooth muscle and endothelial cells, mesangial cells, interstitial fibroblasts, as well as TEC. Recent studies have reported that the expression of TRPC3 and TRPC6 was both increased in UUO kidneys, and inhibition of TRPC6 ameliorates kidney fibrosis and contributes to kidney protection (Wu et al., 2017). Another study showed that TRPC3 was increased in the fibroblasts of obstructed kidney, and TRPC3 knockout could inhibit fibroblast proliferation by regulating the ERK1/2 signaling pathway (Saliba et al., 2015). Of note, we found only TRPC6 was obviously increased in primary TEC treated with TGF-β1 and did not find the increase of TRPC3 (**Supplementary Figure 2A**). Therefore, we focused on TRPC6 in the study of kidney fibrosis on TEC. Furthermore, a study of transdifferentiation of fibroblast to myofibroblast has shown that TRPC6 promoted the transdifferentiation and loss of TRPC6 impeded the process (Davis et al., 2012). However, whether TRPC6 contributes to the transition of TEC to myofibroblast is not clear. To date, no study uncovered the role of TRPC6 on the EMT in renal fibrosis. In our study, coincident results from previous studies were found. TRPC6 expression increased in the injured kidney after UUO in WT mice compared to the contralateral control, and EMT was activated along with the increase of TRPC6. The results revealed TRPC6 expression was strongly related to the activation of EMT in the obstructed kidney. In order to further determine the role of TRPC6 in the process of EMT, TRPC6$^{-/-}$ mice were introduced in the following study. We found the marker change for EMT was partially reversed in obstructed kidney of TRPC6$^{-/-}$ mice compared to that of WT mice. This result suggested EMT was inhibited by the deletion of TRPC6 in fibrotic kidney. With regard to further investigation of EMT and TRPC6, we then aimed to study the primary TEC from kidney tissue.

UUO, a well-established model, enables the study of kidney fibrosis in different pathologic aspects, especially in EMT (Chevalier et al., 2009). When various types of damages from UUO are experienced, TEC become vulnerable, lose some epithelial features, and acquire mesenchymal characteristics leading to the happening of EMT. In the obstructed kidney, an obvious decrease of epithelial markers E-cad and Cadh16 was observed in the TEC as well as the increase of mesenchymal features such as α-SMA and snail1. We also found that an injury cavity appeared that was caused by rampant kidney fibrosis. Importantly, the size of the cavity became larger along with the days of UUO and became smaller following the decrease of EMT. Furthermore, the promotion of EMT augments the damage of TEC, resulting in the decrease of functional capabilities. The kidney function was valued by examination of Na^+/K^+-ATPase and APQ1, which are expressed at the plasma membrane of tubule in the kidney to transport the ion and water (Verkman, 2002). Reduction of the Na^+/K^+-ATPase and APQ1 is closely connected with kidney function and has been proposed to promote fibrosis and increase metabolites and uremic toxin (Rajasekaran et al., 2010; Liu et al., 2012; Ito et al., 2013). As Na^+/K^+-ATPase and APQ1 are necessary to maintain the morphological structure of TEC and filtration function of kidney, so a sharp decrease of them would cause a more serious effect for our engine body. In our study, the low expression of Na^+/K^+-ATPase and APQ1 was found in fibrotic kidney and TGF-β1-induced TEC, which were obviously reversed in TRPC6$^{-/-}$ mice. The results suggested that kidney function was recovered to a certain extent with the inhibition of EMT. Therefore, these results highlight the significance of EMT in the development of kidney fibrosis and that kidney damage was alleviated by the inhibition of EMT.

Recently, a majority of studies about EMT in kidney fibrosis focus on TEC lines such as NRK-52E, HEK293T, and HK-2 (Hu et al., 2018; Zhou T. et al., 2018). Few studies have focused on primary cultured TEC. To further confirm the hypothesis that TRPC6 knockout could alleviate fibrotic damage by inhibition of EMT, most of our work *in vitro* was performed on the primary cultured TEC in parallel with the *in vivo* mice model study. The obvious changes of EMT markers, including the decrease of E-cadherin and Cadh16 along with the increase of α-SMA and snail1, occurred when the primary TEC were stimulated with TGF-β1 for 72 h. For the first time, we have found that TRPC6, not TRPC3, was upregulated in primary TEC treated with TGF-β1 from the WT mice, and the phenotypic changes of EMT were also partially reversed in primary TEC from the TRPC6$^{-/-}$ mice. Immunofluorescence assay showed that primary TEC from the TRPC6$^{-/-}$ mice lack TRPC6 isoforms and had normal TRPC3 expression compared to TEC from the WT mice (**Supplementary Figure 2B**). Additionally, to address the relationship between TRPC6 and EMT, HYP9, the agonist of TRPC6, was used in primary TEC. We found a promotion of EMT in the HYP9-stimulated group compared to the control group (**Supplementary Figure 3A**). These results provide powerful evidence that the anti-fibrotic effect of TRPC6 knockout is related to the inhibition of EMT.

AKT, a serine/threonine protein kinase, acts as a downstream effector for PI3K (Cantrell, 2001) and plays a significant role in biological functions by activating its downstream effectors (Bertacchini et al., 2015; Jiang et al., 2015). mTOR is a key regulator and can be activated by phosphorylated-AKT. The activation of AKT-mTOR is found to be important in contributing to the fibrosis in different organs, including the lungs, liver, and heart (Wang et al., 2015; Reilly et al., 2017; Cui et al., 2019; Wan et al., 2019), which can regulate cell growth and promote EMT in the kidney (Yoo et al., 2011; Xuan et al.,

2014; Carpenter et al., 2015; Yang et al., 2015). Furthermore, the activation of ERK1/2 also significantly contributes to the onset of EMT (Chiu et al., 2017; Sankpal et al., 2017; Jia et al., 2018; Lee et al., 2019). Several studies have shown that the activation of AKT-ERK1/2 plays an important role in the process of EMT in fibrosis and that EMT was initiated through AKT-ERK1/2 activation (Wang et al., 2016; Qu et al., 2019). In order to determine whether the AKT-mTOR and ERK1/2 pathways would be related to the anti-fibrosis effect of TRPC6 knockout in the kidney, the relevant signal molecules were examined in both kidney tissues and primary TEC. In line with previous statements, our data showed that the ratio of phosphorylated-AKT, mTOR, and ERK1/2 was up-regulated strongly in obstructed kidney and TGF-β1-induced TEC. The expression of total AKT, mTOR, and ERK1/2 was also increased in kidney tissues after UUO, and this is consistent with previous studies (Hanatani et al., 2014; Higgins et al., 2017). The results confirmed that the pathways of AKT-mTOR and ERK1/2 were activated in kidney fibrosis. Furthermore, TRPC6$^{-/-}$ mice showed an obvious down-regulation of AKT-mTOR and ERK1/2 after UUO. Beyond that, we found the up-regulation of AKT-mTOR and ERK1/2 pathways in the HYP9-stimulated group compared to the control group (**Supplementary Figure 3B**). Therefore, TRPC6 knockout protects the fibrotic kidney through down-regulation of AKT-mTOR and ERK1/2 pathways. Otherwise, EMT was partially inhibited in TRPC6$^{-/-}$ mice and up-regulated along with the positive regulation of AKT-mTOR and ERK1/2 in the HYP9-stimulated group. We, therefore, concluded that TRPC6 knockout may protect the fibrotic kidney by inhibition of EMT through down-regulation of AKT-mTOR and ERK1/2 pathways. Whether other pathways beside AKT-mTOR and ERK1/2, such as Wnt/β-catenin, GSK3β, and Ras, are involved in the regulation of the phenotypic change of EMT by TRPC6 in kidney fibrosis requires further investigation.

In conclusion, we found that EMT was activated in kidney fibrosis both *in vitro* and *in vivo*. Fibrosis damage was alleviated in TRPC6$^{-/-}$ mice after UUO and in primary TEC treated with TGF-β1. Moreover, EMT was partially reversed along with the down-regulation of AKT-mTOR and ERK1/2 in TRPC6$^{-/-}$ mice. Therefore, we proposed that TRPC6 knockout may ameliorate kidney damage by the inhibition of EMT through down-regulating the AKT-mTOR and ERK1/2 pathways.

DATA AVAILABILITY STATEMENT

The original contributions presented in the study are included in the article/**Supplementary Materials**, further inquiries can be directed to the corresponding author/s.

ETHICS STATEMENT

The animal study was reviewed and approved by the ethics committee of Tongji Medical College of Huazhong University of Science and Technology.

AUTHOR CONTRIBUTIONS

YL, MZ, and YZ designed the research. YZ and NY performed experiments, analyzed data, and wrote the manuscript. AS, QW, WH, XH, and XZ contributed to the interpretation of the results. YL and MZ contributed to the analysis of data and preparation of the manuscript. All authors contributed to revise the article and approved the submitted version.

FUNDING

This research was supported by funding from the National Natural Science Foundation of China Grants 31171087 and 30970662 (to YL), the National Natural Science Foundation of China Grants 81172786, and the Health Committee of Hubei Province of China Grants WJ2019M146 (to MZ).

SUPPLEMENTARY MATERIAL

The Supplementary Material for this article can be found online at: https://www.frontiersin.org/articles/10.3389/fcell.2020.602703/full#supplementary-material

REFERENCES

Barrallo-Gimeno, A., and Nieto, M. A. (2005). The Snail genes as inducers of cell movement and survival: implications in development and cancer. *Development* 132, 3151–3161. doi: 10.1242/dev.01907

Bechtel, W., McGoohan, S., Zeisberg, E. M., Muller, G. A., Kalbacher, H., Salant, D. J., et al. (2010). Methylation determines fibroblast activation and fibrogenesis in the kidney. *Nat. Med.* 16, 544–550. doi: 10.1038/nm.2135

Bertacchini, J., Heidari, N., Mediani, L., Capitani, S., Shahjahani, M., Ahmadzadeh, A., et al. (2015). Targeting PI3K/AKT/mTOR network for treatment of leukemia. *Cell. Mol. Life Sci.* 72, 2337–2347. doi: 10.1007/s00018-015-1867-5

Cantrell, D. A. (2001). Phosphoinositide. 3-kinase signalling pathways. *J. Cell Sci.* 114, 1439–1445.

Carew, R. M., Wang, B., and Kantharidis, P. (2012). The role of EMT in renal fibrosis. *Cell Tissue Res.* 347, 103–116. doi: 10.1007/s00441-011-1227-1

Carpenter, R. L., Paw, I., Dewhirst, M. W., and Lo, H. W. (2015). Akt phosphorylates and activates HSF-1 independent of heat shock, leading to Slug overexpression and epithelial-mesenchymal transition (EMT) of HER2-overexpressing breast cancer cells. *Oncogene* 34, 546–557. doi: 10.1038/onc.2013.582

Chapman, H. A. (2011). Epithelial-mesenchymal interactions in pulmonary fibrosis. *Annu. Rev. Physiol.* 73, 413–435. doi: 10.1146/annurev-physiol-012110-142225

Chen, X., Lu, M., He, X., Ma, L., Birnbaumer, L., and Liao, Y. (2017). TRPC3/6/7 knockdown protects the brain from cerebral ischemia injury via astrocyte apoptosis inhibition and effects on NF-small ka, CyrillicB translocation. *Mol. Neurobiol.* 54, 7555–7566. doi: 10.1007/s12035-016-0227-2

Chevalier, R. L., Forbes, M. S., and Thornhill, B. A. (2009). Ureteral obstruction as a model of renal interstitial fibrosis and obstructive nephropathy. *Kidney Int.* 75, 1145–1152. doi: 10.1038/ki.2009.86

Chiu, L. Y., Hsin, I. L., Yang, T. Y., Sung, W. W., Chi, J. Y., Chang, J. T., et al. (2017). The ERK-ZEB1 pathway mediates epithelial-mesenchymal transition in pemetrexed resistant lung cancer cells with suppression by vinca alkaloids. *Oncogene* 36, 242–253. doi: 10.1038/onc.2016.195

Coresh, J., Selvin, E., Stevens, L. A., Manzi, J., Kusek, J. W., Eggers, P., et al. (2007). Prevalence of chronic kidney disease in the United States. *JAMA* 298, 2038–2047. doi: 10.1001/jama.298.17.2038

Cui, X., Liu, X., Han, Q., Zhu, J., Li, J., Ren, Z., et al. (2019). DPEP1 is a direct target of miR-193a-5p and promotes hepatoblastoma progression by PI3K/Akt/mTOR pathway. *Cell Death Dis.* 10:701. doi: 10.1038/s41419-019-1943-0

Davis, J., Burr, A. R., Davis, G. F., Birnbaumer, L., and Molkentin, J. D. (2012). A TRPC6-dependent pathway for myofibroblast transdifferentiation and wound healing *in vivo*. *Dev. Cell* 23, 705–715. doi: 10.1016/j.devcel.2012.08.017

Du, X., Shimizu, A., Masuda, Y., Kuwahara, N., Arai, T., Kataoka, M., et al. (2012). Involvement of matrix metalloproteinase-2 in the development of renal interstitial fibrosis in mouse obstructive nephropathy. *Lab. Invest.* 92, 1149–1160. doi: 10.1038/labinvest.2012.68

Duffield, J. S. (2014). Cellular and molecular mechanisms in kidney fibrosis. *J. Clin. Invest.* 124, 2299–2306. doi: 10.1172/JCI72267

Eddy, A. A. (1996). Molecular insights into renal interstitial fibrosis. *J. Am. Soc. Nephrol.* 7, 2495–2508.

Geng, X. Q., Ma, A., He, J. Z., Wang, L., Jia, Y. L., Shao, G. Y., et al. (2019). Ganoderic acid hinders renal fibrosis via suppressing the TGF-beta/Smad and MAPK signaling pathways. *Acta Pharmacol. Sin.* 41, 670–677. doi: 10.1038/s41401-019-0324-7

Gewin, L. S. (2018). Renal fibrosis: primacy of the proximal tubule. *Matrix Biol.* 68-69, 248–262. doi: 10.1016/j.matbio.2018.02.006

Grande, M., Franzen, A., Karlsson, J. O., Ericson, L. E., Heldin, N. E., and Nilsson, M. (2002). Transforming growth factor-beta and epidermal growth factor synergistically stimulate epithelial to mesenchymal transition (EMT) through a MEK-dependent mechanism in primary cultured pig thyrocytes. *J. Cell Sci.* 115, 4227–4236. doi: 10.1242/jcs.00091

Grande, M. T., Sánchez-Laorden, B., López-Blau, C., De Frutos, C. A., Boutet, A., Arévalo, M., et al. (2015). Snail1-induced partial epithelial-to-mesenchymal transition drives renal fibrosis in mice and can be targeted to reverse established disease. *Nat. Med.* 21, 989–997. doi: 10.1038/nm.3901

Grille, S. J., Bellacosa, A., Upson, J., Klein-Szanto, A. J., van Roy, F., Lee-Kwon, W., et al. (2003). The protein kinase Akt induces epithelial mesenchymal transition and promotes enhanced motility and invasiveness of squamous cell carcinoma lines. *Cancer Res.* 63, 2172–2178.

Hanatani, S., Izumiya, Y., Araki, S., Rokutanda, T., Kimura, Y., Walsh, K., et al. (2014). Akt1-mediated fast/glycolytic skeletal muscle growth attenuates renal damage in experimental kidney disease. *J. Am. Soc. Nephrol.* 25, 2800–2811. doi: 10.1681/ASN.2013091025

Hay, E. D. (1995). An overview of epithelio-mesenchymal transformation. *Acta Anat.* 154, 8–20. doi: 10.1159/000147748

He, X., Li, S., Liu, B., Susperreguy, S., Formoso, K., Yao, J., et al. (2017). Major contribution of the. 3/6/7 class of TRPC channels to myocardial ischemia/reperfusion and cellular hypoxia/reoxygenation injuries. *Proc. Natl. Acad. Sci. U.S.A.* 114, E4582–E4591. doi: 10.1073/pnas.1621384114

Hertig, A., Anglicheau, D., Verine, J., Pallet, N., Touzot, M., Ancel, P. Y., et al. (2008). Early epithelial phenotypic changes predict graft fibrosis. *J. Am. Soc. Nephrol.* 19, 1584–1591. doi: 10.1681/ASN.2007101160

Higgins, D. F., Ewart, L. M., Masterson, E., Tennant, S., Grebnev, G., Prunotto, M., et al. (2017). BMP7-induced-Pten inhibits Akt and prevents renal fibrosis. *Biochim. Biophys. Acta Mol. Basis Dis.* 1863, 3095–3104. doi: 10.1016/j.bbadis.2017.09.011

Hills, C. E., and Squires, P. E. (2011). The role of TGF-beta and epithelial-to mesenchymal transition in diabetic nephropathy. *Cytokine Growth Factor Rev.* 22, 131–139. doi: 10.1016/j.cytogfr.2011.06.002

Holian, J., Qi, W., Kelly, D. J., Zhang, Y., Mreich, E., Pollock, C. A., et al. (2008). Role of Kruppel-like factor. 6 in transforming growth factor-beta1-induced epithelial-mesenchymal transition of proximal tubule cells. *Am. J. Physiol. Renal Physiol.* 295, F1388–1396. doi: 10.1152/ajprenal.00055.2008

Horikawa, T., Yoshizaki, T., Kondo, S., Furukawa, M., Kaizaki, Y., and Pagano, J. S. (2011). Epstein-Barr virus latent membrane protein 1 induces snail and epithelial-mesenchymal transition in metastatic nasopharyngeal carcinoma. *Br. J. Cancer* 104, 1160–1167. doi: 10.1038/bjc.2011.38

Hou, X., Xiao, H., Zhang, Y., Zeng, X., Huang, M., Chen, X., et al. (2018). Transient receptor potential channel. 6 knockdown prevents apoptosis of renal tubular epithelial cells upon oxidative stress via autophagy activation. *Cell Death Dis.* 9:1015. doi: 10.1038/s41419-018-1052-5

Hu, H., Hu, S., Xu, S., Gao, Y., Zeng, F., and Shui, H. (2018). miR-29b regulates Ang II-induced EMT of rat renal tubular epithelial cells via targeting PI3K/AKT signaling pathway. *Int. J. Mol. Med.* 42, 453–460. doi: 10.3892/ijmm.2018.3579

Ito, S., Higuchi, Y., Yagi, Y., Nishijima, F., Yamato, H., Ishii, H., et al. (2013). Reduction of indoxyl sulfate by AST-120 attenuates monocyte inflammation related to chronic kidney disease. *J. Leukoc. Biol.* 93, 837–845. doi: 10.1189/jlb.0112023

Iwano, M., Plieth, D., Danoff, T. M., Xue, C., Okada, H., and Neilson, E. G. (2002). Evidence that fibroblasts derive from epithelium during tissue fibrosis. *J. Clin. Invest.* 110, 341–350. doi: 10.1172/JCI0215518

Jia, X. W., Li, Z. W., Dong, L. Y., Sun, G. Y., Wang, X., Gao, J., et al. (2018). Lack of hepatic stimulator substance expression promotes hepatocellular carcinoma metastasis partly through ERK-activated epithelial-mesenchymal transition. *Lab. Invest.* 98, 871–882. doi: 10.1038/s41374-018-0039-2

Jiang, L., Dong, P., Zhang, Z., Li, C., Li, Y., Liao, Y., et al. (2015). Akt phosphorylates Prohibitin. 1 to mediate its mitochondrial localization and promote proliferation of bladder cancer cells. *Cell Death Dis.* 6:e1660. doi: 10.1038/cddis.2015.40

Kalluri, R., and Weinberg, R. A. (2009). The basics of epithelial-mesenchymal transition. *J. Clin. Invest.* 119, 1420–1428. doi: 10.1172/JCI39104

Katz, A., Caramori, M. L., Sisson-Ross, S., Groppoli, T., Basgen, J. M., and Mauer, M. (2002). An increase in the cell component of the cortical interstitium antedates interstitial fibrosis in type. 1 diabetic patients. *Kidney Int.* 61, 2058–2066. doi: 10.1046/j.1523-1755.2002.00370.x

Kim, E. Y., Yazdizadeh Shotorbani, P., and Dryer, S. E. (2018). Trpc6 inactivation confers protection in a model of severe nephrosis in rats. *J. Mol. Med.* 96, 631–644. doi: 10.1007/s00109-018-1648-3

Klahr, S., and Morrissey, J. (2003). Obstructive nephropathy and renal fibrosis: The role of bone morphogenic protein-7 and hepatocyte growth factor. *Kidney Int. Suppl.* 64, S105–S112. doi: 10.1046/j.1523-1755.64.s87.16.x

Kong, D., Zhang, F., Shao, J., Wu, L., Zhang, X., Chen, L., et al. (2015). Curcumin inhibits cobalt chloride-induced epithelial-to-mesenchymal transition associated with interference with TGF-beta/Smad signaling in hepatocytes. *Lab. Invest.* 95, 1234–1245. doi: 10.1038/labinvest.2015.107

LeBleu, V. S., Taduri, G., O'Connell, J., Teng, Y., Cooke, V. G., Woda, C., et al. (2013). Origin and function of myofibroblasts in kidney fibrosis. *Nat. Med.* 19, 1047–1053. doi: 10.1038/nm.3218

Lee, M., Kim, D. W., Khalmuratova, R., Shin, S. H., Kim, Y. M., Han, D. H., et al. (2019). The IFN-gamma-p38, ERK kinase axis exacerbates neutrophilic chronic rhinosinusitis by inducing the epithelial-to-mesenchymal transition. *Mucosal Immunol.* 12, 601–611. doi: 10.1038/s41385-019-0149-1

Liang, H., Gu, Y., Li, T., Zhang, Y., Huangfu, L., Hu, M., et al. (2014). Integrated analyses identify the involvement of microRNA-26a in epithelial-mesenchymal transition during idiopathic pulmonary fibrosis. *Cell Death Dis.* 5:e1238. doi: 10.1038/cddis.2014.207

Lin, B. L., Matera, D., Doerner, J. F., Zheng, N., Del Camino, D., Mishra, S., et al. (2019). *In vivo* selective inhibition of TRPC6 by antagonist BI 749327 ameliorates fibrosis and dysfunction in cardiac and renal disease. *Proc. Natl. Acad. Sci. U.S.A.* 116, 10156–10161. doi: 10.1073/pnas.1815354116

Lin, X., Chai, G., Wu, Y., Li, J., Chen, F., Liu, J., et al. (2019). RNA m(6)A methylation regulates the epithelial mesenchymal transition of cancer cells and translation of Snail. *Nat. Commun.* 10:2065. doi: 10.1038/s41467-019-09865-9

Liu, B. C., Tang, T. T., Lv, L. L., and Lan, H. Y. (2018). Renal tubule injury: a driving force toward chronic kidney disease. *Kidney Int.* 93, 568–579. doi: 10.1016/j.kint.2017.09.033

Liu, L., Chen, X., Wang, Y., Qu, Z., Lu, Q., Zhao, J., et al. (2014). Notch3 is important for TGF-β-induced epithelial-mesenchymal transition in non-small cell lung cancer bone metastasis by regulating ZEB-1. *Cancer Gene Ther.* 21, 364–372. doi: 10.1038/cgt.2014.39

Liu, T., Meng, Q., Wang, C., Liu, Q., Guo, X., Sun, H., et al. (2012). Changes in expression of renal Oat1, Oat3 and Mrp2 in cisplatin-induced acute renal failure after treatment of JBP485 in rats. *Toxicol. Appl. Pharmacol.* 264, 423–430. doi: 10.1016/j.taap.2012.08.019

Liu, Y. (2004). Epithelial to mesenchymal transition in renal fibrogenesis: pathologic significance, molecular mechanism, and therapeutic intervention. *J. Am. Soc. Nephrol.* 15, 1–12. doi: 10.1097/01.ASN.0000106015.29070.E7

Liu, Y. (2011). Cellular and molecular mechanisms of renal fibrosis. *Nat. Rev. Nephrol.* 7, 684–696. doi: 10.1038/nrneph.2011.149

Liu, Y., Krueger, K., Hovsepian, A., Tepel, M., and Thilo, F. (2011). Calcium-dependent expression of transient receptor potential canonical type. 3 channels in patients with chronic kidney disease. *Arch. Biochem. Biophys.* 514, 44–49. doi: 10.1016/j.abb.2011.07.011

Liu, Y., Thilo, F., Kreutz, R., Schulz, A., Wendt, N., Loddenkemper, C., et al. (2010). Tissue expression of TRPC3 and TRPC6 in hypertensive munich wistar fromter rats showing proteinuria. *Am. J. Nephrol.* 31, 36–44. doi: 10.1159/000254060

Liu, B., He, X., Li, S., Xu, B., Birnbaumer, L., and Liao, Y. (2017). Deletion of diacylglycerol-responsive TRPC genes attenuates diabetic nephropathy by inhibiting activation of the TGFbeta1 signaling pathway. *Am. J. Transl. Res.* 9, 5619–5630.

Lovisa, S., LeBleu, V. S., Tampe, B., Sugimoto, H., Vadnagara, K., and Carstens, J. L. (2015). Epithelial-to-mesenchymal transition induces cell cycle arrest and parenchymal damage in renal *fibrosis. Nat. Med.* 21, 998–1009. doi: 10.1038/nm.3902

Lovisa, S., Zeisberg, M., and Kalluri, R. (2016). Partial epithelial-to-mesenchymal transition and other new mechanisms of kidney fibrosis. *Trends Endocrinol. Metab.* 27, 681–695. doi: 10.1016/j.tem.2016.06.004

Martinez-Klimova, E., Aparicio-Trejo, O. E., Tapia, E., and Pedraza-Chaverri, J. (2019). Unilateral ureteral obstruction as a model to investigate fibrosis-attenuating treatments. *Biomolecules* 9:141. doi: 10.3390/biom9040141

Masterson, R., Hewitson, T. D., Kelynack, K., Martic, M., Parry, L., Bathgate, R., et al. (2004). Relaxin down-regulates renal fibroblast function and promotes matrix remodelling *in vitro*. *Nephrol. Dial. Transplant.* 19, 544–552. doi: 10.1093/ndt/gfg598

Meng, X. M., Nikolic-Paterson, D. J., and Lan, H. Y. (2016). TGF-beta: the master regulator of fibrosis. *Nat. Rev. Nephrol.* 12, 325–338. doi: 10.1038/nrneph.2016.48

Minke, B. (1977). Drosophila mutant with a transducer defect. *Biophys. Struct. Mech.* 3, 59–64. doi: 10.1007/BF00536455

Moller, C. C., Wei, C., Altintas, M. M., Li, J., Greka, A., Ohse, T., et al. (2007). Induction of TRPC6 channel in acquired forms of proteinuric kidney disease. *J. Am. Soc. Nephrol.* 18, 29–36. doi: 10.1681/ASN.2006091010

Montell, C., Jones, K., Hafen, E., and Rubin, G. (1985). Rescue of the Drosophila phototransduction mutation trp by germline transformation. *Science* 230, 1040–1043. doi: 10.1126/science.3933112

Moustakas, A., and Heldin, C. H. (2005). Non-smad TGF-beta signals. *J. Cell Sci.* 118, 3573–3584. doi: 10.1242/jcs.02554

Neilson, E. G. (2006). Mechanisms of disease: Fibroblasts–a new look at an old problem. *Nat. Clin. Pract. Nephrol.* 2, 101–108. doi: 10.1038/ncpneph0093

Pang, M., Kothapally, J., Mao, H., Tolbert, E., Ponnusamy, M., Chin, Y. E., et al. (2009). Inhibition of histone deacetylase activity attenuates renal fibroblast activation and interstitial fibrosis in obstructive nephropathy. *Am. J. Physiol. Renal Physiol.* 297, F996–F1005. doi: 10.1152/ajprenal.00282.2009

Pang, M., Ma, L., Gong, R., Tolbert, E., Mao, H., Ponnusamy, M., et al. (2010). A novel STAT3 inhibitor, S3I-201, attenuates renal interstitial fibroblast activation and interstitial fibrosis in obstructive nephropathy. *Kidney Int.* 78, 257–268. doi: 10.1038/ki.2010.154

Paniagua-Sierra, J. R., and Galvan-Plata, M. E. (2017). Chronic kidney disease. *Rev. Med. Inst. Mex. Seguro Soc.* 55, S116–117.

Peinado, H., Olmeda, D., and Cano, A. (2007). Snail, Zeb and bHLH factors in tumour progression: an alliance against the epithelial phenotype? *Nat. Rev. Cancer* 7, 415–428. doi: 10.1038/nrc2131

Pillow, T. H., Tien, J., Parsons-Reponte, K. L., Bhakta, S., Li, H., Staben, L. R., et al. (2014). Site-specific trastuzumab maytansinoid antibody-drug conjugates with improved therapeutic activity through linker and antibody engineering. *J. Med. Chem.* 57, 7890–7899. doi: 10.1021/jm500552c

Qu, H., Liu, L., Liu, Z., Qin, H., Liao, Z., Xia, P., et al. (2019). Blocking TBK1 alleviated radiation-induced pulmonary fibrosis and epithelial-mesenchymal transition through Akt-Erk inactivation. *Exp. Mol. Med.* 51, 1–17. doi: 10.1038/s12276-019-0240-4

Quaggin, S. E., and Kapus, A. (2011). Scar wars: mapping the fate of epithelial-mesenchymal-myofibroblast transition. *Kidney Int.* 80, 41–50. doi: 10.1038/ki.2011.77

Radisky, D. C., Kenny, P. A., and Bissell, M. J. (2007). Fibrosis and cancer: do myofibroblasts come also from epithelial cells via EMT? *J. Cell. Biochem.* 101, 830–839. doi: 10.1002/jcb.21186

Rajasekaran, S. A., Huynh, T. P., Wolle, D. G., Espineda, C. E., Inge, L. J., Skay, A., et al. (2010). Na,K-ATPase subunits as markers for epithelial-mesenchymal transition in cancer and fibrosis. *Mol. Cancer Ther.* 9, 1515–1524. doi: 10.1158/1535-7163.MCT-09-0832

Rastaldi, M. P. (2006). Epithelial-mesenchymal transition and its implications for the development of renal tubulointerstitial fibrosis. *J. Nephrol.* 19, 407–412.

Reilly, R., Mroz, M. S., Dempsey, E., Wynne, K., Keely, S. J., McKone, E. F., et al. (2017). Targeting the PI3K/Akt/mTOR signalling pathway in cystic fibrosis. *Sci. Rep.* 7:7642. doi: 10.1038/s41598-017-06588-z

Saliba, Y., Karam, R., Smayra, V., Aftimos, G., Abramowitz, J., Birnbaumer, L., et al. (2015). Evidence of a role for fibroblast transient receptor potential canonical. 3 Ca2+ channel in renal fibrosis. *J. Am. Soc. Nephrol.* 26, 1855–1876. doi: 10.1681/ASN.2014010065

Sankpal, N. V., Fleming, T. P., Sharma, P. K., Wiedner, H. J., and Gillanders, W. E. (2017). A double-negative feedback loop between EpCAM and ERK contributes to the regulation of epithelial-mesenchymal transition in cancer. *Oncogene* 36, 3706–3717. doi: 10.1038/onc.2016.504

Schlondorff, J. (2017). TRPC6 and kidney disease: sclerosing more than just glomeruli? *Kidney Int.* 91, 773–775. doi: 10.1016/j.kint.2016.12.033

Shen, B., Zhou, S., He, Y., Zhao, H., Mei, M., and Wu, X. (2013). Revealing the underlying mechanism of ischemia reperfusion injury using bioinformatics approach. *Kidney Blood Press. Res.* 38, 99–108. doi: 10.1159/000355759

Shen, S., Jin, Y., Li, W., Liu, X., Zhang, T., Xia, W., et al. (2014). Recombinant human erythropoietin pretreatment attenuates acute renal tubular injury against ischemia-reperfusion by restoring transient receptor potential channel-6 expression and function in collecting ducts. *Crit. Care Med.* 42, e663–e672. doi: 10.1097/CCM.0000000000000542

Sugimoto, H., LeBleu, V. S., Bosukonda, D., Keck, P., Taduri, G., Bechtel, W., et al. (2012). Activin-like kinase. 3 is important for kidney regeneration and reversal of fibrosis. *Nat. Med.* 18, 396–404. doi: 10.1038/nm.2629

Tamaki, K., Okuda, S., Ando, T., Iwamoto, T., Nakayama, M., and Fujishima, M. (1994). TGF-beta. 1 in glomerulosclerosis and interstitial fibrosis of adriamycin nephropathy. *Kidney Int.* 45, 525–536. doi: 10.1038/ki.1994.68

Thiery, J. P., Acloque, H., Huang, R. Y., and Nieto, M. A. (2009). Epithelial-mesenchymal transitions in development and disease. *Cell* 139, 871–890. doi: 10.1016/j.cell.2009.11.007

Thiery, J. P., and Sleeman, J. P. (2006). Complex networks orchestrate epithelial-mesenchymal transitions. *Nat. Rev. Mol. Cell Biol.* 7, 131–142. doi: 10.1038/nrm1835

Verkman, A. S. (2002). Renal concentrating and diluting function in deficiency of specific aquaporin genes. *Exp. Nephrol.* 10, 235–240. doi: 10.1159/000063697

Wan, H., Xie, T., Xu, Q., Hu, X., Xing, S., Yang, H., et al. (2019). Thy-1 depletion and integrin beta3 upregulation-mediated PI3K-Akt-mTOR pathway activation inhibits lung fibroblast autophagy in lipopolysaccharide-induced pulmonary fibrosis. *Lab. Invest.* 99, 1636–1649. doi: 10.1038/s41374-019-0281-2

Wang, Z., Qu, L., Deng, B., Sun, X., Wu, S., Liao, J., et al. (2016). STYK1 promotes epithelial-mesenchymal transition and tumor metastasis in human hepatocellular carcinoma through MEK/ERK and PI3K/AKT signaling. *Sci. Rep.* 6:33205. doi: 10.1038/srep33205

Wang, Z. G., Wang, Y., Huang, Y., Lu, Q., Zheng, L., Hu, D., et al. (2015). bFGF regulates autophagy and ubiquitinated protein accumulation induced by myocardial ischemia/reperfusion via the activation of the PI3K/Akt/mTOR pathway. *Sci. Rep.* 5:9287. doi: 10.1038/srep09287

Wes, P. D., Chevesich, J., Jeromin, A., Rosenberg, C., Stetten, G., and Montell, C. (1995). TRPC1, a human homolog of a Drosophila store-operated channel. *Proc. Natl. Acad. Sci. U.S.A* 92, 9652–9656. doi: 10.1073/pnas.92.21.9652

Winn, M. P., Conlon, P. J., Lynn, K. L., Farrington, M. K., Creazzo, T., Hawkins, A. F., et al. (2005). A mutation in the TRPC6 cation channel causes familial focal segmental glomerulosclerosis. *Science* 308, 1801–1804. doi: 10.1126/science.1106215

Woudenberg-Vrenken, T. E., Bindels, R. J., and Hoenderop, J. G. (2009). The role of transient receptor potential channels in kidney disease. *Nat. Rev. Nephrol.* 5, 441–449. doi: 10.1038/nrneph.2009.100

Wu, Y. L., Xie, J., An, S. W., Oliver, N., Barrezueta, N. X., Lin, M. H., et al. (2017). Inhibition of TRPC6 channels ameliorates renal fibrosis and contributes to renal protection by soluble klotho. *Kidney Int.* 91, 830–841. doi: 10.1016/j.kint.2016.09.039

Wynn, T. A. (2008). Cellular and molecular mechanisms of fibrosis. *J. Pathol.* 214, 199–210. doi: 10.1002/path.2277

Xie, L., Law, B. K., Chytil, A. M., Brown, K. A., Aakre, M. E., and Moses, H. L. (2004). Activation of the Erk pathway is required for TGF-beta1-induced EMT *in vitro*. *Neoplasia* 6, 603–610. doi: 10.1593/neo.04241

Xu, J., Lamouille, S., and Derynck, R. (2009). TGF-beta-induced epithelial to mesenchymal transition. *Cell Res.* 19, 156–172. doi: 10.1038/cr.2009.5

Xuan, X., Zeng, Q., Li, Y., Gao, Y., Wang, F., Zhang, H., et al. (2014). Akt-mediated transforming growth factor-beta1-induced epithelial-mesenchymal transition in cultured human esophageal squamous cancer cells. *Cancer Gene Ther.* 21, 238–245. doi: 10.1038/cgt.2014.23

Yang, J., Qin, G., Luo, M., Chen, J., Zhang, Q., Li, L., et al. (2015). Reciprocal positive regulation between Cx26 and PI3K/Akt pathway confers acquired gefitinib resistance in NSCLC cells via GJIC-independent induction of EMT. *Cell Death Dis.* 6:e1829. doi: 10.1038/cddis.2015.197

Yang, Y. Z., Zhao, X. J., Xu, H. J., Wang, S. C., Pan, Y., Wang, S. J., et al. (2019). Magnesium isoglycyrrhizinate ameliorates high fructose-induced liver fibrosis in rat by increasing miR-375-3p to suppress JAK2/STAT3 pathway and TGF-beta1/Smad signaling. *Acta Pharmacol. Sin.* 40, 879–894. doi: 10.1038/s41401-018-0194-4

Yao, F., Wang, X., Cui, Z. K., Lan, H., Ai, X., Song, Q., et al. (2019). ETS2 promotes epithelial-to-mesenchymal transition in renal fibrosis by targeting JUNB transcription. *Lab. Invest.* 100, 438-453. doi: 10.1038/s41374-019-0331-9

Yoo, Y. A., Kang, M. H., Lee, H. J., Kim, B. H., Park, J. K., Kim, H. K., et al. (2011). Sonic hedgehog pathway promotes metastasis and lymphangiogenesis via activation of Akt, EMT, and MMP-9 pathway in gastric cancer. *Cancer Res.* 71, 7061–7070. doi: 10.1158/0008-5472.CAN-11-1338

Zeisberg, M., and Kalluri, R. (2013). Cellular mechanisms of tissue fibrosis. 1. common and organ-specific mechanisms associated with tissue fibrosis. *Am. J. Physiol. Cell Physiol.* 304, C216–C225. doi: 10.1152/ajpcell.00328.2012

Zhang, Y. E. (2018). Mechanistic insight into contextual TGF-beta signaling. *Curr. Opin. Cell Biol.* 51, 1–7. doi: 10.1016/j.ceb.2017.10.001

Zhou, L. F., Chen, Q. Z., Yang, C. T., Fu, Z. D., Zhao, S. T., Chen, Y., et al. (2018). TRPC6 contributes to LPS-induced inflammation through ERK1/2 and p38 pathways in bronchial epithelial cells. *Am. J. Physiol. Cell Physiol.* 314, C278–C288. doi: 10.1152/ajpcell.00117.2017

Zhou, T., Luo, M., Cai, W., Zhou, S., Feng, D., Xu, C., et al. (2018). Runt-related transcription factor. 1 (RUNX1) promotes TGF-beta-induced renal tubular Epithelial-to-Mesenchymal Transition (EMT) and renal fibrosis through the PI3K Subunit p110delta. *EBioMedicine* 31, 217–225. doi: 10.1016/j.ebiom.2018.04.023

Zubair, M., and Ahmad, J. (2019). Role of growth factors and cytokines in diabetic foot ulcer healing: a detailed review. *Rev. Endocr. Metab. Disord.* 20, 207–217. doi: 10.1007/s11154-019-09492-1

Conflict of Interest: The authors declare that the research was conducted in the absence of any commercial or financial relationships that could be construed as a potential conflict of interest.

Copyright © 2021 Zhang, Yin, Sun, Wu, Hu, Hou, Zeng, Zhu and Liao. This is an open-access article distributed under the terms of the Creative Commons Attribution License (CC BY). The use, distribution or reproduction in other forums is permitted, provided the original author(s) and the copyright owner(s) are credited and that the original publication in this journal is cited, in accordance with accepted academic practice. No use, distribution or reproduction is permitted which does not comply with these terms.

frontiers in Cell and Developmental Biology

ORIGINAL RESEARCH
published: 08 April 2021
doi: 10.3389/fcell.2021.648639

Fiber Derived Microbial Metabolites Prevent Acute Kidney Injury Through G-Protein Coupled Receptors and HDAC Inhibition

*Yunzi Liu[1,2†], Yan J. Li[2,3†], Yik W. Loh[2], Julian Singer[2,3], Weiping Zhu[2,4], Laurence Macia[5,6], Charles R. Mackay[7], Weiming Wang[1], Steven J. Chadban[2,3] and Huiling Wu[2,3]**

[1] Department of Nephrology, Ruijin Hospital, Shanghai Jiao Tong University School of Medicine, Shanghai, China, [2] Kidney Node Laboratory, The Charles Perkins Centre, University of Sydney, Camperdown, NSW, Australia, [3] Renal Medicine, Royal Prince Alfred Hospital, Sydney, NSW, Australia, [4] Department of Nephrology, The Fifth Affiliated Hospital of Sun Yat-sen University, Zhuhai, China, [5] Nutritional Immuno-metabolism Laboratory, The Charles Perkins Centre, University of Sydney, Camperdown, NSW, Australia, [6] School of Medical Sciences, Faculty of Medicine and Health, University of Sydney, Sydney, NSW, Australia, [7] Infection and Immunity Program, Biomedicine Discovery Institute, Monash University, Clayton, VIC, Australia

OPEN ACCESS

Edited by:
Nejra Prohic,
Clinical Center University of Sarajevo,
Bosnia and Herzegovina

Reviewed by:
Xin-Ming Chen,
Kolling Institute of Medical Research,
Royal North Shore Hospital, Australia
Angelica Thomaz Vieira,
Federal University of Minas Gerais,
Brazil
Yuan Min Wang,
Children's Hospital at Westmead,
Australia

***Correspondence:**
Huiling Wu
huiling.wu@sydney.edu.au

† These authors have contributed equally to this work and share first authorship

Specialty section:
This article was submitted to Molecular Medicine, a section of the journal Frontiers in Cell and Developmental Biology

Received: 01 January 2021
Accepted: 16 March 2021
Published: 08 April 2021

Citation:
Liu Y, Li YJ, Loh YW, Singer J, Zhu W, Macia L, Mackay CR, Wang W, Chadban SJ and Wu H (2021) Fiber Derived Microbial Metabolites Prevent Acute Kidney Injury Through G-Protein Coupled Receptors and HDAC Inhibition. Front. Cell Dev. Biol. 9:648639. doi: 10.3389/fcell.2021.648639

Short-chain fatty acids (SCFA) derived from gut microbial fermentation of fiber have been shown to exert anti-inflammatory and immune-modulatory properties in acute kidney injury (AKI). However the direct mechanistic link between SCFAs, diet and the gut microbiome is yet to be established. Using the murine model of folic-acid nephropathy (FAN), we examined the effect of dietary fiber on development of AKI (day 2) and subsequent chronic kidney disease (CKD) (day 28). FAN was induced in wild-type and knockout mice lacking G protein–coupled receptors *GPR41*, *GPR43*, or *GPR109A*. Mice were randomized to high-fiber or normal-chow diets, or SCFAs in drinking water. We used 16S rRNA sequencing to assess the gut microbiome and ^{1}H-NMR spectroscopy for metabolic profiles. Mice fed high-fiber were partially protected against development of AKI and subsequent CKD, exhibiting better kidney function throughout, less tubular injury at day 2 and less interstitial fibrosis and chronic inflammation at day 28 vs controls. Fiber modified the gut microbiome and alleviated dysbiosis induced by AKI, promoting expansion of SCFA-producing bacteria *Bifidobacterium* and *Prevotella*, which increased fecal and serum SCFA concentrations. SCFA treatment achieved similar protection, but not in the absence of GPR41 or GPR109A. Histone deacetylase activity (HDAC) was inhibited in kidneys of high-fiber fed mice. We conclude that dietary manipulation of the gut microbiome protects against AKI and subsequent CKD, mediated by HDAC inhibition and activation of GPR41 and GPR109A by SCFAs. This study highlights the potential of the gut microbiome as a modifiable target in the prevention of AKI.

Keywords: gut microbiota, acute kidney injury, dietary fiber, prebiotic, SCFA

INTRODUCTION

Acute kidney injury (AKI) occurs in approximately 10–15% of hospitalized patients (Al-Jaghbeer et al., 2018), with substantial impacts on morbidity, mortality and cost. A variety of pathogenic stimuli in AKI converge on a common cascade of injury-induced events, initiating innate immune responses via damage-associated molecular patterns (DAMPs) which activate Toll like receptors (TLRs) and the NLRP3 inflammasome, forming a vicious cycle of cell death and inflammation driven by pro-inflammatory cytokines, chemokines, and inflammatory cells (Rabb et al., 2016). Characterized initially by an exacerbated innate inflammatory response causing endothelial dysfunction, altered microcirculation, and tubular injury, innate immune cell-derived cytokines facilitate engagement and activation of adaptive immunity. AKI is an independent risk factor for subsequent development of incident chronic kidney disease (CKD), acceleration of pre-existing CKD, cardiovascular disease, heart failure, and death (Coca et al., 2012). Although molecular biomarkers are emerging for risk stratification and early detection, clinically relevant strategies to prevent AKI and associated adverse sequelae are lacking.

The recent surge of interest in gut commensal microbiota and advances in sequencing technologies have greatly changed our understanding of the gut-kidney axis. The potential role of the gut microbiota in the pathogenesis of kidney disorders, through maintenance of intestinal integrity, inflammatory responses, and metabolism has become apparent (Knauf et al., 2019). Short-chain fatty acids (SCFA), gut-derived metabolites produced by bacterial fermentation of non-digestible carbohydrates such as resistant starch, are a key candidate mediator for gut-kidney crosstalk (Sarbini et al., 2014). The most abundant SCFAs generated within the gut are acetate, propionate, and butyrate, of which acetate is present in the highest quantities (mM). In addition to being the main energy source for colonocytes, SCFAs mediate a range of extra-intestinal effects and have the capability to regulate host physiological functions and impact development of immune and inflammatory responses both locally and at distant sites after entering the circulation via active transport mediated by monocarboxylate transporters (Stumpff, 2018). SCFAs exert their effects through binding to metabolite-sensing G-protein-coupled receptors (GPR41, GPR43, and GPR109A) (Tan et al., 2014) or epigenetically via histone deacetylase (HDAC) modulation (Tan et al., 2014).

Experimental models of AKI induced by nephrotoxins (Abdul Hamid et al., 2012; Sun et al., 2013), contrast (Machado et al., 2012), and ischemia (Andrade-Oliveira et al., 2015) have been attenuated by the administration of gut derived SCFAs, highlighting the potential of the gut microbiota as a modifiable target. However, studies to-date have failed to demonstrate a direct mechanistic link between diet, the gut microbiota and response to kidney injury. Drug-induced nephrotoxicity contributes in up to 60% of in-hospital AKI episodes, resulting in substantial morbidity and mortality (Schetz et al., 2005). Murine folic-acid nephropathy (FAN) parallels this common clinical scenario, inducing a toxin-derived AKI through formation of luminal crystals and direct tubular toxicity with subsequent transition to CKD. Here we aimed to obtain deeper insights into how a microbial community responds over time during initiation of AKI and subsequent chronic kidney injury in FAN, and demonstrate how the microbiota's modifiable capacity can be harnessed through diet to prevent kidney injury.

MATERIALS AND METHODS

Animals

Wild-type (WT) C57BL/6 mice were obtained from the Animal Resource Centre (Perth, WA, Australia). *Gpr41*$^{-/-}$, *Gpr43*$^{-/-}$, and *Gpr109A*$^{-/-}$ mice on a C57BL/6 background were bred and maintained in our facility as previously described (Maslowski et al., 2009). Male mice aged 7–9 weeks were used in all experiments and housed in a specific pathogen free facility within the University of Sydney. All animal care and experiments were conducted in accordance with established guidelines and approved by the Animal Ethics Committees of the University of Sydney.

Induction of Folic Acid Nephropathy

Folic Acid Nephropathy (FAN) was induced by a single intraperitoneal injection of folic acid (Sigma, FA 8798) at a dose of 200 mg/kg in 0.3M $NaHCO_3$ (vehicle). Age and body weight matched controls (non-FAN) received volume and pH matched vehicle.

Diet and SCFA Treatment

Custom diets were purchased from Specialty Feeds, Australia (Nutritional Parameters: **Supplementary Table 1**). Mice were fed normal chow (NC) (AIN93G), or a high fiber (HF) modified high-amylose maize starch diet (SF11-025) which is based on AIN93G, commencing 2 weeks prior to FAN induction.

Short-chain fatty acids [150 mM sodium acetate (SA), 150 mM propionate (SP), or 100 mM butyrate (SB)] were dissolved in drinking water pH adjusted to 7.4, and administered to mice fed NC. Control mice received pH-matched control water (Ctrl). SCFA supplemented water was commenced 2 weeks prior to FAN induction and continued *ad libitum* throughout the duration of all experiments.

Study Design

Time-Course Study

To investigate kidney injury events and mechanism, groups of mice were euthanized early (day 2) and late (day 28) after folic acid injection to evaluate acute and chronic kidney injury, respectively.

Diet Experiment

To assess the influence of dietary fiber supplementation, we first conducted a pilot study (**Supplementary Figure 1**). C57BL/6 mice were then randomized to the two different diets commencing 2 weeks prior to FAN induction (**Supplementary Table 1**) in the following experimental groups with six mice per non-FAN control group at each time point: day 2: (1) NC + FAN

$n = 11$; (2) HF + FAN $n = 7$; day 28: (1) NC + FAN $n = 12$; (2) HF + FAN $n = 12$.

SCFA Experiment

C57BL/6 mice were maintained on NC and randomized to receive SA, SP, or SB in drinking water commencing 2 weeks prior to FAN induction in the following groups at each time point: day 2: (1) SA + FAN $n = 10$; (2) SP + FAN $n = 10$, (3) SB + FAN $n = 10$, (4) Ctrl water + FAN $n = 10$; with five mice per non-FAN control group; day 28: (1) SA + FAN $n = 12$; (2) SP + FAN $n = 12$, (3) SB + FAN $n = 12$, (4) Ctrl water + FAN $n = 12$; with six mice per non-FAN control group.

Mechanistic Experiments

Wild-type, GPR41, GPR43, and GPR109A deficient mice were randomized to diet or SCFA treatment commencing 2 weeks prior to FAN induction in the following groups ($n = 5$–15), evaluated at day 2:

- GPR109A: (1) *Gpr109A*$^{-/-}$ + FAN, (2) *Gpr109A*$^{-/-}$ + SB + FAN, (3) *Gpr109A*$^{-/-}$ + HF + FAN, (4) WT + FAN, (5) WT + SB + FAN, (6) WT + HF + FAN.
- GPR41: (1) *Gpr41*$^{-/-}$ + FAN, (2) *Gpr41*$^{-/-}$ + HF + FAN, (3) WT + FAN, (4) WT + HF + FAN.
- GPR43: (1) *Gpr43*$^{-/-}$ + FAN, (2) *Gpr43*$^{-/-}$ + SA + FAN, (3) *Gpr43*$^{-/-}$ + HF + FAN, (4) WT + FAN, (5) WT + SA + FAN, (6) WT + HF + FAN.

Sample Harvest

Blood, kidney tissue, and urine were collected on either day 2 or day 28 after FAN induction. Mouse fecal samples were collected under sterile conditions immediately following extrusion, frozen on dry ice and stored at −80°C.

Assessment of Kidney Function

Serum creatinine was measured by modified Jaffe method and urea was measured using dedicated Urease/GLDH reagents (Roche) at the Biochemistry Department of Royal Prince Alfred Hospital, Sydney, Australia.

Histology

Periodic acid-Schiff's (PAS) and Picro-Sirius Red (PSR) staining were performed on 3 and 5 μm formalin-fixed kidney sections, respectively. Acute tubular injury was assessed on PAS slides in a blinded manner using a scoring system adapted from Martin-Sanchez et al. (2017) containing the following six parameters: loss of brush border, vacuolization, tubular cast formation, tubular epithelial cell edema, cellular infiltration, and tubular dilation. Acute tubular injury was scored on a semi-quantitative zero to three scale for each parameter and the results from each parameter were added to yield the tubular injury score with a maximal value of 18, assessed in at least 15 consecutive fields (×200 magnification). Chronic injury was scored on percentage of renal cortex with tubular atrophy and interstitial fibrosis in 15 randomly chosen, non-overlapping fields at ×200 magnification: 0, none; 0.5, <10%; 1, 10–25%; 2, 26–50%; 3, 51–75%; and 4, >75%. Interstitial collagen deposition was defined as the PSR-positive area, assessed by point counting using a 10 × 10 ocular grid at ×400 magnification in 20 consecutive fields (Li et al., 2020).

Immunohistochemistry and Quantification

Acetone-fixed frozen sections of kidney and spleen were stained for CD4, CD8, CD68, CD11c, and Ly-6B.2 as described previously (Wu et al., 2020). Endogenous peroxidase activity was blocked with 0.06% hydrogen peroxide, followed by application of a biotin blocker system (DAKO). After blocking with 20% normal horse serum (NHS), primary antibodies: anti-CD4 (BD, 550280), anti-CD8 (BD, 550281), anti-CD11c (BD, 550283), anti-CD68 (ABD Serotec Inc., MCA1957), and anti-Ly-6B.2 (ABD Serotec Inc., MCA771GA) were incubated for 60 min. For visualization of bound primary antibodies, sections were washed then incubated with secondary antibodies: biotinylated anti-rat, anti-hamster, and anti-rabbit IgG (BD Pharmingen). Vector stain ABC kit (Vector Laboratories Inc.) was applied, followed by 3,3diaminobenzidine (DAB) solution (DAKO), and counter-staining with Harris' hematoxylin.

Immunohistochemistry staining was assessed in a blinded manner by analysis of 20 consecutive high-power fields (×400 magnification) of renal cortex in each section. Macrophage (CD68$^+$) and dendritic cell (CD11c$^+$) infiltrates were quantified using digital image analysis software (Image Pro Premier 9). T cells (CD4$^+$ or CD8$^+$) and neutrophils (Ly-6B.2$^+$) were counted using an ocular grid and expressed as cells per HPF in a blinded manner as described previously (Wu et al., 2007, 2020).

Gene Expression Analysis

Total RNA was extracted from kidney tissue with Trizol® (Invitrogen). cDNA was synthesized using oligo d(T)$_{16}$ (Applied Biosystems) primers and the SuperScript III Reverse Transcriptase kit (Invitrogen 18080-044). Taqman Real-Time PCR was employed using the Roche Lightcycler 480 (Roche Applied Science) for the following genes: TLR2, TLR4, NLRP3, ASC, TNFα, IL6, IL18, IL1β, IL4, IL10, IFNγ, CXCL2, CCL2, CXCL10, iNOS, KIM1, MMP2, MMP9, TGFβ1, HDAC1-11, and GAPDH (Applied Biosystems). Results were normalized to GAPDH expression.

Bacterial DNA Sequencing and Bioinformatics Analysis

Bacterial genomic DNA was extracted from feces, amplified and sequenced at the Ramaciotti Centre for Genomics (University of New South Wales, Sydney, NSW, Australia) as previously described (Li et al., 2020; Wu et al., 2020). Data was deposited in the European Nucleotide Archive (EMBL-EBI) under accession number PRJEB40433. Bioinformatics analysis was performed using the QIIME2 2020.2 pipeline. Paired-end reads were joined using the fast-q algorithm. Demultiplexed sequences were then denoised and ≥97% similar sequences clustered into operational taxonomic units (OTUs) via DADA2. Taxonomies were assigned with BLAST against the Greengenes v13.8 database at 99% sequence identity using q2-feature-classifier algorithm. Taxa

present at <0.01% were filtered. Rarefaction analysis was used to compare the adequacy of sequencing depth (**Supplementary Figure 2**). Data was log2 transformed to account for non-normal distribution of taxonomic count data. Alpha diversity was measured using Shannon diversity. Bacterial community profiles were compared using Weighted Unifrac clustering of OTU abundances. The differential abundance of microbiota species was determined by ANCOM analysis in Calypso and also on complete libraries using DESeq2 model (R package, phyloseq v1.29.0) (McMurdie and Holmes, 2013). Pearson correlation-based network showing relationships between serum creatinine/BUN and bacterial taxa were visualized. Microbial metagenomes were predicted from 16S rRNA gene data using Phylogenetic Investigation of Communities by Reconstruction of Unobserved States (PICRUSt). Identified Kyoto Encyclopedia of Genes and Genomes (KEGG) orthologous groups (KO) with significant differences were visualized using STAMP (Parks et al., 2014).

SCFA Measurements

Fecal and serum metabolic profiling was performed using ^{1}H NMR spectroscopy on a Bruker 600 MHz AVANCE III spectrometer (Bruker BioSpin) and analyzed using Chenomx NMR Suite v8.4 (Chenomx Inc.) as previously described (Li et al., 2020).

Histone Deacetylase Activity Assay

To determine the activity of HDAC, equal quantities of nuclear fraction proteins (20 μg) were extracted from kidney tissue (Active Motif, 40010), and analyzed using a Fluorometric HDAC Activity Assay Kit (BioVision, k330-100) as described previously (Wu et al., 2020).

Statistical Analyses

Data are presented as mean ± SD or mean ± SEM. Normally distributed data was analyzed using Student's two-tailed *t*-tests, or one- or two-way analysis of variance (ANOVA) with *post hoc* multiple comparisons by Tukey's test. Non-normally distributed data was analyzed using Kruskall–Wallis non-parametric testing with *post hoc* multiple comparisons by Dunn's test (GraphPad Software). A *P*-value of <0.05 was considered statistically significant.

RESULTS

HF Diet Protects Against FA Induced Acute Kidney Injury at Day 2

Folic acid induced AKI was characterized by acute renal dysfunction, tubular injury, and tubulo-interstitial inflammation peaking at 48 h after FA injection. To assess the effect of dietary fiber on AKI, we fed WT mice diets containing standard (NC) or enriched amounts of fiber (resistant starch), commencing 2 weeks before induction of FAN. NC fed mice rapidly developed AKI, marked by elevated serum creatinine (SCr 69.3 ± 54.2 vs 5 ± 1.7 μmol/L, $P < 0.01$) and blood urea nitrogen (BUN 50.1 ± 27.2 vs 8.3 ± 1.7 mmol/L, $P < 0.01$) at day 2 post FA injection compared to non-FAN controls (**Figures 1A,B**). HF fed mice were protected from FA-induced AKI, displaying significantly lower SCr (5.7 ± 3.0 vs 69.3 ± 54.2 μmol/L, $P < 0.01$) and BUN (11.7 ± 5.5 vs 50.1 ± 27.2 mmol/L, $P < 0.001$) compared to those fed NC at day 2, with no difference compared to non-FAN controls (**Figures 1A,B**). HF feeding also afforded protection as assessed by semi-quantitative histopathological scoring. NC fed mice incurred severe tubulo-interstitial damage, with tubular dilation, endothelial injury, interstitial infiltrate, and intra-tubular cast formation at day 2 post FA injection, which was significantly attenuated in HF fed mice (**Figures 1C,D**). Non-FAN mice incurred no tubulo-interstitial injury.

Interstitial Cellular Infiltrates Were Reduced in the Kidneys of HF Fed Mice

Substantial infiltration of Ly6B.2^{+} neutrophils were evident in FAN kidney of NC fed mice at day 2 post FA injection vs non-FAN controls ($P < 0.001$), and this was attenuated in HF fed mice ($P < 0.05$, **Figures 1E,F**). Similarly, significant CD68^{+} macrophage accumulation was evident in FAN kidney in NC fed mice compared to non-FAN controls, but not in HF fed mice at day 2 post FA injection ($P < 0.05$, **Figures 1G,H**).

HF Diet Reduced the Expression of Inflammatory and Tubular Injury Genes Within the Kidney in AKI

Activation of innate immune receptors and the inflammasome by DAMPs, leading to increased expression of downstream proinflammatory genes, is believed to play a major role in the initiation and extension phases of AKI (Leemans et al., 2005; Wu et al., 2007). We next examined the expression of innate immune receptors (TLR2 and TLR4), inflammasome components (NLRP3 and ASC) and downstream inflammatory molecules in the kidney at day 2 post FA-injection by real-time PCR. mRNA expression of TLR2 and TLR4, inflammasome components (NLRP3 and ASC) and downstream pro-inflammatory cytokines (IL6 and TNFα) and chemokines (CCL2 and CXCL2) were significantly upregulated in the kidneys of NC-fed mice at day 2 compared to non-FAN controls. Comparatively, mice fed HF exhibited reduced expression of innate immune receptors and the inflammasome, downstream pro-inflammatory cytokines (IL6 and TNFα) and chemokines (CCL2 and CXCL2) (**Figure 1I**). This was consistent with markedly reduced CD68^{+} macrophage and Ly6B.2^{+} neutrophil accumulation within the kidney (**Figures 1E–H**).

KIM1, a specific marker of tubular epithelial cell injury, was profoundly increased at day 2 in the kidneys of FAN mice fed NC, though markedly less so in kidneys of HF-fed mice (**Figure 1I**), correlating with lower tubular injury scores (**Figure 1D**).

HF Fed Mice Were Protected Against Subsequent Chronic Kidney Injury at Day 28

The FAN model is characterized by partial recovery from AKI, followed by development of CKD by day 28. NC fed FAN

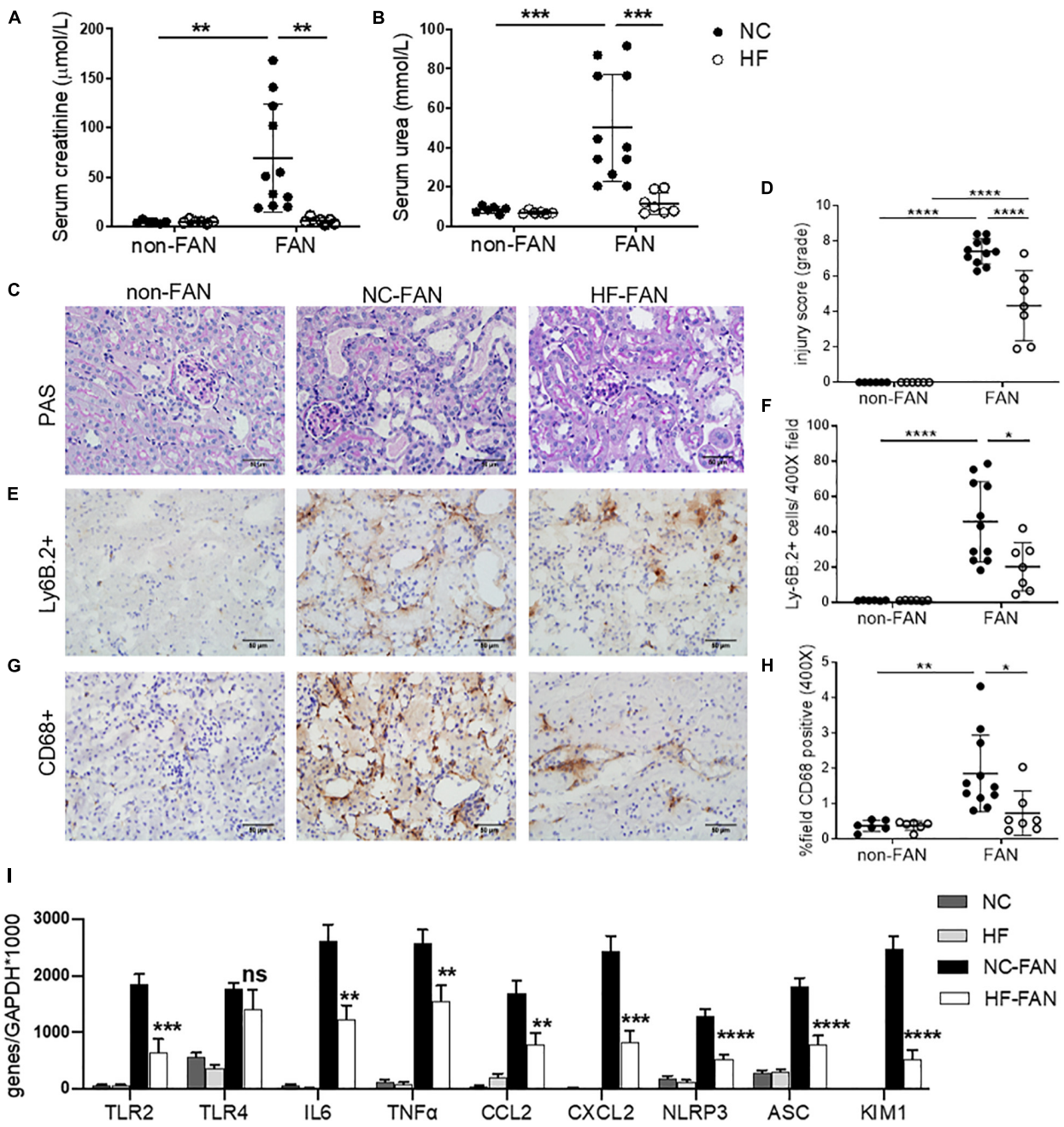

FIGURE 1 | High fiber (HF) diet ameliorates acute kidney injury (AKI) and inflammation in folic acid nephropathy (FAN) at day 2. Folic acid (FA) injection induced AKI in normal chow (NC) fed mice, with peak serum creatinine and blood urea nitrogen (BUN) at day 2. High fiber (HF) fed mice were protected from FA induced AKI with lower serum creatinine **(A)**, BUN **(B)** and tubular injury scores **(D)** compared to NC. **(C)** Representative sections from HF and NC fed FAN and NC fed non-FAN mice at day 2 (PAS stained, ×400 magnification). Representative sections of kidney from mice at day 2 demonstrating increased Ly6B.2^{+} neutrophil **(E)** and CD68^{+} macrophage **(G)** infiltration in NC fed FAN mice compared to controls, which was attenuated by HF feeding **(F,H)**. **(I)** mRNA expression of innate immune receptors (TLR2), pro-inflammatory cytokines (IL6 and TNFα), chemokines (CCL2 and CXCL2), inflammasome components (NLRP3 and ASC), and markers of renal proximal tubular injury (KIM1) were significantly reduced in HF fed mice compared with NC fed FAN controls, as measured by real-time PCR in kidney tissue. NC, vehicle ($n = 6$); HF, vehicle ($n = 6$); NC, FAN ($n = 11$); HF, FAN ($n = 7$). Photomicrographs at 400×, scale bar 50 μm. Data are shown as means ± SD or mean ± SEM; $^{*}P < 0.05$, $^{**}P < 0.01$, $^{***}P < 0.001$, $^{****}P < 0.0001$.

mice exhibited partial recovery in kidney function by day 28, however SCr and BUN remained higher than non-FAN controls (SCr 12.3 ± 4.4 vs 4.3 ± 1.0 μmol/L; BUN 25.1 ± 5.4 vs 8.8 ± 1.1 mmol/L, $P < 0.001$, **Figures 2A,B**). HF fed FAN mice showed a more complete recovery from kidney dysfunction (SCr: 6.6 ± 2.2 vs 12.3 ± 4.4 μmol/L, $P < 0.001$ and BUN: 19.5 ± 4.3

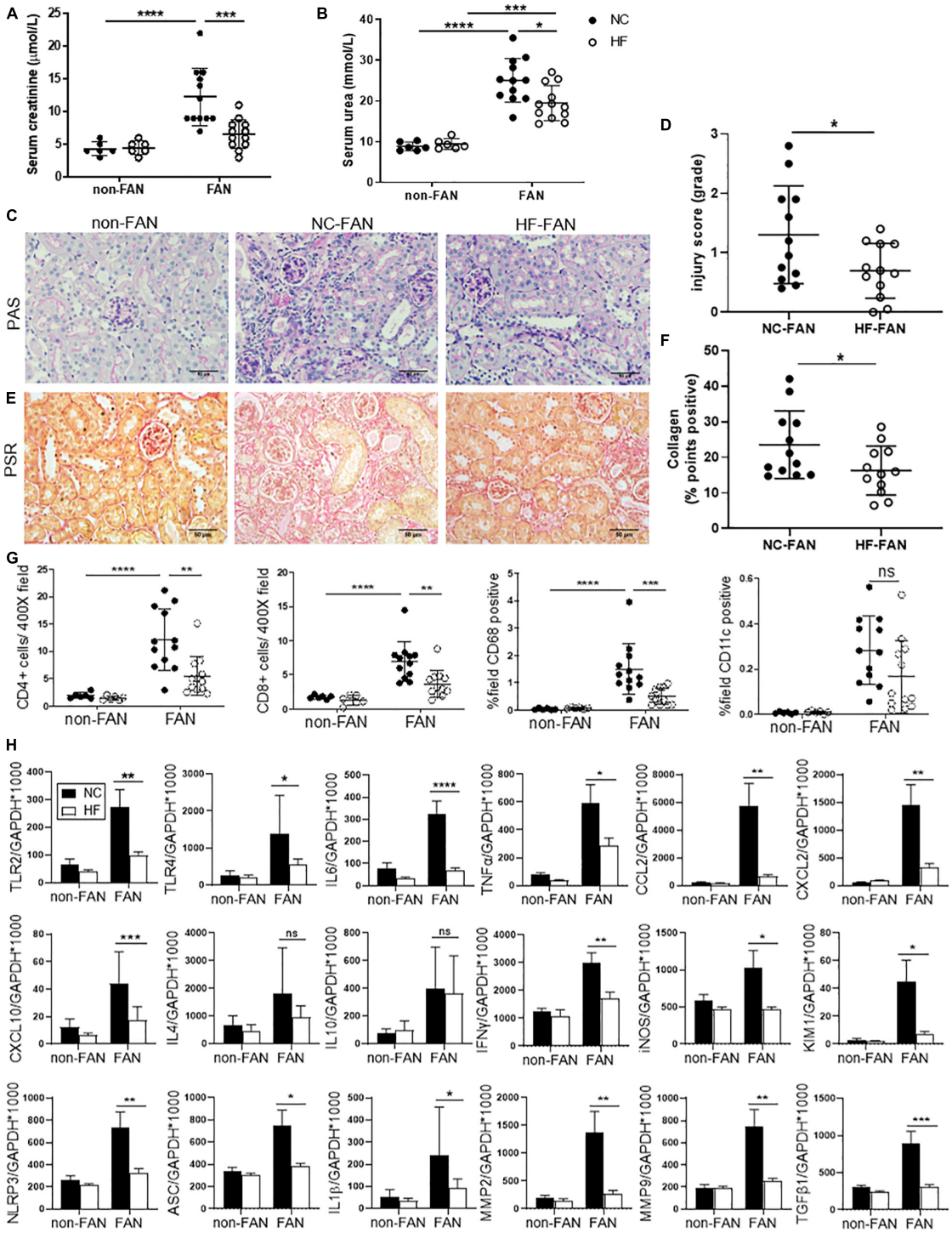

FIGURE 2 | HF fed mice exhibit less chronic inflammation at day 28 after FAN induced AKI. HF fed mice developed less chronic kidney injury at day 28 following FA-induced AKI, with lower serum creatinine **(A)**, BUN **(B)** and histological injury scores assessed on PAS stained kidney sections **(C,D)** compared to NC fed FAN controls. Representative sections of kidney from FAN and non-FAN mice at day 28 demonstrating increased interstitial collagen deposition attenuated by HF feeding on PSR staining **(E,F)**. Quantification of immunostaining for $CD4^+$ and $CD8^+$ T cells, $CD68^+$ macrophages and $CD11c^+$ dendritic cells demonstrates significant infiltration in NC fed FAN kidneys. HF feeding significantly diminished T cell and $CD68^+$ macrophage accumulation in FAN kidneys, with a trend toward diminished $CD11c^+$ infiltrate **(G)**. **(H)** mRNA expression of innate immune receptors (TLR2 and TLR4), pro-inflammatory cytokines (TNFα, IL6, and IFNγ), chemokines (CCL2, CXCL2, and CXCL10), inflammatory mediator (iNOS), inflammasome components (NLRP3, ASC, and IL1β), renal proximal tubular injury marker (KIM1), and fibrosis related genes (TGFβ1, MMP2, and MMP9) were significantly reduced in HF fed FAN mice as compared to NC fed FAN controls. No significant difference was seen in Th2 cytokines (IL4 and IL10) following HF feeding. NC, vehicle ($n = 6$); HF, vehicle ($n = 6$); NC, FAN ($n = 12$); HF, FAN ($n = 12$). Photomicrographs at 400×, scale bar 50 μm. Data are shown as means ± SD or mean ± SEM; $^*P < 0.05$, $^{**}P < 0.01$, $^{***}P < 0.001$, $^{****}P < 0.0001$.

vs 25.1 ± 5.4 mmol/L, $P < 0.05$, for HF vs NC, respectively), with no difference compared to non-FAN controls (**Figures 2A,B**).

Normal chow fed FAN mice demonstrated progression to chronic renal injury (**Figures 2C,D**) and tubulo-interstitial fibrosis following AKI (**Figures 2E,F**) with persistent renal expression of KIM1 at day 28 (**Figure 2H**). HF fed mice developed less chronic tubular injury and interstitial fibrosis, evidenced by decreased morphological chronic injury score (**Figures 2C,D**) and diminished interstitial accumulation of collagen (**Figures 2E,F**).

The innate immune system activates adaptive immune responses in the extension phase of AKI, promoting chronic inflammation and infiltration of T cells and macrophages, drivers of renal fibrosis (Agarwal et al., 2016). Immunohistochemical assessment revealed significant accumulation of $CD4^+$ and $CD8^+$ T cells, $CD68^+$ macrophages and $CD11c^+$ dendritic cells at day 28 in the kidneys of FAN mice fed NC, as compared to non-FAN controls. Accumulation of T cells and macrophages was significantly reduced in kidney from HF fed FAN mice at day 28 (**Figure 2G**).

HF Diet Attenuates Chronic Inflammatory Responses Following AKI

Assessment of gene expression relevant to chronic inflammation in NC fed FAN kidney at day 28 revealed significant upregulation of TLR2, TLR4, inflammasome (NLRP3 and ASC), downstream proinflammatory cytokines (IL6, TNFα, and IL1β), chemokines (CCL2, CXCL2, and CXCL10), Th1 cytokine (IFNγ), inflammatory mediators (iNOS) and genes involved in tissue remodeling (MMP2 and MMP9) and fibrosis (TGFβ1) compared to non-FAN controls (**Figure 2H**). Less chronic inflammation was observed in the kidneys of FAN mice fed HF compared to NC diet, with persistently lower expression of pro-inflammatory and pro-fibrotic genes (**Figure 2H**).

HF Diet Reduces FAN-Induced Dysbiosis and Fosters Expansion of SCFA-Producing Bacteria

We next investigated the influence of diet and kidney injury on gut microbiota composition by performing 16S rRNA sequencing of mouse feces at days 2 and 28 following FAN induction. At day 2, there were clear and significant differences in gut bacterial composition associated with FAN, consistent with a disease-related dysbiosis. Principal coordinate analyses of Unifrac Distances showed cluster separation mice with and without FAN (NC vs NC-FAN, $P < 0.01$; HF vs HF-FAN, $P = 0.032$, **Figure 3A**). This relationship was modified by diet, with additional separation between HF and NC fed groups (NC vs HF $P < 0.01$, NC-FAN vs HF-FAN, $P < 0.01$). Examination of relative abundance at the phylum level found *Bacteroidetes* and *Firmicutes* to be the dominant phyla in all four groups, regardless of diet (**Figure 3B**). The third most-dominant phylum, however, differed significantly according to diet and disease status. FAN mice fed NC revealed expansion of *Verrucomicrobia* (represented by a single genus, *Akkermansia muciniphila*) at the expense of *Actinobacteria* (**Figures 3B,C**), a pattern previously reported as dysbiotic (Tan et al., 2016; Wu et al., 2020). In contrast, HF-fed FAN mice exhibited a stable *Verrucomicrobia* population with no difference compared to non-FAN controls (**Figures 3B,C**). HF diet suppressed the *Firmicutes/Bacteroidetes* ratio and maintained the abundance of *Actinobacteria*, but not *Verrucomicrobia* (**Figures 3C,E**). At the genus level, expansion of the SCFA producing genera *Bifidobacterium* and *Prevotella,* with relative reduction of pathobionts *Odoribacter, Bilophila, Ruminococcus, Dorea*, and *Clostridium*, was also seen in HF fed mice compared to NC fed controls (**Figures 3D,E**). Pearson-correlation analysis to identify bacteria associated with severity of renal dysfunction found *Bifidobacterium* to exhibit a strong negative correlation with increment in serum creatinine ($P < 0.0001$, $R = -0.82$) (**Figure 3F** and **Supplementary Table 2**). A heatmap based on the Pearson-correlation analysis demonstrated that pathobionts *Odoribacter, Bilophila, Ruminococcus, Dorea, Akkermansia*, and *Clostridium* expanded in NC groups were associated with elevated serum creatinine and BUN, whilst "protective bacteria" expanded in HF fed mice, including SCFA producers *Bifidobacterium* and *Prevotella*, were associated with lower SCr and BUN (**Figure 3F** and **Supplementary Table 2**).

We then conducted a gene-centric analysis using the PICRUSt approach to predict functional changes in the gut microbiota that might contribute to improved host renal outcomes. Analysis of 16S-rRNA-inferred metagenomes found a number of metabolic pathways associated with FAN that were modified by diet. Increased activation of pathways associated with damage repair including RNA transcription, repair proteins and alkaloid biosynthesis was seen in FAN mice fed NC compared to HF. Interestingly, we also found greater butyrate and propionate metabolism in FAN mice fed NC compared to a HF diet (**Supplementary Figure 3**). No difference was seen between diets in non-FAN mice (data not shown), indicating that SCFAs might play a role in reactive anti-inflammatory processes after injury.

At day 28, less disease related dysbiosis was evident, with similar microbial composition between FAN and non-FAN groups as determined by principal coordinate analysis of weighted Unifrac distances (NC vs NC-FAN, $P = 0.403$) and similar alpha diversity. However, significant divergence remained between diet groups (**Supplementary Figure 4**). At the phylum and genus levels, the alterations in microbial communities induced by AKI at day 2 were relatively maintained at day 28 post FAN induction (**Supplementary Figures 4B–D**). We used Pearson's correlation analyses to identify bacteria associated with CKD determined by urea and creatinine increment. HF fed mice maintained a "healthier gut microbiota," characterized by expansion of the genera *Bifidobacterium* and *Prevotella*, which negatively corrected with creatinine increment (**Supplementary Figures 4E,F**) and reduction of pathobionts *Odoribacteria* which positively correlated with severity of renal dysfunction and elevated creatinine (**Supplementary Figure 4G**).

HF Diet Promotes Sustained Fecal and Systemic SCFA Production

As dietary fiber is known to be fermented by the gut microbiota to release SCFAs, we next measured SCFA levels in feces and

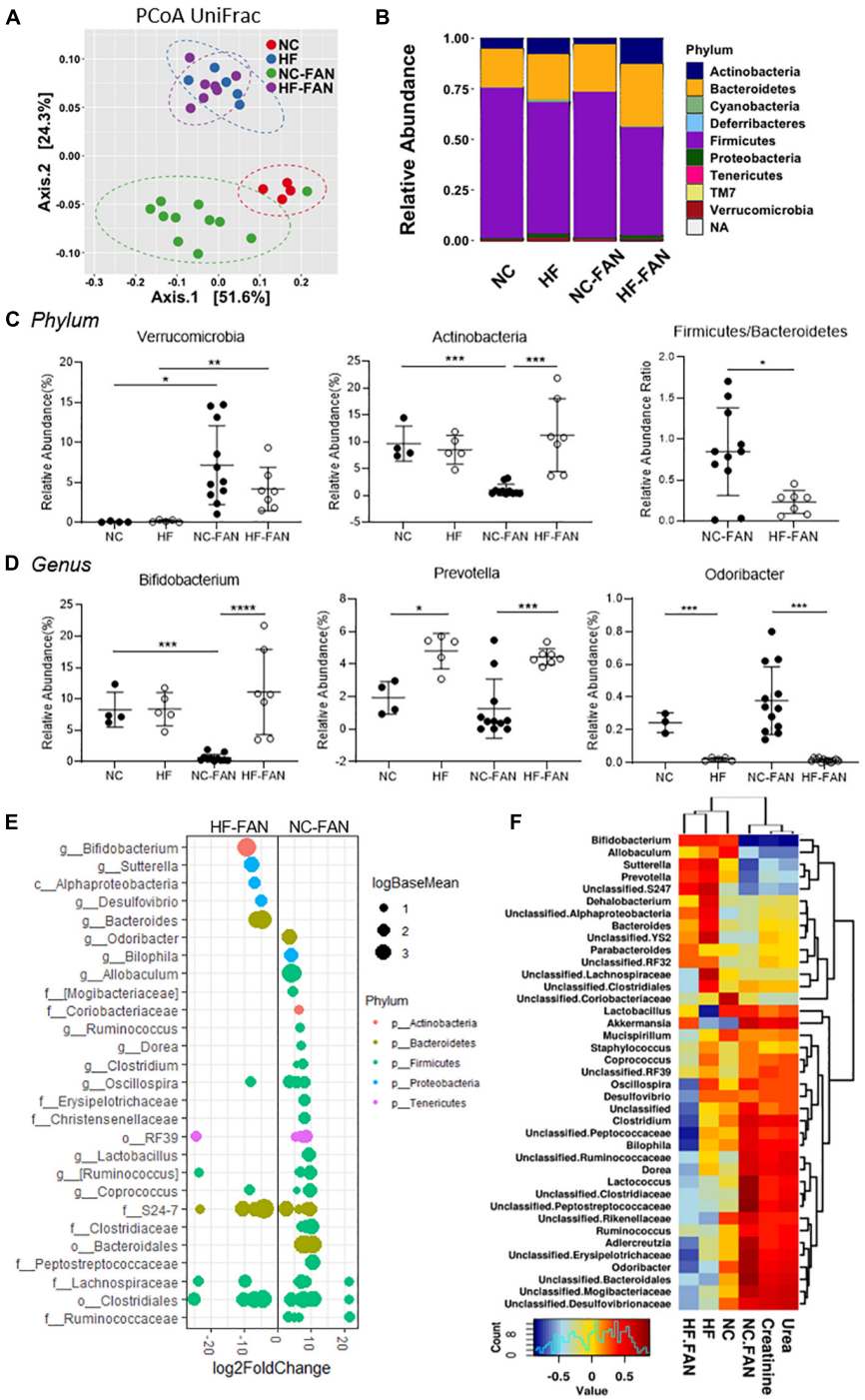

FIGURE 3 | High Fiber diet alters the gut microbial community structure and protects against FAN associated acute dysbiosis at day 2. Fecal DNA analysis using 16S rRNA sequencing was performed on mice fed a NC (FAN: $n = 11$; non-FAN: $n = 4$) and HF (FAN: $n = 7$; non-FAN: $n = 5$) diet at day 2 after FAN induction. **(A)** Principal coordinate analysis of the weighted Unifrac distances demonstrates significant modulation in the microbiota community with cluster separation between diet groups and mice with and without FAN. **(B,C)** Taxonomical composition and relative abundance of different bacteria by ANCOM analysis at the phylum level, depicting "dysbiosis" with expansion of *Verrucomicrobia* at the expense of *Actinobacteria* in NC fed mice, which was modulated by HF feeding. A HF diet suppressed the *Firmicutes* to *Bacteroidetes* ratio. **(D)** At the genus level, NC fed FAN mice had lower levels of the SCFA producers *Bifidobacterium* and *Prevotella*, with relative expansion of the pathobiont *Odoribacter* compared to those fed HF. **(E)** DESeq2 analysis demonstrating differential abundant OTUs (FDR adjusted $P < 0.01$) between dietary groups after FAN induction. OTUs were assigned to their lowest described classification (*y*-axis) and color coded by phylum. Bubble size represents a log fold change in the log base mean of the recorded OTU, with the *x*-axis values demonstrating log2 fold change in relative abundance. **(F)** Pearson-correlation-based heatmap at a genus level, identifying the bacteria associated with increment of serum urea and creatinine. Cool colors represent negative correlation and hot colors represent positive correlations. Data are shown as means ± SD; $^{*}P < 0.05$, $^{**}P < 0.01$, $^{***}P < 0.001$, $^{****}P < 0.0001$.

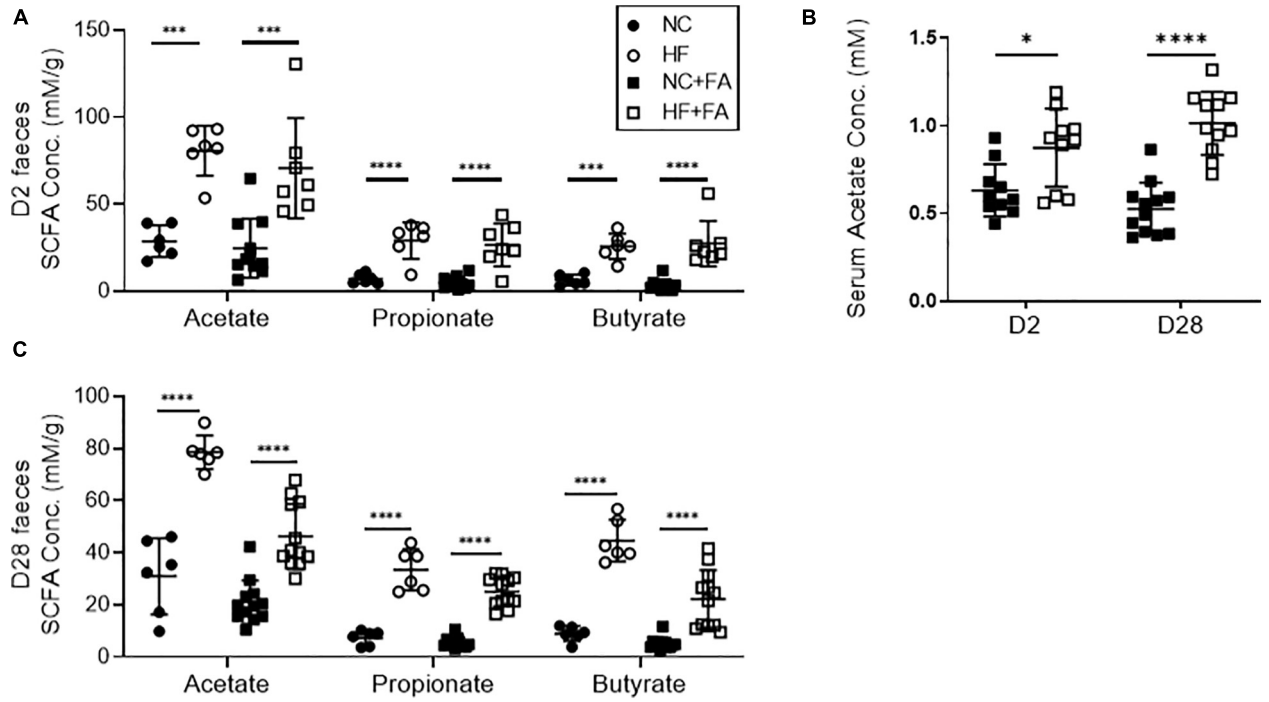

FIGURE 4 | Quantification of SCFA levels in feces and serum by ^{1}H-NMR spectroscopy. HF fed mice had significantly higher levels of fecal SCFAs **(A)** and serum acetate **(B)** at day 2 post FAN induction compared to NC fed counterparts. This diet-induced increases in SCFA concentrations were sustained to day 28 **(C)**. FAN ($n = 7$–12); non-FAN ($n = 6$). Data are shown as means ± SD; $^{*}P < 0.05$, $^{**}P < 0.01$, $^{***}P < 0.001$, $^{****}P < 0.0001$.

serum of FAN mice using ^{1}H NMR. FAN mice fed a HF diet had significantly elevated serum acetate and fecal concentrations of the three main SCFAs (acetate, propionate, and butyrate), as compared to those fed NC at both day 2 and day 28 (**Figure 4**).

SCFA Treatment Protects Against Acute Injury at Day 2 and Chronic Inflammation and Fibrosis at Day 28

To determine whether changes to SCFA levels could account for the protective effect of HF feeding in FAN, we investigated the effect of SCFA supplementation. Mice were treated with a SCFA [150 mM SA, 150 mM propionate (SP), or 100 mM butyrate (SB)] in drinking water, commenced 2 weeks prior to FAN induction. SCFA treated mice developed less FA-induced acute and chronic kidney injury compared to controls, with all three SCFAs yielding similar degrees of protection against loss of renal function, histological injury and cellular infiltration as HF diet at day 2 (**Figures 5A–H**) and day 28 (**Figure 6**). SCFA treatment attenuated both acute and chronic kidney inflammation with downregulated expression of relevant innate immune receptor (TLR2 and TLR4), inflammasome (NLRP3 and ASC), cytokine (IL6 and TNFα), and chemokine (CXCL2 and CCL2) genes in FAN kidneys at day 2 (**Figure 5I**) and day 28 (**Figure 6I**). SCFA treated mice showed reduced expression of inflammasome downstream cytokines (IL18 and IL1β), the Th1 cytokine (IFNγ), and iNOS in FAN kidney at day 28 (**Figure 6I**). Reduced fibrosis, with less interstitial collagen deposition (**Figure 6D**) and down-regulated expression of TGFβ1, MMP2, and MMP9 was also seen in SCFA treated mice at day 28 (**Figure 6I**). We have previously demonstrated that SCFA supplementation in drinking water does not alter gut microbiota composition (Tan et al., 2016), supporting a direct effect of SCFA in mediating protection against FAN.

GPR41 and GPR109A, but Not GPR43 Are Necessary for HF and SCFA Mediated Protection Against FAN

To gain mechanistic insights into how SCFAs influence development of FAN, we treated *Gpr41*$^{-/-}$, *Gpr43*$^{-/-}$, and *Gpr109A*$^{-/-}$ mice with a HF diet, or NC diet plus acetate or butyrate supplemented drinking water. Diet or SCFA treatment had no impact on SCr or BUN in non-FAN mice (data not shown). GPR109A, the primary receptor for butyrate, has previously been shown to potentiate anti-inflammatory pathways (Macia et al., 2015). In the absence of GPR109A, butyrate supplementation did not improve renal function in FAN at day 2, whilst HF diet provided partial protection with a small reduction in SCr and BUN compared to WT controls (**Figures 7A,B**). In contrast, absence of GPR43 yielded no impact on the protective effects of both HF diet and acetate in FAN (**Figures 7C,D**). As all 3 SCFAs tested are agonists of GPR41, HF diet was chosen to be the intervention in *Gpr41*$^{-/-}$ mice. HF feeding did not mitigate renal dysfunction in *Gpr41*$^{-/-}$ mice with no reduction in SCr and BUN compared to WT controls at day 2 (**Figure 7E**).

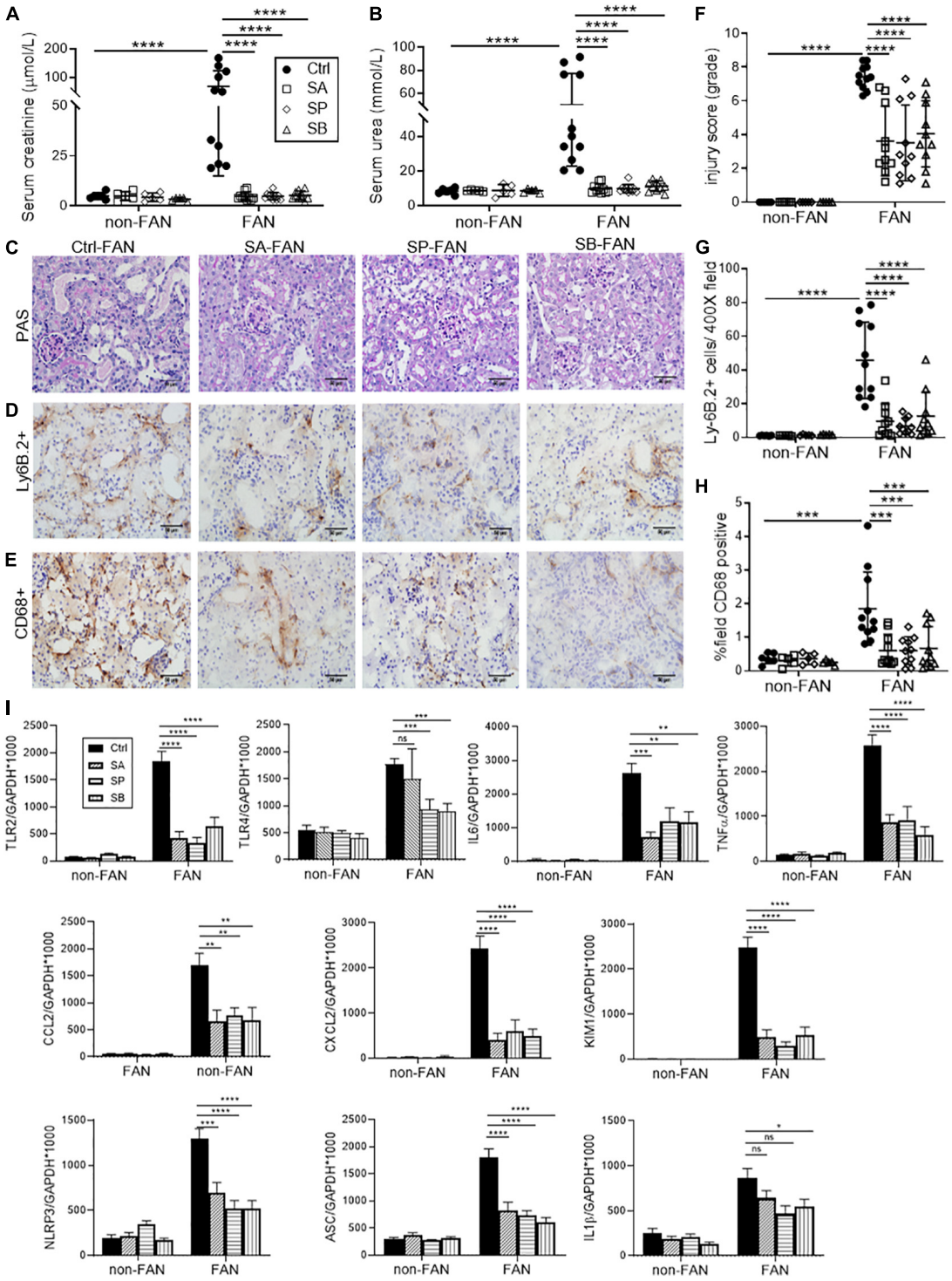

FIGURE 5 | SCFA supplementation attenuates AKI and inflammatory cell infiltrates at day 2. Treatment with SCFAs acetate (SA), butyrate (SB) or propionate (SP) protected against AKI in FAN with lower serum creatinine **(A)**, BUN **(B)** and tubular injury scores **(F)**. Histopathological assessment of PAS stained kidney sections **(C)**, demonstrated protection against kidney damage for all SCFA groups compared to control mice at day 2. Representative sections of immuno-stained kidney for Ly6B.2^{+} neutrophil **(D)** and CD68^{+} macrophages **(E)** demonstrate increased cell infiltrates following FAN induction in control mice, which was significantly diminished by SCFA treatment **(G,H)**. mRNA expression of innate immune receptors (TLR2 and TLR4), pro-inflammatory cytokines (IL6 and TNFα), chemokines (CCL2 and CXCL2), inflammasome components (NLRP3, ASC and IL1β), and the proximal tubule injury marker (KIM1) was diminished by SCFA treatment, as measured by real-time PCR in kidney tissue **(I)**. FAN ($n = 10$); non-FAN ($n = 5$). Photomicrographs at 400×, scale bar 50 μm. Data are shown as means ± SD or mean ± SEM; $^{*}P < 0.05$, $^{**}P < 0.01$, $^{***}P < 0.001$, $^{****}P < 0.0001$.

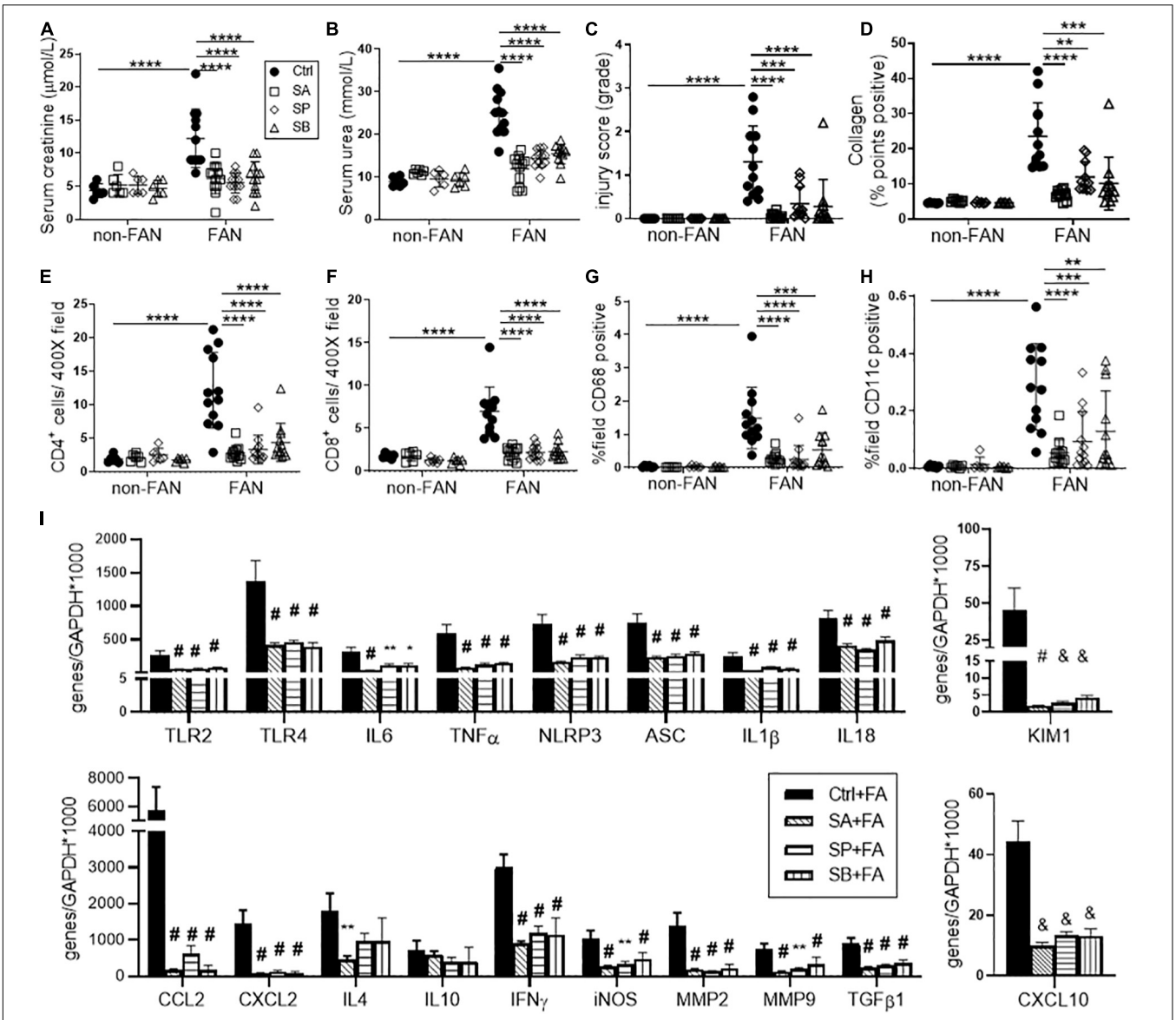

FIGURE 6 | SCFA supplementation resulted in less chronic inflammation at day 28 after FAN induced AKI. SCFA treated mice developed less severe chronic kidney injury, as evidenced by lower serum creatinine **(A)**, BUN **(B)**, histological injury scores **(C)** on PAS staining, and diminished collagen deposition **(D)** on PSR staining at day 28. Reduced $CD4^+$, $CD8^+$ T cell **(E,F)**, $CD68^+$ macrophage **(G)** and $CD11^+$ dendritic cell **(H)** infiltration was seen in SCFA treated FAN kidneys, quantified by immunostaining. **(I)** SCFAs diminished mRNA expression of innate immune receptors (TLR2 and TLR4), pro-inflammatory cytokines (IL6, TNFα, and IFNγ), chemokines (CCL2, CXCL2, and CXCL10), inflammasome components (NLRP3, ASC, IL18, and IL1β), inflammatory mediator (iNOS), proximal tubule injury (KIM1), and fibrosis related genes (TGFβ1, MMP2, and MMP9) measured by real-time PCR in kidney tissue at day 28. FAN ($n = 12$); non-FAN ($n = 6$). Data are shown as means ± SD or mean ± SEM; $^*P < 0.05$, $^{**}P < 0.01$, $^{***\,\&}P < 0.001$, $^{****\,\#}P < 0.0001$.

Taken together, these results indicate that the protective effects of a HF diet and the resultant SCFA metabolites were mediated predominantly through GPR41 and GPR109A.

HF Diet and SCFAs Inhibit Kidney HDAC Activity in FAN

As natural HDAC inhibitors, SCFAs regulate gene transcription through histone modification. To explore the contribution of HDAC in FAN, we tested global HDAC activity in FAN kidney tissue. Mice fed a HF diet, and those on NC diet treated with acetate or propionate, displayed global inhibition of HDAC activity in kidney tissue at day 2 after FAN induction, however no significant difference was seen with butyrate (**Figures 8A,B**). To further clarify the differential importance of various HDAC classes, we next examined mRNA expression of 11 subtypes of HDAC in FAN kidney. HF diet and all three SCFAs reduced mRNA expression of HDAC4 and HDAC10 (class IIa and IIb, respectively) (**Figures 8C–F**). mRNA expression of HDAC3 and HDAC7 was also diminished in the FAN kidney in all three

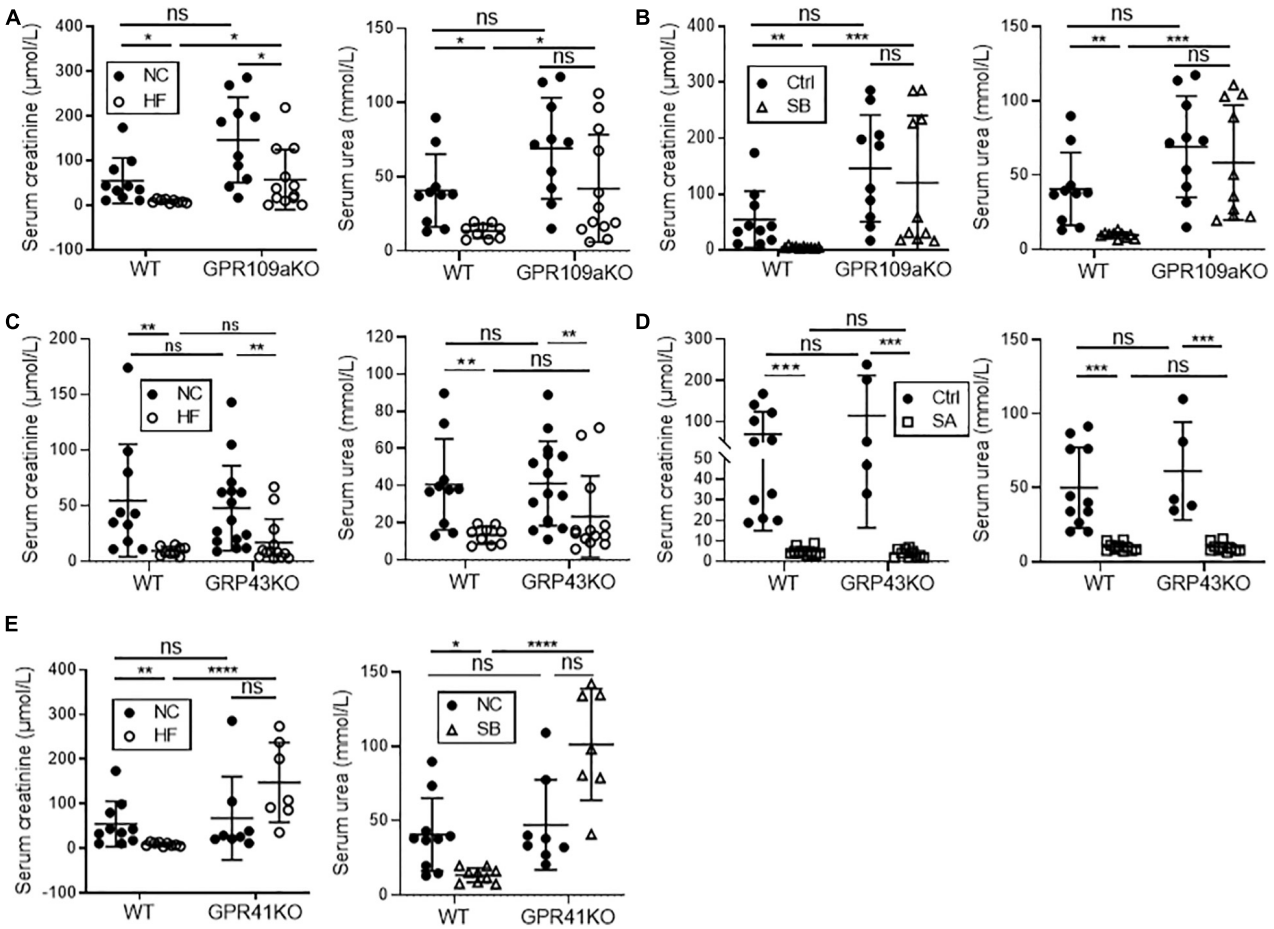

FIGURE 7 | GPR41 and GPR109a play roles in fiber and SCFA mediated reno-protection in FAN at day 2. HF diet provided partial protection against FAN in *Gpr109a*$^{-/-}$ mice **(A)**, however butyrate treatment did not improve renal function at day 2 **(B)** with no significant difference in serum creatinine or BUN compared to WT controls. Both HF diet and oral acetate treatment provided full protection against AKI in *Gpr43*$^{-/-}$ FAN mice **(C,D)**. HF feeding in *Gpr41*$^{-/-}$ FAN mice did not improve renal function at day 2, with no reduction in serum creatinine or BUN compared to WT controls **(E)**. FAN ($n = 6$–12); non-FAN ($n = 5$). Data are shown as means ± SD; $^{*}P < 0.05$, $^{**}P < 0.01$, $^{***}P < 0.001$, $^{****}P < 0.0001$.

groups of SCFA treated mice compared to controls (**Figure 8H**). HDAC 5 expression was lower in FAN kidney in HF and SB treated mice while increased expression of HDAC8 was seen in SB treated FAN mice (**Figures 8G,H**). No reduction was evident in the expression of HDAC 1, 2, 6, 9, and 11 in FAN kidney in response to any treatment. HDAC4 has been shown to be involved in immune regulation, while HDAC10 plays roles in DNA repair, autophagy and anti-cancer responses. These results suggest that dietary fiber may protect against FAN through SCFA mediated HDAC inhibition and downstream changes to gene transcription.

DISCUSSION

The pathophysiology of AKI shares common pathogenic denominators, including hemodynamic alterations, inflammation, and cell injury, followed by a repair process to restore kidney structure and function (Ronco et al., 2019). The gut microbiota and its metabolites are emerging as therapeutic targets in AKI through their ability to regulate inflammatory and immune responses (Jang et al., 2009; Andrade-Oliveira et al., 2015; Emal et al., 2017). Using the murine model of FAN, we demonstrate a novel bi-directional and modifiable relationship between the gut microbiota, AKI and kidney recovery. AKI alters gut microbial composition, promoting dysbiosis with augmented kidney inflammation and progression to CKD. These changes were ameliorated by a HF diet with protection from AKI and less subsequent renal fibrosis. Gut microbial metabolites (SCFA) were integral to this, exerting effects through binding to GPRs and epigenetic modification as HDAC inhibitors. To our knowledge, this is the first study demonstrating the ability to prevent experimental AKI through dietary modification of the gut microbiota. Overall, these findings provide further mechanistic insights into the gut-kidney axis and highlight its importance across the AKI-CKD continuum.

Regional inflammation within the kidney is the hallmark of this model. Folic acid induced tubular necrosis triggers

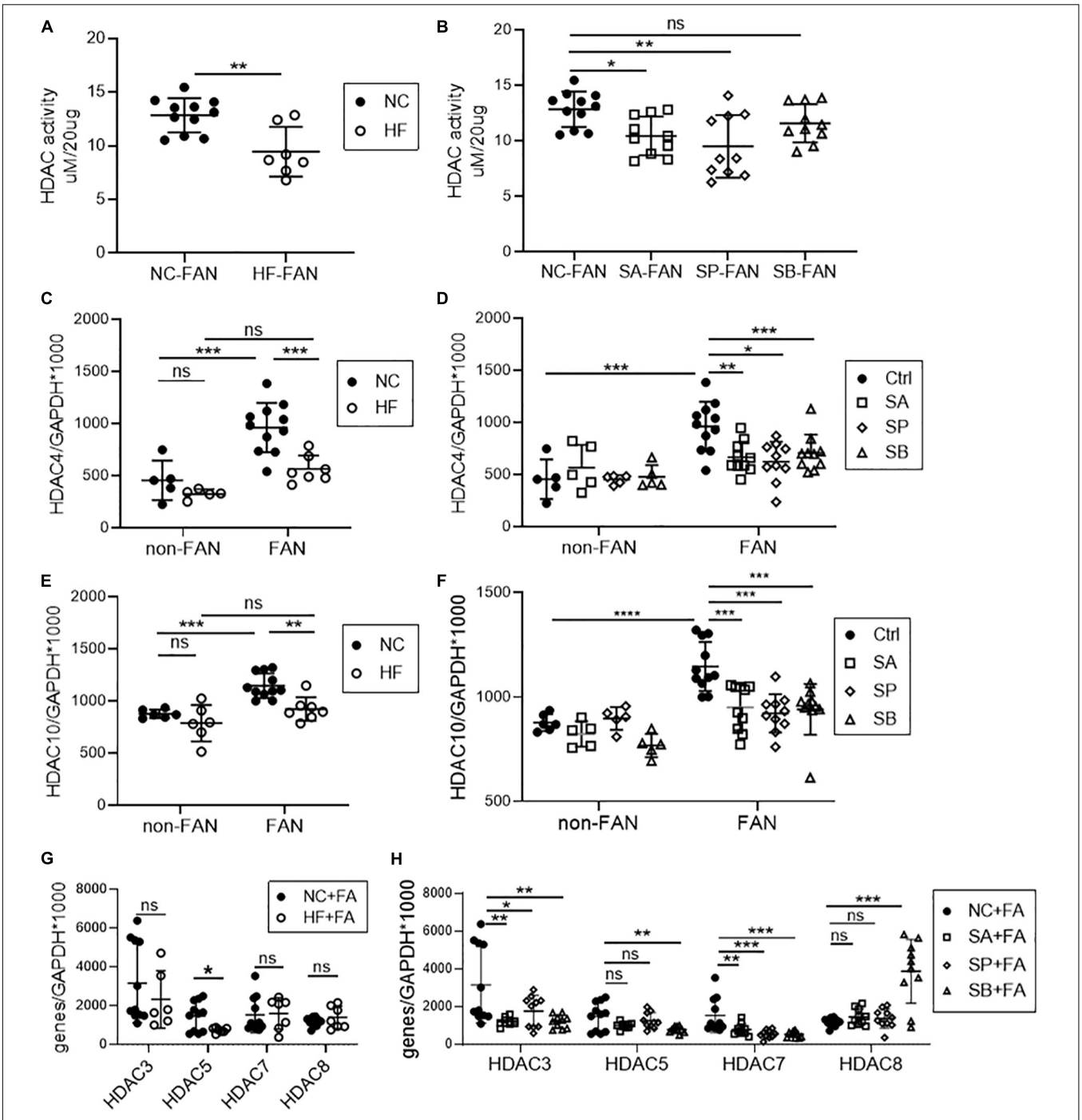

FIGURE 8 | HF and SCFA are involved in epigenetic modification through downregulation of HDAC expression. Downregulation of kidney histone deacetylase (HDAC) activity was seen in HF fed **(A)**, acetate and propionate treated FAN mice **(B)** compared to controls at day 2. **(C–H)** mRNA expression of HDAC subclasses in FAN kidneys. HF diet **(C,E)** and all three SCFAs **(D,F)** reduced kidney mRNA expression of HDAC4 and HDAC10 respectively in FAN. FAN ($n = 10$); non-FAN ($n = 5$). Data are shown as means ± SEM; $^{*}P < 0.05$, $^{**}P < 0.01$, $^{***}P < 0.001$, $^{****}P < 0.0001$.

sterile inflammation, driven by release of DAMPs from injured cells which engage pattern recognition receptors, such as TLRs and NLRs (Rosin and Okusa, 2011), and trigger activation of the inflammasome. Subsequent generation of pro-inflammatory cytokines (including IL1, IL6, IL18, and TNFα) and chemotactic molecules (CXCL2 and CCL2) drives recruitment of neutrophils and macrophages during the early response to injury (Anders and Muruve, 2011; Kurts et al., 2013). The requirement for TLRs and the inflammasome has been demonstrated in studies of mice deficient in TLR2, TLR4, or NLRP3, all of whom were

protected against post-ischemic AKI (Leemans et al., 2005; Wu et al., 2007; Iyer et al., 2009). In the acute phase following FAN-induction, we saw upregulation of innate immune receptors and inflammasome components, however expression of TLR2, NLPR3, and ASC were significantly reduced in kidneys of HF fed mice with AKI, identifying these pathways as potentially important in mediating the protective effects of dietary fiber. TLRs and inflammasomes are involved not only in acute responses, but also in chronic inflammation, tissue repair and fibrosis (Artlett, 2013; Anders and Schaefer, 2014; Yiu et al., 2014). The chronic phase of FAN is characterized by a low-grade inflammatory state, consisting of ongoing innate and evolving adaptive immune responses, culminating in fibrosis. T cells and macrophages actively participate in the development of myofibroblasts, which produce extracellular matrix leading to kidney fibrosis (Duffield, 2014). In our study, HF fed mice had less severe AKI, which translated to reduced chronic tubular damage, inflammatory cell infiltration and renal fibrosis. The NLPR3 inflammasome and caspase 1 substrate IL18 have been found to mediate renal fibrosis. We demonstrated sustained suppression of TLR2, TLR4, NLPR3, and ASC mRNA expression in the kidney at day 28, with reduced IL18 and IL1β expression in HF fed FAN mice compared to NC.

Gut microbiota–host immune maladaptation has been implicated in the rising incidence of inflammatory diseases, with recent evidence highlighting the importance of symbiosis and kidney-microbiota crosstalk in health (Knauf et al., 2019). The gut microbiome has been shown to influence susceptibility to AKI, with transfer of "dysbiotic" microbiota low in SCFAs leading to aggravated post-ischemic kidney injury, whilst microbiota depletion with antibiotics provided partial reno-protection (Yang et al., 2020). Similarly, acute renal dysfunction in our model of FAN induced profound changes in the gut microbiome, characterized by significant accumulation of pathobionts, reduction in the abundance of SCFA producing bacteria, and activated damage repair signaling pathways in the gut microbial metagenome as demonstrated using PICRUSt prediction. Manipulation of the microbiome through a diet high in fiber commenced 2 weeks prior to FAN induction led to a reduced *Firmicutes* to *Bacteroidetes* ratio and expansion of SCFA-producing genera *Prevotella* and *Bifidobacterium*, which has been associated with a healthy gut microbial community (Turnbaugh et al., 2006). This diet induced change in microbial composition was associated with protection against development of AKI and subsequent CKD, with less dysbiosis and increased SCFA levels seen in HF fed mice at day 2, which was sustained to day 28. However further studies are required to assess whether the therapeutic potential of HF can be harnessed following an episode of AKI, to prevent AKI-CKD transition.

The relative abundance of *Bifidobacterium* was not only fostered by HF diet, but closely correlated with reductions in acute and chronic kidney dysfunction. *Bifidobacteria* have been tested as a probiotic in interventional trials targeting surrogate endpoints, however evidence of any impact on clinically relevant outcomes remains lacking, with limitations identified in consistent administration due to toxin accumulation in CKD, variability in the intestinal microenvironment and survival rates of probiotics (Koppe et al., 2015). In our study, fiber fostered increased liberation of all three SCFAs with subsequent protection against FAN, pointing toward non-selective prebiotics such as fiber as an alternative to bypass these limitations. The expansion of SCFA producing bacteria seen in HF fed mice and resultant reno-protection highlights the capacity of diet to mediate extra-intestinal effects (Cummings et al., 1987; Murase et al., 1995). Using PICRUSt prediction, we found that butyrate and propionate metabolic pathways were more active within the gut microbial metagenome after AKI in NC fed mice compared to HF, indicating that SCFAs may play a role in reactive anti-inflammatory processes.

Whilst HF fed mice were protected from dysbiosis and AKI, SCFA supplementation, which does not alter gut microbiota composition (Tan et al., 2016), provided similar degrees of kidney protection. This is consistent with the anti-inflammatory properties of SCFAs previously reported in contract-induced (Machado et al., 2012), IRI (Andrade-Oliveira et al., 2015), and toxin-induced (Abdul Hamid et al., 2012; Sun et al., 2013) experimental models of AKI. Caution in the use of SCFAs is warranted however, given that one study of acetate supplementation in C57BL/6 mice from 3 weeks of age led to ureteritis and hydronephrosis by inducing effector (Th1 and Th17) and regulatory T cells (Park et al., 2016), raising the possibility of pleiotropic age and dose dependent effects which require further investigation.

Two predominant mechanisms have been proposed for the operation of SCFAs at a molecular level: (i) as an HDAC inhibitor or (ii) as a ligand for GPRs. We tested the therapeutic effect of HF diet and SCFA supplementation in *Gpr41*$^{-/-}$, *Gpr43*$^{-/-}$, and *Gpr109A*$^{-/-}$ mice and found that protection was mediated through GPR41 and GPR109A, but not GPR43. Within the kidney, GPR109A is expressed on podocytes, and participates in reno-protective signaling pathways following butyrate treatment in adriamycin nephropathy (Felizardo et al., 2019). GPR41 is found in human colon mucosal enterocytes, enteroendocrine cells, and smooth muscle cells of the small vessels in kidneys (Tazoe et al., 2009). GPR41 has been shown to inhibit TNF-α-induced MCP-1 expression by modulating p38 and JNK signaling pathways in human renal cortical epithelial cells (Kobayashi et al., 2017). Human renal cortical epithelial cells have been found to express both GPR41 and GPR43, with SCFA treatment of these cells *in vitro* lowering TNF-α induced MCP-1 expression (Kobayashi et al., 2017). Whilst we have previously demonstrated GPR43 to be critical in acetate mediated reno-protection and tolerance in murine models of diabetic nephropathy and kidney transplantation respectively (Li et al., 2020; Wu et al., 2020), this was not seen in FAN induced AKI. The role of GPR43 remains less clear in AKI. Acetate was reno-protective through HDAC inhibition and modulation of T-cell function in a model of sepsis induced AKI (Al-Harbi et al., 2018), whilst both GPR43 dependent and independent mechanisms were contributory in IRI (Andrade-Oliveira et al., 2015). We found that both diet and acetate protected against FA-induced AKI independent of GPR43. This may reflect the complex overlapping biochemical, immunologic, and hemodynamic mechanisms involved in both initiation of and

recovery from AKI. Additionally, our knockout mice were not tissue specific, thus it remains to be explored whether HF plays a protective role by modulating immune cells or intrinsic kidney cells through GPR109A and GPR41 in AKI.

In our study, HDAC activity was suppressed in kidney tissues of HF fed mice following AKI, with significant downregulation of HDAC4 and HDAC10 expression. Previous studies have established HDAC4 as playing an essential immunomodulatory role by modifying transcription of immune-related transcription factors, including c-Jun (Gordon et al., 2009), NF-κB and Bcl-6 (Hemmer, 1979; Sandhu et al., 2012), and by regulating the development of various immune cells (Ghisletti et al., 2007; Lu et al., 2015). HDAC10 has been reported to be involved in DNA mismatch repair (Radhakrishnan et al., 2015), cell autophagy (Oehme et al., 2013), and cancer progression (Lee et al., 2010; Fan et al., 2015). However, the functions of HDACs in regulating gene expression and inflammation remain conflicted between different cells and tissues (Liao et al., 2019; Dahiya et al., 2020; Wang et al., 2020). Further studies are required to assess how intrinsic renal and immune cells respond to the suppression of HDAC10 and HDAC4. The relationship between HDAC inhibition and GPRs also remains controversial. Whilst Smith et al. (2013) found HDAC inhibition to be partially GPR43-dependent in colon tissue, others have observed HDAC inhibition independent of GPR-signaling (Aoyama et al., 2010). Further studies are needed to assess the independent or synergistic effects of HDAC inhibition and GPR pathway activation in reno-protection and inflammation.

Our study shows that a high-fiber diet, or supplementation with SCFAs, protects against development of AKI and subsequent kidney fibrosis, and may be a simple and safe means to mitigate susceptibility to AKI. We provide mechanistic insights into the protective actions of dietary fiber, with a specific emphasis on the role of gut derived SCFAs in HDAC and GPR mediated pathways which are integral to inform future translational clinical studies.

DATA AVAILABILITY STATEMENT

The datasets presented in this study can be found in online repositories. The name of the repository and accession number can be found in the article.

ETHICS STATEMENT

The animal study was reviewed and approved by the University of Sydney Animal Ethics Committee.

AUTHOR CONTRIBUTIONS

HW and SC conceived and designed the study. YZL, YJL, YWL, JS, and WZ carried out the experiments. YZL and YJL analyzed and interpreted the data and drafted the manuscript. HW, WW, LM, CM, and SC revised the manuscript. All authors approved the final version of the manuscript.

SUPPLEMENTARY MATERIAL

The Supplementary Material for this article can be found online at: https://www.frontiersin.org/articles/10.3389/fcell.2021.648639/full#supplementary-material

REFERENCES

Abdul Hamid, Z., Budin, S. B., Wen Jie, N., Hamid, A., Husain, K., and Mohamed, J. (2012). Nephroprotective effects of Zingiber zerumbet Smith ethyl acetate extract against paracetamol-induced nephrotoxicity and oxidative stress in rats. *J. Zhejiang Univ. Sci. B.* 13, 176–185. doi: 10.1631/jzus.b1100133

Agarwal, A., Dong, Z., Harris, R., Murray, P., Parikh, S. M., Rosner, M. H., et al. (2016). Cellular and Molecular Mechanisms of AKI. *J. Am. Soc. Nephrol.* 27, 1288–1299.

Al-Harbi, N. O., Nadeem, A., Ahmad, S. F., Alotaibi, M. R., AlAsmari, A. F., Alanazi, W. A., et al. (2018). Short chain fatty acid, acetate ameliorates sepsis-induced acute kidney injury by inhibition of NADPH oxidase signaling in T cells. *Int. Immunopharmacol.* 58, 24–31. doi: 10.1016/j.intimp.2018.02.023

Al-Jaghbeer, M., Dealmeida, D., Bilderback, A., Ambrosino, R., and Kellum, J. A. (2018). Clinical Decision Support for In-Hospital AKI. *J. Am. Soc. Nephrol.* 29, 654–660. doi: 10.1681/asn.2017070765

Anders, H. J., and Muruve, D. A. (2011). The inflammasomes in kidney disease. *J. Am. Soc. Nephrol.* 22, 1007–1018. doi: 10.1681/asn.2010080798

Anders, H. J., and Schaefer, L. (2014). Beyond tissue injury-damage-associated molecular patterns, toll-like receptors, and inflammasomes also drive regeneration and fibrosis. *J. Am. Soc. Nephrol.* 25, 1387–1400. doi: 10.1681/asn.2014010117

Andrade-Oliveira, V., Amano, M. T., Correa-Costa, M., Castoldi, A., Felizardo, R. J. F., de Almeida, D. C., et al. (2015). Gut Bacteria Products Prevent AKI Induced by Ischemia-Reperfusion. *J. Am. Soc. Nephrol.* 26, 1877–1888. doi: 10.1681/asn.2014030288

Aoyama, M., Kotani, J., and Usami, M. (2010). Butyrate and propionate induced activated or non-activated neutrophil apoptosis via HDAC inhibitor activity but without activating GPR-41/GPR-43 pathways. *Nutrition* 26, 653–661. doi: 10.1016/j.nut.2009.07.006

Artlett, C. M. (2013). Inflammasomes in wound healing and fibrosis. *J. Pathol.* 229, 157–167. doi: 10.1002/path.4116

Coca, S. G., Singanamala, S., and Parikh, C. R. (2012). Chronic kidney disease after acute kidney injury: a systematic review and meta-analysis. *Kidney Int.* 81, 442–448. doi: 10.1038/ki.2011.379

Cummings, J. H., Pomare, E. W., Branch, W. J., Naylor, C. P., and Macfarlane, G. T. (1987). Short chain fatty acids in human large intestine, portal, hepatic and venous blood. *Gut* 28, 1221–1227. doi: 10.1136/gut.28.10.1221

Dahiya, S., Beier, U. H., Wang, L., Han, R., Jiao, J., Akimova, T., et al. (2020). HDAC10 deletion promotes Foxp3(+) T-regulatory cell function. *Sci. Rep.* 10:424.

Duffield, J. S. (2014). Cellular and molecular mechanisms in kidney fibrosis. *J. Clin. Invest.* 124, 2299–2306. doi: 10.1172/jci72267

Emal, D., Rampanelli, E., Stroo, I., Butter, L. M., Teske, G. J., Claessen, N., et al. (2017). Depletion of Gut Microbiota Protects against Renal Ischemia-Reperfusion Injury. *J. Am. Soc. Nephrol.* 28, 1450–1461. doi: 10.1681/asn.2016030255

Fan, W., Huang, J., and Xiao, H. (2015). Histone deacetylase 10 suppresses proliferation and invasion by inhibiting the phosphorylation of beta-catenin and serves as an independent prognostic factor for human clear cell renal cell carcinoma. *Int. J. Clin. Exp. Med.* 8, 3734–3742.

Felizardo, R. J. F., de Almeida, D. C., Pereira, R. L., Watanabe, I. K. M., Doimo, N. T. S., Ribeiro, W. R., et al. (2019). Gut microbial metabolite butyrate protects against proteinuric kidney disease through epigenetic- and GPR109a-mediated mechanisms. *FASEB J.* 33, 11894–11908. doi: 10.1096/fj.201901080r

Ghisletti, S., Huang, W., Ogawa, S., Pascual, G., Lin, M. E., Willson, T. M., et al. (2007). Parallel SUMOylation-dependent pathways mediate gene- and signal-specific transrepression by LXRs and PPARgamma. *Mol. Cell.* 25, 57–70. doi: 10.1016/j.molcel.2006.11.022

Gordon, J. W., Pagiatakis, C., Salma, J., Du, M., Andreucci, J. J., Zhao, J., et al. (2009). Protein kinase A-regulated assembly of a MEF2{middle dot}HDAC4 repressor complex controls c-Jun expression in vascular smooth muscle cells. *J. Biol. Chem.* 284, 19027–19042. doi: 10.1074/jbc.m109.000539

Hemmer, R. (1979). Postoperative causes of death in hydrocephalic children. Analysis and conclusions about therapy. *Prog. Pediatr. Surg.* 13, 95–103.

Iyer, S. S., Pulskens, W. P., Sadler, J. J., Butter, L. M., Teske, G. J., Ulland, T. K., et al. (2009). Necrotic cells trigger a sterile inflammatory response through the Nlrp3 inflammasome. *Proc. Natl. Acad. Sci. U S A.* 106, 20388–20393. doi: 10.1073/pnas.0908698106

Jang, H. R., Gandolfo, M. T., Ko, G. J., Satpute, S., Racusen, L., and Rabb, H. (2009). Early exposure to germs modifies kidney damage and inflammation after experimental ischemia-reperfusion injury. *Am. J. Physiol. Renal. Physiol.* 297, F1457–F1465.

Knauf, F., Brewer, J. R., and Flavell, R. A. (2019). Immunity, microbiota and kidney disease. *Nat. Rev. Nephrol.* 15, 263–274. doi: 10.1038/s41581-019-0118-7

Kobayashi, M., Mikami, D., Kimura, H., Kamiyama, K., Morikawa, Y., Yokoi, S., et al. (2017). Short-chain fatty acids, GPR41 and GPR43 ligands, inhibit TNF-alpha-induced MCP-1 expression by modulating p38 and JNK signaling pathways in human renal cortical epithelial cells. *Biochem. Biophys. Res. Commun.* 486, 499–505. doi: 10.1016/j.bbrc.2017.03.071

Koppe, L., Mafra, D., and Fouque, D. (2015). Probiotics and chronic kidney disease. *Kidney Int.* 88, 958–966. doi: 10.1038/ki.2015.255

Kurts, C., Panzer, U., Anders, H. J., and Rees, A. J. (2013). The immune system and kidney disease: basic concepts and clinical implications. *Nat. Rev. Immunol.* 13, 738–753. doi: 10.1038/nri3523

Lee, J. H., Jeong, E. G., Choi, M. C., Kim, S. H., Park, J. H., Song, S. H., et al. (2010). Inhibition of histone deacetylase 10 induces thioredoxin-interacting protein and causes accumulation of reactive oxygen species in SNU-620 human gastric cancer cells. *Mol. Cells.* 30, 107–112. doi: 10.1007/s10059-010-0094-z

Leemans, J. C., Stokman, G., Claessen, N., Rouschop, K. M., Teske, G. J., Kirschning, C. J., et al. (2005). Renal-associated TLR2 mediates ischemia/reperfusion injury in the kidney. *J. Clin. Invest.* 115, 2894–2903. doi: 10.1172/jci22832

Li, Y. J., Chen, X., Kwan, T. K., Loh, Y. W., Singer, J., Liu, Y., et al. (2020). Dietary Fiber Protects against Diabetic Nephropathy through Short-Chain Fatty Acid-Mediated Activation of G Protein-Coupled Receptors GPR43 and GPR109A. *J. Am. Soc. Nephrol.* 31, 1267–1281. doi: 10.1681/asn.2019101029

Liao, W., Sun, J., Liu, W., Li, W., Jia, J., Ou, F., et al. (2019). HDAC10 upregulation contributes to interleukin 1beta-mediated inflammatory activation of synovium-derived mesenchymal stem cells in temporomandibular joint. *J. Cell Physiol.* 234, 12646–12662. doi: 10.1002/jcp.27873

Lu, W., You, R., Yuan, X., Yang, T., Samuel, E. L., Marcano, D. C., et al. (2015). The microRNA miR-22 inhibits the histone deacetylase HDAC4 to promote T(H)17 cell-dependent emphysema. *Nat. Immunol.* 16, 1185–1194. doi: 10.1038/ni.3292

Machado, R. A., Constantino Lde, S., Tomasi, C. D., Rojas, H. A., Vuolo, F. S., Vitto, M. F., et al. (2012). Sodium butyrate decreases the activation of NF-kappaB reducing inflammation and oxidative damage in the kidney of rats subjected to contrast-induced nephropathy. *Nephrol Dial Transplant.* 27, 3136–3140. doi: 10.1093/ndt/gfr807

Macia, L., Tan, J., Vieira, A. T., Leach, K., Stanley, D., Luong, S., et al. (2015). Metabolite-sensing receptors GPR43 and GPR109A facilitate dietary fibre-induced gut homeostasis through regulation of the inflammasome. *Nat. Commun.* 6:6734.

Martin-Sanchez, D., Ruiz-Andres, O., Poveda, J., Carrasco, S., Cannata-Ortiz, P., Sanchez-Nino, M. D., et al. (2017). Ferroptosis, but Not Necroptosis, Is Important in Nephrotoxic Folic Acid-Induced AKI. *J. Am. Soc. Nephrol.* 28, 218–229. doi: 10.1681/asn.2015121376

Maslowski, K. M., Vieira, A. T., Ng, A., Kranich, J., Sierro, F., Yu, D., et al. (2009). Regulation of inflammatory responses by gut microbiota and chemoattractant receptor GPR43. *Nature* 461, 1282–1286. doi: 10.1038/nature08530

McMurdie, P. J., and Holmes, S. (2013). phyloseq: an R package for reproducible interactive analysis and graphics of microbiome census data. *PLoS One* 8:e61217. doi: 10.1371/journal.pone.0061217

Murase, M., Kimura, Y., and Nagata, Y. (1995). Determination of portal short-chain fatty acids in rats fed various dietary fibers by capillary gas chromatography. *J. Chromatogr. B Biomed. Appl.* 664, 415–420. doi: 10.1016/0378-4347(94)00491-m

Oehme, I., Linke, J. P., Bock, B. C., Milde, T., Lodrini, M., Hartenstein, B., et al. (2013). Histone deacetylase 10 promotes autophagy-mediated cell survival. *Proc. Natl. Acad. Sci. U S A.* 110, E2592–E2601.

Park, J., Goergen, C. J., HogenEsch, H., and Kim, C. H. (2016). Chronically Elevated Levels of Short-Chain Fatty Acids Induce T Cell-Mediated Ureteritis and Hydronephrosis. *J. Immunol.* 196, 2388–2400. doi: 10.4049/jimmunol.1502046

Parks, D. H., Tyson, G. W., Hugenholtz, P., and Beiko, R. G. (2014). STAMP statistical analysis of taxonomic and functional profiles. *Bioinformatics* 30, 3123–3124. doi: 10.1093/bioinformatics/btu494

Rabb, H., Griffin, M. D., McKay, D. B., Swaminathan, S., Pickkers, P., Rosner, M. H., et al. (2016). Inflammation in AKI: Current Understanding, Key Questions, and Knowledge Gaps. *J. Am. Soc. Nephrol.* 27, 371–379. doi: 10.1681/asn.2015030261

Radhakrishnan, R., Li, Y., Xiang, S., Yuan, F., Yuan, Z., Telles, E., et al. (2015). Histone deacetylase 10 regulates DNA mismatch repair and may involve the deacetylation of MutS homolog 2. *J. Biol. Chem.* 290, 22795–22804. doi: 10.1074/jbc.m114.612945

Ronco, C., Bellomo, R., and Kellum, J. A. (2019). Acute kidney injury. *Lancet* 394, 1949–1964.

Rosin, D. L., and Okusa, M. D. (2011). Dangers within: DAMP responses to damage and cell death in kidney disease. *J. Am. Soc. Nephrol.* 22, 416–425. doi: 10.1681/asn.2010040430

Sandhu, S. K., Volinia, S., Costinean, S., Galasso, M., Neinast, R., Santhanam, R., et al. (2012). miR-155 targets histone deacetylase 4 (HDAC4) and impairs transcriptional activity of B-cell lymphoma 6 (BCL6) in the Emu-miR-155 transgenic mouse model. *Proc. Natl. Acad. Sci. U S A.* 109, 20047–20052. doi: 10.1073/pnas.1213764109

Sarbini, S. R., Kolida, S., Deaville, E. R., Gibson, G. R., and Rastall, R. A. (2014). Potential of novel dextran oligosaccharides as prebiotics for obesity management through in vitro experimentation. *Br. J. Nutr.* 112, 1303–1314. doi: 10.1017/s0007114514002177

Schetz, M., Dasta, J., Goldstein, S., and Golper, T. (2005). Drug-induced acute kidney injury. *Curr. Opin. Crit. Care* 11, 555–565.

Smith, P. M., Howitt, M. R., Panikov, N., Michaud, M., Gallini, C. A., Bohlooly, Y. M., et al. (2013). The microbial metabolites, short-chain fatty acids, regulate colonic Treg cell homeostasis. *Science* 341, 569–573. doi: 10.1126/science.1241165

Stumpff, F. A. (2018). look at the smelly side of physiology: transport of short chain fatty acids. *Eur. J. Physiol.* 470, 571–598. doi: 10.1007/s00424-017-2105-9

Sun, X., Zhang, B., Hong, X., Zhang, X., and Kong, X. (2013). Histone deacetylase inhibitor, sodium butyrate, attenuates gentamicin-induced nephrotoxicity by increasing prohibitin protein expression in rats. *Eur. J. Pharmacol.* 707, 147–154. doi: 10.1016/j.ejphar.2013.03.018

Tan, J., McKenzie, C., Potamitis, M., Thorburn, A. N., Mackay, C. R., and Macia, L. (2014). The role of short-chain fatty acids in health and disease. *Adv. Immunol.* 121, 91–119. doi: 10.1016/b978-0-12-800100-4.00003-9

Tan, J., McKenzie, C., Vuillermin, P. J., Goverse, G., Vinuesa, C. G., Mebius, R. E., et al. (2016). Dietary Fiber and Bacterial SCFA Enhance Oral Tolerance and Protect against Food Allergy through Diverse Cellular Pathways. *Cell Rep.* 15, 2809–2824. doi: 10.1016/j.celrep.2016.05.047

Tazoe, H., Otomo, Y., Karaki, S., Kato, I., Fukami, Y., Terasaki, M., et al. (2009). Expression of short-chain fatty acid receptor GPR41 in the human colon. *Biomed. Res.* 30, 149–156. doi: 10.2220/biomedres.30.149

Turnbaugh, P. J., Ley, R. E., Mahowald, M. A., Magrini, V., Mardis, E. R., and Gordon, J. I. (2006). An obesity-associated gut microbiome with increased capacity for energy harvest. *Nature* 444, 1027–1031.

Wang, L., Zheng, S., Zhang, L., Xiao, H., Gan, H., Chen, H., et al. (2020). Histone Deacetylation 10 Alleviates Inflammation After Intracerebral Hemorrhage via the PTPN22/NLRP3 Pathway in Rats. *Neuroscience* 432, 247–259. doi: 10.1016/j.neuroscience.2020.02.027

Wu, H., Chen, G., Wyburn, K. R., Yin, J., Bertolino, P., Eris, J. M., et al. (2007). TLR4 activation mediates kidney ischemia/reperfusion injury. *J. Clin. Invest.* 117, 2847–2859. doi: 10.1172/jci31008

Wu, H., Singer, J., Kwan, T. K., Loh, Y. W., Wang, C., Tan, J., et al. (2020). Gut Microbial Metabolites Induce Donor-Specific Tolerance of Kidney Allografts through Induction of T Regulatory Cells by Short-Chain Fatty Acids. *J. Am. Soc. Nephrol.* 2020:2019080852.

Yang, J., Kim, C. J., Go, Y. S., Lee, H. Y., Kim, M. G., Oh, S. W., et al. (2020). Intestinal microbiota control acute kidney injury severity by immune modulation. *Kidney Int.* 98, 932–946. doi: 10.1016/j.kint.2020.04.048

Yiu, W. H., Lin, M., and Tang, S. C. (2014). Toll-like receptor activation: from renal inflammation to fibrosis. *Kidney Int.* 4, 20–25. doi: 10.1038/kisup.2014.5

Conflict of Interest: The authors declare that the research was conducted in the absence of any commercial or financial relationships that could be construed as a potential conflict of interest.

Copyright © 2021 Liu, Li, Loh, Singer, Zhu, Macia, Mackay, Wang, Chadban and Wu. This is an open-access article distributed under the terms of the Creative Commons Attribution License (CC BY). The use, distribution or reproduction in other forums is permitted, provided the original author(s) and the copyright owner(s) are credited and that the original publication in this journal is cited, in accordance with accepted academic practice. No use, distribution or reproduction is permitted which does not comply with these terms.

frontiers in Cell and Developmental Biology

ORIGINAL RESEARCH
published: 13 April 2021
doi: 10.3389/fcell.2021.639127

The Pharmacological Effect and Mechanism of Lanthanum Hydroxide on Vascular Calcification Caused by Chronic Renal Failure Hyperphosphatemia

*Lulu Zhao[1†], Shengnan Wang[1†], Hong Liu[1], Xiaoli Du[1], Ren Bu[1], Bing Li[1], Ruilan Han[1], Jie Gao[1], Yang Liu[1], Jian Hao[2], Jianrong Zhao[2], Yan Meng[2] and Gang Li[1]**

[1] Department of Pharmacology, College of Pharmacy, Inner Mongolia Medical University, Jinshan Development, Hohhot, China, [2] Department of Nephrology, The Affiliated Hospital of Inner Mongolia Medical University, Hohhot, China

OPEN ACCESS

Edited by:
Nejra Prohic,
Clinical Center University of Sarajevo,
Bosnia and Herzegovina

Reviewed by:
Alexander N. Kapustin,
AstraZeneca, United Kingdom
Jianyun Yan,
Southern Medical University, China

***Correspondence:**
Gang Li
cnnmligang@hotmail.com

[†] These authors share first authorship

Specialty section:
This article was submitted to Molecular Medicine, a section of the journal Frontiers in Cell and Developmental Biology

Received: 08 December 2020
Accepted: 24 March 2021
Published: 13 April 2021

Citation:
Zhao L, Wang S, Liu H, Du X, Bu R, Li B, Han R, Gao J, Liu Y, Hao J, Zhao J, Meng Y and Li G (2021) The Pharmacological Effect and Mechanism of Lanthanum Hydroxide on Vascular Calcification Caused by Chronic Renal Failure Hyperphosphatemia. Front. Cell Dev. Biol. 9:639127. doi: 10.3389/fcell.2021.639127

Objective: The present work aimed to explore the efficacy of lanthanum hydroxide in managing the vascular calcification induced by hyperphosphate in chronic renal failure (CRF) as well as the underlying mechanism.

Methods: Rats were randomly allocated to five groups: normal diet control, CKD hyperphosphatemia model, CKD model treated with lanthanum hydroxide, CKD model receiving lanthanum carbonate treatment, together with CKD model receiving calcium carbonate treatment. The serum biochemical and kidney histopathological parameters were analyzed. The aortic vessels were subjected to Von Kossa staining, CT scan and proteomic analysis. *In vitro,* the calcium content and ALP activity were measured, and RT-PCR (SM22α, Runx2, BMP-2, and TRAF6) and Western blot (SM22α, Runx2, BMP-2, TRAF6, and NF-κB) were performed.

Results: In the lanthanum hydroxide group, serum biochemical and kidney histopathological parameters were significantly improved compared with the model group, indicating the efficacy of lanthanum hydroxide in postponing CRF progression and in protecting renal function. In addition, applying lanthanum hydroxide postponed hyperphosphatemia-mediated vascular calcification in CKD. Furthermore, lanthanum hydroxide was found to mitigate vascular calcification via the NF-κB signal transduction pathway. For the cultured VSMCs, lanthanum chloride ($LaCl_3$) alleviated phosphate-mediated calcification and suppressed the activation of NF-κB as well as osteo-/chondrogenic signal transduction. Lanthanum hydroxide evidently downregulated NF-κB, BMP-2, Runx2, and TRAF6 expression.

Conclusion: Lanthanum hydroxide protects against renal failure and reduces the phosphorus level in serum to postpone vascular calcification progression.

Keywords: lanthanum hydroxide, vascular calcification, chronic renal failure, hyperphosphatemia, pharmacological effect, mechanism

INTRODUCTION

Chronic kidney disease (CKD) refers to any abnormality affecting the renal structure and function that lasts for over 3 months (Inker et al., 2014). As reported in a recent systematic analysis, approximately 10.4% of the male and 11.8% of the female adult populations in the world were affected by CKD in 2010, and the incidence is comparatively high among the low/middle-income areas, while low among the developed countries (Mills et al., 2015).

Cardiovascular diseases often result in other comorbidities such as CKD, which may lead to CKD-related death, and this occurs in 30–50% of all CKD-related as well as end-stage renal disease (ESRD)-related deaths globally (Collins et al., 2015; Masakane et al., 2015). Vascular calcification has been identified as the independent risk factor that increases CVD deaths among CKD cases. Many studies have confirmed that hyperphosphatemia can cause cardiovascular complications, such as vascular calcification and left ventricular hypertrophy, thereby increasing the risk of death from CVD in CKD patients (Goodman et al., 2000; Block et al., 2004; Russo et al., 2011; Briet and Burns, 2012; Smith, 2016).

There are four types of vascular calcification: arterial intima calcification, arterial media calcification, aortic valve calcification and calciphylaxis. Arterial intima calcification and media calcification occur in ESRD patients, with intima calcification being the most frequent type (Wang et al., 2001). Therefore, intima and media calcification may be the main reason for the increased risk (10 to 100 fold) of cardiovascular death in patients with ESRD by 10 to 100 times (Huveneers et al., 2015). Intima calcification and media calcification may simultaneously exist in ESRD patients, but their manifestations may be very different. Intima calcification is confined to plaques, and the pathological changes are related to inflammatory reactions and lipid deposition. The main consequences may be plaque rupture and acute vascular occlusion, which may lead to avascular necrosis. Media calcification, which is also called the Monckeberg's sclerosis, usually induces disorders within the inner elastic layer, which is manifested by linear deposition of hydroxyapatite calcium crystals in the inner elastic layer of the arterial media. Compared with intima calcification, there are few inflammatory cells or lipid deposition. The disorder mainly causes arterial stiffness and increased systolic blood pressure, leading to left ventricular hypertrophy, which in turn leads to heart failure. Studies have shown that calcification in the middle layer of arteries is a vital factor for predicting CVD-related mortality among ESRD cases (London et al., 2003).

Among the various causes of vascular calcification in CKD patients, hyperphosphatemia is closely related to vascular calcification. The absorption and excretion of phosphorus by the intestines, renal tubules, intracellular and extracellular fluids, and bones maintains the serum phosphorus levels within the normal range. Among them, the kidney's filtration and absorption of phosphorus are the main factors affecting the steady state of serum phosphorus.

In CKD stage 2–3, the nephron weight decreases and the renal function declines. Phosphate hormones, including fibroblast growth factor 23 (FGF 23) or parathyroid hormone (PTH), are synthesized to resist excessive phosphorus. Such hormones play a major role in the renal proximal tubules, by downregulating type IIa and type IIc sodium-phosphorus transporters, thereby increasing renal phosphorus excretion and maintaining serum phosphorus levels within the normal range (Isakova et al., 2011; Tatsumi et al., 2016). However, as CKD enters the advanced stage, the kidneys can no longer effectively filter the ingested phosphorus, which eventually leads to obvious hyperphosphatemia in CKD stage 4–5. Hyperphosphatemia may lead to the significantly increased morbidity and mortality of vascular calcification, as seen in CKD cases and the general population (Dhingra et al., 2007; Da et al., 2015).

According to the current research on the mechanism of vascular calcification, effective control of serum phosphorus levels has a certain protective effect on the cardiovascular system and kidneys in patients with chronic kidney disease, especially in advanced patients. However, even after, controlling the intake of high-phosphorus foods and administering adequate dialysis, blood phosphorus levels may still not be effectively controlled within the ideal range. The use of phosphorus binders has become an important method to control phosphorus in the blood, mainly by combining with phosphorus in food to reduce phosphorus absorption. Oral phosphate binders combine with dietary phosphates in the intestines to prevent phosphorus absorption and become an important part of the management strategy to decrease and control the level of serum phosphorus in patients with advanced CKD. Some observational research data indicate that the use of phosphate adhesives can prolong the survival time of patients undergoing hemodialysis.

In the current treatment of hyperphosphatemia binders, lanthanum drugs have obvious advantages. Trivalent cations have a high affinity with phosphorus and are easy to form poorly soluble complexes with phosphorus. They are poorly soluble in low water conditions, and it is difficult to pass through the intestinal wall into the blood. They can be excreted through feces to achieve the effect of reducing phosphorus. However, lanthanum does not affect the absorption of fat-soluble vitamins and has no obvious side effects. Lanthanum absorbed into the body is mainly excreted through the liver, and therefore, it is suitable for dialysis patients. In the preliminary research of the research group, it was found that nano-lanthanum hydroxide can satisfactorily reduce phosphorus and also has a protective effect on the kidneys (Ma et al., 2019). The present work aimed to explore the clinical efficacy of lanthanum hydroxide in treating vascular calcification induced by hyperphosphate in the context of chronic renal failure (CRF).

MATERIALS AND METHODS

Reagents and Antibodies

Lanthanum hydroxide (Laboratory synthesis), Adenine (Sigma-Aldrich, Cat. #V900471, United States), Lanthanum carbonate (Sigma-Aldrich, Cat. #325767 United States), Calcium carbonate (Sigma-Aldrich, Cat. #V900138 United States), Human aortic vascular smooth muscle cells (Shanghai Yubo Biological

Technology Co., Ltd., Cat. #C740, China), RNA Simple Total RNA Kit (Tiangen Biochemical Technology (Beijing) Co., Ltd., Cat. #DP419, China), ReverTra Ace qPCR RT Kit (ToYoBo Life Science, Cat. #FSQ-101, China), SYBR Green Realtime PCR Master Mix (ToYoBo Life Science, Cat. #QPK-201), Lipopolysaccharide (LPS, Sigma-Aldrich, Cat. #L4391), Lanthanum chloride (LaCl3, Sigma-Aldrich, Cat. #298182), Sodium pyrophosphate tetrabasic decahydrate (PPI, Sigma-Aldrich, Cat. #S6422), Monoclonal Mouse anti-SM22α (SC-53932, Santa Cruz Biotechnology, RRID: AB_1129519), Monoclonal Mouse anti-BMP-2/4 (SC-137087, Santa Cruz Biotechnology, RRID: AB_2258985), Monoclonal Mouse anti-Runx2 (SC-101145, Santa Cruz Biotechnology, RRID: AB_1128251), Polyclonal Rabbit anti-β-Actin (K101527P, Solarbio), Monoclonal Rabbit anti-TRAF6 (ab40675, Abcam, RRID: AB_778573), Monoclonal Mouse anti-NF-κB (#6956, Cell Signaling Technology, RRID: AB_10828935), Goat anti-Mouse IgG (H + L) (A23910, Abbkine), Goat anti-Rabbit IgG (H + L) (A23920, Abbkine), Polyclonal Rabbit anti-Lamin A (10298-1-AP, Proteintech, RRID:AB_2296961).

Animals and Experimental Protocol

The 6-week-old male wistar rats weighing 200–220 g (SPF, Beijing Vital River Laboratory Animal Technology Co., Ltd., China) were housed under the barrier environment, with constant temperature (21–22°C) and humidity (40–50%). All animals assigned in this study were given free access to their designed diet and tap water. Each rat was acclimatized to the experimental conditions for 1 week ahead of time.

The CKD animal model was established as previously described in **Figure 1**. For 1–2 weeks, the model rats were given 2% adenine gavaged at 200 mg kg^{-1} per day. For 3–4 weeks, all model rats gavaged every other day at the same concentration and dose. After 4 weeks, blood was collected from the fundus venous plexus of the rats, and serum phosphorus, creatinine, and urea nitrogen were detected to determine whether the model was successful. After the CKD rats were successful, the model group is subdivided into Lanthanum hydroxide (0.4 g kg^{-1}, 0.2 g kg^{-1}, and 0.1 g kg^{-1}), lanthanum carbonate (0.3 g kg^{-1}), calcium carbonate (4.2 g kg^{-1}) and model group (n = 12), which was gavaged every day for 8 weeks. During the experimental period, rats were fed with standard chow in the control group or chow containing 1.2% phosphorus (Beijing Keao Xieli Feed Co., Ltd) in the CKD group. Serum phosphorus, creatinine, urea-nitrogen, PTH, FGF23 was measured at 4 and 8 weeks after treatment. On the last day of the 12 weeks, all animals were sacrificed. One day before sacrifice, the 12 h urine samples were collected from rats that were allowed to drink water only. To sacrifice the rats, each animal was injected with 50 mg kg^{-1} pentobarbital for anesthesia, and blood was collected from the abdominal aorta. Thereafter, aorta of every animal was collected and processed below: snap-frozen within liquid nitrogen to carry out RNA analysis and Western blotting assay, right kidney tissues were immersed into 10% phosphate-buffered formalin to conduct histological analysis. Besides, we separate the femoral bone, removed the soft tissues on it and then immersed it into the 10% phosphate-buffered formalin to perform histological analysis. Animal experiments were approved by the Medical Ethics Committee of Inner Mongolia Medical University (Document NO. YKD2019019).

Cell Culture

The human aortic vascular smooth muscle cells (VSMCs) were cultured within the high-glucose (HG) DMEM (Gibco, Cat. #11995-065, United States) that contained 10% fetal bovine serum (FBS, Gibco, Cat. #10099-141, United States) as well as 1% penicillin-streptomycin (Gibco, Cat. #15140122, United States), and this medium was called the growth medium (GM). After achieving cell confluence, cells at passages 5–7 were used in our experiments. The medium was replaced at intervals of 2 days. For the sake of inducing phosphate-induced calcification, the 3 mmol/L inorganic phosphate (namely, the calcification medium, Na_2HPO_4/NaH_2PO_4, pH 7.4) was added into GM with or without La (15–60 μmol L^{-1} of $LaCl_3 \times 6H_2O$) for a period of 6 days.

Serum Biochemistry

Serum calcium, phosphorus, creatinine, and urea levels were measured using biochemical detection kit (Nanjing Jiancheng Bioengineering Institute, China). The Urease-GLDH approach was used to evaluate urea content. The sarcosine oxidase approach was used to measure creatinine content, whereas the MTB approach was used to evaluate calcium content. PTH and FGF23, were measured by a rat ELISA kit (Shanghai Yi Li Biological Technology Co., Ltd., China).

Histologic Analyses

To analyze the histology, we fixed tissues with the 10% phosphate-buffered formalin, followed by paraffin embedding, H&E staining, Von Kossa staining, as well as EVG staining by the standard approaches (Wuhan Saville Biotechnology Co., Ltd., China). Imaging of histological sections was performed using a LEICA DM 2000 (Leica Microsystems GmbH, Wetzlar, Germany) microscope. The specific experimental steps are as follows: Fix the rat kidney and blood vessel in 4% paraformaldehyde for more than 24 h, remove the tissue from the fixative solution, trim the target tissue with a scalpel (the kidney and blood vessel are cut longitudinally), and place the cut tissue in the dehydration box Put the gradient alcohol into the dehydrator for dehydration. Put the melted wax into the embedding frame, take the tissue out of the dehydration box and put it into the embedding frame. Cool in a −20° freezer. After the wax solidifies, remove the wax block from the embedding frame and trim the wax block. The wax block was sliced on a paraffin microtome with a thickness of 4 μm. Float the slices on the spreader's 40°C warm water to flatten the tissues, pick up the tissues with glass slides, and put them in a 60°C oven for baking.

H&E Staining

The sections were deparaffinized to water, stained with hematoxylin for 8 min, and rinsed with tap water. Use 1% hydrochloric acid alcohol to differentiate for 30 s, and rinse with tap water 0.6% ammonia water returns to blue, flushing with running water. Finally, tissue sections were stained with eosin for

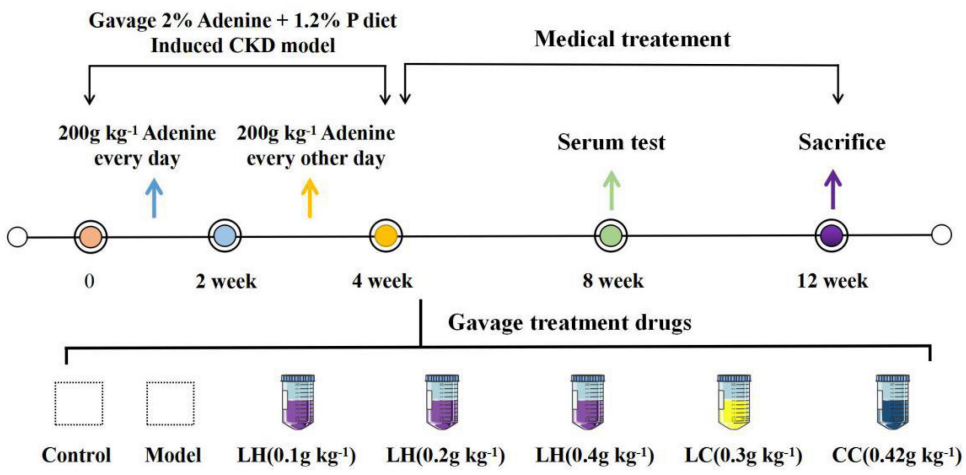

FIGURE 1 | Protocols for the induction of CKD and phosphate loading. Except the control group, all other groups were 1.2% high phosphorus diet for 12 weeks.

3 min, and the water in the sections was replaced with a gradient concentration of alcohol. The sections were put into xylene I for 5 min and then xylene II for 5 min. After covered with neutral gum, the sections were observed under a microscope.

Von-Kossa Staining

Dewax the section to water, shake off the water on the section, and circle the section with a brush, add Von Kossa dye solution dropwise, irradiate it with a UV lamp for 4 h, and distill to clean it. The sections were stained with hematoxylin staining solution for 5 min and washed with tap water; 1% hydrochloric acid alcohol for 30 s, washed with tap water; 0.6% ammonia water returned to blue, washed with running water. Finally, put in 85% and 95% alcohol gradient dehydration for 5 min, and eosin dye solution for 5 min, and then replace the water in the slice with gradient alcohol. The sections were put into xylene I for 5 min and then xylene II for 5 min. After covered with neutral gum, the sections were observed under a microscope.

EVG Staining

The paraffin sections were deparaffinized to water, and the sections were stained with EVG dye solution for 5 min, and rinsed with tap water. Then put the section into EVG dye solution B diluted twice for background differentiation, rinse with tap water, and repeat the operation until the elastic fiber is purple-black and the background is off-white and nearly colorless, and differentiation is over. Re-dye with VG dye solution for 1–3 min, wash in water quickly, and dehydrated quickly in three cylinders with absolute ethanol. Finally, the sections were put into xylene I for 30 s and then xylene II for 5 min. After covered with neutral gum, the sections were observed under a microscope.

Computed Tomography (CT) Analysis

To evaluate the area of aorta calcification, rats were anesthetized by intraperitoneal injection of 20% urethane and subjected to CT imaging using a PET/CT (SIEMENS Inveon MM, Siemens Ltd., Germany).

TMT Modified Quantitative Proteomics

The sample was immediately ground to cell powders with liquid nitrogen, followed by transfer to the 5-mL centrifuge tube. Next, 4 volumes lysis buffer consisting of 1% protease inhibitor cocktail and 8 M urea were used to resuspend cell powders under on ice sonication thrice by the use of the high-intensity ultrasonic processor (Scientz). Thereafter, the obtained samples were subjected to 10 min of centrifugation at 12,000 × *g* under 4°C for removing the rest debris. At last, we obtained the supernatants and determined their protein content through the BCA assay in accordance with specific protocols.

Equal amount of protein of each sample was taken for enzymatic hydrolysis, followed by adding an appropriate amount of standard protein and adjusting the volume to the same with lysis buffer. Add one volume of pre-cooled acetone, vortex to mix. Then, 4 volumes pre-chilled acetone were added to precipitate for 2 h under −20°C, followed by 5 min of centrifugation at 4,500 × *g*, later the supernatants were discarded, and pre-chilled acetone was used to rinse the precipitate for two times. After drying the pellet, add TEAB at a final concentration of 200 mM, ultrasonically disperse the pellet. Later, trypsin was added (protease:protein ratio = 1:50, m m^{-1}) for overnight hydrolysis. Afterward, dithiothreitol (DTT) was added till the 5 mM final concentration for 30 min reduction under 56°C. Later, iodoacetamide (IAA) was added till the 11 mM final concentration, followed by 15 min incubation in dark under ambient temperature. The TMT kit/iTRAQ kit was used to reconstitute peptide within the 0.5 M TEAB, followed by processing following specific instructions.

The Thermo Betasil C18 column (particle size, 5 μm; length, 250 mm; inner diameter, 4.6 mm) was used for high pH reverse-phase HPLC to fractionate tryptic peptides to different fractions. After dissolving in the mobile phase A of liquid chromatography, we adopted the EASY-nLC 1000 ultra-high performance liquid system to separate the different fractions. The mobile phase A was the aqueous solution consisting of 0.1% formic acid along with 2% acetonitrile, whereas mobile phase B was the aqueous solution

consisting of 0.1% formic acid together with 90% acetonitrile. The elution procedure was as follows, 8%∼23% B in 0–38 min; 23%∼35% B in 38–52 min; 35%∼80% B in 52–56 min; and 80% B in 56–60 min, Besides, we fixed the flow rate at 600.00 nL min^{-1}. In addition, the ultra-high performance liquid system was used to separate peptides, which were then ionized with the NSI ion source, followed by analysis using the QE + 1 mass spectrometry. The high-resolution Orbitrap was used to detect and analyze peptide precursor ions together with the secondary fragments, at the voltage of ion source of 2.2 kV.

Mass spectroproteomic data has been placed into the Proteome Xchange Consortium through the PRIDE Partner store inventory with the dataset identifier PXD011610. If any additional data is required, it can be obtained from the corresponding author upon reasonable request[1].

Mass Spectrometry Quality Control Testing

Many peptides had 7–20 amino acids, which conformed to those general rules related to HCD fragmentation as well as trypsin hydrolysis. Nonetheless, peptides that had <5 amino acids only generated few fragment ions, which were unable to generate the valid sequence identification. Peptides that had over 20 amino acids were not appropriate for HCD fragmentation because of their great charges and mass. Upon mass spectrometry, we found that peptide lengths were distributed in a way conforming to the requirements of quality control (**Supplementary Figure 3**).

Quantification of Calcium Deposition

Cells were cultured within the 6-well plates and rinsed by PBS (pH 7.4) thrice, followed by 24 h decalcification using 0.6 mol L^{-1} HCl under 37°C. Afterward, PBS was used to wash cells thrice, followed by 30 min solubilization using the solution consisting of 0.1% SDS and 0.1 mol L^{-1} NaOH. The BCA assay (Beyotime Biotechnology, Cat. #P0012, China) was used to measure protein content. The content of cellular calcium was determined by the QuantiChrom Calcium Assay Kit (Beyotime Biotechnology, Cat. #S1063S, China) and normalized to protein content, which was expressed as μ g/mg protein.

ALP Activity Assay

Cells grown on 6-well plates were washed three times with PBS pH 7.4 and then 150 ul of P0013J (no phosphatase inhibitor) lysis solution was added into each well for 30 min on ice. After lysing cells, we used the alkaline phosphatase (ALP detection kit (Beyotime Biotechnology, Cat. #P0321, China) to determine the ALP activity. Besides, the BCA protein detection kit was utilized to measure protein content. ALP activity was normalized based on protein level and presented in the manner of U/mg protein.

Alizarin Red Staining

PBS (pH, 7.2–7.4) was used to wash cells, followed by 30 min 4% paraformaldehyde fixation under 37°C. After PBS washing again, cells were subjected to 5 min of 1% Alizarin Red S staining (PH 4.2, Solarbio, Cat. #G1452, China). The Alizarin Red S was discarded and washed 5 times with PBS until the Alizarin Red S was washed away. The culture plate was analyzed under the microscope to capture micrographs. Later, 10% acetic acid was used to counter-stain and dissolve calcium precipitates. For quantifying calcification, we used the multi-detection microplate reader (Dynex, Lincoln, United Kingdom) to measure the OD value at 420 nm.

Von Kossa Staining

PBS (pH, 7.2–7.4) was used to wash cells, followed by 30 min 4% paraformaldehyde fixation under 37°C. After PBS washing thrice, cells were treated with reagent A of Von Kossa staining Kit (Solarbio, Cat. #G1452, China) and placed under ultraviolet light until calcium phosphate turned black. The dye was washed with PBS three times to remove the excessive dye. After treating with sodium thiosulfate for 2 min, it was washed three times with PBS. The cell nuclei were counterstained with Eosin staining solution (Solarbio, Cat. #G1120). Finally, the culture plate was analyzed under the microscope.

Western Blot Analysis

The ice-cold cell lysis buffer (Thermo Fisher Scientific) that consisted of the complete phosphatase and protease inhibitor cocktail (Thermo Fisher Scientific) was used to lyse rats' aortic tissue and VSMCs. Then, the samples were centrifuged for 10 min at 12000 rpm, the Roti-Load1 Buffer (Carl Roth GmbH) was used to boil proteins for 10 min under 100°C. Afterward, we separated equivalent volumes of proteins through SDS-PAGE, followed by transfer onto PVDF membranes. Thereafter, the following primary antibodies were used to incubate the membranes under 4°C overnight: Monoclonal Mouse anti-BMP-2/4 (1:600), Goat anti-Rabbit IgG (H + L) (1:5000), Monoclonal Mouse anti-Runx2 (1:600), Goat anti-Mouse IgG (H + L) (1:5000), Polyclonal Rabbit anti-β-Actin (1:2000), Monoclonal Rabbit anti-TRAF6 (1:5000), Monoclonal Mouse anti-NF-κB p65 (1:500). Later, secondary anti-rabbit IgG (H + L) (1:5000) or anti-mouse IgG (H + L) (1:5000) was used to further incubate the membranes under ambient temperature for 1 h. Finally, we used the stripping buffer (Thermo Fisher Scientific) to strip the membranes for 40 min under ambient temperature for subsequent detection of loading controls. The Odyssey CLX two-color infrared laser imaging system (LI-COR) was employed to obtain protein bands, while ImageJ was used for analysis. All data were presented in the manner of total protein/β-actin ratio or nuclear protein/Lamin A ratio after normalization based on controls.

Quantitative Real-Time RT-PCR

The RNA Simple Total RNA Kit [Tiangen Biochemical Technology (Beijing) Co., Ltd., Cat. #DP419, China] was used to extract total cellular and tissue RNA following specific protocols. Thereafter, the ReverTra Ace qPCR RT Kit (ToYoBo Life Science, Cat. #FSQ-101, China) was employed to synthesize cDNA from the extracted total RNA through reverse transcription. In addition, the QuantiTect SYBR Green Realtime PCR Master Mix (ToYoBo Life Science, Cat. #QPK-201) was adopted for RT-qPCR by using the Piko Real-Time PCR Detection System (Thermo

[1]http://www.ebi.ac.uk/pride

Fisher Scientific, Cat. #N11471) in accordance with specific protocols. **Supplementary Table 1** presents primer sequences.

The specificity was confirmed by analysis of the melting curves of the PCR products. Each PCR procedure was repeated twice, and $2^{-\Delta\Delta Ct}$ method was used to determine the fold changes (FCs) of relative mRNA expression, with GAPDH being the internal control.

Immunofluorescence

After preparing the slides and performing induction under different conditions, aspirate the supernatant of the 6-well plate, then rinse it with PBS, 1 mL each time, wash twice, and then add 1 mL of 4% paraformaldehyde solution to each well, Fix on ice for 20 min, wash two times with PBS after fixation, add 1 mL of Triton X-100 to each well for cell permeabilization, and repeat washing with PBS three times after 10 min. Add 1 mL of 10% goat serum to each well for blocking for 60 min, wash once with PBS after blocking, pull out the slides from the well plate, add 200 uL of NF-κB (1:800) to each slide, and incubate overnight at 4°C. Collect the primary antibody, wash three times with PBS, add 200 uL of green fluorescent secondary antibody (1:1000) to each slide in the dark, incubate for 1 h in dark (37°C), wash two times with PBS, Add 1 mL of blue fluorescent antibody DAPI to each slide, incubate for 5 min, and wash three times with PBS. After drying in the dark, pull the slide out of the orifice, mount the slide with 1 to 21 drops of anti-fluorescence quencher on the slide, cover the cover glass, and encapsulate the cover glass with nail polish around the cover glass. Capture photos under a confocal microscope.

Statistical Analysis

Each experiment was carried out for thrice. Data were presented in the manner of mean ± SEM. GraphPad Prism 7.0 was used for statistical analysis and mapping. Multiple group data were analyzed through one-way ANOVA. A difference of $P < 0.05$ indicated statistical significance.

RESULTS

Lanthanum Hydroxide Delays the Development of Renal Failure and Protects Renal Function

The CKD rat modeling method is shown in **Figure 1**. In order to evaluate the protective effect of lanthanum hydroxide on the kidneys of CKD rats, we measured the levels of serum phosphorus, calcium, creatinine, and urea nitrogen at 4 and 8 weeks after treatment. According to **Figures 2**, **4** week compared with the control group, the serum phosphorus, creatinine, and urea nitrogen of the model group increased by 4.85 ± 0.50, 0.31 ± 0.05, 11.88 ± 0.38, respectively, and compared with the normal control group, there were significant differences ($P < 0.01$), suggesting that adenine combined with a 1.2% high-phosphorus diet was successfully modeled. After 4 weeks of administration of lanthanum hydroxide, compared with the model group, serum phosphorus, creatinine, and urea nitrogen levels were significantly reduced. As shown in **Figure 2**, after 8 weeks of treatment, it can be seen that the lanthanum hydroxide 0.4 g kg^{-1} group has the best phosphorus-lowering effect, and the levels of blood urea nitrogen (BUN) and serum creatinine (Scr) decreased depending on its dose. There was no statistical difference in the detection results of serum calcium at 4 and 8 weeks after administration.

According to the results of HE staining of rat kidney in **Figure 3**, compared with the control group, the degeneration and necrosis of the proximal convoluted tubule epithelial cells in the renal cortex and the disappearance of the nuclei can be observed in the other groups. The mesenchyme is accompanied by a large number of mononuclear cell infiltration, glomerular necrosis and disappearance, and visible protein casts and obvious expansion of the renal tubules. The model group exhibited obvious pathological changes, including chronic granulomatous inflammation and purine deposits in some renal tubules (**Figures 3B,I**). At the same time, there were also white blood cell casts and renal mesenchymal fibrous tissue focal hyperplastic lesions in the renal tubules. The pathological results of the lanthanum hydroxide (0.4 g kg^{-1}, 0.2 g kg^{-1}, and 0.1 g kg^{-1}) group showed that compared with the model group, cell deformation and infiltration were lighter, and the degree of renal tubule expansion was significantly improved. Renal interstitial hyperplasia is also effectively controlled, and the glomerular structure is relatively complete (**Figures 3C–E,G,K,L**). It was observed that, lanthanum hydroxide can significantly reduce serum phosphorus levels, protect the kidneys, and slow the development of renal failure.

Lanthanum Hydroxide Inhibits the Development of Vascular Calcification

The above results show that lanthanum hydroxide can effectively reduce serum phosphorus levels and defer the progression of renal failure. Because the increase in blood phosphorus is closely related to vascular calcification, we measured serum PTH, and FGF23 levels, and performed computed tomography (CT) examination of rat thoracic aorta and Von Kossa staining of tissue sections.

Relative to the control group, the CKD model group exhibited markedly elevated serum of levels FGF23 and PTH. After treatment with lanthanum hydroxide, the serum PTH and FGF23 levels decreased, and the difference was significant relative to model group ($P < 0.01$) (**Figures 2E,F**). Elevated blood phosphorus can lead to increased levels of PTH and FGF23, the latter being a major regulator of serum phosphorus synthesized and released by osteoblasts, which plays a role in the metabolism of vitamin D and secondary hyperparathyroidism. It also plays a key role and is directly involved in vascular calcification. Lanthanum hydroxide can slow the occurrence of vascular calcification by reducing serum phosphorus, thereby reducing the levels of PTH and FGF23 in the serum.

Figure 4 shows the EVG and Von Kossa staining of thoracic aortic slices. Vascular calcification was not observed in aortic sections of controls (**Figures 4Aa,h**). In contrast, in the model groups, there was obvious evidence (positive Von Kossa) of

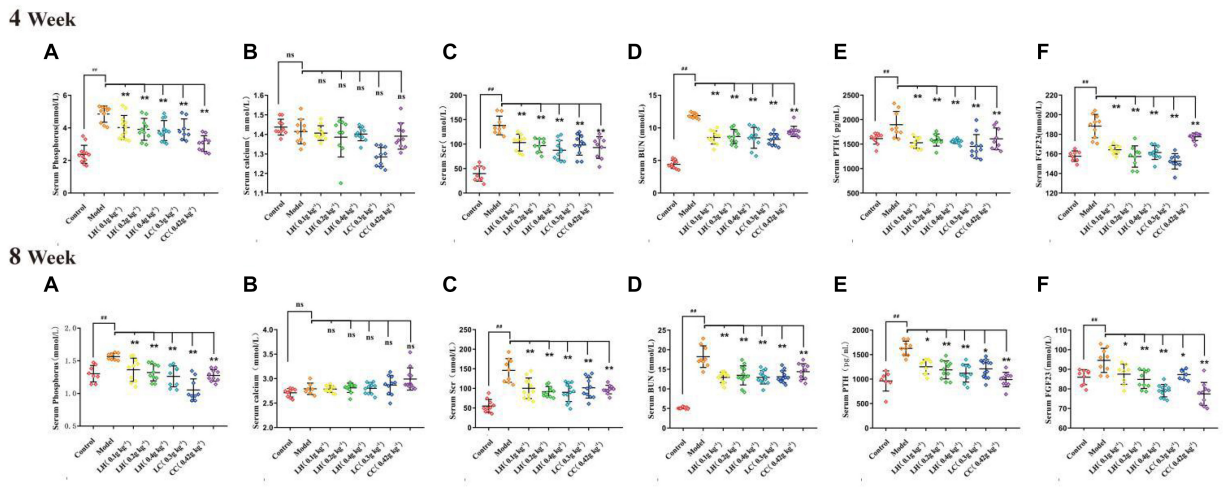

FIGURE 2 | Serum biochemical indicators after lanthanum hydroxide treatment. Serum biochemical examinations for 4 and 8 weeks of drug treatment **(A)** Phosphorus; **(B)** Serum calcium; **(C)** Scr, serum creatinine; **(D)** BUN, serum urea nitrogen; **(E)** PTH, parathyroid hormone; **(F)** FGF23, fibroblast growth factor 23 (mean ± SEM, $^{\#\#}P < 0.01$ compared with the control group; $^{*}P < 0.05$, $^{**}P < 0.01$ compared with the model, NS, not significant, $N = 9$–11).

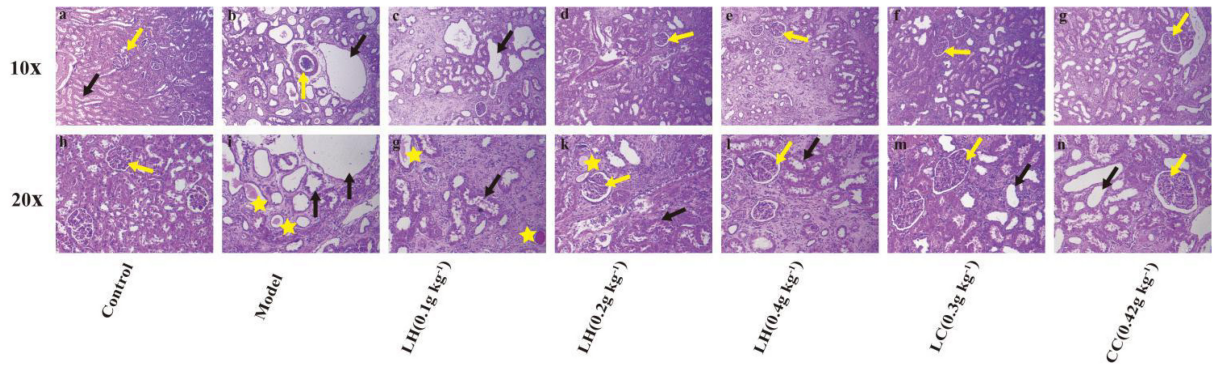

FIGURE 3 | Representative histopathological findings in kidney tissues. As shown in the figure, compared with the control group, the kidney pathology of the model group is: glomerular necrosis and disappearance (yellow arrow), renal tubule dilation (black arrow), protein cast (yellow star), and inflammatory factors Infiltration, and fibrosis of the renal interstitium appears. After treatment with lanthanum hydroxide, the glomerular structure was relatively complete, the degree of renal tubule dilatation was significantly improved, and the inflammatory infiltration was also reduced. **(a–g)** Kidney pathology of each group of animals at 100 times. **(h–n)** Kidney pathology of each group of animals at 200 times.

vascular calcification exclusively in the media. It is noteworthy that the elastin layers in these calcified areas appeared to be disorganized and disrupted in a gross manner (**Figures 4Ab,i**). After 0.4 g kg^{-1} lanthanum hydroxide treatment, a significant reduction in calcification was observed (**Figures 4Ae,l**), as well as less elastic fiber breakage has also been improved. There was obvious aortic calcification in the model group on CT images (**Figure 4Ba**, yellow arrows), and the aortic calcification decreased in the 0.4% lanthanum hydroxide group (**Figure 4Bb**).

The Proteomic Analysis of Aortic Tissue After Lanthanum Hydroxide Treatment *in vivo*

In order to further explore how lanthanum hydroxide delays the occurrence of vascular calcification, we analyzed the effect of lanthanum hydroxide on the CKD rat model through quantitative proteomics technology, and investigated the effect of expression changes due to lanthanum hydroxide on differential proteins in order to verify the relevant signal pathways and provide evidence.

To study the differences in aortic proteomics between the control group and the CKD rat model group, tandem mass tag (TMT) labeling, mass spectrometry-based quantitative proteomics, and high-performance liquid chromatography (HPLC) fractionation technologies were applied. Significantly upregulated proteins were selected at the thresholds of FC > 1.3 and $P < 0.05$, whereas significantly downregulated proteins were selected according to FC < 1/1.3. The differential protein quantitative volcano chart is shown in **Figure 5A**. On the horizontal axis in the figure, the relative protein expression is converted into log2 value,

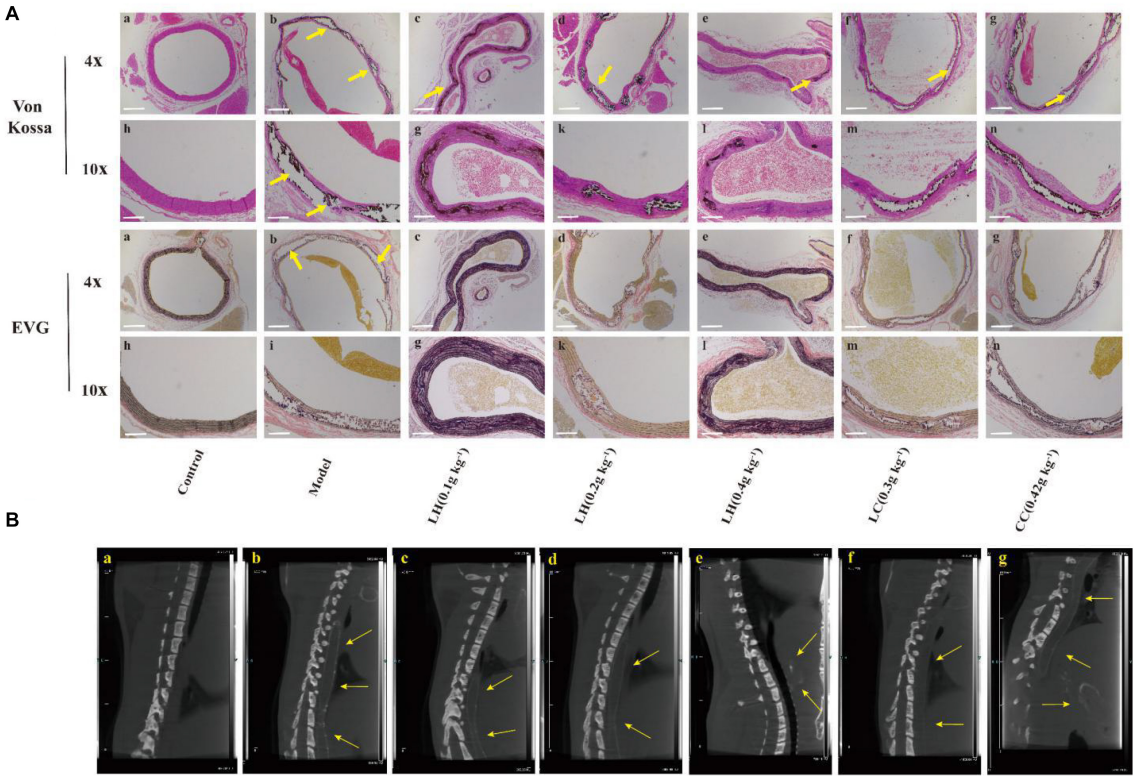

FIGURE 4 | Representative computed tomography (CT) images of ectopic calcification and micrographs of Von Kossa and EVG stained sections of the thoracic aorta after 12 weeks. **(A)** Von Kossa and EVG stained tissue image of thoracic aorta. **(B)** Ectopic calcification was observed in thoracic aortic sections on CT in model group (yellow arrows). **(a)**, control group; **(b)**, model group; **(c)**, lanthanum hydroxide (0.1 g kg^{-1}); **(d)**, lanthanum hydroxide (0.2 g kg^{-1}); **(e)**, lanthanum hydroxide (0.4 g kg^{-1}); **(f)**, lanthanum carbonate (0.3 g kg^{-1}); **(g)**, calcium carbonate (0.42 g kg^{-1}). Von Kossa and EVG staining positive legions were observed in CKD rat (yellow arrows). Scale bar, 200 μm.

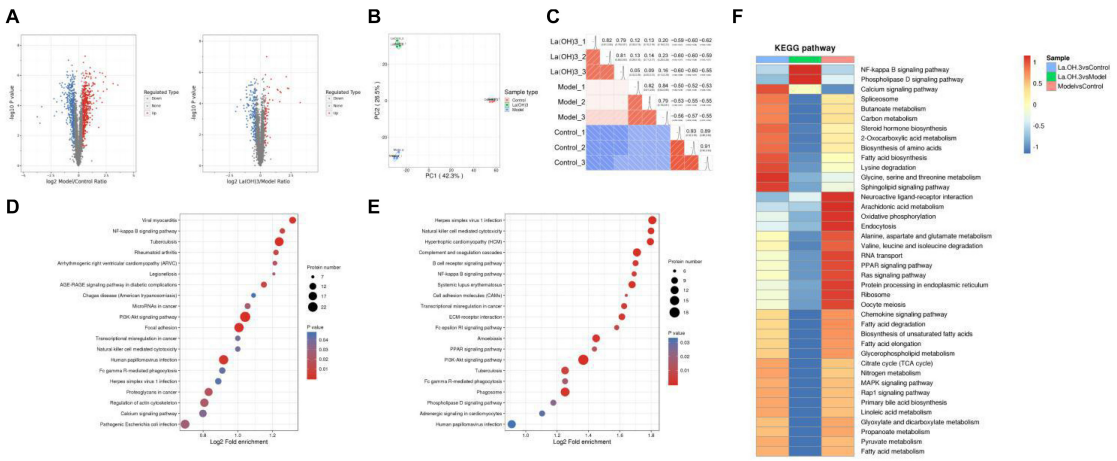

FIGURE 5 | Proteomic analysis of aortic tissues. **(A)** Differential protein quantitative volcano map. The horizontal axis in the figure stands for relative protein level after Log2 conversion, while the vertical axis represents *P*-value obtained upon significance test following -Log10 conversion. In the figure, the red and blue dots stand for significantly upregulated and downregulated proteins, respectively. **(B)** The 2D scatter plot displaying PCA for protein quantification across duplicated samples. **(C)** Pearson's correlation coefficient heat map. **(D)** KEGG pathway enrichment analysis-Model vs. Control. **(E)** KEGG pathway enrichment analysis-$La(OH)_3$ (0.4 g kg^{-1}) vs. Model. **(F)** Cluster analysis heat map of KEGG pathway. The similar functions from diverse groups are clustered and plotted in the heat map based on *P*-values upon enrichment test by the hierarchical clustering approach, where horizontal axis stands for diverse comparison groups, while vertical axis represents functional description of DEPs. The diverse color blocks stand for enrichment levels, where red and blue stand for strong and weak enrichment, respectively.

while the *P*-value obtained from the significance test after being converted to −log10 are on the vertical axis. In the figure, the red and blue dots denote significantly upregulated and downregulated proteins, respectively. Clearly, relative to the control group, there were 448 significantly upregulated and 406 downregulated proteins identified in the CKD model group. Relative to the CKD model group, 69 proteins were significantly upregulated after lanthanum hydroxide administration, and 168 proteins were significantly downregulated.

For biological or technical replicate samples, it is necessary to test the statistical consistency between the results obtained for biological samples and technical duplicate samples. We conducted two analysis methods, principal component analysis (PCA) and Pearson correlation, to evaluate the repeatability of protein quantification. PCA analysis shows that the control, model, and lanthanum hydroxide (0.4 g kg^{-1}) groups have good repeatability and can be completely separated (**Figure 5B**). Pearson correlation analysis also shows that the data has a satisfactory linear correlation (**Figure 5C**). The CKD rat model induced by adenine combined with a 1.2% high-phosphorus diet was successful, and the treatment of lanthanum hydroxide also had a certain effect on the model rats.

For clarifying the enrichment trend of differentially expressed proteins (DEPs) in some functions, the Kyoto Encyclopedia of Genes and Genomes (KEGG) pathway analysis was performed based on all the screened DEPs. A bubble chart was plotted to present the significantly enriched DEPs based on the *p*-values obtained from the enrichment test ($P < 0.05$). The vertical axis in **Figures 5D,E** represents the functional classification or pathway, whereas the horizontal axis denotes the log2-transformed value regarding the proportion of DEPs in a function type to all proteins identified. The circle color indicates the *P*-value upon enrichment significance test, while the circle size represents the number of DEPs involved in the pathway. According to the KEGG enrichment analysis of the control, model, and lanthanum hydroxide (0.4 g kg^{-1}) groups, they can be enriched into the nuclear factor-κB (NF-κB) pathway, PI3K-AKT signaling pathways and cardiovascular disease-related pathways.

To determine the correlation of the differentially modified protein functions after lanthanum hydroxide treatment, we performed KEGG cluster analysis when DEPs were enriched to diverse groups (**Figure 5F**). We clustered similar functions from diverse comparison groups to draw a heat map based on *p*-values acquired upon enrichment test by hierarchical clustering, where the horizontal axis indicated diverse comparison groups, and the vertical axis describes the corresponding differentially expressed gene (DEG) functions. The diverse color blocks indicate the enrichment level, and red and blue denote strong and weak enrichment, respectively. Relative to the model group, DEPs were mostly associated with the NF-κB signal transduction pathway following treatment with lanthanum hydroxide.

The high CVD morbidity and mortality among CKD cases are primarily ascribed to arterial media vascular calcification. Therefore, controlling the occurrence and development of vascular calcification is the key to a positive prognosis for CKD patients. Vascular calcification has been identified as an active process under the regulation of VSMCs. VSMCs can change their phenotype and release stromal vesicles under pathological conditions, which in turn trigger the occurrence of aortic calcification. The signaling pathway regulating the phenotypic transdifferentiation of VSMCs is complex, and it involves systemic inflammation and at least partly depends on the transcription factor NF-κB. It has been demonstrated that NF-κB is a key regulator of vascular calcification. Voelkl et al. (2018b) showed that zinc can inhibit the activation of the NF-κB signal pathway through GPR39-dependent TNFAIP3, thereby inhibiting phosphate-induced osteoblast-like cell transdifferentiation of VSMCs and slowing the development of vascular calcification.

Through a summary of the relevant literature and proteomic analysis of aortic tissue, the NF-κB signal transduction pathway was utilized to investigate how lanthanum hydroxide affects hyperphosphatemia-mediated vascular calcification in the context of CRF.

Lanthanum Hydroxide Inhibits Phosphate-Induced Calcification of VSMCs Through Suppression of NF-κB *in vitro*

To determine whether the promotion of calcification was due to reduced cell viability, the effect of $LaCl_3$ on cytotoxicity was investigated by MTT assay. As shown in **Supplementary Figure 1**, it was determined that the low, medium and high doses for $LaCl_3$ were 15, 30, and 60 μM, respectively, and the incubation time was 48 h. $LaCl_3$ has been shown to treat chronic renal failure and hyperphosphatemia. To examine the inhibitory effect of $LaCl_3$ on Pi-stimulated VSMCs mineralization via suppressing NF-κB under the conditions in this experiment, we grew VSMCs in calcification medium that contained 3 mM inorganic Pi with or without 15–60 μM $LaCl_3$ as well as with or without 1 ug mL^{-1} lipopolysaccharides (LPS) for 6 days. We performed Von Kossa and Alizarin Red Staining to detect granular deposits. Relative to untreated cells, Pi caused a significant 2-fold increase in mineral deposition, while the exposure of VSMCs to $LaCl_3$ decreased Pi-induced mineralization in a dose-dependent manner. Importantly, 60 μM $LaCl_3$ decreased mineral deposition in VSMCs exposed to high Pi, so that it was at the level of cells maintained in growth medium (**Figures 6A,B**). The exposure of VSMCs to $LaCl_3$ resulted in a 2/3 decrease in calcium deposition and alkaline phosphatase (ALP) activity (**Figures 6C,D**). After adding LPS, compared with the high-dose $LaCl_3$ group, the calcium deposition and ALP activity of the LPS group significantly increased, and the calcium deposition almost reached that for the mid-dose level of $LaCl_3$. In addition, differences in ALP activity and calcium level between the 60 μM $LaCl_3$ group (without inorganic Pi) and the control group or between the model group and the NaCl group were not significant, indicating that Cl^- had no effect on calcification, and

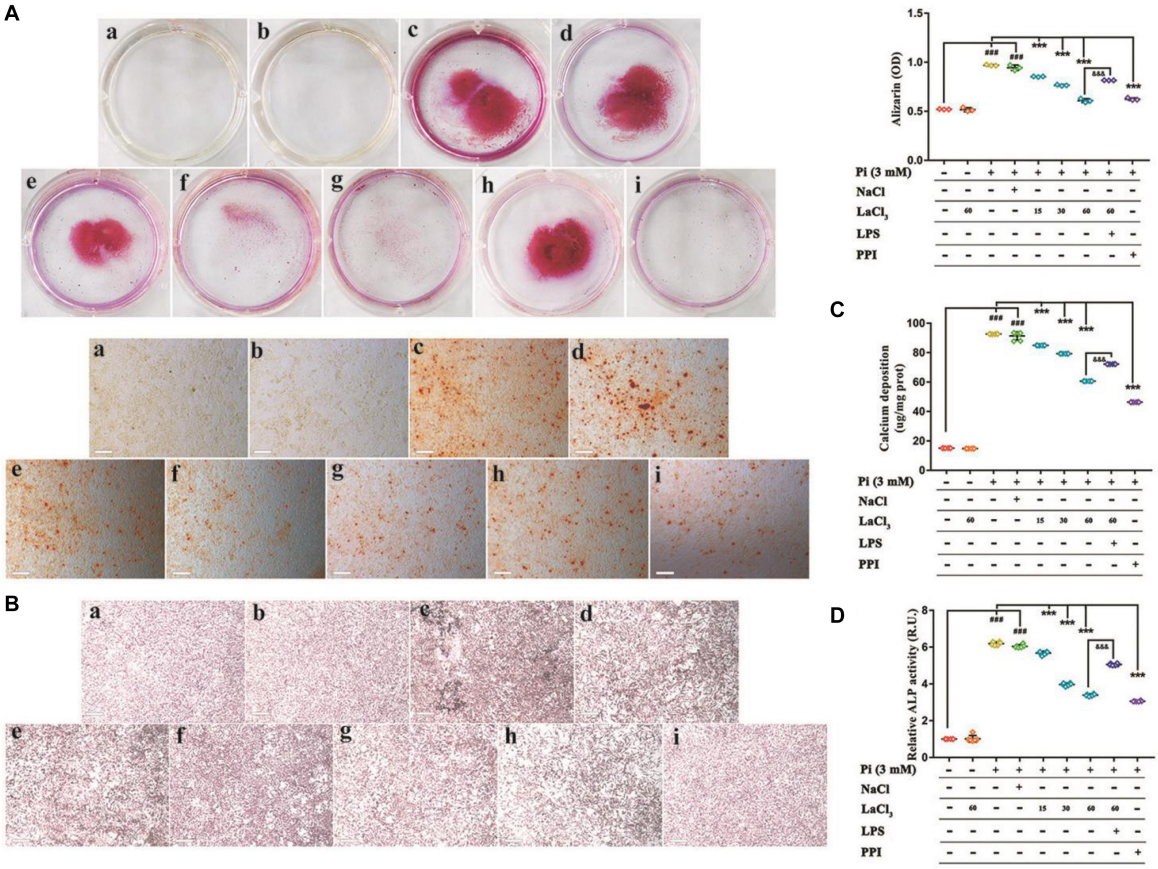

FIGURE 6 | Lanthanum suppresses the phosphate-mediated vascular mineralization depending on its dose by suppressing NF-κB. VSMCs were grown for 6 days within the calcification medium that contained 3 mmol/L phosphate (Pi) with or without 15–60 μM lanthanum **(A–D)**. **(A)** Alizarin Red staining was conducted to visualize calcium deposits. Typical wells as well as images for the stained plates upon 3 individual experiments. Quantification of Alizarin Red to represent the amount of calcium (n = 3). **(a)**, Control group (1 mM phosphate buffer); **(b)**, Control + $LaCl_3$ (60 μM) group; **(c)**, Model group (3 mM phosphate buffer); **(d)**, NaCl group (180 μM); **(e)**, $LaCl_3$ low dose group (15 μM); **(f)**, $LaCl_3$ medium dose group (30 μM); **(g)**, $LaCl_3$ high dose group (60 μM); **(h)**, LPS group (1 ug mL^{-1}); **(i)**, PPI group (100 μM). **(B)** Calcium deposition was visualized by Von Kossa Staining. Typical wells as well as images for the stained plates upon three individual experiments. **(a)**, Control group (1 mM phosphate buffer); **(b)**, Control + $LaCl_3$ (60 μM) group; **(c)**, Model group (3 mM phosphate buffer); **(d)**, NaCl group (180 μM); **(e)**, $LaCl_3$ low dose group (15 μM); **(f)**, $LaCl_3$ medium dose group (30 μM); **(g)**, $LaCl_3$ high dose group (60 μM); **(h)**, LPS group (1 ug mL^{-1}); **(i)**, PPI group (100 μM). **(C)** Scatter plots along with arithmetic means ± SEM (n = 6, ug/mg protein) for calcium deposits within VSMCs following 6 days of treatment with Pi or control, with or without 15–60 μM $LaCl_3$. **(D)** Scatter plots together with arithmetic means ± SEM (n = 6, U/mg protein) for the ALP activity within VSMCs following 6 days of treatment with Pi or control, with or without 15–60 μM $LaCl_3$. All values are presented in the manner of mean ± SEM from four individual experiments. One-way ANOVA test was adopted for statistical analysis. The significance level was set at $p < 0.05$; $^{###}P < 0.001$ versus control VSMCs; $^{***}P < 0.001$ versus Pi-treated VSMCs. $^{\&\&\&}P < 0.001$ versus Pi + $LaCl_3$ (60 μM)-treated VSMCs. Scale bar = 200 μm.

lanthanum was effective. The above findings suggest that $LaCl_3$ efficiently suppressed Pi-mediated mineral deposition by suppressing NF-κB within human VSMCs in a dose-dependent manner.

Effects of Lanthanum Hydroxide Supplementation on Vascular Calcification During Chronic Renal Failure *in vivo* and *in vitro*

To explore the role of lanthanum hydroxide in inhibiting calcification, we initially turned to a robust cell-culture-based −3 mM inorganic Pi-induced Western blot and real-time PCR assay in the VSMCs. The results showed that compared with the control group, after high Pi induced VSMCs, the expression of smooth muscle SM (SM22α) at gene and protein levels was significantly downregulated, and the osteogenic markers runt-related transcription factor 2 (Runx2) and bone morphogenetic protein 2 (BMP-2) markedly increased (**Figures 7A–E**). Therefore, it can be proved that VSMCs underwent osteogenic transdifferentiation. In order to verify whether lanthanum chloride regulates the occurrence of vascular calcification through the NF-κB pathway, we measured NF-κB and TNF receptor associated factor 6 (TRAF6) protein levels. We found that there were markedly elevated nuclear NF-κB and TRAF6 levels in the model group relative to those in control group, while their expression decreased in a concentration-dependent fashion when exposed to $LaCl_3$.

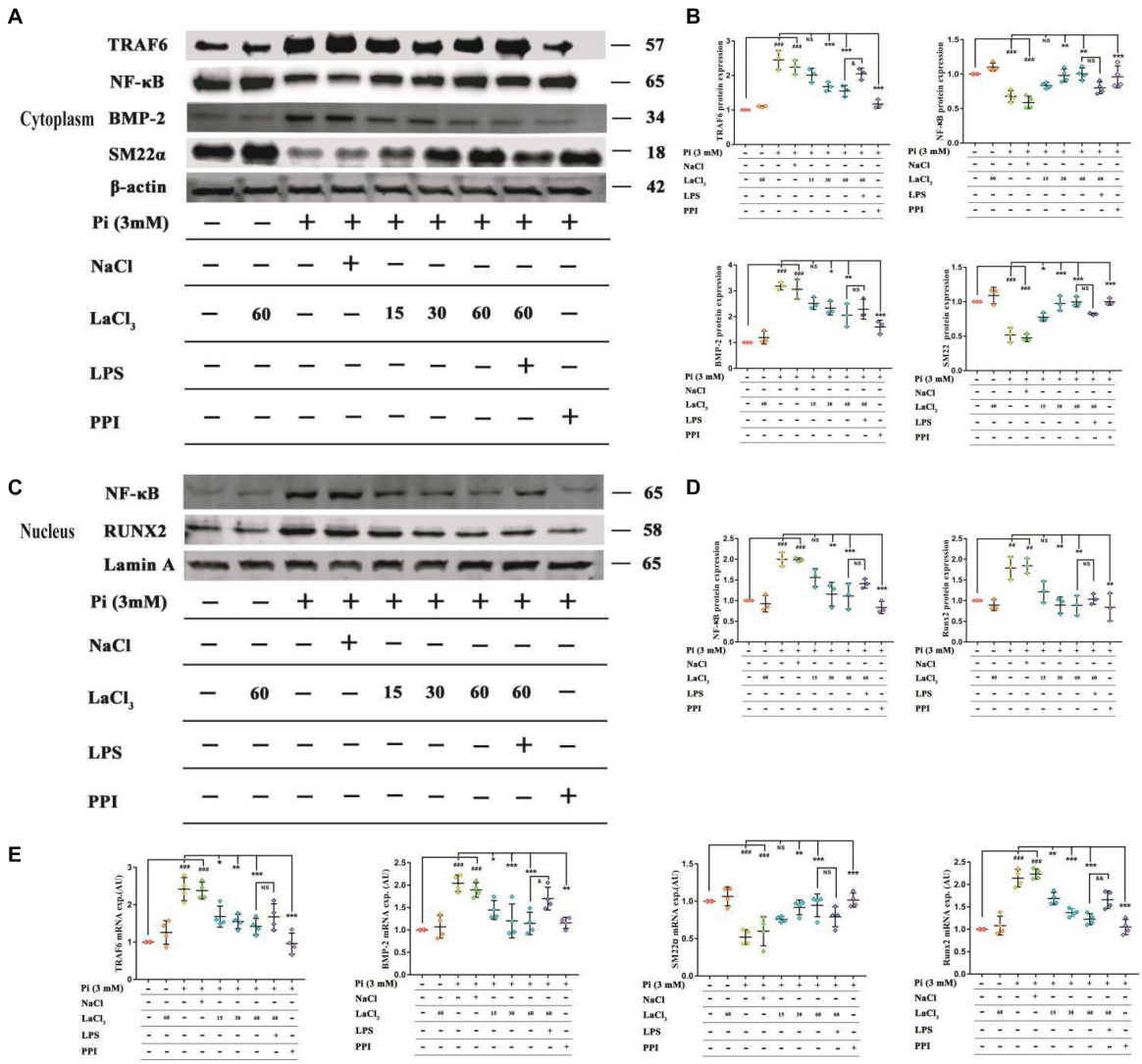

FIGURE 7 | $LaCl_3$ application mitigates vascular calcification and suppresses the osteoinduction signal transduction in the context of CRF. **(A)** Typical Scatter plots, Western blots as well as arithmetic means ± SEM (n = 3) of normalized cytoplasmic TRAF6/β-actin, NF-κB/β-actin, BMP-2/β-actin, and SM22α/β-actin protein ratio in VSMCs with control or with high phosphorus without or with additional treatment with $LaCl_3$. **(B)** Quantification of Western blots to represent the amount of cytoplasmic protein expression (n = 3). **(C)** Typical Scatter plots, Western blots as well as arithmetic means ± SEM (n = 3) for the standardized nuclear NF-κB/Lamin A and Runx2/Lamin A protein ratio in VSMCs with control or with high phosphorus without or with additional treatment with $LaCl_3$. **(D)** Quantification of Western blots to represent the amount of nuclear protein expression (n = 3). **(E)** Scatter plots and arithmetic means ± SEM (n = 3) of TRAF6, BMP-2, SM22α, and Runx2, relative mRNA expression in VSMCs with Pi or control, with or without $LaCl_3$ treatment. $^{\#\#}P < 0.01$; $^{\#\#\#}P < 0.001$ compared with control VSMCs; $^{*}P < 0.05$; $^{**}P < 0.01$; $^{***}P < 0.001$ compared with Pi-treated VSMCs. $^{\&}P < 0.05$; $^{\&\&}P < 0.01$ compared with VSMCs treated with Pi and $LaCl_3$ (60 μM).

After using the NF-κB agonist LPS, compared with $LaCl_3$ (60 μM), there was an increasing trend, but it was not significant (**Figures 7A–D**). Because $LaCl_3$ inhibits the activation of the NF-κB pathway, the expression of SM22α is increased, and the expression of Runx2 and BMP-2 is decreased, thereby preventing the occurrence of VSMCs mineralization. At the same time, we also performed Western blot and realtime PCR detection of the aorta of CKD rats. The expression of TRAF6, nuclear NF-κB, BMP-2, and Runx2 was increased in the established CRF model. After 8 weeks of continuous lanthanum hydroxide treatment, the protein levels of TRAF6, nuclear NF-κB, BMP-2, and Runx2 decreased in a dose-dependent manner in each group (**Figures 8A–E**). In addition, we detected nuclear translocation of NF-κB by immunofluorescence. As shown in **Supplementary Figure 2**, under high phosphorus conditions, nuclear translocation of NF-κB occurred, and after administration of $LaCl_3$ (60 μM), the amount of NF-κB in the nucleus was significantly reduced. The results are basically consistent with the results of *in vitro* studies.

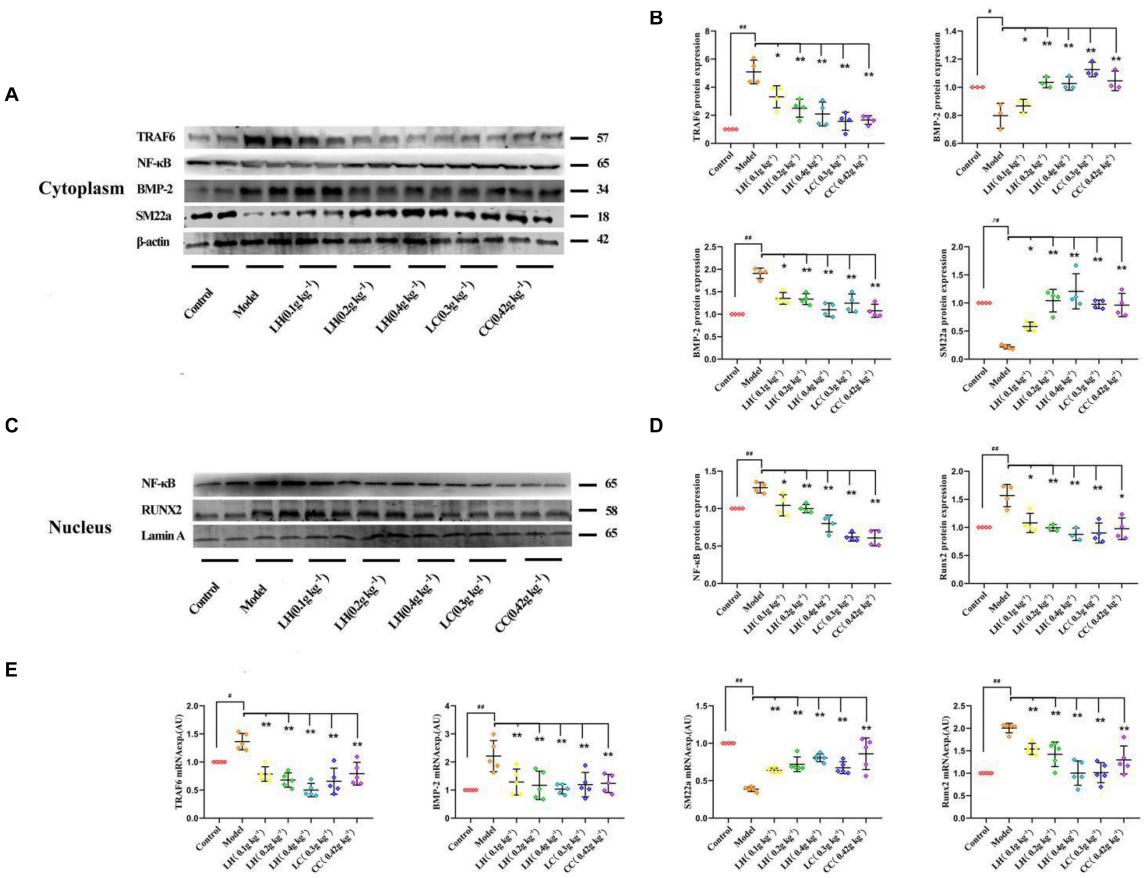

FIGURE 8 | Lanthanum hydroxide supplementation ameliorates vascular calcification and osteoinductive signaling in chronic renal failure. **(A)** Typical Scatter plots, Western blots as well as arithmetic means ± SEM (n = 3) of the standardized cytoplasmic TRAF6/β-actin, NF-κB/β-actin, BMP-2/β-actin, and SM22α/β-actin protein ratio in rats with Pi or control, with or without lanthanum hydroxide treatment. **(B)** Quantification of Western blots to represent the amount of cytoplasmic protein expression (n = 3). **(C)** Typical Scatter plots, Western blots as well as arithmetic means ± SEM (n = 3) for standardized nuclear NF-κB/Lamin A and Runx2/Lamin A protein ratio in rats with control or with high phosphorus without or with additional treatment with lanthanum hydroxide. **(D)** Quantification of Western blots to represent the amount of nuclear protein expression (n = 3). **(E)** Scatter plots and arithmetic means ± SEM (n = 3) of TRAF6, BMP-2, SM22α, and Runx2, relative mRNA expression in rats with Pi or control, with or without lanthanum hydroxide treatment. $^{\#}P < 0.05$; $^{\#\#}P < 0.01$ compared with control rats; $^{*}P < 0.05$; $^{**}P < 0.01$ compared with model rats.

It was observed that lanthanum hydroxide may inhibit the activation of NF-κB, reduce the expression of osteogenic markers, and thereby inhibit the occurrence of calcification.

DISCUSSION

Lanthanum hydroxide, a new phosphate binder, delayed the progression of kidney failure, suppressed the development of vascular calcification; decreased serum PTH and FGF23 levels, and significantly suppressed serum phosphorus. Thus, lanthanum hydroxide inhibited the progression of vascular calcification by decreasing serum phosphorus levels.

Diverse animal models are utilized for investigating the CKD-related MAC formation. Adenine has become an important xanthine dehydrogenase substrate, which can be oxidized to 2,8-dihydroxyadenine. Due to its low solubility, 2,8-dihydroxyadenine can be deposited within renal tubules in the form of stones, giving rise to nephrolithiasis, fibrosis, necrosis, wide tubular dilation, and renal dysfunction (Tamagaki et al., 2006; Tamura et al., 2009). The adenine model has the advantage of inducing renal failure over a short period of time with very little variations between animals (Tamagaki et al., 2006; Massy et al., 2007). We induced a CKD model by combining adenine with a high-phosphorus diet (1.2% -phosphorus), and the weight loss and increases in creatinine and BUN observed in the CKD rats were similar to findings described in previous reports. The findings in this work conformed to those obtained by Jia et al., who discovered that an adenine-supplemented diet increased FGF-23 and PTH as the administration time prolonged (Jia et al., 2013). In the later stages of CKD in animal models, bone abnormalities and vascular calcification were observed. According to human studies, aberrant biochemical changes were detected at the GFR was 40–50 ml min^{-1} (CKD 3–4); meanwhile, bone diseases and vascular calcification lesions were commonly seen among CKD stage 4-5D patients (Block et al., 2005;

Mehrotra and Adler, 2005; Levin et al., 2007; Russo et al., 2007). This model displays the characteristics of progressive onset and the course of chronic renal failure.

In the current study, lanthanum hydroxide treatment provided a satisfactory therapeutic effect in a rat model of hyperphosphatemia renal failure. By measuring physiological and biochemical indicators, the level of serum phosphorus was decreased compared with the model group, and the phosphorus-lowering effect was reduced in a dose-dependent manner after treatment with lanthanum hydroxide. Treatment with 0.2 g kg^{-1} lanthanum hydroxide decreased serum phosphorus, PTH, and FGF23 levels, and delayed the development of renal failure. The same improvements were observed after 0.3 g kg^{-1} lanthanum carbonate and 0.42 g kg^{-1} calcium carbonate treatments were administered. These results indicated that the effect of lanthanum hydroxide was similar to that of existing drugs. However, 0.4 g kg^{-1} lanthanum hydroxide achieved more optimal therapeutic effects when compared to the effects produced by lanthanum carbonate and calcium carbonate, With the use of our renal failure model using hyperphosphatemia rats, the therapeutic advantage of lanthanum hydroxide was determined.

Fibroblast growth factor 23 is secreted by bone cells and osteoblasts, and its main target organs are the kidneys and parathyroid glands. It is a recently discovered important factor that regulates calcium and phosphorus metabolism. Mirza et al. (2009) found that higher or normal serum levels of FGF23 were independently related to the aggravated vasoreactivity impairment and arterial stiffness. CKD patients with high FGF-23 are more likely to have impaired vascular reactivity as well as vascular calcification as compared to patients with a normal glomerular filtration rate. Desjardins et al. (2012) demonstrated that increased FGF-23 levels were positively correlated with the arterial calcification index. Relative to the control group, the model group exhibited elevated FGF23 (94.55 mmol mL^{-1}), and after treatment with 0.4 g kg^{-1} lanthanum hydroxide after 8 weeks, the serum FGF23 decreased to 79.10 mmol mL^{-1} (**Figures 2F**, 8 week). The Von Kossa staining and CT imaging of the thoracic aorta in rats after 8 weeks of treatment showed that the calcification in the 0.4 g kg^{-1} lanthanum hydroxide group markedly decreased relative to that in the model group (**Figure 4**).

NF-κB is a key regulator of vascular calcification. Under *in vitro* conditions, high phosphorus can promote nuclear translocation of NF-κB. The overexpression of glucocorticoid-induced kinase 1 (SGK1) promotes the transdifferentiation and calcification of VSMCs into osteoblasts, and the above process depends on the activation of NF-κB. Under *in vivo* conditions, after knocking out SGK1, NF-κB activity was significantly reduced and calcification was significantly weakened (Voelkl et al., 2018a). Under high phosphorus conditions, the mineral metabolism of mice is disturbed. Growth hormone releasing hormone agonist (GHRH-A) inhibits the production of Runx2 and ALP by inhibiting the activity of NF-κB, thereby inhibiting the transdifferentiation of VSMCs. After injection of GHRH-A, the vascular calcification of mice was also significantly weakened. Therefore, inflammation-mediated VSMCs transdifferentiation into osteoblasts and vascular calcification are blocked (Shen et al., 2018). As for the cultured VSMCs, $LaCl_3$ exposure mitigated

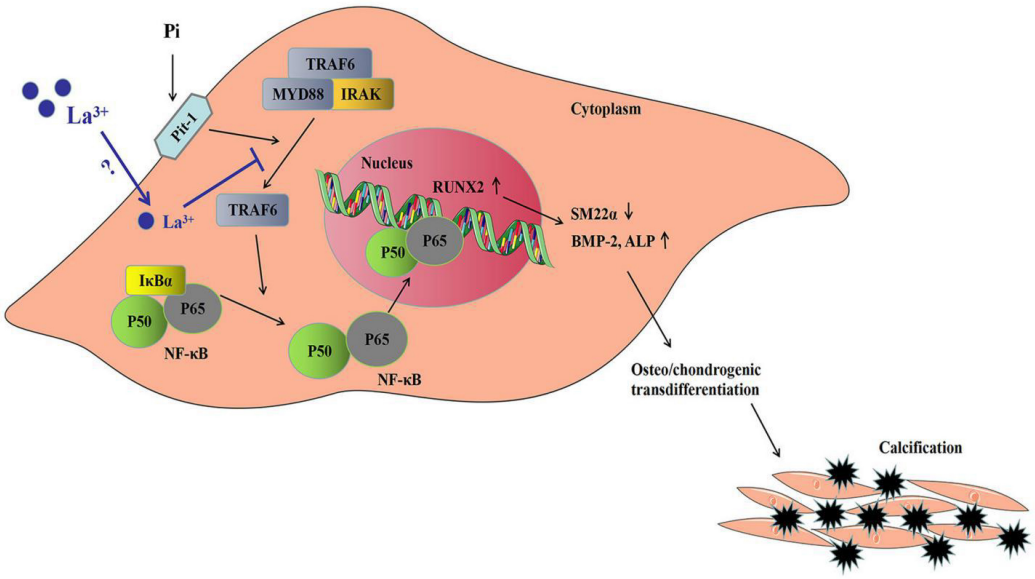

FIGURE 9 | Sketch map regarding the phosphate-mediated VSMC calcification and the suppression by zinc application. Treatment with great phosphate (Pi) content triggers the activation of NF-κB (p50/p65) within VSMCs. The activity of NF-κB is determined by IκBα degradation and ubiquitination according to phosphorylation. The active transcription factor can translocate to the nucleus and induce the target gene expression for promoting VSMCs osteo-/chondrogenic transdifferentiation. Such transdifferentiation can generate the pro-calcifying environment to induce vascular mineralization. Lanthanum supplementation inhibits TRAF6 protein levels. The suppressed TRAF6 protein expression inhibits the activation of NF-κB, thus suppressing VSMCs osteo-/chondrogenic transdifferentiation, decreasing the formation of the pro-calcifying environment as well as the later mineralization.

the phosphate-mediated mineral precipitation. We conducted Alizarin Red and Von Kossa staining to detect granular deposits. Compared with the untreated cells, Pi caused a significant 2-fold increase in mineral deposition, whereas exposure of VSMCs to $LaCl_3$ reduced the Pi-mitigated mineralization in a dose-dependent manner. Importantly, 60 μM $LaCl_3$ decreased mineral deposition in VSMCs treated with high levels of Pi to that maintained within the growth medium (**Figure 6**). Therefore, both *in vitro* and *in vivo* studies have shown that lanthanum hydroxide may inhibit the occurrence and development of vascular calcification. The mechanisms underlying the vascular calcification occurrence and development are similar to those related to physiological osteogenesis, which involve vascular cell apoptosis, osteo-/chondrogenic transdifferentiation, reduced calcification inhibitor, extracellular matrix (ECM) remodeling, and release of extracellular vesicles (Shanahan et al., 2011; Alves et al., 2014; Schlieper et al., 2016). These mechanisms are not mutually exclusive. VSMCs play a key role during vascular calcification (Desjardins et al., 2012; Lanzer et al., 2014; Voelkl et al., 2019). VSMCs can change to the osteo-/chondroblast-like cell phenotype, so as to aggressively respond to increased extracellular phosphate and enhance vascular mineralization (Alesutan et al., 2017; Luong et al., 2018; Voelkl et al., 2019). The transdifferentiated VSMCs have lost the contractile phenotype to develop the mesenchymal phenotype and to obtain characteristics similar to those of chondroblasts or osteoblasts (Demer and Tintut, 2008). In such VSMCs, smooth muscle-specific protein expression decreases, such as smooth muscle SM22α and α-smooth muscle actin (αSMA) (Steitz et al., 2001), whereas osteogenic transcription factor levels are upregulated, like homeobox 2 (MSX2) and core-binding factor α-1 (CBFA1). Among them, CBFA1 (also referred to as Runx2) plays an important role in vascular calcification. Additionally, these osteo-/chondrogenic transcription factors are used to further induce chondrogenic or osteogenic protein expression within VSMCs, such as that which will produce type I collagen, osteocalcin, ALP, and BMP-2 (Lanzer et al., 2014; Leibrock et al., 2016; Voelkl et al., 2019). Therefore, these transdifferentiated VSMCs potentially enhance vascular calcification through generating a local environment that promotes calcification, together with the nidus sites for phosphate/calcium precipitation and calcium phosphate crystal growth. However, additional studies are required to understand the complicated events resulting in vascular calcification within CKD.

In this study, to analyze the mechanisms of lanthanum hydroxide in delaying vascular calcification, Western blotting was performed using the proteins of the thoracic aorta and VSMCs of rats. The results showed that compared with the control group, SM22α decreased and BMP-2 significantly increased in the model group, indicating that VSMCs were transformed into osteoblasts. Subsequently, we identified NF-κB as a key regulator of VSMCs phenotype and calcification. We demonstrated that lanthanum supplementation provides a remarkable protective effect during vascular calcification *in vitro* and in animal models. A high phosphate content may lead to an increased risk of vascular calcification, while the application of lanthanum mitigates osteo-/chondrogenic transdifferentiation of VSMCs. Lanthanum inhibits TRAF6 expression, and later suppresses NF-κB activation or osteo-/chondrogenic reprogramming within VSMCs in the process of hyperphosphatemia. However, the direct inhibitory mechanism of La^{3+} on the NF-κB signaling pathway is not very clear. Therefore, which type of receptor La^{3+} acts on to inhibit vascular calcification needs further study (**Figure 9**).

CONCLUSION

Our study demonstrated that lanthanum hydroxide, a new type of phosphorus binder, can effectively reduce serum phosphorus levels, delay the process of renal failure, and protect renal function. Moreover, lanthanum hydroxide may delay the occurrence and development of vascular calcification through suppressing NF-κB pathway activation via La^{3+}. Therefore, our foundational data can be applied to pre-clinical pharmacological research so that lanthanum hydroxide may become a clinical candidate drug.

DATA AVAILABILITY STATEMENT

The datasets presented in this study can be found in online repositories. The names of the repository/repositories and accession number(s) can be found below: PRIDE database, PXD023081.

ETHICS STATEMENT

The animal study was reviewed and approved by the Inner Mongolian Medical University.

AUTHOR CONTRIBUTIONS

LZ and SW performed the experiments, analyzed the data, and drafted the manuscript. HL, XD, and RB assisted with the experiments. BL, RH, JG, YL, JH, JZ, and YM provided suggestions to the study design and writing of the manuscript. GL designed and financed the study, and wrote and edited the manuscript. All authors contributed to the article and approved the submitted version.

FUNDING

This research was supported by grants from Inner Mongolia Autonomous Region Science and Technology Million Project (no. zdzx201805).

ACKNOWLEDGMENTS

We kindly thank HL in the synthesis of lanthanum hydroxide.

SUPPLEMENTARY MATERIAL

The Supplementary Material for this article can be found online at: https://www.frontiersin.org/articles/10.3389/fcell.2021.639127/full#supplementary-material

REFERENCES

Alesutan, I., Voelkl, J., Feger, M., Kratschmar, D. V., Castor, T., Mia, S., et al. (2017). Involvement of vascular aldosterone synthase in phosphate-induced Osteogenic transformation of vascular smooth muscle cells. *Sci. Rep.* 7:2059. doi: 10.1038/s41598-017-01882-2

Alves, R. D., Eijken, M., van de Peppel, J., and van Leeuwen, J. P. (2014). Calcifying vascular smooth muscle cells and osteoblasts: independent cell types exhibiting extracellular matrix and biomineralization-related mimicries. *BMC Genom.* 15:965. doi: 10.1186/1471-2164-15-965

Block, G. A., Klassen, P. S., Lazarus, J. M., Ofsthun, N., Lowrie, E. G., and Chertow, G. M. (2004). Mineral metabolism, mortality, and morbidity in maintenance hemodialysis. *J. Am. Soc. Nephrol.* 15, 2208–2218. doi: 10.1097/01.ASN.0000133041.27682.A2

Block, G. A., Spiegel, D. M., Ehrlich, J., Mehta, R., Lindbergh, J., Dreisbach, A., et al. (2005). Effects of sevelamer and calcium on coronary artery calcification in patients new to hemodialysis. *Kidney Intern.* 68, 1815–1824. doi: 10.1111/j.1523-1755.2005.00600.x

Briet, M., and Burns, K. D. (2012). Chronic kidney disease and vascular remodelling: molecular mechanisms and clinical implications. *Clin. Sci.* 123, 399–416. doi: 10.1042/CS20120074

Collins, A. J., Foley, R. N., Gilbertson, D. T., and Chen, S. C. (2015). United States renal data system public health surveillance of chronic kidney disease and end-stage renal disease. *Kidney Intern. Suppl.* 5, 2–7. doi: 10.1038/kisup.2015.2

Da, J., Xie, X., Wolf, M., Disthabanchong, S., Wang, J., Zha, Y., et al. (2015). Serum phosphorus and progression of CKD and mortality: a meta-analysis of cohort studies. *Am. J. Kidney Dis.* 66, 258–265. doi: 10.1053/j.ajkd.2015.01.009

Demer, L. L., and Tintut, Y. (2008). Vascular calcification: pathobiology of a multifaceted disease. *Circulation* 117, 2938–2948. doi: 10.1161/CIRCULATIONAHA.107.743161

Desjardins, L., Liabeuf, S., Renard, C., Lenglet, A., Lemke, H. D., Choukroun, G., et al. (2012). FGF23 is independently associated with vascular calcification but not bone mineral density in patients at various CKD stages. *Osteoporos. Intern.* 23, 2017–2025. doi: 10.1007/s00198-011-1838-0

Dhingra, R., Sullivan, L. M., Fox, C. S., Wang, T. J., D'Agostino, R. B. Sr., Gaziano, J. M., et al. (2007). Relations of serum phosphorus and calcium levels to the incidence of cardiovascular disease in the community. *Archiv. Intern. Med.* 167, 879–885. doi: 10.1001/archinte.167.9.879

Goodman, W. G., Goldin, J., Kuizon, B. D., Yoon, C., Gales, B., Sider, D., et al. (2000). Coronary-artery calcification in young adults with end-stage renal disease who are undergoing dialysis. *N. Engl. J. Med.* 342, 1478–1483. doi: 10.1056/NEJM200005183422003

Huveneers, S., Daemen, M. J., and Hordijk, P. L. (2015). Between Rho(k) and a hard place: the relation between vessel wall stiffness, endothelial contractility, and cardiovascular disease. *Circ. Res.* 116, 895–908. doi: 10.1161/CIRCRESAHA.116.305720

Inker, L. A., Astor, B. C., Fox, C. H., Isakova, T., Lash, J. P., Peralta, C. A., et al. (2014). KDOQI US commentary on the 2012 KDIGO clinical practice guideline for the evaluation and management of CKD. *Am. J. Kidney Dis.* 63, 713–735. doi: 10.1053/j.ajkd.2014.01.416

Isakova, T., Wahl, P., Vargas, G. S., Gutiérrez, O. M., Scialla, J., Xie, H., et al. (2011). Fibroblast growth factor 23 is elevated before parathyroid hormone and phosphate in chronic kidney disease. *Kidney Intern.* 79, 1370–1378. doi: 10.1038/ki.2011.47

Jia, T., Olauson, H., Lindberg, K., Amin, R., Edvardsson, K., Lindholm, B., et al. (2013). A novel model of adenine-induced tubulointerstitial nephropathy in mice. *BMC Nephrol.* 14:116. doi: 10.1186/1471-2369-14-116

Lanzer, P., Boehm, M., Sorribas, V., Thiriet, M., Janzen, J., Zeller, T., et al. (2014). Medial vascular calcification revisited: review and perspectives. *Eur. Heart J.* 35, 1515–1525. doi: 10.1093/eurheartj/ehu163

Leibrock, C. B., Alesutan, I., Voelkl, J., Michael, D., Castor, T., Kohlhofer, U., et al. (2016). Acetazolamide sensitive tissue calcification and aging of klotho-hypomorphic mice. *J. Mol. Med.* 94, 95–106. doi: 10.1007/s00109-015-1331-x

Levin, A., Bakris, G. L., Molitch, M., Smulders, M., Tian, J., and Williams, L. A. (2007). Prevalence of abnormal serum vitamin D, PTH, calcium, and phosphorus in patients with chronic kidney disease: results of the study to evaluate early kidney disease. *Kidney Intern.* 71, 31–38. doi: 10.1038/sj.ki.5002009

London, G. M., Guérin, A. P., Marchais, S. J., Métivier, F., Pannier, B., and Adda, H. (2003). Arterial media calcification in end-stage renal disease: impact on all-cause and cardiovascular mortality. *Nephrol. Dialys. Transpl.* 18, 1731–1740. doi: 10.1093/ndt/gfg414

Luong, T., Schelski, N., Boehme, B., Makridakis, M., Vlahou, A., Lang, F., et al. (2018). Fibulin-3 attenuates phosphate-induced vascular smooth muscle cell calcification by inhibition of oxidative stress. *Cell. Physiol. Biochem.* 46, 1305–1316. doi: 10.1159/000489144

Ma, Z., Yu, T., Wu, Y., Liu, D., Zhang, X., Miao, X., et al. (2019). Nano-lanthanum hydroxide, a novel phosphate binder, for treating hyperphosphatemia: a preclinical study. *Biomed. Pharmacother.* 111, 909–916. doi: 10.1016/j.biopha.2018.12.107

Masakane, I., Nakai, S., Ogata, S., Kimata, N., Hanafusa, N., Hamano, T., et al. (2015). An overview of regular dialysis treatment in Japan (As of 31 December 2013). *Therap. Apheresis Dialys.* 19, 540–574. doi: 10.1111/1744-9987.12378

Massy, Z. A., Slama, M., Tribouilloy, C., and Drüeke, T. B. (2007). Animal models–what they can tell us about vascular calcification in CKD. *Semin. Dialys.* 20, 110–112. doi: 10.1111/j.1525-139X.2007.00256.x

Mehrotra, R., and Adler, S. (2005). Coronary artery calcification in nondialyzed patients with chronic kidney diseases. *Am. J. Kidney Dis.* 45:963. doi: 10.1053/j.ajkd.2005.01.041

Mills, K. T., Xu, Y., Zhang, W., Bundy, J. D., Chen, C. S., Kelly, T. N., et al. (2015). A systematic analysis of worldwide population-based data on the global burden of chronic kidney disease in 2010. *Kidney Intern.* 88, 950–957. doi: 10.1038/ki.2015.230

Mirza, M. A., Larsson, A., Lind, L., and Larsson, T. E. (2009). Circulating fibroblast growth factor-23 is associated with vascular dysfunction in the community. *Atherosclerosis* 205, 385–390. doi: 10.1016/j.atherosclerosis.2009.01.001

Russo, D., Corrao, S., Battaglia, Y., Andreucci, M., Caiazza, A., Carlomagno, A., et al. (2011). Progression of coronary artery calcification and cardiac events in patients with chronic renal disease not receiving dialysis. *Kidney Intern.* 80, 112–118. doi: 10.1038/ki.2011.69

Russo, D., Miranda, I., Ruocco, C., Battaglia, Y., Buonanno, E., and Manzi, S. (2007). The progression of coronary artery calcification in predialysis patients on calcium carbonate or sevelamer. *Kidney Intern.* 72, 1255–1261. doi: 10.1038/sj.ki.5002518

Schlieper, G., Schurgers, L., Brandenburg, V., Reutelingsperger, C., and Floege, J. (2016). Vascular calcification in chronic kidney disease: an update. *Nephrol. Dialys. Transpl.* 31, 31–39. doi: 10.1093/ndt/gfv111

Shanahan, C. M., Crouthamel, M. H., Kapustin, A., and Giachelli, C. M. (2011). Arterial calcification in chronic kidney disease: key roles for calcium and phosphate. *Circ. Res.* 109, 697–711. doi: 10.1161/CIRCRESAHA.110.234914

Shen, J., Zhang, N., Lin, Y. N., Xiang, P., Liu, X. B., Shan, P. F., et al. (2018). Regulation of vascular calcification by growth hormone-releasing hormone and its agonists. *Circ. Res.* 122, 1395–1408. doi: 10.1161/CIRCRESAHA.117.312418

Smith, E. R. (2016). Vascular calcification in uremia: new-age concepts about an old-age problem. *Methods Mol. Biol.* 1397, 175–208. doi: 10.1007/978-1-4939-3353-2_13

Steitz, S. A., Speer, M. Y., Curinga, G., Yang, H. Y., Haynes, P., Aebersold, R., et al. (2001). Smooth muscle cell phenotypic transition associated with calcification: upregulation of Cbfa1 and downregulation of smooth muscle lineage markers. *Circ. Res.* 89, 1147–1154. doi: 10.1161/hh2401.101070

Tamagaki, K., Yuan, Q., Ohkawa, H., Imazeki, I., Moriguchi, Y., Imai, N., et al. (2006). Severe hyperparathyroidism with bone abnormalities and metastatic calcification in rats with adenine-induced uraemia. *Nephrol. Dialys. Transpl.* 21, 651–659. doi: 10.1093/ndt/gfi273

Tamura, M., Aizawa, R., Hori, M., and Ozaki, H. (2009). Progressive renal dysfunction and macrophage infiltration in interstitial fibrosis in an adenine-induced tubulointerstitial nephritis mouse model. *Histochem. Cell Biol.* 131, 483–490. doi: 10.1007/s00418-009-0557-5

Tatsumi, S., Miyagawa, A., Kaneko, I., Shiozaki, Y., Segawa, H., and Miyamoto, K. (2016). Regulation of renal phosphate handling: inter-organ communication in health and disease. *J. Bone Min. Metab.* 34, 1–10. doi: 10.1007/s00774-015-0705-z

Voelkl, J., Lang, F., Eckardt, K. U., Amann, K., Kuro-O, M., Pasch, A., et al. (2019). Signaling pathways involved in vascular smooth muscle cell calcification during hyperphosphatemia. *Cell Mol. Life Sci.* 76, 2077–2091. doi: 10.1007/s00018-019-03054-z

Voelkl, J., Luong, T. T., Tuffaha, R., Musculus, K., Auer, T., Lian, X., et al. (2018a). SGK1 induces vascular smooth muscle cell calcification through NF-κB signaling. *J. Clin. Invest.* 128, 3024–3040. doi: 10.1172/JCI96477

Voelkl, J., Tuffaha, R., Luong, T., Zickler, D., Masyout, J., Feger, M., et al. (2018b). Zinc inhibits phosphate-induced vascular calcification through TNFAIP3-mediated suppression of NF-κB. *J. Am. Soc. Nephrol.* 29, 1636–1648. doi: 10.1681/ASN.2017050492

Wang, A. Y., Woo, J., Wang, M., Sea, M. M., Ip, R., Li, P. K., et al. (2001). Association of inflammation and malnutrition with cardiac valve calcification in continuous ambulatory peritoneal dialysis patients. *J. Am. Soc. Nephrol.* 12, 1927–1936.

Conflict of Interest: The authors declare that the research was conducted in the absence of any commercial or financial relationships that could be construed as a potential conflict of interest.

Copyright © 2021 Zhao, Wang, Liu, Du, Bu, Li, Han, Gao, Liu, Hao, Zhao, Meng and Li. This is an open-access article distributed under the terms of the Creative Commons Attribution License (CC BY). The use, distribution or reproduction in other forums is permitted, provided the original author(s) and the copyright owner(s) are credited and that the original publication in this journal is cited, in accordance with accepted academic practice. No use, distribution or reproduction is permitted which does not comply with these terms.

frontiers in Cell and Developmental Biology

REVIEW
published: 13 May 2021
doi: 10.3389/fcell.2021.653138

Renal Ciliopathies: Sorting Out Therapeutic Approaches for Nephronophthisis

Marijn F. Stokman[1,2], Sophie Saunier[2] and Alexandre Benmerah[2]**

[1] Department of Genetics, University Medical Center Utrecht, Utrecht, Netherlands, [2] Université de Paris, Imagine Institute, Laboratory of Inherited Kidney Diseases, INSERM UMR 1163, Paris, France

OPEN ACCESS

Edited by:
Claudia Torino,
Institute of Clinical Physiology, Italian National Research Council, Italy

Reviewed by:
Heon Yung Gee,
Yonsei University, South Korea
Moe R. Mahjoub,
Washington University in St. Louis, United States
Antonio Demetrio Vilasi,
National Research Council (CNR), Italy

***Correspondence:**
Alexandre Benmerah
Alexandre.benmerah@inserm.fr
Marijn F. Stokman
M.F.Stokman@umcutrecht.nl

Specialty section:
This article was submitted to Molecular Medicine, a section of the journal Frontiers in Cell and Developmental Biology

Received: 13 January 2021
Accepted: 19 April 2021
Published: 13 May 2021

Citation:
Stokman MF, Saunier S and Benmerah A (2021) Renal Ciliopathies: Sorting Out Therapeutic Approaches for Nephronophthisis. Front. Cell Dev. Biol. 9:653138. doi: 10.3389/fcell.2021.653138

Nephronophthisis (NPH) is an autosomal recessive ciliopathy and a major cause of end-stage renal disease in children. The main forms, juvenile and adult NPH, are characterized by tubulointerstitial fibrosis whereas the infantile form is more severe and characterized by cysts. NPH is caused by mutations in over 20 different genes, most of which encode components of the primary cilium, an organelle in which important cellular signaling pathways converge. Ciliary signal transduction plays a critical role in kidney development and tissue homeostasis, and disruption of ciliary signaling has been associated with cyst formation, epithelial cell dedifferentiation and kidney function decline. Drugs have been identified that target specific signaling pathways (for example cAMP/PKA, Hedgehog, and mTOR pathways) and rescue NPH phenotypes in *in vitro* and/or *in vivo* models. Despite identification of numerous candidate drugs in rodent models, there has been a lack of clinical trials and there is currently no therapy that halts disease progression in NPH patients. This review covers the most important findings of therapeutic approaches in NPH model systems to date, including hypothesis-driven therapies and untargeted drug screens, approached from the pathophysiology of NPH. Importantly, most animal models used in these studies represent the cystic infantile form of NPH, which is less prevalent than the juvenile form. It appears therefore important to develop new models relevant for juvenile/adult NPH. Alternative non-orthologous animal models and developments in patient-based *in vitro* model systems are discussed, as well as future directions in personalized therapy for NPH.

Keywords: hereditary kidney disease, ciliopathy, nephronophthisis, signaling, cell cycle, drug screen, therapy, gene therapy

INTRODUCTION

Nephronophthisis (NPH) is an autosomal recessive kidney disease that accounts for up to 15% of end-stage renal disease (ESRD) in children (Hamiwka et al., 2008; Salomon et al., 2009). In addition, homozygous deletions in the *NPHP1* gene, the most frequent cause of NPH (≈50% of genetically diagnosed cases), have recently been shown to be an important cause of renal disease in adults (Snoek et al., 2018).

Three clinical subtypes of NPH can be discerned. In juvenile NPH, the most prevalent form, ESRD develops at a median age of 13 years (Hildebrandt et al., 2009). Juvenile NPH is characterized by small to normal-sized kidneys that show marked tubulointerstitial fibrosis, thickened and disrupted tubular basement membranes and, in less than 50% of patients, corticomedullary cysts that arise from distal tubules in advanced stages of the disease (Hildebrandt et al., 2009). Patients present with a urine concentration defect leading to polyuria and polydipsia, anemia, proteinuria (in advanced stages) and progressive renal insufficiency (König et al., 2017; Stokman et al., 2018). The adult form of NPH is clinically and histologically similar to juvenile NPH and leads to adult-onset ESRD (>15 years old). This form is difficult to distinguish clinically from autosomal dominant tubulointerstitial kidney disease (ADTKD) which is also characterized by tubular damage, interstitial fibrosis and corticomedullary microcysts (Devuyst et al., 2019). In contrast, autosomal dominant polycystic kidney disease (ADPKD), which is more prevalent, is typically adult-onset with slow progression to ESRD [onset from 58 to 80 years (Chebib and Torres, 2016)] and characterized by enlarged kidneys with cysts distributed throughout the renal parenchyma (Harris and Torres, 2002).

In contrast to juvenile and adult NPH, infantile NPH leads to ESRD before the age of 5 years and typically presents with enlarged cystic kidneys, severe hypertension and a rapid disease course, making it difficult to distinguish from autosomal recessive polycystic kidney disease (ARPKD) based on renal symptoms only (Gagnadoux et al., 1989; Otto et al., 2003; Waters and Beales, 2011; Bergmann, 2018). Infantile NPH is characterized histologically by cortical cysts, absence of tubular basement membrane thickening and only moderate fibrosis (Gagnadoux et al., 1989; Salomon et al., 2009; Tory et al., 2009). This raises the question whether infantile NPH is really part of the NPH spectrum or rather represents a distinct subtype of cystic kidney disease.

Mutations in more than 20 different genes have been identified to cause NPH (Braun and Hildebrandt, 2017; Devlin and Sayer, 2019). Most of these genes encode proteins that localize to primary cilia and their disruption causes defects in cilia formation, length and/or composition. NPH therefore falls into the category of ciliopathies, a group of multisystemic disorders linked to primary cilia dysfunction. Primary (non-motile or sensory) cilia (PC) are microtubule-based antennae present on the surface of nearly all cell types in vertebrates during development and/or in adult tissues, from where they sense mechanical stress (shear stress), molecules (odor, light) and control key signaling pathways (Hedgehog, Wnt, TGFβ, etc.). PC dysfunction is therefore associated with a variety of phenotypes in different organs including kidney failure, retinal dystrophy, liver fibrosis, skeletal dysplasia, cerebellar vermis hypoplasia and obesity. In the kidney, PC are present on the apical surface of most tubular cells from where they integrate different stimuli during kidney homeostasis and function. The discovery of the ciliary localization and functions of polycystin-1 and polycystin-2, the products of the ADPKD genes *PKD1* and *PKD2*, led to the hypothesis that cilia control oriented cell division and proliferation of tubular cells, and that ciliary defects therefore result in cystic kidneys, which became a classic sign of ciliopathies.

In accordance with the role of PC in most organ systems, 10–20% of NPH patients have extrarenal manifestations defining syndromic forms, including Senior-Løken syndrome (NPH and retinal dystrophy), Bardet-Biedl syndrome (retinal dystrophy, obesity and polydactyly), Joubert syndrome (cerebellar vermis hypoplasia, hypotonia and developmental delay) and cranioectodermal dysplasia (narrow thorax and short stature) (Braun and Hildebrandt, 2017).

Current drug therapy for NPH is merely supportive, aimed at treatment of anemia, hypertension, growth retardation and other symptoms related to chronic kidney disease (CKD) (Braun and Hildebrandt, 2017). Although symptomatic treatment can prevent accelerated decline of renal function (for example due to hypertension) and improve quality of life for NPH patients, it does not target underlying disease mechanisms and ESRD cannot be prevented. The only curative treatment for NPH patients is a renal transplantation, as NPH does not recur in the transplanted kidney (Hamiwka et al., 2008; Tayfur et al., 2011).

Therapy for NPH-related ciliopathies has been an active field of research for more than 15 years. Next-generation sequencing techniques have accelerated gene discovery and uncovered numerous targetable genes and pathways. The most important drug targets for renal ciliopathies (i.e., NPH and PKD) have been reviewed by Molinari and Sayer (2017). Most of these drugs target mechanisms discovered in the context of ADPKD and were subsequently shown to also reduce cystogenesis in mouse or zebrafish models of (mostly infantile) NPH. Contrary to ADPKD, however, tubulointerstitial fibrosis is more important than cystogenesis in the pathophysiology of juvenile NPH. Consequently, aberrant DNA damage-response signaling and proinflammatory signaling, which have been proposed to contribute to fibrosis in juvenile NPH (Slaats et al., 2016), are interesting emerging targets and readouts. However, underlying disease mechanisms and potential targets for therapeutic interventions are not fully elucidated. Moreover, in contrast to ADPKD, thus far no clinical trial has been conducted in NPH patients.

If juvenile NPH is detected in an early disease stage, there is a therapeutic window of a few years in which treatment could delay or prevent renal replacement therapy. Previous reviews of therapies for renal ciliopathies focused on models of PKD and cystic (infantile) NPH or did not discern between renal and extrarenal manifestations. In this review we summarize the results from two main strategies for therapeutic intervention in NPH specifically that have been investigated in *in vitro* and *in vivo* model systems: pharmacotherapy (hypothesis-driven approaches including repurposed medication from PKD and untargeted drug screens) and gene-based therapy, in relation to the pathophysiology of different aspects of the NPH phenotype. Promising developments in personalized disease modeling and drug delivery are discussed, as well as challenges in clinical trials for NPH and orphan-drug

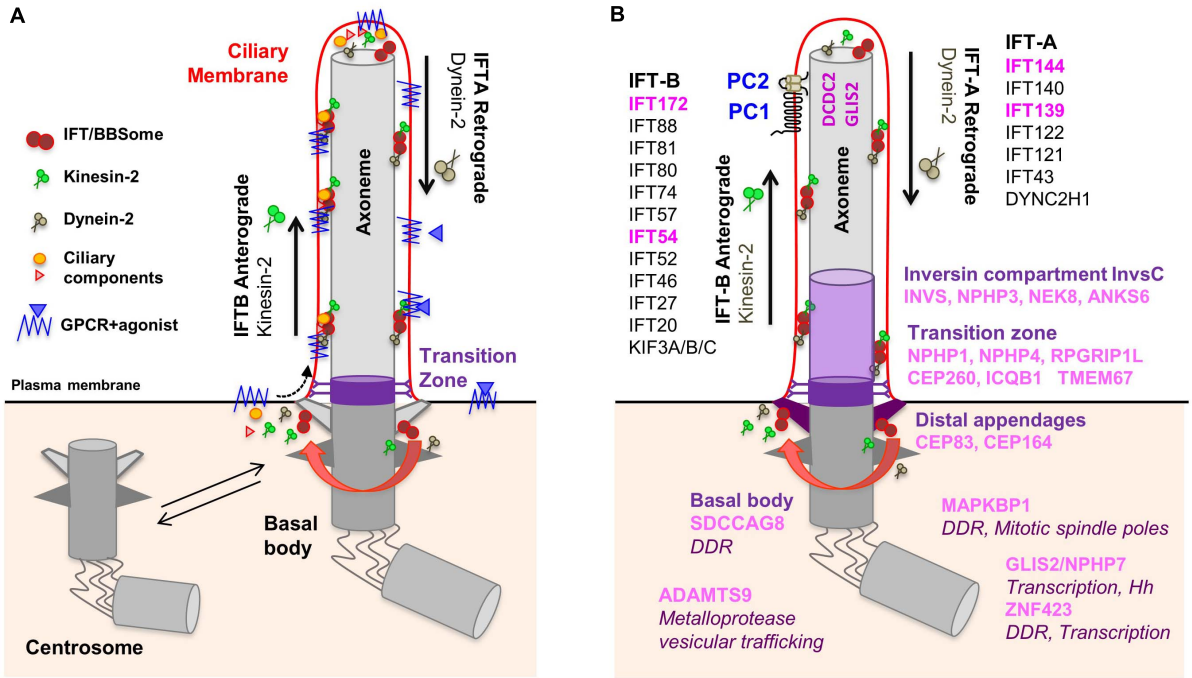

FIGURE 1 | Composition of the primary cilium. **(A)** The mother centriole docks to the apical plasma membrane and forms the basal body which is connected to the plasma membrane by transition fibers. The basal body anchors the ciliary axoneme, consisting of 9+0 microtubule doublets. At the transition zone, Y-linkers connect the axoneme to the ciliary membrane. The transition zone functions as a gate through which membrane receptors and other proteins can enter the cilium. Intraflagellar transport (IFT) inside the cilium is mediated by kinesin-2 motors (anterograde transport) and dynein motors (retrograde transport). **(B)** NPH proteins localize to distinct functional compartments of the primary cilium. IFT proteins in pink are encoded by NPH-associated genes. No ciliary localization was demonstrated for ZNF423 and MAPKBP1.

development. Finally, we provide a rationale for future studies in this field.

PATHOPHYSIOLOGY OF NEPHRONOPHTHISIS

Genetic Basis

Most ciliopathy-associated genes encode proteins that localize to PC which are assembled in quiescent cells (G_0) from the centrosome, called 'basal body' when engaged in ciliogenesis (**Figure 1A**). During this process, the mother centriole docks onto cellular membranes through its distal appendages and then the distal ends of the nine centriolar microtubule doublets extend to form the ciliary axoneme which is surrounded by the ciliary membrane. The generation and maintenance of the unique molecular composition of the ciliary compartment (proteins and lipids) is based on the presence of the transition zone which acts as a gate at the base of the cilium and a highly conserved active transport machinery, the intraflagellar transport (IFT), which mediates in and out trafficking across this barrier through anterograde (IFT-B) and retrograde (IFT-A) transport along axonemal microtubules. The IFT and the BBSome, a protein complex encoded by genes mutated in Bardet-Biedl Syndrome, are also involved in the trafficking of signaling receptors enriched at the ciliary membrane such as G-protein coupled receptors (GPCRs) (Reiter et al., 2017).

Nephronophthisis is caused by mutations in 22 genes (full list in **Table 1**), which encode NPH proteins (NPHP). Of note, not all these genes have an official *NPHP* alias. Most NPHPs localize to and define three functionally important ciliary subdomains: the transition zone (NPHP1, NPHP4, IQCB1/NPHP5, CEP290/NPHP6 and RPGRIP1L/NPHP8), basal body/centrosome (SDCCAG8/NPHP10, CEP164/NPHP14, CEP83/NPHP18) and inversin compartment (**Figure 1B**) (Braun and Hildebrandt, 2017; Reiter et al., 2017; Devlin and Sayer, 2019). The inversin compartment (InvsC) comprises the products of four genes, *INVS/NPHP2, NPHP3, NEK8/NPHP9* and *ANKS6/NPHP16*, all of which have been implicated in infantile-onset NPH in addition to juvenile and/or adult NPH depending on the severity of the mutations (Gagnadoux et al., 1989; Olbrich et al., 2003; Otto et al., 2003, 2008; Bergmann et al., 2008; Tory et al., 2009; Hoff et al., 2013; Rajagopalan et al., 2015; Grampa et al., 2016). In addition to the above ciliary subdomains, NPH-causing mutations were also identified in genes encoding subunits of the IFT-A (*TTC21B/IFT139/NPHP12, WDR19/IFT144/NPHP13)* and IFT-B (*IFT172/NPHP17, TRAF3IP1/IFT54/SLS9*) sub-complexes (Bredrup et al., 2011; Davis et al., 2011; Halbritter et al., 2013a; Bizet et al., 2015). Importantly, NPH-related renal involvement was also reported in individuals harboring mutations in

TABLE 1 | Localization of NPH proteins and associated phenotypes.

Ciliary localization Function	Gene	Locus	Extraciliary localization/function	NPH subtype(s)	Extrarenal features (Halbritter et al., 2013b; Braun and Hildebrandt, 2017; König et al., 2017; Luo and Tao, 2018)	References
Transition zone (TZ)	*NPHP1*	*NPHP1*	Cell junctions	Juvenile, adult	Retinitis pigmentosa, neurologic symptoms, liver disease	Hildebrandt et al. (1997); Saunier et al. (1997)
	NPHP4	*NPHP4*	Cell junctions Hippo signaling	Juvenile, adult	Retinitis pigmentosa, neurologic symptoms, congenital heart disease, liver disease (all infrequent)	Mollet et al. (2002); Otto et al. (2002)
	IQCB1	*NPHP5*	–	Juvenile, adult	Retinitis pigmentosa (in all patients), leber congenital amaurosis, neurologic symptoms	Otto et al. (2005); Estrada-Cuzcano et al. (2011)
	CEP290	*NPHP6*	DDR signaling	Infantile, juvenile, adult	Retinitis pigmentosa, leber congenital amaurosis, neurologic symptoms, liver disease	Sayer et al. (2006); Valente et al. (2006); Helou et al. (2007); Tory et al. (2007)
	RPGRIP1L	*NPHP8*	–	Infantile, juvenile, adult	Retinitis pigmentosa, neurologic symptoms, liver disease, polydactyly	Arts et al. (2007); Delous et al. (2007); Wolf et al. (2007)
	TMEM67	*NPHP11*	–	Infantile, juvenile, adult	Retinitis pigmentosa, neurologic symptoms, liver disease, polydactyly	Smith U. M. et al. (2006)
Intraflagellar transport complex IFT-B	*IFT172*	*NPHP17*	–	Infantile, juvenile, adult	Retinitis pigmentosa, neurologic symptoms, liver disease, skeletal anomalies, polydactyly	Halbritter et al. (2013a)
	TRAF3IP1/IFT54	*SLNS9*	Microtubule dynamics	Infantile, Juvenile	Retinitis pigmentosa, hepatic fibrosis, skeletal anomalies, obesity	Bizet et al. (2015)
Intraflagellar transport complex IFT-A	*TTC21B/IFT139*	*NPHP12*	Microtubule dynamics	Infantile, juvenile	Neurologic symptoms, situs inversus, liver disease, skeletal anomalies	Davis et al. (2011); Cong et al. (2014)
	WDR19/IFT144	*NPHP13*	–	Infantile, juvenile	Retinitis pigmentosa, liver disease (especially Caroli disease), pancreas anomalies, skeletal anomalies	Bredrup et al. (2011)
Inversin compartment	*INVS*	*NPHP2*	Cell junctions; mitotic spindle poles, midbody	Infantile, juvenile	Retinitis pigmentosa, neurologic symptoms, situs inversus, congenital heart disease, liver disease	Otto et al. (2003); O'Toole et al. (2006); Tory et al. (2009)
	NPHP3	*NPHP3*	–	Infantile, juvenile, adult	Retinitis pigmentosa, neurologic symptoms, situs inversus, congenital heart defect, liver disease	Omran et al. (2000); Olbrich et al. (2003); Bergmann et al. (2008); Tory et al. (2009)
	NEK8	*NPHP9*	DDR and Hippo signaling	Infantile, juvenile	Situs inversus, congenital heart disease, liver disease, pancreas anomalies	Otto et al. (2008); Grampa et al. (2016)
	ANKS6	*NPHP16*	–	Infantile, juvenile, adult	Neurologic symptoms, situs inversus, congenital heart disease, liver disease	Hoff et al. (2013); Taskiran et al. (2014)
Basal body	*SDCCAG8*	*NPHP10*	DDR signaling	Infantile, juvenile, adult	Retinitis pigmentosa, neurologic symptoms, obesity, hypogenitalism	Otto et al. (2010); Watanabe et al. (2019)
	CEP164	*NPHP15*	DDR signaling	Juvenile	Retinitis pigmentosa, Leber congenital amaurosis, neurologic symptoms, liver disease, polydactyly	Chaki et al. (2012)
	CEP83	*NPHP18*	–	Infantile, juvenile	Retinitis pigmentosa, neurologic symptoms, liver disease	Failler et al. (2014)
Near basal body	*ADAMTS9*	*NPHP21*	Metalloproteinase function, protein trafficking	Infantile, juvenile	Deafness, short stature, developmental delay	Choi et al. (2019); Nandadasa et al. (2019)

(Continued)

TABLE 1 | Continued

Ciliary localization Function	Gene	Locus	Extraciliary localization/function	NPH subtype(s)	Extrarenal features (Halbritter et al., 2013b; Braun and Hildebrandt, 2017; König et al., 2017; Luo and Tao, 2018)	References
Ciliary axoneme	*GLIS2*	*NPHP7*	Nucleus, role in transcription	Juvenile	–	Attanasio et al. (2007)
	DCDC2	*NPHP19*	Microtubule dynamics, Wnt signaling	Juvenile	Liver disease, deafness	Schueler et al. (2015)
No ciliary localization	*ZNF423*	*NPHP14*	DDR signaling and transcription	Infantile	Neurologic symptoms, situs inversus	Chaki et al. (2012)
	MAPKBP1	*NPHP20*	DDR and JNK signaling; Mitotic spindle poles during mitosis	Juvenile, adult	Scoliosis, facial dysmorphisms[1]	Macia et al. (2017)

Presence and severity of extrarenal features varies between patients. [1]Tentative association in one and two families, respectively.

other IFT-A encoding genes (Perrault et al., 2012; Schmidts et al., 2013). This functional classification of NPH genes also corresponds to specific extrarenal manifestations. For example, genes encoding transition zone proteins are associated with retinal dystrophy, genes encoding InvsC proteins are associated with situs inversus and most genes encoding IFT subunits give rise to skeletal dysplasia.

Interestingly, several NPHPs have not been linked directly to ciliary functions including GLIS2 (*NPHP7*, see below), ZNF423 (*NPHP14*) and the recently discovered gene MAPKBP1 (*NPHP20*). However, ZNF423 has been shown to interact with CEP290 and its murine ortholog *Zfp423* was shown to be involved in the transcription of ciliary genes (Chaki et al., 2012; Hong and Hamilton, 2016). Mutations in *MAPKBP1* were identified in several individuals presenting with late onset juvenile or adult NPH (Macia et al., 2017; Schonauer et al., 2020; Shamseldin et al., 2020). *MAPKBP1* encodes a non-ciliary scaffold protein involved in JNK signaling that localizes to mitotic spindle poles (Macia et al., 2017) as well as to the centrosome (Schonauer et al., 2020). Loss of *MAPKBP1* causes increased DNA-damage response signaling as observed in other NPH subtypes [see section "DNA-Damage Response (DDR)"] but no ciliogenesis defects (Macia et al., 2017), indicating that this may represent a new cilia-independent subtype of isolated NPH.

Of note, NPH can be a feature of syndromic ciliopathies caused by mutations in genes currently not classified as *NPHP* genes (*BBS* genes for example), resulting in more than 90 genes associated with an 'NPH-related ciliopathy' (Braun and Hildebrandt, 2017). In addition, biallelic mutations in *XPNPEP3* and *SLC41A1* can cause an NPH-like phenotype (O'Toole et al., 2010; Hurd et al., 2013). These genes and their functions fall outside the scope of this review.

Pathophysiology

Cilia-Associated Signaling Pathways

The combination of the transition zone at the base of the cilium which limits passive diffusion of molecules and the active transport of ciliary proteins mediated by the IFT/BBSome complexes generates a closed compartment that allows a concentration of signaling molecules and rapid signal transduction independent from rest of the cell body (Hansen et al., 2020). The primary cilium therefore acts as a cellular signaling hub for chemosensory (for example GPCR) and mechanosensory (for example polycystin-1/polycystin-2 receptor-ion channel complex) signaling (Spasic and Jacobs, 2017). PC have also been proposed as a source of a specific subtype of extracellular vesicles or 'ectosomes' which are likely acting as signaling messengers (Wood et al., 2013; Wang and Barr, 2016; Nager et al., 2017; Phua et al., 2017). Ciliary defects can disrupt these pathways, which in turn can impair kidney development and, more importantly in NPH, maintenance of kidney architecture and function. Cilia-dependent signal transduction pathways have been extensively reviewed elsewhere (Wheway et al., 2018; Anvarian et al., 2019). Specific cilia-associated signaling pathways are discussed in more detail in Section

"Targeting Ciliary Signaling Pathways," which summarizes pathways that have been targeted pharmacologically in the context of NPH and/or ADPKD including mTOR, Hedgehog (Hh) and Hippo pathways. Of note, there is mounting evidence for crosstalk between ciliary signaling pathways and DNA-damage response (DDR) signaling discussed below (Wang et al., 2020).

DNA-Damage Response (DDR)

Studies over the past 10 years pointed to an important functional relationship between several NPHP gene products and DDR signaling (Slaats and Giles, 2015; Zhang J. Q. J. et al., 2019). DDR signaling is involved in the detection of DNA damage and activation of appropriate cellular responses including cell cycle arrest and activation of DNA repair mechanisms. Chaki et al. (2012) proposed that disruption of DDR signaling and consequent impairment of cell-cycle checkpoint control early in development leads to depletion of progenitor cells and dysplastic phenotypes, while milder disruptions of DDR signaling associated with hypomorphic mutations lead to a slow accumulation of DNA damage over time resulting in degenerative phenotypes such as NPH. Since the discovery of the role of *ZNF423/NPHP14* and *CEP164/NPHP15* in DDR signaling, this functional link has been confirmed in NPH genes *CEP290/NPHP6*, *NEK8/NPHP9*, *SDCCAG8/NPHP10* and *MAPKBP1/NPHP20* (Otto et al., 2008, 2010; Chaki et al., 2012; Choi et al., 2013; Airik et al., 2014; Slaats et al., 2014, 2015; Slaats and Giles, 2015; Macia et al., 2017). Interestingly, analysis of primary kidney cells from *Cep290*-deficient mice showed increased double-strand breaks, replication fork asymmetry and reduced fork velocity suggestive of increased replication stress, and increased levels of cyclin-dependent kinases (CDKs). These effects could be rescued *in vitro* using CDK inhibitors (Slaats et al., 2015). *Cep164* knockdown in ciliated cells induced epithelial-to-mesenchymal transition (EMT) and upregulation of fibrosis-associated genes, further linking aberrant DDR signaling and S-phase arrest to tubulointerstitial fibrosis in NPH (Slaats et al., 2014). Correspondingly, *MAPKBP1*-deficient cells showed increased DDR, and kidney sections from *MAPKBP1*-related NPH patients revealed tubular atrophy and massive tubulointerstitial fibrosis (Macia et al., 2017).

Polarity

Next to nuclear functions, specific NPH-associated proteins have additional roles outside the cilium. For example, NPHP1, INVS and NPHP4 localize to and regulate cell-cell junctions (Donaldson et al., 2002; Nurnberger et al., 2002; Delous et al., 2009). NPHP1 and NPHP4 are required for timely tight junction formation and interact with the proteins PALS1 and PAR6 involved in establishment of epithelial cell polarity. Knockdown of *NPHP1* and *NPHP4* in MDCK cells resulted in disorganized, multi-lumen structures, and loss of cell polarity (Delous et al., 2009). Similar findings were obtained for other NPHPs in murine IMCD3 kidney cells suggesting a shared function in polarity and epithelialization (Sang et al., 2011; Ghosh et al., 2012). Interestingly, in the case of TRAF3IP1/IFT54, the observed polarity defect could be linked to an increased stability of cytoplasmic microtubules (see below) (Bizet et al., 2015). Finally, the loss of *Glis2/Nphp7* causes NPH in mice through EMT driven by the expression of EMT specific genes such as SNAIL (Attanasio et al., 2007; Kim et al., 2008; Li et al., 2011). Altogether, these data suggest that the crucial roles of NPHP proteins in polarity/epithelialization likely contribute to the tubular atrophy and loss of nephrons observed in juvenile NPH.

Inflammation and Senescence

Most recently, activation of inflammation was proposed to be involved in tubulointerstitial fibrosis in NPH. NPHP1 is part of a protein complex with the kinase LKB1 that regulates cilia-controlled secretion of the chemokine CCL2, and *Nphp1* silencing induced increased Ccl2 expression in kidney cells (Viau et al., 2018). Ccl2 has been associated with macrophage activation and disease progression in CKD (Cao et al., 2015). In addition, mononuclear infiltrates and inflammation have been described in animal models of NPH including *pcy/Nphp3* and *Glis2/Nphp7* mice (Omran et al., 2001; Kim et al., 2008). Interestingly, *Glis2/Nphp7* knockout mice were shown to have increased tubular cell senescence (Jin et al., 2020). Replicative senescence leads to secretion of pro-inflammatory cytokines and activation of the NF-kB pathway, eliciting an inflammatory response, increased senescence in neighboring cells and extensive kidney damage as demonstrated in a *Glis2* knockout mouse and in other mouse models of CKD (Acosta et al., 2013; Docherty et al., 2019; Jin et al., 2020). In addition, senescent tubular epithelial cells were demonstrated to be a source of pro-fibrotic Hh ligands (Jin et al., 2019). Similar processes could contribute to tubulointerstitial damage in other subtypes of juvenile NPH with known defects in DNA-damage response signaling and cell cycle progression, although it is unknown whether tubular cell senescence is a general feature of NPH.

Additional Mechanisms

Additional cilia-independent mechanisms that have been pharmacologically targeted in NPH, including glycosphingolipids and cholesterol, and microtubule dynamics, are discussed in Section "Pharmacotherapy." Other factors were not directly targeted but have been proposed to play a role in the pathophysiology of NPH. For example, oxidative stress, the endoplasmic reticulum (ER) stress response and mitochondrial dynamics were shown to be dysregulated in the *jck* mouse model of NEK8/NPHP9 (Bracken et al., 2016). In addition, the NPH-associated metalloproteinase ADAMTS9 was involved in regulation of ER-Golgi vesicular transport (Yoshina et al., 2012). However, ADAMTS9 was also shown to localize in vesicular structures near the base of the cilium and to be required for ciliogenesis, a function which appears to be distinct from its role in ER-Golgi transport (Choi et al., 2019; Nandadasa et al., 2019). The relationship between the ubiquitin-proteasome system, autophagy and primary cilia has been recently reviewed (Boukhalfa et al., 2019; Wiegering et al., 2019). Finally, increased formation of ciliary extracellular vesicle has been observed in BBS mutant cells suggesting that dysregulation of this process might contribute to ciliopathies (Nager et al., 2017; Akella et al., 2020).

However, for most proposed mechanisms it remains unclear how individual factors contribute to specific NPH phenotypes.

AVAILABLE MODEL SYSTEMS

Animal Models

Although studies in animal models of NPH have provided above-mentioned insights into pathophysiology of NPH, most models do not recapitulate the juvenile NPH phenotypes.

Zebrafish larva (24–72 h post fertilization) is a widely used organism to study renal ciliopathies. This model is low cost, fast and efficient, allowing *in vivo* imaging, functional studies and large-scale screening of small molecules for therapeutic approaches. Most models have been based on morpholino-based knockdown of the respective *nphp* genes, resulting in loss of function like conditions, typically resulting in severe developmental defects including cysts in the proximal pronephros and/or defects in the distal part of the pronephros associated with ciliary defects (Slanchev et al., 2011; Song et al., 2016; Elmonem et al., 2018). It is unlikely that fibrosis could be monitored/observed in early developmental stages in the simple pronephros which is present in the embryo; this would likely require the development of adult fish models. Generation of mutant zebrafish lines to study more slowly progressive juvenile NPH is limited because most described mutants show either too severe phenotypes with early death at larval stages, or no phenotype in the adults (Song et al., 2016; Macia et al., 2017), likely due to compensation mechanisms (El-Brolosy and Stainier, 2017). Interestingly, a recent study described a hypomorphic mutation in *tmem67* (*NPHP11*), leading to ciliary defects and tubular cysts in adult zebrafish kidneys (Zhu et al., 2021), indicating that such models can be generated. Unfortunately, fibrosis was not monitored in this study.

Mouse models more accurately represent human kidney physiology and have been extensively used to characterize mechanisms underlying ciliopathies as well as CKD and associated fibrosis (Norris and Grimes, 2012; Ko and Park, 2013; Nogueira et al., 2017). However, while kidney fibrosis has been observed in mouse models of PKD and after toxic challenges, mice appear to be relatively resistant to NPH-related fibrosis. Indeed, published knockout mouse models corresponding to juvenile NPH including *Nphp1*, *Nphp4*, *Nphp5* and *Mapkbp1* do not show an obvious spontaneous renal phenotype (Jiang et al., 2008; Won et al., 2011; Ronquillo et al., 2016; Macia et al., 2017). Interestingly, only *Glis2/Nphp7*-knockout mice show a phenotype that fully represents juvenile NPH, comprising smaller kidneys with increased apoptosis, immune infiltration, fibrosis and tubular dilations on kidney sections, increased serum creatinine and polyuria (Kim et al., 2008).

Mouse models of InvsC defects (*Invs, pcy/Nphp3*, *jck/Nek8/Nphp9* and *Anks6/Nphp16*-mutated mice) show enlarged cystic kidneys characteristic of infantile NPH, although *pcy/Nphp3* and *Anks6/Nphp16* mice have slow disease progression and (late stage) tubulointerstitial fibrosis (Omran et al., 2001; Bakey et al., 2015). The *pcy/Nphp3* mouse model, which harbors a homozygous missense mutation in *Nphp3*, is characterized by cysts at the corticomedullary junction (later throughout the kidney), kidney enlargement and late-stage fibrosis (Takahashi et al., 1991; Omran et al., 2001; Olbrich et al., 2003). Consequently, *pcy/Nphp3* mice show more resemblance to ADPKD than to juvenile NPH. This is relevant because contrary to ADPKD, cyst formation in juvenile NPH likely occurs secondary to tissue degeneration and atrophy instead of being a driving mechanism, so targetable mechanisms in both conditions could diverge (Braun and Hildebrandt, 2017; Srivastava et al., 2018). Similarly, *jck/Nek8/Nphp9* mice, which show enlarged cystic kidneys and rapid disease progression, have been used as a model for (AR)PKD (Bukanov et al., 2006). These differences between human and animal phenotypes should be taken into account in pharmacological studies in NPH.

With the exception of juvenile NPHP genes mentioned above, genetic invalidation of most NPHP genes causes cystic kidney enlargement in mice (**Table 2**). These severe phenotypes could partly be explained by predominantly complete loss of function mutations in the mice models, which do not correspond to the (often hypomorphic) mutations in (at least) part of patients with juvenile NPH. The same limitations are found in the Lewis polycystic kidney (LPK), Wistar polycystic kidney (Wpk) and *Cy* rat models, with mutations in the orthologs of human *NEK8/NPHP9*, *TMEM67/NPHP11* and *ANKS6/NPHP16* genes, respectively. These all show rapidly progressive cystic kidney enlargement reminiscent of infantile NPH or ARPKD phenotypes (Cowley et al., 1993; Gattone et al., 2004; Brown et al., 2005; Smith U. M. et al., 2006; Phillips et al., 2007; McCooke et al., 2012; Taskiran et al., 2014).

It is important to note that the type of genetic defect in animal models (knockout/loss of function or missense mutations) and the genetic background strain with associated genetic modifiers impact the severity of the phenotype and the utility of the model for human disease, as was demonstrated in mouse models of *Cep290*-associated ciliopathies (Ramsbottom et al., 2015, 2020). Patient-derived *in vitro* systems, for example urinary renal epithelial cells (URECs), kidney tubuloids and organoids, could partly solve these issues (Schutgens et al., 2019; Steichen et al., 2020).

Kidney Organoids and Tubuloids

Primary kidney tubular epithelial organoids, or 'tubuloids,' can be efficiently established from adult stem cells derived from kidney biopsy material and from URECs. Tubuloids were employed to study infectious kidney disease in a personalized fashion and test the efficacy of cystic fibrosis treatment using a forskolin (cAMP) swelling assay, illustrating its utility in (personalized) drug screening (Schutgens et al., 2019). In contrast to tubuloids, which are restricted to epithelial tubular cells, kidney organoids were generated from human induced pluripotent stem cells (iPSC) that contained different parts of the nephron (glomerulus, proximal and distal tubule) and interstitial cells (Yousef Yengej et al., 2020). While these organoids lack collecting ducts, other protocols were recently setup to generate ureteric bud-derived collecting ducts enriched organoids (Kuraoka et al., 2020; Uchimura et al., 2020). Kidney organoids were also generated from adult differentiated kidney cells which incorporated extracellular matrix (ECM) cells,

TABLE 2 | Rodent models of NPH discussed in this review.

Species	Name	Human ortholog	Type of mutation	Renal disease progression	Survival	Tubular phenotype	Interstitial phenotype	Urine concentration defect	Kidney size	Extrarenal phenotypes	References
Mouse	*Nphp1*	*NPHP1*	Out-of-frame deletion exon 20	NA	Normal	–	–	NA	Normal	Male infertility	Jiang et al. (2008)
	Invs	*INVS/NPHP2*	Out-of-frame deletion exon 3–11	Rapid (kidney failure around age 1 week)	Around 1 week	Absence of tubular atrophy and tubular basement membrane irregularities; corticomedullary cysts arising from proximal tubule and collecting duct;	–	NA	Enlarged	Situs inversus, biliary obstruction/ atresia	Yokoyama et al. (1993); Lowe et al. (1996); Mochizuki et al. (1998); Morgan et al. (1998); Phillips et al. (2004)
	Polycystic kidney disease (Pcy)	*NPHP3*	Missense	Slow (kidney failure in adult mice)	NA	Tubular atrophy and tubular basement membrane thickening; corticomedullary cysts followed by entire kidney, tubular dilations arising predominantly from distal tubules and collecting duct	Tubulointerstitial fibrosis and inflammation (late stage)	NA	Enlarged	Cerebral vascular aneurysms	Takahashi et al. (1991); Omran et al. (2001); Olbrich et al. (2003)
	Nphp4	*NPHP4*	Missense	NA	Normal	–	–	NA	Normal	Retinal disease, male infertility	Won et al. (2011)
	Iqcb1	*IQCB1/ NPHP5*	Gene trap leading to loss of function	NA	NA	–	–	NA	Normal	Retinal disease	Ronquillo et al. (2016)
	Cep290	*CEP290/ NPHP6*	Gene trap inserted in intron 25 leading to premature stop codon	NA	129/Ola background: survival past age 1 year	Small cysts in cortex arising from collecting duct	–	Evidence of polyuria and polydipsia	NA	Retinal disease, cerebral abnormalities	Hynes et al. (2014)
			Rd16: deletion of exons 35 to 39	NA	NA	–	–	NA	Normal	Retinal disease	Chang et al. (2006)

(Continued)

TABLE 2 | Continued

Species	Name	Human ortholog	Type of mutation	Renal disease progression	Survival	Tubular phenotype	Interstitial phenotype	Urine concentration defect	Kidney size	Extrarenal phenotypes	References
			Knockout	Slow	Mixed C57BL/6 and 129/SvJ background: 80% lethality within first weeks due to hydrocephalus; surviving mice lived until age 2 years	Corticomedullary cysts develop after 12 months	–	NA	Enlarged	Retinal disease, cerebral and cerebellar abnormalities	Rachel et al. (2015)
			Gene trap inserted in intron 25 leading to premature stop codon	Rapid	C57BL/6 and 129/SvJ backgrounds: majority dies prenatally; mice that survive to age 2–3 weeks show severe cystic kidney disease	Loss of tubules (not further specified); corticomedullary cysts	Cellular infiltrate	NA	Enlarged	Retinal disease, hepatic pallor	
	Glis2	*GLIS2/NPHP7*	Knockout	NA	>40% lethality by age 10 months	Atrophy of proximal tubules, minimal tubular basement membrane thickening; corticomedullary and glomerular cysts	Tubulointerstitial inflammation and fibrosis starting at age 8 weeks	NA	Reduced	–	Attanasio et al. (2007); Kim et al. (2008)
	Rpgrip1l (Ftm)	*RPGRIP1L/ NPHP8*	Knockout	NA	Embryonically lethal	Cortical microcysts arising from proximal tubule at 18.5 days post conception	–	NA	NA	Exencephaly, microphthalmia, situs inversus, liver abnormalities, polydactyly	Delous et al. (2007)

(Continued)

TABLE 2 | Continued

Species	Name	Human ortholog	Type of mutation	Renal disease progression	Survival	Tubular phenotype	Interstitial phenotype	Urine concentration defect	Kidney size	Extrarenal phenotypes	References
	Juvenile cystic kidneys (Jck)	*NEK8/NPHP9*	Missense	NA	100% lethality by age 25 weeks in males and age 80 weeks in females	Basement membrane disruptions; corticomedullary cysts followed by entire kidney, arising from collecting duct, in later stage also from distal tubule and loop of Henle	–	NA	Enlarged	–	Atala et al. (1993); Liu et al. (2002); Smith L. A. et al. (2006); Otto et al. (2008)
			Knockout	NA	Die within hours after birth due to congenital heart defect	Proximal tubule dilation; glomerular cysts and (few cysts develop in kidney explant culture)	–	NA	Normal	Situs inversus, cardiac anomalies	Manning et al. (2013)
	Sdccag8	*SDCCAG8/ NPHP10*	Gene trap leading to loss of function	Slow	Survival > 250 days	Initial cortical cysts followed by corticomedullary cysts, arising from distal convoluted tubule and collecting duct; glomerular cysts	Tubulointerstitial fibrosis (late stage)	NA	Enlarged (late stage)	Retinal disease	Airik et al. (2014)
	Bilateral polycystic kidneys (Bpck)	*TMEM67/ NPHP11*	Deletion	Rapid (kidney failure around age 3 weeks)	Survive to age 3 weeks	Corticomedullary cysts arising from distal tubule and collecting duct, later mild dilation of some proximal tubules	–	NA	Enlarged	Hydrocephalus, spermatogenesis defects	Cook et al. (2009)

(Continued)

TABLE 2 | Continued

Species	Name	Human ortholog	Type of mutation	Renal disease progression	Survival	Tubular phenotype	Interstitial phenotype	Urine concentration defect	Kidney size	Extrarenal phenotypes	References
	Ttc21b (Thm1)	*TTC21B/ NPHP12*	Loss of function mutation	NA	Embryonically lethal	Cystic dilations of glomeruli, proximal tubules and ascending loops of Henle	–	NA	NA	–	Tran et al. (2008, 2014)
			Conditional *Ttc21b* knockout using ROSA26Cre ERT+	Rapid (cystic kidney disease and elevated BUN by age 6 weeks when *Ttc21b* is inactivated before P12-14)	NA	Cortical cysts arising from proximal tubule, loop of Henle and collecting duct	–	NA	Enlarged	–	Tran et al. (2014)
	Cep164	*CEP164/ NPHP15*	Kidney-specific *Cep164* inactivation using Hoxb7-Cre (collecting duct)	Rapid (kidney failure around 3 weeks)	Median survival 25 days	Cysts in medulla followed by cortex and entire kidney, arising from collecting duct	–	NA	Enlarged	–	Airik et al. (2019)
	Anks6	*ANKS6/ NPHP16*	Missense mutation	Slow	Survival to age 18 months	Cysts arising from collecting duct, thick ascending limb of loop of Henle, to a lesser extent from distal tubule; glomerular cysts	Interstitial fibrosis	NA	Enlarged	–	Bakey et al. (2015)
	Mapkbp1	*MAPKBP1/ NPHP20*	Knockout	NA	Normal	–	–	NA	Normal	–	Macia et al. (2017)
	Ofd1	*OFD1*	Kidney-specific *Ofd1* inactivation using Ksp-Cre (distal tubule and collecting duct)	Severely impaired kidney function at age 1–3 months	Animals sacrificed at age 3 months	Cysts in medulla followed by cortex, arising from distal tubules; later glomerular cysts and proximal tubular cysts	–	NA	Enlarged	–	Zullo et al. (2010)

(Continued)

TABLE 2 | Continued

Species	Name	Human ortholog	Type of mutation	Renal disease progression	Survival	Tubular phenotype	Interstitial phenotype	Urine concentration defect	Kidney size	Extrarenal phenotypes	References
	Ahi1	*AHI1*	Knockout	Slow (kidney function impairment at age 1 year or older)	80% did not survive into adulthood	Tubular basement membrane disruption and thickening; corticomedullary microcysts and tubular dilations, mainly arising from proximal tubule	Interstitial cell infiltrate and fibrosis	Urinary concentration defect	Reduced by age 5 months	–	Lancaster et al. (2009)
Non-orthologous mouse models	*Fan1*	*FAN1*	Knockout mice treated with 2 mg/kg cisplatin	Rapid (kidney failure within 5 weeks after start of treatment)	NA	Tubular basement membrane thickening; tubular dilation; karyomegalic nuclei in proximal tubule	Tubulointerstitial inflammation and fibrosis	NA	NA	Bone marrow failure	Airik et al. (2016)
	Prkar1a	*PRKAR1A*	Kidney-specific *Prka1a* inactivation using Pkhd1-Cre (collecting duct)	NA	Animals sacrificed at age 3 months	Small cysts primarily arising from distal tubule and collecting duct	Interstitial fibrosis	NA	Normal (enlarged in 2/16 mice)	–	Ye et al. (2017)
	Lkb1	*STK11/LKB1*	Kidney-specific Lkb1 inactivation using Ksp-Cre (distal tubule and collecting duct)	Rapid (kidney failure around age 5 weeks)	50% survival around age 11 months	Tubular basement membrane thickening, tubular dilation, corticomedullary cysts at late stage	Tubulointerstitial inflammation and fibrosis	Impaired urine concentration at age 5 weeks	Reduced size at age 5 weeks	–	Viau et al. (2018)
	Aatf	*AATF*	Kidney-specific *Aatf* inactivation using Ksp-Cre (distal tubule and collecting duct)	Rapid (kidney failure around age 10 weeks)	Survival 10–15 weeks	Tubular basement membrane disruption and thickening; corticomedullary cysts arising from distal tubule, later glomerular cysts	Interstitial fibrosis	Urinary concentration defect	Reduced size at age 10 weeks	–	Jain et al. (2019)

(Continued)

TABLE 2 | Continued

Species	Name	Human ortholog	Type of mutation	Renal disease progression	Survival	Tubular phenotype	Interstitial phenotype	Urine concentration defect	Kidney size	Extrarenal phenotypes	References
Rat	Lewis polycystic kidney (LPK)	*NEK8/NPHP9*	Missense	Slow (kidney failure around 12–24 weeks)	No survival beyond age 26 weeks	Corticomedullary cysts, predominantly arising from collecting duct	Tubulointerstitial inflammation and fibrosis	NA	Enlarged	–	Phillips et al. (2007); McCooke et al. (2012)
	Wistar polycystic kidney (Wpk)	*TMEM67/NPHP11*	Missense	Rapid (kidney failure around age 3 weeks)	NA	Cysts in proximal tubule and collecting duct	–	NA	Enlarged	Cerebral abnormalities, hypoplastic spleen	Gattone et al. (2004); Smith U. M. et al. (2006)
	Cy	*ANKS6/NPHP16*	Missense	Homozygous: rapid (kidney failure around age 3 weeks)	Survive to age 3 weeks	Cysts in cortex and outer medulla	–	NA	Enlarged	–	Cowley et al. (1993); Brown et al. (2005)
			Missense	Heterozygous: slow	Males die of kidney failure within 1 year, females survive past 1 year	Thickened tubular basement membranes; dilatations of proximal and distal tubule and collecting duct	Tubulointerstitial fibrosis and inflammation	NA	Moderately enlarged	–	Cowley et al. (1993); Brown et al. (2005)

Severity of the phenotype can depend on background strain. Presence of a renal phenotype was not reported for mouse models of WDR19/NPHP13, ZNF423/NPHP14, IFT172/NPHP17, DCDC2/NPHP19 and ADAMTS9/NPHP21 (Alcaraz et al., 2006; Cheng et al., 2007; Gorivodsky et al., 2009; Kern et al., 2010; Wang et al., 2011; Ashe et al., 2012; Dubail et al., 2014; Nandadasa et al., 2015; Schueler et al., 2015; Casoni et al., 2017). For CEP83/NPHP18, a cortical radial glial progenitor cell-specific conditional knockout was created that did not permit study of renal phenotypes (Shao et al., 2020). NPH can be a feature of other syndromic ciliopathies. Corresponding mouse models were not included in this table unless they were discussed in the main text. NA, not available/not reported.

making them suitable to study interstitial phenotypes (Takasato et al., 2015; Ding et al., 2020). Although kidney organoids have mainly been studied as models of cyst development (ADPKD and ARPKD), with forskolin treatment inducing cystogenesis (Cruz et al., 2017; Low et al., 2019; Kuraoka et al., 2020), they have also been used to monitor fibrosis and myofibroblasts expansion upon IL-1β treatment (Lemos et al., 2018).

Limitations are that kidney organoids do not recapitulate the overall kidney morphology and do not take into account interactions between organs including vascularization of the glomeruli (unless they are transplanted into a host organism), an essential step required for generation of intratubular flow. In addition, only one study reported the generation of iPSCs-derived kidney organoid in the context of an NPH-related condition. The generated organoids were used as a source of tubular epithelial cells in which transciptomic and functional analyses confirmed major defects in polarity (Forbes et al., 2018), as previously reported for other NPHP genes in kidney epithelial cell lines (see section "Polarity"). However, these organoids did not show a cystic phenotype (Forbes et al., 2018). Further improvement of NPH patient-derived kidney organoids is required before these can be used in drug tests.

PHARMACOTHERAPY

Hypothesis-Driven Therapies

In NPH, pharmacological targeting of the defective gene product is challenging because NPH-associated mutations typically lower expression of the protein and/or result in expression of a truncated protein. This is especially the case for homozygous deletion of *NPHP1*, the most frequent genetic event in NPH. Possibilities for targeted therapies therefore include enhancing stability/function of remaining mutated NPHP protein and/or of the complex in which it functions, or targeting the signaling pathway in which the protein plays a role, downstream pathophysiological mechanisms or modifier gene products (Kim and Kim, 2019).

Despite efforts to uncover specific approaches, many drugs investigated for the treatment of NPH were discovered in animal models of other renal ciliopathies, mainly ADPKD. ADPKD is the most prevalent inherited kidney disease and has a partly shared pathophysiology with NPH (cysts and fibrosis). As a result, important findings in the ADPKD field may be relevant for NPH.

Of note, some therapies listed below are aimed at prevention of NPH manifestations. While this approach in animal models could provide important insights, in practice most patients are symptomatic upon diagnosis therefore precluding any preventive treatment until the identification of relevant biomarkers in asymptomatic individuals.

Targeting Ciliary Signaling Pathways

Targeting GPCR/cAMP signaling

G-protein coupled receptors are a large family of signaling receptors, many of which localize to the ciliary membrane (Mykytyn and Askwith, 2017). Examples include odor receptors in olfactory neurons, rhodopsin in photoreceptors and smoothened (SMO) in various tissues. Key ciliary GPCRs are positively coupled to adenylate cyclases (AC) through GαS and their activation leads to production of cyclic AMP (cAMP), a key signaling intermediate which was shown to drive renal cyst formation in ADPKD and other renal ciliopathies (Mangoo-Karim et al., 1989; Ye and Grantham, 1993; Ghosh et al., 2012). Indeed, polycystin-2 was shown to interact with and inhibit AC while activating phosphodiesterase activity both resulting in a decreased amount of cAMP. In addition to the loss of this negative regulation in PKD conditions, dysregulation of calcium signaling may also contribute to elevated levels of cAMP through overactivation of ciliary AC and cAMP production leading to increased downstream signaling and cell proliferation (Sussman et al., 2020). Interestingly, NEK8/NPHP9 was shown to positively regulate polycystin-2 expression and ciliary localization (Smith L. A. et al., 2006; Sohara et al., 2008; Manning et al., 2013), in agreement with the cystic kidneys observed in infantile NPH linked to mutations in InvsC genes.

One of the main targetable sources of cAMP is the vasopressin receptor type 2 (V2R) encoded by *AVPR2*. V2R is an important GPCR in renal physiology that localizes to the basolateral membrane and to cilia of renal tubular epithelial cells (Sherpa et al., 2019). Activation of V2R by vasopressin leads to cAMP-dependent activation of PKA which in turn phosphorylates aquaporin 2 (AQP2), causing its translocation to the apical membrane where it controls water reabsorption, and upregulates AQP2 transcription (**Figure 2A**) (Nielsen et al., 2002). Disruption of this pathway could explain the urine concentration defect observed in NPH which partially mimics nephrogenic diabetes insipidus caused by mutations in *AVPR2* (Rosenthal et al., 1992; Van den Ouweland et al., 1992). Indeed, AQP2 targeting to the apical membrane in response to vasopressin was shown to be defective in human collecting duct cells in the context of Bardet-Biedl syndrome (Marion et al., 2011). Alternatively, decreased water reabsorption could result from disruption of tubular architecture and medullary osmotic gradient through defects in cell junctions and fibrosis as in other CKD (Krishnan et al., 2008; Bockenhauer et al., 2010).

In addition to its role in water reabsorption, V2R was involved in cystic kidney diseases (PKD). Its activation was shown to stimulate cyst growth through several cAMP-mediated mechanisms including activation of PKA leading to Cl^--dependent fluid secretion by cystic cells, and extracellular signal-regulated protein kinase (ERK) pathway-induced epithelial cell proliferation (Yamaguchi et al., 2000; Reif et al., 2011; Sherpa et al., 2019). The use of V2R antagonists such as tolvaptan, which inhibits V2R signaling reducing cAMP levels in renal collecting duct cells (**Figure 2A**), has proven to be a successful strategy in ADPKD. This approach was first shown to markedly reduce renal cyst formation and fibrosis and limit disease progression in a polycystic kidney rat model of ARPKD (PCK) and the *pcy/Nphp3* mouse model (Gattone et al., 2003). The V2R antagonist OPC31260 was subsequently shown to mitigate cystogenesis and renal function decline in a mouse model of ADPKD (Torres et al., 2004). Tolvaptan was shown to be effective in clinical trials (Torres et al., 2012, 2017, 2018) and is the first

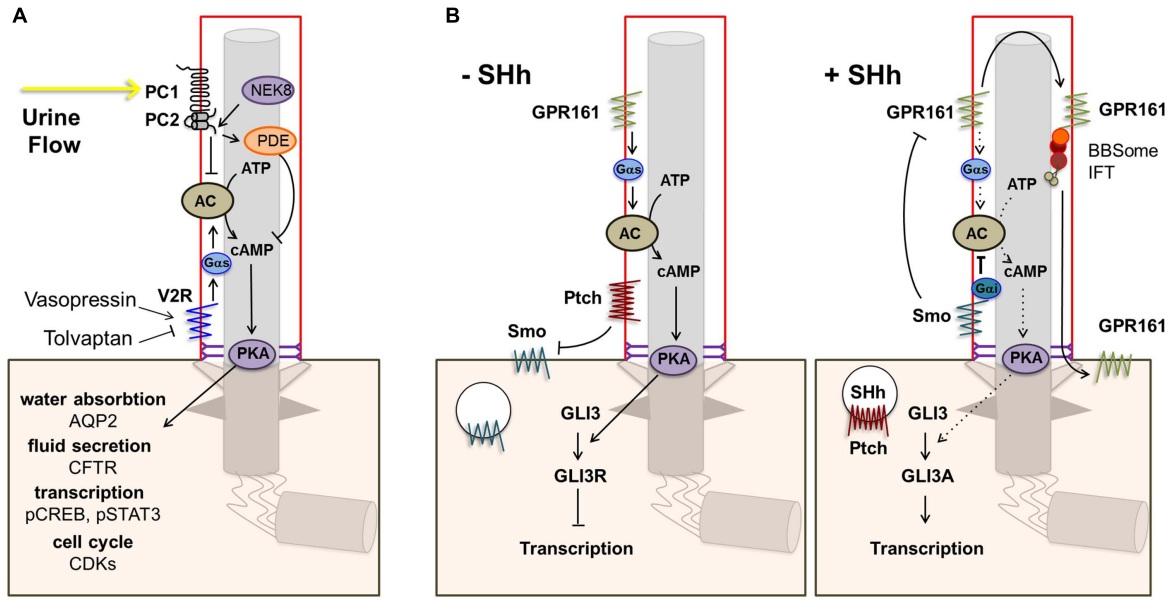

FIGURE 2 | Ciliary GPCR signaling. **(A)** The vasopressin receptor type 2 (V2R) is located in the ciliary membrane. When activated, signal transduction via Gs alpha subunit (Gαs) leads to increased production of cAMP by adenylate cyclase (AC) and subsequent activation of protein kinase A (PKA). PKA phosphorylates aquaporin 2 (AQP2), which translocates to the apical cell membrane leading to increased water reabsorption. In addition, PKA phosphorylates the cystic fibrosis transmembrane conductance regulator (CFTR), leading to transport of Cl^- ions and fluid secretion into the lumen, and CREB and STAT3, enhancing transcription. Other downstream effects include increased CDK signaling. Opening of the polycystin-1/polycystin-2 (PC1/PC2) complex in response to urine flow inhibits the cAMP/PKA pathway via inhibition of AC5/6 and through PDE4C. **(B)** Other main ciliary GPCRs are Smo and the constitutively active Shh receptor GPR161. In the absence of Shh, Ptch1 excludes and inhibits Smo, leading to repression of Gli transcription factors by SuFu, and GPR161 signaling leads to increased cAMP-dependent activation of PKA. Elevated PKA further represses Gli transcription factors. Binding of a Hh ligand leads to entry of Smo and consequent removal of GPR161 from the ciliary membrane, resulting in decreased cAMP/PKA activity and activation of Gli transcription factors.

drug registered for treatment of adult ADPKD patients below 55 years of age and at risk of rapidly progressive disease as defined by clinical and/or genetic criteria (Chebib et al., 2018). There are no clinical trials registered for use of Tolvaptan in patients with NPH and there is only one case report in which Tolvaptan is described for the treatment of *NPHP3*-related infantile NPH without an effect on the very rapid renal function decline in this specific severe case (Strong et al., 2018). Such an approach could theoretically be used in the case of cystic infantile NPH, although the therapeutic window is small (mean age under 5), while its relevance in juvenile NPH is less apparent. Indeed, the presence of cysts is a late event in the juvenile/adult form and the potential role of cAMP remains to be investigated.

Another class of drugs that modulate renal cAMP levels by binding to GPCRs are somatostatin analogs, which activate somatostatin receptors and inhibit AC through the inhibitory G protein Gαi (Günther et al., 2018). Somatostatin analogs such as octreotide are used in the treatment of neuroendocrine tumors as inhibitors of growth hormone and several pancreatic and gastrointestinal hormones. In the context of kidney disease, octreotide was first shown to be well-tolerated and slow renal volume expansion in a 6-month trial with 14 adult patients with ADPKD (Ruggenenti et al., 2005). Octreotide was later shown to inhibit hepatic cyst development in the PCK rat model and reduce liver volume in *post hoc* analysis of the above-mentioned study in ADPKD patients (Masyuk et al., 2007; Caroli et al., 2010). It also reduced kidney volume in patients with ADPKD compared to placebo-treated patients (Hogan et al., 2010). In the context of NPH, octreotide was shown to significantly decrease cAMP levels and to rescue cilia defects and abnormal 3D spheroid phenotypes in *Nphp3*, *Cep290/Nphp6* and *Rpgrip1l/Nphp8* knockdown IMCD3 cells (Ghosh et al., 2012). These results suggest a positive effect of treatment with somatostatin analogs in NPH, although results have not been replicated in an animal model. Similarly, targeting the calcium-sensing receptor (CasR), a GPCR expressed in renal tubular cells, also leads to decreased production of cAMP through inhibition of AC (Riccardi and Valenti, 2016). Administration of the calcimimetic R-568 CasR agonist was shown to decrease cystogenesis and renal fibrosis in *pcy/Nphp3* mice (Chen et al., 2011). The above examples clearly show that decreasing cAMP levels is an effective therapeutic option in models of cystic kidney disease including ADPKD and (mostly infantile) NPH. The relevance of targeting cAMP in the context of juvenile NPH remains an open question as cystogenesis through proliferation and fluid secretion could be a less critical mechanism in this form of NPH (Srivastava et al., 2018).

A class of bioactive lipid metabolites called cyclooxygenase (COX) oxylipins (e.g., prostaglandins, leukotrienes) has been shown to be elevated in diseased kidneys of rodent models of NPH (*pcy/Nphp3* and *jck/Nek8/Nphp9* mice and Han:SPRD-*Cy/Anks6/Nphp16* rats) and other cystic kidney diseases

(Ibrahim et al., 2014; Yamaguchi et al., 2014; Monirujjaman et al., 2017). A flax oil-enriched diet effectively reduced levels of COX-derived oxylipins compared to a control diet and mitigated interstitial fibrosis and cyst growth in *pcy/Nphp3* mice (Sankaran et al., 2004; Yamaguchi et al., 2015). In addition, treatment with COX inhibitors or dietary soy protein slowed disease progression in a heterozygous Han:SPRD-*Cy/Anks6/Nphp16* rat model (Sankaran et al., 2007; Ibrahim et al., 2014, 2015). Interestingly, the COX inhibitor Ibuprofen is used to treat patients presenting with Bartter Syndrome which is characterized by water and salt loss associated with elevated urinary prostaglandin E2 (PGE2). However, treatment of PCK rats with a COX inhibitor did not show any improvement of the cystic index or of kidney function (Sussman et al., 2020).

Although the exact role of COX-derived oxylipins in CKD remains unclear, PGE2 is known to exert its effect partly through increasing levels of cAMP through activation of tubular EP2/4 receptors (Elberg et al., 2007; Monirujjaman et al., 2017). The GPCR EP4 is one of the PGE2 receptors which control water and salt reabsorption (Li et al., 2018). Interestingly, EP4, which is also involved in AQP2 trafficking and could functionally compensate for the loss of V2R (Li et al., 2009), is present at cilia where it is involved in cAMP production and positive regulation of ciliogenesis through positive regulation of IFT (Jin et al., 2014; Jiang et al., 2019). It has however to be noticed that PGE2 acts through activation of four distinct receptors (EP1-4, see above) which control opposite downstream signaling pathways, complicating the understanding of the role of PGE2 in renal ciliopathies. Indeed, a recent study indicate that while PGE2 is pro-cystogenic *in vitro*, inhibition of EP2 and EP4 with antagonists resulted in a more severe disease in a *Pkd1* model due to increased inflammation (Lannoy et al., 2020). Even if among oxylipins PGE2 is an interesting candidate in the context of NPH (see above), evidence for increased or decreased production of PGE2, or of any other COX-derived oxylipins, in NPH patients is lacking so far.

mTOR inhibition

Next to cAMP signaling, an important signaling pathway that is inappropriately activated in ciliopathies is the mammalian target of rapamycin (mTOR) which functions as a central regulator in cellular metabolism, growth, proliferation, cell cycle and survival. It has been shown that cilia-dependent flow sensing negatively regulates mTORC1 through the kinase LKB1 (Boehlke et al., 2010). In ciliopathies like PKD, flow sensing is altered leading to mTOR pathway activation and uncontrolled cell growth and proliferation which induces cystogenesis (Lai and Jiang, 2020).

Administration of the mTOR pathway inhibitor rapamycin was shown to decrease proliferation, cystogenesis, kidney enlargement and renal function decline in heterozygous Han:SPRD-*Cy/Anks6/Nphp16* rats (Tao et al., 2005). In addition, ADPKD patients who had received kidney transplants were observed to have reduced volumes of affected kidney and liver if an mTOR inhibitor was included in the immunosuppressive regimen (Shillingford et al., 2006; Qian et al., 2008). However, 18-month rapamycin treatment of adults with early stage ADPKD did not halt disease progression and a clinically effective dose could not be achieved without systemic adverse effects (Serra et al., 2010; Shillingford et al., 2012). A study in zebrafish with morpholino-based knockdown of ciliopathy-associated genes including *nphp2, nphp5, nphp6* and *nphp11* provided additional evidence for the potential efficacy of mTOR inhibition in NPH-related ciliopathies. Treatment with rapamycin restored renal size and morphology in all morphants and partially rescued renal filtration decrease (Tobin and Beales, 2008). Treatment of *pcy/Nphp3* mice with rapamycin did not prevent initial cyst development but significantly reduced cyst enlargement, fibrosis and renal insufficiency (Gattone et al., 2009). This suggests an application in late-stage progression of NPH, the stage in which NPH is typically detected, if future targeted delivery can prevent systemic side effects of rapamycin.

Modulators of Hedgehog signaling

The ciliary GPCRs SMO and GPR161 are key players in the Hh signaling pathway, which is essential in embryonic development and adult tissue homeostasis and regeneration (Kopinke et al., 2020). In the absence of Hh, patched (PTCH1) localizes to the ciliary membrane and excludes and inhibits SMO. In addition, constitutive GPR161 activity in the cilium stimulates AC leading to increased cAMP-dependent activation of PKA which further leads to repressor forms of the GLI3 transcription factor (GLI3R). Upon binding of Hh to PTCH1, SMO enters the cilium whereas GPR161 is removed from the ciliary membrane, leading to decreased cAMP/PKA activity and activation of GLI3 (GLI3A; **Figure 2B**).

Hh signaling is involved in kidney development and preservation of the differentiated state of renal tubular epithelial cells (Li et al., 2011). Interestingly, Hh signaling has been implicated in fibrosis in different tissues through involvement in proliferation of myofibroblasts which expand in fibrotic tissues and secrete ECM components (Distler et al., 2019). In the kidney, Hh was shown to be produced in high amount by tubular cells in different models of kidney injury, stimulating interstitial mesenchymal cells which leads to fibrosis (Tan et al., 2016). In contrast, activation or downregulation of Hh signaling did not affect cyst formation in a *Pkd1* mouse model (Ma et al., 2019). NPHP proteins were shown to play important roles in Hh signaling including RPGRIP1L and ZNF423 as well as IFT involved in the transport of GPR161 and GLI transcription factors in and out of cilia (Vierkotten et al., 2007; Qin et al., 2011; Hong and Hamilton, 2016). Indeed, the Hh pathway has been shown to be dysregulated in numerous ciliopathies (Ruiz-Perez et al., 2007; Aguilar et al., 2012). Of note, a CRISPR-based screen to identify regulators of Hh signaling detected among many ciliopathy genes few genes mutated exclusively in NPH, not including *NPHP1* and *NPHP4* or the genes encoding InvsC proteins, suggesting that disrupted Hh signaling plays a less prominent role in isolated NPH than in other ciliopathies (Breslow et al., 2018).

A *Cep290*-gene trap mouse model of Joubert syndrome revealed increased Gli3 repressor isoform in the kidney, in agreement with decreased Hh signaling. Modulation of this pathway with the Hh agonist purmorphamine reconstituted impaired spheroid formation in collecting duct cells from *Cep290*-mutant mice and in URECs derived from a patient

with Joubert syndrome (Hynes et al., 2014) as well the elongated cilia phenotype (Srivastava et al., 2017). In contrast, inhibition of Hh signaling using GLI and SMO small molecule antagonists Gant61 and Sant2 respectively prevented cyst formation in kidney explants from *Ttc21b/Ift139*-conditional knockout, *jck/Nek8/Nphp9* and *Pkd1* mutant mice (Tran et al., 2014). In contrast to CEP290, TTC21B/IFT139 is a negative regulator of Hh signaling (Tran et al., 2008), similar to other IFT-A subunits which control ciliary transport of GPR161 (Kopinke et al., 2020). The impact of ciliopathies on Hh signaling is therefore complex and appears to be gene and tissue dependent and may rely on its impact on the level of ciliary cAMP production. Although *in vitro* modulation of Hh signaling yielded promising results, pharmacological studies in patients are unlikely to be executed because of the risk of serious side effects including medulloblastoma associated with Hh stimulation (Molinari and Sayer, 2017).

YAP inhibition

The Hippo pathway controls numerous biological processes and is an important modulator of cell proliferation and organ size (Müller and Schermer, 2020). NPHP4 represses the Hippo signaling pathways through inhibition of LATS1/2-mediated phosphorylation of YAP and TAZ transcription factors, thereby stimulating transcription of target genes and cell proliferation (Habbig et al., 2011). In addition, InvsC proteins including NEK8/NPHP9 and NPHP3 form a complex that controls nuclear translocation of YAP/TAZ and transcription of target genes (Habbig et al., 2012; Frank et al., 2013). Dysregulation of the Hippo pathway can cause antiproliferative signaling resulting in hypodysplastic phenotypes and loss of differentiation, or increased proliferation leading to cystic phenotypes depending on the type of mutation (Habbig et al., 2011; Grampa et al., 2016; Müller and Schermer, 2019; Xu et al., 2020).

Transient *Nek8* knockdown in mIMCD3 cells resulted in increased YAP activation and enlarged spheroids, which could be rescued by administration of Verteporfin, an inhibitor of YAP transcriptional activity. Verteporfin additionally rescued pronephric cysts in zebrafish embryos overexpressing human NEK8 (Grampa et al., 2016). Verteporfin also reduced fibrosis in the unilateral ureteral obstruction mouse model (Szeto et al., 2016). Interestingly, Hippo components *Mst1/Mst2* double knockout mice presented with an NPH-resembling phenotype comprising fibrosis, tubular dilation and thickening of tubular basement membranes. Additional knockout of YAP rescued this kidney phenotype (Xu et al., 2020), further indicating that targeting of the Hippo pathway could be an interesting approach for NPH.

Wnt inhibition

Another key developmental pathway is the Wingless-Int-1 (Wnt) pathway, although the role of cilia in canonical, β-catenin-dependent Wnt signaling remains controversial (Wheway et al., 2018). Proteins from the InvsC disrupted in infantile NPH including INVS/NPHP2 and NPHP3 have been proposed to be required for the switch from canonical Wnt signaling, involved in cell proliferation, to non-canonical Wnt signaling which maintains planar cell polarity, although the precise role in cystogenesis is debated (Simons et al., 2005; Bergmann et al., 2008; Sugiyama et al., 2011; Wang et al., 2018). Planar cell polarity is essential for oriented cell division which controls tubule elongation and is impaired in most murine renal ciliopathy models (Fischer and Pontoglio, 2009). Interestingly, RPGRIP1L and NPHP4 were also involved in Wnt signaling through their functional interaction with INVS (Burckle et al., 2011; Mahuzier et al., 2012).

Increased canonical Wnt signaling has been suggested to induce cystogenesis in PKD and NPH (Malik et al., 2020). Knockdown of *DCDC2/NPHP19* has been shown to activate the canonical Wnt pathway and cause pronephric cyst formation in zebrafish, a phenotype which could be rescued by a β-catenin inhibitor (Schueler et al., 2015).

Targeting Cilia-Independent Signaling Pathways and Cell Cycle Regulation

CDKs

Specific ciliary proteins are involved in DDR signaling and consequent cell cycle regulation. Although drugs that interfere directly with DDR signaling have not been studied in this context, the dysregulated cell cycle has been investigated as a target for the treatment of cysts and fibrosis in renal ciliopathies (Ibraghimov-Beskrovnaya, 2007; Choi et al., 2013).

Administration of the broad CDK inhibitor roscovitine (which targets CDK1, CDK2, CDK5 and CDK7, arresting the cell cycle) effectively arrested kidney volume expansion, cyst progression and renal insufficiency in *jck/Nek8/Nphp9* and *cpk* (cystin) mouse models of infantile NPH and PKD, respectively, with long-lasting effects. Analysis of the targets of roscovitine revealed induction of a G1/S cell-cycle block, transcriptional regulation and inhibition of apoptosis as mechanisms of action (Bukanov et al., 2006). In addition to the mouse models, roscovitine treatment also showed partial rescue of pronephric cysts and improved renal filtration capacity in zebrafish morphants of ciliopathy-associated genes (Tobin and Beales, 2008). Another study in *jck/Nek8/Nphp9* mice demonstrated that roscovitine ameliorated the elongated cilia phenotype and restored tubular epithelial differentiation, while conditional inactivation of CDK5 reduced cilia length, total kidney volume and cyst formation (Husson et al., 2016). In contrast, *Cdk2*-deficient *jck/Nek8/Nphp9* mice showed no improvement of renal cyst growth, inflammation and fibrosis, likely due to compensatory upregulation of *Cdk1*. In addition, treatment with the mTOR inhibitor rapamycin reduced Cdk1 and Cdk2 activity and attenuated the cystic phenotype, suggesting that the effect of mTOR inhibition is partly mediated by CDK inhibition (Zhang et al., 2020). Finally, roscovitine was demonstrated to attenuate renal cyst progression in a kidney-specific *Cep164*-knockout mouse model characterized by rapidly progressive cystic kidney enlargement (Airik et al., 2019). In summary, studies performed mostly in models of infantile NPH have demonstrated that targeting cell cycle dysregulation and proliferation using CDK inhibitors is an efficient approach to limit cyst growth. Of note, part of the effects of roscovitine, and also of its derivative CR8, could however be linked to its potent

inhibition of Casein Kinase 1 family members which expression pattern is perturbed in cystic mouse model including infantile NPH models (*pcy/Nphp3*, *Jck/Nek8/Nphp9)* (Billot et al., 2018). Interestingly, this study also indicates that the expression of the cell cycle regulator p21cip1/WAF1, which inhibits CDK2, is decreased in all cystic models while it is increased in the kidneys of *Nphp4* mutant mice, again suggesting differential pathophysiological mechanisms between cystic infantile and juvenile forms of NPH.

Interestingly, targeting of CDK1/2 was also shown to be effective in a *Cep290/Nphp6* mouse model characterized by slowly progressive kidney disease. Treatment of kidney cells from *Cep290*-deficient mice with CDK1/2 inhibitor rescued DNA-damage signaling, supernumerary centrioles and ciliation defects (Slaats et al., 2015). Furthermore, knockdown of CDK5 in URECs from a patient with Joubert syndrome with compound heterozygous mutations in *CEP290* mitigated the elongated cilia phenotype observed in these cells. In addition, treatment of the cells with the Hh agonist purmorphamine reduced expression of CDK5, suggesting a convergence of the Hh and CDK signaling pathways (Srivastava et al., 2017).

Calmodulin and Ca^{2+}/calmodulin-dependent protein kinase II

Ca^{2+}/calmodulin-dependent protein kinase II (CaMKII) is an important mediator of the endoplasmic reticulum stress response, oxidative stress and the mitochondrial apoptotic pathway, which were shown to be upregulated in kidneys from *jck/Nek8/Nphp9* mice. Pharmacological inhibition of CaMKII restored these pathways and significantly reduced kidney volume and cystogenesis (Bracken et al., 2016). CaMKII additionally has a role in cell cycle progression (Skelding et al., 2011). CaMKII inhibition could therefore also reduce cystogenesis through a mechanism similar to CDK inhibitors. Interestingly, calmodulin is known to bind to IQCB1/NPHP5 (Otto et al., 2005) and was recently shown to negatively regulate the amount of NPHP5 present at the transition zone (Kim et al., 2018). Eupatilin, a compound able to rescue ciliogenesis in *CEP290* invalidated cells (see below), directly modulates the calmodulin/NPHP5 interaction therefore increasing the amount of NPHP5 at the transition zone in the absence of CEP90 (Kim et al., 2018). Interestingly, Eupatilin was recently shown to improve cilia-related phenotypes in the context of *RPGRIP1L/NPHP8* suggesting that it might present broader potential in transition zone-related NPH (Wiegering et al., 2021).

ERK and p38-MAPK inhibition

The ERK pathway (downstream of receptor tyrosine kinases and GPCR signaling), is involved in regulation of cell cycle and proliferation and was shown to be activated as a consequence of increased cAMP in ADPKD (Yamaguchi et al., 2003). Inhibition of ERK activation slowed down disease progression in *pcy/Nphp3* mice (Omori et al., 2006). It also resulted in decreased fibrosis and cystogenesis in an *Invs/Nphp2* mouse model (Okumura et al., 2009). The same group later showed that a p38 mitogen-activated protein kinase (MAPK) inhibitor reduced renal fibrosis but not cystogenesis independently of ERK activation, however, this did not improve kidney function and survival rate of *Invs* mice (Sugiyama et al., 2012).

Inflammation and Senescence

In addition to ciliary signaling pathways and cystogenesis, specific interventions directly target development of tubulointerstitial fibrosis, a hallmark histopathological feature of juvenile and adult NPH. The role of inflammation in fibrosis has been discussed in section "Inflammation and Senescence." Several groups have targeted the immune response in NPH. For example, rodent models of infantile NPH (Han:SPRD-*Cy/Anks6/Nphp16* rats and *pcy/nphp3* mice) treated with the anti-inflammatory drug methylprednisolone showed reduced fibrosis and preserved kidney function compared to untreated animals (Gattone et al., 1995). Treatment of Han:SPRD-*Cy/Anks6/Nphp16* rats with the anti-inflammatory drug resveratrol attenuated cyst formation, elevated serum creatinine and macrophage infiltration partly through inhibition of mTOR signaling and the NF-kB pathway (Wu et al., 2016). Furthermore, a study using LPK/*Nek8/Nphp9* mutant rats found that treatment with the immunomodulatory drug dimethyl fumarate, which activates the Nrf2 pathway and inhibits NF-kB signaling, reduced macrophage infiltration but did not ameliorate cyst progression or renal insufficiency (Oey et al., 2018).

Replicative senescence in tubular cells, which leads to secretion of pro-inflammatory molecules, has been shown to cause extensive kidney damage in *Glis2/Nphp7* knockout mice (Jin et al., 2020) (see section "Pathophysiology of Nephronophthisis"). The senolytic (anti-aging) drug forkhead box protein O4 D-retro inverso (FOXO4-DRI), which induces apoptosis of senescent cells through inhibition of FOXO4/P53 interaction (Baar et al., 2017), effectively eliminated senescent cells in mouse models for acute kidney disease and reduced inflammation and tubulointerstitial fibrosis while preserving renal function in *Glis2*-knockout mice (Jin et al., 2019, 2020). The role of senescence and the efficacy of senolytic drugs in other types of NPH is unknown and should be investigated further.

Glycosphingolipids and Cholesterol

Several studies demonstrated that glycosphingolipid metabolism is perturbed in PKD (Deshmukh et al., 1994; Chatterjee et al., 1996). Interestingly, glycosphingolipids are components of rafts, membrane microdomains involved in the assembly of signaling platforms at the plasma membrane that are also present at the ciliary membrane. Dysregulated production of those lipids may therefore contribute to perturbed signaling and therefore to cystogenesis (Natoli et al., 2020). Interestingly, glucosylceramides, which are glycosphingolipid precursors, were found to be highly increased in the kidneys of cystic mouse models including in *pcy/Nphp3* and *Jck/Nek8/Nphp9* mice and pharmacological or genetic inhibition of glucosylceramide synthase activity efficiently reduced renal cysts in *Jck/Nek8/Nphp9* mice (Natoli et al., 2010, 2012).

Besides glycosphingolipids, cholesterol is also involved in many cellular functions including in signaling through Ras and plasma membrane lipid rafts (Ahmadi et al., 2020). Cholesterol synthesis can be modulated by statins, a family of molecules

which have been widely used to treat hypercholesterolemia. In addition to its classical well-established functions, cholesterol is enriched in the ciliary membrane and was revealed to play an important role in ciliogenesis (Maerz et al., 2019) as well as in Hh signaling as a direct modulator of SMO activity (Kong et al., 2019). Interestingly, and in agreement with those observations, mutations in genes encoding actors of the cholesterol biosynthesis pathway were associated with skeletal disorders (Suzuki et al., 2020) resembling those associated with mutations in IFT-A subunit encoding genes (see introduction). Statins were shown to improve CKD in various animal models (Ecder, 2016) and were also shown to improve renal function in the *Cy/Anks6/Nphp16* rat model, likely through an effect on the renin-angiotensin system (Gile et al., 1995; Zafar et al., 2007). Several studies obtained conflicting results on the beneficial effects of statins in PKD patients (Fassett et al., 2010; Cadnapaphornchai et al., 2014; Brosnahan et al., 2017; Müller and Schermer, 2019). It is currently not known if cholesterol dysregulation is associated with NPH or if modulating cholesterol synthesis could be an interesting approach in the context of NPH other than in infantile NPH rodent models.

Microtubule Dynamics

Cytoplasmic microtubule dynamics directly influences ciliogenesis (Sharma et al., 2011) and their reorganization tightly controls polarity establishment in epithelia (Toya and Takeichi, 2016). Interestingly, ciliopathy conditions were associated with increased stability of cytoplasmic microtubules (Berbari et al., 2013), a phenotype which was more deeply investigated in the context of NPH and *TRAF3IP1/IFT54* mutant conditions (Berbari et al., 2011; Bizet et al., 2015). Impaired IFT54 function led to overexpression of the microtubule associated protein MAP4 and lowering MAP4 expression rescued polarity defects *in vitro* and partially rescued ciliopathy phenotypes in zebrafish morphants (Bizet et al., 2015). It would be interesting to investigate if stabilization of the microtubules is a phenotype shared with other NPHP defects. These results indicate that modulators of cytoplasmic microtubule dynamics could be a potential therapeutic approach for NPH.

Interestingly, expression of HDAC6 was found to be increased in various kidney conditions including fibrotic, ADPKD and CKD models, and HDAC6 inhibitors showed a positive effect on disease evolution (Ke et al., 2018). HDAC6 is a histone deacetylase which is key regulator of the cytoskeleton through deacetylation of α-tubulin and cortactin. HADC6 was also found to be involved in cilia disassembly through destabilization of axonemal microtubules (Pugacheva et al., 2007; Loktev et al., 2008). Functions of HDAC6 are wide and complex, however, and its overexpression likely yields deacetylation which is expected to result in destabilization of microtubules (contrary to increased stability of microtubules observed in *TRAF3IP1/IFT54* mutant conditions). This suggests differential microtubule involvement between NPH and other renal disorders.

Drug Screens for Nephronophthisis

Pharmacological screens for ciliopathies comprise small molecule compound screens and high-throughput testing of chemical libraries such as United States Food and Drug Administration (FDA)-approved drugs with the aim of drug repurposing. The latter is an attractive option because it is cheaper, faster, and has a higher success rate than development of novel drugs (Forsythe et al., 2018). Thus far, compound screens in cystic renal disease have mostly been performed for ADPKD, the most common ciliopathy affecting the kidney (Booij et al., 2017, 2019). High-throughput drug screens for NPH-related ciliopathies are scarce in the literature and findings have not been replicated (Kim and Kim, 2019).

One of the few published compound screens was conducted by Kim et al. (2018), who screened a library of 2,789 synthetic and natural compounds in *CEP290*-invalidated human RPE1 cells and identified 22 compounds that restored ciliogenesis, of which the flavonoid eupatilin showed the strongest effect. Eupatilin was demonstrated to restore IQCB1/NPHP5 levels at the ciliary transition zone in the absence of CEP290 (see above). Eupatilin treatment did not significantly rescue ciliogenesis defects associated with the knockdown of other NPH-associated genes, including *NPHP4*, *CEP164/NPHP15* and *CEP83/NPHP18*, suggesting a *CEP290*-specific effect. Treatment of rd16 mice harboring a *Cep290* in-frame deletion with eupatilin improved cone photoreceptor function, showing its efficacy *in vivo* (Kim et al., 2018). However, because this *Cep290* mouse model of Leber congenital amaurosis (LCA) does not present a kidney phenotype (Chang et al., 2006), the effect of eupatilin on NPH was not investigated.

Two compound screens were performed in zebrafish models. A library of 115 compounds targeting cilia specific pathways was screened in *pkd2*- and *ift172*-morphant embryos which present pronephric cysts (Cao et al., 2009). A histone deacetylase (HDAC) inhibitor was identified that suppressed cyst formation in *pkd2*- but not in *ift172*-morphants, making this finding less relevant for NPH. Cox2-inhibitors and a CaMKII inhibitor were identified to affect extrarenal ciliopathy phenotypes in both models (Cao et al., 2009). In addition, an automated imaging pipeline was recently developed to efficiently profile a large compound library in *ift172*-morphant zebrafish embryos, however, identified pronephric cyst-modifying compounds were not reported (Pandey et al., 2019).

Another strategy that has been employed is an untargeted small interfering RNA (siRNA) screen to identify genes that modulate ciliogenesis and can be targeted pharmacologically. For example, an siRNA screen in RPE1 cells targeting 7,784 therapeutically relevant genes identified 36 positive modulators of ciliogenesis including proteins involved in the regulation of actin cytoskeleton dynamics. Pharmacological inhibition of actin polymerization using cytochalasin D rescued ciliogenesis in *Ift88*-mutant mouse embryonic fibroblasts (Kim et al., 2010). However, cytochalasin D is likely not specific enough for treatment of ciliopathies. In addition, a recent genome-wide siRNA screen identified 10 genes that rescued aberrant Wnt signaling in *BBS4*-depleted cells (Tsai et al., 2019). One of the identified genes encoded USP35, a negative regulator of the ubiquitin proteasome system. Suppression of USP35 improved the kidney phenotype in *bbs4*-morphant zebrafish embryos, suggesting that impaired clearance of signaling molecules could play a role in NPH

pathophysiology. Next, a small molecule inhibitor of another deubiquitinase (USP14; IU1) was tested in zebrafish and did not have a significant effect on the kidney phenotype, consistent with the results from the screen (Tsai et al., 2019). High-throughput phenotype-based screening methods using zebrafish and cell models have been outlined for renal ciliopathies (Gehrig et al., 2018; Pandey et al., 2019; Zhang P. et al., 2019).

GENE-BASED THERAPY

A promising gene-based strategy makes use of antisense-oligonucleotides (ASO) to modulate splicing. This approach was first employed to correct a recurrent intronic *CEP290/NPHP6* mutation present in 10–15% of LCA cases, which introduces a cryptic splice site leading to inclusion of a pseudo exon with a premature stop codon (Collin et al., 2012). ASO targeting of this mutation successfully restored mRNA splicing, CEP290 expression and cilia in patient cells and patient iPSC-derived retinal organoids (Gerard et al., 2012; Parfitt et al., 2016) and led to vision improvement in LCA patients (Cideciyan et al., 2019). ASO was also used to induce skipping of nonsense mutation-bearing exons as well as treat non-retinal manifestations. For example, systemic ASO treatment of a *Cep290* mouse model of Joubert syndrome resulted in reduced kidney cyst burden compared to untreated mice (Ramsbottom et al., 2018). While *CEP290* is unique in that it contains numerous in-frame exons that can be targeted by ASO, basal exon skipping has also been shown to modify the phenotype in *CC2D2A*-related Joubert syndrome and could be induced in other ciliopathy-associated genes (Drivas et al., 2015; Ramsbottom et al., 2018). Although ASO cannot be applied in case of a homozygous *NPHP1* deletion which is the most common cause of NPH, it can be used to target downstream dysregulated genes as was demonstrated for *Agt* encoding angiotensinogen in the treatment of *Pkd1* mice (Saigusa et al., 2016; Fitzgibbon et al., 2018). An advantage of ASO-based treatment for NPH is that circulating ASO are cleared by and accumulate in the kidney where they are taken up especially but not exclusively by tubular cells, facilitating delivery to target tissue (Oberbauer et al., 1996; Lakhia et al., 2019). Research into ligand-based targeted ASO delivery is ongoing (Kim and Kim, 2019).

Additionally, CRISPR/Cas9 has shown promising results for the treatment of NPH in *in vitro* systems. In contrast to classical gene therapy in which a wild-type copy of the gene is integrated into the host genome, CRISPR/Cas9 is a precise genome-editing technique that allows use of a repair template. This correction approach is widely used to obtain isogenic control iPSCs and it was shown to efficiently restore the cilia phenotype in iPSC-derived kidney organoids from a patient with *IFT140*-related Mainzer-Saldino syndrome. In addition, spheroids from epithelial cells sorted from uncorrected organoids were less polarized than spheroids from gene-corrected cells (Forbes et al., 2018). However, implementation in patients with renal ciliopathies is met by technical challenges (for example off-target effects, delivery to the kidney and evading an immune response) and ethical obstacles. In addition, the extreme genetic heterogeneity in NPH-related ciliopathies, i.e., the absence of mutation hot spots except for the homozygous *NPHP1* deletion, and possible role of modifier variants, limit the practical and financial feasibility of gene-targeted therapies (Kim and Kim, 2019).

DEVELOPMENTS AND FUTURE DIRECTIONS

Nephronophthisis is an important hereditary cause of ESRD in children and young adults for which there is currently no targeted therapy. Pharmacological interventions aimed at restoring aberrant signal transduction (for example V2R antagonists) or dysregulated cell cycle (for example CDK inhibitors) as well as the use of immunomodulatory drugs (for example senolytic drugs) have improved cystic phenotypes in zebrafish and rodent models of NPH (Gattone et al., 2003; Bukanov et al., 2006; Jin et al., 2020). In addition, ASO therapy partly restored gene expression and reversed cyst burden in a *Cep290* mouse model of Joubert syndrome (Ramsbottom et al., 2018). ASO therapy has been approved by the FDA for clinical use in several human diseases including spinal muscular atrophy and Duchenne muscular dystrophy, suggesting that application in NPH is feasible (Fay et al., 2020). However, the *Cep290* mouse model, like most rodent and zebrafish models reviewed here, does not exhibit the massive tubulointerstitial fibrosis observed in NPH patients, which severely limits conclusions about efficacy of potential therapy for juvenile NPH (Hynes et al., 2014; Ramsbottom et al., 2018).

Truly representative models for juvenile NPH are not available yet except for *Glis2/Nphp7* knockout mice, and *GLIS2* mutations are an atypical and rare cause of NPH (Lu et al., 2016). In fact, most mouse models used in research on NPH therapy correspond genetically and phenotypically mainly to infantile NPH, which represents a minor fraction of NPH patients, is histologically different from the more prevalent juvenile NPH and shows a more rapid disease course (see introduction).

Alternative non-orthologous animal models that mimic juvenile/adult NPH could also be explored. For example, mice with kidney-specific knockout of *Lkb1* showed a urine concentration defect, diminished kidney size, cysts at the corticomedullary junction, tubular basement membrane thickening, inflammation and fibrosis (Han et al., 2016; Viau et al., 2018). Interestingly, LKB1 (STK11) was shown to be part of a ciliary module comprising NPHP1, NEK7, ANKS3 and polycystin-1 that regulates cilia-controlled secretion of CCL2, a chemokine that promotes macrophage recruitment and consequent cyst growth and interstitial inflammation (Viau et al., 2018). In addition, mice with kidney-specific knockout of *Prkar1a,* a regulatory subunit of PKA, presented with normal-sized kidneys with small cysts and interstitial fibrosis (Ye et al., 2017), suggesting that cAMP signaling defects not only play a role in cystogenesis but also in the development of juvenile NPH-specific phenotypes. Kidney-specific knockout of *Aatf* (DNA damage response target Apoptosis Antagonizing Transcription Factor), encoding a regulator of p53 during DDR, also leads to phenotypes similar to juvenile NPH including tubular atrophy,

interstitial fibrosis and cysts at the corticomedullary junction (Jain et al., 2019). Lastly, *Fan1* knockout mice treated with cisplatin showed a histological phenotype that included tubular dilations, tubular basement membrane thickening and interstitial fibrosis, resembling juvenile NPH except for the presence of karyomegalic nuclei (Zhou et al., 2012; Airik et al., 2016). These models might point to key signaling pathways and might prove more useful for testing fibrosis-modulating drugs for juvenile NPH than genetically identical models.

During the past 5 years, an increasing number of pharmacological studies in NPH have focused on fibrosis-associated pathways and fibrosis-modulating agents. Drugs that interfere with cell cycle progression such as CDK inhibitors typically affect ubiquitous and essential cellular processes, which limits their application in NPH treatment. Alternatively, the pro-inflammatory response downstream of cell cycle arrest can be targeted to prevent tubular damage and fibrosis (Jin et al., 2020). Specifically, the role of cellular senescence and efficacy of senolytic drugs remains to be investigated in prevalent NPH subtypes. Of note, the CDK inhibitor roscovitine was shown to promote apoptosis of neutrophils and enhance resolution of inflammation, indicating crosstalk between both mechanisms (Rossi et al., 2006). Additional progress can be gained from repurposing of medication approved for other fibrotic kidney diseases, for example COX inhibitors which have shown potential in the prevention of diabetic nephropathy in addition to ameliorating NPH in rodent models (Goru, 2018).

Despite *in vitro* and *in vivo* evidence for drugs that ameliorate (part of) the NPH phenotype, there is a striking lack of clinical trials for NPH. To exclude possible publication bias, ClinicalTrials.gov was queried for registered ongoing and future clinical trials in ciliopathies. This yielded trials for ADPKD, ARPKD, primary ciliary dyskinesia, Von Hippel Lindau disease and various extrarenal manifestations of ciliopathies, including obesity in Bardet-Biedl and Alström syndromes (clinicaltrials.gov – access date 2021 April 12). There are several possible reasons for the absence of clinical trials in NPH, including challenges related to the genetic and phenotypic heterogeneity in NPH, for example small sample sizes and variability within cohorts, the relatively short therapeutic window compared to ADPKD, challenges of clinical trials in a pediatric population and financial aspects of orphan drug development.

In light of this, research groups should capitalize on available data in renal ciliopathies and investigate associations between medication for (extra)renal symptoms and fluctuation in renal phenotype, for example statins which can be prescribed to treat hypercholesterolemia in patients with Bardet-Biedl or Alström syndrome have shown promising but inconsistent results in ADPKD (Fassett et al., 2010; Cadnapaphornchai et al., 2014; Brosnahan et al., 2017; Müller and Schermer, 2019). In addition, data should be collected to gain insight into ciliopathy-specific symptomatic treatment. For example, in a patient with *NPHP3*-related infantile NPH isosorbide dinitrate was used to treat hypertension by restoring nitric oxide generation (Strong et al., 2018). Nitric oxide is produced by vascular endothelial cells in response to ciliary sensation of shear stress and causes compensatory vasodilatation, a process that is impaired in ciliopathies. Targeting this cilia-specific cause of hypertension was more effective in this patient than classic anti-hypertensive medication (Strong et al., 2018).

Another consequence of the low prevalence and phenotypic heterogeneity in NPH is the need for personalized therapy. Developments in *in vitro* modeling, for example the use of URECs or the generation of kidney organoids from iPSCs, enable testing of medication directly in NPH patient-derived cells that harbor the causal mutation and the genetic background of the patient including modifier gene variants. This should facilitate translation of findings back to therapy in individual patients. Despite current limitations, improvement of NPH-kidney organoids can aid drug development in NPH, as has been successfully illustrated in a kidney organoid model of cystinosis (Hollywood et al., 2020).

Patient-derived organoids can be combined with CRISPR/Cas9 technology to correct the NPH phenotype for various applications (Steichen et al., 2020). To overcome technical and ethical hurdles associated with *in vivo* therapeutic application of CRISPR/Cas9, genome editing can be applied *ex vivo,* for example to populate bioartificial kidneys with corrected patient-derived renal epithelial cells as a future alternative for donor kidneys if safety issues of cell-based therapies have been sufficiently resolved (McKee and Wingert, 2016; Mihajlovic et al., 2019a,b). Bioengineering strategies in kidney regeneration have been reviewed by Peired et al. (2020).

Besides *ex vivo* applications, developments in targeted delivery methods bring gene therapy in NPH patients one step closer (Liu et al., 2019). Whereas adeno-associated virus (AAV)-vector delivery of wildtype gene and CRISPR/Cas9 to retinal cells via subretinal injection has been demonstrated in *Bbs4* and *Cep290* mouse models, respectively, delivery of viral vector to the kidney via systemic injection is limited because AAV particles do not pass the glomerular filtration barrier (Simons et al., 2011; Ruan et al., 2017; Rubin et al., 2019). Targeted delivery and nephron segment-specific gene expression has been achieved via retrograde ureteral infusion of AAV9 vector in combination with segment-specific promoters in mice (Asico et al., 2018). This system of targeted delivery could be used for gene-based therapy in NPH. In addition, systemic administration of (artificial) extracellular vesicles or nanoparticles has been proposed for targeted delivery of siRNA or drugs to kidney cells (Barile and Vassalli, 2017; Oroojalian et al., 2020).

CONCLUSION

Many potential therapies for NPH have been explored in model systems, from targeted treatments aimed at restoring ciliary signaling, CDK inhibition, immune system suppression and ASO therapy to untargeted drug screens. Translation of results is limited by the lack of animal models that recapitulate the juvenile NPH phenotype and in the case of infantile NPH, for which models exist, by the short therapeutic window. Employment of non-orthologous animal models and developments in organoid

technology can potentially fill this gap and provide new opportunities for personalized treatments. Ultimately, safety and efficacy of potential NPH therapies will have to be tested in clinical trials. Given obstacles of genetic and phenotypic heterogeneity in renal ciliopathies and clinical trials in children, repurposing of medication used in other cystic or chronic kidney diseases could be the most viable approach. In addition to identification of effective drugs, successful treatment or prevention of NPH depends on the discovery of biomarkers that identify NPH patients in an early disease stage.

AUTHOR CONTRIBUTIONS

MS and AB conceived the idea and wrote the manuscript. AB and SS provided critical feedback. All authors contributed to the article and approved the submitted version.

FUNDING

The researchers received funding from the Dutch Kidney Foundation under grant agreement 19OK001 TACTICS to MS, the European Molecular Biology Organization (EMBO) Short-Term Fellowship to MS and the Academy Ter Meulen grant of the Academy Medical Sciences Fund of the Royal Netherlands Academy of Arts and Sciences (KNAW) to MS, and from the Agence Nationale de la Recherche (ANR) to AB and SS, including the "Investissements d'Avenir" program (ANR-10-IAHU-01), and the "RHU-C'IL-LICO" as part of the second "Investissements d'Avenir" program (reference: ANR-17-RHUS-0002).

ACKNOWLEDGMENTS

The authors thank Amandine Viau for her constructive criticism of the manuscript.

REFERENCES

Acosta, J. C., Banito, A., Wuestefeld, T., Georgilis, A., Janich, P., Morton, J. P., et al. (2013). A complex secretory program orchestrated by the inflammasome controls paracrine senescence. *Nat. Cell Biol.* 15, 978–992.

Aguilar, A., Meunier, A., Strehl, L., Martinovic, J., Bonniere, M., Attie-Bitach, T., et al. (2012). Analysis of human samples reveals impaired SHH-dependent cerebellar development in Joubert syndrome/Meckel syndrome. *Proc. Natl. Acad. Sci. U.S.A.* 109, 16951–16956. doi: 10.1073/pnas.1201408109

Ahmadi, M., Amiri, S., Pecic, S., Machaj, F., Rosik, J., Łos, M. J., et al. (2020). Pleiotropic effects of statins: a focus on cancer. *Biochim. Biophys. Acta Mol. Basis Dis.* 2020:1866. doi: 10.1016/j.bbadis.2020.165968

Airik, R., Airik, M., Schueler, M., Bates, C. M., and Hildebrandt, F. (2019). Roscovitine blocks collecting duct cyst growth in Cep164-deficient kidneys. *Kidney Int.* 96, 320–326. doi: 10.1016/j.kint.2019.04.014

Airik, R., Schueler, M., Airik, M., Cho, J., Porath, J. D., Mukherjee, E., et al. (2016). A FANCD2/FANCI-associated nuclease 1-knockout model develops karyomegalic interstitial nephritis. *J. Am. Soc. Nephrol.* 27, 3552–3559. doi: 10.1681/ASN.2015101108

Airik, R., Slaats, G. G., Guo, Z., Weiss, A. C., Khan, N., Ghosh, A., et al. (2014). Renal-retinal ciliopathy gene Sdccag8 regulates DNA damage response signaling. *J. Am. Soc. Nephrol.* 25, 2573–2583. doi: 10.1681/ASN.2013050565

Akella, J. S., Carter, S. P., Nguyen, K., Tsiropoulou, S., Moran, A. L., Silva, M., et al. (2020). Ciliary rab28 and the BBSome negatively regulate extracellular vesicle shedding. *eLife* 9, 1–27. doi: 10.7554/eLife.50580

Alcaraz, W. A., Gold, D. A., Raponi, E., Gent, P. M., Concepcion, D., and Hamilton, B. A. (2006). *Zfp423* controls proliferation and differentiation of neural precursors in cerebellar vermis formation. *Proc. Natl. Acad. Sci. USA* 103, 19424–19429. doi: 10.1073/pnas.0609184103

Anvarian, Z., Mykytyn, K., Mukhopadhyay, S., Pedersen, L. B., and Christensen, S. T. (2019). Cellular signalling by primary cilia in development, organ function and disease. *Nat. Rev. Nephrol.* 15, 199–219. doi: 10.1038/s41581-019-0116-9

Arts, H. H., Doherty, D., Van Beersum, S. E. C., Parisi, M. A., Letteboer, S. J. F., Gorden, N. T., et al. (2007). Mutations in the gene encoding the basal body protein RPGRIP1L, a nephrocystin-4 interactor, cause Joubert syndrome. *Nat. Genet.* 39, 882–888. doi: 10.1038/ng2069

Ashe, A., Butterfield, N. C., Town, L., Courtney, A. D., Cooper, A. N., Ferguson, C., et al. (2012). Mutations in mouse *Ift144* model the craniofacial, limb and rib defects in skeletal ciliopathies. *Hum. Mol. Genet.* 21, 1808–1823. doi: 10.1093/hmg/ddr613

Asico, L. D., Cuevas, S., Ma, X., Jose, P. A., Armando, I., and Konkalmatt, P. R. (2018). Nephron segment-specific gene expression using AAV vectors. *Biochem. Biophys. Res. Commun.* 497, 19–24. doi: 10.1016/j.bbrc.2018.01.169

Atala, A., Freeman, M. R., Mandell, J., and Beier, D. R. (1993). Juvenile cystic kidneys (jck): a new mouse mutation which causes polycystic kidneys. *Kidney Int.* 43, 1081–1085. doi: 10.1038/ki.1993.151

Attanasio, M., Uhlenhaut, N. H., Sousa, V. H., O'Toole, J. F., Otto, E., Anlag, K., et al. (2007). Loss of GLIS2 causes nephronophthisis in humans and mice by increased apoptosis and fibrosis. *Nat. Genet.* 39, 1018–1024.

Baar, M. P., Brandt, R. M., Putavet, D. A., Klein, J. D., Derks, K. W., Bourgeois, B. R., et al. (2017). Targeted apoptosis of senescent cells restores tissue homeostasis in response to chemotoxicity and aging. *Cell* 196, 132–147. doi: 10.1016/j.cell.2017.02.031

Bakey, Z., Bihoreau, M. T., Piedagnel, R., Delestré, L., Arnould, C., De Villiers, A. D., et al. (2015). The SAM domain of ANKS6 has different interacting partners and mutations can induce different cystic phenotypes. *Kidney Int.* 88, 299–310. doi: 10.1038/ki.2015.122

Barile, L., and Vassalli, G. (2017). Exosomes: therapy delivery tools and biomarkers of diseases. *Pharmacol. Ther.* 174, 63–78. doi: 10.1016/j.pharmthera.2017.02.020

Berbari, N. F., Kin, N. W., Sharma, N., Michaud, E. J., Kesterson, R. A., and Yoder, B. K. (2011). Mutations in Traf3ip1 reveal defects in ciliogenesis, embryonic development, and altered cell size regulation. *Dev. Biol.* 360, 66–76. doi: 10.1016/j.ydbio.2011.09.001

Berbari, N. F., Sharma, N., Malarkey, E. B., Pieczynski, J. N., Boddu, R., Gaertig, J., et al. (2013). Microtubule modifications and stability are altered by cilia perturbation and in cystic kidney disease. *Cytoskeleton* 70, 24–31. doi: 10.1002/cm.21088

Bergmann, C. (2018). Genetics of autosomal recessive polycystic kidney disease and its differential diagnoses. *Front. Pediatr.* 5:221. doi: 10.3389/fped.2017.00221

Bergmann, C., Fliegauf, M., Brüchle, N. O., Frank, V., Olbrich, H., Kirschner, J., et al. (2008). Loss of Nephrocystin-3 function can cause embryonic lethality, meckel-gruber-like syndrome, situs inversus, and renal-hepatic-pancreatic Dysplasia. *Am. J. Hum. Genet.* 82, 959–970. doi: 10.1016/j.ajhg.2008.02.017

Billot, K., Coquil, C., Villiers, B., Josselin-Foll, B., Desban, N., Delehouzé, C., et al. (2018). Casein kinase 1ε and 1α as novel players in polycystic kidney disease and mechanistic targets for (R)-roscovitine and (S)-CR8. *Am. J. Physiol. Ren. Physiol.* 315, F57–F73. doi: 10.1152/ajprenal.00489.2017

Bizet, A. A., Becker-Heck, A., Ryan, R., Weber, K., Filhol, E., Krug, P., et al. (2015). Mutations in TRAF3IP1/IFT54 reveal a new role for IFT proteins in microtubule stabilization. *Nat. Commun.* 6, 1–14. doi: 10.1038/ncomms9666

Bockenhauer, D., van 't Hoff, W., Dattani, M., Lehnhardt, A., Subtirelu, M., Hildebrandt, F., et al. (2010). Secondary nephrogenic diabetes insipidus as a complication of inherited renal diseases. *Bone* 23, 1–7. doi: 10.1159/000320117

Boehlke, C., Kotsis, F., Patel, V., Braeg, S., Bredt, S., Beyer, T., et al. (2010). Primary cilia regulate mTORC1 activity and cell size through Lkb1. *Nat. Cell Biol.* 12, 1115–1122. doi: 10.1038/ncb2117.Primary

Booij, T. H., Bange, H., Leonhard, W. N., Yan, K., Fokkelman, M., Kunnen, S. J., et al. (2017). High-throughput phenotypic screening of kinase inhibitors to identify drug targets for polycystic kidney disease. *SLAS Discov.* 22, 974–984. doi: 10.1177/2472555217716056

Booij, T. H., Leonhard, W. N., Bange, H., Yan, K., Fokkelman, M., Plugge, A. J., et al. (2019). In vitro 3D phenotypic drug screen identifies celastrol as an effective in vivo inhibitor of polycystic kidney disease. *J. Mol. Cell Biol.* 12, 644–653. doi: 10.1093/jmcb/mjz029

Boukhalfa, A., Miceli, C., Ávalos, Y., Morel, E., and Dupont, N. (2019). Interplay between primary cilia, ubiquitin-proteasome system and autophagy. *Biochimie* 166, 286–292. doi: 10.1016/j.biochi.2019.06.009

Bracken, C., Beauverger, P., Duclos, O., Russo, R. J., Rogers, K. A., Husson, H., et al. (2016). CaMKII as a pathological mediator of ER stress, oxidative stress, and mitochondrial dysfunction in a murine model of nephronophthisis. *Am. J. Physiol. Ren. Physiol.* 310, F1414–F1422. doi: 10.1152/ajprenal.00426.2015

Braun, D. A., and Hildebrandt, F. (2017). Ciliopathies. *Cold Spring Harb. Perspect. Biol.* 9:a028191.

Bredrup, C., Saunier, S., Oud, M. M., Fiskerstrand, T., Hoischen, A., Brackman, D., et al. (2011). Ciliopathies with skeletal anomalies and renal insufficiency due to mutations in the IFT-A gene WDR19. *Am. J. Hum. Genet.* 89, 634–643. doi: 10.1016/j.ajhg.2011.10.001

Breslow, D. K., Hoogendoorn, S., Kopp, A. R., Morgens, D. W., Vu, B. K., Kennedy, M. C., et al. (2018). A CRISPR-based screen for Hedgehog signaling provides insights into ciliary function and ciliopathies. *Nat. Genet.* 50, 460–471. doi: 10.1038/s41588-018-0054-7.A

Brosnahan, G. M., Abebe, K. Z., Rahbari-Oskoui, F. F., Patterson, C. G., Bae, K. T., Schrier, R. W., et al. (2017). Effect of statin therapy on the progression of autosomal dominant polycystic kidney disease. a secondary analysis of the HALT PKD Trials. *Curr. Hypertens. Rev.* 13, 109–120. doi: 10.2174/1573402113666170427142815

Brown, J. H., Bihoreau, M. T., Hoffmann, S., Kranzlin, B., Tychinskaya, I., Obermuller, N., et al. (2005). Missense mutation in sterile alpha motif of novel protein SamCystin is associated with polycystic kidney disease in (cy/+) rat. *J. Am. Soc. Nephrol.* 16, 3517–3526. doi: 10.1681/ASN.2005060601

Bukanov, N. O., Smith, L. A., Klinger, K. W., and Ledbetter, S. R. (2006). Long-lasting arrest of murine polycystic kidney disease with CDK inhibitor roscovitine. *Nature* 444, 949–952. doi: 10.1038/nature05348

Burckle, C., Gaude, H. M., Vesque, C., Silbermann, F., Salomon, R., Jeanpierre, C., et al. (2011). Control of the Wnt pathways by nephrocystin-4 is required for morphogenesis of the zebrafish pronephros. *Hum. Mol. Genet.* 20, 2611–2627. doi: 10.1093/hmg/ddr164

Cadnapaphornchai, M. A., George, D. M., McFann, K., Wang, W., Gitomer, B., Strain, J. D., et al. (2014). Effect of pravastatin on total kidney volume, left ventricular mass index, and microalbuminuria in pediatric autosomal dominant polycystic kidney disease. *Clin. J. Am. Soc. Nephrol.* 9, 889–896. doi: 10.2215/CJN.08350813

Cao, Q., Harris, D. C. H., and Wang, Y. (2015). Macrophages in kidney injury, inflammation, and fibrosis. *Physiology* 30, 183–194. doi: 10.1152/physiol.00046.2014

Cao, Y., Semanchik, N., Lee, S. H., Somlo, S., Barbano, P. E., Coifman, R., et al. (2009). Chemical modifier screen identifies HDAC inhibitors as suppressors of PKD models. *Proc. Natl. Acad. Sci. U.S.A.* 106, 21819–21824. doi: 10.1073/pnas.0911987106

Caroli, A., Antiga, L., Cafaro, M., Fasolini, G., and Remuzzi, A. (2010). Reducing polycystic liver volume in ADPKD: effects of somatostatin analogue octreotide. *Clin. J. Am. Soc. Nephrol.* 5, 783–789. doi: 10.2215/CJN.05380709

Casoni, F., Croci, L., Bosone, C., D'Ambrosio, R., Badaloni, A., Gaudesi, D., et al. (2017). *Zfp423/ZNF423* regulates cell cycle progression, the mode of cell division and the DNA-damage response in purkinje neuron progenitors. *Dev.* 144, 3686–3697. doi: 10.1242/dev.155077

Chaki, M., Airik, R., Ghosh, A. K., Giles, R. H., Chen, R., Slaats, G. G., et al. (2012). Exome capture reveals ZNF423 and CEP164 mutations, linking renal ciliopathies to DNA damage response signaling. *Cell* 150, 533–548. doi: 10.1016/j.cell.2012.06.028.Exome

Chang, B., Khanna, H., Hawes, N., Jimeno, D., He, S., Lillo, C., et al. (2006). In-frame deletion in a novel centrosomal/ciliary protein CEP290/ NPHP6 perturbs its interaction with RPGR and results in early- onset retinal degeneration in the rd16 mouse. *Hum. Mol. Genet.* 15, 1847–1857.

Chatterjee, S., Shi, W. Y., Wilson, P., and Mazumdar, A. (1996). Role of lactosylceramide and MAP kinase in the proliferation of proximal tubular cells in human polycystic kidney disease. *J. Lipid Res.* 37, 1334–1344.

Chebib, F. T., Perrone, R. D., Chapman, A. B., Dahl, N. K., Harris, P. C., Mrug, M., et al. (2018). A practical guide for treatment of rapidly progressive ADPKD with tolvaptan. *J. Am. Soc. Nephrol.* 29, 2458–2470. doi: 10.1681/ASN.2018060590

Chebib, F. T., and Torres, V. E. (2016). Autosomal dominant polycystic kidney disease: core curriculum 2016. *Am. J. Kidney Dis.* 67, 792–810. doi: 10.1053/j.ajkd.2015.07.037

Chen, N. X., Moe, S. M., Eggleston-Gulyas, T., Chen, X., Hoffmeyer, W. D., Bacallao, R. L., et al. (2011). Calcimimetics inhibit renal pathology in rodent nephronophthisis. *Kidney Int.* 80, 612–619. doi: 10.1038/ki.2011.139

Cheng, L. E., Zhang, J., and Reed, R. R. (2007). The transcription factor *Zfp423/OAZ* is required for cerebellar development and CNS midline patterning. *Dev. Biol.* 307, 43–52. doi: 10.1016/j.ydbio.2007.04.005

Choi, H. J. C., Lin, J. R., Vannier, J. B., Slaats, G. G., Kile, A. C., Paulsen, R. D., et al. (2013). NEK8 links the ATR-regulated replication stress response and S phase CDK activity to renal ciliopathies. *Mol. Cell* 51, 423–439. doi: 10.1016/j.molcel.2013.08.006

Choi, Y. J., Halbritter, J., Braun, D. A., Schueler, M., Schapiro, D., Rim, J. H., et al. (2019). Mutations of ADAMTS9 cause nephronophthisis-related ciliopathy. *Am. J. Hum. Genet.* 104, 45–54. doi: 10.1016/j.ajhg.2018.11.003

Cideciyan, A. V., Jacobson, S. G., Drack, A. V., Ho, A. C., Charng, J., Garafalo, A. V., et al. (2019). Effect of an intravitreal antisense oligonucleotide on vision in Leber congenital amaurosis due to a photoreceptor cilium defect. *Nat. Med.* 25, 225–228. doi: 10.1038/s41591-018-0295-0

Collin, R. W., Den Hollander, A. I., Der Velde-Visser, S. D. V., Bennicelli, J., Bennett, J., and Cremers, F. P. (2012). Antisense oligonucleotide (AON)-based therapy for leber congenital amaurosis caused by a frequent mutation in CEP290. *Mol. Ther. Nucleic Acids* 1, e14. doi: 10.1038/mtna.2012.3

Cong, E. H., Bizet, A. A., Boyer, O., Woerner, S., Gribouval, O., Filhol, E., et al. (2014). A Homozygous missense mutation in the ciliary gene TTC21B causes familial FSGS. *J. Am. Soc. Nephrol.* 25, 1–9. doi: 10.1681/ASN.2013101126

Cook, S. A., Collin, G. B., Bronson, R. T., Naggert, J. K., Liu, D. P., Akeson, E. C., et al. (2009). A mouse model for meckel syndrome type 3. *J. Am. Soc. Nephrol.* 20, 753–764. doi: 10.1681/ASN.2008040412

Cowley, B. D., Gudapaty, S., Kraybill, A. L., Barash, B. D., Harding, M. A., Calvet, J. P., et al. (1993). Autosomal-dominant polycystic kidney disease in the rat. *Kidney Int.* 43, 522–534. doi: 10.1038/ki.1993.79

Cruz, N. M., Song, X., Czerniecki, S. M., Gulieva, R. E., Churchill, A. J., Kim, Y. K., et al. (2017). Organoid cystogenesis reveals a critical role of microenvironment in human polycystic kidney disease. *Nat. Mater.* 16, 1112–1119. doi: 10.1038/NMAT4994

Davis, E. E., Zhang, Q., Liu, Q., Diplas, B. H., Davey, L. M., Hartley, J., et al. (2011). TTC21B contributes both causal and modifying alleles across the ciliopathy spectrum. *Nat. Genet.* 43, 189–196. doi: 10.1038/ng.756

Delous, M., Baala, L., Salomon, R., Laclef, C., Vierkotten, J., Tory, K., et al. (2007). The ciliary gene RPGRIP1L is mutated in cerebello-oculo-renal syndrome (Joubert syndrome type B) and Meckel syndrome. *Nat. Genet.* 39, 875–881.

Delous, M., Hellman, N. E., Gaudé, H. M., Silbermann, F., Le Bivic, A., Salomon, R., et al. (2009). Nephrocystin-1 and nephrocystin-4 are required for epithelial morphogenesis and associate with PALS1/PATJ and Par6. *Hum. Mol. Genet.* 18, 4711–4723. doi: 10.1093/hmg/ddp434

Deshmukh, G. D., Radin, N. S., Gattone, V. H., and Shayman, J. A. (1994). Abnormalities of glycosphingolipid, sulfatide, and ceramide in the polycystic (cpk/cpk) mouse. *J. Lipid Res.* 35, 1611–1618.

Devlin, L. A., and Sayer, J. A. (2019). Renal ciliopathies. *Curr. Opin. Genet. Dev.* 56, 49–60. doi: 10.1016/j.gde.2019.07.005

Devuyst, O., Olinger, E., Weber, S., Eckardt, K. U., Kmoch, S., Rampoldi, L., et al. (2019). Autosomal dominant tubulointerstitial kidney disease. *Nat. Rev. Dis. Prim.* 5:60. doi: 10.1038/s41572-019-0109-9

Ding, B., Sun, G., Liu, S., Peng, E., Wan, M., Chen, L., et al. (2020). Three-dimensional renal organoids from whole kidney cells: generation, optimization,

and potential application in nephrotoxicology in vitro. *Cell Transplant.* 29, 1–10. doi: 10.1177/0963689719897066

Distler, J. H. W., Györfi, A. H., Ramanujam, M., Whitfield, M. L., Königshoff, M., and Lafyatis, R. (2019). Shared and distinct mechanisms of fibrosis. *Nat. Rev. Rheumatol.* 15, 705–730. doi: 10.1038/s41584-019-0322-7

Docherty, M. H., O'Sullivan, E. D., Bonventre, J. V., and Ferenbach, D. A. (2019). Cellular senescence in the kidney. *J. Am. Soc. Nephrol.* 30, 726–736. doi: 10.1681/ASN.2018121251

Donaldson, J. C., Dise, R. S., Ritchie, M. D., and Hanks, S. K. (2002). Nephrocystin-conserved domains involved in targeting to epithelial cell-cell junctions, interaction with filamins, and establishing cell polarity. *J. Biol. Chem.* 277, 29028–29035. doi: 10.1074/jbc.M111697200

Drivas, T. G., Wojno, A. P., Tucker, B. A., Stone, E. M., and Bennett, J. (2015). Basal exon skipping and genetic pleiotropy: a predictive model of disease pathogenesis. *Sci. Transl. Med.* 7:291ra97. doi: 10.1126/scitranslmed.aaa5370

Dubail, J., Aramaki-Hattori, N., Bader, H. L., Nelson, C. M., Katebi, N., Matuska, B., et al. (2014). A new *Adamts9* conditional mouse allele identifies its non-redundant role in interdigital web regression. *Genesis* 52, 702–712. doi: 10.1002/dvg.22784

Ecder, T. (2016). Statins in the treatment of autosomal dominant polycystic kidney disease. *Nephrol. Dial. Transplant.* 31, 1194–1196. doi: 10.1093/ndt/gfv449

Elberg, G., Elberg, D., Lewis, T. V., Guruswamy, S., Chen, L., Logan, C. J., et al. (2007). EP2 receptor mediates PGE2-induced cystogenesis of human renal epithelial cells. *Am. J. Physiol. Ren. Physiol.* 293, 1622–1632. doi: 10.1152/ajprenal.00036.2007

El-Brolosy, M. A., and Stainier, D. Y. R. (2017). Genetic compensation: a phenomenon in search of mechanisms. *PLoS Genet.* 13:e1006780. doi: 10.1371/journal.pgen.1006780

Elmonem, M., Berlingerio, S., van den Heuvel, L., de Witte, P., Lowe, M., and Levtchenko, E. (2018). Genetic renal diseases: the emerging role of zebrafish models. *Cells* 7:130. doi: 10.3390/cells7090130

Estrada-Cuzcano, A., Koenekoop, R. K., Coppieters, F., Kohl, S., Lopez, I., Collin, R. W. J., et al. (2011). IQCB1 mutations in patients with leber congenital amaurosis. *Investig. Ophthalmol. Vis. Sci.* 52, 834–839. doi: 10.1167/iovs.10-5221

Failler, M., Gee, H. Y., Krug, P., Joo, K., Halbritter, J., Belkacem, L., et al. (2014). Mutations of CEP83 cause infantile nephronophthisis and intellectual disability. *Am. J. Hum. Genet.* 94, 905–914. doi: 10.1016/j.ajhg.2014.05.002

Fassett, R. G., Coombes, J. S., Packham, D., Fairley, K. F., and Kincaid-Smith, P. (2010). Effect of pravastatin on kidney function and urinary protein excretion in autosomal dominant polycystic kidney disease. *Scand. J. Urol. Nephrol.* 44, 56–61. doi: 10.3109/00365590903359908

Fay, A. J., Knox, R., Neil, E. E., and Strober, J. (2020). Targeted treatments for inherited neuromuscular diseases of childhood. *Semin. Neurol.* 40, 335–341.

Fischer, E., and Pontoglio, M. (2009). Planar cell polarity and cilia. *Semin. Cell Dev. Biol.* 20, 998–1005. doi: 10.1016/j.semcdb.2009.09.016

Fitzgibbon, W. R., Dang, Y., Bunni, M. A., Baicu, C. F., Zile, M. R., Mullick, A. E., et al. (2018). Attenuation of accelerated renal cystogenesis in pkd1 mice by renin-angiotensin system blockade. *Am. J. Physiol. Ren. Physiol.* 314, F210–F218. doi: 10.1152/ajprenal.00389.2017

Forbes, T. A., Howden, S. E., Lawlor, K., Phipson, B., Maksimovic, J., Hale, L., et al. (2018). Patient-iPSC-derived kidney organoids show functional validation of a ciliopathic renal phenotype and reveal underlying pathogenetic mechanisms. *Am. J. Hum. Genet.* 102, 816–831. doi: 10.1016/j.ajhg.2018.03.014

Forsythe, E., Kenny, J., Bacchelli, C., and Beales, P. L. (2018). Managing bardet - biedl syndrome - now and in the future. *Front. Pediatr.* 6:23. doi: 10.3389/fped.2018.00023

Frank, V., Habbig, S., Bartram, M. P., Eisenberger, T., Veenstra-Knol, H. E., Decker, C., et al. (2013). Mutations in NEK8 link multiple organ dysplasia with altered Hippo signalling and increased c-MYC expression. *Hum. Mol. Genet.* 22, 2177–2185. doi: 10.1093/hmg/ddt070

Gagnadoux, M. F., Bacri, J. L., Broyer, M., and Habib, R. (1989). Infantile chronic tubulo-interstitial nephritis with cortical microcysts: variant of nephronophthisis or new disease entity? *Pediatr. Nephrol.* 3, 50–55. doi: 10.1007/BF00859626

Gattone, V. H. II, Sinders, R. M., Hornberger, T. A., and Robling, A. G. (2009). Late progression of renal pathology and cyst enlargement is reduced by rapamycin in a mouse model of nephronophthisis. *Kidney Int.* 76, 178–182. doi: 10.1038/ki.2009.147

Gattone, V. H. II, Wang, X., Harris, P. C., and Torres, V. E. (2003). Inhibition of renal cystic disease development and progression by a vasopressin V2 receptor antagonist. *Nat. Med.* 9, 1323–1326. doi: 10.1038/nm935

Gattone, V. H., Cowley, B. D., Barash, B. D., Nagao, S., Takahashi, H., Yamaguchi, T., et al. (1995). Methylprednisolone retards the progression of inherited polycystic kidney disease in rodents. *Am. J. Kidney Dis.* 25, 302–313. doi: 10.1016/0272-6386(95)90013-6

Gattone, V. H., Tourkow, B. A., Trambaugh, C. M., Yu, A. C., Whelan, S., Phillips, C. L., et al. (2004). Development of multiorgan pathology in the wpk rat model of polycystic kidney disease. *Anat. Rec. Part A Discov. Mol. Cell. Evol. Biol.* 277, 384–395. doi: 10.1002/ar.a.20022

Gehrig, J., Pandey, G., and Westhoff, J. H. (2018). Zebrafish as a model for drug screening in genetic kidney diseases. *Front. Pediatr.* 6:183. doi: 10.3389/fped.2018.00183

Gerard, X., Perrault, I., Hanein, S., Silva, E., Bigot, K., Defoort-Delhemmes, S., et al. (2012). AON-mediated exon skipping restores ciliation in fibroblasts harboring the common leber congenital amaurosis CEP290 mutation. *Mol. Ther. Nucleic Acids* 1:e29. doi: 10.1038/mtna.2012.21

Ghosh, A. K., Hurd, T., and Hildebrandt, F. (2012). 3D spheroid defects in NPHP knockdown cells are rescued by the somatostatin receptor agonist octreotide. *Am. J. Physiol. Ren. Physiol.* 303, 1225–1229. doi: 10.1152/ajprenal.00135.2012

Gile, R. D., Cowley, B. D., Gattone, V. H., O'Donnell, M. P., Swan, S. K., and Grantham, J. J. (1995). Effect of lovastatin on the development of polycystic kidney disease in the han:SPRD rat. *Am. J. Kidney Dis.* 26, 501–507. doi: 10.1016/0272-6386(95)90497-2

Gorivodsky, M., Mukhopadhyay, M., Wilsch-Braeuninger, M., Phillips, M., Teufel, A., Kim, C., et al. (2009). Intraflagellar transport protein 172 is essential for primary cilia formation and plays a vital role in patterning the mammalian brain. *Dev. Biol.* 325, 24–32. doi: 10.1016/j.ydbio.2008.09.019

Goru, S. K. S. (2018). Novel reno-protective mechanism of aspirin involves H2AK119 monoubiquitination and Set7 in preventing type 1 diabetic nephropathy. *Pharmacol. Rep.* 70, 497–502.

Grampa, V., Delous, M., Zaidan, M., Odye, G., Thomas, S., Elkhartoufi, N., et al. (2016). Novel NEK8 mutations cause severe syndromic renal cystic dysplasia through YAP Dysregulation. *PLoS Genet.* 12:e1005894. doi: 10.1371/journal.pgen.1005894

Günther, T., Tulipano, G., Dournaud, P., Bousquet, C., Csaba, Z., Kreienkamp, H. J., et al. (2018). International union of basic and clinical pharmacology. CV. somatostatin receptors: structure, function, ligands, and new nomenclature. *Pharmacol. Rev.* 70, 763–835. doi: 10.1124/pr.117.015388

Habbig, S., Bartram, M. P., Muller, R. U., Schwarz, R., Andriopoulos, N., Chen, S., et al. (2011). NPHP4, a cilia-associated protein, negatively regulates the Hippo pathway. *J. Cell Biol.* 193, 633–642. doi: 10.1083/jcb.201009069

Habbig, S., Bartram, M. P., Sägmüller, J. G., Griessmann, A., Franke, M., Müller, R. U., et al. (2012). The ciliopathy disease protein NPHP9 promotes nuclear delivery and activation of the oncogenic transcriptional regulator TAZ. *Hum. Mol. Genet.* 21, 5528–5538. doi: 10.1093/hmg/dds408

Halbritter, J., Bizet, A. A., Schmidts, M., Porath, J. D., Braun, D. A., Gee, H. Y., et al. (2013a). Defects in the IFT-B component IFT172 cause jeune and mainzer-saldino syndromes in humans. *Am. J. Hum. Genet.* 93, 915–925. doi: 10.1016/j.ajhg.2013.09.012

Halbritter, J., Porath, J. D., Diaz, K. A., Braun, D. A., Kohl, S., Chaki, M., et al. (2013b). Identification of 99 novel mutations in a worldwide cohort of 1,056 patients with a nephronophthisis-related ciliopathy. *Hum. Genet.* 132, 865–884. doi: 10.1007/s00439-013-1297-0

Hamiwka, L. A., Midgley, J. P., Wade, A. W., Martz, K. L., and Grisaru, S. (2008). Outcomes of kidney transplantation in children with nephronophthisis: an analysis of the North American Pediatric Renal Trials and Collaborative Studies (NAPRTCS) Registry. *Pediatr. Transplant.* 12, 878–882. doi: 10.1111/j.1399-3046.2008.00942.x

Han, S. H., Malaga-DIeguez, L., Chinga, F., Kang, H. M., Tao, J., Reidy, K., et al. (2016). Deletion of Lkb1 in renal tubular epithelial cells leads to CKD by altering metabolism. *J. Am. Soc. Nephrol.* 27, 439–453. doi: 10.1681/ASN.2014121181

Hansen, J. N., Kaiser, F., Klausen, C., Stüven, B., Chong, R., Bönigk, W., et al. (2020). Nanobody-directed targeting of optogenetic tools reveals differential

regulation of cilia length. *bioRxiv* [Preprint]. doi: 10.1101/2020.02.04.933440

Harris, P. C., and Torres, V. E. (2002). Autosomal dominant polycystic kidney disease. *Gene Rev.* 2, 2645–2688. doi: 10.1016/B978-0-12-381462-3.00080-X

Helou, J., Otto, E. A., Attanasio, M., Allen, S. J., Parisi, M. A., Glass, I., et al. (2007). Mutation analysis of NPHP6/CEP290 in patients with Joubert syndrome ana Senior-Løken syndrome. *J. Med. Genet.* 44, 657–663. doi: 10.1136/jmg.2007.052027

Hildebrandt, F., Attanasio, M., and Otto, E. (2009). Nephronophthisis: disease mechanisms of a ciliopathy. *J. Am. Soc. Nephrol.* 20, 23–35. doi: 10.1681/ASN.2008050456

Hildebrandt, F., Otto, E., Rensing, C., Nothwang, H. G., Vollmer, M., Adolphs, J., et al. (1997). A novel gene encoding an SH3 domain protein is mutated in nephronophthisis type 1. *Nat. Genet.* 17, 149–153. doi: 10.1038/ng1097-149

Hoff, S., Halbritter, J., Epting, D., Frank, V., Nguyen, T.-M. T., van Reeuwijk, J., et al. (2013). ANKS6 is a central component of a nephronophthisis module linking NEK8 to INVS and NPHP3. *Nat. Genet.* 45, 951–958.

Hogan, M. C., Masyuk, T. V., Page, L. J., Kubly, V. J., Bergstralh, E. J., Li, X., et al. (2010). Randomized clinical trial of long-acting somatostatin for autosomal dominant polycystic kidney and liver disease. *J. Am. Soc. Nephrol.* 21, 1052–1061. doi: 10.1681/ASN.2009121291

Hollywood, J. A., Przepiorski, A., D'Souza, R. F., Sreebhavan, S., Wolvetang, E. J., Harrison, P. T., et al. (2020). Use of human induced pluripotent stem cells and kidney organoids to develop a Cysteamine/mTOR inhibition combination therapy for cystinosis. *J. Am. Soc. Nephrol.* 2020:712. doi: 10.1681/asn.2019070712

Hong, C. J., and Hamilton, B. A. (2016). Zfp423 regulates sonic hedgehog signaling via primary cilium function. *PLoS Genet.* 12:e1006357. doi: 10.1371/journal.pgen.1006357

Hurd, T. W., Otto, E. A., Mishima, E., Gee, H. Y., Inoue, H., Inazu, M., et al. (2013). Mutation of the Mg2+ transporter SLC41A1 results in a nephronophthisis-like phenotype. *J. Am. Soc. Nephrol.* 24, 967–977. doi: 10.1681/ASN.2012101034

Husson, H., Moreno, S., Smith, L. A., Smith, M. M., Russo, R. J., Pitstick, R., et al. (2016). Reduction of ciliary length through pharmacologic or genetic inhibition of CDK5 attenuates polycystic kidney disease in a model of nephronophthisis. *Hum. Mol. Genet.* 25, 2245–2255. doi: 10.1093/hmg/ddw093

Hynes, A. M., Giles, R. H., Srivastava, S., Eley, L., Whitehead, J., Danilenko, M., et al. (2014). Murine Joubert syndrome reveals Hedgehog signaling defects as a potential therapeutic target for nephronophthisis. *Proc. Natl. Acad. Sci. U.S.A.* 111, 9893–9898. doi: 10.1073/pnas.1322373111

Ibraghimov-Beskrovnaya, O. (2007). Targeting dysregulated cell cycle and apoptosis for polycystic kidney disease therapy. *Cell Cycle* 6, 776–779. doi: 10.4161/cc.6.7.4047

Ibrahim, N. H. M., Gregoire, M., Devassy, J. G., Wu, Y., Yoshihara, D., Yamaguchi, T., et al. (2015). Cyclooxygenase product inhibition with acetylsalicylic acid slows disease progression in the Han:SPRD-Cy rat model of polycystic kidney disease. *Prostagland. Other Lipid Mediat.* 116–117, 19–25. doi: 10.1016/j.prostaglandins.2014.10.005

Ibrahim, N. H. M., Jia, Y., Devassy, J. G., Yamaguchi, T., and Aukema, H. M. (2014). Renal cyclooxygenase and lipoxygenase products are altered in polycystic kidneys and by dietary soy protein and fish oil treatment in the Han: SPRD-Cy rat. *Mol. Nutr. Food Res.* 58, 768–781. doi: 10.1002/mnfr.201300332

Jain, M., Kaiser, R. W. J., Bohl, K., Hoehne, M., Göbel, H., Bartram, M. P., et al. (2019). Inactivation of apoptosis antagonizing transcription factor in tubular epithelial cells induces accumulation of DNA damage and Nephronophthisis. *Kidney Int.* 95, 846–858. doi: 10.1016/j.kint.2018.10.034

Jiang, J. Y., Falcone, J. L., Curci, S., and Hofer, A. M. (2019). Direct visualization of cAMP signaling in primary cilia reveals up-regulation of ciliary GPCR activity following Hedgehog activation. *Proc. Natl. Acad. Sci. U.S.A.* 116, 12066–12071. doi: 10.1073/pnas.1819730116

Jiang, S. T., Chiou, Y. Y., Wang, E., Lin, H. K., Lee, S. P., Lu, H. Y., et al. (2008). Targeted disruption of Nphp1 causes male infertility due to defects in the later steps of sperm morphogenesis in mice. *Hum. Mol. Genet.* 17, 3368–3379. doi: 10.1093/hmg/ddn231

Jin, D., Ni, T. T., Sun, J., Wan, H., Amack, J. D., Yu, G., et al. (2014). Prostaglandin signalling regulates ciliogenesis by modulating intraflagellar transport. *Nat. Cell Biol.* 16, 841–851. doi: 10.1038/ncb3029

Jin, H., Zhang, Y., Ding, Q., Wang, S. S., Rastogi, P., Dai, D. F., et al. (2019). Epithelial innate immunity mediates tubular cell senescence after kidney injury. *JCI Insight* 4, 1–14. doi: 10.1172/jci.insight.125490

Jin, H., Zhang, Y., Liu, D., Wang, S. S., Ding, Q., Rastogi, P., et al. (2020). Innate immune signaling contributes to tubular cell senescence in the glis2 knockout mouse model of Nephronophthisis. *Am. J. Pathol.* 190, 176–189. doi: 10.1016/j.ajpath.2019.09.013

Ke, B., Chen, Y., Tu, W., Ye, T., Fang, X., and Yang, L. (2018). Inhibition of HDAC6 activity in kidney diseases: a new perspective. *Mol. Med.* 24, 1–6. doi: 10.1186/s10020-018-0027-4

Kern, C. B., Wessels, A., McGarity, J., Dixon, L. J., Alston, E., Argraves, W. S., et al. (2010). Reduced versican cleavage due to *Adamts9* haploinsufficiency is associated with cardiac and aortic anomalies. *Matrix Biol.* 29, 304–316. doi: 10.1016/j.matbio.2010.01.005

Kim, J., Lee, J. E., Heynen-Genel, S., Suyama, E., Ono, K., Lee, K., et al. (2010). Functional genomic screen for modulators of ciliogenesis and cilium length. *Nature* 464, 1048–1051. doi: 10.1038/nature08895

Kim, Y. J., and Kim, J. (2019). Therapeutic perspectives for structural and functional abnormalities of cilia. *Cell. Mol. Life Sci.* 76, 3695–3709. doi: 10.1007/s00018-019-03158-6

Kim, Y. J., Kwon, H. J., Kim, J., Kim, Y. J., Kim, S., Jung, Y., et al. (2018). Eupatilin rescues ciliary transition zone defects to ameliorate ciliopathy-related phenotypes. *J. Clin. Invest.* 128, 3642–3648.

Kim, Y.-S., Kang, H. S., Herbert, R., Beak, J. Y., Collins, J. B., Grissom, S. F., et al. (2008). Krüppel-like zinc finger protein Glis2 is essential for the maintenance of normal renal functions. *Mol. Cell. Biol.* 28, 2358–2367. doi: 10.1128/mcb.01722-07

Ko, J. Y., and Park, J. H. (2013). Mouse models of polycystic kidney disease induced by defects of ciliary proteins. *BMB Rep.* 46, 73–79. doi: 10.5483/BMBRep.2013.46.2.022

Kong, J. H., Siebold, C., and Rohatgi, R. (2019). Biochemical mechanisms of vertebrate hedgehog signaling. *Development* 146:dev.166892. doi: 10.1242/dev.166892

König, J., Kranz, B., König, S., Schlingmann, K. P., Titieni, A., Tönshoff, B., et al. (2017). Phenotypic spectrum of children with nephronophthisis and related Ciliopathies. *Clin. J. Am. Soc. Nephrol.* 12, 1974–1983. doi: 10.2215/CJN.01280217

Kopinke, D., Norris, A. M., and Mukhopadhyay, S. (2020). Developmental and regenerative paradigms of cilia regulated hedgehog signaling. *Semin. Cell Dev. Biol.* 110, 89–103. doi: 10.1016/j.semcdb.2020.05.029

Krishnan, R., Eley, L., and Sayer, J. A. (2008). Urinary concentration defects and mechanisms underlying nephronophthisis. *Kidney Blood Press. Res.* 31, 152–162. doi: 10.1159/000129648

Kuraoka, S., Tanigawa, S., Taguchi, A., Hotta, A., Nakazato, H., Osafune, K., et al. (2020). PKD1-dependent renal cystogenesis in human induced pluripotent stem cell-derived ureteric bud/collecting duct organoids. *J Am Soc Nephrol* 31, 2355–2371. doi: 10.1681/ASN.2020030378

Lai, Y., and Jiang, Y. (2020). Reciprocal regulation between primary cilia and mtorc1. *Genes* 11, 1–15. doi: 10.3390/genes11060711

Lakhia, R., Mishra, A., and Patel, V. (2019). *Manipulation of Renal Gene Expression using Oligonucleotides*, 1st Edn, Amsterdam: Elsevier Inc, doi: 10.1016/bs.mcb.2019.05.006

Lancaster, M. A., Louie, C. M., Silhavy, J. L., Sintasath, L., DeCambre, M., Nigam, S. K., et al. (2009). Impaired Wnt-β-catenin signaling disrupts adult renal homeostasis and leads to cystic kidney ciliopathy. *Nat. Med.* 15, 1046–1054. doi: 10.1038/nm.2010.Impaired

Lannoy, M., Valluru, M. K., Chang, L., Abdela-Ali, F., Peters, D. J. M., Streets, A. J., et al. (2020). The positive effect of selective prostaglandin E2 receptor EP2 and EP4 blockade on cystogenesis in vitro is counteracted by increased kidney inflammation in vivo. *Kidney Int.* 98, 404–419. doi: 10.1016/j.kint.2020.02.012

Lemos, D. R., McMurdo, M., Karaca, G., Wilflingseder, J., Leaf, I. A., Gupta, N., et al. (2018). Interleukin-1b activates a MYC-dependent metabolic switch in kidney stromal cells necessary for progressive tubulointerstitial fibrosis. *J. Am. Soc. Nephrol.* 29, 1690–1705. doi: 10.1681/ASN.2017121283

Li, B., Rauhauser, A. A., Dai, J., Sakthivel, R., Igarashi, P., Jetten, A. M., et al. (2011). Increased hedgehog signaling in postnatal kidney results in aberrant activation of nephron developmental programs. *Hum. Mol. Genet.* 20, 4155–4166. doi: 10.1093/hmg/ddr339

Li, J. H., Chou, C. L., Li, B., Gavrilova, O., Eisner, C., Schnermann, J., et al. (2009). A selective EP4 PGE2 receptor agonist alleviates disease in a new mouse model of X-linked nephrogenic diabetes insipidus. *J. Clin. Invest.* 119, 3115–3126. doi: 10.1172/JCI39680

Li, Y., Xia, W., Zhao, F., Wen, Z., Zhang, A., Huang, S., et al. (2018). Prostaglandins in the pathogenesis of kidney diseases. *Oncotarget* 9, 26586–26602. doi: 10.18632/oncotarget.25005

Liu, C. P., Hu, Y., Lin, J. C., Fu, H. L., Lim, L. Y., and Yuan, Z. X. (2019). Targeting strategies for drug delivery to the kidney: from renal glomeruli to tubules. *Med. Res. Rev.* 39, 561–578. doi: 10.1002/med.21532

Liu, S., Lu, W., Obara, T., Kuida, S., Lehoczky, J., Dewar, K., et al. (2002). A defect in novel Nek-family kinase causes cystic kidney disease in the mouse and in zebrafish. *Development* 129, 5839–5846. doi: 10.1242/dev.00173

Loktev, A. V., Zhang, Q., Beck, J. S., Searby, C. C., Scheetz, T. E., Bazan, J. F., et al. (2008). A BBSome subunit links ciliogenesis, microtubule stability, and Acetylation. *Dev. Cell* 15, 854–865. doi: 10.1016/j.devcel.2008.11.001

Low, J. H., Li, P., Chew, E. G. Y., Zhou, B., Suzuki, K., Zhang, T., et al. (2019). Generation of human PSC-derived kidney organoids with patterned nephron segments and a de novo vascular network. *Cell Stem Cell* 25, 373–387.e9. doi: 10.1016/j.stem.2019.06.009

Lowe, L. A., Supp, D. M., Sampath, K., Yokoyama, T., Wright, C. V. E., Potter, S. S., et al. (1996). Conserved left-right asymmetry of nodal expression and alterations in murine situs inversus. *Nature* 381, 158–161. doi: 10.1038/381158a0

Lu, D., Rauhauser, A., Li, B., Ren, C., McEnery, K., Zhu, J., et al. (2016). Loss of Glis2/NPHP7 causes kidney epithelial cell senescence and suppresses cyst growth in the Kif3a mouse model of cystic kidney disease. *Kidney Int.* 89, 1307–1323. doi: 10.1016/j.kint.2016.03.006

Luo, F., and Tao, Y. H. (2018). Nephronophthisis: A review of genotype-phenotype correlation. *Nephrology* 23, 904–911. doi: 10.1111/nep.13393

Ma, M., Legué, E., Tian, X., Somlo, S., and Liem, K. F. (2019). Cell-autonomous hedgehog signaling is not required for cyst formation in autosomal dominant polycystic kidney disease. *J. Am. Soc. Nephrol.* 30, 2103–2111. doi: 10.1681/ASN.2018121274

Macia, M. S., Halbritter, J., Delous, M., Bredrup, C., Gutter, A., Filhol, E., et al. (2017). Mutations in MAPKBP1 cause juvenile or late-onset cilia-independent Nephronophthisis. *Am. J. Hum. Genet.* 100, 323–333. doi: 10.1016/j.ajhg.2016.12.011

Maerz, L. D., Burkhalter, M. D., Schilpp, C., Wittekindt, O. H., Frick, M., and Philipp, M. (2019). Pharmacological cholesterol depletion disturbs ciliogenesis and ciliary function in developing zebrafish. *Commun. Biol.* 2, 1–13. doi: 10.1038/s42003-018-0272-7

Mahuzier, A., Gaudé, H. M., Grampa, V., Anselme, I., Silbermann, F., Leroux-Berger, M., et al. (2012). Dishevelled stabilization by the ciliopathy protein rpgrip1l is essential for planar cell polarity. *J. Cell Biol.* 198, 927–940. doi: 10.1083/jcb.201111009

Malik, S. A., Modarage, K., and Goggolidou, P. (2020). The role of WNT signalling in chronic kidney disease (CKD). *Genes* 11, 1–19. doi: 10.3390/genes11050496

Mangoo-Karim, R., Uchic, M. E., Grant, M., Shumate, W. A., Calvet, J. P., Park, C. H., et al. (1989). Renal epithelial fluid secretion and cyst growth: the role of cyclic AMP. *FASEB J.* 3, 2629–2632. doi: 10.1096/fasebj.3.14.2480260

Manning, D. K., Sergeev, M., Van Heesbeen, R. G., Wong, M. D., Oh, J. H., Liu, Y., et al. (2013). Loss of the ciliary kinase Nek8 causes left-right asymmetry defects. *J. Am. Soc. Nephrol.* 24, 100–112. doi: 10.1681/ASN.2012050490

Marion, V., Schlicht, D., Mockel, A., Caillard, S., Imhoff, O., Stoetzel, C., et al. (2011). Bardet-Biedl syndrome highlights the major role of the primary cilium in efficient water reabsorption. *Kidney Int.* 79, 1013–1025. doi: 10.1038/ki.2010.538

Masyuk, T. V., Masyuk, A. I., Torres, V. E., Harris, P. C., and Larusso, N. F. (2007). Octreotide inhibits hepatic cystogenesis in a rodent model of polycystic liver disease by reducing Cholangiocyte adenosine. *Gastroenterology* 132, 1104–1116. doi: 10.1053/j.gastro.2006.12.039

McCooke, J. K., Appels, R., Barrero, R. A., Ding, A., Ozimek-Kulik, J. E., Bellgard, M. I., et al. (2012). A novel mutation causing nephronophthisis in the lewis polycystic kidney rat localises to a conserved RCC1 domain in Nek8. *BMC Genom.* 13:393. doi: 10.1186/1471-2164-13-393

McKee, R. A., and Wingert, R. A. (2016). Repopulating decellularized kidney scaffolds: an avenue for ex vivo organ generation. *Materials* 9:190. doi: 10.3390/ma9030190

Mihajlovic, M., Hariri, S., Westphal, K. C. G., Janssen, M. J., Oost, M. J., Bongiovanni, L., et al. (2019a). Safety evaluation of conditionally immortalized cells for renal replacement therapy. *Oncotarget* 10, 5332–5348.

Mihajlovic, M., Wever, K. E., van der Made, T. K., de Vries, R. B. M., Hilbrands, L. B., and Masereeuw, R. (2019b). Are cell-based therapies for kidney disease safe? A systematic review of preclinical evidence. *Pharmacol. Ther.* 197, 191–211. doi: 10.1016/j.pharmthera.2019.01.004

Mochizuki, T., Saijoh, Y., Tsuchiya, K., Shirayoshi, Y., Takai, S., Taya, C., et al. (1998). Cloning of inv, a gene that controls left/right asymmetry and kidney development. *Nature* 395, 177–181. doi: 10.1038/255243a0

Molinari, E., and Sayer, J. A. (2017). Emerging treatments and personalised medicine for ciliopathies associated with cystic kidney disease. *Expert Opin. Orphan. Drugs* 5, 785–798. doi: 10.1080/21678707.2017.1372282

Mollet, G., Salomon, R., Gribouval, O., Silbermann, F., Bacq, D., Landthaler, G., et al. (2002). The gene mutated in juvenile nephronophthisis type 4 encodes a novel protein that interacts with nephrocystin. *Nat. Genet.* 32, 300–305. doi: 10.1038/ng996

Monirujjaman, M., Devassy, J. G., Yamaguchi, T., Sidhu, N., Kugita, M., Gabbs, M., et al. (2017). Distinct oxylipin alterations in diverse models of cystic kidney diseases. *Biochim. Biophys. Acta Mol. Cell Biol. Lipids* 1862, 1562–1574. doi: 10.1016/j.bbalip.2017.08.005

Morgan, D., Turnpenny, L., Goodship, J., Dai, W., Majumder, K., Matthews, L., et al. (1998). Inversin, a novel gene in the vertebrate left-right axis pathway, is partially deleted in the inv mouse. *Nat. Genet.* 20, 149–156. doi: 10.1038/2450

Müller, R. U., and Schermer, B. (2019). Hippo signaling—a central player in cystic kidney disease? *Pediatr. Nephrol.* 35, 1143–1152.

Müller, R. U., and Schermer, B. (2020). Hippo signaling—a central player in cystic kidney disease? *Pediatr. Nephrol.* 35, 1143–1152. doi: 10.1007/s00467-019-04299-3

Mykytyn, K., and Askwith, C. (2017). G-Protein-Coupled receptor signaling in cilia. *Cold Spring Harb. Perspect. Biol.* 9, 1–16. doi: 10.1101/cshperspect.a028183

Nager, A. R., Goldstein, J. S., Herranz-Pérez, V., Portran, D., Ye, F., Garcia-Verdugo, J. M., et al. (2017). An Actin network dispatches ciliary GPCRs into extracellular vesicles to modulate signaling. *Cell* 168, 252–263.e14. doi: 10.1016/j.cell.2016.11.036

Nandadasa, S., Kraft, C. M., Wang, L. W., O'Donnell, A., Patel, R., Gee, H. Y., et al. (2019). Secreted metalloproteases ADAMTS9 and ADAMTS20 have a non-canonical role in ciliary vesicle growth during ciliogenesis. *Nat. Commun.* 10:953. doi: 10.1038/s41467-019-08520-7

Nandadasa, S., Nelson, C. M., and Apte, S. S. (2015). *ADAMTS9*-mediated extracellular matrix dynamics regulates umbilical cord vascular smooth muscle differentiation and rotation. *Cell Rep.* 11, 1519–1528. doi: 10.1016/j.celrep.2015.05.005

Natoli, T. A., Husson, H., Rogers, K. A., Smith, L. A., Wang, B., Budman, Y., et al. (2012). Loss of GM3 synthase gene, but not sphingosine kinase 1, is protective against murine nephronophthisis-related polycystic kidney disease. *Hum. Mol. Genet.* 21, 3397–3407. doi: 10.1093/hmg/dds172

Natoli, T. A., Modur, V., and Ibraghimov-Beskrovnaya, O. (2020). Glycosphingolipid metabolism and polycystic kidney disease. *Cell. Signal.* 69:109526. doi: 10.1016/j.cellsig.2020.109526

Natoli, T. A., Smith, L. A., Rogers, K. A., Wang, B., Komarnitsky, S., Budman, Y., et al. (2010). Inhibition of glucosylceramide accumulation results in effective blockade of polycystic kidney disease in mouse models. *Nat. Med.* 16, 788–792. doi: 10.1038/nm.2171.Inhibition

Nielsen, S., Frøkiær, J., Marples, D., Kwon, T. H., Agre, P., and Knepper, M. A. (2002). Aquaporins in the kidney: from molecules to medicine. *Physiol. Rev.* 82, 205–244. doi: 10.1152/physrev.00024.2001

Nogueira, A., Pires, M. J., and Oliveira, P. A. (2017). Pathophysiological mechanisms of renal fibrosis: a review of animal models and therapeutic strategies. *In Vivo* 31, 1–22. doi: 10.21873/invivo.11019

Norris, D. P., and Grimes, D. T. (2012). Mouse models of ciliopathies: the state of the art. *DMM Dis. Model. Mech.* 5, 299–312.

Nurnberger, J., Bacallao, R. L., and Phillips, C. L. (2002). Inversin forms a complex with catenins and N-cadherin in polarized epithelial cells. *Mol. Biol. Cell* 13, 3096–3106. doi: 10.1091/mbc.E02

Oberbauer, R., Schreiner, G. F., Biber, J., Murer, H., and Meyer, T. W. (1996). In vivo suppression of the renal Na+/Pi cotransporter by antisense oligonucleotides. *Proc. Natl. Acad. Sci. U.S.A.* 93, 4903–4906.

Oey, O., Rao, P., Luciuk, M., Mannix, C., Rogers, N. M., Sagar, P., et al. (2018). Effect of dimethyl fumarate on renal disease progression in a genetic ortholog of nephronophthisis. *Exp. Biol. Med.* 243, 428–436. doi: 10.1177/1535370218759313

Okumura, Y., Sugiyama, N., Tanimura, S., Nishida, M., Hamaoka, K., Kohno, M., et al. (2009). ERK regulates renal cell proliferation and renal cyst expansion in inv mutant mice. *Acta Histochem. Cytochem.* 42, 39–45. doi: 10.1267/ahc.08040

Olbrich, H., Fliegauf, M., Hoefele, J., Kispert, A., Otto, E., Volz, A., et al. (2003). Mutations in a novel gene, NPHP3, cause adolescent nephronophthisis, tapeto-retinal degeneration and hepatic fibrosis. *Nat. Genet.* 34, 455–459. doi: 10.1038/ng1216

Omori, S., Hida, M., Fujita, H., Takahashi, H., Tanimura, S., Kohno, M., et al. (2006). Extracellular signal-regulated kinase inhibition slows disease progression in mice with polycystic kidney disease. *J. Am. Soc. Nephrol.* 17, 1604–1614. doi: 10.1681/ASN.2004090800

Omran, H., Fernandez, C., Jung, M., Haffner, K., Fargier, B., Villaquiran, A., et al. (2000). Identification of a new gene locus for adolescent nephronophthisis, on chromosome 3q22 in a large Venezuelan pedigree. *Am. J. Hum. Genet.* 66, 118–127. doi: 10.1086/302705

Omran, H., Häffner, K., Burth, S., Fernandez, C., Fargier, B., Villaquiran, A., et al. (2001). Human adolescent nephronophthisis: gene locus synteny with polycystic kidney disease in pcy mice. *J. Am. Soc. Nephrol.* 12, 107–113.

Oroojalian, F., Charbgoo, F., Hashemi, M., Amani, A., Yazdian-Robati, R., Mokhtarzadeh, A., et al. (2020). Recent advances in nanotechnology-based drug delivery systems for the kidney. *J. Control. Release* 321, 442–462. doi: 10.1016/j.jconrel.2020.02.027

O'Toole, J. F., Liu, Y., Davis, E. E., Westlake, C. J., Attanasio, M., Otto, E. A., et al. (2010). Individuals with mutations in XPNPEP3, which encodes a mitochondrial protein, develop a nephronophthisis-like nephropathy John. *J. Clin. Invest.* 120, 791–802. doi: 10.1172/JCI40076.Introduction

O'Toole, J. F., Otto, E. A., Frishberg, Y., and Hildebrandt, F. (2006). Retinitis pigmentosa and renal failure in a patient with mutations in INVS. *Nephrol. Dial. Transplant.* 21, 1989–1991. doi: 10.1093/ndt/gfl088

Otto, E., Hoefele, J., Ruf, R., Mueller, A. M., Hiller, K. S., Wolf, M. T., et al. (2002). A gene mutated in nephronophthisis and retinitis pigmentosa encodes a novel protein, nephroretinin, conserved in evolution. *Am. J. Hum. Genet.* 71, 1161–1167. doi: 10.1086/344395

Otto, E. A., Hurd, T. W., Airik, R., Chaki, M., Zhou, W., Stoetzel, C., et al. (2010). Candidate exome capture identifies mutation of SDCCAG8 as the cause of a retinal-renal ciliopathy. *Nat. Genet.* 42, 840–850. doi: 10.1038/ng.662

Otto, E. A., Loeys, B., Khanna, H., Hellemans, J., Sudbrak, R., Fan, S., et al. (2005). Nephrocystin-5, a ciliary IQ domain protein, is mutated in Senior-Loken syndrome and interacts with RPGR and calmodulin. *Nat. Genet.* 37, 282–288. doi: 10.1038/ng1520

Otto, E. A., Schermer, B., Obara, T., Toole, J. F. O., Hiller, K. S., Mueller, A. M., et al. (2003). Mutations in INVS encoding inversin cause nephronophthisis type 2, linking renal cystic disease to the function of primary cilia and left-right axis determination. *Nat. Genet.* 34, 413–420. doi: 10.1038/ng1217.Mutations

Otto, E. A., Trapp, M. L., Schultheiss, U. T., Helou, J., Quarmby, L. M., and Hildebrandt, F. (2008). NEK8 mutations affect ciliary and centrosomal localization and may cause nephronophthisis. *J. Am. Soc. Nephrol.* 19, 587–592. doi: 10.1681/ASN.2007040490

Pandey, G., Westhoff, J. H., Schaefer, F., and Gehrig, J. (2019). A smart imaging workflow for organ-specific screening in a cystic kidney Zebrafish disease model. *Int. J. Mol. Sci.* 20:1290. doi: 10.3390/ijms20061290

Parfitt, D. A., Lane, A., Ramsden, C. M., Carr, A. J. F., Munro, P. M., Jovanovic, K., et al. (2016). Identification and Correction of Mechanisms Underlying Inherited Blindness in Human iPSC-Derived Optic Cups. *Cell Stem Cell* 18, 769–781. doi: 10.1016/j.stem.2016.03.021

Peired, A. J., Mazzinghi, B., De Chiara, L., Guzzi, F., Lasagni, L., Romagnani, P., et al. (2020). Bioengineering strategies for nephrologists: kidney was not built in a day. *Expert Opin. Biol. Ther.* 20, 467–480. doi: 10.1080/14712598.2020.1709439

Perrault, I., Saunier, S., Hanein, S., Filhol, E., Bizet, A. A., Collins, F., et al. (2012). Mainzer-saldino syndrome is a ciliopathy caused by IFT140 mutations. *Am. J. Hum. Genet.* 90, 864–870. doi: 10.1016/j.ajhg.2012.03.006

Phillips, C. L., Miller, K. J., Filson, A. J., Nurnberger, J., Clendenon, J. L., Cook, G. W., et al. (2004). Renal cysts of inv/inv mice resemble early infantile nephronophthisis. *J. Am. Soc. Nephrol.* 15, 1744–1755.

Phillips, J. K., Hopwood, D., Loxley, R. A., Ghatora, K., Coombes, J. D., Tan, Y. S., et al. (2007). Temporal relationship between renal cyst development, hypertension and cardiac hypertrophy in a new rat model of autosomal recessive polycystic kidney disease. *Kidney Blood Press. Res.* 30, 129–144. doi: 10.1159/000101828

Phua, S. C., Chiba, S., Suzuki, M., Su, E., Roberson, E. C., Pusapati, G. V., et al. (2017). Dynamic remodeling of membrane composition drives cell cycle through primary cilia excision. *Cell* 168, 264–279.e15. doi: 10.1016/j.cell.2016.12.032

Pugacheva, E. N., Jablonski, S. A., Hartman, T. R., Henske, E. P., and Golemis, E. A. (2007). HEF1-dependent aurora a activation induces disassembly of the primary cilium. *Cell* 129, 1351–1363. doi: 10.1016/j.cell.2007.04.035

Qian, Q., Du, H., King, B. F., Kumar, S., Dean, P. G., Cosio, F. G., et al. (2008). Sirolimus reduces polycystic liver volume in ADPKD patients. *J. Am. Soc. Nephrol.* 19, 631–638. doi: 10.1681/ASN.2007050626

Qin, J., Lin, Y., Norman, R. X., Ko, H. W., Eggenschwiler, J. T., Anderson, K. V., et al. (2011). Intraflagellar transport protein 122 antagonizes sonic hedgehog signaling and controls ciliary localization of pathway components. *Proc. Natl. Acad. Sci. U.S.A.* 108, 1456–1461.

Rachel, R. A., Yamamoto, E. A., Dewanjee, M. K., May-Simera, H. L., Sergeev, Y. V., Hackett, A. N., et al. (2015). CEP290 alleles in mice disrupt tissue-specific cilia biogenesis and recapitulate features of syndromic ciliopathies. *Hum. Mol. Genet.* 24, 3775–3791. doi: 10.1093/hmg/ddv123

Rajagopalan, R., Grochowski, C. M., Gilbert, M. A., Falsey, A. M., Coleman, K., Romero, R., et al. (2015). Compound heterozygous mutations in NEK8 in siblings with end-stage renal disease with hepatic and cardiac anomalies. *Am. J. Med. Genet. Part A* 170, 750–753. doi: 10.1002/ajmg.a.37512

Ramsbottom, S. A., Miles, C., and Sayer, J. A. (2015). Murine Cep290 phenotypes are modified by genetic backgrounds and provide an impetus for investigating disease modifier alleles. *F1000Research* 4:590. doi: 10.12688/f1000research.6959.1

Ramsbottom, S. A., Molinari, E., Srivastava, S., Silberman, F., Henry, C., Alkanderi, S., et al. (2018). Targeted exon skipping of a CEP290 mutation rescues Joubert syndrome phenotypes in vitro and in a murine model. *Proc. Natl. Acad. Sci. U.S.A.* 115, 12489–12494. doi: 10.1073/pnas.1809432115

Ramsbottom, S. A., Thelwall, P. E., Wood, K. M., Clowry, G. J., Devlin, L. A., Silbermann, F., et al. (2020). Mouse genetics reveals Barttin as a genetic modifier of Joubert syndrome. *Proc. Natl. Acad. Sci. U.S.A.* 117, 1113–1118. doi: 10.1073/pnas.1912602117

Reif, G. A., Yamaguchi, T., Nivens, E., Fujiki, H., Pinto, C. S., and Wallace, D. P. (2011). Tolvaptan inhibits ERK-dependent cell proliferation, Cl - secretion, and in vitro cyst growth of human ADPKD cells stimulated by vasopressin. *Am. J. Physiol. Ren. Physiol.* 301, 1005–1013. doi: 10.1152/ajprenal.00243.2011

Reiter, J. F., Leroux, M. R., Francisco, S., Francisco, S., and Columbia, B. (2017). Genes and molecular pathways underpinning ciliopathies. *Nat. Rev. Mol. Cell Biol.* 18, 533–547. doi: 10.1038/nrm.2017.60.Genes

Riccardi, D., and Valenti, G. (2016). Localization and function of the renal calcium-sensing receptor. *Nat. Rev. Nephrol.* 12, 414–425.

Ronquillo, C. C., Hanke-Gogokhia, C., Revelo, M. P., Frederick, J. M., Jiang, L., and Baehr, W. (2016). Ciliopathy-associated IQCB1/NPHP5 protein is required for mouse photoreceptor outer segment formation. *FASEB J.* 30, 3400–3412. doi: 10.1096/fj.201600511R

Rosenthal, W., Seibold, A., Antaramian, A., Lonergan, M., Arthus, M.-F., Hendy, G. N., et al. (1992). Molecular identification of the gene responsible for congenital nephrogenic diabetes insipidus. *Nature* 359, 233–235.

Rossi, A. G., Sawatzky, D. A., Walker, A., Ward, C., Sheldrake, T. A., Riley, N. A., et al. (2006). Cyclin-dependent kinase inhibitors enhance the resolution of inflammation by promoting inflammatory cell apoptosis. *Nat. Med.* 12, 1056–1064. doi: 10.1038/nm1468

Ruan, G. X., Barry, E., Yu, D., Lukason, M., Cheng, S. H., and Scaria, A. (2017). CRISPR/Cas9-mediated genome editing as a therapeutic approach for leber congenital amaurosis 10. *Mol. Ther.* 25, 331–341. doi: 10.1016/j.ymthe.2016.12.006

Rubin, J. D., Nguyen, T. V., Allen, K. L., Ayasoufi, K., and Barry, M. A. (2019). Comparison of Gene Delivery to the Kidney by adenovirus, adeno-associated virus, and lentiviral vectors after intravenous and direct Kidney Injections. *Hum. Gene Ther.* 30, 1559–1571. doi: 10.1089/hum.2019.127

Ruggenenti, P., Remuzzi, A., Ondel, P., Fasolini, G., Antiga, L., Ene-Iordache, B., et al. (2005). Safety and efficacy of long-acting somatostatin treatment in autosomal-dominant polycystic kidney disease. *Kidney Int.* 68, 206–216. doi: 10.1111/j.1523-1755.2005.00395.x

Ruiz-Perez, V. L., Blair, H. J., Rodriguez-andres, M. E., Blanco, M. J., Wilson, A., Liu, Y., et al. (2007). Evc is a positive mediator of Ihh-regulated bone growth that localises at the base of chondrocyte cilia. *Development* 134, 2903–2912. doi: 10.1242/dev.007542

Saigusa, T., Dang, Y., Mullick, A. E., Yeh, S. T., Zile, M. R., Baicu, C. F., et al. (2016). Suppressing angiotensinogen synthesis attenuates kidney cyst formation in a Pkd1 mouse model. *FASEB J.* 30, 370–379. doi: 10.1096/fj.15-279299

Salomon, R., Saunier, S., and Niaudet, P. (2009). Nephronophthisis. *Pediatr. Nephrol.* 24, 2333–2344. doi: 10.1007/s00467-008-0840-z

Sang, L., Miller, J. J., Corbit, K. C., Giles, R. H., Brauer, M. J., Otto, E. A., et al. (2011). Mapping the Nephronophthisis-joubert-meckel-gruber protein network reveals ciliopathy disease genes and pathways. *Cell* 145, 513–528. doi: 10.1016/j.cell.2011.04.019.Mapping

Sankaran, D., Bankovic-Calic, N., Ogborn, M. R., Crow, G., and Aukema, H. M. (2007). Selective COX-2 inhibition markedly slows disease progression and attenuates altered prostanoid production in Han:SPRD-cy rats with inherited kidney disease. *Am. J. Physiol. Ren. Physiol.* 293, 821–830. doi: 10.1152/ajprenal.00257.2006

Sankaran, D., Lu, J., Bankovic-Calic, N., Ogborn, M. R., and Aukema, H. M. (2004). Modulation of renal injury in pcy mice by dietary fat containing n-3 fatty acids depends on the level and type of fat. *Lipids* 39, 207–214. doi: 10.1007/s11745-004-1221-7

Saunier, S., Calado, J., Heilig, R., Silbermann, F., Benessy, F., Morin, G., et al. (1997). A novel gene that encodes a protein with a putative src homology 3 domain is a candidate gene for familial juvenile nephronophthisis. *Hum. Mol. Genet.* 6, 2317–2323.

Sayer, J. A., Otto, E. A., O'Toole, J. F., Nurnberg, G., Kennedy, M. A., Becker, C., et al. (2006). The centrosomal protein nephrocystin-6 is mutated in Joubert syndrome and activates transcription factor ATF4. *Nat. Genet.* 38, 674–681. doi: 10.1038/ng1786

Schmidts, M., Frank, V., Eisenberger, T., Al Turki, S., Bizet, A. A., Antony, D., et al. (2013). Combined NGS approaches identify mutations in the intraflagellar transport gene IFT140 in skeletal ciliopathies with early progressive kidney disease. *Hum. Mutat.* 34, 714–724. doi: 10.1126/scitranslmed.3008882. Plasmodium

Schonauer, R., Jin, W., Ertel, A., Nemitz-Kliemchen, M., Panitz, N., Hantmann, E., et al. (2020). Novel nephronophthisis-associated variants reveal functional importance of MAPKBP1 dimerization for centriolar recruitment. *Kidney Int.* 98, 958–969. doi: 10.1016/j.kint.2020.05.027

Schueler, M., Braun, D. A., Chandrasekar, G., Gee, H. Y., Klasson, T. D., Halbritter, J., et al. (2015). DCDC2 mutations cause a renal-hepatic ciliopathy by disrupting Wnt signaling. *Am. J. Hum. Genet.* 96, 81–92. doi: 10.1016/j.ajhg.2014.12.002

Schutgens, F., Rookmaaker, M. B., Margaritis, T., Rios, A., Ammerlaan, C., Jansen, J., et al. (2019). Tubuloids derived from human adult kidney and urine for personalized disease modeling. *Nat. Biotechnol.* 37, 303–313. doi: 10.1038/s41587-019-0048-8

Serra, A. L., Poster, D., Kistler, A. D., Krauer, F., Raina, S., Young, J., et al. (2010). Sirolimus and kidney growth in autosomal dominant polycystic kidney disease. *N. Engl. J. Med.* 363, 820–829. doi: 10.1056/NEJMoa0907419

Shamseldin, H. E., Shaheen, R., Ewida, N., Bubshait, D. K., Alkuraya, H., Almardawi, E., et al. (2020). The morbid genome of ciliopathies: an update. *Genet. Med.* 22, 1051–1060. doi: 10.1038/s41436-020-0761-1

Shao, W., Yang, J., He, M., Yu, X. Y., Lee, C. H., Yang, Z., et al. (2020). Centrosome anchoring regulates progenitor properties and cortical formation. *Nature* 580, 106–112. doi: 10.1038/s41586-020-2139-6

Sharma, N., Kosan, Z. A., Stallworth, J. E., Berbari, N. F., and Yoder, B. K. (2011). Soluble levels of cytosolic tubulin regulate ciliary length control. *Mol. Biol. Cell* 22, 806–816. doi: 10.1091/mbc.E10-03-0269

Sherpa, R. T., Mohieldin, A. M., Pala, R., Wachten, D., Ostrom, R. S., and Nauli, S. M. (2019). Sensory primary cilium is a responsive cAMP microdomain in renal epithelia. *Sci. Rep.* 9, 1–16. doi: 10.1038/s41598-019-43002-2

Shillingford, J. M., Leamon, C. P., Vlahov, I. R., and Weimbs, T. (2012). Folate-conjugated rapamycin slows progression of polycystic kidney disease. *J. Am. Soc. Nephrol.* 23, 1674–1681. doi: 10.1681/ASN.2012040367

Shillingford, J. M., Murcia, N. S., Larson, C. H., Low, S. H., Hedgepeth, R., Brown, N., et al. (2006). The mTOR pathway is regulated by polycystin-1, and its inhibition reverses renal cystogenesis in polycystic kidney disease. *Proc. Natl. Acad. Sci. U.S.A.* 103, 5466–5471. doi: 10.1073/pnas.0509694103

Simons, D. L., Boye, S. L., Hauswirth, W. W., and Wu, S. M. (2011). Gene therapy prevents photoreceptor death and preserves retinal function in a Bardet-Biedl syndrome mouse model. *Proc. Natl. Acad. Sci. U.S.A.* 108, 6276–6281. doi: 10.1073/pnas.1019222108

Simons, M., Gloy, J., Ganner, A., Bullerkotte, A., Bashkurov, M., Kronig, C., et al. (2005). Inversin, the gene product mutated in nephronophthisis type II, functions as a molecular switch between Wnt signaling pathways. *Nat. Genet.* 37, 537–543. doi: 10.1038/ng1552

Skelding, K. A., Rostas, J. A. P., and Verrills, N. M. (2011). Controlling the cell cycle: the role of calcium/calmodulin-stimulated protein kinases I and II. *Cell Cycle* 10, 631–639. doi: 10.4161/cc.10.4.14798

Slaats, G. G., Ghosh, A. K., Falke, L. L., Le Corre, S., Shaltiel, I. A., van de Hoek, G., et al. (2014). Nephronophthisis-associated CEP164 regulates cell cycle progression, apoptosis and epithelial-to-mesenchymal transition. *PLoS Genet.* 10:e1004594. doi: 10.1371/journal.pgen.1004594

Slaats, G. G., and Giles, R. H. (2015). Are renal ciliopathies (replication) stressed out? *Trends Cell Biol.* 25, 317–319. doi: 10.1016/j.tcb.2015.03.005

Slaats, G. G., Lilien, M. R., and Giles, R. H. (2016). Nephronophthisis: should we target cysts or fibrosis? *Pediatr. Nephrol.* 31, 545–554. doi: 10.1007/s00467-015-3162-y

Slaats, G. G., Saldivar, J. C., Bacal, J., Zeman, M. K., Kile, A. C., Hynes, A. M., et al. (2015). DNA replication stress underlies renal phenotypes in CEP290 - associated Joubert syndrome. *J. Clin. Invest.* 125, 1–10. doi: 10.1172/JCI80657. of

Slanchev, K., Pütz, M., Schmitt, A., Kramer-Zucker, A., and Walz, G. (2011). Nephrocystin-4 is required for pronephric duct-dependent cloaca formation in zebrafish. *Hum. Mol. Genet.* 20, 3119–3128. doi: 10.1093/hmg/ddr214

Smith, L. A., Bukanov, N. O., Husson, H., Russo, R. J., Barry, T. C., Taylor, A. L., et al. (2006). Development of polycystic kidney disease in juvenile cystic kidney mice: insights into pathogenesis, ciliary abnormalities, and common features with human disease. *J. Am. Soc. Nephrol.* 17, 2821–2831. doi: 10.1681/ASN.2006020136

Smith, U. M., Consugar, M., Tee, L. J., McKee, B. M., Maina, E. N., Whelan, S., et al. (2006). The transmembrane protein meckelin (MKS3) is mutated in Meckel-Gruber syndrome and the wpk rat. *Nat. Genet.* 38, 191–196. doi: 10.1038/ng1713

Snoek, R., van Setten, J., Keating, B. J., Israni, A. K., Jacobson, P. A., Oetting, W. S., et al. (2018). NPHP1 (Nephrocystin-1) gene deletions cause adult-onset ESRD. *J. Am. Soc. Nephrol.* 29, 1772–1779. doi: 10.1681/asn.2017111200

Sohara, E., Luo, Y., Zhang, J., Manning, D. K., Beier, D. R., and Zhou, J. (2008). Nek8 regulates the expression and localization of polycystin-1 and polycystin-2. *J. Am. Soc. Nephrol.* 19, 469–476. doi: 10.1681/ASN.2006090985

Song, Z., Zhang, X., Jia, S., Yelick, P. C., and Zhao, C. (2016). Zebrafish as a model for human ciliopathies. *J. Genet. Genom.* 43, 107–120. doi: 10.1016/j.jgg.2016.02.001

Spasic, M., and Jacobs, C. R. (2017). Primary cilia: cell and molecular mechanosensors directing whole tissue function. *Semin. Cell Dev. Biol.* 71, 42–52. doi: 10.1016/j.semcdb.2017.08.036.Primary

Srivastava, S., Molinari, E., Raman, S., and Sayer, J. A. (2018). Many genes-one disease? Genetics of nephronophthisis (NPHP) and NPHP-associated disorders. *Front. Pediatr.* 5:287. doi: 10.3389/fped.2017.00287

Srivastava, S., Ramsbottom, S. A., Molinari, E., Alkanderi, S., Filby, A., White, K., et al. (2017). A human patient-derived cellular model of Joubert syndrome reveals ciliary defects which can be rescued with targeted therapies. *Hum. Mol. Genet.* 26, 4657–4667. doi: 10.1093/hmg/ddx347

Steichen, C., Giraud, S., and Hauet, T. (2020). Combining kidney Organoids and genome editing technologies for a better understanding of physiopathological mechanisms of renal diseases: state of the art. *Front. Med.* 7:10. doi: 10.3389/fmed.2020.00010

Stokman, M. F., Van der Zwaag, B., Van de Kar, N. C. A. J., Van Haelst, M. M., Van Eerde, A. M., Van der Heijden, J. W., et al. (2018). Clinical and genetic analyses of a Dutch cohort of 40 patients with a nephronophthisis-related ciliopathy. *Pediatr. Nephrol.* 33, 1701–1712. doi: 10.1007/s00467-018-3958-7

Strong, A., Muneeruddin, S., Parrish, R., Lui, D., and Conley, S. B. (2018). Isosorbide dinitrate in nephronophthisis treatment. *Am. J. Med. Genet. Part A* 176, 1023–1026. doi: 10.1002/ajmg.a.38650

Sugiyama, N., Kohno, M., and Yokoyama, T. (2012). Inhibition of the p38 MAPK pathway ameliorates renal fibrosis in an NPHP2 mouse model. *Nephrol. Dial. Transplant.* 27, 1351–1358. doi: 10.1093/ndt/gfr550

Sugiyama, N., Tsukiyama, T., Yamaguchi, T. P., and Yokoyama, T. (2011). The canonical Wnt signaling pathway is not involved in renal cyst development in the kidneys of inv mutant mice. *Kidney Int.* 79, 957–965.

Sussman, C. R., Wang, X., Chebib, F. T., and Torres, V. E. (2020). Modulation of polycystic kidney disease by G-protein coupled receptors and cyclic AMP signaling. *Cell. Signal.* 72:109649. doi: 10.1016/j.cellsig.2020.109649

Suzuki, A., Ogata, K., Yoshioka, H., Shim, J., Wassif, C. A., Porter, F. D., et al. (2020). Disruption of Dhcr7 and Insig1/2 in cholesterol metabolism causes defects in bone formation and homeostasis through primary cilium formation. *Bone Res.* 8:1. doi: 10.1038/s41413-019-0078-3

Szeto, S. G., Narimatsu, M., Lu, M., He, X., Sidiqi, A. M., Tolosa, M. F., et al. (2016). YAP/TAZ are mechanoregulators of TGF-b-smad signaling and renal fibrogenesis. *J. Am. Soc. Nephrol.* 27, 3117–3128. doi: 10.1681/ASN.2015050499

Takahashi, H., Calvet, J. P., Dittemore-Hoover, D., Yoshida, K., Grantham, J. J., and Gattone, V. H. (1991). A hereditary model of slowly progressive polycystic kidney disease in the mouse. *J. Am. Soc. Nephrol.* 1, 980–989.

Takasato, M., Er, P. X., Chiu, H. S., Maier, B., Baillie, G. J., Ferguson, C., et al. (2015). Kidney organoids from human iPS cells contain multiple lineages and model human nephrogenesis. *Nature* 526, 564–569.

Tan, R. J., Zhou, D., and Liu, Y. (2016). Signaling crosstalk between tubular epithelial cells and interstitial fibroblasts after kidney injury. *Kidney Dis.* 2, 136–144. doi: 10.1159/000446336

Tao, Y., Kim, J., Schrier, R. W., and Edelstein, C. L. (2005). Rapamycin markedly slows disease progression in a rat model of polycystic kidney disease. *J. Am. Soc. Nephrol.* 16, 46–51. doi: 10.1681/ASN.2004080660

Taskiran, E. Z., Korkmaz, E., Gucer, S., Kosukcu, C., Kaymaz, F., Koyunlar, C., et al. (2014). Mutations in ANKS6 cause a nephronophthisis-like phenotype with ESRD. *J. Am. Soc. Nephrol.* 25, 1653–1661. doi: 10.1681/ASN.2013060646

Tayfur, A. C., Besbas, N., Bilginer, Y., Ozaltin, F., Duzova, A., Bakkaloglu, M., et al. (2011). Follow-up of patients with juvenile nephronophthisis after renal transplantation: a single center experience. *Transplant. Proc.* 43, 847–849.

Tobin, J. L., and Beales, P. L. (2008). Restoration of renal function in zebrafish models of ciliopathies. *Pediatr. Nephrol.* 23, 2095–2099. doi: 10.1007/s00467-008-0898-7

Torres, V. E., Chapman, A. B., Devuyst, O., Gansevoort, R. T., Grantham, J. J., Higashihara, E., et al. (2012). Tolvaptan in patients with autosomal dominant polycystic kidney disease. *N. Engl. J. Med.* 367, 2407–2418. doi: 10.1056/NEJMoa1205511

Torres, V. E., Chapman, A. B., Devuyst, O., Gansevoort, R. T., Perrone, R. D., Dandurand, A., et al. (2018). Multicenter, open-label, extension trial to evaluate the long-term efficacy and safety of early versus delayed treatment with tolvaptan in autosomal dominant polycystic kidney disease: the TEMPO 4:4 Trial. *Nephrol. Dial. Transplant.* 33, 477–489. doi: 10.1093/ndt/gfx043

Torres, V. E., Chapman, A. B., Devuyst, O., Gansevoort, R. T., Perrone, R. D., Koch, G., et al. (2017). Tolvaptan in later-stage autosomal dominant polycystic kidney disease. *N. Engl. J. Med.* 377, 1930–1942. doi: 10.1056/NEJMoa1710030

Torres, V. E., Wang, X., Qian, Q., Somlo, S., Harris, P. C., and Ii, V. H. G. (2004). Effective treatment of an orthologous model of autosomal dominant polycystic kidney disease. *Nat. Med.* 10, 363–364. doi: 10.1038/nm1004

Tory, K., Lacoste, T., Burglen, L., Morinière, V., Boddaert, N., Macher, M. A., et al. (2007). High NPHP1 and NPHP6 mutation rate in patients with Joubert syndrome and nephronophthisis: potential epistatic effect of NPHP6 and AHI1 mutations in patients with NPHP1 mutations. *J. Am. Soc. Nephrol.* 18, 1566–1575. doi: 10.1681/ASN.2006101164

Tory, K., Rousset-Rouvière, C., Gubler, M. C., Morinière, V., Pawtowski, A., Becker, C., et al. (2009). Mutations of NPHP2 and NPHP3 in infantile nephronophthisis. *Kidney Int.* 75, 839–847. doi: 10.1038/ki.2008.662

Toya, M., and Takeichi, M. (2016). Organization of non-centrosomal microtubules in epithelial cells. *Cell Struct. Funct.* 41, 127–135. doi: 10.1247/csf.16015

Tran, P. V., Haycraft, C. J., Besschetnova, T. Y., Turbe-Doan, A., Scottmann, R. W., Herron, B. J., et al. (2008). THM1 negatively modulates mouse sonic hedgehog signal transduction and affects retrograde intraflagellar transport in cilia. *Nat. Genet.* 40, 403–410.

Tran, P. V., Talbott, G. C., Turbe-Doan, A., Jacobs, D. T., Schonfeld, M. P., Silva, L. M., et al. (2014). Downregulating hedgehog signaling reduces renal cystogenic potential of mouse models. *J. Am. Soc. Nephrol.* 25, 2201–2212. doi: 10.1681/ASN.2013070735

Tsai, I. C., Adams, K. A., Tzeng, J. A., Shennib, O., Tan, P. L., and Katsanis, N. (2019). Genome-wide suppressor screen identifies USP35/USP38 as therapeutic candidates for ciliopathies. *JCI Insight* 4:e130516. doi: 10.1172/jci.insight.130516

Uchimura, K., Wu, H., Yoshimura, Y., and Humphreys, B. D. (2020). Human pluripotent stem cell-derived kidney organoids with improved collecting duct maturation and injury modeling. *Cell Rep.* 33:108514. doi: 10.1016/j.celrep.2020.108514

Valente, E. M., Silhavy, J. L., Brancati, F., Barrano, G., Krishnaswami, S. R., Castori, M., et al. (2006). Mutations in CEP290, which encodes a centrosomal protein, cause pleiotropic forms of Joubert syndrome. *Nat. Genet.* 38, 623–625.

Van den Ouweland, A. M., Dreesen, J. C., Verdijk, M., Knoers, N. V., Monnens, L. A., Rocchi, M., et al. (1992). Mutations in the vasopressin type 2 receptor gene (AVPR2) associated with nephrogenic diabetes insipidus. *Nat. Genet.* 2, 99–102.

Viau, A., Bienaimé, F., Lukas, K., Todkar, A. P., Knoll, M., Yakulov, T. A., et al. (2018). Cilia-localized LKB 1 regulates chemokine signaling, macrophage recruitment, and tissue homeostasis in the kidney. *EMBO J.* 37, 1–21. doi: 10.15252/embj.201798615

Vierkotten, J., Dildrop, R., Peters, T., Wang, B., and Rüther, U. (2007). Ftm is a novel basal body protein of cilia involved in Shh signalling. *Development* 134, 2569–2577. doi: 10.1242/dev.003715

Wang, J., and Barr, M. M. (2016). Ciliary extracellular vesicles: Txt msg orgnlls. *Cell. Mol. Neurobiol.* 36, 449–457. doi: 10.1016/j.gde.2016.03.011

Wang, K., Li, L., Zhang, Y., and Gao, D. (2020). Crosstalk between signaling pathways and DNA damage response. *Genome Instab. Dis.* 1, 81–91. doi: 10.1007/s42764-019-00005-7

Wang, Y., Yin, X., Rosen, G., Gabel, L., Guadiana, S. M., Sarkisian, M. R., et al. (2011). *Dcdc2* knockout mice display exacerbated developmental disruptions following knockdown of doublecortin. *Neurosci.* 190, 398–408. doi: 10.1016/j.neuroscience.2011.06.010

Wang, Y., Zhou, C. J., and Liu, Y. (2018). Wnt signaling in kidney development and disease. *Prog. Mol. Biol. Transl. Sci.* 153, 181–207. doi: 10.1016/bs.pmbts.2017.11.019

Watanabe, Y., Fujinaga, S., Sakuraya, K., Morisada, N., Nozu, K., and Iijima, K. (2019). Rapidly progressive nephronophthisis in a 2-year-old boy with a homozygous SDCCAG8 mutation. *Tohoku J. Exp. Med.* 249, 29–32. doi: 10.1620/tjem.249.29

Waters, A. M., and Beales, P. L. (2011). Ciliopathies: an expanding disease spectrum. *Pediatr. Nephrol.* 26, 1039–1056. doi: 10.1007/s00467-010-1731-7

Wheway, G., Nazlamova, L., and Hancock, J. T. (2018). Signaling through the primary cilium. *Front. Cell Dev. Biol.* 6:8. doi: 10.3389/fcell.2018.00008

Wiegering, A., Dildrop, R., Vesque, C., Schneider-Maunoury, S., and Gerhardt, C. (2021). Rpgrip1l controls ciliary gating by ensuring the proper amount of Cep290 at the vertebrate transition zone. *Mol Biol Cell* 2, 675–689. doi: 10.1101/2020.02.10.942300

Wiegering, A., Rüther, U., and Gerhardt, C. (2019). The role of primary cilia in the crosstalk between the Ubiquitin-proteasome system and autophagy. *Cells* 8:241. doi: 10.3390/cells8030241

Wolf, M. T., Saunier, S., O'Toole, J. F., Wanner, N., Groshong, T., Attanasio, M., et al. (2007). Mutational analysis of the RPGRIP1L gene in patients with Joubert

syndrome and nephronophthisis. *Kidney Int.* 72, 1520–1526. doi: 10.1038/sj.ki.5002630

Won, J., de Evsikova, C. M., Smith, R. S., Hicks, W. L., Edwards, M. M., Longo-Guess, C., et al. (2011). NPHP4 is necessary for normal photoreceptor ribbon synapse maintenance and outer segment formation, and for sperm development. *Hum. Mol. Genet.* 20, 482–496. doi: 10.1093/hmg/ddq494

Wood, C. R., Huang, K., Diener, D. R., and Rosenbaum, J. L. (2013). The cilium secretes bioactive ectosomes. *Curr. Biol.* 23, 906–911. doi: 10.1016/j.cub.2013.04.019

Wu, M., Gu, J., Mei, S., Xu, D., Jing, Y., Yao, Q., et al. (2016). Resveratrol delays polycystic kidney disease progression through attenuation of nuclear factor κb-induced inflammation. *Nephrol. Dial. Transplant.* 31, 1826–1834. doi: 10.1093/ndt/gfw058

Xu, C., Wang, L., Zhang, Y., Li, W., Li, J., Wang, Y., et al. (2020). Tubule-Specific Mst1/2 Deficiency Induces CKD via YAP and Non-YAP Mechanisms. *J Am Soc Nephrol* 31, 946–961. doi: 10.1681/ASN.2019101052

Yamaguchi, T., Devassy, J. G., Gabbs, M., Ravandi, A., Nagao, S., and Aukema, H. M. (2015). Dietary flax oil rich in α-linolenic acid reduces renal disease and oxylipin abnormalities, including formation of docosahexaenoic acid derived oxylipins in the CD1-pcy/pcy mouse model of nephronophthisis. *Prostaglandins Leukot. Essent. Fat. Acids* 94, 83–89. doi: 10.1016/j.plefa.2014.11.009

Yamaguchi, T., Lysecki, C., Reid, A., Nagao, S., and Aukema, H. M. (2014). Renal cyclooxygenase products are higher and lipoxygenase products are lower in early disease in the pcy mouse model of adolescent nephronophthisis. *Lipids* 49, 39–47. doi: 10.1007/s11745-013-3859-2

Yamaguchi, T., Nagao, S., Wallace, D. P., Belibi, F. A., Cowley, B. D., Pelling, J. C., et al. (2003). Cyclic AMP activates B-Raf and ERK in cyst epithelial cells from autosomal-dominant polycystic kidneys. *Kidney Int.* 63, 1983–1994. doi: 10.1046/j.1523-1755.2003.00023.x

Yamaguchi, T., Pelling, J. C., Ramaswamy, N. T., Eppler, J. W., Wallace, D. P., Nagao, S., et al. (2000). cAMP stimulates the in vitro proliferation of renal cyst epithelial cells by activating the extracellular signal-regulated kinase pathway. *Kidney Int.* 57, 1460–1471. doi: 10.1046/j.1523-1755.2000.00991.x

Ye, H., Wang, X., Constans, M. M., Sussman, C. R., Chebib, F. T., Irazabal, M. V., et al. (2017). The regulatory 1α subunit of protein kinase a modulates renal cystogenesis. *Am. J. Physiol. Ren. Physiol.* 313, F677–F686. doi: 10.1152/ajprenal.00119.2017

Ye, M., and Grantham, J. J. (1993). The secretion of fluid by renal cysts from patients with autosomal dominant polycystic kidney disease. *New Engl. J. Med.* 329, 310–313.

Yokoyama, T., Copeland, N. G., Jenkins, N. A., Charles, A., Elder, F. F. B., Overbeek, P. A., et al. (1993). Reversal of Left-right asymmetry: a situs inversus mutation. *Science* 260, 679–682.

Yoshina, S., Sakaki, K., Yonezumi-Hayashi, A., Gengyo-Ando, K., Inoue, H., Iino, Y., et al. (2012). Identification of a novel ADAMTS9/GON-1 function for protein transport from the ER to the Golgi. *Mol. Biol. Cell* 23, 1728–1741. doi: 10.1091/mbc.E11-10-0857

Yousef Yengej, F. A., Jansen, J., Rookmaaker, M. B., Verhaar, M. C., and Clevers, H. (2020). Kidney Organoids and Tubuloids. *Cells* 9, 1–20. doi: 10.3390/cells9061326

Zafar, I., Tao, Y., Falk, S., McFann, K., Schrier, R. W., and Edelstein, C. L. (2007). Effect of statin and angiotensin-converting enzyme inhibition on structural and hemodynamic alterations in autosomal dominant polycystic kidney disease model. *Am. J. Physiol. Ren. Physiol.* 293, 854–859. doi: 10.1152/ajprenal.00059.2007

Zhang, J. Q. J., Burgess, J., Stepanova, D., Saravanabavan, S., Wong, A. T. Y., Kaldis, P., et al. (2020). Role of cyclin-dependent kinase 2 in the progression of mouse juvenile cystic kidney disease. *Lab. Investig.* 100, 696–711. doi: 10.1038/s41374-019-0360-4

Zhang, J. Q. J., Saravanabavan, S., Munt, A., Wong, A. T. Y., Harris, D. C., Harris, P. C., et al. (2019). The role of DNA damage as a therapeutic target in autosomal dominant polycystic kidney. *Expert Rev. Mol. Med.* 21:e6.

Zhang, P., Kiseleva, A. A., Korobeynikov, V., Liu, H., and Liebau, M. C. (2019). Microscopy-based automated live cell screening for small molecules that affect ciliation. *Front. Genet.* 10:75. doi: 10.3389/fgene.2019.00075

Zhou, W., Otto, E. A., Cluckey, A., Airik, R., Hurd, T. W., Chaki, M., et al. (2012). FAN1 mutations cause karyomegalic interstitial nephritis, linking chronic kidney failure to defective DNA damage repair. *Nat. Genet.* 44, 910–917.

Zhu, P., Qiu, Q., Harris, P. C., Xu, X., and Lin, X. (2021). *mtor* Haploinsufficiency ameliorates renal cysts and cilia abnormality in adult Zebrafish tmem67 mutants. *J Am Soc Nephrol* 2021:ASN.2020070991.

Zullo, A., Iaconis, D., Barra, A., Cantone, A., Messaddeq, N., Capasso, G., et al. (2010). Kidney-specific inactivation of Ofd1 leads to renal cystic disease associated with upregulation of the mTOR pathway. *Hum. Mol. Genet.* 19, 2792–2803. doi: 10.1093/hmg/ddq180

Conflict of Interest: The authors declare that the research was conducted in the absence of any commercial or financial relationships that could be construed as a potential conflict of interest.

Copyright © 2021 Stokman, Saunier and Benmerah. This is an open-access article distributed under the terms of the Creative Commons Attribution License (CC BY). The use, distribution or reproduction in other forums is permitted, provided the original author(s) and the copyright owner(s) are credited and that the original publication in this journal is cited, in accordance with accepted academic practice. No use, distribution or reproduction is permitted which does not comply with these terms.

Advantages of publishing in Frontiers

OPEN ACCESS
Articles are free to read for greatest visibility and readership

FAST PUBLICATION
Around 90 days from submission to decision

HIGH QUALITY PEER-REVIEW
Rigorous, collaborative, and constructive peer-review

TRANSPARENT PEER-REVIEW
Editors and reviewers acknowledged by name on published articles

Frontiers
Avenue du Tribunal-Fédéral 34
1005 Lausanne | Switzerland

Visit us: www.frontiersin.org
Contact us: frontiersin.org/about/contact

REPRODUCIBILITY OF RESEARCH
Support open data and methods to enhance research reproducibility

DIGITAL PUBLISHING
Articles designed for optimal readership across devices

FOLLOW US
@frontiersin

IMPACT METRICS
Advanced article metrics track visibility across digital media

EXTENSIVE PROMOTION
Marketing and promotion of impactful research

LOOP RESEARCH NETWORK
Our network increases your article's readership